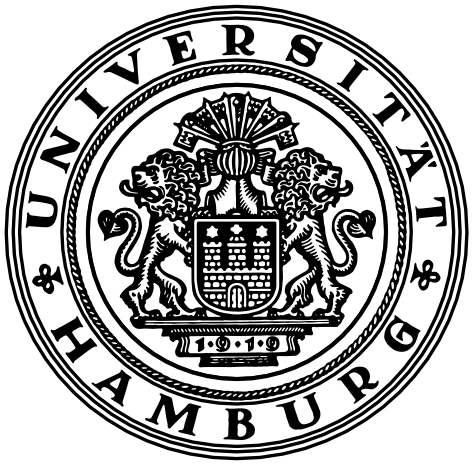
Hantzsch Esters: Versatile Reagents for Light-Driven C_1 Functionalization

Dissertation

zur Erlangung des Doktorgrades der Naturwissenschaften

Dr. rer. nat.

am Institut für Anorganische und Angewandte Chemie der Universität Hamburg



vorgelegt von

Mattis-Ole W. S. Schmotz

aus Hamburg

Hamburg, 2025

The experimental part of this work was performed from October 2020 to July 2025 at the Institute of Inorganic and Applied Chemistry, University of Hamburg. This work was supervised by Prof. Dr. Axel Jacobi von Wangelin.

Date of thesis submission:	15.09.2025
Board of examiners:	1.) Prof. Dr. Axel Jacobi von Wangelin
	2.) Prof. Dr. Gerrit Luinstra
Date of thesis defense:	30.10.2025
Board of examiners:	1.) Prof. Dr. Axel Jacobi von Wangelin
	2.) Prof. Dr. Ralph Holl
	3.) Prof. Dr. Lisa Vondung

“And if in a distant future the supply of coal becomes completely exhausted, civilization will not be checked by that, for life and civilization will continue as long as the sun shines!

If our black and nervous civilization, based on coal, shall be followed by a quieter civilization based on the utilization of solar energy, that will not be harmful to progress and to human happiness.

The photochemistry of the future should not however be postponed to such distant times; I believe that industry will do well in using from this very day all the energies that nature puts at its disposal. So far, human civilization has made use almost exclusively of fossil solar energy.

Would it not be advantageous
to make better use of radiant energy?”

GIACOMO LUIGI CIAMICIAN

The Photochemistry of the Future, **1912**

Table of Contents

List of Publications I
List of Abbreviations II
Abstract III
Zusammenfassung IV
1 Introduction and Theoretical Foundations 1
1.1 Let there be Light: Photochemistry 1
1.1.1 A Brief History of Photochemistry 1
1.1.2 Photocatalysis 6
1.1.3 The Basics of Photoredox Catalysis 7
1.1.4 What Qualifies as a Photoredox Catalyst? 9
1.1.5 The Photoinduced Electron Transfer 13
1.1.6 Applications of Photoredox Catalysis 17
1.2 Hantzsch Esters 21
1.2.1 What are Hantzsch Esters? 21
1.2.2 Applications of Hantzsch Esters: Pharmaceuticals 22
1.2.3 Applications of Hantzsch Esters: Transfer Hydrogenation 23
1.2.4 Applications of Hantzsch Esters: Radical Alkylation 25
1.2.5 Applications of Hantzsch Esters: C_1 Functionalization 28
2 Photoredox-Catalyzed Synthesis of α-Amino Acid Amides by Imine Carbamoylation 37
2.1 Results and Discussion 37
2.2 Experimental Section 46
3 Catalyst-Free Photo-Hydroformylation of Olefins 129
3.1 Results and Discussion 129
3.2 Experimental Section 140
4 Nickel-Catalyzed Photoformylation of Aryl Bromides 260
4.1 Results and Discussion 260
4.2 Experimental Section 268
5 Hydroformylation of Electron-Deficient Olefins by Photoredox Catalysis 290
5.1 Results and Discussion 290
5.2 Experimental Section 299
6 Hydroformylation of Electron-Deficient Olefins via Thioacetal Intermediates 344
6.1 Results and Discussion 344
6.2 Experimental Section 351
Appendix 398
List of Used Chemicals 398
Acknowledgements 420
Eidesstattliche Erklärung 421

List of Publications

[1] L. Cardinale,[†] M.-O. W. S. Schmotz,[†] M. O. Konev, A. Jacobi von Wangelin*, Photoredox-Catalyzed Synthesis of α-Amino Acid Amides by Imine Carbamoylation, *Org. Lett.* **2021**, *24*, 506–510.

[2] B. J. Gregori, M.-O. W. S. Schmotz, A. Jacobi von Wangelin*, Stereoselective Semi-Hydrogenations of Alkynes by First-Row (3d) Transition Metal Catalysts, *ChemCatChem* **2022**, *14*, e202200886.

List of Abbreviations

3DPA2FBN	2,4,6-Tris(diphenylamino)-3,5-difluorobenzonitrile
3DPAFIPN	2,4,6-Tris(diphenylamino)-5-fluoroisophthalonitrile
4CzIPN	2,4,5,6-Tetrakis(9*H*-carbazol-9-yl)-isophthalonitrile
A	Acceptor
Acr	Acridine
AIBN	Azobisisobutyronitrile
BAIB	Bis(acetoxy)iodobenzene
BINOL	1,1‘-Bi-2-naphthol
Boc	*tert*-Butyloxycarbonyl
BOX	Bis(oxazoline)
bpy	2,2‘-Bipyridine
cat.	Catalytic
CHANT	*N*-Cyclohexyl-2-(((2,2,6,6-tetramethylpiperidin-1-yl)oxy)methyl)acrylamide
D	Donor
DCC	*N*,*N*‘-Dicyclohexylcarbodiimide
DDQ	2,3-Dichloro-5,6-dicyano-1,4-benzoquinone
DIPEA	Diisopropylethylamine
DMAP	*N*,*N*-Dimethylaminopyridine
DMA	*N*,*N*-Dimethylacetamide
DME	1,2-Dimethoxyethane
DMF	*N*,*N*-Dimethylformamide
DMI	1,3-Dimethyl-2-imidazolidinone
DMP	Dess-Martin periodinane
dMeObpy	4,4‘-Dimethoxy-2,2‘-bipyridine
DMSO	Dimethyl sulfoxide
dr	Diastereomeric ratio
dtbbpy	4,4‘-Di-*tert*-butyl-2,2‘-bipyridine
EC	Encounter complex
EDA	Electron donor-acceptor
EDG	Electron-donating group
ee/*e.e.*	Enantiomeric excess
EnT	Energy Transfer
ESI	Electrospray ionization
ET	Electron transfer
EWG	Electron-withdrawing group
EY	Eosin Y
GC-MS	Gas chromatography-mass spectrometry
GP	Gas phase
HAT	Hydrogen atom transfer
HFIP	Hexafluoroisopropanol
HOMO	Highest occupied molecular orbital
HPLC	High-performance liquid chromatography
HRMS	High-resolution mass spectrometry
IC	Internal conversion
Ipc	Isopinocampheyl
IR	Infrared
ISC	Intersystem Crossing
LED	Light-emitting diode
LUMO	Lowest unoccupied molecular orbital
Mes	Mesityl
MLCT	Metal-to-ligand charge transfer
m.p.	Melting point
MS	Mass spectrometry
NADP	Nicotinamide adenine dinucleotide phosphate
NBS	*N*-Bromosuccinimide
NMR	Nuclear magnetic resonance
PC	Photocatalyst
PET	Photoinduced electron transfer
phen	1,10-Phenanthroline
PIFA	Phenyliodine bis(trifluoroacetate)
Piv	Pivaloyl
PMP	*para*-Methoxyphenyl
ppy	2-Phenylpyridine
PRC	Photoredox catalyst
Py	Pyridine
SCE	Saturated calomel electrode
SET	Single-electron transfer
SSIP	Solvent-separated ion pair
STY	Space-time yield
TEMPO	(2,2,6,6-Tetramethylpiperidin-1-yl)oxyl
Tf	Triflate/Trifluoromethanesulfonate
TFA	Trifluoroacetic acid
THF	Tetrahydrofuran
TLC	Thin-layer chromatography
TMEDA	*N*,*N*,*N‘*,*N‘*-Tetramethylethylenediamine
Tol	Tolyl
Ts	Tosyl/toluenesulfonyl
UV	Ultraviolet
Vis	Visible (light)
XAT	X-atom transfer
XRD	X-ray diffraction

Abstract

The present thesis aims to explore novel methods for photochemical C_1 functionalization of various substrates using Hantzsch ester derivatives as the C_1 source. Particular emphasis is placed on synthetic utility and ease of operation.

Chapter 1 provides a theoretical overview to the reader, including an introduction to the world of photochemistry, a brief outline of key historical developments, the fundamentals of photoredox catalysis, a theoretical approach to photoinduced electron transfer, as well as applications of photoredox catalysis in comparison to traditional methods. This is followed by an introduction to Hantzsch esters, including their discovery, synthesis, and various applications such as transfer hydrogenation, free-radical alkylation, and C_1 functionalization.

In **Chapter 2**, a blue-light photoredox-catalyzed approach towards amino acid amides/peptides is detailed. The protocol starts from easily accessible imines and employs 4-carbamoyl-substituted Hantzsch esters as the amide source in this radical-variant STRECKER reaction. All three substituents (side chain, *N*-substituent, amide moiety) are freely selectable, making this modular approach particularly attractive.

A novel strategy for a fully (photo)catalyst- and additive-free olefin hydroformylation is presented in **Chapter 3**. Upon direct ultraviolet irradiation, a dimethoxymethyl-substituted Hantzsch ester transfers the acetal moiety onto electron-deficient olefins. This results in protected aldehydes, which can be easily deprotected using non-aqueous trifluoroacetic acid.

Chapter 4 seeks to extend the scope of this photocatalyst-free Hantzsch ester reactivity towards the synthesis of aromatic aldehydes. By addition of a simple [Ni] catalyst ($NiBr_2 \cdot$DME, 2,2'-bipyridine), aryl bromides are converted in a free-radical cross-coupling. With a substituted ligand (4,4'-dimethoxy-2,2'-bipyridine) even notoriously challenging electron-rich aryl bromides are converted in satisfactory yields.

In **Chapter 5**, an extension of the olefin hydroformylation of Chapter 3 is reported. Upon green-light photoredox catalysis using Eosin Y, yields and reaction times are significantly improved. Additionally, a continuous-flow protocol allows for effortless scale-up.

Two alternate approaches for olefin hydroformylation are presented in **Chapter 6**. In both a photocatalyst-free UV-mediated and a blue-light photoredox-catalyzed strategy, thioacetals are obtained instead of oxoacetals. They exhibit orthogonal reactivity and are particularly of interest in synthetic organic chemistry. The scope of these reactions shows complementarity to those presented in Chapter 3 and 5, as also substrates bearing additional electron-withdrawing groups are converted smoothly.

Zusammenfassung

Die vorliegende Dissertation befasst sich mit der Entwicklung neuartiger Methoden zur photochemischen C_1-Funktionalisierung verschiedenster Substrate mit Hantzsch-Ester-Derivaten als C_1-Quelle. Besonderer Wert wird dabei auf synthetische Anwendungsbreite und einfache Handhabung gelegt.

Kapitel 1 bietet einen theoretischen Überblick, einschließlich einer Einführung in die Welt der Photochemie, eines kurzen Abrisses historischer Meilensteine, der Grundlagen der Photoredox-Katalyse, einer theoretischen Herleitung des photoinduzierten Elektronentransfers, sowie Anwendungen der Photoredox-Katalyse im Vergleich zu traditionellen Methoden. Es folgt ein Überblick über Hantzsch-Ester, einschließlich ihrer Entdeckung, Synthese, und der vielseitigen Anwendungen wie bspw. Transferhydrierungen, radikalische Alkylierungen und C_1-Funktionalisierungen.

In **Kapitel 2** wird eine photoredox-katalysierte Synthese von Aminosäureamiden/Peptiden mittels blauen Lichts beschrieben. Diese radikalische Variante der STRECKER-Reaktion nutzt leicht zugängliche Imine und 4-Carbamoyl-substituierte Hantzsch-Ester als Amidquelle. Alle drei Substituenten (Seitenkette, *N*-Substituent, Amidrest) sind frei wählbar, was diesen modularen Ansatz besonders attraktiv gestaltet.

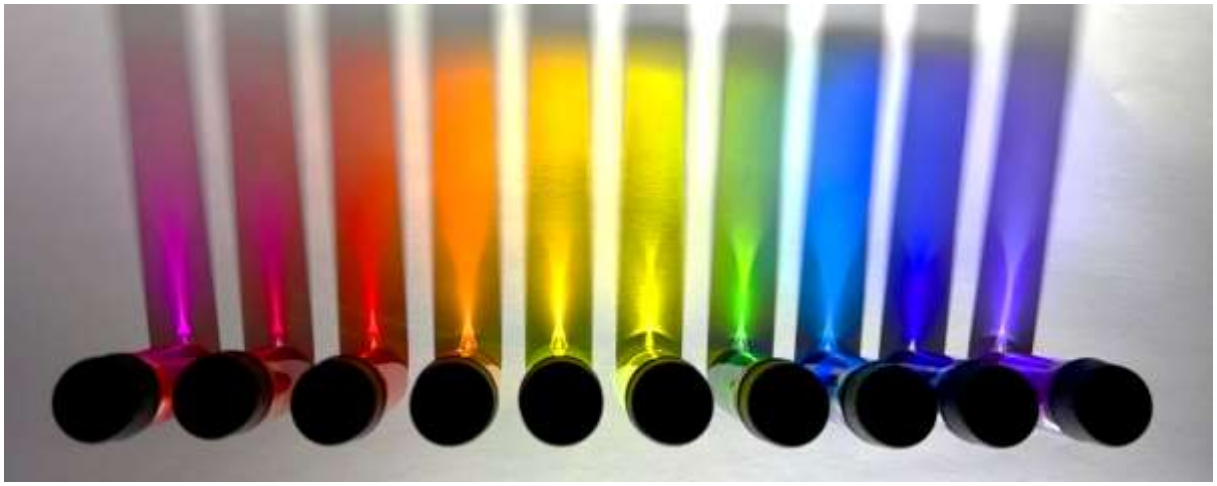
Eine neuartige Strategie zur völlig (photo)katalysator- und additivfreien Hydroformylierung von Olefinen wird in **Kapitel 3** vorgestellt. Unter direkter Ultraviolettbestrahlung überträgt ein Dimethoxymethyl-substituierter Hantzsch-Ester die Acetalgruppe auf elektronenarme Olefine. Dabei entstehen geschützte Aldehyde, die sich leicht mittels wasserfreier Trifluoressigsäure entschützen lassen.

In **Kapitel 4** wird das Anwendungsspektrum dieser photokatalysatorfreien Hantzsch-Ester-Reaktion auf die Synthese aromatischer Aldehyde erweitert. In Gegenwart eines simplen [Ni]-Katalysators ($NiBr_2$·DME, 2,2'-Bipyridin) werden Arylbromide in einer radikalischen Kreuzkupplung umgesetzt. Durch Verwendung eines substituierten Liganden (4,4'-Dimethoxy-2,2'-bipyridin) können selbst anspruchsvolle elektronenreiche Arylbromide zufriedenstellend umgesetzt werden.

In **Kapitel 5** wird eine Erweiterung der in Kapitel 3 beschriebenen Olefin-Hydroformylierung vorgestellt. Unter Einsatz von Photoredox-Katalyse mittels grünen Lichts und Eosin Y werden sowohl Ausbeuten als auch Reaktionszeiten signifikant verbessert. Des Weiteren erlaubt eine *Continuous-Flow*-Methode mühelose Hochskalierung.

Zwei alternative Ansätze zur Olefin-Hydroformylierung werden in **Kapitel 6** präsentiert. Sowohl in einer UV-vermittelten, photokatalysatorfreien als auch einer photoredox-katalysierten Strategie werden Thioacetale anstelle von Oxoacetalen erhalten. Diese zeigen orthogonale Reaktivität und sind besonders aus organisch-synthetischer Sicht interessant. Die Substratpalette ergänzt sich mit der aus Kapitel 3 und 5, da auch Substrate mit zusätzlichen elektronenziehenden Gruppen glatt umgesetzt werden.

Chapter 1.1



Let there be Light: Photochemistry

1.1.1 A Brief History of Photochemistry

In its earliest days, photochemistry was dominated by light from the sun, the most abundant and intense light source on earth. The solar radiation at sea level closely resembles the emission spectrum of an ideal black body at 5722 K minus the absorption bands of atmospheric components, mainly water, oxygen, ozone, and carbon dioxide (Fig. 1).

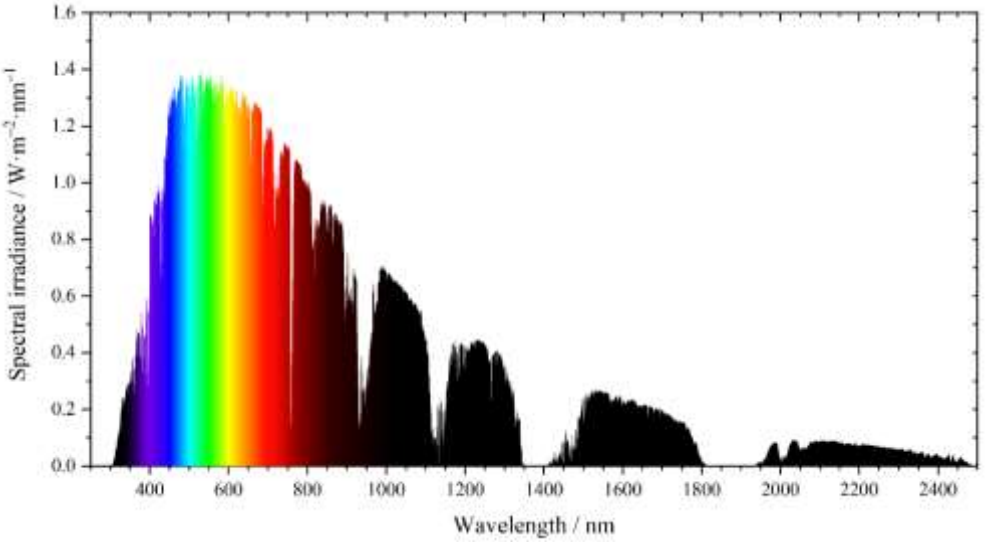


Fig. 1. *Solar radiation spectrum at sea level plotted from ASTM G173-03 reference data (Direct Normal). Colors may not be accurately reproduced in the printed version of this work.*

Ultraviolet light (<400 nm) merely accounts for 3–5% of the solar energy received on earth's surface, yet it is the major factor in sunlight-driven photochemistry. The latter likely first emerged in the form of undesired bleaching of colors, paints, and dyes in ancient times. Allegedly, Alexander the Great (356 BC–323 BC), King of Macedon, found a clever way to exploit this phenomenon: He reportedly supplied his soldiers with wristbands containing a dye that turned purple upon exposure to sunlight.[1] This apparently predictable and reproducible color shift signaled the start of a coordinated attack at a specific time, essentially functioning as the world's first wristwatch. The exact dye remains unknown, but is believed to be a colorless precursor to Tyrian purple (6,6'-dibromoindigo) obtained from the purple dye murex (*Bolinus brandaris*), a sea snail (Fig. 2).[2]

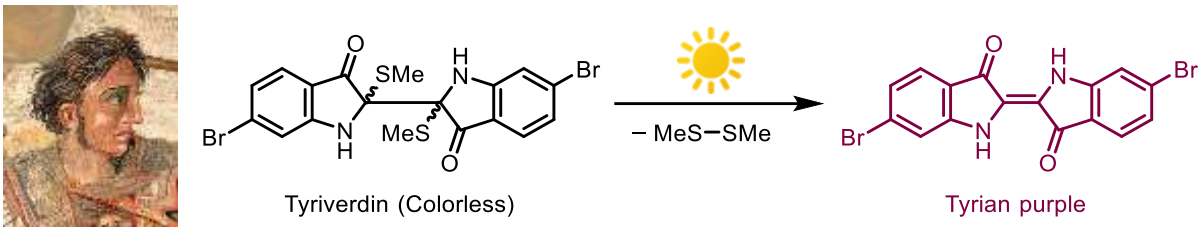


Fig. 2. *Colorless Tyriverdin is converted into Tyrian Purple by the action of sunlight, an effect allegedly exploited by Alexander the Great.*[3]

One of the first non-dye compounds that attracted special attention to its photochemistry is santonin, a sesquiterpene lactone from Levant wormseed (*Artemisia cina*) which has been used as an anthelminthic for over 2,000 years.[4] Santonin was first isolated and its properties investigated in 1830.[5,6] The colorless crystals were observed to yellow and eventually burst when exposed to sunlight. This peculiar observation caught the attention of German pharmacist Hermann Trommsdorff, who began investigating this phenomenon in 1834.[7] In groundbreaking pioneering work, he became one of the first scientists to identify a wavelength-dependent photochemical reaction: Trommsdorff used a prism to separate the sunlight into its individual colors and discovered that santonin was changed by the action of the violet and blue beams, while the yellow, green, and red beams had no effect at all – an observation which he could not have possibly explained with the state of chemistry and physics in his time. The photochemistry of santonin in solution was not fully elucidated until 1958[8] and its complex solid-phase photochemistry (including the "exploding crystal" phenomenon) remained unsolved until 1968 (Fig. 3).[9]

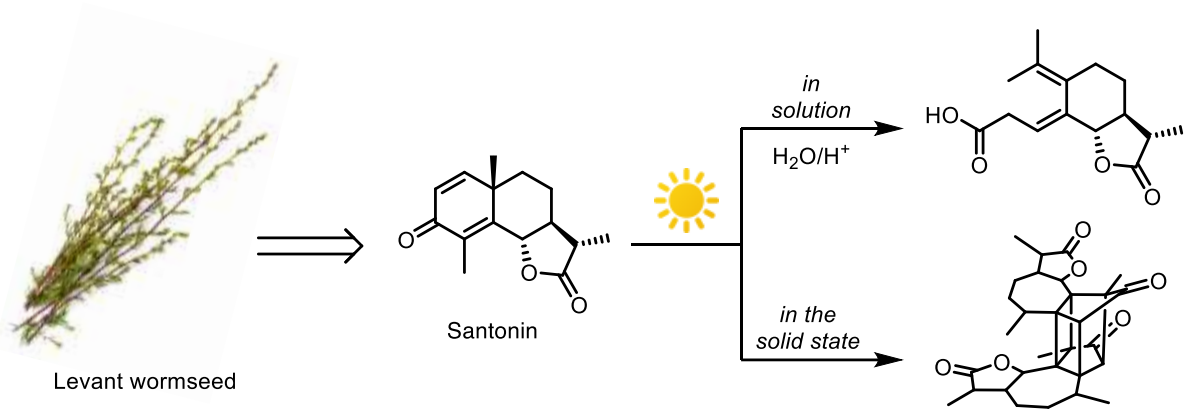


Fig. 3. *Santonin from the Levant wormseed undergoes complex photoinduced rearrangements in solution (towards photosantonic acid)*[8] *or in the solid state.*[9]

As early as 1867, Carl Fritzsche observed that an anthracene solution exposed to sunlight separated small crystals of a substance distinct from anthracene yet capable of regenerating it upon heating above the melting point.[10] In 1891, Karl Elbs identified this "paranthracene" as a dimer based on molecular weight measurements[11] and the first correct structure was proposed by Orndorff and Cameron in 1895 (Fig. 4, top).[12] This marks the first documented case of a photodimerization reaction.

The first photo**iso**merization was reported in 1881 by William Perkin, who discovered that violet and ultraviolet rays from sunlight could reversibly isomerize 2-methoxycinnamic acid between its *E* and *Z* form (Fig. 4, bottom).[13] However, Perkin was unaware of the stereochemical nature of the isomerism at hand, simply referring to them as "α-" and "β-methylorthoxyphenylacrylic acid" without structural proposals.

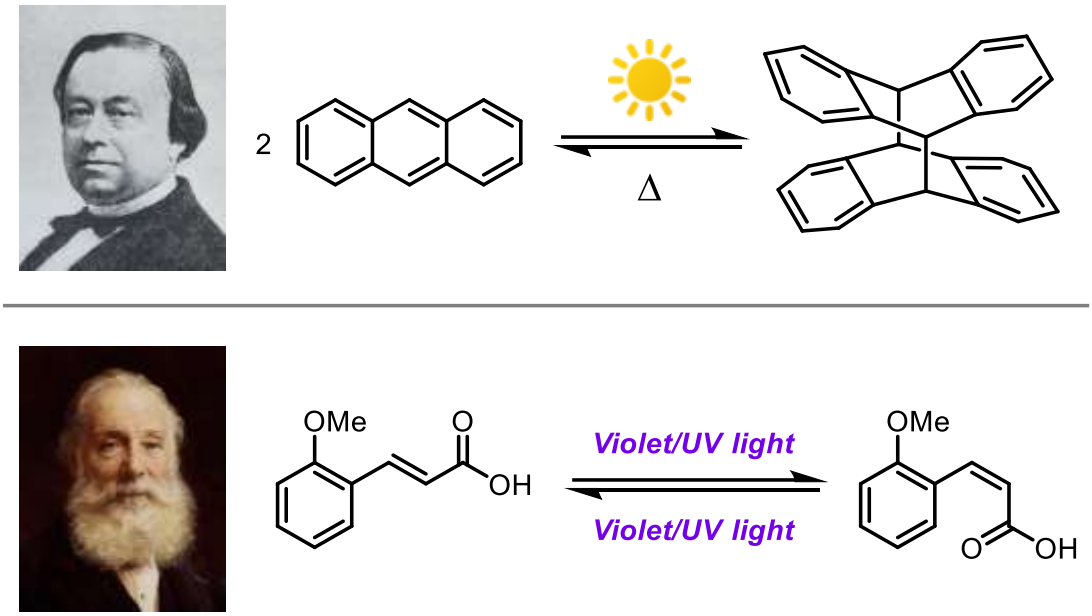


Fig. 4. *Top: Photodimerization of anthracene by sunlight (Carl Fritzsche, 1867),[10] Bottom: E/Z isomerization of 2-methoxycinnamic acid by violet or UV light (William Perkin, 1881).[13]*

In the beginning of the 20th century, Giacomo Ciamician and his assistant Paul Silber (commonly referred to as *Paolo Silber* in Italian) conducted numerous systematic studies on the role of light in chemical transformations with unparalleled fervor, skill, and expertise. Between 1900 and 1915, they published over thirty groundbreaking works in their comprehensive series "*Chemische Lichteinwirkungen*", comprising well over a hundred individual experiments. This monumental body of work helped establish photochemistry as a fundamental branch of chemistry. Their studies include, but are by far not limited to, the addition of methanol to acetone,[14] the conversion of *o*-nitrobenzaldehyde to *o*-nitrosobenzoic acid,[15] the intramolecular [2+2]-cycloaddition of carvone (remarkably, Ciamician correctly deduced the structure of the product),[16] and the photo-mediated oxidation of alcohols by *p*-benzoquinone (Fig. 5).[17]

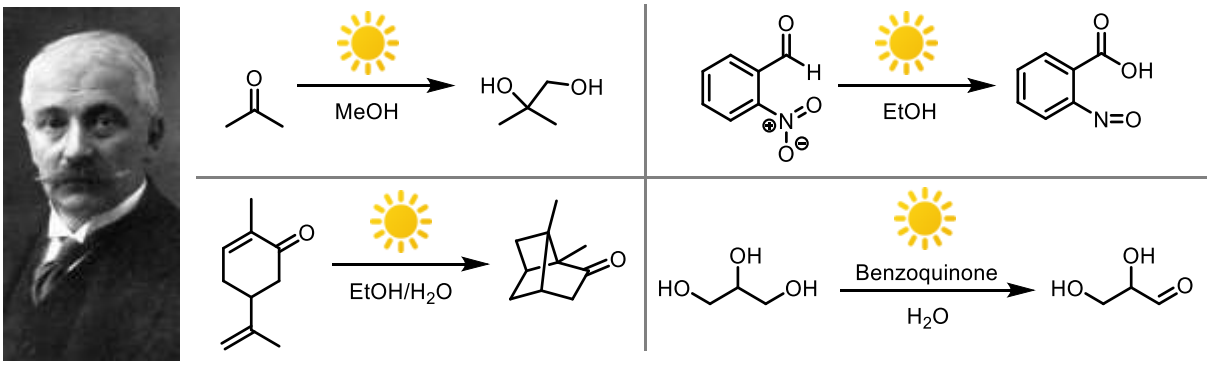


Fig. 5. *Selected experiments from Ciamician and Silber's series "Chemische Lichteinwirkungen" (1900–1915).[14–17]*

For his pioneering contributions, Ciamician is often referred to as the “father of photochemistry”[18,19] and was nominated nine times for the Nobel Prize in chemistry.[19] Fig. 6 impressively demonstrates Ciamician’s default work setting. Sadly, the advent of World War I brought his photochemical research to an abrupt halt and Ciamician passed away not long after in 1922.

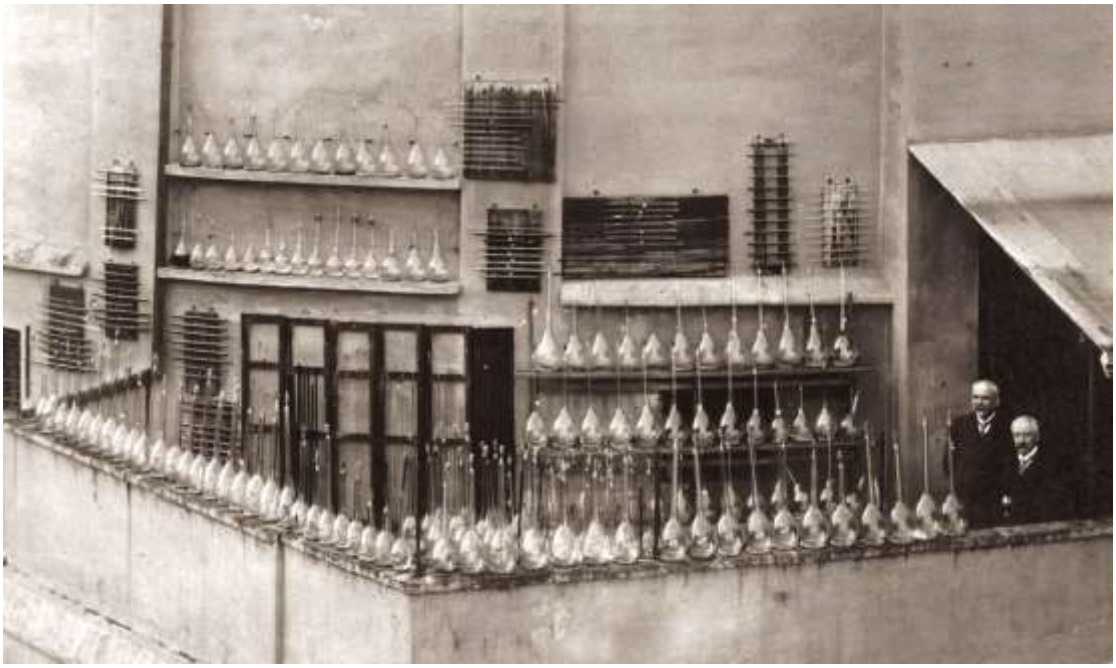


Fig. 6. *Giacomo Ciamician and Paul Silber on the balcony of their laboratory in sunny Bologna, Italy conducting a multitude of photochemical experiments (ca. 1910–1915).*

With the emergence of quantum theory in the 1910’s to 1930’s, photochemical reactions were gradually being understood on a deeper molecular level as it provided a framework to explain light-matter-interactions. A rapid development of fundamental photophysical concepts such as fluorescence or phosphorescence, but also concepts such as electron transfer was seen in this time. This increasingly physical approach attracted physical chemists to the field who focused primarily on the photolysis of small molecules rather than the synthetic applications of photochemistry. Among them, the English chemist and Nobel laureate Ronald G. W. Norrish used these emerging theories to his advantage which culminated in several groundbreaking publications from 1932 onwards. Armed with modern mercury vapor ultraviolet lamps and state-of-the-art spectroscopic equipment, he and his co-workers provided in-depth insight into carbonyl photochemistry from both chemical and physical perspectives. While studying the photodecomposition of aldehydes and ketones, they identified two major pathways which they dubbed Type I and Type II reactions,[20] nowadays accompanied by Norrish’s name.

Norrish Type I reactions involve a simple homolytic *α*-bond cleavage, leading to an acyl and an alkyl radical (Fig. 7, top). In 1934, Norrish and his team found that gas-phase ultraviolet photodecomposition of acetone at 60 °C near-exclusively yields carbon monoxide and ethane.[21] Two years later, Spence and Wild discovered that at room temperature, the reaction

instead yields large quantities of diacetyl and less CO.[22] Similar carbonyl reactivity had already been described to some degree by Ciamician and Silber, for example in the photolysis of cyclohexanone[23] or menthone.[24] Norrish Type II reactions occur when the carbonyl group features an accessible hydrogen atom in the γ-position (Fig. 7, bottom). When 4-heptanone is irradiated, butanone and ethylene are readily produced in near quantitative amounts via an initial 1,5-hydrogen shift and fragmentation of the intermediate diradical.[20]

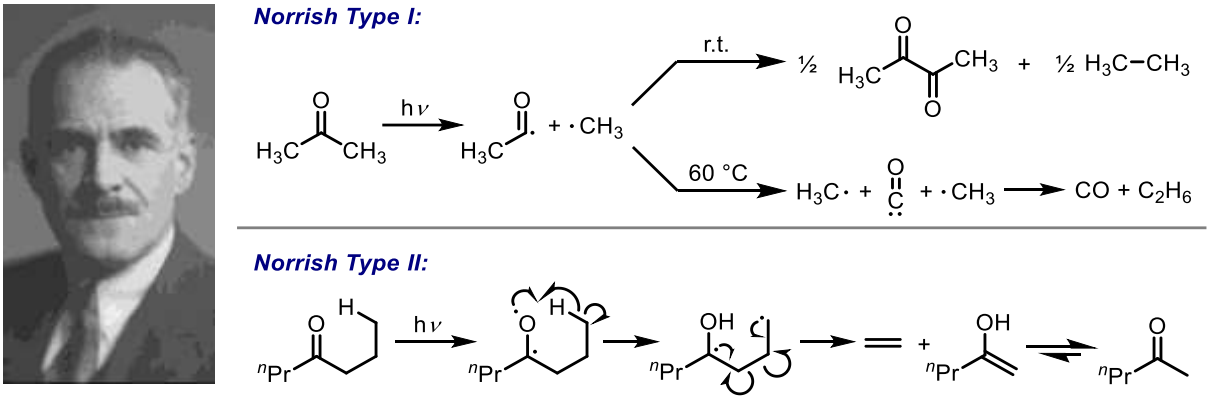


Fig. 7. *Top: Ultraviolet photolysis of acetone in a Norrish Type I reaction, Bottom: UV photolysis of 4-heptanone in a Norrish Type II reaction (Ronald Norrish, 1934).*[21,25]

Norrish's investigation of the photolysis of acetone remains one of the earliest applications of modern quantum-mechanical theories in photochemistry. He provided detailed accounts of the photophysical behavior of acetone,[21] including its UV and infrared absorption spectra. He thoroughly described its fluorescence, building on the emerging concept of discrete energy states akin to Aleksander Jabłoński's proposal one year prior in 1933.[26] Norrish proposed a photo-mechanistic rationale for acetone's Type I decomposition – a novelty in this time. The original diagram from Norrish's 1934 publication is reproduced in Fig. 8.

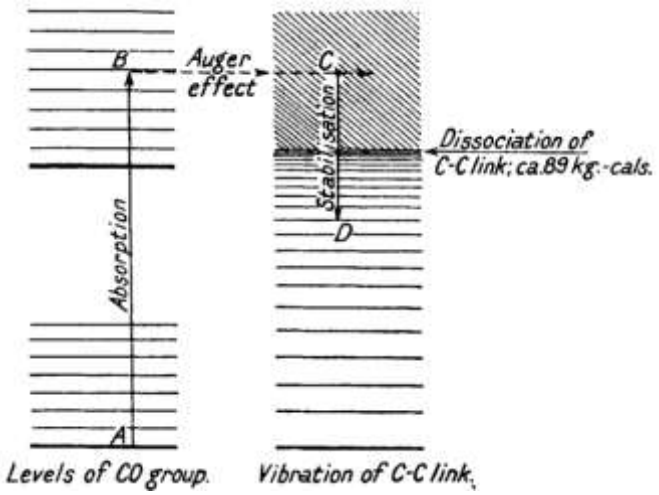


Fig. 8. *Photo-mechanistic proposal for the Norrish Type I reaction of acetone as an early example of the application of quantum mechanics in photochemistry (original figure from Ronald Norrish's 1934 publication).*[21]

In 1949, Norrish and George Porter introduced flash photolysis,[27] which brought a revolutionary new technology into the field and ultimately earned them the 1967 Nobel Prize in chemistry. For several years afterwards, photochemistry mostly remained the domain of physical chemists who sought to (re-)investigate a large portion of photochemical reactions of small molecules. It was not until the 1960's through the 1990's that the development and commercialization of light-emitting diodes (LEDs) sparked a renewed surge of research interest and reattracted synthetic chemists to the field. Unlike incandescent light bulbs, fluorescent lights, or even sunlight, LEDs were compact, inexpensive, energy-efficient, and were capable of emitting specific wavelengths at reasonable intensities. This was eventually the final nail in the coffin for traditional light sources in visible-light photochemistry. These developments ultimately led to the advent of *photocatalysis* for molecules that do not even absorb visible light.

Today, in an era of growing environmental awareness and desire for sustainability, solar photochemistry is once again being pursued with renewed vigor.[28,29] In a way, photochemistry has come full circle.

1.1.2 Photocatalysis

Light energy can only drive a chemical transformation if the photons are absorbed by the system (GROTTHUSS-DRAPER law[30]). This presents a serious disadvantage for the use of ordinary visible light in photochemistry: a sizeable portion of organic molecules is colorless (or pale-yellow at best) and accordingly does not absorb visible photons. To harness the energy of visible light for photoreactions of such colorless molecules, a colored reaction partner is obligatory. This is the fundamental concept behind *photocatalysis*: The use of a colored molecule to mediate the reaction between colorless substrates. Photocatalysis can be classified into three major types, categorized by the manner in which the *photocatalyst* (PC) harnesses the light energy:

1.) Direct energy transfer (EnT) onto the substrate
    ⇒ *Photosensitization*, the PC is a *photosensitizer.*

2.) Electron transfer (ET) from or onto the substrate
    ⇒ *Photoredox catalysis*, the PC is a *photoredox catalyst.*

3.) Atom transfer from or onto the substrate
    ⇒ *Hydrogen-atom transfer* (HAT) or *halogen-atom transfer* (XAT) are the most common; the PC is a *HAT/XAT agent.*

This work will focus primarily on photoredox catalysis.

1.1.3 The Basics of Photoredox Catalysis

As mentioned above, photoredox catalysis describes a reaction in which a colored photoredox catalyst (PRC) absorbs the energy of the light, then induces an electron transfer and consequently the desired reaction of the substrates. How does this work and what is the role of light in this scenario? The underlying principle of photoredox catalysis may be illustrated by the molecular orbital diagram of one such catalyst, the archetypical PRC $[Ru^{II}(bpy)_3]^{2+}$ (hereinafter abbreviated as [Ru], Fig. 9).[31] The highest occupied molecular orbitals (HOMOs) of this complex are three fully occupied metal-centered π orbitals, whereas the antibonding ligand-centered π* level contains the lowest unoccupied molecular orbitals (the LUMOs). A symmetry-allowed HOMO-LUMO transition leads to a strong absorption band at ~450 nm, corresponding to blue light; this produces the vibrant red color of the molecule. This type of transition is called a *metal-to-ligand charge transfer (MLCT)* and is characteristic of numerous strongly colored metal complexes (e.g. the deep purple permanganate anion). Formally, this transition can be viewed as an oxidation of the central Ru(II) to Ru(III) coupled with a reduction of the ligand sphere.

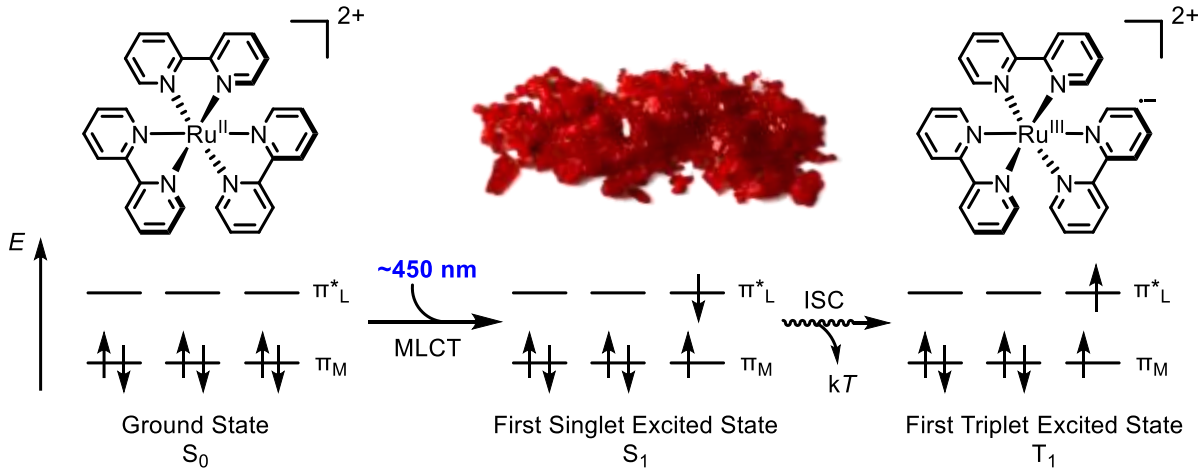


Fig. 9. *Partial and simplified molecular orbital diagram of $[Ru(bpy)_3]^{2+}$ showcasing its electronic properties upon photoexcitation.*[31]

When [Ru] absorbs a blue photon, it is promoted from the ground state to an electronically excited state, denoted [Ru]*. Due to the ground state being a *singlet* state (called S_0) with a spin multiplicity of 1 (according to $M = 2S + 1$), the excited state reached immediately after excitation will also be a singlet state (called S_1) because of the spin conservation rule of transitions. This radiative transition will be denoted here with a bold solid arrow as $S_0 \rightarrow S_1$. Each electronic state contains vibrational sublevels $v = n \in \mathbb{N}_0$ with smaller energetic separation. Upon $S_0 \rightarrow S_1$, the molecule may occupy any of the n vibrational states of S_1; the likelihood of each transition is described by the FRANCK-CONDON principle. Typically, the molecule rapidly relaxes to $v = 0$ before any further processes occur (KASHA's rule). The subsequent fate of

$[Ru]^{S1}$ (or any other excited molecule) is dictated by probabilities, as is customary within the realm of quantum mechanics. Every possible process has a unique probability known as the *quantum yield* of that process. All quantum yields of a species must add up to 1.

The processes available to the metastable $[Ru]^{S1}$ are numerous: The simplest is the radiative relaxation $S_1 \rightarrow S_0$ by emission of a photon, known as *fluorescence* (essentially the "reverse reaction" of the excitation). Another possibility is the isoenergetic *internal conversion* (IC) into a vibrationally excited state of S_0 followed again by vibrational relaxation to $v = 0$. This non-radiative transition will be denoted here as $S_1 \rightsquigarrow S_0$. A third, slightly more complex but all the more important possibility is the spin flip of either unpaired electron, known as *intersystem crossing* (ISC). This now leads to a total multiplicity of 3, hence the molecule reaches a *triplet* state called T_1. The latter is lower in energy than S_1 because of decreased repulsion between the two unpaired electrons, an effect which may only fully be explained quantum-mechanically. The transition $S_1 \rightsquigarrow T_1$ is technically forbidden: The quantum mechanical selection rules for transitions demand that $\Delta S = 0$, otherwise the final wave function would mathematically be zero and hence not exist at all. Several factors can nonetheless enable an ISC, which are described below (Chapter 1.1.4).

It is in fact this triple state T_1 which holds the key to photoredox catalysis. As can be seen in Fig. 9, the excited state [Ru] now has an electron in an antibonding orbital – a state reminiscent of single-electron reductants such as cobaltocene. Contemporaneously, it features a *hole* in its bonding t_{2g} orbitals, providing the prerequisites for oxidative reactivity. As a result, PRCs in their excited state show dual reactivity as both a stronger single-electron reductant and as a stronger single-electron oxidant than in their ground state. This enables an incredible versatility of photoredox-catalyzed reactions. Upon redox reaction with a substrate S, the PRC is transformed either into a radical anion or cation by two pathways: In a *reductive quenching cycle*, the excited PRC is reacting as an oxidant according to $[PRC]^* + S \longrightarrow [PRC]^{\bullet -} + S^{\bullet +}$. In an *oxidative quenching cycle*, it instead acts as a reductant according to $[PRC]^* + S \longrightarrow [PRC]^{\bullet +} + S^{\bullet -}$. This first electron transfer is always followed by a regular, non-light-induced electron transfer which re-forms the original PRC and closes the catalytic cycle. From the point of view of the PRC, photoredox-catalyzed reactions are always redox-neutral: The role of the PRC is perhaps best described as that of an "electron mediator" which formally facilitates the electron flow from substrate A to substrate B.

1.1.4 What Qualifies as a Photoredox Catalyst?

An important clarification should be made: Merely the absorption of a photon and subsequent formation of an electron-hole-pair does not a photoredox catalyst make. By this rule alone, *every* substance in the universe could act as a PRC, as *every* substance absorbs photons at some wavelength. Three principal criteria must be fulfilled to qualify as a useful PRC:

Criterion 1.) *The substance must absorb photons at sensible wavelengths at a reasonable rate.*

Visible or near-infrared light (400–800 nm) is the most favorable; the higher the coefficient of absorption, the better. Ultraviolet or near-ultraviolet (~300–400 nm) photoredox catalysis is possible (e.g. using 10-phenylphenothiazine), but less common due to increased risk of species other than the photocatalyst absorbing the light, as well as the generally higher reactivity of such excited photocatalysts.

We have now sorted out substances such as water, polyethylene, sodium chloride, helium, glucose, or ammonia from being photoredox catalysts.

Criterion 2.) *The substance must exhibit a relatively long-lived excited state.*

The substrates must be able to interact with the excited PRC. This requires that the excited-state lifetime of the PRC's lie on a timescale that allows for two species to approach each other by diffusion to initiate the photoreaction. Triplet states are usually sufficiently long-lived and fulfill this criterion, and thus a rapid $S_1 \rightsquigarrow T_1$ intersystem crossing with a high quantum yield is beneficial. This shifts the favor towards molecules with a large conjugated π system or heavy atoms (especially 4d or 5d transition metals), which cause an increased amount of spin-orbit-coupling within the molecule. Spin-orbit coupling is a quantum-mechanical "mathematical" phenomenon that slightly alters the selection rules, which will not be further discussed here. As a result, the spin-forbidden ISC becomes "less forbidden".

This sorts out most remaining organic substances, including for example benzene, indole, xanthone, azobenzene, benzoquinone, epothilone A, or vanillin. In certain cases, however, molecules with an inefficient ISC may act as photoredox catalysts from S_1, an example being rhodamine dyes,[32] but this is not the norm.

Criterion 3.) *The substance must exhibit appropriate redox behavior in its excited state.*

Photo**redox** catalysis can only happen when a **redox** event takes place. The redox potentials of the excited photocatalyst are governed by the relative energies of S_0, S_1, and T_1, as well as the ground state redox potential (Chapter 1.1.5).

This is obviously highly dependent on the specific reaction, but a general trend is observed that some dyes give consistently better results in photoredox catalysis than others.

In addition to other trivial criteria (such as: the molecule must be stable and must not be reactive towards the substrates on its own), the library of competent photocatalysts available to the chemist is reduced to just a handful. Typical photoredox catalysts include the above-mentioned $[Ru^{II}(bpy)_3]X_2$ or $[Ir^{III}(ppy)_3]$ and ligand variations thereof,[33] but also organic dyes such as Eosin Y,[34] Rhodamine B,[35] Safranin,[36] Rose Bengal,[37] as well as acridinium salts,[38] pyrylium salts,[39] or tailor-made hexasubstituted benzene derivatives popularized by the Zeitler group such as 4CzIPN, 3DPAFIPN, or 3DPA2FBN that contain a specific substitution pattern of electron-withdrawing (F, CN) and -donating substituents (NPh_2, N-Carbazol).[40] An overview of the most common photoredox catalysts is given in Fig. 10 and Fig. 11. In accordance with criterion 3, not all photoredox catalysts can be used interchangeably for every reaction. As can be seen from the redox potentials in Fig. 10 and Fig. 11, some PRCs tend to be strong photoreductants but weak photooxidants (e.g. $[Ir(ppy)_3]$), some are strong photooxidants (e.g. pyrylium salts), while some are both decent photooxidants and photoreductants (e.g. 4CzIPN). This behavior is dictated by the ground-state redox potentials. The astute reader may notice that both the excited-state oxidation and reduction potential of a particular PRC shift by the same numerical value from their respective ground-state potentials. How does this oddity come about and how are excited-state redox potentials determined in the first place?

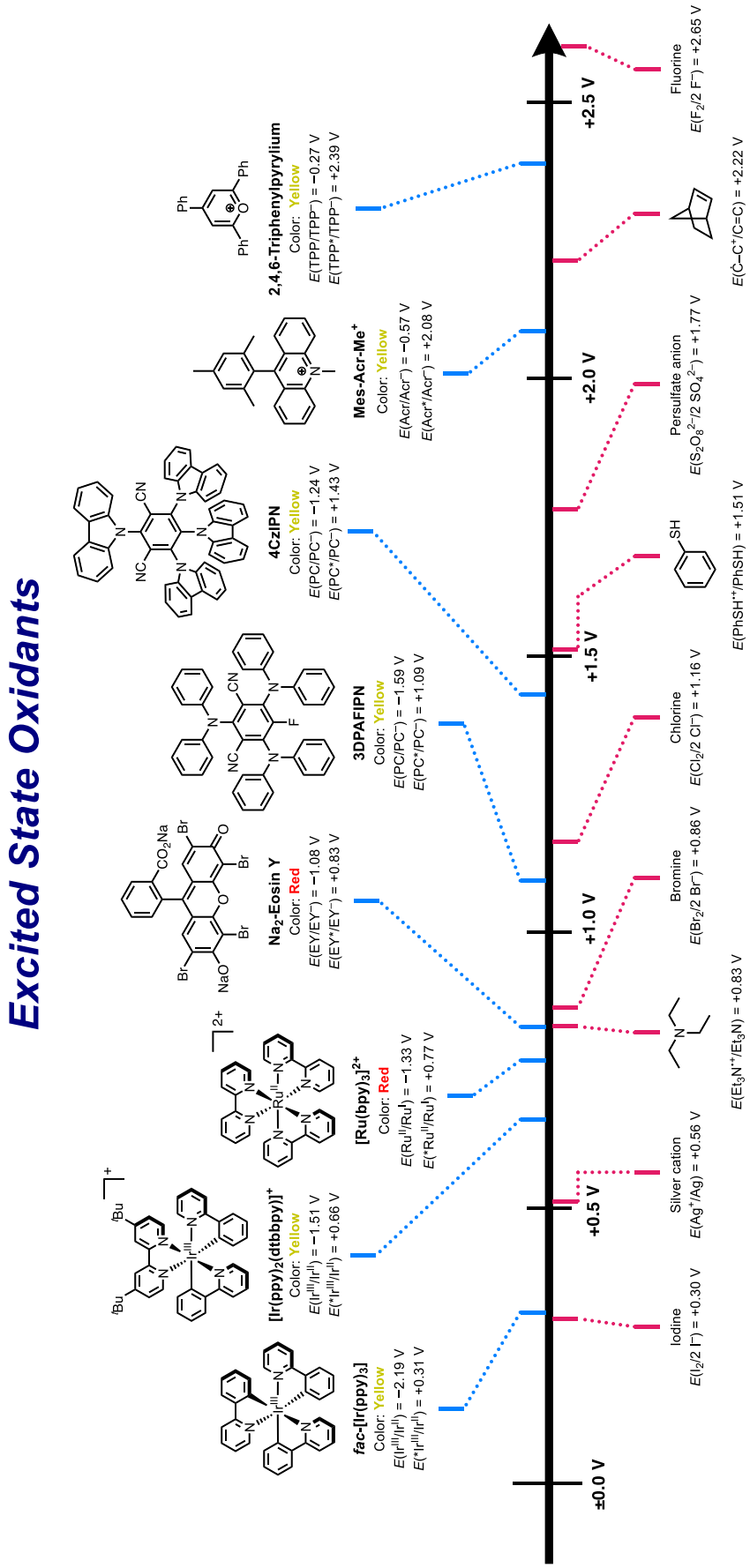


Fig. 10. *Overview of common photoredox catalysts which are excited-state oxidants and comparison with other common oxidants. All potentials vs. SCE.*

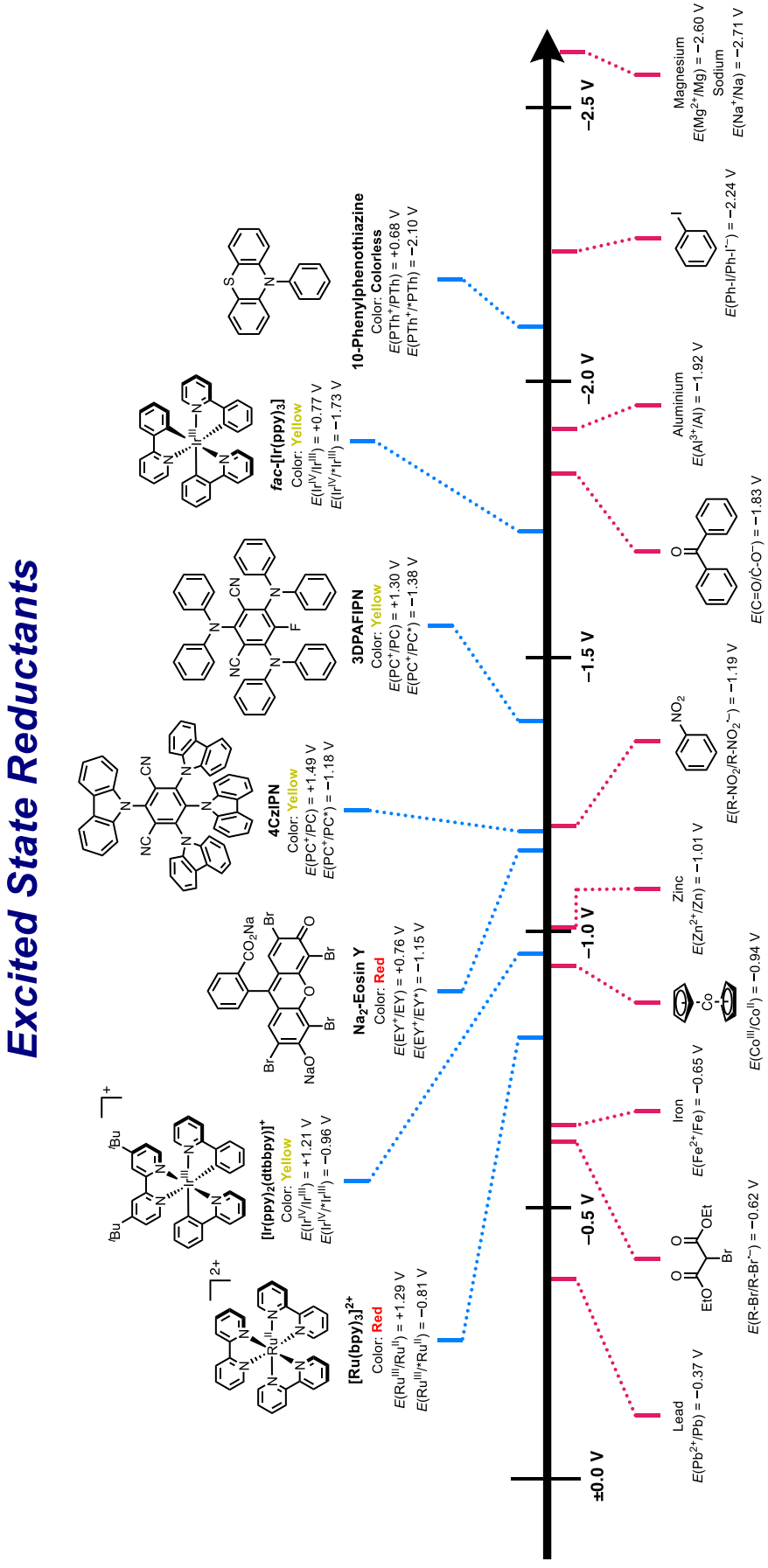


Fig. 11. *Overview of common photoredox catalysts which are excited-state reductants and comparison with other common reductants. All potentials vs. SCE.*

1.1.5 The Photoinduced Electron Transfer

The term photo**redox** catalysis implies redox processes – that is the transfer of electrons from a donor D to an acceptor A. In our case, one of these two species will be excited, giving rise to the term *photoinduced electron transfer (PET)*.

In general, any electron transfer (ET) in the gas phase (GP) is thermodynamically feasible (i.e. its GIBBS energy ΔG is negative) if the *electron affinity* E_{ea} of the acceptor A exceeds the *ionization energy* E_{i} of the donor D.[41]

$$\Delta G_{\mathrm{ET,GP}} = E_{\mathrm{i,D}} - E_{\mathrm{ea,A}} \tag{1}$$

Upon absorption of a photon, either $E_{\mathrm{i,D}}$ or $E_{\mathrm{ea,A}}$ will change, depending on whether D or A have been excited. According to KOOPMANS' theorem, which relates the magnitudes of ionization energies and electron affinities directly to the HOMO and LUMO energies,[42] $E^*_{\mathrm{i,D}}$ and $E^*_{\mathrm{ea,A}}$ are derived from $E_{\mathrm{i,D}}$ and $E_{\mathrm{ea,A}}$ by mere addition (or subtraction) of a simple energy term. Thus, for a *photoinduced* electron transfer in the gas phase two equations are derived from eq. 1, depending on whether D or A is excited:

$$\Delta G_{\mathrm{PET,GP}} = E^*_{\mathrm{i,D}} - E_{\mathrm{ea,A}} = \left(E_{\mathrm{i,D}} - E_{0,0}\right) - E_{\mathrm{ea,A}} \tag{2}$$

$$\Delta G'_{\mathrm{PET,GP}} = E_{\mathrm{i,D}} - E^*_{\mathrm{ea,A}} = E_{\mathrm{i,D}} - \left(E_{ea,A} + E_{0,0}\right) \tag{3}$$

$E_{0,0}$ is known as the *zero-zero transition energy* of a particular excited state. More accurately it describes the energy difference between the thermal ground state ($v = 0$) of the electronic ground state and the thermal ground state ($v' = 0$) of the excited electronic state, hence the term "zero-zero". Evidently, eq. 2 and eq. 3 are identical ($E_{0,0}$ is, of course, different for D and A, so the specific value used in the calculation will differ). Fig. 12 shows how previously inaccessible electron transfers (from D to A) could become accessible by excitation of either D or A. Simply put, the additional "availability" of the energy $E_{0,0}$, brought upon externally through the absorption of a photon, can be enough to overturn the otherwise endergonic electron transfer by causing $\Delta G < 0$.

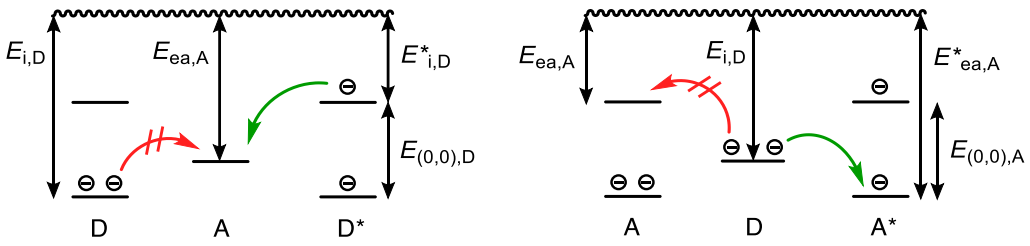


Fig. 12. *Schematic representation of ground-state and analogous excited-state electron transfer from a donor D to an acceptor A upon excitation of either D or A.*

This model is only valid for gas phase reactions. In solution, solvation effects must be taken into account. ΔG of an electron transfer reaction that leads to a solvent-separated ion pair (SSIP) is that of the gas phase reaction with the addition of the GIBBS energy of solvation ΔG_{sol} as well as a Coulombic energy term C that describes the electrostatic attraction between the two newly created charges.[41]

$$\begin{aligned}\Delta G_{\mathrm{PET,SSIP}} &= \Delta G_{\mathrm{PET,GP}} + \Delta G_{\mathrm{sol}} + C \\ &= (E_{\mathrm{i,D}} - E_{ea,A} - E_{0,0}) + \Delta G_{\mathrm{sol}} + C\end{aligned} \tag{4}$$

The ionization energy and electron affinity of the species in solution differ from those in the gas phase and are experimentally inaccessible. In solution they are instead described by the *redox potentials*, which are directly related to E_{i} and E_{ea} by the addition of solvation terms. In eq. 4, the latter are conveniently already contained within ΔG_{sol}. If ΔG_{PET} is treated in the unit of eV, eq. 4 can be rewritten (the index SSIP will now be omitted) as

$$\Delta G_{\mathrm{PET}}[\mathrm{eV}] = E(\mathrm{D}^+/\mathrm{D}) - E(\mathrm{A}/\mathrm{A}^-) - E_{0,0} + C \tag{5}$$

This key equation is commonly referred to as the "REHM-WELLER equation",[43–51] however, current IUPAC guidelines recommend against using this name for this equation, instead reserving it for the correlation of the PET's kinetic rate constant and its GIBBS energy (see eq. 13 below).[52] This form of the equation is permissible despite an apparent unit mismatch, because for single electrons 1 eV and 1 V are equivalent, i.e. an electron accelerated by 1 V will gain an energy of 1 eV. Eq. 5 represents a simple way to determine the feasibility of a PET reaction from easily determined quantities: The redox potentials of the two reactants are measured by cyclic voltammetry whereas $E_{0,0}$ of the excited species can be approximated from absorption and fluorescence/phosphorescence spectroscopy. In polar solvents, the Coulombic term C is negligibly small (e.g. ~0.06 eV in acetonitrile) and is typically excluded.[32]

To gain further insight into the nature of the redox potentials involved in PET, some additional derivatizations will be made. The GIBBS energy of a regular dark redox reaction is given by the well-known equation

$$\Delta G_{\mathrm{ET}}[\mathrm{J}\cdot\mathrm{mol}^{-1}] = -n\mathcal{F}E_{\mathrm{cell}} \tag{6}$$

with n being the number of transferred electrons, $\mathcal{F}$ being the FARADAY constant (the charge of a mole of electrons) and E_{cell} being the cell potential.[53] For reactions of two molecules with the transfer of a single electron ($n = 1$), eq. 6 simplifies to

$$\Delta G_{\mathrm{ET}}[\mathrm{J}] = -eE_{\mathrm{cell}} \tag{7}$$

with e being the charge of a *single* electron. As 1 eV is equal to 1 J · e^{-1}, this leads to

$$\Delta G_{\mathrm{ET}}[\mathrm{eV}] = -E_{\mathrm{cell}} \tag{8}$$

Because E_{cell} is merely the difference of the cathode potential and the anode potential,[53] it follows for our bimolecular photoinduced electron transfer reaction that

$$\Delta G_{\mathrm{PET}}[\mathrm{eV}] = E(\mathrm{D}^{+}/\mathrm{D}^{*}) - E(\mathrm{A}/\mathrm{A}^{-}) \tag{9}$$

$$\Delta G'_{\mathrm{PET}}[\mathrm{eV}] = E(\mathrm{D}^{+}/\mathrm{D}) - E(\mathrm{A}^{*}/\mathrm{A}^{-}) \tag{10}$$

featuring the excited state redox potentials of either D or A. Consequently, if eq. 09/10 are inserted into eq. 5, it follows that any excited-state redox potential E^* may simply be determined by subtracting $E_{0,0}$ from the ground-state redox potential E (if C is neglected):

$$E^* = E - E_{0,0} \tag{11}$$

This correlation is particularly important in a practical sense since E^* is a common quantity used by photochemists especially in the context of photoredox catalysis. Eq. 11 rationalizes the above-mentioned observation that excited-state oxidation and reduction potentials of a molecule shift by the same numerical value from the respective ground-state potentials, this "numerical value" being precisely $E_{0,0}$.

The equations given above deal with the energetics, i.e. the *thermodynamics* of PET. No information is contained about the *kinetics* of such reactions. In 1956 Rudolph Marcus set out to expand upon prior work of Willard Libby[54] and formulated the rate constant of any electron transfer *in solution* as

$$k_{\mathrm{ET}} = A \cdot \exp\left[\frac{(\Delta G_{\mathrm{ET}} + \lambda_{\mathrm{S}})^2}{4\lambda_{\mathrm{S}} k_{\mathrm{B}} T}\right] \tag{12}$$

with A being a frequency factor, ΔG_{ET} being the GIBBS energy of the electron transfer, λ_{S} being the "solvent reorganization energy" describing the change in the solvation shell upon relocation of the charge, k_{B} being the BOLTZMANN constant, and T being the absolute temperature.[55] A remarkable consequence of this equation is that if $\Delta G_{\mathrm{ET}} = \lambda_{\mathrm{S}}$, the reaction rate tends to a maximum with the activation energy being 0. This implies that if the GIBBS energy, i.e. the driving force, increases further, the reaction *slows down again* – this is known as the "inverted region". In a photochemical context, Rehm and Weller have investigated the kinetics of fluorescence quenching by electron transfer of over 60 organic donor/acceptor pairs.[43] Their results showed no indication of any "inverted region" and gave the perhaps more intuitive result in that an increase in driving force will lead to a faster reaction until the diffusion limit is reached and the reaction cannot physically become any faster. Rehm and Weller's original results are shown in Fig. 13.

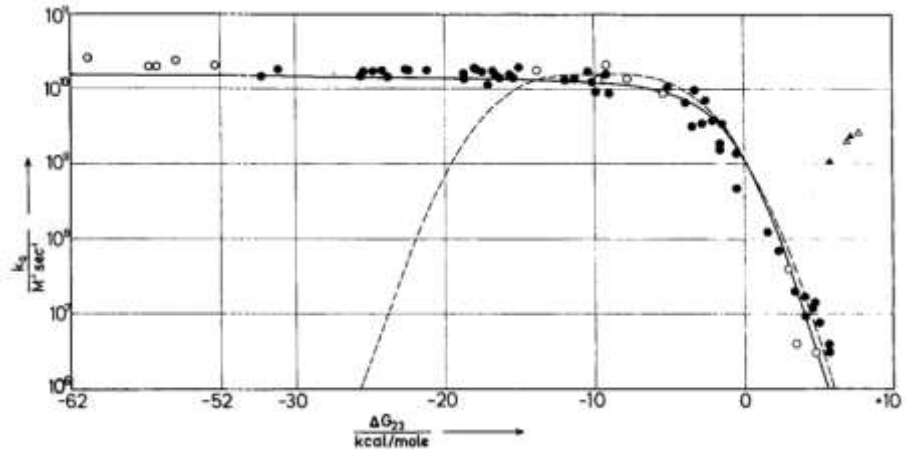


Fig. 13. *Experimentally found correlation of GIBBS energy ΔG and fluorescence quenching rate constant k_q. The dashed line describes the "inverted region" as predicted by Marcus' theory (original figure from Rehm and Weller's 1970 publication).*[43]

A solution for this dilemma was proposed within the confines of Marcus' theory: Strongly exergonic reactions with highly negative ΔG could lead to electronically excited products instead of ground-state products. In accordance with the free energy curves of reactant and product, the activation energy is lowered, thus circumventing the rate-slowing activation barriers predicted by the inverted region. This effect will not be further discussed here.

Based on their results, Rehm and Weller incorporated the absence of an inverted region from a practical viewpoint into the derivatization of an alternative equation for the rate constant of a photoinduced electron transfer based on its GIBBS energy:

$$k_{\mathrm{PET}} = \frac{k_{\mathrm{EC}}}{1 + \frac{k_{-\mathrm{EC}}}{A}\left(e^{\frac{\Delta G_{\mathrm{PET}}}{\mathrm{R}T}} + e^{\frac{\Delta G^{\ddagger}_{\mathrm{PET}}}{\mathrm{R}T}}\right)} \tag{13}$$

where k_{EC} and $k_{-\mathrm{EC}}$ are the respective rate constants for the formation and separation of the encounter complex between the two substrates, A is the collision frequency factor, R is the ideal gas constant, ΔG_{PET} is the GIBBS energy of the photoinduced electron transfer as described above, $\Delta G^{\ddagger}_{\mathrm{PET}}$ is the activation GIBBS energy, and T is the absolute temperature. In the original publication, a value of $\frac{k_{-\mathrm{EC}}}{A}$ = 0.25 was used for acetonitrile.[43,56]

Almost 30 years after Marcus' original proposal, the existence of the inverted region was first unequivocally experimentally verified by Miller and co-workers in 1984.[57] By attaching the donor and acceptor moieties onto opposite ends of a sterane scaffold, they investigated **intra**molecular electron transfer, thus eliminating diffusion effects.

1.1.6 Applications of Photoredox Catalysis

The central dogma of photoredox catalysis – and photochemistry in general – is that it is inherently *radical chemistry.* The notion of "radical chemistry" in the context of traditional organic chemistry tends to evoke a sense of unease among chemists. And justifiably so; conventional means of generating radicals frequently encompass high temperatures, harsh oxidants or reductants, exotic starting materials, or toxic reagents. In stark contrast, photoredox catalysis provides a completely novel way of generating radicals under extremely mild conditions without any of the drawbacks. This not only opens up new pathways towards known molecules, but also new pathways towards brand-new molecules that are difficult or even impossible to synthesize by standard means.

The NEWMAN-KWART rearrangement of *O*-aryl dimethylthiocarbamates is a well-established way to convert phenols into thiophenols (Fig. 14, bottom).[58] The major drawback is that high temperatures not rarely in excess of 200 °C are required. In 2015, the Nicewicz group presented an alternative approach based on blue-light photoredox catalysis using a strongly photooxidizing pyrylium salt (Fig. 14, top).[59] Instead of a neutral zwitterionic intermediate, this method proceeds through a radical cation which allows for an efficient conversion at room temperature.[60] Most strikingly, the novel approach offers a complementary substrate scope compared to the original thermolytic approach. While the traditional rearrangement gives the best results with electron-withdrawing substituents on the aromatic ring, the photoredox-catalyzed variant shows the best performance with electron-rich substrates. This observation is explained by the intermediate structures: a carbanion in the traditional rearrangement vs. an electrophilic radical in the photoredox-catalyzed variant.

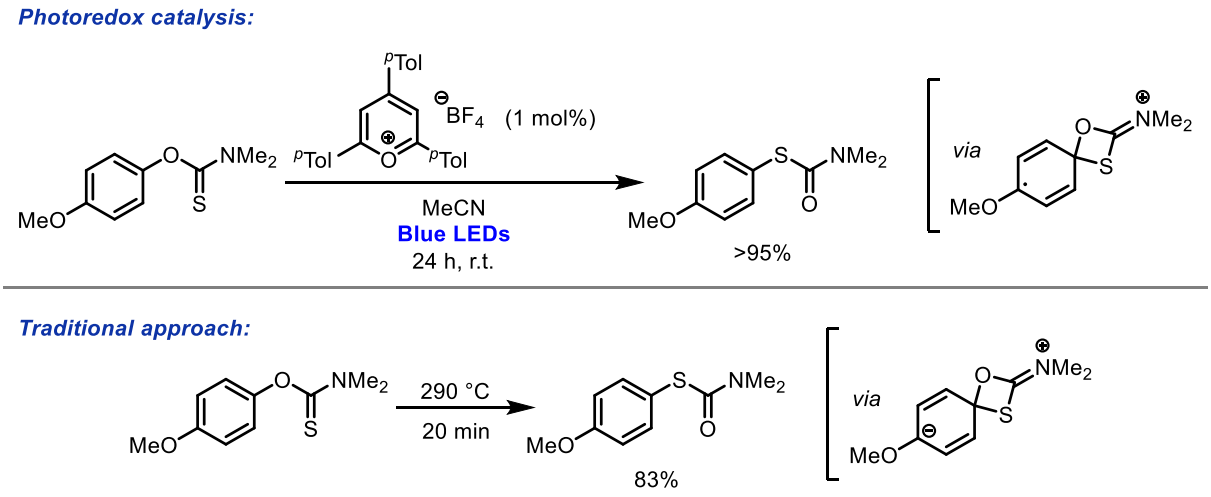


Fig. 14. *Top: Photoredox-catalyzed variant of the NEWMAN-KWART rearrangement.*[59] *Bottom: Original thermal NEWMAN-KWART reaction.*[58]

In 2013, the Zeitler group developed a photoredox-catalyzed cyclization of bis-enones using the common dye Eosin Y (Fig. 15, top).[61] A thiourea-derived hydrogen-bond organocatalyst activates the enone for photoreduction. The reaction is rapid (0.5–4.5 h) and gives >90% yield for all reported substrates, with excellent diastereoselectivity. A non-photoredox approach involves a reductive cyclization mediated by tributylstannane,[62,63] which is also a radical reaction (Fig. 15, bottom). Due to the harsh conditions (refluxing benzene), the selectivity is poor: A bicyclic side product from a second cyclization after initial 5-*exo*-trig-cyclization is observed.

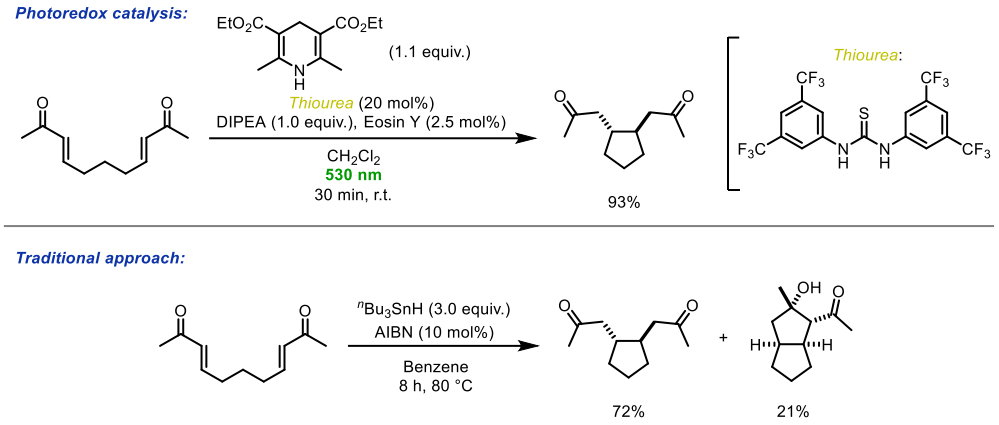


Fig. 15. *Top: Cooperative photoredox and hydrogen bond catalysis for the intramolecular cyclization of bisenones.*[61] *Bottom: Cyclization of bisenones by action of tributylstannane.*[62]

Photoredox catalysis is frequently paired with other forms of catalysis, like HAT or transition metal catalysis, to extend the scope even further. HAT catalysis is primarily used for C-H activation, as demonstrated in 2015 by the MacMillan group. The group presented a smooth alkylation of six-membered N-heterocycles via the combination of an [Ir] photoredox catalyst and a thiol as a HAT agent, which enables the use of alcohols as alkylating agents (Fig. 16, top).[64]. The traditional approach involves nucleophilic addition of alkyllithium species followed by oxidation of the resulting dihydro-heterocycle (Fig. 16, bottom),[65] or total *de novo* synthesis of the heterocyclic moiety.[66]

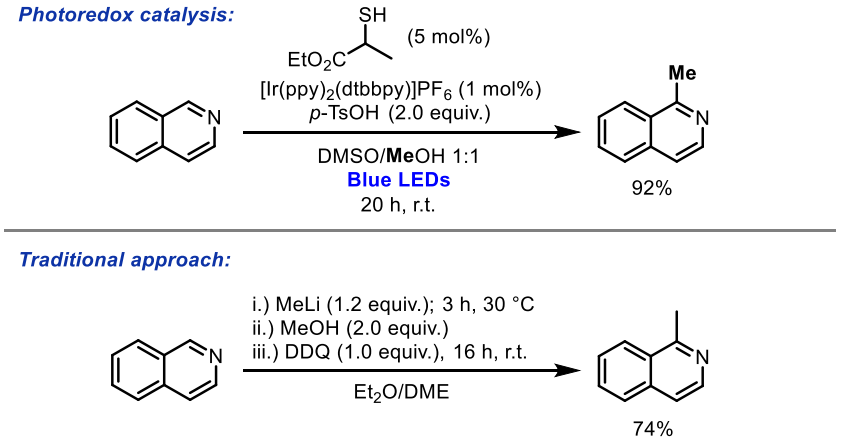


Fig. 16. *Top: Alkylation of N-heterocycles by dual photoredox and HAT catalysis using alcohols as the alkyl source.*[64] *Bottom: Alkylation of N-heterocycles by addition of alkyllithium followed by oxidation.*[65]

In 2009, Du and Yoon reported a crossed [2+2]-cycloaddition of two distinct enones using combined visible-light-photoredox and Lewis acid catalysis (Fig. 17).[67] This transformation has been replicated by the Zeitler group using Eosin Y and LiBr under green light irradiation.[61] The Yoon group later presented an enantioselective variant of this cycloaddition using $Eu(OTf)_3$ bearing a chiral ligand – hitherto the second reported enantioselective [2+2]-cycloaddition. The reaction was proposed to proceed via a radical anion, leading to a stepwise rather than a concerted [2+2]-cycloaddition.[67,68] This reaction represents an example of a novel transformation enabled by photoredox catalysis: Irradiation of the olefin mixture at 300 nm yields no cycloaddition products and merely causes *E*/*Z* isomerization of the phenylbutenone.[67] As a result, no direct traditional photochemical synthesis of the depicted product is known. Any conceivable non-photoredox-catalyzed synthesis would encompass several steps which have not been devised as of now.

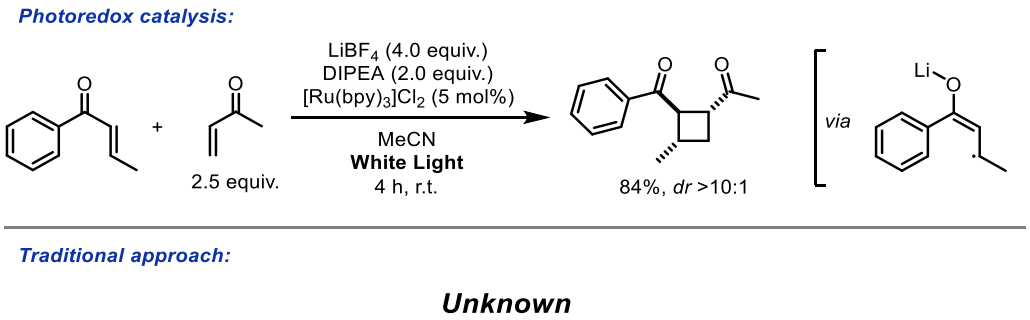


Fig. 17. *Crossed enone [2+2]-cycloaddition of enones mediated by Lewis acid and photoredox catalysis.*[67]

Photoredox catalysis has found its way into total synthesis routes of several complex natural products,[69] one such example being the total synthesis of the indole alkaloid gliocladin C by the group of Corey Stephenson (Fig. 18).[70] The key bond between the indole and pyrroloindoline moiety was constructed by generation of a radical from the respective tertiary bromide and concomitant addition onto 2-formylindole. The formyl group directed the radical addition and was removed in the subsequent step.

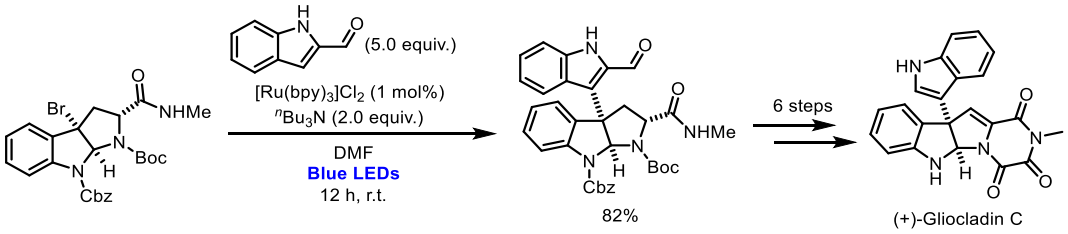


Fig. 18. *Application of photoredox catalysis in the total synthesis of (+)-gliocladin C.*[70]

In summary, photoredox catalysis bears the potential to profoundly reshape the landscape of synthetic organic chemistry in terms of efficiency, sustainability, accessibility, and molecular diversity. Interest in photoredox catalysis is growing steadily, along with the number of publications presenting efficient, mild, and selective transformations. As a result, it will likely take on an increasingly prominent role in the synthesis of natural products and fine chemicals in the near future. As it becomes progressively more accessible, it is not implausible that photoredox catalysis will eventually persuade even the most “old school” organic chemists to abandon obsolete pathways.

Chapter 1.2



Hantzsch Esters

1.2.1 What are Hantzsch Esters?

Just after obtaining his doctorate, the young Arthur Rudolf Hantzsch reacted ethyl acetoacetate ("*Acetessigäther*") with a solution of acetaldehyde in aqueous ammonia ("*Aldehydammoniak*") in the presence of zinc chloride in 1881 (Fig. 19, top).[71] He obtained a well-defined product which was easily oxidized to the hitherto unknown diethyl 2,4,6-collidine-3,5-dicarboxylate. He conducted further investigations on the *strange and unique*[a] intermediate in his following post-doctoral thesis.[72] He correctly identified it as a dihydropyridine derived from a three-component condensation reaction, albeit with an incorrect structural proposal and mechanistic elucidation – he believed it to be a 1,2-dihydropyridine (Fig. 19, bottom).

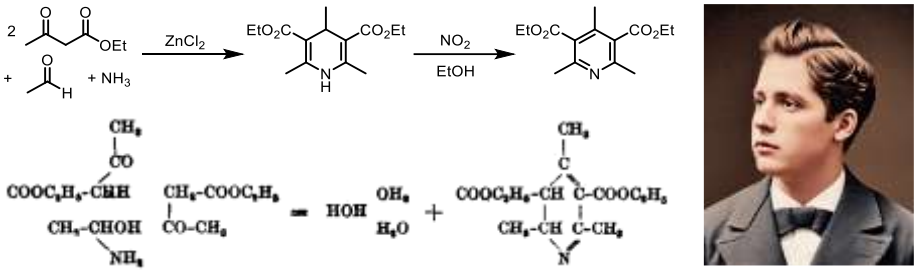


Fig. 19. *Top: Zinc(II) chloride-catalyzed condensation of ethyl acetoacetate, acetaldehyde, and ammonia and subsequent oxidation (Arthur Hantzsch, 1881),*[71] *Bottom: Hantzsch's mechanistic and structural proposal (original figure from Hantzsch's 1882 publication).*[72]

On its own, the trivial name "Hantzsch ester" commonly refers to the simplest contender of dihydropyridine dicarboxylates, namely the formaldehyde-derived diethyl 1,4-dihydro-2,6-dimethyl-3,5-pyridinedicarboxylate (also known as *diludine*). In this work, the term "Hantzsch ester" will exclusively refer to the general group of 1,4-dihydropyridine-3,5-dicarboxylates and never to a specific compound.

The actual formation mechanism of the 1,4-dihydropyridine ring includes two separate preceding reactions of the β-ketoester (Fig. 20). One of the two equivalents reacts with ammonia to form an enamine, whereas the other equivalent reacts with the aldehyde via ammonia catalysis in a standard KNOEVENAGEL condensation. This condensate is a classic MICHAEL acceptor and is easily attacked by the nucleophilic enamine previously formed. The adduct undergoes cyclization followed by facile base-promoted elimination of water to yield the 1,4-dihydropyridine. Three equivalents of water are the only byproducts, which has already been correctly identified by Hantzsch himself. This proposed stepwise reaction can be verified by separately

[a] „Das Product der Condensation von Aldehydammoniak mit Acetessigäther […] ist ein so merkwürdiger und […] so isolirt dastehender Körper, daſs es sich als zweckmäſsig erweist, zuerst über seine Bildung […] einen kurzen Ueberblick zu geben […]"

synthesizing the enamine and KNOEVENAGEL condensate and then reacting them, which leads to an identical product. This strategy is commonly used if unsymmetrical products are desired.

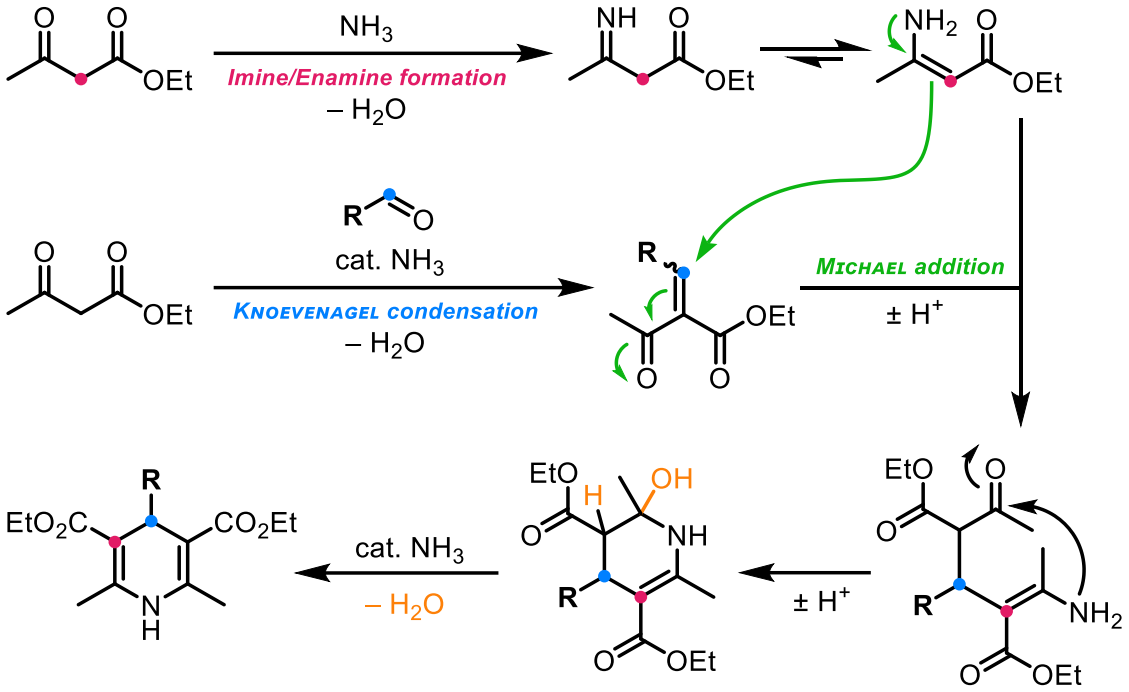


Fig. 20. *Proposed stepwise mechanism of the Hantzsch dihydropyridine synthesis.*

1.2.2 Applications of Hantzsch Esters: Pharmaceuticals

1,4-Dihydropyridines, especially Hantzsch esters, are valuable lead motifs in medicinal and pharmaceutical chemistry. As calcium antagonist, this motif binds to voltage-gated L-type calcium channels in the membrane of smooth muscle cells.[73,74] This prevents the influx of Ca^{2+} during cell depolarization, which normally leads to muscle contraction and vasoconstriction.[73] As a result, the dihydropyridine motif regulates the mechanism causing hypertension, i.e. elevated blood pressure. The first Hantzsch ester to find widespread use as an antihypertensive is Nifedipine, which was developed by Bayer in the 1960's and was launched in 1975 under the brand name *Adalat*.[75] Due to the facile synthesis of the dihydropyridine backbone, a plethora of analogues have been prepared to date. Consequently, the structure-activity relationship especially with regards to antihypertensive activity is well-developed and a large multitude of 1,4-dihydropyridine-containing drugs is available on the market (Fig. 21). Beyond their role as antihypertensiva, certain dihydropyridine scaffolds have been explored for antimicrobial (especially tuberculosis,[76,77] leishmaniasis,[78,79] and malaria[80]), antioxidant,[81] anticoagulant,[82] and antiepileptic[83,84] properties. They even show activity as neuroprotective agents in the treatment of Alzheimer's disease by partial inhibition of the aggregative effect of acetylcholinesterase on β-amyloid.[85]

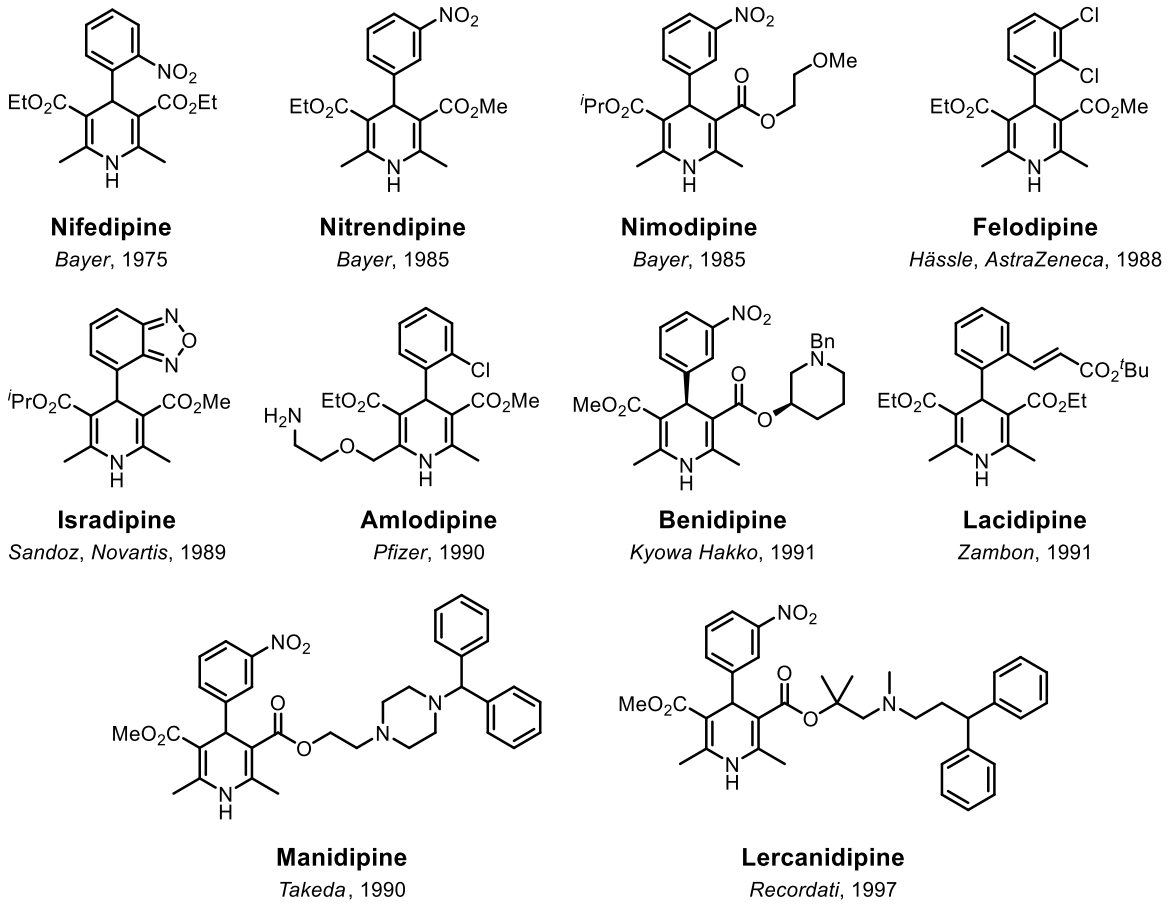


Fig. 21. *Structures of important 1,4-dihydropyridine-based antihypertensive pharmaceuticals and the year of their market launch.*[86]

1.2.3 Applications of Hantzsch Esters: Transfer Hydrogenation

Dihydropyridines, as their name implies, are merely a formal dihydrogen elimination away from achieving aromaticity. This raises the question: Can they serve as hydrogen sources/reductants in chemical reactions? A glance into nature reveals that life has preempted humanity by millions of years in this regard. In the form of nicotinamide adenine dinucleotide phosphate (NADP) all organisms utilize its dihydropyridine motif as an essential reducing agent and hydride source, generally represented as $H^+ + 2\ e^-$ in a biochemical context (Fig. 22, top). It is thus not surprising that Hantzsch esters exhibit similar reactivity. A look at the structure reveals the reason behind their high hydride-donating tendency – expulsion of a H^- leads directly to an aromatic pyridinium (Fig. 22, center).

Diludine is commonly used as a transfer hydrogenation agent due to its low cost, bench stability, and mildness of its hydride transfer. Common targets include C=O bonds, C=N bonds, and C=C bonds, both isolated and in conjugation (Fig. ***22***, bottom). A *Z*-selective semi-hydrogenation of C≡C bonds has also been reported.[87] The relative bulkiness of diludine combined with the requirement of a catalyst (Lewis/Brønsted acid, transition metals) make it the perfect

candidate for stereoselective reactions – not surprisingly, a plethora of asymmetric transfer hydrogenation protocols have been reported. Several comprehensive review articles and review chapters about Hantzsch ester-mediated transfer hydrogenation have been published, both regular and enantioselective.[88–94]

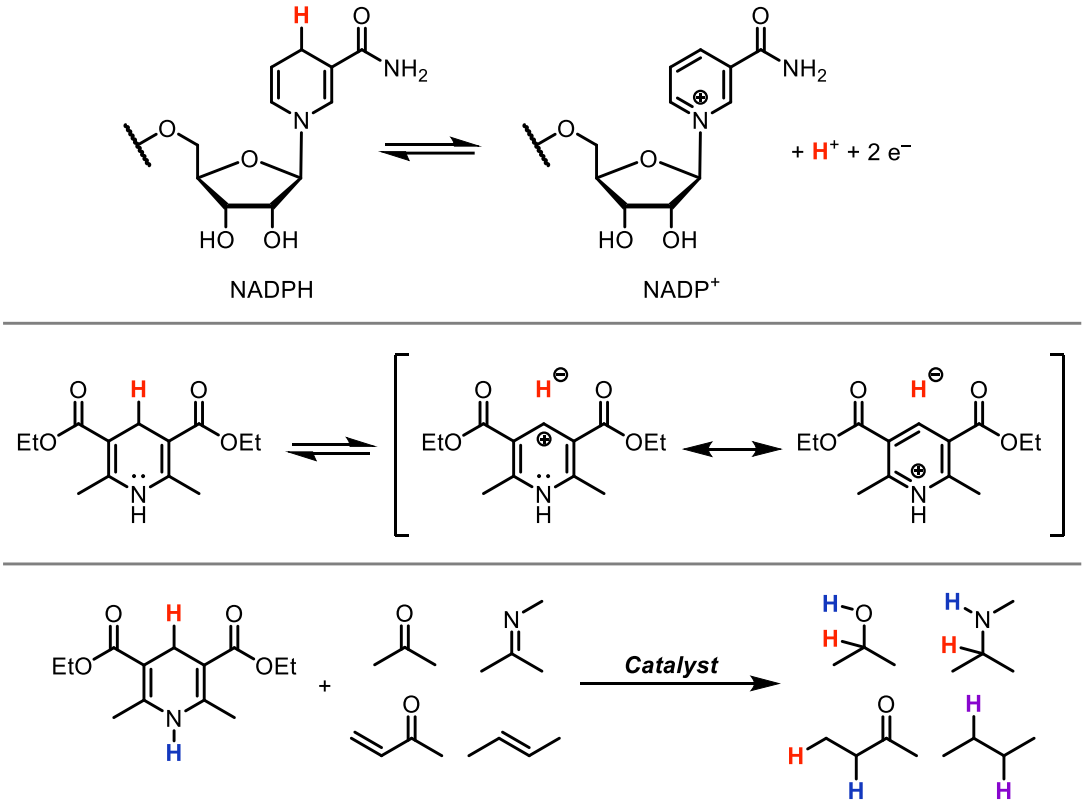


Fig. 22. *Top: Partial structure of the biological cofactor NADP, Center: Hydride expulsion from a Hantzsch ester results in a pyridinium ion, Bottom: Some prototypical applications for Hantzsch ester-mediated transfer hydrogenations*

1.2.4 Applications of Hantzsch Esters: Radical Alkylation

While the biomimetic hydride-donating capability of Hantzsch esters is well-established, their reactivity potential extends far beyond two-electron processes. Aromaticity can also be achieved by *two separate one-electron processes*, which invokes the prerequisite for radical chemistry. If one electron is removed from the dihydropyridine core by single-electron oxidation, we end up in a similar starting situation as in the hydride transfer shown in Fig. 22. The difference is that now the expulsion of a radical rather than an anion is favored – this implies that Hantzsch esters can function as radical reservoirs (Fig. 23). Oxidation can be achieved by traditional means such as persulfate or bis(acetoxy)iodobenzene (BAIB), but as shown in chapter 1.1.6, photoredox catalysis enables milder access to single-electron redox chemistry.

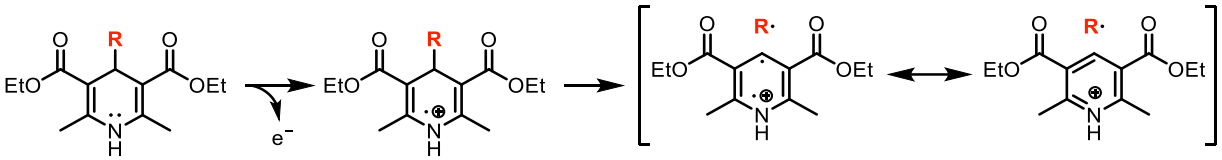


Fig. 23. *Radical expulsion from an oxidized Hantzsch ester leads to a pyridinium ion.*

The group of Zhou Tang was one of the first to recognize the potential of Hantzsch esters for alkylation reactions. After having successfully transferred alkyl groups onto imines via Lewis/Brønsted catalysis in 2013 (Fig. 24, top),[95] they hypothesized that the mechanism may involve free alkyl radicals based on reactivity observations. One year later, when they intended to extend their scope to β-nitrostyrenes, they found that the addition of the radical initiator AIBN greatly improved the efficiency (Fig. 24, center).[96] In the same year, Huang and co-workers treated $[Mn^{I}(\eta^{6}\text{-}C_6H_6)(CO)_3]PF_6$ with an isopropyl-substituted Hantzsch ester and observed a transfer of the isopropyl group onto the activated benzene ligand (Fig. 24, bottom).[97] The authors postulated an SET event followed by alkyl radical transfer.

In 2016, the Nishibayashi group sought to combine this novel reactivity of Hantzsch esters with the emerging trend of photoredox catalysis. Upon subjecting dicyanoarenes or cyanoheteroarenes to $[Ir(ppy_3)]$, NaOAc, and visible light in the presence of alkyl-substituted Hantzsch esters, *ipso*-substituted alkyl arenes were obtained (Fig. 25, top).[98] Intermediate free radicals were trapped by TEMPO. Shortly after, the same group reported a similar reaction in the presence of $NiCl_2$ and 4,4'-di-*tert*-butyl-2,2'-bipyridine (dtbbpy) to enable cross-coupling with aryl iodides (Fig. 25, bottom).[99]

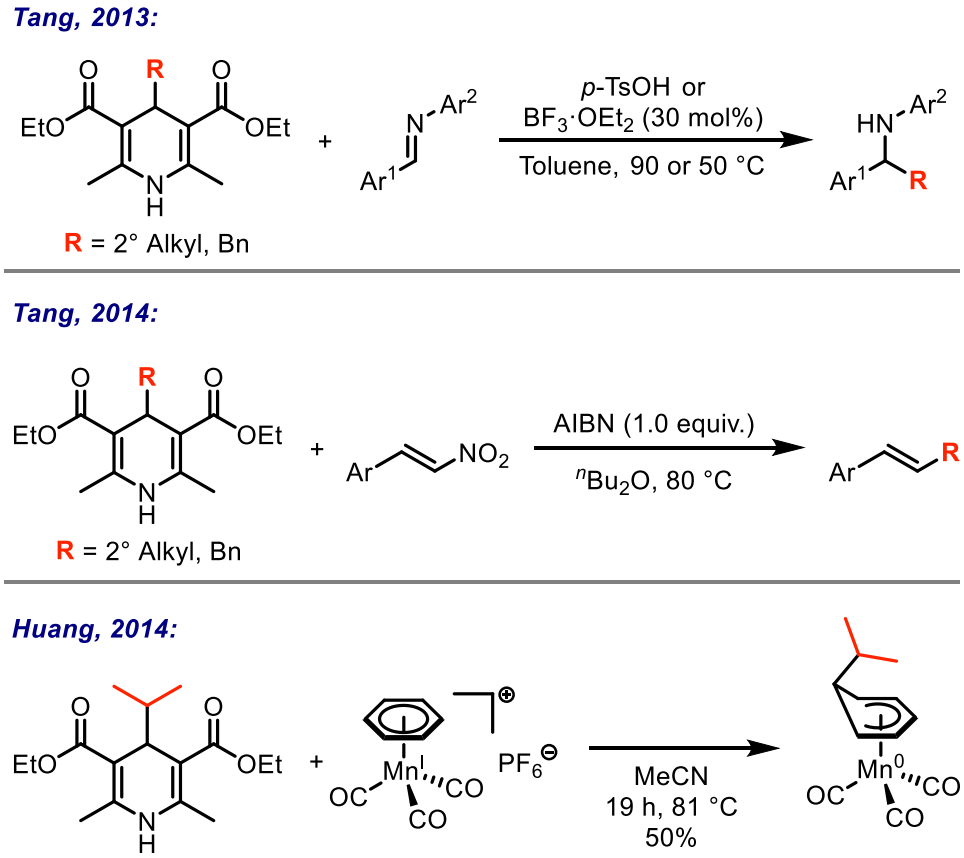


Fig. 24. *Top: Acid-mediated alkylation of imines (Tang, 2013),*[95] *Center: AIBN-mediated substitution of the nitro group in β-nitrostyrenes (Tang, 2014),*[96] *Bottom: Isopropyl transfer onto* $[Mn(\eta^6\text{-}C_6H_6)(CO)_3]PF_6$ *(Huang, 2014).*[97]

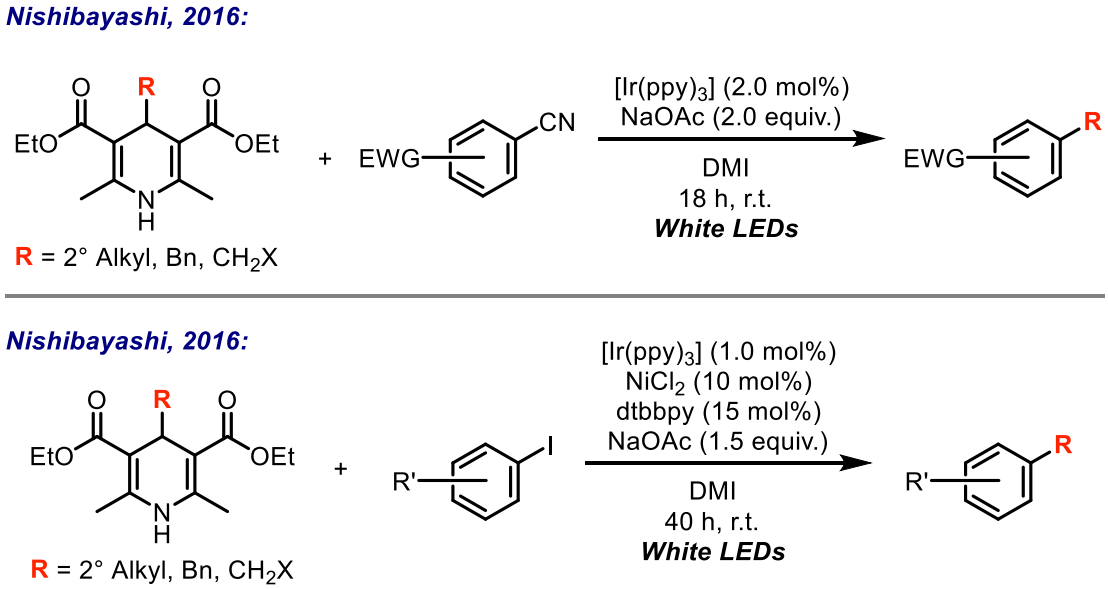


Fig. 25. *Top: ipso-substitution of cyanoarenes under visible-light photoredox catalysis (Nishibayashi, 2016),*[98] *Bottom: Nickel-photoredox-cocatalyzed cross coupling of aryl iodides (Nishibayashi, 2016).*[99]

These groundbreaking works laid the foundation for further studies in the field of photoredox-catalyzed Hantzsch ester-mediated transformations. Multiple review articles have been published on this matter.[100,101]

In certain circumstances, a Hantzsch ester may react photochemically with a substrate in the absence of any photocatalyst. This occurs when the occupied π orbitals of the electron-rich dihydropyridine core overlap with the unoccupied π orbitals of an electron-deficient substrate as a result of π stacking interactions. This is a special type of charge-transfer complex known as an *electron donor-acceptor complex*, or EDA complex. As a result, an electron transfer between the Hantzsch ester and the substrate is facilitated, as it is now intramolecular rather than intermolecular. An EDA complex generally shows an extended absorption spectrum and a characteristic bathochromic shift compared to the sum of its constituents and may usually be excited with longer wavelengths. This effect has been extensively exploited for reductions using diludine,[102] but can also be applied to alkylation reactions. Hong and co-workers described a synthesis of substituted pyridines from Hantzsch esters and *N*-aminopyridinium salts in 2020 (Fig. 26, top).[103] They found that a mixture of these two substrates gave a deep-yellow solution, despite the substrates themselves being colorless or pale-yellow; a result of a bathochromic shift upon EDA complex formation. Further studies revealed a 1:1 stoichiometry of the complex. Blue light irradiation of the complex induces an SET followed by radical transfer in the absence of any additive or photocatalyst. In certain cases, a third molecule may participate in EDA complex formation. For example, in 2021 the Tripathi group reported a free-radical alkylation of quinone methides that proceeds via a yellow EDA complex mediated by diphenylphosphoric acid. No complex formation is observed in the absence of the acid (Fig. 26, bottom).[104]

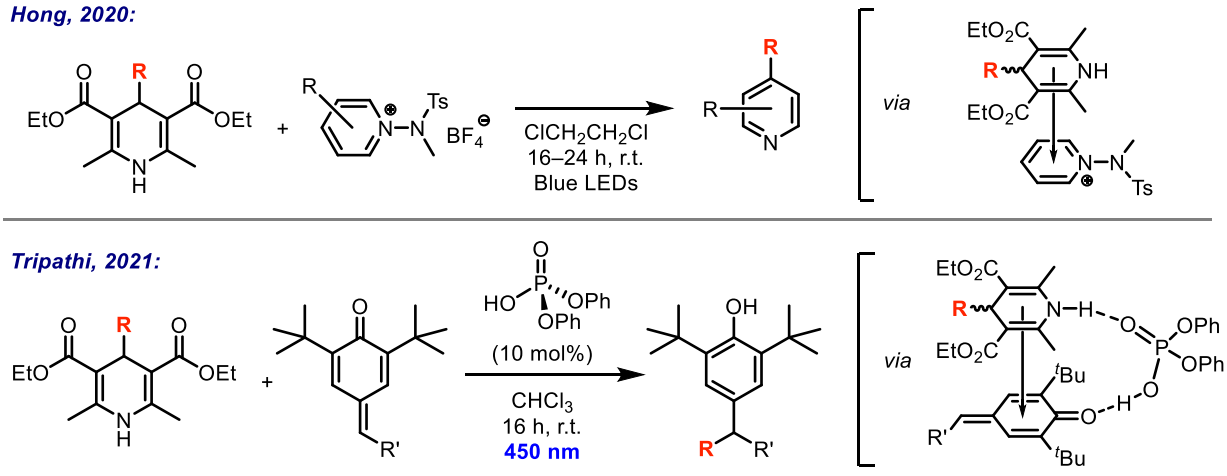


Fig. 26. *Top: Alkylation of N-Aminopyridinium salts via a directly irradiated EDA complex (Hong, 2020), Bottom: Alkylation of quinone methides via an EDA complex mediated by a Brønsted acid catalyst (Tripathi, 2021).*[104]

1.2.5 Applications of Hantzsch Esters: C_1 Functionalization

C_1 functionalization describes the addition of a functional group containing a singular carbon atom to a substrate. This concept has been known for centuries and has been intensively studied ever since. Traditional C_1 building blocks include, but are not limited to: $CO_{(2)}$, methyl halides, cyanide, diazomethane, nitromethane, formaldehyde, and methyl anion equivalents (MeMgX, MeLi). In such reactions, either their inherent reactivity is exploited (e.g. the nucleophilicity of cyanide) or they are incorporated by the action of an additional reagent or catalyst (e.g. transition metal-catalyzed carbonylation with CO). In order to combine the radical reservoir potential of Hantzsch esters with C_1 functionalization, the expelled fragment must form a rather stable radical. For instance, unstable methyl radicals cannot be formed as the energy gained from aromatization is insufficient.[105] Heteroatom stabilization is therefore the key to unlocking free-radical C_1 fragments. Depending on the number of heteroatoms, the substituted methyl group can either have a degree of oxidation of 1, 2, or 3 (not to be confused with the oxidation *number*).

Degree of oxidation of 3 (≙ Carboxylic acid)

The majority of C_1 radicals transferred by Hantzsch esters possesses a degree of oxidation of 3. Carbamoylations are predominant in this category as a result of the relatively high stability of free carbamoyl radicals (Fig. 27, top). In 2020, the Jacobi von Wangelin group reported a carbamoyl transfer onto electron-deficient olefins using photoredox catalysis mediated by 3DPAFIPN.[106] In parallel, the Melchiorre group showcased a dual nickel/photoredox-cocatalyzed cross-coupling of aryl bromides yielding benzamides.[107] In the same year, Hong and co-workers described the photocatalyst- and additive-free functionalization of *N*-aminopyridinium salts via an EDA complex featuring 4-carboxamido Hantzsch esters as part of the scope (cf. Fig. 26).[103] An example of a dark carbamoylation was reported in 2023 by Zhou *et al.* *N*-Arylacrylamides and *N*-arylcinnamides were carbamoylated via a persulfate-mediated oxidation of the Hantzsch ester, following by intramolecular cyclization.[108] In contrast, the transfer of ester groups using 4-oxycarbonyl-substituted Hantzsch esters remains considerably more challenging. The corresponding radicals show significantly lower stability compared to their carbamoyl counterparts and are prone to rapid decarboxylation or decarbonylation pathways. To date, only a single report by Bandyopadhyay and co-workers has demonstrated a Hantzsch ester-mediated oxycarbonylation as part of a Pd-catalyzed functionalization of azoles using stoichiometric BAIB.[109] The carboxyl-substituted[107] and trichloromethyl-substituted[110] Hantzsch ester have been synthesized, though they have not yet found application in any C_1 functionalization reactions.

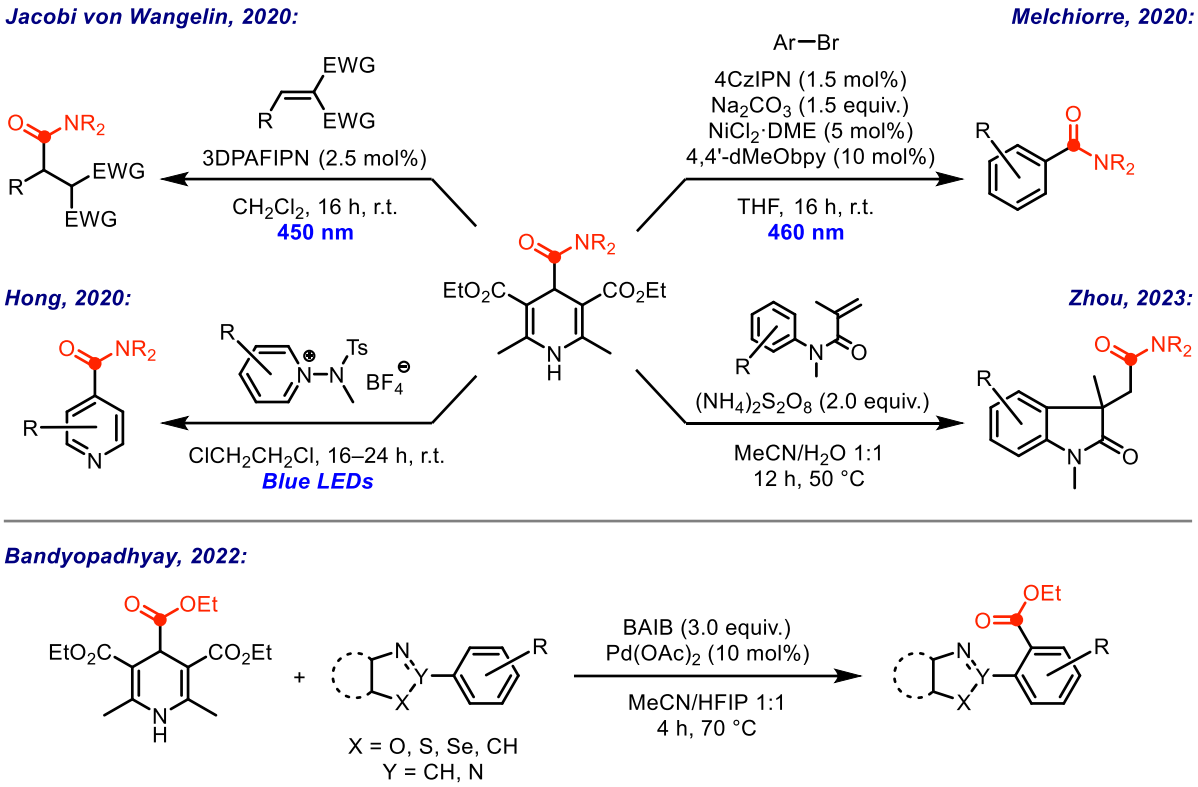


Fig. 27. *Top: Selected examples for Hantzsch ester-mediated carbamoylations,*[103,106–108] *Bottom: Pd-catalyzed oxycarbonylation of azoles using BAIB (Bandyopadhyay, 2022).*[109]

Degree of oxidation of 2 (≙ Aldehyde)

Transfer of C_1 radicals with a degree of oxidation of 2 is limited to oxygen-bearing methyl groups. Three reports with a total of five reactions featuring a dimethoxymethyl-substituted Hantzsch ester as part of a substrate scope have been reported (Fig. 28), including an iridium-photoredox-catalyzed functionalization of α,β-unsaturated carboxylates,[111] a Safranin-photoredox-catalyzed synthesis of a substituted phenylacetylene,[112] and a desulfonative alkylation of *N*-heteroaryl sulfones using 4CzIPN photoredox catalysis.[113] Three reaction examples for a direct formylation of 2-arylquinazolines under electrochemical conditions have been reported by Das and co-workers in 2023 (Fig. 28, bottom).[114] Hantzsch esters substituted with other di(heteroatom)-substituted methyl groups such as halogens, nitrogen, or sulfur have not been synthesized as of today.

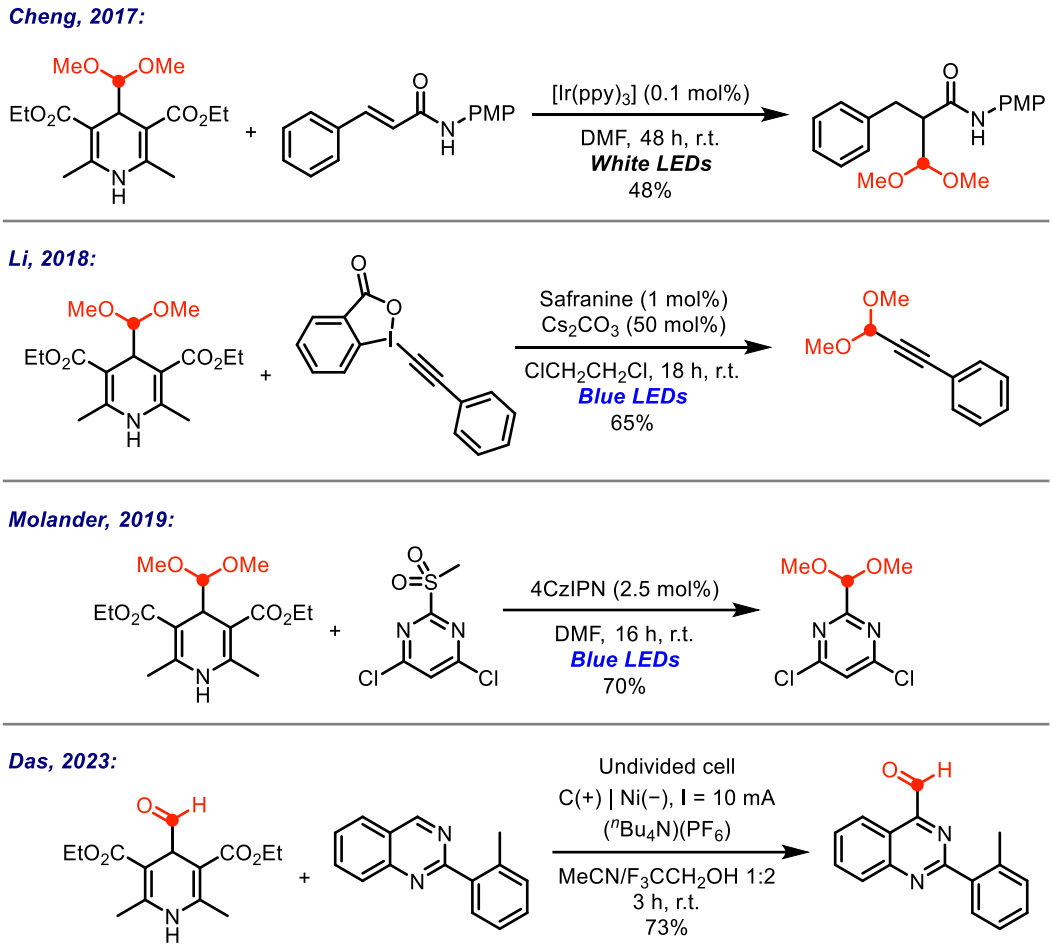


Fig. 28. *Every reported example of a Hantzsch ester-mediated C_1 functionalization reaction within a degree of oxidation of 2.*[111–114]

Degree of oxidation of 1 (≙ Alcohol)

Sporadic examples of methoxymethylation reactions have been reported,[98,99,115] for example as part of the substrate scope of Nishibayashi's 2016 publication concerning nickel/photoredox-cocatalysis (Fig. 29, top; cf. Fig. 25).[99] Aminomethylations are slightly more common,[98,99,116–122] mostly featuring Boc-protected or dibenzyl-substituted amino groups. An example is the enantioselective substitution of allylic acetate groups reported by Yu and co-workers in 2018 (Fig. 29, center).[117] The reaction proceeds via palladium/iridium-photoredox-cocatalysis featuring the axially chiral ligand Garphos. A single example of a chloromethylation is given in a 2019 report by Zhao *et al.* regarding a manganese and di-*tert*-butylperoxide-driven alkyl-alkyl cross-coupling of β-chloroketones (Fig. 29, bottom).[123] Single substitution of the methyl group on 4-methyl Hantzsch esters with other heteroatoms such as sulfur,[124,125] phosphorus,[126,127] bromine,[128,129] or iodine[125,130] is known, but these structures have not yet been reported in alkylation reactions.

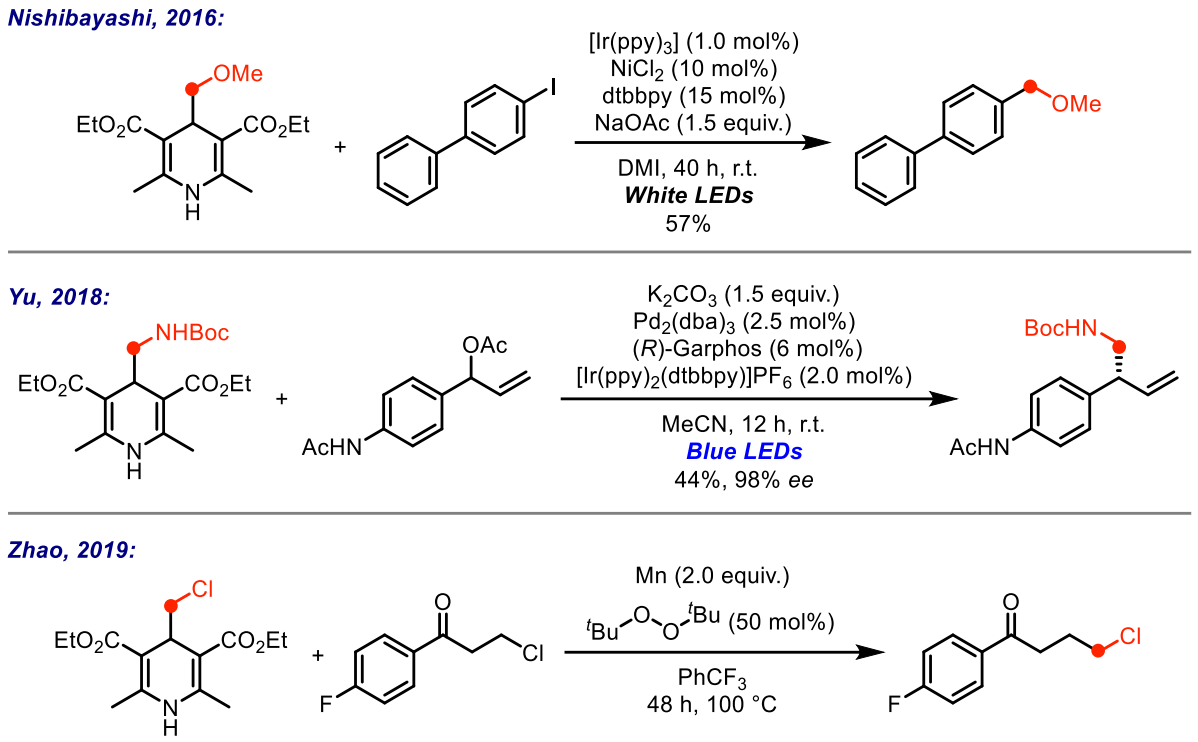


Fig. 29. *Selected examples of Hantzsch ester-mediated C_1 functionalization reactions within a degree of oxidation of 1.*[99,117,123]

Literature References

[1] K. Nakatani, J. Piard, P. Yu, R. Métivier, Introduction: Organic Photochromic Molecules in *Photochromic Materials: Preparation, Properties and Applications* (Eds.: H. Tian, J. Zhang), Wiley-VCH Verlag, Weinheim, Germany, **2016**, pp. 1–45.

[2] V. Durasevic, D. Parac, A. Sutlovic, From Murex Purpura to Sensory Photochromic Textiles in *Textile Dyeing* (Ed.: P. Hauser), InTech, **2011**, pp. 60–61.

[3] C. Christophersen, F. Wätjen, O. Buchardt, U. Anthoni, *Tetrahedron* **1978**, *34*, 2779–2781.

[4] M. Grieve, *A Modern Herbal (Volume 2, I-Z and Indexes)*, Dover Publications, **1971**.

[5] Kahler, *Arch. Pharm.* **1830**, *34*, 318–319.

[6] A. Alms, *Arch. Pharm.* **1830**, *34*, 319–320.

[7] H. Trommsdorff, *Ann. Pharm.* **1834**, *11*, 190–207.

[8] E. E. van Tamelen, S. H. Levin, G. Brenner, J. Wolinsky, P. Aldrich, *J. Am. Chem. Soc.* **1958**, *80*, 501–502.

[9] T. Matsuura, Y. Sata, K. Ogura, M. Mori, *Tetrahedron Lett.* **1968**, *9*, 4627–4630.

[10] C. J. Fritzsche, *J. Prakt. Chem.* **1867**, *101*, 333–343.

[11] K. Elbs, *J. Prakt. Chem.* **1891**, *44*, 467–469.

[12] W. R. Orndorff, F. K. Cameron, *Am. Chem. J.* **1895**, *17*, 658–681.

[13] W. H. Perkin, *J. Chem. Soc. Trans.* **1881**, *39*, 409–452.

[14] G. Ciamician, P. Silber, *Ber. Dtsch. Chem. Ges.* **1910**, *43*, 945–949.

[15] G. Ciamician, P. Silber, *Ber. Dtsch. Chem. Ges.* **1901**, *34*, 2040–2046.

[16] G. Ciamician, P. Silber, *Ber. Dtsch. Chem. Ges.* **1908**, *41*, 1928–1935.

[17] G. Ciamician, P. Silber, *Ber. Dtsch. Chem. Ges.* **1901**, *34*, 1530–1543.

[18] Royal Society of Chemistry, "One hundred years on, the RSC celebrates progress towards realising father of photochemistry's vision," can be found under https://www.rsc.org/news-events/articles/2012/09-september/one-hundred-years-on-the-rsc-celebrates-progress-towards-realising-father-of-photochemistrys-vision/, **2012**, accessed on November 16, 2024.

[19] Università di Bologna, "Giacomo Luigi Ciamician," can be found under https://www.unibo.it/en/university/who-we-are/our-history/famous-people-and-students/giacomo-luigi-ciamician-1, **n.d.**, accessed on November 16, 2024.

[20] R. G. W. Norrish, C. H. Bamford, *Nature* **1936**, *138*, 1016–1016.

[21] R. G. W. Norrish, H. G. Crone, O. D. Saltmarsh, *J. Chem. Soc.* **1934**, 1456.

[22] R. Spence, W. Wild, *Nature* **1936**, *138*, 206–206.

[23] G. Ciamician, P. Silber, *Ber. Dtsch. Chem. Ges.* **1908**, *41*, 1071–1080.

[24] G. Ciamician, P. Silber, *Ber. Dtsch. Chem. Ges.* **1909**, *42*, 1510–1515.

[25] R. G. W. Norrish, M. E. S. Appleyard, *J. Chem. Soc.* **1934**, 874.

[26] A. Jabłoński, *Nature* **1933**, *131*, 839–840.

[27] R. G. W. Norrish, G. Porter, *Nature* **1949**, *164*, 658–658.

[28] M. Oelgemöller, *Chem. Rev.* **2016**, *116*, 9664–9682.

[29] D. Cambié, T. Noël, *Top. Curr. Chem.* **2018**, *376*, 1–27.

[30] J. Law, R. Rennie, *A Dictionary of Chemistry*, Oxford University Press, **2020**.

[31] S. Campagna, F. Puntoriero, F. Nastasi, G. Bergamini, V. Balzani, Photochemistry and Photophysics of Coordination Compounds: Ruthenium in *Photochemistry and Photophysics of Coordination Compounds I*, Springer Berlin Heidelberg, Berlin, Heidelberg, **2007**, pp. 117–214.

[32] N. A. Romero, D. A. Nicewicz, *Chem. Rev.* **2016**, *116*, 10075–10166.

[33] K. Teegardin, J. I. Day, J. Chan, J. Weaver, *Org. Process Res. Dev.* **2016**, *20*, 1156–1163.

[34] D. P. Haria, B. König, *Chem. Commun.* **2014**, *50*, 6688–6699.

[35] E. Yoshioka, S. Kohtani, T. Jichu, T. Fukazawa, T. Nagai, Y. Takemoto, H. Miyabe, *Synlett* **2014**, *26*, 265–270.

[36] C. H. Liu, J. J. Wang, M. Xu, Q. Luo, Z. Wang, W. Tan, X. Zhao, X. Jia, *New J. Chem.* **2024**, *48*, 2367–2370.

[37] Z. Y. Yu, J. N. Zhao, F. Yang, X. F. Tang, Y. F. Wu, C. F. Ma, B. Song, L. Yun, Q. W. Meng, *RSC Adv.* **2020**, *10*, 4825–4831.

[38] A. Joshi-Pangu, F. Lévesque, H. G. Roth, S. F. Oliver, L. C. Campeau, D. Nicewicz, D. A. DiRocco, *J. Org. Chem.* **2016**, *81*, 7244–7249.

[39] W. Zhang, Y. Guo, Z. Liu, X. Jin, L. Yang, Z. L. Liu, *Tetrahedron* **2005**, *61*, 1325–1333.

[40] E. Speckmeier, T. G. Fischer, K. Zeitler, *J. Am. Chem. Soc.* **2018**, *140*, 15353–15365.

[41] G. J. Kavarnos, Fundamental Concepts of Photoinduced Electron Transfer in *Photoinduced Electron Transfer I* (Ed.: J. Mattay), Springer, **1990**, pp. 21–58.

[42] T. Koopmans, *Physica* **1934**, *1*, 104–113.

[43] D. Rehm, A. Weller, *Isr. J. Chem.* **1970**, *8*, 259–271.

[44] G. J. Kavarnos, *Fundamentals of Photoinduced Electron Transfer*, VCH, **1993**.

[45] A. Taherpour, *Arab. J. Chem.* **2017**, *10*, S609–S616.

[46] P. Suppan, E. Vauthey, *J. Photochem. Photobiol. A* **1989**, *49*, 239–248.

[47] T. Caronna, S. Morrocchi, B. M. Vittimberga, *J. Am. Chem. Soc.* **1986**, *108*, 2205–2208.

[48] A. Rosspeintner, G. Angulo, E. Vauthey, *J. Am. Chem. Soc.* **2014**, *136*, 2026–2032.

[49] S. Schieffer, *Dissertation*, Universität zu Köln, **2002**.

[50] D. Rau, *Dissertation*, Universität Bonn, **2005**.

[51] J. M. Haimerl, *Dissertation*, Universität Regensburg, **2018**.

[52] S. E. Braslavsky, *Pure Appl. Chem.* **2007**, *79*, 293–465.

[53] P. Atkins, J. de Paula, J. Keeler, *Atkin's Physical Chemistry*, Oxford University Press, Oxford, **2022**.

[54] W. F. Libby, *J. Phys. Chem.* **1952**, *56*, 863–868.

[55] H. D. Roth, A Brief History of Photoinduced Electron Transfer and Related Reactions in *Photoinduced Electron Transfer I* (Ed.: J. Mattay), **1990**, pp. 1–20.

[56] D. Rehm, A. Weller, *Ber. Bunsenges. Phys. Chem.* **1969**, *73*, 834–839.

[57] J. R. Miller, L. T. Calcaterra, G. L. Closs, *J. Am. Chem. Soc.* **1984**, *106*, 3047–3049.

[58] M. S. Newman, H. A. Karnes, *J. Org. Chem.* **1966**, *31*, 3980–3984.

[59] A. J. Perkowski, C. L. Cruz, D. A. Nicewicz, *J. Am. Chem. Soc.* **2015**, *137*, 15684–15687.

[60] C. L. Cruz, D. A. Nicewicz, *ACS Catal.* **2019**, *9*, 3926–3935.

[61] M. Neumann, K. Zeitler, M. Neumann, K. Zeitler, *Chem. Eur. J.* **2013**, *19*, 6950–6955.

[62] E. J. Enholm, K. S. Kinter, *J. Am. Chem. Soc.* **1991**, *113*, 7784–7785.

[63] D. S. Hays, G. C. Fu, *Tetrahedron* **1999**, *55*, 8815–8832.

[64] J. Jin, D. W. C. MacMillan, *Nature* **2015**, *525*, 87–90.

[65] F. Louërat, Y. Fort, V. Mamane, *Tetrahedron Lett.* **2009**, *50*, 5716–5718.

[66] E. Späth, F. Berger, W. Kuntara, *Ber. Dtsch. Chem. Ges.* **1930**, *63*, 134–141.

[67] J. Du, T. P. Yoon, *J. Am. Chem. Soc.* **2009**, *131*, 14604–14605.

[68] J. Du, K. L. Skubi, D. M. Schultz, T. P. Yoon, *Science* **2014**, *344*, 392–396.

[69] S. P. Pitre, L. E. Overman, *Chem. Rev.* **2022**, *122*, 1717–1751.

[70] L. Furst, J. M. R. Narayanam, C. R. J. Stephenson, *Angew. Chem. Int. Ed.* **2011**, *50*, 9655–9659.

[71] A. Hantzsch, *Ber. Dtsch. Chem. Ges.* **1881**, *14*, 1637–1638.

[72] A. Hantzsch, *Liebigs Ann. Chem.* **1882**, *215*, 1–82.

[73] M. Schubert-Zsilavecz, H. Stark, *Pharm. Unserer Zeit* **2005**, *34*, 374–379.

[74] I. Huber, E. Wappl, A. Herzog, J. Mitterdorfer, H. Glossmann, T. Langer, J. Striessing, *Biochem. J.* **2000**, *347*, 829–836.

[75] E. Verg, *Meilensteine - 125 Jahre Bayer*, Bayer AG Selbstverlag, Leverkusen, **1988**.

[76] M. Khoshneviszadeh, N. Edraki, K. Javidnia, A. Alborzi, B. Pourabbas, J. Mardaneh, R. Miri, *Bioorg. Med. Chem.* **2009**, *17*, 1579–1586.

[77] A. Fassihi, Z. Azadpour, N. Delbari, L. Saghaie, H. R. Memarian, R. Sabet, A. Alborzi, R. Miri, B. Pourabbas, J. Mardaneh, *Eur. J. Med. Chem.* **2009**, *44*, 3253–3258.

[78] A. G. Tempone, N. N. Taniwaki, J. Q. Reimão, *Parasitol. Res.* **2009**, *105*, 499–505.

[79] V. P. Pandey, S. S. Bisht, M. Mishra, A. Kumar, M. I. Siddiqi, A. Verma, M. Mittal, S. A. Sane, S. Gupta, R. P. Tripathi, *Eur. J. Med. Chem.* **2010**, *45*, 2381–2388.

[80] K. S. Van Horn, Y. Zhao, P. T. Parvatkar, J. Maier, T. Mutka, A. Lacrue, F. Brockmeier, D. Ebert, W. Wu, D. R. Casandra, N. Namelikonda, J. Yacoub, M. Sigal, S. Knapp, D. Floyd, D. Waterson, J. N. Burrows, J. Duffy, J. L. DeRisi, D. E. Kyle, R. K. Guy, R. Manetsch, *Eur. J. Med. Chem.* **2024**, *275*, 116599.

[81] A. M. Vijesh, A. M. Isloor, S. K. Peethambar, K. N. Shivananda, T. Arulmoli, N. A. Isloor, *Eur. J. Med. Chem.* **2011**, *46*, 5591–5597.

[82] R. S. Kumar, A. Idhayadhulla, A. J. Abdul Nasser, J. Selvin, *Eur. J. Med. Chem.* **2011**, *46*, 804–810.

[83] L. Navidpour, H. Shafaroodi, R. Miri, A. R. Dehpour, A. Shafiee, *Farmaco* **2004**, *59*, 261–269.

[84] A. Samzadeh-Kermani, H. Shafaroodi, R. Miri, H. Mirkhani, M. Vosooghi, A. Shafiee, *Med. Chem. Res.* **2009**, *18*, 112–126.

[85] J. Marco-Contelles, R. León, C. de los Ríos, A. Samadi, M. Bartolini, V. Andrisano, O. Huertas, X. Barril, F. J. Luque, M. I. Rodríguez-Franco, B. López, M. G. López, A. G. García, M. do Carmo Carreiras, M. Villarroya, *J. Med. Chem.* **2009**, *52*, 2724–2732.

[86] J. Fischer, C. Robin Ganellin, *Analog. Drug Discov.* **2006**, 464–466.

[87] Y. Zhao, Q. Liu, J. Li, Z. Liu, B. Zhou, *Synlett* **2010**, *2010*, 1870–1872.

[88] S. J. Connon, *Org. Biomol. Chem.* **2007**, *5*, 3407–3417.

[89] J. G. De Vries, N. Mršić, *Catal. Sci. Technol.* **2011**, *1*, 727–735.

[90] M. Rueping, J. Dufour, F. R. Schoepke, *Green Chem.* **2011**, *13*, 1084–1105.

[91] A. Mc Skimming, S. B. Colbran, *Chem. Soc. Rev.* **2013**, *42*, 5439–5488.

[92] D. Wang, D. Astruc, *Chem. Rev.* **2015**, *115*, 6621–6686.

[93] S. G. Ouellet, A. M. Walji, D. W. C. MacMillan, *Acc. Chem. Res.* **2007**, *40*, 1327–1339.

[94] C. Zheng, S. L. You, *Chem. Soc. Rev.* **2012**, *41*, 2498–2518.

[95] G. Li, R. Chen, L. Wu, Q. Fu, X. Zhang, Z. Tang, *Angew. Chem. Int. Ed.* **2013**, *52*, 8432–8436.

[96] G. Li, L. Wu, G. Lv, H. Liu, Q. Fu, X. Zhang, Z. Tang, *Chem. Commun.* **2014**, *50*, 6246–6248.

[97] L. Cao, L. Zheng, Q. Huang, *J. Organomet. Chem.* **2014**, *768*, 56–60.

[98] K. Nakajima, S. Nojima, K. Sakata, Y. Nishibayashi, *ChemCatChem* **2016**, *8*, 1028–1032.

[99] K. Nakajima, S. Nojima, Y. Nishibayashi, *Angew. Chem. Int. Ed.* **2016**, *55*, 14106–14110.

[100] P. Z. Wang, J. R. Chen, W. J. Xiao, *Org. Biomol. Chem.* **2019**, *17*, 6936–6951.

[101] A. M. Faisca Phillips, A. J. L. Pombeiro, *Catalysts* **2023**, *13*, 419.

[102] G. Suresh Yedase, S. Venugopal, A. P., V. Reddy Yatham, *Asian J. Org. Chem.* **2022**, *11*, e202200478.

[103] I. Kim, S. Park, S. Hong, *Org. Lett.* **2020**, *22*, 8730–8734.

[104] S. S. Patel, D. Kumar, C. B. Tripathi, *Chem. Commun.* **2021**, *57*, 5151–5154.

[105] G. Bin Shen, L. Xie, H. Y. Yu, J. Liu, Y. H. Fu, M. Yan, *RSC Adv.* **2020**, *10*, 31425–31434.

[106] L. Cardinale, M. O. Konev, A. Jacobi von Wangelin, *Chem. Eur. J.* **2020**, *26*, 8239–8243.

[107] N. Alandini, L. Buzzetti, G. Favi, T. Schulte, L. Candish, K. D. Collins, P. Melchiorre, *Angew. Chem.* **2020**, *132*, 5286–5291.

[108] Q. Jing, F. C. Qiao, J. Sun, J. Y. Wang, M. D. Zhou, *Org. Biomol. Chem.* **2023**, *21*, 7530–7534.

[109] A. Sarkar, M. Saha, A. R. Das, A. Banerjee, R. Majumder, D. Bandyopadhyay, *ChemistrySelect* **2022**, *7*, e202203959.

[110] F. Aydin, R. Ozen, *Molbank* **2006**, *2006*, M471.

[111] F. Gu, W. Huang, X. Liu, W. Chen, X. Cheng, *Adv. Synth. Catal.* **2018**, *360*, 925–931.

[112] X. Liu, R. Liu, J. Dai, X. Cheng, G. Li, *Org. Lett.* **2018**, *20*, 6906–6909.

[113] Z. J. Wang, S. Zheng, J. K. Matsui, Z. Lu, G. A. Molander, *Chem. Sci.* **2019**, *10*, 4389–4393.

[114] R. D. Mandal, M. Saha, D. Das, A. R. Das, *J. Org. Chem.* **2023**, *88*, 6071–6095.

[115] Y. Liu, W. Luo, T. Xia, Y. Fang, C. Du, X. Jin, Y. Li, L. Zhang, W. Lei, H. Wu, *Org. Chem. Front.* **2021**, *8*, 1732–1738.

[116] K. Nakajima, X. Guo, Y. Nishibayashi, *Chem. Asian J.* **2018**, *13*, 3653–3657.

[117] H. H. Zhang, J. J. Zhao, S. Yu, *J. Am. Chem. Soc.* **2018**, *140*, 16914–16919.

[118] K. Zhang, L. Q. Lu, Y. Jia, Y. Wang, F. D. Lu, F. Pan, W. J. Xiao, *Angew. Chem. Int. Ed.* **2019**, *58*, 13375–13379.

[119] Y. Liu, W. Luo, T. Xia, Y. Fang, C. Du, X. Jin, Y. Li, L. Zhang, W. Lei, H. Wu, *Org. Chem. Front.* **2021**, *8*, 1732–1738.

[120] J. P. Malval, S. Achelle, L. Bodiou, A. Spangenberg, L. C. Gomez, O. Soppera, F. R. Le Guen, *J. Mater. Chem. C* **2014**, *2*, 7869–7880.

[121] Y. Zhang, Y. Tanabe, S. Kuriyama, Y. Nishibayashi, *J. Org. Chem.* **2021**, *86*, 12577–12590.

[122] S. Xue, À. Cristòfol, B. Limburg, Q. Zeng, A. W. Kleij, *ACS Catal.* **2022**, *12*, 3651–3659.

[123] J. Wang, Y. B. Pang, N. Tao, R. S. Zeng, Y. Zhao, *J. Org. Chem.* **2019**, *84*, 15315–15322.

[124] L. F. Lee, G. L. Stikes, J. M. Molyneaux, Y. L. Sing, J. P. Chupp, S. S. Woodard, *J. Org. Chem.* **1990**, *55*, 2872–2877.

[125] M. E. M. Baggs, B. Gregory, *Can. J. Chem.* **1980**, *58*, 794–802.

[126] M. M. Cid, *Tetrahedron Lett.* **1996**, *37*, 6033–6036.

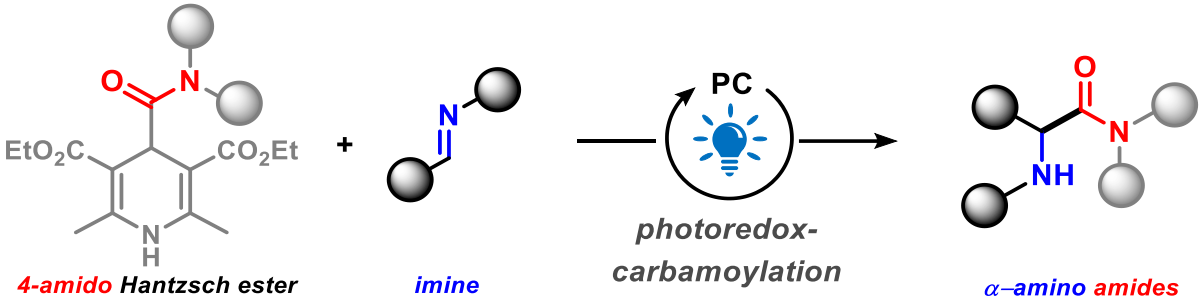
[127] A. I. Razumov, M. P. Sokolov, B. G. Liorber, T. V. Zykova, R. A. Salakhutdinov, G. V. Urmancheeva, *Zh. Obshch. Khim.* **1977**, *47*, 2717–2722.

[128] P. J. Brignell, E. Bullock, U. Eisner, B. Gregory, A. W. Johnson, H. Williams, *J. Chem. Soc.* **1963**, 4819–4827.

[129] M. Anderson, A. W. Johnson, *J. Chem. Soc.* **1965**, 2411–2422.

[130] J. Ashby, U. Eisner, *J. Chem. Soc. C* **1967**, *53*, 1706.

Chapter 2



Photoredox-Catalyzed Synthesis of α-Amino Acid Amides by Imine Carbamoylation

Abstract: *An operationally simple protocol for the photocatalytic carbamoylation of imines is reported. Easily available, bench-stable 4-amido Hantzsch ester derivatives serve as precursors to carbamoyl radicals which undergo rapid addition to N-aryl imines. The reaction proceeds under blue light irradiation in the presence of the photocatalyst 3DPAFIPN and Brønsted/Lewis acid additives. Mechanistic studies indicated a photoredox mechanism that involves carbamoyl radicals.*

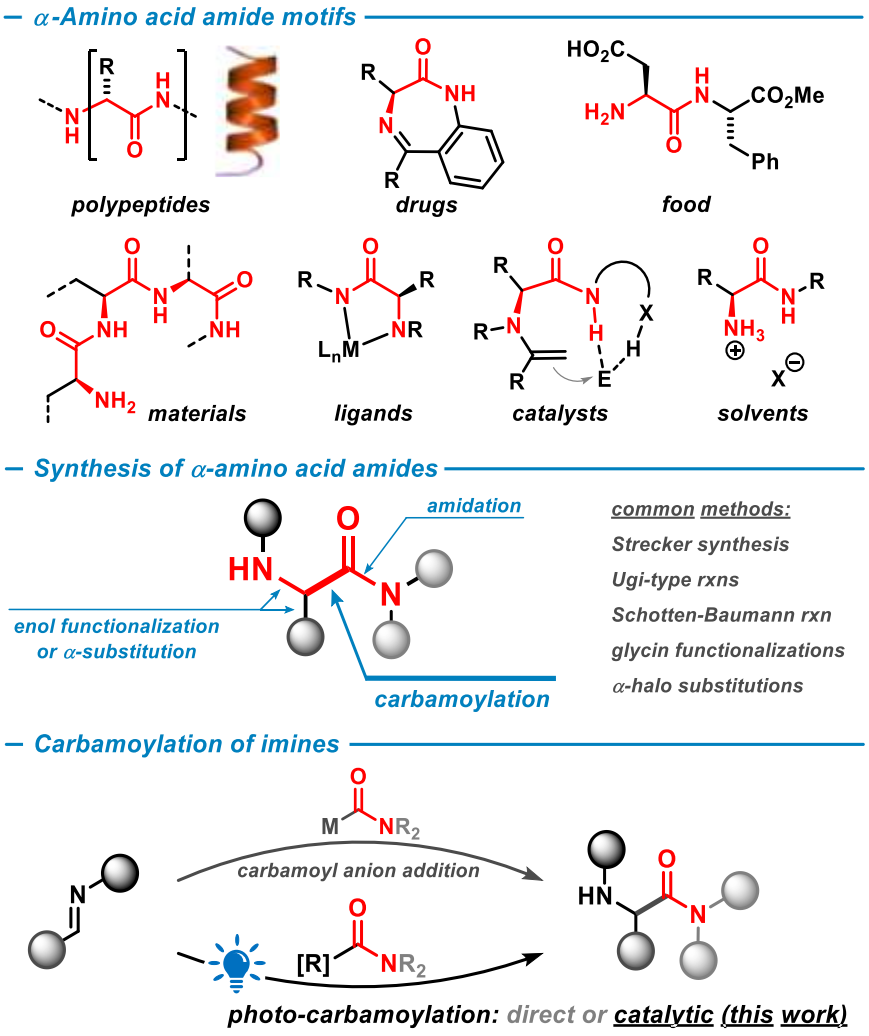
This chapter has been published in and reproduced with minor formatting adjustments from L. Cardinale, M.-O. W. S. Schmotz, M. O. Konev, A. Jacobi von Wanglin, *Org. Lett.* **2022**, *24*, 506–510, DOI: 10.1021/acs.orglett.1c03908, with permission of ACS.
Copyright **2021** American Chemical Society.

Part of this work constitutes the bachelor thesis “Photoredox-catalyzed Synthesis of Unnatural α-Amino Acid Amides”, Mattis-Ole W. S. Schmotz, **2020**. This chapter is also part of the doctoral thesis “Small Molecule Activation through Radical Formation by Visible Light Photoredox Catalysis”, Luana Cardinale, **2021**.

Author contributions: **Luana Cardinale** wrote the manuscript and performed experimental work, **Mattis-Ole W. S. Schmotz** assisted in writing the manuscript, performed experimental work, and wrote the experimental section, **Mikhail O. Konev** performed experimental work, **Axel Jacobi von Wangelin** supervised this work.

Introduction

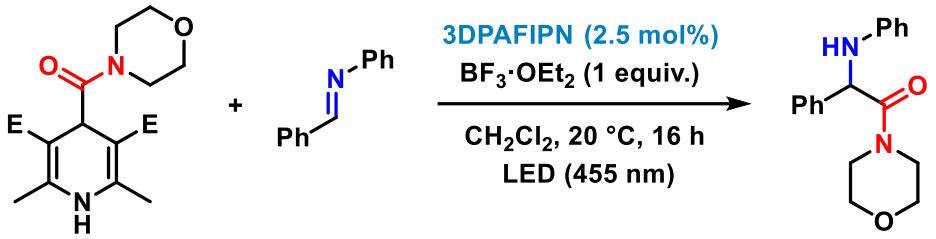
Amino acid derivatives undoubtedly are among the most abundant, most versatile, and most studied functional molecules.[1] They form the molecular basis of biological life and find diverse applications as pharmaceuticals, food, materials, fine chemicals, and catalysts. α-Amino acid amides are the formal monomeric entities of polypeptides and a recurrent structural motif in numerous natural and synthetic molecules (Scheme 1, top). This molecular skeleton displays high density of functionalization (i.e. amine, proton, carbonyl, amide, and substituents) and high thermodynamic stability. Numerous syntheses have been developed to access α-amino acid am-ides with most methodologies involving peripheral manipulations of pre-functionalized core structures (e.g. Schotten-Baumann, α-carbonyl substitutions).[2] The *de novo* construction of the amino carboxamide motif by construction of the central C-C bond in a formal addition to imines displays high modularity and enables high product diversity. The most prominent methods include Strecker reactions, Ugi reactions, and aminocarbonylations.[3–5] Direct carbamoylations of imines have remained very rare due to the limited availability of reactive carbamoyl precursors and low functional group compatibility. Nucleophilic additions of carbamoylmetal reagents (Li, Si) were reported.[6,7] Photoredox catalysis has recently emerged as a powerful tool to access functionalized radical species from stable and available synthetic precursors under mild conditions. Successful applications to photoredox-carbamoylations furnished new syntheses of carboxamides and anilides.[8] 4-Amido-Hantzsch esters were demonstrated to serve as convenient precursors to various acyl radicals under photoredox conditions, including carbamoyl radicals.[9] Here, we report on the development of mild conditions that enable the visible light-mediated carbamoylation of imines with Hantzsch ester derivatives (HEH-$CONR_2$) and the implementation of such synthetic strategy to the synthesis of a diverse set of α-amino acid amides (Scheme 1, bottom).[10]



Scheme 1. *α-Amino Acid Amide Motifs: General Occurrence, General Synthetic Methods, and Carbamoylations of Imines.*

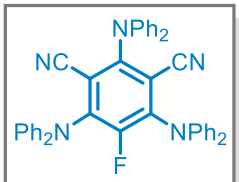
Results and Discussion

Initially, 4-morpholinocarbonyl-substituted Hantzsch ester (**1a**) and benzylideneaniline (**2a**) were reacted in the presence of 3DPAFIPN (Scheme 2). The organic catalyst is commercially available and displays oxidative and reductive reactivity under visible light irradiation, so that either mechanistic scenario may operate with the employed combination of electrophilic (imine) and nucleophilic (Hantzsch ester) reagents.[11] The addition of Brønsted/Lewis acids was beneficial, most likely due to higher reducibility (for imine, $E \sim -2$ V vs. SCE; for iminium ion, $E \sim -1$ V vs. SCE) or higher electrophilicity.[12,13] No reaction proceeded in the dark (entry 7). Direct irradiation of catalyst-free reactions gave low yields (entry 8; see Experimental Section for UV−Vis spectra of the EDA complex).



1a (E = CO_2Et) **2a** **3a**

entry	deviation from standard conditions	yield (%)[a]
1	none	85
2	no $BF_3{\cdot}OEt_2$	10
3	$BF_3{\cdot}OEt_2$ (20 mol%)	54
4	TFA instead of $BF_3{\cdot}OEt_2$	77
5	$Sc(OTf)_3$ instead of $BF_3{\cdot}OEt_2$	51
6	$PhCO_2H$ instead of $BF_3{\cdot}OEt_2$	24
7	no 3DPAFIPN, dark	0
8	no 3DPAFIPN, 365 nm or 455 nm	20

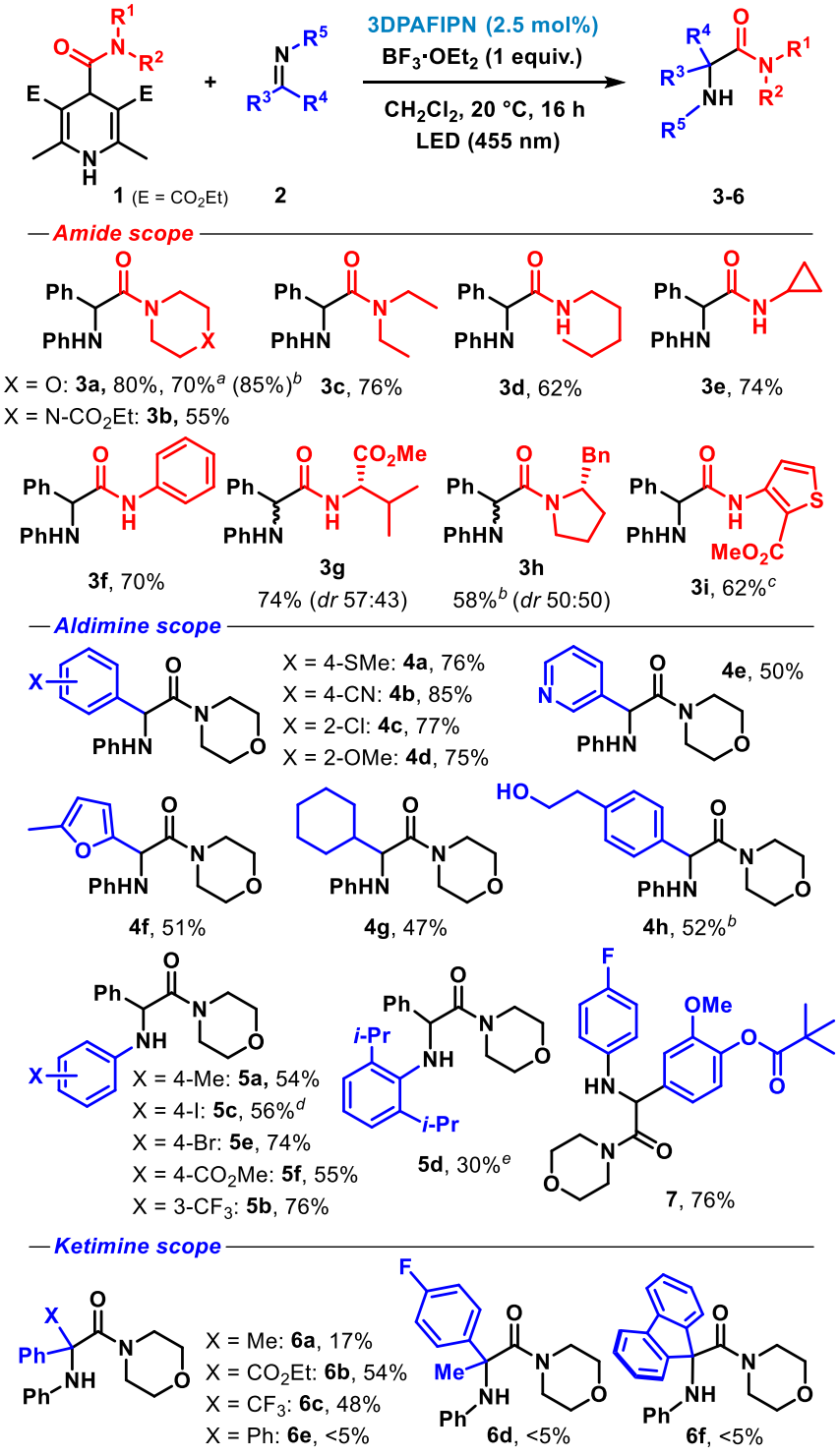


3DPAFIPN

E(PC$^{\bullet+}$/PC*)= -1.38 V
E(PC*/PC$^{\bullet-}$)= +1.09 V
E(PC$^{\bullet+}$/PC)= +1.30 V
E(PC/PC$^{\bullet-}$)= -1.59 V

Scheme 2. *Key Experiments for Method Development.* [a] *Yields determined by* ^1H *NMR vs. 1,3,5-trimethoxybenzene. 0.10 mmol scale reactions, 0.1 M in* CH_2Cl_2*, 1.3 equiv.* ***1a*** *under* N_2 *in dry solvents.*

A diverse set of carboxamido-Hantzsch esters, aldimines, and ketimines were subjected to the optimized conditions (Scheme 3). Tertiary and secondary carboxamides bearing (hetero)aryl and (cyclo)alkyl substituents were cleanly installed in the amino acid derivatives (**3a–i**). Electron-deficient aldimines afforded good yields (e.g., **4b**), which is in accord with an electrophilic or oxidizing reactivity of the imine. Reactions of aliphatic imines, due to their instability at room temperature and their tendency to undergo further condensation, were shown with *N*-cyclohexylcarboxamide **4g**. Variations of the N-substituents of the imines were limited to aryl groups. Tosyl, benzyl, *n*/*tert*-alkyl, and pyridyl substituents at the imine nitrogen afforded no products. Hydrazones and/or oximes were not tolerated. The electron-rich *N*-(4-methoxyphenyl)-benzaldimine underwent competing oxidation of the PMP moiety. Ketimine reactions were sensitive to stereoelectronic properties. Generally lower yields were observed (**6a–f**), and electron-deficient ketimines still gave moderate yields (**6b** and **6c**). The mild reaction conditions tolerated halides (F, Cl, Br, and I), electron-rich and electron-deficient heteroarenes, alcohols, esters, and nitriles. This documents high chemoselectivity of a presumably operating reductive electron transfer event within the reaction mechanism.[14] Only in the case of 4-iodoaniline **5c** was minor deiodination observed (~9% **3a**).

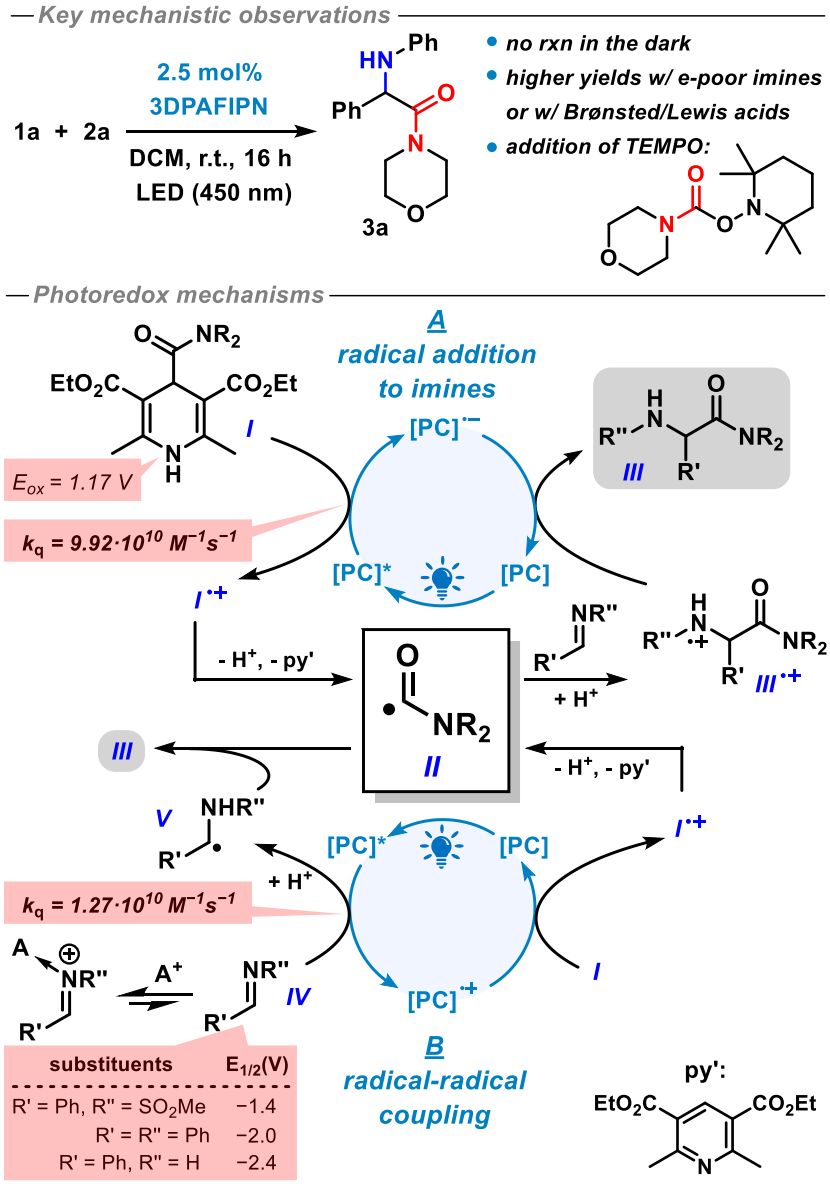


Scheme 3. *Substrate Scope. 0.30 mmol scale reactions, 0.1 M in CH_2Cl_2. Isolated yields are given.* [a] *1.5 mmol scale.* [b] *NMR yields vs. 1,3,5-trimethoxybenzene.* [c] *Recrystallized from MeOH.* [d] *Isolated as mixture with 9% **3a** (HPLC).* [e] *72 h.*

The reaction could be scaled up by a factor of 5 (1.5 mmol) with an only minor decrease in yield (**3a**, 70% instead of 80%). A one-pot reaction was performed, starting from benzaldehyde and aniline without isolating the imine, then adding **1a** and TFA, and furnishing **3a** in lower yields [50% (see the Experimental Section)].

Key mechanistic data were collected during the optimization of reaction conditions (Scheme 4, top). The reaction did not proceed in the dark. Higher yields were obtained from electron-deficient imines. The presence of Brønsted/Lewis acids gave faster reactions and higher yields. These observations rule out a free carbamoyl anion mechanism.[15] Upon addition of 1 equiv. of the radical scavenger TEMPO (2,2,6,6-tetramethylpiperidine-*N*-oxyl), the reaction was completely inhibited and the carbamoyl-TEMPO adduct was detected. The visible light-mediated reaction with the organic catalyst 3DPAFIPN (= PC) may operate via two distinct photoredox mechanisms that both involve the intermediacy of a carbamoyl radical species. The first (Scheme 4, A) proceeds through reductive photocatalyst quenching by the Hantzsch ester (**I**) followed by aromatization-driven fragmentation to give carbamoyl radical **II**.[16] Addition of this nucleophilic radical to the imine (or better the more electrophilic iminium ion) and a successive SET reduction of the presumably formed amino amide radical cation **III**$^{\bullet+}$ furnish the desired α-amino amide **III**. Another scenario (Scheme 4, B) may involve initial oxidative PC quenching by the imine/iminium (**IV**) to give nucleophilic α-amino radical **V**.[17] Product formation results from radical−radical coupling with **II**, which was generated by SET oxidation of **I** with the radical cation PC$^{\bullet+}$. Both mechanistic scenarios align well with the redox potentials of the photocatalyst.[11,17c] Stern−Volmer studies of the quenching events of the excited state PC* with the imine and the Hantzsch ester amide (in the absence of acid additives) documented that both SET events are rapid and on the same order of magnitude: $k_q = 1.27 \times 10^{10}$ M^{-1} s^{-1} for **2a**, and $k_q = 9.22 \times 10^{10}$ M^{-1} s^{-1} (**1a**).[9b] It is likely that the oxidative PC quenching by the imine may experience a dramatic acceleration by acid additives (A^+, Scheme 4, bottom), so that mechanism B may become dominant under such conditions. The quantum yield Φ of the reaction was found to be 0.86%, which may exclude mechanistic scenarios based on radical chain propagations.

The presence of Brønsted/Lewis acid additives in the photocarbamoylation of imines could be potentially exploited for stereoselective reactions.[18] We envisioned three possible approaches: (i) the use of chiral *N*-alkyl imines (not explored due the incompatibility of the reaction with *N*-alkyl substituents),[19] (ii) the use of chiral acids (Brønsted or Lewis), and (iii) the use of chiral Hantzsch ester amides. Chiral Lewis acids [(+)-(Ipc)BCl_2 and $Sc(OTf)_3$/$Yb(OTf)_3$ with BOX/PyBOX ligands (see the Experimental Section)] afforded low to moderate yields of essentially racemic product mixtures. Low stereocontrol (~10% *ee*) was obtained from a chiral BINOL-derived phosphoric acid (see the Experimental Section). Diastereoselective reactions were attempted with chiral Hantzsch ester amides. A tethered Evans auxiliary did not undergo photoredox fragmentation. The L-valine and (*S*)-2-benzylpyrrolidine derivatives gave low levels of stereoinduction [**3g**, *dr* 57:43; **3h**, *dr* 50:50 (Scheme 3)].



Scheme 4. *Mechanistic Proposal.*

Conclusion

In conclusion, we have developed a photoredox-catalyzed C−C bond-forming amino acid synthesis that utilizes easily available Hantzsch ester derivatives and imines. The protocol proceeds with the organic photocatalyst 3DPAFIPN under blue light irradiation at room temperature. Combined mechanistic studies support the notion of a photoredox mechanism via intermediate carbamoyl radicals.

Literature References

1. a) Greenberg, G. The Amide Linkage: Selected Structural Aspects in Chemistry, Biochemistry, and Materials Science (Wiley-Interscience, **2000**); b) Soloshonok, V. A.; Izawa, K. Asymmetric Synthesis and Application of α-Amino Acids (Oxford University Press: Washington, DC, **2009**); c) Blaskovich, M. A. Handbook on Syntheses of Amino Acids: General Routes for the Syntheses of Amino Acids (Oxford University Press: Oxford; New York, **2010**).

2. a) Krauch, H.; Kunz, H., Reaktionen der Organischen Chemie, 6. Aufl.; Hüthig: Heidelberg, **1997**, 22–23; b) Rogers, S. A.; Bero, J. D.; Melander, C. Chemical Synthesis and Biological Screening of 2-Aminoimidazole-Based Bacterial and Fungal Antibiofilm Agents. *Chem. Bio. Chem*. **2010**, *11*, 396–410; c) Smith, A. M. R.; Hii, K. K. Transition Metal Catalyzed Enantioselective α-Heterofunctionalization of Carbonyl Compounds. *Chem. Rev.* **2011**, *111*, 1637–1656; d) Tona, V.; de la Torre, A.; Padmanaban, M.; Ruider, S.; González, L.; Maulide, N. Chemo- and Stereoselective Transition-Metal-Free Amination of Amides with Azides. *J. Am. Chem. Soc.* **2016**, *138*, 8348−8351.

3. a) Pattabiraman, V. R.; Bode, J. W. Rethinking Amide Bond Synthesis. *Nature* **2011**, *480*, 471–479; b) Marcia de Figueiredo, R.; Suppo, J.-S.; Campagne, J.-M. Nonclassical Routes for Amide Bond Formation. *Chem. Rev.* **2016**, *116*, 12029–12122; c) Wang, J.; Liu, X.; Feng, X. Asymmetric Strecker Reactions. *Chem. Rev.* **2011**, *111* (11), 6947–6983.

4. a) Ngouansavanh, T.; Zhu, J. P. IBX-Mediated Oxidative Ugi-Type Multicomponent Reactions: Application to the N and C1 functionalization of Tetrahydroisoquinoline. *Angew. Chem. Int. Ed*. **2007**, *46*, 5775–5778; b) Jiang, G. X.; Chen, J.; Huang, J. S.; Che, C. M. Highly Efficient Oxidation of Amines to Imines by Singlet Oxygen and Its Application in Ugi-Type Reactions. *Org. Lett.* **2009**, *11*, 4568–4571; c) Ye, X.; Xie, C.; Pan, Y.; Han, L.; Xie, T. Copper-Catalyzed Synthesis of α-Amino Imides from Tertiary Amines: Ugi-Type Three-Component Assemblies Involving Direct Functionalization of sp3 C−Hs Adjacent to Nitrogen Atoms. *Org. Lett.* **2010**, *12*, 4240–4243; d) Ye, X.; Xie, C.; Huang, R.; Liu, J. Direct Synthesis of α-Amino Amides from N-Alkyl Amines by the Copper-Catalyzed Oxidative Ugi-Type Reaction. *Synlett* **2012**, *23*, 409–412.

5. Lin, Y.-Z.; Alper, H. A Novel Approach for the One-Pot Preparation of α-Amino Amides by Pd-Catalyzed Double Carbohydroamination. *Angew. Chem. Int. Ed.* **2001**, *40*, 779–781.

6. J. T. Reeves, Z. Tan, M. A. Herbage, Z. S. Han, M. A. Marsini, Z. Li, G. Li, Y. Xu, K. R. Fandrick, N. C. Gonnella, S. Campbell, S. Ma, N. Grinberg, H. Lee, B. Z. Lu, C. H. Senanayake. Carbamoyl Anion Addition to N-Sulfinyl Imines: Highly Diastereoselective Synthesis of α-Amino Amides. *J. Am. Chem. Soc.* **2013**, *135*, 5565–5568.

7. a) Chen, J.; Cunico, R. F. α-Amino Amides from a Carbamoylsilane and Aldehyde Imines. *Tetrahedron Lett.* **2003**, *44*, 8025–8027; b) Chen, J.; Pandey, R. K.; Cunico, R.F. Diastereoselective formation of α-Amino Amides from Carbamoylsilanes and Aldehyde Imines. *Tetrahedron Asymm.* **2005**, *16*, 941–947; c) Cunico, R. F.; Pandey, R.K.; Chen, J.; Motta, A. R. Copper(II) Trifluoromethanesulfonate Catalyzed Addition of a Carbamoylsilane to Aldehyde Imines. *Synlett* **2005**, 3157–3159; d) Pastori, N.; Greco, C.; Clerici, A.; Punta, C.; Porta, O. Free-Radical Addition to Ketimines Generated In Situ. New One-Pot Synthesis of Quaternary α-Aminoamides Promoted by a H_2O_2/$TiCl_4$−Zn/$HCONH_2$ System. *Org. Lett.* **2010**, *12*, 17, 3898–3901.

8. Photoredox-catalyzed carboxamide syntheses have also been realized by an Umpolung approach with imines and isocyanates: a) Rueping, M.; Vila, C. Visible Light Photoredox-Catalyzed Multicomponent Reactions. *Org. Lett.* **2013**, *15*, 2092–2095; b) Zhu, J.; Dai, C.; Ma, M.; Yue, Y.; Fan, X. Visible Light-Mediated Cross-Coupling of Electrophiles: Synthesis of α-Amino Amides from Isocyanates and Ketimines. *Org. Chem. Front*. **2021**, *8*, 1227–1232.

9. a) Alandini, N.; Buzzetti, L.; Favi, G.; Schulte, T.; Candish, L.; Collins, K. D.; Melchiorre P. Amide Synthesis by Nickel/Photoredox-Catalyzed Direct Carbamoylation of (Hetero)Aryl Bromides. *Angew. Chem. Int. Ed*. **2020**, *59*, 5248–5253; b) Cardinale, L.; Konev, M. O.; Jacobi von Wangelin, A. Photoredox-Catalyzed Addition of Carbamoyl Radicals to Olefins: A 1,4-Dihydropyridine Approach. *Chem. Eur. J.* **2020**, *26*, 8239–8243; c) Kim, I.; Park, S.; Hong, S. Functionalization of Pyridinium Derivatives with 1,4- Dihydropyridines Enabled by Photoinduced Charge Transfer. *Org. Lett.* **2020**, *22*, 8730–8734.

10. a) Parallel to this work, another manuscript reported a complementary substrate scope of imine carbamoylation: Matsuo, B. T.; Oliveira, P. H. R.; Correira, J. T. M.; Paixão, M. W. Carbamoylation of Azomethine Imines via Visible-Light Photoredox Catalysis. *Org. Lett.* **2021**, DOI: 10.1021/acs.orglett.1c02353; b) two carboxamides were prepared by a photo-acylation in: Zhang, H.-H.; Yu, S. Visible-Light-Induced Radical Acylation of Imines with α-Ketoacids Enabled by Electron-Donor–Acceptor Complexes. *Org. Lett*. **2019**, *21*, 10, 3711–3715; c) a single entry of carboxamide synthesis was reported in: Liu, D.; Mao, J.; Rong, G.; Yan, H.; Zheng, Y.; Chen, J. Concise Synthesis of Semicarbazides and Formylhydrazines via Direct Addition Reaction between Aromatic Azoarenes and N-substituted Formamides. *RSC Adv.* **2015**, *5*, 19301-19305.

11. Speckmeier, E.; Fischer, T. G.; Zeitler, K. A Toolbox Approach to Construct Broadly Applicable Metal-Free Catalysts for Photoredox Chemistry: Deliberate Tuning of Redox Potentials and Importance of Halogens in Donor–Acceptor Cyanoarenes. *J. Am. Chem. Soc*. **2018**, *140*, 15353–15365.

12. a) Leitch, J. A.; Rossolini, T.; Rogova, T.; Maitland, J. A. P.; Dixon, D. J. α-Amino Radicals via Photocatalytic Single-Electron Reduction of Imine Derivatives. *ACS Catal.* **2020**, *10*, 2009−2025; b) Garrido-Castro, A. F.; Maestro, M. C.; Alemán, J. α-Functionalization of Imines via Visible Light Photoredox Catalysis. *Catalysts* **2020**, *10*, 562.

13. a) Rong, J.; Seeberger, P. H.; Gilmore, K. Chemoselective Photoredox Synthesis of Unprotected Primary Amines Using Ammonia. *Org. Lett.* **2018**, *20*, 4081−4085; b) Gentry, E. C.; Knowles, R. R. Synthetic Applications of Proton-Coupled Electron Transfer. *Acc. Chem. Res*. **2016**, *49*, 1546−1556.

14. Kim, H.; Lee, C. Visible-Light-Induced Photocatalytic Reductive Transformations of Organohalides. *Angew. Chem. Int. Ed.* **2012**, *51*, 12303–12306.

15. Li, G.; Chen, R.; Wu, L.; Fu, Q.; Zhang, X.; Tang, Z. Alkyl Transfer from C−C Cleavage. *Angew. Chem. Int. Ed.* **2013**, *52*, 8432–8436.

16. Li, Z.; Yang, J.-D.; Cheng, J.-P. Thermodynamic and Kinetic Studies of Hydride Transfer from Hantzsch Ester under the Promotion of Organic Bases. *Org. Chem. Front*. **2021**, *8*, 876–882.

17. a) Studer, A. The Persistent Radical Effect in Organic Synthesis. *Chem. Eur. J.* **2001**, *7*, 1159−1164; b) Fischer, H. The Persistent Radical Effect: A Principle for Selective Radical Reactions and Living Radical Polymerizations. *Chem. Rev.* **2001**, *101*, 3581−3610; c) Patel, N. R.; Kelly, C. B.; Siegenfeld, A. P.; Molander, G. A. Mild, Redox-Neutral Alkylation of Imines Enabled by an Organic Photocatalyst. *ACS Catal.* **2017**, *7*, 1766−1770.

18. For enantioselective synthesis of α-amino amides see: a) Hacking, M. A. P. J.; Wegman, M. A.; Rops, J.; van Rantwijk, F.; Sheldon, R. A. Enantioselective Synthesis of Amino Acid Amides via Enzymatic Ammonolysis of Amino Acid Esters. *J. Mol. Catal. B Enzym.* **1998**, *5*, 155−157; b) Nanayakkara, P.; Alper, H. Asymmetric Synthesis of α-Amino Amides by Pd-Catalyzed Double Carbohydroamination. *Chem. Commun*. **2003**, 2384−2385; c) Wang, J.; Liu, X.; Feng, X. Asymmetric Strecker Reactions. *Chem. Rev.* **2011**, *111*, 6947; d) Schwieter, K. E.; Johnston, J. N. Enantioselective Synthesis of D-α-Amino Amides from Aliphatic Aldehydes. *Chem. Sci.* **2015**, *6*, 2590−2595.

19. a) Shatskiy, A.; Axelsson, A.; Stepanova, E. V.; Liu, J.-Q.; Temerdashev, A. Z.; Kore, B. P.; Blomkvist, B.; Gardner, J. M.; Dinér, P.; Kärkäs, M. D. Stereoselective Synthesis of Unnatural α-Amino Acid Derivatives through Photoredox Catalysis. *Chem. Sci.* **2021**, *12*, 5430–5437; b) Morton, D.; Stockman, R. A. Chiral non-racemic sulfinimines: versatile reagents for asymmetric synthesis. *Tetrahedron* **2006**, *62*, 8869–8905; c) Robak, M. T.; Herbage, M. A.; Ellman, J. A. Synthesis and Applications of *tert*-Butanesulfinamide, *Chem. Rev.* **2010**, *110*, 3600−3740.

Experimental Section

General Information

Chemicals and solvents: All reagents (≥95% purity) and solvents (≥99% purity) were purchased from commercial suppliers (Acros, Alfa Aesar, Fisher, Fluka, Grüssing, Merck, Sigma-Aldrich, TCI, Th. Geyer) and used as received unless otherwise indicated.

Reaction setup: All reactions were carried out in LABSOLUTE 4 mL Screw Neck Vials, 45 x 14.7 mm, clear glass, 1st hydrolytic class unless otherwise stated. Irradiation was performed in an air-cooled EvoluChem™ PhotoRedOx Box fitted with a blue (450 nm) EvoluChem™ 450DX LED (55 mW/cm^2).

Nuclear magnetic resonance (NMR) spectroscopy: ^{1}H-NMR, ^{13}C-NMR and ^{19}F-NMR were used for purity and structure determination of products. NMR spectral data were collected on a Bruker Avance 300 (300 MHz for ^{1}H, 75 MHz for ^{13}C, 282 MHz for ^{19}F) spectrometer, a Bruker Avance 400 (400 MHz for ^{1}H, 100 MHz for ^{13}C) spectrometer or a Bruker Avance III 600 (600 MHz for ^{1}H, 565 MHz for ^{19}F) spectrometer at 20 °C. Chemical shifts are reported in δ/ppm, coupling constants *J* are given in Hertz. Solvent residual peaks were used as internal standard for all NMR measurements. The quantification of ^{1}H nuclei was performed by integration of appropriate resonance signals. Abbreviations used in NMR spectra: s – singlet, d – doublet, t – triplet, q – quartet, pent – pentet, sept – septet, m – multiplet, br. s – broad singlet.

High-resolution mass spectrometry (HRMS): HRMS was carried out by the Central Analytics at the department of chemistry, Universität Hamburg. Abbreviations used in MS spectra: *m/z* – mass-to-charge ratio, ESI – electrospray ionization.

Thin-layer chromatography (TLC) and column chromatography: TLC was performed on commercial SiO_2-coated aluminum plates (DC60 F254, Merck). The spots were visualized by UV light (365 nm and/or 254 nm) or alkaline potassium permanganate solution. Column chromatography was performed using SiO_2 (Acros Organics, 35-70 mesh, 60 Å pore size).

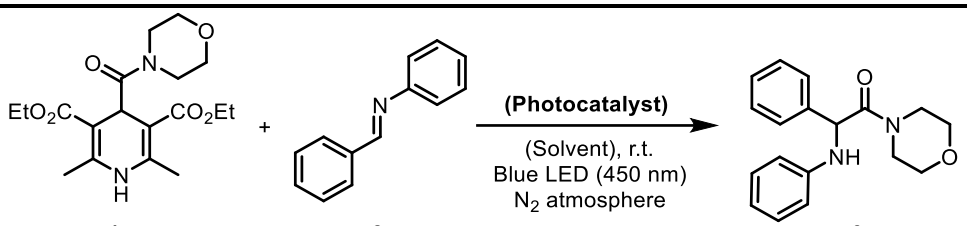
UV-Vis absorption spectroscopy: UV-Vis absorption spectroscopy was performed at room temperature on an Agilent Cary 5000 UV-Vis-NIR double beam spectrometer with a 10 mm quartz cuvette.

Fluorescence spectroscopy: The fluorescence spectra were recorded at room temperature using an Agilent Cary Eclipse Fluorescence Spectrophotometer in quartz cuvettes fitted with a rubber septum. The excitation slit was opened to 5 nm and the emission slit to 10 nm.

Polarimetry: Specific rotations were obtained using an A.KRÜSS Optronic P8000 at 20 °C using the sodium D-line (589.3 nm) and a cuvette with a length of 1 dm. Concentrations *c* are given in g/100 mL.

Analytical chiral HPLC: The ratio of enantiomers in chiral experiments was determined *via* HPLC using a CHIRALPAK® IB (250 x 4.6 mm, 5 µm) column after isolation of the mixture of enantiomers using column chromatography as indicated.

Optimization Studies



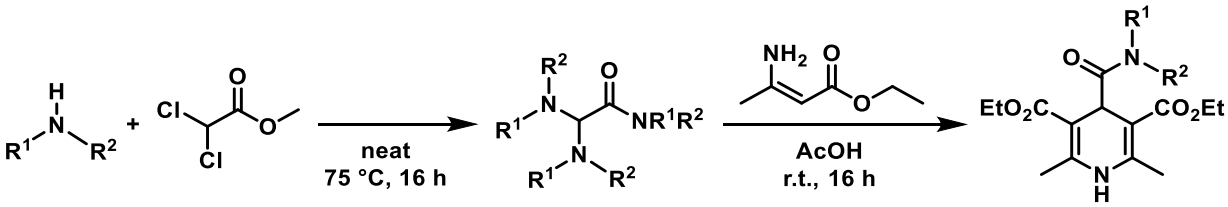
1a 1.3 eq. | **2a** 1.0 eq. | **3a**

Solvent (M)	Photocatalyst (mol%)	Additives (equiv.)	Yield of **3a**[a] [%]
CH_2Cl_2 (0.2)	3DPAFIPN (2.5)	–	10
DMA (0.2)	3DPAFIPN (2.5)	–	22
Acetone (0.2)	3DPAFIPN (2.5)	–	26
CH_2Cl_2 (0.2)	3DPA2FBN (2.5)	–	10
CH_2Cl_2 (0.2)	4CzIPN (2.5)	–	31
CH_2Cl_2 (0.1)	3DPAFIPN (2.5)	TFA (2)	71
CH_2Cl_2 (0.2)	3DPAFIPN (2.5)	TFA (2)	77
CH_2Cl_2 (0.2)	3DPAFIPN (2.5)	TFA (10)	96
CH_2Cl_2 (0.1)	3DPAFIPN (2.5)	TFA (1)	77
CH_2Cl_2 (0.1)	3DPAFIPN (2.5)	TFA (1)	59[b]
CH_2Cl_2 (0.1)	3DPAFIPN (2.5)	$MgCl_2$ (1)	26
CH_2Cl_2 (0.1)	3DPAFIPN (2.5)	$Sc(OTf)_3$ (1)	51
CH_2Cl_2 (0.1)	3DPAFIPN (2.5)	PhCOOH (1)	24
CH_2Cl_2 (0.1)	3DPAFIPN (2.5)	$ZnCl_2$ (0.2)	46
CH_2Cl_2 (0.5)	3DPAFIPN (2.5)	TFA (1)	60
Toluene (0.1)	3DPAFIPN (2.5)	TFA (1)	61
CH_2Cl_2 (0.2)	–	TFA (1)	13[c]
CH_2Cl_2 **(0.1)**	**3DPAFIPN (2.5)**	**$BF_3{\cdot}OEt_2$ (1)**	**85**
CH_2Cl_2 (0.1)	3DPAFIPN (2.5)	$BF_3{\cdot}OEt_2$ (0.2)	54
CH_2Cl_2 (0.1)	3DPAFIPN (2.5)	$BF_3{\cdot}OEt_2$ (1.5)	81
CH_2Cl_2 (0.2)	4CzIPN (2.5)	TFA (1)	36
CH_2Cl_2 (0.2)	3DPA2FBN (2.5)	TFA (1)	42
MeCN/MeOH 4:1 (0.2)	3DPAFIPN (2.5)	TFA (1)	14
CH_2Cl_2 (0.2)	3DPAFIPN (2.5)	TFA (1)	*n. r.*[d]
CH_2Cl_2 (0.1)	3DPAFIPN (2.5)	$BF_3{\cdot}OEt_2$ (1)	*n. r.*[d]

[a] ^{1}H-NMR yield using 1,3,5-trimethoxybenzene as an external standard. [b] Under non-inert conditions. [c] Direct photoexcitation of **1a** at 365 nm. [d] No light irradiation. *n. r.*: no reaction.

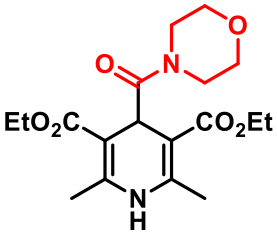
Synthesis and characterization of all compounds

General Procedure 1.A: Synthesis of 4-Amido-1,4-Dihydropyridines



Methyl dichloroacetate (1.0 equiv.) and the corresponding amine (5.0 equiv.) were mixed and heated to 75 °C overnight, during which the mixture crystallized to form an orange, waxy solid. The solid was broken up using a glass rod and dissolved in glacial acetic acid (0.5 M with regard to methyl dichloroacetate). Ethyl 3-aminocrotonate (2.0 equiv.) was added and the mixture was stirred at room temperature overnight. The resultant suspension was diluted with water and the precipitate was removed by filtration, washed with water and dried *in vacuo* to yield the Hantzsch esters **1a**–**1b.**

Diethyl 2,6-dimethyl-4-(morpholine-4-carbonyl)-1,4-dihydropyridine-3,5-dicarboxylate (1a)

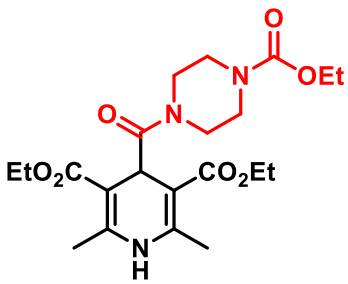


Starting from methyl dichloroacetate (718 mg, 520 µL, 5.00 mmol), morpholine (2.18 g, 219 µL, 25.0 mmol), ethyl 3-aminocrotonate (1.29 g, 1.26 mL, 10.0 mmol), and following the general procedure 1.A, **1a** was obtained as a light beige powder (831 mg, 45 %).

^{1}H-NMR (600 MHz, $CDCl_3$): δ [ppm] = 7.35 (s, 1H), 5.01 (s, 1H), 4.20 (dq, J = 10.9, 7.1 Hz, 2H), 4.14 (dq, J = 10.9, 7.1 Hz, 2H), 3.93 (t, J = 4.8 Hz, 2H), 3.75 (t, J = 4.7 Hz, 2H), 3.65 (t, J = 4.8 Hz, 2H), 3.60 (t, J = 4.7 Hz, 2H), 2.24 (s, 6H), 1.28 (*pseudo*-t, J = 7.1 Hz, 6H).

L. Cardinale, M. O. Konev, A. Jacobi von Wangelin, *Chem. Eur. J.* **2020**, *26*, 8239–8243.

Diethyl 4-(4-(ethoxycarbonyl)piperazine-1-carbonyl)-2,6-dimethyl-1,4-dihydro-pyridine-3,5-dicarboxylate (1b)



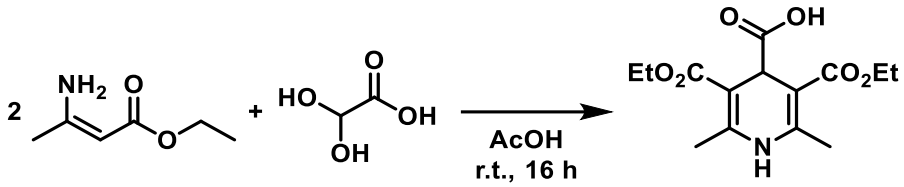
Starting from methyl dichloroacetate (0.72 g, 0.52 mL, 5.0 mmol), ethyl 1-piperazinecarboxylate (4.0 g, 3.7 mL, 25 mmol), ethyl 3-aminocrotonate (1.3 g, 1.3 mL, 10 mmol) and following the general procedure 1.A, **1b** was obtained as a pale-yellow powder (710 mg, 32 %).

^{1}H-NMR (300 MHz, $CDCl_3$): δ [ppm] = 7.66 (br. s, 1H), 5.03 (s, 1H), 4.25 – 4.06 (m, 6H), 3.95 – 3.86 (m, 2H), 3.64 – 3.53 (m, 4H), 3.49 – 3.39 (m, 2H), 2.21 (s, 6H), 1.26 (*pseudo*-t, J = 7.1, 1.0 Hz, 9H).

L. Cardinale, M. O. Konev, A. Jacobi von Wangelin, *Chem. Eur. J.* **2020**, *26*, 8239–8243.

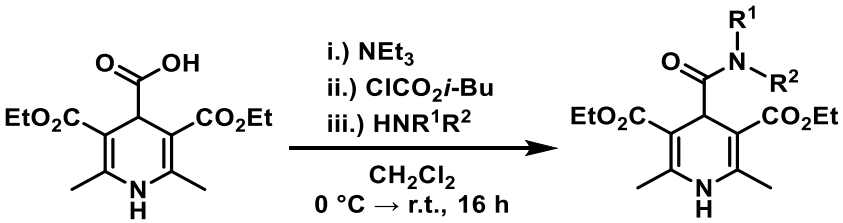
General Procedure 1.B: Synthesis of 4-Amido-1,4-dihydropyridines

*Synthesis of **I** (HE-COOH):*



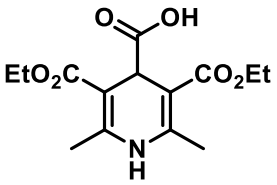
Ethyl 3-aminocrotonate (14.9 g, 115 mmol, 2.3 equiv.) was dissolved in glacial acetic acid (5 mL) and the solution was cooled to 0 °C. A solution of glyoxylic acid monohydrate (4.6 g, 50 mmol, 1.0 equiv.) in glacial acetic acid (30 mL)[a] was added dropwise, leading to a yellow suspension. The mixture was warmed to room temperature and stirred overnight. The resultant suspension was diluted with water and the precipitate was removed by filtration and washed with acetic acid. The solid was dried *in vacuo* to yield the Hantzsch ester carboxylic acid **I** (HE-COOH) as a colorless to pale-yellow powder (2.99 g, 10 mmol, 20 %).

*Synthesis of **1a**–**1g**:*



The Hantzsch ester carboxylic acid **I** was suspended in CH_2Cl_2 (0.20 M) and triethylamine (1.2–2.0 equiv.) was added dropwise, leading to dissolution of **I**. The solution was cooled to 0 °C and isobutyl chloroformate (1.2 equiv.) was added dropwise. After 10 minutes of stirring at 0 °C, the mixture was warmed to room temperature and stirred for additional 20 minutes. Subsequently, the amine (1.2–3.0 equiv.) was added and the mixture was stirred for 1 hour (primary amines) or overnight (secondary amines). The mixture was concentrated *in vacuo* and the residue purified by silica column chromatography (pentane/acetone or pentane/ethyl acetate) to yield the Hantzsch esters **1c**–**1g**.

3,5-Bis(ethoxycarbonyl)-2,6-dimethyl-1,4-dihydropyridine-4-carboxylic acid (I)



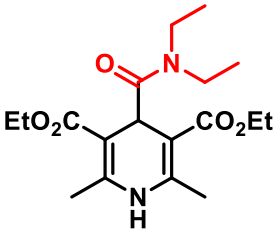
Colorless to pale-yellow powder.

^{1}H-NMR (300 MHz, DMSO-d_6): δ [ppm] = 11.81 (s, 1H), 8.84 (s, 1H), 4.58 (s, 1H), 4.16 – 4.00 (m, 4H), 2.22 (s, 6H), 1.19 (t, J = 7.1, 6H).

L. Cardinale, M. O. Konev, A. Jacobi von Wangelin, *Chem. Eur. J.* **2020**, *26*, 8239–8243.

[a] Dissolution of the glyoxylic acid monohydrate in the glacial acetic acid may take as long as 10–20 minutes and may require manual breaking of the crystal chunks into smaller pieces.

Diethyl (4-diethylcarbamoyl)-2,6-dimethyl-1,4-dihydropyridine-3,5-dicarboxylate (1c)

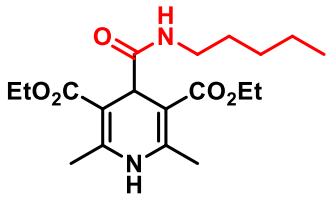


Starting from HE-COOH **I** (500 mg, 1.68 mmol), triethylamine (203 mg, 280 µL, 2.01 mmol, 1.2 equiv.), diethylamine (247 mg, 350 µL, 3.38 mmol, 2.0 equiv.), isobutyl chloroformate (274 mg, 260 µL, 2.00 mmol, 1.2 equiv.) and following the general procedure 1.B, **1d** was obtained as a pale-yellow powder (100 mg, 14 %).

^{1}H-NMR (300 MHz, $CDCl_3$): δ [ppm] = 8.44 (br. s, 1H), 5.08 (s, 1H), 4.17 (qq, *J* = 10.9, 7.1 Hz, 4H), 3.77 (q, *J* = 7.1 Hz, 2H), 3.34 (q, *J* = 7.0 Hz, 2H), 2.20 (s, 6H), 1.27 (t, *J* = 7.1 Hz, 8H), 1.03 (t, *J* = 7.0 Hz, 3H).

N. Alandini, L. Buzzetti, G. Favi, T. Schulte, L. Candish, K. D. Collins, P. Melchiorre, *Angew. Chem. Int. Ed.* **2020**, *59*, 5248 –5253, *Angew. Chem.* **2020**, *132*, 5286–5291.

Diethyl 2,6-dimethyl-4-(pentylcarbamoyl)-1,4-dihydropyridine-3,5-dicarboxylate (1d)



Starting from HE-COOH **I** (297 mg, 1.0 mmol), triethylamine (123 mg, 170 µL, 1.22 mmol, 1.2 equiv.), pentylamine (174 mg, 230 µL, 2.00 mmol, 2.0 equiv.), isobutyl chloroformate (158 mg, 150 µL, 1.16 mmol, 1.2 equiv.) and following the general procedure 1.B, **1d** was obtained as a pale-yellow powder (140 mg, 0.382 mmol, 38 %). Instead of column chromatography, **1d** was purified by recrystallization from diethyl ether (hot filtration required).

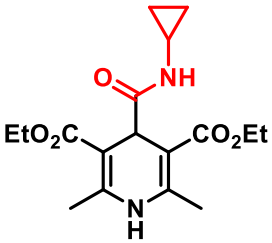
m.p. = 146–148 °C

^{1}H-NMR (500 MHz, $CDCl_3$): δ [ppm] = 7.89 (s, 1H), 6.67 (t, *J* = 5.8 Hz, 1H), 4.55 (s, 1H), 4.18 (q, *J* = 7.1 Hz, 4H), 3.18 (td, *J* = 6.9, 5.7 Hz, 2H), 2.21 (s, 6H), 1.61 (s, 2H), 1.46 (pent, *J* = 7.1 Hz, 2H), 1.28 (t, *J* = 7.1 Hz, 8H), 0.88 (t, *J* = 7.0 Hz, 3H).

^{13}C-{^{1}H}-NMR (75 MHz, $CDCl_3$): δ [ppm] = 174.9, 168.2, 147.7, 97.9, 60.2, 41.8, 39.6, 29.4, 29.1, 22.5, 19.0, 14.5, 14.1.

HRMS (ESI): *m/z* = calcd. for $C_{19}H_{31}N_2O_5^+$: 367.2227, found: 367.2220.

Diethyl (4-cyclopropylcarbamoyl)-2,6-dimethyl-1,4-dihydropyridine-3,5-dicarboxylate (1e)

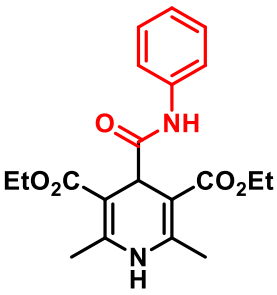


Starting from HE-COOH **I** (446 mg, 1.50 mmol), triethylamine (182 mg, 250 µL, 1.84 mmol, 1.2 equiv.), cyclopropylamine (107 mg, 130 µL, 1.87 mmol, 1.2 equiv.), isobutyl chloroformate (242 mg, 230 µL, 1.77 mmol, 1.2 equiv.) and following the general procedure 1.B, **1e** was obtained as a pale-yellow powder (272 mg, 0.809 mmol, 54 %).

^{1}H-NMR (300 MHz, $CDCl_3$): δ [ppm] = 8.05 (s, 1H), 6.82 (d, *J* = 3.3 Hz, 1H), 4.49 (s, 1H), 4.17 (qd, *J* = 7.2, 0.9 Hz, 4H), 2.67 (tq, *J* = 7.4, 3.7 Hz, 1H), 2.21 (s, 6H), 1.27 (t, *J* = 7.1 Hz, 6H), 0.76–0.68 (m, 2H), 0.47 – 0.39 (m, 2H).

L. Cardinale, M. O. Konev, A. Jacobi von Wangelin, *Chem. Eur. J.* **2020**, *26*, 8239–8243.

Diethyl 2,6-dimethyl-4-(phenylcarbamoyl)-1,4-dihydropyridine-3,5-dicarboxylate (1f)

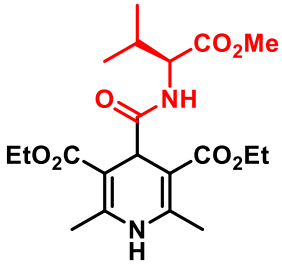


Starting from HE-COOH **I** (1.02 g, 3.43 mmol), triethylamine (682 mg, 940 µL, 6.78 mmol, 2.0 equiv.), aniline (949 mg, 930 µL, 5.04 mmol, 1.5 equiv.), isobutyl chloroformate (558 mg, 530 µL, 4.09 mmol, 1.2 equiv.) and following the general procedure 1.B, **1f** was obtained as a pale-yellow powder (760 mg, 2.04 mmol, 58 %).

^{1}H-NMR (300 MHz, $CDCl_3$): δ [ppm] = 8.81 (s, 1H), 7.61 – 7.50 (m, 2H), 7.35 – 7.24 (m, 2H), 7.11 – 7.00 (m, 1H), 4.72 (s, 1H), 4.21 (q, *J* = 7.1 Hz, 4H), 2.27 (s, 4H), 1.58 – 1.56 (m, 1H), 1.28 (t, *J* = 7.1 Hz, 6H).

N. Alandini, L. Buzzetti, G. Favi, T. Schulte, L. Candish, K. D. Collins, P. Melchiorre, *Angew. Chem. Int. Ed.* **2020**, *59*, 5248 –5253, *Angew. Chem.* **2020**, *132*, 5286–5291.

Diethyl 2,6-dimethyl-4-((*S*)-valine-*N*-carbonyl)-1,4-dihydropyridine-3,5-dicarboxylate (1g)

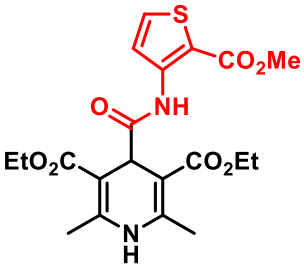


Starting from HE-COOH **I** (297 mg, 1.00 mmol), triethylamine (203 mg, 280 µL, 2.00 mmol, 2.0 equiv.), (*S*)-valine methyl ester hydrochloride (201 mg, 1.20 mmol, 1.2 equiv.), isobutyl chloroformate (158 mg, 150 µL, 1.16 mmol, 1.2 equiv.) and following the general procedure 1.B, **1g** was obtained as yellow solid (290 mg, 0.707 mmol, 71 %).

^{1}H-NMR (300 MHz, $CDCl_3$): δ [ppm] = 8.10 (br. s, 1H), 7.12 (d, *J* = 9.0 Hz, 1H), 4.67 (br. s, 1H), 4.44 – 4.39 (m, 1H), 4.18 – 4.13 (m, 4H), 3.67 (s, 3H), 2.17 (s, 3H), 2.10 (s, 3H), 1.29 – 1.23 (m, 6H), 0.91 – 0.88 (m, 6H).

N. Alandini, L. Buzzetti, G. Favi, T. Schulte, L. Candish, K. D. Collins, P. Melchiorre, *Angew. Chem. Int. Ed.* **2020**, *59*, 5248 –5253, *Angew. Chem.* **2020**, *132*, 5286–5291.

Diethyl 4-((2-(methoxycarbonyl)thiophen-3-yl)carbamoyl)-2,6-dimethyl-1,4-dihydropyridine-3,5-dicarboxylate (1h)



Starting from HE-COOH **I** (446 mg, 1.50 mmol), triethylamine (182 mg, 250 µL, 1.84 mmol, 1.2 equiv.), methyl 3-aminothiophene-2-carboxylate (283 mg, 1.80 mmol, 1.2 equiv.), isobutyl chloro-formate (242 mg, 230 µL, 1.77 mmol, 1.2 equiv.) and following the general procedure 1.B, **1h** was obtained as small, pale-yellow needles (424 mg, 0.971 mmol, 65 %).

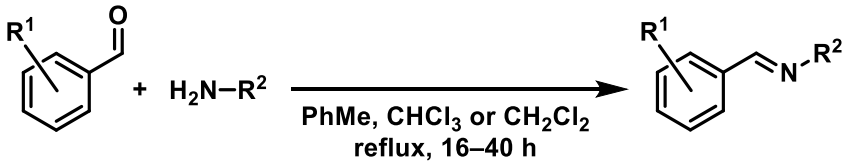
m.p. = 189–191 °C

^{1}H-NMR (300 MHz, $CDCl_3$): δ [ppm] = 10.53 (s, 1H, CONH), 8.12 (d, *J* = 5.4 Hz, 1H), 7.42 (d, *J* = 5.5 Hz, 1H), 7.14 (br. s, 1H, NH), 4.82 (s, 1H), 4.29 – 4.10 (m, 4H), 3.90 (s, 3H), 2.29 (s, 6H), 1.24 (t, *J* = 7.1 Hz, 6H).

^{13}C-{^{1}H}-NMR (75 MHz, $CDCl_3$): δ [ppm] = 172.8, 167.2, 164.1, 147.2, 144.5, 131.3, 122.7, 111.2, 98.5, 60.3, 52.0, 43.5, 19.4, 14.4.

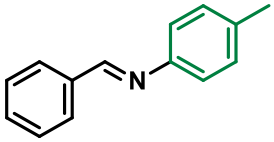
HRMS (ESI): *m/z* = calcd. for $C_{20}H_{24}N_2NaO_7S^+$: 459.1196, found: 459.1197.

General Procedure 2: Synthesis of Aldimines



In a SOXHLET apparatus with anhydrous calcium chloride in the extraction thimble, the aldehyde (10 mmol, 1.0 equiv.) and the amine (10 mmol, 1.0 equiv.) were refluxed in 50 mL[a] of toluene, chloroform, or dichloromethane for 16–40 hours until complete conversion of the starting material was observed (determined *via* GC-MS). The solvent was removed *in vacuo* and the imines **2b–2k** were obtained. In some cases, further purification was necessary.

Benzylidene(4-methylphenyl)amine (2b)

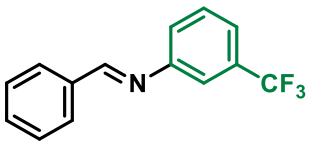


Starting from benzaldehyde (1.06 g, 1.01 mL) and *p*-toluidine (1.07 g), was obtained as a beige solid after 16 hours of reflux in toluene (1.34 g, 69 %).

^{1}H-NMR (300 MHz, $CDCl_3$): δ [ppm] = 8.49 (s, 1H), 7.96 – 7.88 (m, 2H), 7.53 – 7.45 (m, 3H), 7.27 – 7.13 (m, 4H), 2.40 (s, 3H).

X. Hong, H. Wang, B. Liu, B. Xu, *Chem. Comm.* **2014**, *50*, 14129–14132.

Benzylidene(3-(trifluoromethyl)phenyl)amine (2c)



Starting from benzaldehyde (1.06 g, 1.01 mL) and 3-(trifluoro-methyl)aniline (1.61 g, 1.25 mL), the crude product was obtained after 16 hours of reflux in chloroform. Recrystallization from hexane yielded pure **2c** as colorless crystals (1.95 g, 78 %).

m.p. = 66–67 °C

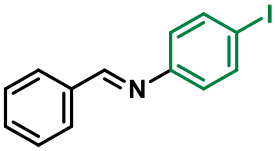
^{1}H-NMR (600 MHz, $CDCl_3$): δ [ppm] = 8.46 (s, 1H), 7.95 – 7.89 (m, 2H), 7.56 – 7.48 (m, 5H), 7.48 – 7.45 (m, 1H), 7.40 – 7.35 (m, 1H)

^{19}F-NMR (565 MHz, $CDCl_3$): δ [ppm] = −62.61.

L. J. Silverberg, C. Pacheco, D. Sahu, P. Scholl, H. F. Sobhi, J. T. Bachert, K. Bandholz, R. V. Bendinsky, H. G. Bradley, B. K. Colburn, D. J. Coyle, J. R. Dahl, M. Felty, R. F. Fox, K. M. Gonzalez, J. M. Islam, S. E. Koperna, Q. J. Moyer, D. J. Noble, M. E. Ramirez, Z. Yang, *J. Heterocyclic Chem.* **2020**, *57*, 1797–1805.

[a] This corresponds to a concentration of 0.2 M, however the volume of solvent was chosen to be 50 mL because the Soxhlet chamber has a volume of 30 mL.

Benzylidene(4-iodophenyl)amine (2d)

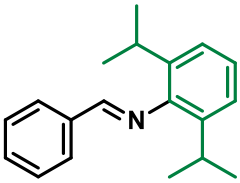


Starting from benzaldehyde (1.06 g, 1.01 mL) and 4-iodoaniline (2.19 g), **2d** was obtained as a grey solid after 16 hours of reflux in toluene (2.90 g, 94 %).

^{1}H-NMR (300 MHz, $CDCl_3$): δ [ppm] = 8.42 (s, 1H), 7.93 – 7.86 (m, 2H), 7.74 – 7.67 (m, 2H), 7.53 – 7.44 (m, 3H), 7.00 – 6.94 (m, 2H).

J. Bhattacharjee, M. Sachdeva, T. K. Panda, *Z. Anorg. Allg. Chem.* **2016**, *17*, 937–940.

Benzylidene(2,6-diisopropylphenyl)amine (2e)

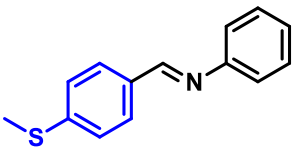


Starting from benzaldehyde (1.06 g, 1.01 mL) and 2,6-diisopropylaniline (1.77 g, 1.88 mL), the crude product was obtained after 40 hours of reflux in toluene. Crystallisation from hexane at –20 °C yielded pure **2e** as yellow crystals (1.32 g, 50 %).

^{1}H-NMR (300 MHz, $CDCl_3$): δ [ppm] = 8.20 (s, 1H), 7.97 – 7.87 (m, 2H), 7.59 – 7.45 (m, 3H), 7.21 – 7.03 (m, 3H), 2.98 (sept, J = 6.8 Hz, 2H), 1.17 (d, J = 6.9 Hz, 12H).

G. Verardo, A. G. Giumanini, P. Strazzolini, M. Poiana, *Synthesis* **1993**, *1*, 121–125.

N-Phenyl-1-(4-methylthio)methanimine (2f)

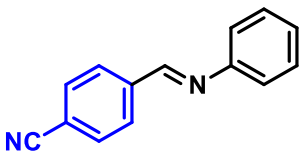


Starting from 4-(methylthio)benzaldehyde (1.52 g, 1.33 mL) and aniline (931 mg, 913 µL), **2f** was obtained as a bright orange solid after 16 hours of reflux in toluene (2.30 g, 100 %).

^{1}H-NMR (300 MHz, $CDCl_3$): δ [ppm] = 8.40 (s, 1H), 7.84 – 7.81 (m, 2H), 7.39 – 7.33 (m, 2H), 7.30-7.26 (m, 2H), 7.23 – 7.20 (m, 3H), 2.54 (s, 3H).

R. D. Chakravarthy, V. Ramkumar, D. K. Chand, *Green Chem*. **2014**, *16*, 2190–2196.

N-Phenyl-1-(4-cyanophenyl)methanimine (2g

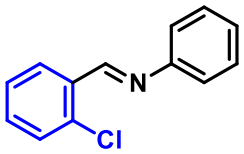


Starting from 4-cyanobenzaldehyde (1.31 g) and aniline (931 mg, 913 µL), the crude product was obtained after 16 hours of reflux in chloroform. Recrystallization from dry methanol yielded pure **2g** as large yellow crystals (1.46 g, 71 %).

^{1}H-NMR (400 MHz, $CDCl_3$): δ [ppm] = 8.50 (s, 1H), 8.05 – 7.98 (m, 2H), 7.80 – 7.73 (m, 2H), 7.47 – 7.38 (m, 2H), 7.32–7.27 (m, 1H), 7.27 – 7.21 (m, 2H).

D. J. Dibble, R. Kurakake, A. G. Wardrip, A. Bartlett, R. Lopez, J. A. Linares, M. Firstman, A. M. Schmidt, M. J. Umerani, A. A. Gorodetsky, *Org. Lett.* **2018**, *20*, 3, 502–505.

N-Phenyl-1-(2-chlorophenyl)methanimine (2h)

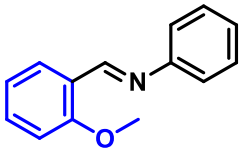


Starting from 2-chlorobenzaldehyde (1.41 g, 1.13 mL) and aniline (931 mg, 913 µL) **2h** was obtained as a pale-brown oil after 16 hours of reflux in toluene (1.90 g, 88 %).

^{1}H-NMR (300 MHz, $CDCl_3$): δ [ppm] = 8.92 (s, 1H), 8.29 – 8.22 (m, 1H), 7.44 – 7.34 (m, 5H), 7.29 – 7.22 (m, 3H).

E. Zhang, H. Tian, S. Xu, X. Yu, Q. Xu, *Org. Lett.* **2013**, *15*, 2704–2707.

N-Phenyl-1-(2-methoxyphenyl)methanimine (2i)

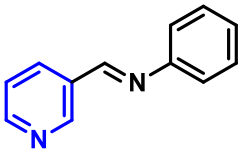


Starting from 2-methoxybenzaldehyde (1.36 g) and aniline (931 mg, 913 µL) **2i** was obtained after 16 hours of reflux in chloroform as a pale-yellow solid (2.10 g, 100 %).

^{1}H-NMR (300 MHz, $CDCl_3$): δ [ppm] = 9.00 (s, 1H), 8.25 – 8.21 (m, 1H), 7.54 – 7.43 (m, 3H), 7.32 – 7.26 (m, 3H), 7.14 – 7.09 (m, 1H), 7.04 – 7.00 (m, 1H), 3.96 (s, 3H).

L. Han, P. Xing, B. Jiang, *Org. Lett.* **2014**, *16*, 3428–3431.

N-Phenyl-1-(3-pyridinyl)methanimine (2j)

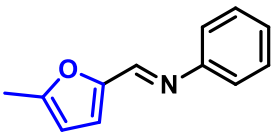


Starting from 3-formylpyridine (1.07 g, 938 µL) and aniline (931 mg, 913 µL), **2j** was obtained as a yellow oil after 16 hours of reflux in chloroform (1.51 g, 83 %).

^{1}H-NMR (300 MHz, $CDCl_3$): δ [ppm] = 8.97 (d, J = 2.1 Hz, 1H), 8.65 (dd, J = 4.8, 1.7 Hz, 1H), 8.42 (s, 1H), 8.22 (dt, J = 7.9, 1.9 Hz, 1H), 7.40 – 7.29 (m, 3H), 7.25 – 7.15 (m, 3H).

R. R. Donthiri, R. D. Patil, S. Adimurty, *Eur. J. Org. Chem.* **2012**, *24*, 4457–4460.

N-Phenyl-1-(5-methylfuran-2-yl)methanimine (2k)



Starting from 5-methylfurfural (1.10 g, 994 µL) and aniline (931 mg, 913 µL), the crude product was obtained as a dark brown oil after 16 hours of reflux in toluene. Vacuum Kugelrohr distillation yielded pure **2k** as a yellow oil (1.33 g, 72 %).

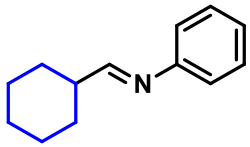
b.p. = 220–225 °C / 9 Torr

^{1}H-NMR (400 MHz, $CDCl_3$): δ [ppm] = 8.18 (s, 1H), 7.39 – 7.35 (m, 2H), 7.24 – 7.19 (m, 3H), 6.39 (d, J = 3.3 Hz, 1H), 6.17 (dq, J = 3.2, 1.0 Hz, 1H), 2.44 – 2.43 (m, 3H).

I. Sasaki, T. Ikeda, T. Amou, J. Taguchi, H. Ito, T. Ishiyama, *Synlett*, **2016**, *27*, 1582–1586.

3.4 Syntheses of ketimines and aldimines by other procedures

N-Phenyl-1-(cyclohexyl)methanimine (2l)



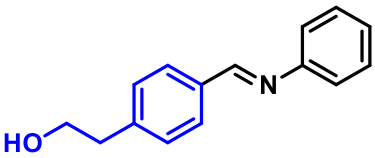
A mixture of cyclohexanecarboxaldehyde (927 mg, 1.00 mL, 8.26 mmol) and anhydrous Na_2SO_4 (11.7 g, 82.6 mmol) in acetonitrile (4.25 mL) was cooled to –40 °C using a cryostat. A solution of aniline (769 mg, 0.75 mL, 8.26 mmol) in acetonitrile (6.25 mL) was added dropwise and the mixture was subsequently stirred for 45 minutes at –40 °C. The cooling bath was removed and the mixture stirred for further 30 minutes while slowly warming to room temperature. The mixture was filtered and concentrated *in vacuo* to yield a yellow, viscous oil, which was vacuum-distilled to give pure **2l** as a pale-yellow liquid (758 mg, 51 %).

b.p. = 95–105 °C / 0.1 Torr

^{1}H-NMR (300 MHz, $CDCl_3$): δ [ppm] = 7.71 (d, J = 5.0 Hz, 1H), 7.38 – 7.28 (m, 2H), 7.20 – 7.13 (m, 1H), 7.05 – 6.98 (m, 2H), 2.44 – 2.31 (m, 1H), 2.00 – 1.65 (m, 6H), 1.46 – 1.31 (m, 4H).

G. J. T. Kuster, L. W. A. van Berkom, M. Kalmoua, A. van Loevezijn, L. A. J. M. Sliedregt, B. J. van Steen, C. G. Kruse, F. P. J. T., Rutjes, H. W. Scheeren, *J. Comb. Chem.* **2006**, *8*, 85–94.

N-Phenyl-1-(4-(2-hydroxyethyl)phenyl)methanimine (2m)



A mixture of 4-(2-hydroxyethyl)benzaldehyde (see section 3.6) (309 mg, 2.05 mmol) and aniline (191 mg, 190 µL, 2.05 mmol) in CH_2Cl_2 (15 mL) was stirred overnight at room temperature over activated 4 Å molecular sieves. The mixture was filtered and concentrated *in vacuo*. The residue was purified by column chromatography on basic silica (deactivated with NEt_3, pentane/ethyl acetate 1:1) to yield **2m** as a yellow solid, which was dried at 40–50 °C and 10^{-2} mbar to remove last traces of the starting materials (202 mg, 0.896 mmol, 44 %). The product may turn orange upon storage.

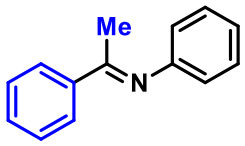
m.p. = 56–57 °C

^{1}H-NMR (300 MHz, $CDCl_3$): δ [ppm] = 8.44 (s, 1H), 7.91 – 7.84 (m, 2H), 7.43 – 7.33 (m, 4H), 7.27 – 7.20 (m, 3H), 3.91 (t, J = 6.5 Hz, 2H), 2.95 (t, J = 6.5 Hz, 2H).

^{13}C-{^{1}H}-NMR (75 MHz, $CDCl_3$): δ [ppm] = 160.3, 152.1, 142.6, 134.7, 129.6, 129.3, 129.2, 126.0, 121.0, 63.5, 39.3.

HRMS (ESI): m/z = calcd. for $C_{15}H_{16}NO^+$: 226.1226, found: 226.1226.

N,1-Diphenylethan-1-imine (2n)

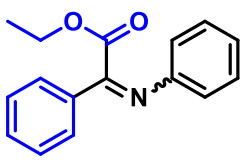


A mixture of acetophenone (1.20 g, 1.17 mL, 10 mmol) and aniline (931 mg, 910 µL, 10 mmol) was refluxed overnight in toluene (20 mL) over activated 4 Å molecular sieves. The mixture was filtered and concentrated *in vacuo*. The yellow residue was dissolved in a minimal amount of methanol and **2n** was crystallized at –20 °C overnight as a pale-yellow solid (1.04 g, 5.33 mmol, 53 %).

^{1}H-NMR (300 MHz, $CDCl_3$): δ [ppm] = 8.02 – 7.96 (m, 2H), 7.51 – 7.43 (m, 3H), 7.40 – 7.32 (m, 2H), 7.13 – 7.06 (m, 1H), 6.86 – 6.77 (m, 2H), 2.25 (s, 3H).

Y. Xie, T. Chen, S. Fu, X.-S. Li, Y. Deng, H. Jiang, W. Zeng, *Chem. Commun.* **2014**, *50*, 10699–10702.

2-Phenyl-2-(phenylimino)acetate (2o)



A mixture of ethyl benzoylformate (885 mg, 790 µL, 4.98 mmol), aniline (459 mg, 450 µL, 4.98 mmol) and *p*-toluenesulfonic acid monohydrate (95 mg, 0.50 mmol, 10 mol%) in toluene (50 mL) was refluxed for 16 hours in a SOXHLET apparatus with anhydrous calcium chloride in the extraction thimble. The mixture was filtered and concentrated *in vacuo*. The brown residue was purified by column chromatography on silica (pentane/diethyl ether) to yield a mixture of (*E*)-**2o** and (*Z*)-**2o** as a yellow oil (975 mg, 77 %). The ratio of isomers was determined *via* ^{1}H-NMR spectroscopy to be 2.5/1, however, the isomers were not assigned.

Major isomer:

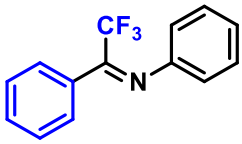
^{1}H-NMR (300 MHz, $CDCl_3$): *δ* [ppm] = 7.92 – 7.86 (m, 2H), 7.53 – 7.43 (m, 3H), 7.36 – 7.29 (m, 2H), 7.17 – 7.09 (m, 1H), 6.99 – 6.93 (m, 2H), 4.13 (q, *J* = 7.1 Hz, 2H), 0.99 (t, *J* = 7.1 Hz, 3H).

Minor isomer:

^{1}H-NMR (300 MHz, $CDCl_3$): *δ* [ppm] = 8.05 – 7.98 (m, 2H), 7.70 – 7.63 (m, 1H), 4.46 (q, *J* = 7.1 Hz, 2H), 1.43 (t, *J* = 7.1 Hz, 3H), other aromatic signals could not accurately be determined due to overlapping.

D. Enders, A. Rembiak, B. A. Stöckel, *Adv. Synth. Catal.* **2013**, *335*, 1937–1942.

2,2,2-Trifluoro-*N*,1-diphenylethan-1-imine (2p)



In a SOXHLET apparatus with anhydrous calcium chloride in the extraction thimble, a mixture of 2,2,2-trifluoroacetophenone (500 mg, 400 µL, 2.87 mmol), aniline (267 mg, 260 µL, 2.85 mmol) and *p*-toluenesulfonic acid monohydrate (27 mg, 0.15 mmol, 5 mol%) in toluene (50 mL) was refluxed for 40 hours. The mixture was filtered, concentrated *in vacuo* and the brown residue was purified by Kugelrohr distillation. The obtained liquid was dried at 70 °C at 5 mbar for one hour using a rotary evaporator to remove traces of the starting materials to yield pure **2p** as a yellow liquid (232 mg, 931 mmol, 32 %).

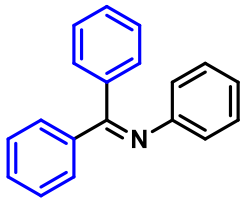
b.p. = 190–200 °C / 7.5 Torr

^{1}H-NMR (600 MHz, $CDCl_3$): *δ* [ppm] = 7.37 – 7.34 (m, 1H), 7.32 – 7.28 (m, 2H), 7.23 – 7.17 (m, 4H), 7.06 – 7.02 (m, 1H), 6.76 – 6.72 (m, 2H).

^{19}F-NMR (565 MHz, $CDCl_3$): *δ* [ppm] = −70.00.

M. Abid, M. Savolainen, S. Landge, J. Hu, G. K. S. Prakash, G. A. Olah, B. Török, *J. Fluor. Chem.* **2007**, *128*, 587–594.

N,1,1-Triphenylmethanimine (2q)

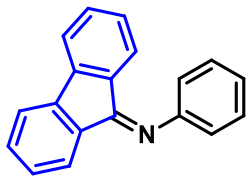


In a SOXHLET apparatus with anhydrous calcium chloride in the extraction thimble, a mixture of benzophenone (1.82 g, 10.0 mmol), aniline (931 mg, 910 µL, 10.0 mmol) and *p*-toluenesulfonic acid monohydrate (114 mg, 0.60 mmol, 6 mol%) in toluene (50 mL) was refluxed for 40 hours. The mixture was filtered, washed with water (20 mL), dried over Na_2SO_4, filtered and concentrated *in vacuo*. The residual dark yellow solid was recrystallized from diethyl ether to yield **2q** as light-yellow crystal plates (809 mg, 3.14 mmol, 31 %).

^{1}H-NMR (300 MHz, $CDCl_3$): *δ* [ppm] = 7.79 – 7.72 (m, 2H), 7.50 – 7.37 (m, 3H), 7.30 – 7.22 (m, 3H), 7.18 – 7.09 (m, 4H), 6.97 – 6.89 (m, 1H), 6.79 – 6.68 (m, 2H).

T. Ogata, J. F. Hartwig, *J. Am. Chem. Soc.* **2008**, *42*, 13848–13849.

N-Phenyl-9*H*-fluoren-9-imine (2r)

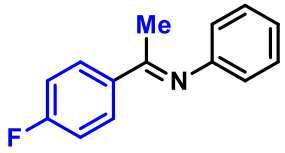


In a SOXHLET apparatus with anhydrous calcium chloride in the extraction thimble, a mixture of fluorenone (1.81 g, 10.0 mmol), aniline (931 mg, 910 µL, 10.0 mmol) and *p*-toluenesulfonic acid monohydrate (97 mg, 0.51 mmol, 5 mol%) in toluene (50 mL) was refluxed for 40 hours. The mixture was filtered, washed with water (20 mL), dried over Na_2SO_4, filtered and concentrated *in vacuo*. The residual dark-orange solid was recrystallized from diethyl ether to yield **2r** as yellow-orange needles (1.52 g, 5.95 mmol, 60 %).

^{1}H-NMR (300 MHz, $CDCl_3$): *δ* [ppm] = 7.98 – 7.88 (m, 1H), 7.63 – 7.57 (m, 2H), 7.51 – 7.29 (m, 5H), 7.25 – 7.18 (m, 1H), 7.04 – 6.97 (m, 2H), 6.93 (td, *J* = 7.6, 1.1 Hz, 1H), 6.57 (dt, *J* = 7.8, 0.9 Hz, 1H).

D. J. van As, T. U. Connell, M. Brzozowski, A. D. Scully, A. Polyzos, *Org. Lett.* **2018**, *20*, 905–908.

1-(4-Fluorophenyl)-*N*-phenylethan-1-imine (2s)



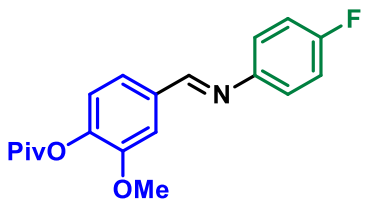
A mixture of 4-fluoroacetophenone (570 mg, 0.50 mL, 4.14 mmol), aniline (388 mg, 0.38 mL, 4.14 mmol) and *p*-toluenesulfonic acid monohydrate (21 mg, 0.207 mmol, 5 mol%) in toluene (10 mL) was stirred overnight at room temperature over activated 4 Å molecular sieves. The mixture was filtered and concentrated *in vacuo*. The residue was recrystallized from ethanol to yield **2s** as white crystal plates (290 mg, 1.36 mmol, 33 %).

^{1}H-NMR (300 MHz, $CDCl_3$): *δ* [ppm] = 8.05 – 7.92 (m, 2H), 7.42 – 7.30 (m, 2H), 7.18 – 7.06 (m, 3H), 6.85 – 6.73 (m, 2H), 2.23 (s, 3H).

^{19}F-NMR (565 MHz, $CDCl_3$): *δ* [ppm] = −110.35.

N. Nghia Pham, T. T. Dang, N. T. Ngo, A. Villinger, P. Ehlers, P. Langer, *Org. Biomol. Chem.* **2015**, *13*, 6047–6058.

4-(((4-Fluorophenyl)imino)methyl)-2-methoxyphenyl pivalate (2t)



A mixture of 4-formyl-2-methoxyphenyl pivalate (see section 3.6) (681 mg, 2.88 mmol, 1.0 equiv.) and 4-fluoroaniline (381 mg, 325 µL, 3.43 mmol, 1.2 equiv.) in methanol (5 mL) was stirred overnight at room temperature over activated 3 Å molecular sieves, then heated to 45 °C for 30 minutes. The mixture was filtered through Celite, which was washed thoroughly with CH_2Cl_2, and the filtrate was concentrated *in vacuo*. The residual yellow solid was recrystallized from boiling methanol to yield **2t** as a pale-yellow solid (707 mg, 2.15 mmol, 75 %).

m.p. = 82–83 °C

^{1}H-NMR (300 MHz, $CDCl_3$): δ [ppm] = 8.39 (s, 1H), 7.64 (d, J = 1.8 Hz, 1H), 7.34 (dd, J = 8.1, 1.8 Hz, 1H), 7.23 – 7.15 (m, 2H), 7.13 – 7.03 (m, 3H), 3.91 (s, 3H), 1.39 (s, 9H).

^{13}C-{^{1}H}-NMR (151 MHz, $CDCl_3$): δ [ppm] = 176.6, 161.4 (d, J = 244.7 Hz), 159.5, 152.0, 148.1 (d, J = 3.4 Hz), 143.3, 134.9, 123.3, 123.1, 122.4 (d, J = 8.5 Hz), 116.0 (d, J = 22.6 Hz), 110.6, 56.2, 39.3, 27.3.

^{19}F-NMR (565 MHz, $CDCl_3$): δ [ppm] = −117.24 (tt, J = 9.0, 4.5 Hz).

HRMS (ESI): *m/z* = calcd. for $C_{19}H_{21}FNO_3^+$: 330.1500, found: 330.1504.

General Procedure 3: Synthesis of α-Amino Amides

A 4 mL glass vial was charged with a magnetic stir bar, the corresponding imine (0.30 mmol, 1.0 equiv.), the corresponding Hantzsch ester (0.39 mmol, 1.3 equiv.) and 3DPAFIPN (4.9 mg, 7.5 µmol, 2.5 mol%) and closed with a septum screw cap. The vial was evacuated and flushed with nitrogen three times before adding dry CH_2Cl_2 (3 mL, results in a 0.1 M soln. of the imine) and $BF_3{\cdot}OEt_2$ (37 µL, 0.30 mmol, 1.0 equiv.). The vial was shaken and the mixture was stirred for 16 hours at room temperature under blue light irradiation (λ = 450 nm, EvoluChem™ 450DX). The mixture was then washed with water (5 mL), the aqueous phase was extracted with CH_2Cl_2 (3× 5 mL) and the combined organic phases were dried over $MgSO_4$ or Na_2SO_4. After filtration and removal of the solvent *in vacuo*, the residue was purified using silica column chromatography (gradient of pentane/ethyl acetate, generally starting from 9:1) to yield the α-amino amides **3**–**7**.

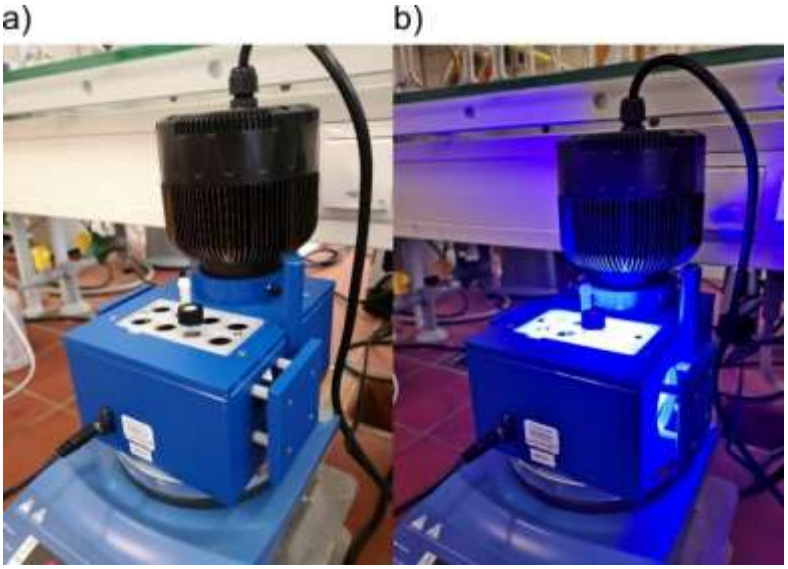
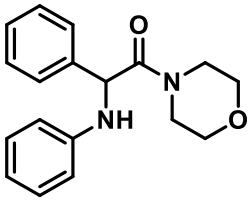


Figure 1. *a) Experimental setup for the photoredox-catalyzed carbamoylation of imines using an EvoluChem™ PhotoRedOx Box fitted with a blue EvoluChem™ 450DX LED (450 nm) with the light turned off. b) With the light turned on.*

1-Morpholino-2-phenyl-2-(phenylamino)ethan-1-one (3a)



Starting from benzylideneaniline (54 mg), HE **1a** (143 mg), and following the general procedure 3, **3a** was obtained as a brown solid (70 mg, 80 %).

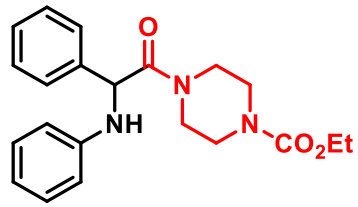
m.p. = 103–104 °C

^{1}H-NMR (400 MHz, $CDCl_3$): δ [ppm] = 7.45 – 7.39 (m, 2H), 7.39 – 7.32 (m, 2H), 7.32 – 7.27 (m, 1H), 7.18 – 7.08 (m, 2H), 6.75 – 6.62 (m, 3H), 5.27 (s, 1H), 4.44 (br. s, 1H, NH), 3.78 – 3.43 (m, 7H), 3.29 – 3.13 (m, 1H).

^{13}C-{^{1}H}-NMR (75 MHz, $CDCl_3$): δ [ppm] = 169.5, 146.0, 138.1, 129.4, 129.2, 128.4, 127.8, 118.4, 114.1, 66.8, 66.3, 58.5, 46.1, 43.0.

HRMS (ESI): *m/z* = calcd. for $C_{18}H_{21}N_2O_2^+$: 297.1598, found: 297.1600.

Ethyl 4-(2-phenyl-2-(phenylamino)acetyl)piperazine-1-carboxylate (3b)



Starting from benzylideneaniline (54 mg), HE **1b** (171 mg), and following the general procedure 3, **3b** was obtained as a beige solid (61 mg, 55 %).

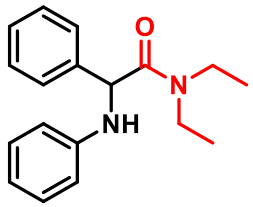
m.p. = 109–111 °C

^{1}H-NMR (400 MHz, $CDCl_3$): δ [ppm] = 7.43 – 7.39 (m, 2H), 7.38 – 7.32 (m, 2H), 7.31 – 7.26 (m, 1H), 7.16 – 7.10 (m, 2H), 6.75 – 6.67 (m, 3H), 5.30 (s, 1H), 5.20 (br. s, 1H, NH), 4.11 (q, *J* = 7.1 Hz, 2H), 3.83 – 3.71 (m, 1H), 3.60 – 3.39 (m, 5H), 3.28 – 3.17 (m, 1H), 2.89 – 2.77 (m, 1H), 1.23 (t, *J* = 7.1 Hz, 3H).

^{13}C-{^{1}H}-NMR (101 MHz, $CDCl_3$): δ [ppm] = 169.5, 155.4, 145.5, 137.7, 129.6, 129.4, 129.3, 128.6, 127.9, 118.9, 114.5, 61.9, 59.1, 45.3, 43.3, 42.5, 14.7.

HRMS (ESI): *m/z* = calcd. for $C_{21}H_{26}N_3O_3^+$: 368.1969, found: 368.1967.

N,*N*-Diethyl-2-phenyl-2-(phenylamino)acetamide (3c)



Starting from benzylideneaniline (54 mg), HE **1c** (138 mg), and following the general procedure 3, **3c** was obtained as a yellow solid (65 mg, 76 %).

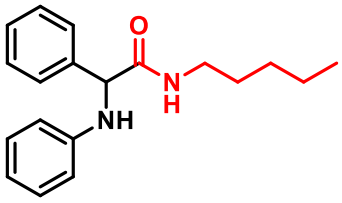
m.p. = 103–105 °C

^{1}H-NMR (300 MHz, $CDCl_3$): δ [ppm] = 7.50 – 7.47 (m, 2H), 7.40 – 7.25 (m, 3H), 7.17 – 7.12 (m, 2H), 6.72 – 6.67 (m, 3H), 5.48 (br. s, 1H, NH), 5.25 (s, 1H), 3.48 (dq, *J* = 14.2, 7.1 Hz, 2H), 3.31 (dq, *J* = 13.9, 7.0 Hz, 2H), 1.12 (t, *J* = 7.1 Hz, 3H), 1.02 (t, *J* = 7.1 Hz, 3H).

^{13}C-{^{1}H}-NMR (101 MHz, $CDCl_3$): δ [ppm] = 169.9, 146.6, 138.9, 129.3, 129.0, 128.0, 127.9, 117.0, 113.8, 58.4, 41.6, 40.8, 14.0, 12.8.

HRMS (ESI): *m/z* = calcd. for $C_{18}H_{23}N_2O^+$: 283.1805, found: 283.1798.

N-Pentyl-2-phenyl-2-(phenylamino)acetamide (3d)



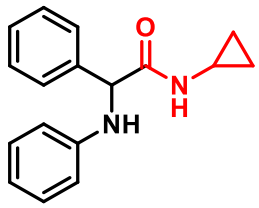
Starting from benzylideneaniline (54 mg), HE **1d** (143 mg), and following the general procedure 3, **3d** was obtained as a brown gum (55 mg, 62 %).

^{1}H-NMR (300 MHz, $CDCl_3$): *δ* [ppm] = 7.43 – 7.36 (m, 5H), 7.19 – 7.16 (m, 2H), 6.83 – 6.78 (m, 1H), 6.66 – 6.63 (m, 2H), 4.73 (s, 1H), 4.44 (br. s, 1H), 3.30 – 3.23 (m, 2H), 1.45 – 1.42 (m, 2H), 1.25 – 1.20 (m, 4H), 0.84 (t, 3H, *J* = 7.0 Hz).

^{13}C-{^{1}H}-NMR (75 MHz, $CDCl_3$): *δ* [ppm] = 171.1, 146.8, 139.1, 129.5, 129.3, 128.7, 127.5, 119.3, 114.0, 64.4, 39.6, 29.3, 29.0, 22.4, 14.1.

HRMS (ESI): m/z = calcd. for $C_{19}H_{25}N_2O^+$: 297.1961, found: 297.1965.

N-Cyclopropyl-2-phenyl-2-(phenylamino)acetamide (3e)



Starting from benzylideneaniline (54 mg), HE **1e** (131 mg), and following the general procedure 3, **3e** was obtained as a yellow solid (65 mg, 74 %).

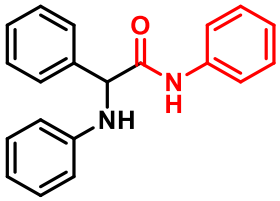
m.p. = 134–136 °C

^{1}H-NMR (300 MHz, $CDCl_3$): *δ* [ppm] = 7.41 – 7.35 (m, 4H), 7.21 – 7.16 (m, 2H), 6.87 – 6.77 (m, 2H), 6.63 – 6.59 (m, 2H), 4.72 (s, 1H), 4.59 (br. s, 1H, NH), 2.76 – 2.67 (m, 1H), 0.76 – 0.71 (m, 2H), 0.46 – 0.42 (m, 2H).

^{13}C-{^{1}H}-NMR (101 MHz, $CDCl_3$): *δ* [ppm] = 172.7, 146.7, 138.8, 129.4, 129.2, 128.6, 127.4, 119.1, 113.8, 64.0, 22.7, 6.8, 6.5.

HRMS (ESI): *m/z* = calcd. for $C_{17}H_{19}N_2O^+$: 267.1492, found: 267.1499.

N,2-Diphenyl-2-(phenylamino)acetamide (3f)



Starting from benzylideneaniline (54 mg), HE **1c** (145 mg), and following the general procedure 3, **3f** was obtained as a pale-yellow solid (64 mg, 70 %).

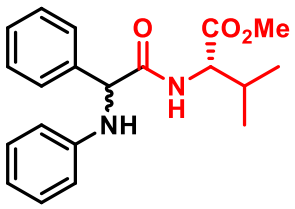
m.p. = 130–135 °C (dec.)

^{1}H-NMR (300 MHz, $CDCl_3$): δ [ppm] = 8.75 (s, 1H, CONH), 7.59 – 7.50 (m, 4H), 7.48 – 7.38 (m, 3H), 7.38 – 7.22 (m, 4H), 7.18 – 7.10 (m, 1H), 6.94 – 6.85 (m, 1H), 6.79 – 6.72 (m, 2H), 4.86 (s, 1H), 4.52 (s, 1H, NH).

^{13}C-{^{1}H}-NMR (75 MHz, $CDCl_3$): δ [ppm] = 169.6, 146.7, 138.6, 137.4, 129.7, 129.5, 129.1, 129.0, 127.6, 124.8, 120.1, 120.0, 114.3, 65.6.

HRMS (ESI): *m/z* = calcd. for $C_{20}H_{19}N_2O^+$: 303.1492, found: 303.1495.

Methyl (2-phenyl-2-(phenylamino)acetyl)-(*S*)-valinate (3g)



Starting from benzylideneaniline (54 mg), HE **1e** (156 mg), and following the general procedure 3, **3g** was obtained as a mixture of the two diastereomers (1:1.3 ratio) as a yellow powder (75 mg, 74 %).

Major diastereomer:

^{1}H-NMR (300 MHz, $CDCl_3$): δ [ppm] = 7.49 – 7.46 (m, 2 H), 7.40 – 7.36 (m, 3H), 7.22 – 7.18 (m, 2H), 6.83 – 6.77 (m, 1H), 6.67 – 6.65 (m, 2H), 4.80 (d, *J* = 3.9 Hz, 1H), 4.58 (dd, *J* = 9.3, 4.5 Hz), 3.73 (s, 3H), 2.26 – 2.06 (m, 1H), 0.79 (d, *J* = 6.7 Hz), 0.67 (d, *J* = 6.8 Hz).

^{13}C-{^{1}H}-NMR (75 MHz, $CDCl_3$): δ [ppm] = 172.3, 171.1, 146.5, 138.9, 129.3, 128.7, 127.6, 119.2, 113.9, 64.1, 57.0, 52.3, 31.2, 19.0, 17.3.

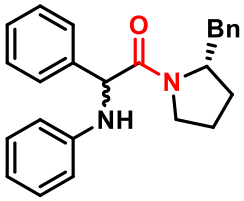
Minor diastereomer:

^{1}H-NMR (300 MHz, $CDCl_3$): δ [ppm] = 7.49 – 7.46 (m, 2 H), 7.40 – 7.36 (m, 3H), 7.22 – 7.18 (m, 2H), 6.83 – 6.77 (m, 1H), 6.67 – 6.65 (m, 2H), 4.80 (d, *J* = 3.9 Hz, 1H), 4.53 (dd, *J* = 8.9, 4.9 Hz, 1H), 3.59 (s, 3H), 0.89 (t, *J* = 7.2 Hz, 6H).

^{13}C-{^{1}H}-NMR (75 MHz, $CDCl_3$): δ [ppm] = 171.7, 171.5, 146.7, 138.7, 129.4, 129.3, 127.4, 119.3, 114.2, 64.5, 57.3, 52.1, 31.3, 19.1, 17.9.

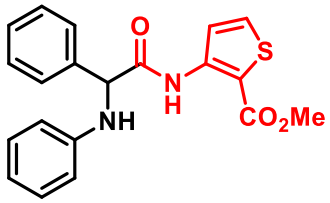
HRMS (ESI): *m/z* = calcd. for $C_{20}H_{25}N_2O_3^+$: 341.1860, found: 341.1864.

1-((*S*)-2-Benzylpyrrolidin-1-yl)-2-phenyl-2-(phenylamino)ethan-1-one (3h)



Starting from benzylideneaniline (54 mg), HE-(Bn-Pyrrolidine) (see section 3.6) (168 mg), and following the general procedure 3, **3h** was obtained as a mixture of the two diastereomers (near 1:1) as a yellow, fluorescent gum (58 %). The yield was determined *via* ^{1}H-NMR using 1,3,5-trimethoxybenzene as an external standard. Attempts to obtain a pure sample *via* crystallization or preparative HPLC were unsuccessful.

Methyl 3-(2-phenyl-2-(phenylamino)acetamido)thiophene-2-carboxylate (3i)



Starting from benzylideneaniline (54 mg), HE **1h** (170 mg), and following the general procedure 3, impure **3i** was obtained after elution with pentane/ethyl acetate 9:1. Pure **3i** was obtained as a pale-yellow solid after recrystallization from boiling methanol (68 mg, 62 %).

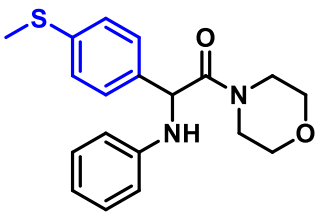
m.p. = 165–168 °C

^{1}H-NMR (300 MHz, $CDCl_3$): δ [ppm] = 11.19 (s, 1H, NH), 8.14 (d, J = 5.5 Hz, 1H), 7.59 – 7.56 (m, 2H), 7.45 – 7.35 (m, 3H), 7.23 – 7.18 (m, 2H), 6.84 – 6.78 (m, 2H), 6.75 – 6.71 (m, 2H), 4.95 (s, 1H), 4.82 (br. s, 1H, NH), 3.82 (s, 3H).

^{13}C-{^{1}H}-NMR (75 MHz, $CDCl_3$): δ [ppm] = 169.6, 164.3, 146.6, 143.7, 138.3, 131.7, 129.5, 128.9, 127.5, 122.4, 119.3, 114.0, 111.6, 65.0, 52.1.

HRMS (ESI): *m/z* = calcd. for $C_{20}H_{19}N_2O_3S^+$: 367.1111, found: 367.1113.

2-(4-(Methylthio)phenyl)-1-morpholino-2-(phenylamino)ethan-1-one (4a)



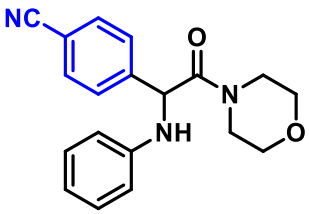
Starting from imine **2f** (65 mg), HE **1a** (143 mg), and following the general procedure 3, **4a** was obtained as a brownish gum (78 mg, 76 %).

^{1}H-NMR (300 MHz, $CDCl_3$): δ [ppm] = 7.36 – 7.33 (m, 2H), 7.22–7.20 (m, 2H), 7.15 – 7.10 (m, 2H), 6.71 – 6.61 (m, 3H), 5.33 (br. s, 1H, NH), 5.22 (s, 1H), 3.65 – 3.48 (m, 7H), 3.29 – 3.25 (m, 1H), 2.46 (s, 3H).

^{13}C-{^{1}H}-NMR (75 MHz, $CDCl_3$): δ [ppm] = 169.4, 146.1, 138.8, 134.8, 129.3, 128.1, 126.8, 118.0, 113.7, 66.7, 66.2, 57.5, 45.9, 42.9, 15.5.

HRMS (ESI): *m/z* = calcd. for $C_{19}H_{22}N_2O_2S^+$: 343.1475, found: 343.1477.

2-(4-Cyanophenyl)-1-morpholino-2-(phenylamino)ethan-1-one (4b)



Starting from imine **2g** (65 mg), HE **1a** (143 mg), and following the general procedure 3, **4b** was obtained as a pale-yellow solid (82 mg, 85 %).

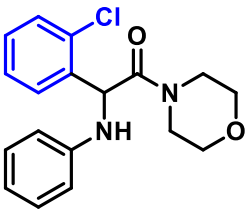
m.p. = 69–70 °C

^{1}H-NMR (500 MHz, $CDCl_3$): δ [ppm] = 7.68 – 7.62 (m, 2H), 7.59 – 7.54 (m, 2H), 7.16 – 7.09 (m, 2H), 6.75 – 6.68 (m, 1H), 6.61 – 6.56 (m, 2H), 5.39 (d, *J* = 7.2 Hz, 1H), 5.33 (d, *J* = 6.4 Hz, 1H), 3.72 – 3.54 (m, 6H), 3.51 – 3.42 (m, 1H), 3.42 – 3.34 (m, 1H).

^{13}C-{^{1}H}-NMR (75 MHz, $CDCl_3$): δ [ppm] = 168.4, 145.2, 143.6, 132.9, 129.4, 128.4, 118.7, 118.3, 113.7, 112.3, 66.6, 66.2, 57.5, 46.1, 43.0.

HRMS: *m/z* = calcd. for $C_{19}H_{20}N_3O_2^+$: 322.1550, found: 322.1552.

2-(2-Chlorophenyl)-1-morpholino-2-(phenylamino)ethan-1-one (4c)



Starting from imine **2h** (62 mg), HE **1a** (143 mg), and following the general procedure 3, **4c** was obtained as a cream-colored solid (76 mg, 77 %).

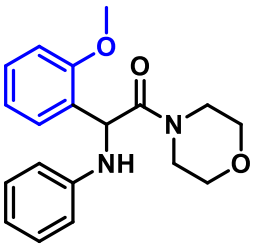
m.p. = 161–162 °C

^{1}H-NMR (300 MHz, $CDCl_3$): δ [ppm] = 7.55 – 7.48 (m, 1H), 7.43 – 7.36 (m, 1H), 7.31 – 7.21 (m, 2H), 7.20 – 7.11 (m, 2H), 6.77 – 6.69 (m, 3H), 5.71 (s, 1H), 5.16 (br. s, 1H, NH), 3.77 – 3.48 (m, 7H), 3.35 – 3.20 (m, 1H).

^{13}C-{^{1}H}-NMR (75 MHz, $CDCl_3$): δ [ppm] = 169.5, 146.2, 136.0, 133.0, 129.9, 129.7, 129.4, 129.2, 128.1, 118.7, 114.2, 66.8, 66.5, 54.6, 45.9, 43.3.

HRMS: *m/z* = calcd. for $C_{18}H_{20}ClN_2O_2^+$: 331.1208, found: 331.1209.

2-(2-Methoxyphenyl)-1-morpholino-2-(phenylamino)ethan-1-one (4d)



Starting from imine **2i** (62 mg), HE **1a** (143 mg), and following the general procedure 3, **4d** was obtained as a yellow solid (73 mg, 75 %).

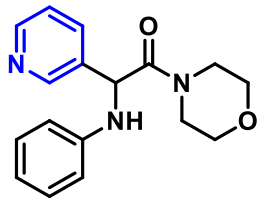
m.p. = 114–116 °C

^{1}H-NMR (300 MHz, $CDCl_3$): δ [ppm] = 7.44 – 7.41 (m, 1H), 7.35 – 7.21 (m, 1H), 7.16 – 7.11 (m, 2H), 6.98 – 6.92 (m, 2H), 6.72 – 6.68 (m, 3H), 5.76 (s, 1H), 5.45 (br. s, 1H, NH), 4.00 (s, 3H), 3.73 – 3.52 (m, 7H), 3.18 – 3.14 (m, 1H).

^{13}C-{^{1}H}-NMR (75 MHz, $CDCl_3$): δ [ppm] = 170.3, 155.7, 146.5, 129.5, 129.2, 128.2, 126.6, 121.9, 117.7, 113.7, 110.7, 66.8, 66.4, 55.7, 50.3, 45.4, 43.1.

HRMS (ESI): *m/z* = calcd. for $C_{19}H_{23}N_2O_3^+$: 327.1703, found: 327.1703.

1-Morpholino-2-(phenylamino)-2-(pyridin-3-yl)ethan-1-one (4e)



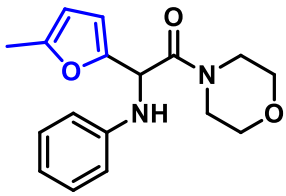
Starting from imine **2j** (55 mg), HE **1a** (143 mg), and following the general procedure 3 (elution: pentane/ethyl acetate 9:1 to 1:9), **4e** was obtained as a yellow gum (45 mg, 50 %).

^{1}H-NMR (300 MHz, DMSO-d_6): δ [ppm] = 8.70 (s, 1H), 8.46 (d, J = 4.8 Hz, 1H), 7.85 (d, J = 7.9 Hz, 1H), 7.36 (dd, J = 7.9, 4.8 Hz, 1H), 7.04 (t, J = 7.7 Hz, 2H), 6.74 (d, J = 7.9 Hz, 2H), 6.54 (t, J = 7.3 Hz, 1H), 6.32 (d, J = 8.8 Hz, 1H), 5.72 (d, J = 8.8 Hz, 1H), 3.86 – 3.68 (m, 1H), 3.68 – 3.40 (m, 7H).

^{13}C-{^{1}H}-NMR: (75 MHz, DMSO-d_6): δ [ppm] = 168.6, 149.3, 148.7, 146.7, 135.3, 134.6, 128.8, 123.6, 116.8, 113.3, 66.0, 65.8, 53.7, 45.6, 42.3.

HRMS: m/z = calcd. for $C_{17}H_{20}N_3O_2^+$: 298.1550, found: 298.1550.

2-(5-Methylfuran-2-yl)-1-morpholino-2-(phenylamino)ethan-1-one (4f)



Starting from imine **2k** (56 mg), HE **1a** (143 mg), and following the general procedure 3, **4f** was obtained as a brown solid (46 mg, 51 %).

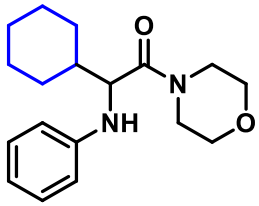
m.p. = 121–123 °C

^{1}H-NMR (300 MHz, $CDCl_3$): δ [ppm] = 7.20 – 7.12 (m, 2H), 6.78 – 6.62 (m, 3H), 6.17 (d, J = 3.1 Hz, 1H), 5.90 (dd, J = 3.1, 1.2 Hz, 1H), 5.32 (s, 1H), 5.26 (br. s, 1H, NH), 3.89 – 3.77 (m, 1H), 3.77 – 3.40 (m, 7H), 2.27 (s, 3H).

^{13}C-{^{1}H}-NMR (75 MHz, $CDCl_3$): δ [ppm] = 167.7, 152.2, 149.5, 146.4, 129.3, 118.3, 113.8, 108.9, 106.8, 66.8, 66.5, 52.6, 46.2, 43.1, 13.7.

HRMS (ESI): m/z = calcd. for $C_{17}H_{21}N_2O_3^+$: 301.1547, found: 301.1545.

2-Cyclohexyl-1-morpholino-2-(phenylamino)ethan-1-one (4g)



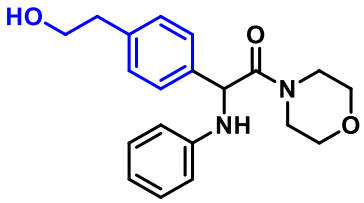
Starting from imine **2l** (57 mg), HE **1a** (143 mg), and following the general procedure 3, **4g** was obtained as a pale-yellow gum (44 mg, 47 %).

^{1}H-NMR (300 MHz, $CDCl_3$): δ [ppm] = 7.17 – 7.12 (m, 2H), 6.73 – 6.68 (m, 1H), 6.64 – 6.61 (m, 2H), 4.55 (br. s, NH), 4.10 (d, J = 5.6 Hz, 1H), 3.69 – 3.52 (m, 8H), 1.91 – 1.65 (m, 6H), 1.26 – 1.17 (m, 5H).

^{13}C-{^{1}H}-NMR (75 MHz, $CDCl_3$): δ [ppm] = 172.0, 148.2, 129.4, 118.2, 114.0, 67.1, 66.8, 58.5, 46.4, 42.5, 42.1, 30.4, 28.8, 26.4, 26.3, 26.2.

HRMS: m/z = calcd. for $C_{18}H_{27}N_2O_2^+$: 303.2067, found: 303.2066.

2-(4-(2-Hydroxyethyl)phenyl)-1-morpholino-2-(phenylamino)ethan-1-one (4h)



Starting from imine **2m** (67 mg), HE **1a** (143 mg), and following the general procedure 3 using TFA (23 µL, 1 equiv.) instead of $BF_3{\cdot}OEt_2$, **4h** was obtained as a brown solid (52 %). The yield was determined *via* ^{1}H-NMR using 1,3,5-trimethoxybenzene as an external standard. An analytical sample was crystallized from CH_2Cl_2 (colorless crystals).

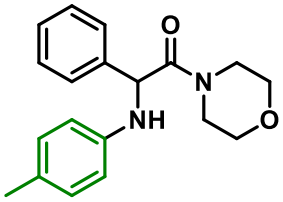
m.p. = 166–167 °C

^{1}H-NMR (300 MHz, $CDCl_3$): δ [ppm]= 7.38 –7.35 (m, 2H), 7.22 – 7.19 (m, 2H), 7.15 – 7.10 (m, 2H), 6.71 – 6.63 (m, 3H), 5.25 (br. s, 1H), 3.82 (t, 2H, *J* = 6.56 Hz), 3.64 – 3.42 (m, 7H), 3.29 – 2.18 (m, 1H), 2.83 (t, 2H, *J* = 6.56 Hz).

^{13}C-{^{1}H}-NMR (75 MHz, $CDCl_3$): δ [ppm] = 169.6, 146.2, 138.9, 136.3, 129.8, 129.4, 127.9, 118.2, 113.8, 66.8, 66.3, 63.5, 57.9, 46.1, 42.9, 38.9.

HRMS (ESI): *m/z* = calcd. for $C_{20}H_{25}N_2O_3^+$: 341.1860, found: 341.1863.

1-Morpholino-2-phenyl-2-((4-methylphenyl)amino)ethan-1-one (5a)



Starting from imine **2b** (59 mg), HE **1a** (143 mg), and following the general procedure 3, **5a** was obtained as an orange-brown solid (50 mg, 54 %).

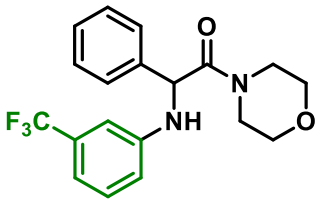
m.p. = 137–138 °C

^{1}H-NMR (500 MHz, $CDCl_3$): *δ* [ppm] = 7.44 – 7.40 (m, 2H), 7.37 – 7.33 (m, 2H), 7.30 – 7.26 (m, 1H), 6.96 – 6.92 (m, 2H), 6.60 – 6.55 (m, 2H), 5.24 (s, 1H), 3.76 – 3.43 (m, 7H), 3.25 – 3.16 (m, 1H), 2.20 (s, 3H).

^{13}C-{^{1}H}-NMR (75 MHz, $CDCl_3$): *δ* [ppm] = 169.7, 144.1, 138.4, 129.8, 129.2, 128.3, 127.8, 127.4, 114.0, 66.8, 66.3, 58.6, 46.0, 43.0, 20.5.

HRMS (ESI): *m/z* = calcd. for $C_{19}H_{23}N_2O_2^+$: 311.1754, found: 311.1756.

1-Morpholino-2-phenyl-2-((3-(trifluoromethyl)phenyl)amino)ethan-1-one (5b)



Starting from imine **2c** (63 mg), HE **1a** (143 mg), and following the general procedure 3, **5b** was obtained as a colorless solid (83 mg, 76 %).

m.p. = 110–111 °C

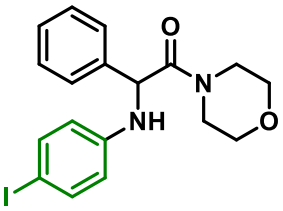
^{1}H-NMR (300 MHz, $CDCl_3$): *δ* [ppm] = 7.45 – 7.27 (m, 5H), 7.23 – 7.16 (m, 1H), 6.94 – 6.75 (m, 3H), 5.25 (s, 1H), 3.77 – 3.38 (m, 7H), 3.28 – 3.11 (m, 1H).

^{13}C-{^{1}H}-NMR (75 MHz, $CDCl_3$): *δ* [ppm] = 168.9, 146.4, 137.6, 131.4 (q, *J* = 31.7 Hz), 129.7, 129.3, 128.5, 127.7, 124.3 (q, *J* = 272.7 Hz), 116.6 (q, *J* = 1.1 Hz), 114.2 (q, *J* = 3.9 Hz), 109.6 (q, *J* = 4.0 Hz), 66.7, 66.1, 57.8, 46.0, 43.0.

^{19}F-NMR (565 MHz, $CDCl_3$): *δ* [ppm] = −62.89.

HRMS (ESI): *m/z* = calcd. for $C_{19}H_{20}F_3N_2O_2^+$: 365.1471, found: 365.1472.

1-Morpholino-2-phenyl-2-((4-iodophenyl)amino)ethan-1-one (5c)



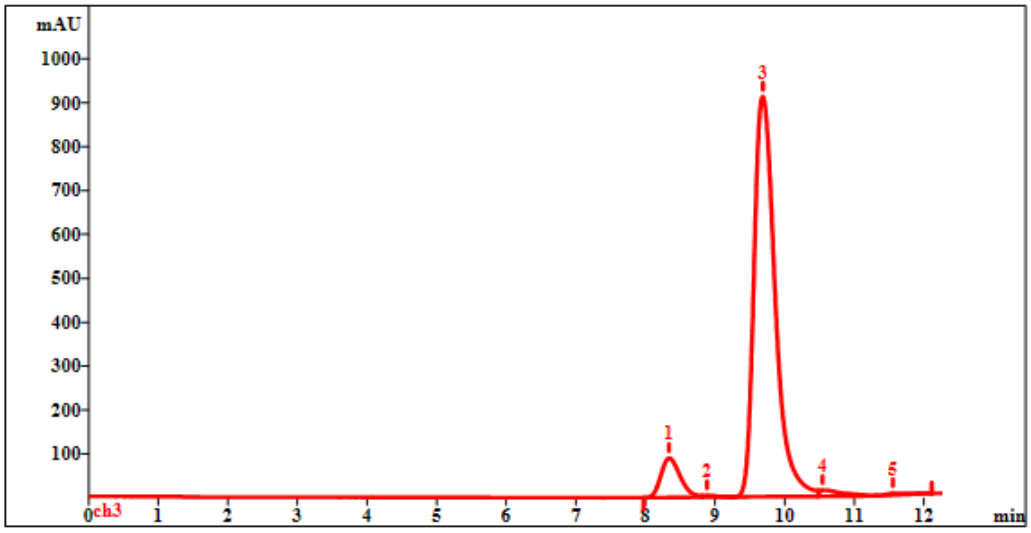
Starting from imine **2d** (92 mg), HE **1a** (143 mg), and following the general procedure 3, a mixture of **5c** and **3a** inseparable by preparative column chromatography was obtained due to deiodination of the product during the photoreaction as a white-brown solid (75 mg). The ratio of **5c** to **3a** was determined as 11/1 *via* HPLC (Fig. 2), which corresponds to a yield of 56 % for **5c**.

Due to the large excess of **5c**, it could nonetheless be characterized by NMR spectroscopy and mass spectrometry.

^{1}H-NMR (300 MHz, $CDCl_3$): *δ* [ppm] = 7.31 – 7.18 (m, 7H), 6.35 – 6.32 (m, 2H), 5.33 (br. s, 1H, NH), 5.11 (s, 1H), 3.60 – 3.40 (m, 7H), 3.12 – 3.09 (m, 1H).

^{13}C-{^{1}H}-NMR (75 MHz, $CDCl_3$): *δ* [ppm] = 169.1, 145.7, 137.9, 137.7, 129.3, 128.5, 127.7, 115.9, 78.8, 66.7, 66.2, 57.9, 46.0, 43.0.

HRMS (ESI): *m/z* = calcd. for $C_{18}H_{20}IN_2O_2^+$: 423.0564, found: 423.0560.

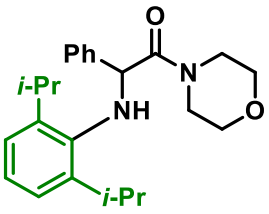


Quantitation method: Custom

Peak	Retention min	Height mAU	Area mAU*sec	Conc.	Component
1	8.34	89.59	1732.232	86.61	
2	8.89	3.63	53.514	2.68	
3	9.68	910.44	19218.891	960.94	
4	10.54	13.89	327.177	16.36	
5	11.55	3.81	89.503	4.48	
5	12.26	1021.36	21421.318	1071.07	

Figure 2. *Chromatogram of the mixture of **5c** and **3a** obtained via HPLC (ProntoSIL, C_{18} column, MeCN 100 %, 5 mL/min).*

2-((2,6-Diisopropylphenyl)amino)-1-morpholino-2-phenylethan-1-one (5d)



Starting from imine **2e** (77 mg), HE **1a** (143 mg), and following the general procedure 3, **5d** was obtained as a colorless solid after 40 hours of reaction time (35 mg, 30 %).

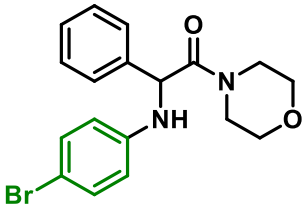
m.p. = 119–121 °C

^{1}H-NMR (300 MHz, $CDCl_3$): δ [ppm] = 7.31 – 7.24 (m, 3H), 7.19 – 7.12 (m, 2H), 7.04 (s, 3H), 4.92 (s, 1H), 4.63 (br. s, 1H), 3.95 – 3.81 (m, 1H), 3.79 – 3.53 (m, 3H), 3.52 – 3.31 (m, 2H), 3.29 – 3.18 (m, 1H), 3.18 – 3.05 (m, 3H), 1.22 (d, *J* = 7.3 Hz, 6H), 0.99 (d, *J* = 7.3 Hz, 6H).

^{13}C-{^{1}H}-NMR (75 MHz, $CDCl_3$): δ [ppm] = 170.6, 142.8, 140.4, 138.3, 128.9, 128.1, 127.5, 123.9, 123.6, 66.8, 66.2, 63.9, 45.9, 42.7, 27.9, 24.5, 24.1.

HRMS (ESI): *m/z* = calcd. for $C_{24}H_{33}N_2O_2^+$: 381.2537, found: 381.2535.

1-Morpholino-2-phenyl-2-((4-bromophenyl)amino)ethan-1-one (5e)



Starting from *N*-Phenyl-1-(4-bromophenyl)methanimine (74 mg), HE **1a** (143 mg), and following the general procedure 3, **5e** was obtained as an off-white powder (83 mg, 74 %).

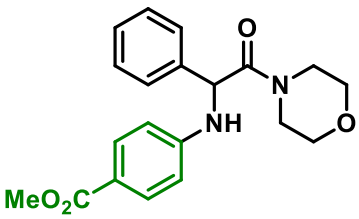
m.p. = 175–176 °C

^{1}H-NMR (300 MHz, $CDCl_3$): δ [ppm] = 7.34 – 7.16 (m, 5H), 7.13 – 7.06 (m, 2H), 6.45 – 6.37 (m, 2H), 5.35 (d, *J* = 7.2 Hz, 1H), 5.09 (d, *J* = 7.2 Hz, 1H), 3.66 – 3.34 (m, 7H), 3.16 – 3.02 (m, 1H).

^{13}C-{^{1}H}-NMR (75 MHz, $CDCl_3$): δ [ppm] = 169.1, 145.2, 137.7, 131.9, 129.2, 128.4, 127.6, 115.2, 109.5, 66.6, 66.1, 58.0, 45.9, 42.9.

HRMS (ESI): *m/z* = calcd. for $C_{18}H_{20}BrN_2O_2^+$: 375.0703, found: 375.0704.

Methyl 4-((2-morpholino-2-oxo-1-phenylethyl)amino)benzoate (5f)



Starting from methyl 4-(benzylideneamino)benzoate (76 mg), HE **1a** (143 mg), and following the general procedure 3, **5f** was obtained as a yellow solid (42 mg, 55 %).

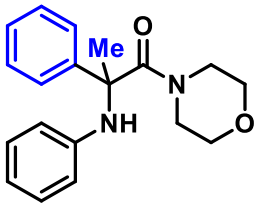
m.p. = 174–176 °C

^{1}H-NMR (300 MHz, $CDCl_3$): δ [ppm] = 7.85 – 7.77 (m, 2H), 7.47 – 7.26 (m, 5H), 6.64 – 6.56 (m, 2H), 6.00 (s, 1H), 5.29 (s, 1H), 3.82 (s, 3H), 3.78 – 3.42 (m, 7H), 3.26 – 3.10 (m, 1H).

^{13}C-{^{1}H}-NMR (75 MHz, $CDCl_3$): δ [ppm] = 168.8, 167.3, 149.8, 137.6, 131.6, 129.3, 128.6, 127.7, 118.9, 112.3, 66.7, 66.1, 57.3, 51.6, 46.0, 43.1.

HRMS (ESI): *m/z* = calcd. for $C_{20}H_{23}N_2O_4^+$: 355.1652, found: 355.1652.

1-Morpholino-2-phenyl-2-(phenylamino)propan-1-one (6a)



Starting from imine **2n** (47 mg, 0.24 mmol, 1.0 equiv.), HE **1a** (114 mg, 0.311 mmol, 1.3 equiv.), and following the general procedure 3 with adjusted scale, **6a** was obtained as a beige solid (12 mg, 17 %).

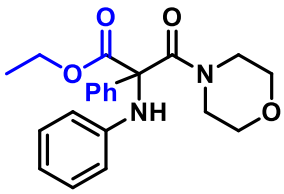
m.p. = 148–150 °C

^{1}H-NMR (300 MHz, $CDCl_3$): δ [ppm] = 7.51 – 7.35 (m, 4H), 7.35 – 7.27 (m, 1H), 7.18 – 7.06 (m, 2H), 6.78 – 6.59 (m, 3H), 5.07 (br. s, 1H, NH), 3.77 – 3.05 (m, 8H), 1.86 (s, 3H).

^{13}C-{^{1}H}-NMR (75 MHz, $CDCl_3$): δ [ppm] = 172.2, 144.9, 143.4, 129.3, 129.2, 127.8, 125.3, 118.4, 115.3, 77.6, 77.2, 76.7, 66.4, 63.9, 45.7 (br. s), 25.7.

HRMS: *m/z* = calcd. for $C_{19}H_{23}N_2O_2^+$: 311.1754, found: 311.1750.

Ethyl 3-morpholino-3-oxo-2-phenyl-2-(phenylamino)propanoate (6b)



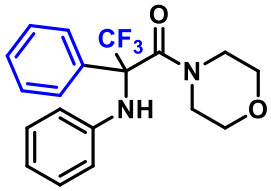
Starting from imine **2o** (76 mg), HE **1a** (143 mg), and following the general procedure 3, **6b** was obtained as a yellow gum (60 mg, 54 %).

^{1}H-NMR (300 MHz, $CDCl_3$): δ [ppm] = 7.68 – 7.65 (m, 2H), 7.34 – 7.29 (m, 3H), 7.11 – 7.06 (m, 2H), 6.75 – 6.72 (m, 1H), 6.62 – 6.59 (m, 2H), 4.28 (dq, 2H, *J* = 7.2, 1.8 Hz), 3.76 – 3.23 (m, 8H), 1.25 (t, *J* = 7.2 Hz, 3H).

^{13}C-{^{1}H}-NMR: (75 MHz, $CDCl_3$): δ [ppm] = 169.9, 166.2, 143.9, 135.7, 129.6, 129.2, 128.9, 128.2, 127.9, 118.6, 114.6, 70.4, 66.4, 63.1, 14.1.

HRMS (ESI): *m/z* = calcd. for $C_{21}H_{25}N_2O_4^+$: 369.1809, found: 369.1803.

1-Morpholino-2-phenyl-2-(phenylamino)-2-(trifluoromethyl)propan-1-one (6c)



Starting from imine **2p** (75 mg), HE **1a** (143 mg), and following the general procedure 3, **6c** was obtained as a pale-yellow solid (52 mg, 48 %).

m.p. = 189–191 °C

^{1}H-NMR (300 MHz, $CDCl_3$): δ [ppm] = 7.59 – 7.38 (m, 5H), 7.23– 7.09 (m, 2H), 6.92 – 6.79 (m, 3H), 5.02 (s, 1H), 3.82 – 2.67 (m, 8H).

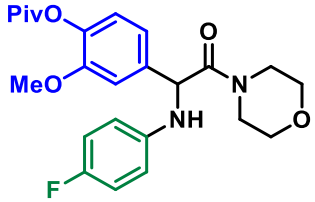
^{13}C-{^{1}H}-NMR (101 MHz, $CDCl_3$, −20 °C): δ [ppm] = 164.9, 143.0, 133.1, 129.8, 129.3, 129.2, 126.1, 123.1 (q, *J* = 288.9 Hz), 120.1, 115.4, 68.8 (q, *J* = 26.0 Hz), 66.3[a], 65.2[a], 46.6[a], 42.8[a].

^{19}F-NMR (565 MHz, $CDCl_3$): δ [ppm]: = −71.02.

HRMS (ESI): *m/z* = calcd. for $C_{19}H_{20}F_3N_2O_2^+$: 365.1471, found: 365.1478.

[a] At room temperature, these signals (corresponding to the carbon atoms of the morpholine moiety) are almost not visible, even when 50 mg of substance is used for the ^{13}C-NMR measurement.

4-(1-((4-Fluorophenyl)amino)-2-morpholino-2-oxoethyl)-2-methoxyphenyl pivalate (7)



Starting from imine **2t** (99 mg), HE **1a** (143 mg), and following the general procedure 3, **7** was obtained as an off-white powder (101 mg, 76 %).

m.p. = 171–172 °C

^{1}H-NMR (300 MHz, $CDCl_3$): δ [ppm] = 7.04 – 6.92 (m, 3H), 6.89 – 6.77 (m, 2H), 6.63 – 6.50 (m, 2H), 5.15 (s, 2H), 3.77 (s, 3H), 3.73 – 3.39 (m, 7H), 3.38 – 3.20 (m, 1H), 1.35 (s, 9H).

^{13}C-{^{1}H}-NMR (75 MHz, $CDCl_3$): *δ* [ppm] = 176.6, 169.2, 156.2 (d, *J* = 236.1 Hz), 152.1, 142.7, 140.3, 136.5, 122.9, 120.1, 115.7 (d, *J* = 22.4 Hz), 114.8 (d, *J* = 7.5 Hz), 111.2, 66.7, 66.2, 58.7, 56.1, 39.1, 27.2.

^{19}F-NMR (565 MHz, $CDCl_3$): δ [ppm]: = −126.96 (tt, *J* = 8.5, 4.2 Hz).

HRMS (ESI): *m/z* = calcd. for $C_{24}H_{30}FN_2O_5^+$: 445.2133, found: 445.2130.

Large-Scale Reaction and One-Pot Experiments

- **Large-scale synthesis of 3a**

A 30 mL glass vial was charged with a magnetic stir bar, benzylideneaniline (272 mg, 1.50 mmol, 1.0 equiv.), Hantzsch ester **1a** (714 mg, 1.95 mmol, 1.3 equiv.) and 3DPAFIPN (24 mg, 38 µmol, 2.5 mol%), and closed with a rubber septum. After evacuating and flushing with nitrogen three times, dry, degassed CH_2Cl_2 (15 mL) was added, resulting in a bright yellow solution. $BF_3{\cdot}OEt_2$ (190 µL, 1.50 mmol, 1.0 equiv.) was added in one portion, during which the solution turned orange. The vial was shaken, and the mixture was irradiated with blue light (450 nm) for 16 hours at room temperature. The resultant yellow solution was washed with water (20 mL) and the aqueous phase was extracted with CH_2Cl_2 (3× 20 mL). The combined organic phases were dried over Na_2SO_4, filtered, and concentrated *in vacuo*, yielding a dark yellow, almost black gum as residue. The crude product was purified by silica column chromatography (pentane/ethyl acetate 9:1, then 8:2), yielding **3a** as a pale-yellow powder (311 mg, 1.05 mmol, 70 %).

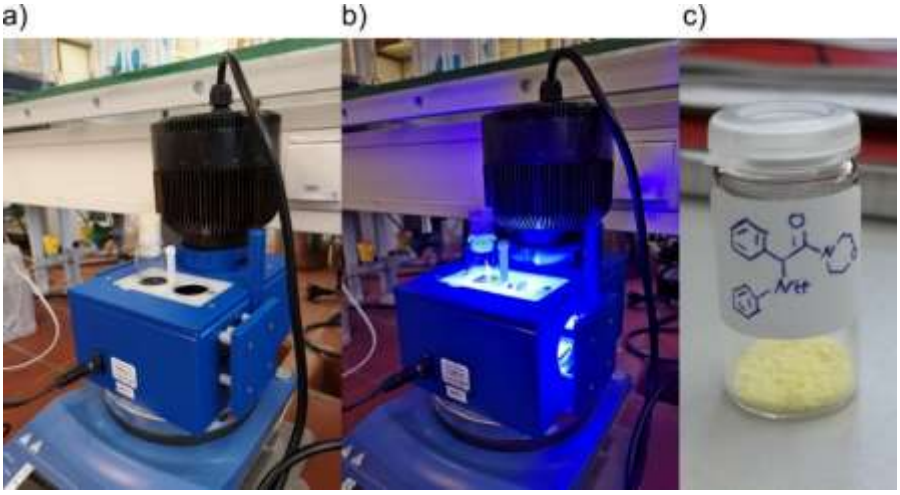
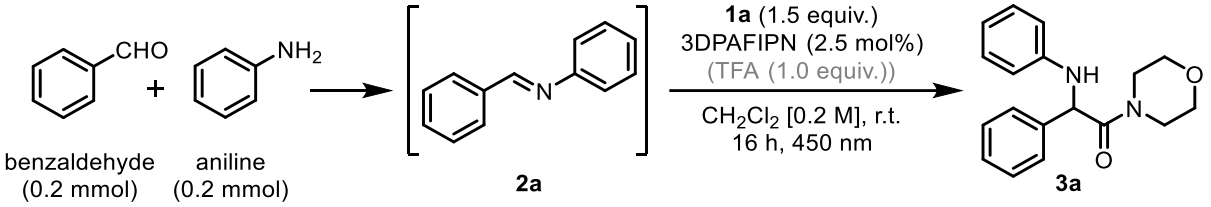


Figure 3. *a) Experimental setup of the large-scale synthesis of **3a** with the light turned off. b) With the light turned on. c) Ca. 300 mg of **3a** as a pale-yellow powder.*

- **One-pot experiments**

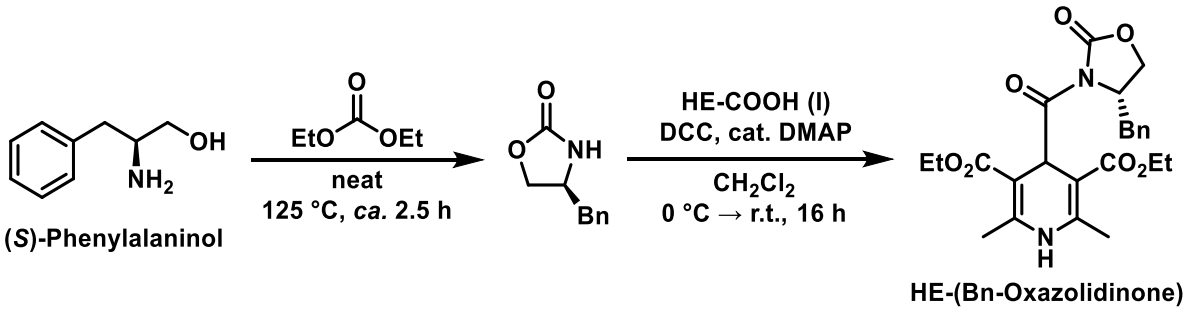


Experiment 1: Benzaldehyde (20 µL, 1.0 equiv.), aniline (18 µL, 1.0 equiv.) and 3DPAFIPN (3.2 mg, 2.5 mol%) were dissolved in CH_2Cl_2 (1 mL, 0.2 M) over activated 4 Å molecular sieves. The reaction was stirred for 1 hour in the dark, then transferred to another vial containing **1a** (104 mg, 1.5 equiv.) under nitrogen. The mixture was irradiated for 16 h. Yield was determined using ^{1}H-NMR based on 1,3,5-trimethoxybenzene as external standard. Yield: 30 %.

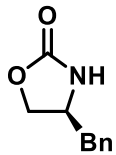
Experiment 2: Benzaldehyde (20 µL, 1.0 equiv.), aniline (18 µL, 1.0 equiv.) and 3DPAFIPN (3.2 mg, 2.5 mol%) were solubilized in CH_2Cl_2 (1 mL, 0.2 M). The reaction was stirred for 1 hour in the dark, then transferred to another vial containing **1a** (104 mg, 1.5 equiv.) under nitrogen. Trifluoroacetic acid (15 µL, 1.0 equiv.) was added and the mixture was irradiated for 16 h. Yield was determined using ^{1}H-NMR based on 1,3,5-trimethoxybenzene as external standard. Yield: 50 %.

Syntheses of Other Starting Materials

Diethyl (*S*)-4-(4-benzyl-2-oxooxazolidine-3-carbonyl)-2,6-dimethyl-1,4-dihydropyridine-3,5-dicarboxylate (HE-(Bn-Oxazolidinone))



(*S*)-4-Benzyl-2-oxazolidinone

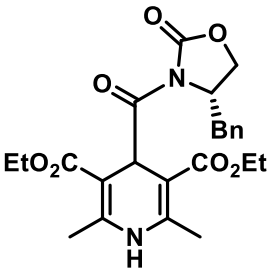


A mixture of (*S*)-phenylalaninol (1.00 g, 6.61 mmol, 1.0 equiv.), anhydrous potassium carbonate (935 mg, 1.0 equiv.) and diethyl carbonate (1.60 mL, 13.2 mmol, 2.0 equiv.) was heated to 125 °C in a distillation apparatus fitted with a 10 cm Vigreux column until no more ethanol was obtained in the receiving flask (*ca.* 2.5 hours). The mixture was diluted with CH_2Cl_2 (20 mL), washed with water (2× 10 mL) and brine (10 mL), dried over Na_2SO_4 and filtered. The solvent was removed *in vacuo* and the residue purified by flash column chromatography on silica (pentane/ethyl acetate) to yield (*S*)-4-benzyl-2-oxazolidinone as a colorless solid (876 mg, 4.94 mmol, 75 %).

^{1}H-NMR (300 MHz, $CDCl_3$): δ [ppm] = 7.38 – 7.23 (m, 3H), 7.21 – 7.14 (m, 2H), 5.53 (s, 1H), 4.46 (t, J = 8.1 Hz, 1H), 4.19 – 4.05 (m, 2H), 2.88 (d, J = 6.7 Hz, 2H).

X.-Y. Tian, J.-W. Han, Q. Zhao, H. N. C. Wong, *Org. Biomol. Chem.* **2014**, *12*, 3686–3700.

HE-(Bn-Oxazolidinone)



A suspension of (*S*)-4-benzyloxazolidin-2-one (494 mg, 2.79 mmol, 1.0 equiv.), HE-COOH **I** (1.09 g, 3.67 mmol, 1.3 equiv.), and 4-(di-methylamino)-pyridine (51.9 mg, 0.425 mmol, 15 mol%) in dry CH_2Cl_2 (10 mL) was cooled to 0 °C and dicyclohexylcarbodiimide (749 mg, 3.63 mmol, 1.3 equiv.) was added in one portion. The mixture was stirred at 0 °C for 10 minutes, after which it was warmed to room temperature and stirred for 16 hours. The bright-yellow suspension was filtered, the filter cake was washed with CH_2Cl_2 (10 mL) and the filtrate was washed with sat. aq. $NaHCO_3$ (10 mL). The organic phase was dried over Na_2SO_4, filtered and concentrated *in vacuo*. The residue was purified by column chromatography on silica (pentane/ethyl acetate 7:3, two columns were necessary) to yield HE-(Bn-Oxazolidinone) as a pale-brown solid (158 mg, 0.346 mmol, 12 %).

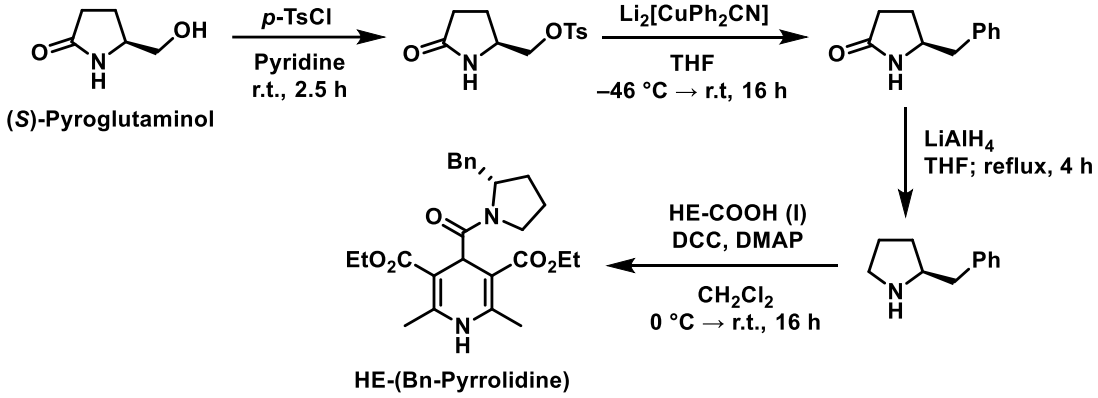
m.p. = 140–141 °C

^{1}H-NMR (300 MHz, $CDCl_3$): δ [ppm] = 7.30 – 7.24 (m, 5H), 6.06 (br. s, 1H, NH), 6.00 (s, 1H), 4.68 – 4.61 8m, 1H), 4.22 – 4.08 8m, 6H), 3.37 (dd, *J* = 13.1, 3.1 Hz, 1H), 2.62 (dd, *J* = 13.1, 10.7 Hz, 1H), 2.28 (d, *J* = 4.5 Hz, 6H), 1.25 (dt, *J* = 11.9, 7.1, 6H).

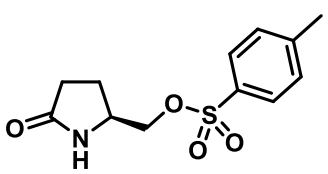
^{13}C-{^{1}H}-NMR (75 MHz, $CDCl_3$): δ [ppm] = 166.9, 152.3, 135.9, 129.3, 128.9, 127.1, 65.5, 60.13, 60.07, 56.3, 38.6, 37.9, 19.7, 19.5, 14.3, 14.1.

HRMS (ESI): *m/z* = calcd. for $C_{24}H_{28}N_2NaO_7^+$: 479.1789, found: 479.1783.

Diethyl (*S*)-4-(2-benzylpyrrolidine-1-carbonyl)-2,6-dimethyl-1,4-dihydropyridine-3,5-dicarboxylate (HE-(Bn-Pyrrolidine))



(*S*)-(5-Oxopyrrolidin-2-yl)methyl 4-toluenesulfonate

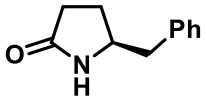


(*S*)-Pyroglutaminol (600 mg, 5.21 mmol, 1.0 equiv.) was dissolved in pyridine (4.5 mL) and *p*-toluenesulfonyl chloride (1.49 g, 7.82 mmol, 1.5 equiv.) was added. The mixture was stirred for 2.5 hours at room temperature, after which water (3 mL) was added and the mixture stirred for additional 30 minutes. Then aq. HCl (2 M, 20 mL) was added and the organics were extracted with CH_2Cl_2 (8× 30 mL). The combined organic phases were dried over Na_2SO_4, filtered and concentrated *in vacuo*. The solid residue was recrystallized from CH_2Cl_2/Hexane to yield (*S*)-(5-oxopyrrolidin-2-yl)methyl 4-toluene-sulfonate as a pinkish solid (565 mg, 2.10 mmol, 40 %).

^{1}H-NMR (300 MHz, $CDCl_3$): δ [ppm] = 7.82 – 7.75 (m, 2H), 7.39 – 7.33 (m, 2H), 6.00 (br. s, NH), 4.05 (dd, *J* = 9.4, 3.3 Hz), 3.94 – 3.83 (m, 2H), 2.46 (s, 3H), 2.38 – 2.20 (m, 3H), 1.80 – 1.75 (m, 1H).

S. Lebrun, A. Couture, E. Deniau, P. Grandclaudon, *Tetrahedron Asymmetry* **2003**, *14*, 2625–2632.

(*S*)-5-Benzyl-2-pyrrolidinone

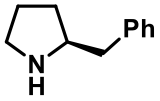


A suspension of cuprous cyanide (dried twice azeotropically with toluene, 505 mg, 5.64 mmol, 2.7 equiv.) in dry THF (5 mL) was cooled to –84 °C using an ethyl acetate/liquid N_2 bath and phenyllithium (1.9 M in dibutyl ether, 5.90 mL, 11.2 mmol, 5.4 equiv.) was added slowly. The mixture was stirred for 5 minutes at –84 °C, after which it was warmed to –46 °C using an acetonitrile/liquid N_2 bath and stirred for further 5 minutes. A suspension of (*S*)-(oxopyrrolidin-2-yl)methyl 4-toluenesulfonate (557 mg, 2.07 mmol, 1.0 equiv.) in dry THF (5 mL) was cannulated to the mixture which was then stirred for 3 hours at –46 °C and then overnight at room temperature. The clear, yellow mixture was poured into NH_4Cl/NH_3 buffer (*ca.* 20 mL, adjusted to pH 8 by adding dilute aq. NaOH to sat. aq. NH_4Cl) and the organic layer was diluted with ethyl acetate (20 mL) and washed with water (2× 20 mL). The combined deep blue aqueous layers were extracted with ethyl acetate (2× 30 mL) and the combined organic phases were dried over Na_2SO_4, filtered and concentrated *in vacuo*. The residue was purified by column chromatography on silica (100% pentane, then 100% ethyl acetate) to yield (*S*)-5-benzyl-2-pyrrolidinone as a colorless solid (257 mg, 1.47 mmol, 71 %).

^{1}H-NMR (300 MHz, $CDCl_3$): δ [ppm] = 7.36 – 7.21 (m, 3H), 7.20 – 7.14 (m, 2H), 5.66 (br. s, 1H, NH), 3.94 – 3.83 (m, 1H), 2.86 (dd, *J* = 13.4, 5.3 Hz, 1H), 2.70 (dd, *J* = 13.4, 8.4 Hz, 1H), 2.41 – 2.21 (m, 3H), 1.91 – 1.79 (m, 1H).

S. Lebrun, A. Couture, E. Deniau, P. Grandclaudon, *Tetrahedron Asymmetry* **2003**, *14*, 2625–2632.

(*S*)-2-Benzylpyrrolidine

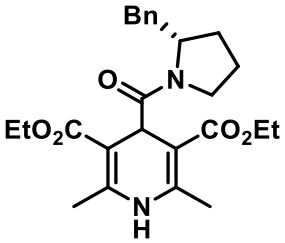


A solution of (*S*)-5-benzyl-2-pyrrolidinone (251 mg, 1.43 mmol, 1.0 equiv.) in dry THF (5 mL) was cooled to 0 °C and a suspension of lithium aluminium hydride (108 mg, 2.85 mmol, 2.0 equiv.) in dry THF (5 mL) was added dropwise. After stirring for 10 more minutes at 0 °C the mixture was refluxed for 4 hours. The mixture was then cooled to 0 °C and water (0.1 mL), then 15 % aq. NaOH (0.1 mL), then water (0.3 mL) were added under vigorous stirring. The mixture was stirred for 15 minutes at room temperature, then Na_2SO_4 was added and the mixture was stirred for further 15 minutes, upon which it was filtered and concentrated *in vacuo*. The residue was purified by column chromatography on silica (CH_2Cl_2/MeOH 20:1 containing 1 % of NEt_3) to yield (*S*)-2-benzylpyrrolidine as a yellow liquid (175 mg, 0.997 mmol, 70 %).

^{1}H-NMR (300 MHz, $CDCl_3$): δ [ppm] = 7.33 – 7.17 (m, 5H), 3.32 – 3.19 (m, 1H), 3.06 (ddd, *J* = 10.3, 7.6, 5.1 Hz, 1H), 2.90 – 2.74 (m, 3H), 2.31 (br. s, 1H, NH), 1.91 – 1.65 (m, 3H), 1.48 – 1.37 (m, 1H).

S. Lebrun, A. Couture, E. Deniau, P. Grandclaudon, *Tetrahedron Asymmetry* **2003**, *14*, 2625–2632.

HE-(Bn-Pyrrolidine)



A mixture of HE-COOH **I** (288 mg, 0.968 mmol, 1.0 equiv.), (*S*)-2-benzylpyrrolidine (170 mg, 0.968 mmol, 1.0 equiv.) and 4-(dimethylamino)pyridine (118 mg, 0.968 mmol, 1.0 equiv.) in dry CH_2Cl_2 (5 mL) was cooled to 0 °C and dicyclohexylcarbodiimide (200 mg, 0.968 mmol, 1.0 equiv.) was added in one portion. The mixture was stirred at 0 °C for 30 minutes, after which it was slowly warmed to room temperature and stirred overnight. The bright yellow suspension was stored at –20 °C for several hours to precipitate as much dicyclohexylurea as possible, then filtered cold. The filtrate was washed with aq. HCl (1 M, 15 mL) and water (15 mL) and the combined aqueous phases were extracted with CH_2Cl_2 (3× 15 mL). The organic phases were combined, dried over Na_2SO_4, filtered, and concentrated *in vacuo*. The solid residue was purified by column chromatography on silica (pentane/ethyl acetate 7:3 to 6:4, each containing 0.5 % of AcOH) to yield HE-(Bn-Pyrrolidine) as a yellow solid (186 mg, 0.422 mmol, 44 %).

m.p. = 117–119 °C

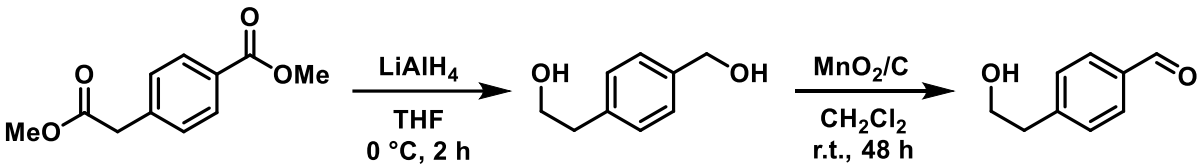
^{1}H-NMR (300 MHz, $CDCl_3$): δ [ppm] = 8.49 (s, 1H, NH), 7.35 – 7.14 (m, 5H), 4.84 (s, 1H), 4.31 – 4.11 (m, 5H), 4.09 – 3.96 (m, 2H), 3.12 (dd, *J* = 13.0, 3.2 Hz, 1H), 2.49 (dd, *J* = 12.9, 9.4 Hz, 1H), 2.31 (s, 3H), 2.24 (s, 3H), 1.91 – 1.65 (m, 4H), 1.27 (t, *J* = 7.1 Hz, 6H).

^{13}C-{^{1}H}-NMR (75 MHz, $CDCl_3$): δ [ppm] = 174.1, 167.9, 148.3, 147.9, 139.5, 129.6, 128.4, 126.2, 98.8, 98.7, 77.2, 60.0, 59.9, 59.3, 47.4, 39.8, 38.9, 28.6, 24.1, 19.7, 19.5, 14.73, 14.68.

HRMS (ESI): *m/z* = calcd. for $C_{25}H_{33}N_2O_5^+$: 441.2389, found: 441.2387.

$[\boldsymbol{\alpha}]_{\mathbf{D}}^{\mathbf{20}}$ = –26.2° (*c* 0.455, $CHCl_3$).

4-(2-Hydroxyethyl)benzaldehyde



Synthesis of activated MnO_2 on carbon (MnO_2/C):

In a 600 mL beaker, potassium permanganate (20.0 g, 127 mmol, 1.0 equiv.) was dissolved in water (250 mL) and the solution was brought to a boil. Activated carbon (6.25 g, 520 mmol, 4.1 equiv.) was added portionwise under strong stirring and mild gas evolution. The mixture was boiled until the purple color disappeared (*ca.* 20–30 min) and the mixture had turned brown. The beaker was taken off the hot plate and left at room temperature for 10-15 min upon which it was filtered warm. The filter cake was dried at 105 °C for 18 hours to yield 18.5 g of MnO_2/C as a lightweight black powder.

Synthesis of 4-(2-hydroxyethyl)benzyl alcohol:

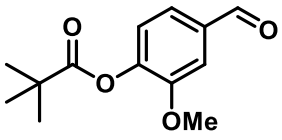
A solution of dimethyl homoterephthalate (2.00 g, 9.61 mmol, 1.0 equiv.) in dry THF (10 mL) was cooled to 0 °C and a suspension of $LiAlH_4$ (567 mg, 14.8 mmol, 1.5 equiv.) in dry THF (15 mL) was added dropwise. After stirring the mixture for 2 hours at 0 °C, water (0.6 mL), then aq. NaOH (15 %, 0.6 mL), then water (1.8 mL) were added at 0 °C under vigorous stirring.

After 15 minutes of stirring at room temperature, $MgSO_4$ was added and the mixture was stirred for another 15 minutes, followed by filtration. The filtrate was washed with brine (10 mL) and the organic phase was dried over $MgSO_4$ and filtered. Removal of the solvent *in vacuo* yielded crude 4-(2-hydroxyethyl)benzyl alcohol as a yellow oil, which was used without characterization or further purification (*ca.* 1.40 g).

Synthesis of 4-(2-hydroxyethyl)benzaldehyde:

The oil was dissolved in CH_2Cl_2 (50 mL) and MnO_2/C (18.5 g) was added, followed by vigorous stirring at room temperature for 48 hours (monitored by GC-MS). The mixture was filtered and the filter cake was washed thoroughly with CH_2Cl_2 and ethyl acetate. Removal of the solvent *in vacuo* yielded 4-(2-hydroxyethyl)benzaldehyde as a yellow oil (*ca.* 502 mg), which was used without further purification in the synthesis of **2m**.

4-Formyl-2-methoxyphenyl pivalate

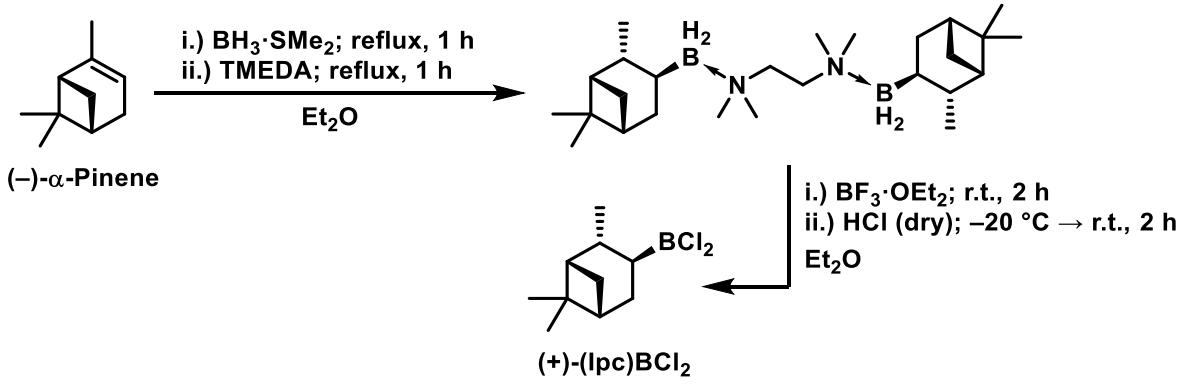


Vanillin (761 mg, 5.00 mmol, 1.0 equiv.) was dissolved in dry pyridine (10 mL). The mixture was cooled to 0 °C and pivaloyl chloride (1.21 g, 1.24 mL, 10.0 mmol, 2.0 equiv.) was added dropwise. The resultant greyish suspension was stirred for 30 minutes at 0 °C, then warmed to room temperature and stirred for further 60 minutes. The mixture was diluted with ethyl acetate and washed with aq. HCl (1 M, 4× 10 mL), sat. aq. $NaHCO_3$ (10 mL), aq. NaOH (0.5 M, 10 mL) and water (10 mL). The organic phase was dried over $MgSO_4$, filtered and concentrated *in vacuo* to yield 4-formyl-2-methoxyphenyl pivalate as a yellow powder (734 mg, 3.11 mmol, 62 %).

^{1}H-NMR (300 MHz, $CDCl_3$): δ [ppm] = 9.94 (s, 1H), 7.50 – 7.44 (m, 2H), 7.21 – 7.16 (m, 1H), 3.88 (s, 3H), 1.38 (s, 9H).

W. Gao, Q. Li, J. Chen, Z. Wang, C. Hua, *Molecules* **2013**, *18*, 15613–15623.

Monoisopinocampheylboron dichloride



Synthesis of the monoisopinocampheylborane TMEDA complex:

To a solution of borane dimethylsulfide (401 mg, 500 µL, 5.26 mmol, 1.0 equiv.) in dry diethyl ether (5 mL) was added dropwise (−)-□-pinene (1.65 g, 1.92 mL, 12.0 mmol, 2.3 equiv.) so as to maintain gentle reflux, after which the mixture was refluxed for 1 hour. To the cooled down mixture was added tetramethylenediamine (306 mg, 0.39 mL, 2.62 mmol, 0.5 equiv.) and the mixture was subsequently refluxed for 1 hour. After the mixture had cooled to room temperature, a slow stream of nitrogen was passed through the flask to evaporate a small amount of

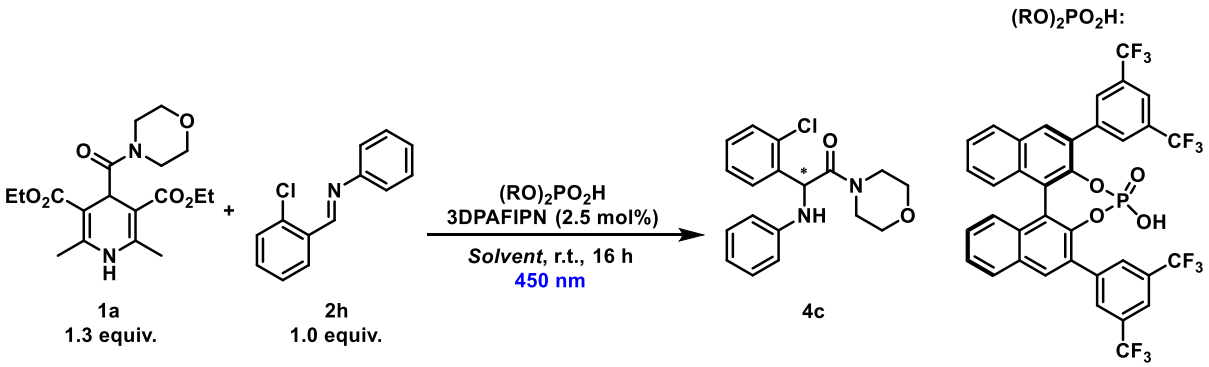
the diethyl ether to generate seed crystals on the inner walls. The mixture was stored in the freezer overnight to induce complete crystallization. The solidified mixture was broken up using a glass rod and washed several times with cold pentane to yield the monoisopinocampheylborane TMEDA complex as a colorless powder which was used in the next step without further purification or characterization (259 mg, 0.621 mmol, 24 %).

Synthesis of monoisopinocampheylboron dichloride:

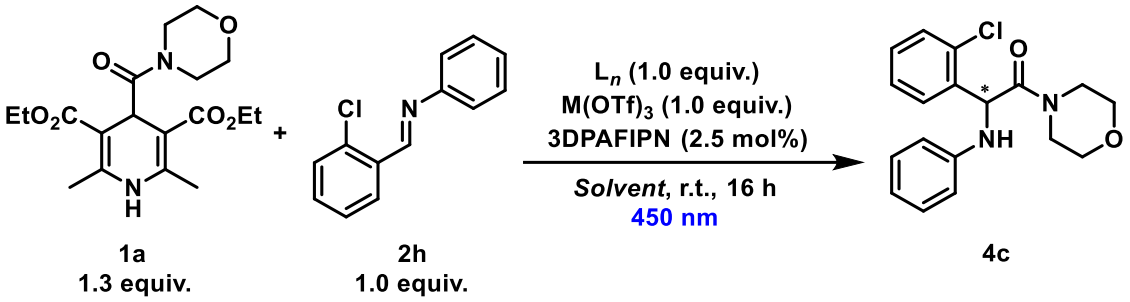
To a solution of the monoisopinocampheylborane TMEDA complex (259 mg, 0.621 mmol, 1.0 equiv.) in dry diethyl ether (5 mL) was added boron trifluoride diethyl etherate (171 mg, 0.15 mL, 1.22 mmol, 1.96 equiv.), after which the mixture was stirred at room temperature for 2 hours, during which a colorless precipitate formed. The suspension was filtered and the filtrate containing the monoisopinocampheylborane was cooled down to –20 °C using an ice/salt bath. A solution of HCl in diethyl ether (1.0 M, 2.48 mL, 2.48 mmol, 4.0 equiv.) was added dropwise under gas evolution. After complete addition, the mixture was stirred for 10 minutes at –20 °C, then for 2 hours at room temperature. The solvent was subsequently removed *in vacuo* at 0 °C to yield ether-free monoisopinocampheylboron dichloride as a viscous oil which was used without further purification (234 mg, 1.07 mmol, 86 %). The identity of the product was confirmed by a signal at 61 ppm in the ^{11}B-NMR spectrum (193 MHz, dry $CDCl_3$).

H. C. Brown, P. V. Ramachandran, J. Chandrasekharan, *Heteroat. Chem.* **1995**, *6*, 117–131.

Chiral Experiments



Solvent	Equiv. of $(RO)_2PO_2H$	Yield of 4c [%]	*ee* [%]
Toluene	1.0	80	10
Toluene	0.2	61	10
CH_2Cl_2	1.0	52	0

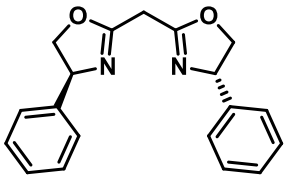


1a
1.3 equiv.

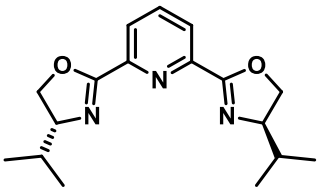
2h
1.0 equiv.

4c

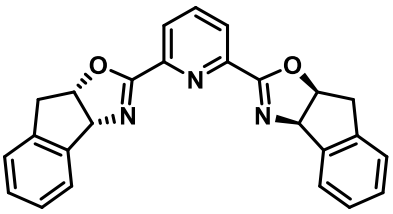
L_1:



L_2:

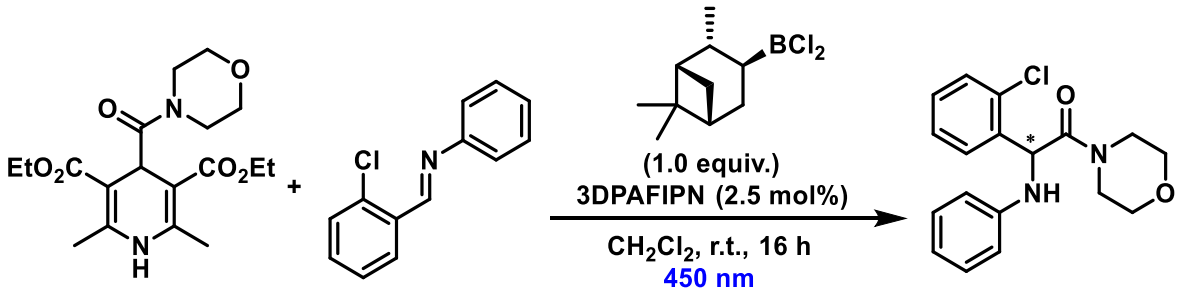


L_3:



Note: $Sc(OTf)_3$ and $Yb(OTf)_3$ are sparingly soluble in aromatic or apolar solvents, also under irradiation.

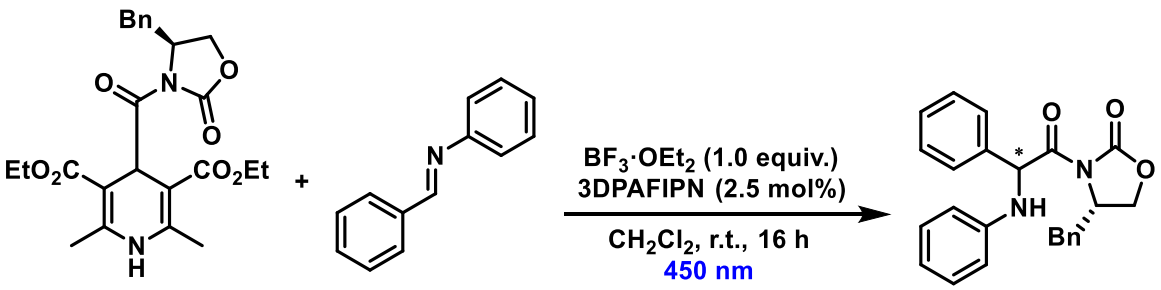
M	L_n	Solvent	Yield of 4c [%]	*ee* [%]
Sc	L_1	CH_2Cl_2	39	0
Sc	L_2	MeCN	59	0
Yb	L_3	CH_2Cl_2	34	0
Yb	L_3	*o*-Xylene	0	–



1a
1.3 equiv.

2h
1.0 equiv.

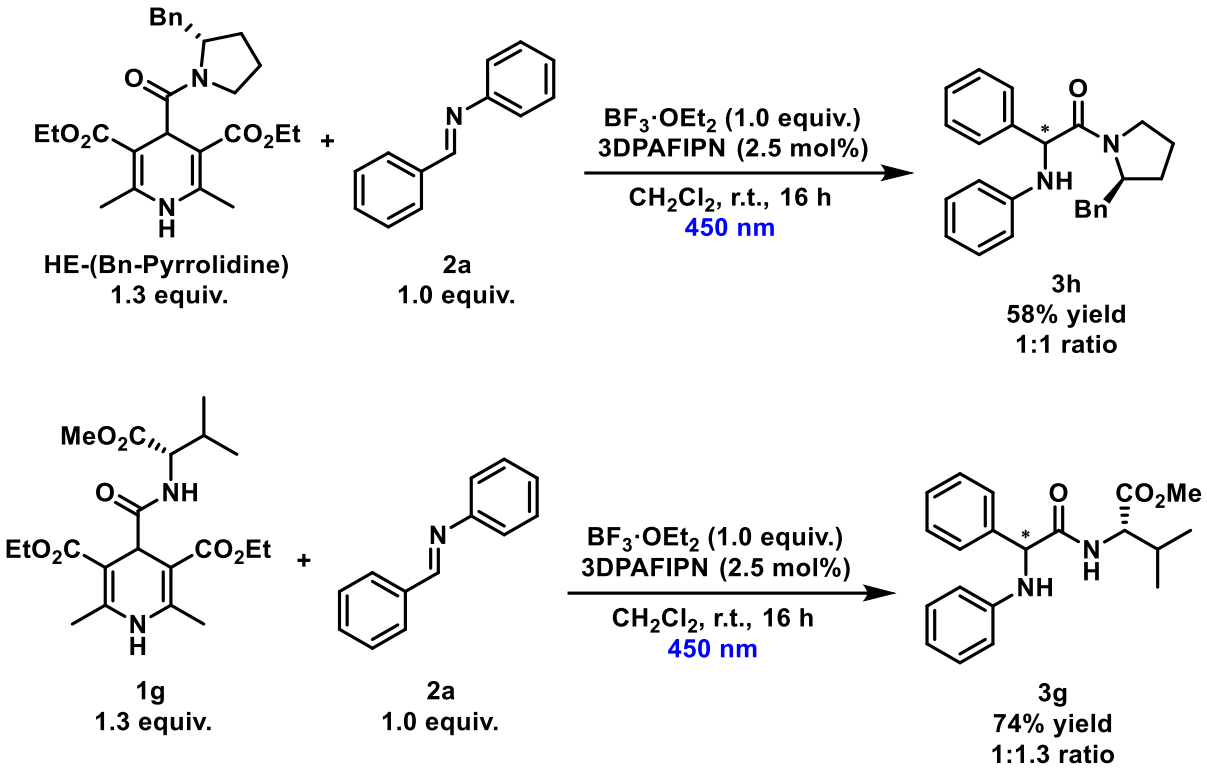
4c
24% yield
0% *ee*



HE-(Bn-Oxazolidinone)
1.3 equiv.

2a
1.0 equiv.

0% yield



Mechanistic Experiments

Fluorescence-Quenching Experiments

The stock solutions were prepared by dissolving 0.61 mg of 3DPAFIPN in 100 mL of DMSO (0.01 mM) and by dissolving 90.2 mg of benzylideneaniline **2a** in 25.0 mL of the previously prepared 3DPAFIPN solution (0.02 M of the imine). All stock solutions were degassed for 10 minutes by purging with argon and transferred to the cuvette through the rubber septum fitted with an argon-filled balloon.

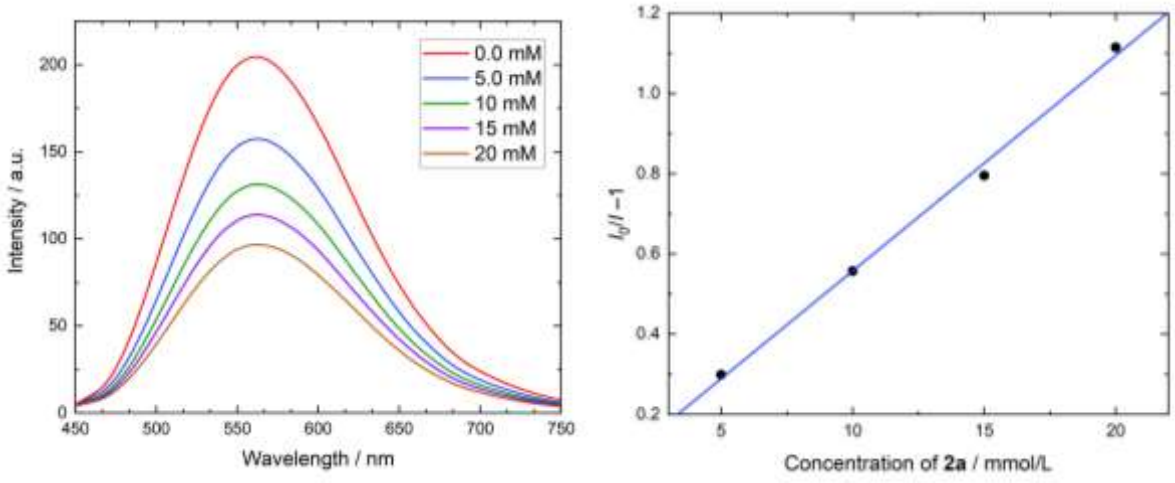
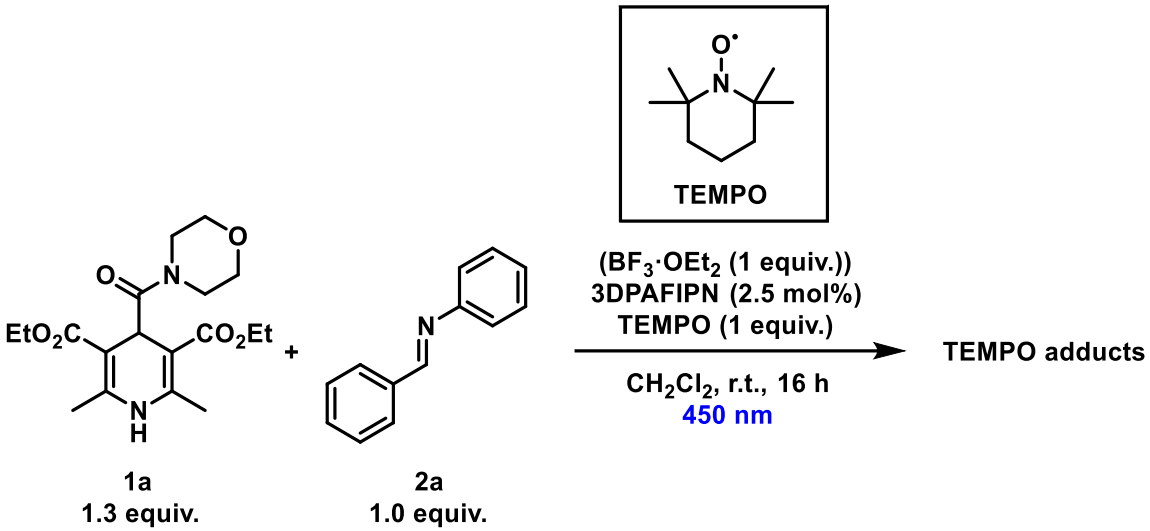


***Figure 4**. Left: The fluorescence intensity of a 3DPAFIPN solution (0.01 mM in DMSO) containing increasing amounts of benzylideneaniline **2a** as the quencher. Excitation wavelength: 400 nm. Right: STERN-VOLMER plot of the above data (y = 0.05369·x + 0.02059, R^2 = 0.9960). The quenching constant K_q was determined using the STERN-VOLMER equation $K_{sv} = K_q \cdot \tau$ and a lifetime of τ = 4.2 ns for 3DPAFIPN as $K_q = 1.27 \cdot 10^{10}$ L·mol^{-1}·s^{-1}.*

Radical-Trapping Experiments

The radical trapping experiments were conducted analogously to general procedure 3 on a 0.1 mmol scale in the presence of 1 equiv. of TEMPO. Experiments were conducted in the presence and absence of the Hantzsch ester and both in the presence or absence of $BF_3{\cdot}OEt_2$. The reaction mixtures were analyzed *via* GC-MS after quenching the mixtures containing $BF_3{\cdot}OEt_2$ as described in general procedure 3.



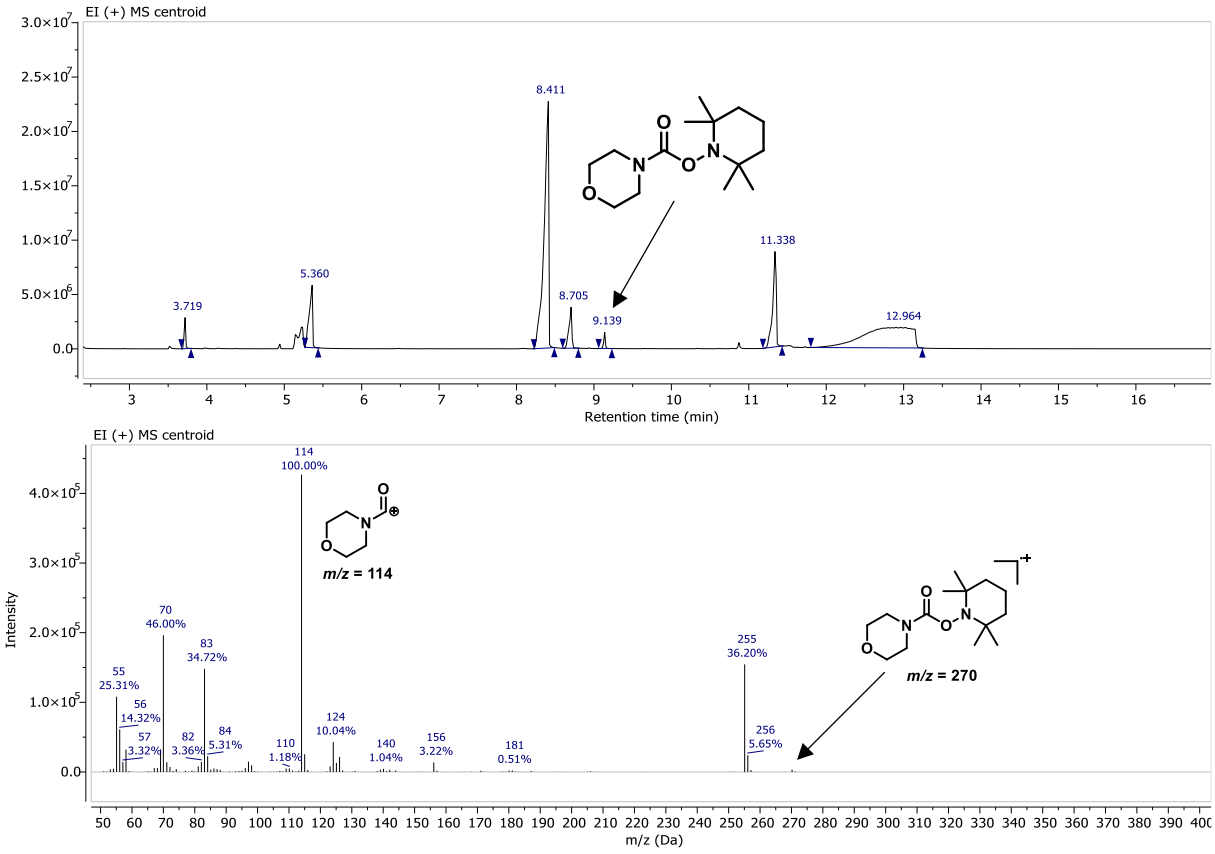


Figure 5. *GC-MS chromatogram of the crude reaction mixture and the EI-mass spectrum of the detected TEMPO adduct.*

UV-Vis Experiments

The samples were prepared by diluting 1.5 mL of a 0.06 M stock solution of the respective substance in CH_2Cl_2 with 1.5 mL of CH_2Cl_2 in a quartz cuvette. For the mixtures of both substrates, 1.5 mL of both 0.06 M stock solutions were combined. The samples containing BF_3 were prepared in a quartz cuvette fitted with a rubber septum and an argon balloon by adding 1.0 eq of $BF_3{\cdot}OEt_2$ (11 µL) to the solutions. To all solutions was added 0.1 mL of DMSO to solubilize precipitates, which results in a 0.028 M solution in CH_2Cl_2/DMSO 15/1.

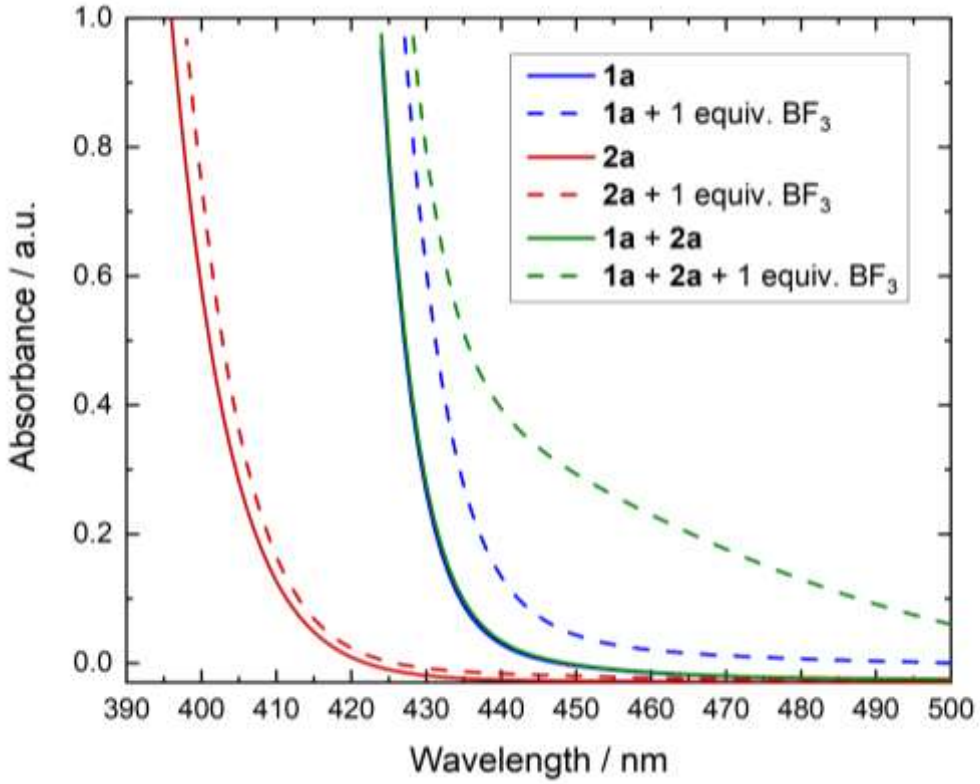


***Figure S5**. The UV-Vis absorption spectra of HE **1a**, benzylideneaniline **2a** and **1a** + **2a** (1:1) without $BF_3{\cdot}OEt_2$ as well as **1a**, **2a** and **1a** + **2a** (1:1) with 1 equivalent of $BF_3{\cdot}OEt_2$ each, all 0.028 M in CH_2Cl_2/DMSO 15/1, in the range of 390–500 nm.*

Quantum Yield Measurements

The quantum yield (QY) Φ was measured in a self-built, shaded catalysis setup. The illumination was performed with a Thorlabs SOLIS-445C (High-Power LED for Microscopy, 445 nm (Royal Blue), 5.4 W (Min)) and a constant current. The area-dependent illumination power P_0 was measured at the spot of the reaction quartz cuvette with a Thorlabs S120C (Standard Photodiode Power Sensor, Si, 400–1100 nm, 50 mW). After the reaction was stopped, the absorption A_λ was measured at the excitation wavelength λ by an Agilent Cary 5000.

$$\Phi = \frac{r \cdot hc}{(1 - 10^{-A_\lambda}) \cdot P_0 \cdot \lambda} \quad (1)$$

The QY was calculated with the production rate r (molecules/s), Planck's constant h and the speed of light c.

Experiment 1: The reaction between **1a** and **2a** was set up under standard conditions (0.3 mmol scale) following general procedure 3. The cuvette was irradiated for 262 minutes

and the yield of formed product was determined *via* ^{1}H-NMR using 1,3,5-trimethoxybenzene as external standard. Yield of **3a** after 262 minutes was of 26% (0.077 mmol). According to equation 1, $\Phi = 0.86\%$

Experiment 2: The reaction between **1a** and **2a** was set up under standard conditions (0.3 mmol scale) following general procedure 3. The cuvette was irradiated for 16 h and the yield of formed product was determined *via* ^{1}H-NMR using 1,3,5-trimethoxybenzene as external standard. Yield of **3a** after 16 h was of 79% (0.217 mmol). According to equation 1, $\Phi = 0.66\%$

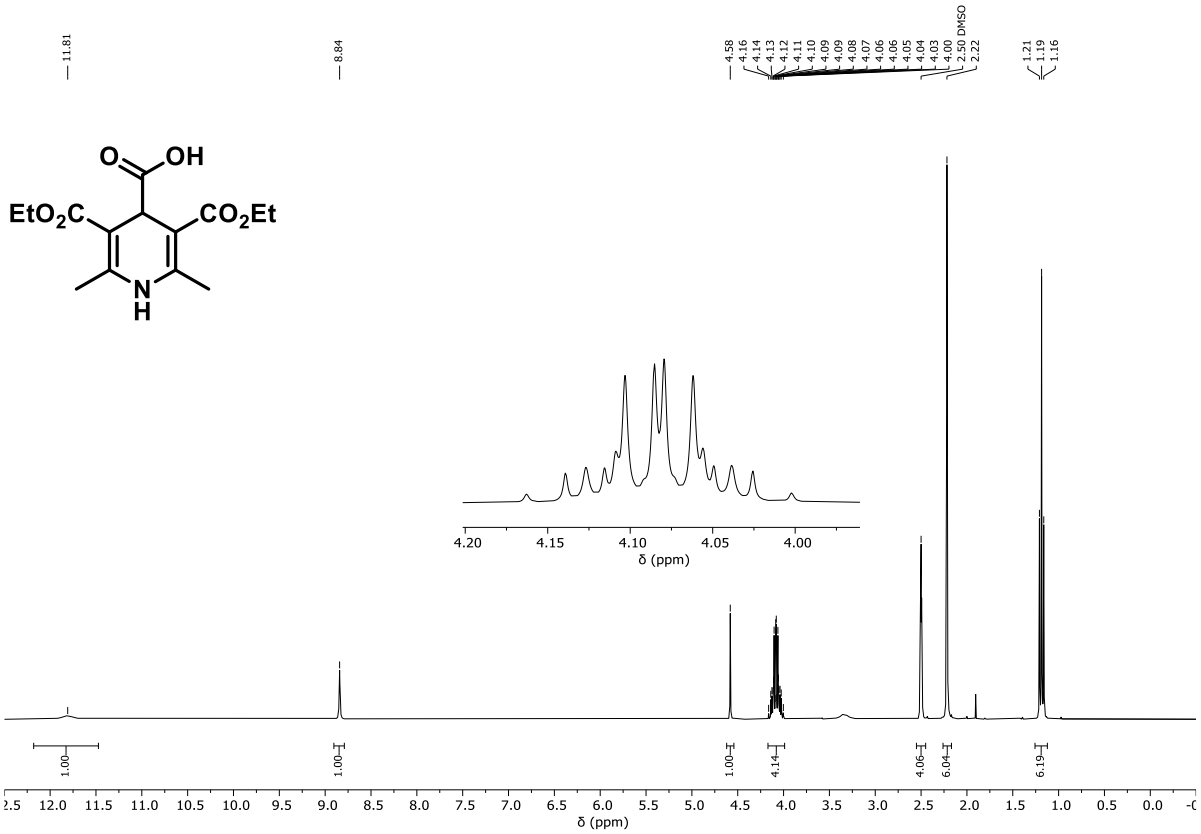
The obtained QYs could be improved by a decrease of the illumination power and time. For the QY experiments a power was set which corresponds to the power in the “normal” reactor. Due to saturation of the excited states in the photocatalyst, it might be possible that some photons are not absorbed. Therefore, a smaller power can still produce the same yield of product, while obtaining a larger QY. Additionally, the time is considered in the calculation. If the reaction reaches a saturation in the production formation, the QY is decreased. Thus, the product formation should be monitored or determined and/or the QY should be measured for several reaction times.

With a QY of less than 1 %, the presence of radical chain mechanisms seems unlikely. The low value accounts for a non-efficient process where few of the absorbed photons are effective in the product formation.

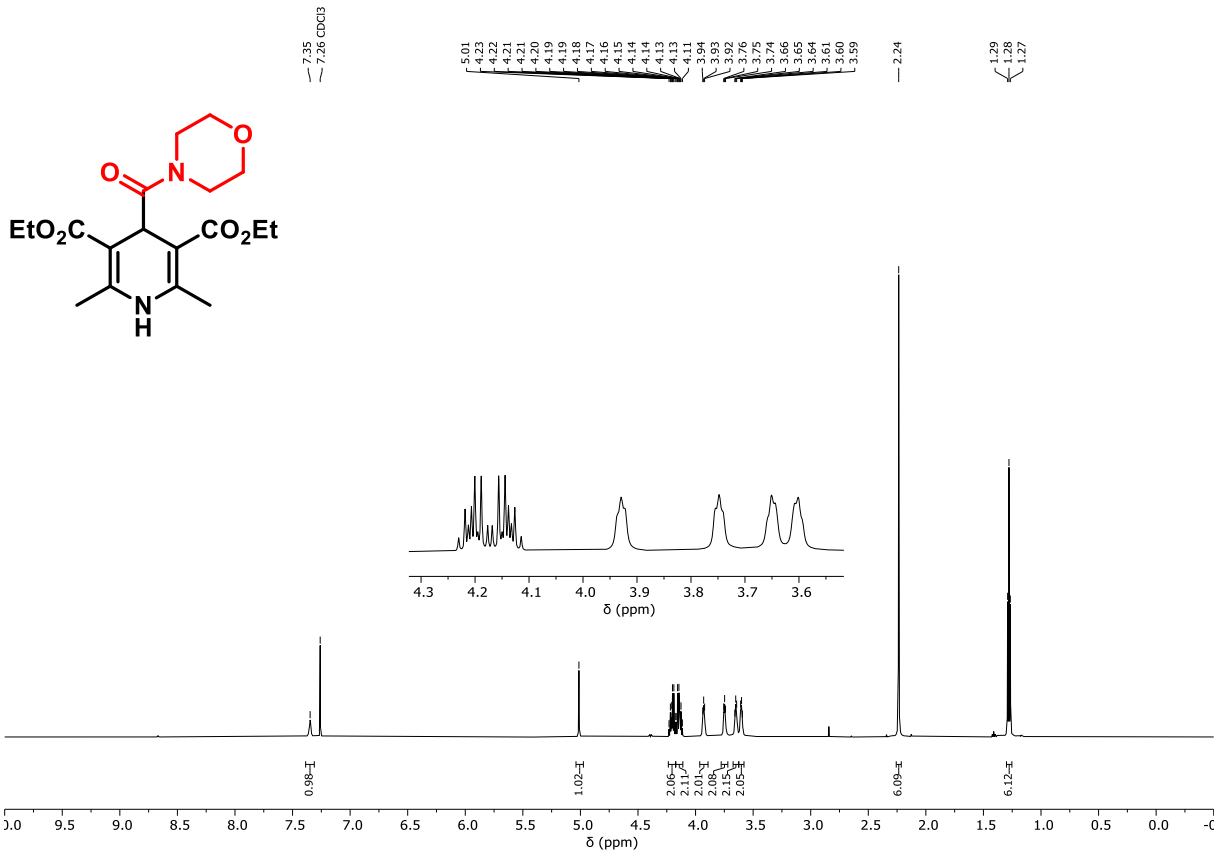
Literature for the development of the QY equation (1):

a) H. Kisch, D. Bahnemann, *J. Phys. Chem. Lett.* **2015**, *6*, 1907; b) Z. Chen, H. N. Dinh, E. Miller, *Photoelectrochemical water splitting*. *Standards, experimental methods, and protocols*, Springer, New York, Heidelberg, Dordrecht, London, **2013**.

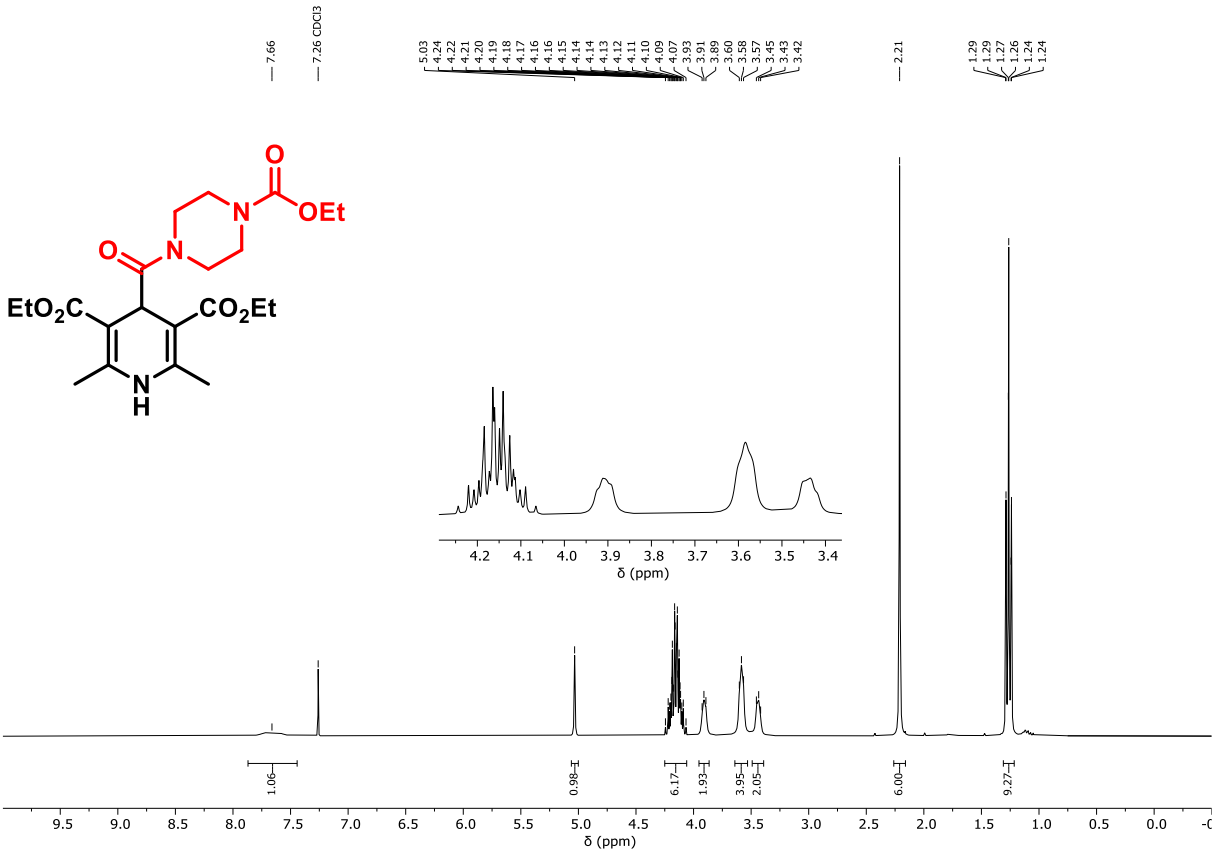
NMR Spectra of all Compounds



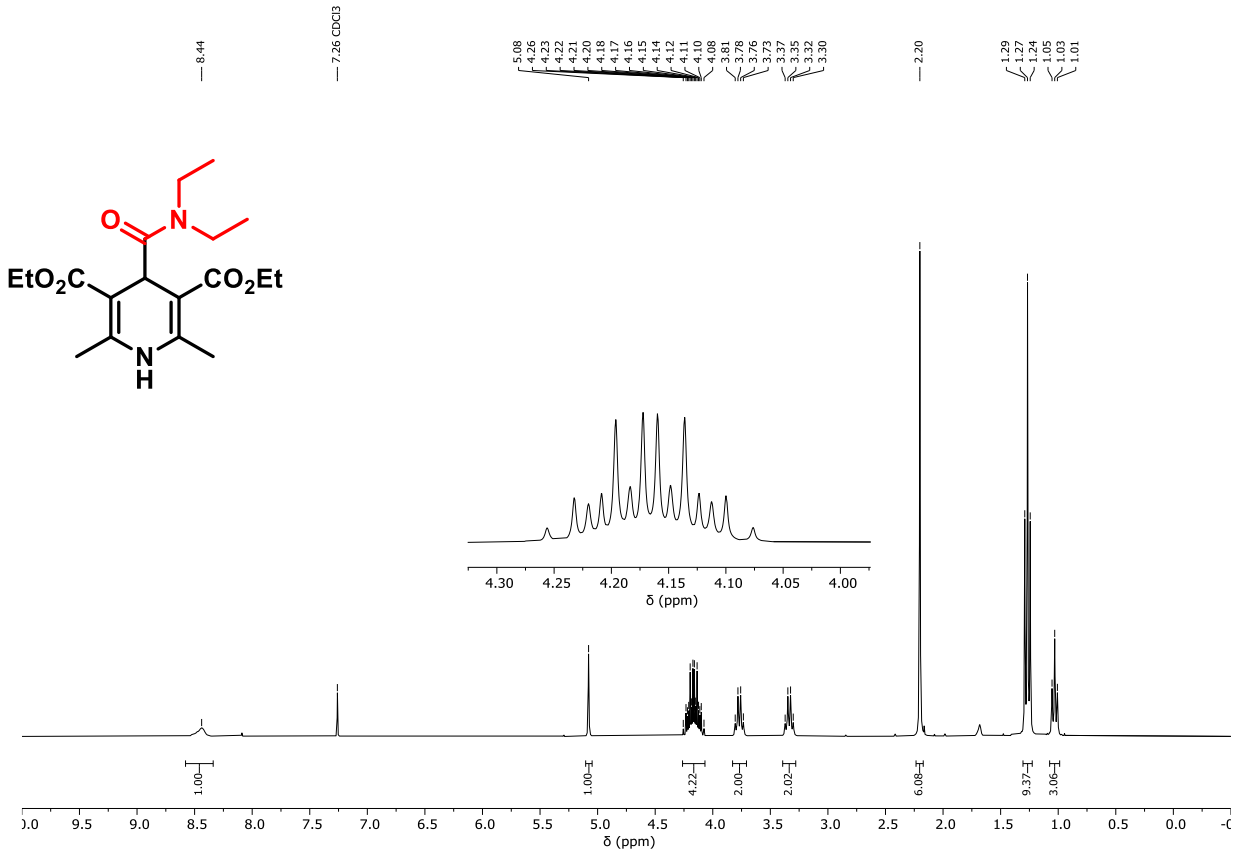
^{1}H-NMR (300 MHz) of 3,5-bis(ethoxycarbonyl)-2,6-dimethyl-1,4-dihydropyridine-4-carboxylic acid (HE-COOH, **I**).



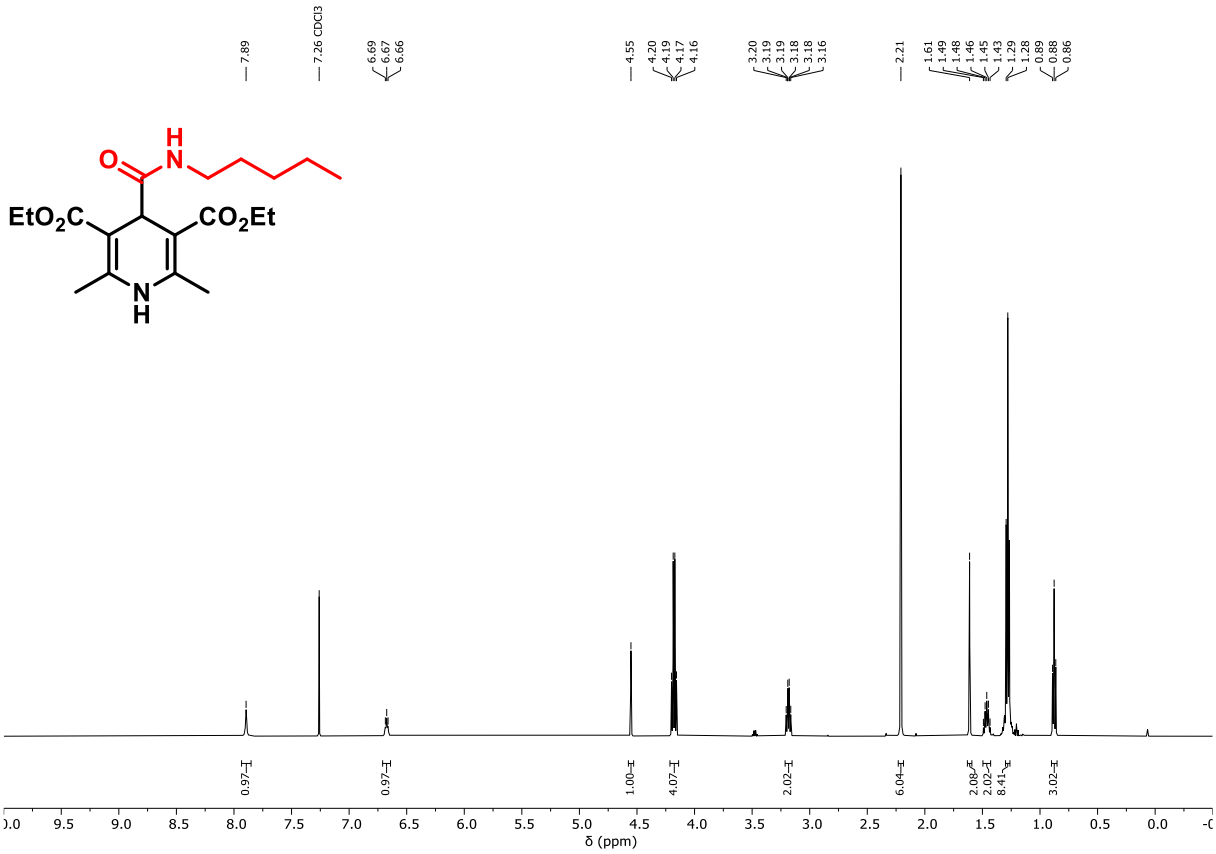
^{1}H-NMR (600 MHz) of diethyl 2,6-dimethyl-4-(morpholine-4-carbonyl)-1,4-dihydropyridine-3,5-dicarboxylate (**1a**).



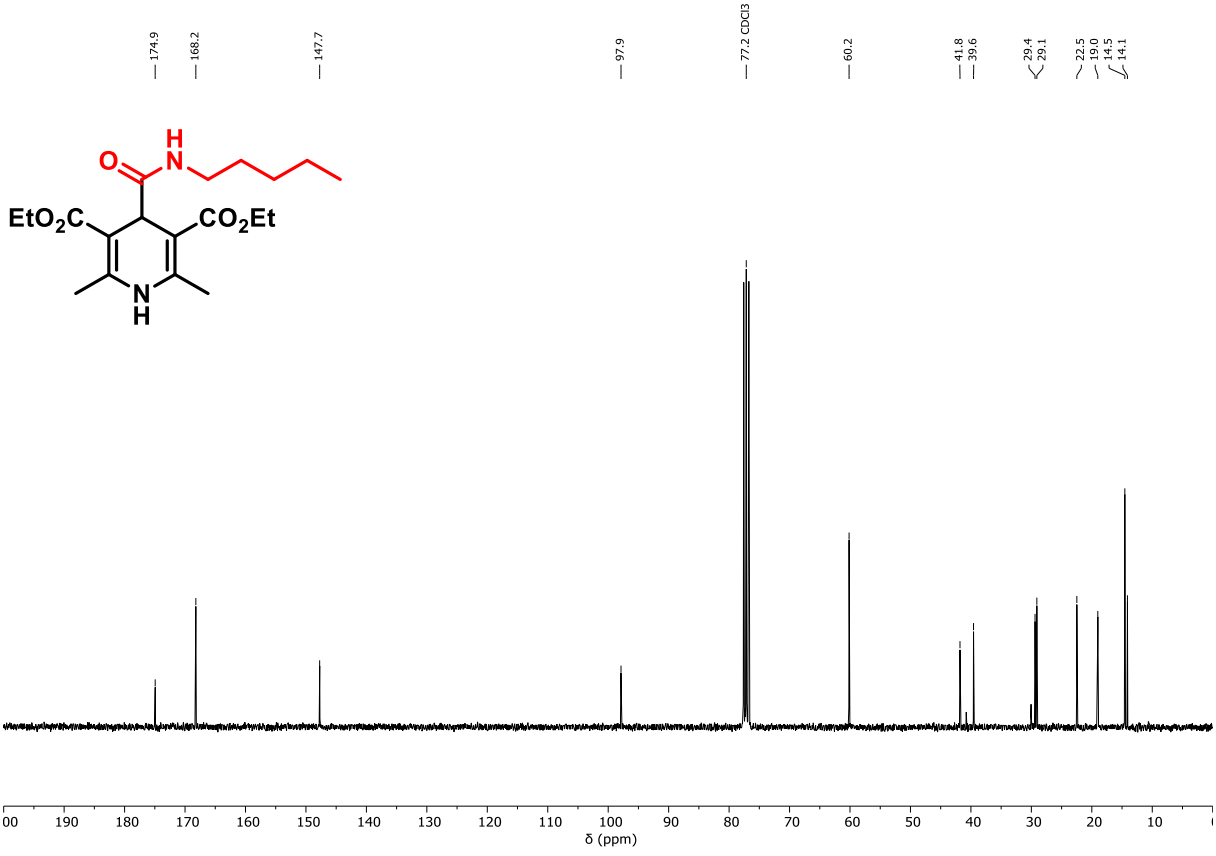
^{1}H-NMR (300 MHz) of diethyl 4-(4-(ethoxycarbonyl)piperazine-1-carbonyl)-2,6-dimethyl-1,4-dihydropyridine-3,5-dicarboxylate (**1b**).



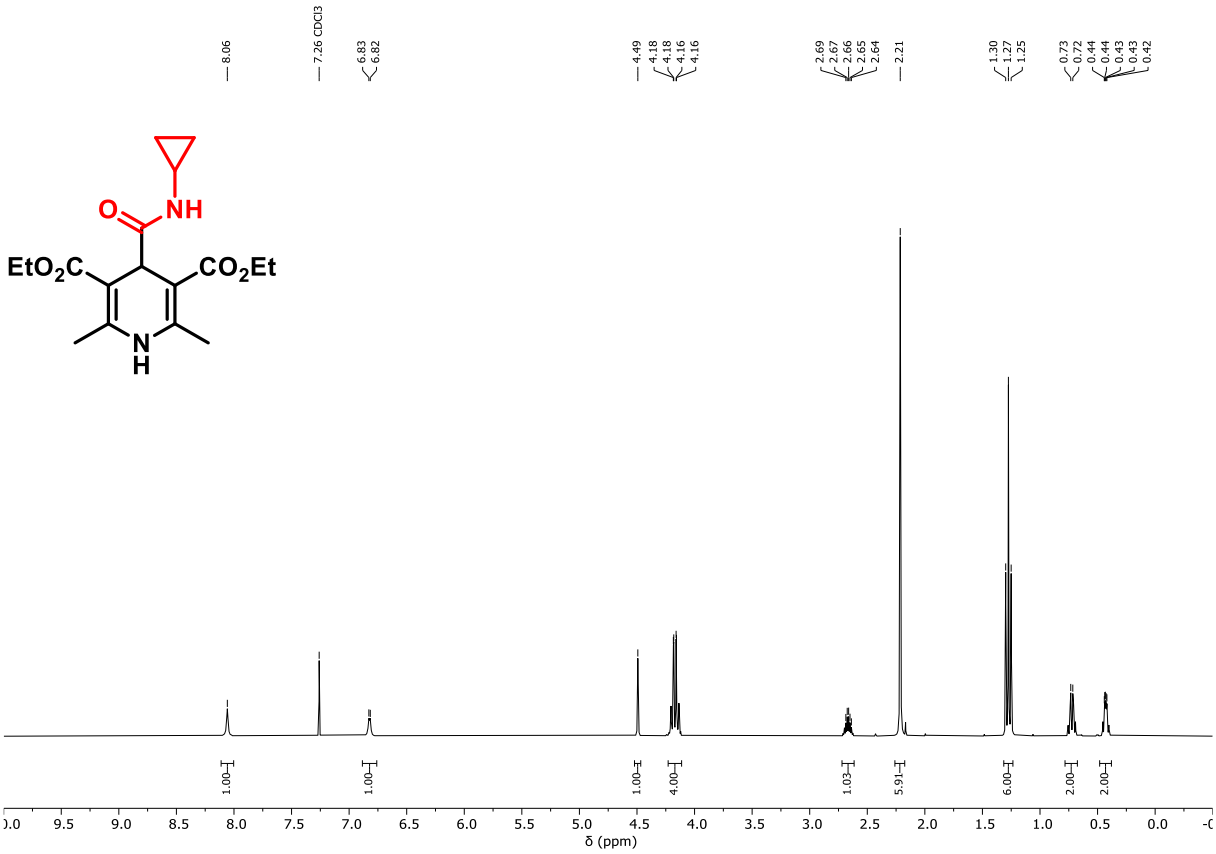
^{1}H-NMR (300 MHz) of diethyl (4-diethylcarbamoyl)-2,6-dimethyl-1,4-dihydropyridine-3,5-dicarboxylate (**1c**)



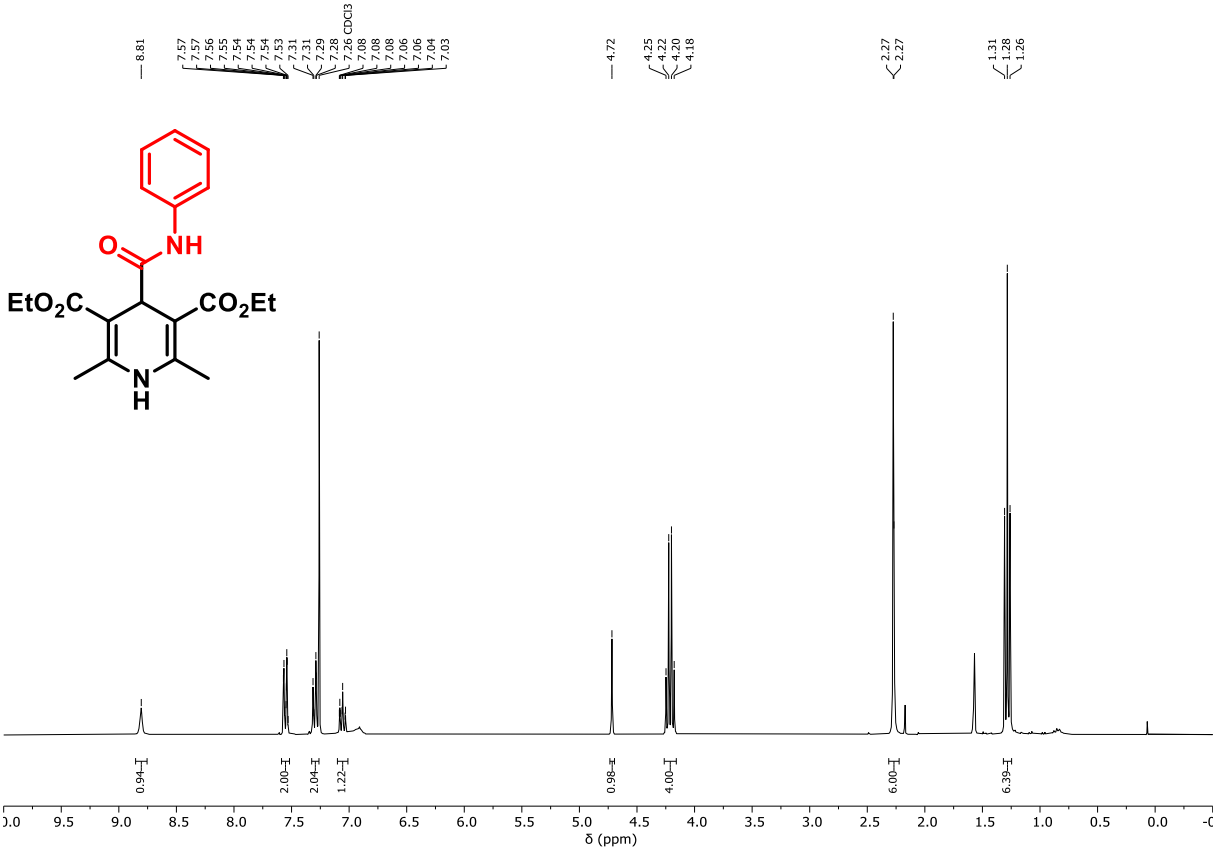
^{1}H-NMR (500 MHz) of diethyl 2,6-dimethyl-4-(pentylcarbamoyl)-1,4-dihydropyridine-3,5-dicarboxylate (**1d**).



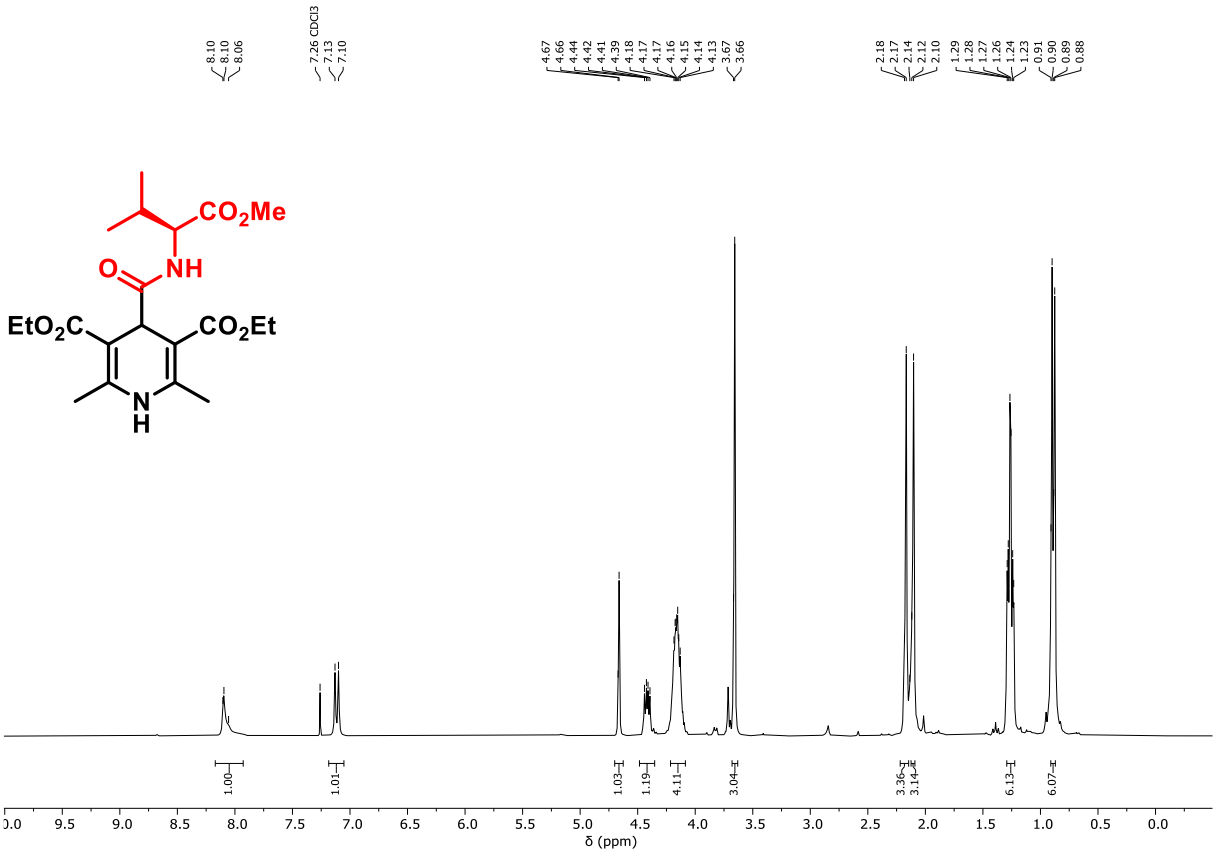
^{13}C-{^{1}H}-NMR (75 MHz) of diethyl 2,6-dimethyl-4-(pentylcarbamoyl)-1,4-dihydropyridine-3,5-dicarboxylate (**1d**).



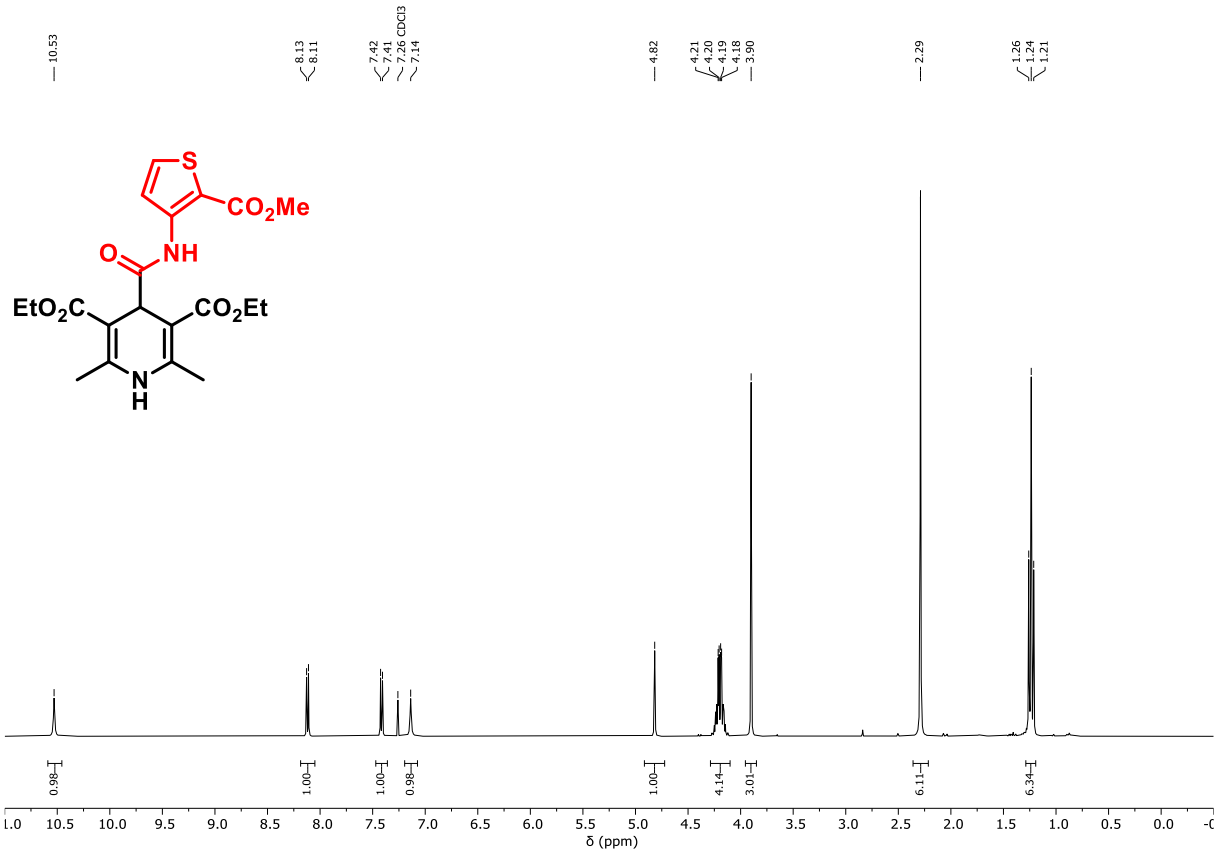
^{1}H-NMR (300 MHz) of diethyl (4-cyclopropylcarbamoyl)-2,6-dimethyl-1,4-dihydropyridine-3,5-dicarboxylate (**1e**).



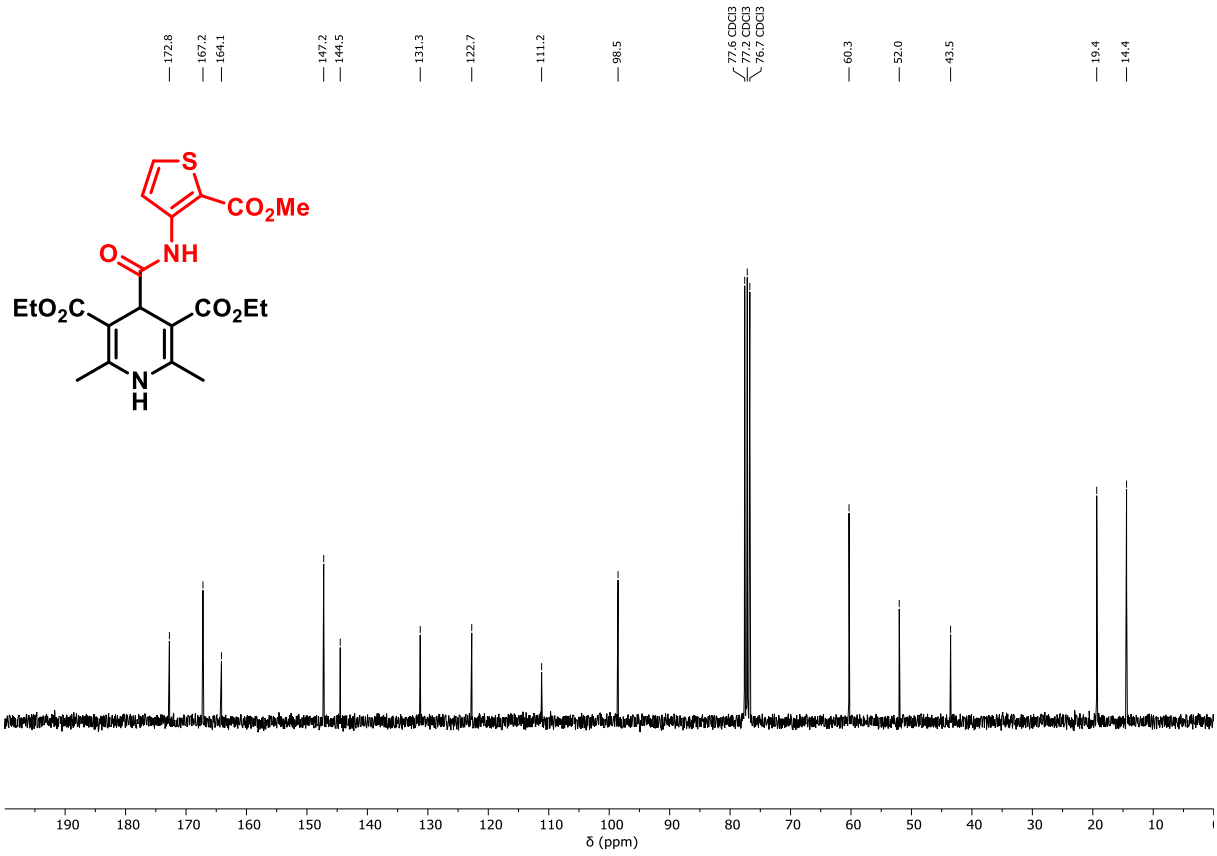
^{1}H-NMR (300 MHz) of diethyl 2,6-dimethyl-4-(phenylcarbamoyl)-1,4-dihydropyridine-3,5-dicarboxylate (**1f**).



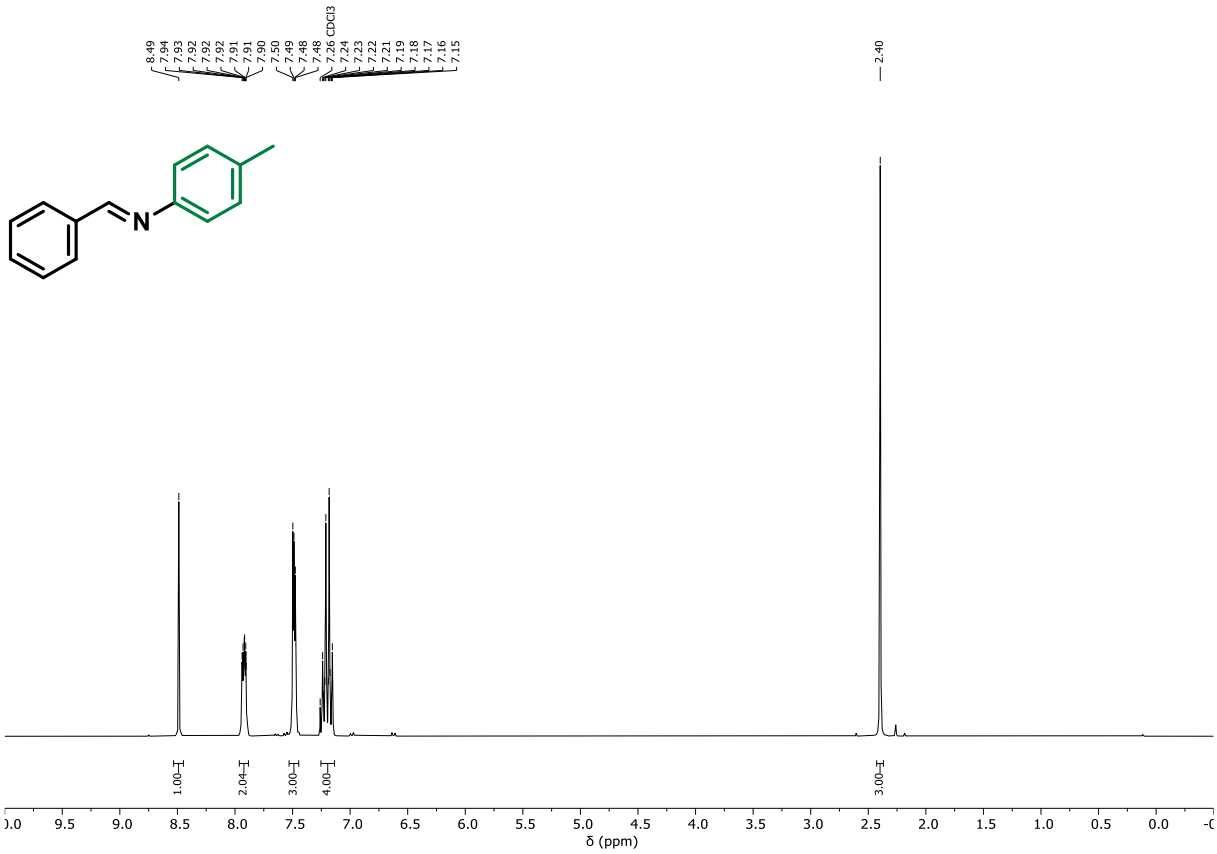
^{1}H-NMR (300 MHz) of diethyl 2,6-dimethyl-4-((*S*)-valine-*N*-carbonyl)-1,4-dihydropyridine-3,5-dicarboxylate (**1g**).



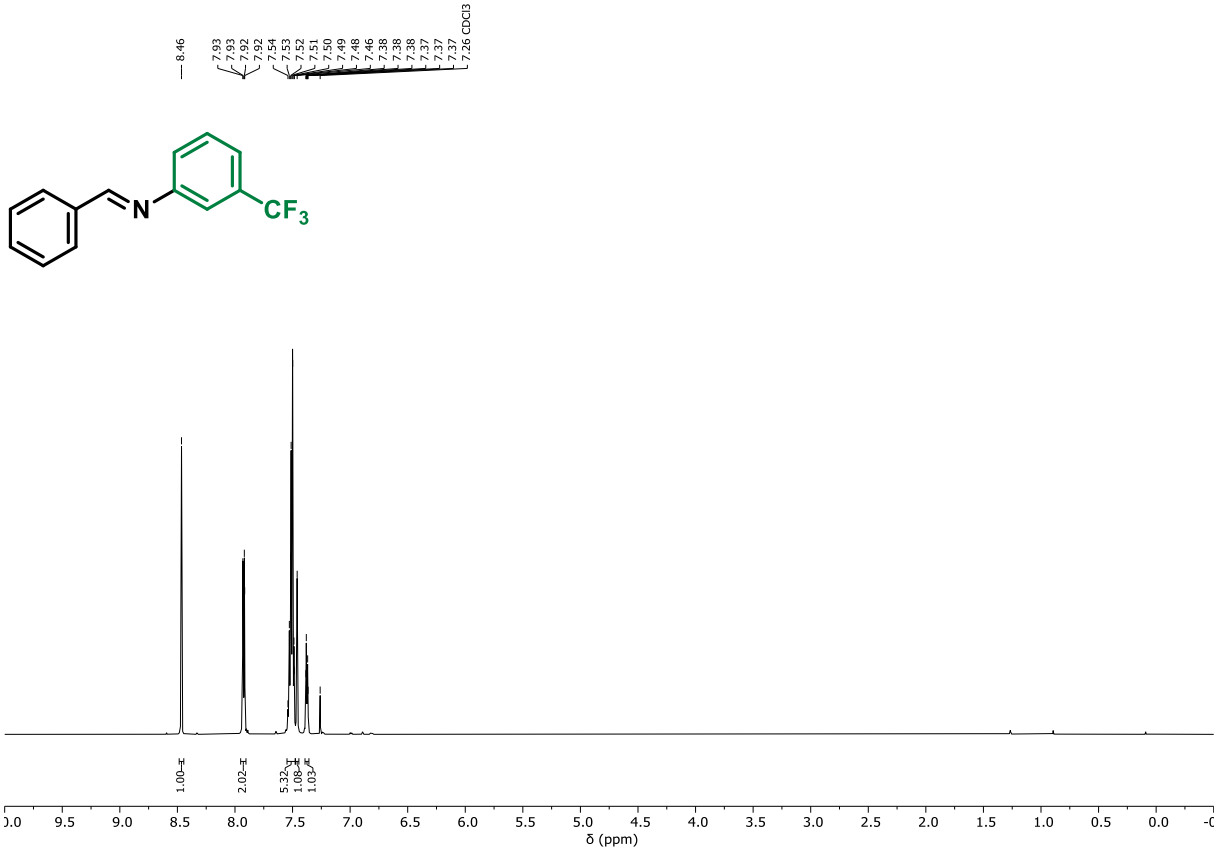
^{1}H-NMR (300 MHz) of diethyl 4-((2-(methoxycarbonyl)thiophen-3-yl)carbamoyl)-2,6-dimethyl-1,4-dihydropyridine-3,5-dicarboxylate (**1h**).



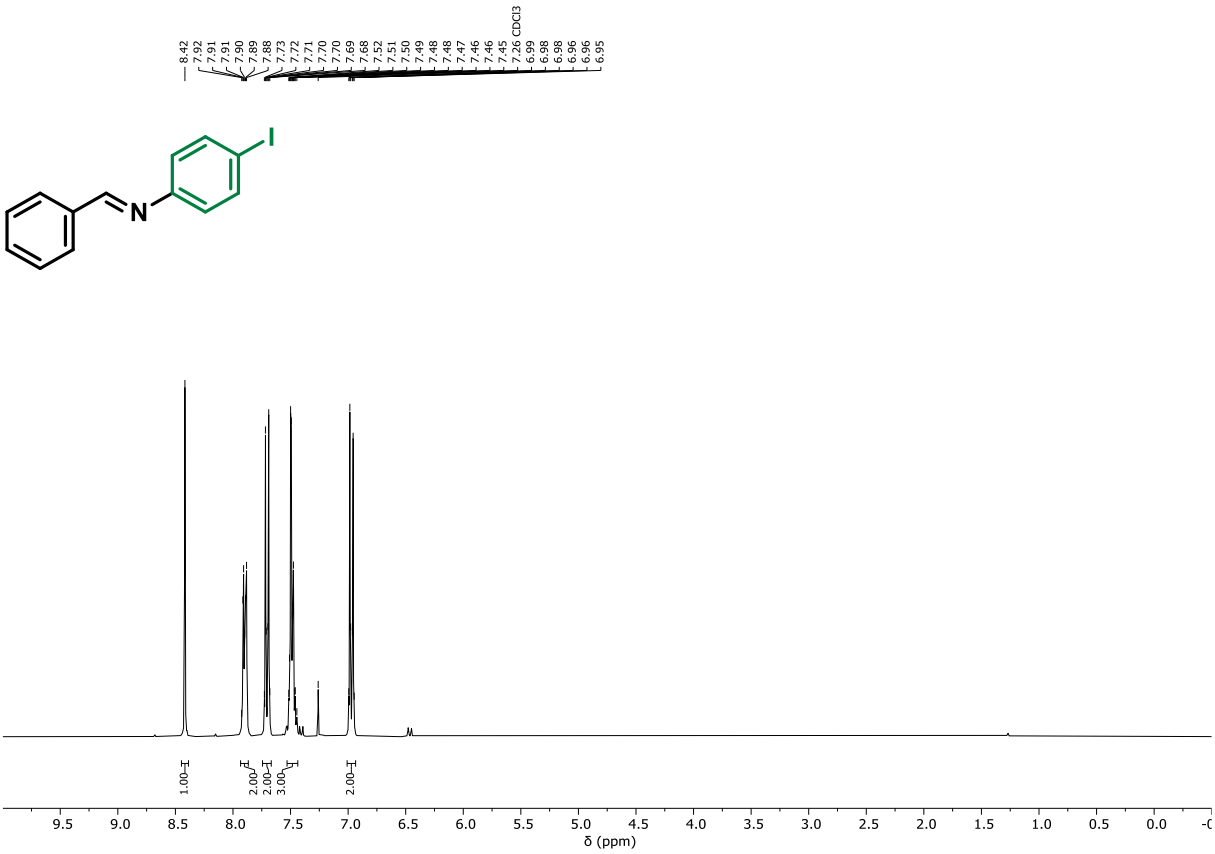
^{13}C-{^{1}H}-NMR (75 MHz) of diethyl 4-((2-(methoxycarbonyl)thiophen-3-yl)carbamoyl)-2,6-dimethyl-1,4-dihydro-pyridine-3,5-dicarboxylate (**1h**).



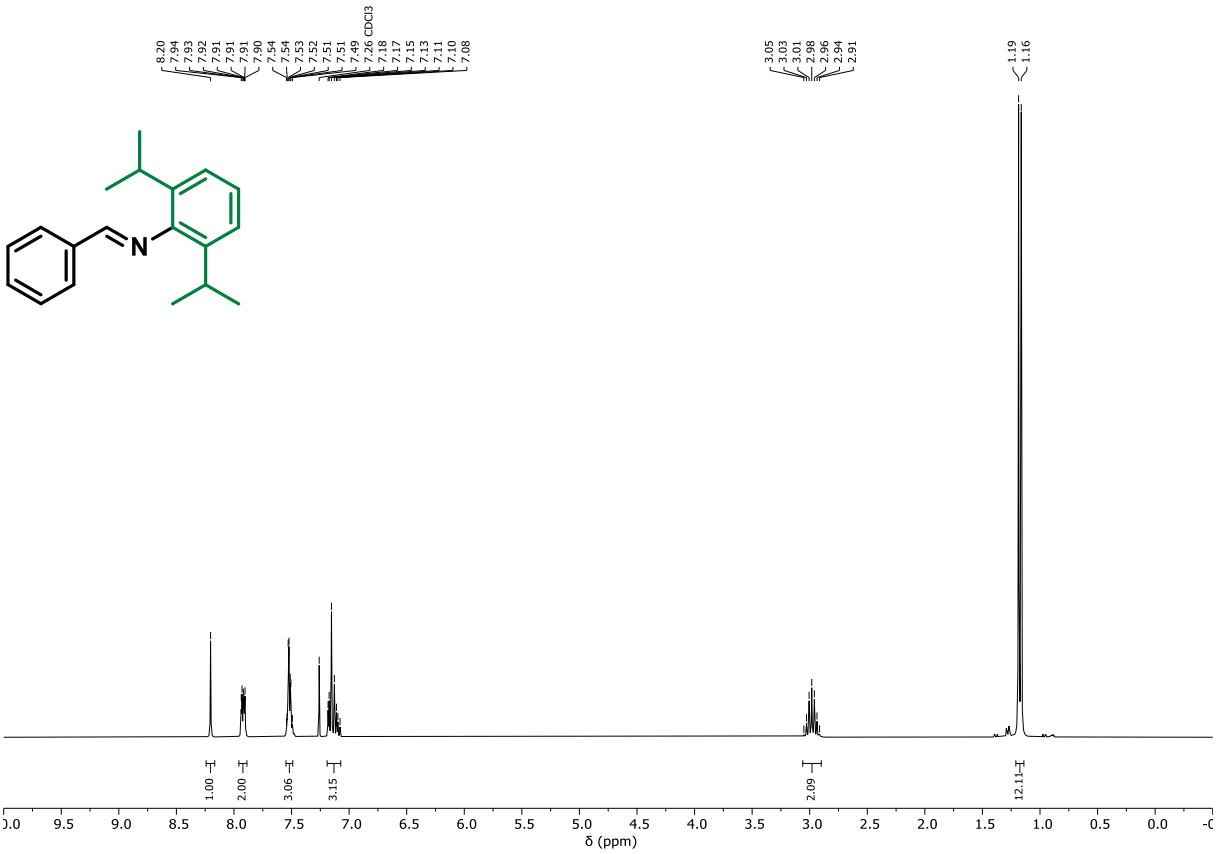
^{1}H-NMR (300 MHz) of benzylidene(4-methylphenyl)amine (**2b**).



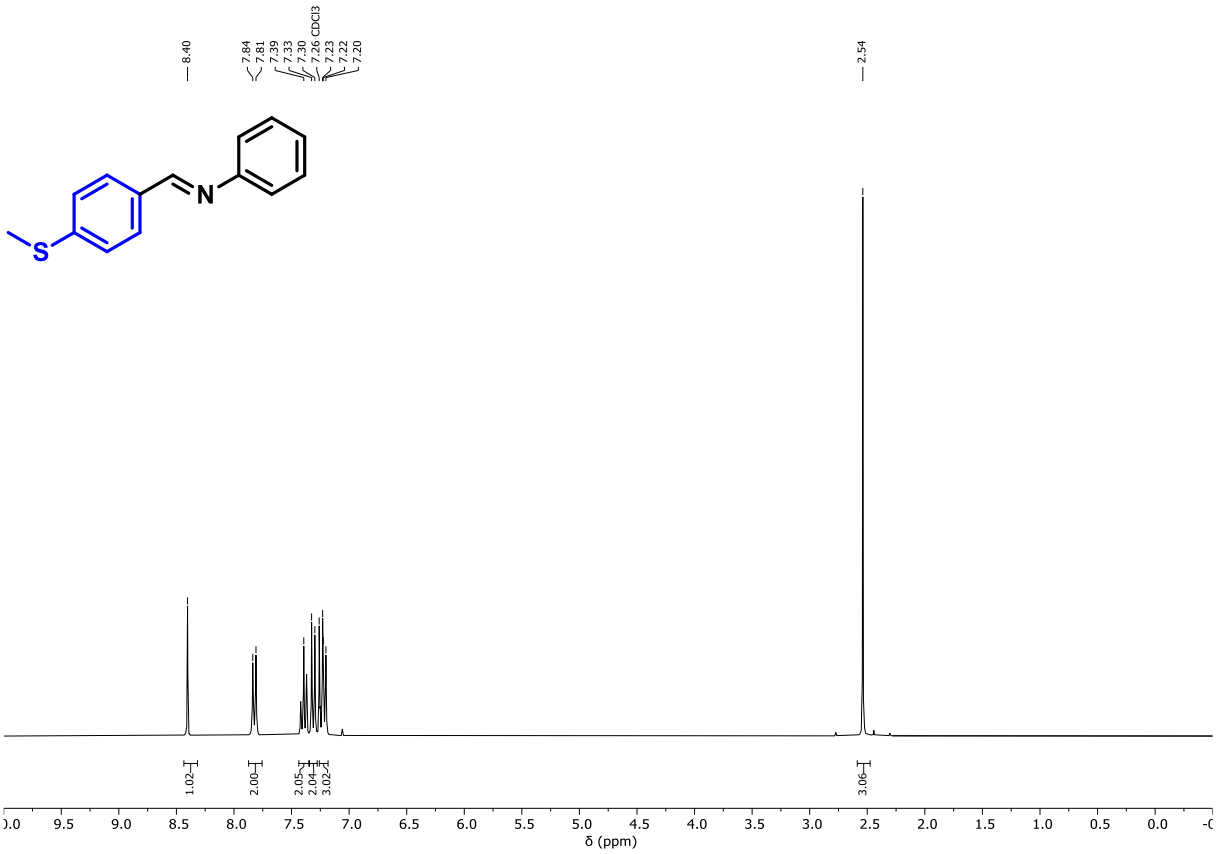
^{1}H-NMR (600 MHz) of benzylidene(3-(trifluoromethyl)phenyl)amine (**2c**).



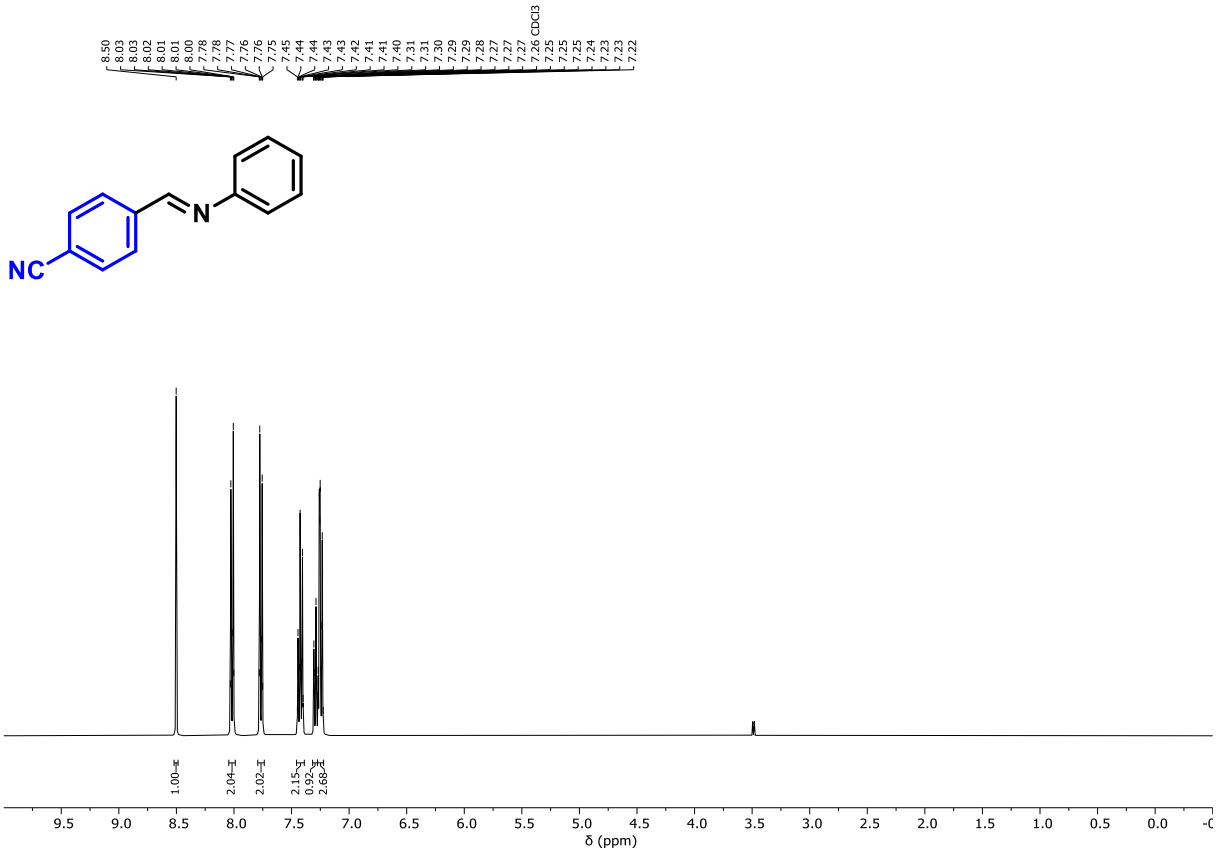
^{1}H-NMR (300 MHz) of benzylidene(4-iodophenyl)amine (**2d**).



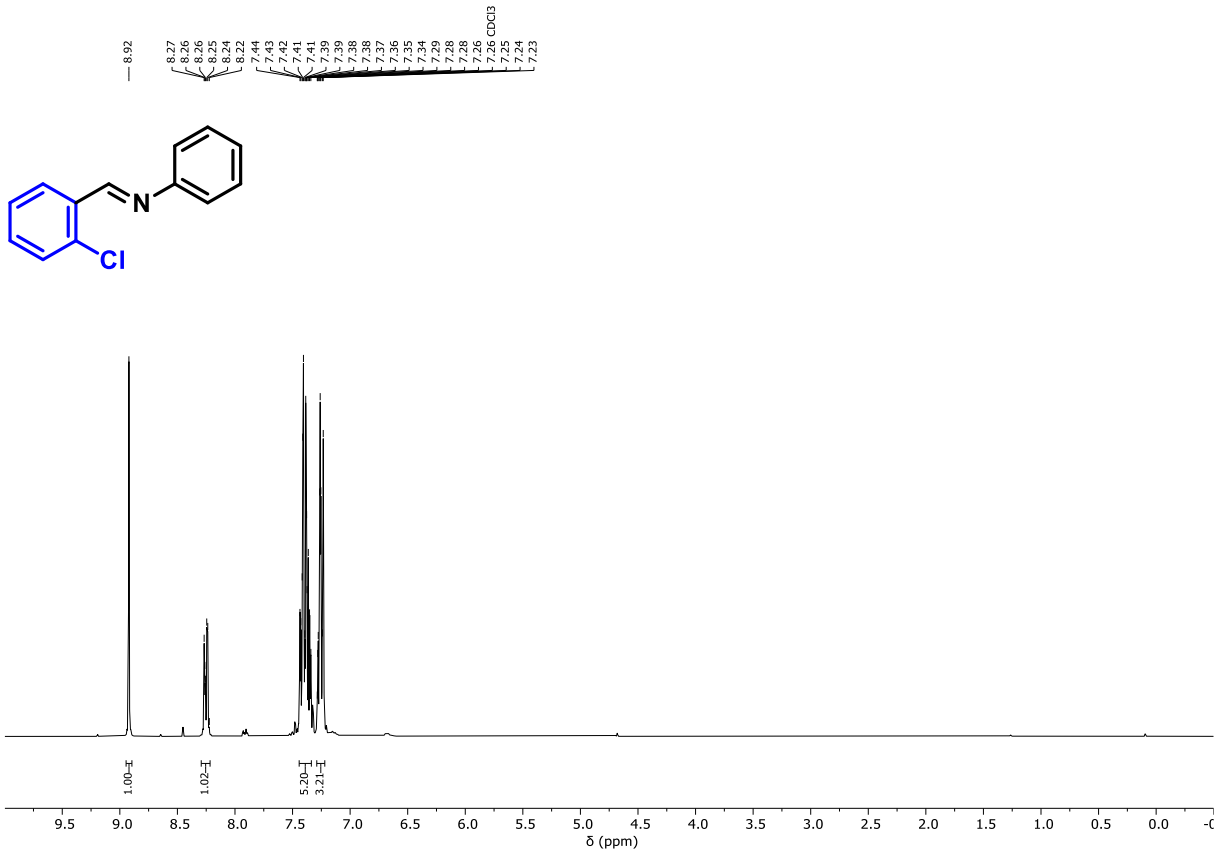
^{1}H-NMR (300 MHz) of benzylidene(2,6-diisopropylphenyl)amine (**2e**).



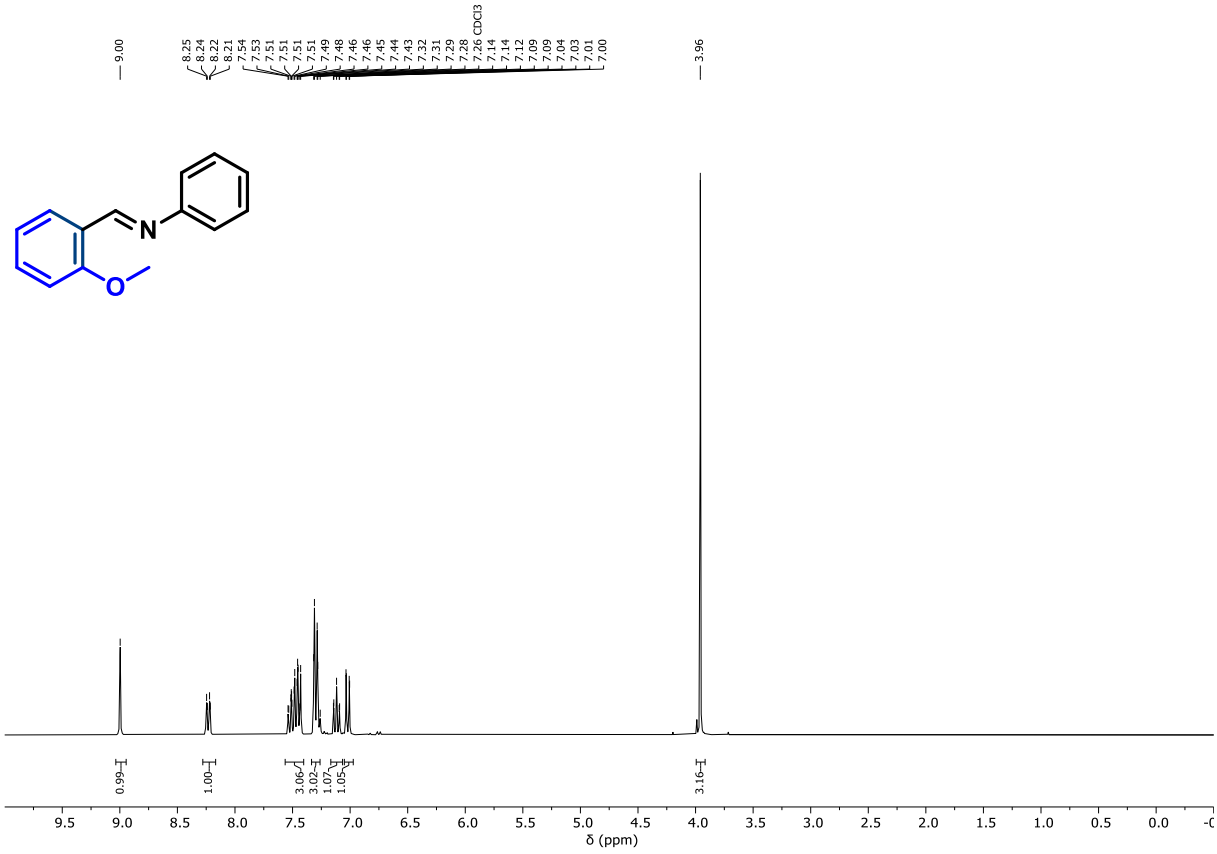
^{1}H-NMR (300 MHz) of *N*-phenyl-1-(4-methylthio)methanimine (**2f**).



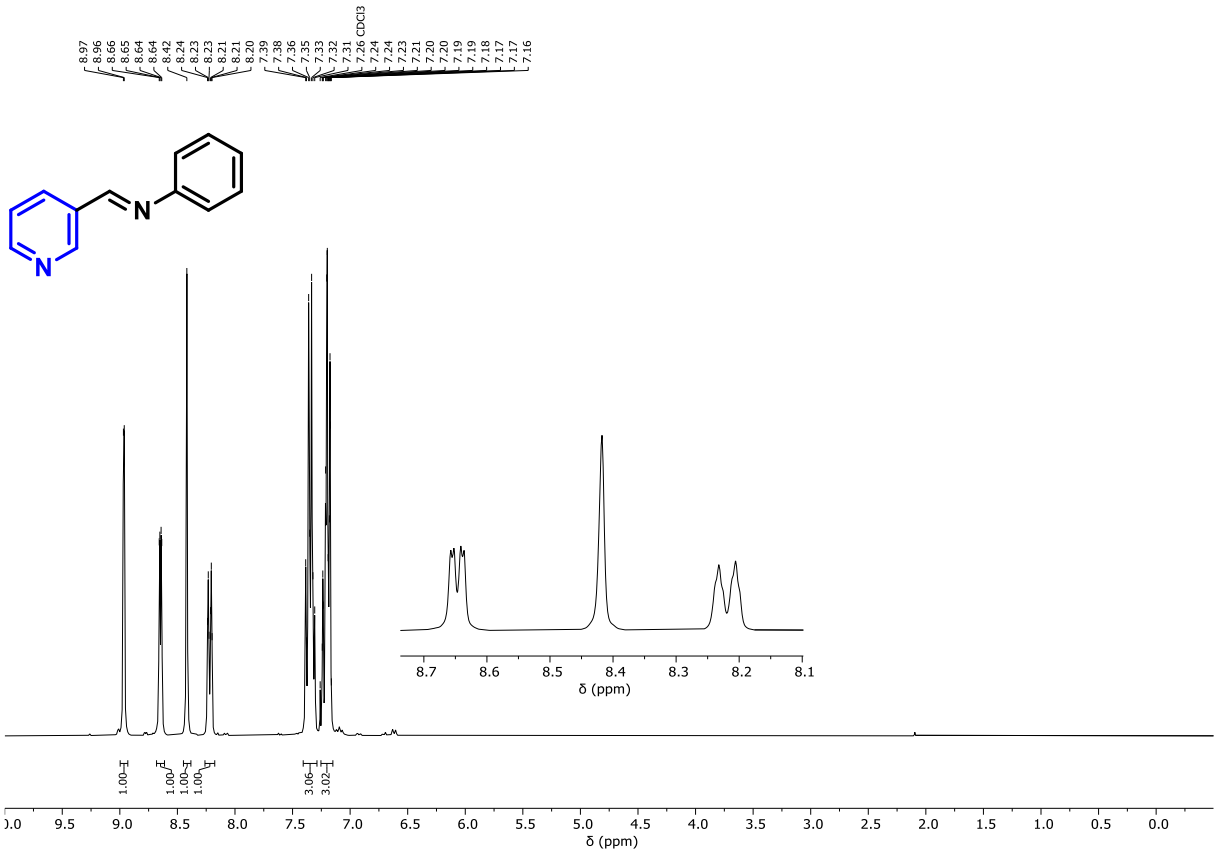
^{1}H-NMR (400 MHz) of *N*-phenyl-1-(4-cyanophenyl)methanimine (**2g**).



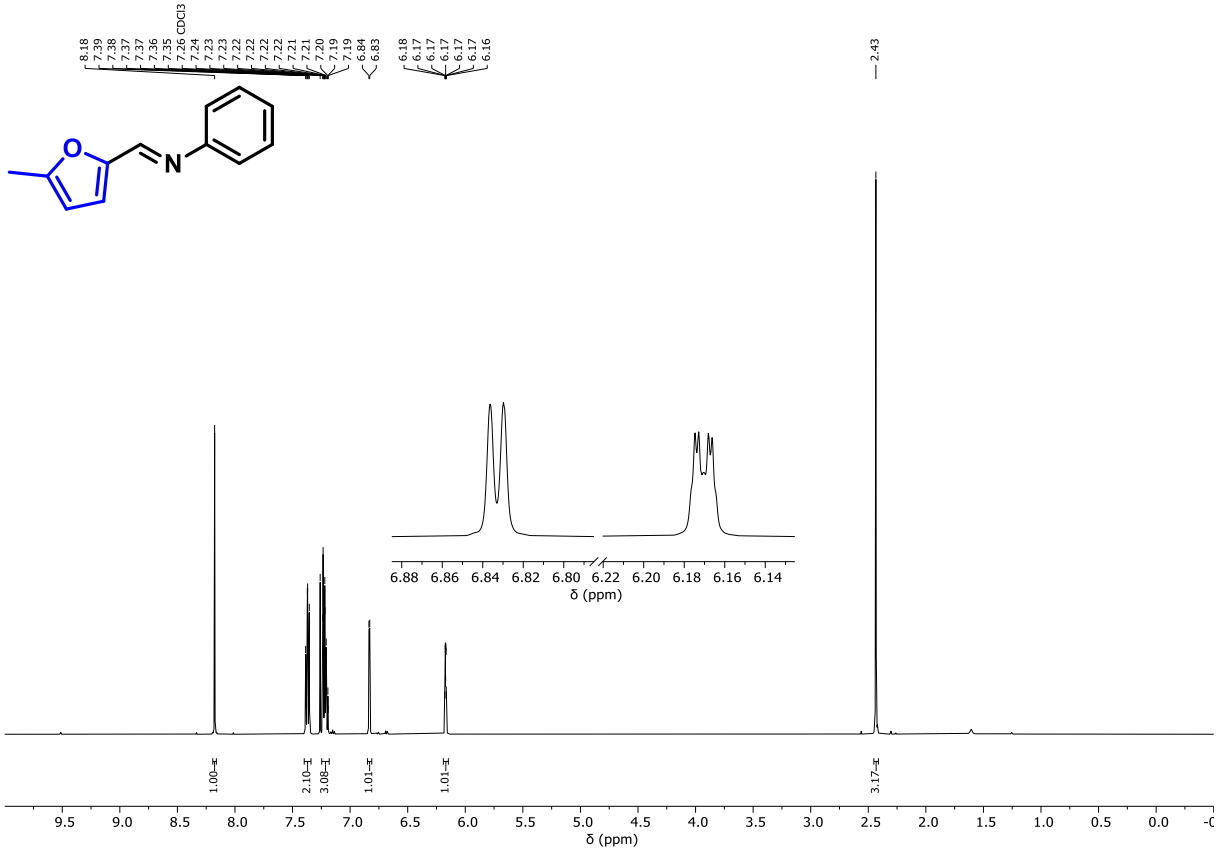
^{1}H-NMR (300 MHz) of *N*-phenyl-1-(2-chlorophenyl)methanimine (**2h**).



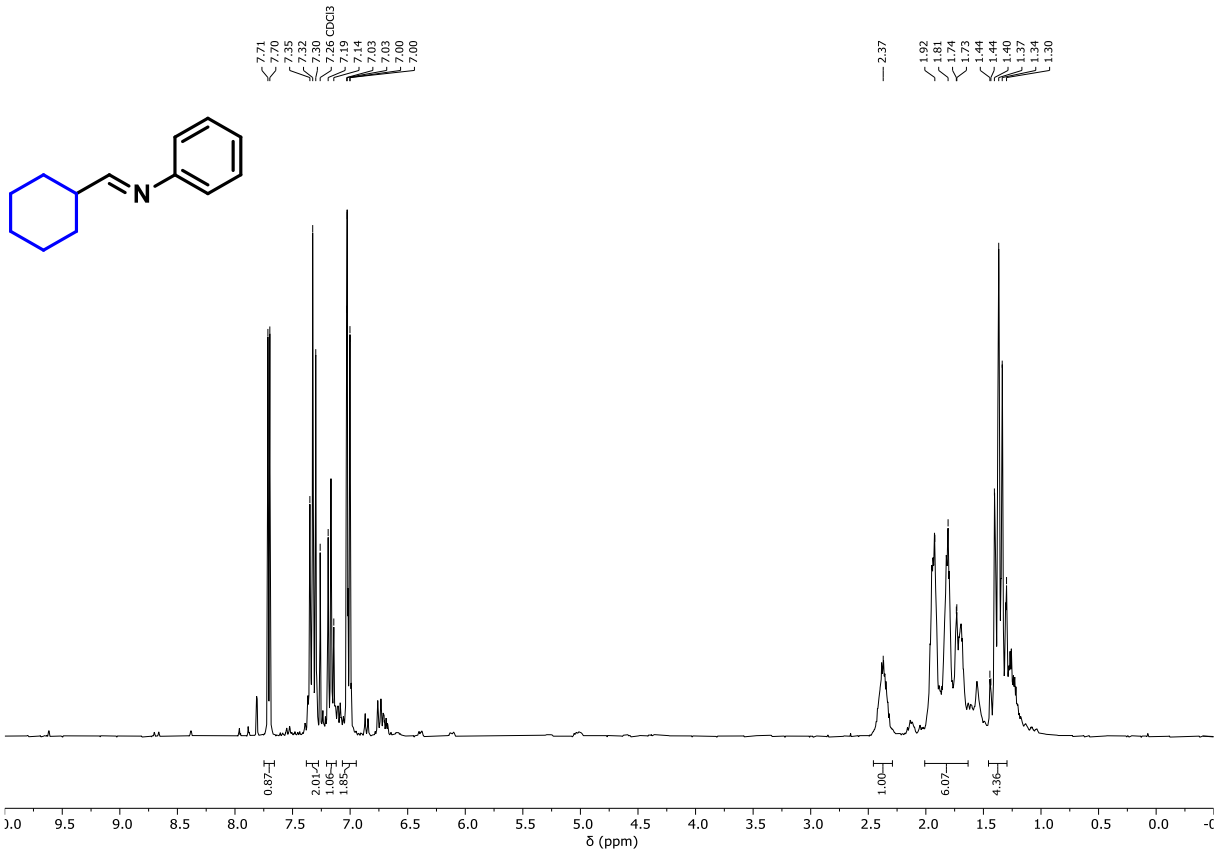
^{1}H-NMR (300 MHz) of *N*-phenyl-1-(2-methoxyphenyl)methanimine (**2i**).



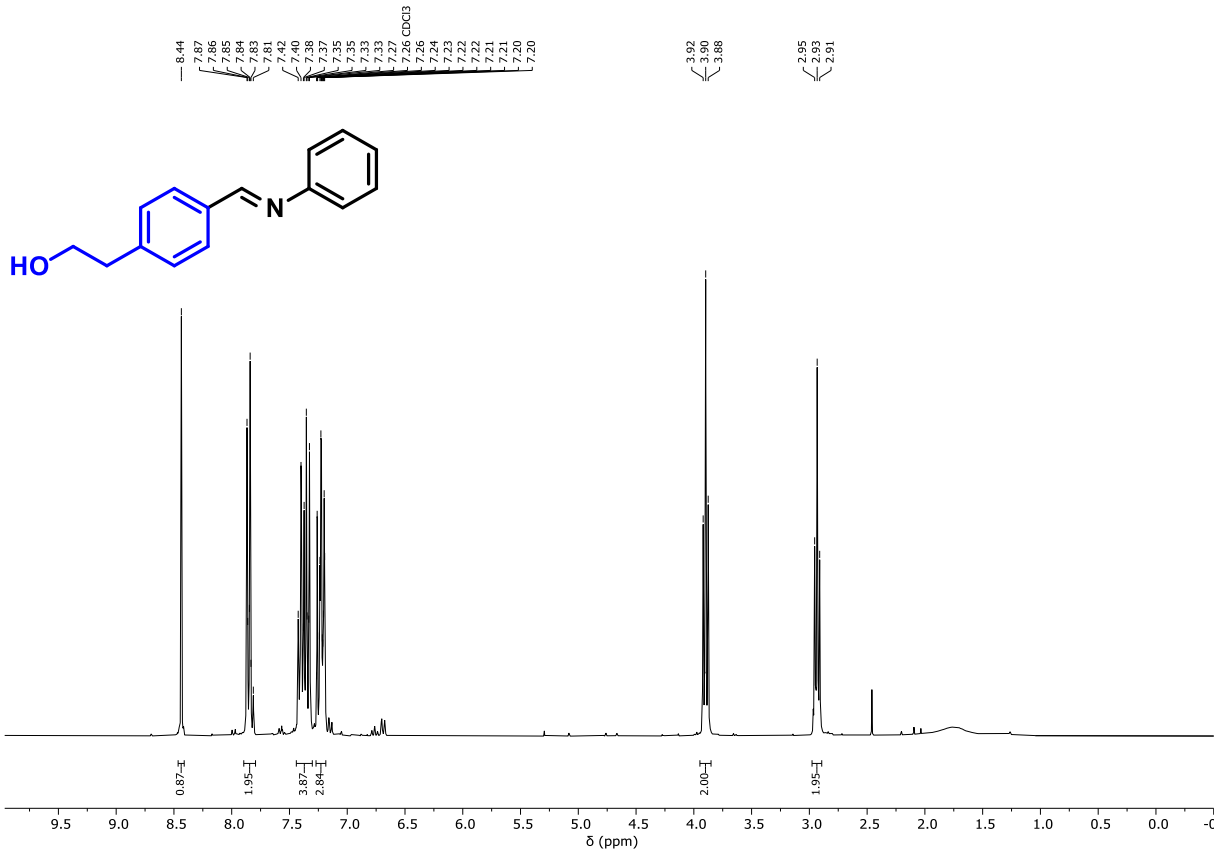
^{1}H-NMR (300 MHz) of *N*-phenyl-1-(3-pyridinyl)methanimine (**2j**).



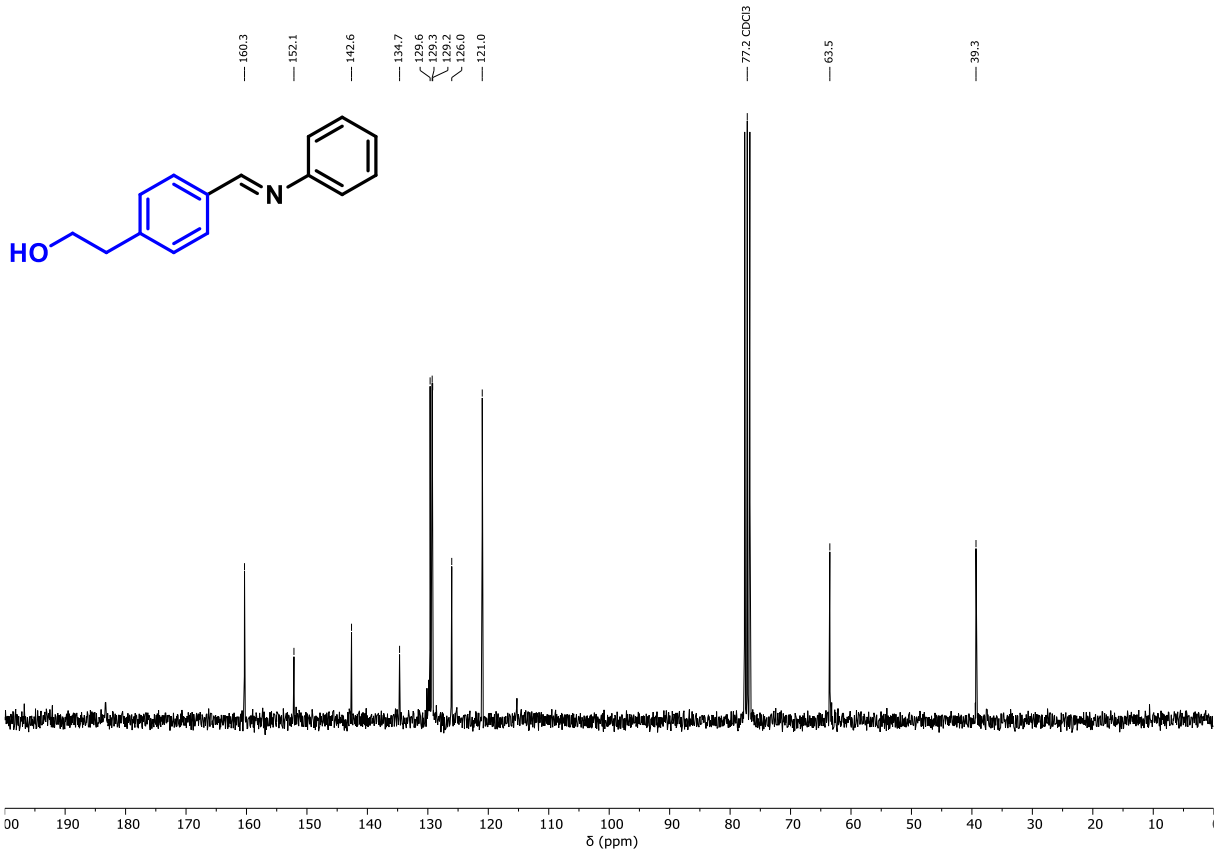
^{1}H-NMR (400 MHz) of *N*-phenyl-1-(5-methylfuran-2-yl)methanimine (**2k**).



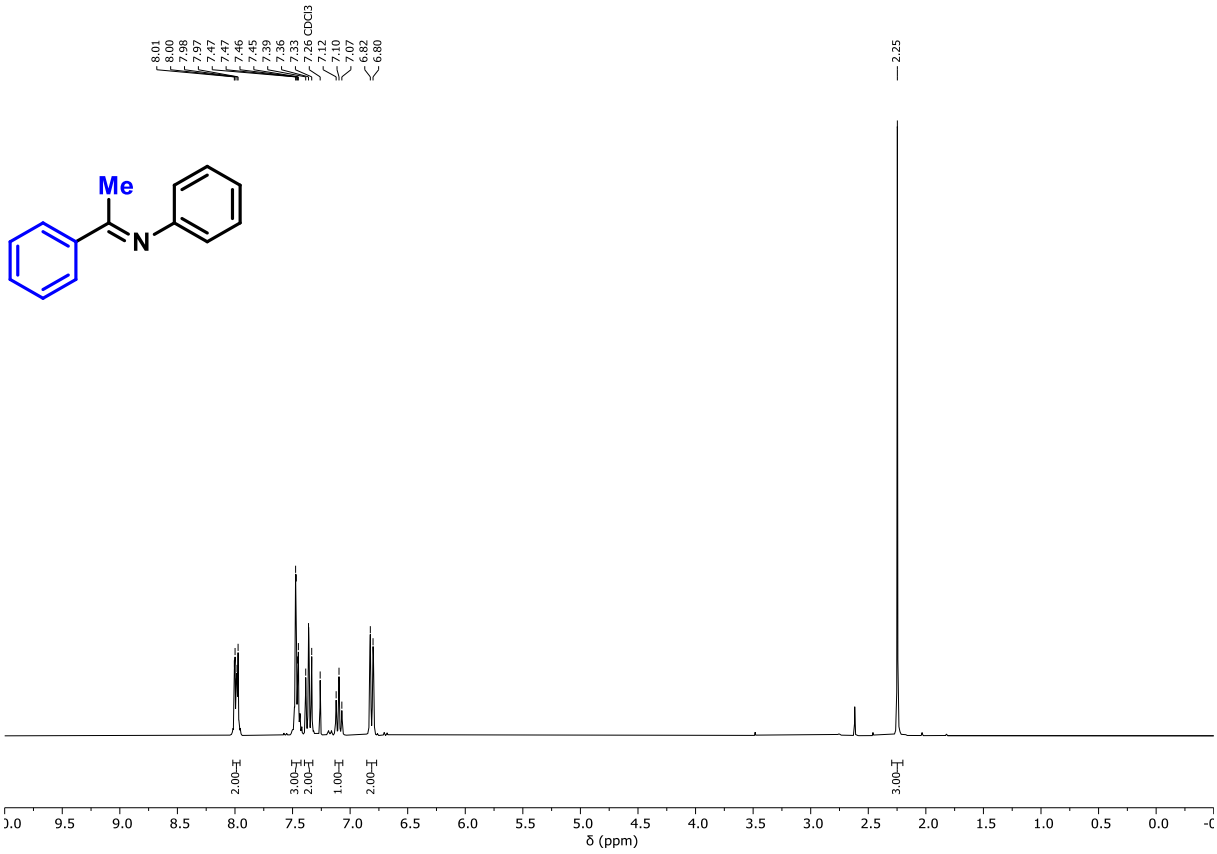
^{1}H-NMR (300 MHz) of *N*-phenyl-1-(cyclohexyl)methanimine (**2l**).



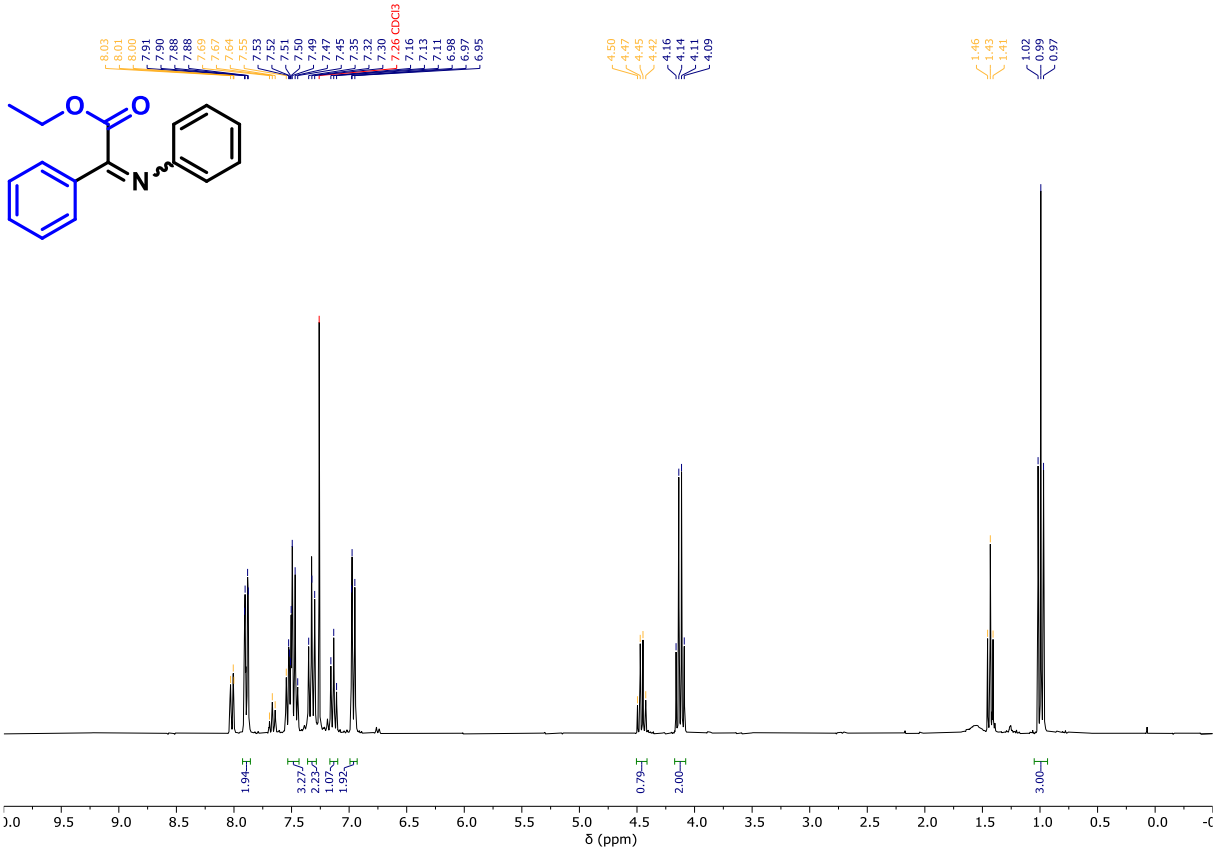
^{1}H-NMR (300 MHz) of *N*-phenyl-1-(4-(2-hydroxyethyl)phenyl)methanimine (**2m**).



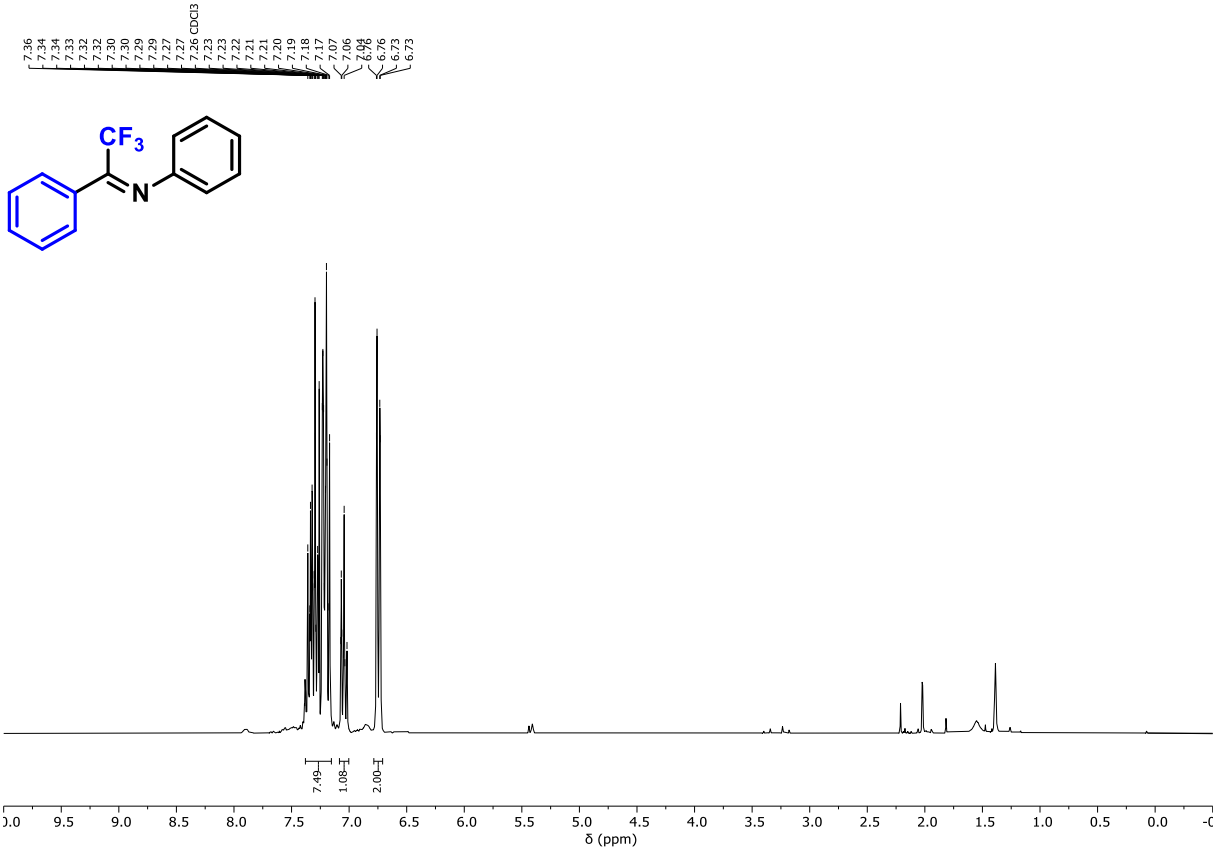
^{13}C-{^{1}H}-NMR (75 MHz) of *N*-phenyl-1-(4-(2-hydroxyethyl)phenyl)methanimine (**2m**).



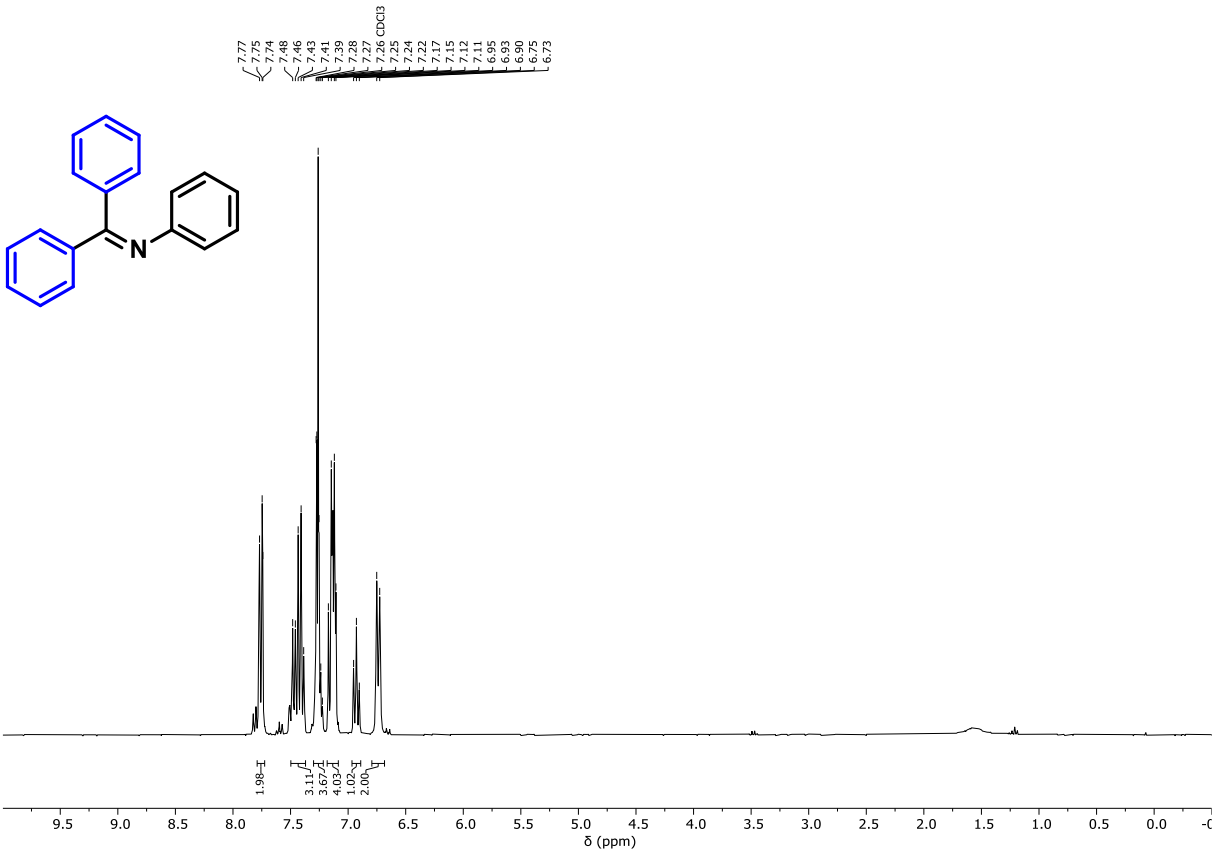
^{1}H-NMR (300 MHz) of *N*,1-diphenylethan-1-imine (**2n**).



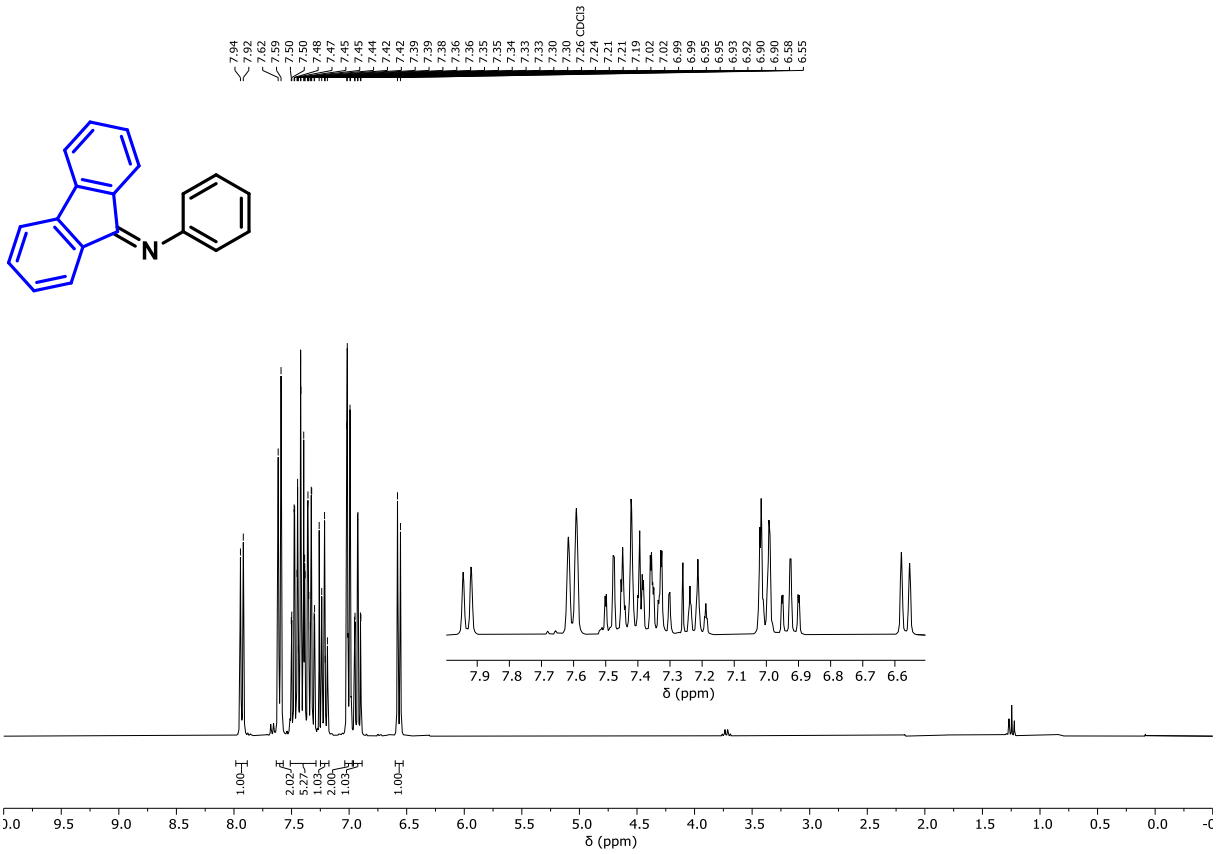
^{1}H-NMR (300 MHz) of (*E*)-2-phenyl-2-(phenylimino)acetate and (*Z*)-2-phenyl-2-(phenylimino)acetate (**2o**).



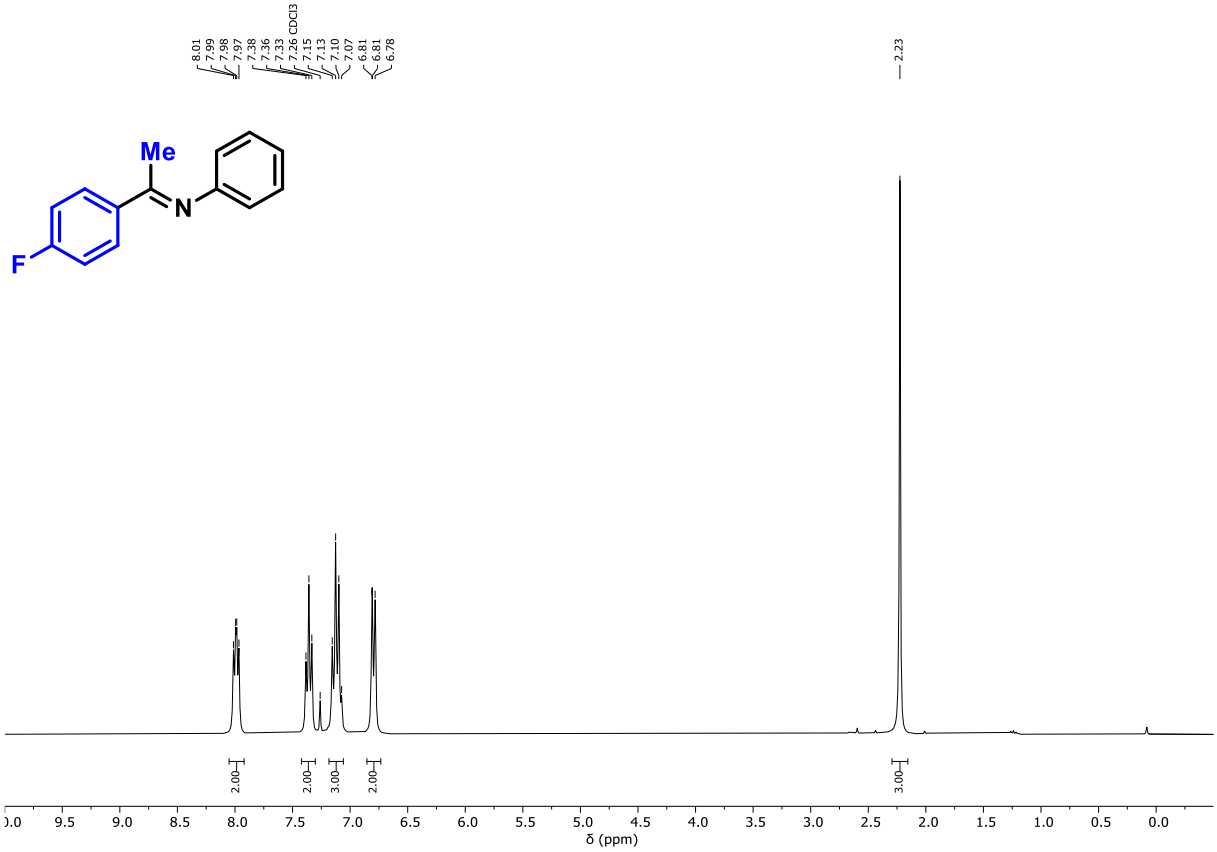
^{1}H-NMR (600 MHz) of 2,2,2-trifluoro-*N*,1-diphenylethan-1-imine (**2p**).



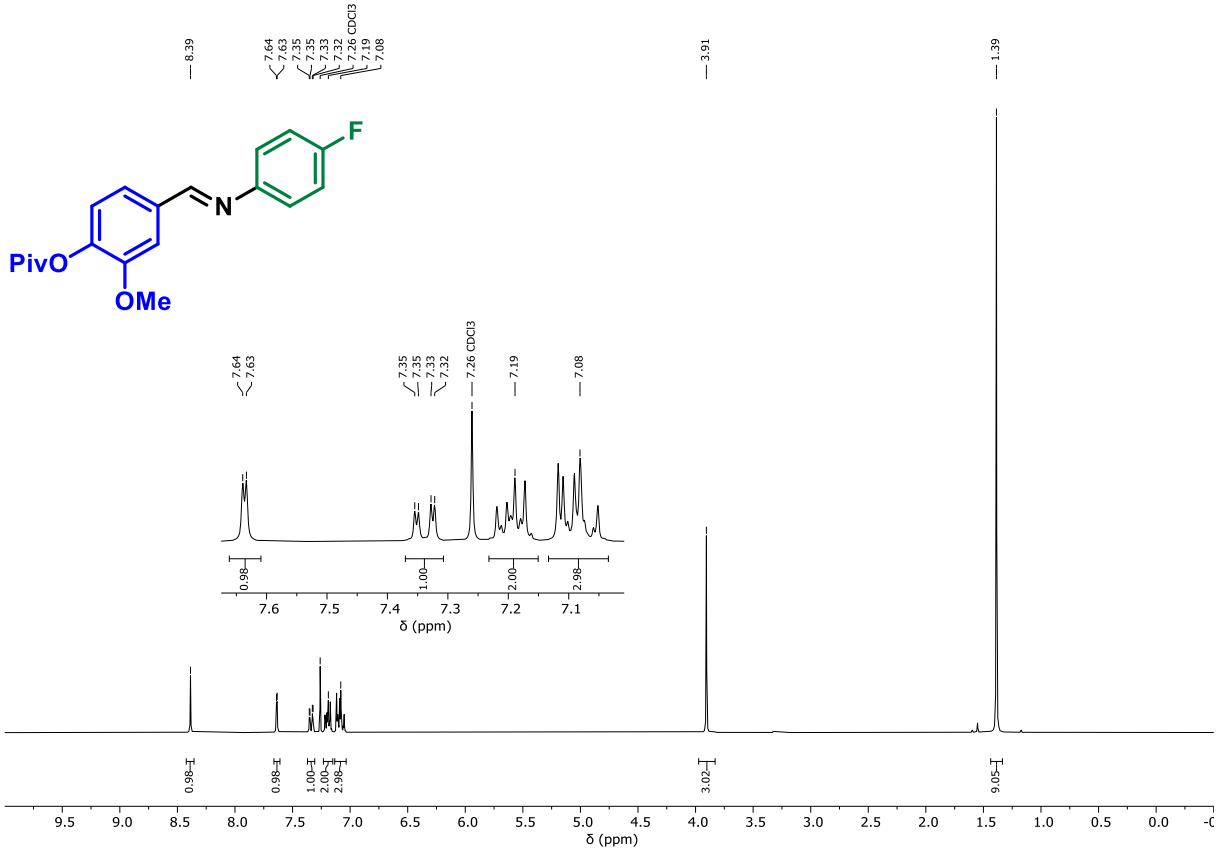
H-NMR (300 MHz) of *N*,1,1-triphenylmethanimine (**2q**).



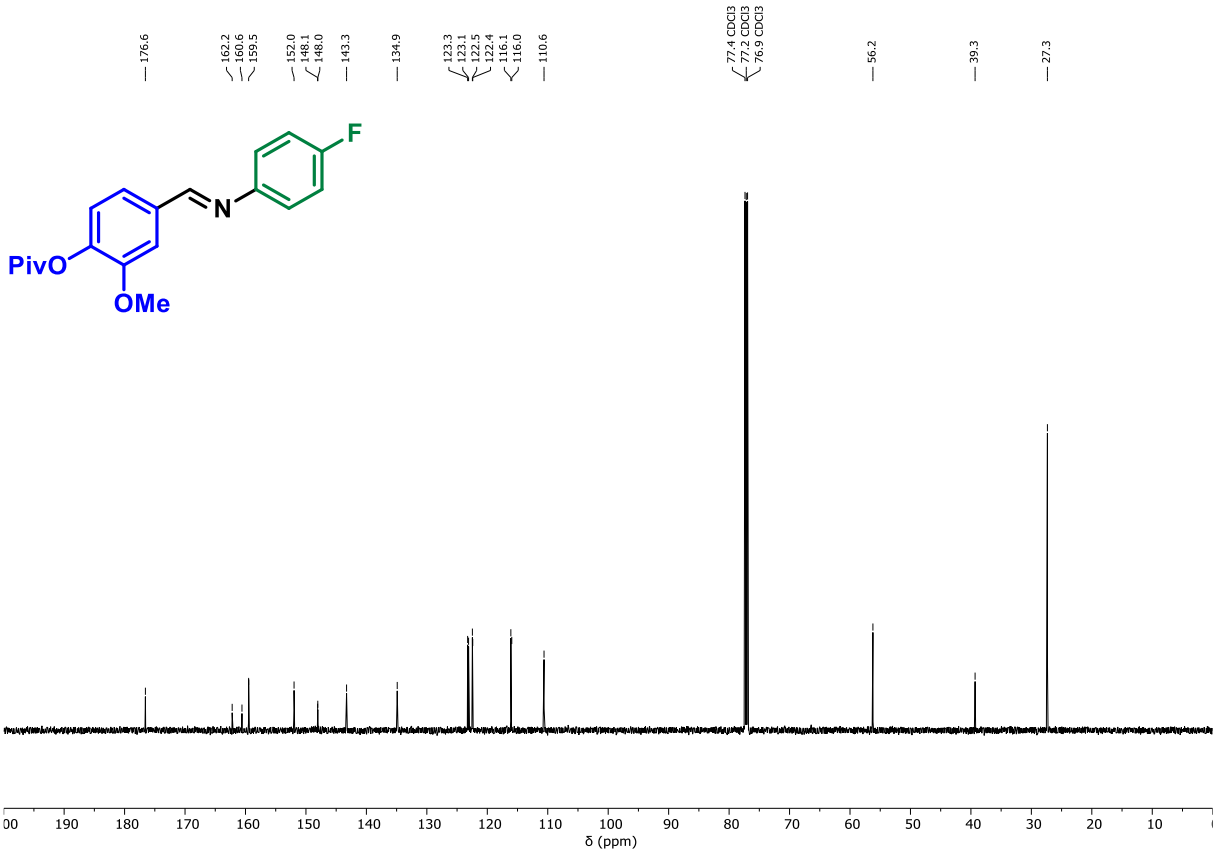
^{1}H-NMR (300 MHz) of *N*-phenyl-9*H*-fluoren-9-imine (**2r**).



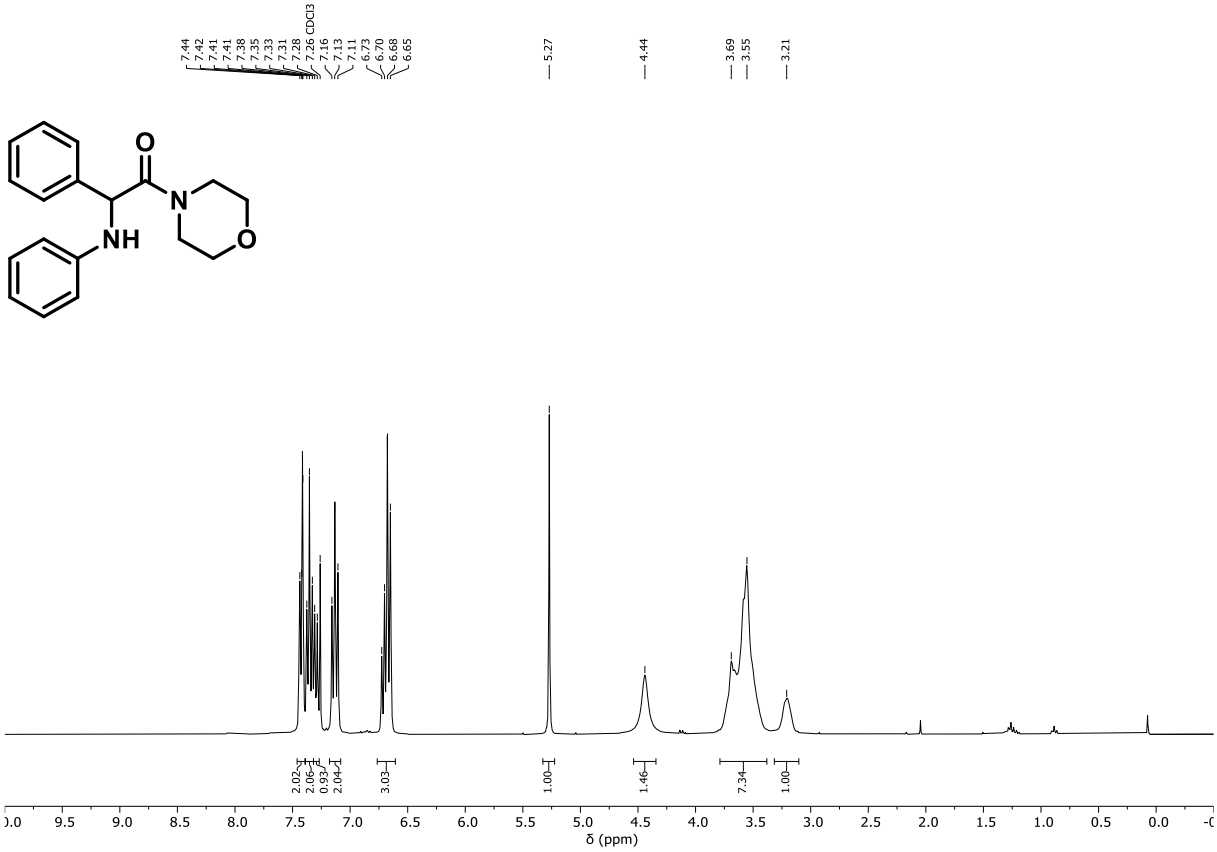
^{1}H-NMR (300 MHz) of 1-(4-fluorophenyl)-*N*-phenylethan-1-imine (**2s**).



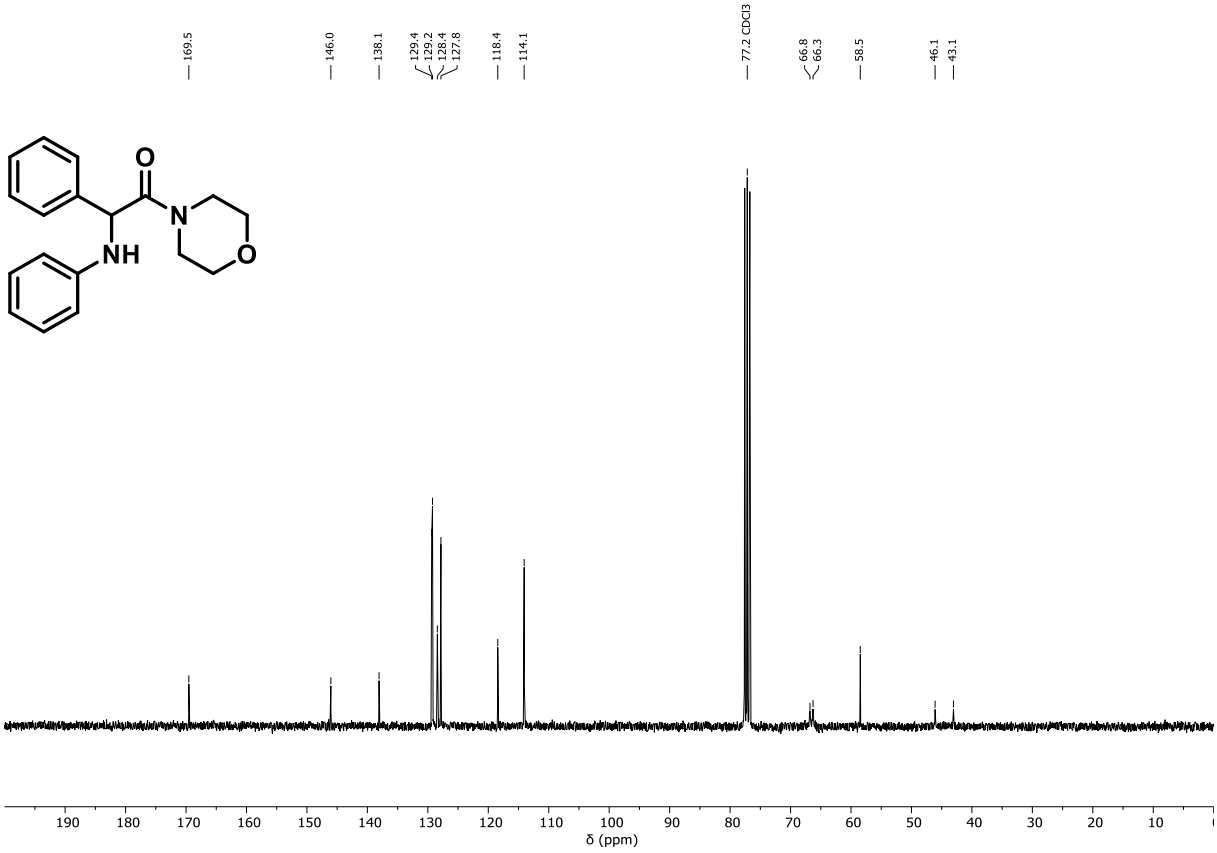
^{1}H-NMR (300 MHz) of 4-(((4-fluorophenyl)imino)methyl)-2-methoxyphenyl pivalate (**2t**).



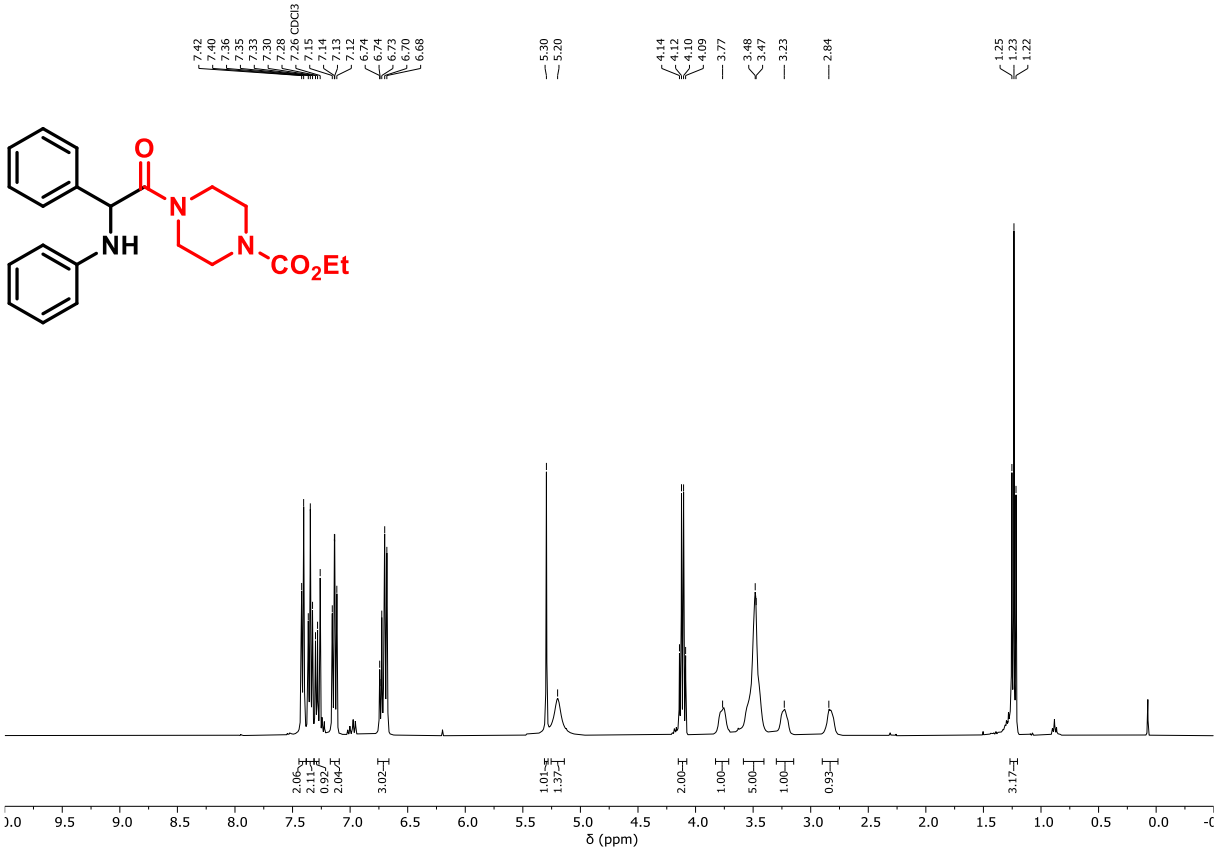
^{13}C-{^{1}H}-NMR (151 MHz) of 4-(((4-fluorophenyl)imino)methyl)-2-methoxyphenyl pivalate (**2t**).



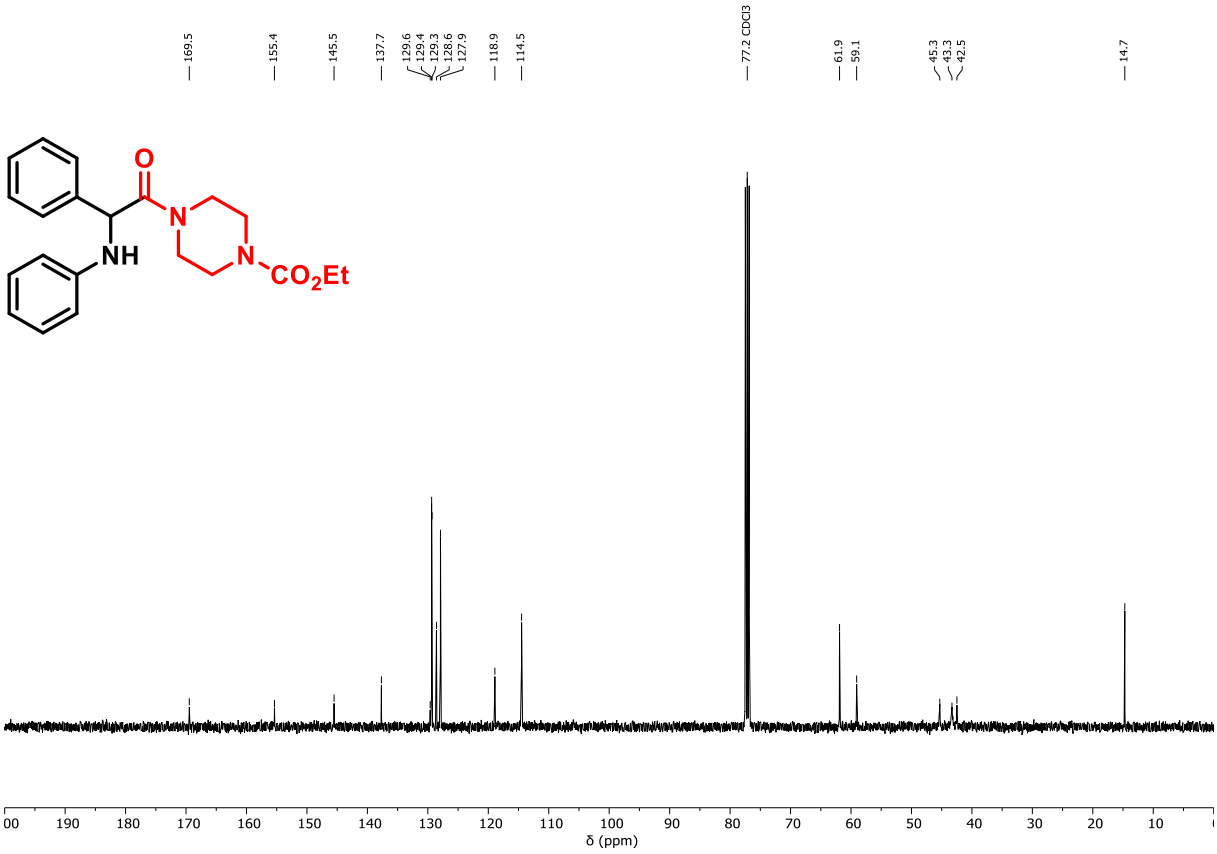
^{1}H-NMR (400 MHz) of 1-morpholino-2-phenyl-2-(phenylamino)ethan-1-one (**3a**).



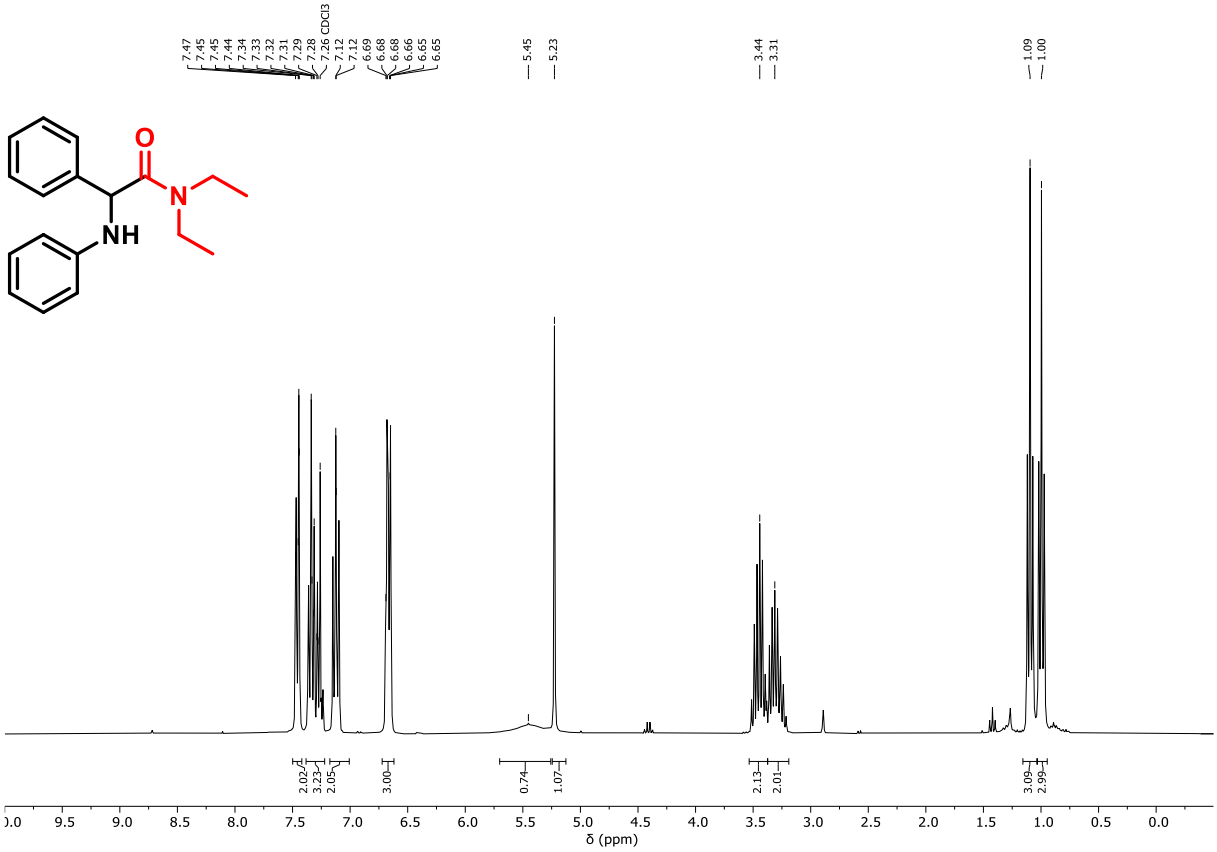
^{13}C-{^{1}H}-NMR (75 MHz) of 1-morpholino-2-phenyl-2-(phenylamino)ethan-1-one (**3a**).



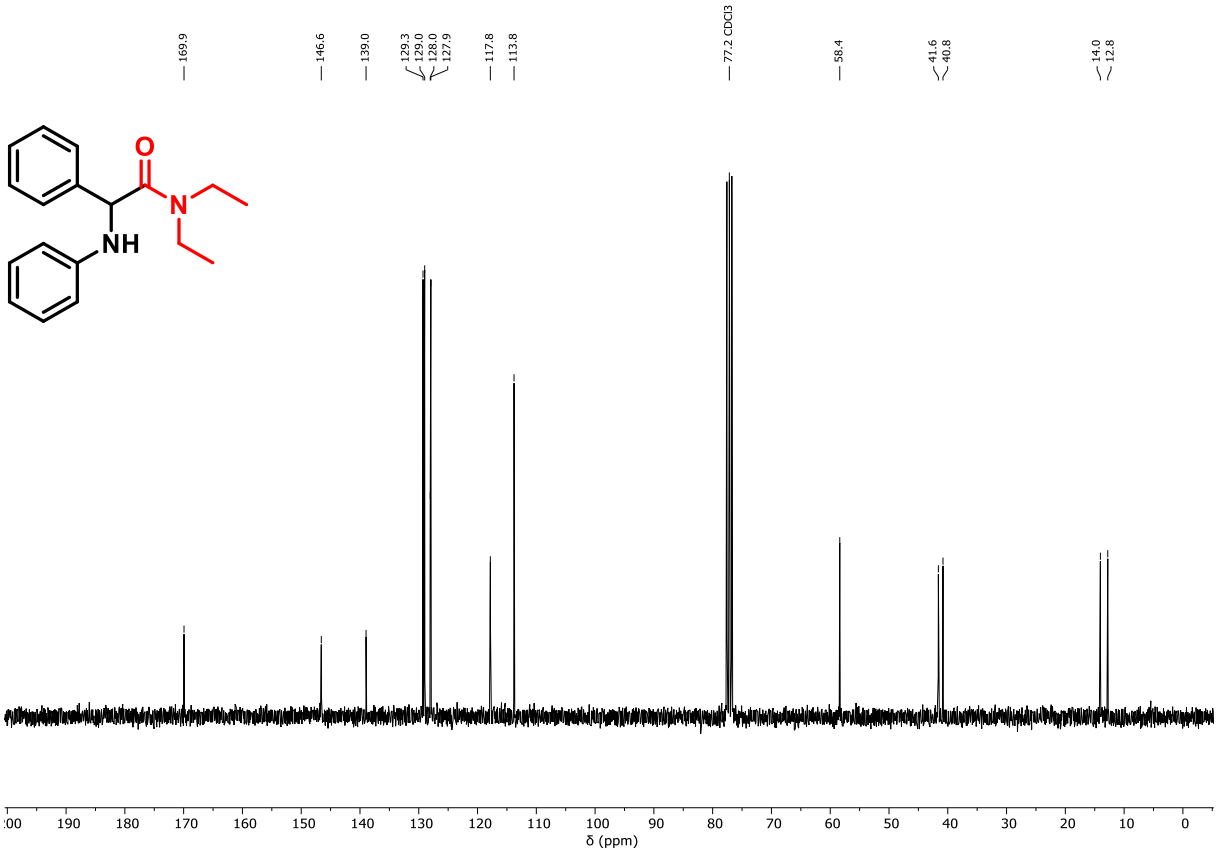
^{1}H-NMR (400 MHz) of ethyl 4-(2-phenyl-2-(phenylamino)acetyl)piperazine-1-carboxylate (**3b**).



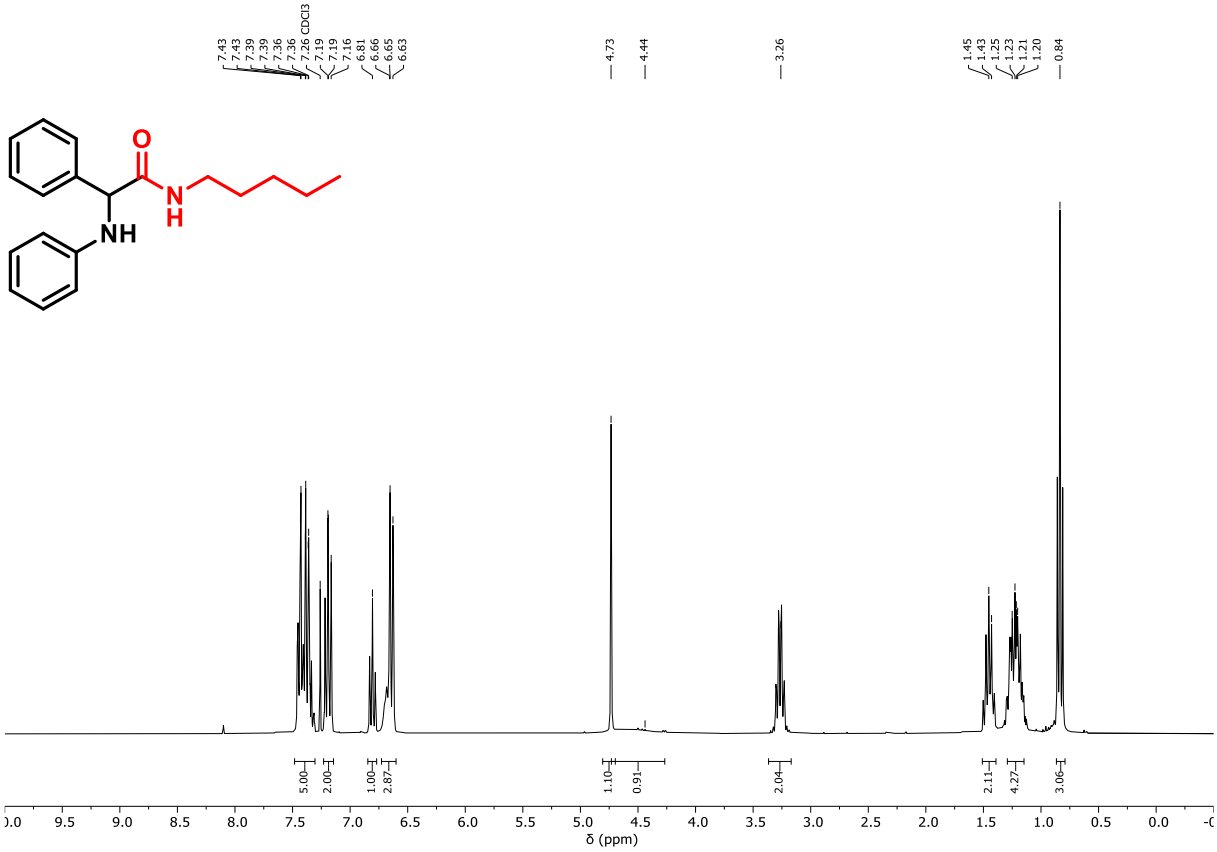
^{13}C-{^{1}H}-NMR (101 MHz) of ethyl 4-(2-phenyl-2-(phenylamino)acetyl)piperazine-1-carboxylate (**3b**).



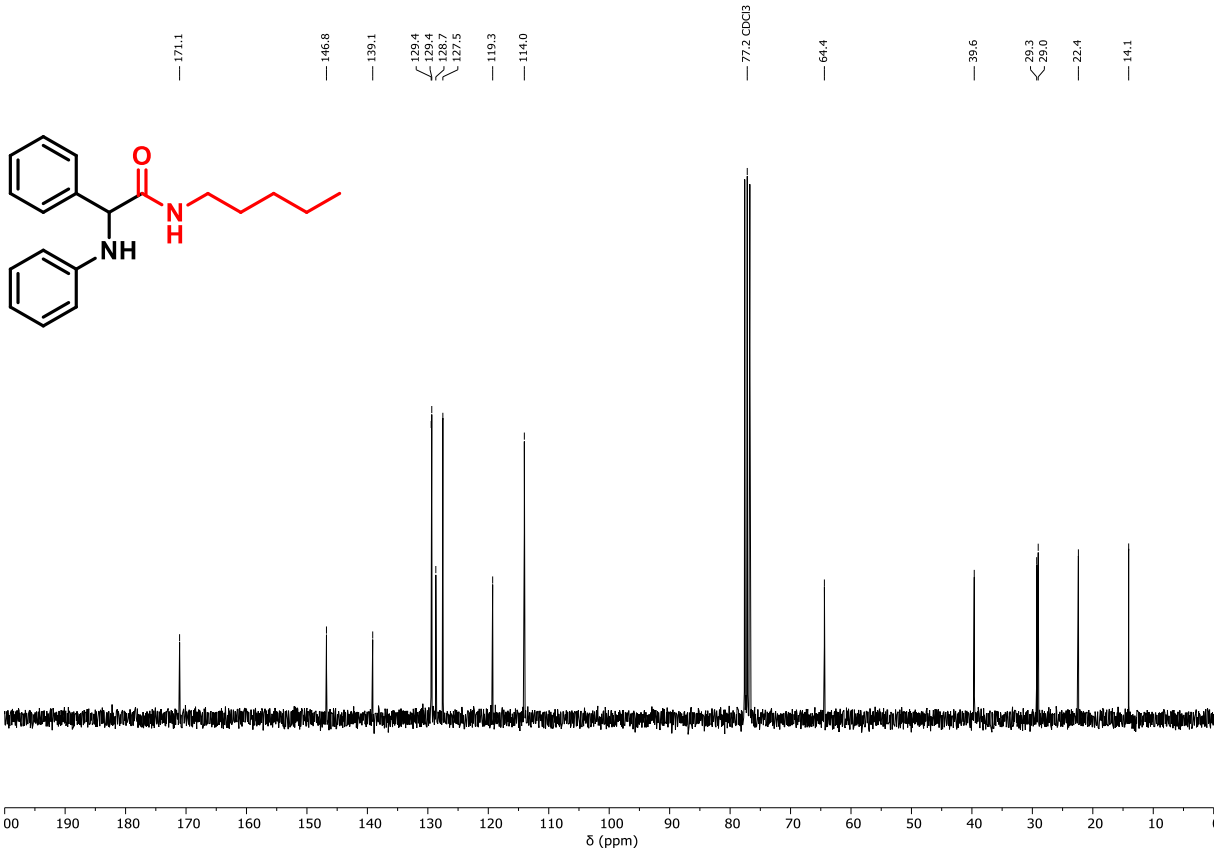
^{1}H-NMR (300 MHz) of *N*,*N*-diethyl-2-phenyl-2-(phenylamino)acetamide (**3c**).



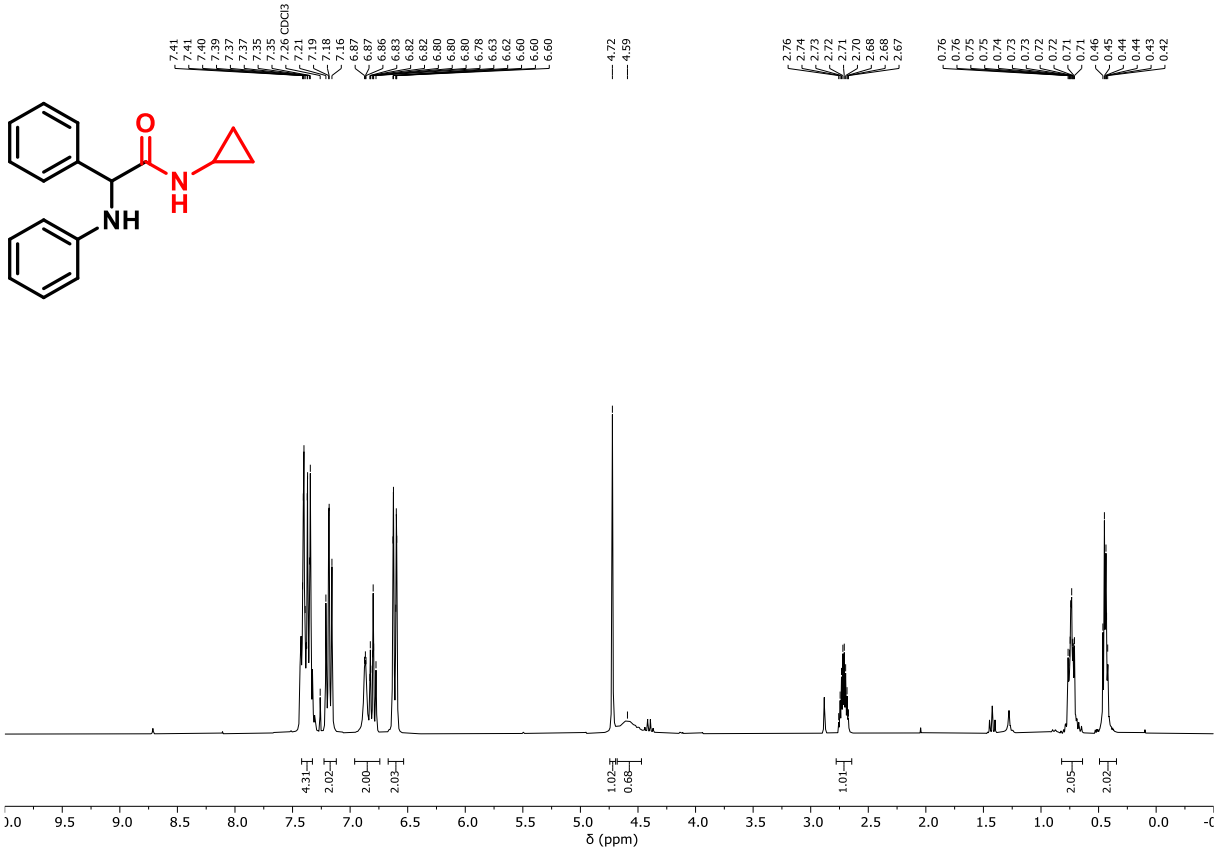
^{13}C-{^{1}H}-NMR (101 MHz) of *N*,*N*-diethyl-2-phenyl-2-(phenylamino)acetamide (**3c**).



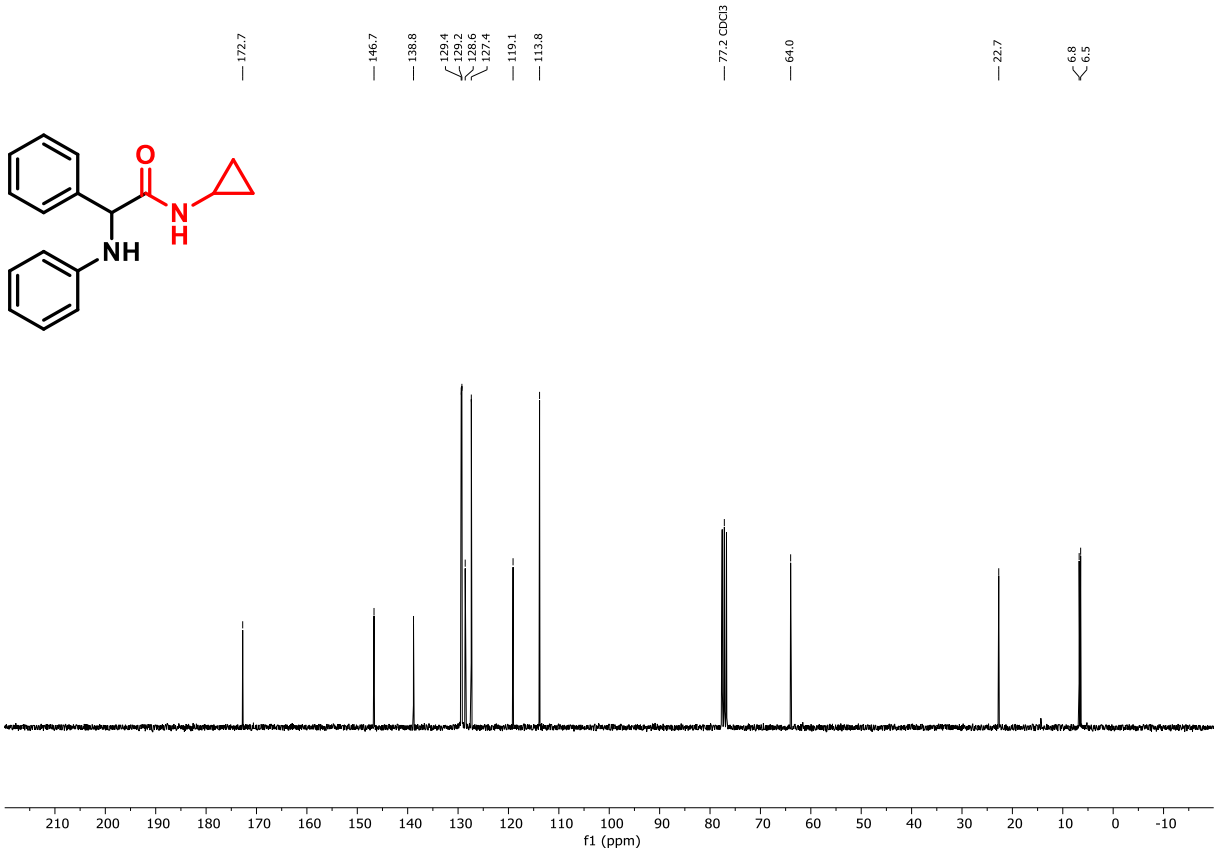
^{1}H-NMR (300 MHz) of *N*-pentyl-2-phenyl-2-(phenylamino)acetamide (**3d**).



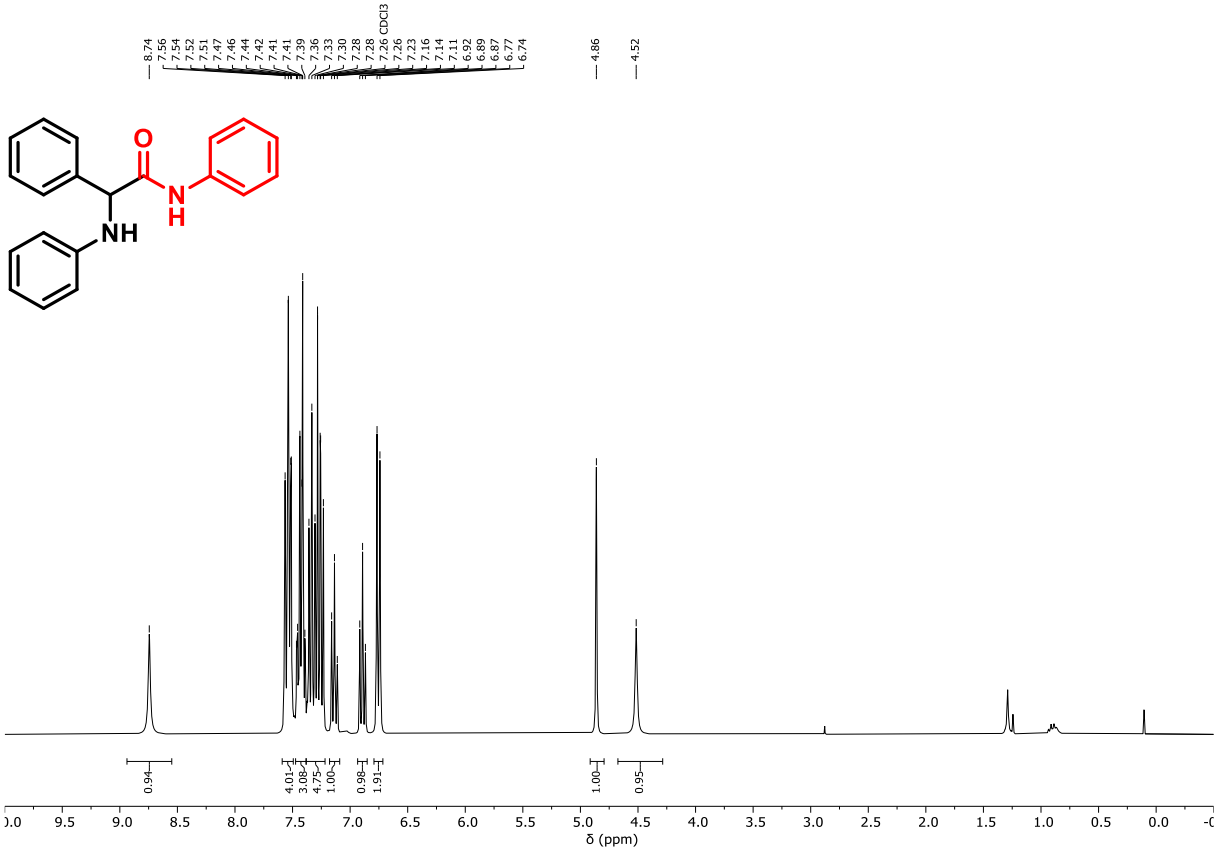
^{13}C-{^{1}H}-NMR (75 MHz) of *N*-pentyl-2-phenyl-2-(phenylamino)acetamide (**3d**).



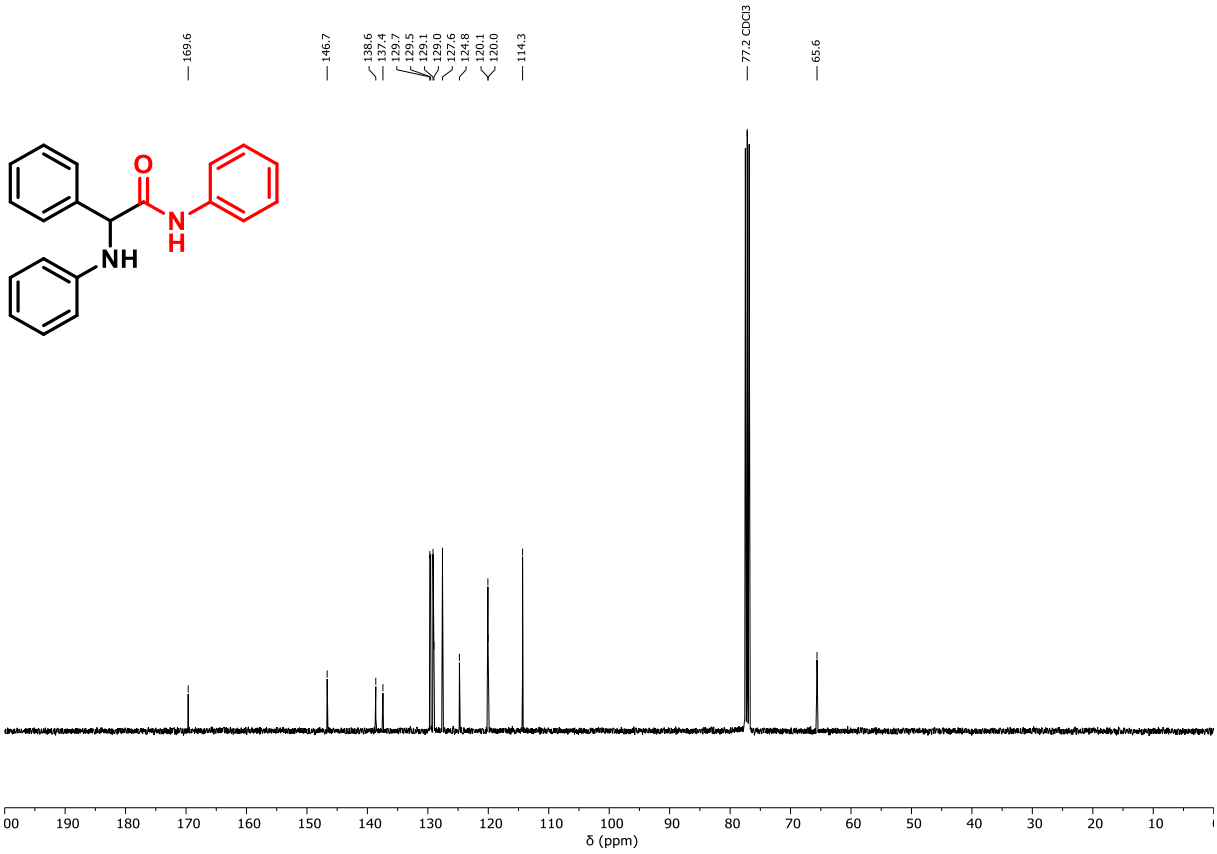
^{1}H-NMR (300 MHz) of *N*-cyclopropyl-2-phenyl-2-(phenylamino)acetamide (**3e**).



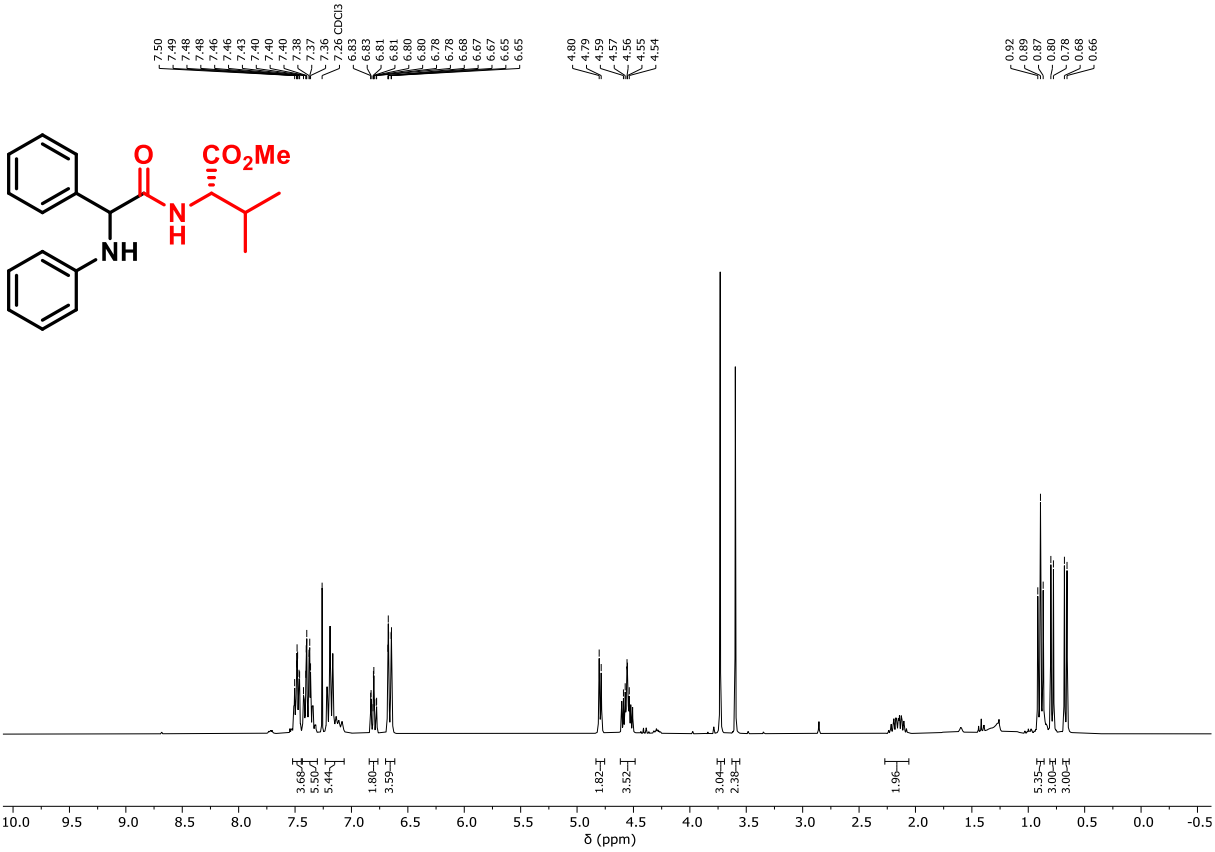
^{13}C-{^{1}H}-NMR (101 MHz) of *N*-cyclopropyl-2-phenyl-2-(phenylamino)acetamide (**3e**).



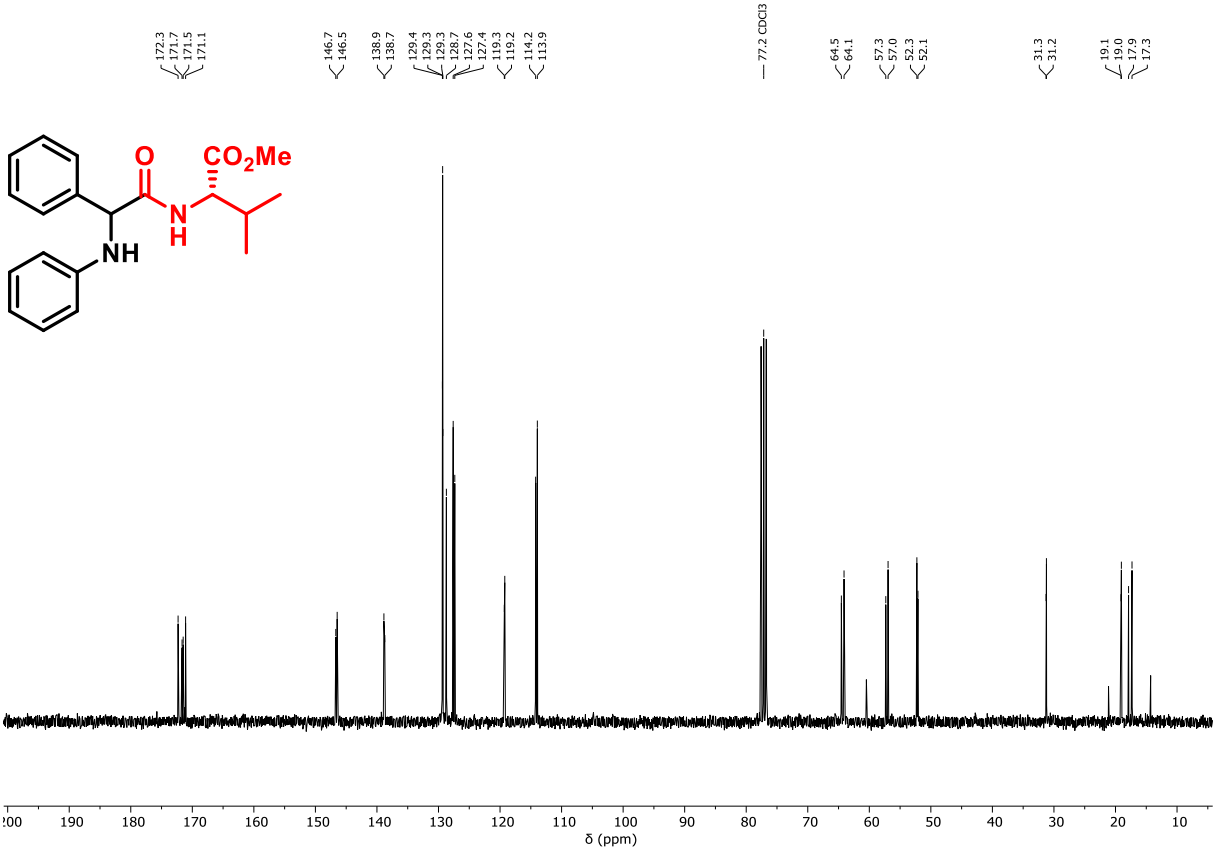
^{1}H-NMR (300 MHz) of *N*,2-diphenyl-2-(phenylamino)acetamide (**3f**).



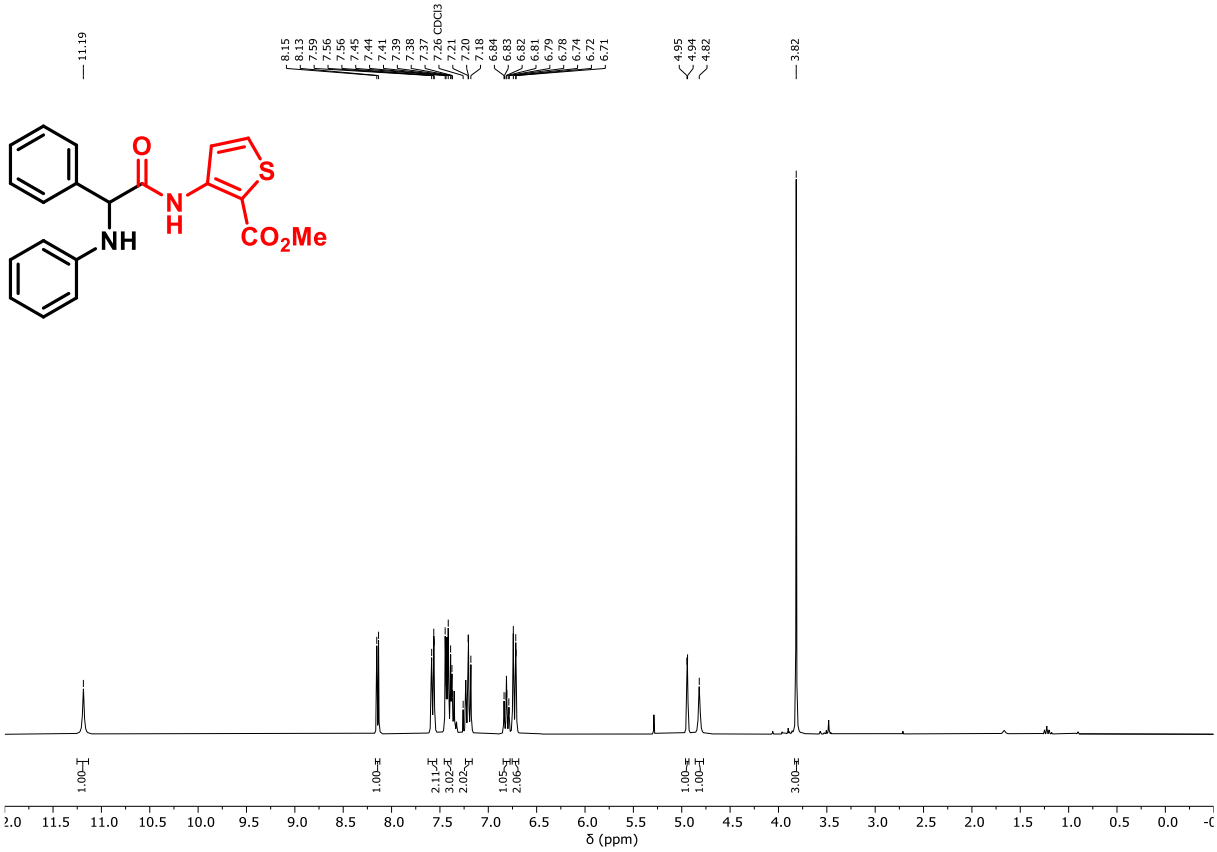
^{13}C-{^{1}H}-NMR (75 MHz) of *N*,2-diphenyl-2-(phenylamino)acetamide (**3f**).



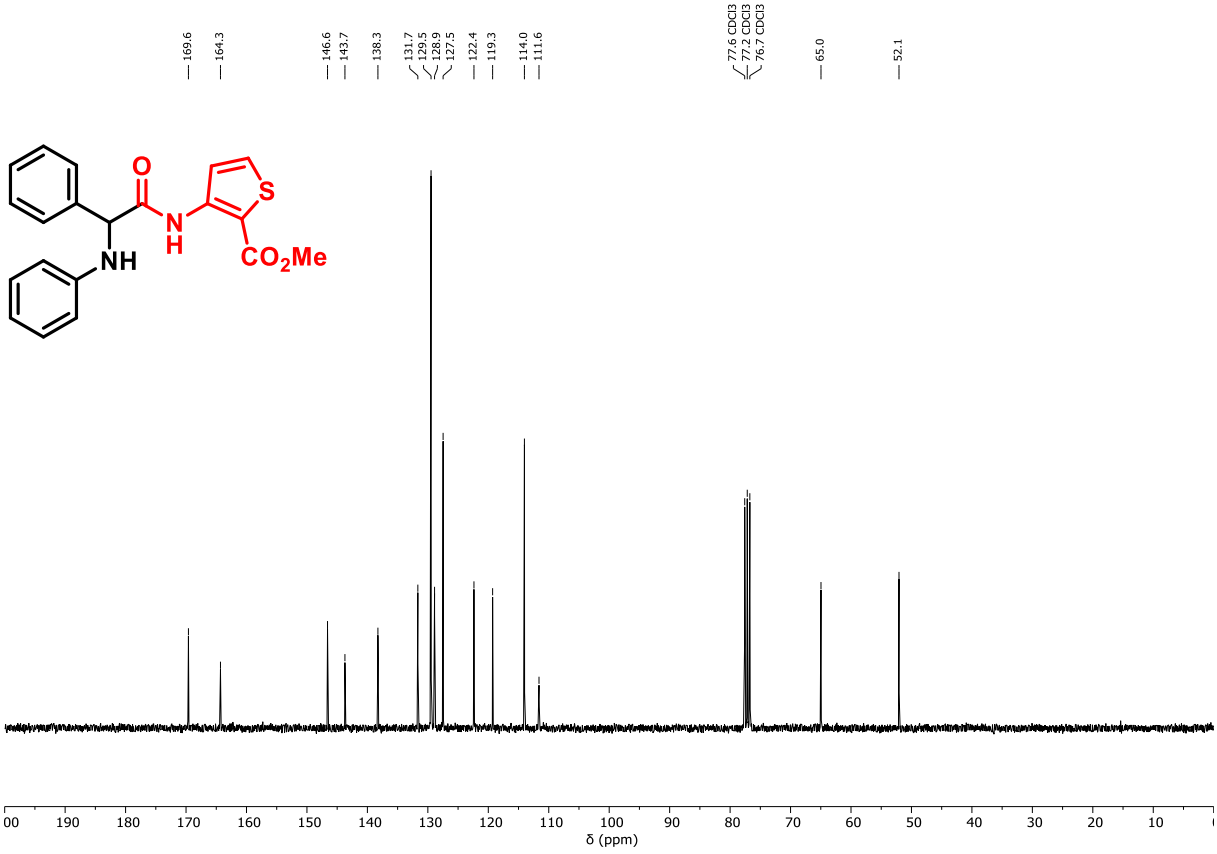
^{1}H-NMR (300 MHz) of methyl (2-phenyl-2-(phenylamino)acetyl)-(*S*)-valinate (diastereomeric mixture) (**3g**).



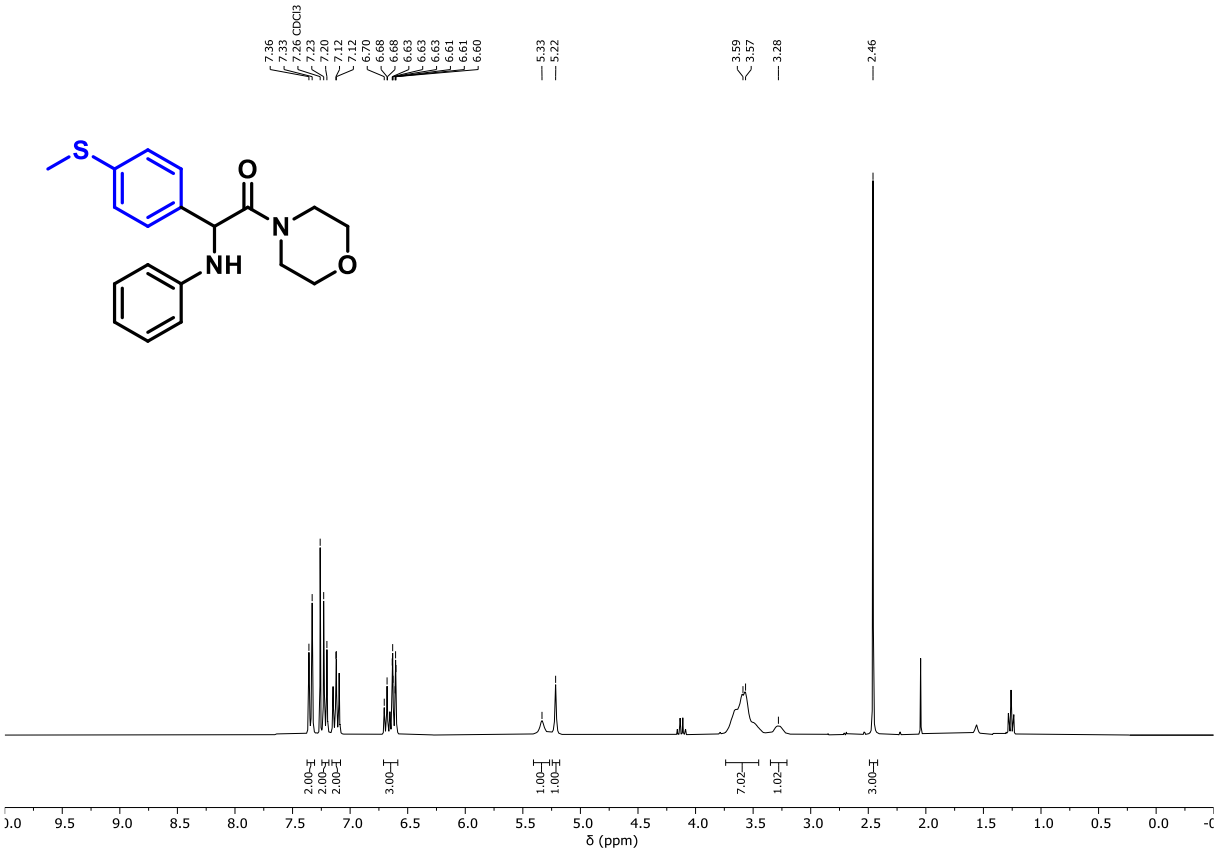
^{13}C-{^{1}H}-NMR (75 MHz) of methyl (2-phenyl-2-(phenylamino)acetyl)-(*S*)-valinate (diastereomeric mixture) (**3g**).



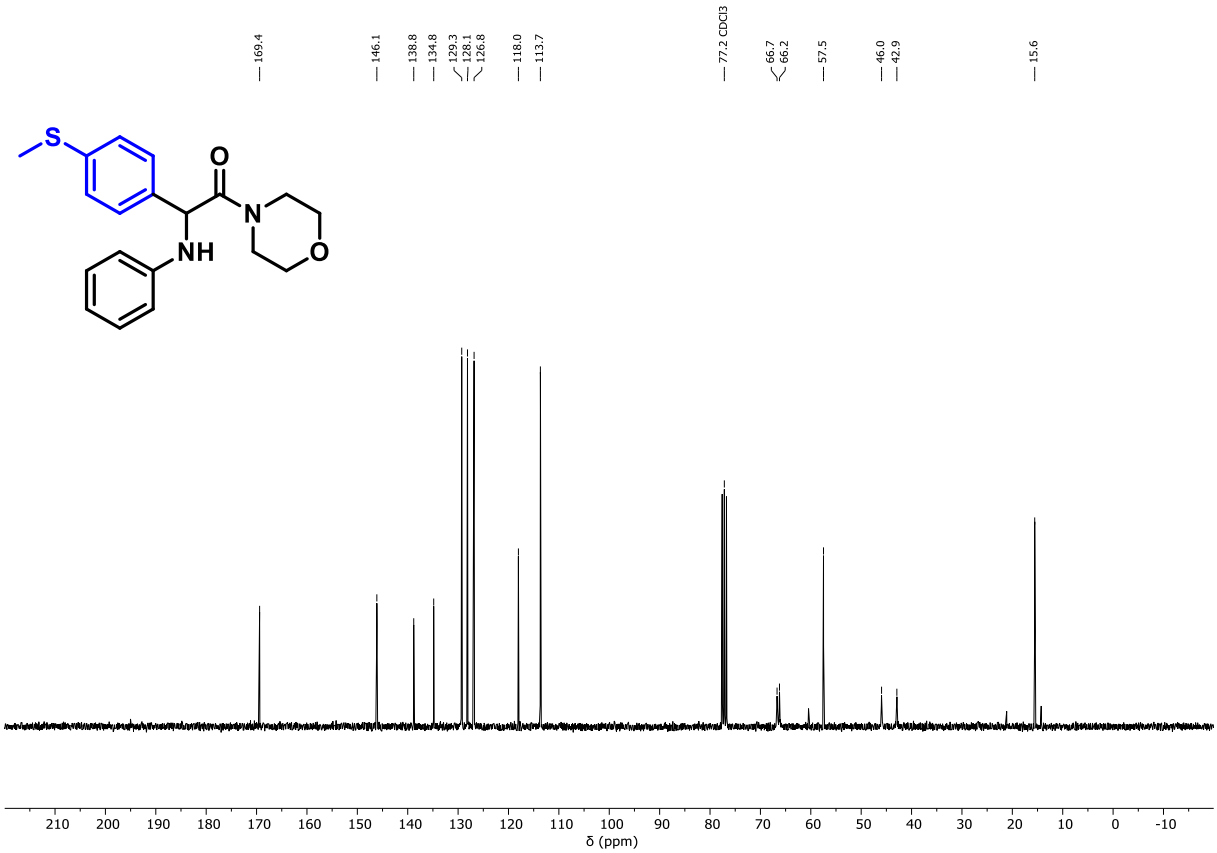
^{1}H-NMR (300 MHz) of methyl 3-(2-phenyl-2-(phenylamino)acetamido)thiophene-2-carboxylate (**3i**).



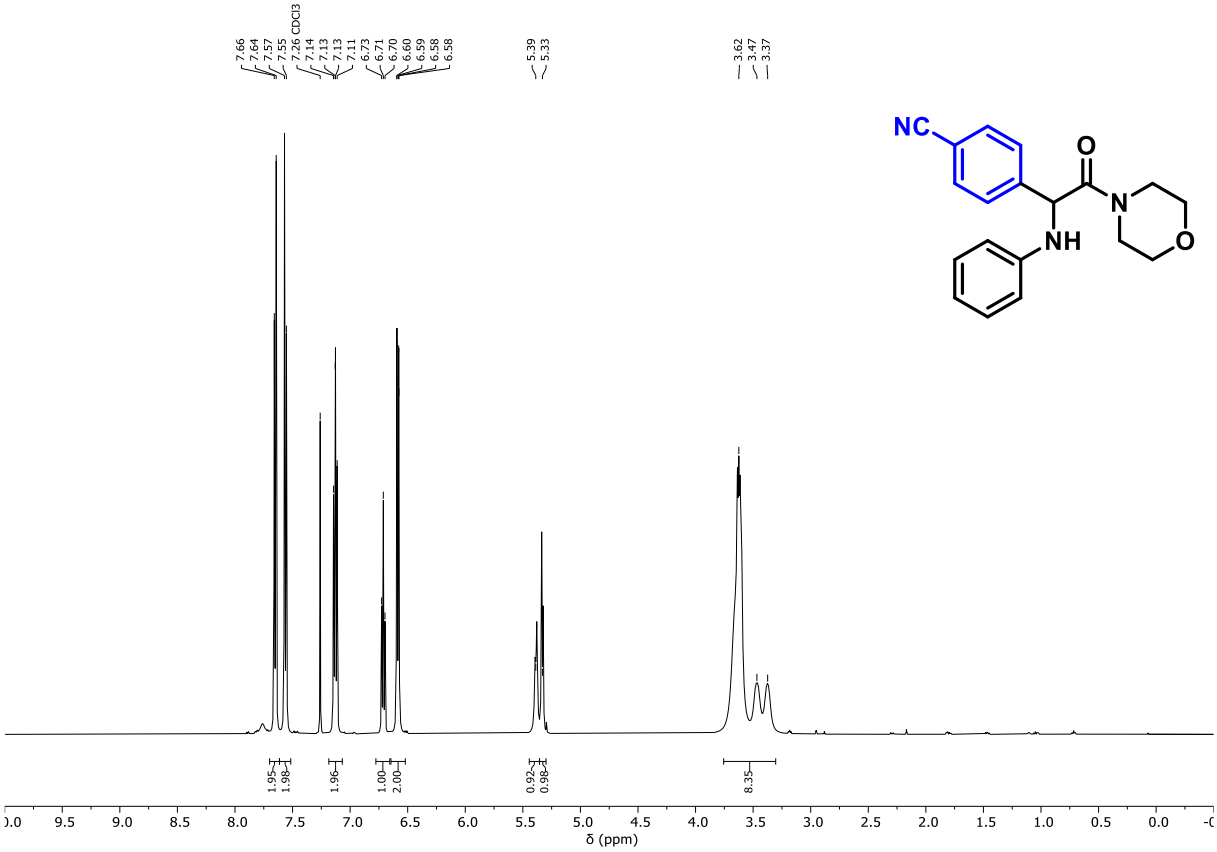
^{13}C-{^{1}H}-NMR (75 MHz) of methyl 3-(2-phenyl-2-(phenylamino)acetamido)thiophene-2-carboxylate (**3i**).



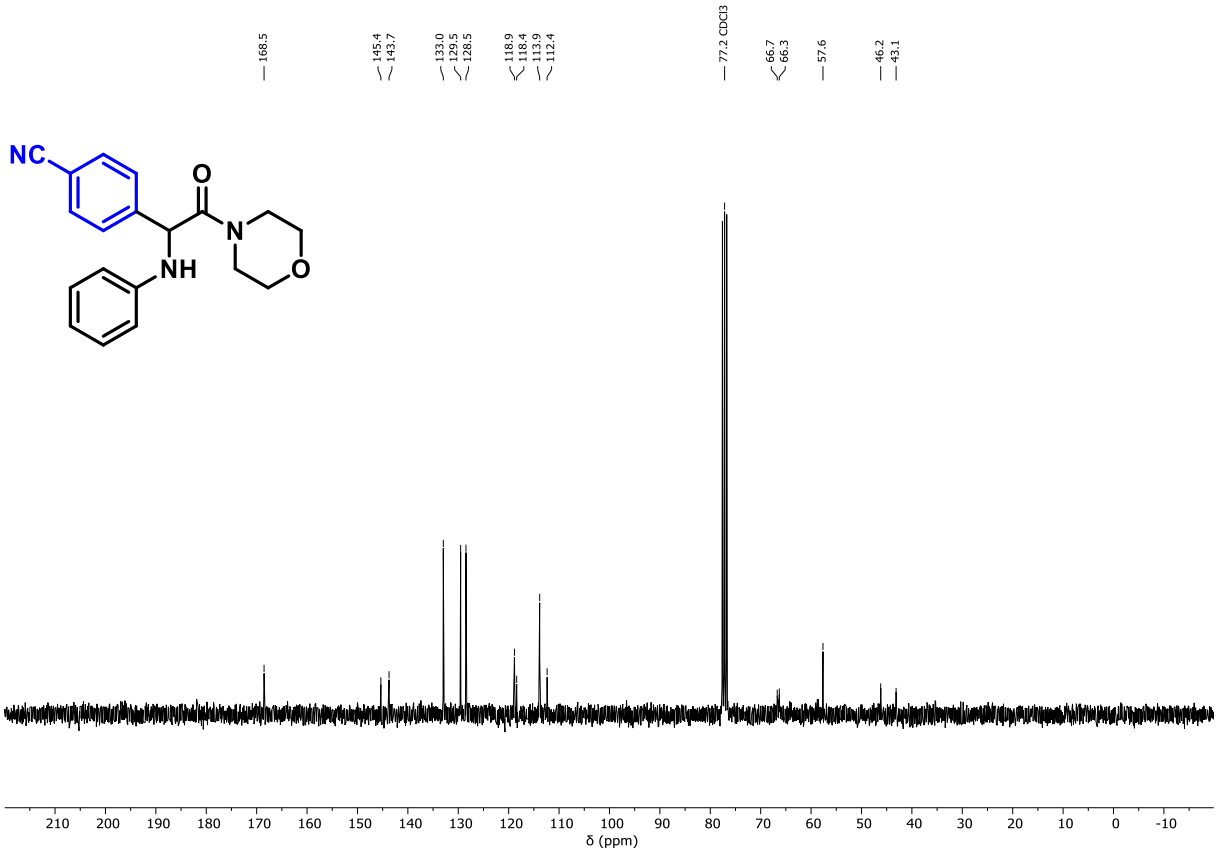
^{1}H-NMR (300 MHz) of 2-(4-(methylthio)phenyl)-1-morpholino-2-(phenylamino)ethan-1-one (**4a**).



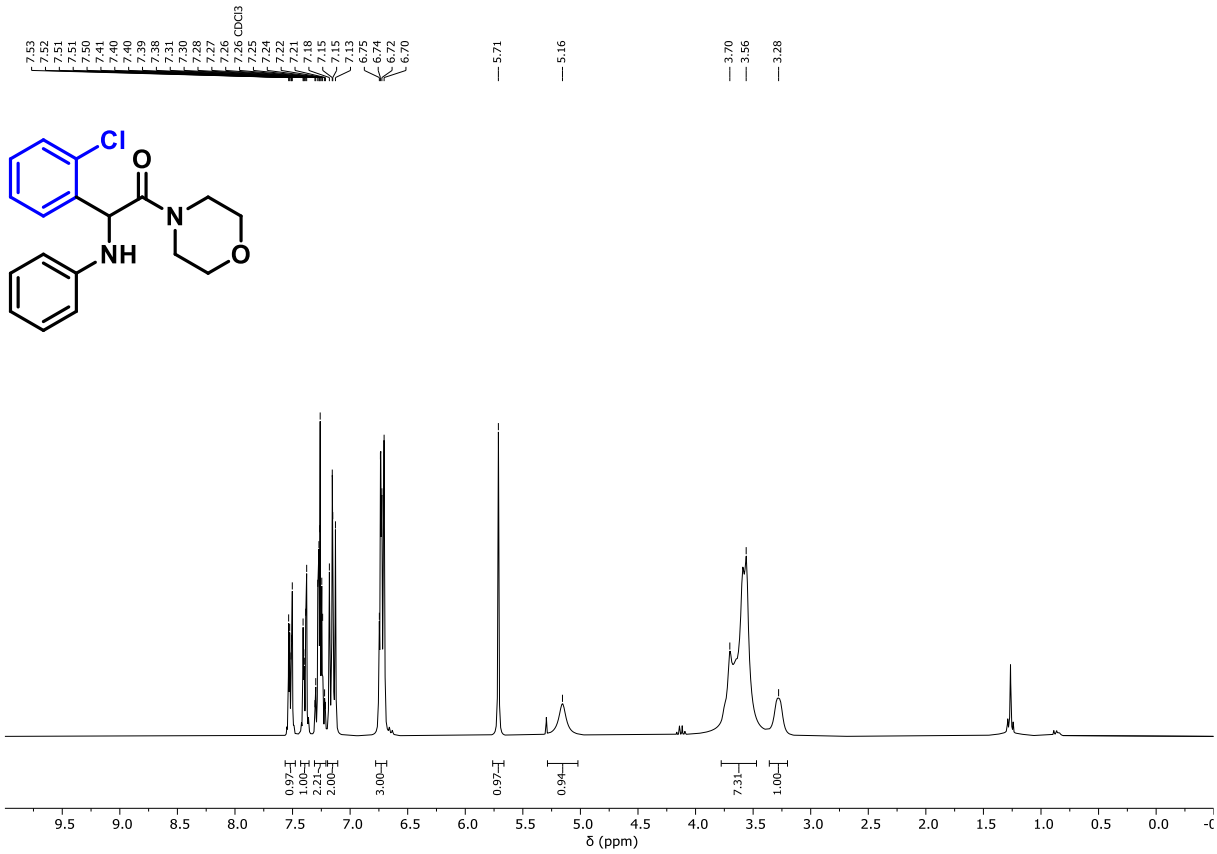
^{13}C-{^{1}H}-NMR (75 MHz) of 2-(4-(methylthio)phenyl)-1-morpholino-2-(phenylamino)ethan-1-one (**4a**).



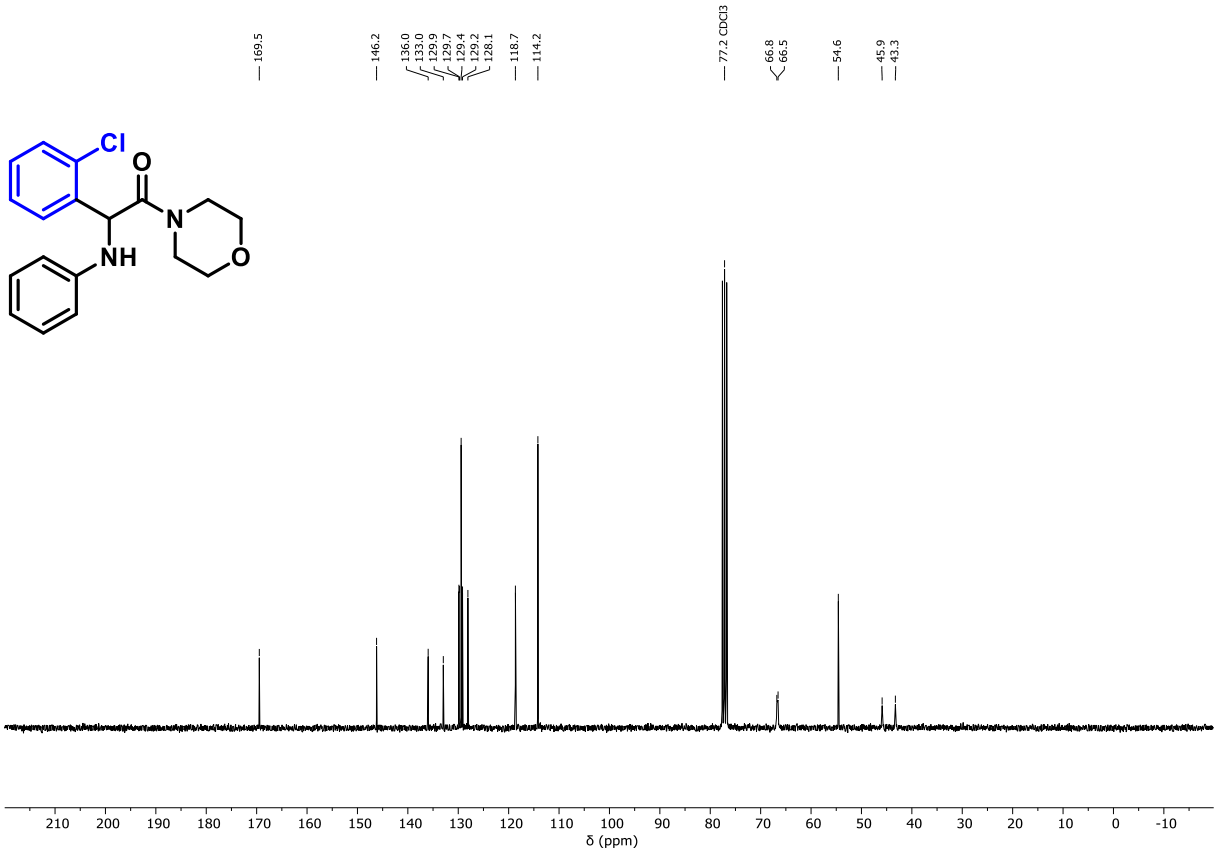
^{1}H-NMR (500 MHz) of 2-(4-cyanophenyl)-1-morpholino-2-(phenylamino)ethan-1-one (**4b**).



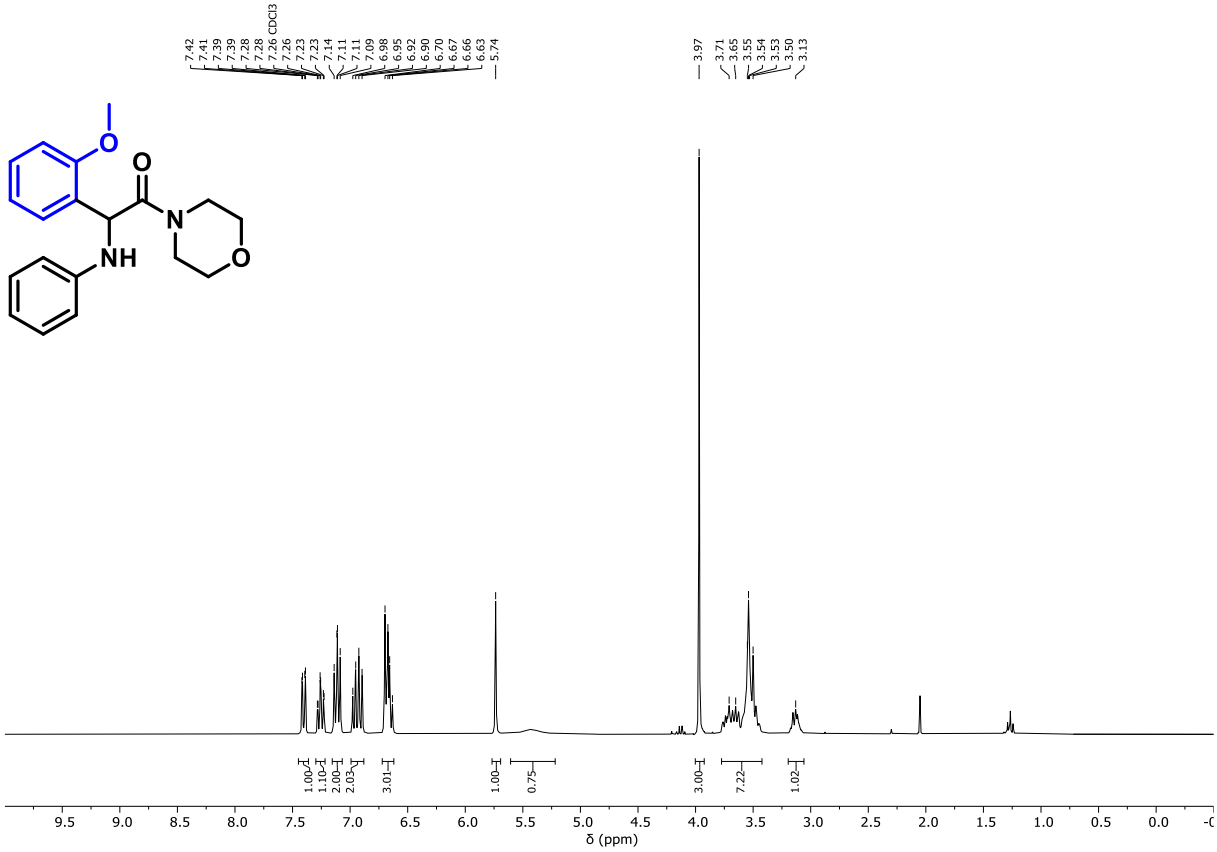
^{13}C-{^{1}H}-NMR (75 MHz) of 2-(4-cyanophenyl)-1-morpholino-2-(phenylamino)ethan-1-one (**4b**).



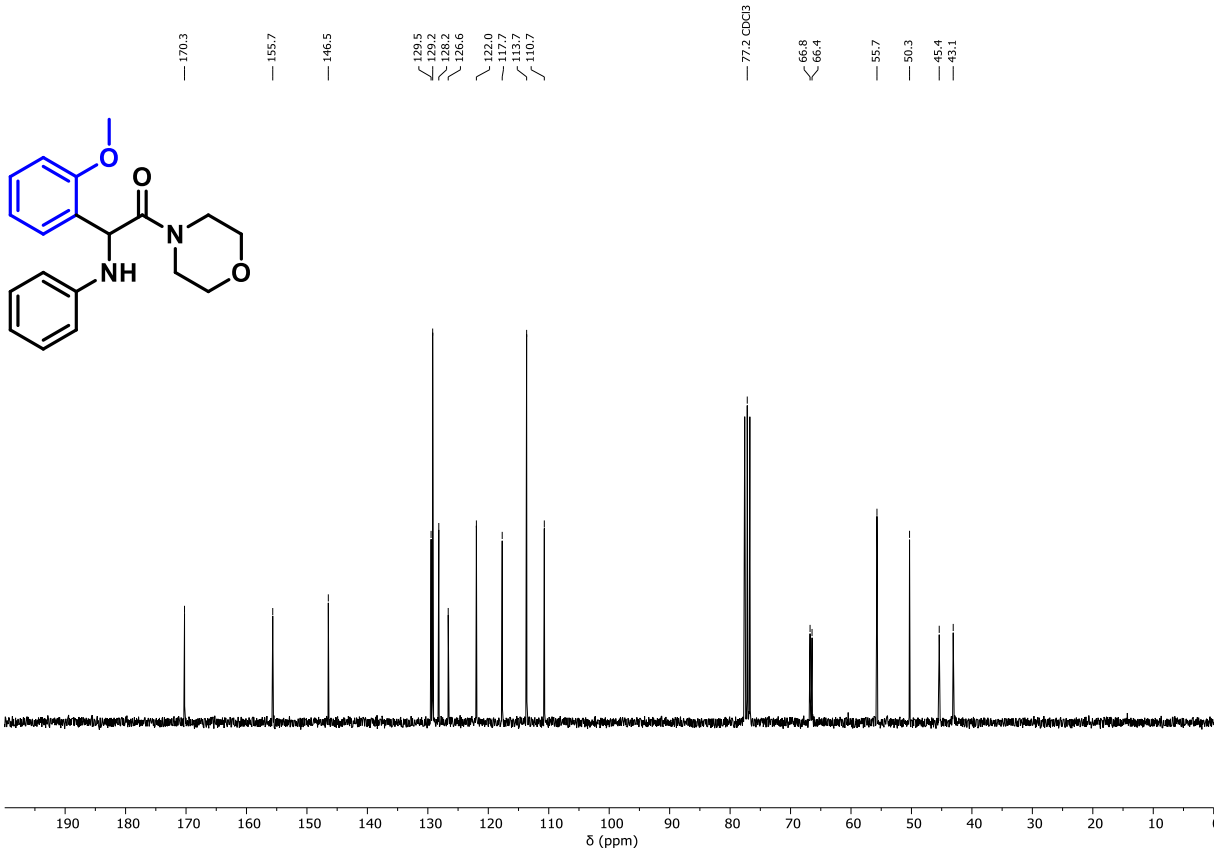
^{1}H-NMR (300 MHz) of 2-(2-chlorophenyl)-1-morpholino-2-(phenylamino)ethan-1-one (**4c**).



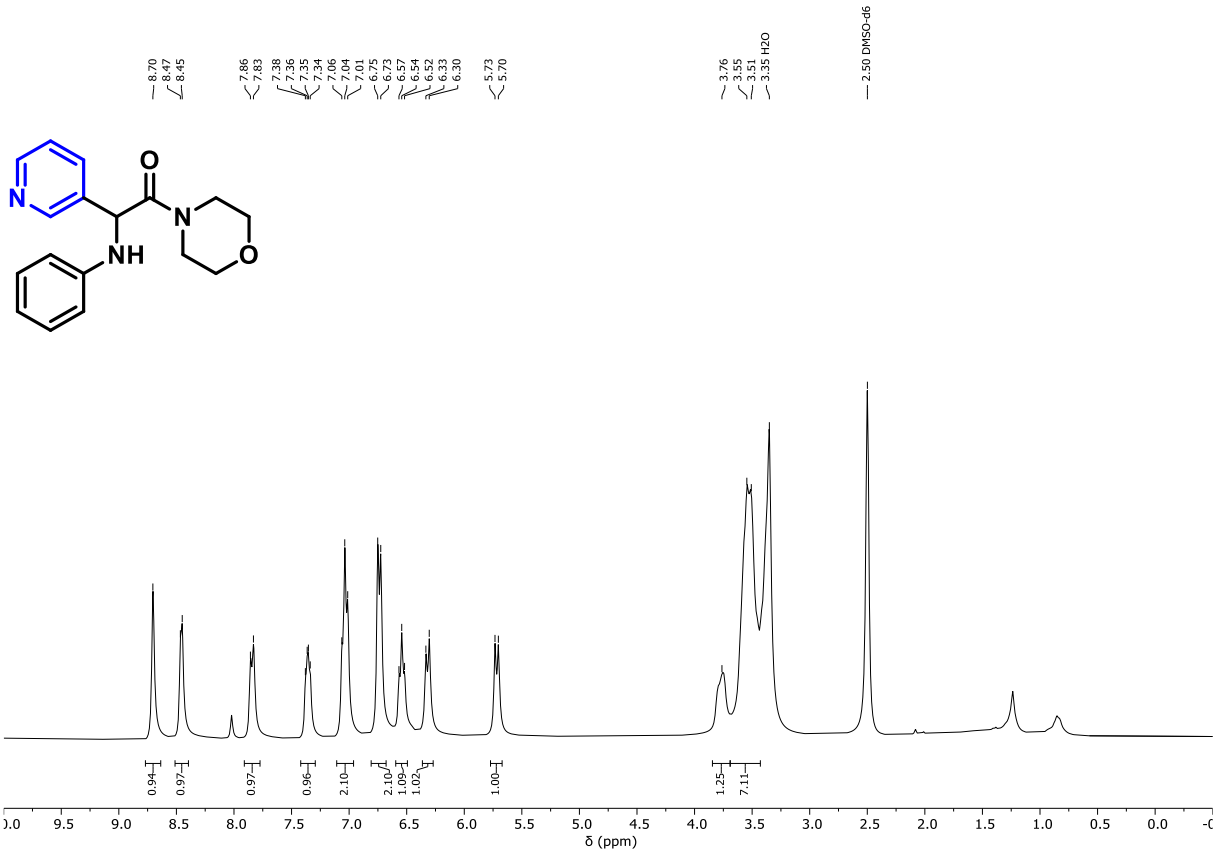
^{13}C-{^{1}H}-NMR (75 MHz) of 2-(2-chlorophenyl)-1-morpholino-2-(phenylamino)ethan-1-one (**4c**).



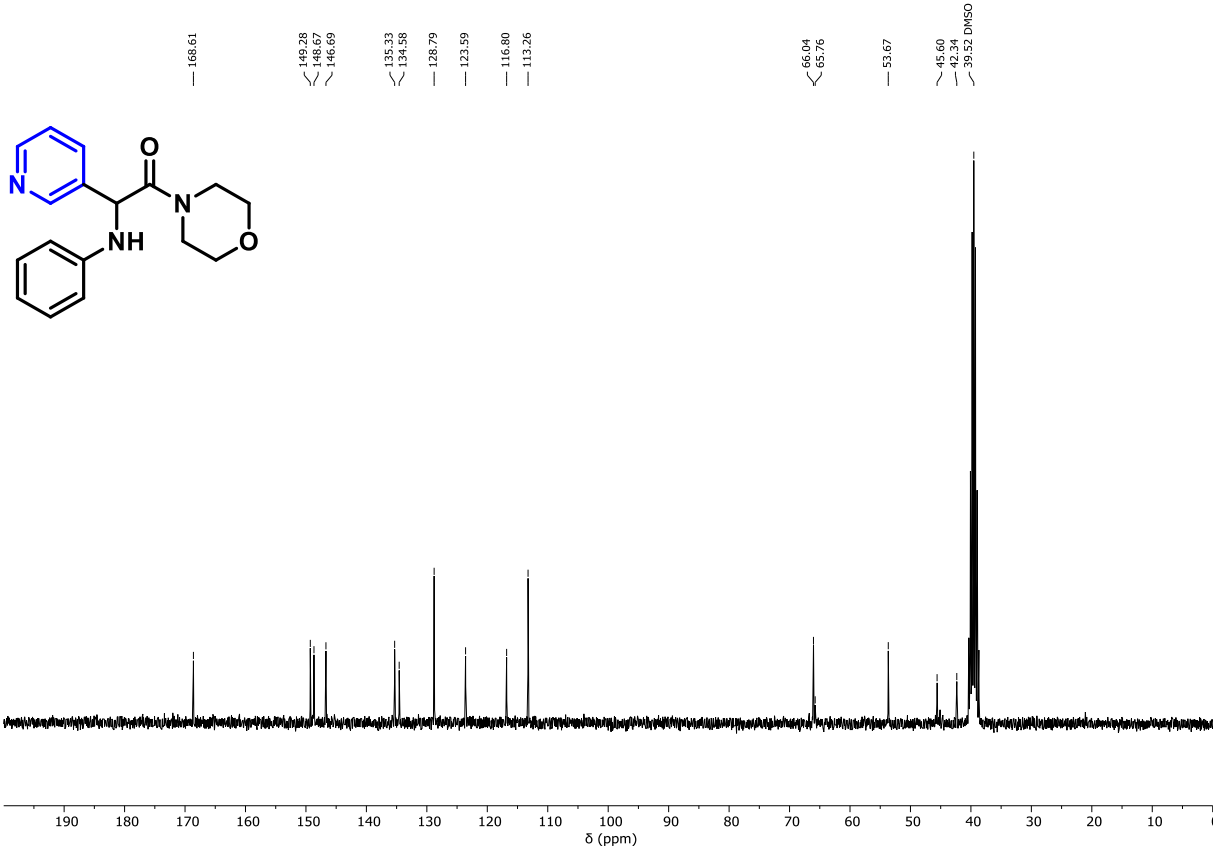
^{1}H-NMR (300 MHz) of 2-(2-methoxyphenyl)-1-morpholino-2-(phenylamino)ethan-1-one (**4d**).



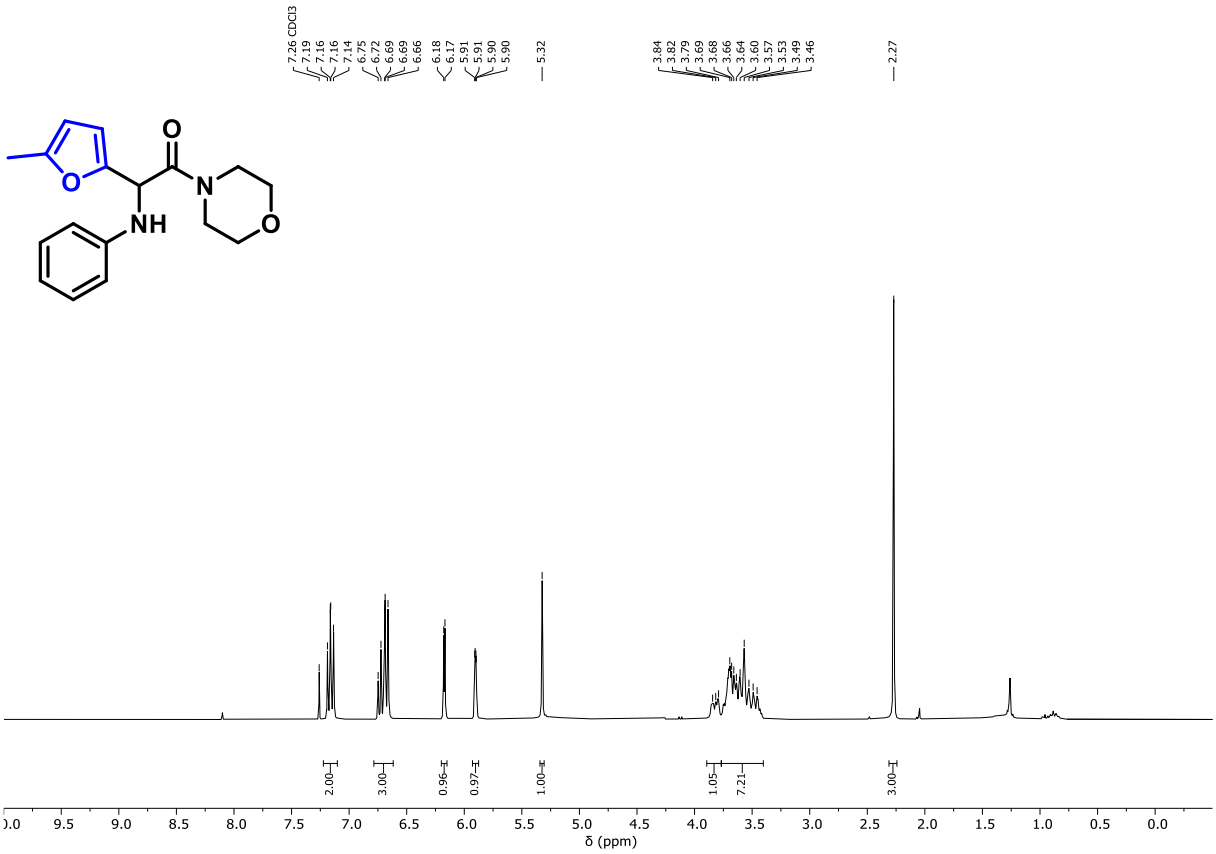
^{13}C-{^{1}H}-NMR (75 MHz) of 2-(2-methoxyphenyl)-1-morpholino-2-(phenylamino)ethan-1-one (**4d**).



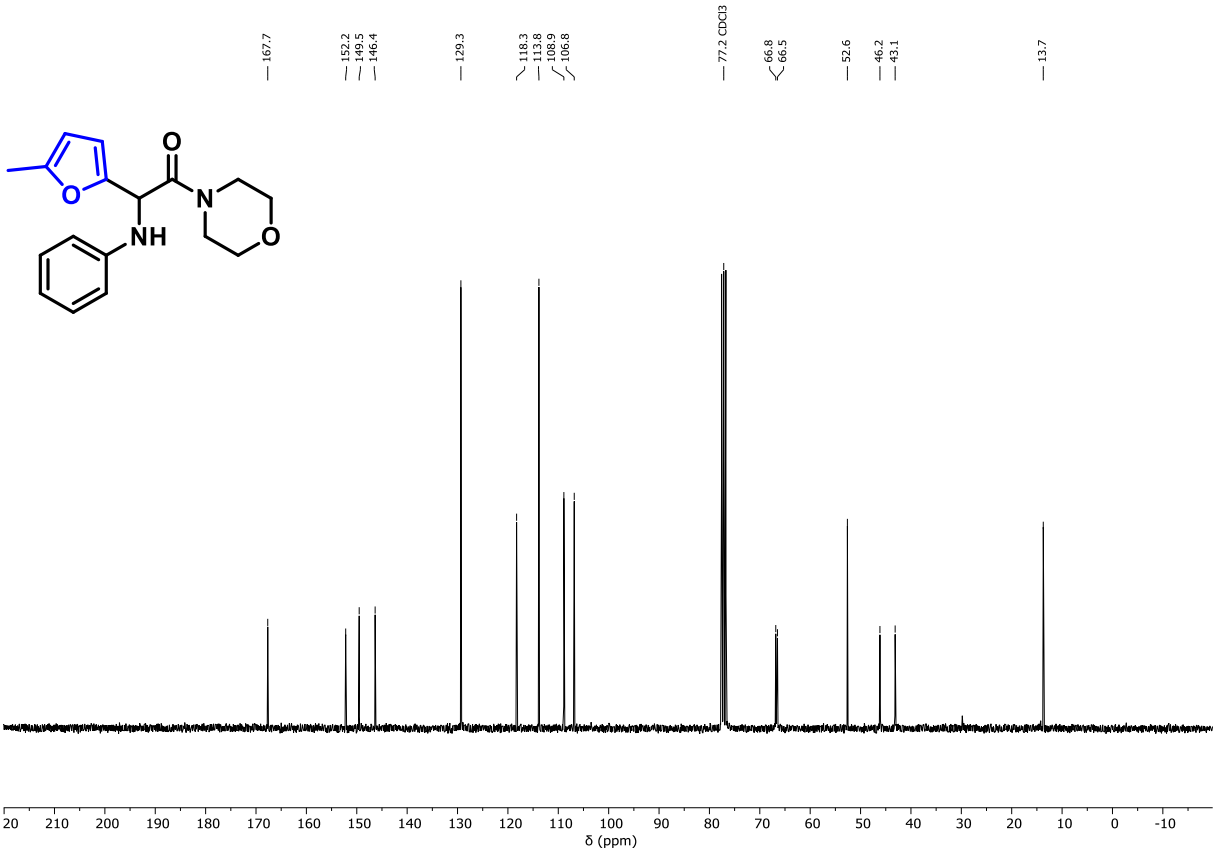
^{1}H-NMR (300 MHz) of 1-morpholino-2-(phenylamino)-2-(pyridin-3-yl)ethan-1-one (**4e**).



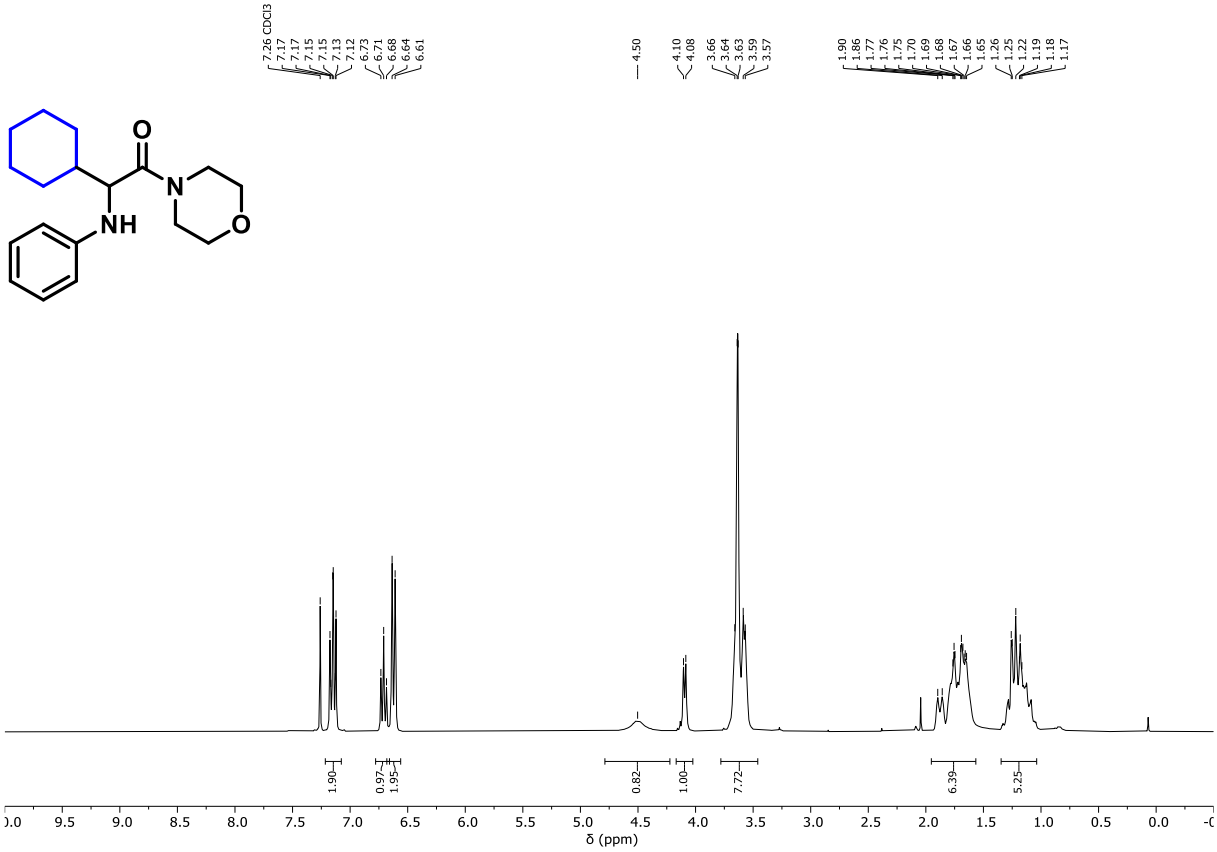
^{13}C-{^{1}H}-NMR (75 MHz) of 1-morpholino-2-(phenylamino)-2-(pyridin-3-yl)ethan-1-one (**4e**).



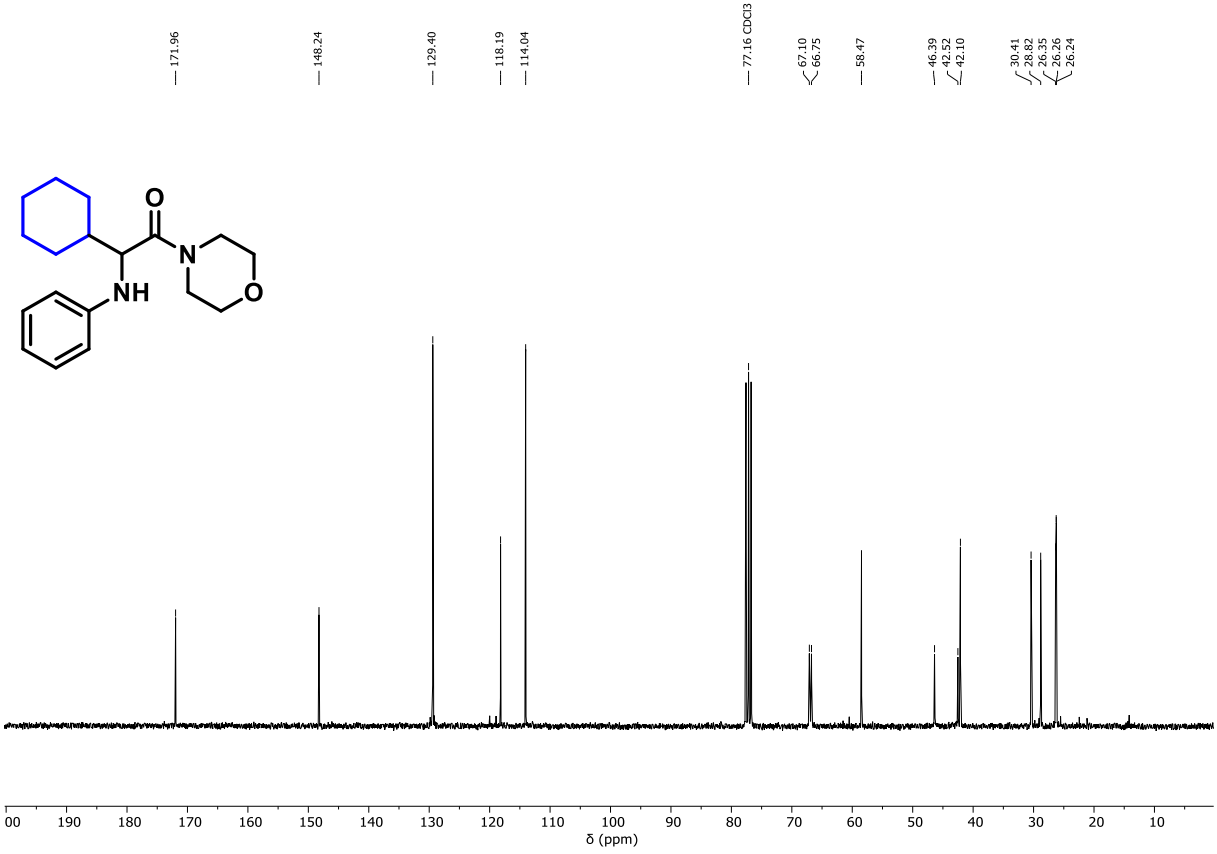
^{1}H-NMR (300 MHz) of 2-(5-methylfuran-2-yl)-1-morpholino-2-(phenylamino)ethan-1-one (**4f**).



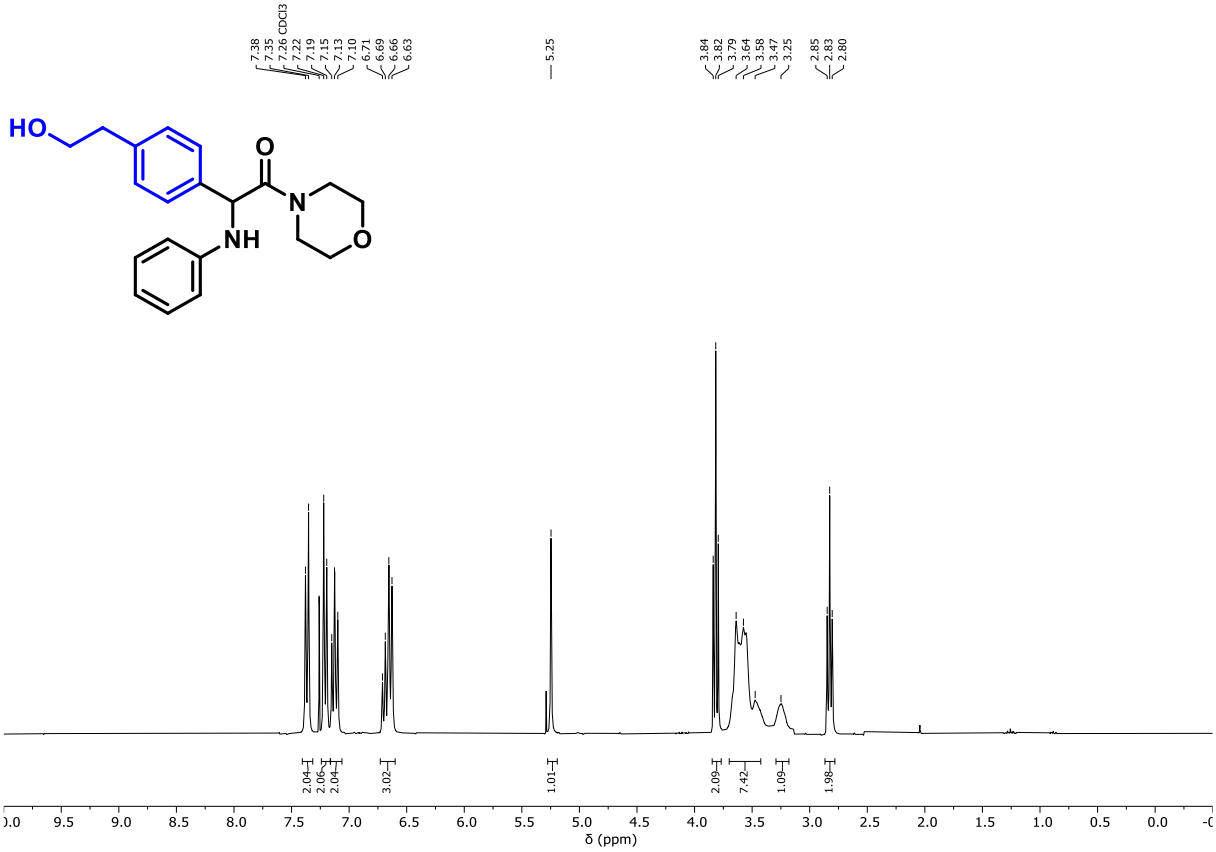
^{13}C-{^{1}H}-NMR (75 MHz) of 2-(5-methylfuran-2-yl)-1-morpholino-2-(phenylamino)ethan-1-one (**4f**).



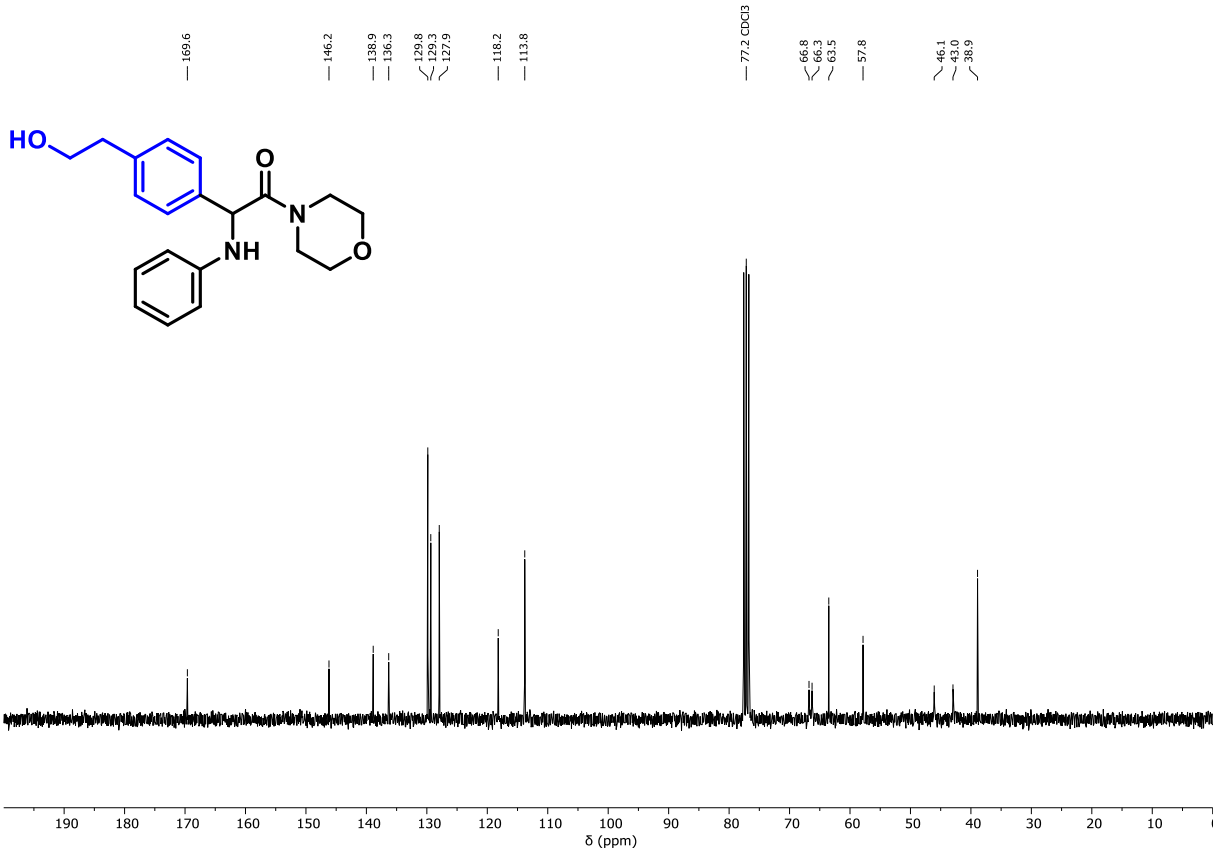
^{1}H-NMR (300 MHz) of 2-cyclohexyl-1-morpholino-2-(phenylamino)ethan-1-one (**4g**)



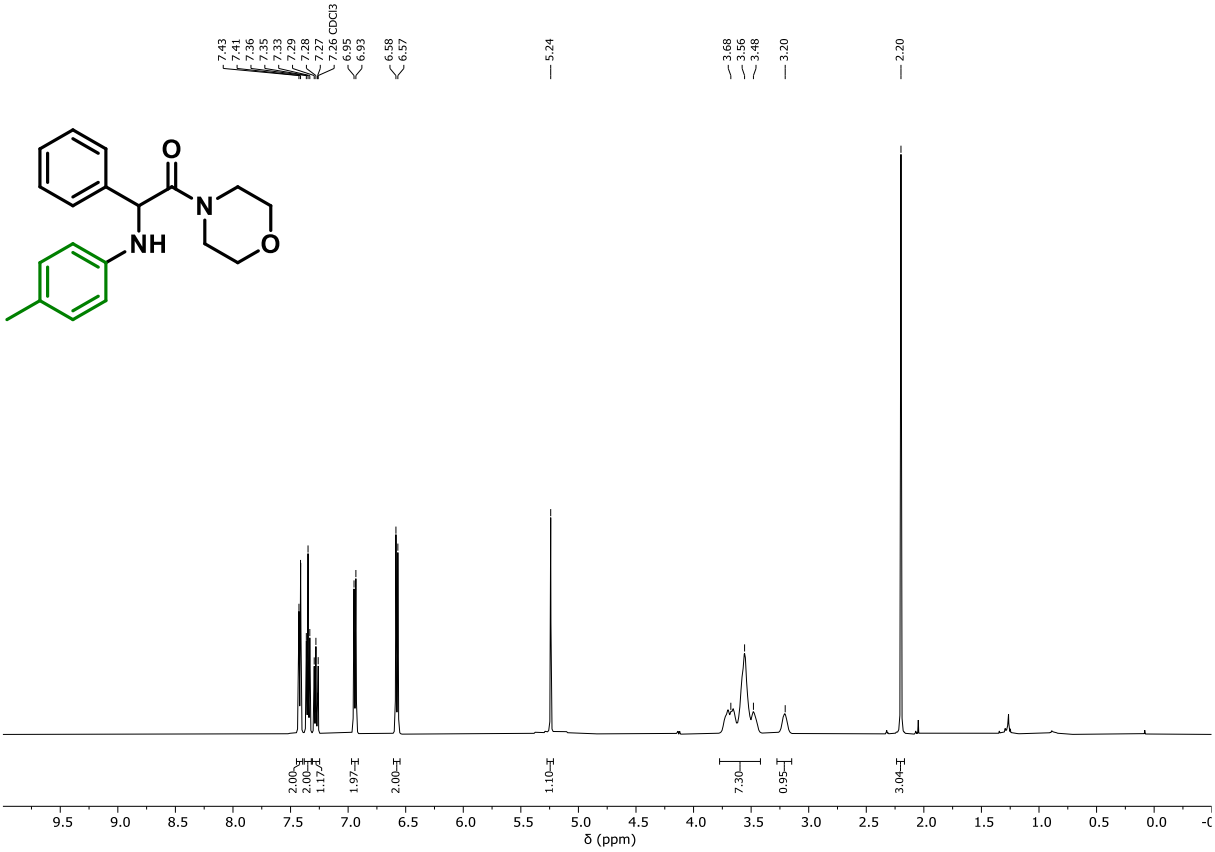
^{13}C-{^{1}H}-NMR (75 MHz) of 2-cyclohexyl-1-morpholino-2-(phenylamino)ethan-1-one (**4g**).



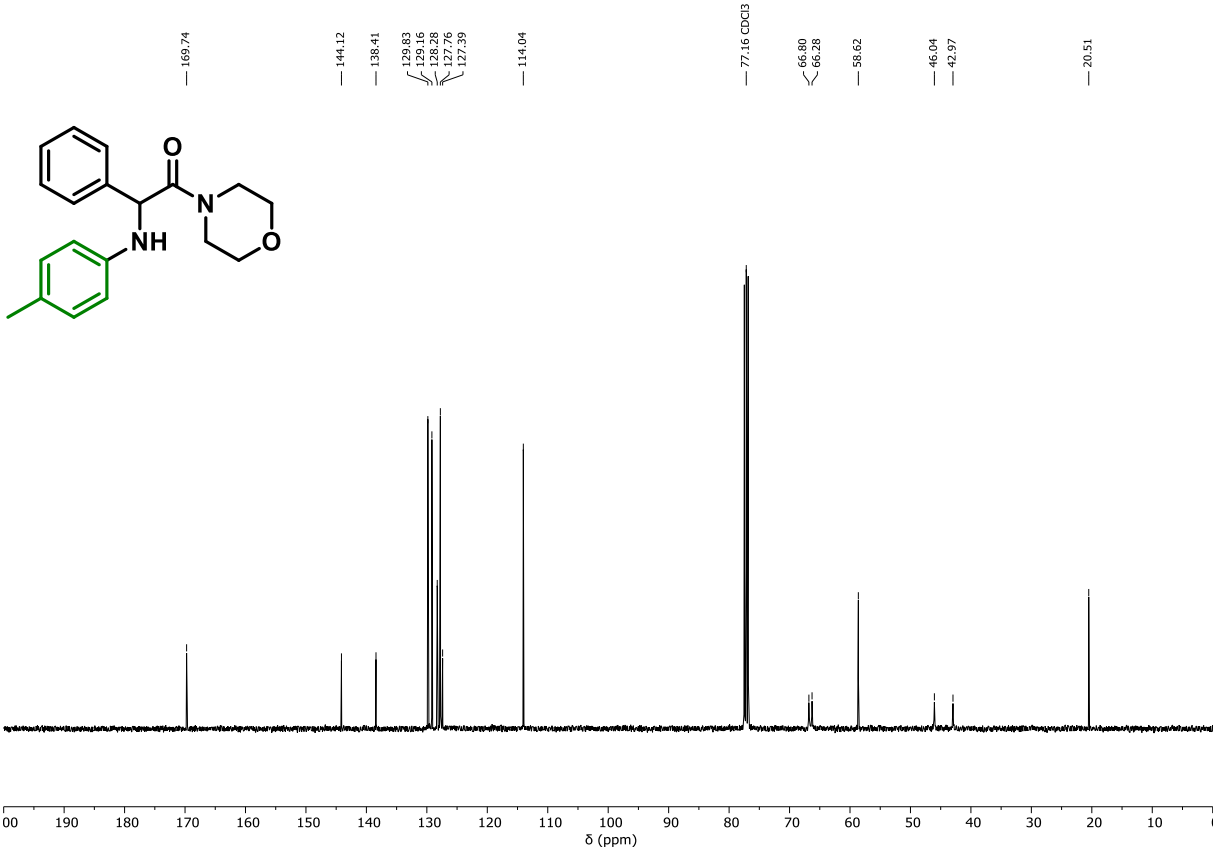
^{1}H-NMR (300 MHz) of 2-(4-(2-hydroxyethyl)phenyl)-1-morpholino-2-(phenylamino)ethan-1-one (**4h**).



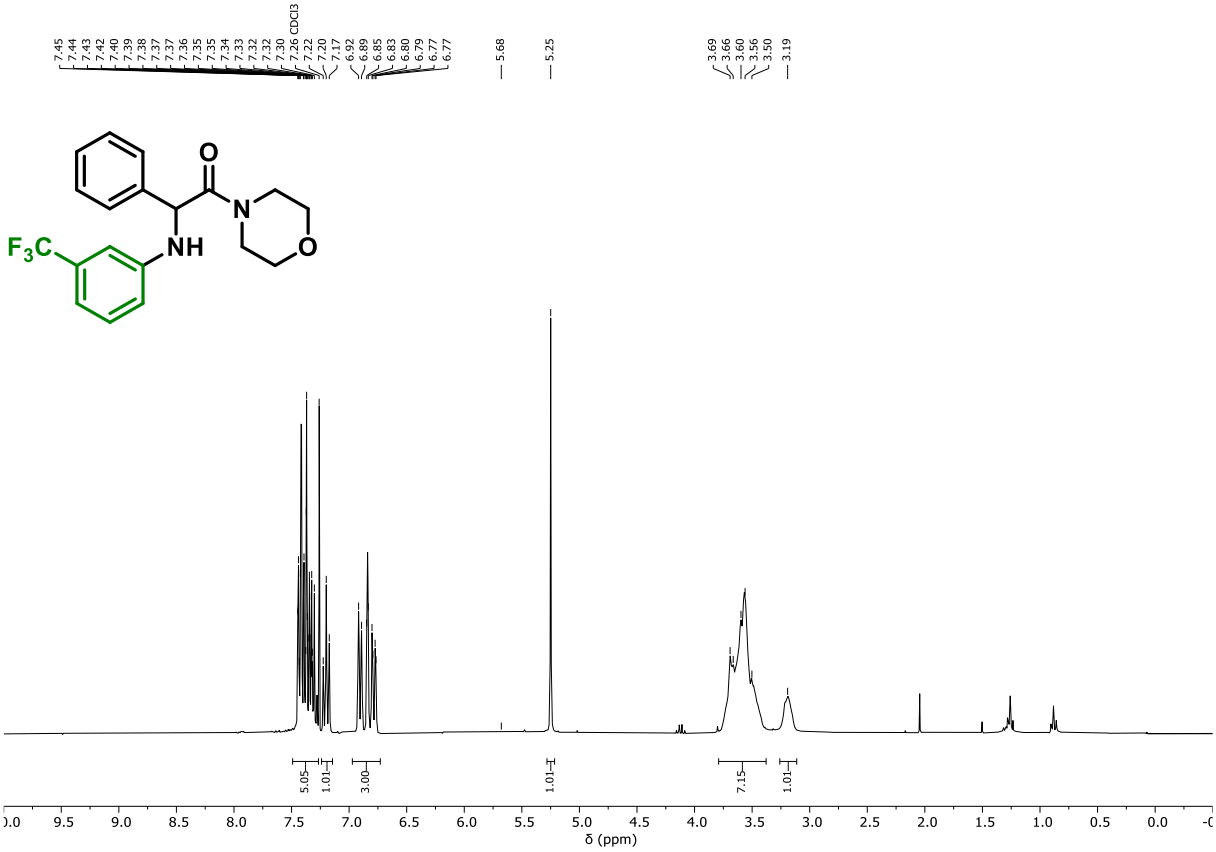
^{13}C-{^{1}H}-NMR (75 MHz) of 2-(4-(2-hydroxyethyl)phenyl)-1-morpholino-2-(phenylamino)ethan-1-one (**4h**).



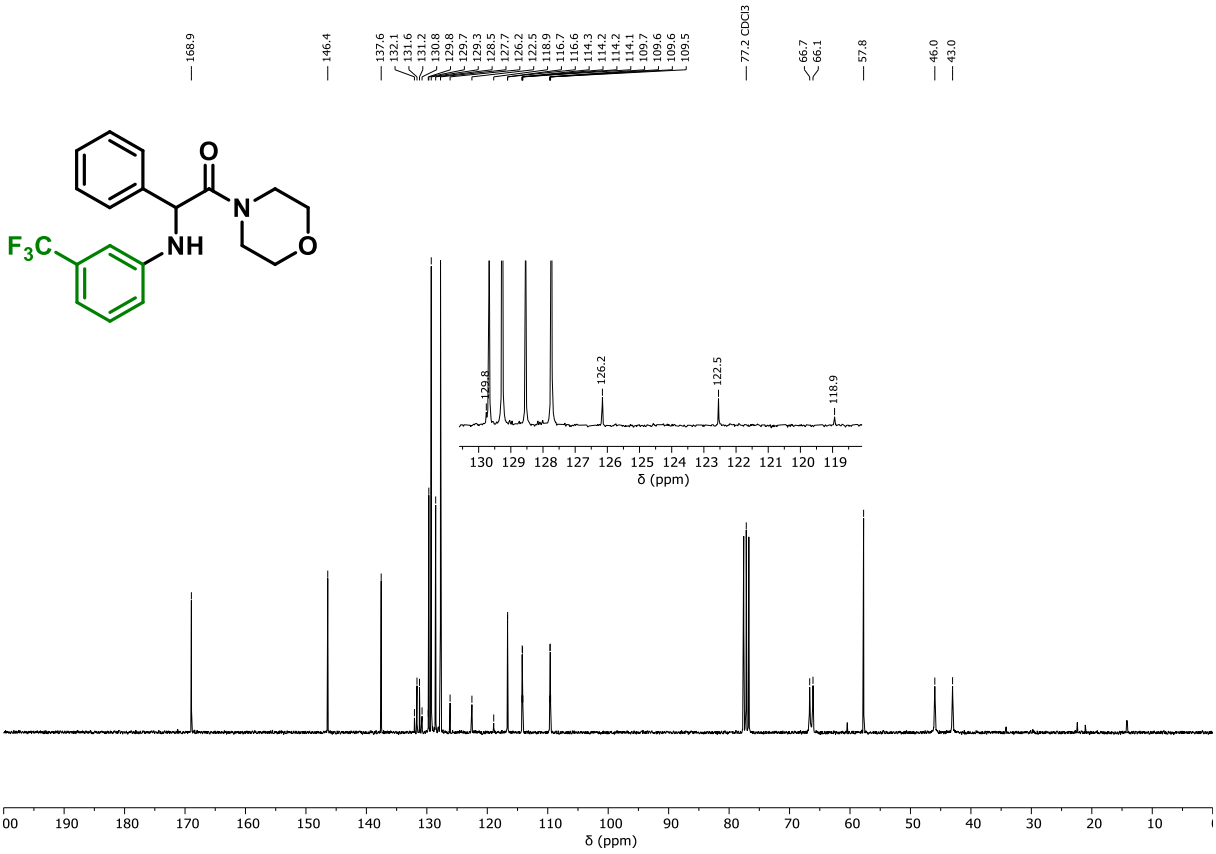
^{1}H-NMR (500 MHz) of 1-morpholino-2-phenyl-2-((4-methylphenyl)amino)ethan-1-one (**5a**).



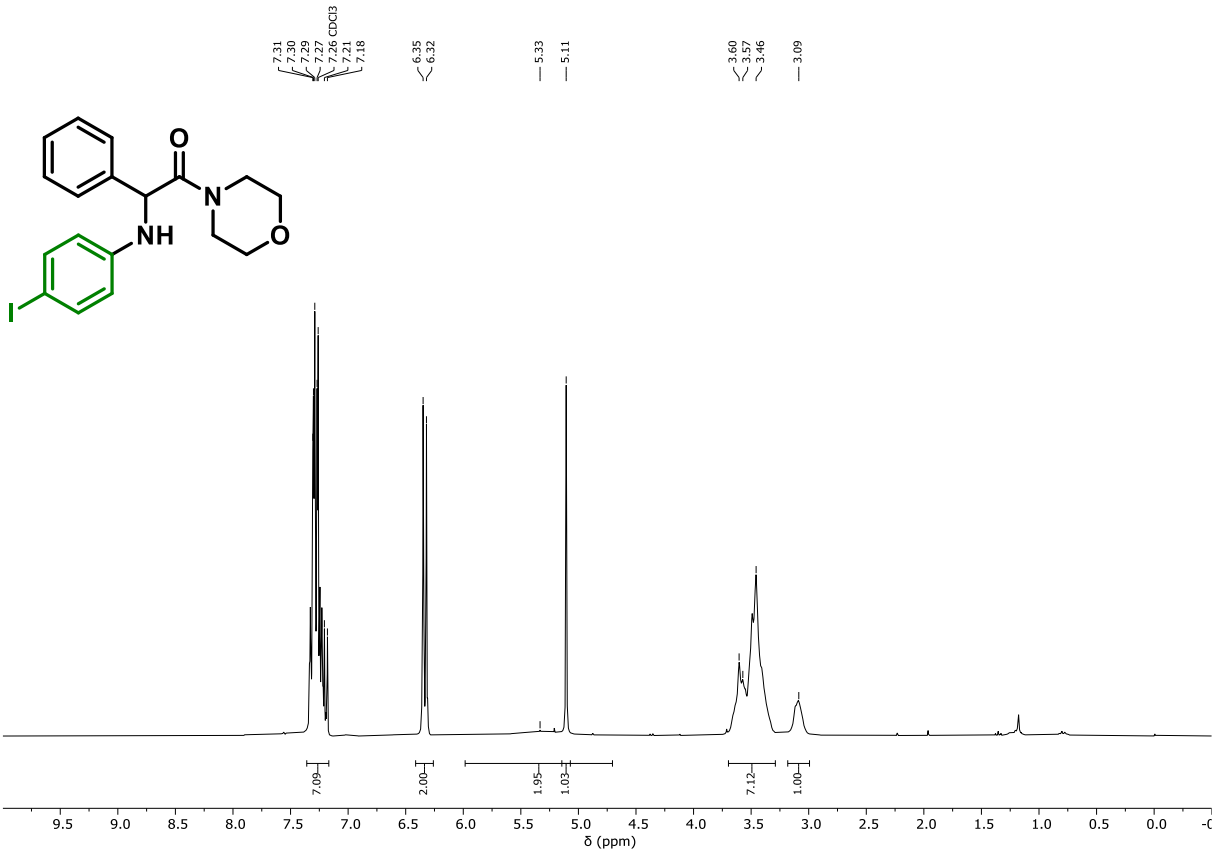
^{13}C-{^{1}H}-NMR (75 MHz) of 1-morpholino-2-phenyl-2-((4-methylphenyl)amino)ethan-1-one (**5a**).



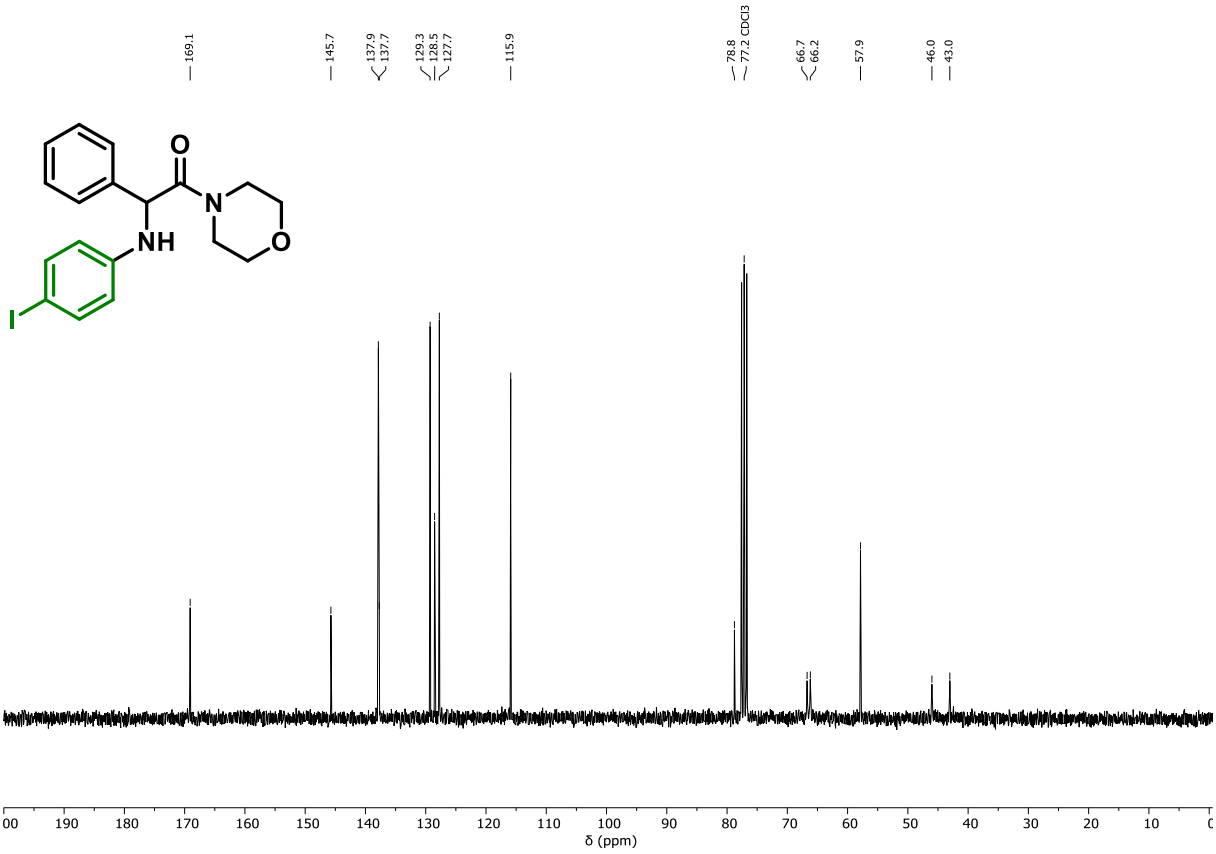
^{1}H-NMR (300 MHz) of 1-morpholino-2-phenyl-2-((3-(trifluoromethyl)phenyl)amino)ethan-1-one (**5b**).



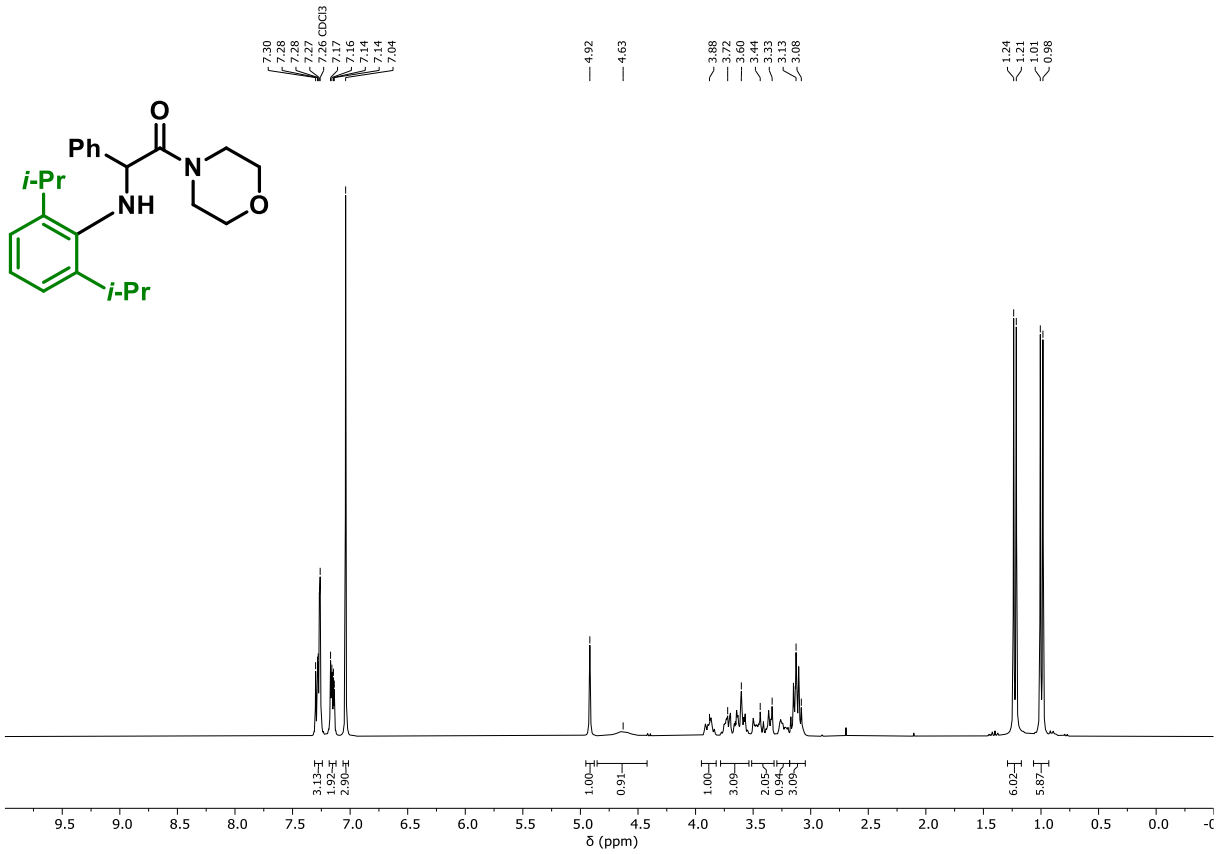
^{13}C-{^{1}H}-NMR (75 MHz) of 1-morpholino-2-phenyl-2-((3-(trifluoromethyl)phenyl)amino)ethan-1-one (**5b**).



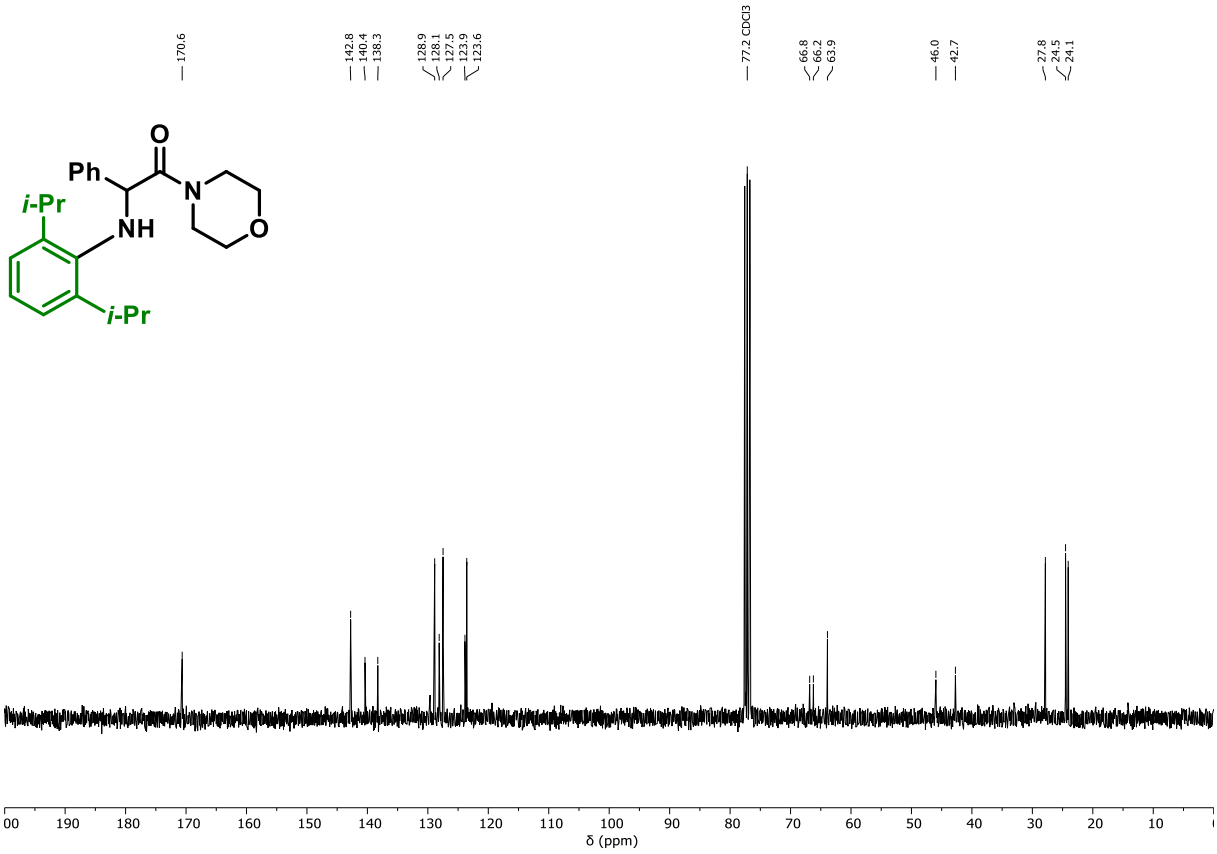
^{1}H-NMR (300 MHz) of 1-morpholino-2-phenyl-2-((4-iodophenyl)amino)ethan-1-one (**5c**).



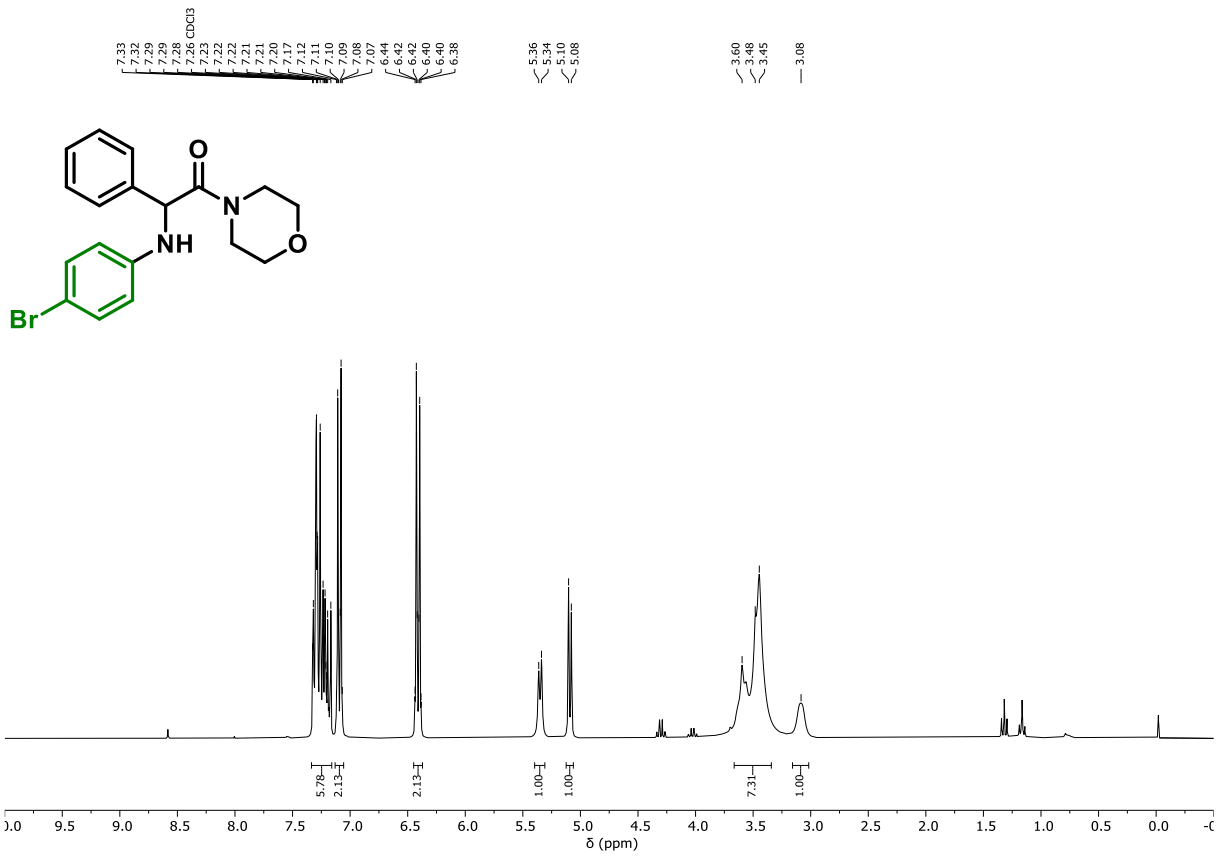
^{13}C-{^{1}H}-NMR (75 MHz) of 1-morpholino-2-phenyl-2-((4-iodophenyl)amino)ethan-1-one (**5c**).



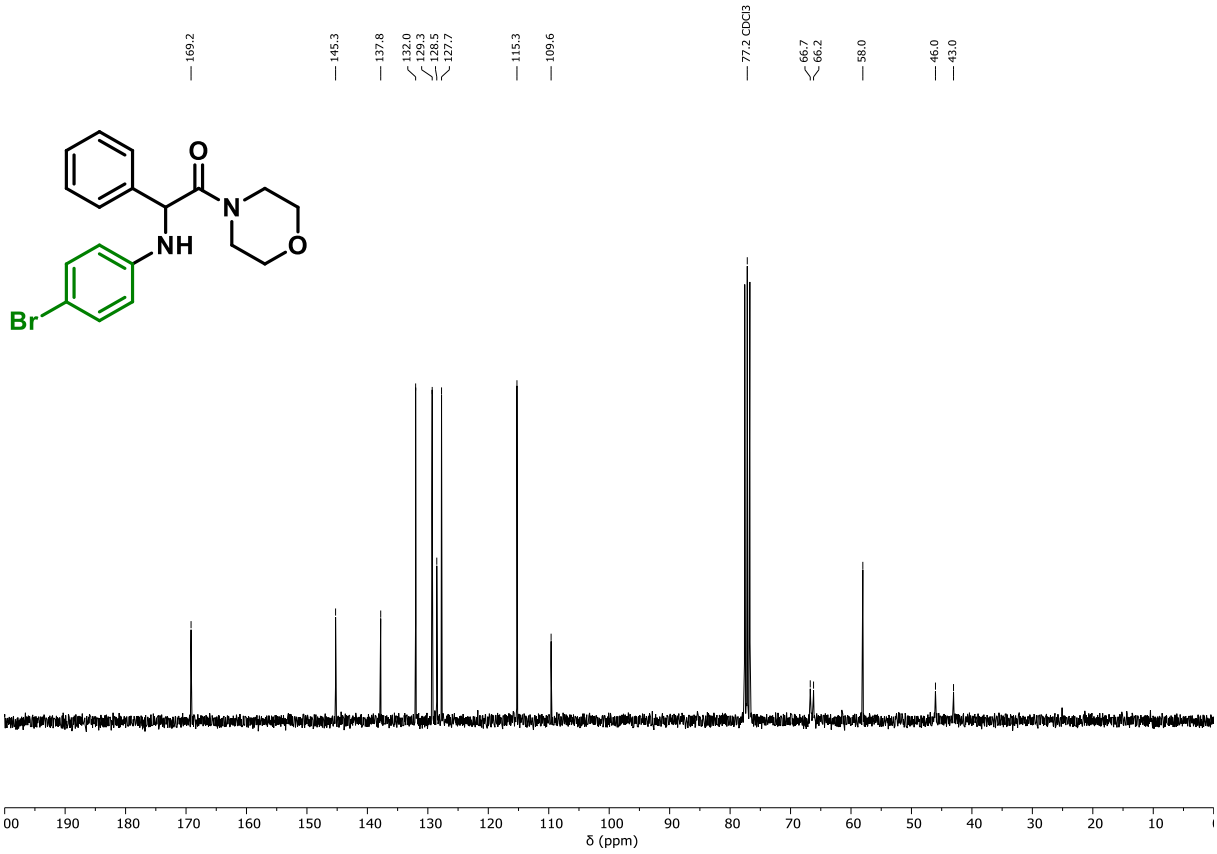
^{1}H-NMR (300 MHz) of 2-((2,6-diisopropylphenyl)amino)-1-morpholino-2-phenylethan-1-one (**5d**).



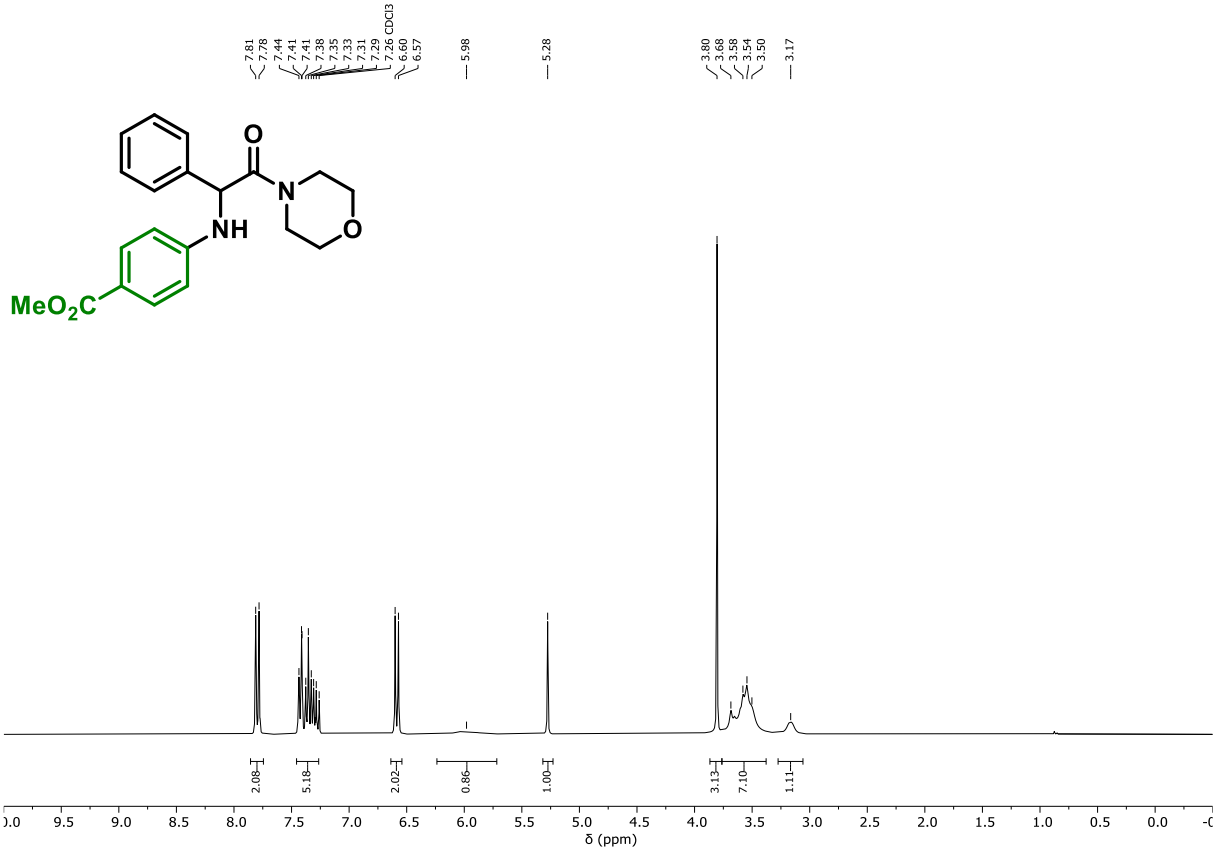
^{13}C-{^{1}H}-NMR (75 MHz) of 2-((2,6-diisopropylphenyl)amino)-1-morpholino-2-phenylethan-1-one (**5d**).



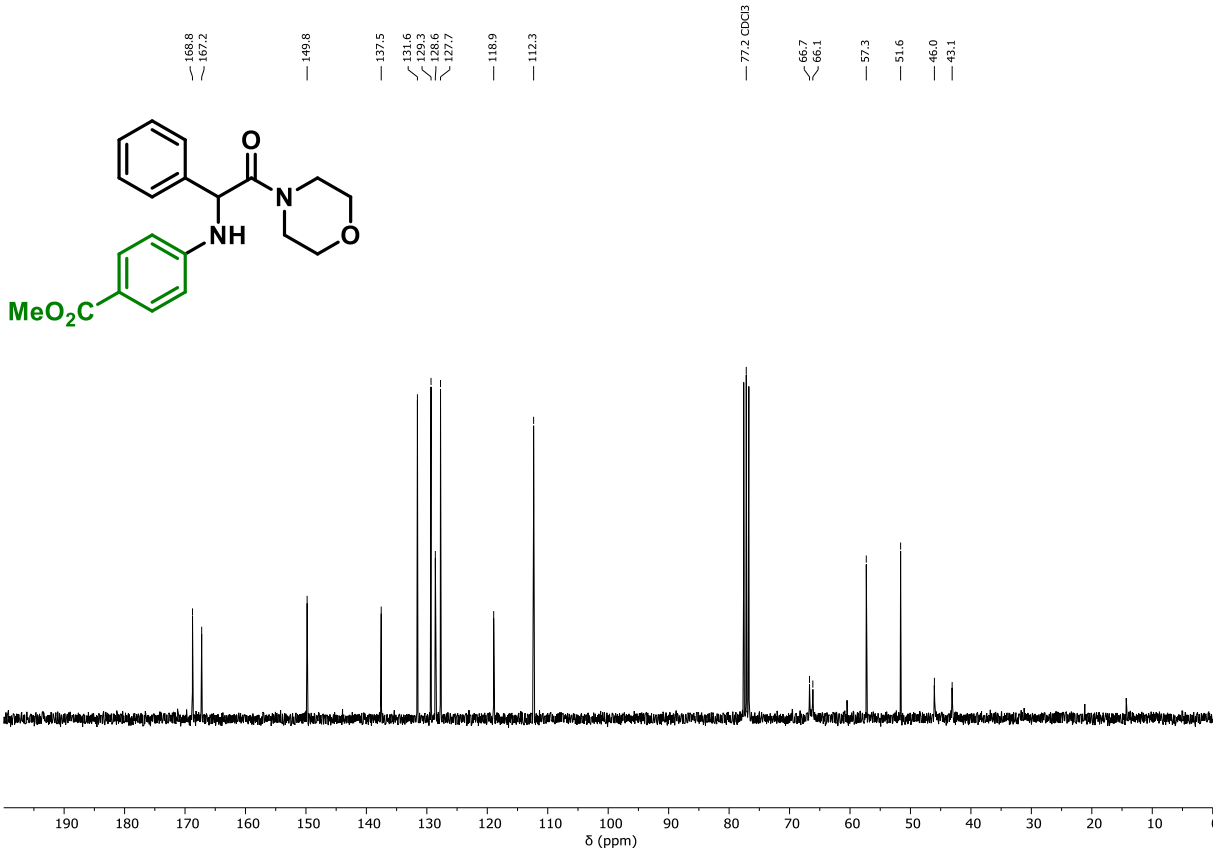
^{1}H-NMR (300 MHz) of 1-morpholino-2-phenyl-2-((4-bromophenyl)amino)ethan-1-one (**5e**).



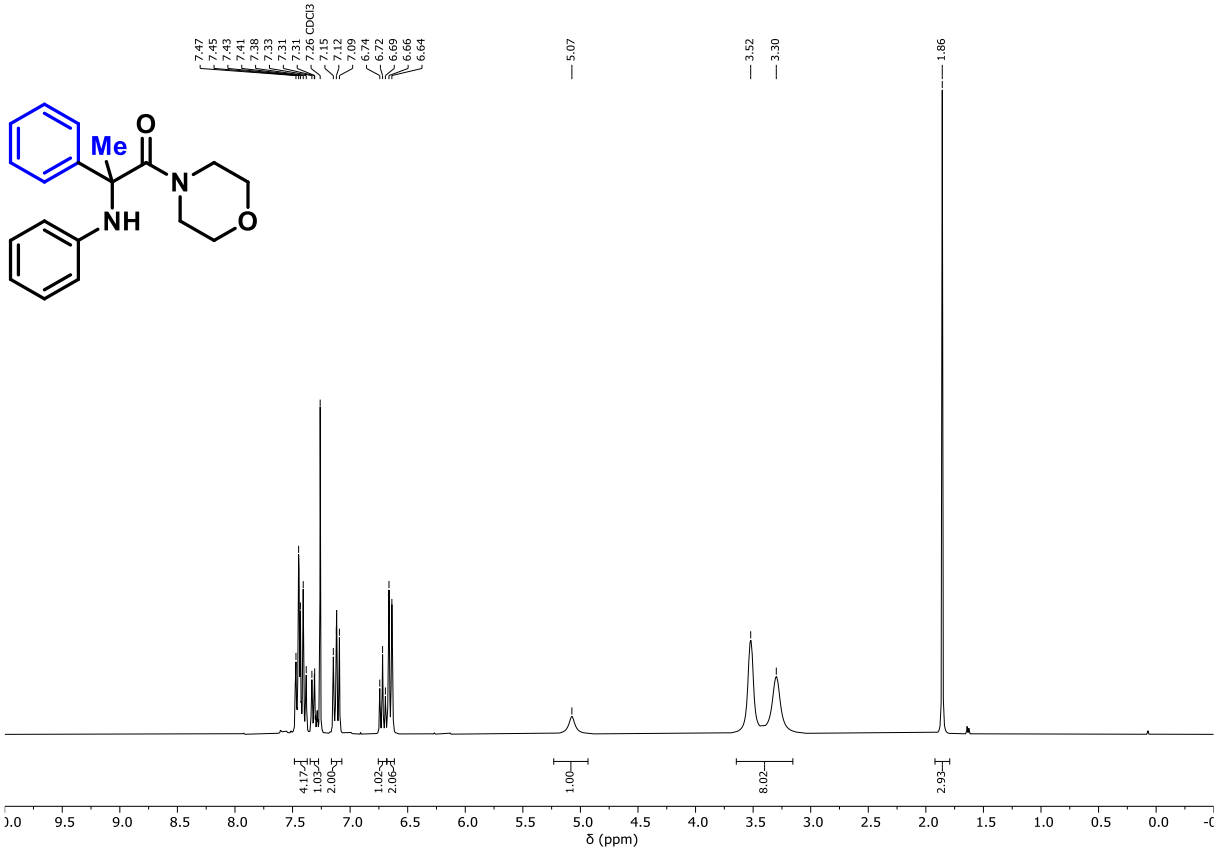
^{13}C-{^{1}H}-NMR (75 MHz) of 1-morpholino-2-phenyl-2-((4-bromophenyl)amino)ethan-1-one (**5e**).



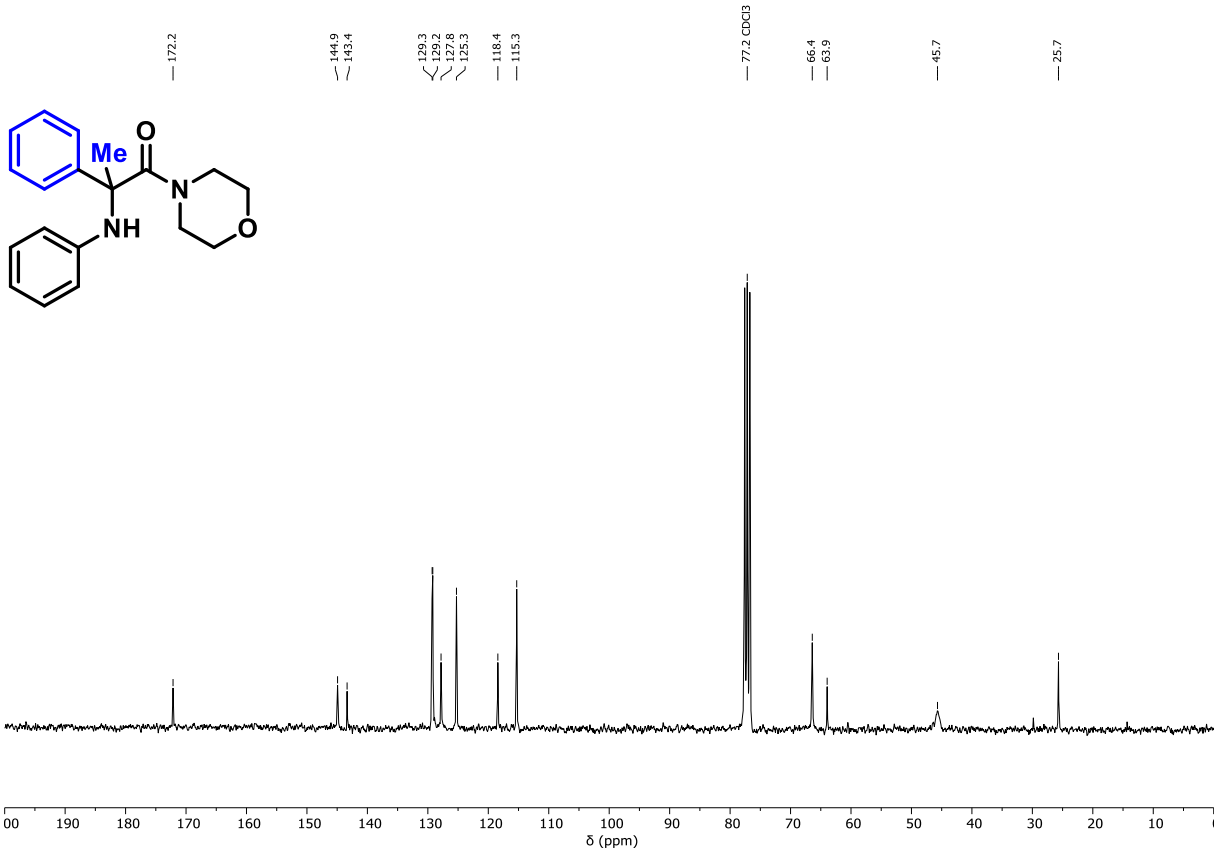
^{1}H-NMR (300 MHz) of methyl 4-((2-morpholino-2-oxo-1-phenylethyl)amino)benzoate (**5f**).



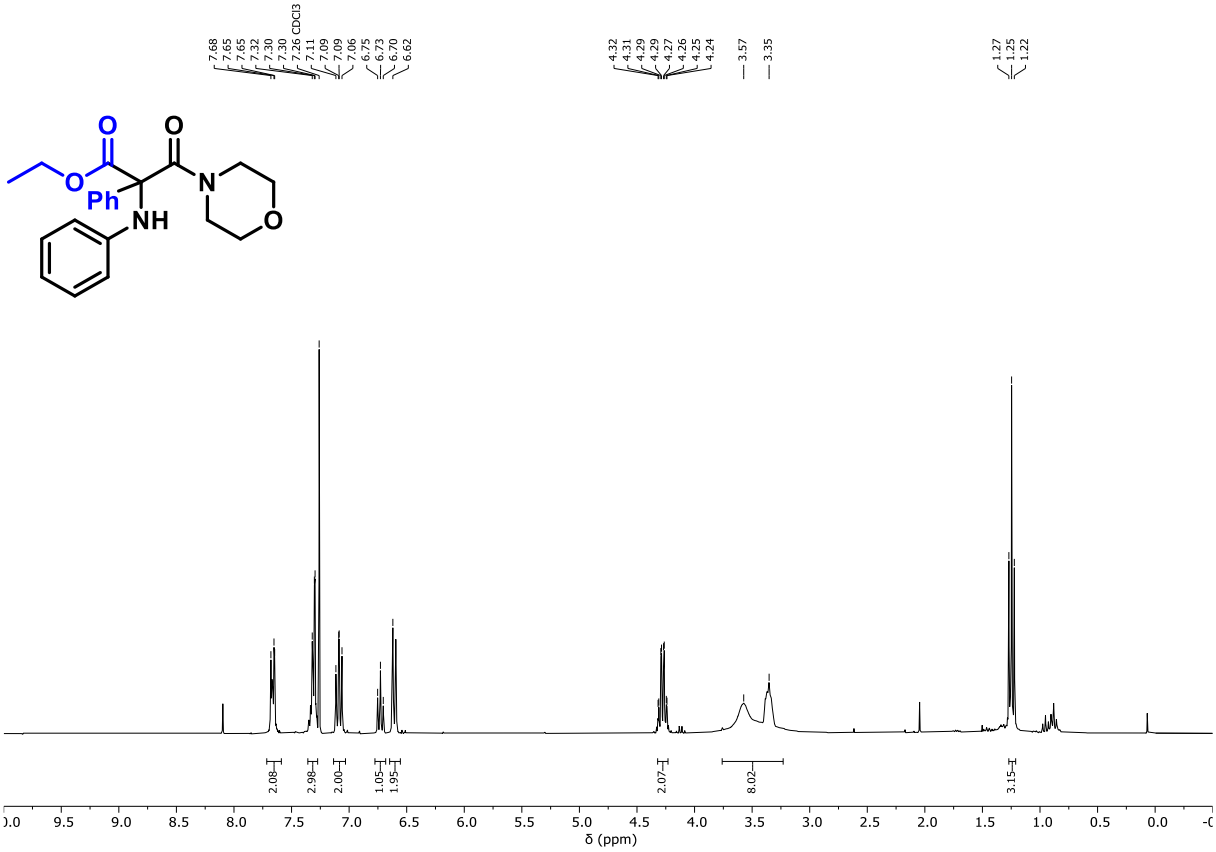
^{13}C-{^{1}H}-NMR (75 MHz) of methyl 4-((2-morpholino-2-oxo-1-phenylethyl)amino)benzoate (**5f**).



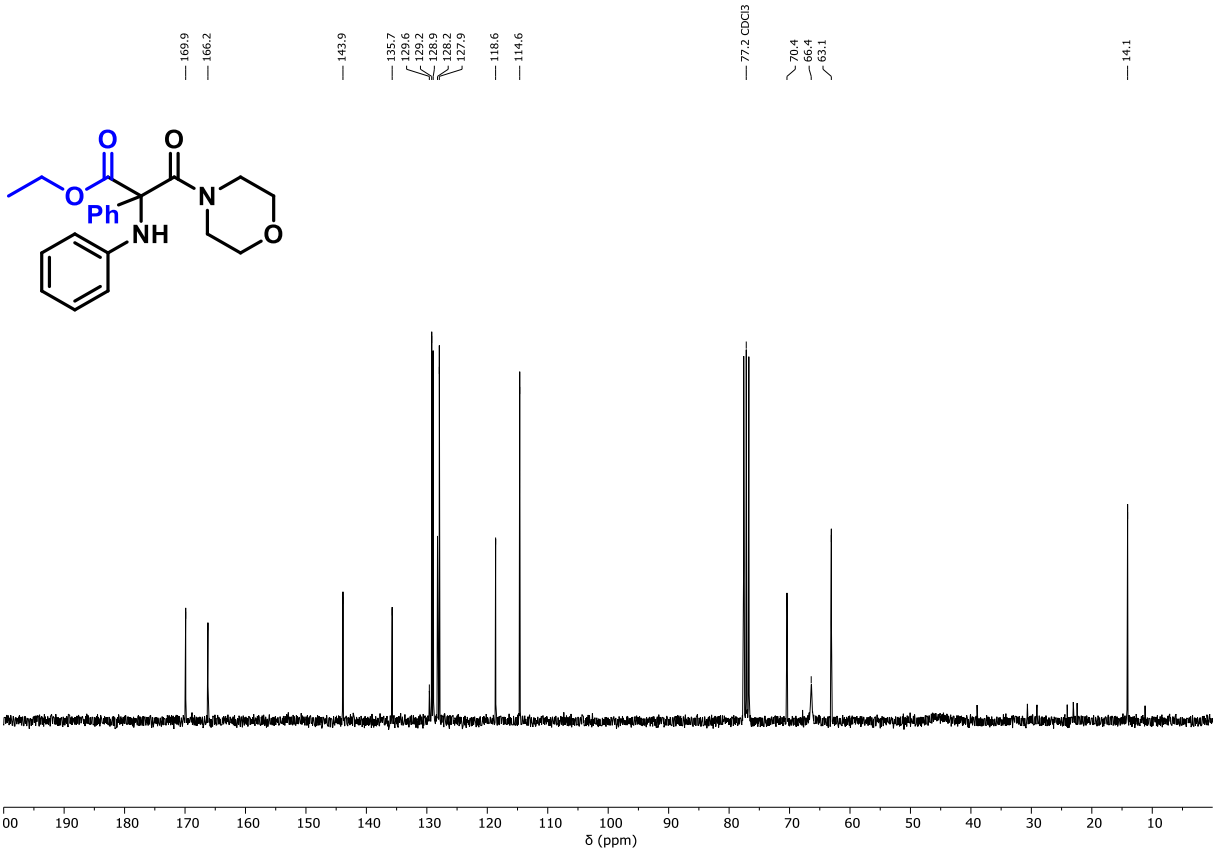
^{1}H-NMR (300 MHz) of 1-morpholino-2-phenyl-2-(phenylamino)propan-1-one (**6a**).



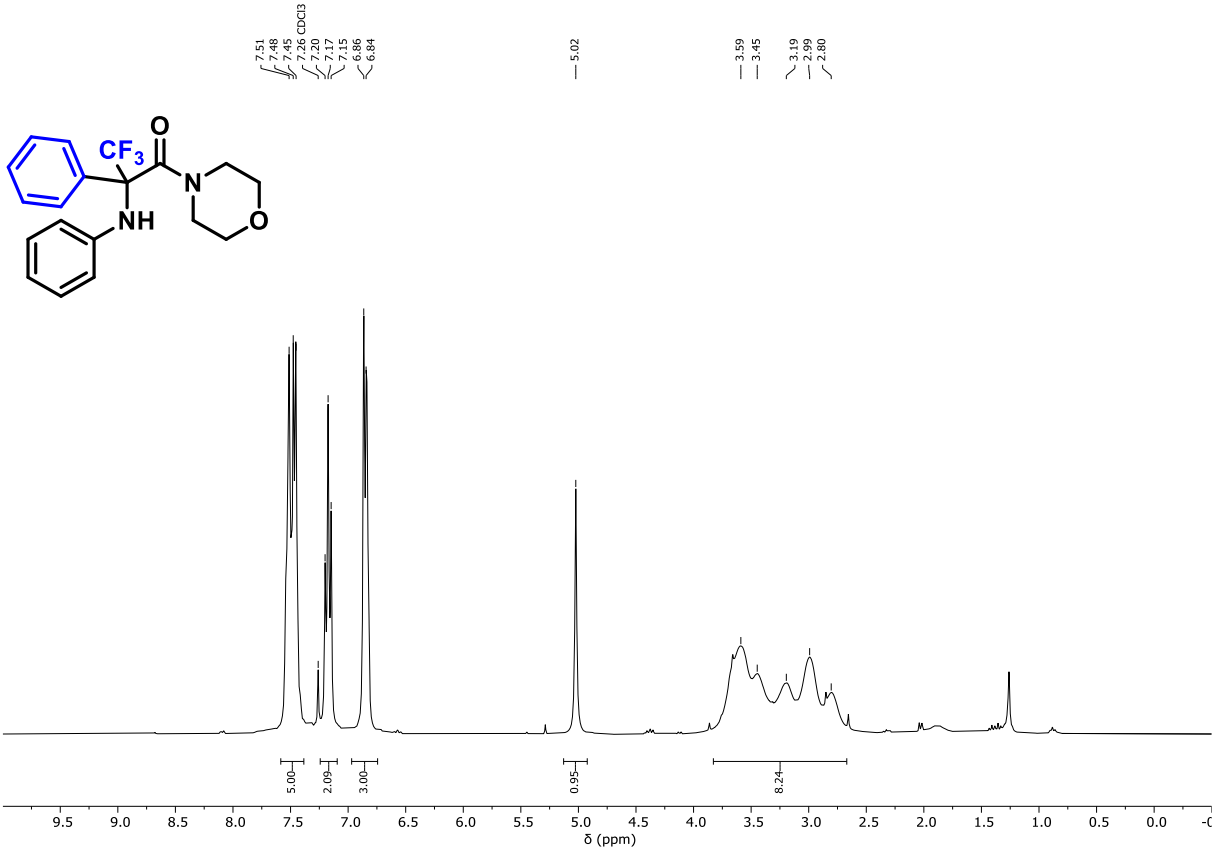
^{13}C-{^{1}H}-NMR (75 MHz) of 1-morpholino-2-phenyl-2-(phenylamino)propan-1-one (**6a**).



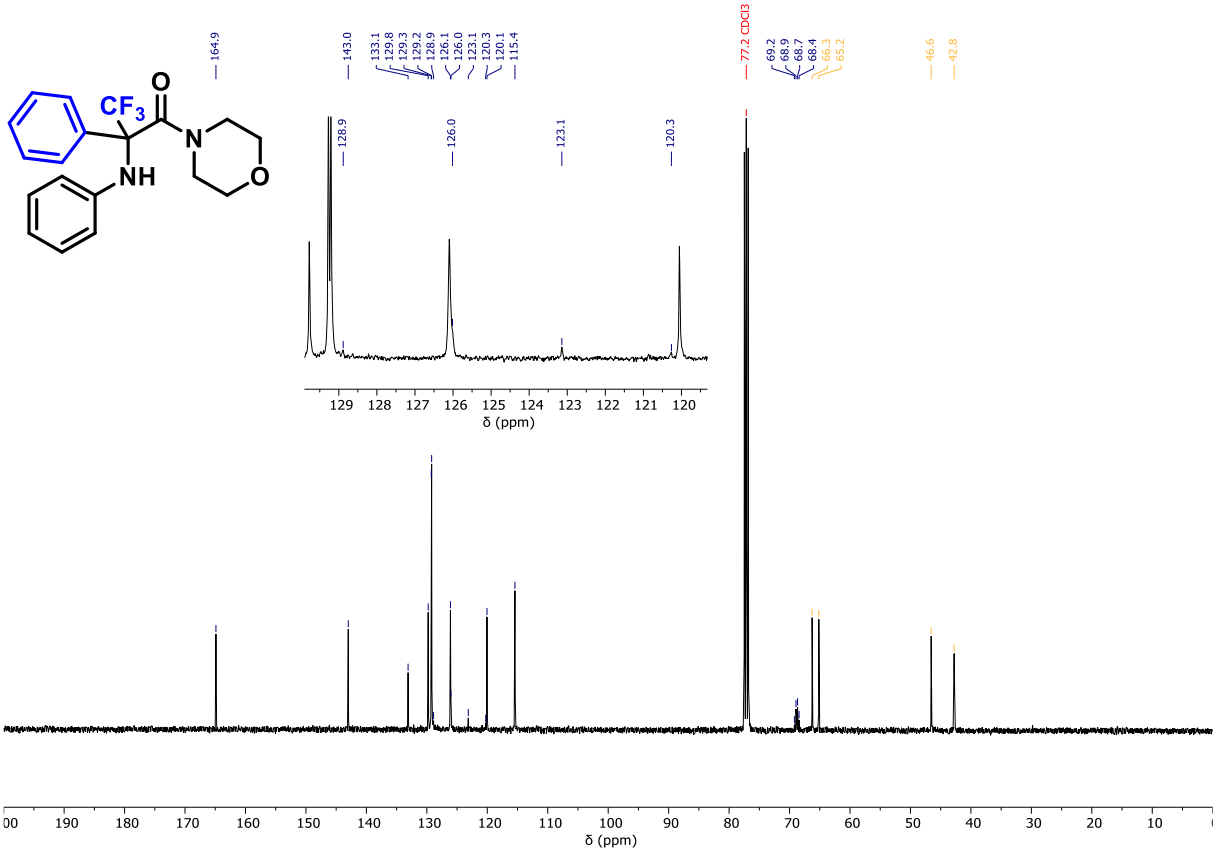
^{1}H-NMR (300 MHz) of ethyl 3-morpholino-3-oxo-2-phenyl-2-(phenylamino)propanoate (**6b**).



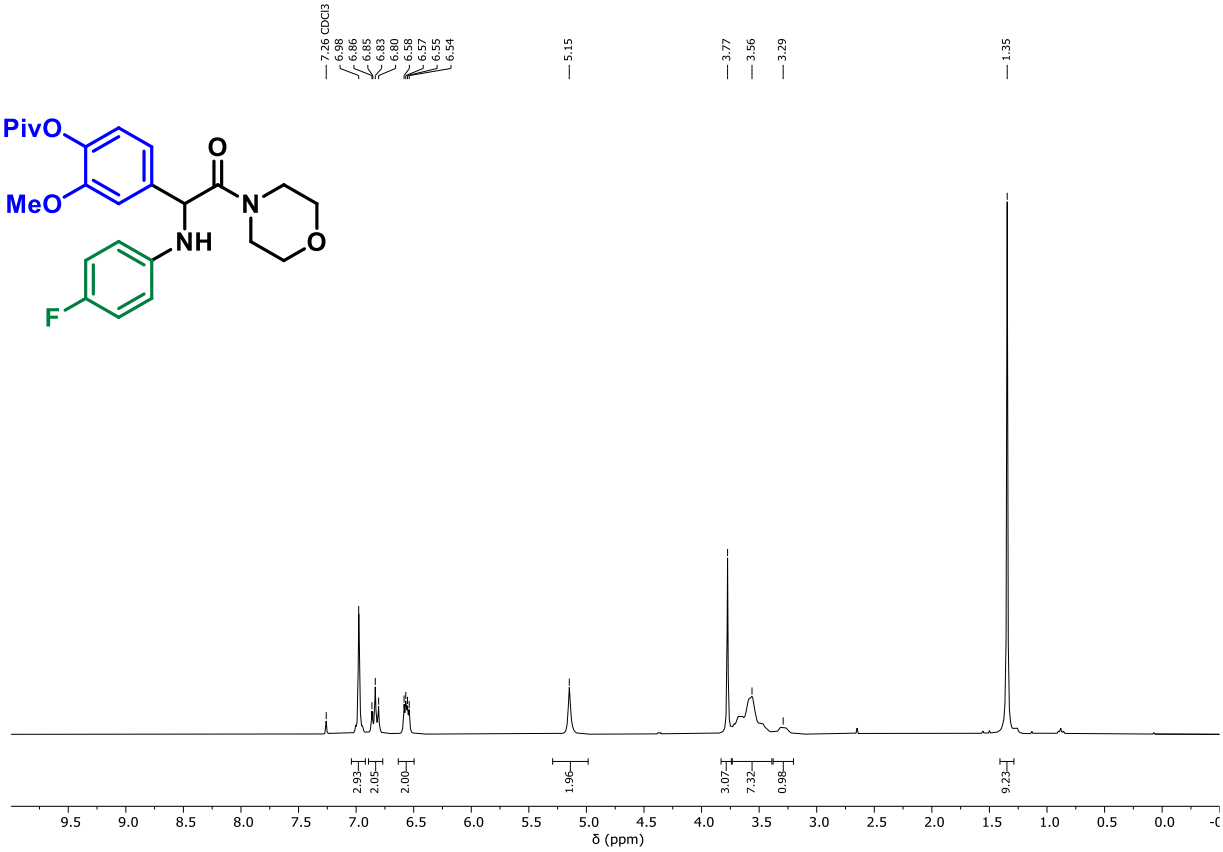
^{13}C-{^{1}H}-NMR (75 MHz) of ethyl 3-morpholino-3-oxo-2-phenyl-2-(phenylamino)propanoate (**6b**).



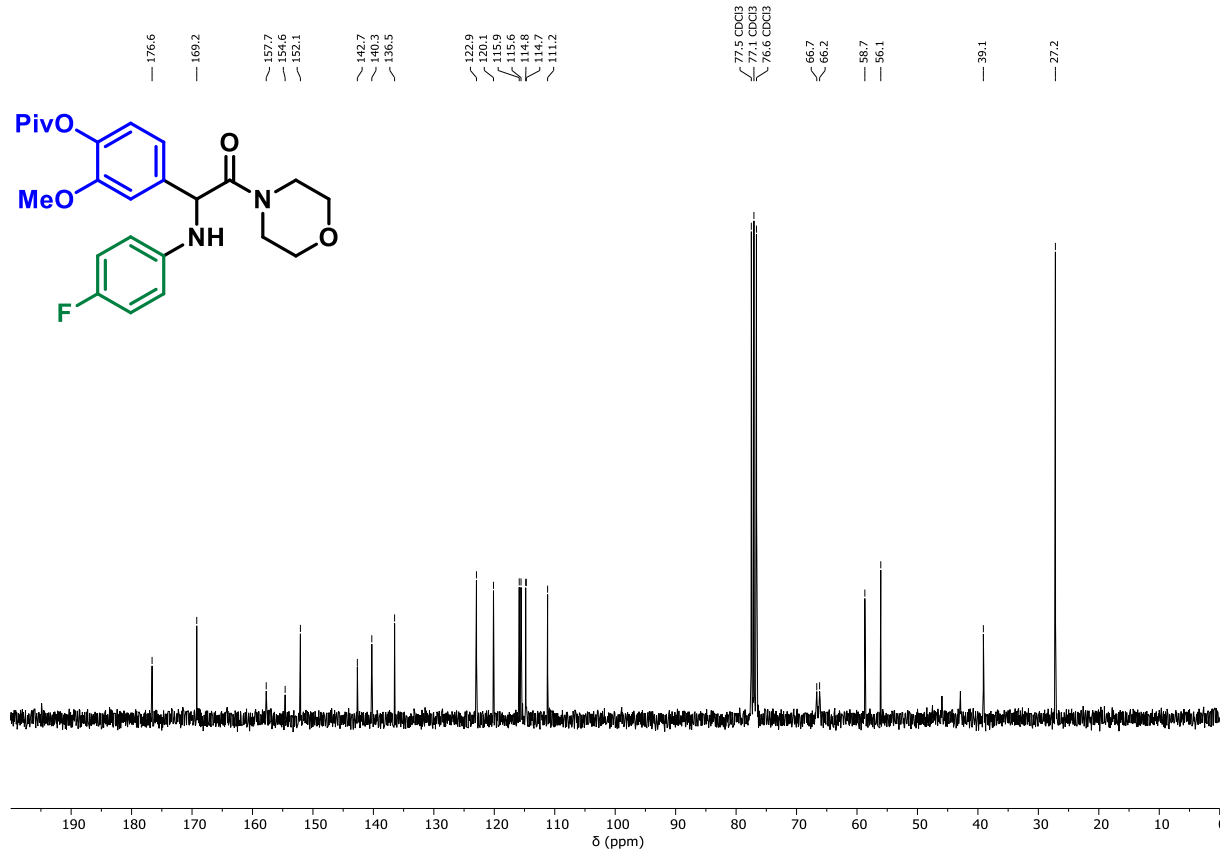
^{1}H-NMR (300 MHz) of 1-morpholino-2-phenyl-2-(phenylamino)-2-(trifluoromethyl)propan-1-one (**6c**).



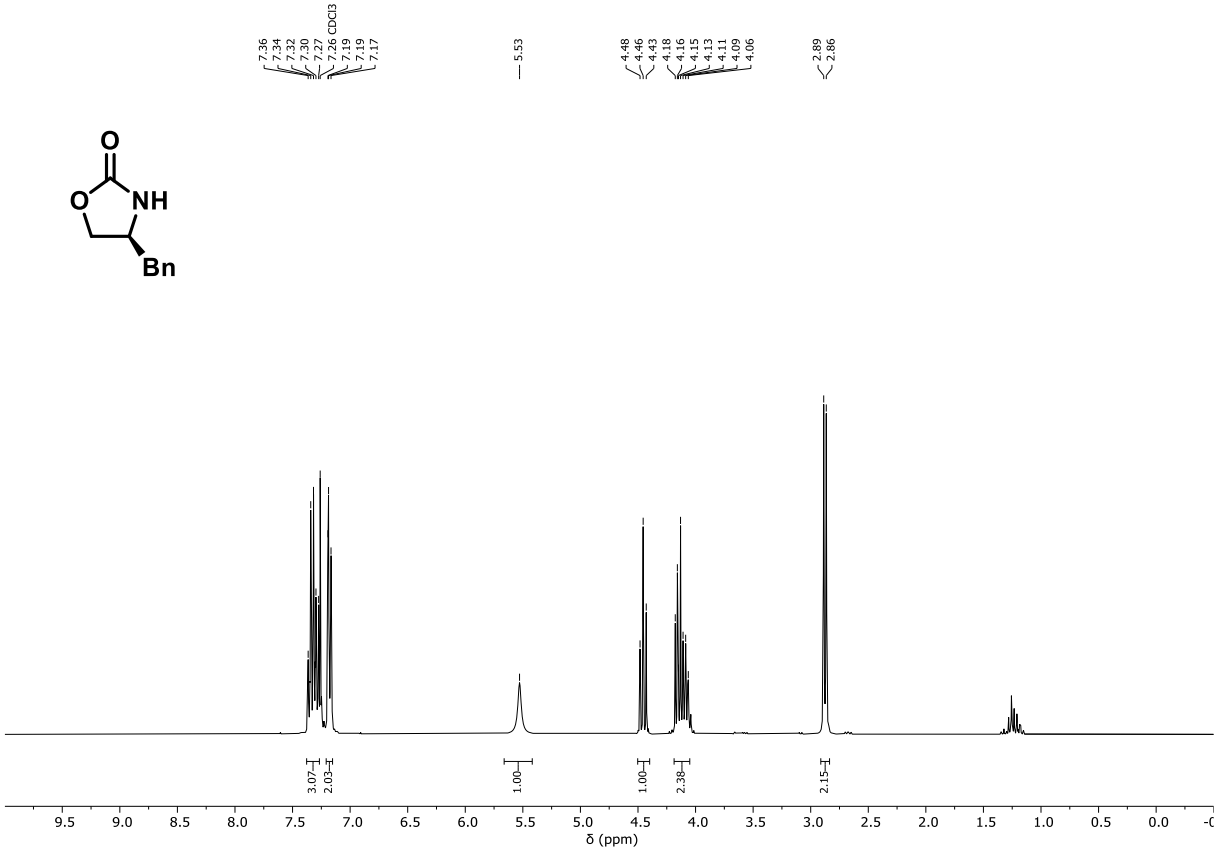
^{13}C-{^{1}H}-NMR (101 MHz) of 1-morpholino-2-phenyl-2-(phenylamino)-2-(trifluoromethyl)propan-1-one (**6c**) at –20 °C. The signals labeled in yellow are not or just barely visible at room temperature.



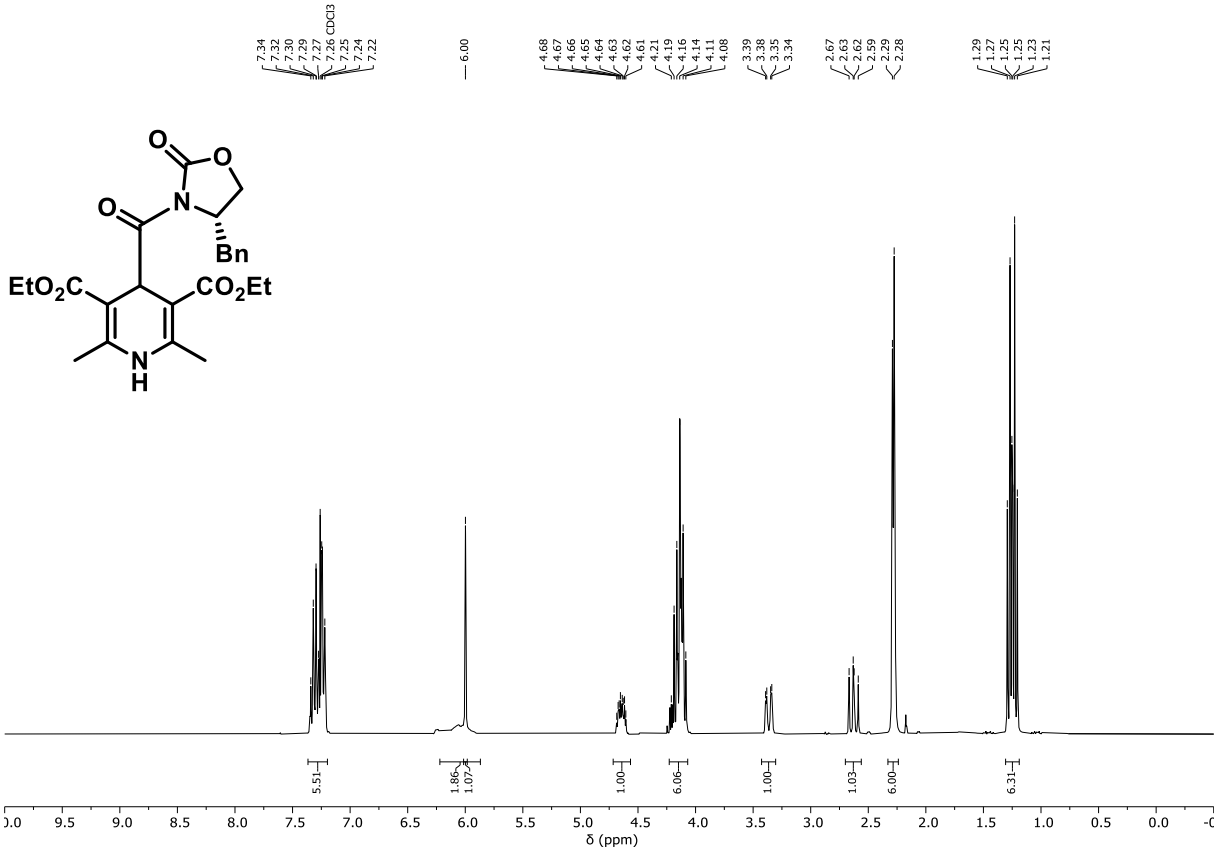
^{1}H-NMR (300 MHz) of 4-(1-((4-Fluorophenyl)amino)-2-morpholino-2-oxoethyl)-2-methoxyphenyl pivalate (**7**).



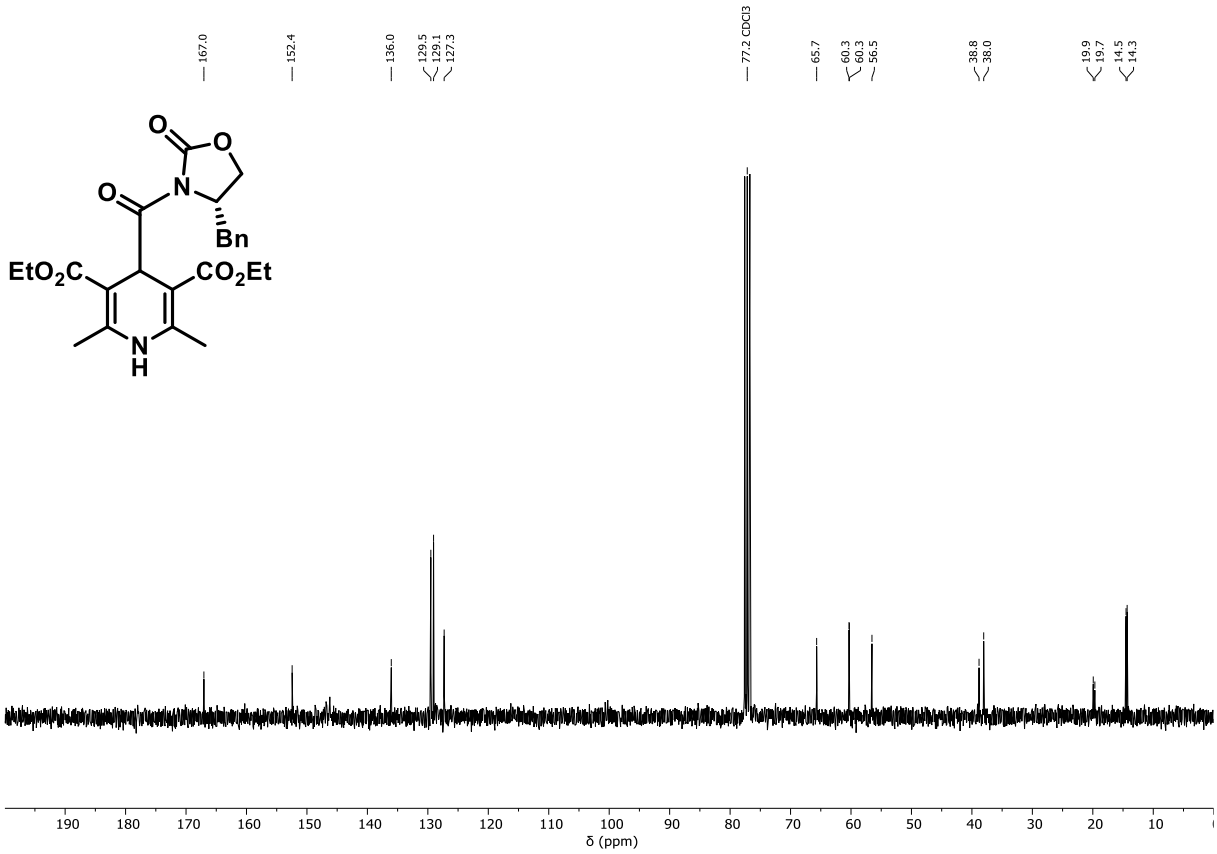
^{13}C-{^{1}H}-NMR (75 MHz) of 4-(1-((4-Fluorophenyl)amino)-2-morpholino-2-oxoethyl)-2-methoxyphenyl pivalate (**7**).



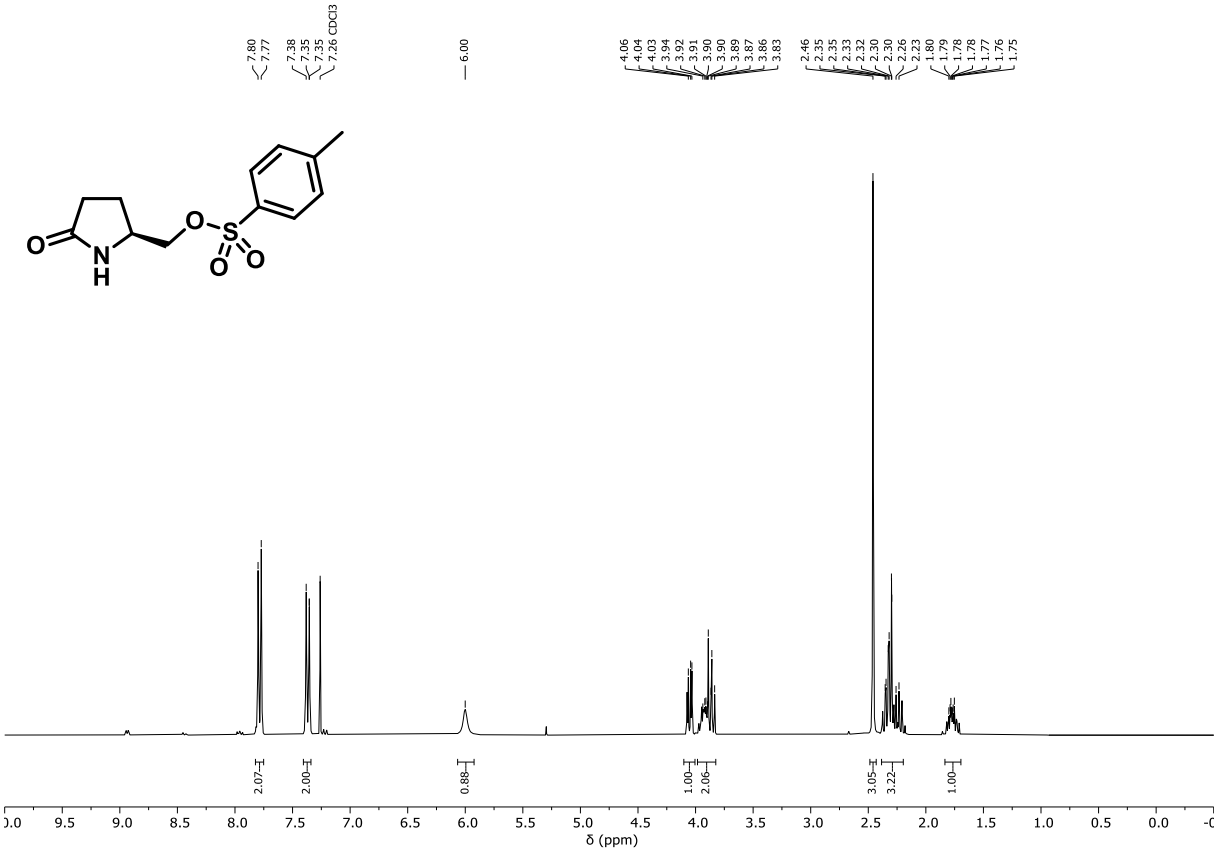
^{1}H-NMR (300 MHz) of (*S*)-4-benzyl-2-oxazolidinone.



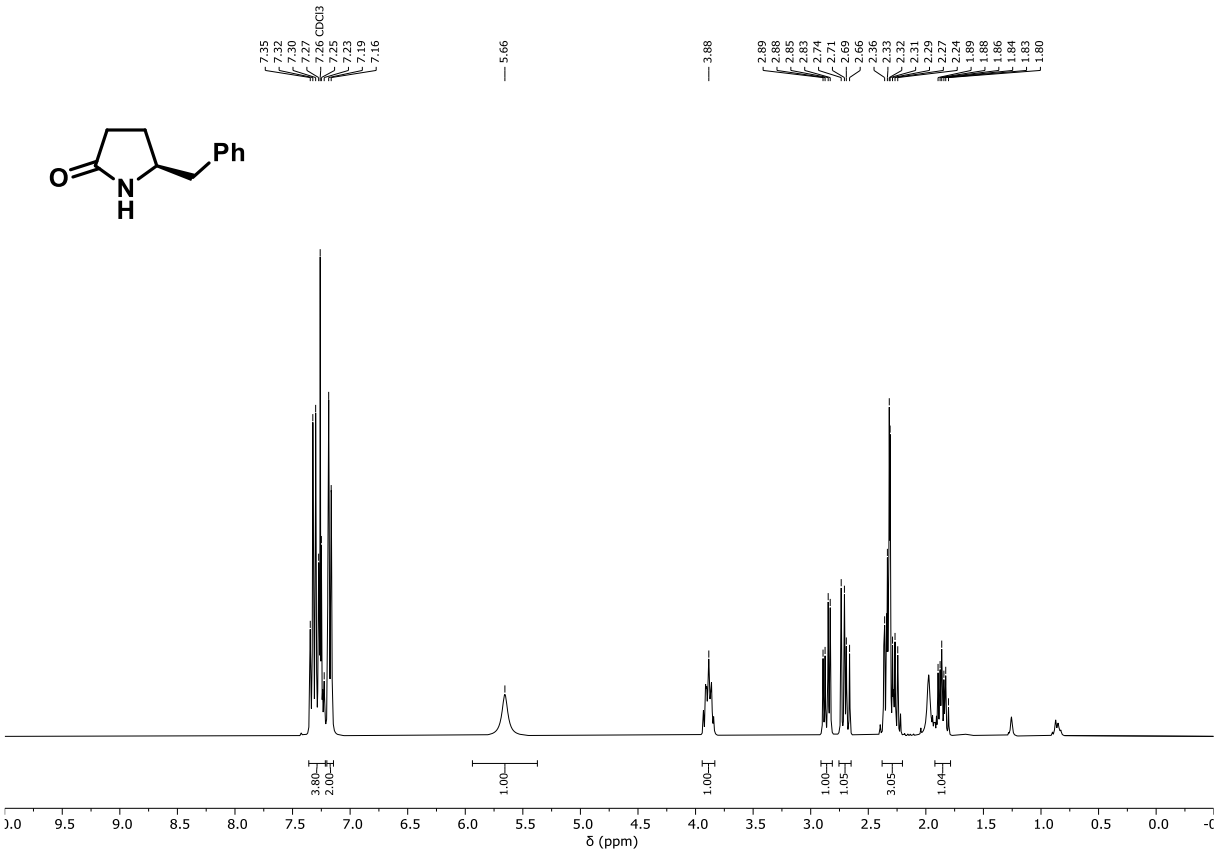
^{1}H-NMR (300 MHz) of diethyl (*S*)-4-(4-benzyl-2-oxooxazolidine-3-carbonyl)-2,6-dimethyl-1,4-dihydropyridine-3,5-dicarboxylate (**HE-(Bn-Oxazolidinone)**).



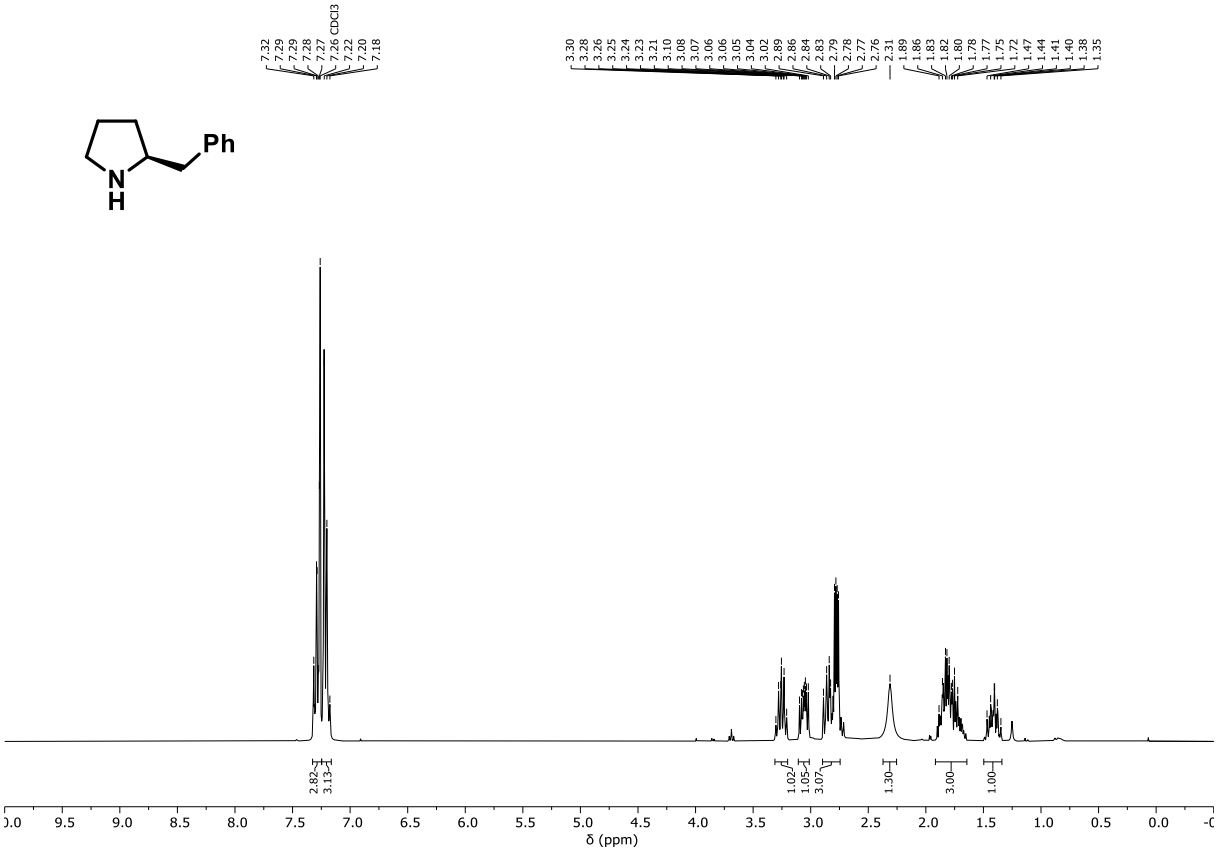
^{13}C-{^{1}H}-NMR (75 MHz) of diethyl (*S*)-4-(4-benzyl-2-oxooxazolidine-3-carbonyl)-2,6-dimethyl-1,4-dihydropyridine-3,5-dicarboxylate (**HE-(Bn-Oxazolidinone)**).



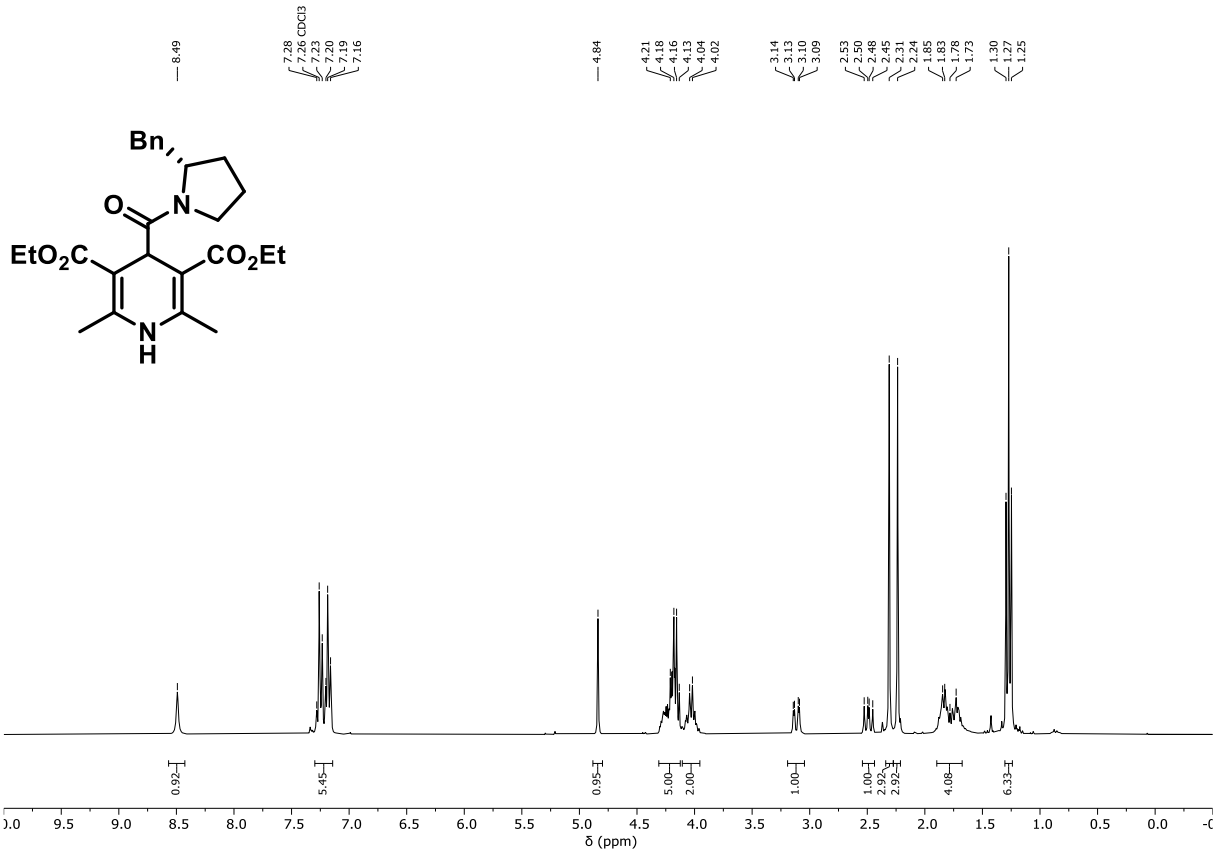
^{1}H-NMR (300 MHz) of (*S*)-(5-oxopyrrolidin-2-yl)methyl 4-toluenesulfonate.



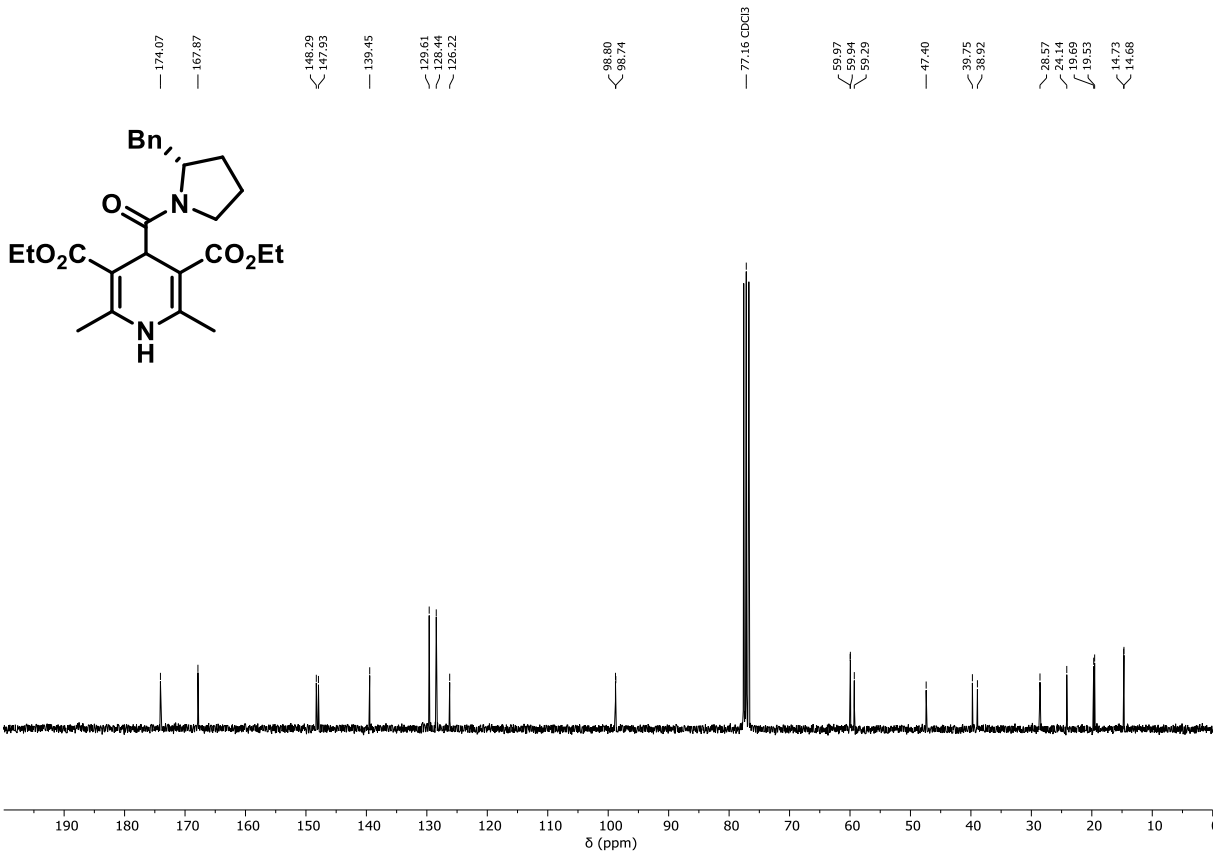
^{1}H-NMR (300 MHz) of (*S*)-5-benzyl-2-pyrrolidinone.



^{1}H-NMR (300 MHz) of (*S*)-2-benzylpyrrolidine.



^{1}H-NMR (300 MHz) of diethyl (S)-4-(2-benzylpyrrolidine-1-carbonyl)-2,6-dimethyl-1,4-dihydropyridine-3,5-dicarboxylate (**HE-(Bn-Pyrrolidine)**).

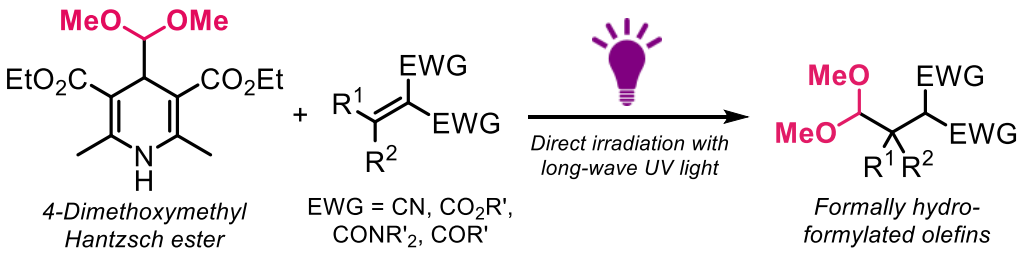


^{13}C-{^{1}H}-NMR (75 MHz) of diethyl (S)-4-(2-benzylpyrrolidine-1-carbonyl)-2,6-dimethyl-1,4-dihydropyridine-3,5-dicarboxylate (**HE-(Bn-Pyrrolidine)**).



^{1}H-NMR (300 MHz) of 4-formyl-2-methoxyphenyl pivalate.

Chapter 3



★ *Just two ingredients:* ***No*** *catalysts, photocatalysts, or additives*

★ ***Mild*** *conditions, high chemoselectivity, broad functional group tolerance*

★ *Applicable to* ***late-stage*** *derivatization of highly functionalized molecules*

★ ***Quaternary*** *centers possible* ★ *Easily* ***accessible*** *starting materials*

Catalyst-Free Photo-Hydroformylation of Olefins

Abstract: *We report a novel catalyst-free photochemical hydroformylation of electron-deficient olefins using a bench stable, easily prepared 1,4-dihydropyridine derivative (a Hantzsch ester). The transformation proceeds under long-wave ultraviolet light (365 nm) and requires no additives or photocatalysts. The operationally simple protocol tolerates a broad array of functional groups important for synthetic applications and can be used for late-stage functionalization. Mechanistic investigations suggest that the Hantzsch ester acts as a strong photoreductant, generating free dimethoxymethyl radicals as the key intermediates. The resulting acetals are easily deprotected by trifluoroacetic acid and yield unnatural 1,4-functional group distances.*

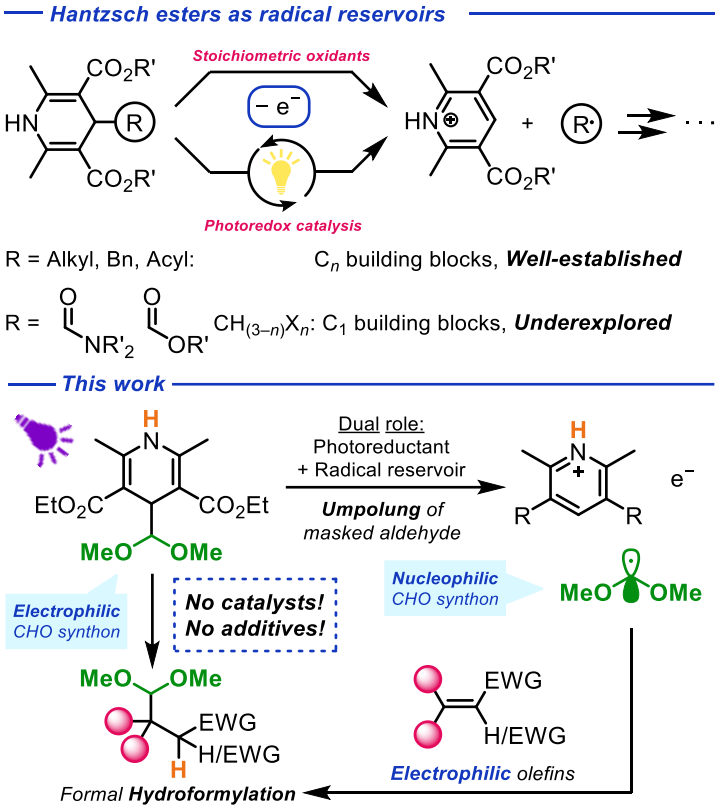
The work outlined in this chapter is scheduled for publication.

Author contributions: **Mattis-Ole W. S. Schmotz** wrote the manuscript and experimental section, and performed experimental work, **Fabian B. Lüttchens** performed experimental work, **Axel Jacobi von Wangelin** supervised this work.

Aldehydes are indubitably among the most versatile and prevalent functional groups due to their unique reactivity. Their pivotal role across most fields of chemistry is reflected in their usage as key intermediates and products in numerous laboratory and industrial synthesis routes of natural products, pharmaceuticals, agrochemicals, fragrances, materials, and more. Over the last 150 years, a wide variety of synthetic routes has accordingly been developed, ranging from classical electrophilic aromatic substitutions (e.g. Vilsmeier-Haack reaction[1–4]) to the reaction of organometallic species with formamides (Bouveault reaction).[5–8] Further approaches include redox reactions of suitable precursors (alcohols,[9] carboxylates[10–12]), and transition-metal-catalyzed carbonylation reactions employing syngas such as the Roelen hydroformylation reaction.[13–15] Despite their widespread adoption, many of these methods suffer from significant limitations, including harsh reaction conditions leading to a narrow substrate scope, poor atom economy, the use of toxic or costly reagents, or the need for elaborate purification procedures. There remains a constant high demand for novel synthetic strategies towards aldehydes to address these challenges.

Throughout the 2010's, 1,4-dihydropyridine-3,5-dicarboxylates (*Hantzsch esters*) arose as versatile radical precursors for carbon-carbon bond-forming reactions. Initially used in conjunction with stoichiometric oxidants such as persulfate, this methodology benefited greatly from the concurrent emergence of photoredox catalysis, which enabled milder and more selective single-electron oxidation processes.[16,17] This significantly expanded the synthetic scope of Hantzsch ester-mediated transformations. Several applications of radical alkylation and benzylation with a wide variety of radical acceptors have since been reported.[18] Notably, the group of Melchiorre reported the photocatalyst-free generation of alkyl radicals by direct irradiation of Hantzsch esters and their subsequent nickel-catalyzed cross-coupling with aryl and acyl halides.[19] However, despite significant progress in C–C bond-forming reactions employing Hantzsch esters, C_1 functionalization has remained comparatively underexplored. This is especially true for transformations aimed at delivering heteroatom-substituted methyl groups $CH_{(3-n)}X_n$. Driven by our interest in C_1 functionalization and photocarbonylation reactions combined with our expertise in radical dihydropyridine chemistry, we envisioned a user-friendly formylation protocol utilizing Hantzsch esters as the formyl source. Given the difficult accessibility and high reactivity of the formyl radical ·CHO we devised a more controlled approach based on acetalyl radicals – masked formyl equivalents. This has the additional effect of yielding protected aldehydes, which are easier to handle due to the reactivity of free aldehydes which could lead to undesired side reactions. We opted for the 4-dimethoxymethyl Hantzsch ester motif **1** due to the commercial availability of the reagents. This motif has appeared sporadically in literature, primarily as a single example of the substrate scope for the functionalization of cinnamides using [Ir] photoredox catalysis,[20] the desulfonative alkylation of *N*-heteroaryl sulfones using 4CzIPN photoredox catalysis,[21] and the synthesis of disubstituted

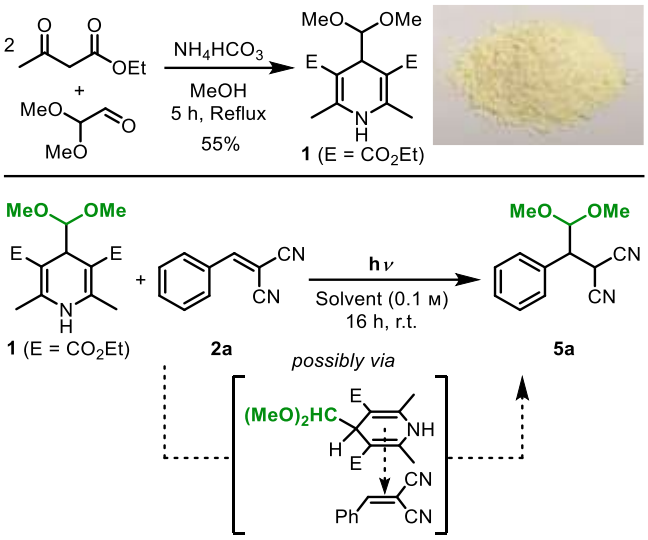
acetylenes using Safranin photoredox catalysis.[22] However, it has never been systematically explored as a platform for aldehyde synthesis and its full application-oriented potential in delivering structurally diverse aldehydes has remained untapped.



Scheme 1. *Hantzsch esters as radical reservoirs in light-driven functionalization reactions.*

Based on the divergent electronic structures of electron-rich **1** and electron-deficient olefins as well as our previous observation of direct radical transfer from Hantzsch esters,[23,24] we reasoned that electron donor-acceptor (EDA) complex formation between **1** and the olefins could occur, enabling a catalyst-free acetalyl transfer by direct irradiation. We prepared **1** on a multi-decagram scale in a standard Hantzsch dihydropyridine synthesis from inexpensive 2,2-dimethoxyacetaldehyde, ethyl acetoacetate, and ammonium bicarbonate (Scheme 2, top) and commenced our investigation by reacting **1** with benzylidenemalononitrile (**2a**) under violet light irradiation (405 nm) in acetonitrile (entry 1). Indeed, to our delight, product **5a** was obtained in 78% ^{1}H NMR yield after 16 h. After testing a range of different solvents (entries 1–7), the best results were obtained in acetonitrile and acetone (entries 1 and 7). We then discovered that blue light (450 nm) is ineffective (entry 8), but ultraviolet light (365 nm) not only accelerated the reaction (from 16 h to 8 h), but gave consistently higher yields (entries 9–10). We chose acetone as the optimal solvent due to its higher environmental benignity and lower noxiousness (higher "greenness") compared to acetonitrile.[25,26] Changes in concentration had no beneficial effect (entries 11–12). No product formation was observed in the absence of light (entry 13), confirming the photochemical aspect of the reaction.

Scheme 2. *Top: Synthesis of* ***1****. Bottom: Optimization of Reaction Conditions.*



Entry	Solvent	λ [nm]	Yield [%][a]
1	MeCN	405	78
2	DMF	405	8
3	CH_2Cl_2	405	10
4	Toluene	405	20
5	DMA	405	26
6	$ClCH_2CH_2Cl$	405	51
7	Acetone	405	74
8	MeCN	450	0
9	MeCN	365	85
10	**Acetone**	**365**	**85**[b]
11	Acetone (0.2 M)	365	77[c]
12	Acetone (0.05 M)	365	84[c]
13	Acetone	–	0

0.10 mmol scale reactions, 1.2 equiv. of **1**, under Ar/N_2 in dry solvents. [a] Yields determined by ^{1}H NMR *vs.* 1,3,5-trimethoxybenzene. [b] Identical yield at 16 h and 8 h of reaction time. [c] 8 h of reaction time. DMF = *N*,*N*-Dimethylformamide, DMA = *N*,*N*-Dimethylacetamide.

A robustness screening[27] (Figure 1) revealed that the reaction remains impervious to elevated temperatures (50 °C) as well as a high intensity of light. Low temperatures (0 °C) and a low concentration (½×) hamper conversion, but do not affect the relative yield based on converted starting material. The presence of water or oxygen leads to incomplete conversion with diminished yields. A high concentration (2×) gives a slightly lowered yield with full conversion.

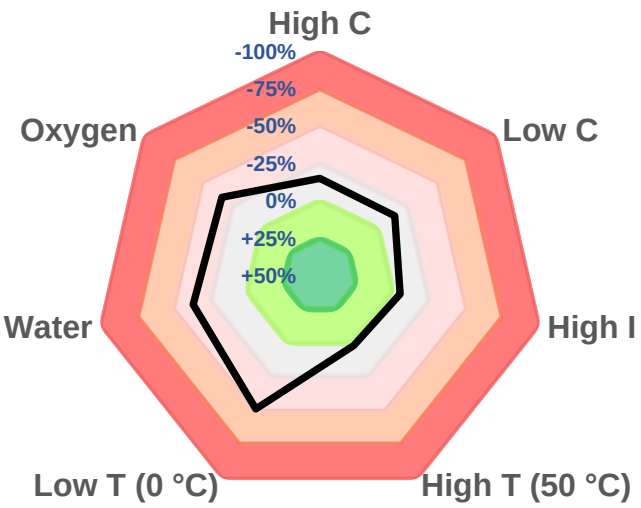
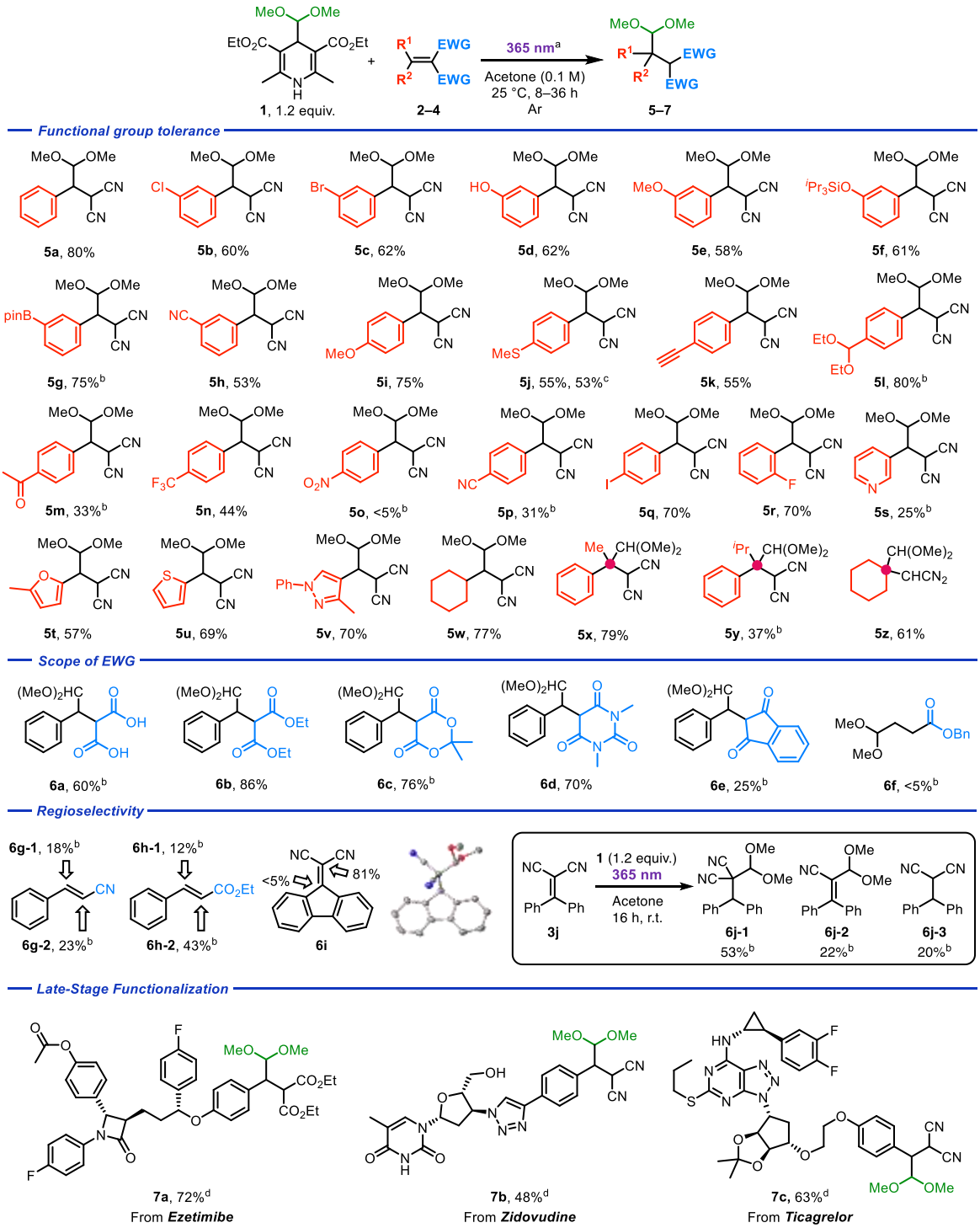


Figure 1. *Robustness screening.*

With the optimized conditions in hand, we proceeded to investigate the scope of this reaction on a diverse set of arylidene malononitriles (Scheme 3). A large variety of functional groups was tolerated to give the corresponding aldehyde dimethyl acetal in good to excellent yields. Functional groups frequently encountered by synthetic chemists such as silyl ethers (**5f**), boronates (**5g**), terminal alkynes (**5k**), or phenols (**5d**) were well tolerated by the mild reaction conditions. Five-membered N-, O-, and S-heterocycles were also smoothly converted (**5t**–**v**), as were aryl fluorides, chlorides, and bromides (**5r**, **5b**, **5c**). Aryl iodides, which are well-known to easily undergo reductive cleavage, exhibited some hydrodeiodination after 16 h of reaction time (8–10% of **5a** detected by ^{1}H NMR). Notably, this side reaction occurred only after complete consumption of the dicyanovinyl moiety and was entirely suppressed by careful monitoring of the reaction progress to yield **5a**-free **5q** in 70% yield after 6 h of irradiation. This underscores the high chemoselectivity of this transformation even in the presence of potentially labile functional groups. Substrates bearing further electron-withdrawing groups on the aromatic core showed diminished yields under standard conditions. ^{1}H NMR analysis of the crude reaction mixtures revealed additional dimethoxymethyl-containing side products alongside what we presume to be the intended product. We hypothesize that side reactions on the aromatic moiety (e.g. *ipso*-substitution of the nitrile group in **5p**)[19] and/or free-radical polymerization accelerated by the additional electron-deficient character become significant. This effect is less pronounced when the electron-withdrawing group is *meta* to the dicyanovinyl group (**5h**).

Excitingly, ylidenemalononitriles derived from both dialkyl and alkyl aryl ketones were converted to the respective acetals bearing quaternary carbon centers (**5x**–**z**), albeit limited by pronounced steric bulk (**5y**). Similarly, activated olefins derived from malonic acid, diethyl malonate, Meldrum's acid – a valuable synthon – and *N*,*N*'-dimethylbarbituric acid showed similar good yields compared to those derived from malononitrile (**6a**–**d**). A 1,3-indanedione-derived

substrate resulted in a dark-orange complex mixture accompanied by formation of an insoluble precipitate and diminished product yield (**6e**). Benzyl acrylate yielded only polymerization products (**6f**). Cinnamonitrile and ethyl cinnamate reacted sluggishly and gave a mixture of two regioisomers derived from competitive benzylic and homobenzylic formylations with ratios of 1/1.3 and 1/3.6, respectively (**6g–h**).



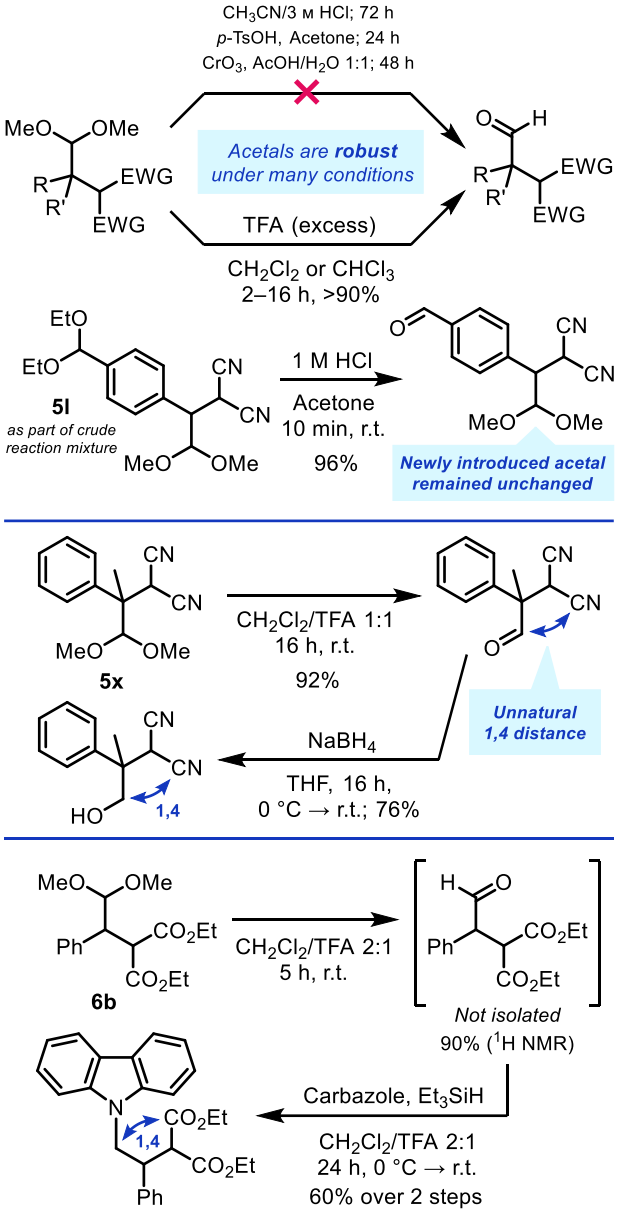
Scheme 3. *Substrate scope. 100 µmol scale reactions, isolated yields are given. [a] EvoluChem 365PF LED, [b] ^{1}H NMR yield vs. 1,3,5-trimethoxybenzene. [c] Isolated yield on a 3.0 mmol scale (72 h of irradiation). [d] Isolated yield on a 50 µmol scale reaction.*

To assess the synthetic utility of our method, we examined its applicability to late-stage functionalization of large molecules bearing biologically relevant motifs. Under standard conditions, an Ezetimibe derivative gave **7a** in good 72% yield. An azide-alkyne cycloadduct of Zidovudine (AZT), gave **7b** in 48% yield. **4c**, derived from the platelet aggregation inhibitor Ticagrelor, gave **7c** in 63% yield. These results further demonstrate the mildness and selectivity of this reaction. The reaction was successfully scaled up by a factor of 30 in the case of **5j** with 72 h of irradiation and a minimal change in yield.

When diphenylmethylidene malononitrile (**3j**) was employed as the substrate, we observed a mixture of three major species in the crude ^{1}H NMR spectrum: The homobenzylic formylation product (**6j-1**), its corresponding formal HCN elimination product (**6j-2**), as well as the hydrogenation product of the starting material (**6j-3**). Remarkably, no regular benzylic formylation was observed. To gain further insight, we conducted control experiments to probe the origin of **6j-2** and **6j-3**. The hydrogenation of **3j** via hydride-transfer/protonation by unsubstituted Hantzsch ester is a known reaction which has been reported on multiple occasions.[28–30] We found that **1** does not reduce **3j** in the dark to yield **6j-3**, neither in the absence of any additives nor in the presence of the photoreaction byproducts such as the side product diethyl 2,6-dimethylpyridine-3,5-dicarboxylate. Furthermore, **6j-1** did not eliminate HCN to yield **6j-2** upon prolonged stirring of the reaction mixture at room temperature (72 h) or 50 °C (24 h) after irradiation. These findings indicate that **6j-2** and **6j-3** are formed during the photochemical process itself rather than via parallel dark side reactions. In stark contrast, fluorenone-derived malononitrile **3i** was smoothly converted to the analogous homobenzylic acetal **6i** in 81% isolated yield. The position of the dimethoxymethyl group was unequivocally confirmed by single-crystal X-ray diffraction. Notably, hydrogenation or HCN elimination was not observed in this case.

The dimethyl acetals obtained by our method are robust towards a large portion of acidic conditions normally employed to deprotect other acetals as a result of their acyclic, aldehyde-derived, and α-substituted nature (Scheme 4, top).[31] For example, addition of an equal volume of 3 M hydrochloric acid or *para*-toluenesulfonic acid to the irradiated reaction mixture resulted in minimal conversion after three days. The stability is further attested by the rapid orthogonal deprotection of the aromatic diethyl acetal in **5l**. The newly introduced dimethoxymethyl moiety is smoothly deprotected in a non-aqueous fashion by excess trifluoroacetic acid in dichloromethane or chloroform within 3–16 h. We found that the free aldehydes are rather unstable and degrade rapidly upon isolation or purification. To mitigate this, they should be concentrated swiftly at or below ambient temperature and immediately used in the next step in their crude form, or more ideally kept dissolved in the deprotecting CH_2Cl_2/TFA medium in which they remain stable for ~8–24 h at room temperature. More hindered aldehydes like that derived from **5x** can be kept in their isolated crude form for at least 6 months at −25 °C, but still exhibit

decomposition during further purification attempts. The newly obtained unnatural 1,4-functional group distance as a result of the umpolung of the formyl synthon is useful in organic synthesis. Combined with typical aldehyde reactivity, this enables vast subsequent functionalization potential. The aldehyde derived from **5x** was reduced to the corresponding alcohol using a standard $NaBH_4$ protocol (Scheme 4, middle). Deprotection of **6b** gave a solution of the free aldehyde with a yield of ~90% after 5 h (confirmed by ^1H NMR spectroscopy in a separate run), which could immediately be treated with carbazole and triethylsilane in a reductive amination[32] (Scheme 4, bottom).

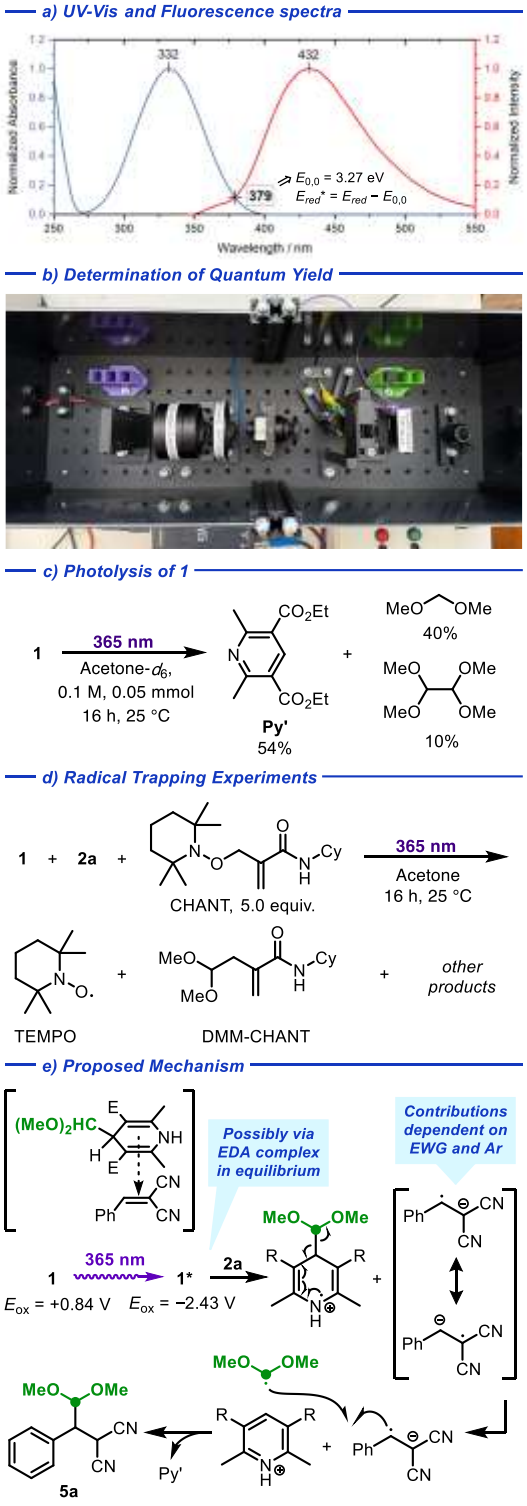


Scheme 4. *Top: Demonstration of the robustness of the newly introduced dimethoxymethyl moiety. Middle, Bottom: Demonstration of the deprotection and follow-up reactions of* ***5x*** *and* ***6b****. Yields and conditions have not been optimized.*

After establishing the synthetic potential of our reaction, we sought to gain insight into its mechanism. UV-Vis spectroscopy revealed that Hantzsch ester **1** shows an absorption band with λ_{max} = 332 nm, likely an $n \rightarrow \pi^*$ transition.[33] Within the model system, only **1** was found to absorb at 365 nm. UV-Vis spectroscopy showed no indication of a persistent electron donor-acceptor (EDA) complex between **1** and **2a** due to the absence of a bathochromic shift. However, transient EDA complex formation with a low equilibrium constant cannot be ruled out. A direct involvement of acetone, a known hydrogen abstractor in its triplet state,[34] is unlikely based on its absorption spectrum (<330 nm) and the fact that the reaction progresses similarly in acetonitrile (<190 nm). Cyclic voltammetry studies revealed an irreversible oxidation of **1** with $E(\mathbf{1}^{\bullet+}/\mathbf{1})$ = +0.84 V vs. SCE and an irreversible reduction of **2a** with $E(\mathbf{2a}/\mathbf{2a}^{\bullet-})$ = −1.16 V vs. SCE (see experimental section for details). Using 3.27 eV (≙ 379 nm, 323 kJ·mol^{-1}) for the singlet energy of **1** derived from spectroscopic measurements, the redox potential in S_1 is approximated as $E(\mathbf{1}^{\bullet+}/^1\mathbf{1})$ ≈ 0.84 – 3.27 = −2.43 V vs. SCE (Scheme 5a). Involvement of the triplet excited state T_1 is improbable given the low intersystem crossing rates typically observed for (alkyl) Hantzsch esters. Access to their triplet states generally requires either sensitization or intramolecular charge transfer through a 4-aryl substituent.[35] A light-initiated long-lived radical chain mechanism may be excluded on the basis of a reaction quantum yield Φ_R of 1.1% (Scheme 5b). Direct ultraviolet irradiation of **1** in oxygen-free acetone-d_6 led to full decomposition within 16 h (Scheme 5c). As expected, diethyl 2,6-dimethylpyridine-3,5-dicarboxylate (**Py'**) was formed as the major product. In addition to other unidentified side products, dimethoxymethane (40%) and glyoxal tetramethyl acetal (10%) were identified by ^{1}H and ^{13}C NMR analysis. The formation of the latter provides strong evidence for the generation of free dimethoxymethyl radicals under these conditions. Additional support for the involvement of radical intermediates was obtained through trapping experiments employing the radical scavenger CHANT (Scheme 5d).[36] GC-MS revealed the presence of free TEMPO, which is only formed upon reaction of CHANT with free radical species. Furthermore, the adduct of CHANT and the dimethoxymethyl radical was detected by GC-MS and ESI-MS, conclusively supporting its intermediacy throughout the reaction.

Based on our observations and mechanistic experiments, we propose the following mechanism (Scheme 5e): Initially, **1** is excited by an ultraviolet photon to yield the strong one-electron reductant **1***. The latter reduces the π-system of **2a**, which is thermodynamically feasible based on their redox potentials (*vide supra*). This reaction yields $\mathbf{1}^{\bullet+}$ and the relatively long-lived benzylic radical $\mathbf{2a}^{\bullet-}$. The dimethoxymethyl radical is liberated by $\mathbf{1}^{\bullet+}$ upon a rapid aromatization-driven fragmentation. The product **5a** is then formed by radical recombination and protonation. No homodimerization of either radical has been detected under the reaction conditions, presumably due to the near-concomitant formation of benzylic radical $\mathbf{2a}^{\bullet-}$ and the dimethoxymethyl radical. Spatial proximity as well as advantageous kinetics due to the persistent radical

effect[37] may enable an efficient radical cross-coupling. An alternative mechanism based on direct photo-homolysis of the Hantzsch ester followed by a Giese-type addition of the di-methoxymethyl radical to the neutral olefin cannot be fully excluded as of now.



Scheme 5. *a) Normalized UV-Vis spectrum (blue) and normalized fluorescence spectrum (red) of **1** in acetonitrile (see experimental section for full details). b) Experimental setup for the determination of the reaction quantum yield. c) Photodecomposition of **1** under ultraviolet irradiation. d) Radical trapping experiments using TEMPO-CHANT. e) Postulated reaction mechanism, R = CO_2Et.*

The observed homobenzylic formylations in the case of **6e**–**f** as well as **8a**–**b** may be rationalized by an altered electronic distribution within the resonance-stabilized radical anion. In the case of **2a**$^{\bullet-}$, the radical seems to be mainly localized on the benzylic position with the anionic character in the α-position of the two nitrile groups. The loss of one of the two electron-withdrawing groups or the addition of a second aryl group leads to a less pronounced difference or a reversal of the radical and anionic sites. The observation that **6j-1** is not converted into **6j-2** by HCN elimination suggests that protonation occurs after radical recombination as the final step. This order of events would lead to an anionic intermediate from which cyanide is eliminated in an E1cb fashion.

In conclusion, we have developed a catalyst-free radical hydroformylation of electron-deficient olefins that utilizes easily accessible starting materials. Under ultraviolet irradiation (365 nm), the Hantzsch ester derivative becomes a strong photoreductant and presumably reduces the olefin. Upon fragmentation of the former, a dimethoxymethyl radical is released which recombines with the olefin radical anion. Numerous functional groups are well-tolerated and the applicability to late-stage functionalization was demonstrated. The acetals are easily deprotected into the respective aldehyde by trifluoroacetic acid, which enables further functionalization. Further research regarding the application of Hantzsch esters as formylation reagents is currently being undertaken in our group.

Literature References

[1] A. Vilsmeier, A. Haack, *Ber. Dtsch. Chem. Ges.* **1927**, *60*, 119–122.

[2] R. M. Garbaccio, S. J. Stachel, D. K. Baeschlin, S. J. Danishefsky, *J. Am. Chem. Soc.* **2001**, *123*, 10903–10908.

[3] K. C. Nicolaou, Q. Kang, S. Y. Ng, D. Y. K. Chen, *J. Am. Chem. Soc.* **2010**, *132*, 8219–8222.

[4] C. A. Kuttruff, H. Zipse, D. Trauner, *Angew. Chem. Int. Ed.* **2011**, *50*, 1402–1405.

[5] L. Bouveault, *Bull. Soc. Chim. Paris* **1904**, 1306–1322.

[6] D. L. Comins, H. Hong, G. Jianhua, *Tetrahedron Lett.* **1994**, *35*, 5331–5334.

[7] X. Lin, R. W. Kavash, P. S. Mariano, *J. Org. Chem.* **1996**, *61*, 7335–7347.

[8] H. Weinstabl, M. Suhartono, Z. Qureshi, M. Lautens, *Angew. Chem. Int. Ed.* **2013**, *52*, 5305–5308.

[9] G. Tojo, M. Fernández, *Oxidation of Alcohols to Aldehydes and Ketones. A Guide to Current Common Practice*, Springer, **2006**.

[10] N. D. Smith, P. J. Kocienski, S. D. A. Street, *Synthesis* **1996**, *1996*, 652–666.

[11] R. V. Stevens, P. M. Lesko, R. Lapalme, *J. Org. Chem.* **1975**, *40*, 3495–3498.

[12] A. Zakarian, A. Batch, R. A. Holton, *J. Am. Chem. Soc.* **2003**, *125*, 7822–7824.

[13] O. Roelen, *Verfahren Zur Herstellung von Sauerstoffhaltigen Verbindungen*, **1938**, DE849548C.

[14] B. Cornils, W. A. Herrmann, M. Rasch, *Angew. Chem. Int. Ed.* **1994**, *33*, 2144–2163.

[15] R. Franke, D. Selent, A. Börner, *Chem. Rev.* **2012**, *112*, 5675–5732.

[16] C. K. Prier, D. A. Rankic, D. W. C. MacMillan, *Chem. Rev.* **2013**, *113*, 5322–5363.

[17] N. A. Romero, D. A. Nicewicz, *Chem. Rev.* **2016**, *116*, 10075–10166.

[18] P. Z. Wang, J. R. Chen, W. J. Xiao, *Org. Biomol. Chem.* **2019**, *17*, 6936–6951.

[19] L. Buzzetti, A. Prieto, S. R. Roy, P. Melchiorre, *Angew. Chem. Int. Ed.* **2017**, *56*, 15039–15043.

[20] F. Gu, W. Huang, X. Liu, W. Chen, X. Cheng, *Adv. Synth. Catal.* **2018**, *360*, 925–931.

[21] Z. J. Wang, S. Zheng, J. K. Matsui, Z. Lu, G. A. Molander, *Chem. Sci.* **2019**, *10*, 4389–4393.

[22] X. Liu, R. Liu, J. Dai, X. Cheng, G. Li, *Org. Lett.* **2018**, *20*, 6906–6909.

[23] L. Cardinale, M. O. Konev, A. Jacobi von Wangelin, *Chem. Eur. J.* **2020**, *26*, 8239–8243.

[24] L. Cardinale, M.-O. W. S. Schmotz, M. O. Konev, A. Jacobi von Wangelin, *Org. Lett.* **2022**, *24*, 506–510.

[25] D. Prat, J. Hayler, A. Wells, *Green Chem.* **2014**, *16*, 4546.

[26] F. P. Byrne, S. Jin, G. Paggiola, T. H. M. Petchey, J. H. Clark, T. J. Farmer, A. J. Hunt, C. Robert McElroy, J. Sherwood, *Sustain. Chem. Process. 2016 41* **2016**, *4*, 1–24.

[27] L. Pitzer, F. Schäfers, F. Glorius, *Angew. Chem. Int. Ed.* **2019**, *58*, 8572–8576.

[28] X. Q. Fang, H. J. Xu, H. Jiang, Y. C. Liu, Y. Fu, Y. D. Wu, *Tetrahedron Lett.* **2009**, *50*, 312–315.

[29] J. Che, Y. Lam, *Adv. Synth. Catal.* **2010**, *352*, 1752–1758.

[30] Z. Li, J. D. Yang, J. P. Cheng, *Org. Chem. Front.* **2021**, *8*, 876–882.

[31] D. P. N. Satchell, R. S. Satchell, *Chem. Soc. Rev.* **1990**, *19*, 55.

[32] M. Righi, A. Bedini, G. Piersanti, F. Romagnoli, G. Spadoni, *J. Org. Chem.* **2011**, *76*, 704–707.

[33] P. Pávez, M. V. Encinas, *Photochem. Photobiol.* **2007**, *83*, 722–729.

[34] G. Porter, S. K. Dogra, R. O. Loutfy, S. E. Sugamori, R. W. Yip, *J. Chem. Soc. Faraday Trans.* **1973**, *69*, 1462–1474.

[35] E. Fasani, M. Fagnoni, D. Dondi, A. Albini, *J. Org. Chem.* **2006**, *71*, 2037–2045.

[36] P. J. H. Williams, G. A. Boustead, D. E. Heard, P. W. Seakins, A. R. Rickard, V. Chechik, *J. Am. Chem. Soc.* **2022**, *144*, 15969–15976.

[37] D. Leifert, A. Studer, *Angew. Chem. Int. Ed.* **2020**, *59*, 74–108.

Experimental Section

General Information

Nuclear magnetic resonance (NMR) spectroscopy: ^{1}H NMR spectra (300 MHz) and ^{13}C-NMR spectra (75.5 MHz) were recorded on a *Bruker Fourier HD 300.* ^{1}H NMR spectra (400 MHz) and ^{13}C-NMR spectra (101 MHz) were recorded on a *Bruker Avance III HD 400*. ^{1}H NMR spectra (600 MHz), ^{13}C-NMR spectra (151 MHz), and ^{19}F-NMR spectra (565 MHz) were recorded on a *Bruker Avance III HD 600*. All spectra were recorded at 25 °C unless otherwise stated. Chemical shifts δ are reported in parts per million (ppm) relative to tetramethylsilane for ^{1}H and ^{13}C NMR spectra, and relative to $CFCl_3$ for ^{19}F NMR spectra. Coupling constants *J* are given in Hertz (Hz). *MestReNova 14* (Mnova) by *Mestrelab* was used for analysis of the NMR spectra. Abbreviations used for NMR data: s = singlet; br. s = broad singlet; d = doublet; t = triplet; q = quartet, m = multiplet and combinations thereof.

Infrared (IR) spectroscopy: Infrared spectra were recorded using a *Bruker VERTEX 70* FTIR spectrometer using a *Specac Golden Gate* ATR unit.

UV-Vis spectroscopy: UV-Vis spectra were measured at room temperature on an *Agilent Cary 5000* UV-Vis-NIR Spectrophotometer in double-beam mode using 10 mm SUPRASIL quartz cuvettes by *Hellma*.

Fluorescence spectroscopy: Fluorescence spectra were measured at room temperature on an *Agilent Cary Eclipse Fluorescence Spectrophotometer* at a 90° angle using 10 mm SUPRASIL quartz fluorescence cuvettes by *Hellma*.

Mass spectrometry: High-resolution mass spectra (electrospray ionization, ESI) were measured using an *Agilent 6224 ESI-TOF* or a *Bruker maXis ESI-Q-TOF* by direct injection in positive or negative ion mode. Abbreviations used for MS data: *m/z* mass-to-charge ratio; M = exact mass of the target compound. *MestReNova 14* (Mnova) by *Mestrelab* was used for analysis of the MS spectra.

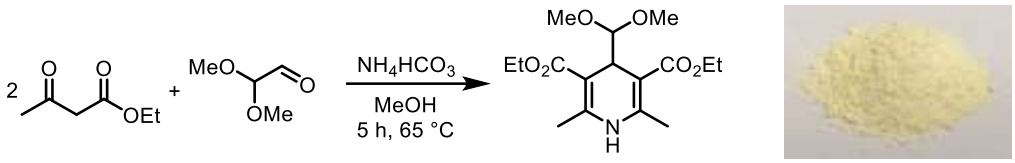
Melting points: Melting points (m.p.) were measured using a *DigiMelt MPA160* by *Stanford Research Systems*.

Cyclic voltammetry (CV): CV measurements were performed with a potentiostat galvanostat *PGSTAT101* from *Metrohm Autolab* using a glassy carbon working electrode, a platinum wire counter electrode, a silver/silver(I) chloride reference electrode and N(*n*-Bu)$_4$PF$_6$ (0.1 M) as supporting electrolyte.

Thin-layer chromatography (TLC) and column chromatography: TLC was performed using aluminium plates coated with UV-fluorescence-indicator-doped stationary phase by *Macherey-Nagel* (*ALUGRAM® Xtra Sil G/UV$_{254}$* for SiO_2, *ALUGRAM® ALOX N / UV254* for neutral Al_2O_3). Preparative column chromatography was performed using silica by *Acros Organics* (35–70 µm, 60 Å pore size) or neutral alumina by *Macherey-Nagel* (50–200 µm, 90 Å pore size) using distilled technical grade solvents.

Synthesis of Compounds

Diethyl 4-(dimethoxymethyl)-2,6-dimethyl-1,4-dihydropyridin-3,5-dicarboxylate (1)



A suspension of ammonium bicarbonate (2.37 g, 30.0 mmol, 1.0 equiv.), ethyl acetoacetate (7.81 g, 60.0 mmol, 2.0 equiv.) and 2,2-dimethoxyacetaldehyde (60 wt.% soln. in water, 5.21 g, 30.0 mmol, 1.0 equiv.) in methanol (30 mL) was refluxed. Within 10–20 minutes the solid ammonium bicarbonate dissolves and the mixture turns homogeneous and bright yellow. After 5 h of reflux, the solvent was removed and the orange syrupy residue was thoroughly dried *in vacuo*, during which slow solidification to a waxy solid eventually occurs (scratching the flask wall is often required to induce crystallization). The product crystallizes slowly (after ~30 min) from boiling diethyl ether (~25–30 mL) upon cooling to r.t., then to −25 °C overnight, initially as small pale-yellow needles which merge into solid clumps. **1** is obtained as a pale-yellow solid after filtration and washing with cold diethyl ether and room-temperature pentane until the distinct odor of ethyl acetoacetate is no longer perceptible (5.37 g, 16.4 mmol, 55 %). The solid thus obtained melts at 88–89 °C and is sufficiently pure for the photoreaction. A purer, almost colorless product melting at 90–91 °C is obtained after a second recrystallization or careful silica column chromatography (SiO_2, Pentane/EtOAc 3:2). This synthesis was also conducted several times on a 5.0, 60, and 150 mmol scale with consistent yields (50–60 %).

^{1}H NMR (600 MHz, $CDCl_3$): δ [ppm] = 5.85 (s, 1H), 4.34 (d, J = 5.2 Hz, 1H), 4.25 – 4.11 (m, 4H), 3.94 (d, J = 5.2 Hz, 1H), 3.29 (s, 6H), 2.27 (s, 6H), 1.28 (t, J = 7.2 Hz, 6H).

^{13}C{^{1}H} NMR (151 MHz, $CDCl_3$): δ [ppm] = 168.4, 145.1, 107.9, 99.2, 59.8, 55.3, 36.9, 19.4, 14.5.

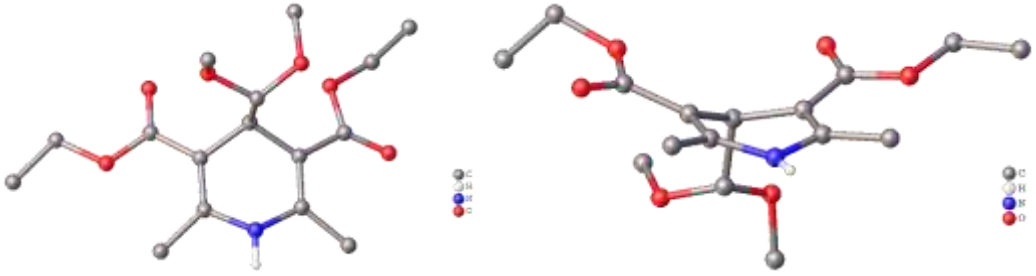
IR (ATR): $\tilde{\upsilon}$ [cm^{-1}] = 3346 (ν(N–H)), 2990, 2938, 2889, 2837, 1699, 1649 (ν(C=O)), 1484, 1474, 1448, 1391, 1368, 1335, 1321, 1291, 1272, 1258, 1210 (ν(C–O–C)), 1166, 1150, 1122, 1099, 1044, 1016, 981, 916, 863, 776, 741, 711, 699, 643, 628.

UV-Vis (MeCN): λ_{max} [nm] (ε [$L \cdot mol^{-1} \cdot cm^{-1}$]) = 230, 248, 332 (6496).

HRMS (ESI): *m/z* calcd. for $C_{16}H_{25}NNaO_6^+$ ([M+Na]$^+$): 350.1574, found.: 350.1571; calcd. for $C_{32}H_{50}N_2NaO_{12}^+$ ([2M+Na]$^+$): 677.3256, found.: 677.3260.

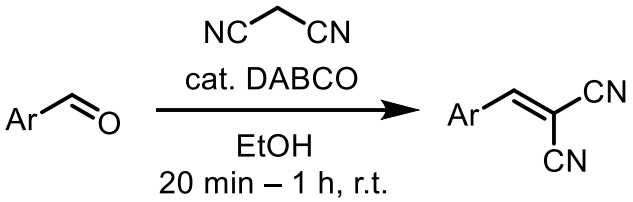
m.p. = 90–91 °C.

XRD (Non heteroatom-bonded hydrogen atoms omitted for clarity):



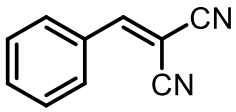
Synthesis of electron-deficient olefins

General procedure for the synthesis of arylidenemalononitriles (GP1)



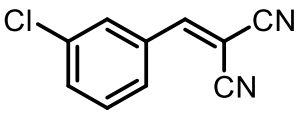
To a solution or suspension of the corresponding aldehyde (3.00 mmol, 1.0 equiv.) and malononitrile (198 mg, 3.00 mmol, 1.0 equiv.) in ethanol (3.0 mL) was added a spatula tip of 1,4-diazabicyclo-[2.2.2]octane (DABCO). Generally, a color change is observed and the products precipitates within 30–90 seconds. The mixture was stirred for a total of 20 minutes (1 hour if the starting aldehyde did not fully dissolve in ethanol), then diluted with water to induce further precipitation. The solid was filtered off and washed with water and a small amount of cold ethanol (−25 °C). The products required no further purification unless stated otherwise.

Benzylidenemalononitrile (**2a**)



Purchased from Sigma-Aldrich and used as received.

(3-Chlorobenzylidene)malononitrile (**2b**)



By GP1 starting from 3-chlorobenzaldehyde (422 mg) with a reaction time of 20 min.

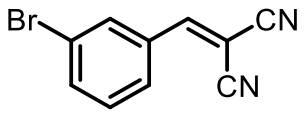
Yield: 58% (331 mg, 1.75 mmol).

Appearance: Colorless powder.

^{1}H NMR (300 MHz, $CDCl_3$): δ [ppm] = 7.88 – 7.80 (m, 2H), 7.72 (s, 1H), 7.64 – 7.57 (m, 1H), 7.54 – 7.45 (m, 1H).

Literature: D. Z. Xu, S. Shi, Y. Wang, *RSC Adv.* **2013**, *3*, 23075–23079.

(3-Bromobenzylidene)malononitrile (**2c**)



By GP1 starting from 3-bromobenzaldehyde (555 mg) with a reaction time of 20 min.

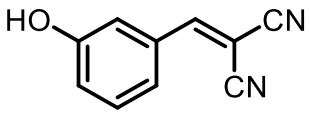
Yield: 67% (471 mg, 2.02 mmol).

Appearance: Colorless powder.

^{1}H NMR (300 MHz, $CDCl_3$): δ [ppm] = 8.00 – 7.94 (m, 1H), 7.93 – 7.87 (m, 1H), 7.79 – 7.73 (m, 1H), 7.71 (s, 1H), 7.47 – 7.39 (m, 1H).

Literature: R. Jin, Z. Bian, J. Li, M. Ding, L. Gao, *Dalt. Trans.* **2013**, *42*, 3936–3940.

(3-Hydroxybenzylidene)malononitrile (**2d**)



By GP1 on an adjusted scale starting from 3-hydroxybenzaldehyde (1.22 g, 10.0 mmol) and malononitrile (661 mg, 10.0 mmol) in ethanol (10 mL) with a reaction time of 20 min. Purified by recrystallization from water/EtOH.

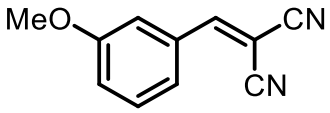
Yield: 63% (1.07 g, 6.30 mmol).

Appearance: Yellow powder.

^{1}H NMR (400 MHz, DMSO-d_6): δ [ppm] = 10.10 (s, 1H), 8.44 (s, 1H), 7.45 – 7.33 (m, 3H), 7.12 – 7.05 (m, 1H).

Literature: S. Chakraborty, A. Rudra Paul, S. Majumdar, *Results Chem.* **2022**, *4*, 100294.

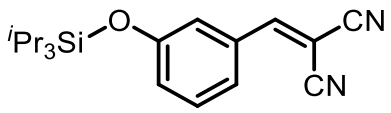
(3-Methoxybenzylidene)malononitrile (**2e**)



The synthesis and characterization of the batch used in this work is described in:

L. Cardinale, M. O. Konev, A. Jacobi von Wangelin, *Chem. Eur. J.* **2020**, *26*, 8239–8243.

(3-((Triisopropylsilyl)oxy)benzylidene)malononitrile (**2f**)



To a suspension of (3-hydroxybenzylidene)malononitrile (**2d**, 119 mg, 700 µmol, 1.0 equiv.) in CH_2Cl_2 (5.0 mL) was added imidazole (71.0 mg, 1.05 mmol, 1.5 equiv.), leading to a yellow solution. Triisopropylsilyl chloride (0.18 mL, 0.84 mmol, 1.2 equiv.) was added dropwise. Shortly after complete addition, the mixture became turbid. The mixture was stirred at room temperature for 16 hours, after which water (5.0 mL) was added to the yellow suspension. The aqueous phase was extracted with CH_2Cl_2 (3× 5.0 mL) and the combined organic phases were washed with brine (10 mL), dried over Na_2SO_4, filtered, and concentrated. The yellow residue was purified by column chromatography (SiO_2, Pentane/EtOAc 20:1) and thoroughly dried at 0.01 mbar and 45 °C to remove residual traces of triisopropylsilanol.

Yield: 86% (196 mg, 600 µmol).

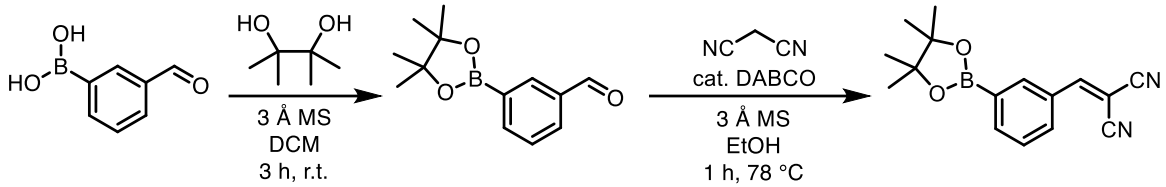
Appearance: Pale-yellow oil.

^{1}H NMR (300 MHz, $CDCl_3$): δ [ppm] = 7.70 (s, 1H), 7.46 – 7.35 (m, 3H), 7.17 – 7.11 (m, 1H), 1.35 – 1.22 (m, 3H), 1.14 – 1.08 (m, 18H).

^{13}C{^{1}H} NMR (75.5 MHz, $CDCl_3$): δ [ppm] = 159.9, 157.1, 132.3, 130.8, 126.8, 124.2, 121.0, 113.9, 112.6, 83.0, 18.0, 12.7;

HRMS (ESI): *m/z* calcd. for $C_{19}H_{27}N_2OSi^+$: 327.1887, found: 327.1888, calcd. for $C_{19}H_{26}N_2NaOSi^+$ ($[M+Na]^+$): 349.1707, found: 349.1705.

3-(2,2-Dicyanovinyl)phenylboronic acid pinacol ester (**2g**)



3-Formylboronic acid pinacol ester. To a suspension of 3-formylphenylboronic acid (525 mg, 3.50 mmol, 1.0 equiv.) in CH_2Cl_2 (5.0 mL) was added pinacol (414 mg, 3.50 mmol, 1.0 equiv.) and molecular sieves (3 Å). The mixture was stirred for 3 hours, during which the undissolved starting material disappeared. The mixture was filtered through Celite and concentrated.

Yield: 93% (751 mg, 3.24 mmol)

Appearance: Colorless solid.

^{1}H NMR (300 MHz, $CDCl_3$): δ [ppm] = 10.04 (s, 1H), 8.32 – 8.28 (m, 1H), 8.08 – 8.02 (m, 1H), 8.01 – 7.95 (m, 1H), 7.57 – 7.48 (m, 1H), 1.36 (s, 12H).

Literature = P. B. Dzhevakov, M. A. Topchiy, D. A. Zharkova, O. S. Morozov, A. F. Asachenko, M. S. Nechaev, *Adv. Synth. Catal.* **2016**, *358*, 977–983.

3-(2,2-Dicyanovinyl)phenylboronic acid pinacol ester. To a solution of 3-formylboronic acid pinacol ester (464 mg, 2.00 mmol, 1.0 equiv.) in ethanol (2 mL) over molecular sieves (3 Å) was added malononitrile (145 mg, 2.20 mmol, 1.1 equiv.) and a spatula tip of DABCO. The mixture was refluxed for one hour and the resulting dark red mixture was filtered, diluted with dichloromethane (5.0 mL), and washed with water (5.0 mL). The organic phase was dried over Na_2SO_4, filtered, and concentrated. The dark red residue was re-dissolved in a small amount of CH_2Cl_2 and passed through a silica plug. After elution with additional CH_2Cl_2, the colorless eluate was concentrated.

Yield: 70% (388 mg, 1.39 mmol)

Appearance: Colorless solid.

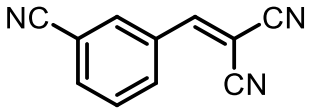
^{1}H NMR (300 MHz, $CDCl_3$): δ [ppm] = 8.22 – 8.16 (m, 1H), 8.12 – 8.07 (m, 1H), 8.06 – 8.00 (m, 1H), 7.79 (s, 1H), 7.58 – 7.51 (m, 1H), 1.36 (s, 12H).

^{13}C{^{1}H} NMR (101 MHz, $CDCl_3$): δ [ppm] = 160.2, 140.9, 138.7, 131.6, 130.5, 129.1, 113.9, 112.6, 84.6, 82.9, 25.0.

HRMS (ESI): *m/z* calcd. for $C_{16}H_{18}BN_2O_2^+$ ($[M+H]^+$): 281.1456, found: 281.1460; calcd. for $C_{16}H_{17}BN_2NaO_2^+$ ($[M+Na]^+$): 303.1275, found: 303.1292.

m.p. = 98–99 °C.

(3-Cyanobenzylidene)malononitrile (**2h**)



By GP1 starting from 3-cyanobenzaldehyde (393 mg) with a reaction time of 20 min.

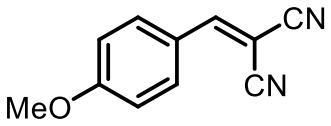
Yield: 75% (401 mg, 2.24 mmol).

Appearance: Colorless powder.

^{1}H NMR (300 MHz, $CDCl_3$): δ [ppm] = 8.23 – 8.16 (m, 1H), 8.10 – 8.04 (m, 1H), 7.94 – 7.86 (m, 1H), 7.79 (s, 1H), 7.76 – 7.66 (m, 1H).

Literature: W. J. Ang, Y. S. Chng, Y. Lam, *RSC Adv.* **2015**, *5*, 81415–81428.

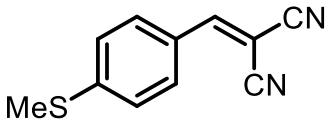
(4-Methoxybenzylidene)malononitrile (**2i**)



The synthesis and characterization of the batch used in this work is described in:

L. Cardinale, M. O. Konev, A. Jacobi von Wangelin, *Chem. Eur. J.* **2020**, *26*, 8239–8243.

(4-(Methylthio)benzylidene)malononitrile (**2j**)



By GP1 starting from 4-(methylthio)benzaldehyde (457 mg) with a reaction time of 20 min.

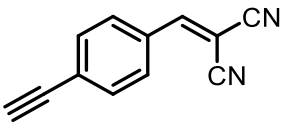
Yield: 87% (522 mg, 2.61 mmol).

Appearance: Bright yellow powder.

^{1}H NMR (300 MHz, $CDCl_3$): δ [ppm] = 7.86 – 7.77 (m, 2H), 7.66 (s, 1H), 7.35 – 7.27 (m, 2H), 2.55 (s, 3H).

Literature: Z. H. Zhang, B. B. Qian, P. P. Sheng, S. Yang, X. F. Huang, J. L. Wang, Q. Chen, L. Wang, M. Y. He, *Appl. Organomet. Chem.* **2019**, *33*, e4788.

(4-Ethynylbenzylidene)malononitrile (**2k**)



By GP1 starting from 4-ethynylbenzaldehyde (390 mg) with a reaction time of 1 h.

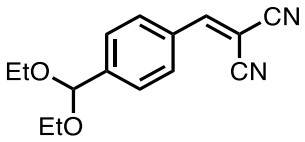
Yield: 91% (486 mg, 2.73 mmol).

Appearance: Ochre powder.

^{1}H NMR (300 MHz, $CDCl_3$): δ [ppm] = 7.92 – 7.81 (m, 2H), 7.74 (s, 1H), 7.68 – 7.57 (m, 2H), 3.37 (s, 1H).

Literature: P. D. Jarowski, Y. L. Wu, C. Boudon, J. P. Gisselbrecht, M. Gross, W. B. Schweizer, F. Diederich, *Org. Biomol. Chem.* **2009**, *7*, 1312–1322.

(4-(Diethoxymethyl)benzylidene)malononitrile (**2l**)



Terephthalaldehyde mono(diethyl acetal) (1.041 g, 5.00 mmol, 1.0 equiv.), malononitrile (330 mg, 5.00 mmol, 1.0 equiv.) and a spatula tip of DABCO were dissolved in EtOH (5.0 mL). The mixture was stirred at 1 h at room temperature, during which the product separated as small oil droplets. The mixture was stored at 3 °C for ca. 1 h, during which it solidified. The mixture was diluted with water and the solid was filtered off, washed with plenty of water, and twice with a small amount of cold (–18 °C) EtOH.

Yield: 48% (611 mg, 2.39 mmol).

Appearance: Off-white powder.

^{1}H NMR (300 MHz, $CDCl_3$): δ [ppm] = 7.97 – 7.82 (m, 2H), 7.77 (s, 1H), 7.73 – 7.56 (m, 2H), 5.55 (s, 1H), 3.69 – 3.47 (m, 4H), 1.25 (t, J = 7.1 Hz, 6H).

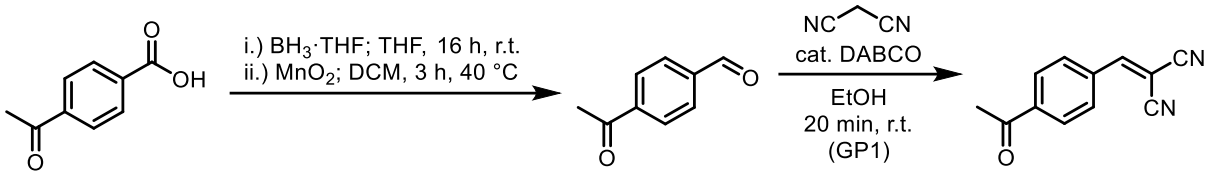
^{13}C{^{1}H} NMR (75.5 MHz, $CDCl_3$): δ [ppm] = 159.6, 146.0, 130.9, 130.8, 128.1, 113.9, 112.7, 100.5, 83.0, 61.5, 15.3.

MS (EI): *m/z* (%): 256 (2) $[M]^+$, 211 (100) $[M-(C_2H_4O)]$, 183 (50), 155 (61), 128 (15)

IR (ATR): $\tilde{\nu}$ [cm^{-1}] = 3024 (ν(=C–H)), 2976 (ν(C–H)), 2934, 2892, 2226 (ν(C≡N)), 1590 (ν(C=C)), 1561, 1479, 1447 ($\delta(CH_3)$), 1409, 1372 ($\delta(CH_3)$), 1351, 1341, 1301, 1216, 1180, 1154, 1130, 1089, 1037 (ν(C–O–C)), 1018, 999, 985, 951, 925, 872, 855, 836, 802, 776 (δ(=C–H)), 729, 694, 616.

m.p. = 53–54 °C.

(4-Acetylbenzylidene)malononitrile (**2m**)



4-Acetylbenzaldehyde. 4-Acetylbenzoic acid (492 mg, 3.00 mmol, 1.0 equiv.) was suspended in dry THF (5.0 mL) under nitrogen atmosphere. The mixture was cooled to 0 °C and BH_3 (1.0 M in THF, 6.00 mL, 6.00 mmol, 2.0 equiv.) was added dropwise, resulting in effervescence due to evolution of hydrogen as well as gradual dissolution of the starting material. The ice bath was removed and the mixture was stirred at room temperature for 16 hours. The reaction mixture was carefully poured into a 1:1 mixture of THF (5.0 mL) and ice water (5.0 mL) in a separatory funnel. When the hydrogen evolution had ceased, the water was saturated with solid K_2CO_3, the THF phase was separated, and the aqueous phase was extracted with ethyl acetate (3× 10 mL). The combined organic phases were dried over $MgSO_4$, filtered and concentrated to yield crude 4-(1-hydroxyethyl)benzyl alcohol as a colorless oil as confirmed by GC-MS analysis. The 4-(1-hydroxyethyl)benzyl alcohol was taken up in CH_2Cl_2 (10 mL) and manganese dioxide (5.22 g, 60.0 mmol, 20.0 equiv. based on 4-acetylbenzoic acid) was added. The mixture was refluxed for 3 hours (GC-MS control). The mixture was filtered through a silica plug and concentrated. The residue was purified by column chromatography (SiO_2, Pentane/Et_2O 5:1).

Yield: 44% (194 mg, 1.31 mmol).

Appearance: Colorless solid.

^{1}H NMR (300 MHz, $CDCl_3$): δ [ppm] = 10.11 (s, 1H), 8.13 – 8.07 (m, 2H), 8.01 – 7.95 (m, 2H), 2.66 (s, 3H).

Literature: V. Hornillos, M. Giannerini, C. Vila, M. Fañanás-Mastral, B. L. Feringa, *Chem. Sci.* **2015**, *6*, 1394–1398.

(4-Acetylbenzylidene)malononitrile. By GP1 on an adjusted scale starting from 4-acetylbenzaldehyde (187 mg, 1.26 mmol) and malononitrile (83.0 mg, 1.26 mmol) in ethanol (1.30 mL) with a reaction time of 20 min.

Yield: 78% (193 mg, 984 µmol).

Appearance: Yellow powder.

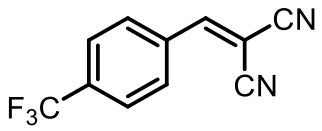
^{1}H NMR (300 MHz, $CDCl_3$): δ [ppm] = 10.11 (s, 1H), 8.13 – 8.07 (m, 2H), 8.01 – 7.95 (m, 2H), 2.66 (s, 3H).

$^{13}C\{^{1}H\}$ NMR (151 MHz, $CDCl_3$): δ [ppm] = 196.7, 158.5, 140.9, 134.4, 130.9, 129.3, 113.3, 112.2, 85.6, 27.0.

HRMS (ESI): *m/z* calcd. for $C_{12}H_9N_2O^+$: 197.0709, found: 197.0704.

m.p. = 136–138 °C.

(4-(Trifluoromethyl)benzylidene)malononitrile (**2n**)



By GP1 starting from 4-(trifluoromethyl)benzaldehyde (522 mg) with a reaction time of 20 min. Purified by recrystallization from water/EtOH.

Yield: 67% (449 mg, 2.02 mmol).

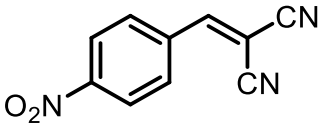
Appearance: Long colorless needles.

^{1}H NMR (600 MHz, $CDCl_3$): δ [ppm] = 8.03 – 8.00 (m, 2H), 7.84 (s, 1H), 7.83 – 7.79 (m, 2H).

^{19}F NMR (565 MHz, $CDCl_3$): δ [ppm] = −63.48.

Literature: N. Zengin, H. Burhan, A. Şavk, H. Göksu, F. Şen, *Sci. Reports* **2020**, *10*, 12758.

(4-Nitrobenzylidene)malononitrile (**2o**)



By GP1 starting from 4-nitrobenzaldehyde (453 mg) with a reaction time of 20 min.

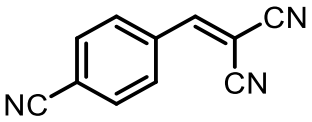
Yield: 82% (492 mg, 2.47 mmol).

Appearance: Orange-brown powder.

^{1}H NMR (300 MHz, $CDCl_3$): δ [ppm] = 8.44 – 8.34 (m, 2H), 8.12 – 8.03 (m, 2H), 7.88 (s, 1H).

Literature: N. Zengin, H. Burhan, A. Şavk, H. Göksu, F. Şen, *Sci. Reports* **2020**, *10*, 12758.

(4-Cyanobenzylidene)malononitrile (**2p**)



By GP1 starting from 4-cyanobenzaldehyde (393 mg) with a reaction time of 20 min.

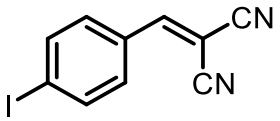
Yield: 79% (426 mg, 2.38 mmol).

Appearance: Off-white powder.

^{1}H NMR (300 MHz, $CDCl_3$): δ [ppm] = 8.03 – 7.96 (m, 2H), 7.87 – 7.79 (m, 3H).

Literature: L. Cardinale, M. O. Konev, A. Jacobi von Wangelin, *Chem. Eur. J.* **2020**, *26*, 8239–8243.

(4-Iodobenzylidene)malononitrile (**2q**)



By GP1 starting from 4-iodobenzaldehyde (696 mg) with a reaction time of 20 min.

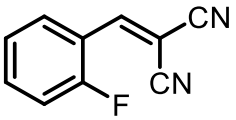
Yield: 77% (647 mg, 2.31 mmol).

Appearance: Off-white powder.

^{1}H NMR (300 MHz, $CDCl_3$): δ [ppm] = 7.95 – 7.86 (m, 2H), 7.69 (s, 1H), 7.64 – 7.57 (m, 2H).

Literature: S. Kuwano, T. Masuda, K. Yamaguchi, T. Arai, *Heterocycles* **2017**, *95*, 232–242.

(2-Fluorobenzylidene)malononitrile (**2r**)



By GP1 starting from 2-fluorobenzaldehyde (372 mg) with a reaction time of 20 min.

Yield: 83% (430 mg, 2.50 mmol).

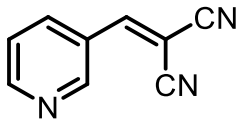
Appearance: Colorless powder.

^{1}H NMR (600 MHz, $CDCl_3$): δ [ppm] = 8.31 – 8.26 (m, 1H), 8.10 (s, 1H), 7.68 – 7.61 (m, 1H), 7.37 – 7.31 (m, 1H), 7.26 – 7.20 (m, 1H);

^{19}F NMR (565 MHz, $CDCl_3$): δ [ppm] = −110.9 – −111.0 (m).

Literature: M. D. Harvey, T. D. Crawford, G. T. Yee, *Inorg. Chem.* **2008**, *47*, 5649–5655.

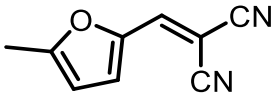
(Pyridin-3-ylmethylidene)malononitrile (**2s**)



The synthesis and characterization of the batch used in this work is described in:

L. Cardinale, M. O. Konev, A. Jacobi von Wangelin, *Chem. Eur. J.* **2020**, *26*, 8239–8243.

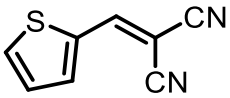
(5-Methylfuran-2-ylmethylidene)malononitrile (**2t**)



The synthesis and characterization of the batch used in this work is described in:

L. Cardinale, M. O. Konev, A. Jacobi von Wangelin, *Chem. Eur. J.* **2020**, *26*, 8239–8243.

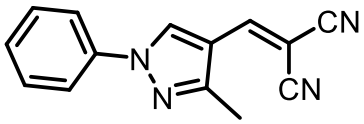
(Thiophen-2-ylmethylidene)malononitrile (**2u**)



The synthesis and characterization of the batch used in this work is described in:

L. Cardinale, M. O. Konev, A. Jacobi von Wangelin, *Chem. Eur. J.* **2020**, *26*, 8239–8243.

((3-Methyl-1-phenyl-1*H*-pyrazol-4-yl)methylene)malononitrile (**2v**)



By GP1 starting from 3-methyl-1-phenyl-1*H*-pyrazole-4-carboxaldehyde (559 mg) with a reaction time of 1 h.

Yield: 83% (583 mg, 2.49 mmol).

Appearance: Yellow powder.

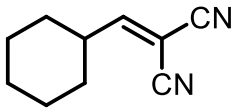
^{1}H NMR (300 MHz, $CDCl_3$): δ [ppm] = 8.89 (s, 1H), 7.76 – 7.65 (m, 3H), 7.54 – 7.45 (m, 2H), 7.44 – 7.36 (m, 1H), 2.46 (s, 3H).

^{13}C{^{1}H} NMR (151 MHz, $CDCl_3$): δ [ppm] = 153.6, 150.1, 138.6, 129.9, 129.1, 128.5, 120.0, 116.0, 114.1, 114.1, 77.5, 11.8.

HRMS (ESI): *m/z* calcd. for $C_{14}H_{12}N_4^+$: 235.0978, found: 235.0983.

m.p. = 192–193 °C.

Cyclohexylmethylidenemalononitrile (**2w**)



A solution of cyclohexylcarboxaldehyde (337 mg, 3.00 mmol, 1.0 equiv.), malononitrile (297 mg, 4.5 mmol, 1.5 equiv.) and a spatula tip of DABCO in ethanol (3.0 mL) was stirred for 16 hours at room temperature over molecular sieves (3 Å). The orange mixture was decanted from the molecular sieves, diluted with ethyl acetate (30 mL), and washed with water (3× 10 mL). The combined aqueous phases were extracted with ethyl acetate (3× 10 mL). The combined organic phases were washed with brine (10 mL), dried over Na_2SO_4, filtered, and concentrated. The dark red residue was purified by column chromatography (SiO_2, Pentane/EtOAc 15:1).

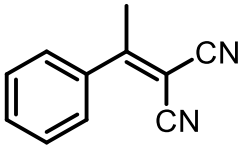
Yield: 59% (284 mg, 1.77 mmol).

Appearance: Pale-yellow oil.

^{1}H NMR (600 MHz, $CDCl_3$): δ [ppm] = 7.15 (d, J = 10.5 Hz, 1H), 2.84 – 2.62 (m, 1H), 1.87 – 1.69 (m, 5H), 1.45 – 1.14 (m, 5H).

Literature: L. Cardinale, M. O. Konev, A. Jacobi von Wangelin, *Chem. Eur. J.* **2020**, *26*, 8239–8243.

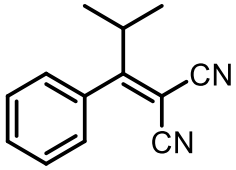
(1-Phenylethylidene)malononitrile (**2x**)



The synthesis and characterization of the batch used in this work is described in:

L. Cardinale, M. O. Konev, A. Jacobi von Wangelin, *Chem. Eur. J.* **2020**, *26*, 8239–8243.

(2-Methyl-1-phenylpropylidene)malononitrile (**2y**)



Isobutyrophenone (445 mg, 3.00 mmol, 1.0 equiv.) and malononitrile (396 mg, 6.00 mmol, 2.0 equiv.) were dissolved in dry dichloromethane (15 mL) and cooled to 0 °C using an ice bath. Titanium tetrachloride (295 µL, 6.00 mmol, 2.0 equiv.) was slowly added dropwise at this temperature. Dry pyridine (0.73.0 mL, 9.0 mmol, 3.0 equiv.) was then added at 0 °C over

30 min using a syringe pump. After complete addition, the mixture was slowly warmed to room temperature and stirred for 16 h. Aq. HCl (0.5 M, 20 mL) was added slowly and the organic phase was separated. The aqueous phase was extracted with CH_2Cl_2 (2× 20 mL) and the combined org. phases were washed with sat. aq. $NaHCO_3$ (20 mL), water (20 mL), and brine (20 mL), dried over Na_2SO_4, filtered, and concentrated. The residual dark orange-brown oil was purified by column chromatography (SiO_2, Pentane/EtOAc 12:1).

Yield: 33% (192 mg, 978 µmol).

Appearance: Colorless solid.

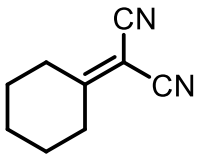
^{1}H NMR (300 MHz, $CDCl_3$): δ [ppm] = 7.54 – 7.43 (m, 3H), 7.24 – 7.14 (m, 2H), 3.46 (hept, *J* = 7.9 Hz, 1H), 1.19 (d, *J* = 7.9 Hz, 6H).

^{13}C{^{1}H} NMR (75.5 MHz, $CDCl_3$): δ [ppm] = 186.9, 135.9, 134.1, 130.6, 129.0, 127.0, 112.1, 111.9, 86.9, 36.4, 20.7.

HRMS (ESI): *m/z* calcd. for $C_{13}H_{13}N_2^+$: 197.1073, found: 197.1083.

m.p. = 57–58 °C.

Cyclohexylidenemalononitrile (**2z**)



To a neat mixture of cyclohexanone (9.82 g, 100 mmol, 1.0 equiv.) and malononitrile (6.61 g, 100 mmol, 1.0 equiv.) was added DABCO (112 mg, 1.00 mmol, 1 mol%). An immediate color change to yellow and then orange was observed within a minute, followed by a significant exothermic reaction and condensation of water on the flask wall. The mixture was stirred for 3 h, then diluted with diethyl ether (200 mL) and washed with brine (100 mL), dried over Na_2SO_4, filtered, and concentrated. The yellow-greenish residue was fractionally vacuum-distilled at 0.16 mbar with an oil bath temperature of 130–150 °C. The forerun boiling <89 °C/0.16 mbar was discarded and the product was collected at 89–93 °C/0.16 mbar.

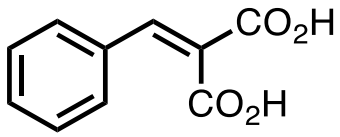
Yield: 86% (12.50 g, 85.5 mmol).

Appearance: Pale-straw liquid.

^{1}H NMR (300 MHz, $CDCl_3$): δ [ppm] = 2.70 – 2.60 (m, 4H), 1.86 – 1.74 (m, 4H), 1.73 – 1.63 (m, 2H).

Literature: A. A. Sysoeva, M. V. Il'in, D. S. Bolotin, *ChemCatChem* **2024**, *16*, e202301668.

Benzylidenemalonic acid (**3a**)



Freshly distilled benzaldehyde (10.61 g, 100 mmol, 1.0 equiv.) and malonic acid (10.41 g, 100 mmol, 1.0 equiv.) were stirred at 100 °C in a slight stream of nitrogen. After 45 min the mixture had become a yellow semi-solid mass. Heating was continued for 4 h in total with occasional manual mixing using a spatula. The yellow solid was recrystallized from $CHCl_3$/MeCN and the mother liquor was stored at −25 °C for three days.

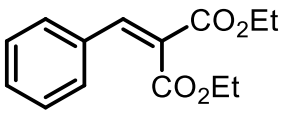
Yield: 44% (8.45 g, 44.0 mmol).

Appearance: Colorless crystals.

^{1}H NMR (600 MHz, DMSO-d_6): δ [ppm] = 13.15 (br. s, 2H), 7.64 – 7.51 (m, 3H), 7.51 – 7.39 (m, 3H).

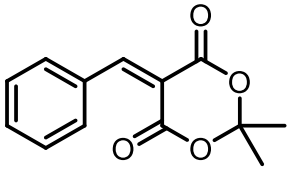
Literature: Y. Ogiwara, K. Takahashi, T. Kitazawa, N. Sakai, *J. Org. Chem.* **2015**, *80*, 3101–3110.

Diethyl benzylidenemalonate (**3b**)



Purchased from TCI Chemicals and used as received.

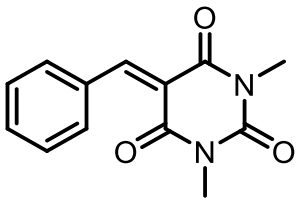
5-Benzylidene-2,2-dimethyl-1,3-dioxane-4,6-dione (**3c**)



The synthesis and characterization of the batch used in this work is described in:

L. Cardinale, M. O. Konev, A. Jacobi von Wangelin, *Chem. Eur. J.* **2020**, *26*, 8239–8243.

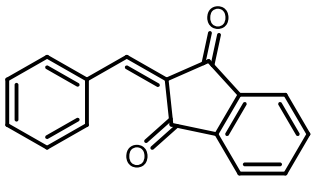
N,*N'*-Dimethyl-4-benzylidenebarbituric acid (**3d**)



The synthesis and characterization of the batch used in this work is described in:

L. Cardinale, M. O. Konev, A. Jacobi von Wangelin, *Chem. Eur. J.* **2020**, *26*, 8239–8243.

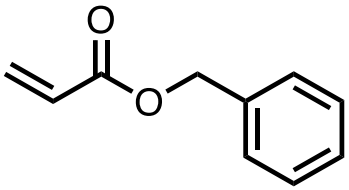
2-Benzylideneindane-1,3-dione (**3e**)



The synthesis and characterization of the batch used in this work is described in:

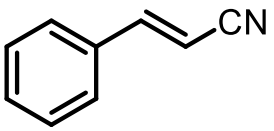
L. Cardinale, M. O. Konev, A. Jacobi von Wangelin, *Chem. Eur. J.* **2020**, *26*, 8239–8243.

Benzyl acrylate (**3f**)



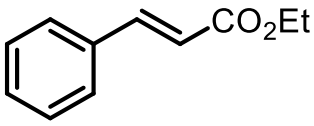
Purchased from TCI Chemicals and vacuum-distilled before use.

Cinnamonitrile (**3g**)



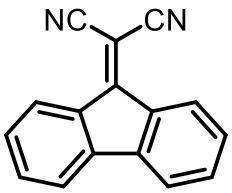
Purchased from J&K Scientific and used as received.

Ethyl cinnamate (**3h**)



Purchased from TCI Chemicals and used as received.

(9*H*-Fluoren-9-ylidene)malononitrile (**3i**)



By GP1 starting from fluorenone (541 mg) with a reaction time of 1 h. Purified by recrystallization from ethanol/chloroform.

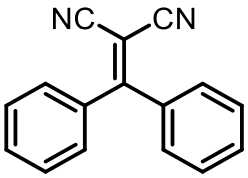
Yield: 58% (400 mg, 1.75 mmol).

Appearance: Vibrantly orange-red needles.

^{1}H NMR (600 MHz, $CDCl_3$): δ [ppm] = 8.39 – 8.33 (m, 2H), 7.57 – 7.52 (m, 2H), 7.52 – 7.46 (m, 2H), 7.35 – 7.28 (m, 2H).

Literature: B. Kubendiran, G. Pramanik, G. K. Kole, *J. Mol. Struct.* **2023**, *1294*, 136397.

(Diphenylmethylidene)malononitrile (**3j**)



To stirred solid malononitrile (3.30 g, 50.0 mmol, 1.0 equiv.) under nitrogen atmosphere was added benzophenone imine (8.40 mL, 9.06 g, 50.0 mmol, 1.0 equiv.) in one portion. Immediately, a red coloration and vigorous evolution of gaseous NH_3 was observed, and the mixture turned into a semi-solid paste within seconds. The mixture was stirred neat for 5 minutes before dry THF (30 mL) was added and stirring was continued at room temperature for 1 h. The mixture was concentrated and the residual solid was recrystallized from ethanol/water.

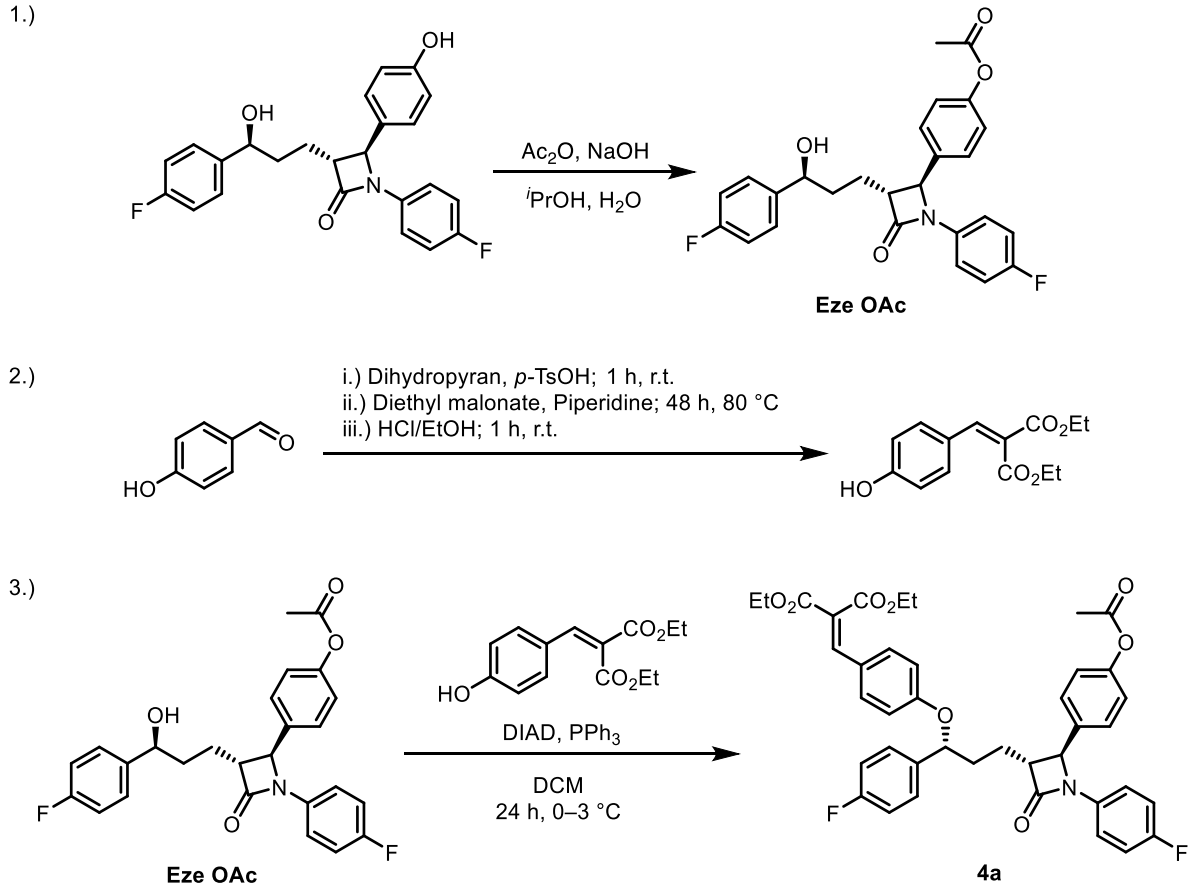
Yield: 83% (9.50 g, 41.3 mmol).

Appearance: Large colorless flat needles.

^{1}H NMR (300 MHz, $CDCl_3$): δ [ppm] = 7.62 – 7.55 (m, 2H), 7.53 – 7.41 (m, 8H).

Literature: K. Jain, S. Chaudhuri, K. Pal, K. Das, *New J. Chem.* **2019**, *43*, 1299–1304.

Diethyl 2-(4-((*R*)-3-((2*S*,3*R*)-2-(4-acetoxyphenyl)-1-(4-fluorophenyl)-4-oxoazetidin-3-yl)-1-(4-fluorophenyl)propoxy)benzylidene)malonate (**4a**)



1.) *4-((2S,3R)-1-(4-Fluorophenyl)-3-((S)-3-(4-fluorophenyl)-3-hydroxypropyl)-4-oxoazetidin-2-yl)-phenyl acetate (**Eze OAc**)*. To a solution of Ezetimibe (819 mg, 2.00 mmol, 1.0 equiv.) in isopropanol (10 mL), was added a solution of NaOH (176 mg, 4.40 mmol, 2.2 equiv.) in water (2 mL). Acetic anhydride (454 µL, 4.80 mmol, 2.4 equiv.) was then added dropwise. The mixture was stirred at room temperature. After 2 h, the mixture had completely solidified. At this point, it was diluted with sat. aq. $NaHCO_3$ (50 mL) and the colorless solid was obtained by filtration and thorough washing with water (4×).

Yield: 86% (781 mg, 1.73 mmol).

Appearance: Colorless solid.

^{1}H NMR (600 MHz, $CDCl_3$): δ [ppm] = 7.34 – 7.31 (m, 2H), 7.31 – 7.26 (m, 2H), 7.24 – 7.19 (m, 2H), 7.12 – 7.08 (m, 2H), 7.04 – 6.99 (m, 2H), 6.96 – 6.90 (m, 2H), 4.73 – 4.68 (m, 1H), 4.62 (d, *J* = 2.4 Hz), 3.08 (td, *J* = 7.5, 2.5 Hz, 1H), 2.30 (s, 3H), 2.27 (d, *J* = 3.7 Hz, 1H), 2.03 – 1.85 (m, 4H).

Literature: L. Kværnø, M. Werdern, H. Hauser, E. M. Carreira, *J. Med. Chem.* **2005**, *48*, 6035–6053.

2.) *Diethyl (4-hydroxybenzylidene)malonate*. To a suspension of 4-hydroxybenzaldehyde (1.22 g, 10.0 mmol, 1.0 equiv.) and dihydropyran (1.68 g, 20.0 mmol, 2.0 equiv.) in benzene (100 mL) was added *para*-toluenesulfonic acid monohydrate (95.1 mg, 500 µmol, 5.0 mol%) and the mixture was stirred at room temperature for 1 h. To this deep purple solution was added piperidine (170 mg, 2.00 mmol, 20 mol%) in one portion, resulting in an immediate pale-yellow color. After the addition of diethyl malonate (1.60 g, 10.0 mmol, 1.0 equiv.) the mixture was refluxed for 48 h in a Soxhlet apparatus containing 3 Å molecular sieves in the thimble. To this mixture was added at room temperature a ~0.5 M solution of HCl in EtOH (prepared by carefully dissolving 10 mmol of acetyl chloride in 20 mL of ethanol) and the mixture was stirred for 1 h. The near-black mixture was washed with water (2× 50 mL) and brine (50 mL), dried over Na_2SO_4, filtered, and concentrated. The residual dark brown oil was purified by column chromatography (SiO_2, Pentane/EtOAc 2:1). The product is contaminated with about ~8% of difficult to separate 4-hydroxybenzaldehyde and was used in subsequent reactions without further purification.

Yield: 73% adj. for purity (2.00 g total/1.93 g adj. for purity, 7.30 mmol).

Appearance: Pale-yellow solid.

^{1}H NMR (300 MHz, DMSO-d_6): δ [ppm] = 10.25 (s, 1H), 7.58 (s, 1H), 7.41 – 7.30 (m, 2H), 6.86 – 6.76 (m, 2H), 4.29 (q, J = 7.2 Hz, 2H), 4.21 (q, J = 7.1 Hz, 2H), 1.23 (t, J = 7.1 Hz, 6H).

Literature: A. V. Narsaiah, K. Nagaiah, *Synth. Commun.* **2003**, *33*, 3825–3832.

3.) *Diethyl 2-(4-((R)-3-((2S,3R)-2-(4-acetoxyphenyl)-1-(4-fluorophenyl)-4-oxoazetidin-3-yl)-1-(4-fluorophenyl)propoxy)benzylidene)malonate (**4a**)*. A solution of **Eze OAc** (677 mg, 1.50 mmol, 1.0 equiv.), diethyl (4-hydroxybenzylidene)malonate (451 mg, 1.95 mmol, 1.3 equiv.), and triphenylphosphine (551 mg, 2.10 mmol, 1.4 equiv.) in dichloromethane (15 mL) was cooled to 0 °C using an ice bath. Diisopropyl azodicarboxylate (0.41 mL, 210 µmol, 1.4 equiv.) was added dropwise at this temperature. After complete addition, the mixture was stirred at 0 °C for 2 h, then stored in the fridge at 3 °C for 22 h. The mixture was washed with water (10 mL), and the aq. phase was extracted with CH_2Cl_2 (3× 10 mL). The combined organic phases were washed with brine (10 mL), dried over Na_2SO_4, filtered, and concentrated. The residual yellow oil was purified by automated flash chromatography (C_{18}-SiO_2, 20% MeCN in H_2O → 100% MeCN) and lyophilized.

Yield: 58% (605 mg, 868 µmol), *dr* 25:1.

Appearance: Colorless fluffy solid (lyophilisate).

^{1}H NMR (600 MHz, $CDCl_3$): δ [ppm] = 7.52 (s, 1H), 7.26 – 7.18 (m, 6H), 7.16 – 7.12 (m, 2H), 7.04 – 7.01 (m, 2H), 6.97 – 6.91 (m, 2H), 6.89 – 6.83 (m, 2H), 6.71 – 6.64 (m, 2H), 5.10 (dd, J

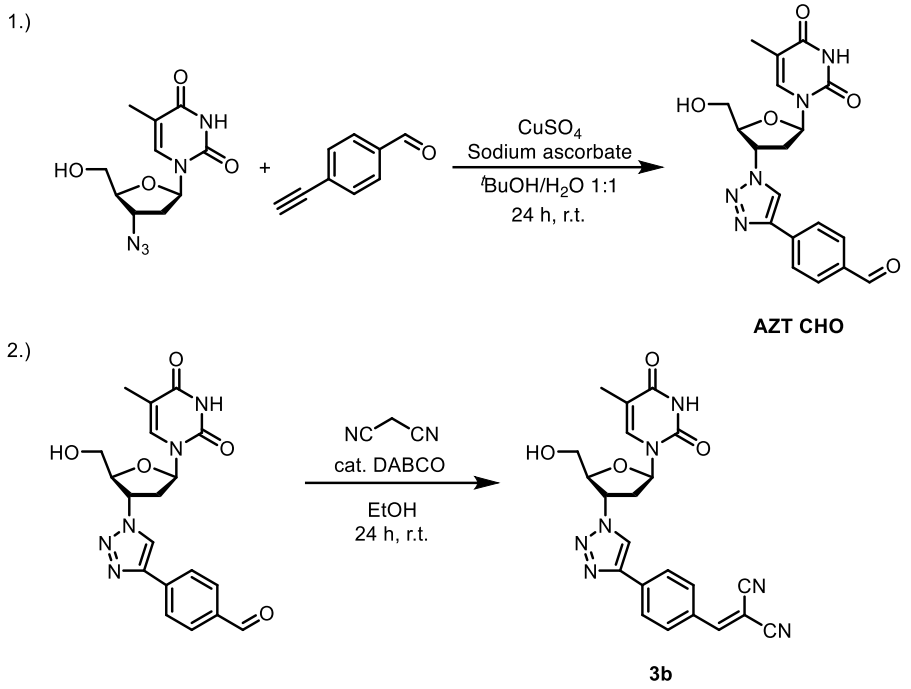
= 7.6, 4.6 Hz, 1H), 4.53 (d, *J* = 2.4 Hz, 1H), 4.24 (q, *J* = 7.2 Hz, 2H), 4.19 (q, *J* = 7.2 Hz, 2H), 2.23 (s, 3H), 2.14 (dddd, *J* = 12.8, 9.9, 7.4, 4.6 Hz, 1H), 2.09 – 2.00 (m, 1H), 1.97 – 1.83 (m, 2H), 1.23 (t, *J* = 7.1 Hz, 3H), 1.19 (t, *J* = 7.2 Hz, 3H).

^{13}C{^{1}H} NMR (151 MHz, $CDCl_3$): *δ* [ppm] = 169.4, 167.2, 167.0, 164.5, 162.4 (d, *J* = 246.4 Hz), 159.8, 159.2 (d, *J* = 243.0 Hz), 151.0, 141.7, 136.4 (d, *J* = 2.8 Hz), 135.1, 133.8 (d, *J* = 2.8 Hz), 131.6, 127.6 (d, *J* = 8.5 Hz), 127.1, 125.8, 123.9, 122.7, 118.5 (d, *J* = 7.9 Hz), 116.2, 116.1 (d, *J* = 14.1 Hz), 115.9 (d, *J* = 13.6 Hz), 79.0, 61.7, 61.6, 60.9, 60.4, 35.9, 24.9, 21.2, 14.3, 14.0.

^{19}F NMR (565 MHz, $CDCl_3$): *δ* [ppm] = −113.96 – −114.05 (m), −117.74 – −117.83 (m).

HRMS (ESI): *m/z* calcd. for $C_{40}H_{37}F_2NNaO_8^+$: 720.2379, found: 720.2391.

3'-(4-(4-(Dicyanovinyl)phenyl)-(1,2,3-triazol-1-yl))-3'-deoxythymidine (**4b**)



1.) *3'-(4-(4-Formylphenyl)-(1,2,3-triazol-1-yl))-3'-deoxythymidine (**AZT CHO**)*. Zidovudine (267 mg, 1.00 µmol, 1.0 equiv.), 4-ethynylbenzaldehyde (195 mg, 1.50 mmol, 1.5 equiv.), and sodium ascorbate (59.4 mg, 300 µmol, 0.3 equiv.) were suspended in a mixture of *tert*-butanol (5.0 mL) and water (5.0 mL). The mixture was degassed by N_2 sparging for 10 minutes. Copper(II) sulfate (16.0 mg, 100 µmol, 10 mol%) was added and the mixture was stirred for 24 h. The resulting orange suspension was partitioned between water (10 mL) and EtOAc (30 mL). The organic phase was removed and the aq. phase was extracted with EtOAc (3× 30 mL). The combined organic phases were dried over Na_2SO_4, filtered, and concentrated. The residue was purified by column chromatography (SiO_2, CH_2Cl_2/MeOH 20/1 to 14/1).

Yield: 71% (281 mg, 707 µmol).

Appearance: Colorless solid.

^{1}H NMR (600 MHz, DMSO-d_6): δ [ppm] = 11.37 (s, 1H), 10.02 (s, 1H), 8.99 (s, 1H), 8.14 – 8.06 (m, 2H), 8.04 – 7.96 (m, 2H), 7.84 (q, *J* = 1.0 Hz, 1H), 6.46 (t, *J* = 6.7 Hz, 1H), 5.44 (dt, *J* = 8.7, 5.3 Hz, 1H), 5.31 (t, *J* = 5.3 Hz, 1H), 4.30 (dt, *J* = 5.3, 3.6 Hz, 1H), 3.74 (ddd, *J* = 12.0, 5.3, 3.5 Hz, 1H), 3.68 (ddd, *J* = 12.0, 5.3, 3.8 Hz, 1H), 2.82 (ddd, *J* = 14.1, 6.7, 5.2 Hz, 1H), 2.72 (ddd, *J* = 14.1, 8.8, 6.7 Hz, 1H), 1.82 (d, *J* = 1.0 Hz, 6H).

^{13}C-NMR (151 MHz, DMSO-d_6): δ [ppm] = 192.5, 163.7, 150.4, 145.5, 136.2, 136.2, 135.5, 130.3, 125.6, 122.6, 109.6, 84.4, 83.9, 60.8, 59.6, 37.1, 12.2.

HRMS (ESI): *m/z* calcd. for $C_{19}H_{20}N_5O_5^+$: 398.1459, found: 389.1471.

m.p. = >250 °C.

2.) *3'-(4-(4-(Dicyanovinyl)phenyl)-(1,2,3-triazol-1-yl))-3'-deoxythymidine (**4b**)*. To a stirred suspension of **AZT CHO** (59.6 mg, 150 µmol, 1.0 equiv.) and malononitrile (9.91 mg, 150 µmol, 1.0 equiv.) in ethanol (0.50 mL) was added a spatula tip of DABCO. The mixture was stirred for 16 h at room temperature and the solvent was removed. The residue was purified by automated flash chromatography (C_{18}-SiO_2, 10% MeCN in H_2O → 100% MeCN) and lyophilized.

Yield: 85% (57.1 mg, 128 µmol).

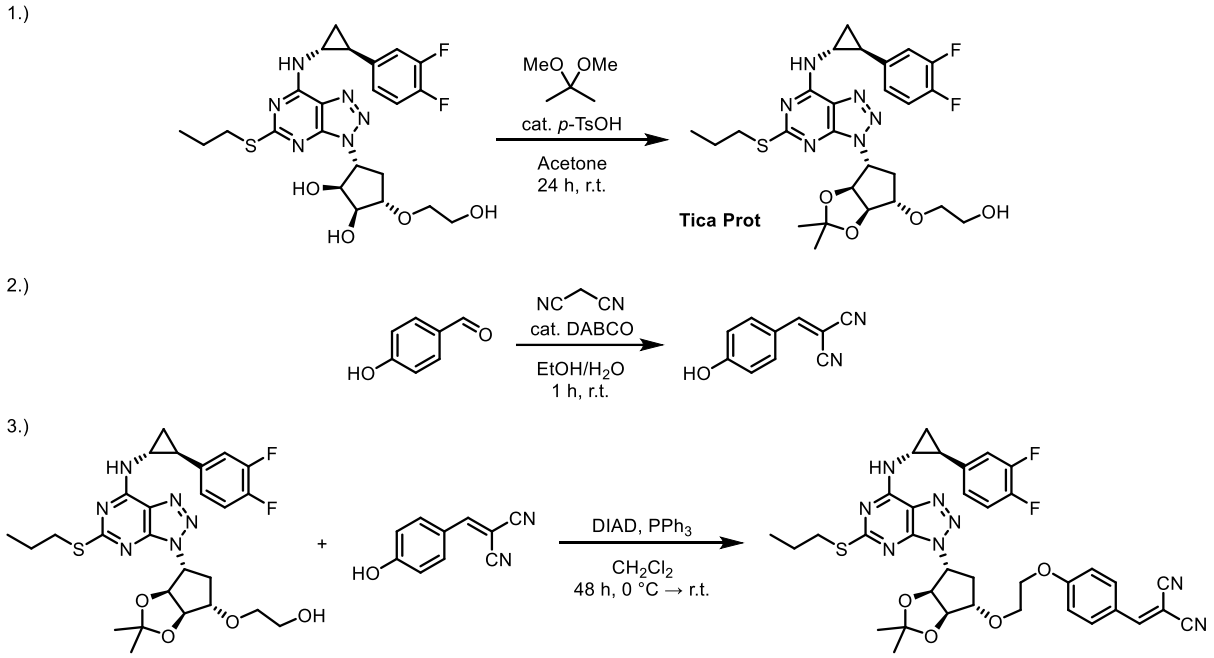
Appearance: Pale-yellow fluffy solid (lyophilisate).

^{1}H NMR (600 MHz, DMSO-d_6): δ [ppm] = 11.38 (s, 1H), 8.99 (s, 1H), 8.55 (s, 1H), 8.14 – 8.08 (m, 2H), 8.09 – 8.05 (m, 2H), 7.85 (q, *J* = 1.6 Hz, 1H), 6.47 (t, *J* = 6.7 Hz, 1H), 5.45 (dt, *J* = 8.8, 5.3 Hz, 1H), 5.32 (t, *J* = 5.3 Hz, 1H), 4.31 (dt, *J* = 5.5, 3.7 Hz, 1H), 3.78 – 3.72 (m, 1H), 3.72 – 3.65 (m, 1H), 2.82 (ddd, *J* = 14.0, 6.9, 5.2 Hz, 1H), 2.72 (ddd, *J* = 13.9, 8.7, 6.5 Hz, 1H), 1.83 (d, *J* = 1.3 Hz, 3H).

^{13}C-NMR (151 MHz, DMSO-d_6): δ [ppm] = 163.7, 160.6, 150.5, 145.2, 136.2, 136.0, 131.5, 130.7, 125.8, 123.0, 114.4, 113.4, 109.7, 84.4, 83.9, 80.8, 60.8, 59.7, 40.1, 37.1, 12.3.

HRMS (ESI): *m/z* calcd. for $C_{22}H_{18}N_7O_4^-$: 444.1426, found: 444.1427.

(4-(2-(((3a*R*,4*S*,6*R*,6a*S*)-6-(7-(((1*R*,2*S*)-2-(3,4-Difluorophenyl)cyclopropyl)amino)-5-(propylthio)-3*H*-[1,2,3]triazolo[4,5-*d*]pyrimidin-3-yl)-2,2-dimethyltetrahydro-4*H*-cyclopenta[*d*][1,3]dioxol-4-yl)oxy)ethoxy)benzylidene)malononitrile (**4c**)



1.) *2-(((3aR,4S,6R,6aS)-6-(7-(((1R,2S)-2-(3,4-difluorophenyl)cyclopropyl)amino)-5-(propylthio)-3H-[1,2,3]triazolo[4,5-d]pyrimidin-3-yl)-2,2-dimethyltetrahydro-4H-cyclopenta[d][1,3]dioxol-4-yl)oxy)ethan-1-ol (**Tica Prot**).* Ticagrelor (1.05 g, 2.00 mmol, 1.0 equiv.) was dissolved in acetone (10 mL) and 2,2-dimethoxypropane (0.49 mL, 4.00 mmol, 2.0 equiv.) and *para*-toluenesulfonic acid monohydrate (38.0 mg, 200 µmol, 10 mol%) were added. The mixture was stirred at room temperature for 24 h, then partitioned between dilute aq. $NaHCO_3$ (50 mL) and ethyl acetate (50 mL). The aqueous phase was extracted with EtOAc (3× 25 mL) and the combined organic phases were washed with brine (50 mL), dried over Na_2SO_4, filtered, and concentrated. The residue was purified by column chromatography (SiO_2, CH_2Cl_2/MeOH 50/1 to 33/1).

Yield: 96% (1.08 g, 1.92 mmol).

Appearance: Colorless foam.

The product is a mixture of two rotamers in DMSO-d_6 solution (Ratio 80%/20%), as is known for Ticagrelor and its derivatives, including this compound.

^{1}H NMR (600 MHz, DMSO-d_6): δ [ppm] = 9.38 (d, *J* = 4.2 Hz, 0.8H), 8.99 (d, *J* = 4.5 Hz, 0.2), 7.37 – 7.27 (m, 1.8H), 7.27 – 7.20 (m, 0.2H), 7.10 – 7.04 (m, 0.8H), 7.03 – 6.99 (m, 0.2H), 5.21 (dd, *J* = 7.3, 4.8 Hz, 0.8H), 5.18 – 5.15 (m, 0.2H), 5.01 (ddd, *J* = 9.7, 6.9, 4.7 Hz, 1H), 4.67 (dd, *J* = 7.4, 3.3 Hz, 0.8H), 4.64 (dd, *J* = 7.2, 2.8 Hz, 0.2H), 4.56 (t, *J* = 5.4 Hz, 1H), 4.00 (ddd, *J* = 9.4, 6.1, 3.2 Hz, 1H), 3.76 – 3.70 (m, 0.2H), 3.51 – 3.47 (m, 1H), 3.45 – 3.39 (m, 3H), 3.17 – 3.13 (m, 0.8H), 3.12 – 3.08 (m, 0.2H), 3.08 – 3.02 (m, 0.2H), 2.96 – 2.84 (m, 1.6H), 2.69 – 2.62 (m, 1H), 2.55 – 2.51 (m, 1H), 2.27–2.21 (m, 0.2H), 2.13 (ddd, *J* = 9.5, 6.3. 3.3 Hz, 0.8H), 1.70 (h, *J* = 7.0 Hz, 0.4H), 1.56 – 1.50 (m, 2.6H), 1.48 (s, 3H), 1.37 (dt, *J* = 7.9, 5.9 Hz, 1H), 1.26 (s, 2.4H), 1.25 (s, 0.6H), 0.99 (t, *J* = 7.3 Hz, 0.6H), 0.84 (t, *J* = 7.4 Hz, 2.4H).

Literature: E. Goffin, N. Jacques, L. Musumeci, A. Nchimi, C. Oury, P. Lancellotti, B. Pirotte, *Eur. J. Med. Chem.* **2020**, *208*, 112767.

2.) *(4-Hydroxybenzylidene)malononitrile*. To a solution of 4-hydroxybenzaldehyde (366 mg, 3.00 mmol, 1.0 equiv.) and malononitrile (198 mg, 3.00 mmol, 1.0 equiv.) in ethanol (3.0 mL) was added a spatula tip of DABCO. The mixture was stirred for 20 min at room temperature. The vibrantly yellow mixture was diluted with water (20 mL), upon which a yellow solid precipitated after a few seconds. The suspension was stirred for an additional hour and then stored in the fridge at 3 °C for 3 h to induce further precipitation. The mixture was filtered and the solid was washed with water (3×).

Yield: 71% (361 mg, 2.12 mmol).

Appearance: Pale-yellow solid.

^{1}H NMR (300 MHz, DMSO-d_6): δ [ppm] = 11.06 (br. s, 1H), 8.30 (s, 1H), 7.93 – 7.84 (m, 2H), 7.02 – 6.92 (m, 2H).

Literature: L. Jedinák, V. Kryštof, P. Cankař, *Heterocycles* **2011**, *83*, 371–383.

3.) *(4-(2-(((3aR,4S,6R,6aS)-6-(7-(((1R,2S)-2-(3,4-Difluorophenyl)cyclopropyl)amino)-5-(propylthio)-3H-[1,2,3]triazolo[4,5-d]pyrimidin-3-yl)-2,2-dimethyltetrahydro-4H-cyclopenta[d][1,3]dioxol-4-yl)oxy)ethoxy)benzylidene)malononitrile (**4c**).* A suspension of **Tica Prot** (281 mg, 500 µmol, 1.0 equiv.), (4-hydroxybenzylidene)malononitrile (204 mg, 1.20 mmol, 2.4 equiv.), and triphenylphosphine (184 mg, 700 µmol, 1.4 equiv.) in dichloromethane (5.0 mL) was cooled to 0 °C using an ice bath. Diisopropyl azodicarboxylate (138 µL, 700 µmol, 1.40 equiv.) was added dropwise at this temperature. After complete addition, the mixture was stirred at 0 °C for 4 h, then stored in the fridge at 3 °C for 20 h, then warmed to room temperature and stirred for further 24 h. The mixture was washed with water (5.0 mL) and the aq. phase was extracted with CH_2Cl_2 (3× 5.0 mL). The combined organic phases were dried over Na_2SO_4,

filtered, and concentrated. The residue was purified by automated flash chromatography (C_{18}-SiO_2, 20% MeCN in H_2O → 100% MeCN) and lyophilized.

Yield: 56% (200 mg, 280 µmol).

Appearance: Pale-yellow fluffy solid (lyophilisate).

The product is a mixture of two rotamers in DMSO-d_6 solution (Ratio 80%/20%), as is known for Ticagrelor and its derivatives.

^{1}H NMR (600 MHz, DMSO-d_6): δ [ppm] = 9.36 (d, *J* = 4.1 Hz, 0.8H), 8.96 (d, *J* = 5.5 Hz, 0.2H), 8.38 (s, 1H), 7.98 – 7.92 (m, 2H), 7.36 – 7.25 (m, 1.8H), 7.24 – 7.18 (m, 0.2H), 7.17 – 7.11 (m, 2H), 7.08 – 7.03 (m, 0.8H), 7.01 – 6.97 (m, 0.2H), 5.28 (dd, *J* = 7.2, 4.4 Hz, 0.8H), 5.23 (dd, *J* = 6.8, 4.4 Hz, 0.2H), 5.07 – 4.99 (m, 1H), 4.71 (dd, *J* = 7.2, 3.1 Hz, 0.8H), 4.68 (dd, *J* = 7.5, 3.1 Hz, 0.2H), 4.20 – 4.12 (m, 2H), 4.11 – 4.05 (m, 1H), 3.85 – 3.79 (m, 1H), 3.77 – 3.71 (m, 1H), 3.72 – 3.67 (m, 0.2H), 3.15 – 3.06 (m, 1H), 3.03 (dt, *J* = 13.7, 7.1 Hz, 0.2H), 2.96 – 2.83 (m, 1.6H), 2.71 – 2.62 (m, 1H), 2.63 – 2.52 (m, 1H), 2.25 – 2.18 (m, 0.2H), 2.09 (ddd, *J* = 9.7, 6.4, 3.3 Hz, 0.8H), 1.73 – 1.64 (m, 0.4H), 1.57 – 1.49 (m, 2.4H), 1.51 – 1.46 (m, 3H), 1.42 (dt, *J* = 9.5, 5.5 Hz, 0.2H), 1.39 – 1.33 (m, 1H), 1.26 (s, 2.4H), 1.25 (s, 0.6H), 0.97 (t, *J* = 7.3 Hz, 0.6H), 0.82 (t, *J* = 7.3 Hz, 2.4H).

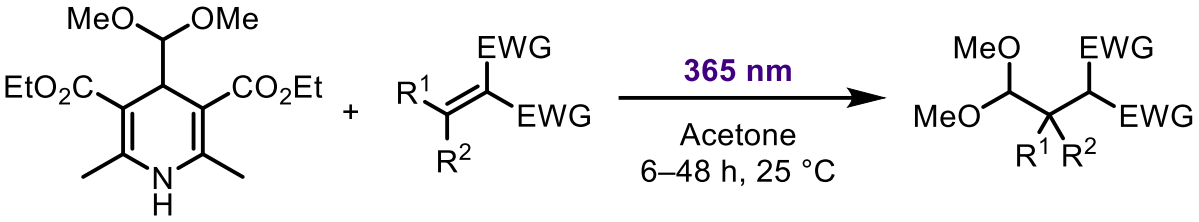
^{19}F NMR (565 MHz, DMSO-d_6): δ [ppm] = −139.25 – −139.43 (m, 1F), −142.99) – −143.11 (m, 0.8F), −143.11 – −143.20 (m, 0.2F).

^{13}C-NMR (151 MHz, DMSO-d_6, only major signals): δ [ppm] = 169.5, 163.6, 160.4, 154.0, 149.5 (dd, *J* = 238.8, 12.7 Hz), 149.1, 147.9 (dd, *J* = 237.4, 12.4 Hz) 139.2 (dd, *J* = 6.2, 3.4 Hz), 133.4, 124.2, 123.2, 122.9 (dd, *J* = 5.9, 3.1 Hz), 117.1 (d, *J* = 17.0 Hz), 115.6, 115.0 (d, *J* = 17.0 Hz), 114.9, 114.0, 112.4, 83.7, 82.5, 81.9, 76.9, 67.7, 67.1, 61.7, 35.2, 34.0, 32.5, 26.8, 24.7, 24.0, 22.4, 15.0, 13.1.

HRMS (ESI): *m/z* calcd. for $C_{36}H_{37}F_2N_8O_4S^+$: 715.2621, found: 715.2610.

Synthesis of Substituted Acetaldehyde Dimethyl Acetals

General procedure for the light-driven synthesis of substituted acetaldehyde dimethyl acetals (GP2)



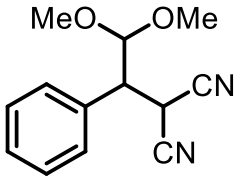
The corresponding olefin (100 µmol, 1.0 equiv.) and Hantzsch ester **1** (39.2 mg, 120 µmol, 1.2 equiv.) were weighed into a 4 mL glass vial, equipped with a stir bar and closed with a septum screw cap which was punctured by a cannula. The vial was transferred into an argon-filled glove box and acetone[a] (1.0 mL, 0.1 M) was added. The vial was closed, removed from the glove box, and placed inside the photoreactor (*EvoluChem PhotoRedOx Box TC*) filled with silicone oil that was kept at 25.0 °C. The mixture was vigorously stirred under irradiation (**365 nm**, *EvoluChem LED 365DX*) for the corresponding time.

Isolation of the product: The mixture after complete irradiation was directly transferred to a round-bottom flask and Celite® (~100 mg) was added. The solvent was removed and the crude product adsorbed on Celite® was purified by column chromatography on silica or neutral alumina using an appropriate solvent mixture as determined by TLC (generally Pentane/Ethyl acetate).

NMR yield determination: An exactly weighed amount of 1,3,5-trimethoxybenzene (>99 % purity, 1.50–5.00 mg) was added to the reaction mixture after complete irradiation and the vial was shaken well. The mixture was transferred to a round-bottom flask, the solvent was removed, the residue was dissolved in $CDCl_3$, and a ^1H NMR spectrum was recorded. By integration of a suitable product signal in comparison with the signal of the internal standard, the amount of substance and thus the yield was determined.

[a] Acetone (technical grade) was stirred over activated 3 Å molecular sieves for a maximum of **16 hours**, distilled off, and degassed using the Freeze-Pump-Thaw technique under nitrogen (3–4 cycles). The solvent was stored in an argon-filled glove box.

2-(Dicyanomethyl)-2-phenylacetaldehyde dimethyl acetal (**5a**)



By GP2 starting from benzylidenemalononitrile (**2a**, 15.4 mg) with an irradiation time of 8 h. Purified by column chromatography (Neutral Al_2O_3, Pentane/EtOAc 5:1).

Yield: 80% (18.4 mg, 79.9 µmol).

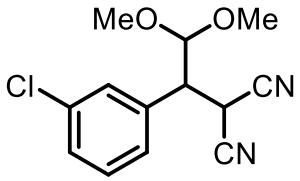
Appearance: Colorless oil.

^{1}H NMR (300 MHz, $CDCl_3$): δ [ppm] = 7.46 – 7.38 (m, 5H), 4.81 (d, *J* = 6.7 Hz, 1H), 4.34 (d, *J* = 5.7 Hz, 1H), 3.52 (s, 3H), 3.42 (dd, *J* = 6.7, 5.6 Hz, 1H), 3.31 (s, 3H).

^{13}C{^{1}H} NMR (101 MHz, $CDCl_3$): δ [ppm] = 133.6, 129.3, 128.9, 112.1, 112.0, 104.4, 56.5, 55.1, 49.3, 26.0.

HRMS (ESI): *m/z* calcd. for $C_{13}H_{15}N_2O_2^+$: 231.1128, found: 231.1137.

2-(3-Chlorophenyl)-2-dicyanomethylacetaldehyde dimethyl acetal (**5b**)



By GP2 starting from (3-chlorobenzylidene)malononitrile (**2b**, 18.9 mg) with an irradiation time of 8 h. Purified by column chromatography (Neutral Al_2O_3, Pentane/EtOAc 4:1).

Yield: 60% (16.0 mg, 60.4 µmol).

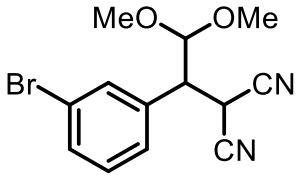
Appearance: Colorless syrup.

^{1}H NMR (300 MHz, $CDCl_3$): δ [ppm] = 7.43 – 7.28 (m, 4H), 4.76 (d, *J* = 6.3 Hz, 1H), 4.33 (d, *J* = 5.9 Hz, 1H), 3.52 (s, 3H), 3.40 (t, *J* = 6.2 Hz, 1H), 3.34 (s, 3H).

^{13}C{^{1}H} NMR (75.5 MHz, $CDCl_3$): δ [ppm] = 135.5, 135.2, 130.6, 129.7, 129.2, 127.1, 111.8, 111.7, 104.2, 56.6, 55.5, 49.0, 25.7.

HRMS (ESI): *m/z* calcd. for $C_{13}H_{14}ClN_2O_2^+$: 265.0739, found: 265.0745.

2-(3-Bromophenyl)-2-dicyanomethylacetaldehyde dimethyl acetal (**5c**)



By GP2 starting from (3-bromobenzylidene)malononitrile (**2c**, 23.3 mg) with an irradiation time of 8 h. Purified by column chromatography (Neutral Al_2O_3, Pentane/EtOAc 4:1).

Yield: 62% (19.2 mg, 62.1 µmol).

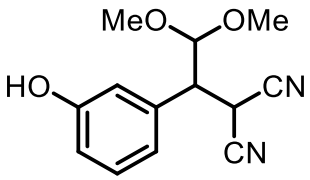
Appearance: Colorless gum.

^{1}H NMR (600 MHz, $CDCl_3$): δ [ppm] = 7.57 – 7.53 (m, 2H), 7.39 – 7.35 (m, 1H), 7.34 – 7.28 (m, 1H), 4.76 (d, J = 6.3 Hz, 1H), 4.32 (d, J = 5.9 Hz, 1H), 3.52 (s, 3H), 3.38 (t, J = 6.1 Hz, 1H), 3.35 (s, 3H).

^{13}C{^{1}H} NMR (75.5 MHz, $CDCl_3$): δ [ppm] = 135.7, 132.6, 132.1, 130.8, 127.5, 123.3, 111.8, 111.6, 104.2, 56.7, 55.5, 48.9, 25.7.

HRMS (ESI): *m/z* calcd. for $C_{13}H_{14}BrN_2O_2^+$: 309.0233, found: 309.0241.

2-(Dicyanomethyl)-2-(3-hydroxyphenyl)acetaldehyde dimethyl acetal (**5d**)



By GP2 starting from (3-hydroxybenzylidene)malononitrile (**2d**, 17.0 mg) with an irradiation time of 8 h. Purified by column chromatography (SiO_2, Pentane/EtOAc 2:1).

Yield: 62% (15.3 mg, 62.1 µmol).

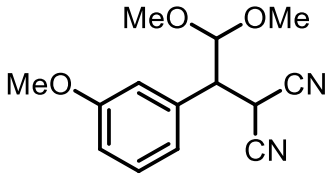
Appearance: Colorless gum.

^{1}H NMR (300 MHz, $CDCl_3$): δ [ppm] = 7.34 – 7.18 (m, 1H), 7.02 – 6.94 (m, 1H), 6.94 – 6.80 (m, 2H), 5.49 (br. s, 1H), 4.77 (d, J = 6.6 Hz, 1H), 4.32 (d, J = 5.7 Hz, 1H), 3.52 (s, 3H), 3.37 (t, J = 5.6 Hz, 1H), 3.33 (s, 3H).

^{13}C{^{1}H} NMR (75.5 MHz, $CDCl_3$): δ [ppm] = 156.3, 135.2, 130.7, 121.2, 116.5, 115.8, 112.1, 112.0, 104.5, 56.5, 55.3, 49.1, 25.9.

HRMS (ESI): *m/z* calcd. for $C_{13}H_{13}N_2O_3^-$: 245.0921, found: 245.0922.

2-(Dicyanomethyl)-2-(3-methoxyphenyl)acetaldehyde dimethyl acetal (**5e**)



By GP2 starting from (3-methoxybenzylidene)malononitrile (**2e**, 18.4 mg) with an irradiation time of 8 h. Purified by column chromatography (Neutral Al_2O_3, Pentane/EtOAc 4:1).

Yield: 58% (15.0 mg, 57.6 µmol).

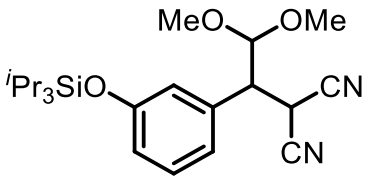
Appearance: Colorless oil.

^{1}H NMR (400 MHz, $CDCl_3$): *δ* [ppm] = 7.38 – 7.30 (m, 1H), 7.03 – 6.89 (m, 3H), 4.79 (d, *J* = 6.7 Hz, 1H), 4.32 (d, *J* = 5.7 Hz, 1H), 3.83 (s, 3H), 3.52 (s, 3H), 3.38 (t, *J* = 6.1 Hz, 1H), 3.32 (s, 3H).

^{13}C{^{1}H} NMR (101 MHz, $CDCl_3$): *δ* [ppm] = 160.1, 135.0, 130.4, 121.0, 114.8, 114.6, 112.1, 112.0, 104.4, 56.5, 55.4, 55.2, 49.3, 25.9.

HRMS (ESI): *m/z* calcd. for $C_{14}H_{17}N_2O_3^+$: 261.1234, found: 261.1227.

2-(Dicyanomethyl)-2-(3-((triisopropylsilyl)oxy)phenyl)acetaldehyde dimethyl acetal (**5f**)



By GP2 starting from (3-((triisopropylsilyl)oxy)benzylidene)malononitrile (**2f**, 32.7 mg) with an irradiation time of 8 h. Purified by column chromatography (Neutral Al_2O_3, Pentane/EtOAc 10:1).

Yield: 61% (24.5 mg, 60.9 µmol).

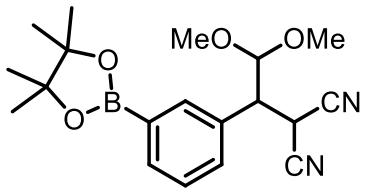
Appearance: Colorless syrup.

^{1}H NMR (300 MHz, $CDCl_3$): *δ* [ppm] = 7.32 – 7.21 (m, 1H), 7.05 – 6.85 (m, 3H), 4.74 (d, *J* = 6.7 Hz, 1H), 4.30 (d, *J* = 5.8 Hz, 1H), 3.51 (s, 3H), 3.34 (t, *J* = 6.2 Hz, 4H), 3.30 (s, 3H), 1.33 – 1.22 (m, 3H), 1.15 – 1.07 (m, 18H).

^{13}C{^{1}H} NMR (75.5 MHz, $CDCl_3$): *δ* [ppm] = 156.8, 135.1, 130.3, 121.5, 121.0, 120.4, 112.0, 112.0, 104.7, 56.4, 55.4, 49.2, 25.8, 18.0, 12.8.

HRMS (ESI): *m/z* calcd. for $C_{22}H_{34}N_2NaO3Si^+$: 425.2231, found: 425.2236.

2-(Dicyanomethyl)-2-(3-(4,4,5,5-tetramethyl-1,3,2-dioxaborolan-2-yl)phenyl)acetaldehyde dimethyl acetal (**5g**)



By GP2 starting from (3-(2,2-dicyanovinyl)phenylboronic acid pinacol ester (**2g**, 28.0 mg) with an irradiation time of 8 h. An analytical sample was obtained by automated flash column chromatography (C_{18}-SiO_2, 20% MeCN in H_2O → 100% MeCN) and lyophilization.

Yield: 75% (^{1}H NMR yield *vs.* 1,3,5-trimethoxybenzene).

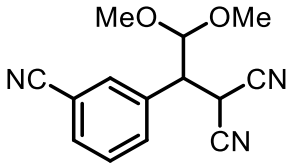
Appearance: Colorless fluffy solid (lyophilisate).

^{1}H NMR (400 MHz, $CDCl_3$): *δ* [ppm] = 7.88 – 7.80 (m, 1H), 7.80 – 7.73 (m, 1H), 7.58 – 7.51 (m, 1H), 7.46 – 7.39 (m, 1H), 4.81 (d, *J* = 6.5 Hz, 1H), 4.32 (d, *J* = 6.0 Hz, 1H), 3.52 (s, 3H), 3.46 (t, *J* = 6.3 Hz, 1H), 3.31 (s, 3H), 1.35 (s, 12H).

^{13}C{^{1}H} NMR (101 MHz, $CDCl_3$): *δ* [ppm] = 135.8, 135.5, 133.0, 131.1, 128.7, 112.1, 112.0, 104.5, 84.2, 56.5, 55.0, 49.3, 25.8, 25.0.

HRMS (ESI): *m/z* calcd. for $C_{19}H_{25}BN_2NaO_4^+$: 378.1836, found: 378.1828.

2-(Dicyanomethyl)-2-(3-cyanophenyl)acetaldehyde dimethyl acetal (**5h**)



By GP2 starting from (3-cyanobenzylidene)malononitrile (**2h**, 17.9 mg) with an irradiation time of 8 h. Purified by column chromatography (Neutral Al_2O_3, Pentane/EtOAc 2:1).

Yield: 53% (13.6 mg, 53.3 µmol).

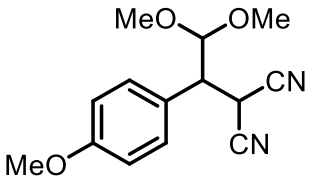
Appearance: Pale-yellow gum.

^{1}H NMR (300 MHz, $CDCl_3$): *δ* [ppm] = 7.75 – 7.65 (m, 3H), 7.62 – 7.52 (m, 1H), 4.78 (d, *J* = 6.1 Hz, 1H), 4.35 (d, *J* = 6.2 Hz, 1H), 3.53 (s, 3H), 3.47 (t, *J* = 6.1 Hz, 1H), 3.37 (s, 3H).

^{13}C{^{1}H} NMR (75.5 MHz, $CDCl_3$): *δ* [ppm] = 135.0, 133.5, 133.0, 132.7, 130.2, 118.2, 113.6, 111.6, 111.4, 103.9, 56.8, 55.7, 48.9, 25.5.

HRMS (ESI): *m/z* calcd. for $C_{14}H_{14}N_3O_2^+$: 256.1081, found: 256.1088.

2-(Dicyanomethyl)-2-(4-methoxyphenyl)acetaldehyde dimethyl acetal (**5i**)



By GP2 starting from (4-methoxybenzylidene)malononitrile (**2i**, 18.4 mg) with an irradiation time of 20 h. Purified by column chromatography (Neutral Al_2O_3, Pentane/EtOAc 5:1).

Yield: 75% (19.6 mg, 75.3 µmol).

Appearance: Colorless solid.

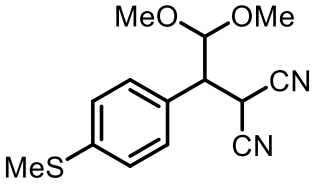
^{1}H NMR (400 MHz, $CDCl_3$): *δ* [ppm] = 7.38 – 7.31 (m, 2H), 6.98 – 6.91 (m, 2H), 4.76 (d, *J* = 6.6 Hz, 1H), 4.31 (d, *J* = 5.5 Hz, 1H), 3.82 (s, 3H), 3.51 (s, 3H), 3.38 (t, *J* = 6.1 Hz, 1H), 3.31 (s, 3H).

^{13}C{^{1}H} NMR (101 MHz, $CDCl_3$): *δ* [ppm] = 160.3, 130.1, 125.4, 114.7, 112.2, 112.0, 104.5, 56.4, 55.4, 55.0, 48.7, 26.2.

HRMS (ESI): *m/z* calcd. for $C_{14}H_{17}N_2O_3^+$: 261.1234, found: 261.1226.

m.p. = 55–57 °C.

2-(Dicyanomethyl)-2-(4-(methylthio)phenyl)acetaldehyde dimethyl acetal (**5j**)



By GP2 starting from (4-(methylthio)benzylidene)malononitrile (**2j**, 20.0 mg) with an irradiation time of 16 h. Purified by column chromatography (Neutral Al_2O_3, Pentane/EtOAc 4:1).

Yield: 55% (15.3 mg, 55.3 µmol).

Appearance: Pale-yellow solid.

^{1}H NMR (300 MHz, $CDCl_3$): *δ* [ppm] = 7.39 – 7.30 (m, 2H), 7.30 – 7.24 (m, 3H), 4.77 (d, *J* = 6.7 Hz, 1H), 4.32 (d, *J* = 5.6 Hz, 1H), 3.51 (s, 3H), 3.38 (t, *J* = 6.1 Hz, 1H), 3.31 (s, 3H), 2.49 (s, 3H).

^{13}C{^{1}H} NMR (75.5 MHz, $CDCl_3$): *δ* [ppm] = 140.3, 129.9, 129.3, 126.8, 112.1, 111.9, 104.3, 56.5, 55.1, 48.9, 26.0, 15.5.

HRMS (ESI): *m/z* calcd. for $C_{14}H_{17}N_2O_2S^+$: 277.1005, found: 277.0992.

m.p. = 67–68 °C.

This compound was also prepared on a 3.00 mmol scale, starting from **2j** (601 mg) and **1** (1.18 g) in acetone (30 mL) in a 100 mL Schlenk tube, with 72 h of irradiation time (Fig. 2). The ultraviolet LED was placed with a distance of ca. 2 cm and a standard desk fan was used for air cooling. The mixture warmed up to ~30–40 °C during the reaction, which did not affect the yield (cf. sensitivity screening). After irradiation, the mixture was treated as usual. **Yield**: 53% (439 mg, 1.59 mmol).

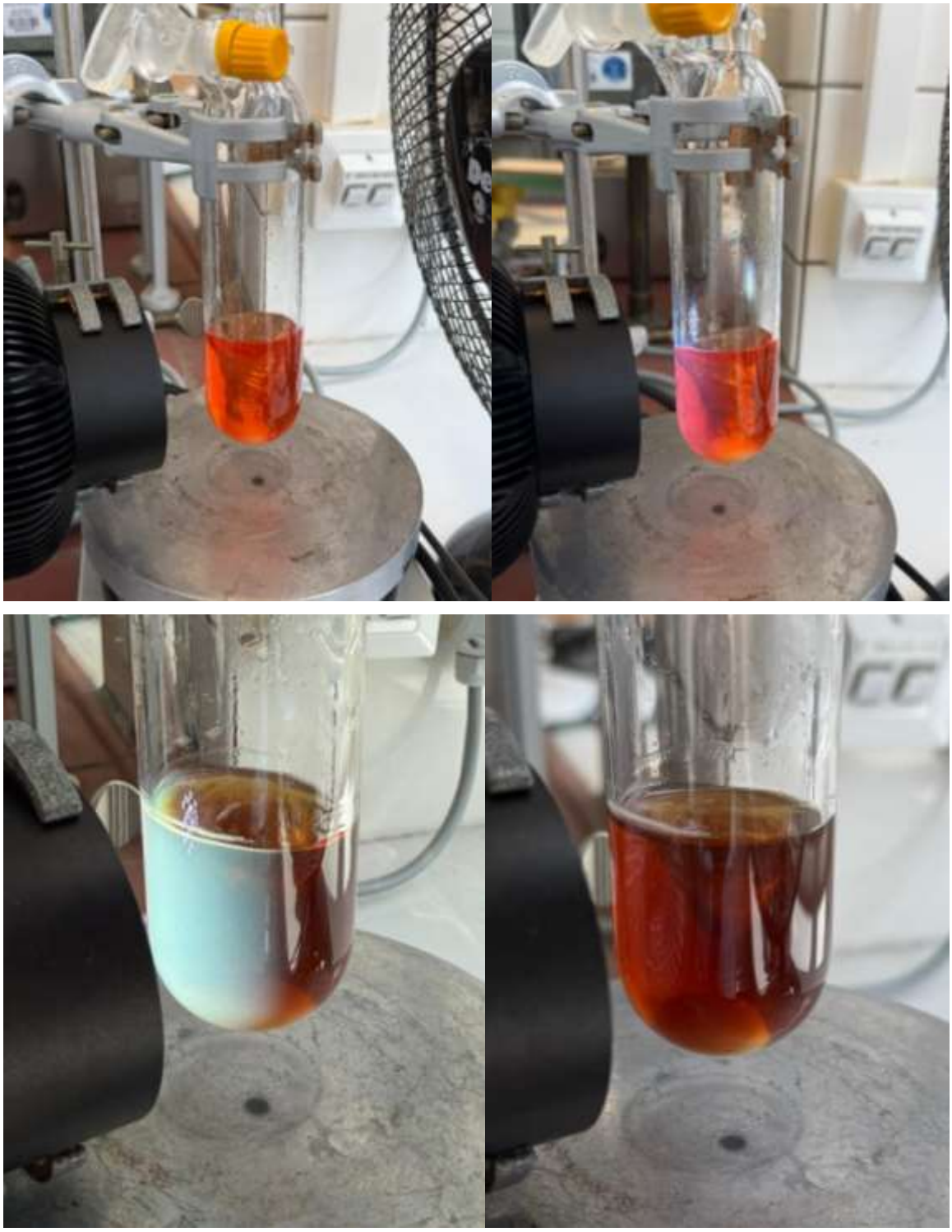
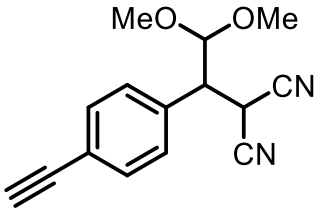


Figure 2. *Large-scale synthesis of* ***5j*** *before (top) and after (bottom) 72 h of irradiation.*

2-(Dicyanomethyl)-2-(4-ethynylphenyl)acetaldehyde dimethyl acetal (**5k**)



By GP2 starting from (4-ethynylbenzylidene)malononitrile (**2k**, 17.8 mg) with an irradiation time of 8 h. Purified by column chromatography (Neutral Al_2O_3, Pentane/EtOAc 4:1).

Yield: 55% (14.1 mg, 55.4 µmol).

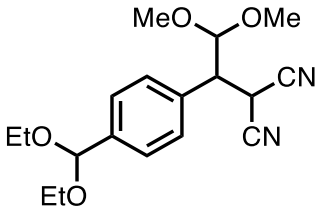
Appearance: Pale-yellow gum.

^{1}H NMR (300 MHz, $CDCl_3$): δ [ppm] = 7.59 – 7.49 (m, 2H), 7.44 – 7.34 (m, 2H), 4.78 (d, *J* = 6.6 Hz, 1H), 4.33 (d, *J* = 5.8 Hz, 1H), 3.52 (s, 3H), 3.42 (t, *J* = 6.1 Hz, 1H), 3.32 (s, 3H), 3.13 (s, 1H).

^{13}C{^{1}H} NMR (75.5 MHz, $CDCl_3$): δ [ppm] = 134.1, 133.0, 129.0, 123.4, 111.9, 111.7, 104.3, 82.9, 78.6, 56.6, 55.4, 49.2, 25.7.

HRMS (ESI): *m/z* calcd. for $C_{15}H_{15}N_2O_2^+$: 255.1128, found: 255.1143.

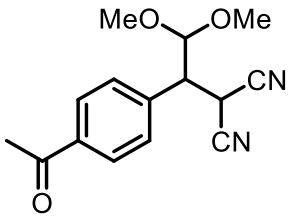
2-(Dicyanomethyl)-2-(4-(diethoxymethyl)phenyl)acetaldehyde dimethyl acetal (**5l**)



By GP2 starting from (4-acetylbenzylidene)malononitrile (**2l**, 19.6 mg) with an irradiation time of 8 h.

Yield: 80% (^{1}H NMR yield *vs.* 1,3,5-trimethoxybenzene).

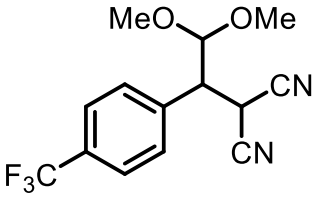
2-(Dicyanomethyl)-2-(4-acetylphenyl)acetaldehyde dimethyl acetal (**5m**)



By GP2 starting from (4-acetylbenzylidene)malononitrile (**2m**, 19.6 mg) with an irradiation time of 8 h.

Yield: 33% (^{1}H NMR yield *vs.* 1,3,5-trimethoxybenzene).

2-(Dicyanomethyl)-2-(4-(trifluoromethyl)phenyl)acetaldehyde dimethyl acetal (**5n**)



By GP2 starting from (4-(trifluoromethyl)benzylidene)malononitrile (**2n**, 22.2 mg) with an irradiation time of 8 h. Purified by column chromatography (Neutral Al_2O_3, Pentane/EtOAc 6:1).

Yield: 44% (13.1 mg, 43.9 µmol).

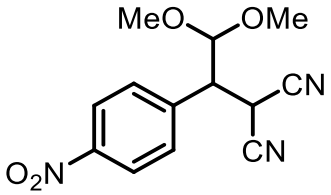
Appearance: Pale-yellow syrup.

^{1}H NMR (300 MHz, $CDCl_3$): δ [ppm] = 7.74 – 7.66 (m, 2H), 7.60 – 7.52 (m, 2H), 4.81 (d, J = 6.5 Hz, 1H), 4.37 (d, J = 5.8 Hz, 1H), 3.54 (s, 3H), 3.50 (t, J = 6.1 Hz, 1H), 3.34 (s, 3H).

^{13}C{^{1}H} NMR (75.5 MHz, $CDCl_3$): δ [ppm] = 137.4 (q, J = 1.3 Hz), 131.6 (q, J = 33.2 Hz), 129.5, 126.3 (q, J = 3.7 Hz), 123.9 (q, J = 272.3 Hz), 111.7, 111.6, 104.1, 56.7, 55.4, 49.1, 25.6.

HRMS (ESI): *m/z* calcd. for $C_{14}H_{14}F_3N_2O_2^+$: 299.1002, found: 299.1000.

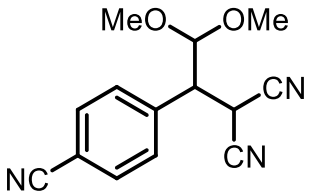
2-(Dicyanomethyl)-2-(4-nitrophenyl)acetaldehyde dimethyl acetal (**5o**)



By GP2 starting from (4-nitrobenzylidene)malononitrile (**2o**, 19.9 mg) with an irradiation time of 8 h.

Yield: <5% (^{1}H NMR yield *vs.* 1,3,5-trimethoxybenzene).

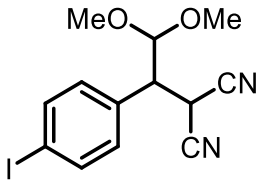
2-(Dicyanomethyl)-2-(4-cyanophenyl)acetaldehyde dimethyl acetal (**5p**)



By GP2 starting from (4-cyanobenzylidene)malononitrile (**2p**, 17.9 mg) with an irradiation time of 8 h.

Yield: 31% (^{1}H NMR yield *vs.* 1,3,5-trimethoxybenzene).

2-(Dicyanomethyl)-2-(4-iodophenyl)acetaldehyde dimethyl acetal (**5q**)



By GP2 starting from (4-iodobenzylidene)malononitrile (**2q**, 28.0 mg) with an irradiation time of 8 h. Purified by column chromatography (Neutral Al_2O_3, Pentane/EtOAc 4:1).

Yield: 70% (24.9 mg, 69.9 µmol).

Appearance: Colorless solid.

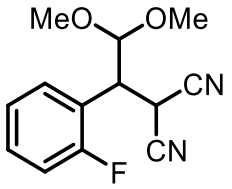
^{1}H NMR (300 MHz, $CDCl_3$): δ [ppm] = 7.82 – 7.69 (m, 2H), 7.21 – 7.11 (m, 2H), 4.75 (d, J = 6.6 Hz, 1H), 4.32 (d, J = 5.7 Hz, 1H), 3.52 (s, 3H), 3.37 (t, J = 6.1 Hz, 1H), 3.32 (s, 3H).

^{13}C{^{1}H} NMR (151 MHz, $CDCl_3$): δ [ppm] = 138.5, 133.1, 130.7, 111.9, 111.7, 104.1, 95.5, 56.6, 55.3, 49.0, 25.7.

HRMS (ESI): *m/z* calcd. for $C_{13}H_{14}IN_2O_2^+$: 357.0094, found: 357.0119.

m.p. = 59–61 °C.

2-(Dicyanomethyl)-2-(2-fluorophenyl)acetaldehyde dimethyl acetal (**5r**)



By GP2 starting from (2-fluorobenzylidene)malononitrile (**2r**, 17.2 mg) with an irradiation time of 8 h. Purified by column chromatography (Neutral Al_2O_3, Pentane/EtOAc 5:1).

Yield: 70% (17.3 mg, 69.7 µmol).

Appearance: Colorless oil.

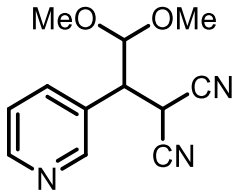
^{1}H NMR (300 MHz, $CDCl_3$): δ [ppm] = 7.58 – 7.46 (m, 1H), 7.45 – 7.33 (m, 1H), 7.26 – 7.10 (m, 2H), 4.83 (d, J = 6.8 Hz, 1H), 4.33 (d, J = 6.3 Hz, 1H), 3.95 (t, J = 6.5 Hz, 1H), 3.52 (s, 3H), 3.33 (s, 3H).

^{13}C{^{1}H} NMR (75.5 MHz, $CDCl_3$): δ [ppm] = 161.1 (d, J = 247.4 Hz), 131.0 (d, J = 8.8 Hz), 129.3 (d, J = 3.0 Hz), 125.1 (d, J = 3.9 Hz), 120.9 (d, J = 13.8 Hz), 116.3 (d, J = 22.7 Hz), 111.8, 111.7, 103.7 (d, J = 1.7 Hz), 56.4, 54.5, 41.2 (d, J = 2.8 Hz), 25.2.

^{19}F NMR (565 MHz, $CDCl_3$): δ [ppm] = −110.91 – −110.99 (m).

HRMS (ESI): *m/z* calcd. for $C_{13}H_{14}FN_2O_2^+$: 249.1034, found: 249.1028.

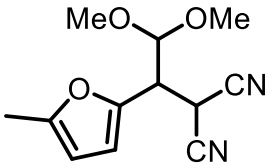
2-(Dicyanomethyl)-2-(pyridin-3-yl)acetaldehyde dimethyl acetal (**5s**)



By GP2 starting from (pyridin-3-ylmethylidene)malononitrile (**2s**, 15.5 mg) with an irradiation time of 8 h.

Yield: 25% (^{1}H NMR yield *vs.* 1,3,5-trimethoxybenzene).

2-(Dicyanomethyl)-2-(5-methylfuran-2-yl)acetaldehyde dimethyl acetal (**5t**)



By GP2 starting from ((5-methylfuran-2-yl)methylidene)malononitrile (**2t**, 15.8 mg) with an irradiation time of 36 h. Purified by column chromatography (Neutral Al_2O_3, Pentane/EtOAc 5:1).

Yield: 57% (13.4 mg, 57.2 µmol).

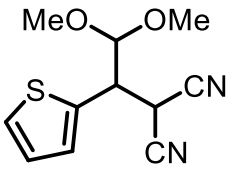
Appearance: Pale-yellow gum.

^{1}H NMR (400 MHz, $CDCl_3$): δ [ppm] = 6.35 (d, *J* = 3.2 Hz, 1H), 5.99 (dd, *J* = 3.2, 1.0 Hz, 1H), 4.76 (d, *J* = 7.0 Hz, 1H), 4.29 (d, *J* = 5.0 Hz, 1H), 3.54 (dd, *J* = 7.0, 5.0 Hz, 1H), 3.50 (s, 3H), 3.35 (s, 3H), 2.31 (d, *J* = 1.0 Hz, 3H).

^{13}C{^{1}H} NMR (101 MHz, $CDCl_3$): δ [ppm] = 153.4, 145.1, 111.9, 111.6, 111.2, 107.0, 103.3, 56.4, 55.1, 43.8, 24.6, 13.7.

HRMS (ESI): *m/z* calcd. for $C_{12}H_{15}N_2O_3^+$: 235.1077, found: 235.1070.

2-(Dicyanomethyl)-2-(thiophen-2-yl)acetaldehyde dimethyl acetal (**5u**)



By GP2 starting from (thiophen-2-ylmethylidene)malononitrile (**2u**, 16.0 mg) with an irradiation time of 20 h. Purified by column chromatography (Neutral Al_2O_3, Pentane/EtOAc 5:1).

Yield: 69% (16.4 mg, 69.4 µmol).

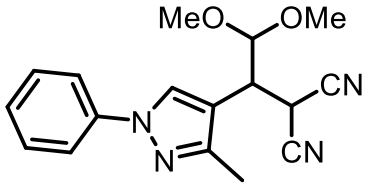
Appearance: Yellow syrup.

^{1}H NMR (300 MHz, $CDCl_3$): δ [ppm] = 7.37 (dd, *J* = 5.1, 1.3 Hz, 1H), 7.21 (dd, *J* = 3.7, 1.4 Hz, 1H), 7.07 (dd, *J* = 5.1, 3.6 Hz, 1H), 4.70 (d, *J* = 5.8 Hz, 1H), 4.35 (d, *J* = 5.5 Hz, 1H), 3.78 (t, *J* = 5.5 Hz, 1H), 3.54 (s, 3H), 3.41 (s, 3H).

^{13}C{^{1}H} NMR (75.5 MHz, $CDCl_3$): δ [ppm] = 134.7, 128.4, 127.4, 127.0, 112.0, 111.7, 104.9, 56.9, 55.9, 45.5, 26.4.

HRMS (ESI): *m/z* calcd. for $C_{11}H_{13}N_2O_2S^+$: 237.0692, found: 237.0692.

2-(Dicyanomethyl)-2-(3-methyl-1-phenyl-1*H*-pyrazol-4-yl)acetaldehyde dimethyl acetal (**5v**)



By GP2 starting from ((3-methyl-1-phenyl-1*H*-pyrazol-4-yl)methylene)malononitrile (**2v**, 23.4 mg) with an irradiation time of 20 h. Purified by column chromatography (Neutral Al_2O_3, Pentane/EtOAc 5:1).

Yield: 70% (21.8 mg, 70.2 µmol).

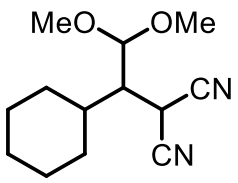
Appearance: Yellow syrup.

^{1}H NMR (300 MHz, $CDCl_3$): δ [ppm] = 8.06 (s, 1H), 7.70 – 7.65 (m, 2H), 7.48 – 7.41 (m, 2H), 7.32 – 7.25 (m, 1H), 4.61 (d, *J* = 5.9 Hz, 1H), 4.32 (d, *J* = 4.8 Hz, 1H), 3.52 (s, 3H), 3.50 (dd, *J* = 5.9, 4.7 Hz, 1H), 3.39 (s, 3H), 2.40 (s, 3H).

^{13}C{^{1}H} NMR (75.5 MHz, $CDCl_3$): δ [ppm] = 149.9, 139.9, 129.6, 126.8, 126.3, 119.3, 113.8, 112.3, 112.2, 105.0, 56.8, 55.7, 40.7, 25.9, 12.0.

HRMS (ESI): *m/z* calcd. for $C_{17}H_{19}N_4O_2^+$: 311.1503, found: 311.1496.

2-(Dicyanomethyl)-2-cyclohexylacetaldehyde dimethyl acetal (**5w**)



By GP2 starting from cyclohexylmethylidenemalononitrile (**2w**, 16.0 mg) with an irradiation time of 16 h. Purified by column chromatography (Neutral Al_2O_3, Pentane/Diethyl ether 2:1).

Yield: 77% (18.1 mg, 76.7 µmol).

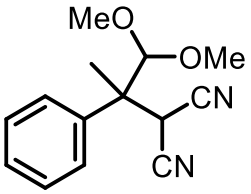
Appearance: Colorless oil.

^{1}H NMR (600 MHz, $CDCl_3$): δ [ppm] = 4.49 (d, *J* = 4.3 Hz, 1H), 4.20 (d, *J* = 2.7 Hz, 1H), 3.48 (s, 3H), 3.41 (s, 3H), 2.04 (ddd, *J* = 7.1, 4.3, 2.7 Hz, 1H), 1.98 – 1.92 (m, 1H), 1.87 – 1.76 (m, 4H), 1.74 – 1.68 (m, 1H), 1.37 – 1.27 (m, 2H), 1.25 – 1.09 (m, 3H).

^{13}C{^{1}H} NMR (151 MHz, $CDCl_3$): δ [ppm] = 113.9, 112.8, 103.4, 57.0, 55.2, 49.4, 37.2, 31.0, 30.7, 26.18, 26.15, 20.3.

HRMS (ESI): *m/z* calcd. for $C_{13}H_{21}N_2O_2^+$: 237.1598, found: 237.1604.

2-(Dicyanomethyl)-2-phenylpropionaldehyde dimethyl acetal (**5x**)



By GP2 starting from (1-phenylethylidene)malononitrile (**2x**, 16.8 mg) with an irradiation time of 8 h. Purified by column chromatography (Neutral Al_2O_3, Pentane/EtOAc 5:1).

Yield: 79% (19.3 mg, 79.0 µmol).

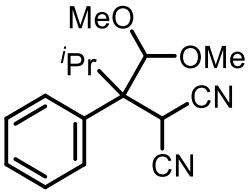
Appearance: Colorless oil.

^{1}H NMR (400 MHz, $CDCl_3$): δ [ppm] = 7.57 – 7.49 (m, 2H), 7.45 – 7.36 (m, 3H), 4.64 (s, 1H), 4.36 (s, 1H), 3.54 (s, 3H), 3.41 (s, 3H), 1.72 (s, 3H).

^{13}C{^{1}H} NMR (101 MHz, $CDCl_3$): δ [ppm] = 137.3, 129.1, 128.9, 128.7, 127.3, 112.2, 112.0, 109.3, 59.4, 59.0, 49.6, 32.4, 18.4.

HRMS (ESI): *m/z* calcd. for $C_{14}H_{17}N_2O_2^+$: 245.1285, found: 245.1282.

2-(Dicyanomethyl)-2-phenyl-3-methylbutyraldehyde dimethyl acetal (**5y**)



By GP2 on a 200 µmol scale, starting from (2-methyl-1-phenylpropylidene)malononitrile (**2y**, 39.3 mg, 200 µmol) and **1** (78.4 mg, 240 µmol) in acetone (2.0 mL) with an irradiation time of 24 h. An analytical sample was obtained by twofold column chromatography (SiO_2, Pentane/EtOAc, gradient from 30:1 → 7:1; SiO_2, Pentane/THF, gradient from 30:1 → 7:1).

Yield: 37% (^{1}H NMR yield *vs.* 1,3,5-trimethoxybenzene).

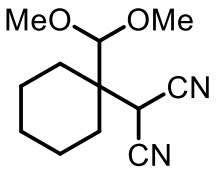
Appearance: Colorless gum.

^{1}H NMR (300 MHz, $CDCl_3$): δ [ppm] = 7.54 – 7.46 (m, 1H), 7.45 – 7.37 (m, 1H), 7.36 – 7.29 (m, 1H), 4.75 (s, 1H), 4.51 (s, 1H), 3.57 (s, 3H), 3.53 (s, 3H), 2.75 (hept, *J* = 7.0 Hz, 1H), 1.03 (t, *J* = 6.9 Hz, 6H).

^{13}C{^{1}H} NMR (75.5 MHz, $CDCl_3$): δ [ppm] = 137.2, 128.6, 128.0, 127.6, 113.5, 113.2, 109.3, 59.6, 59.1, 56.3, 32.6, 26.8, 19.1, 19.0.

HRMS (ESI): *m/z* calcd. for $C_{16}H_{21}N_2O_2^+$: 273.1598, found: 273.1593.

(1-(Dimethoxymethyl)cyclohexyl)malononitrile (**5z**)



By GP2 starting from cyclohexylidenemalononitrile (**2z**, 14.6 mg) with an irradiation time of 16 h. Purified by column chromatography (SiO_2, Pentane/EtOAc 6:1).

Yield: 61% (13.5 mg, 60.7 µmol).

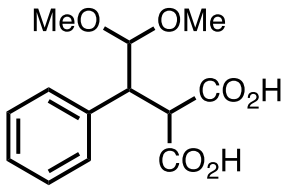
Appearance: Colorless oil.

^{1}H NMR (300 MHz, $CDCl_3$): δ [ppm] = 4.42 (s, 1H), 4.07 (s, 1H), 3.58 (s, 6H), 1.94 – 1.81 (m, 1H), 1.69 – 1.41 (m, 8H).

^{13}C{^{1}H} NMR (75.5 MHz, $CDCl_3$): δ [ppm] = 112.5, 107.6, 59.0, 45.9, 29.1, 28.2, 25.1, 21.4.

HRMS (ESI): *m/z* calcd. for $C_{12}H_{19}N_2O_2^+$: 223.1441, found: 223.1450.

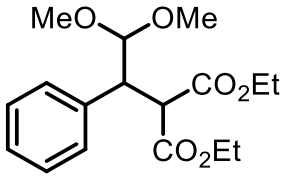
(2,2-Dimethoxy-1-phenylethyl)malonic acid (**6a**)



By GP2 starting from benzylidenemalonic acid (**3a**, 19.2 mg) with an irradiation time of 16 h.

Yield: 60% (^{1}H NMR yield *vs.* 1,3,5-trimethoxybenzene).

Diethyl (2,2-dimethoxy-1-phenylethyl)malonate (**6b**)



By GP2 starting from diethyl benzylidenemalonate (**3b**, 24.8 mg) with an irradiation time of 16 h. Purified by column chromatography (Neutral Al_2O_3, Pentane/EtOAc 8:1).

Yield: 86% (27.8 mg, 85.7 µmol).

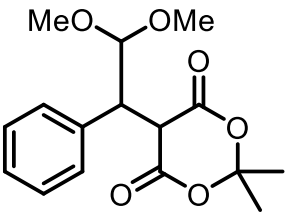
Appearance: Colorless oil.

^{1}H NMR (400 MHz, $CDCl_3$): δ [ppm] = 7.30 – 7.15 (m, 5H), 4.59 (d, *J* = 5.9 Hz, 1H), 4.23 – 4.14 (m, 2H), 3.93 – 3.82 (m, 3H), 3.76 (dd, *J* = 10.2, 5.9 Hz, 1H), 3.34 (s, 3H), 3.24 (s, 3H), 1.26 (t, *J* = 7.1 Hz, 3H), 0.92 (t, *J* = 7.1 Hz, 3H).

^{13}C{^{1}H} NMR (101 MHz, $CDCl_3$): δ [ppm] = 168.4, 167.9, 137.4, 129.5, 128.2, 127.3, 106.6, 61.5, 61.3, 56.0, 54.6, 54.4, 48.5, 14.2, 13.8.

HRMS (ESI): *m/z* calcd. for $C_{17}H_{24}NaO_6^+$: 347.1465, found: 347.1468.

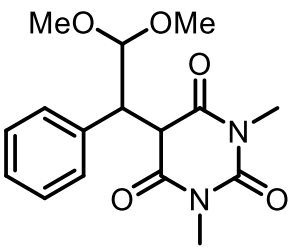
5-(2,2-Dimethoxy-1-phenylethyl)-2,2-dimethyl-1,3-dioxane-4,6-dione (**6c**)



By GP2 starting from 5-benzylidene-2,2-dimethyl-1,3-dioxane-4,6-dione (**3c**, 23.2 mg) with an irradiation time of 16 h.

Yield: 76% (^{1}H NMR yield *vs.* 1,3,5-trimethoxybenzene).

N,*N'*-Dimethyl-5-(2,2-dimethoxy-1-phenylethyl)barbituric acid (**6d**)



By GP2 starting from *N*,*N'*-dimethyl-4-benzylidenebarbituric acid (**3d**, 24.4 mg) with an irradiation time of 16 h. Purified by automated flash chromatography (C_{18}-SiO_2, 10% MeCN in H_2O → 100% MeCN).

Yield: 70% (22.5 mg, 70.2 µmol).

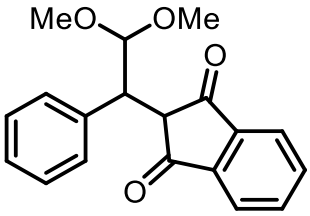
Appearance: Pale-yellow gum.

^{1}H NMR (300 MHz, $CDCl_3$): δ [ppm] = 7.32 – 7.23 (m, 3H), 7.14 – 7.06 (m, 2H), 5.25 (d, J = 9.2 Hz, 1H), 4.03 (d, J = 2.9 Hz, 1H), 3.87 (dd, J = 9.2, 2.9 Hz, 1H), 3.52 (s, 3H), 3.20 (s, 3H), 3.13 (s, 3H), 3.12 (s, 3H).

^{13}C{^{1}H} NMR (75.5 MHz, $CDCl_3$): δ [ppm] = 168.4, 167.8, 151.1, 135.8, 128.8, 128.4, 128.3, 103.0, 54.9, 52.8, 51.7, 51.4, 28.4, 28.3.

HRMS (ESI): *m/z* calcd. for $C_{16}H_{20}N_2NaO_5^+$: 343.1264, found: 343.1276.

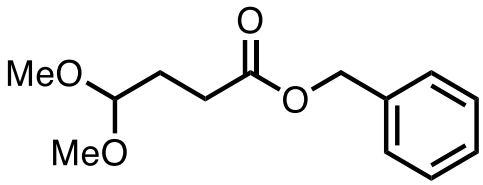
2-(2,2-Dimethoxy-1-phenylethyl)indane-1,3-dione (**6e**)



By GP2 starting from 2-benzylideneindane-1,3-dione (**3e**, 23.4 mg) with an irradiation time of 16 h. Attempts at separating the product from side products were unsuccessful.

Yield: 25% (^{1}H NMR yield *vs.* 1,3,5-trimethoxybenzene).

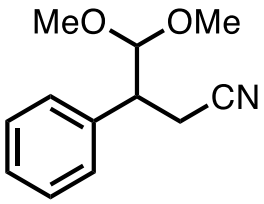
Benzyl 4,4-dimethoxybutanoate (**6f**)



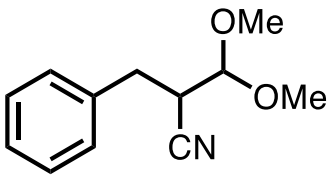
By GP2 starting from benzyl acrylate (**3f**, 16.2 mg) with an irradiation time of 16 h. Full conversion but no product formation was observed in the ^{1}H NMR spectrum of the crude reaction mixture, likely due to polymerization.

Yield: <5% (^{1}H NMR yield *vs.* 1,3,5-trimethoxybenzene).

2-(Cyanomethyl)-2-phenylacetaldehyde dimethyl acetal (**6g-1**) and 2-Cyano-3-phenyl-2-propionaldehyde dimethyl acetal (**6g-2**)



6g-1



6g-2

By GP2 on a 300 µmol scale, starting from cinnamonitrile (**3g**, 38.7 mg) and **1** (118 mg, 360 µmol) in acetone (3.0 mL) with an irradiation time of 72 h. The isomers were separated by automated flash chromatography (C_{18}-SiO_2, 30% MeCN in H_2O → 100% MeCN). Structures were assigned based on 2D-NMR spectroscopy and EI fragmentation patterns.

*2-(Cyanomethyl)-2-phenylacetaldehyde dimethyl acetal (**6g-1**)*

Yield: 12% (7.4 mg, 36 µmol); 18% (^{1}H NMR yield *vs.* 1,3,5-trimethoxybenzene after 48 h on a 100 µmol scale).

Appearance: Colorless syrup.

^{1}H NMR (300 MHz, $CDCl_3$): δ [ppm] = 7.37 – 7.18 (m, 4H), 4.46 (d, *J* = 5.7 Hz, 1H), 3.36 (s, 3H), 3.26 (s, 3H), 3.17 (dt, *J* = 8.9, 5.4 Hz, 1H), 2.78 (dd, *J* = 16.9, 5.0 Hz, 1H), 2.68 (dd, *J* = 16.9, 9.0 Hz, 1H).

^{13}C{^{1}H} NMR (75.5 MHz, $CDCl_3$): δ [ppm] = 137.8, 128.9, 128.3, 128.0, 118.9, 106.5, 56.0, 55.2, 45.6, 19.6.

HRMS (ESI): *m/z* calcd. for $C_{12}H_{16}NO_2^+$: 206.1176, found: 206.1175.

*2-Cyano-3-phenyl-2-propionaldehyde dimethyl acetal (**6g-2**)*

Yield: 16% (9.9 mg, 48 µmol); 23% (^{1}H NMR yield *vs.* 1,3,5-trimethoxybenzene after 48 h on a 100 µmol scale).

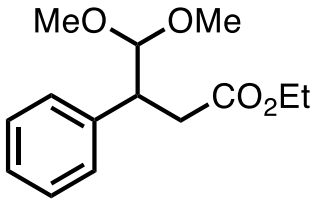
Appearance: Colorless syrup.

^{1}H NMR (300 MHz, $CDCl_3$): δ [ppm] = 7.38 – 7.19 (m, 4H), 4.43 – 4.30 (m, 1H), 3.45 (s, 3H), 3.41 (s, 3H), 3.07 – 2.94 (m, 2H), 2.92 – 2.81 (m, 1H).

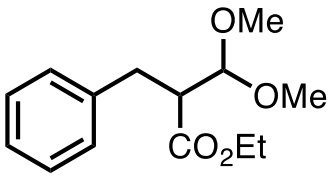
^{13}C{^{1}H} NMR (75.5 MHz, $CDCl_3$): δ [ppm] = 136.6, 129.2, 128.9, 127.4, 119.0, 102.6, 55.5, 54.8, 38.6, 33.8.

HRMS (ESI): *m/z* calcd. for $C_{12}H_{15}NNaO_2^+$: 228.0995, found: 228.0995.

Ethyl 4,4-dimethoxy-3-phenylbutanoate (**6h-1**) and Ethyl 2-benzyl-3,3-dimethoxypropanoate (**6h-2**)



6h-1



6h-2

By GP2 on a 300 µmol scale, starting from ethyl cinnamate (**3h**, 52.9 mg) and **1** (118 mg, 360 µmol) in acetone (3.0 mL) with an irradiation time of 72 h. Analytical samples were obtained by column chromatography (SiO_2, Pentane/$CHCl_3$ 1:1 → 1:3), which yielded **6h-2** as well as a mixture of **6h-1** and the Hantzsch ester-derived pyridine byproduct. Preparative TLC (SiO_2, Benzene/Et_2O 10:1) afforded **6h-1**. Structures were assigned based on 2D-NMR spectroscopy.

*Ethyl 4,4-dimethoxy-3-phenylbutanoate (**6h-1**)*

Yield: 12% (^{1}H NMR yield *vs.* 1,3,5-trimethoxybenzene after 48 h on a 100 µmol scale).

Appearance: Colorless oil.

^{1}H NMR (300 MHz, $CDCl_3$): δ [ppm] = 7.27 (d, *J* = 3.3 Hz, 6H), 4.42 (d, *J* = 6.1 Hz, 1H), 4.02 (qd, *J* = 7.1, 2.4 Hz, 2H), 3.46 (dt, *J* = 9.0, 6.0 Hz, 1H), 3.36 (s, 3H), 3.28 (s, 3H), 2.86 (dd, *J* = 15.6, 5.9 Hz, 1H), 2.61 (dd, *J* = 15.6, 9.0 Hz, 1H), 1.12 (t, *J* = 7.2 Hz, 3H).

^{13}C{^{1}H} NMR (75.5 MHz, $CDCl_3$): δ [ppm] = 172.4, 140.1, 128.6, 128.5, 127.0, 107.6, 60.4, 55.2, 54.7, 45.4, 36.4, 14.2.

HRMS (ESI): *m/z* calcd. for $C_{14}H_{20}NaO_4^+$: 275.1254, found: 275.1246.

*Ethyl 2-benzyl-3,3-dimethoxypropanoate (**6h-2**)*

Yield: 43% (^{1}H NMR yield *vs.* 1,3,5-trimethoxybenzene after 48 h on a 100 µmol scale).

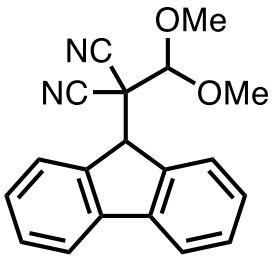
Appearance: Colorless oil.

^{1}H NMR (600 MHz, $CDCl_3$): δ [ppm] = 7.29 – 7.23 (m, 2H), 7.21 – 7.15 (m, 3H), 4.59 (d, *J* = 7.9 Hz, 1H), 4.08 – 3.97 (m, 2H), 3.40 (s, 3H), 3.38 (s, 3H), 3.05 – 2.95 (m, 2H), 2.88 (dd, *J* = 13.5, 10.8 Hz, 1H), 1.06 (t, *J* = 7.1 Hz, 3H).

^{13}C{^{1}H} NMR (151 MHz, $CDCl_3$): δ [ppm] = 172.3, 138.7, 128.9, 128.5, 126.5, 104.6, 60.5, 54.4, 53.1, 51.4, 34.5, 14.1.

HRMS (ESI): *m/z* calcd. for $C_{14}H_{20}NaO_4^+$: 275.1254, found: 275.1259.

2,2-Dicyano-2-(9*H*-fluoren-9-yl)acetaldehyde dimethyl acetal (**6i**)



By GP2 starting from (9*H*-fluoren-9-yl)malononitrile (**3i**, 22.8 mg) with an irradiation time of 16 h. Purified by column chromatography (Neutral Al_2O_3, Pentane/EtOAc 6:1).

Yield: 24.8 mg (81.4 µmol, 81%).

Appearance: Colorless solid.

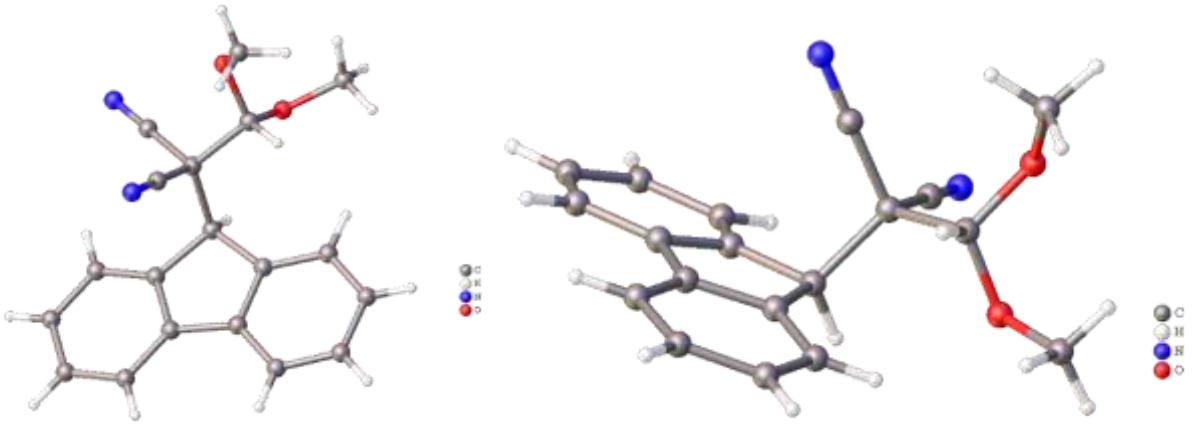
^{1}H NMR (300 MHz, $CDCl_3$): δ [ppm] = 7.90 – 7.71 (m, 5H), 7.56 – 7.45 (m, 2H), 7.43 – 7.32 (m, 1H), 4.65 (s, 1H), 4.54 (s, 1H), 3.57 (s, 6H).

^{13}C{^{1}H} NMR (75.5 MHz, $CDCl_3$): δ [ppm] = 142.1, 139.2, 130.1, 129.7, 127.8, 126.1, 120.7, 113.0, 103.6, 57.5, 48.9, 48.0.

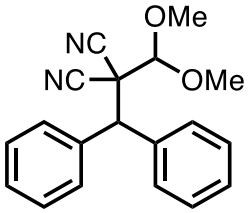
HRMS (ESI): *m/z* calcd. for $C_{19}H_{16}N_2NaO_2^+$: 327.1104, found: 327.1103.

m.p. = 152–154 °C.

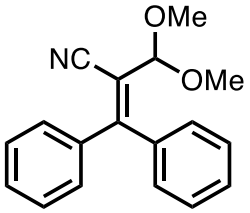
XRD:



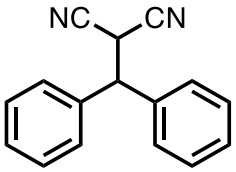
2,2-Dicyano-3,3-diphenylpropionaldehyde dimethyl acetal (**6j-1**), 2-Cyano-3,3-diphenyl-acrolein dimethyl acetal (**6j-2**), and Benzhydrylmalononitrile (**6j-3**)



6j-1



6j-2



6j-3

By GP2 on four parallel 300 µmol scales using (diphenylmethylidene)malononitrile **6j** (4× 69.1 mg = 1.20 mmol) and **1** (4× 118 mg = 1.44 mmol) in acetone (4× 3.0 mL) with an irradiation time of 48 h. Analytical samples were obtained by automated flash chromatography (15 µm spherical SiO_2, 7% Et_2O in pentane → 40% Et_2O in pentane), which yielded pure **6j-2** and a mixture of **6j-1** and **6j-3**. The latter two were separated by a second column chromatography (SiO_2, Pentane/THF 4:1). Structural assignments of the products were made based on 2D-NMR spectroscopy and EI fragmentation patterns. **6j-3** is a known compound.

*2,2-Dicyano-3,3-diphenylpropionaldehyde dimethyl acetal (**6j-1**)*

Yield: 53% (^{1}H NMR yield *vs.* 1,3,5-trimethoxybenzene after 24 h on a 100 µmol scale).

Appearance: Colorless solid.

^{1}H NMR (300 MHz, $CDCl_3$): δ [ppm] = 7.61 – 7.51 (m, 4H), 7.45 – 7.27 (m, 6H), 4.60 (s, 1H), 4.23 (s, 1H), 3.55 (s, 6H).

^{13}C{^{1}H} NMR (75.5 MHz, $CDCl_3$): δ [ppm] = 136.7, 129.3, 129.1, 128.6, 113.5, 104.1, 58.3, 53.9, 48.8.

HRMS (ESI): *m/z* calcd. for $C_{19}H_{18}N_2NaO_2^+$: 329.1260, found: 329.1267.

m.p. = 107–109 °C.

*2-Cyano-3,3-diphenylacrolein dimethyl acetal (**6j-2**)*

Yield: 22% (^{1}H NMR yield *vs.* 1,3,5-trimethoxybenzene after 24 h on a 100 µmol scale).

Appearance: Colorless solid.

^{1}H NMR (300 MHz, $CDCl_3$): δ [ppm] = 7.43 – 7.36 (m, 8H), 7.27 – 7.22 (m, 2H), 4.76 (s, 1H), 3.42 (s, 6H).

^{13}C{^{1}H} NMR (75.5 MHz, $CDCl_3$): δ [ppm] = 160.8, 138.9, 138.0, 130.2, 129.8, 129.8, 129.7, 128.6, 128.5, 117.5, 111.0, 100.8, 54.1.

HRMS (ESI): *m/z* calcd. for $C_{18}H_{17}NNaO_2^+$: 302.1151, found: 302.1153.

m.p. = 102–103 °C.

*Benzhydrylmalononitrile (**6j-3**)*

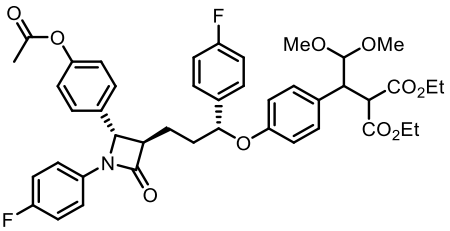
Yield: 20% (^{1}H NMR yield *vs.* 1,3,5-trimethoxybenzene after 24 h on a 100 µmol scale).

Appearance: Colorless solid.

^{1}H NMR (300 MHz, $CDCl_3$): *δ* [ppm] = 7.45 – 7.30 (m, 10H), 4.63 (d, *J* = 8.2 Hz, 1H), 4.41 (d, *J* = 8.1 Hz, 1H).

Literature: J. Che, Y. Lam, *Adv. Synth. Catal.* **2010**, *352*, 1752–1758.

Diethyl 2-(1-(4-((*R*)-3-((2*S*,3*R*)-2-(4-acetoxyphenyl)-1-(4-fluorophenyl)-4-oxoazetidin-3-yl)-1-(4-fluorophenyl)propoxy)phenyl)-2,2-dimethoxyethyl)malonate (**7a**)



By GP2 on a 50 µmol scale starting from **4a** (34.9 mg) with an irradiation time of 36 h. Purified by automated flash chromatography (C_{18}-SiO_2, 20% MeCN in H_2O → 100% MeCN).

Yield: 27.8 mg (35.9 µmol, 72%).

Appearance: Fluffy colorless solid (lyophilisate).

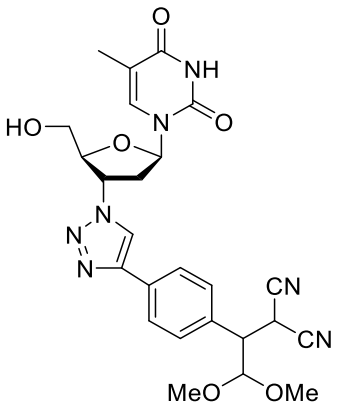
^{1}H NMR (600 MHz, C_6D_6): *δ* [ppm] = 7.31 – 7.26 (m, 2H), 7.25 – 7.21 (m, 2H), 7.01 – 6.91 (m, 4H), 6.88 – 6.83 (m, 2H), 6.79 – 6.75 (m, 2H), 6.73 – 6.68 (m, 2H), 6.64 – 6.59 (m, 2H), 4.86 – 4.82 (m, 1H), 4.61 (t, *J* = 5.9 Hz, 1H), 4.23 (dd, *J* = 10.0, 5.5 Hz, 1H), 4.10 – 4.05 (m, 2H), 4.05 – 3.96 (m, 2H), 3.75 – 3.67 (m, 2H), 3.11 (d, *J* = 2.7 Hz, 3H), 3.03 (d, *J* = 3.1 Hz, 3H), 2.77 – 2.73 (m, 0H), 2.09 – 2.00 (m, 1H), 1.95 – 1.87 (m, 1H), 1.79 – 1.73 (m, 1H), 1.72 (s, 3H), 1.69 – 1.61 (m, 1H), 0.95 (td, *J* = 7.2, 1.6 Hz, 3H), 0.65 (td, *J* = 7.1, 6.1 Hz, 3H).

^{13}C{^{1}H} NMR (101 MHz, C_6D_6): *δ* [ppm] = 168.4, 168.4, 168.0, 167.9, 166.5, 162.5 (d, *J* = 245.3 Hz), 159.3 (d, *J* = 242.4 Hz), 157.43, 157.40, 151.3, 137.6 (d, *J* = 3.4 Hz), 137.6 (d, *J* = 2.9 Hz), 135.59, 135.58, 134.7 (d, *J* = 2.7 Hz), 131.3, 130.91, 130.87, 128.3, 128.1 (d, *J* = 24.3 Hz), 127.1, 122.7, 118.4 (d, *J* = 7.9 Hz), 116.1 (d, *J* = 22.6 Hz), 115.8 (d, *J* = 21.5 Hz), 115.8, 115.7, 106.77, 106.76, 78.99, 78.97, 61.3, 61.1, 61.0, 60.9, 60.8, 60.7, 55.32, 55.31, 55.0, 54.8, 54.1, 54.0, 48.0, 47.9, 36.10, 36.08, 25.10, 25.08, 20.5, 14.1, 13.8.

^{19}F NMR (565 MHz, C_6D_6): *δ* [ppm] = −114.55 – −114.63 (m), −118.17 – −118.25 (m).

HRMS (ESI): *m/z* calcd. for $C_{43}H_{45}F_2NNaO_{10}^+$: 796.2904, found: 796.2960.

2-(1-(4-(1-((2*S*,3*S*,5*R*)-2-(Hydroxymethyl)-5-(5-methyl-2,4-dioxo-3,4-dihydropyrimidin-1(2*H*)-yl)tetrahydrofuran-3-yl)-1*H*-1,2,3-triazol-4-yl)phenyl)-2,2-dimethoxyethyl)malononitrile (**7b**)



By GP2 on a 50 µmol scale starting from **4b** (22.3 mg) with an irradiation time of 8 h. Purified by automated flash chromatography (C_{18}-SiO_2, 10% MeCN in H_2O → 100% MeCN).

Yield: 12.4 mg (23.8 µmol, 48%).

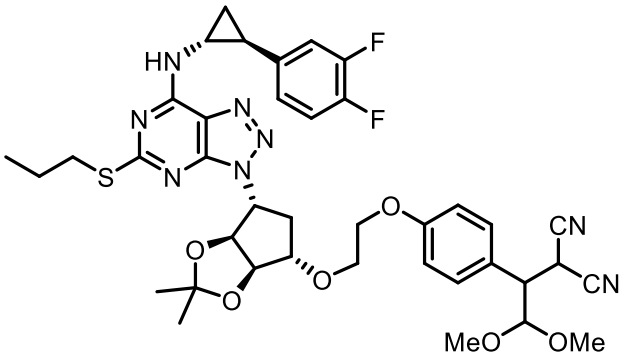
Appearance: Fluffy colorless solid (lyophilisate).

^{1}H NMR (600 MHz, DMSO-d_6): δ [ppm] = 11.37 (s, 1H), 8.80 (s, 1H), 7.90 – 7.85 (m, 2H), 7.86 – 7.82 (m, 1H), 7.56 – 7.49 (m, 2H), 6.45 (t, *J* = 6.6 Hz, 1H), 5.42 (dt, *J* = 8.7, 5.5 Hz, 1H), 5.31 (t, *J* = 5.3 Hz, 1H), 5.26 (d, *J* = 6.9 Hz, 1H), 4.83 (d, *J* = 6.8 Hz, 1H), 4.28 (dt, *J* = 5.5, 3.6 Hz, 1H), 3.87 (t, *J* = 6.9 Hz, 1H), 3.74 (ddd, *J* = 12.0, 5.4, 3.4 Hz, 1H), 3.67 (ddd, *J* = 12.1, 5.3, 3.8 Hz, 1H), 3.41 (s, 3H), 3.25 (s, 3H), 2.81 (ddd, *J* = 14.0, 6.9, 5.4 Hz, 1H), 2.71 (ddd, *J* = 14.0, 8.8, 6.5 Hz, 1H), 1.82 (d, *J* = 1.3 Hz, 3H).

^{13}C{^{1}H} NMR (101 MHz, DMSO-d_6): δ [ppm] = 163.8, 150.5, 146.1, 136.3, 135.0, 130.6, 129.5, 125.4, 121.3, 113.5, 109.7, 104.0, 84.5, 83.9, 60.8, 59.4, 55.1, 54.4, 46.3, 37.2, 25.5, 12.3.

HRMS (ESI): *m/z* calcd. for $C_{25}H_{28}N_7O_6^+$: 522.2096, found: 522.2073.

2-(1-(4-(2-(((3a*R*,4*S*,6*R*,6a*S*)-6-(7-(((1*R*,2*S*)-2-(3,4-Difluorophenyl)cyclopropyl)amino)-5-(propylthio)-3*H*-[1,2,3]triazolo[4,5-*d*]pyrimidin-3-yl)-2,2-dimethyltetrahydro-4*H*-cyclopenta[*d*]-[1,3]dioxol-4-yl)oxy)ethoxy)phenyl)-2,2-dimethoxyethyl)malononitrile (**7c**)



By GP2 on a 50 µmol scale starting from **4c** (35.7 mg) with an irradiation time of 24 h. Purified by automated flash chromatography (C_{18}-SiO_2, 20% MeCN in H_2O → 100% MeCN).

Yield: 25.1 mg (31.7 µmol, 63%).

Appearance: Fluffy colorless solid (lyophilisate).

The product is a mixture of two rotamers in DMSO-d_6 solution (Ratio 80%/20%), as is known for Ticagrelor and its derivatives.

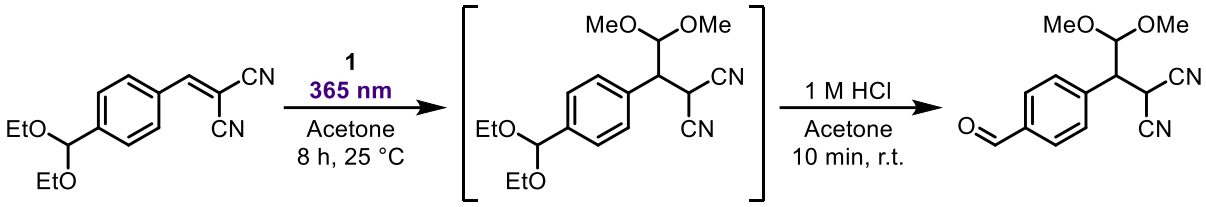
^{1}H NMR (600 MHz, DMSO-d_6): δ [ppm] = 9.38 (d, *J* = 4.1 Hz, 0.8H), 8.98 (d, *J* = 5.1 Hz, 0.2H), 7.35 – 7.27 (m, 3.8H), 7.25 – 7.19 (m, 0.2H), 7.09 – 7.03 (m, 0.8H), 7.02 – 6.97 (m, 0.2H), 6.96 – 6.91 (m, 2H), 5.25 (dd, *J* = 7.3, 4.5 Hz, 0.8H), 5.20 (dd, *J* = 7.2, 4.4 Hz, 0.2H), 5.15 (d, *J* = 6.7 Hz, 1H), 5.04 (ddd, *J* = 9.6, 6.9, 4.5 Hz, 1H), 4.76 – 4.70 (m, 1.8H), 4.69 (dd, *J* = 7.3, 3.1 Hz, 0.2H), 4.12 – 4.01 (m, 3H), 3.80 (ddd, *J* = 11.1, 5.5, 3.7 Hz, 1H), 3.76 – 3.71 (m, 2.2H), 3.38 (s, 3H), 3.21 (s, 3H), 3.17 – 3.12 (m, 0.8H), 3.11 – 3.08 (m, 0.2H), 3.04 (dt, *J* = 13.2, 7.2 Hz, 0.2H), 2.97 – 2.85 (m, 1.6H), 2.69 (dt, *J* = 13.0, 6.5 Hz, 1H), 2.58 (ddd, *J* = 13.0, 9.7, 8.2 Hz, 1H), 2.26 – 2.21 (m, 0.2H), 2.12 (ddd, *J* = 9.5, 6.3, 3.3 Hz, 0.8H), 1.73 – 1.66 (m, 0.4H), 1.57 – 1.51 (m, 2.4H), 1.49 (s, 3H), 1.46 – 1.42 (m, 0.2H), 1.42 – 1.32 (m, 1H), 1.26 (s, 2.4H), 1.25 (s, 0.6H), 0.98 (t, *J* = 7.3 Hz, 0.6H), 0.83 (t, *J* = 7.3 Hz, 2.4H).

^{19}F NMR (565 MHz, DMSO-d_6): δ [ppm] = −139.21 – −139.50 (m), −142.98 – −143.28 (m).

^{13}C{^{1}H} NMR (151 MHz, DMSO-d_6, only major signals): δ [ppm] = 169.5, 158.3, 153.9, 149.4 (dd, *J* = 240.8, 12.9 Hz), 149.1, 147.8 (dd, *J* = 239.3, 12.7 Hz), 139.2 (dd, *J* = 6.3, 3.8 Hz), 130.0, 127.2, 123.2, 122.9 (dd, *J* = 6.0, 3.0 Hz), 117.0 (d, *J* = 17.0 Hz), 114.9 (d, *J* = 17.5 Hz), 114.5, 113.6, 113.5, 112.5, 104.1, 83.7, 82.2, 81.9, 67.4, 66.8, 61.5, 55.0, 54.2, 45.9, 35.2, 34.0, 32.4, 26.8, 24.7, 23.9, 22.4, 14.9, 13.0.

HRMS (ESI): *m/z* calcd. for $C_{39}H_{45}F_2N_8O_6S^+$: 791.3146, found: 791.3122.

2-(Dicyanomethyl)-2-(4-formylphenyl)acetaldehyde dimethyl acetal



(4-(Diethoxymethyl)benzylidene)malononitrile (**2l**, 25.6 mg, 100 µmol) was irradiated for 8 h according to GP2. 1,3,5-Trimethoxybenzene was added as a standard and the ^{1}H NMR yield of the bisacetal was determined to be 80%. The $CDCl_3$ solution was concentrated and the residue was re-dissolved in acetone (1.0 mL). Aqueous hydrochlorid acid (1 M, 0.1 mL) was added and the mixture was stirred for 10 min at room temperature. The solvent was evaporated and the residue was purified by column chromatography (Neutral Al_2O_3, Pentane/EtOAc 3:1).

Yield: 19.8 mg (76.7 µmol, 96% based on the intermediate bisacetal, 77% over 2 steps).

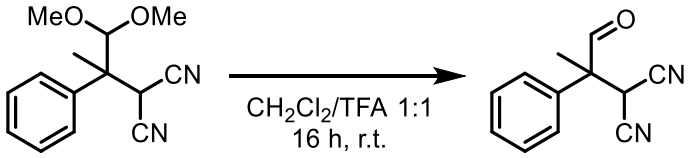
Appearance: Colorless syrup.

^{1}H NMR (300 MHz, $CDCl_3$): δ [ppm] = 10.05 (s, 1H), 8.05 – 7.87 (m, 2H), 7.68 – 7.54 (m, 2H), 4.83 (d, J = 6.5 Hz, 1H), 4.38 (d, J = 5.9 Hz, 1H), 3.59 – 3.48 (m, 4H), 3.34 (s, 3H).

^{13}C{^{1}H} NMR (75.5 MHz, $CDCl_3$): δ [ppm] = 191.6, 139.9, 136.9, 130.5, 129.8, 111.7, 111.6, 104.1, 56.7, 55.5, 49.3, 25.6.

HRMS (ESI): *m/z* calcd. for $C_{14}H_{15}N_2O_3^+$: 259.1077, found: 259.1060.

2-(Dicyanomethyl)-2-phenylpropionaldehyde



To a solution of **5w** (73.3 mg, 300 µmol) in dichloromethane (1.5 mL) was added trifluoroacetic acid (1.5 mL) in one portion. The mixture was stirred for 16 h at room temperature and concentrated using a stream of nitrogen, upon which the product solidified. The purity of the product was determined to be 92% by ^{1}H NMR *vs.* 1,3,5-trimethoxybenzene. Any purification attempts yielded a more impure product in severely diminished yields.

Yield: 92% adj. for purity (59.5 mg total/54.7 mg adj. for purity, 276 µmol).

Appearance: Yellow solid.

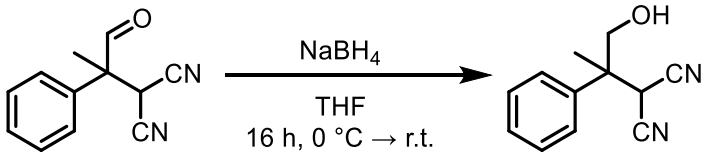
^{1}H NMR (300 MHz, $CDCl_3$): δ [ppm] = 9.42 (s, 1H), 7.56 – 7.46 (m, 2H), 7.34 – 7.28 (m, 2H), 4.34 (s, 1H), 1.93 (s, 3H).

$^{13}C\{^{1}H\}$ NMR (75.5 MHz, $CDCl_3$): δ [ppm] = 194.9, 131.8, 130.3, 130.1, 127.5, 111.2, 111.0, 56.2, 31.0, 16.3.

HRMS (ESI): *m/z* calcd. for $C_{12}H_{11}N_2O^+$: 199.0866, found: 199.0871.

m.p. = 80–87 °C.

1-Hydroxy-2-phenylpropan-2-yl)malononitrile



A solution of 2-(dicyanomethyl)-2-phenylpropionaldehyde (32.3 mg, 29.7 mg adj. for purity, 150 µmol, 1.0 equiv.) in dry tetrahydrofuran (1.5 mL) was cooled to 0 °C. Sodium borohydride (8.5 mg, 225 µmol, 1.5 equiv.) was slowly added portionwise. The mixture was kept in the slowly melting ice bath and stirred for a total of 16 h. Sat. aq. NH_4Cl (1.0 mL) was added and the mixture was partitioned between water (10 mL) and dichloromethane (10 mL). The organic phase was removed and the aqeous phase was extracted with dichloromethane (3× 5 mL). The combined organic phases were dried over Na_2SO_4, filtered, and concentrated. The residue was purified by automated flash chromatography (C_{18}-SiO_2, 10% MeCN in H_2O → 100% MeCN), followed by lyophilization.

Yield: 22.9 mg (114 µmol, 76%).

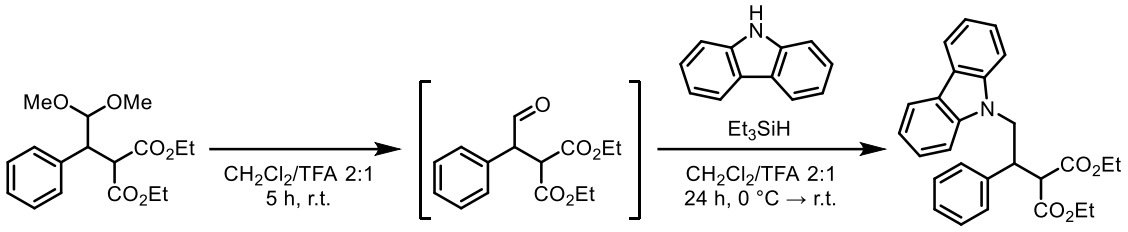
Appearance: Fluffy colorless solid (lyophilisate).

^{1}H NMR (600 MHz, DMSO-d_6): δ [ppm] = 7.40 – 7.33 (m, 4H), 7.26 – 7.22 (m, 1H), 7.14 (s, 2H), 4.33 (d, J = 8.8 Hz, 1H), 4.30 (d, J = 8.8 Hz, 1H), 1.54 (s, 3H).

$^{13}C\{^{1}H\}$ NMR (151 MHz, DMSO-d_6): δ [ppm] = 168.2, 147.2, 128.9, 127.0, 126.2, 120.0, 83.5, 59.7, 49.8, 26.7.

HRMS (ESI): *m/z* calcd. for $C_{12}H_{12}N_2NaO^+$: 223.0842, found: 223.0836.

Diethyl 2-(2-(9*H*-carbazol-9-yl)-1-phenylethyl)malonate



To a solution of **6a** (48.7 mg, 150 µmol, 1.0 equiv.) in dichloromethane (1.0 mL) was added trifluoroacetic acid (0.5 mL) in one portion. The mixture was stirred at room temperature for 5 h. Carbazole (37.6 mg, 225 µmol, 1.5 equiv.) was added in one portion and the mixture was cooled to 0 °C in an ice bath. A solution of triethylsilane (48 µL, 300 µmol, 2.0 equiv.) in dichloromethane (0.3.0 mL) was added dropwise over 30 min using a syringe pump. The mixture was stirred in the slowly melting ice bath for a total of 24 h. The straw-colored solution was concentrated by a stream of nitrogen and purified by automated flash chromatography (C_{18}-SiO_2, 25% MeCN in H_2O → 100% MeCN), followed by lyophilization.

Yield: 38.4 mg (89.4 µmol, 60%).

Appearance: Fluffy colorless solid (lyophilisate).

^{1}H NMR (300 MHz, $CDCl_3$): δ [ppm] = 7.99 – 7.87 (m, 2H), 7.67 – 7.60 (m, 1H), 7.41 – 7.30 (m, 2H), 7.23 – 7.04 (m, 7H), 6.99 – 6.90 (m, 1H), 4.26 (q, *J* = 7.2 Hz, 2H), 3.95 – 3.82 (m, 3H), 3.77 (ddd, *J* = 10.8, 10.2, 4.1 Hz, 1H), 3.28 (dd, *J* = 13.3, 4.0 Hz, 1H), 3.00 (dd, *J* = 13.4, 9.6 Hz, 1H), 1.33 (t, *J* = 7.2 Hz, 3H), 0.93 (t, *J* = 7.1 Hz, 3H).

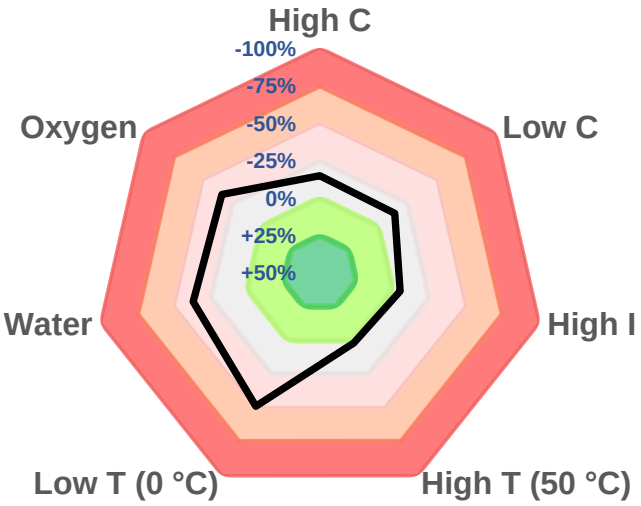
^{13}C{^{1}H} NMR (75.5 MHz, $CDCl_3$): δ [ppm] = 168.8, 168.0, 140.4, 139.8, 138.2, 130.1, 128.8, 128.2, 127.6, 126.9, 125.8, 123.4, 123.3, 120.9, 120.4, 119.4, 110.6, 110.1, 61.8, 61.3, 58.0, 48.4, 41.1, 14.3, 13.8.

HRMS (ESI): *m/z* calcd. for $C_{27}H_{28}NO_4^+$: 430.2013, found: 430.2017.

Sensitivity Assessment

The reactions were set up using the standard conditions (0.10 mmol scale, 1.0 equiv. **2a**, 1.2 equiv. **1**, Acetone (0.1 M), 365 nm, 8 h, r.t.) in combination with the deviations shown below. The yields were determined *via* ^{1}H NMR spectroscopy using 1,3,5-trimethoxybenzene as the standard.

Entry	Deviations from standard conditions	Yield of 5a [%]	Difference in yield to standard conditions (85%) [%]
High *c*	0.2 M	70	−15
Low *c*	0.05 M	71 (85% conv.)	−14
High *I*	Vial placed ~1 cm in front of the LED, cooled by a desk fan	80	−5
High *T*	50 °C	83	−2
Low *T*	0 °C	36 (42% conv.)	−49
Water	+ 1 vol.% degassed water	59 (incompl. conv.)	−37
Oxygen	+ 2 mL of dry air added	51 (68% conv.)	−34



Determination of the Excited-State Redox Potential of 1

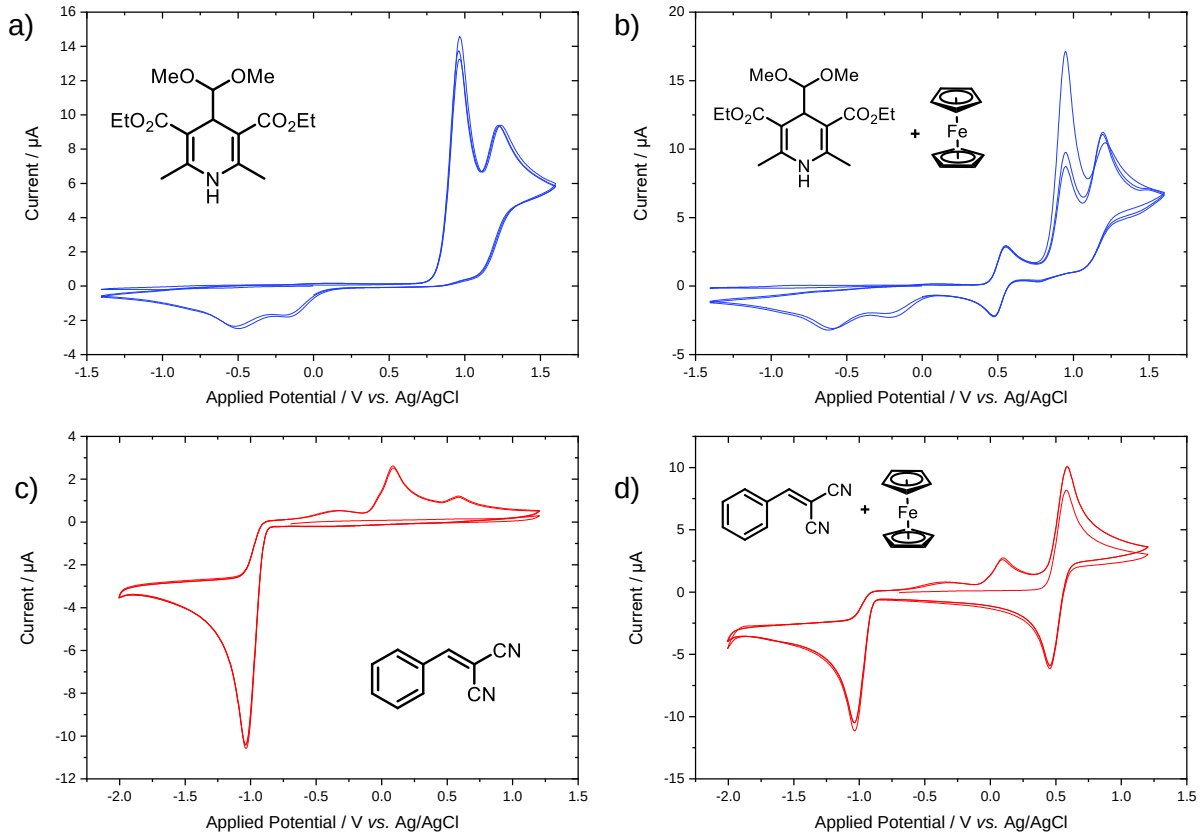


Figure 3. *Cyclic voltammograms (CVs) of* ***1*** *and* ***2a****. Scan rates 100 mV·s^{-1}, 5 cycles each. a) CV of* ***1*** *(1.0 mM) in 0.10 M Bu_4NPF_6 in MeCN (7.0 mL). ±0.00 V → +1.60 V → –1.40 V → ±0.00 V. b) Same as a), but with a spatula tip of ferrocene added as internal reference. c) CV of* ***2a*** *(1.0 mM) in 0.10 M Bu_4NPF_6 in MeCN (7.0 mL). –0.70 V → +1.20 V → –2.00 V → –0.70 V. d) Same as c), but with a spatula tip of ferrocene added as internal reference.*

Cyclic voltammetry was performed to investigate the oxidation/reduction behavior of **1** and **2a** (Fig. 3). Hantzsch ester **1** shows an irreversible oxidation with an anodic peak potential of $E_{pa} \approx$ +0.95 V. Using ferrocene as an internal standard ($E^{1/2}$ = +0.51 V), the redox potential of **1** was determined as $E(\mathbf{1}^{\cdot+}/\mathbf{1})$ = +0.44 V *vs.* Fc/Fc$^+$. Using the conversion factor of $E^{1/2}$(Fc$^+$/Fc) = +0.40 V vs. SCE:

$$E(\mathbf{1}^{\cdot+}/\mathbf{1}) = +0.84 \text{ V vs. SCE}$$

Benzylidenemalononitrile (**2a**) shows an irreversible reduction with a cathodic peak potential of $E_{pc} \approx$ –1.04 V. Using ferrocene as an internal standard ($E^{1/2}$ = +0.52 V), the redox potential of **2a** was determined as $E(\mathbf{2a}/\mathbf{2a}^{\cdot-})$ = –1.56 V vs. Fc/Fc$^+$. Using the conversion factor of $E^{1/2}$(Fc$^+$/Fc) = +0.40 V vs. SCE:

$$E(\mathbf{2a}/\mathbf{2a}^{\cdot-}) = -1.16 \text{ V vs. SCE}$$

To approximate the redox potential of **1** in its singlet excited state, the equation

$$E(\mathbf{1}^{\cdot+}/\mathbf{1}^{*}) = E(\mathbf{1}^{\cdot+}/\mathbf{1}) - E_{0,0}$$

where $E_{0,0}$ is the singlet energy, also known as the zero-zero-transition energy (that is the energy of the lowest vibrational state of the first singlet excited state), was used. $E_{0,0}$ is approximated from the UV-Vis (absorption) and fluorescence (emission) spectrum according to the mirror image rule as the intersection of the normalized curves (Fig 4).

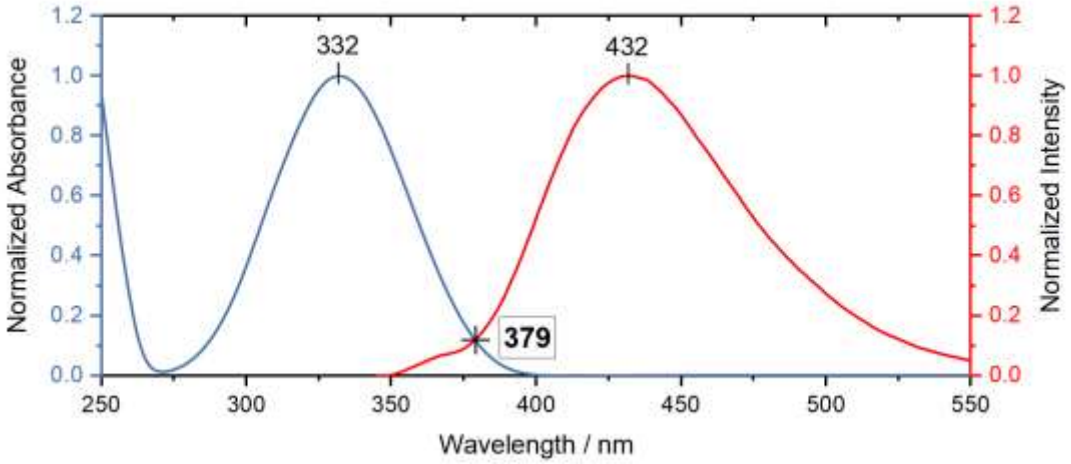
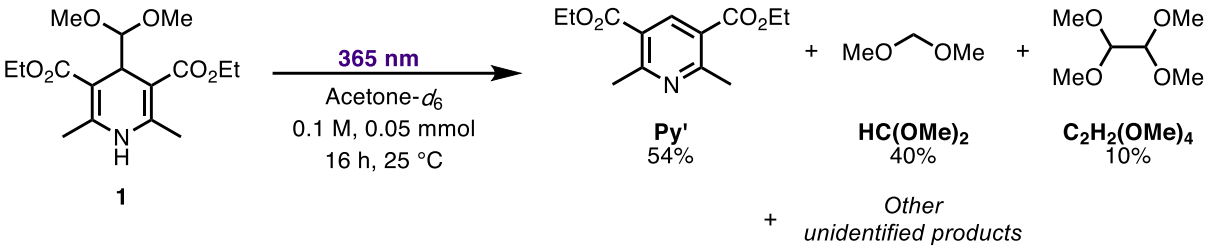


Figure 4. *Blue: Normalized UV-Vis absorption spectrum of **1**, 0.3 mM in MeCN, path length 10 mm. Red: Normalized fluorescence spectrum of **1**, 90 degree mode, 0.3 mM in MeCN, 10 mm cuvette, excitation wavelength: 330 nm, excitation slit: 10 nm, emission slit: 10 nm.*

The intersection was found to be 379 nm, which corresponds to an energy of 77.1 kcal·mol^{-1}, or 323 kJ·mol^{-1}, or 3.27 eV (≙ 3.27 V for one electron). The excited state redox potential in the singlet state S_1 is thus approximately

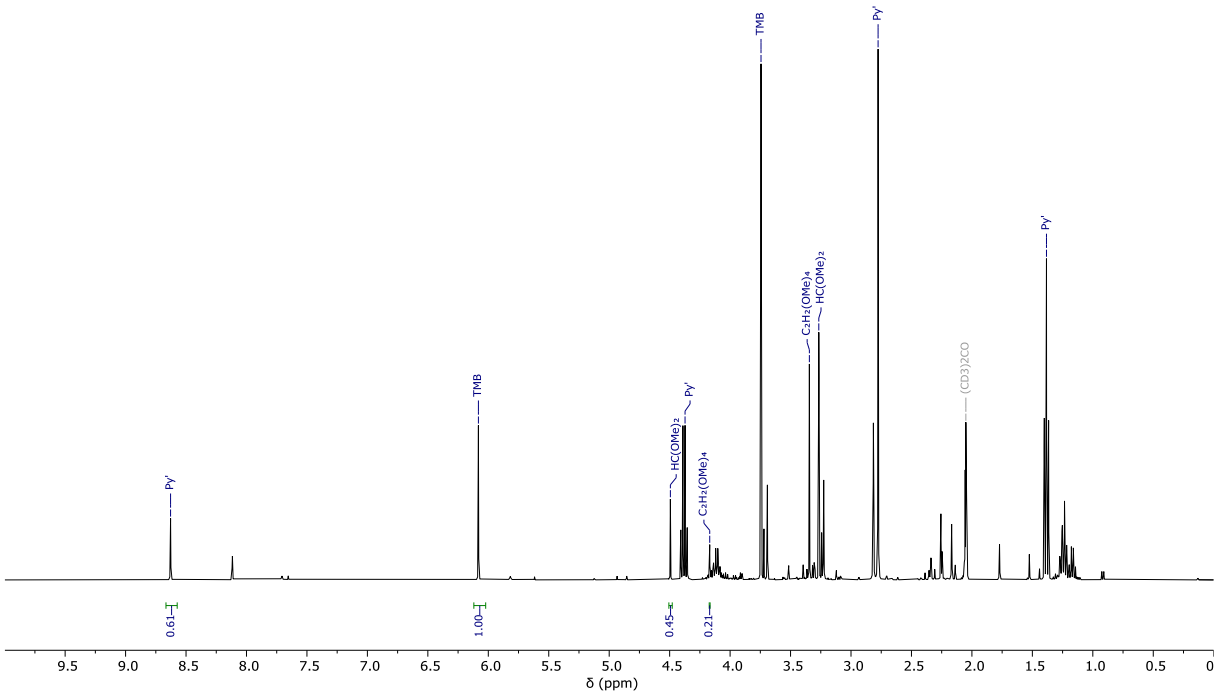
$$E(\mathbf{1}^{\cdot+}/\mathbf{1}^{*}) = 0.84\ \text{V} - 3.27\ \text{V} = \underline{-2.40\ \text{V vs. SCE}}.$$

Photolysis of 1

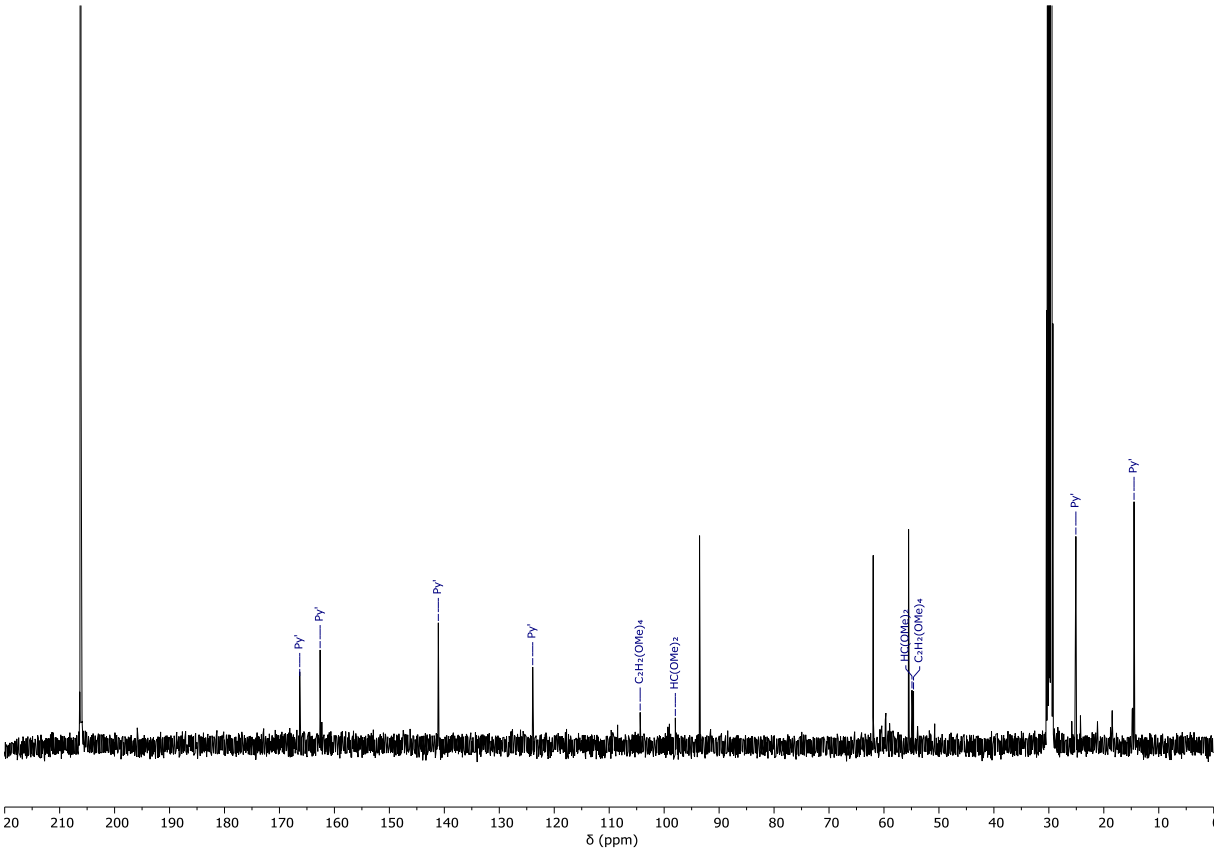


Hantzsch ester **1** (16.4 mg, 50.0 µmol) was weighed into a 4 mL glass vial, equipped with a stir bar and closed with a septum screw cap which was punctured by a cannula. The vial was transferred into an argon-filled glove box and dry, degassed acetone-d_6 (0.5 mL, 0.1 M) was added. The vial was closed, removed from the glove box, and placed into an *EvoluChem PhotoRedOx Box TC* filled with silicone oil that was kept at 25.0 °C. The mixture was vigorously stirred under irradiation (**365 nm**) for 16 h. 1,3,5-Trimethoxybenzene (2.50 mg) was added as an internal standard and an ^{1}H and ^{13}C NMR spectrum was recorded. The presence of dimethoxymethane and glyoxal tetramethyl acetal was proven by comparison with authentic spectra in acetone-d_6 and quantified *vs.* 1,3,5-trimethoxybenzene.

The corresponding spectra of the crude reaction mixtures are shown below. Py' = Diethyl 2,6-dimethylpyridine-3,5-dicarboxylate, TMB = 1,3,5-trimethoxybenzene, $HC(OMe)_2$ = Dimethoxymethane, $C_2H_2(OMe)_4$ = Glyoxal tetramethyl acetal.

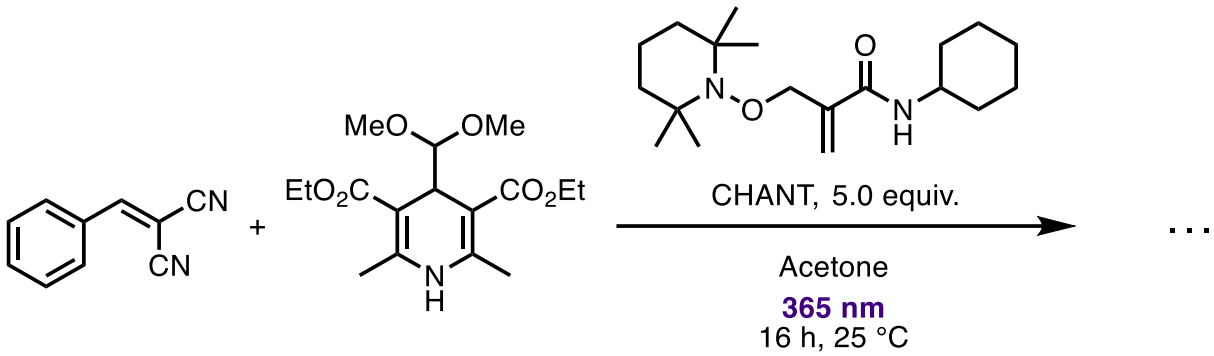


^{1}H NMR spectrum (400 MHz, acetone-d_6) of the crude reaction mixture after irradiation of **1**.



^{13}C NMR spectrum (101 MHz, acetone-d_6) of the crude reaction mixture after irradiation of **1**.

Radical-Trapping Experiments



A standard reaction on a 100 µmol scale according to GP2 was set up using benzylidenemalononitrile with the addition of *N*-cyclohexyl-2-(((2,2,6,6-tetramethylpiperidin-1-yl)oxy)methyl)acrylamide (CHANT, 161 mg, 500 µmol, 5.0 equiv.). The crude reaction mixture after irradiation for 16 h was analyzed by both GC-EI-MS and by ESI-MS (Figs. 5–7).

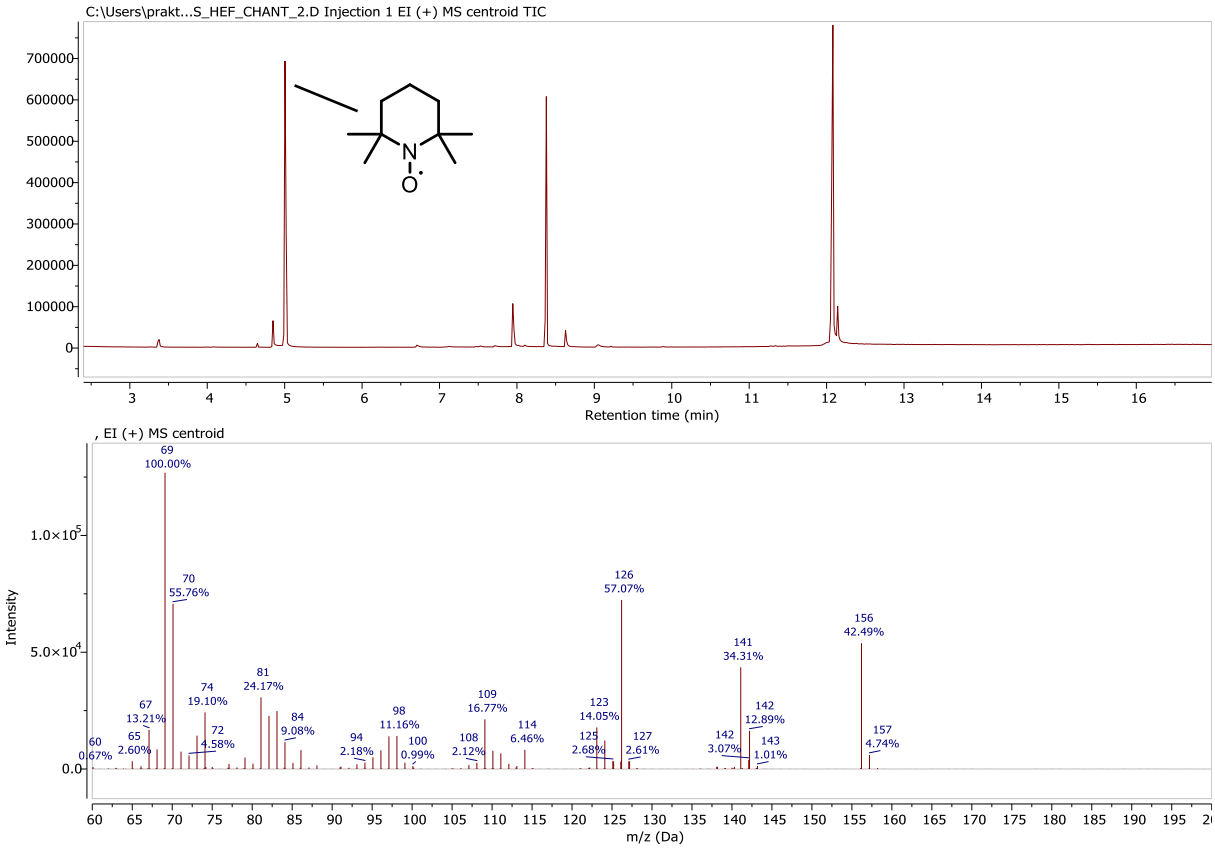


Figure 5. *GC-MS chromatogram of the crude reaction mixture and the EI-mass spectrum of detected TEMPO.*

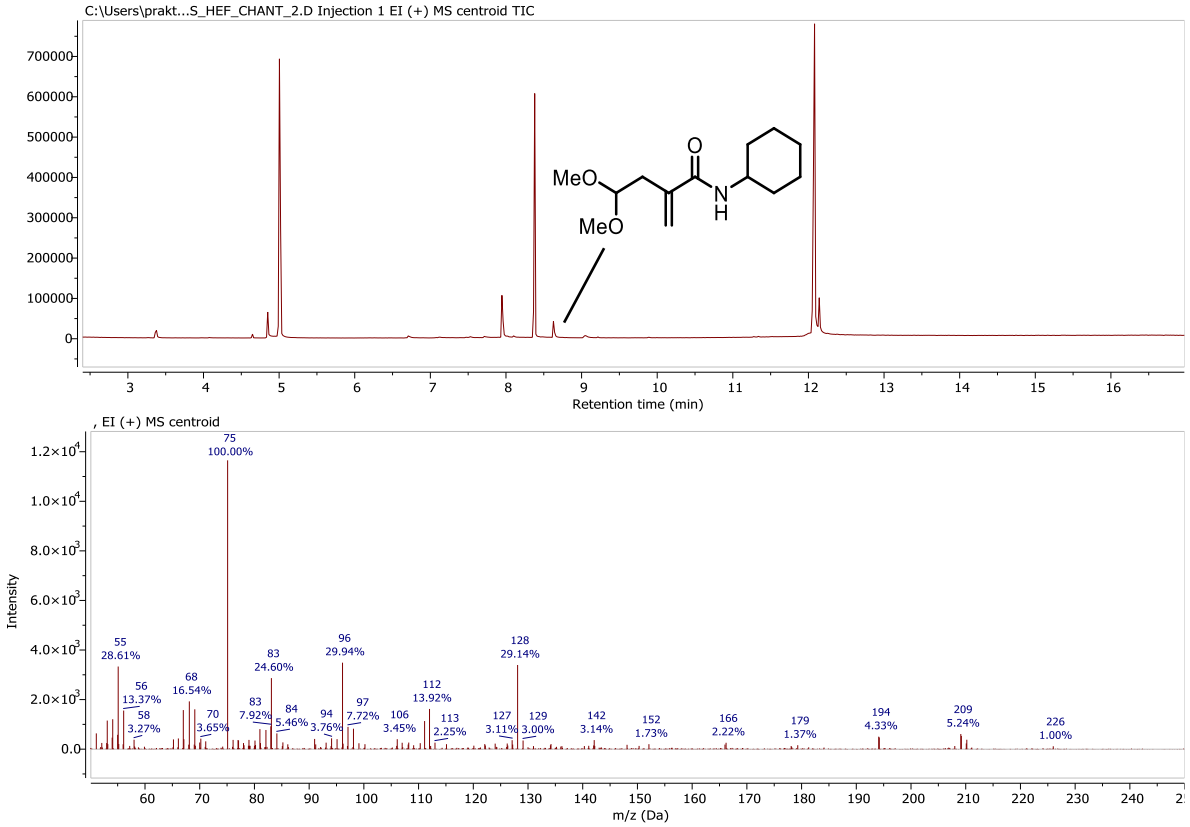


Figure 6. *GC-MS chromatogram of the crude reaction mixture and the EI-mass spectrum of detected TEMPO-CHANT.*

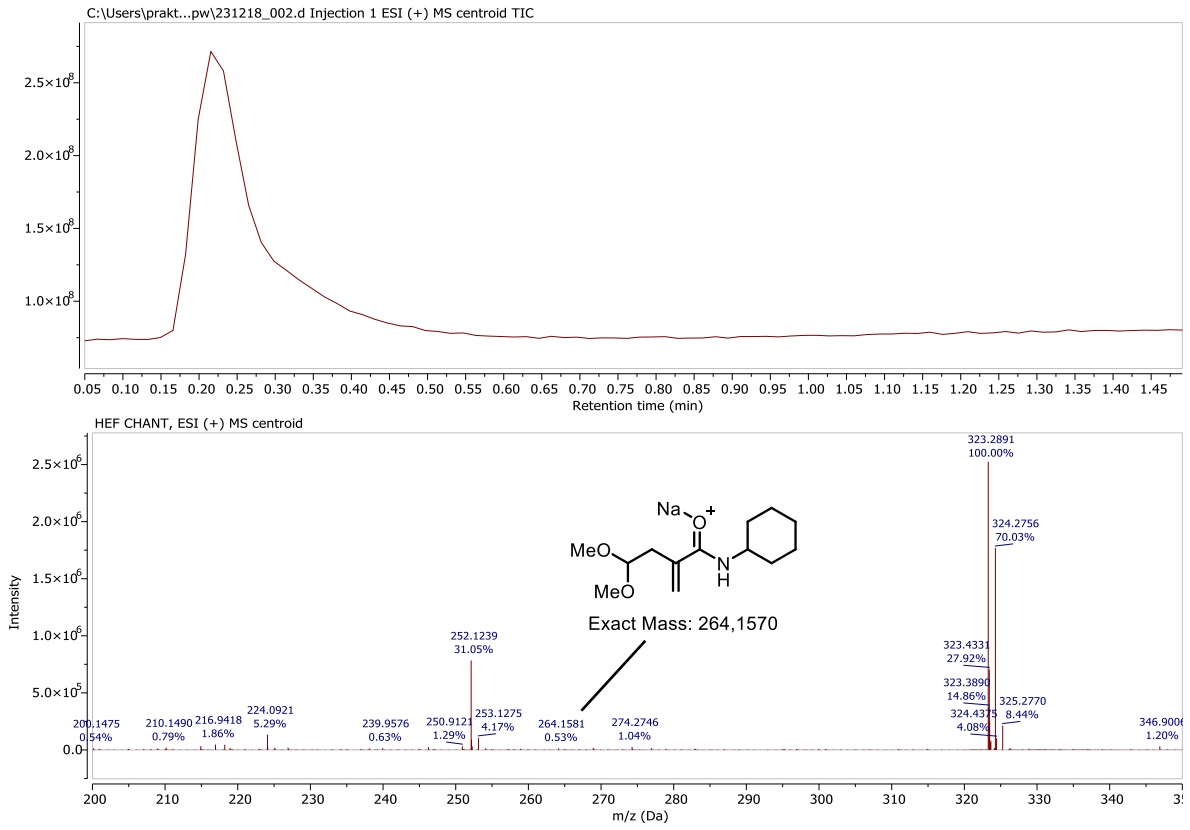


Figure 7. *ESI-mass spectrum of the crude reaction mixture and the highlighted signal of detected TEMPO-CHANT.*

Quantum Yield Determination

The reaction quantum yield Φ_R was measured using a *Quantum Yield Determination Setup* (*QYDS*) by Eberhard Riedle *et al.* (U. Megerle, R. Lechner, B. König, E. Riedle, *Photochem. Photobiol. Sci.* **2010**, *9*, 1400–1406, see www.qyds.info for further details). The setup is shown schematically in Figure 8 below. The LED light source (*Seoul Viosys* CUN6GB21A, 370 nm) is powered by a *Korad* KA3005P DC Power Supply. The light is passed through a sample cuvette onto a standard solar cell. The voltage is read by a *PicoScope* 2204A USB Oscilloscope and converted to a power reading after prior calibration using a *Coherent* PowerMax USB PS19Q.

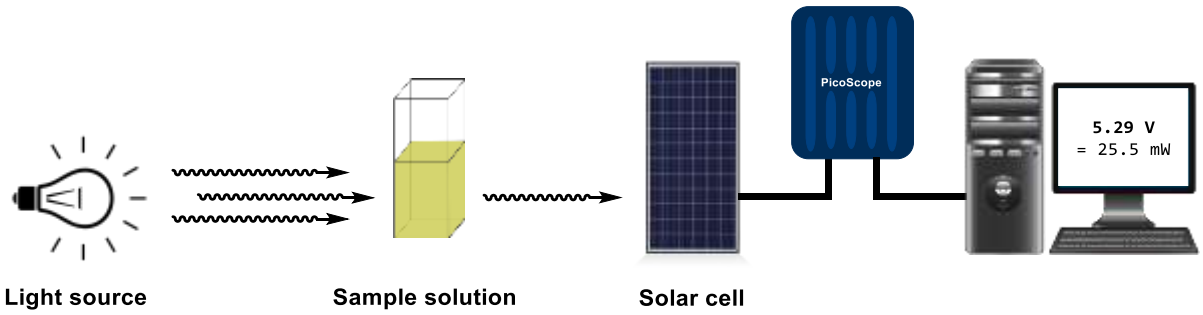


Figure 8. *Schematic depiction of the setup used for quantum yield determination.*

The energy of the light that has been absorbed by the reaction mixture is

$$E_{abs} = \mathrm{h}\upsilon \cdot N_{\mathrm{Photons}} = \frac{\mathrm{hc}}{\lambda} \cdot N_{\mathrm{Photons}} \tag{1}$$

and also

$$E_{abs} = P_{\mathrm{beam}} t - \int_{t=0}^{t} P(t)\, dt \tag{2}$$

with P_{beam} being the radiant flux of the pure beam and $P(t)$ being the power of the solar cell measured over time throughout the irradiation of the sample. This leads to

$$N_{\mathrm{Photons}} = \frac{\lambda}{\mathrm{hc}} \left(P_{\mathrm{beam}} t - \int_{t=0}^{t} P(t)\, dt \right) \tag{3}$$

Using the definition of the reaction quantum yield

$$\Phi_R = \frac{N_{\mathrm{Molecules}}}{N_{\mathrm{Photons}}} \tag{4}$$

results in

$$\Phi_R = \frac{\mathrm{hc} \cdot N_{\mathrm{Molecules}}}{\lambda \left(P_{\mathrm{beam}} t - \int_{t=0}^{t} P(t)\, dt \right)} \tag{5}$$

Combining the constants, including unit conversions, and using $N_{\mathrm{Molecules}} = n \cdot \mathrm{N_A}$:

$$\Phi_{\mathrm{R}} = 1994000 \cdot \frac{n}{\lambda \left(P_{\mathrm{beam}} t - \int_{t=0}^{t} P(t)\, dt \right)} \tag{6}$$

with n being the amount of product in **mmol**, λ being the wavelength of the light in **nm**, P_{beam} being the radiant flux of the light beam in **mW**, t being the irradiation time in **min**, and $\int_{t=0}^{t} P(t)\, dt$ being the integral of the radiant flux vs. time plot in **mW·min**.

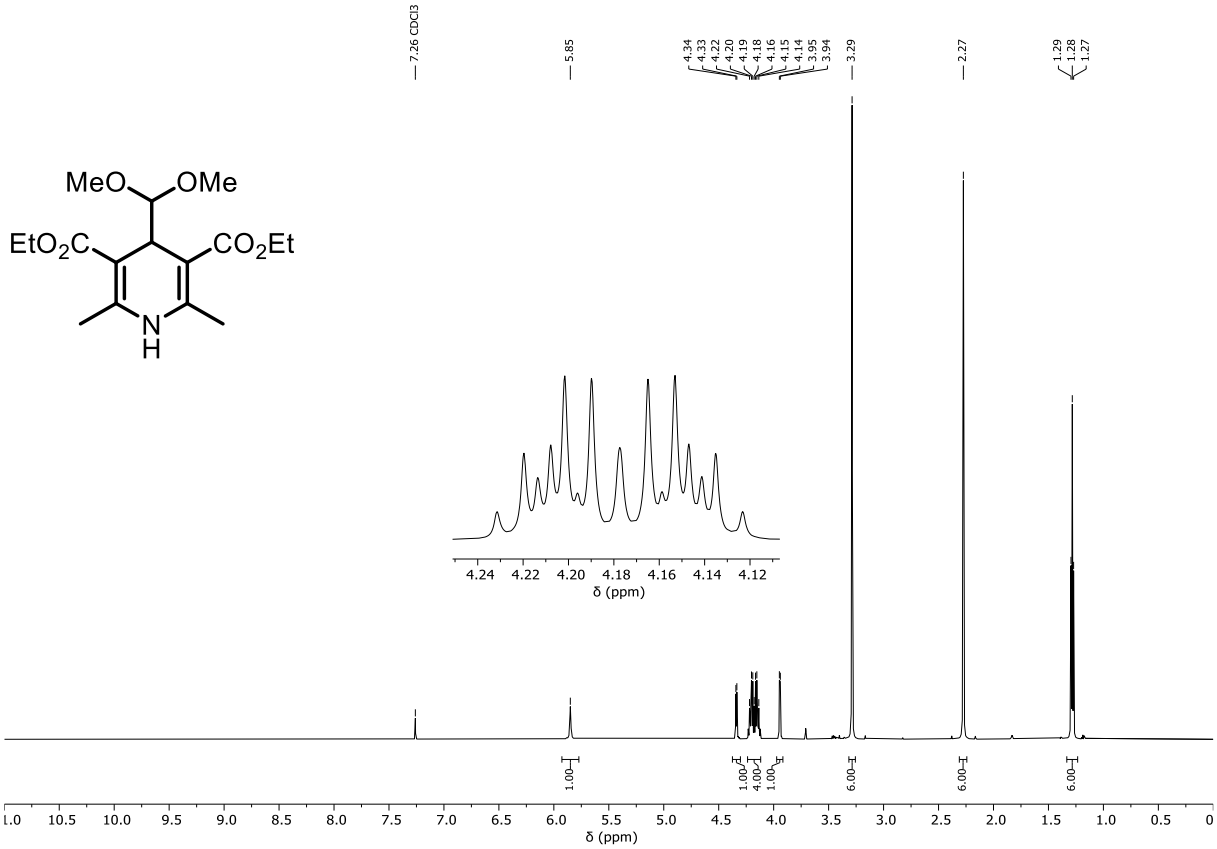
Illumination was performed at λ = 370 nm at a constant current of 96.0 mA and a voltage of 3.29 V. The radiant flux of the beam after passing through the cuvette containing the solvent P_{beam} was found to be 48.0 mW with a voltage of 9.97 V being measured (calibration factor: 4.814 mW·V^{-1} at 370 nm).

The reaction between **1** and **2a** was set up under standard conditions on a scale of 70.0 µmol in a *Hellma* QS Transmission Cuvette (4 mm, screw cap) equipped with a stir bar. The reaction was irradiated for t = 60.0 min in total while stirring and measuring the radiant flux of the light beam after passing through the reaction mixture. The measured voltage fluctuated between 0 and 10 mV, which means that the sample cuvette absorbed practically all the incident light ($P(t) \approx 0$).

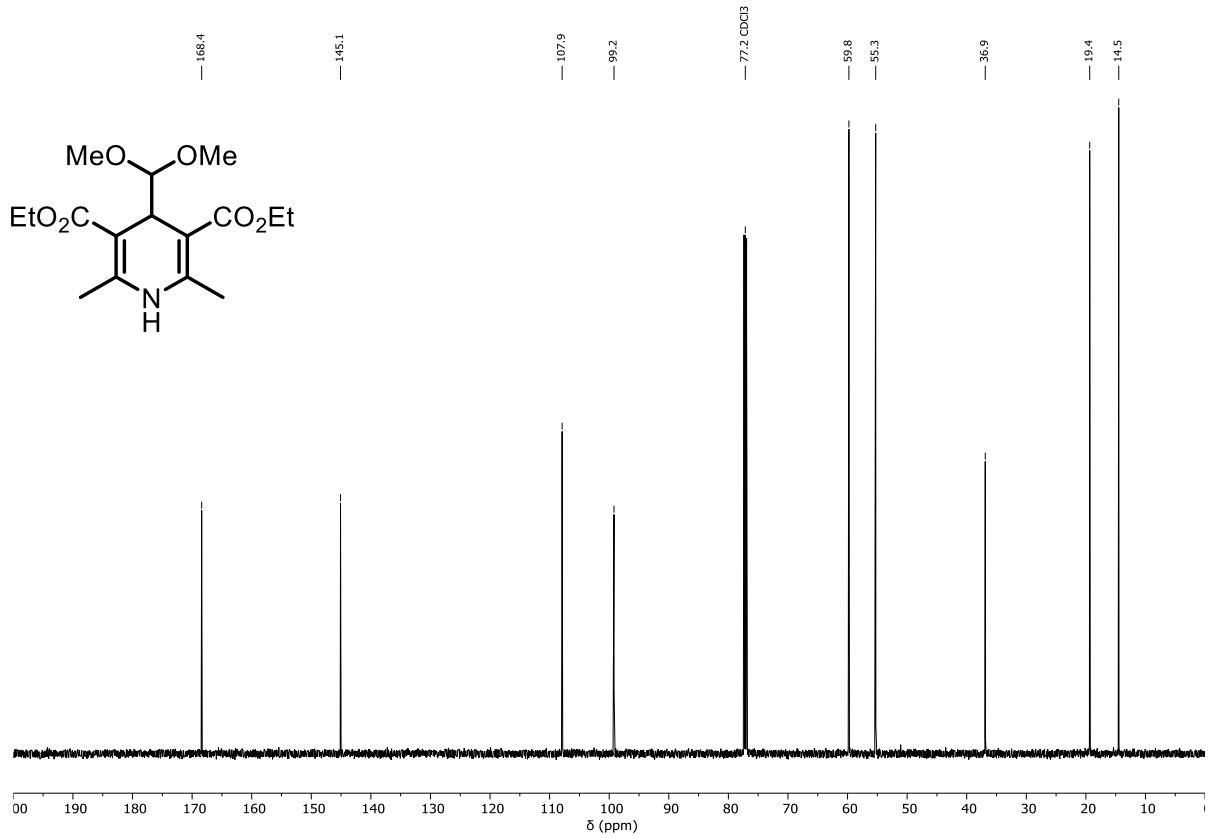
After irradiation, 1,3,5-trimethoxybenzene was added to the mixture as a standard and the yield was determined by ^{1}H NMR. A yield of 8.2% was found, that is 5.7·10^{-3} mmol.

According to equation 6: $\Phi_{\mathrm{R}} = 0.011 = 1.1\%$.

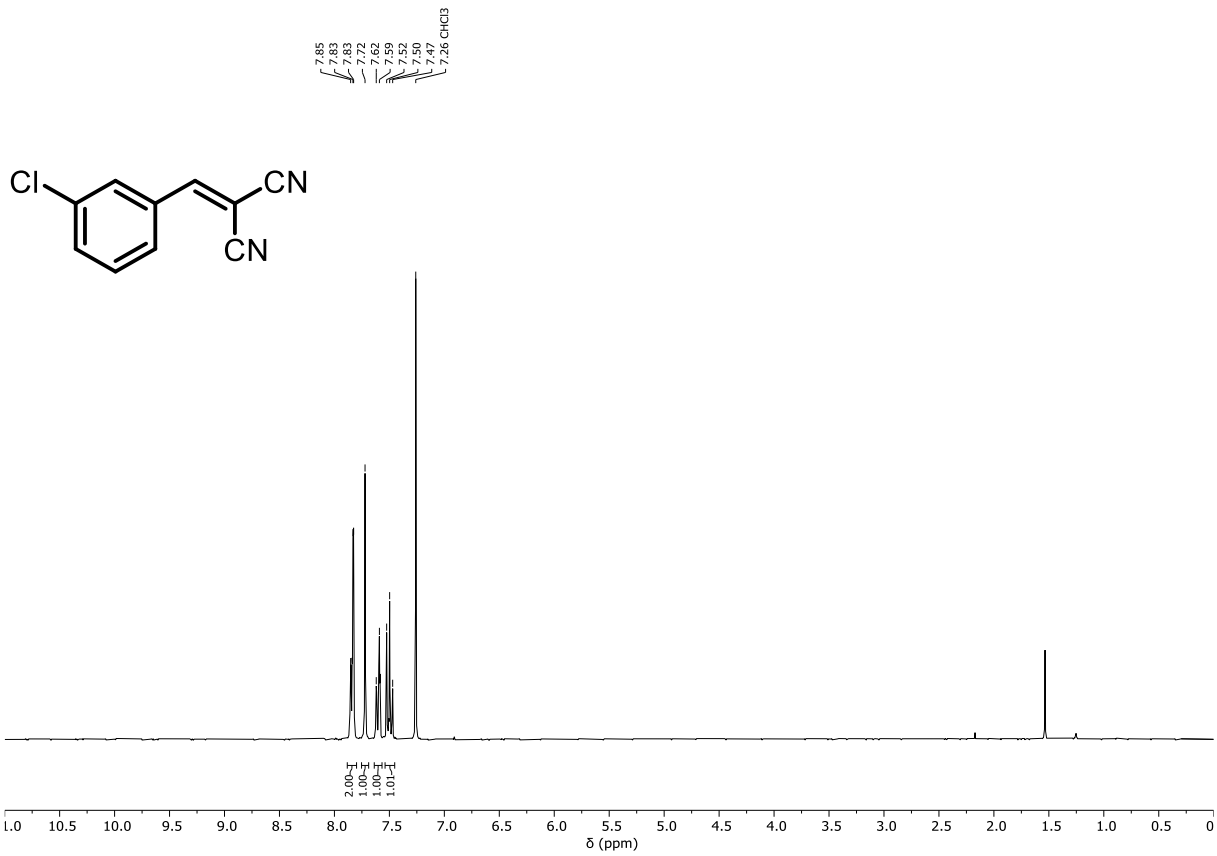
NMR Spectra of all Compounds



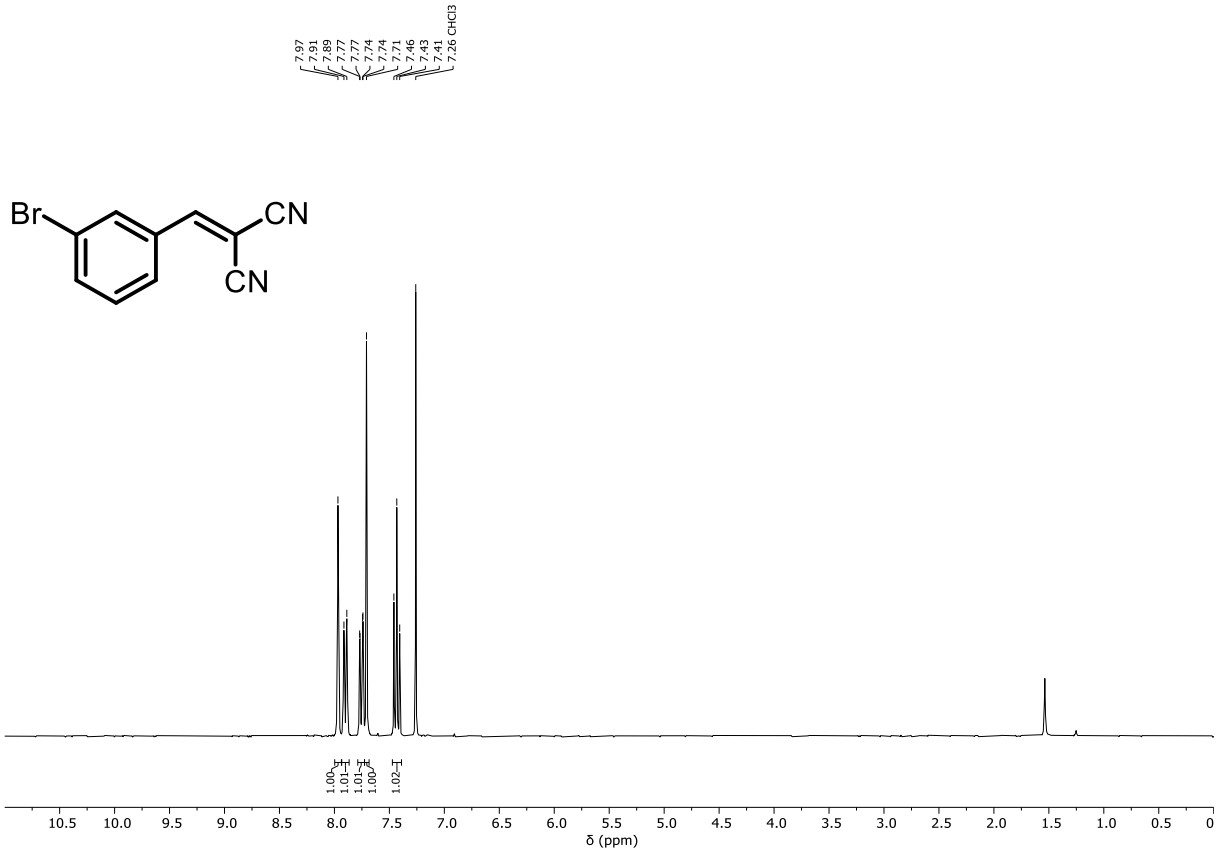
^{1}H NMR spectrum (600 MHz, $CDCl_3$) of **1**



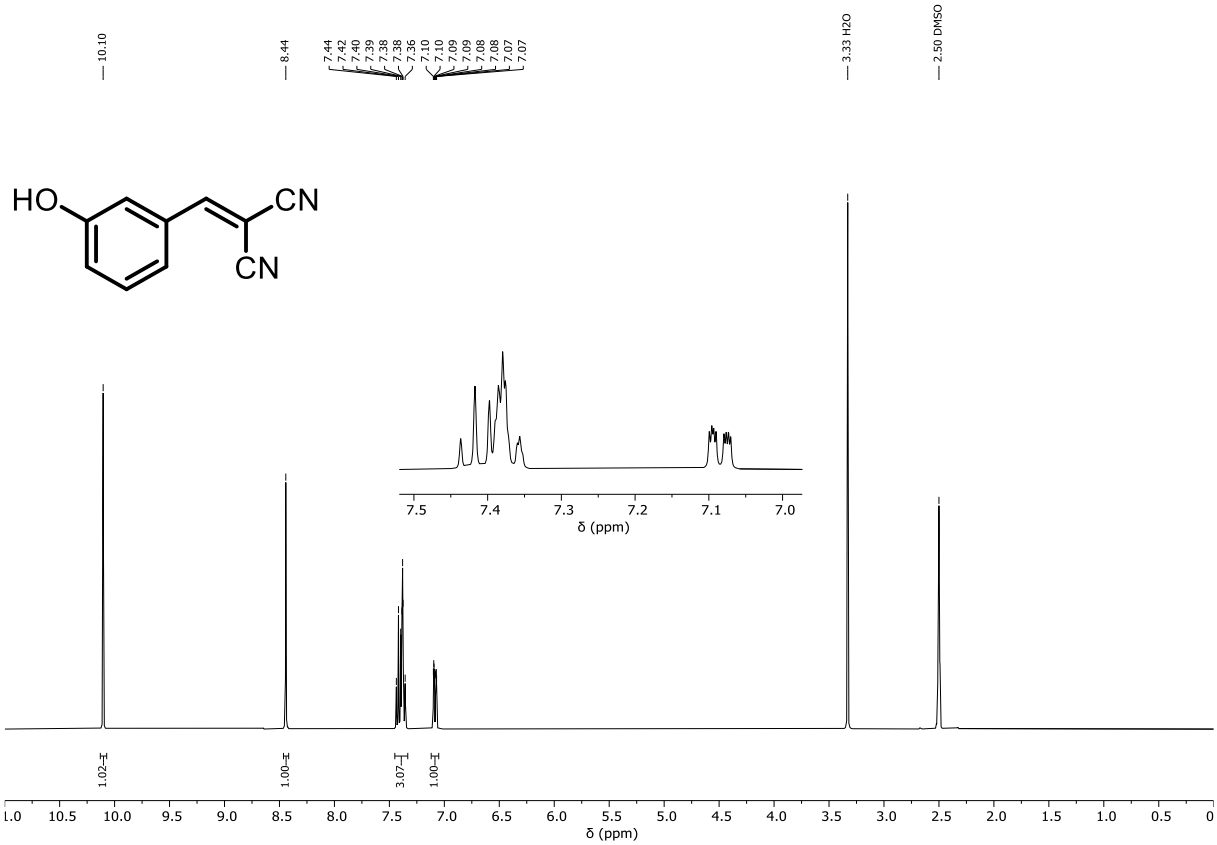
^{13}C NMR spectrum (151 MHz, $CDCl_3$) of **1**



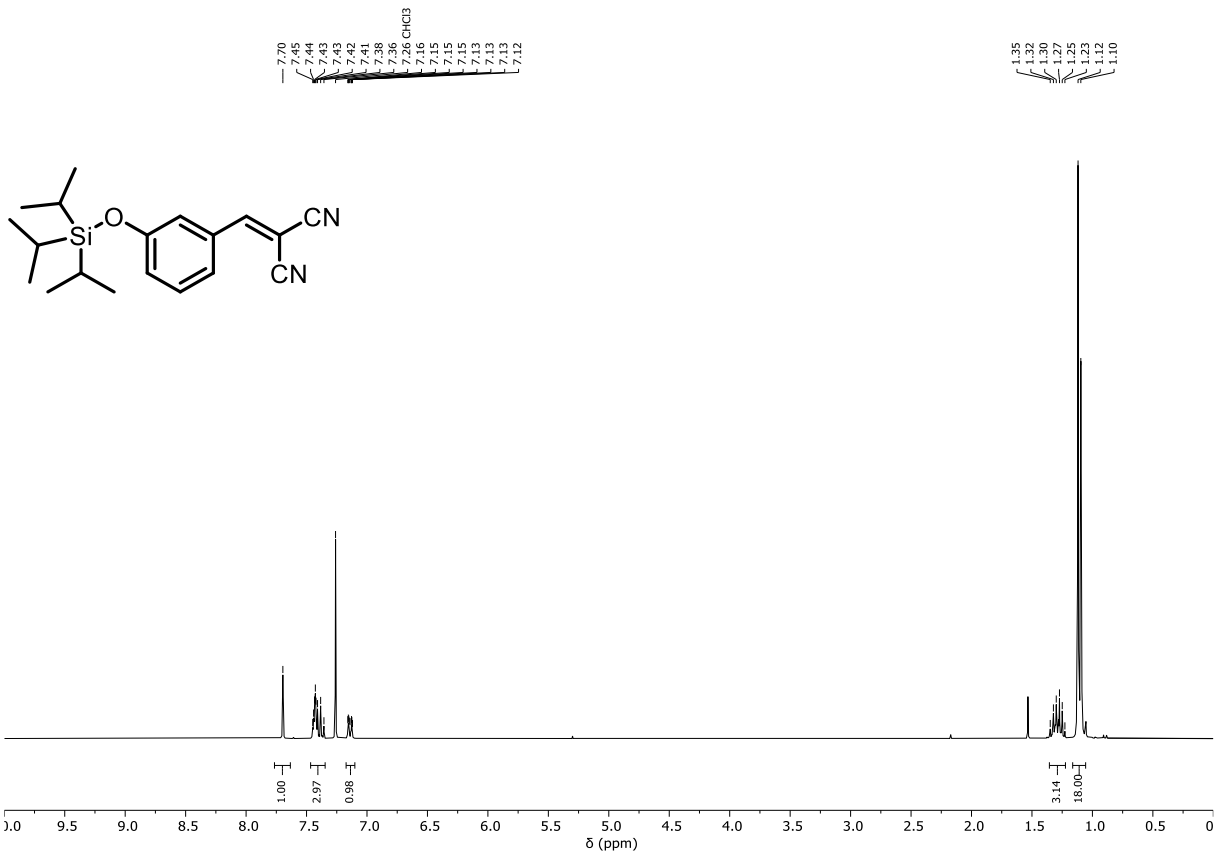
^{1}H NMR spectrum (300 MHz, $CDCl_3$) of **2b**



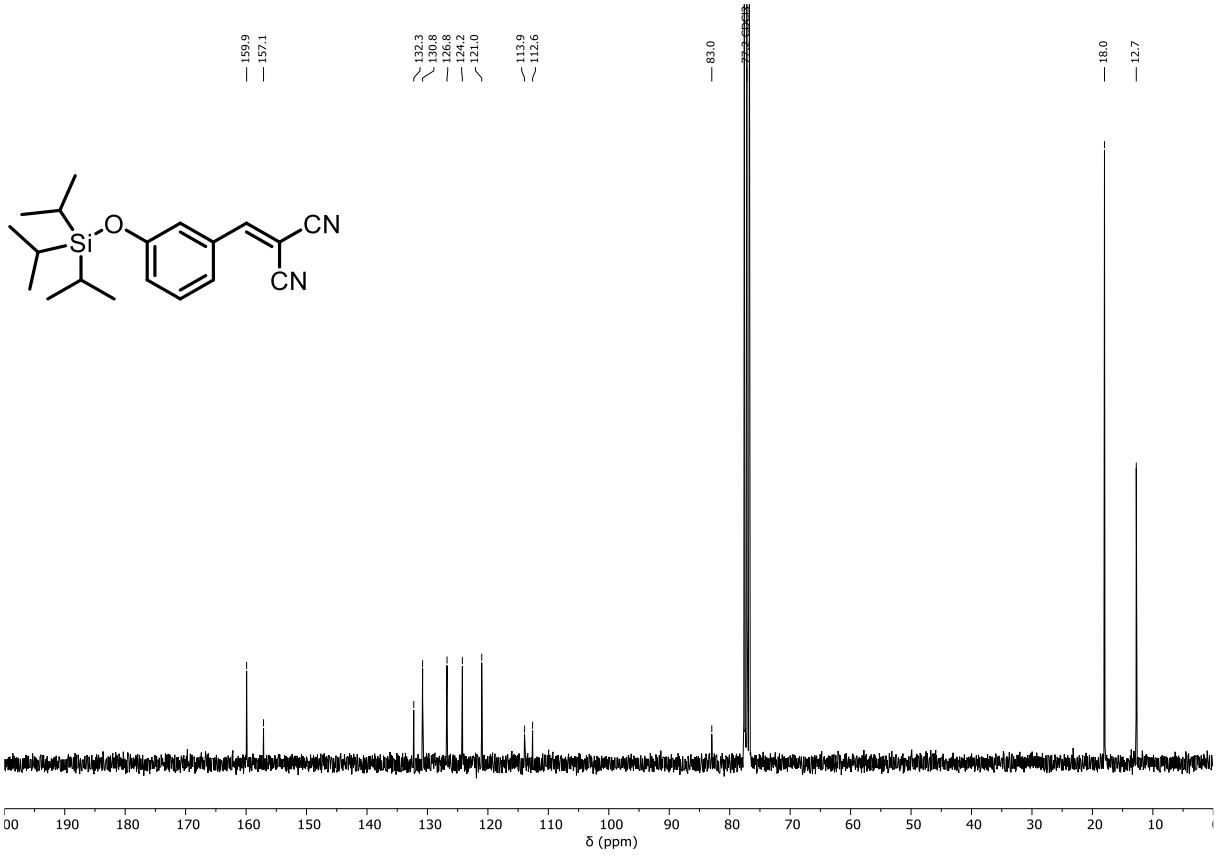
^{1}H NMR spectrum (300 MHz, $CDCl_3$) of **2c**



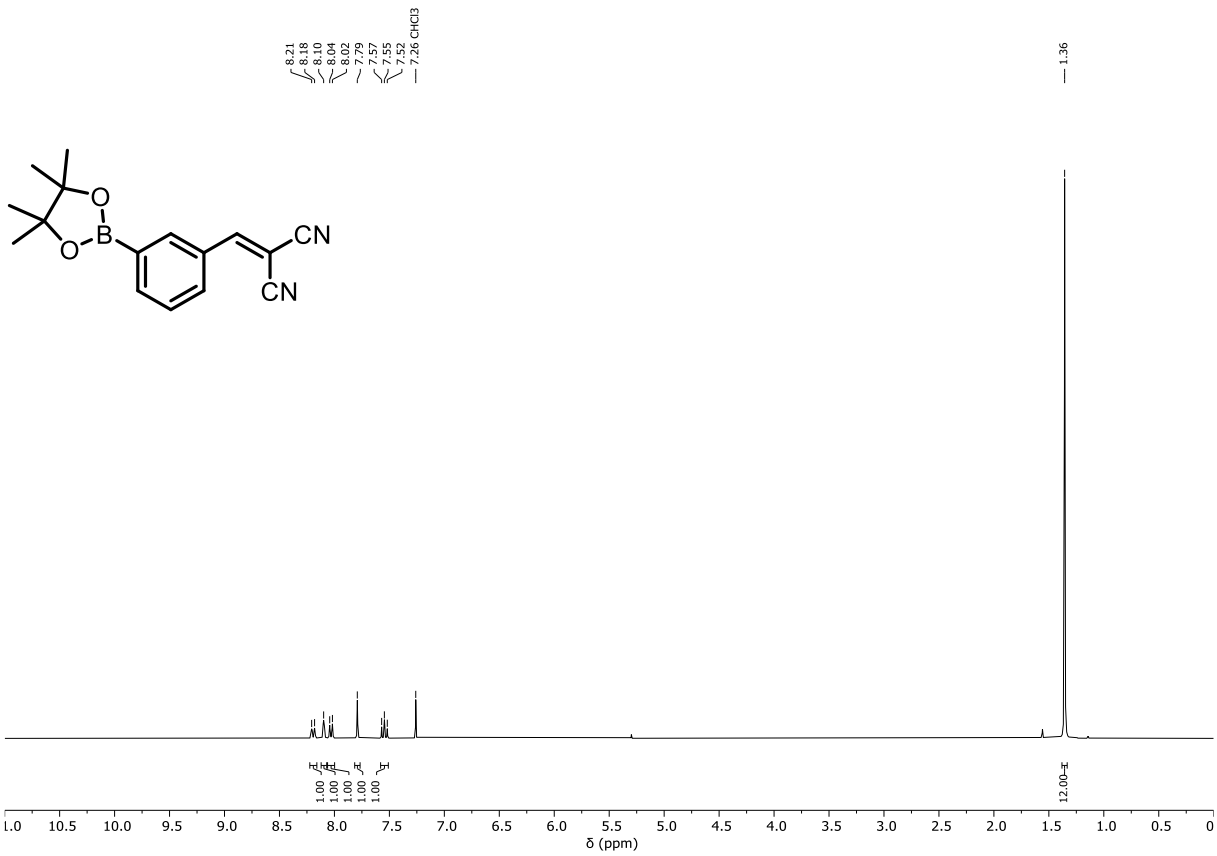
^{1}H NMR spectrum (400 MHz, DMSO-d_6) of **2d**



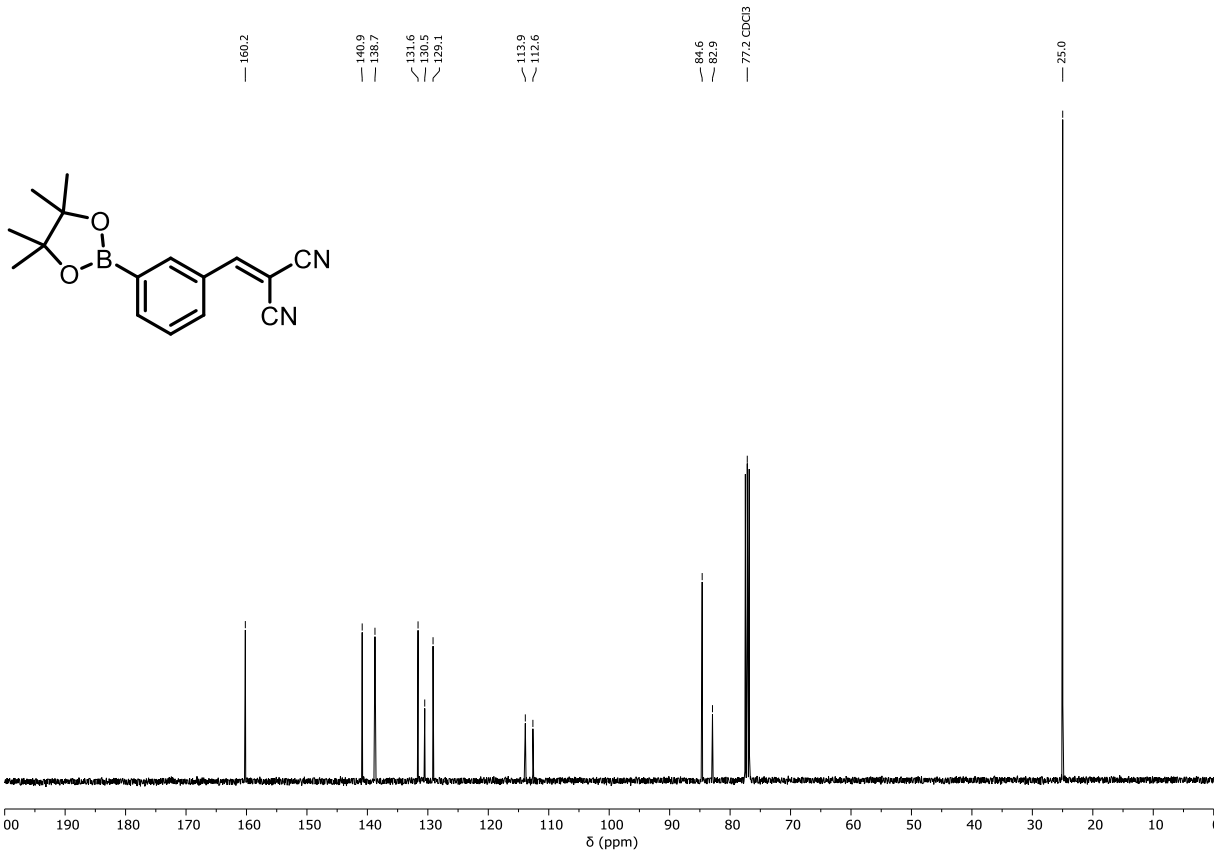
^{1}H NMR spectrum (300 MHz, $CDCl_3$) of **2f**



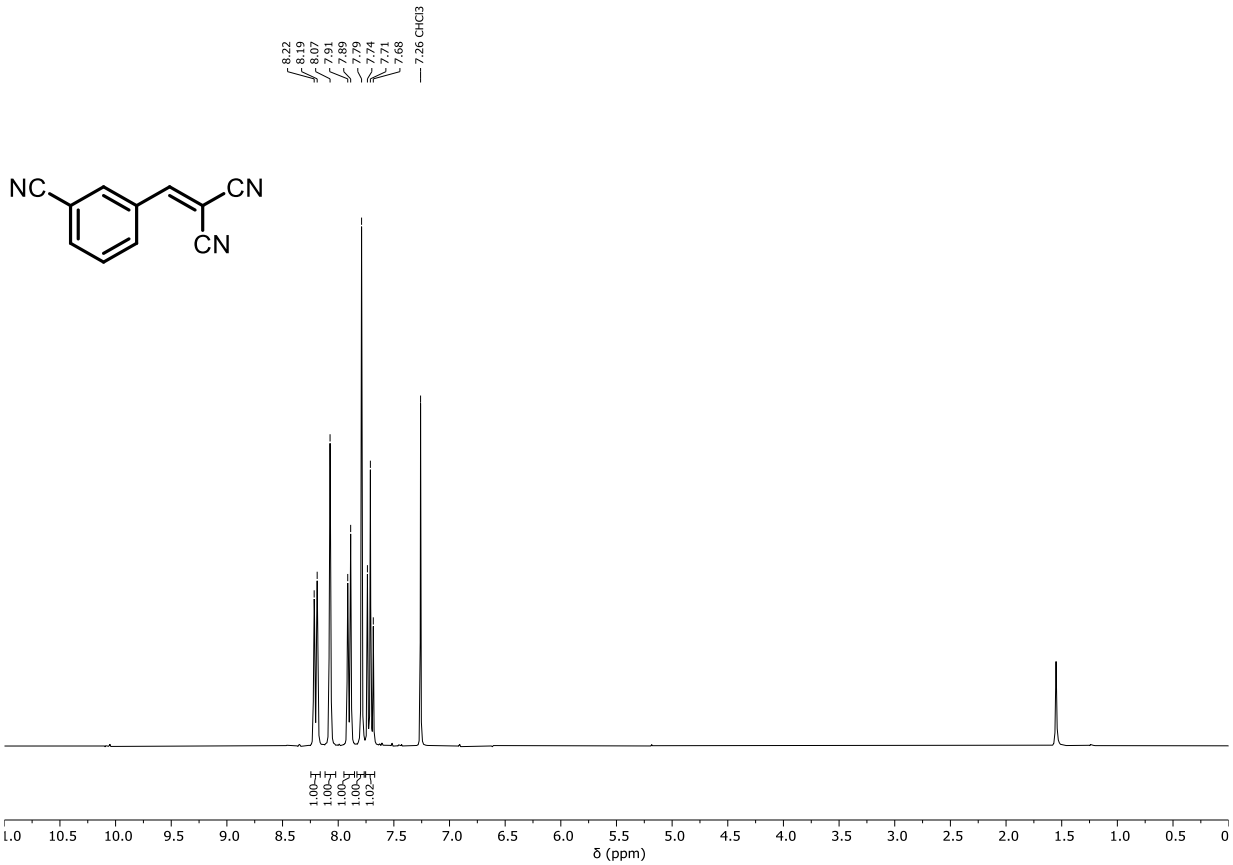
^{13}C NMR spectrum (75.5 MHz, $CDCl_3$) of **2f**



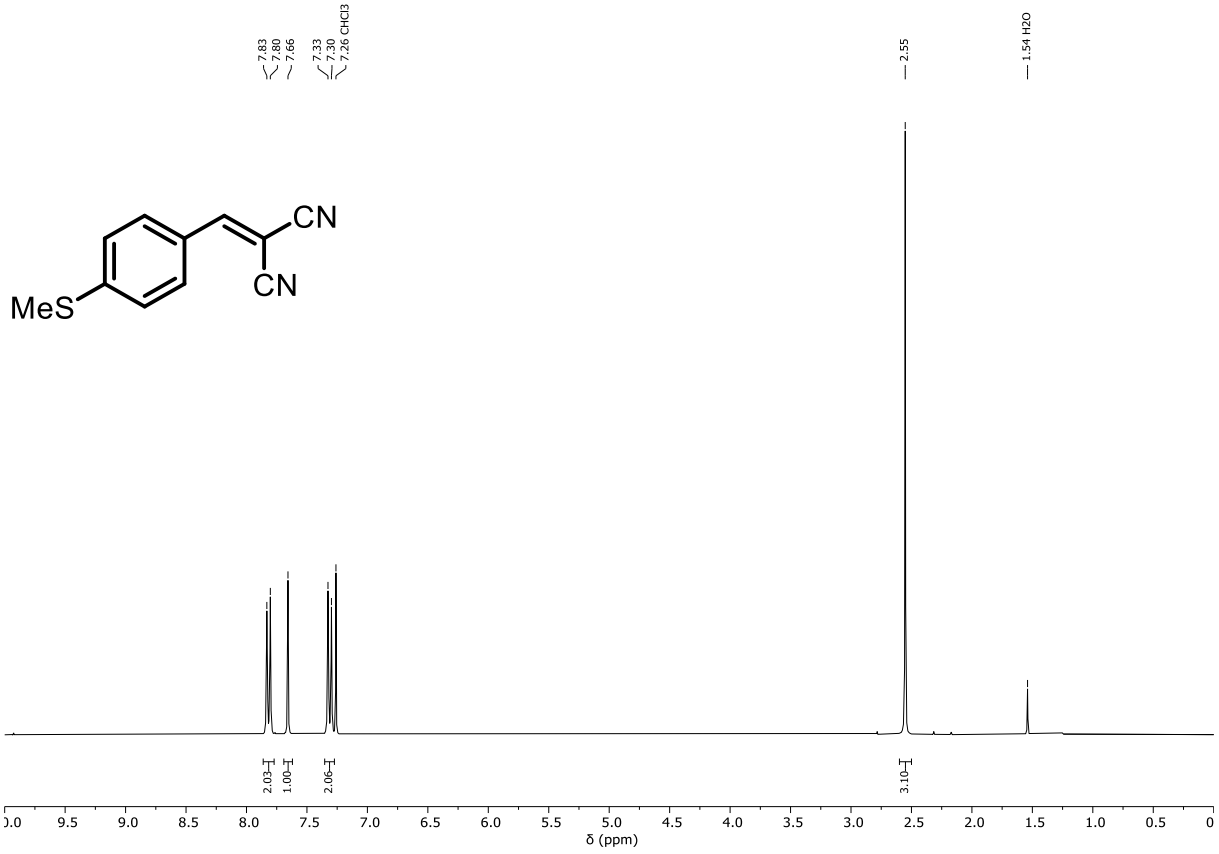
^{1}H NMR spectrum (300 MHz, $CDCl_3$) of **2g**



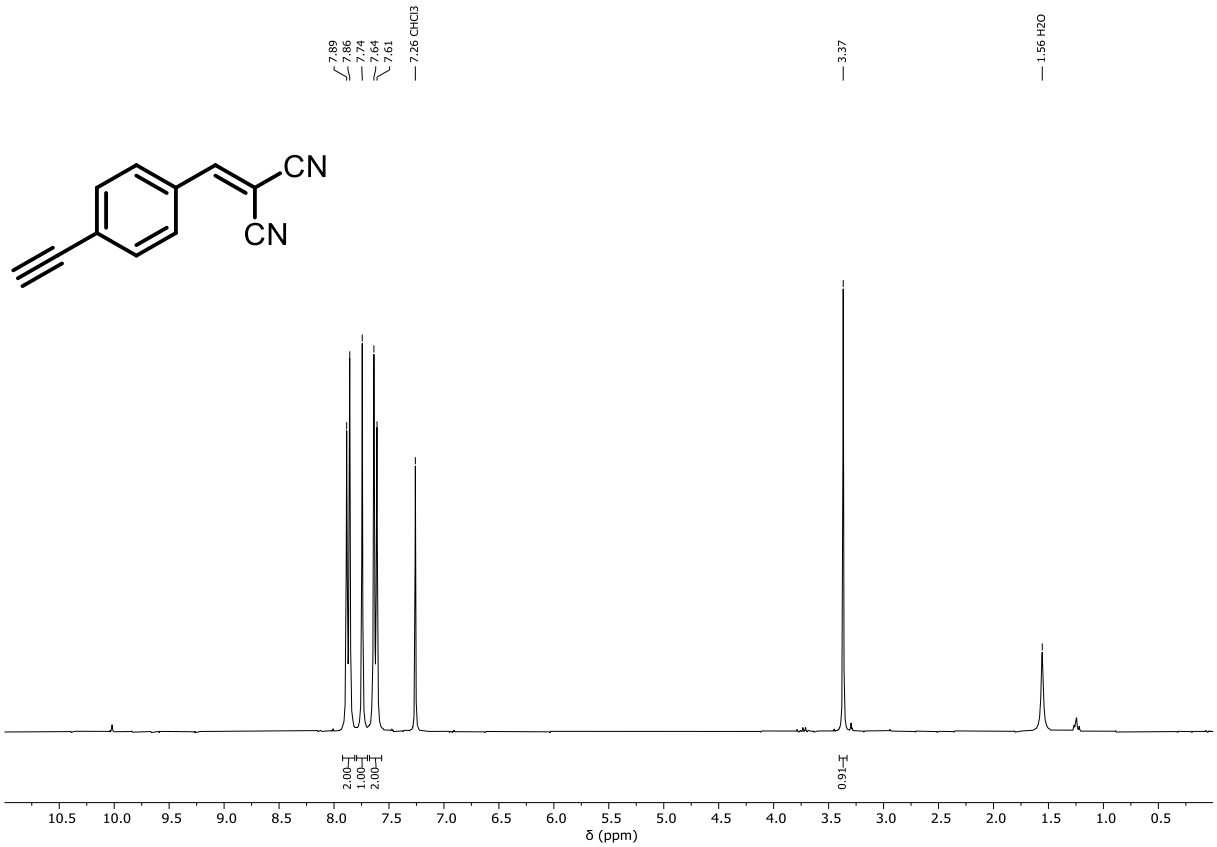
^{13}C NMR spectrum (101 MHz, $CDCl_3$) of **2g**



^{1}H NMR spectrum (300 MHz, $CDCl_3$) of **2h**



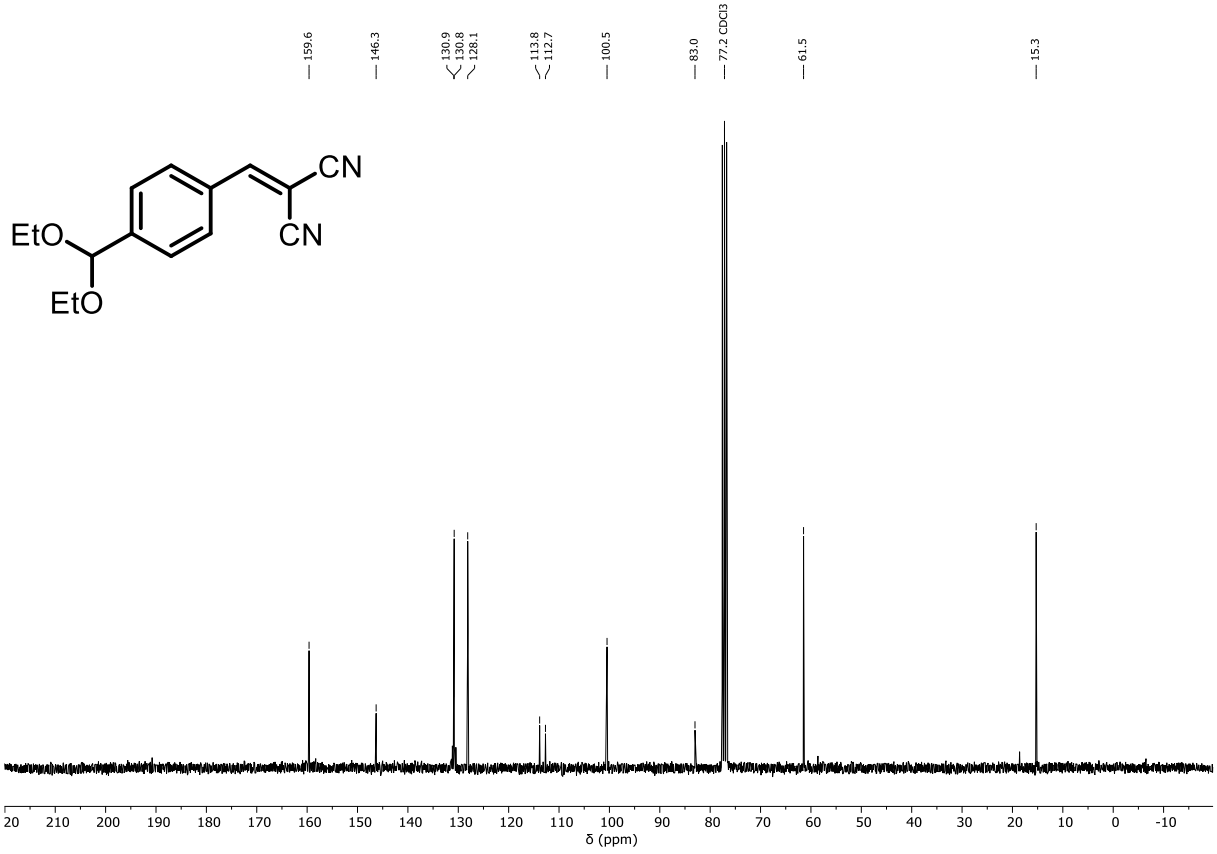
^{1}H NMR spectrum (300 MHz, $CDCl_3$) of **2j**



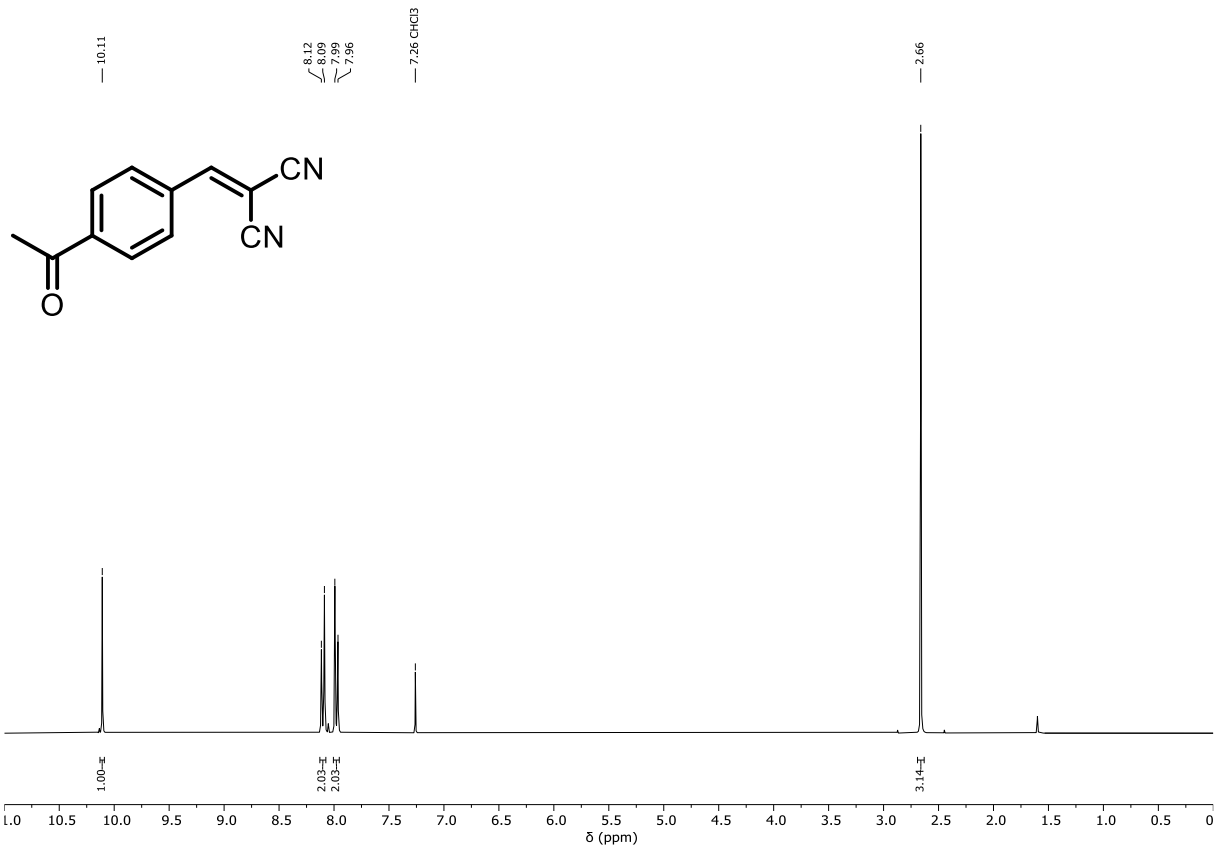
^{1}H NMR spectrum (300 MHz, $CDCl_3$) of **2k**



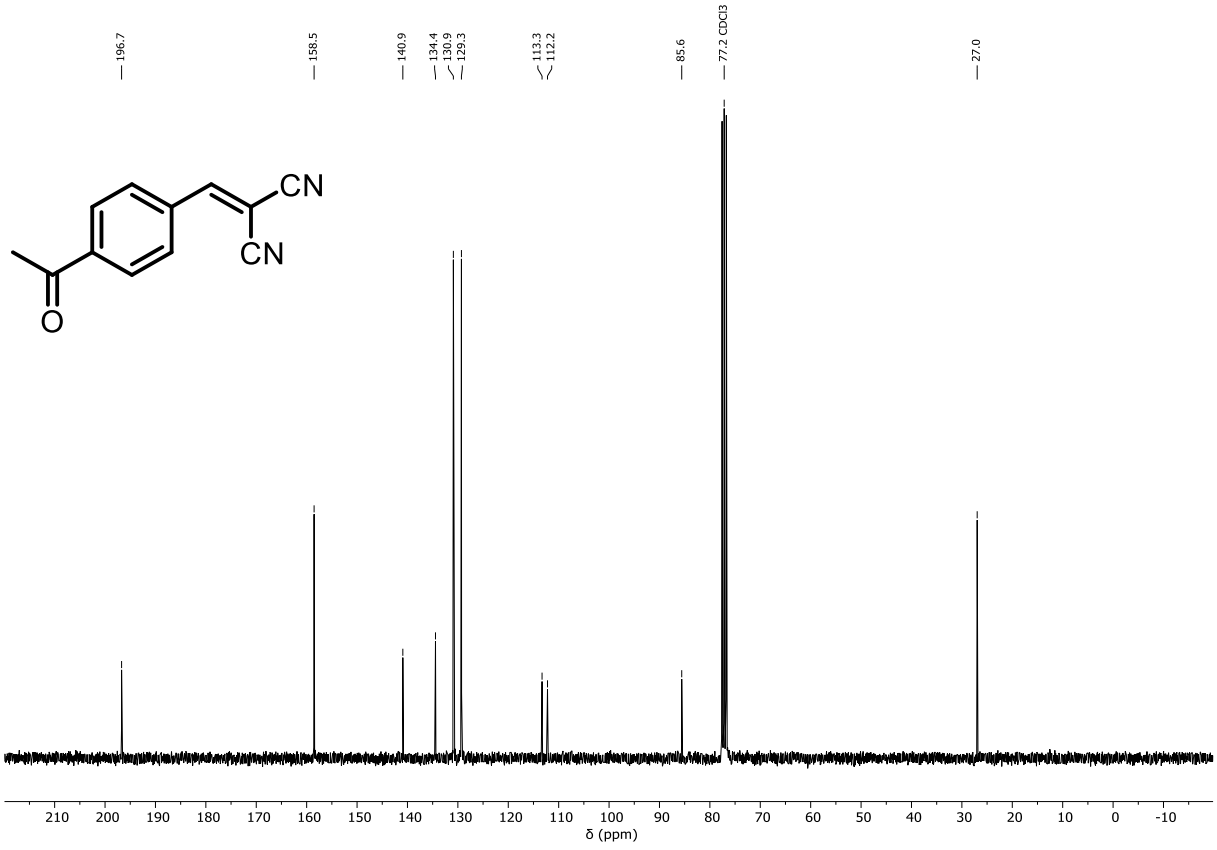
^{1}H NMR spectrum (300 MHz, $CDCl_3$) of **2l**



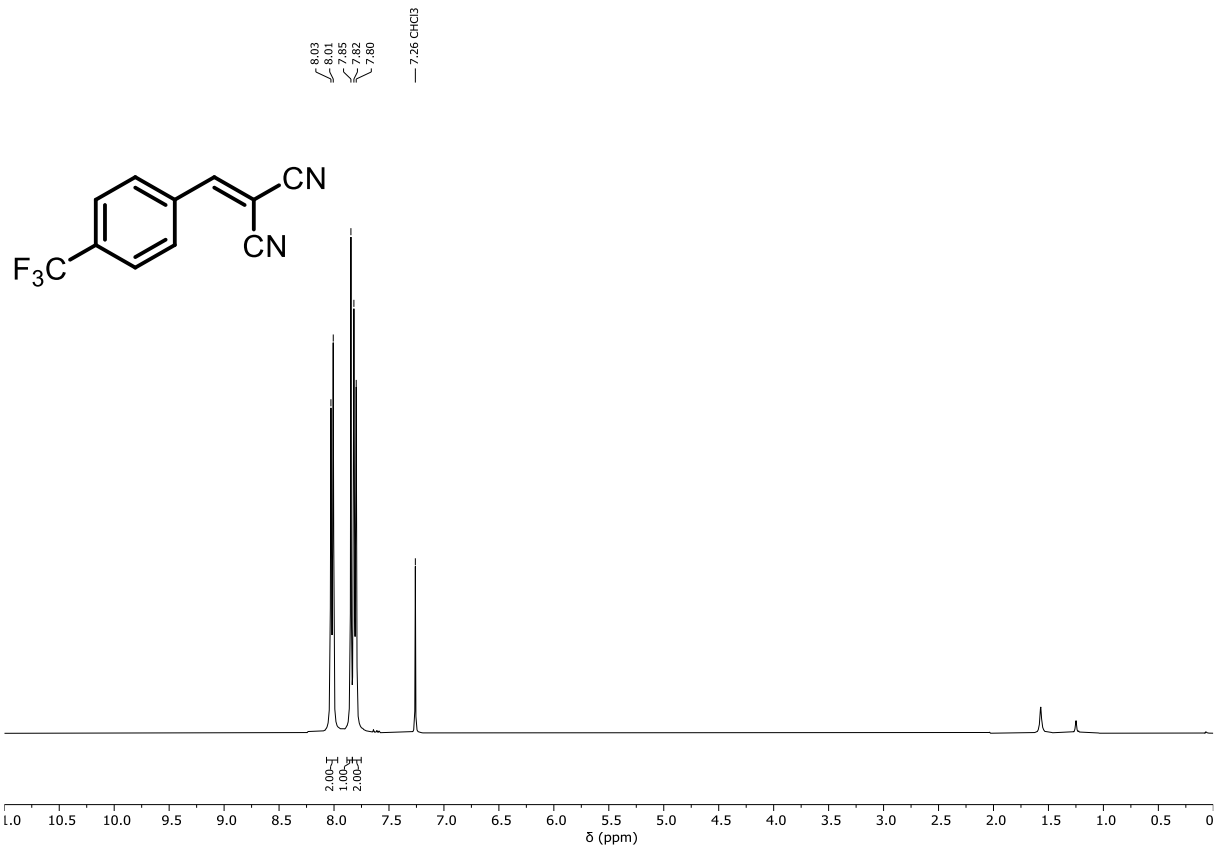
^{13}C NMR spectrum (75.5 MHz, $CDCl_3$) of **2l**



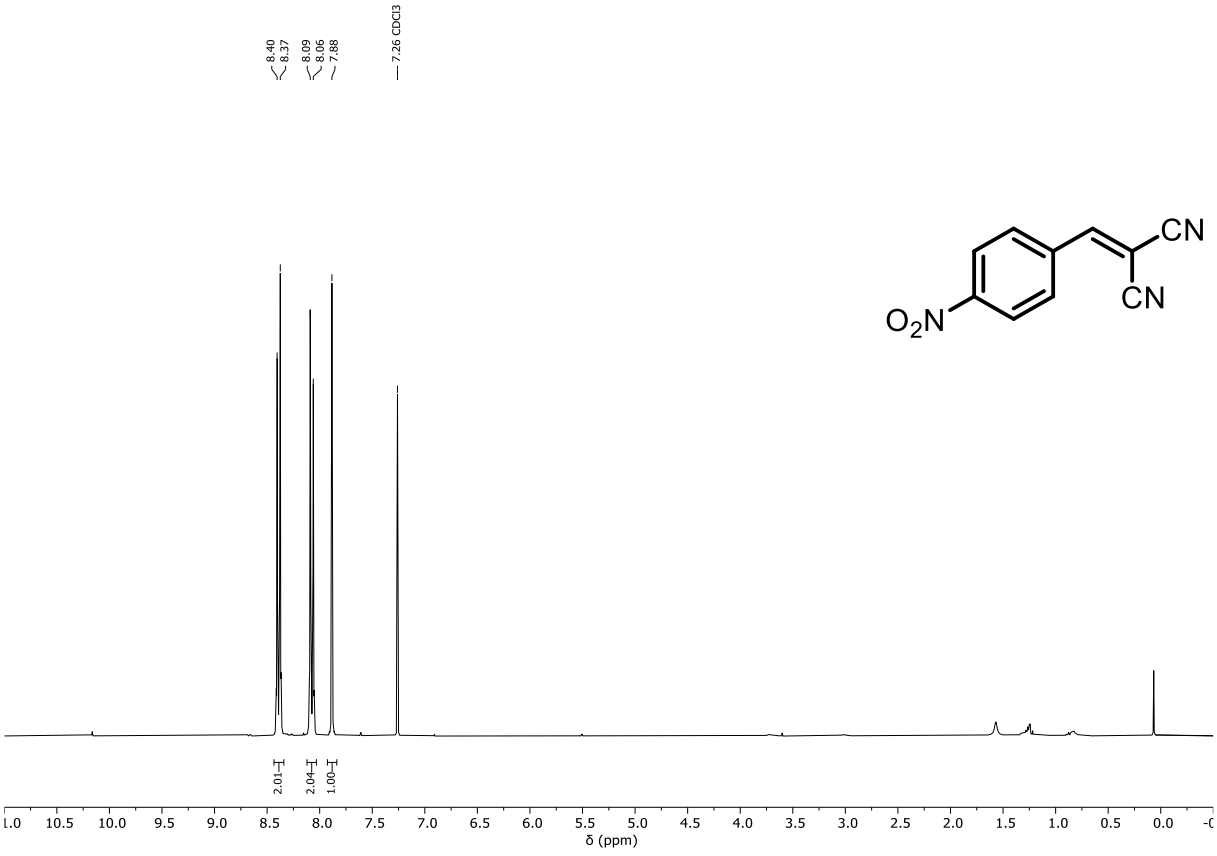
^{1}H NMR spectrum (300 MHz, $CDCl_3$) of **2m**



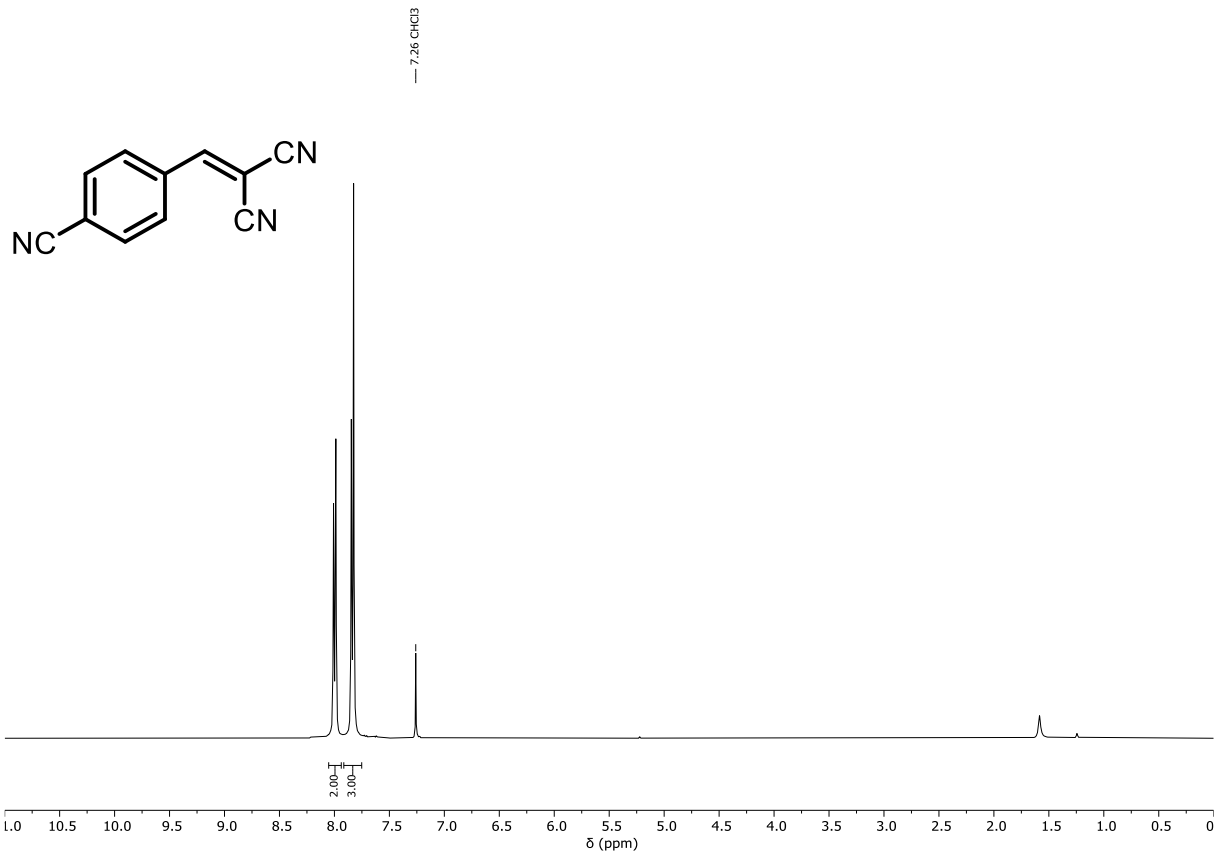
^{13}C NMR spectrum (75.5 MHz, $CDCl_3$) of **2m**



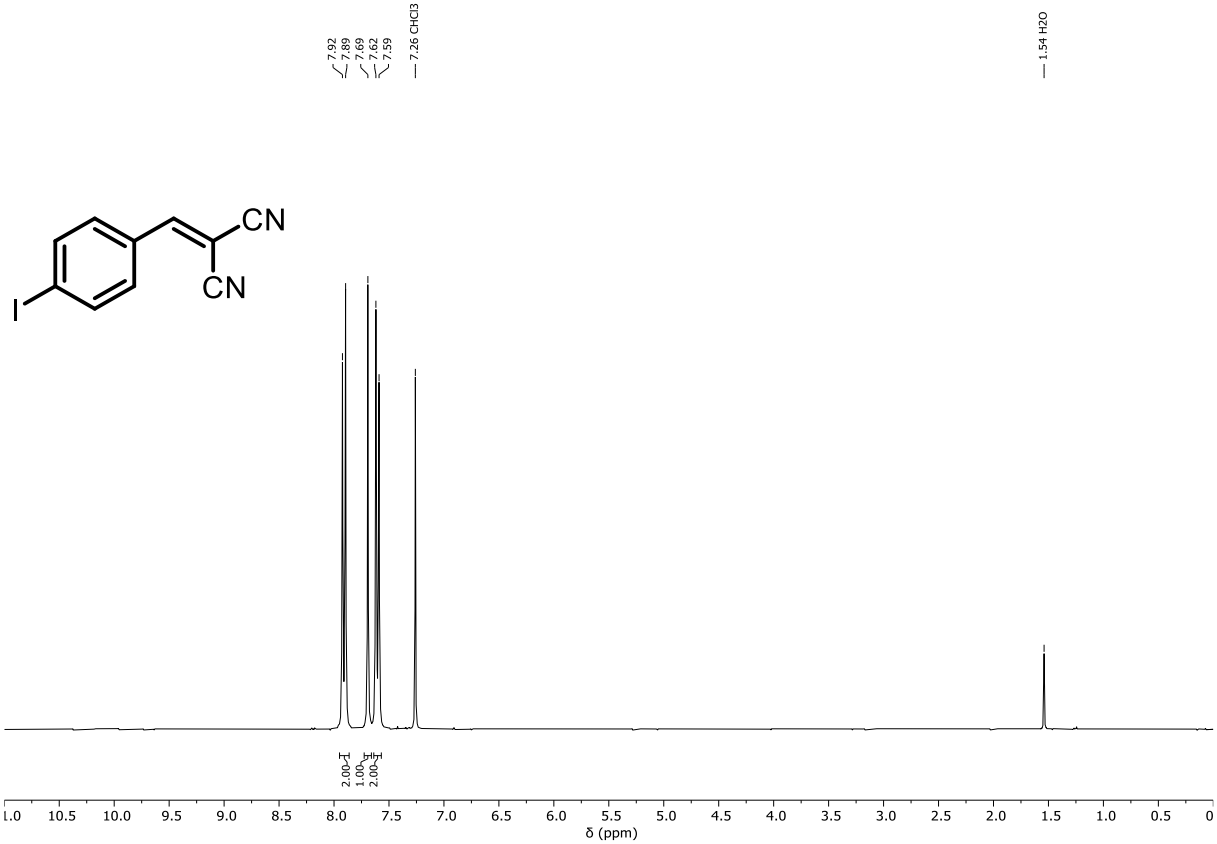
^{1}H NMR spectrum (400 MHz, $CDCl_3$) of **2n**



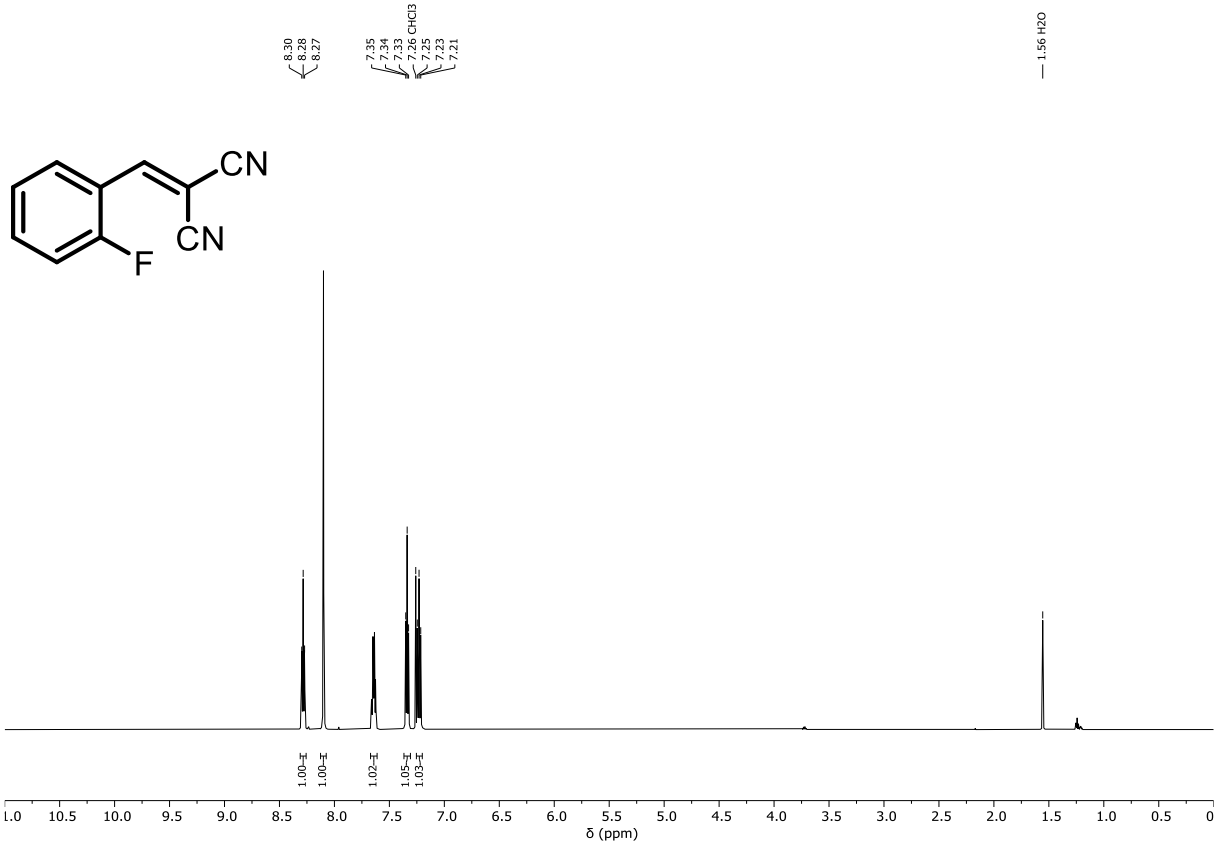
^{1}H NMR spectrum (300 MHz, $CDCl_3$) of **2o**



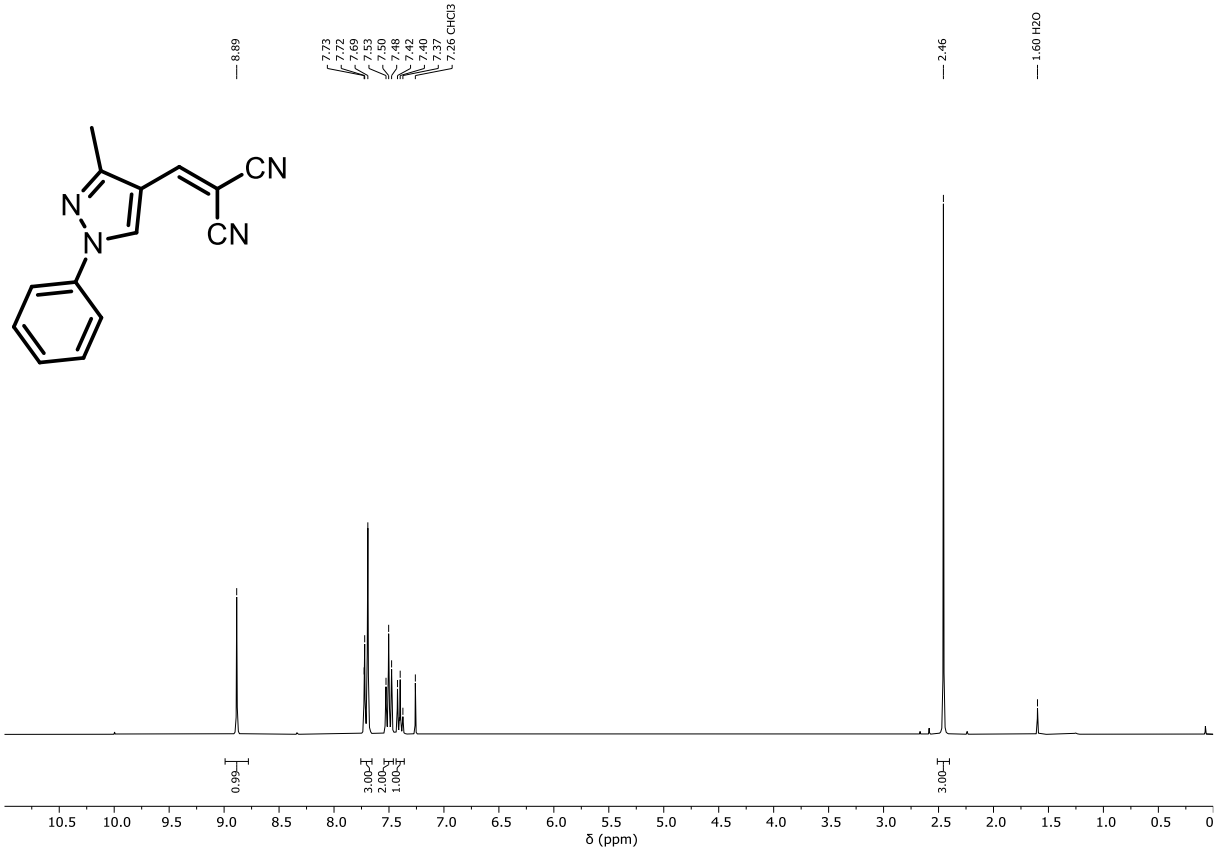
^{1}H NMR spectrum (300 MHz, $CDCl_3$) of **2p**



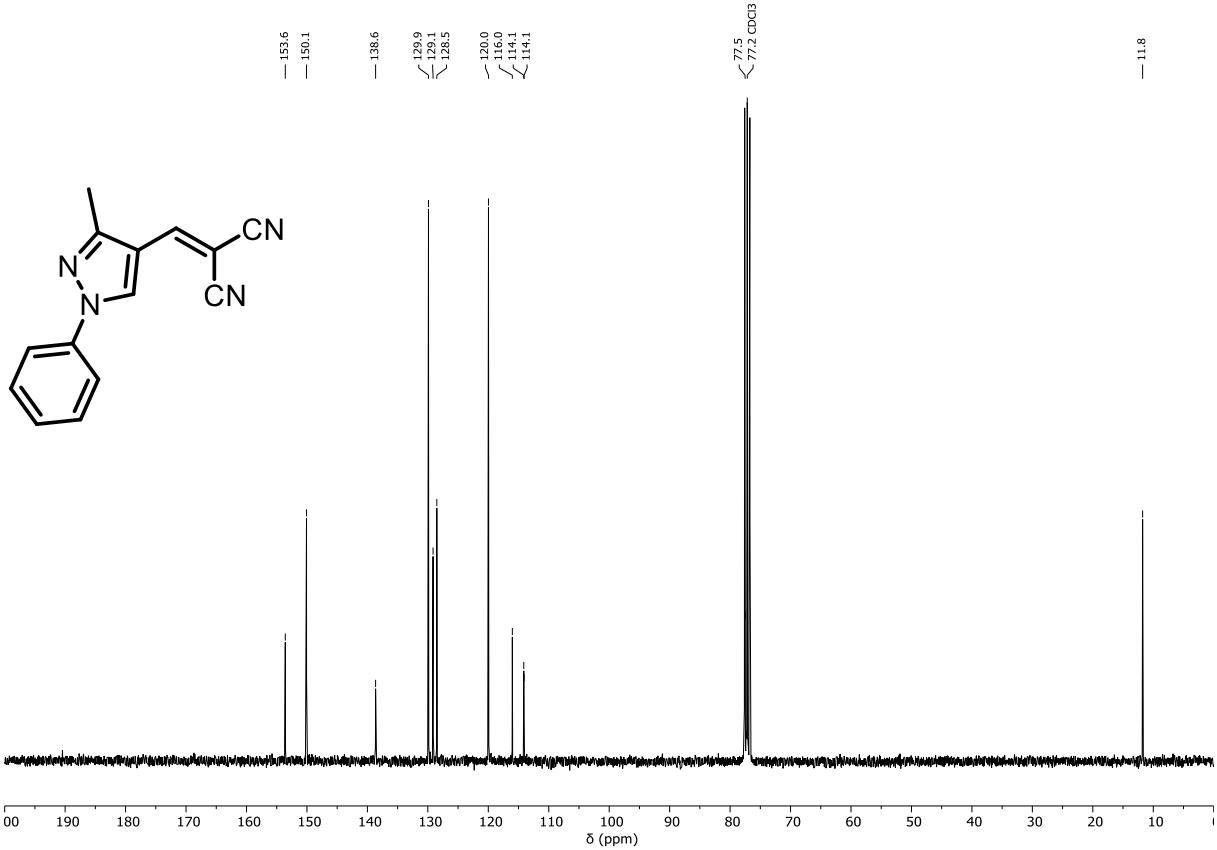
^{1}H NMR spectrum (300 MHz, $CDCl_3$) of **2q**



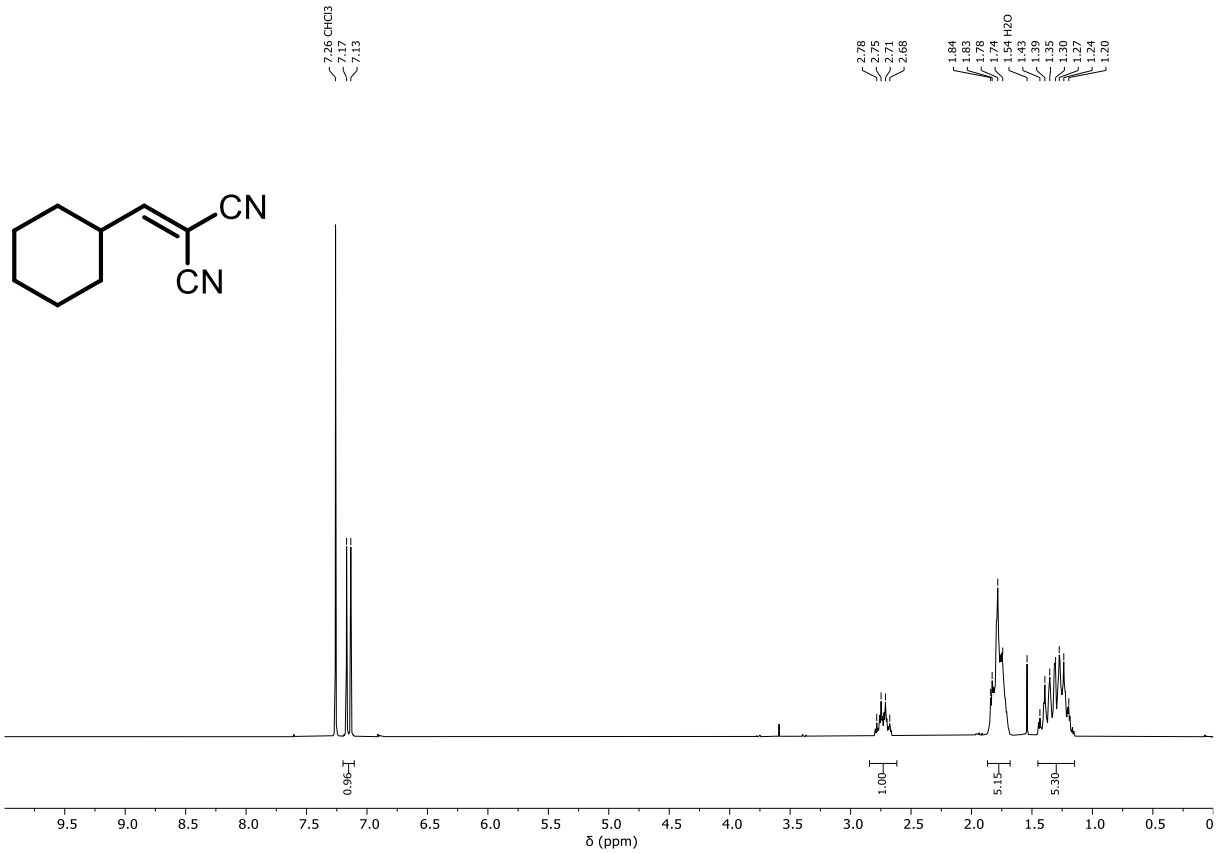
^{1}H NMR spectrum (600 MHz, $CDCl_3$) of **2r**



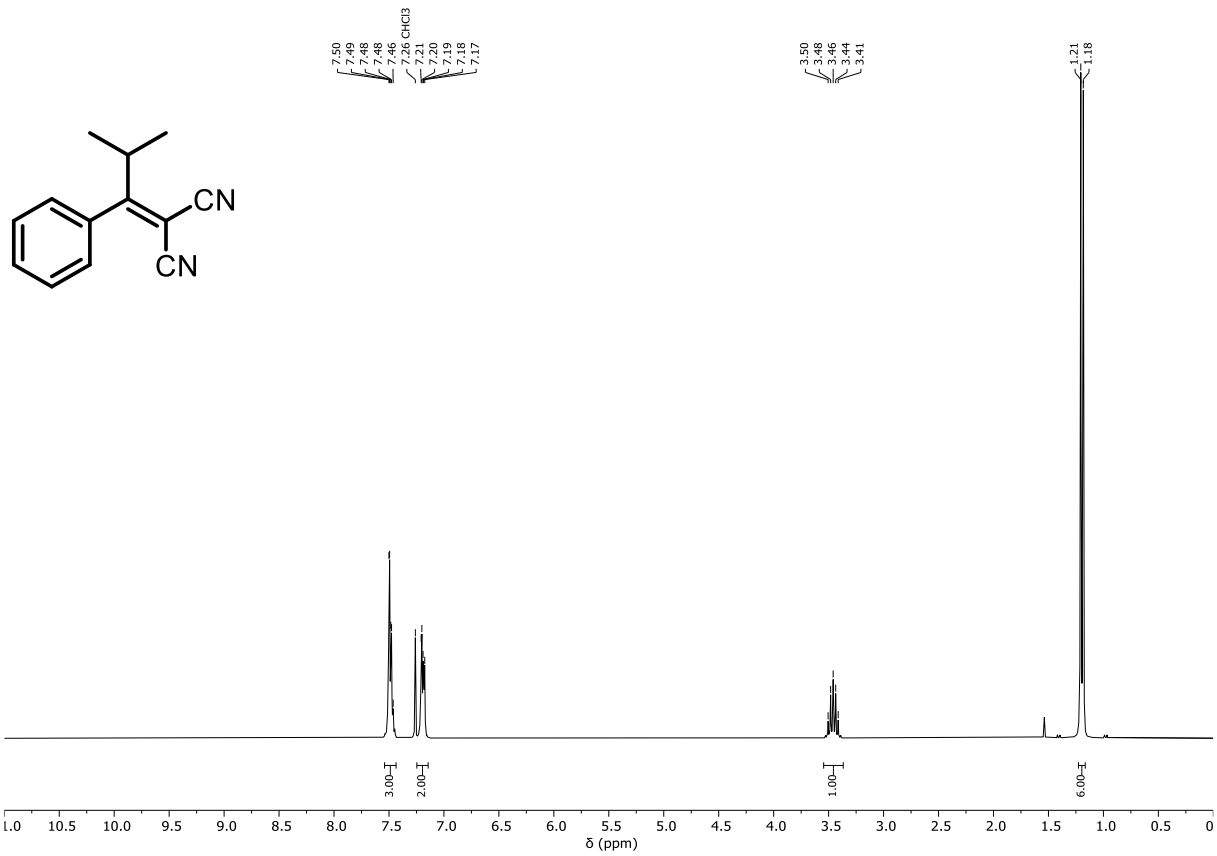
^{1}H NMR spectrum (300 MHz, $CDCl_3$) of **2v**



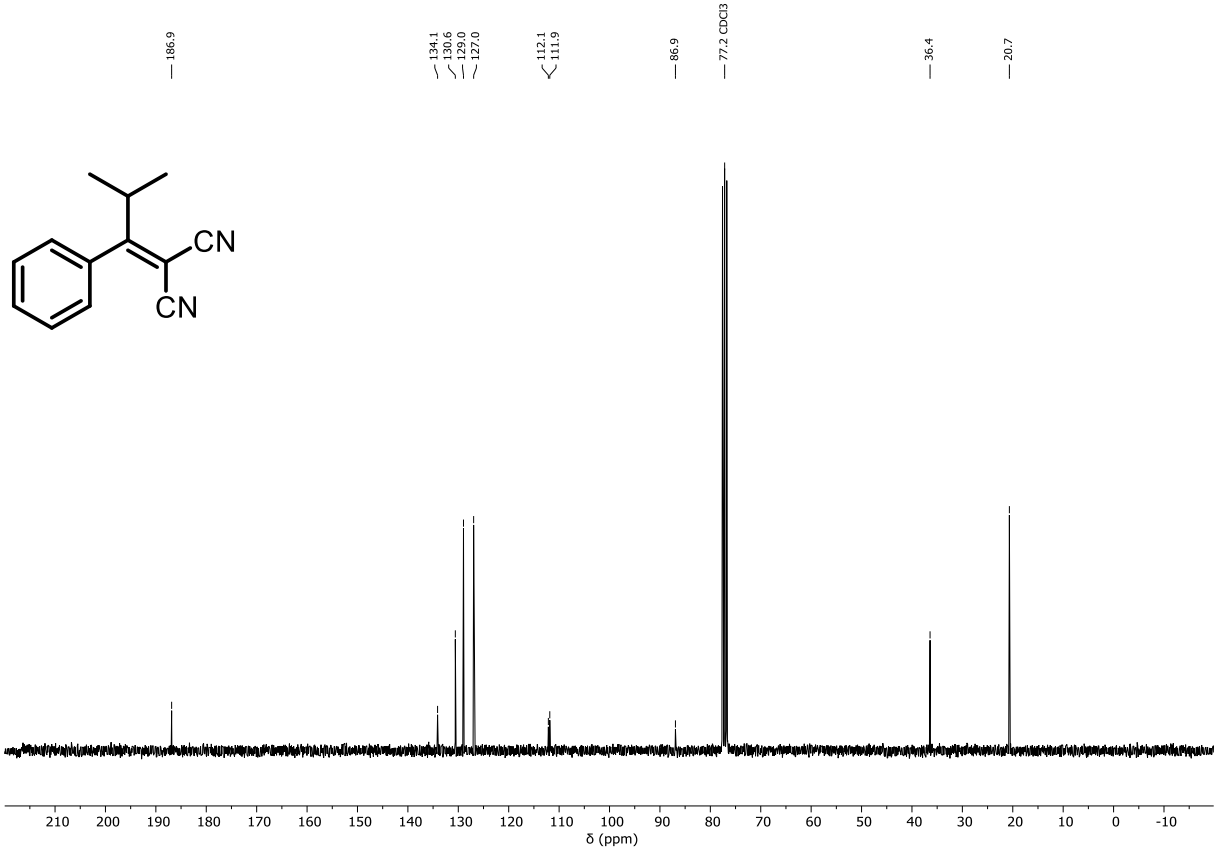
^{13}C NMR spectrum (75.5 MHz, $CDCl_3$) of **2v**



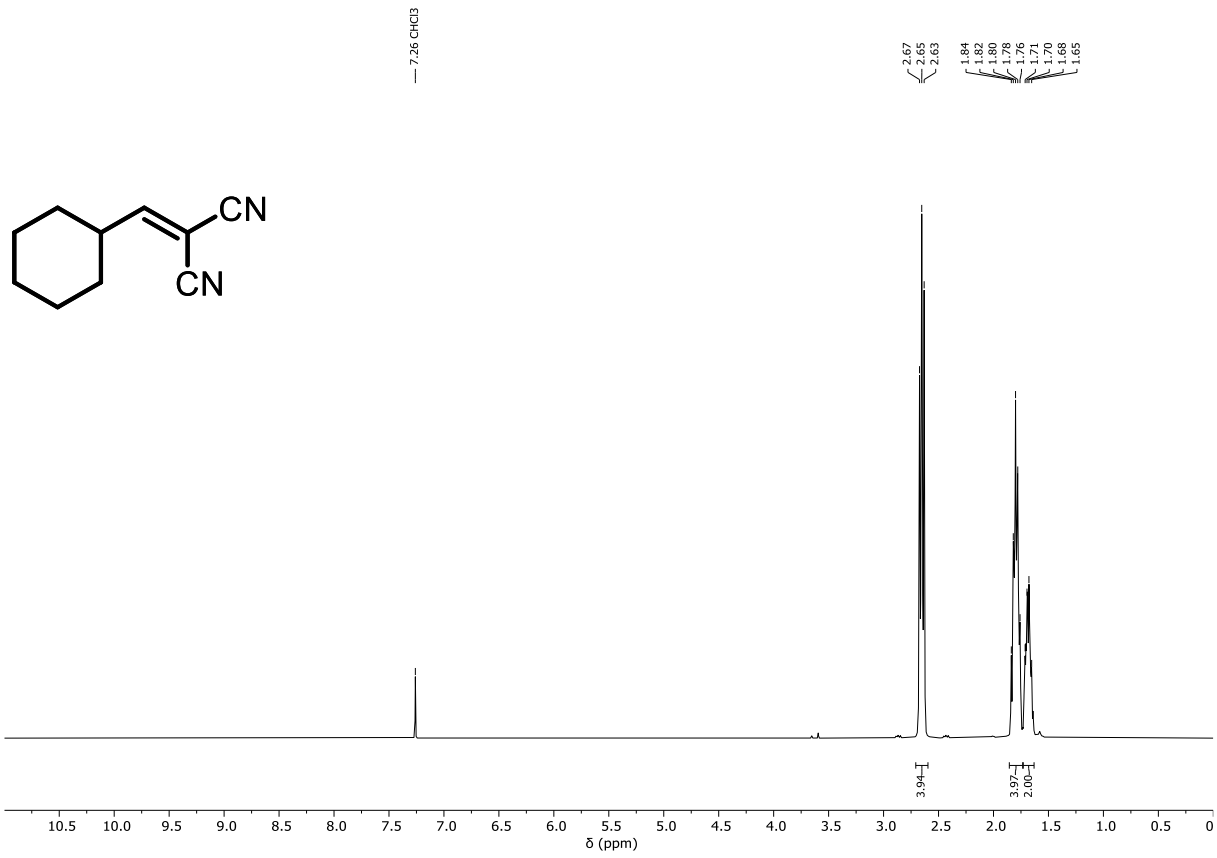
^{1}H NMR spectrum (300 MHz, $CDCl_3$) of **2w**



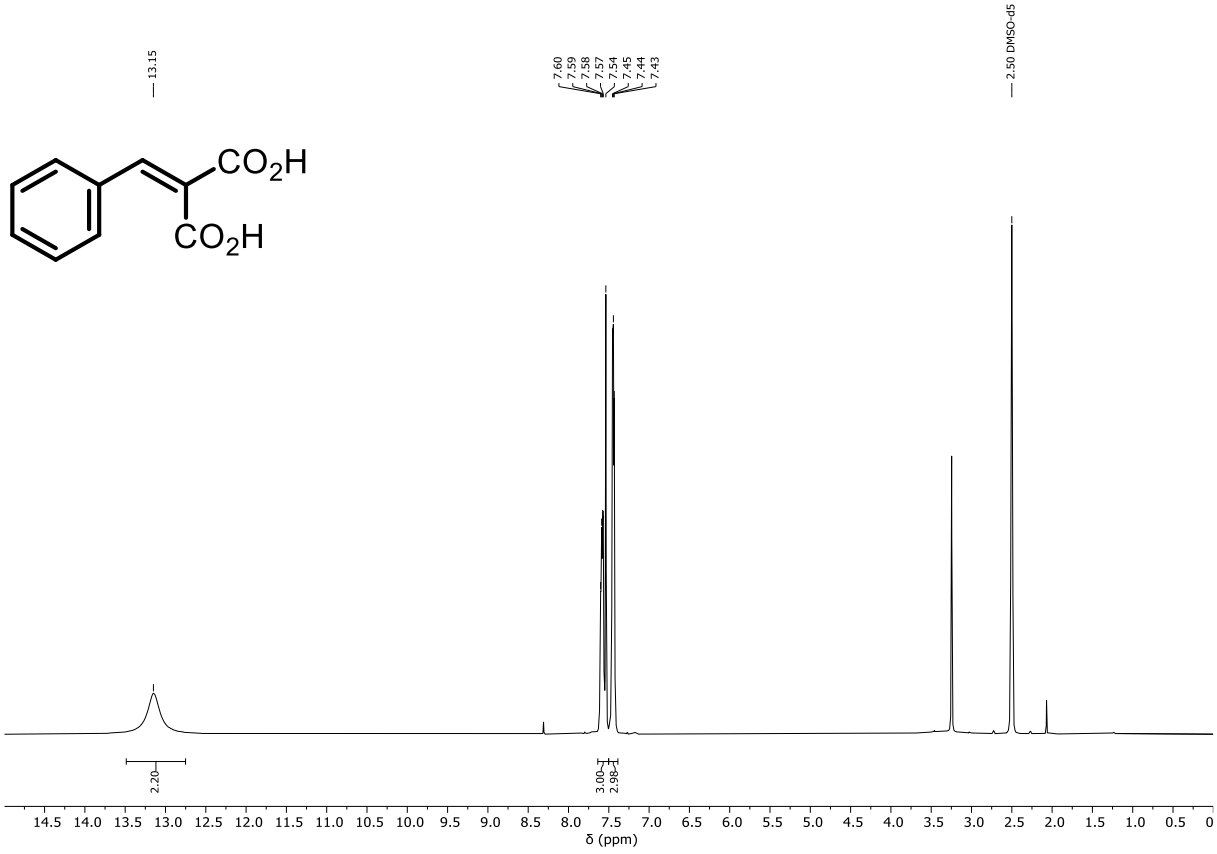
^{1}H NMR spectrum (300 MHz, $CDCl_3$) of **2y**



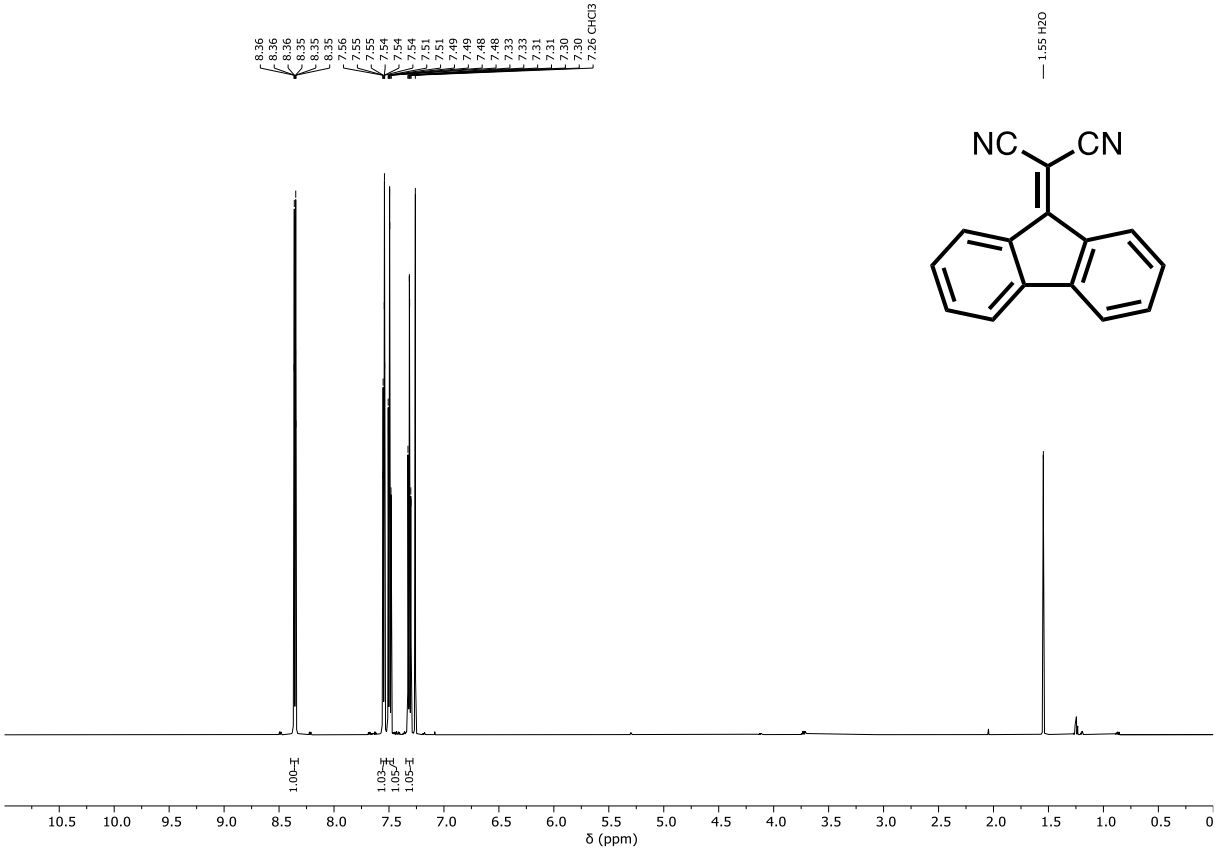
^{13}C NMR spectrum (75.5 MHz, $CDCl_3$) of **2y**



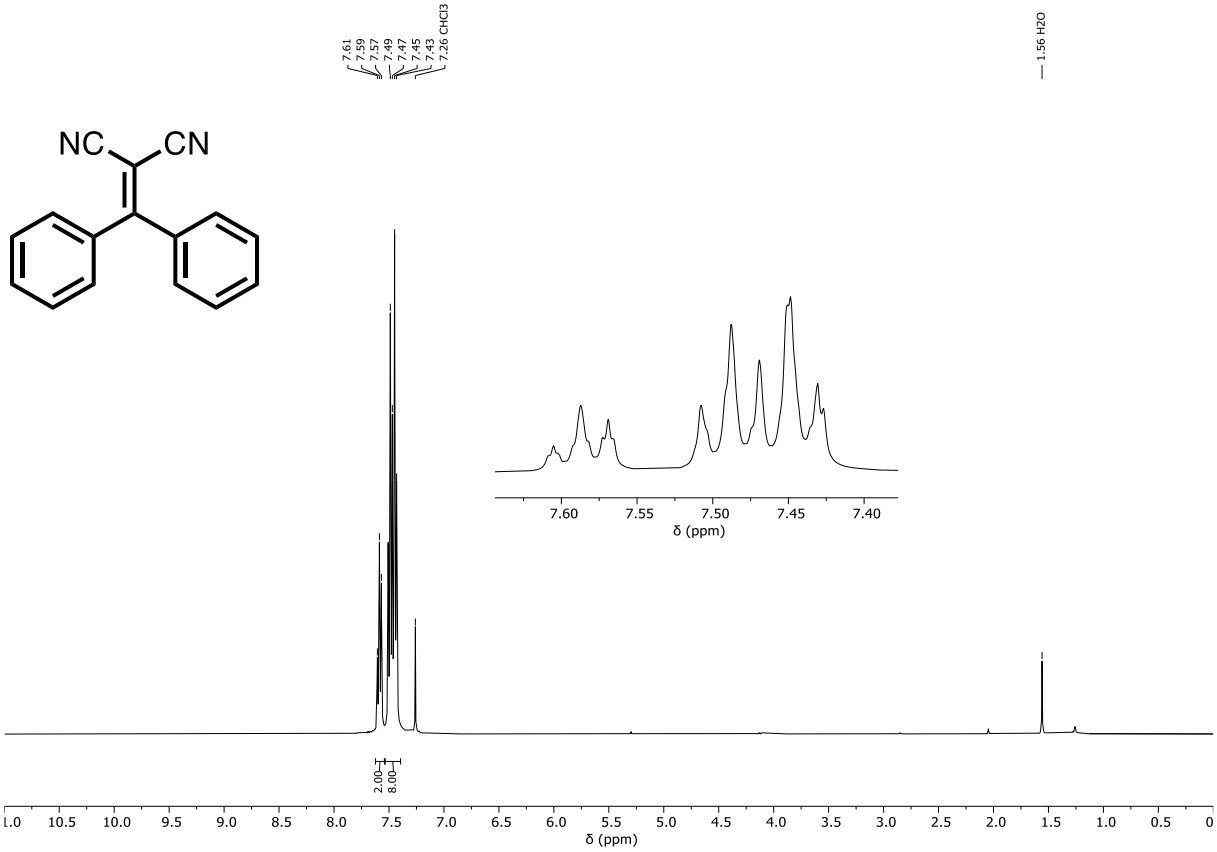
^{1}H NMR spectrum (300 MHz, $CDCl_3$) of **2z**



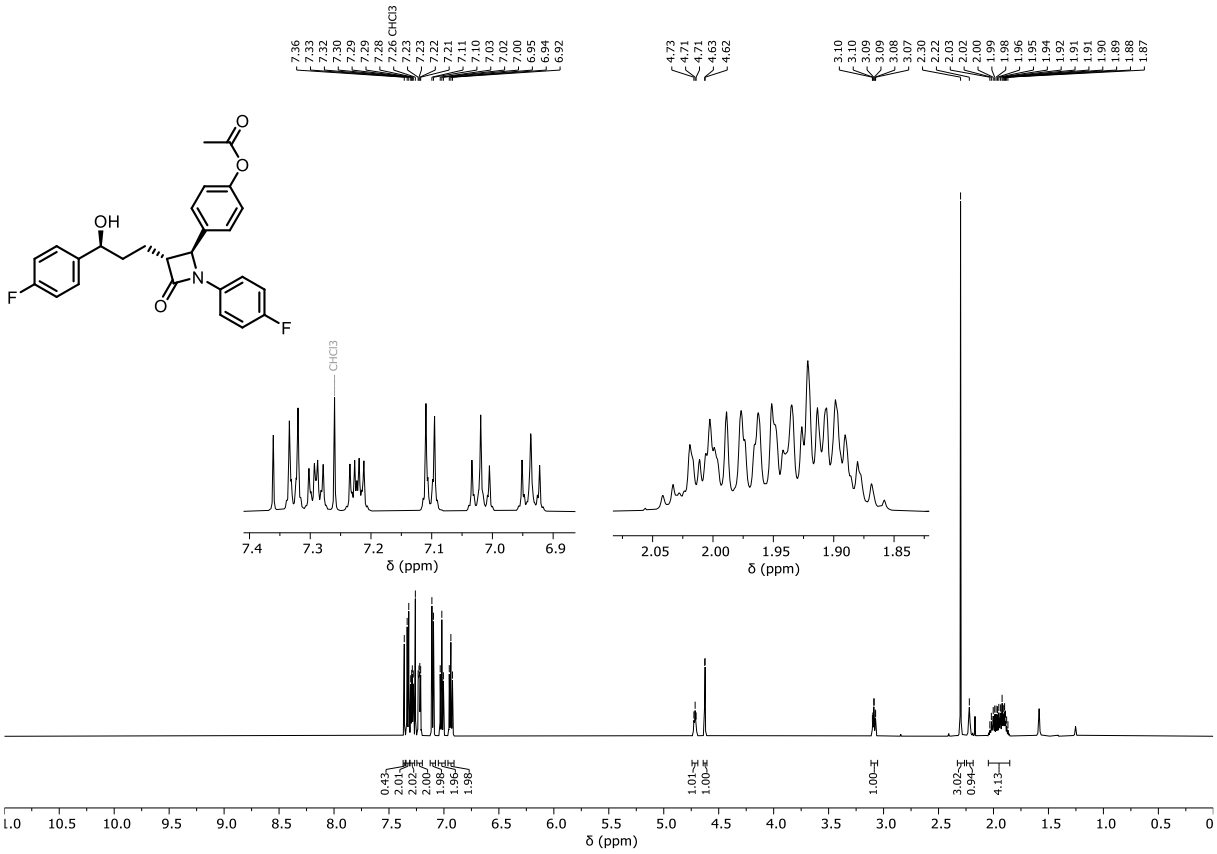
^{1}H NMR spectrum (300 MHz, DMSO-d_6) of **3a**



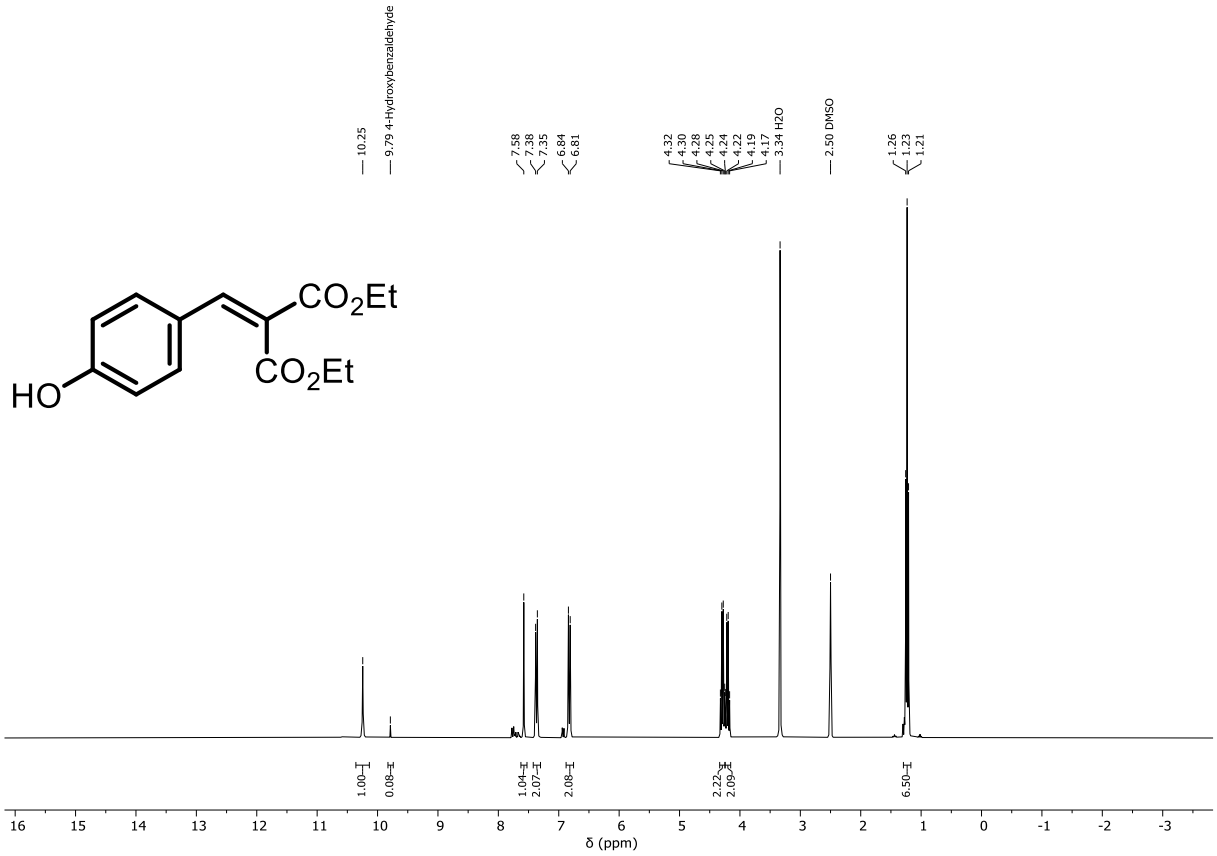
^{1}H NMR spectrum (600 MHz, $CDCl_3$) of **3i**



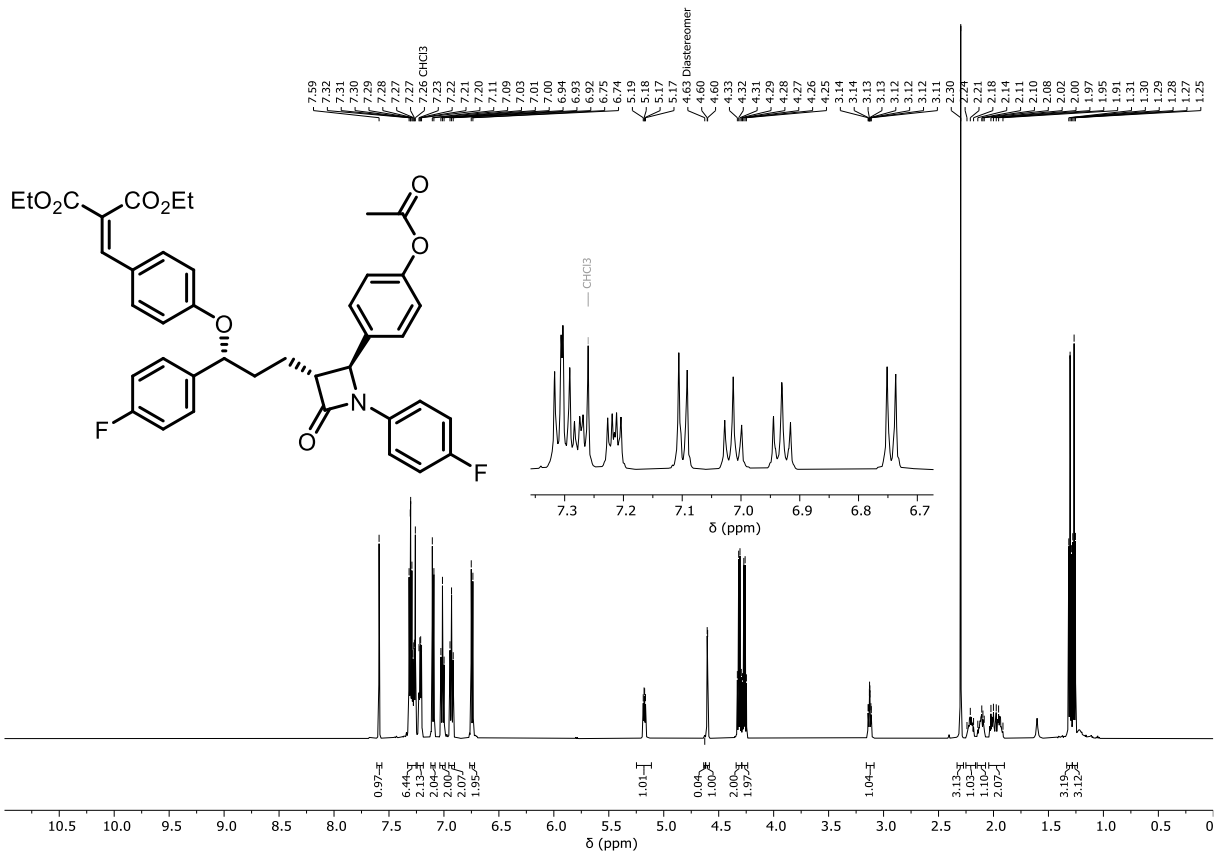
^{1}H NMR spectrum (300 MHz, $CDCl_3$) of **3j**



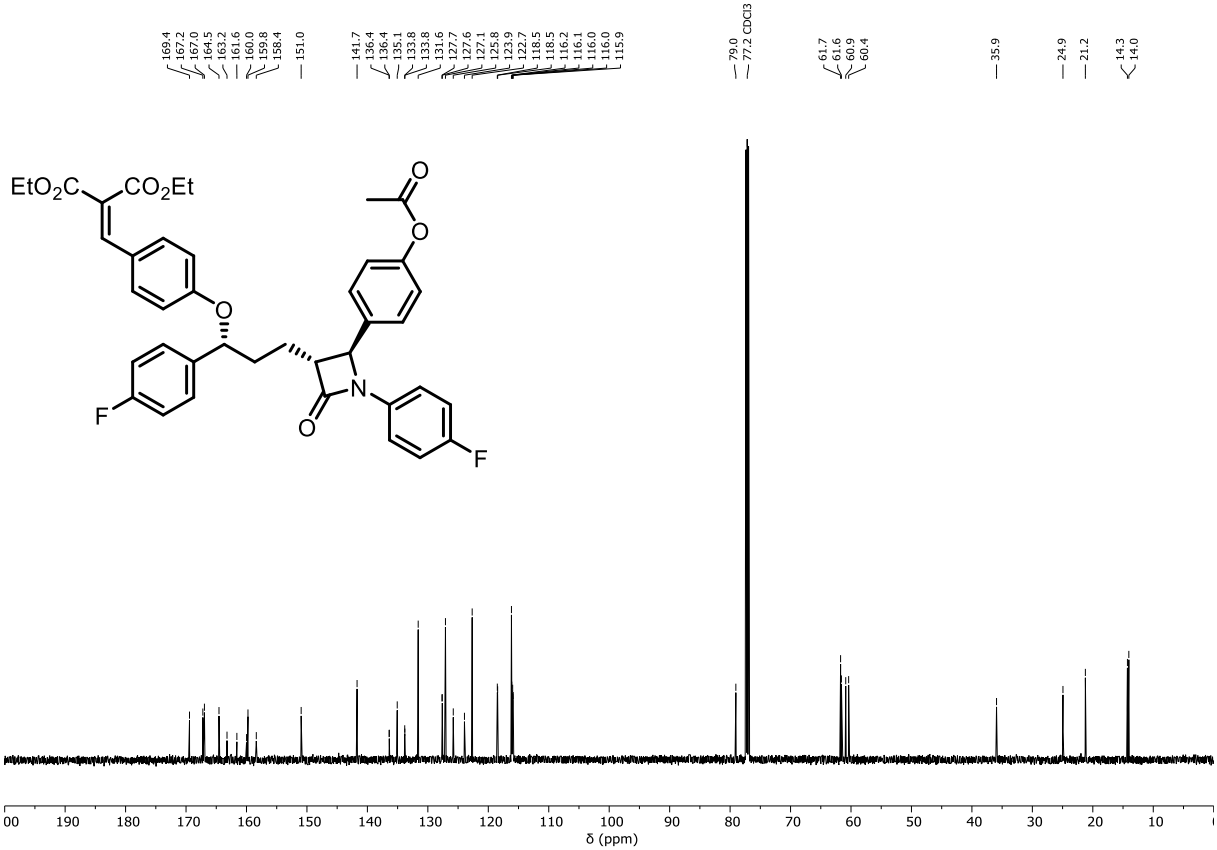
^{1}H NMR spectrum (600 MHz, $CDCl_3$) of **Eze OAc**



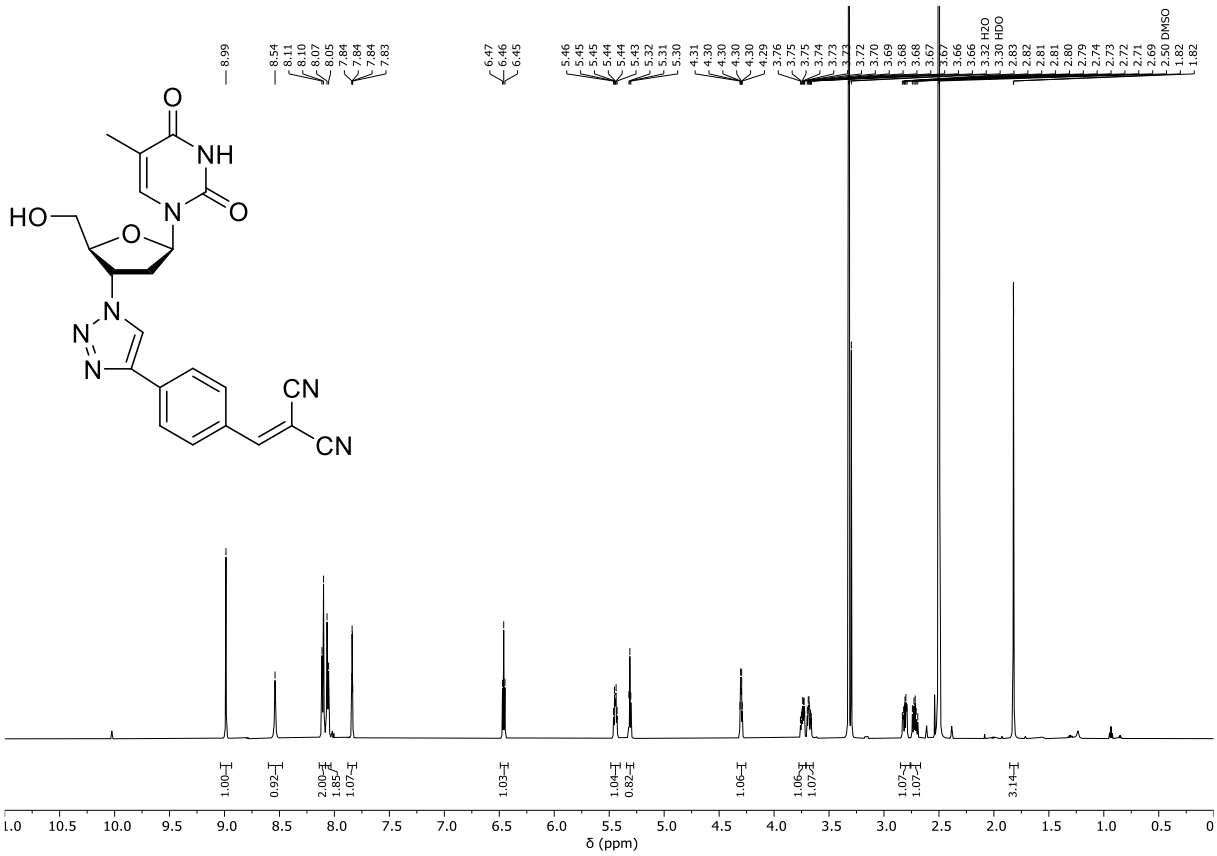
^{1}H NMR spectrum (300 MHz, DMSO-d_6) of diethyl (4-hydroxybenzylidene)malonate



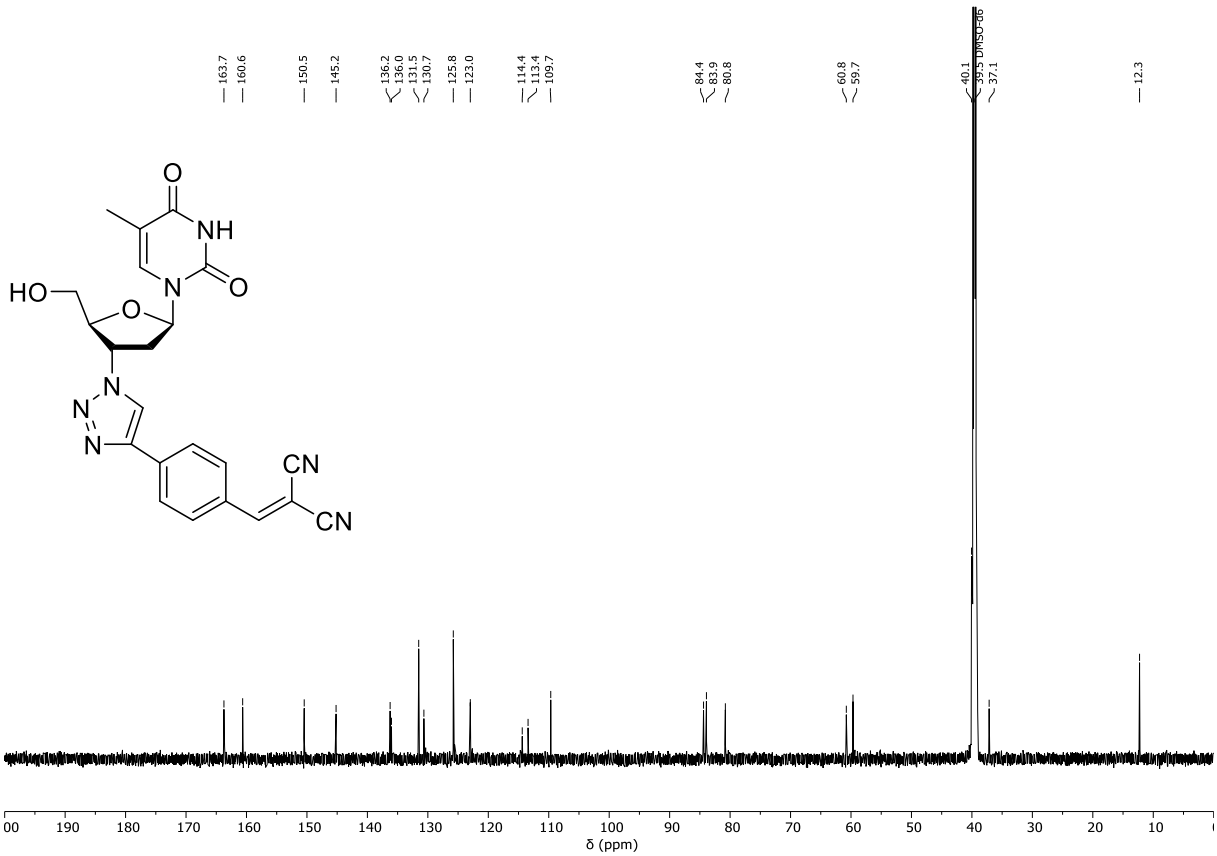
^{1}H NMR spectrum (600 MHz, $CDCl_3$) of **4a**



^{13}C NMR spectrum (151 MHz, $CDCl_3$) of **4a**



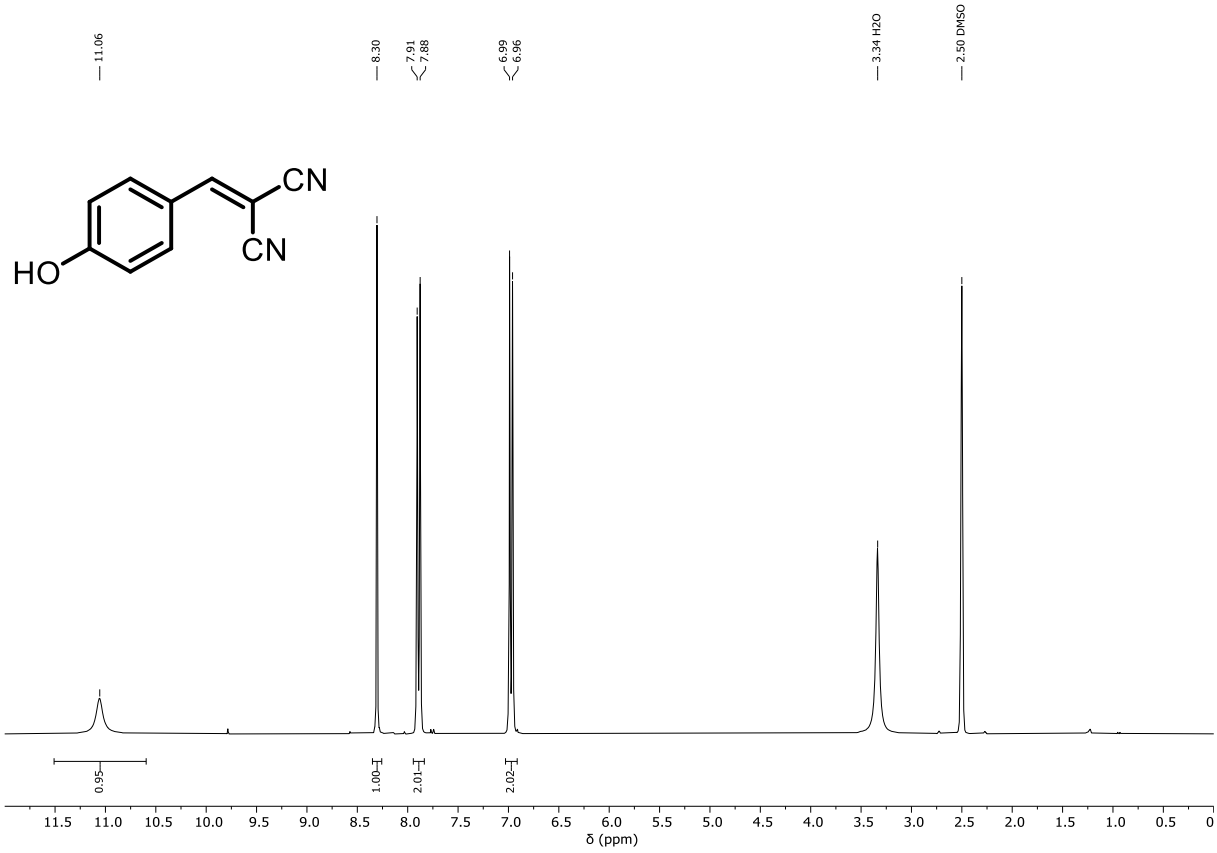
^{1}H NMR spectrum (600 MHz, DMSO-d_6) of **4b**



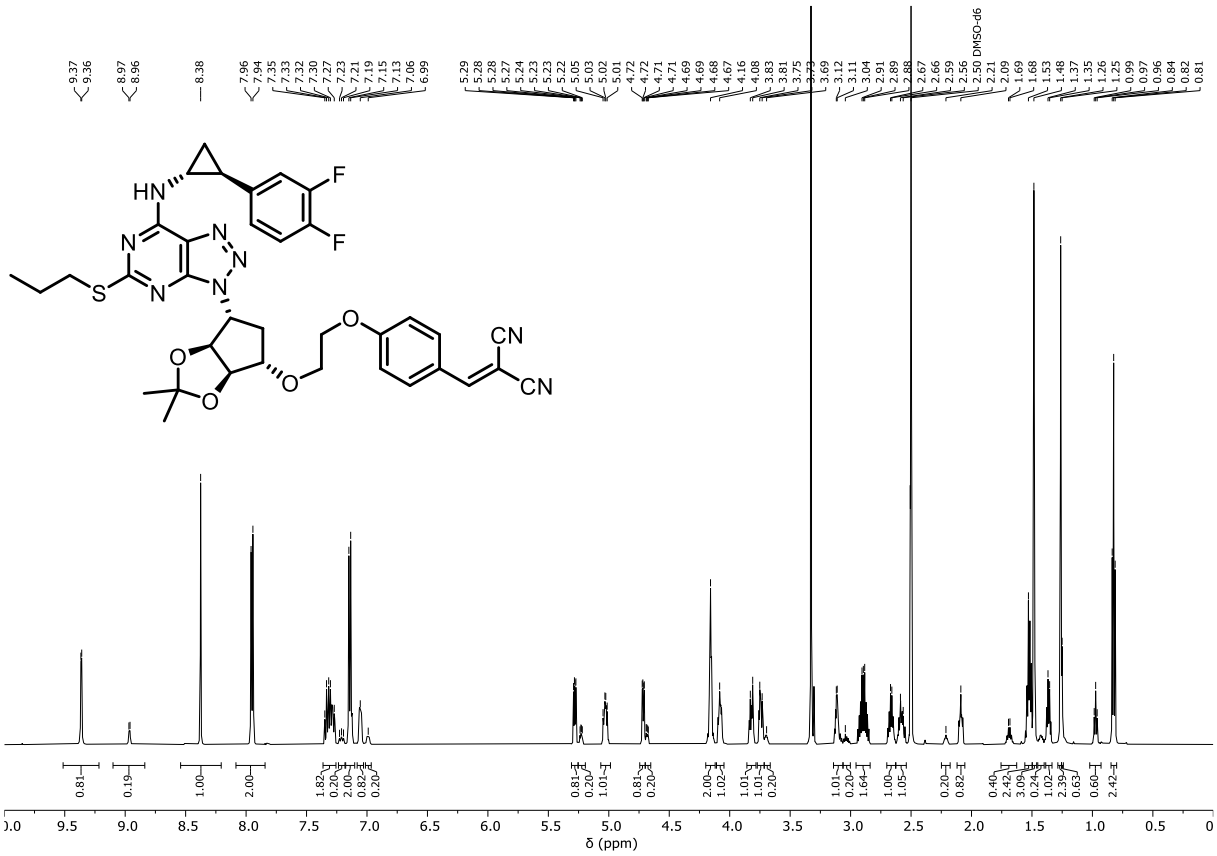
^{13}C NMR spectrum (151 MHz, DMSO-d_6) of **4b**



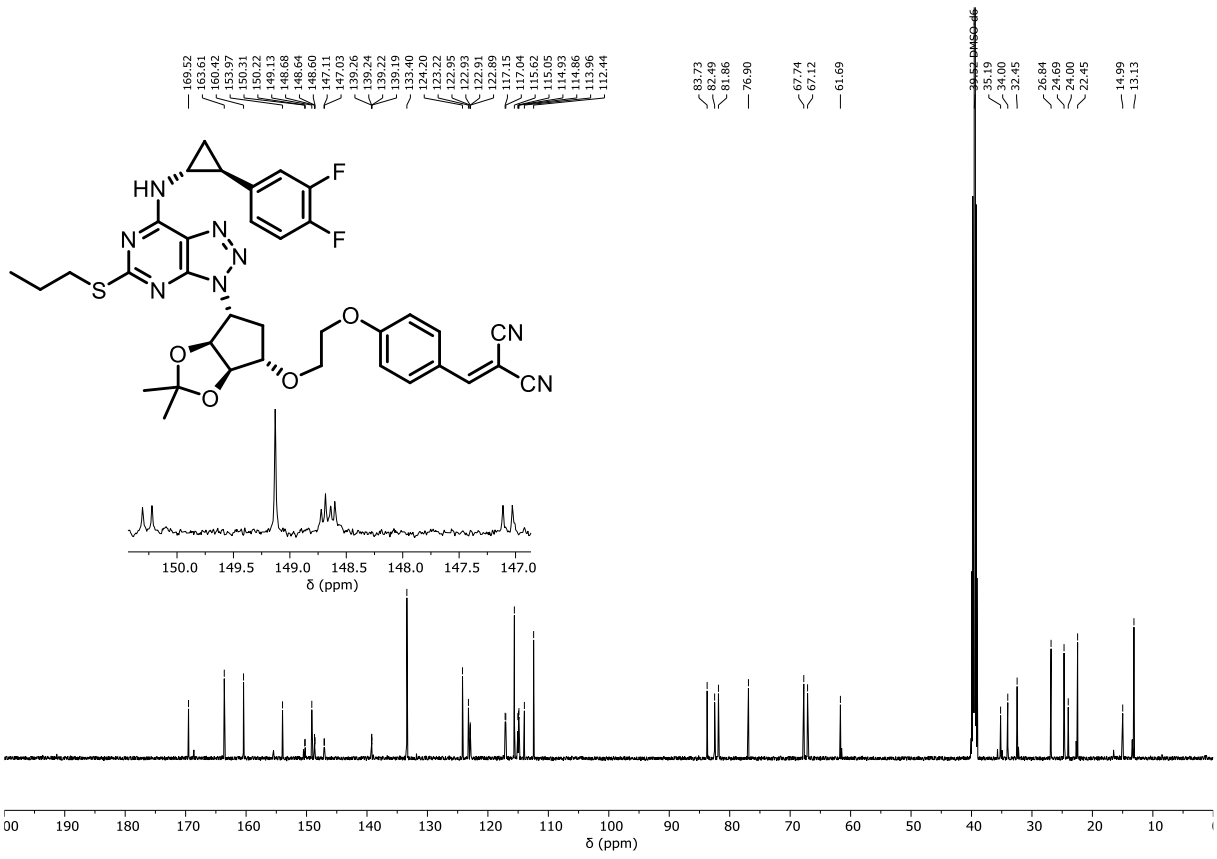
^{1}H NMR spectrum (600 MHz, DMSO-d_6) of **Tica Prot** (major + minor rotamer signals highlighted)



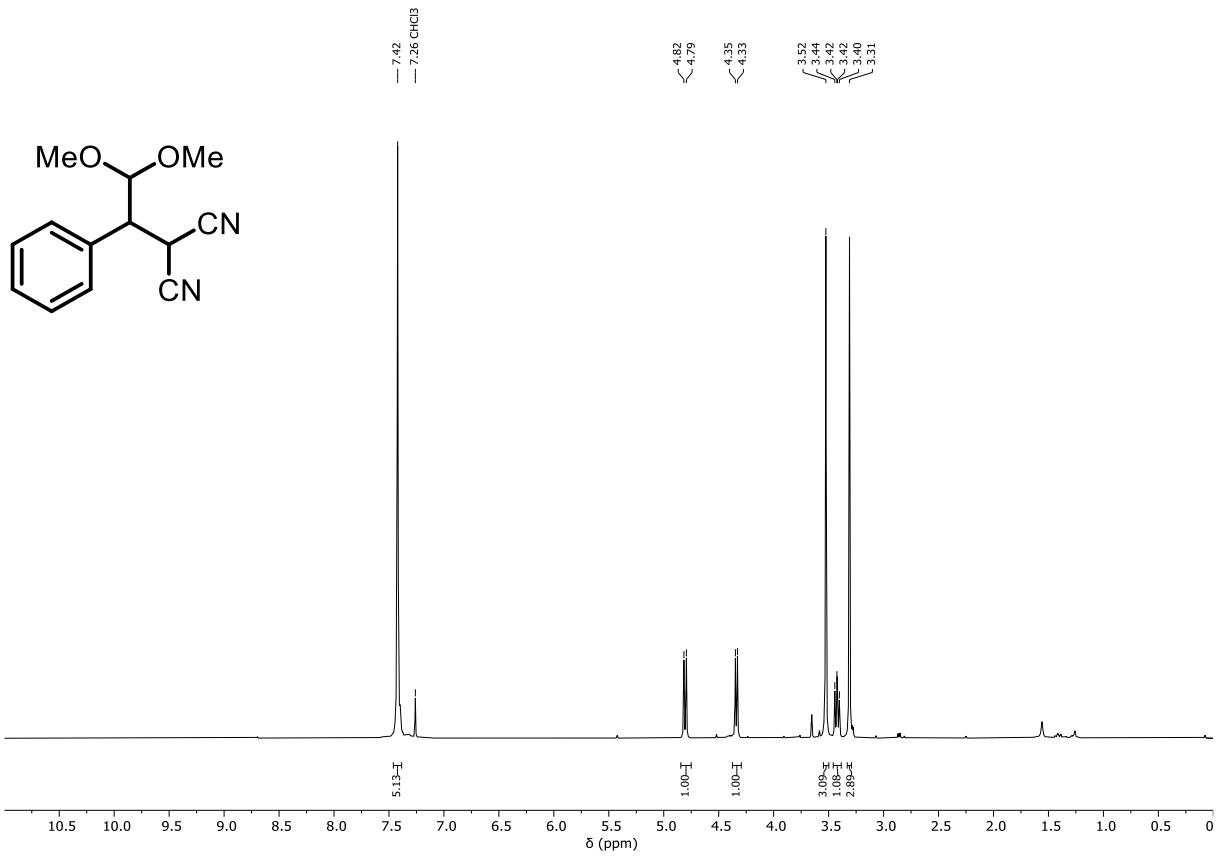
^{1}H NMR spectrum (300 MHz, DMSO-d_6) of (4-hydroxybenzylidene)malononitrile



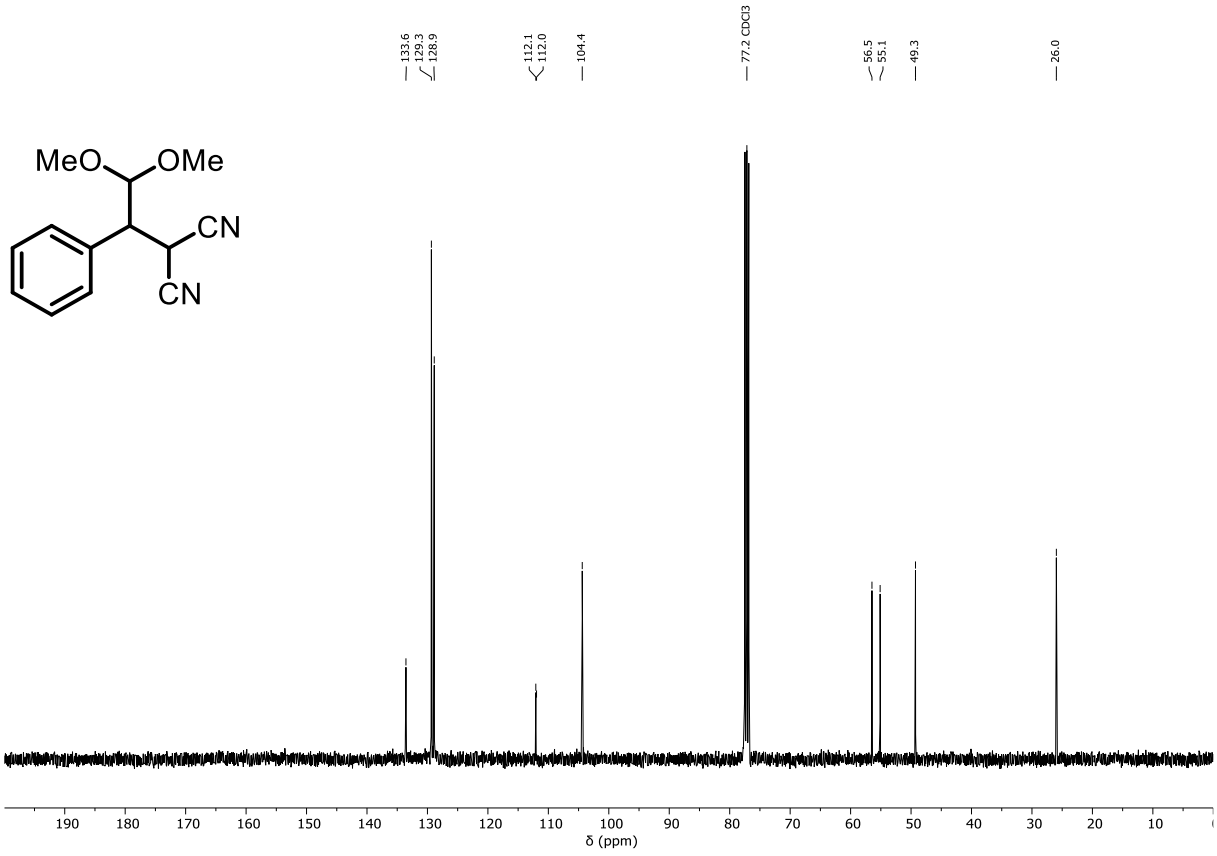
^{1}H NMR spectrum (600 MHz, DMSO-d_6) of **4c** (major + minor rotamer signals highlighted)



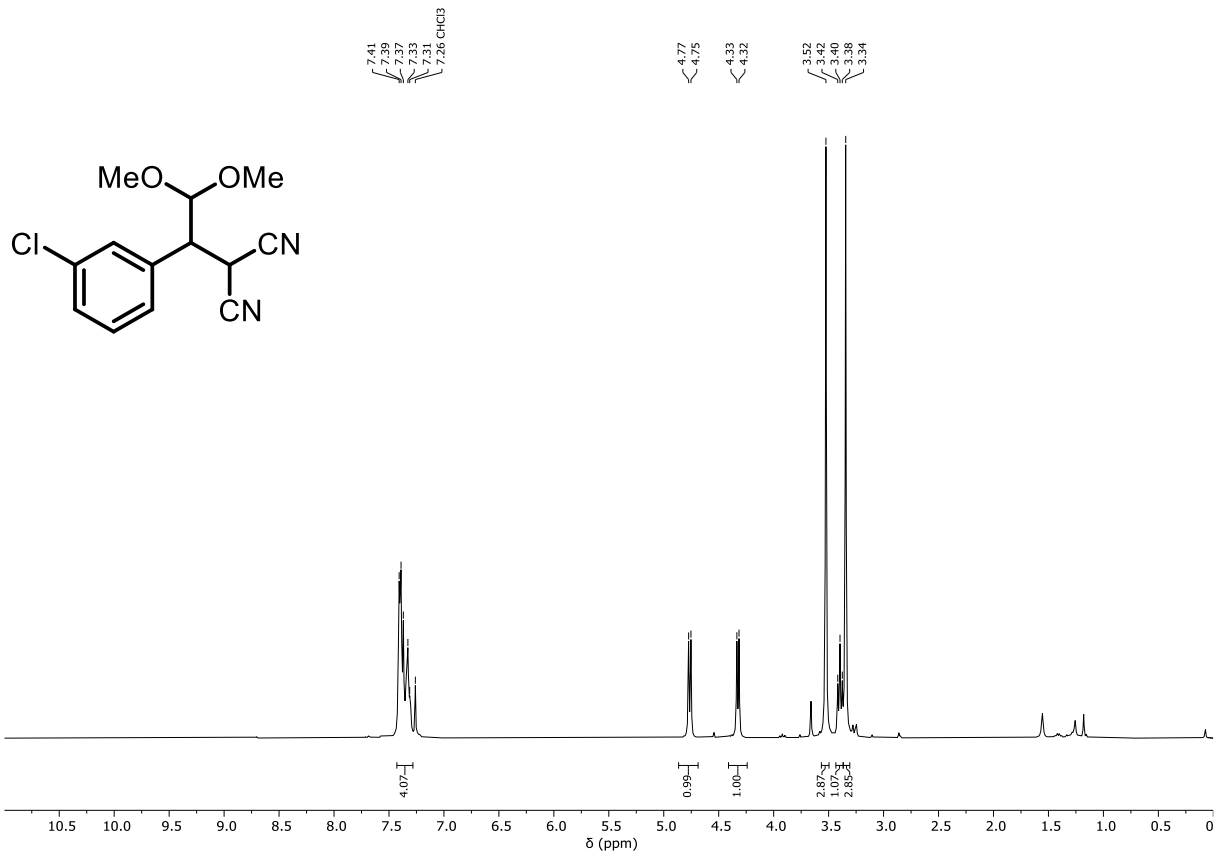
^{13}C{^{1}H} NMR spectrum (151 MHz, DMSO-d_6) of **4c** (only major rotamer signals highlighted)



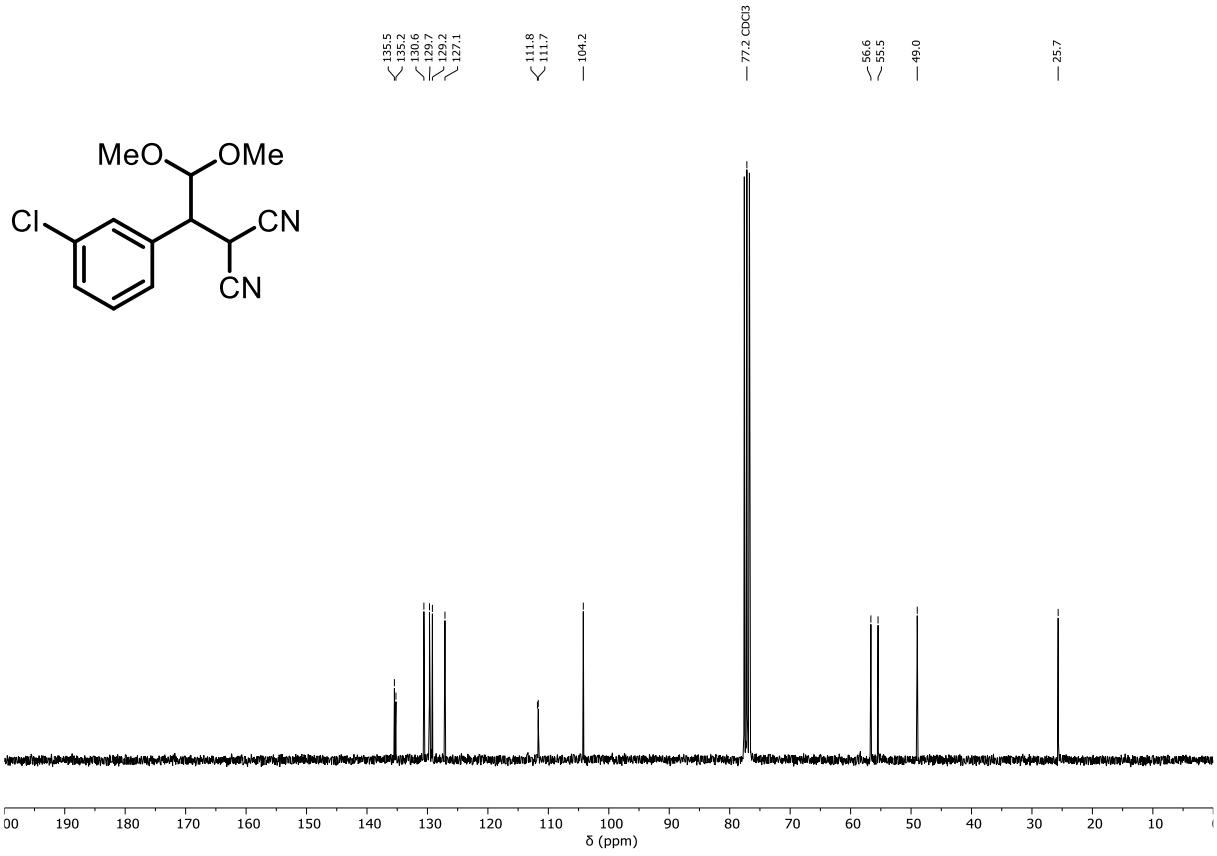
^{1}H NMR spectrum (300 MHz, $CDCl_3$) of **5a**



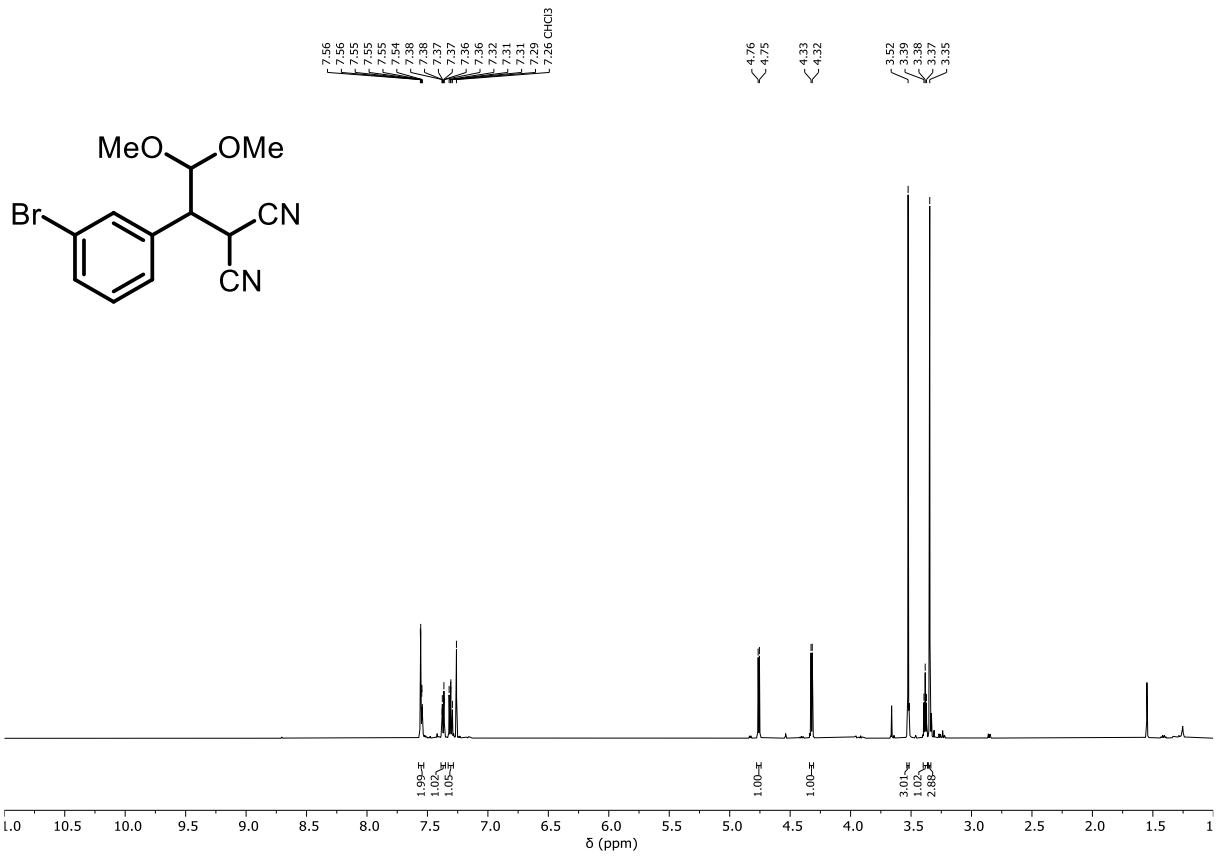
^{13}C{^{1}H} NMR spectrum (101 MHz, $CDCl_3$) of **5a**



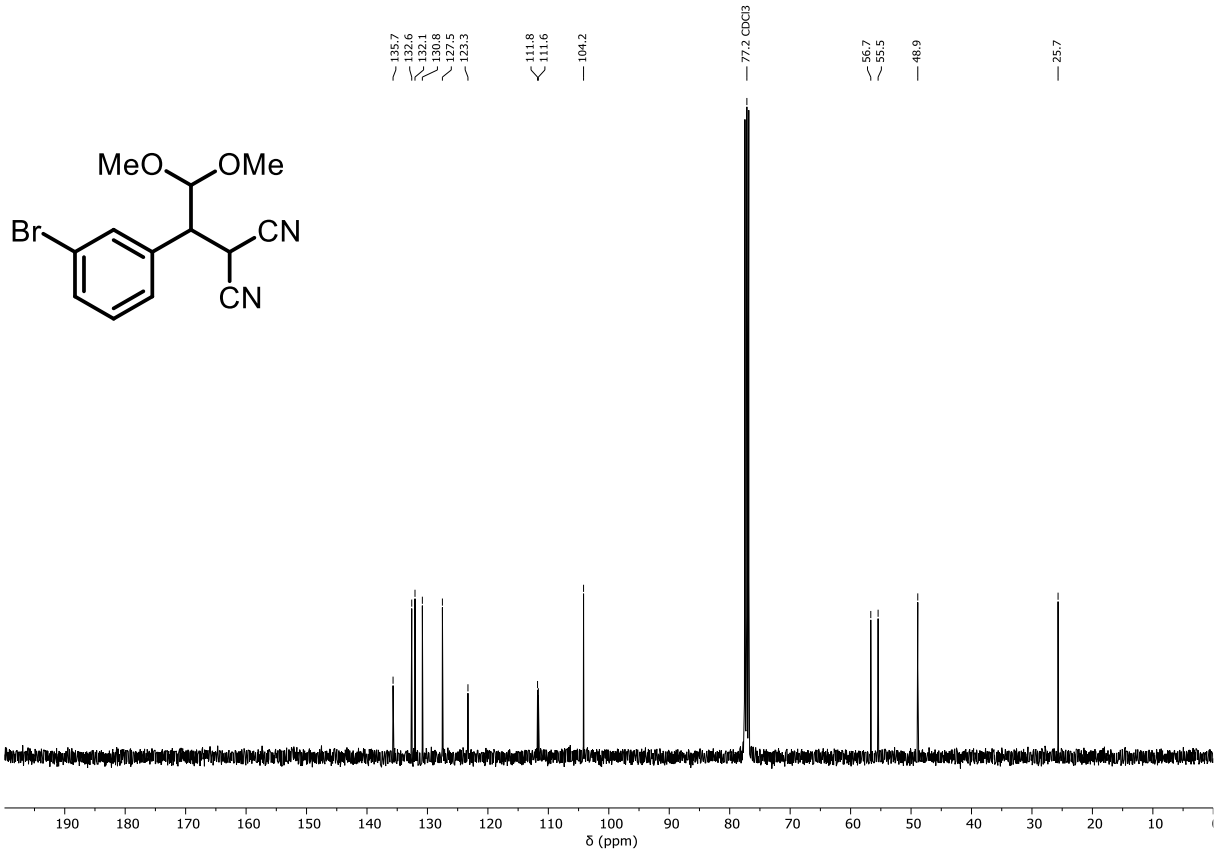
^{1}H NMR spectrum (300 MHz, $CDCl_3$) of **5b**



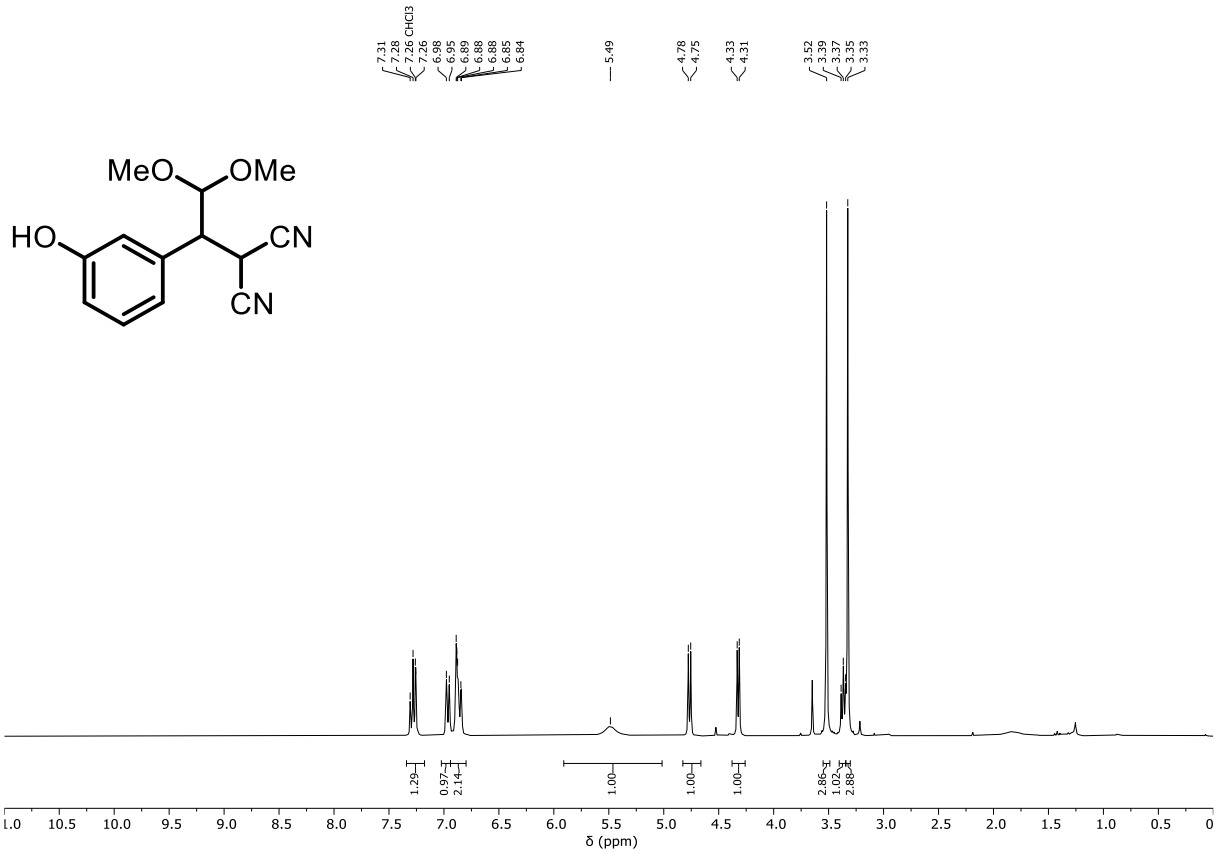
^{13}C{^{1}H} NMR spectrum (75.5 MHz, $CDCl_3$) of **5b**



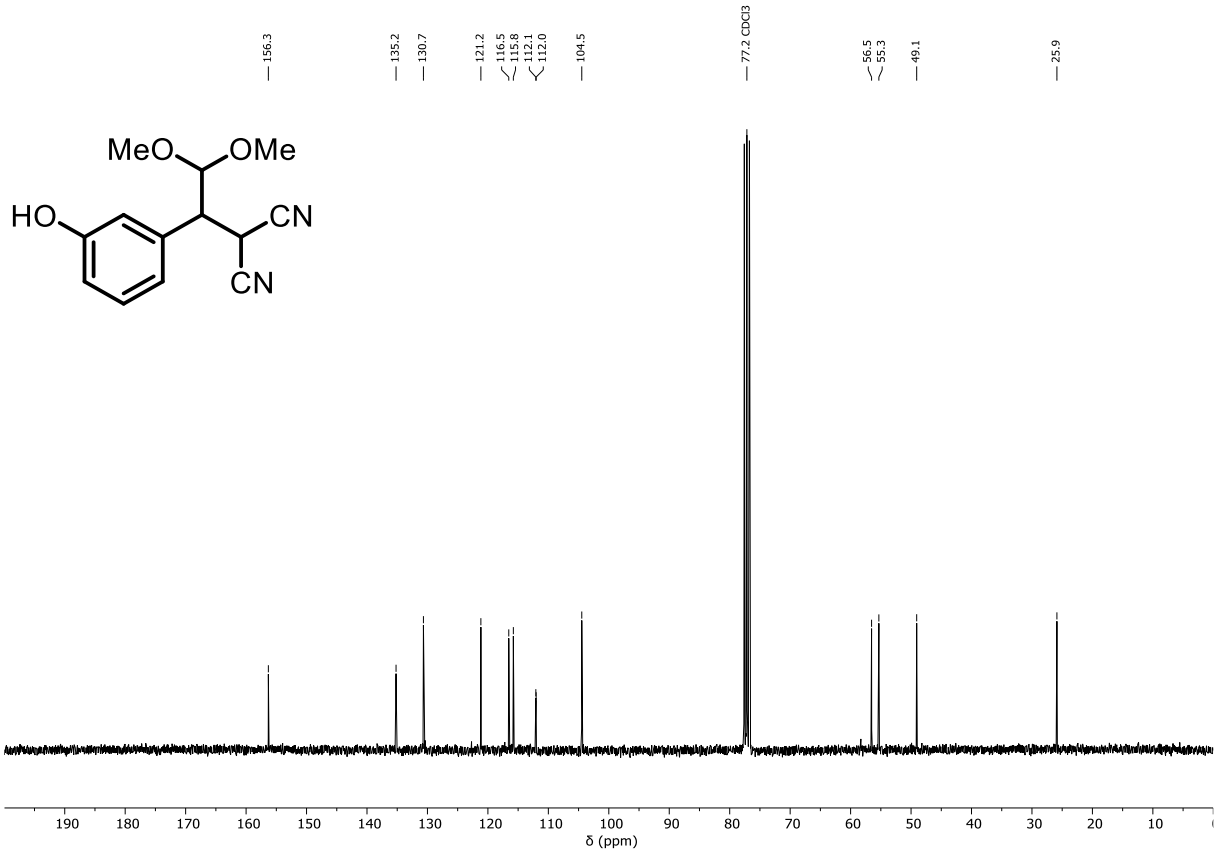
^{1}H NMR spectrum (600 MHz, $CDCl_3$) of **5c**



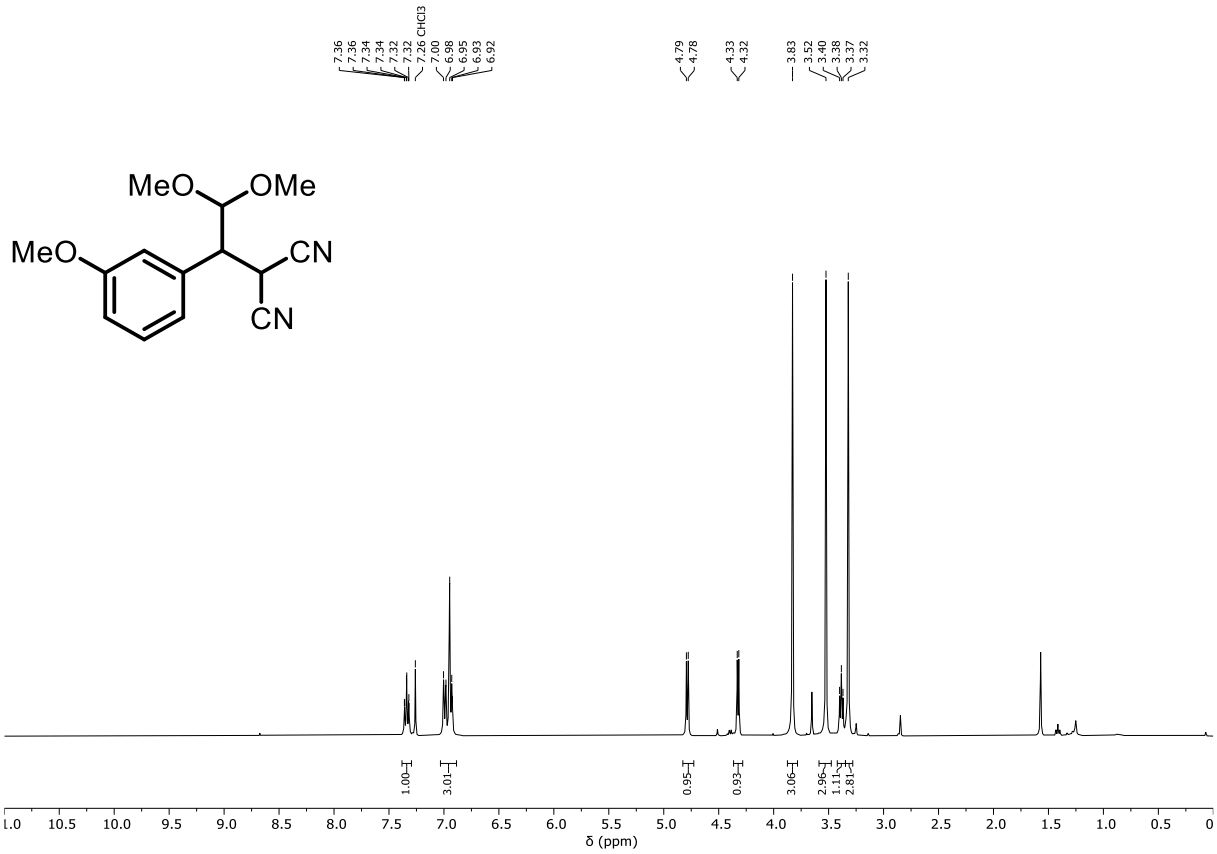
^{13}C{^{1}H} NMR spectrum (101 MHz, $CDCl_3$) of **5c**



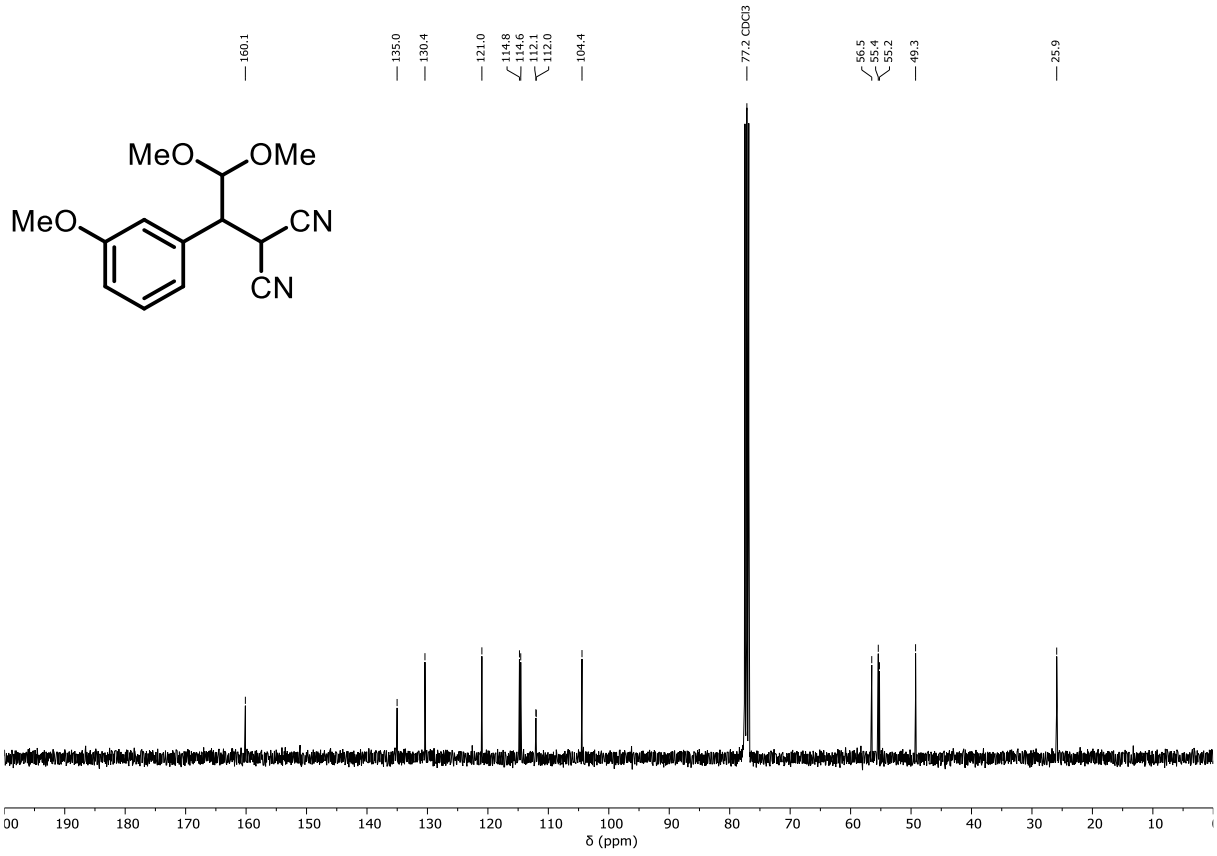
^{1}H NMR spectrum (300 MHz, $CDCl_3$) of **5d**



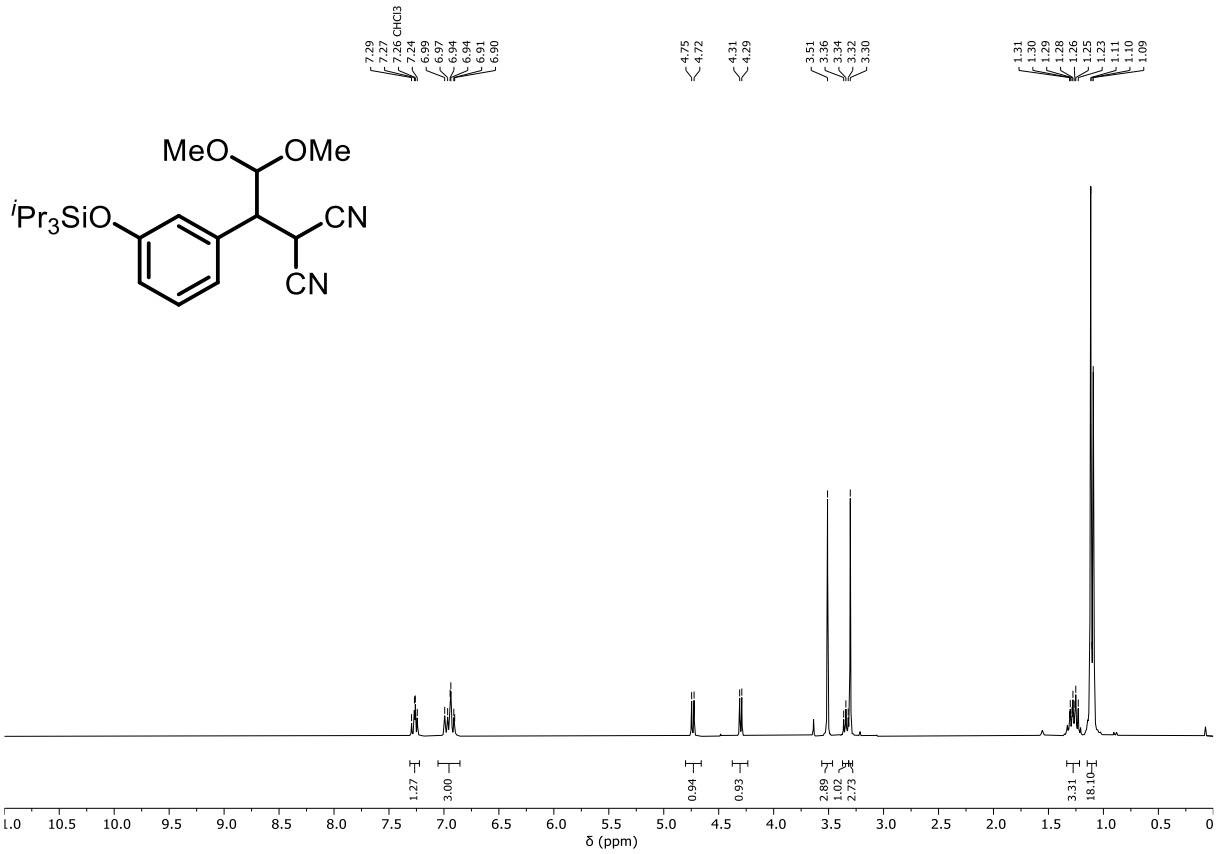
^{13}C{^{1}H} NMR spectrum (75.5 MHz, $CDCl_3$) of **5d**



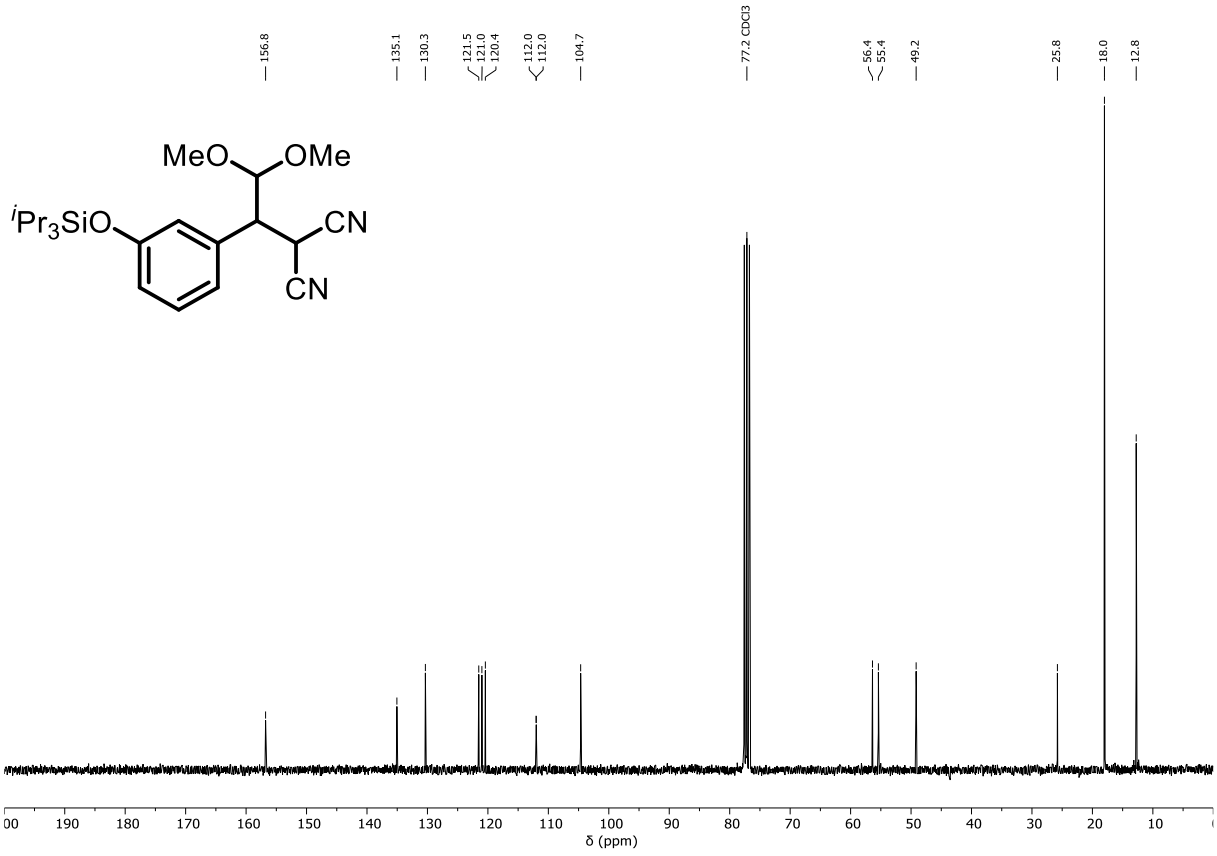
^{1}H NMR spectrum (400 MHz, $CDCl_3$) of **5e**



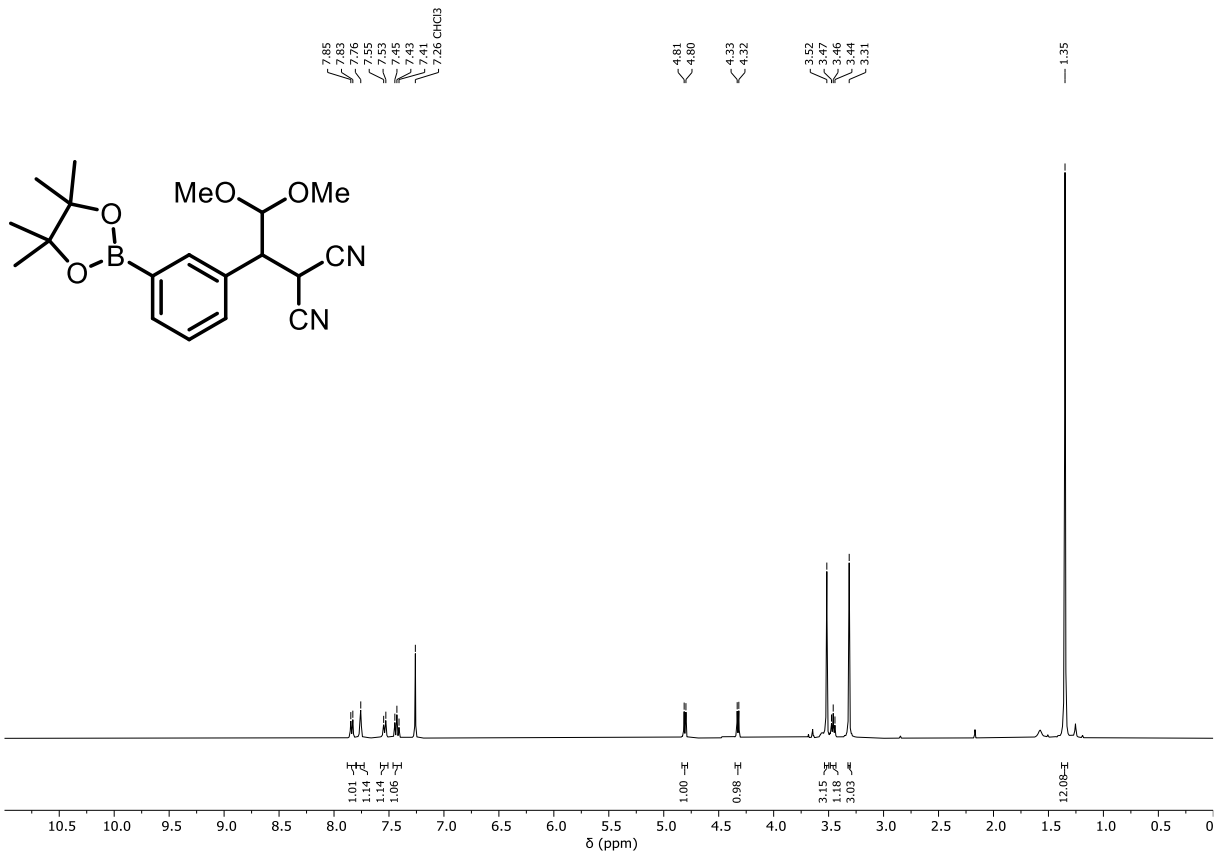
^{13}C{^{1}H} NMR spectrum (101 MHz, $CDCl_3$) of **5e**



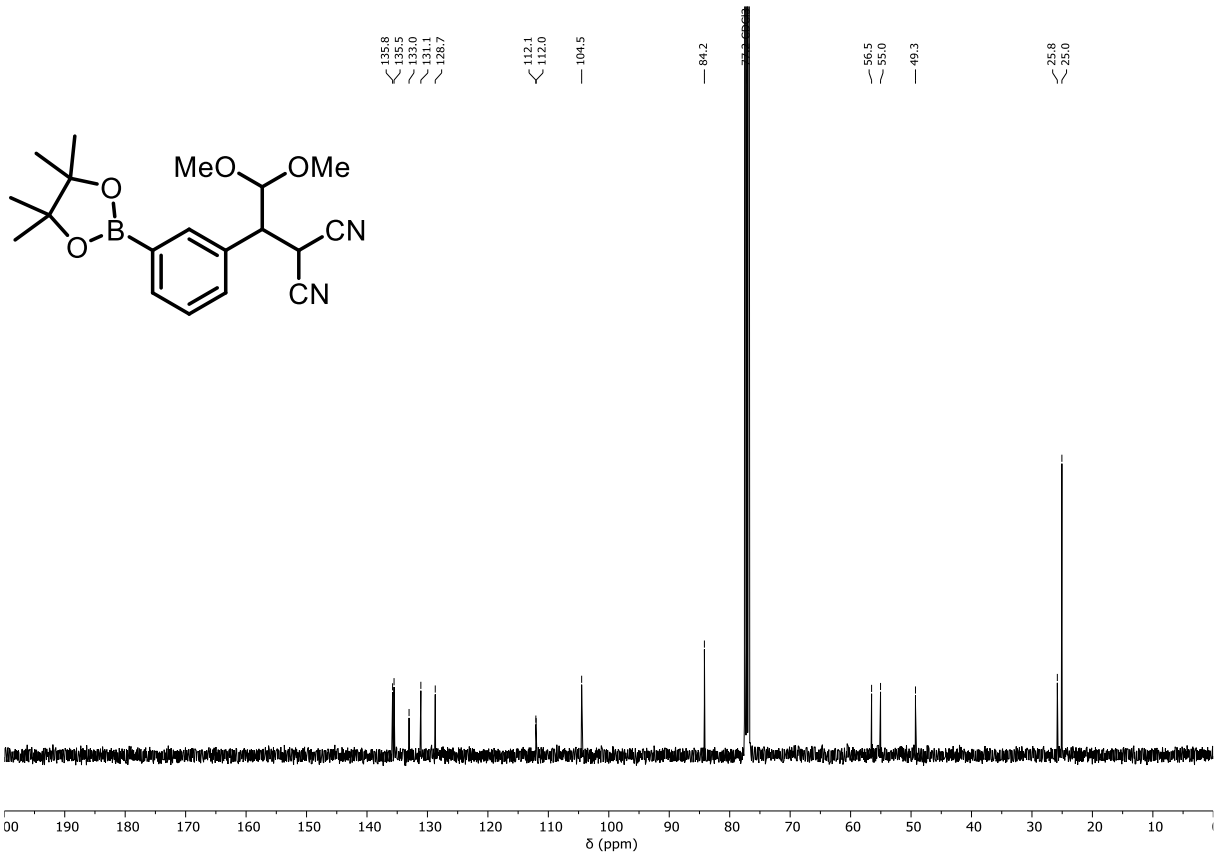
^{1}H NMR spectrum (300 MHz, $CDCl_3$) of **5f**



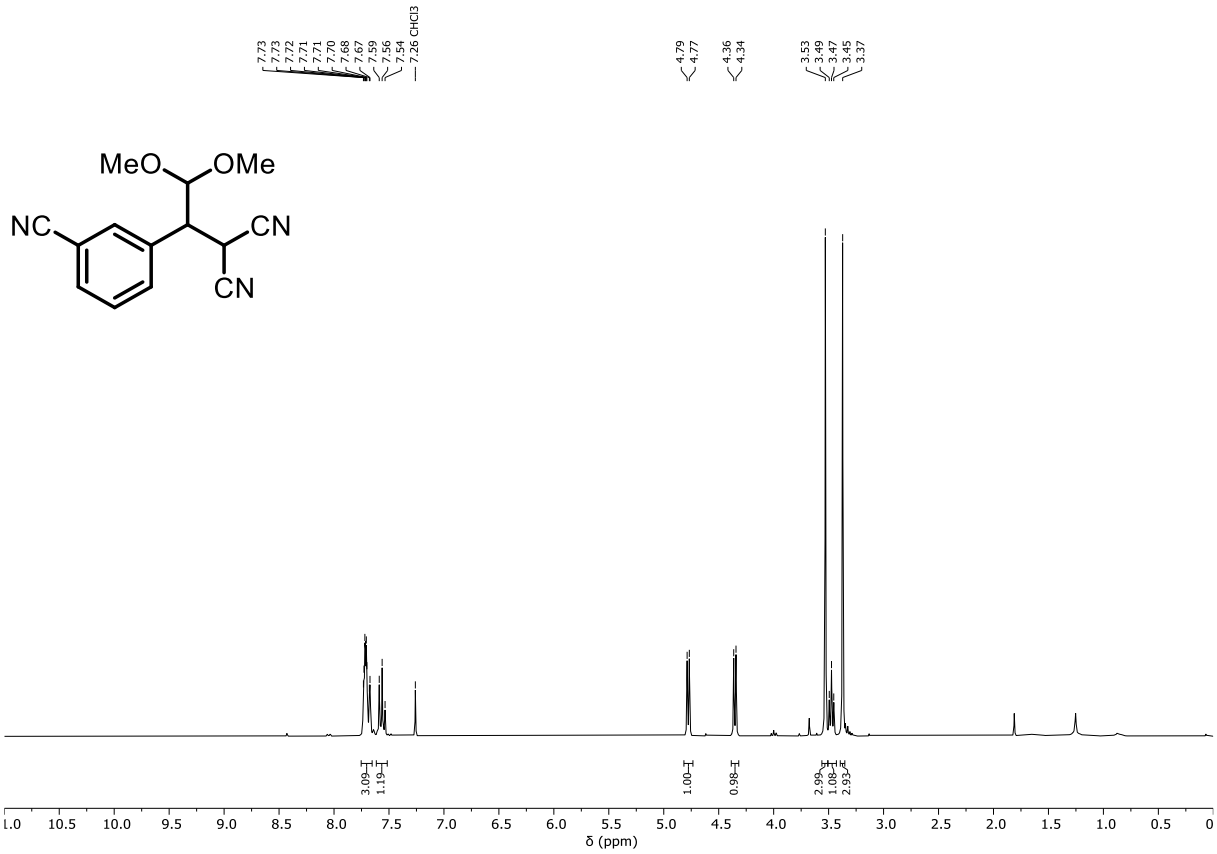
^{13}C{^{1}H} NMR spectrum (75.5 MHz, $CDCl_3$) of **5f**



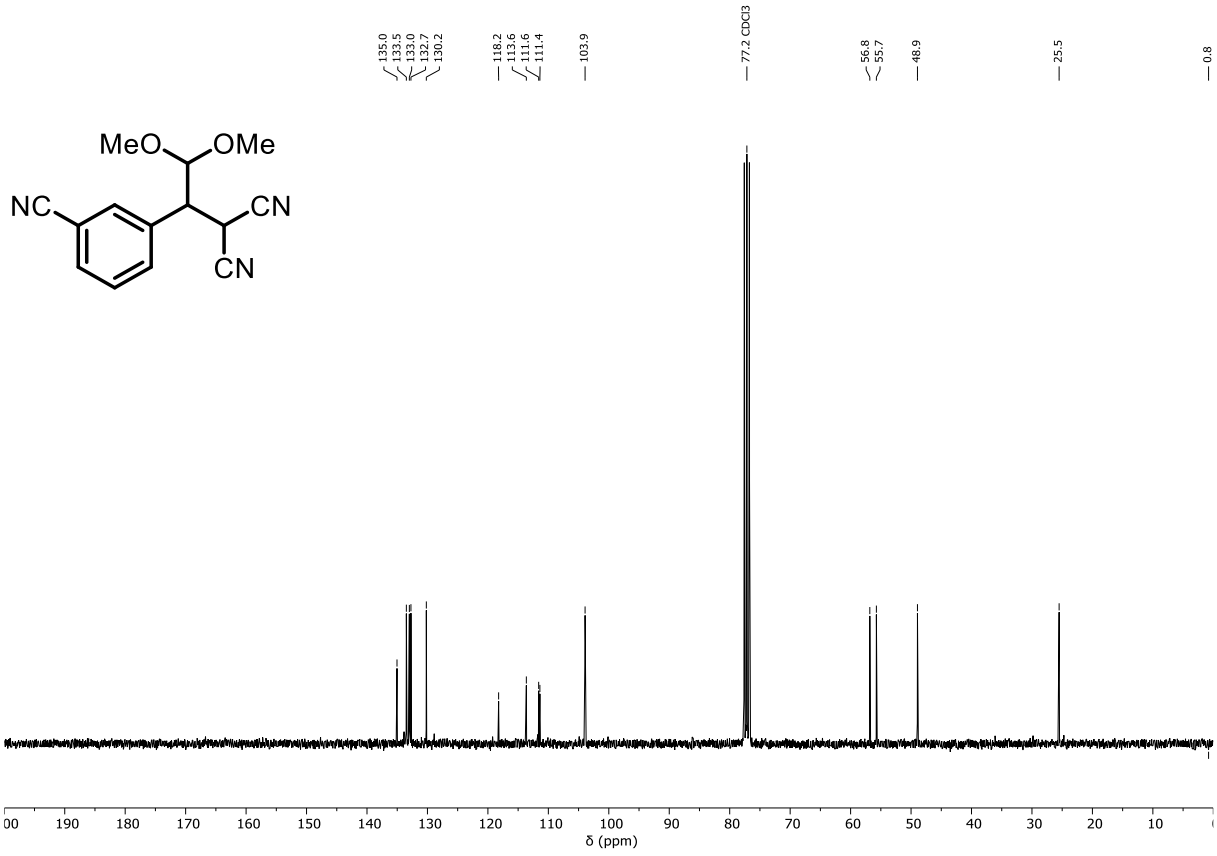
^{1}H NMR spectrum (400 MHz, $CDCl_3$) of **5g**



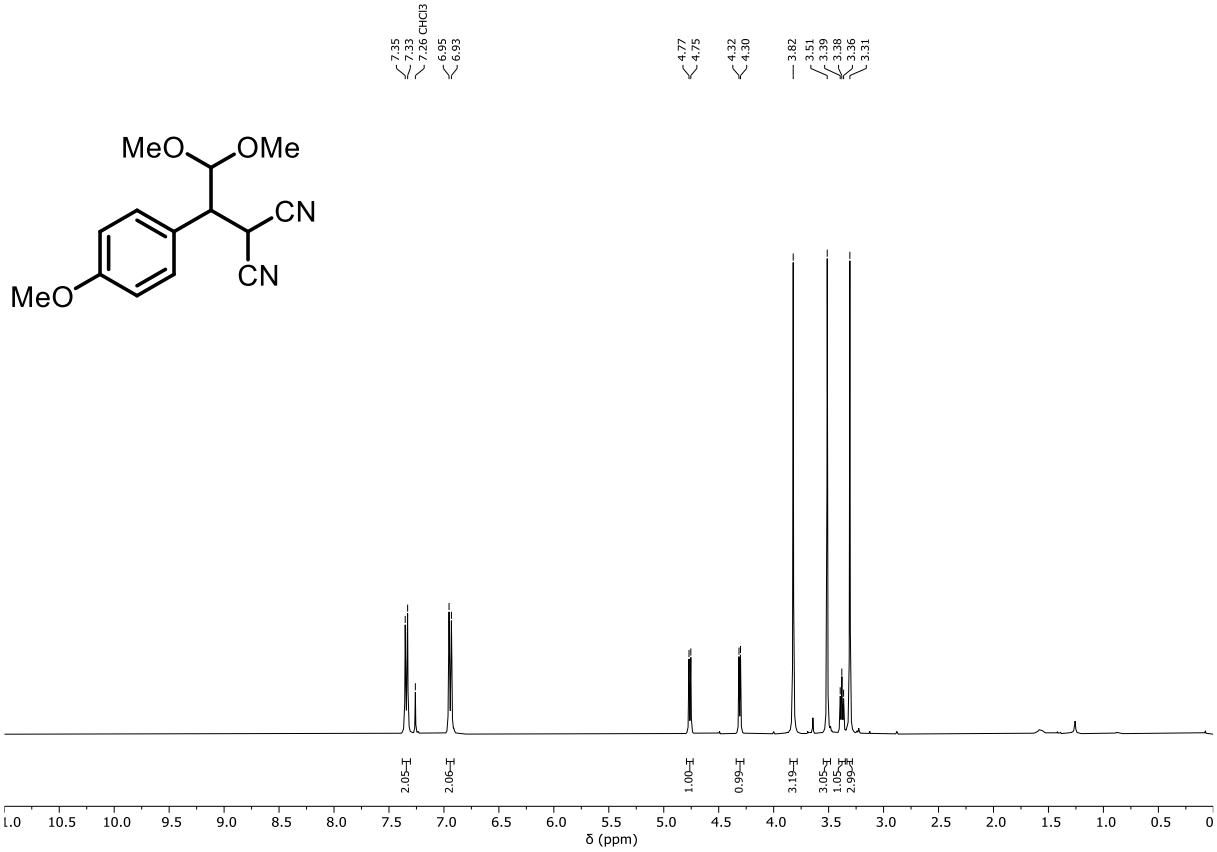
^{13}C{^{1}H} NMR spectrum (101 MHz, $CDCl_3$) of **5g**



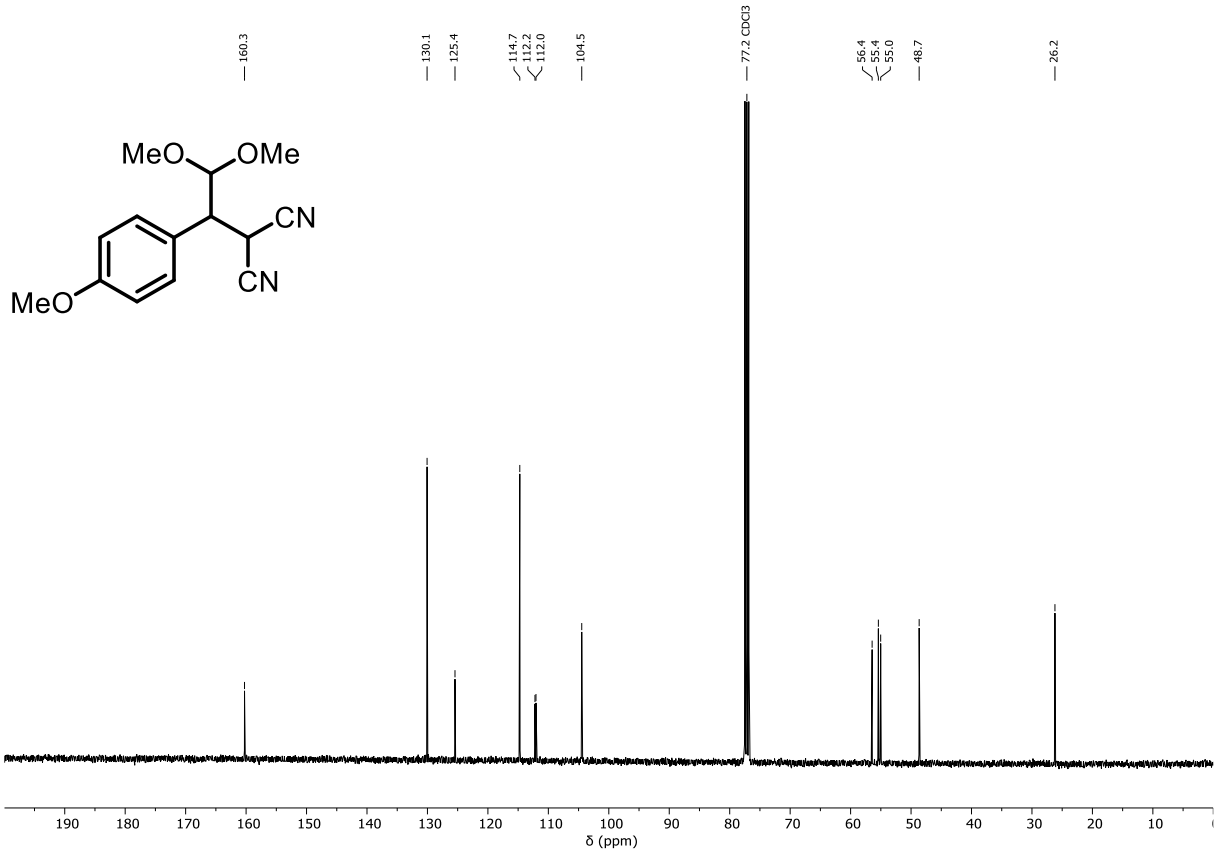
^{1}H NMR spectrum (300 MHz, $CDCl_3$) of **5h**



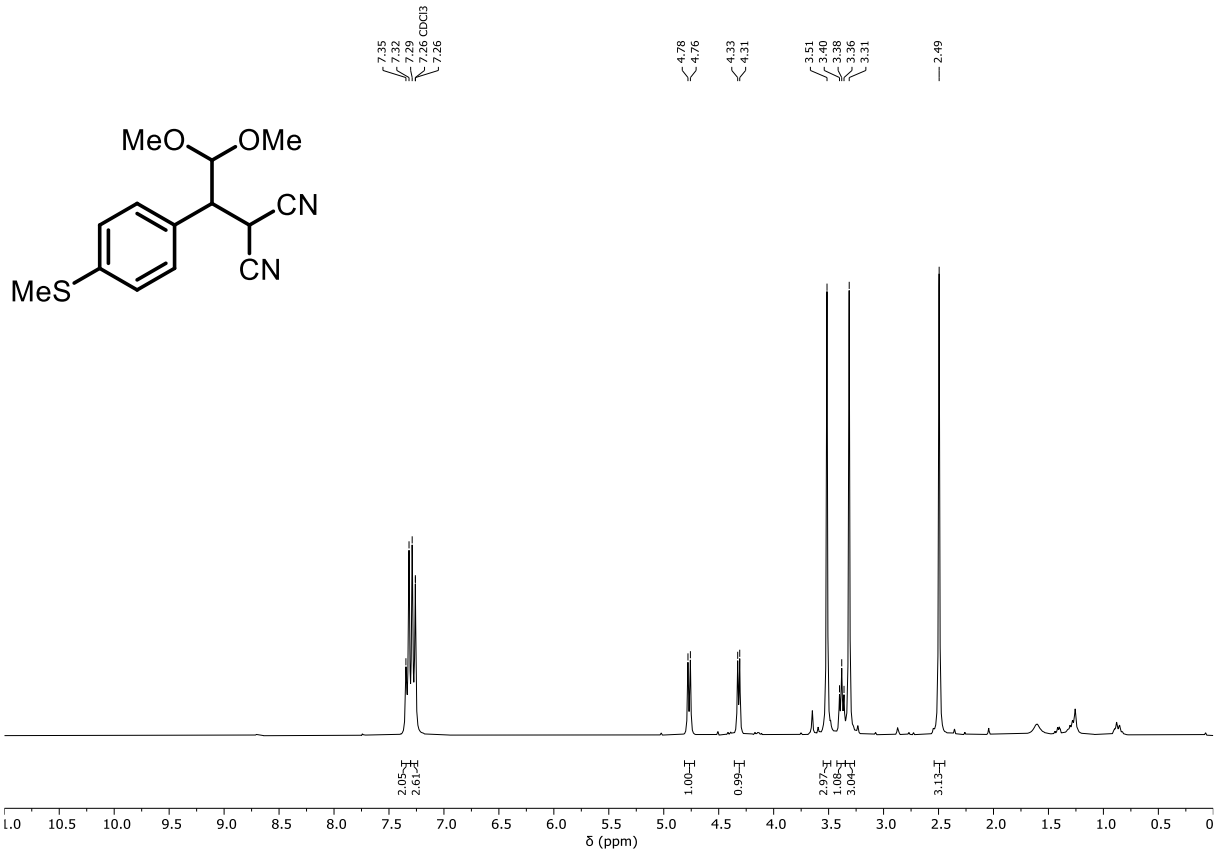
^{13}C{^{1}H} NMR spectrum (75.5 MHz, $CDCl_3$) of **5h**



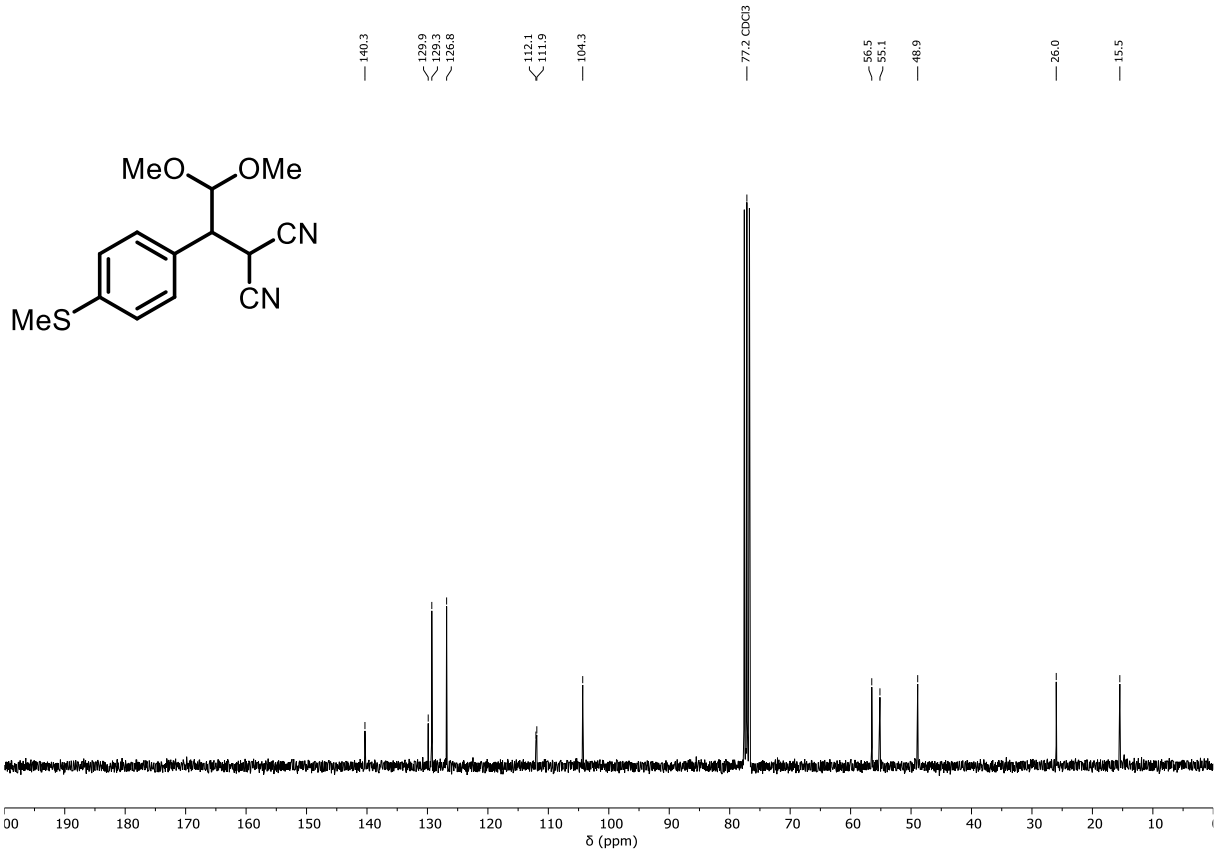
^{1}H NMR spectrum (400 MHz, $CDCl_3$) of **5i**



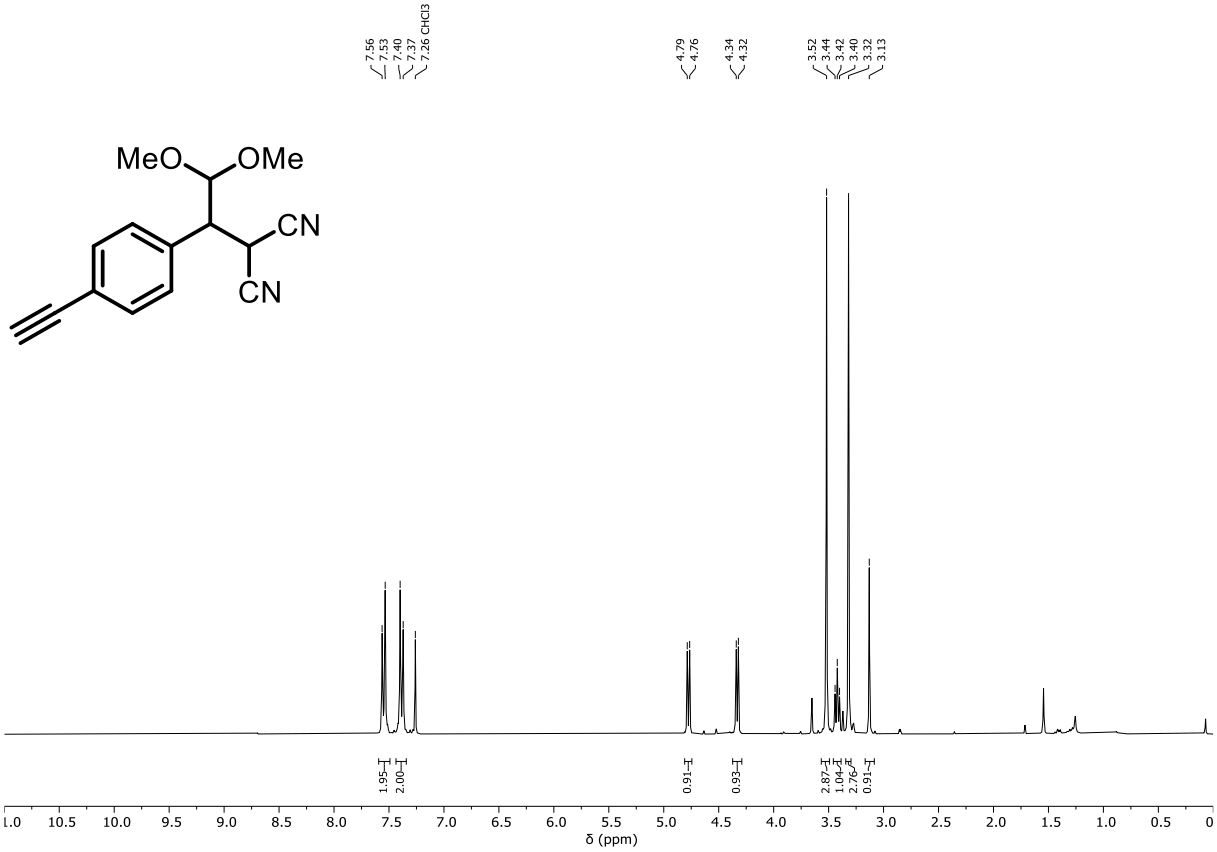
^{13}C{^{1}H} NMR spectrum (101 MHz, $CDCl_3$) of **5i**



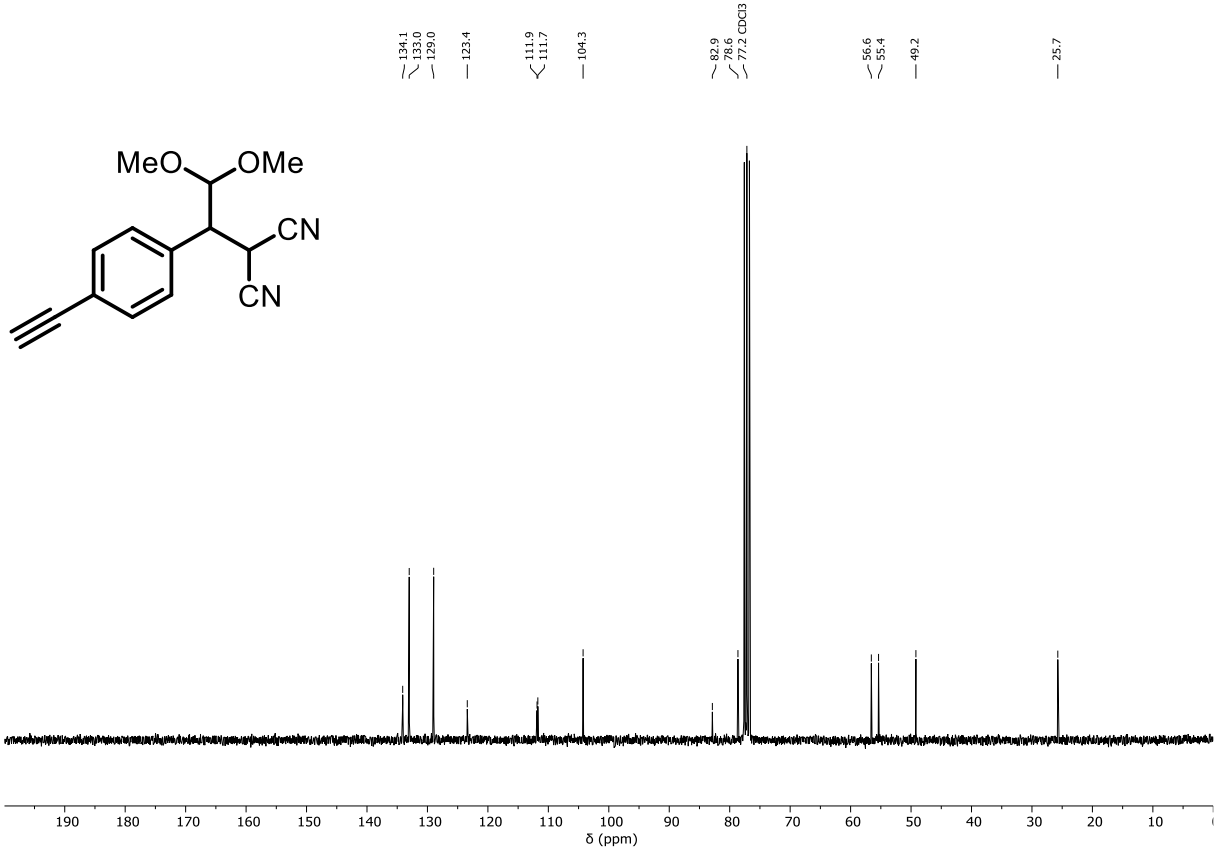
^{1}H NMR spectrum (300 MHz, $CDCl_3$) of **5j**



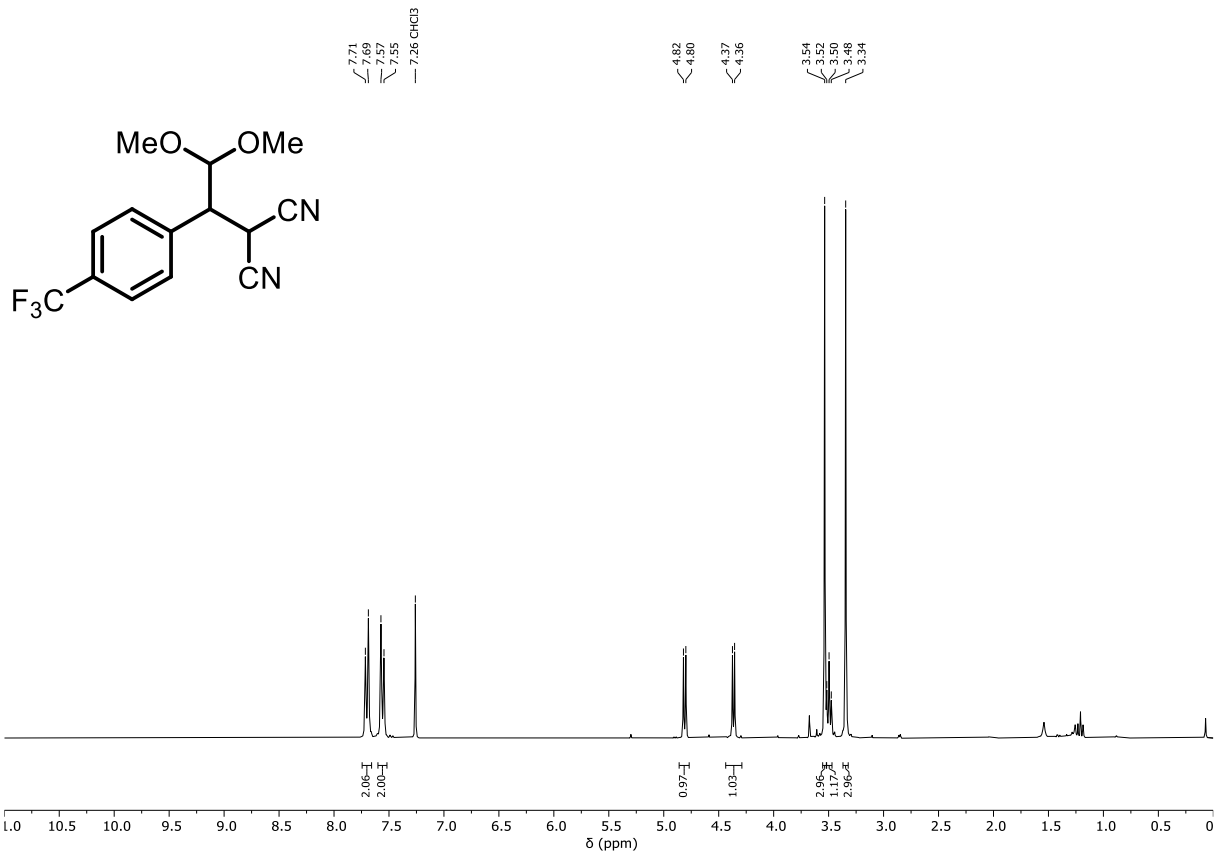
^{13}C{^{1}H} NMR spectrum (101 MHz, $CDCl_3$) of **5j**



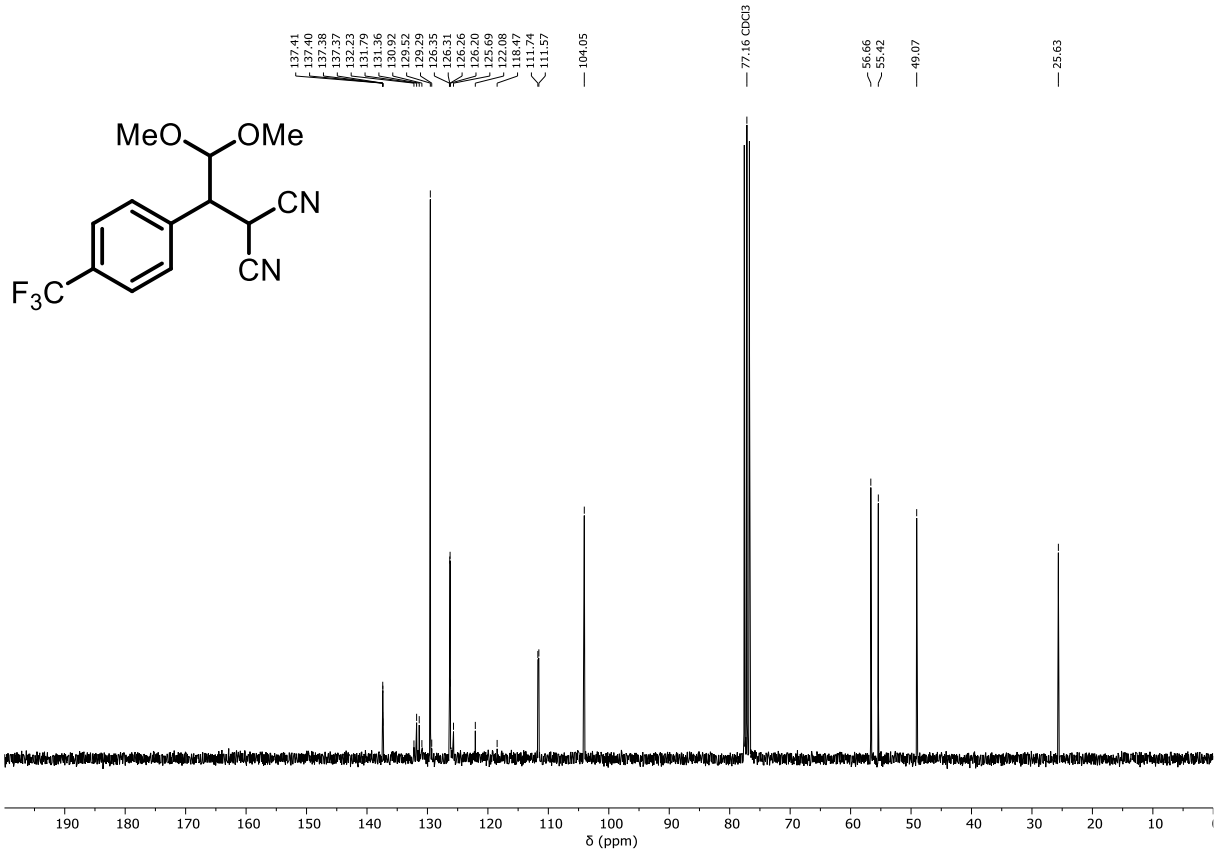
^{1}H NMR spectrum (300 MHz, $CDCl_3$) of **5k**



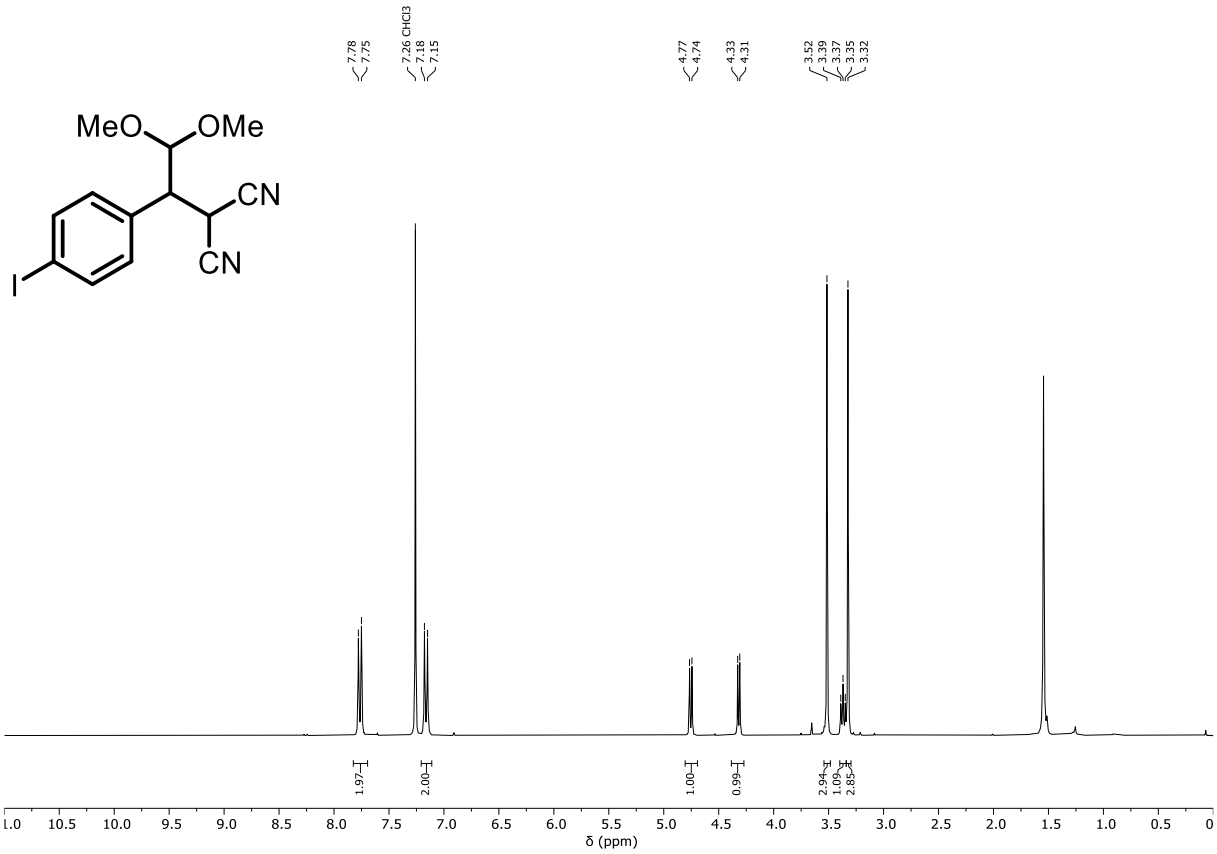
^{13}C{^{1}H} NMR spectrum (75.5 MHz, $CDCl_3$) of **5k**



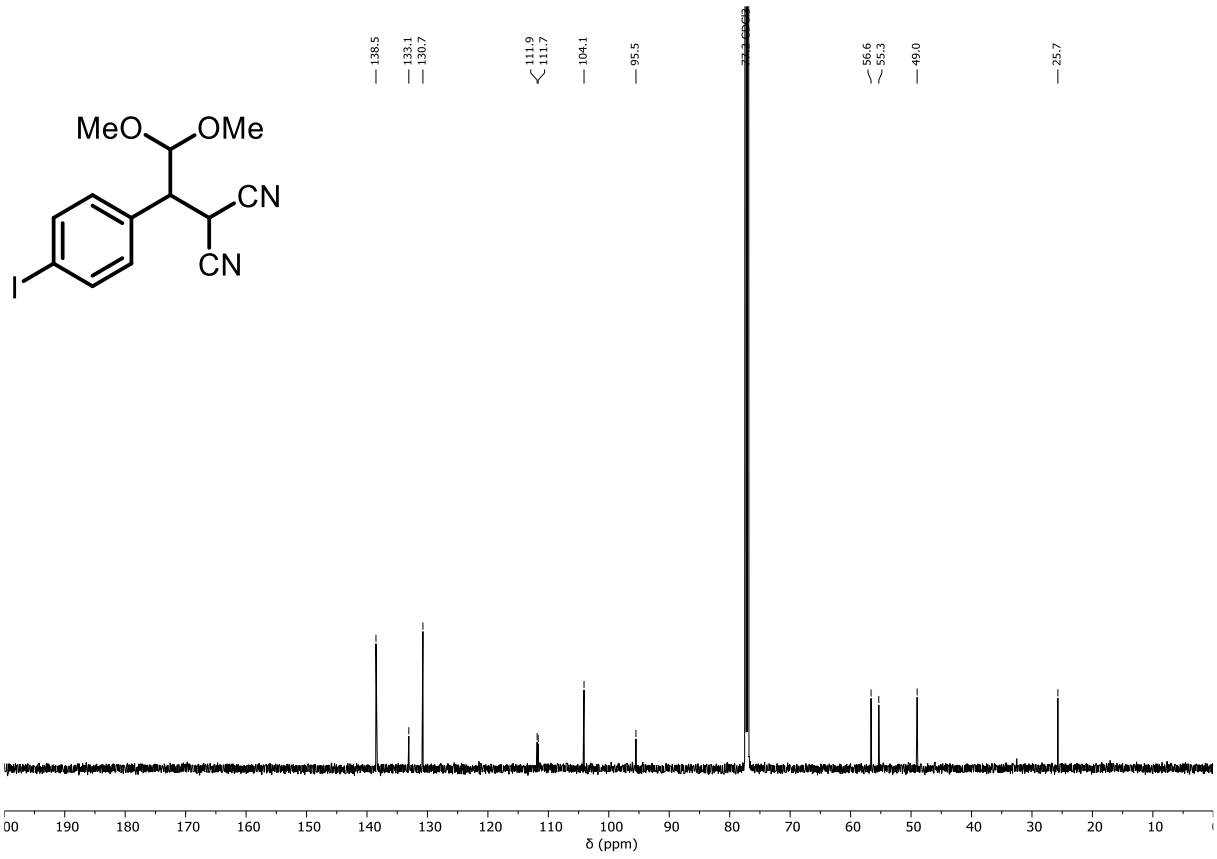
^{1}H NMR spectrum (300 MHz, $CDCl_3$) of **5n**



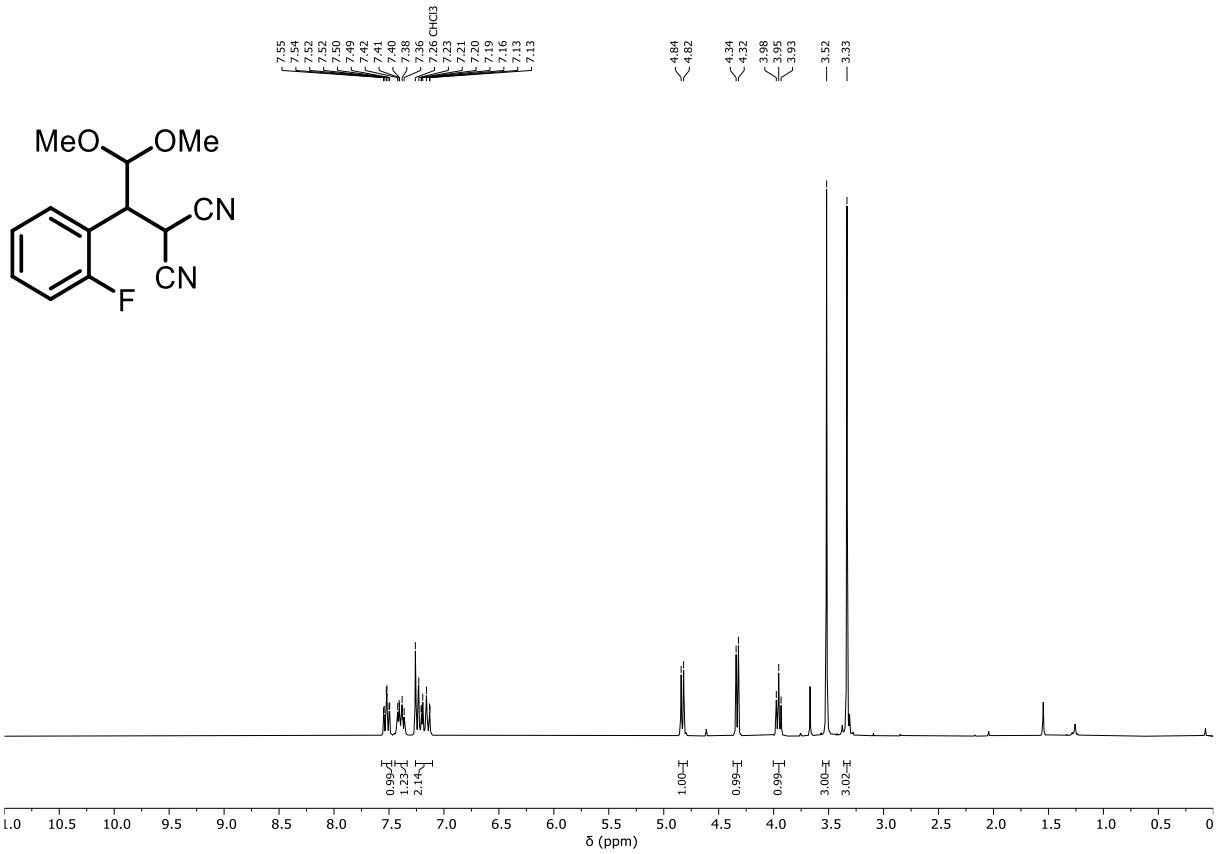
^{13}C{^{1}H} NMR spectrum (75.5 MHz, $CDCl_3$) of **5n**



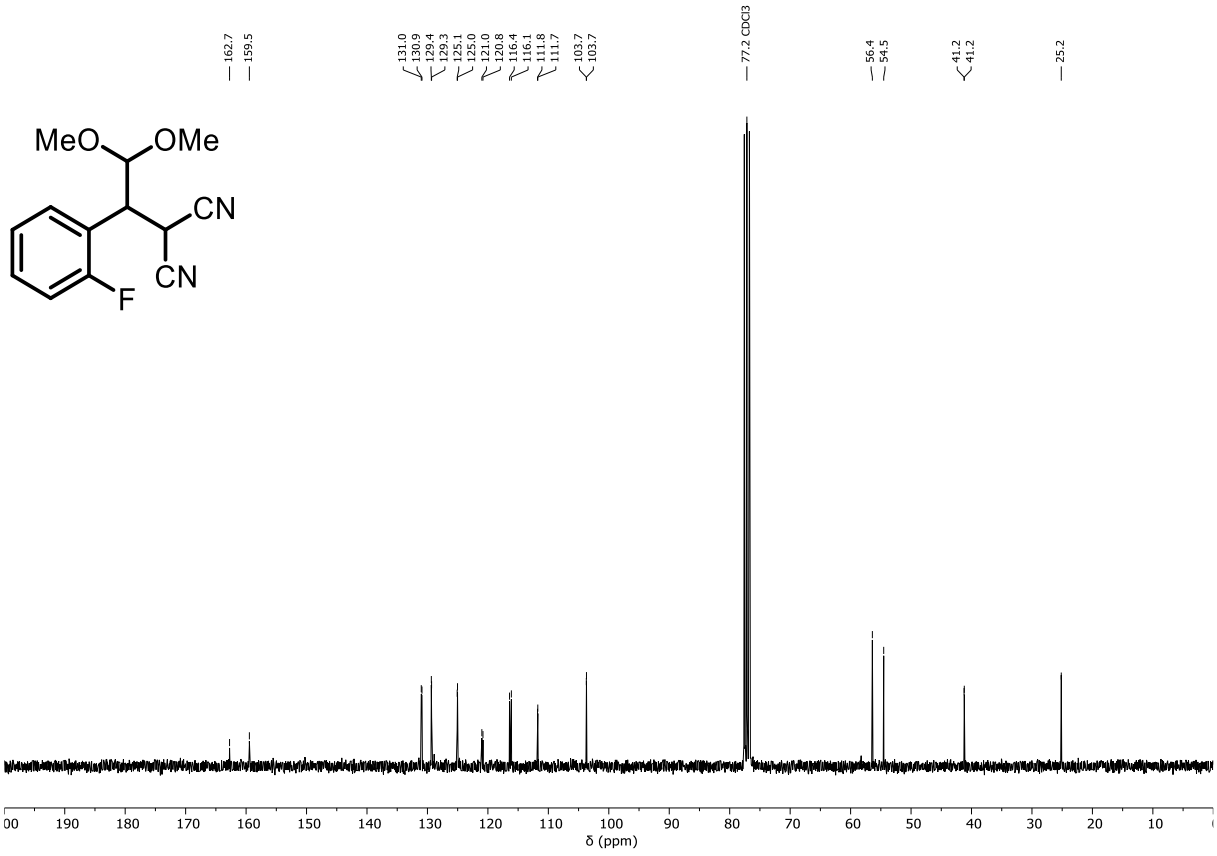
^{1}H NMR spectrum (300 MHz, $CDCl_3$) of **5q**



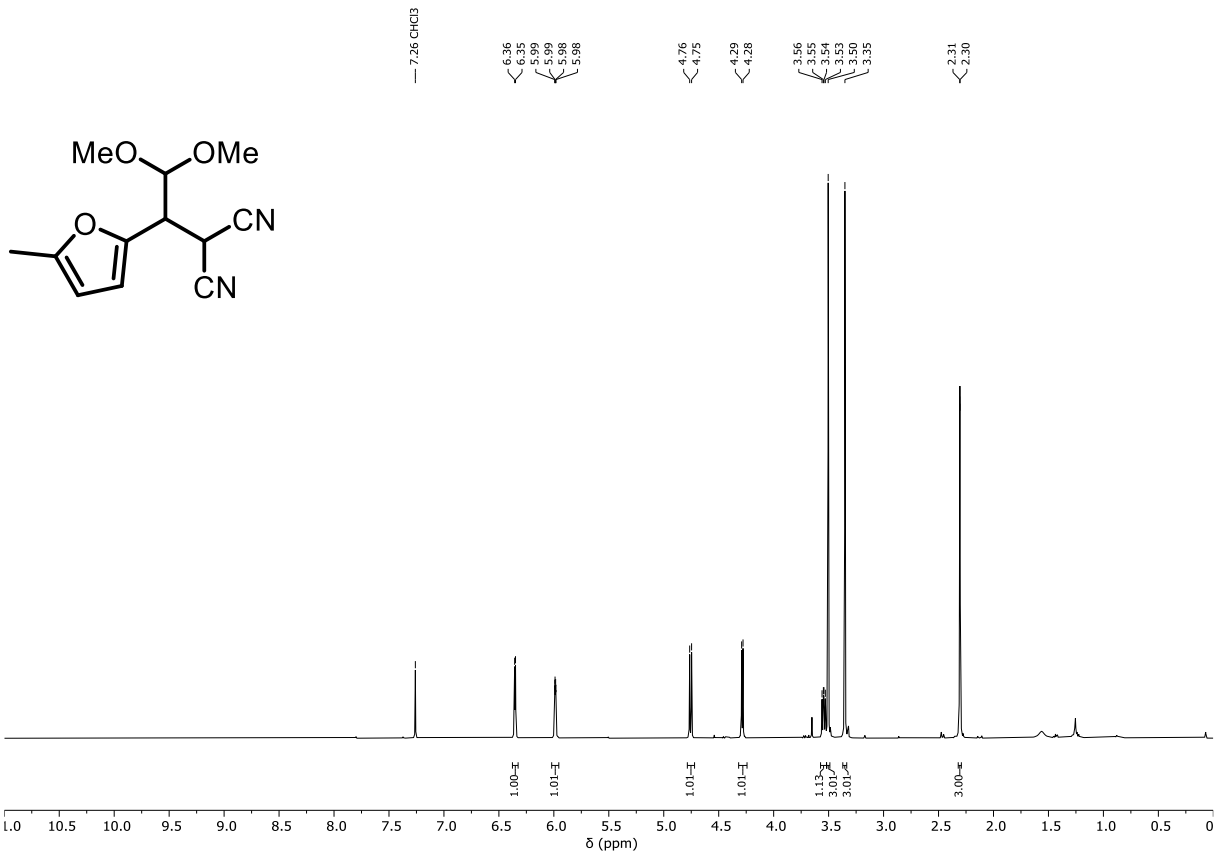
^{13}C{^{1}H} NMR spectrum (151 MHz, $CDCl_3$) of **5q**



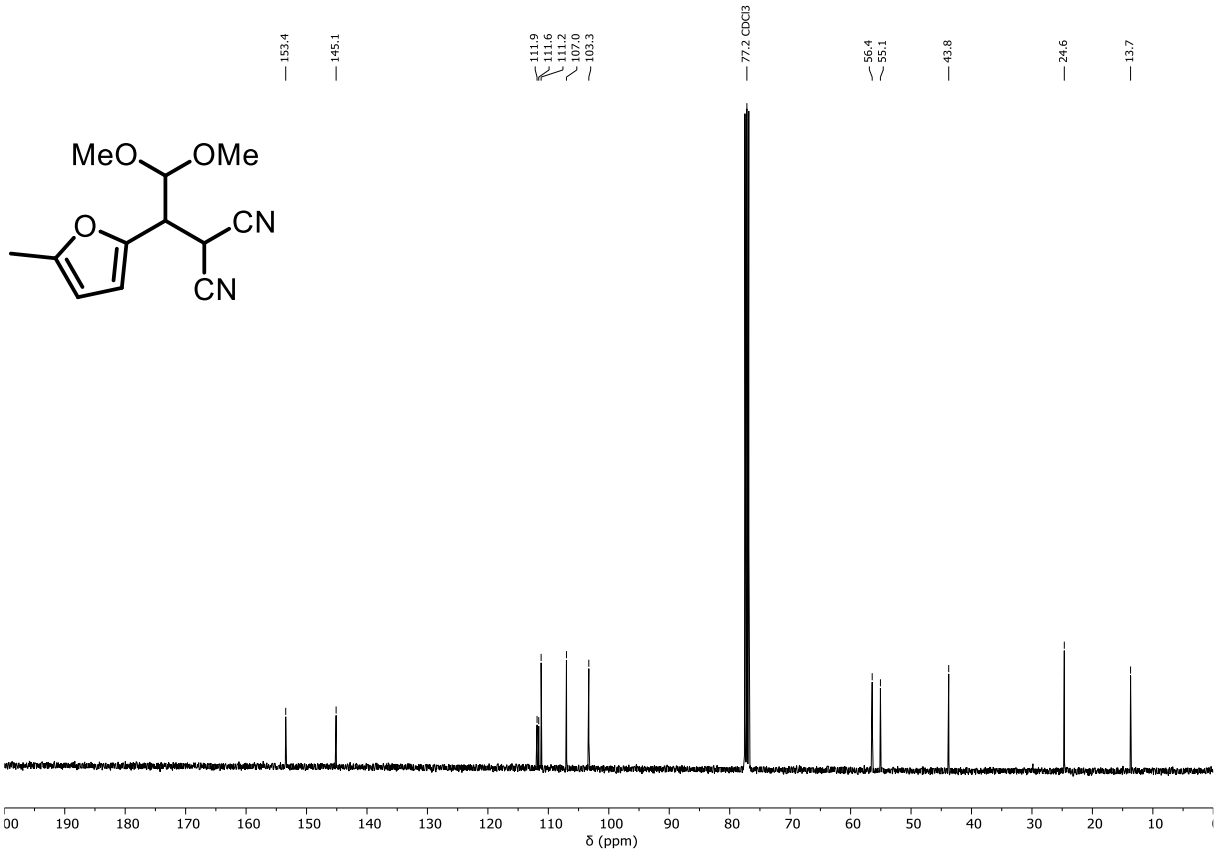
^{1}H NMR spectrum (300 MHz, $CDCl_3$) of **5r**



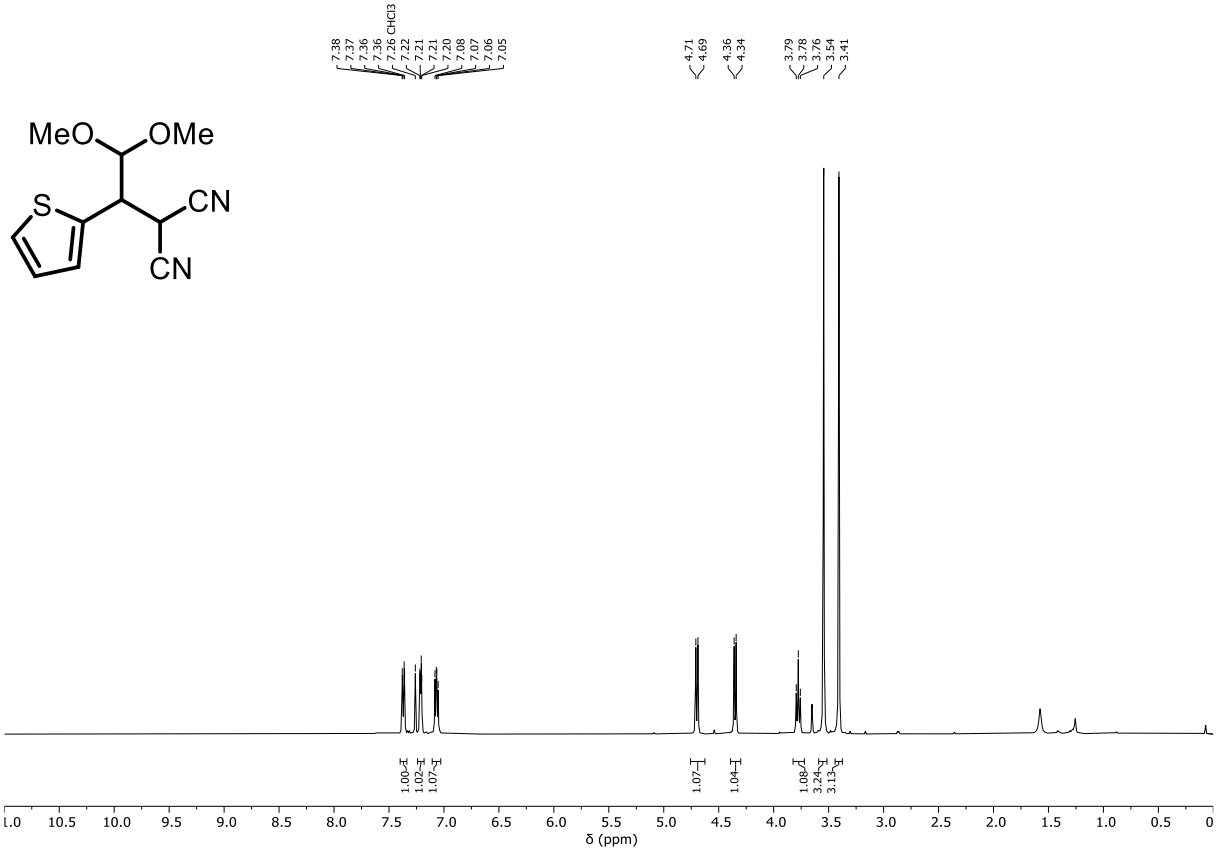
^{13}C{^{1}H} NMR spectrum (75.5 MHz, $CDCl_3$) of **5r**



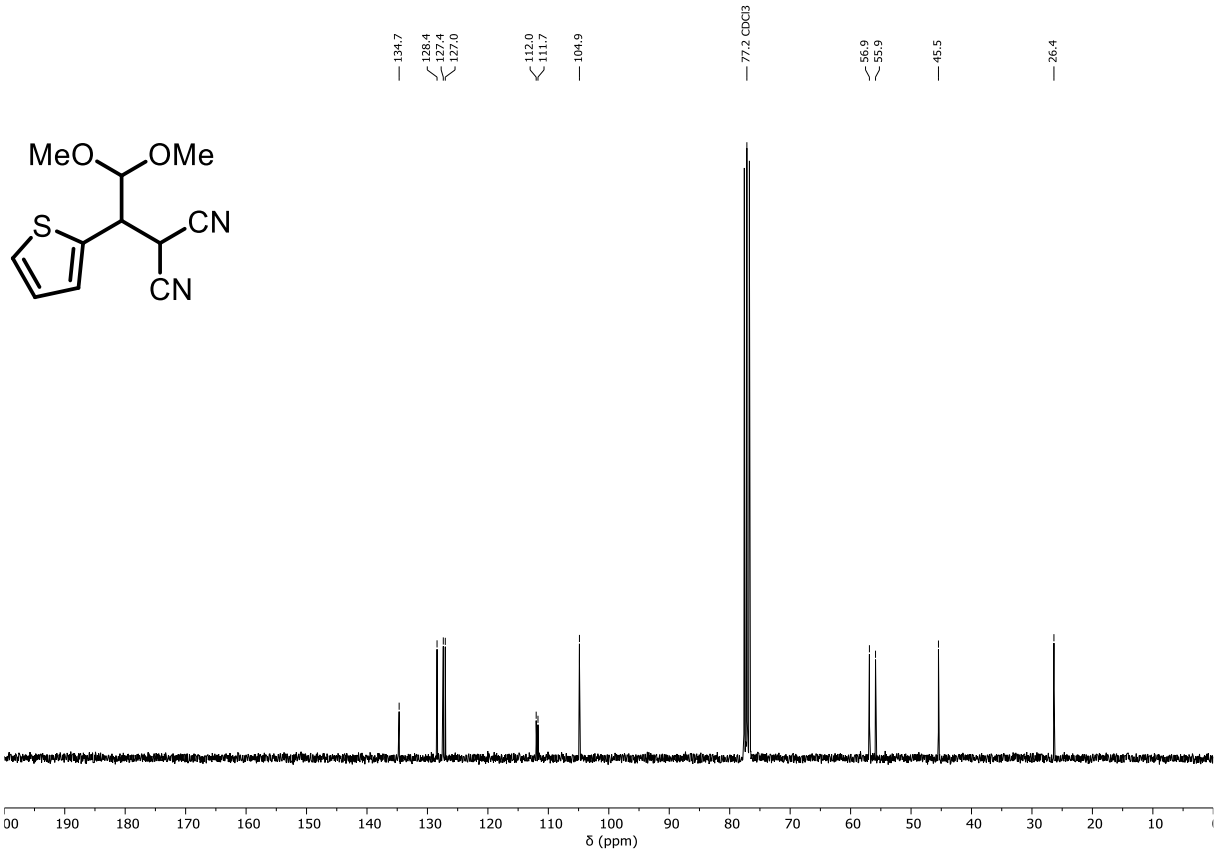
^{1}H NMR spectrum (400 MHz, $CDCl_3$) of **5t**



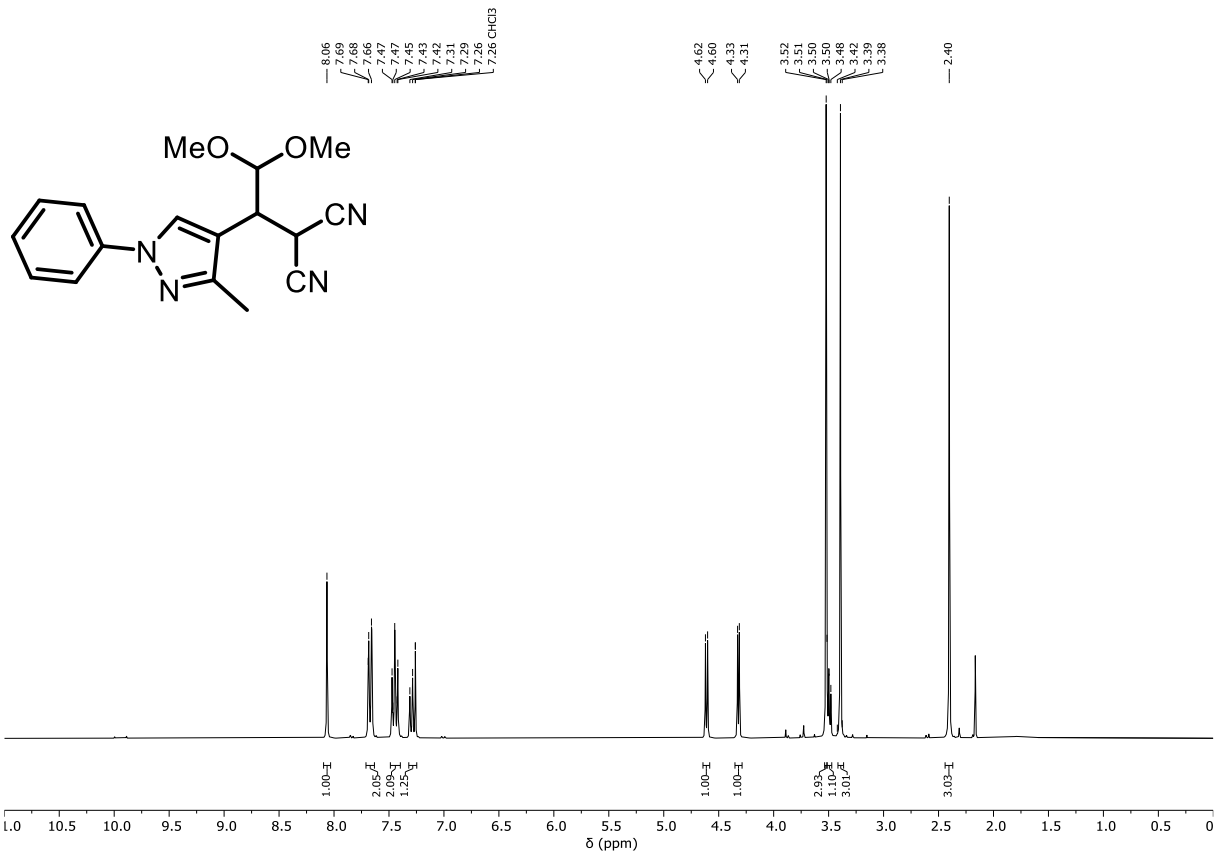
^{13}C{^{1}H} NMR spectrum (101 MHz, $CDCl_3$) of **5t**



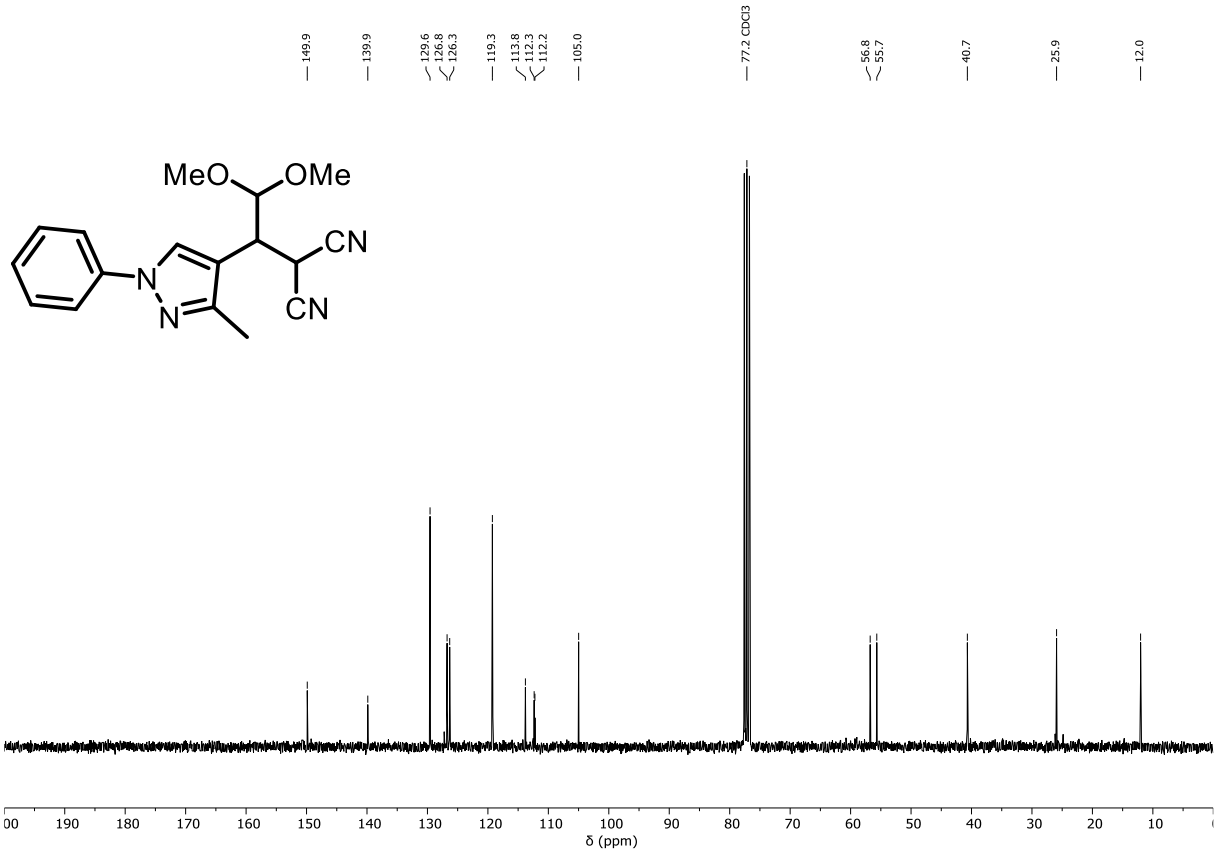
^{1}H NMR spectrum (300 MHz, $CDCl_3$) of **5u**



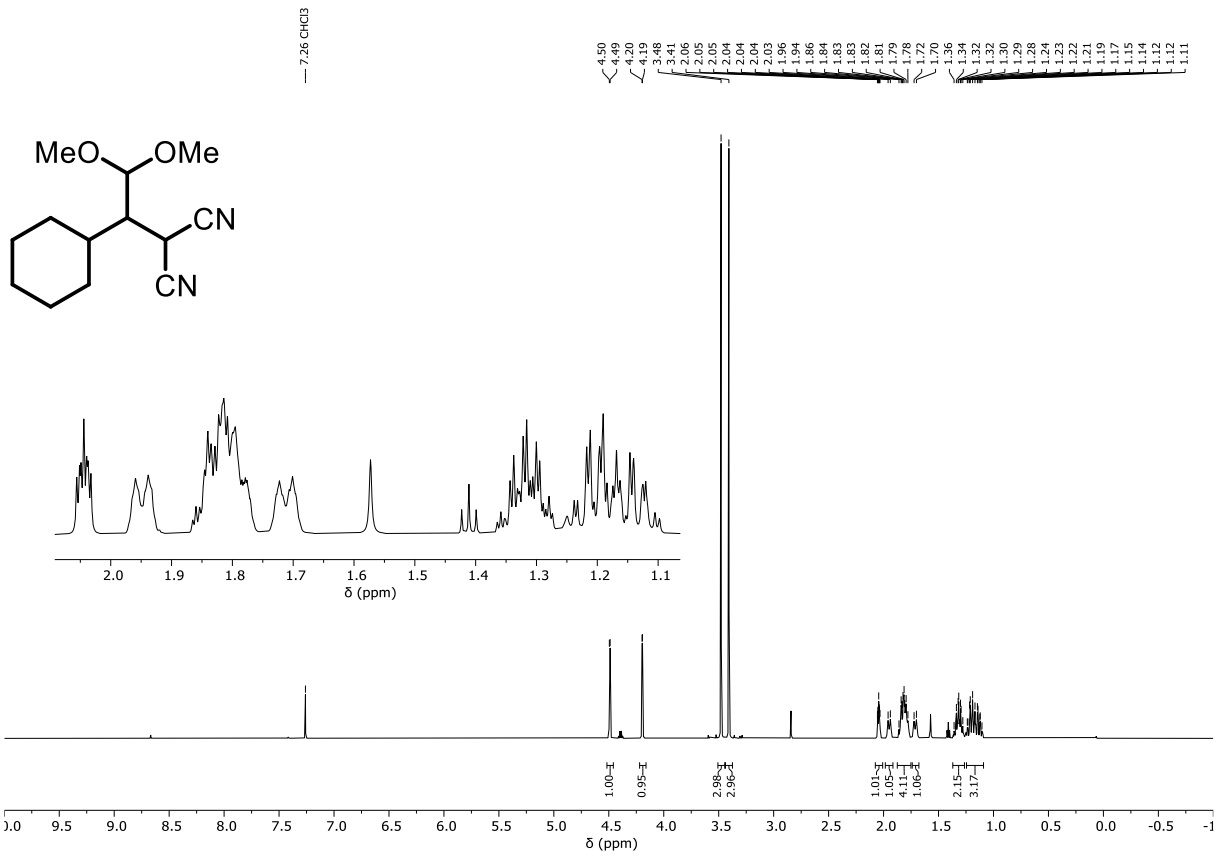
^{13}C{^{1}H} NMR spectrum (75.5 MHz, $CDCl_3$) of **5u**



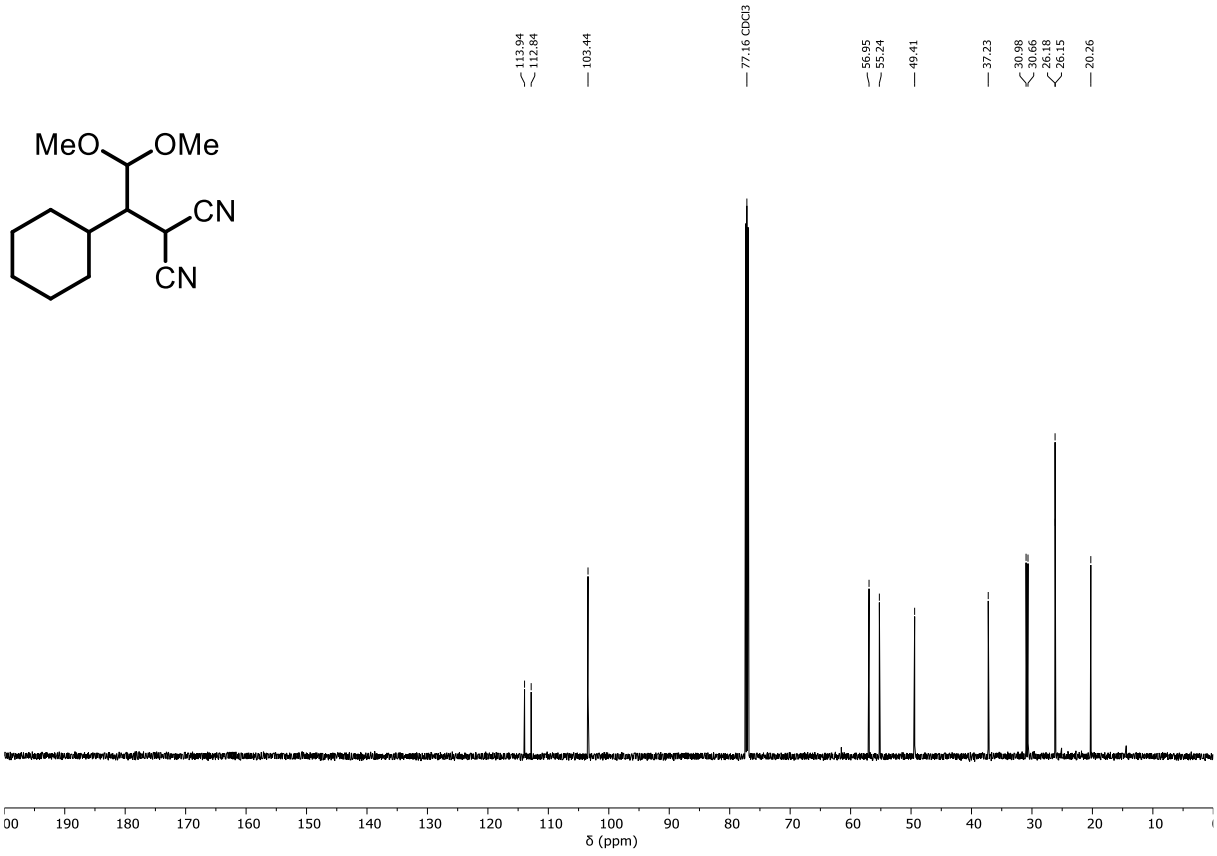
^{1}H NMR spectrum (300 MHz, $CDCl_3$) of **5v**



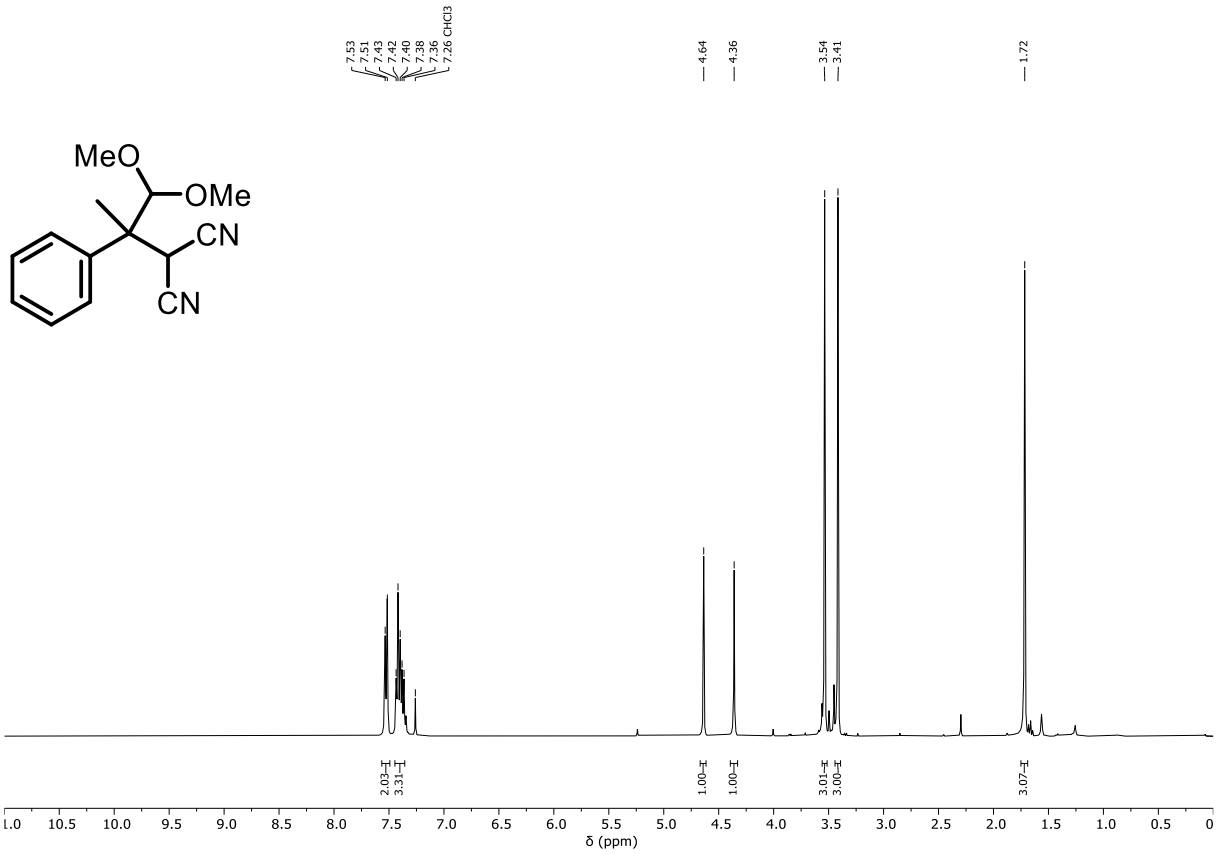
^{13}C{^{1}H} NMR spectrum (101 MHz, $CDCl_3$) of **5v**



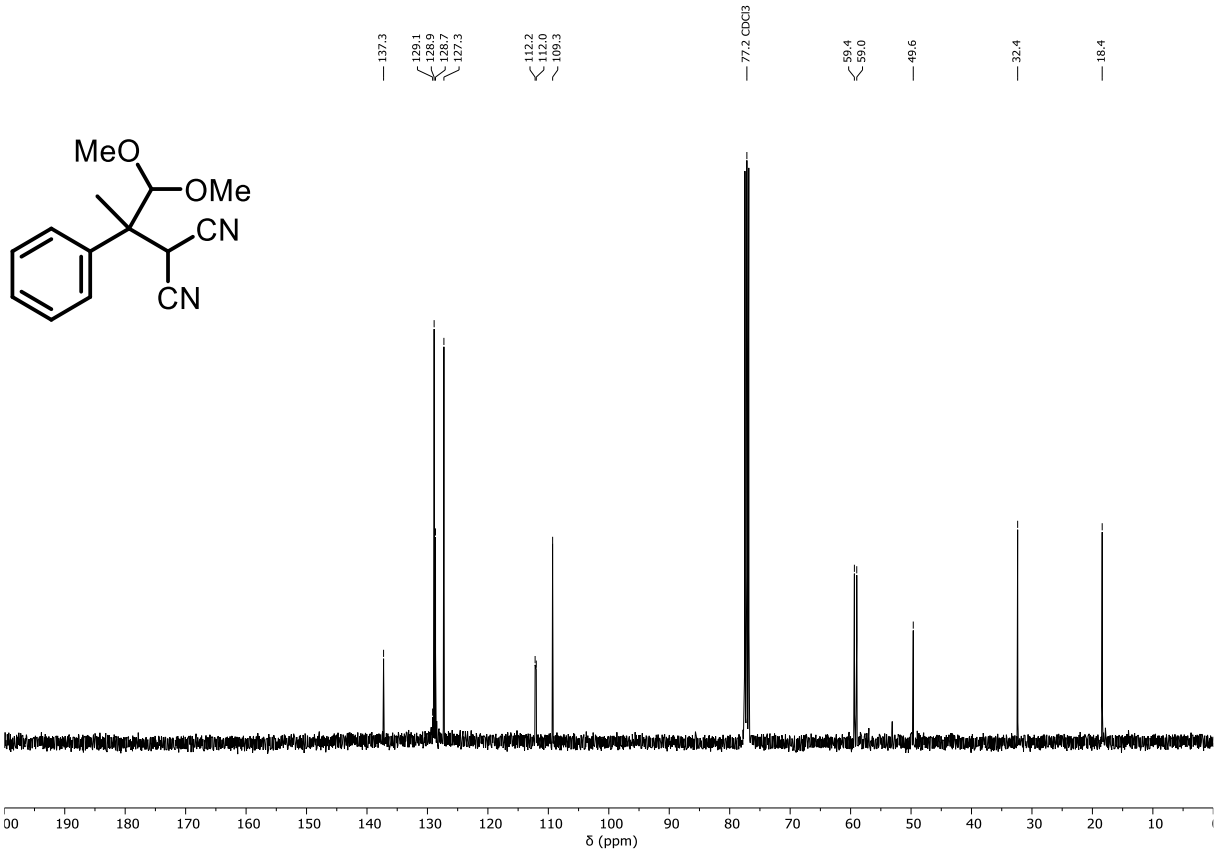
^{1}H NMR spectrum (600 MHz, $CDCl_3$) of **5w**



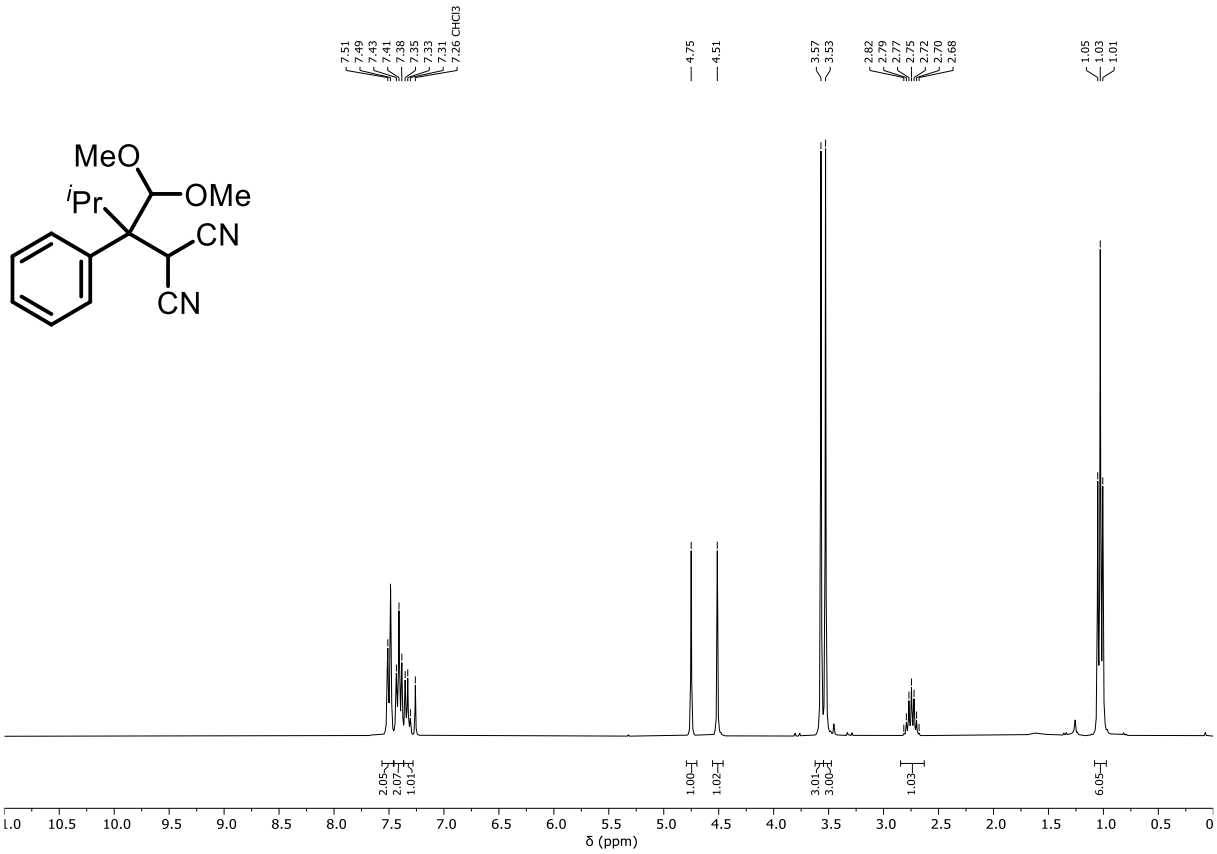
^{13}C{^{1}H} NMR spectrum (151 MHz, $CDCl_3$) of **5w**



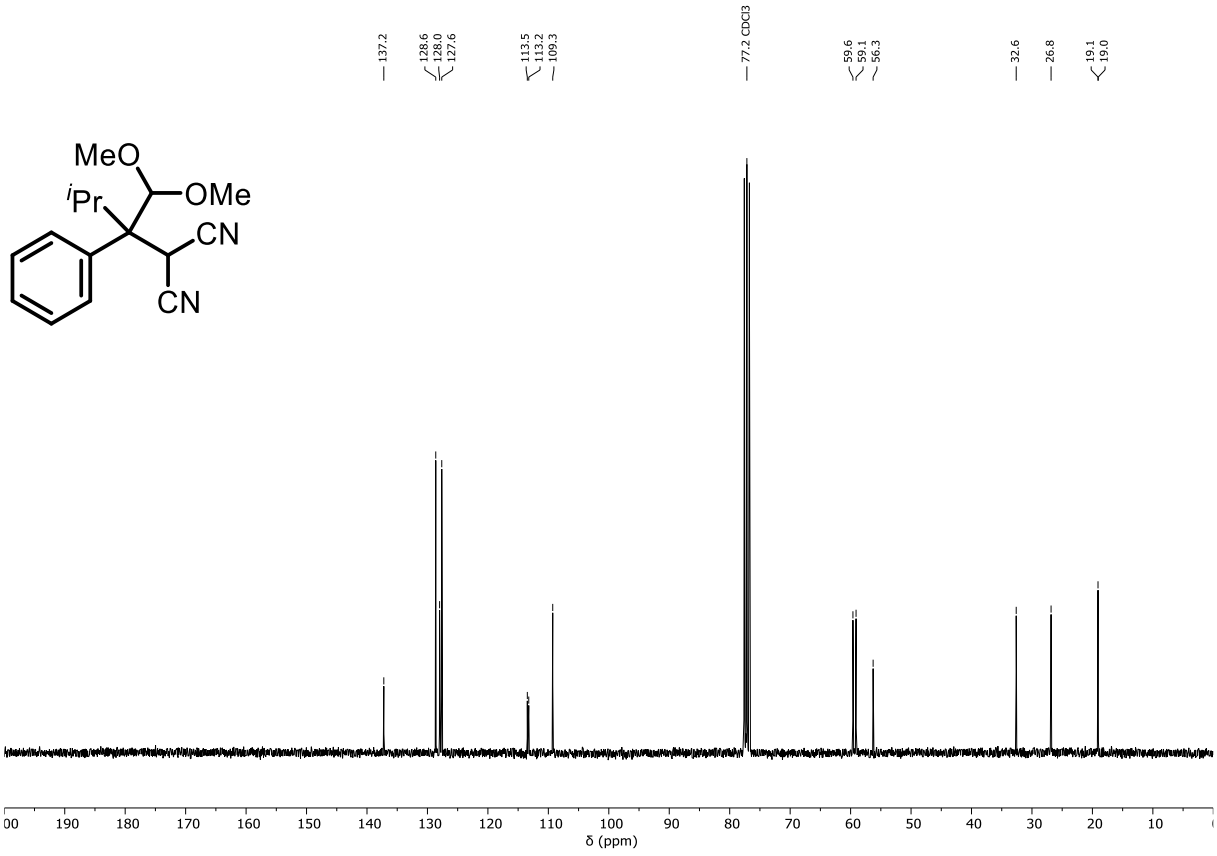
^{1}H NMR spectrum (400 MHz, $CDCl_3$) of **5x**



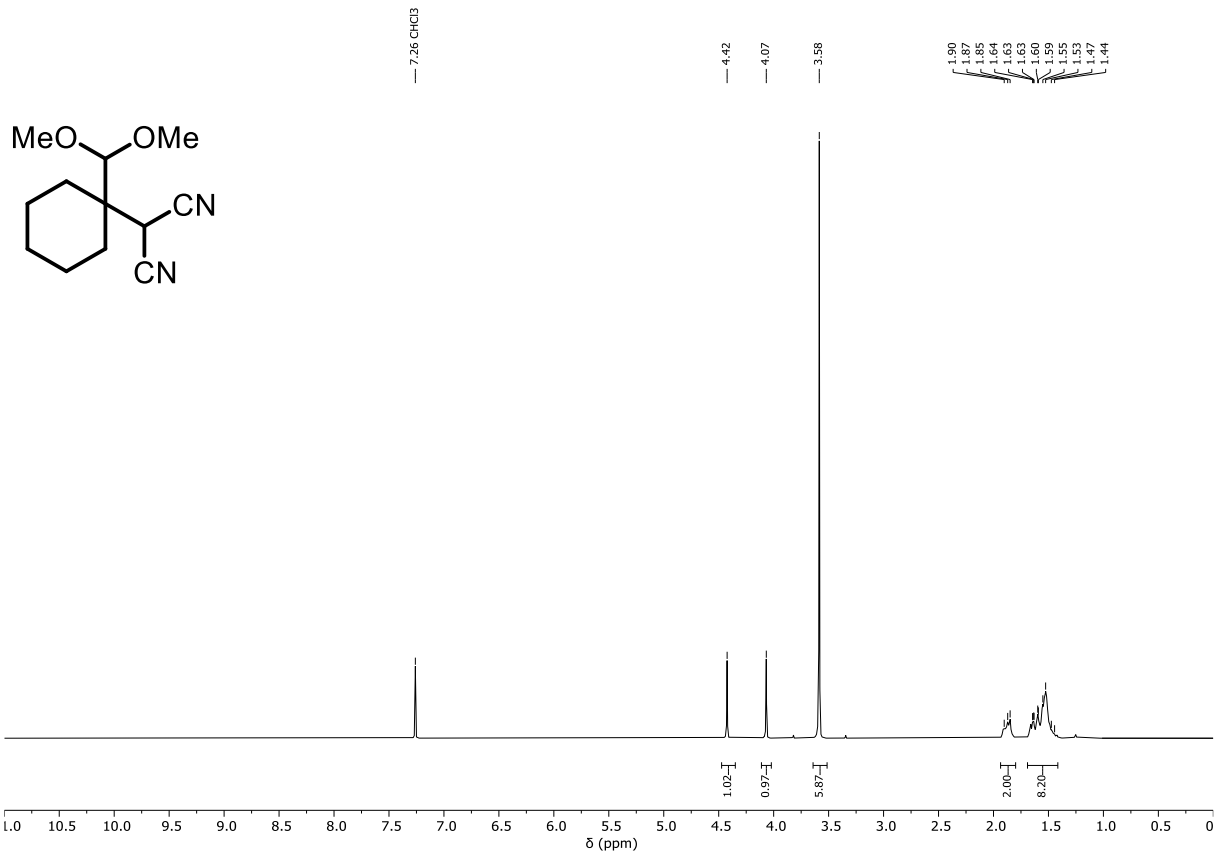
^{13}C{^{1}H} NMR spectrum (101 MHz, $CDCl_3$) of **5x**



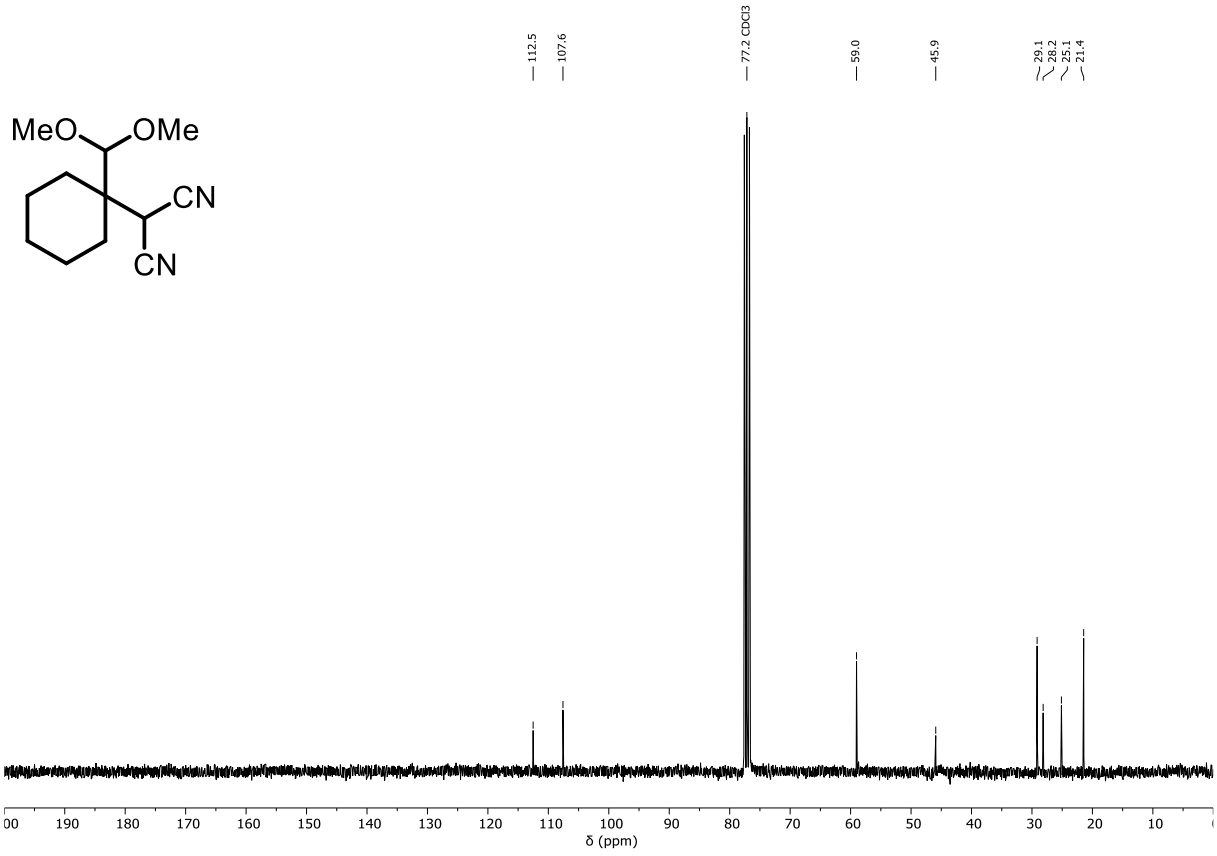
^{1}H NMR spectrum (300 MHz, $CDCl_3$) of **5y**



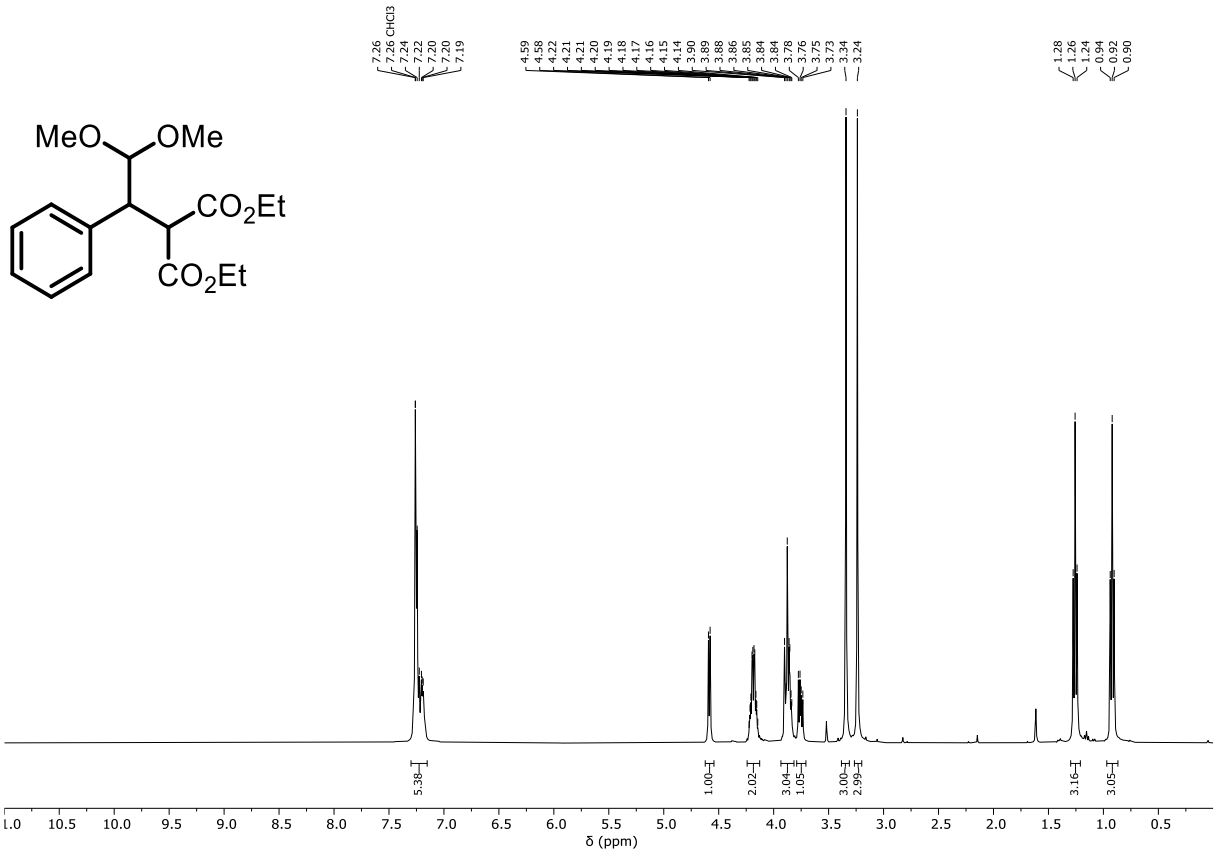
$^{13}C\{^{1}H\}$ NMR spectrum (75.5 MHz, $CDCl_3$) of **5y**



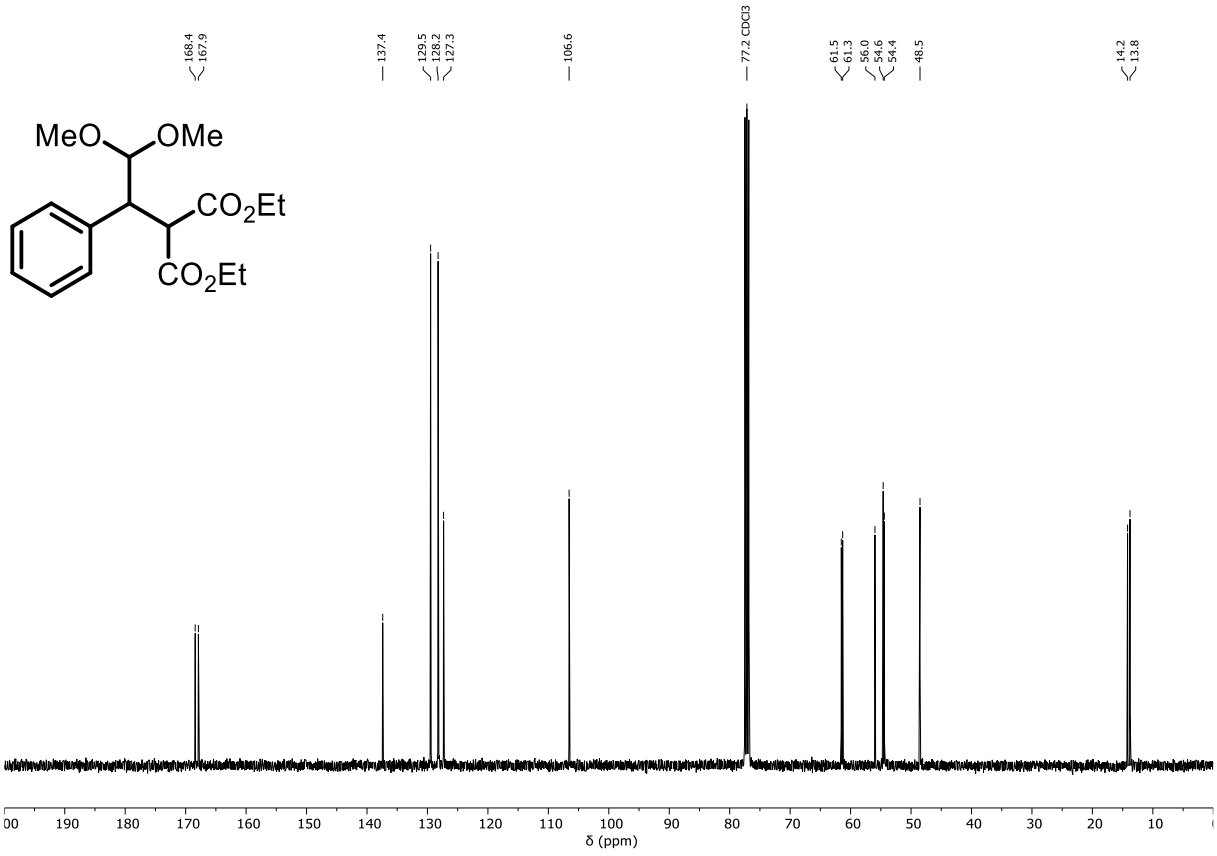
^{1}H NMR spectrum (300 MHz, $CDCl_3$) of **5z**



^{13}C{^{1}H} NMR spectrum (75.5 MHz, $CDCl_3$) of **5z**



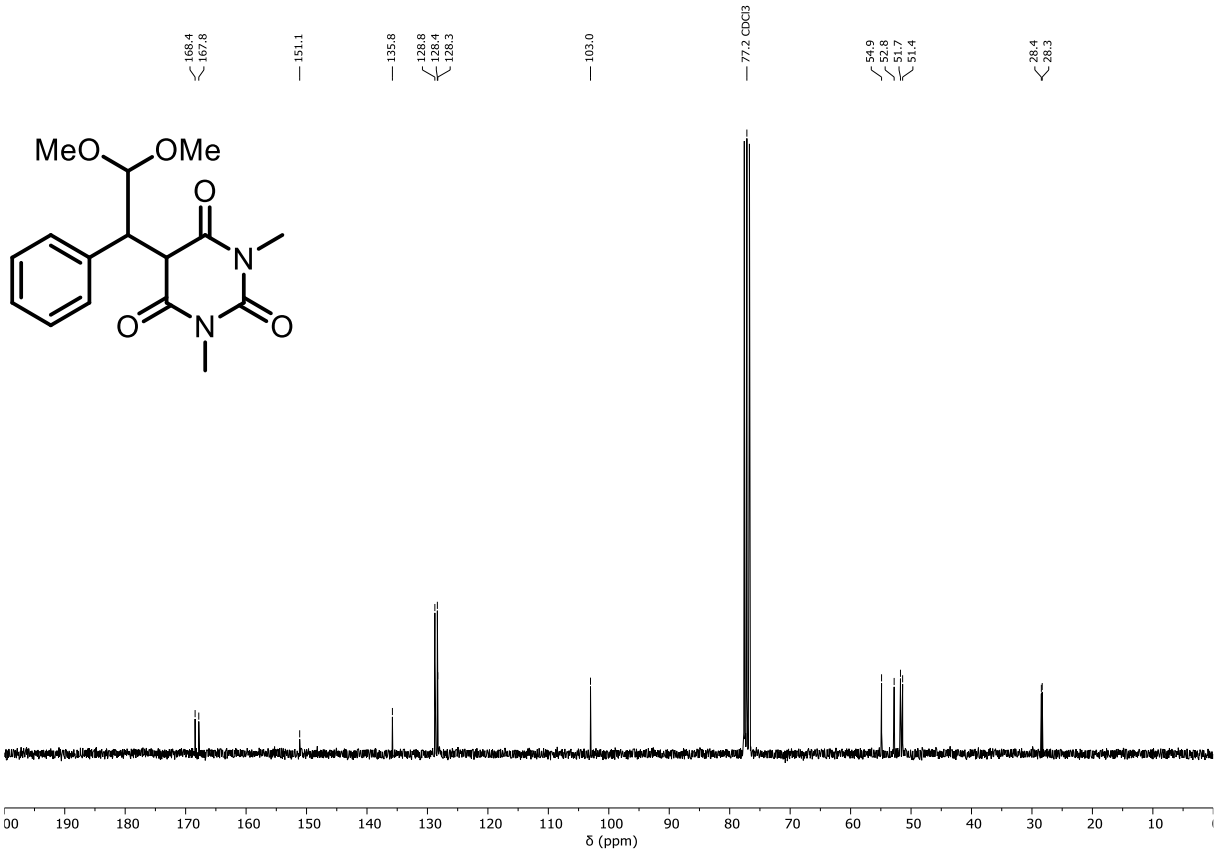
^{1}H NMR spectrum (400 MHz, $CDCl_3$) of **6b**



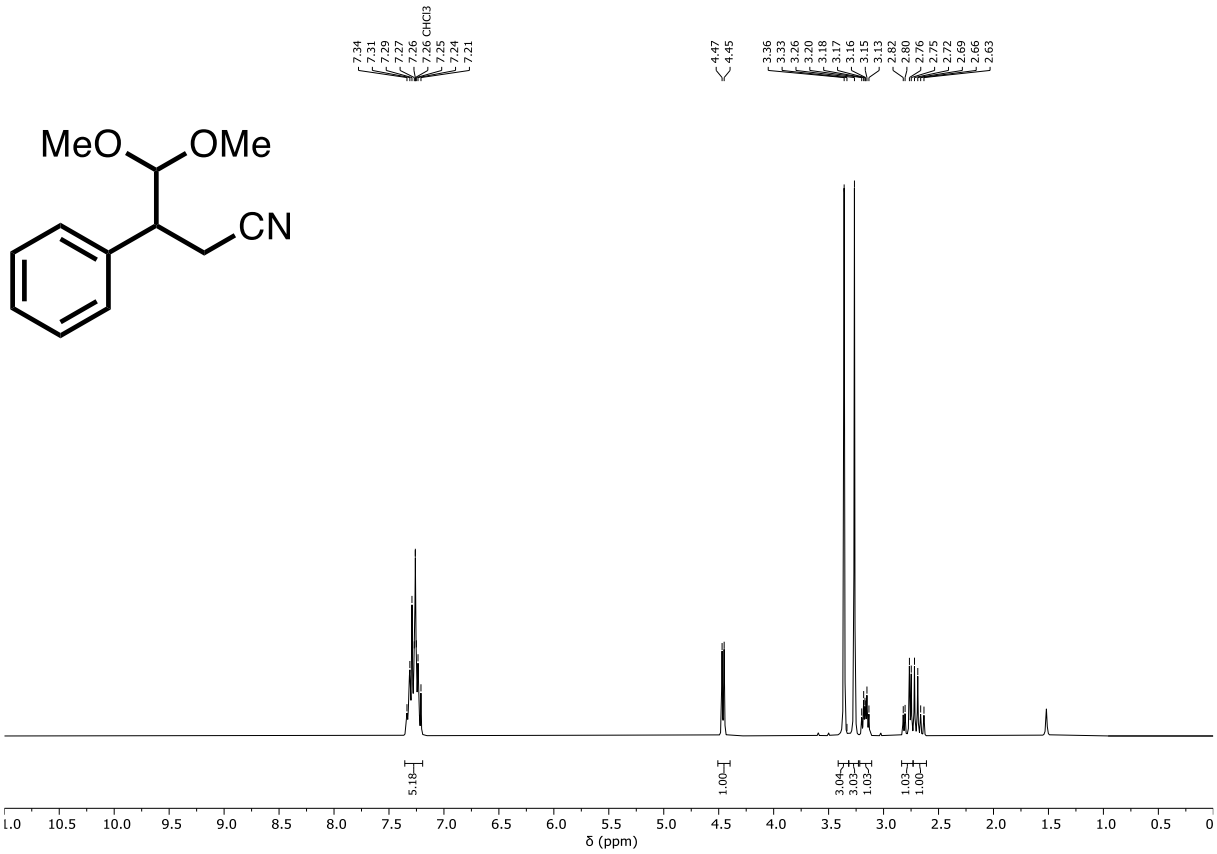
^{13}C{^{1}H} NMR spectrum (101 MHz, $CDCl_3$) of **6b**



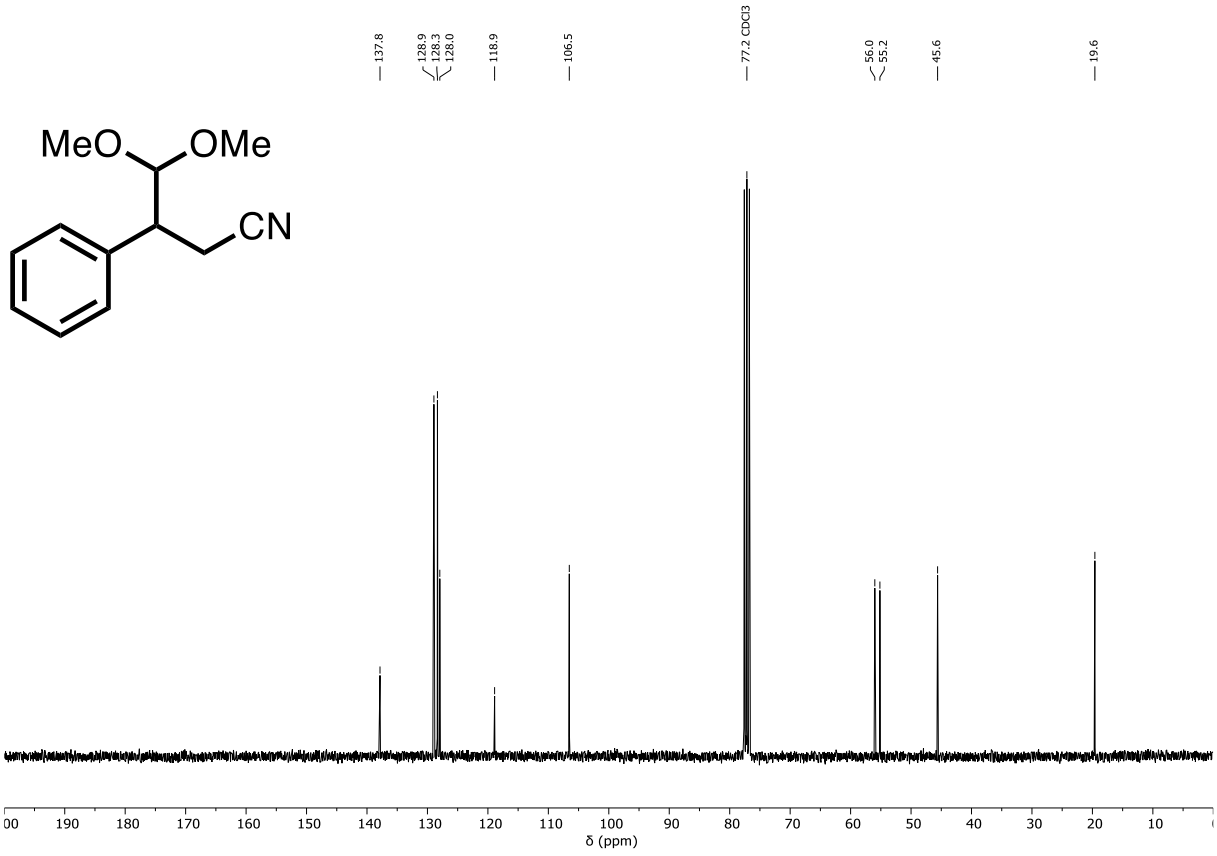
^{1}H NMR spectrum (300 MHz, $CDCl_3$) of **6d**



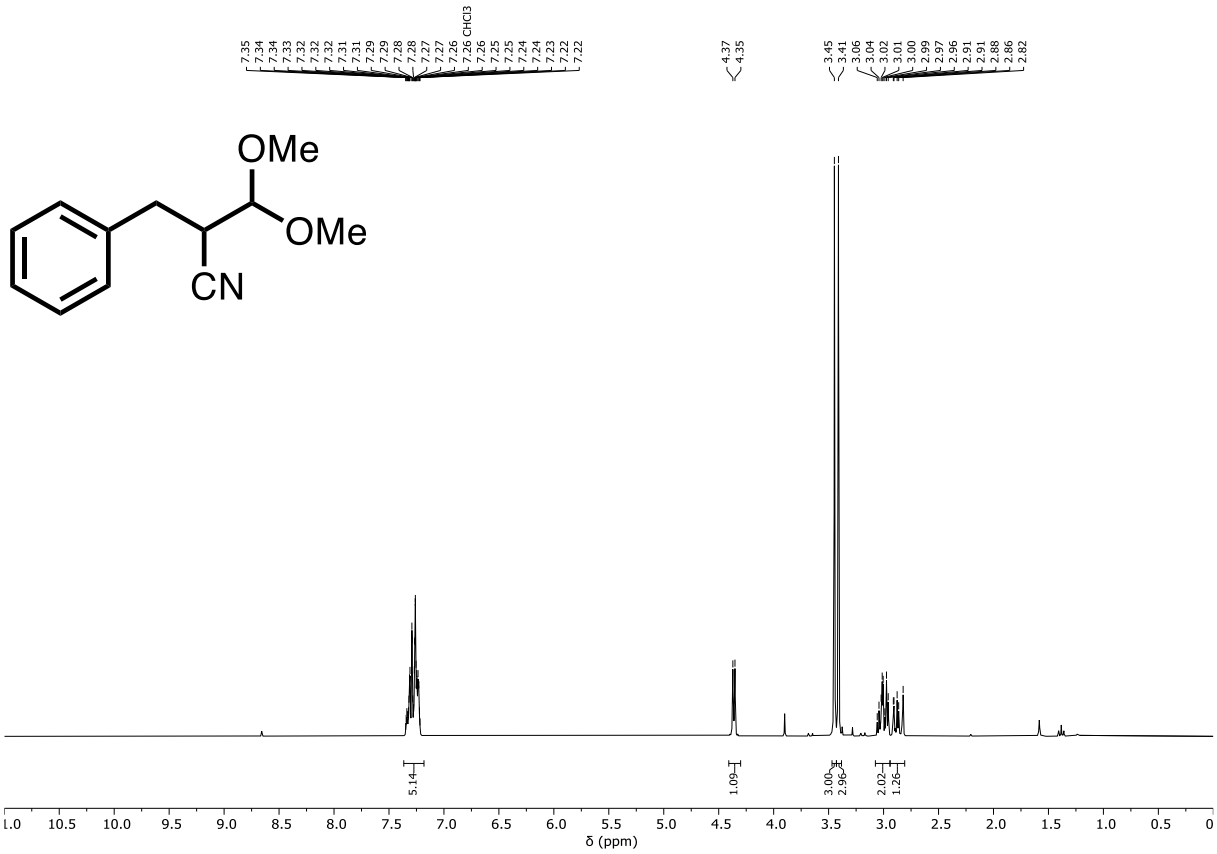
^{13}C{^{1}H} NMR spectrum (75.5 MHz, $CDCl_3$) of **6d**



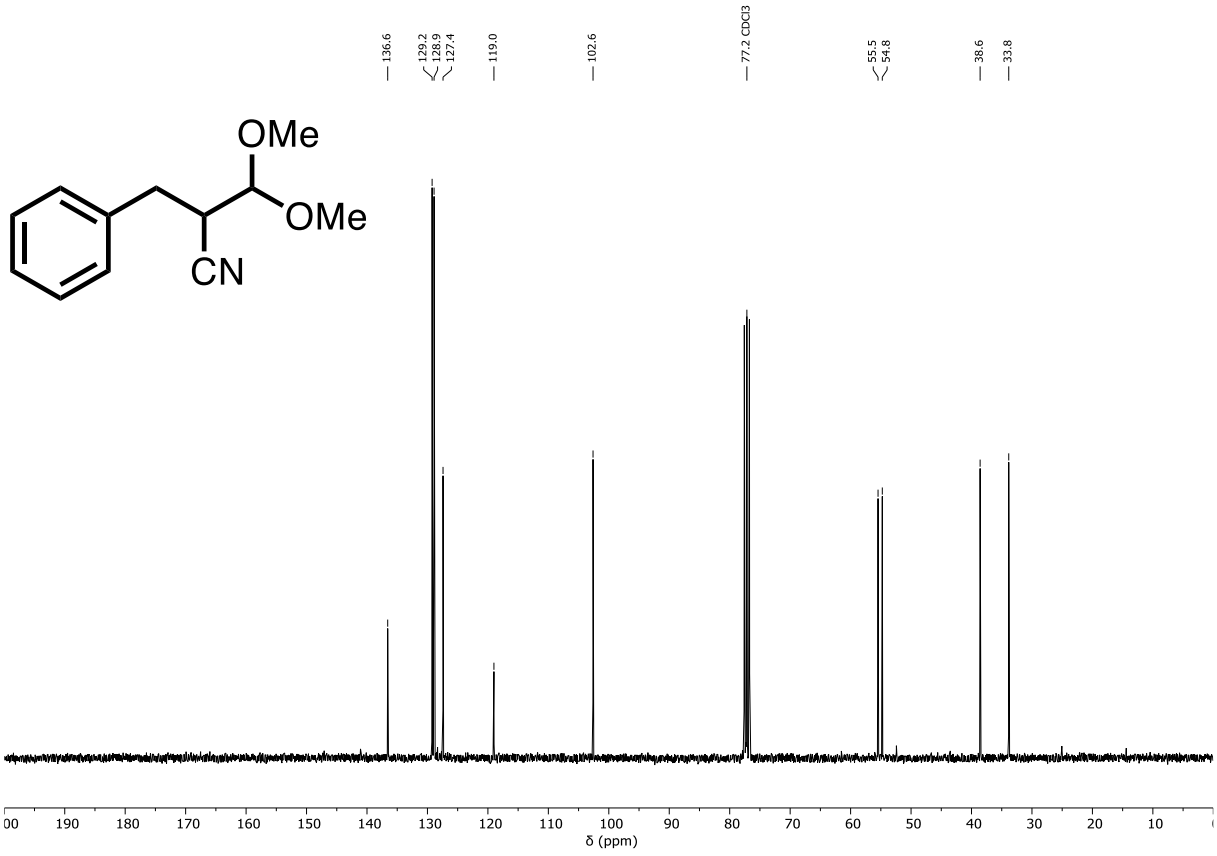
^{1}H NMR spectrum (300 MHz, $CDCl_3$) of **6g-1**



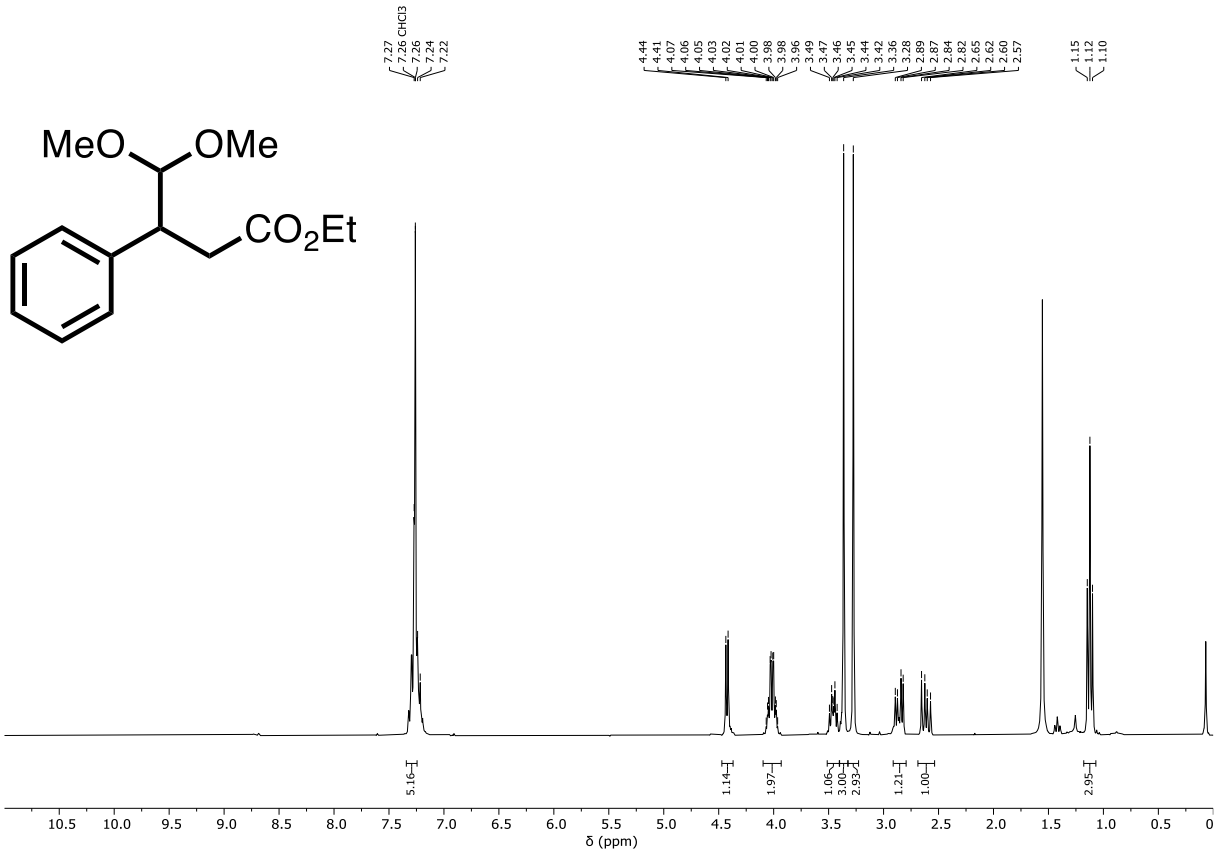
$^{13}C\{^{1}H\}$ NMR spectrum (75.5 MHz, $CDCl_3$) of **6g-1**



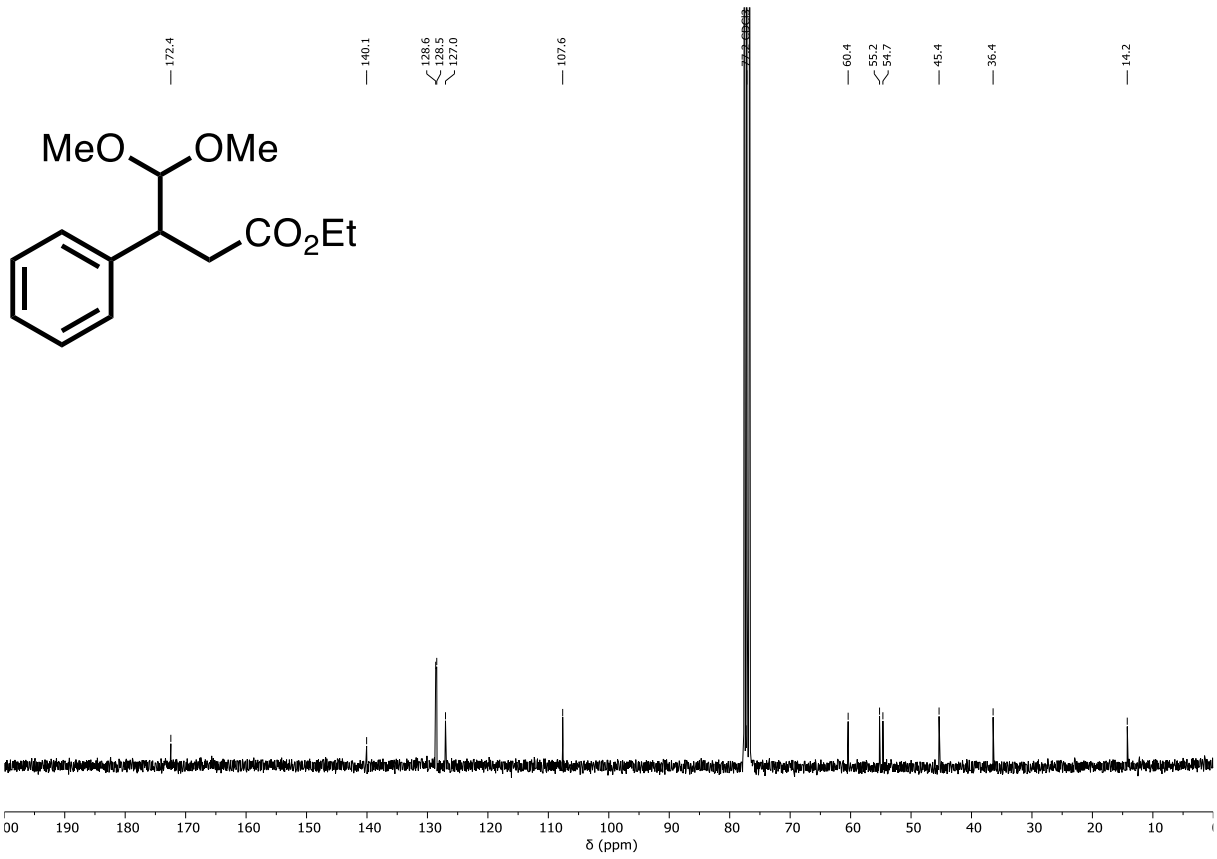
^{1}H NMR spectrum (300 MHz, $CDCl_3$) of **6g-2**



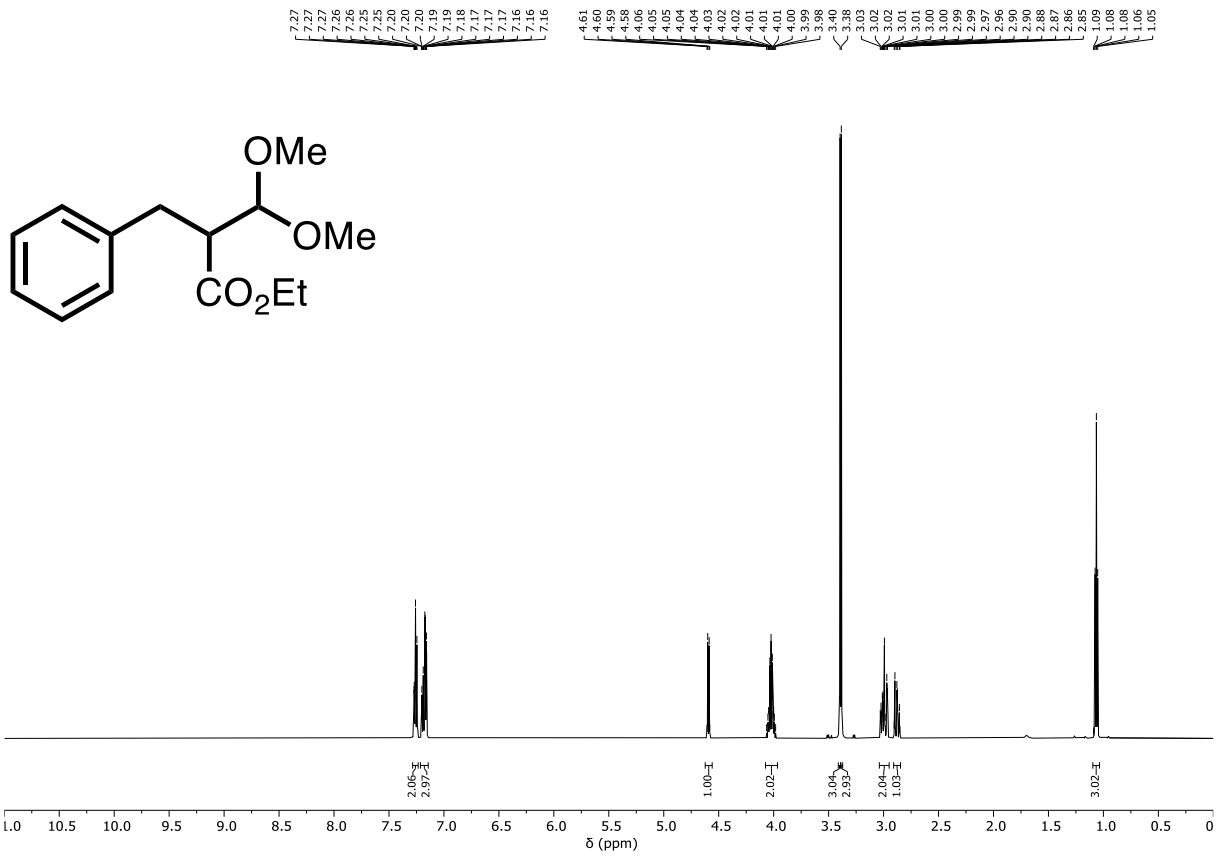
$^{13}C\{^{1}H\}$ NMR spectrum (75.5 MHz, $CDCl_3$) of **6g-2**



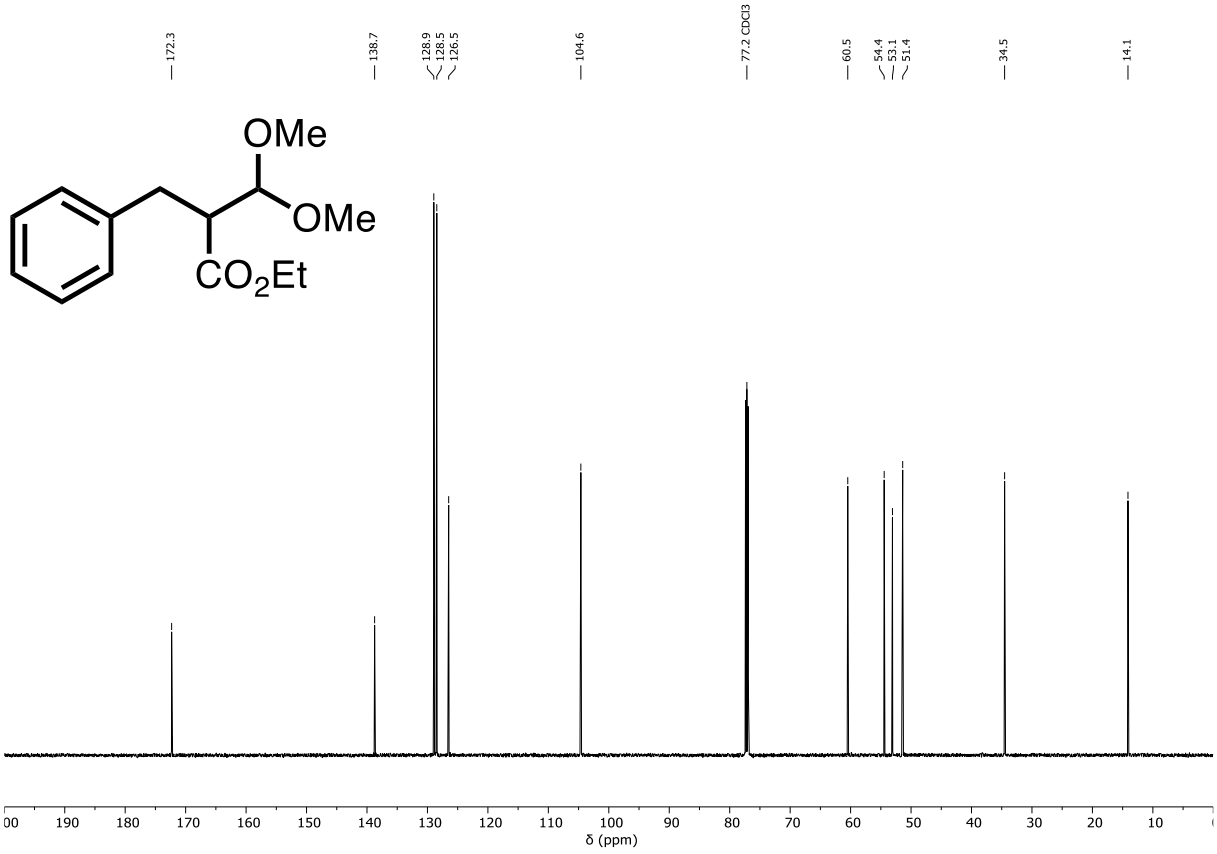
^{1}H NMR spectrum (300 MHz, $CDCl_3$) of **6h-1**



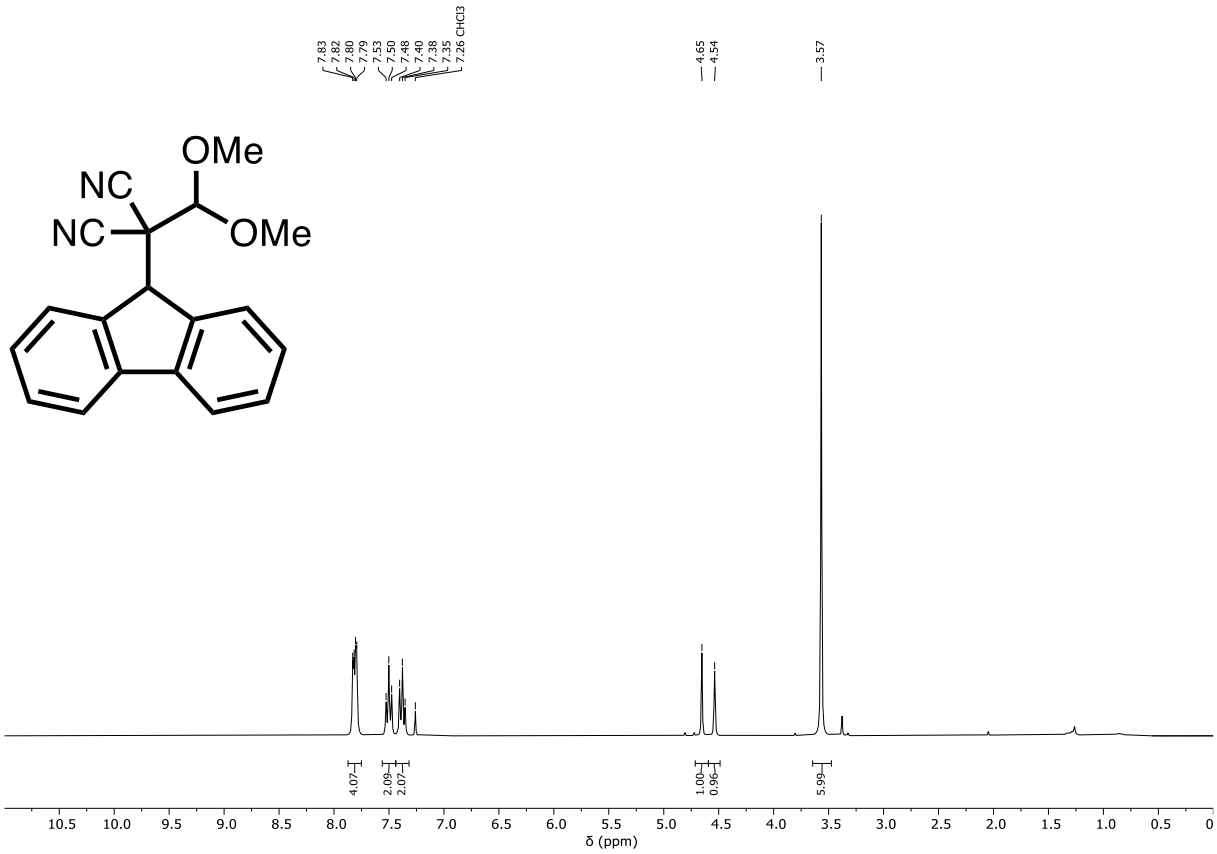
$^{13}C\{^{1}H\}$ NMR spectrum (75.5 MHz, $CDCl_3$) of **6h-1**



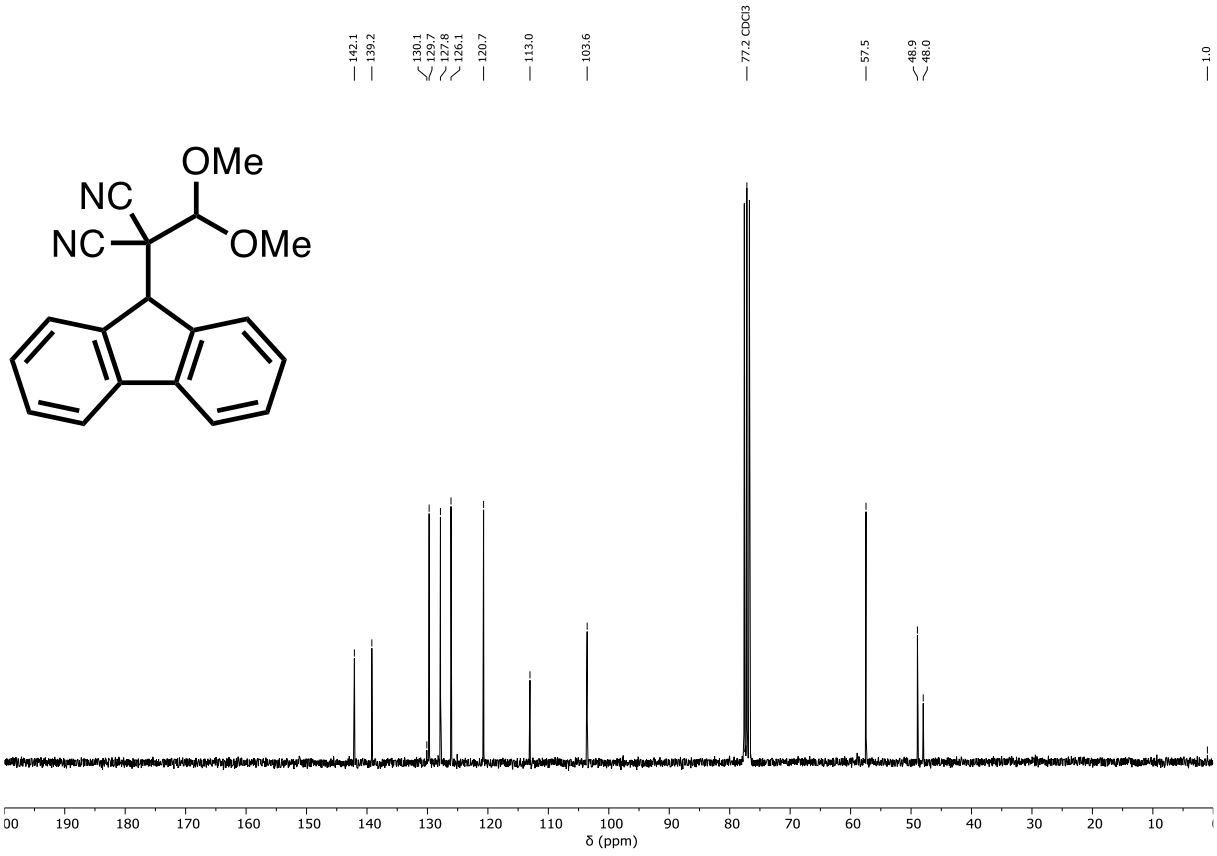
^{1}H NMR spectrum (300 MHz, $CDCl_3$) of **6h-2**



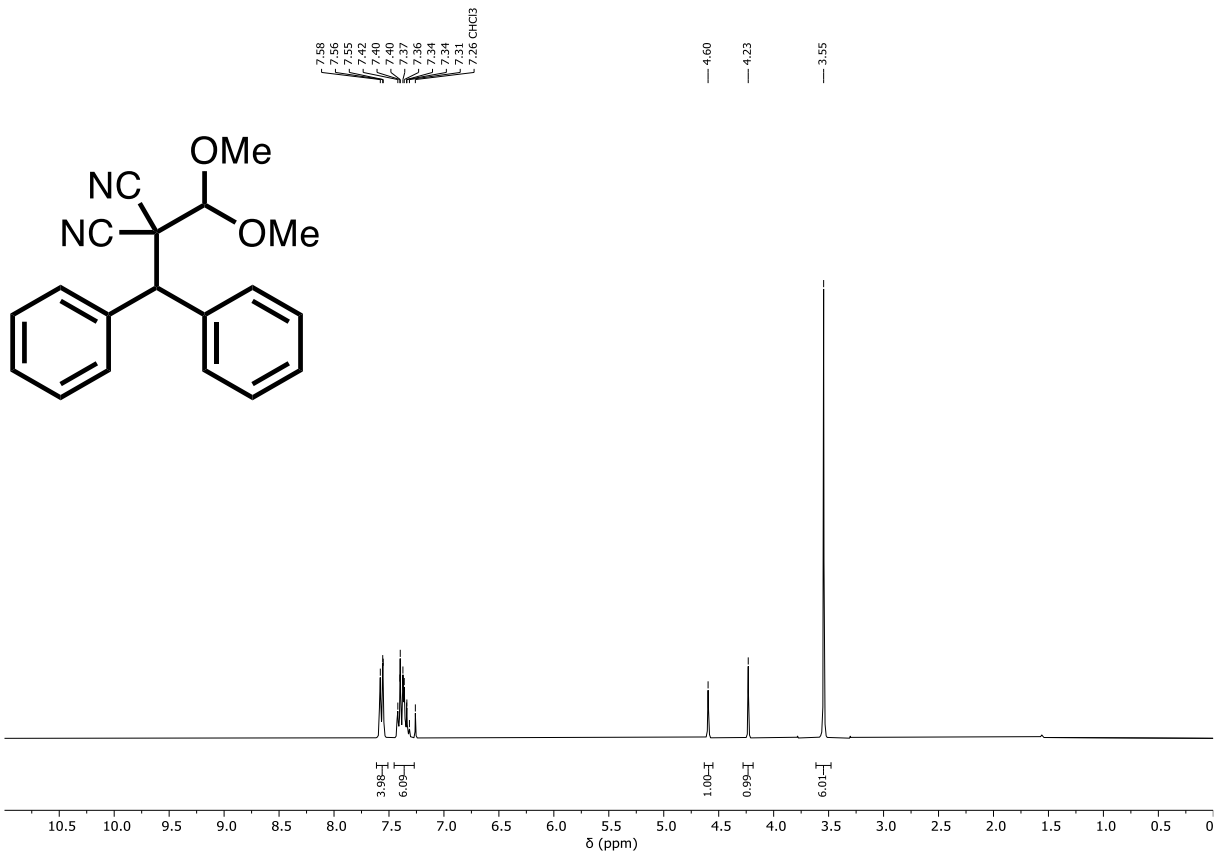
$^{13}C\{^{1}H\}$ NMR spectrum (75.5 MHz, $CDCl_3$) of **6h-2**



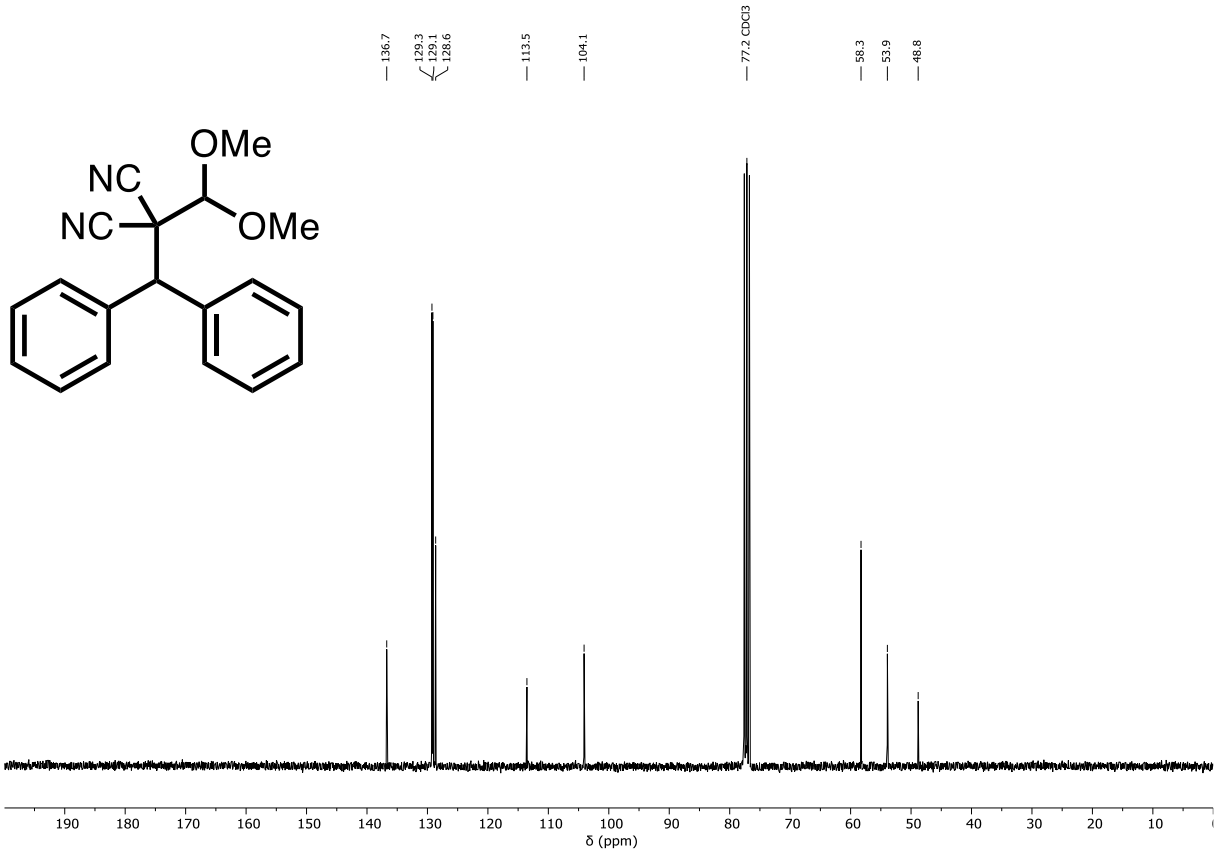
^{1}H NMR spectrum (300 MHz, $CDCl_3$) of **6i**



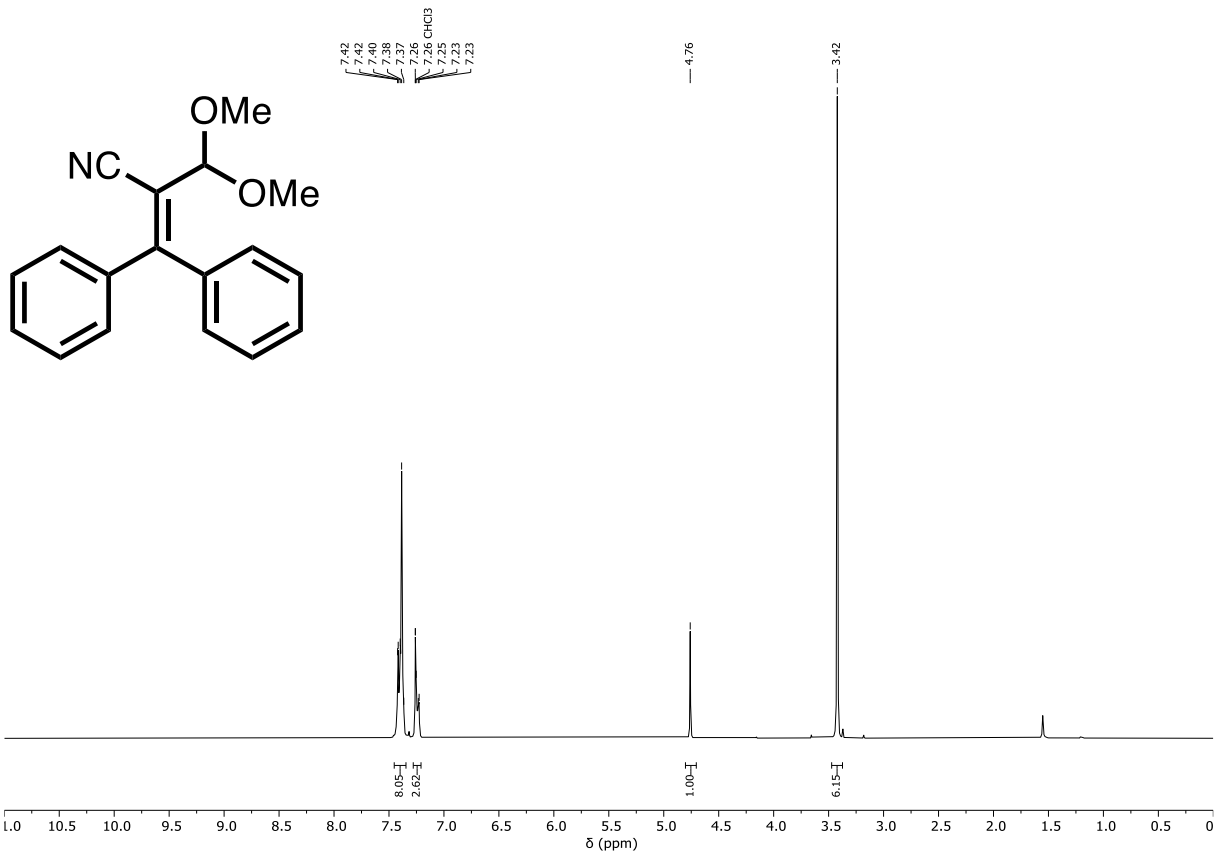
^{13}C{^{1}H} NMR spectrum (75.5 MHz, $CDCl_3$) of **6i**



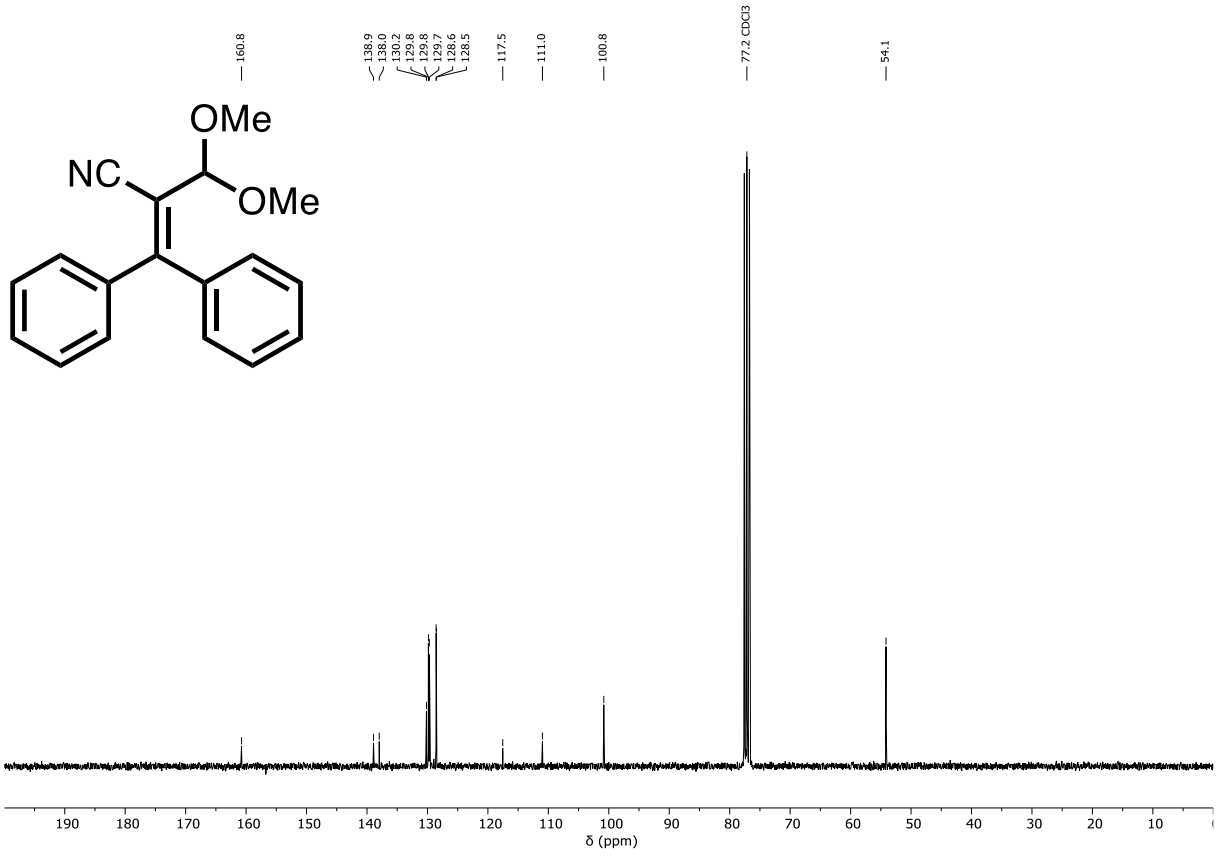
^{1}H NMR spectrum (300 MHz, $CDCl_3$) of **6j-1**



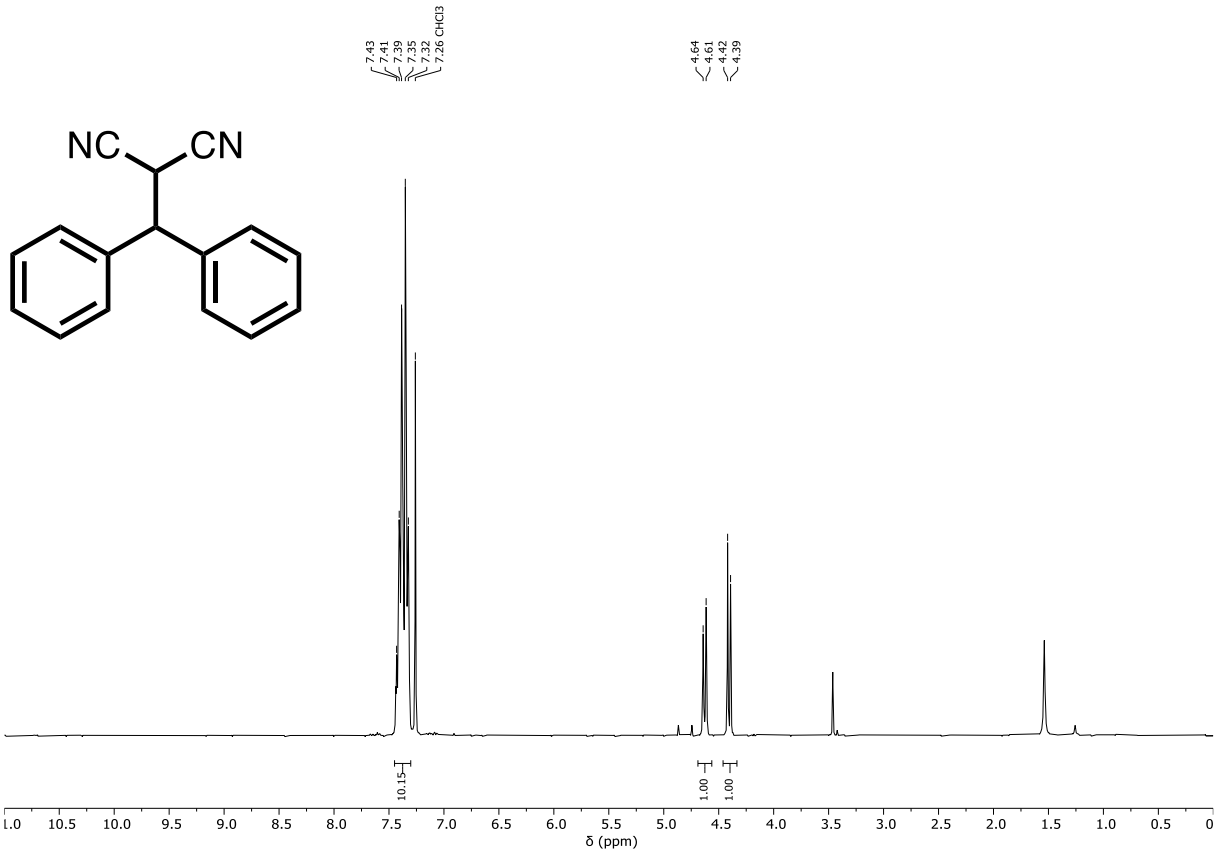
^{13}C{^{1}H} NMR spectrum (75.5 MHz, $CDCl_3$) of **6j-1**



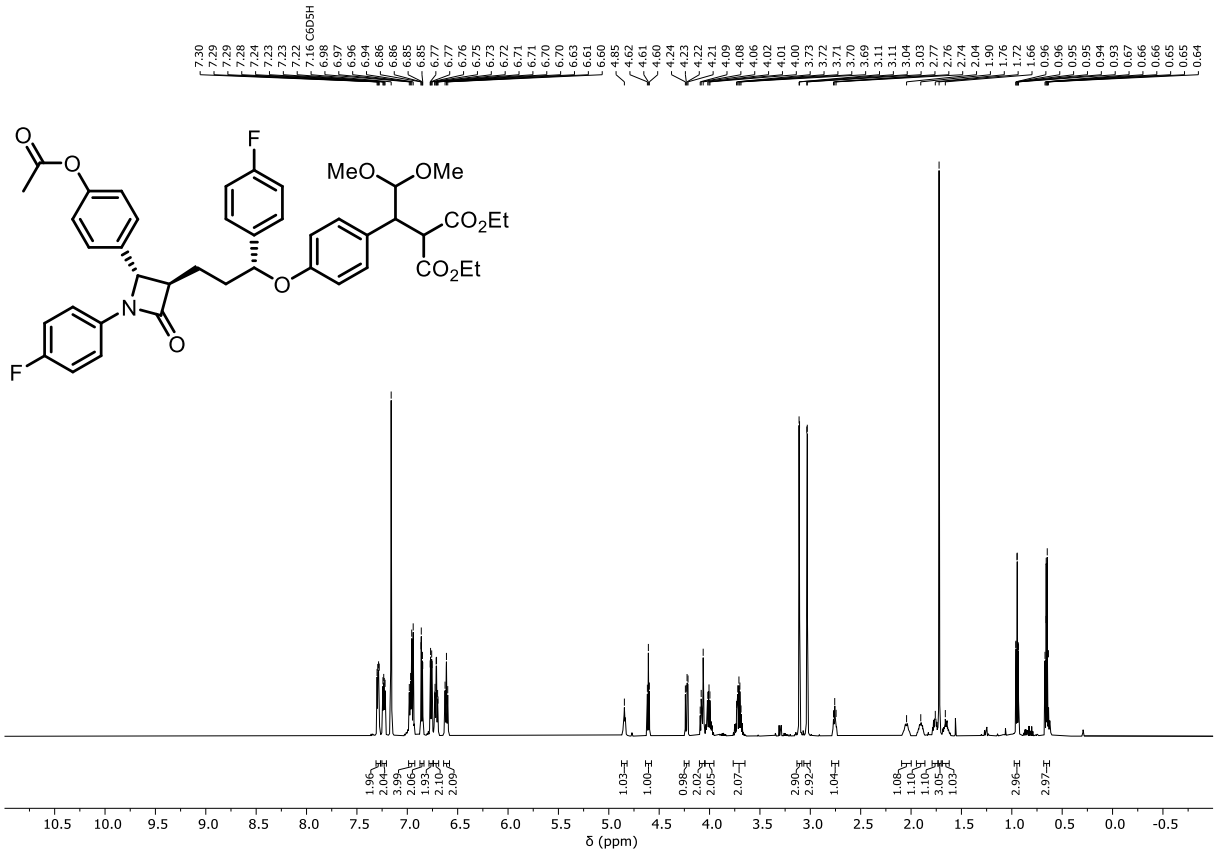
^{1}H NMR spectrum (300 MHz, $CDCl_3$) of **6j-2**



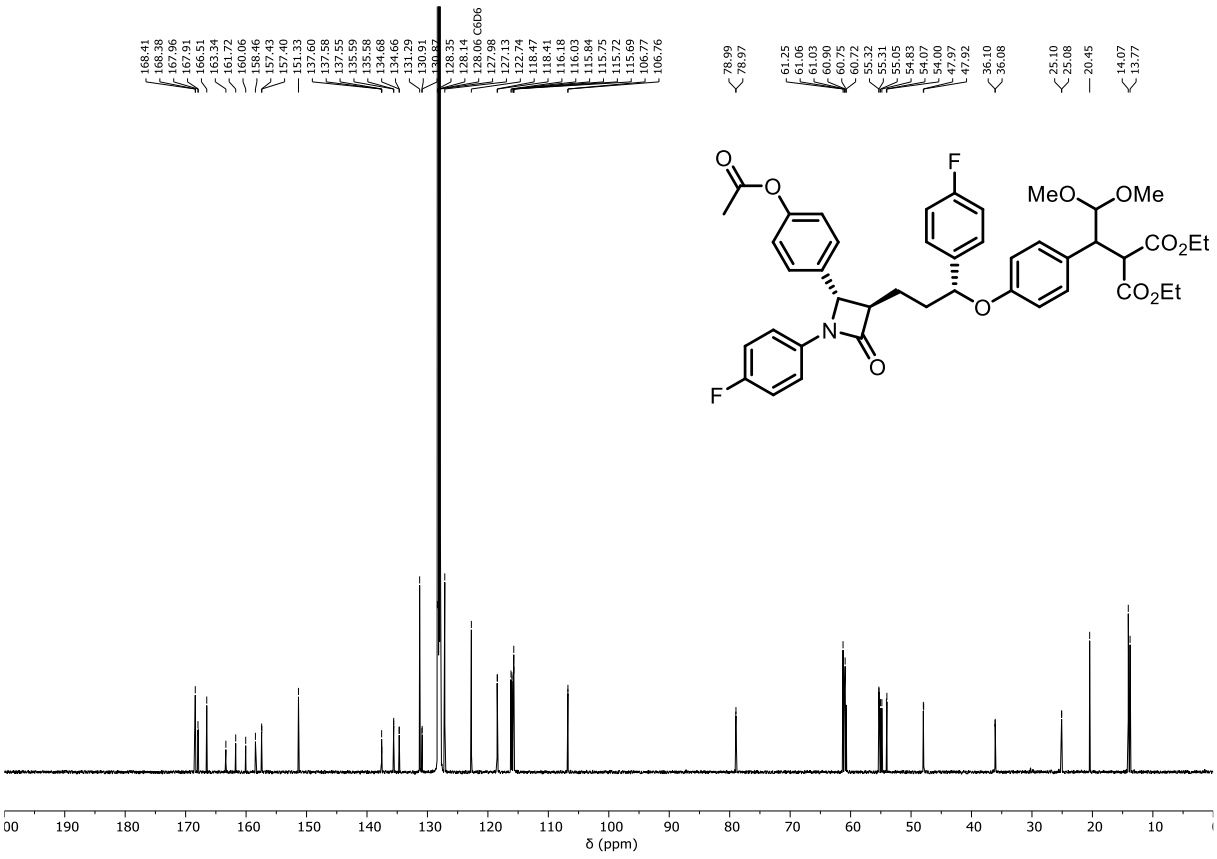
^{13}C{^{1}H} NMR spectrum (75.5 MHz, $CDCl_3$) of **6j-2**



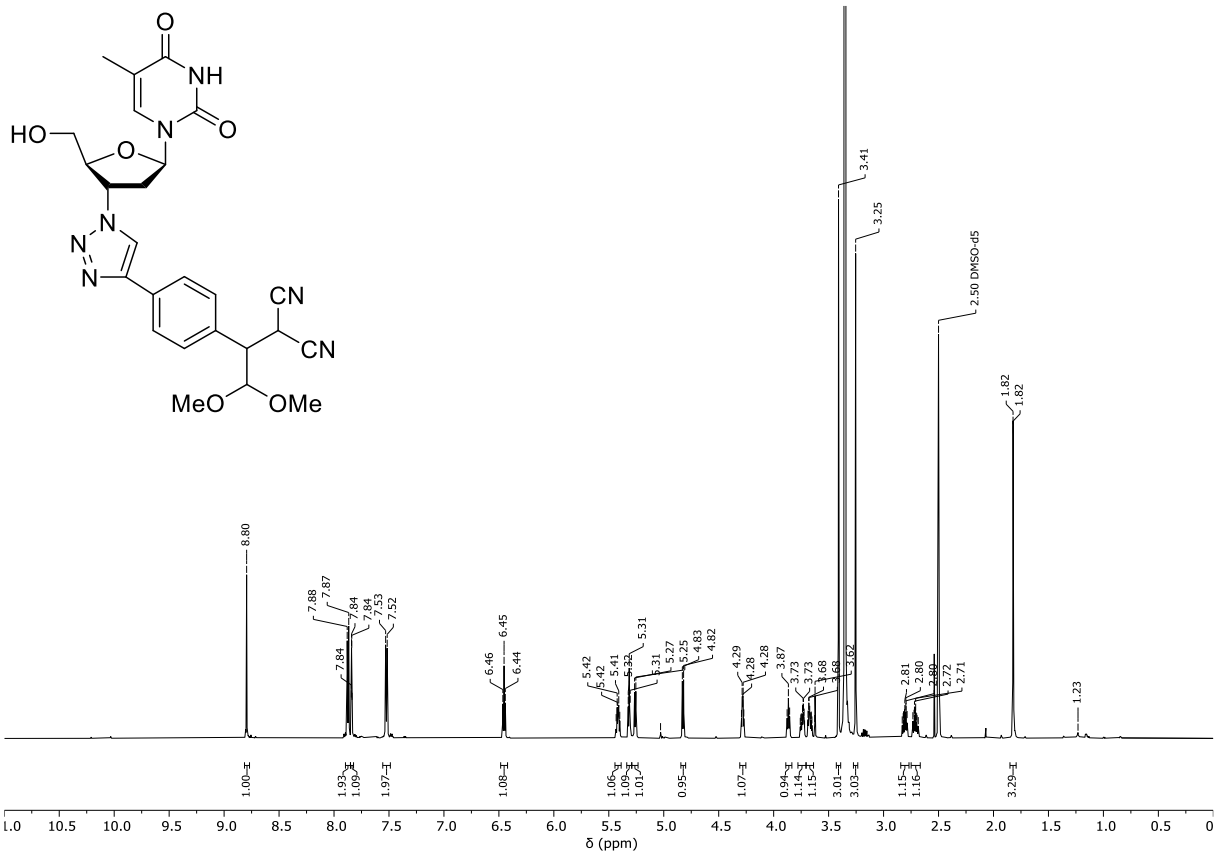
^{1}H NMR spectrum (300 MHz, $CDCl_3$) of **6j-3**



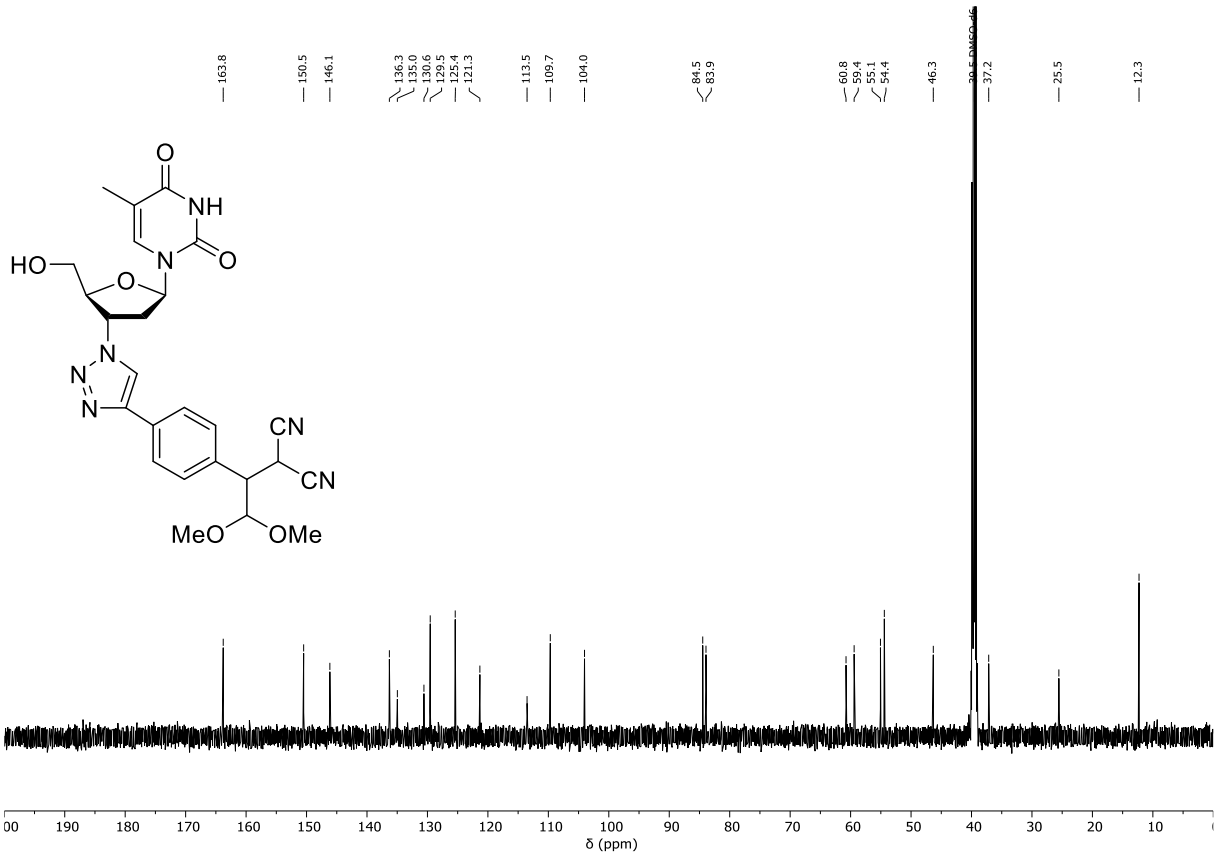
^{1}H NMR spectrum (600 MHz, C_6D_6) of **7a**



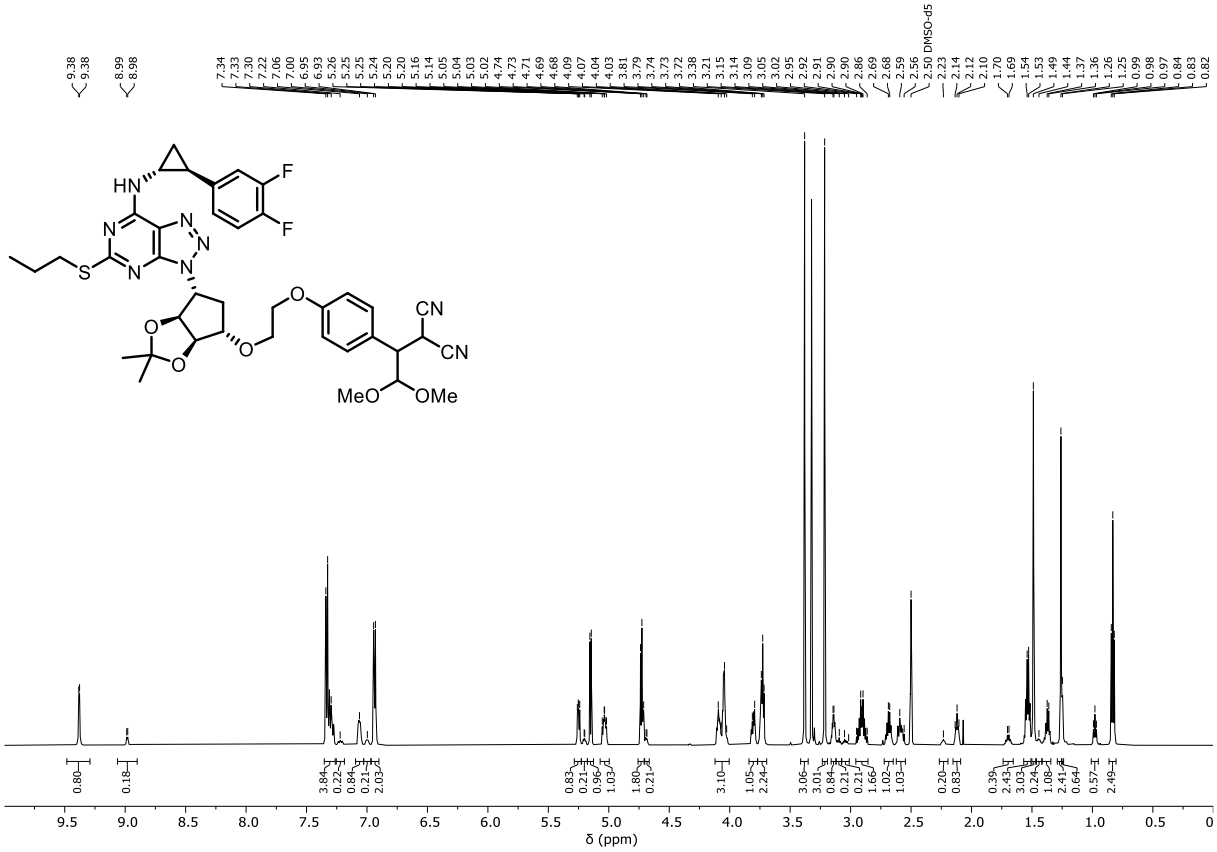
^{13}C{^{1}H} NMR spectrum (151 MHz, C_6D_6) of **7a**



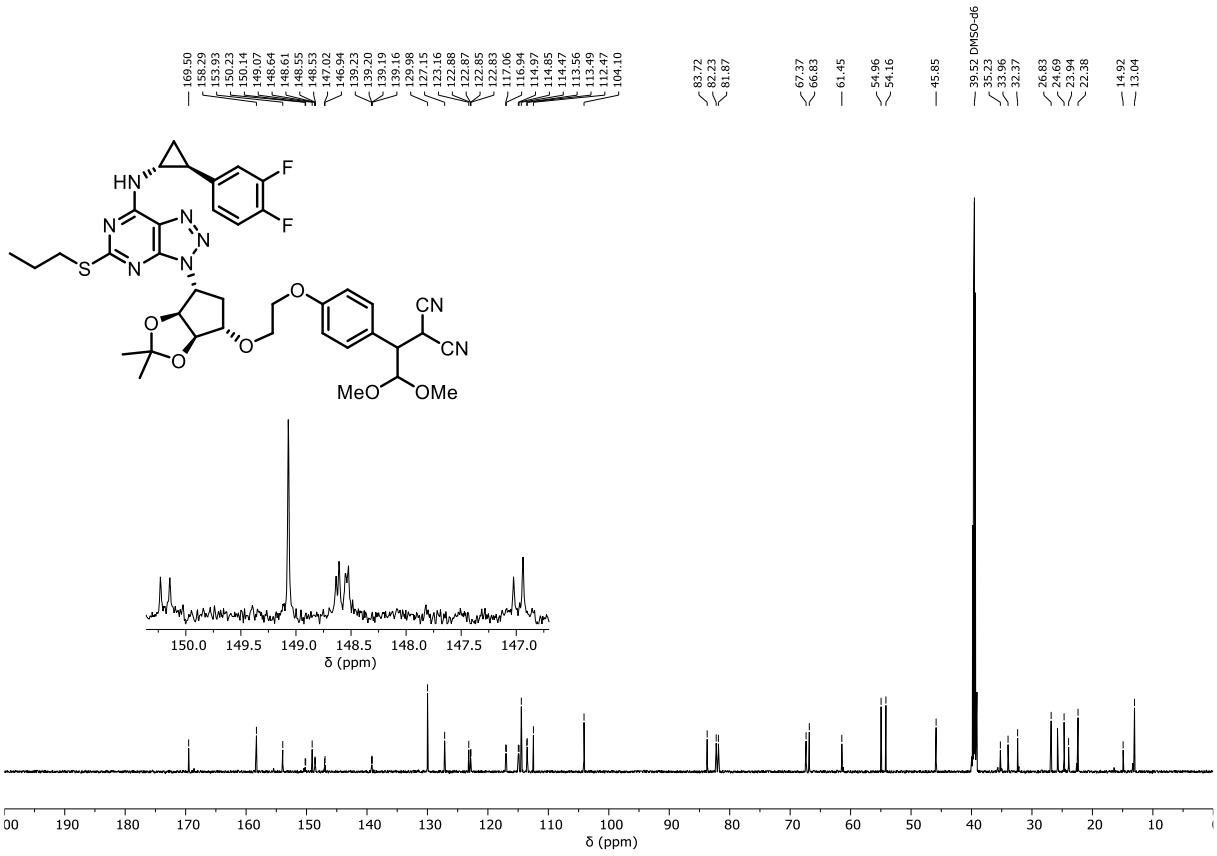
^{1}H NMR spectrum (600 MHz, DMSO-d_6) of **7b**



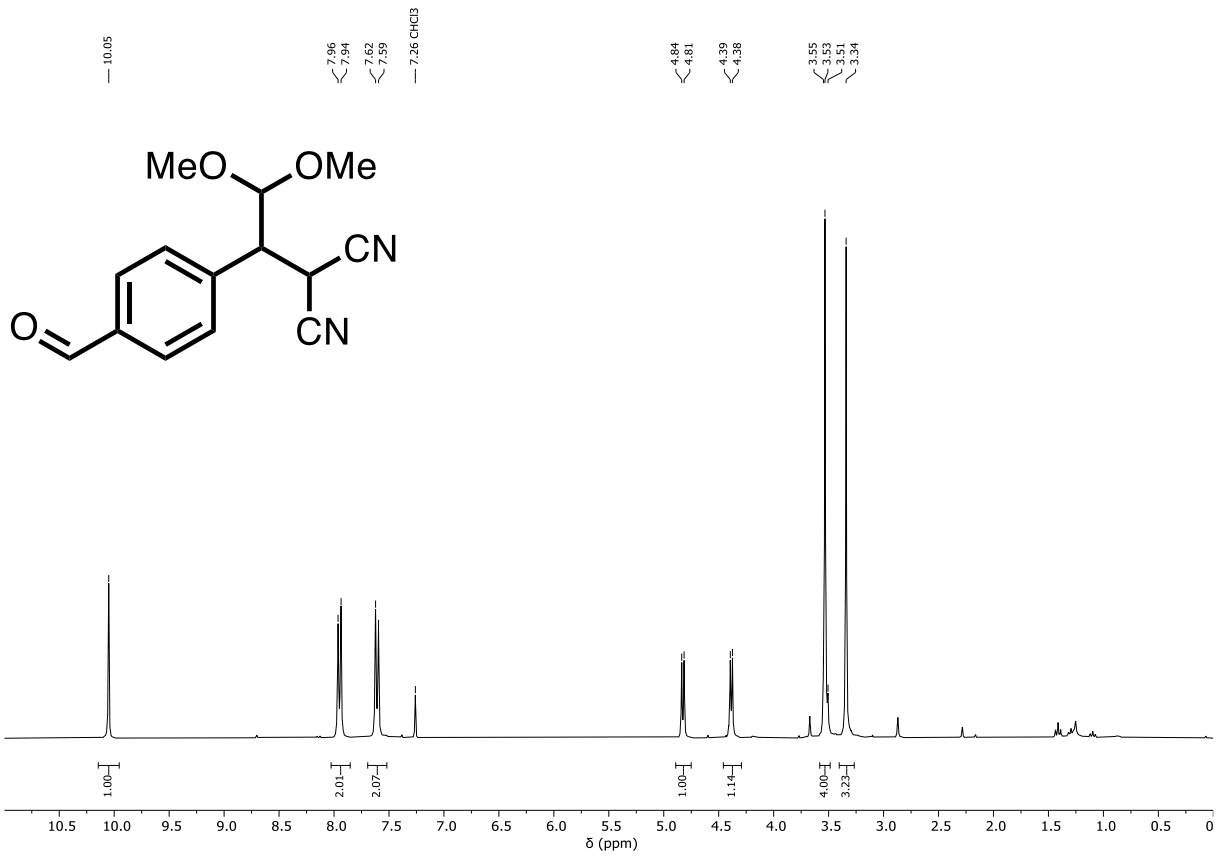
^{13}C{^{1}H} NMR spectrum (151 MHz, DMSO-d_6) of **7b**



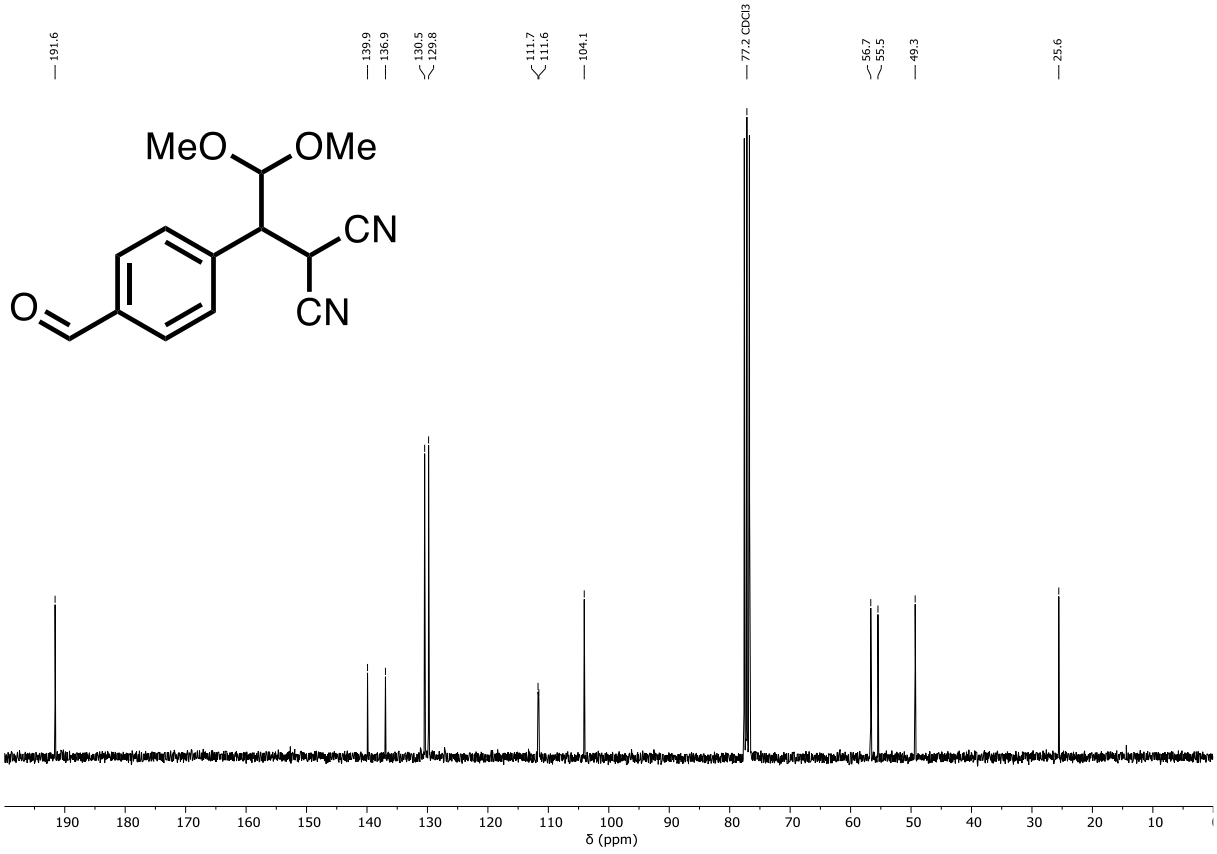
^{1}H NMR spectrum (600 MHz, DMSO-d_6) of **7c** (major + minor rotamer signals highlighted)



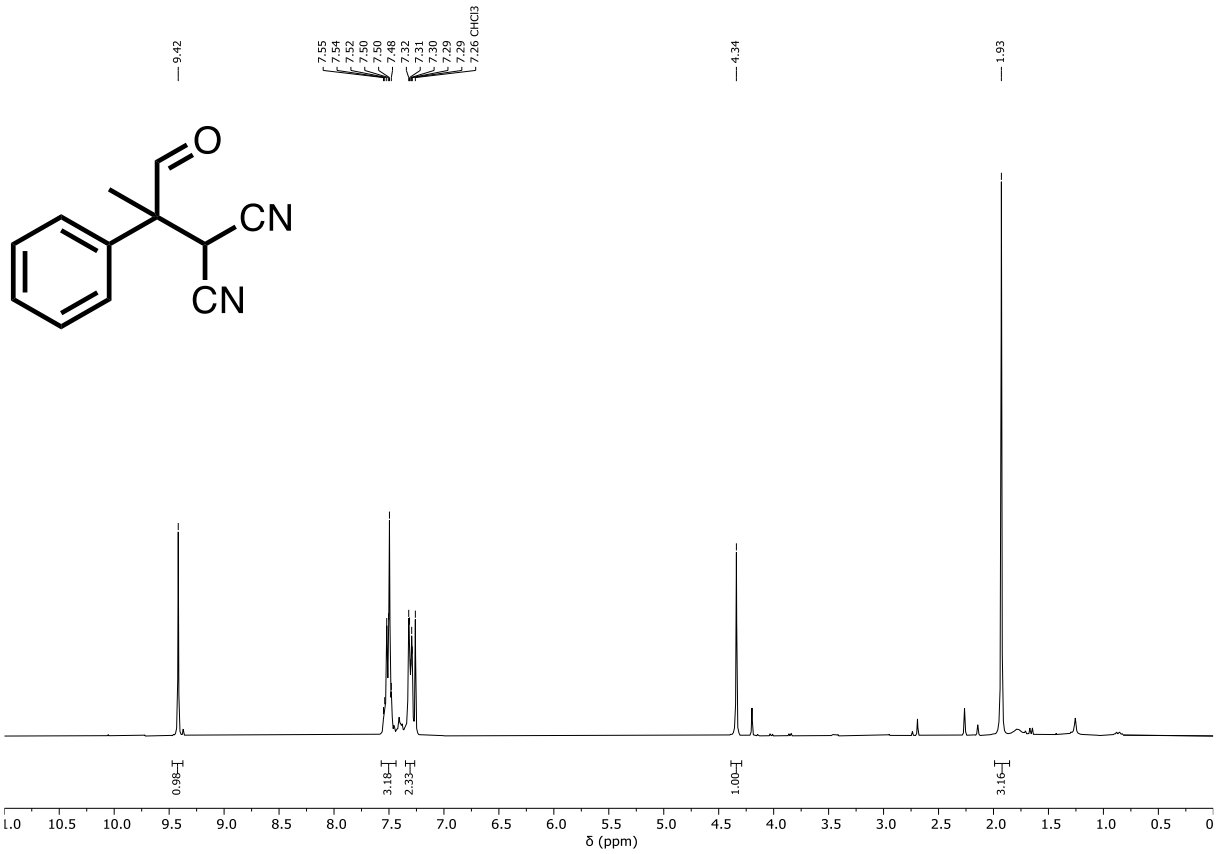
^{13}C{^{1}H} NMR spectrum (151 MHz, DMSO-d_6) of **7c** (only major rotamer signals highlighted)



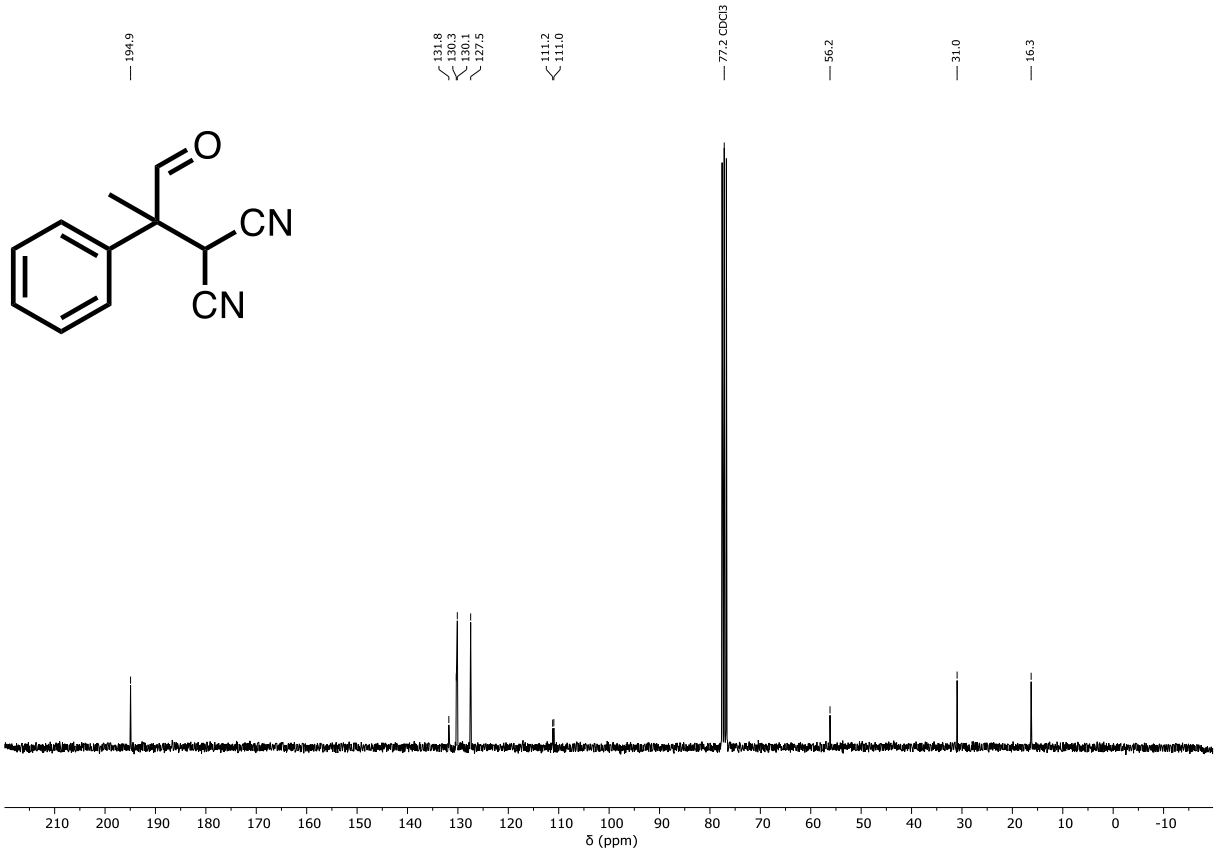
^{1}H NMR spectrum (300 MHz, $CDCl_3$) of 2-(dicyanomethyl)-2-(4-formylphenyl)acetaldehyde dimethyl acetal



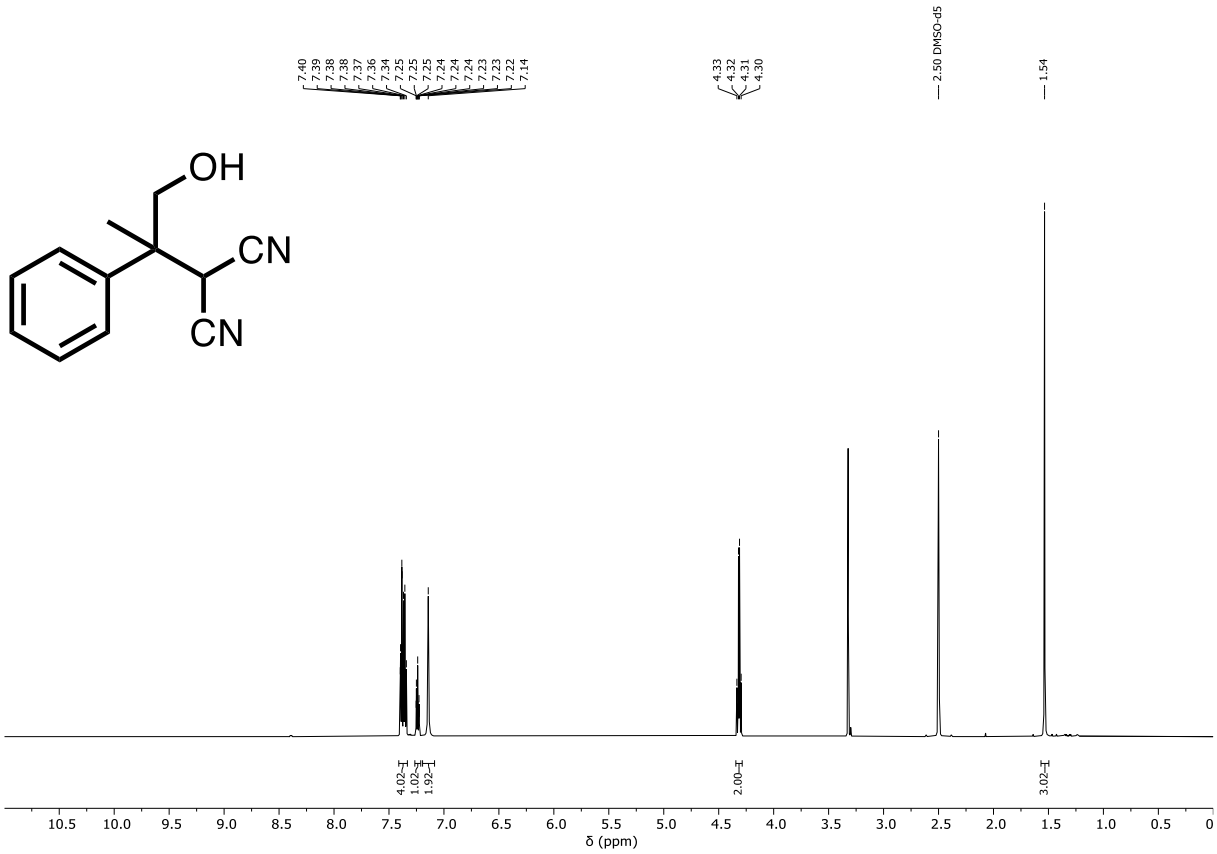
^{13}C{^{1}H} NMR spectrum (75.5 MHz, $CDCl_3$) of 2-(dicyanomethyl)-2-(4-formylphenyl)acetaldehyde dimethyl acetal



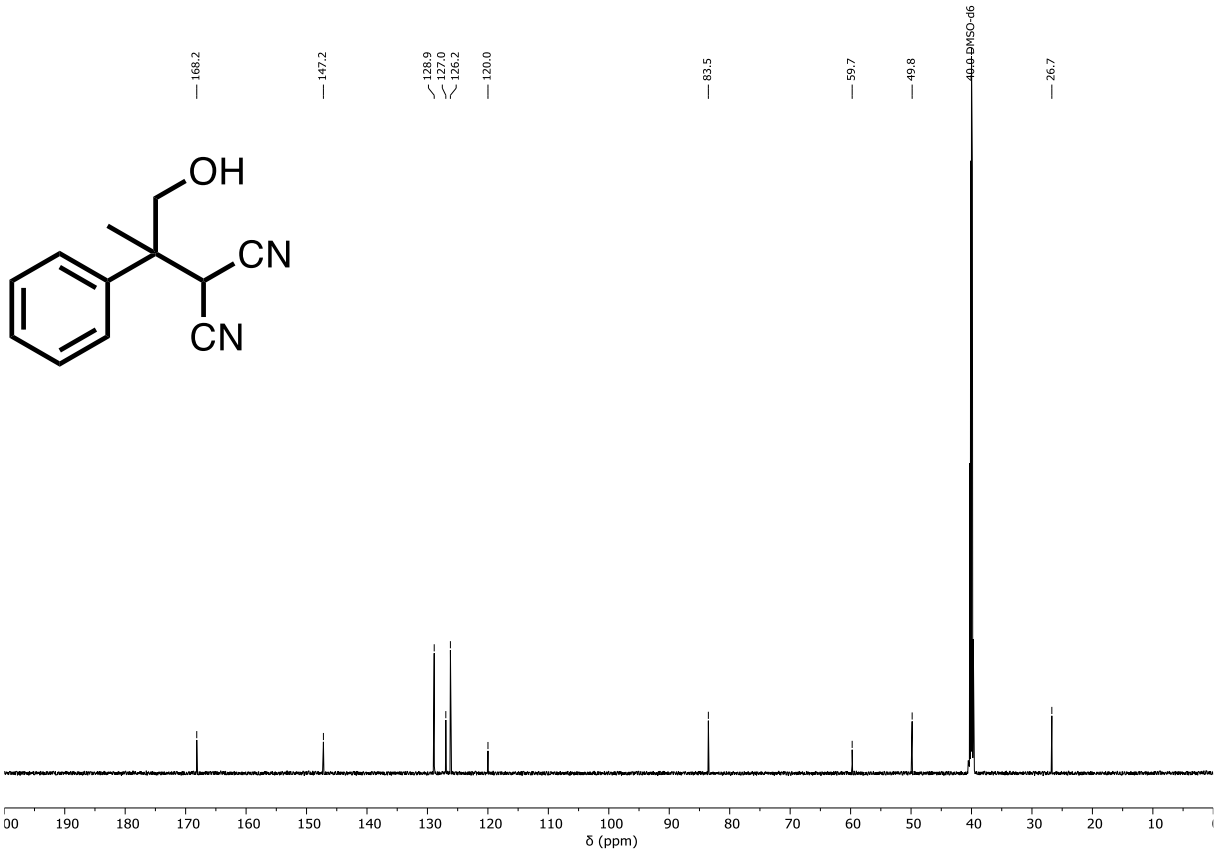
^{1}H NMR spectrum (300 MHz, $CDCl_3$) of 2-(dicyanomethyl)-2-phenylpropionaldehyde



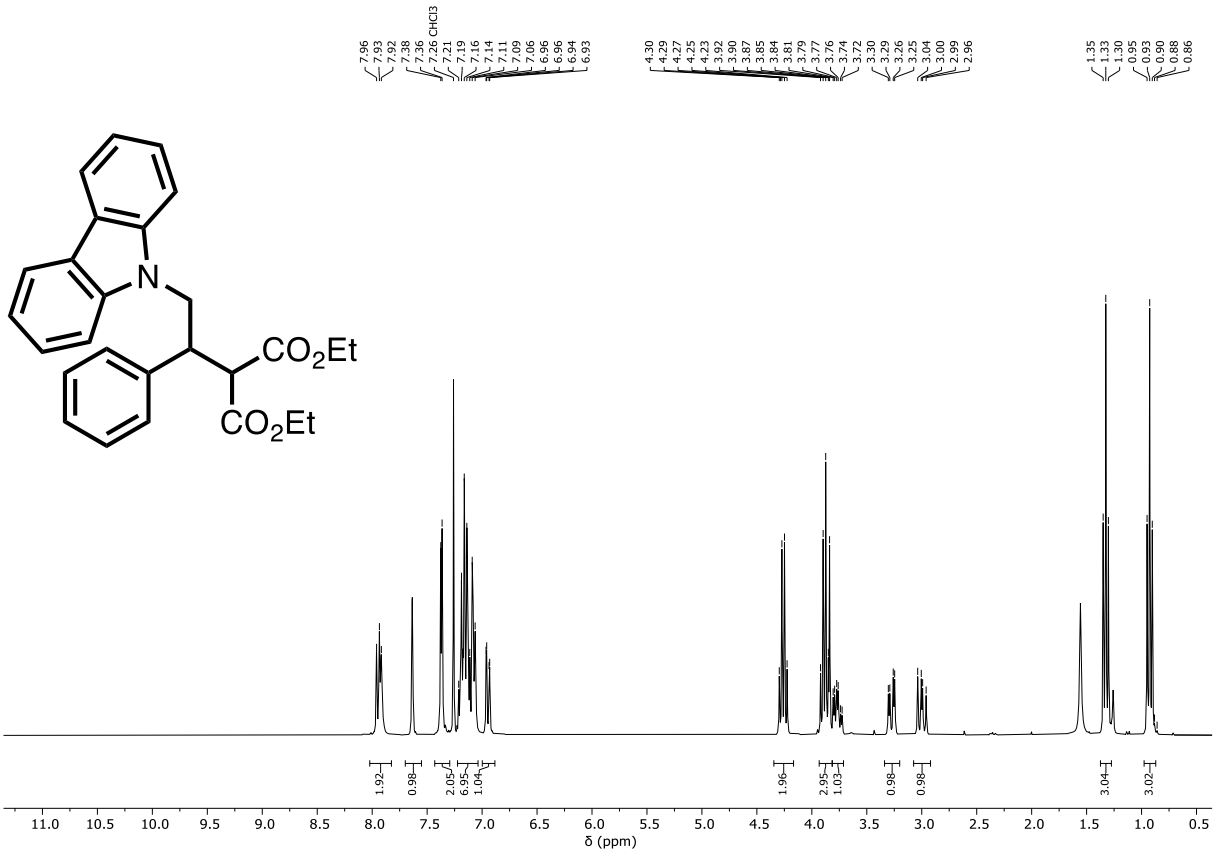
$^{13}C\{^{1}H\}$ NMR spectrum (75.5 MHz, $CDCl_3$) of 2-(dicyanomethyl)-2-phenylpropionaldehyde



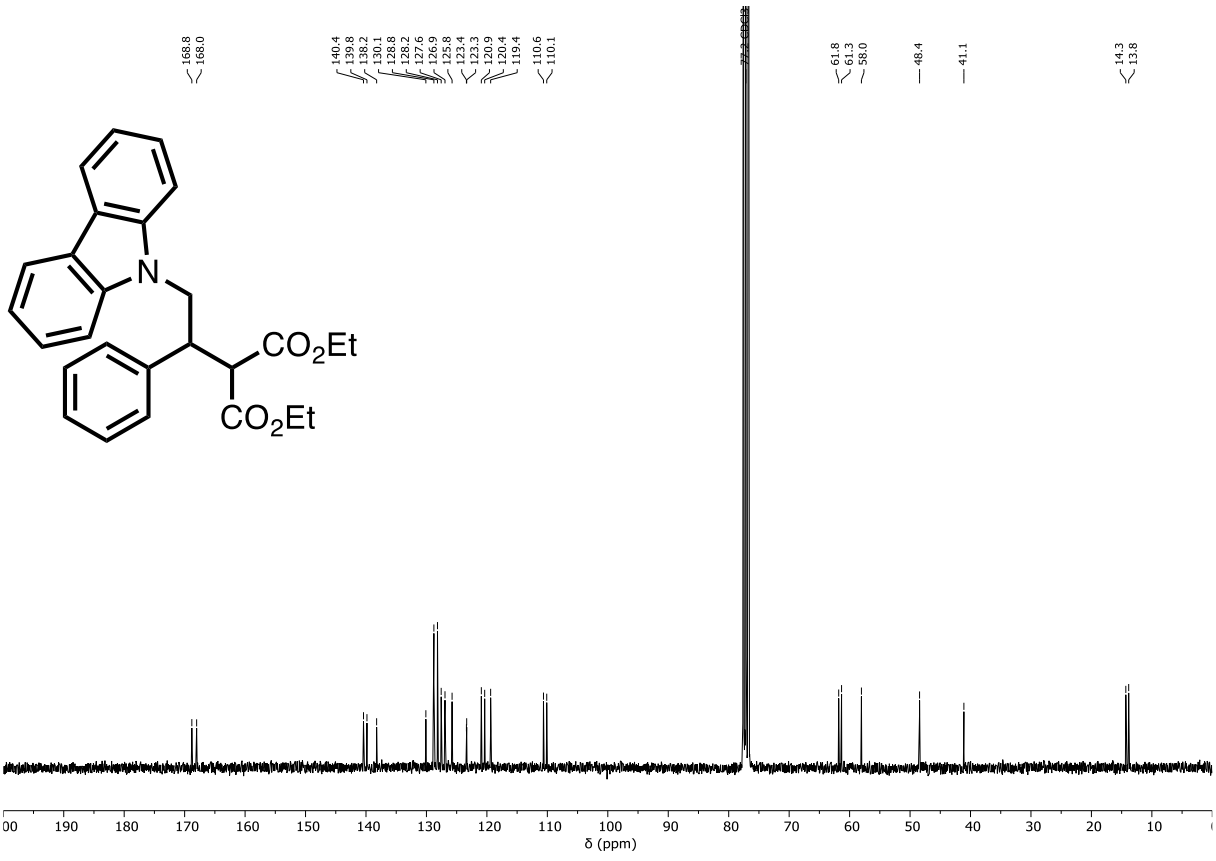
^{1}H NMR spectrum (600 MHz, DMSO-d_6) of (1-hydroxy-2-phenylpropan-2-yl)malononitrile



^{13}C{^{1}H} NMR spectrum (75.5 MHz, DMSO-d_6) of (1-hydroxy-2-phenylpropan-2-yl)malononitrile

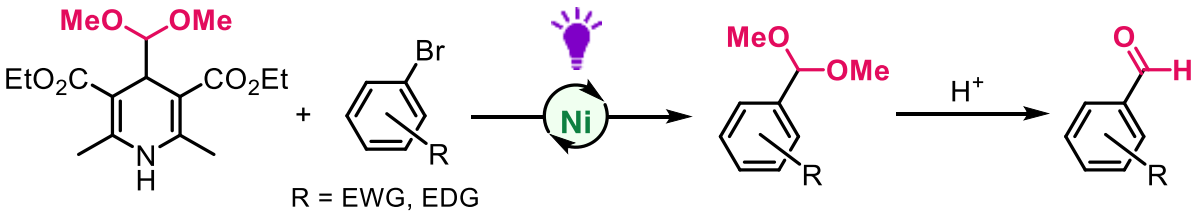


^{1}H NMR spectrum (300 MHz, $CDCl_3$) of diethyl 2-(2-(9*H*-carbazol-9-yl)-1-phenylethyl)malonate



^{13}C{^{1}H} NMR spectrum (75.5 MHz, $CDCl_3$) of diethyl 2-(2-(9*H*-carbazol-9-yl)-1-phenylethyl)malonate

Chapter 4



★ *Violet light-driven, **photocatalyst-free*** ★ *Inexpensive 3d metal catalyst system*
★ *Mild conditions, high chemoselectivity* ★ *20+ unique functional groups tolerated*
★ *Both aryl and heteroaryl substrates* ★ *Electron-poor and electron-rich substrates*
★ *Easily synthesized, low-cost precursor* ★ *Straightforward separation of byproduct*

Nickel-Catalyzed Photoformylation of Aryl Bromides

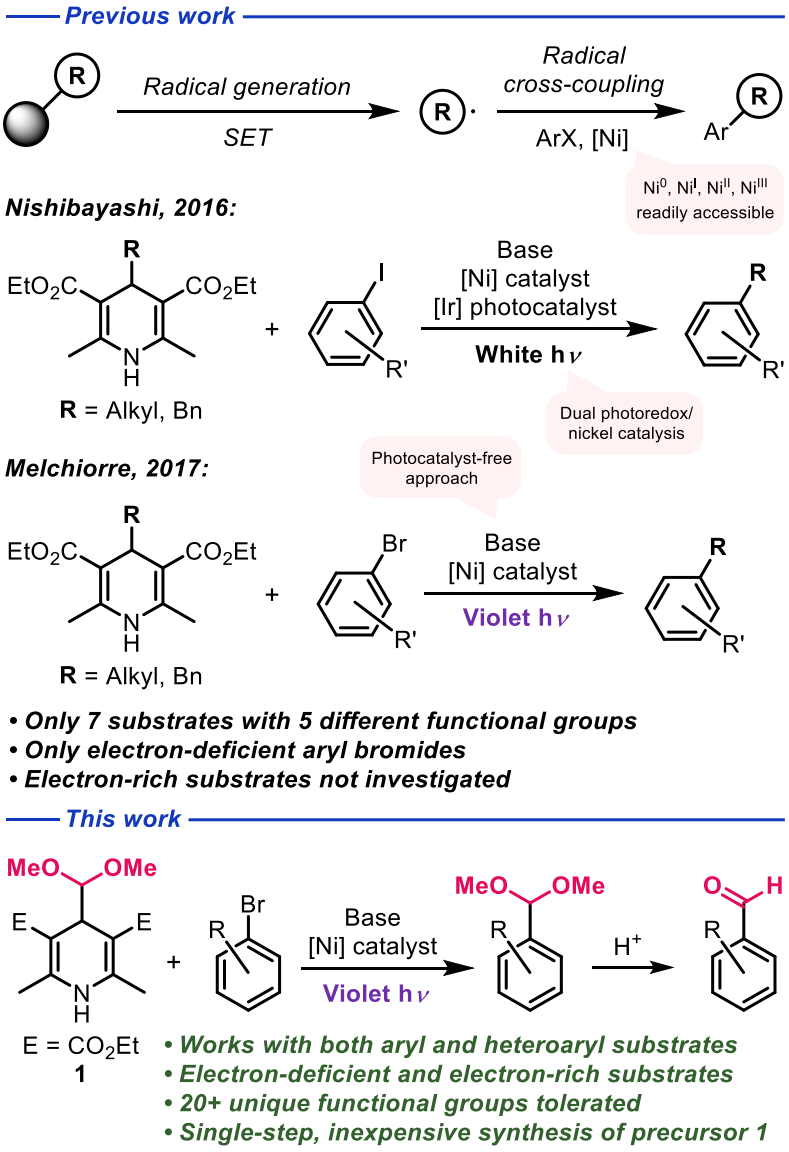
Abstract: *The versatile Hantzsch ester reagent diethyl 4-dimethoxymethyl-2,6-dimethyl-1,4-dihydropyridine-3,5-dicarboxylate (**1**) was applied in the formylation of (hetero)aryl bromides. Upon violet light irradiation, **1** liberates a dimethoxymethyl radical as a synthetic equivalent to a formyl radical. Subsequent cross-coupling occurs under the catalytic influence of a simple nickel/ligand system ($NiBr_2$·DME/2,2'-bipyridine). Despite the occurrence of free-radical intermediates, the reaction proceeds under mild conditions and high selectivity with a broad tolerance of important functional groups and without the need for reactive organometallic species, cryogenic temperatures, or toxic carbon monoxide. The use of a substituted ligand (2,2'-dMeObpy) enables formylation of notoriously challenging electron-rich aryl bromides.*

The work outlined in this chapter is scheduled for publication.

Author contributions: **Mattis-Ole W. S. Schmotz** wrote the manuscript and performed experimental work, **Axel Jacobi von Wangelin** supervised this work.

In **Chapter 3**, we reported that irradiation of Hantzsch ester **1** in the presence of a suitable acceptor led to the release of a dimethoxymethyl radical as a masked formyl equivalent. This strategy was successfully applied to a photocatalyst-free synthesis of aliphatic aldehydes from electron-deficient olefins. Recognizing the comparable synthetic importance of aryl aldehydes, we sought to extend this methodology to aromatic substrates. Despite the wide availability of well-established methods for aryl aldehyde synthesis, numerous traditional approaches suffer from significant limitations. Electrophilic aromatic substitutions (Vilsmeier-Haack,[1–4] Duff,[5–8] Gattermann(-Koch),[9,10] Rieche[11,12]) generally require strongly electron-rich arenes and frequently lack regioselectivity. The reaction of organometallic species with formamide derivatives (Bouveault reaction) is commonplace in organic synthesis,[13–16] but exhibits poor functional group tolerance and requires cryogenic temperatures. Transition metal-catalyzed reductive carbonylations of aryl (pseudo)halides using carbon monoxide and a hydrogen source[17–20] are impractical for routine use on a laboratory scale. In the last 15 years, light-driven nickel-(co)catalyzed cross-coupling reactions between C(sp^2)-halides and free radicals obtained from suitable reservoirs have shown a rising trend.[21–25] The choice of nickel as a catalyst is not only cost-effective, but also practical due to its redox flexibility: In contrast to higher transition metals such as palladium, $Ni^{0/I/II/III}$ oxidation states are easily accessible.[26] In 2016, Nishibayashi and co-workers reported one of the first uses of Hantzsch esters as radical reservoirs in a dual iridium-photoredox/nickel catalysis approach towards the alkylation of aryl iodides under white light irradiation.[27] Inspired by our previous photoformylation methodology, we envisioned a similar protocol for the nickel-catalyzed formylation of aryl halides by **1** in the absence of any photocatalyst. In 2017, a related photocatalyst-free approach for the Hantzsch ester-mediated alkylation of aryl bromides was reported by the Melchiorre group.[28] However, their method displayed a highly limited functional group diversity and does not accommodate substrates without electron-withdrawing substituents.

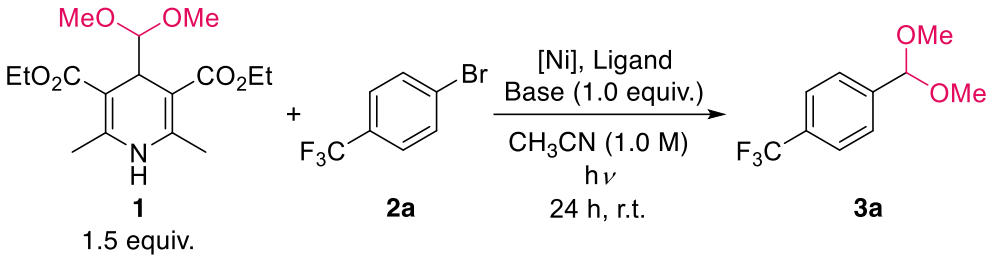
We commenced our investigation by irradiating an acetonitrile solution of **1** and 4-bromobenzotrifluoride (**2a**) with ultraviolet light at 365 nm in the presence of nickel(II) chloride dimethoxyethane adduct ($NiCl_2$·DME) as soluble nickel source, 2,2'-bipyridine (bpy) as ligand, and 2,4,6-collidine as base (Scheme 2, entry 1). The desired cross-coupling product **3a** was not observed in the crude ^{1}H NMR spectrum; additionally, a deposition of a Ni^0 mirror on the inner wall of the reaction vial was observed, indicating catalyst decomposition. Upon employing violet light (405 nm), we were delighted to detect **3a** in 60% yield (entry 2). Replacing the $NiCl_2$ precursor with its corresponding $NiBr_2$ analogue increased the yield to 83% (entry 3). The use of 4,4'-di-*tert*-butyl-2,2'-bipyridine (dtbbpy) as ligand delivered comparable good yields to bpy, but was deemed less favorable due to its higher cost (entry 4). Other bipyridine/phenanthroline-derived ligands performed worse (entry 5 + further entries in the experimental section).



Scheme 1. *Hantzsch esters in nickel-catalyzed light-driven cross-coupling reactions.*

A variety of bases, including other pyridine derivatives, aliphatic amines, and inorganic salts were evaluated, among which 2,4,6-collidine consistently afforded the highest yields (entries 6–9 + experimental section). Conducting the reaction in the absence of a base dramatically decreased the yield, highlighting its necessity (entry 10). 4-Chlorobenzotrifluoride as the coupling partner resulted in low conversion (entry 11), whereas 4-iodobenzotrifluoride led to a dark, complex mixture (entry 12). When the stoichiometry of nickel to ligand is reduced to 1:1, the yield is significantly decreased, accompanied by slight Ni^0 formation (entry 13). Halving the catalyst loading from 10 mol% to 5.0 mol% considerably decelerated the reaction, requiring several days of irradiation at 405 nm to achieve completion. Fortunately, irradiating at a slightly shorter wavelength at 390 nm sufficiently accelerated the reaction to reach completion within 24 hours with the same yield (entry 15) without causing catalyst decomposition (cf. entry 1). Control experiments revealed that the nickel precursor, the ligand, as well as light irradiation are essential for product formation (entries 16–18).

Scheme 2. *Selected optimization experiments (full list in the experimental section).*



№	Ni source (mol%)	Ligand (mol%)	Base	λ / nm	Yield of 3a[a] / %
1	$NiCl_2$·DME (10)	bpy (20)	Collidine	**365**	<5
2	$NiCl_2$·DME (10)	bpy (20)	Collidine	**405**	60
3	**$NiBr_2$·DME (10)**	bpy (20)	Collidine	405	83
4	$NiBr_2$·DME (10)	**dtbbpy (20)**	Collidine	405	80
5	$NiBr_2$·DME (10)	**phen (20)**	Collidine	405	35
6	$NiBr_2$·DME (10)	bpy (20)	**Lutidine**	405	74
7	$NiBr_2$·DME (10)	bpy (20)	**DIPEA**	405	67
8	$NiBr_2$·DME (10)	bpy (20)	**K_3PO_4**	405	61
9	$NiBr_2$·DME (10)	bpy (20)	**Cs_2CO_3**	405	6
10	$NiBr_2$·DME (10)	bpy (20)	**–**	405	12
11	$NiBr_2$·DME (10)	bpy (20)	Collidine	405	5[b]
12	$NiBr_2$·DME (10)	bpy (20)	Collidine	405	16[c]
13	$NiBr_2$·DME (10)	bpy (**10**)	Collidine	405	42
14	$NiBr_2$·DME (**5**)	bpy (10)	Collidine	405	22
15	$NiBr_2$·DME (5)	bpy (10)	Collidine	**390**	83
16	–	bpy (10)	Collidine	390	0
17	$NiBr_2$·DME (5.0)	–	Collidine	390	<5
18	$NiBr_2$·DME (5.0)	bpy (10)	Collidine	–	<5

[a] ^{1}H-NMR yield *vs.* 1,3,5-trimethoxybenzene. [b] 4-Chlorobenzotrifluoride instead of **2a**. [c] 4-Iodobenzotrifluoride instead of **2a**.

We next evaluated the robustness of the reaction through a sensitivity assessment.[29] The yield of **3a** remained unchanged upon varying the concentration by either a factor of 2 or ½ (83% under optimized conditions). High-intensity light had no discernible effect, whereas a decreased irradiance led to a lower yield due to incomplete conversion. The presence of water caused a more substantial drop in yield (−24%) than oxygen (−12%), however care should nonetheless be taken to exclude both from the reaction. The reaction proceeded efficiently at 0 °C with virtually unchanged yield. In contrast, elevating the temperature to 50 °C resulted in a decreased yield (−35%).

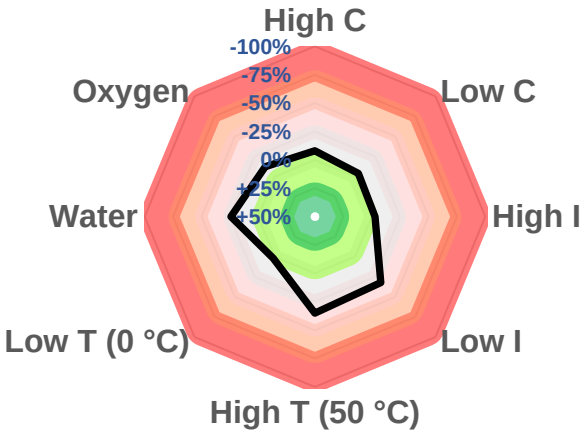
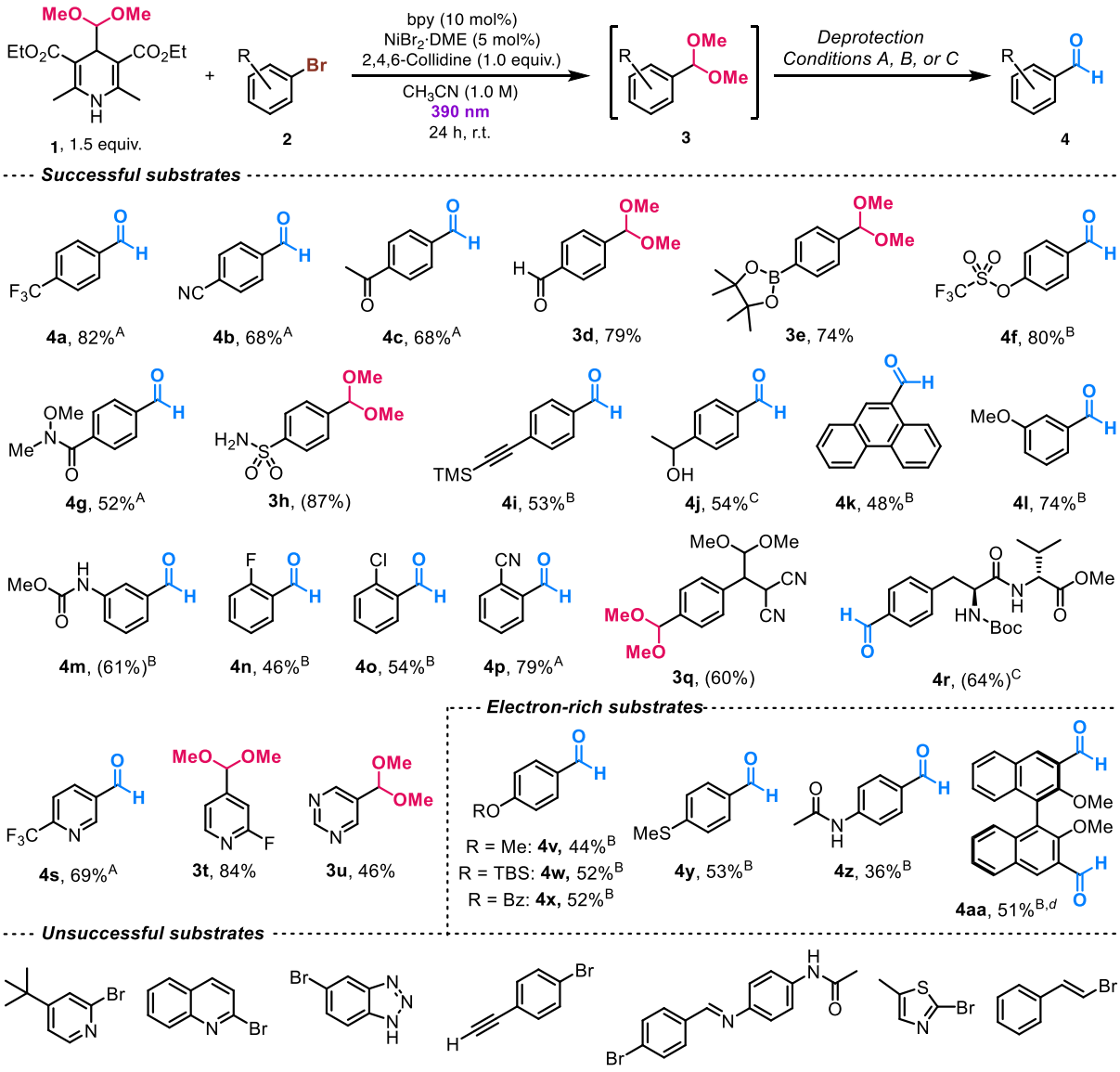


Figure 1. *Robustness screening.*

Having established the optimal conditions, we explored the substrate scope of our reaction using a diverse array of aryl and heteroaryl bromides (Scheme 3). The reaction demonstrated good tolerance towards common functional groups, accommodating trifluoromethyl (**4a**), nitriles (**4b**, **4p**, **3q**), ketones (**4c**), aldehydes (**3d**), carbamates (**4m**), benzylic alcohols (**4j**), and Weinreb amides (**4g**). Notably, common cross-coupling sites such as boronates and triflates were well-tolerated, facilitating follow-up functionalization (**3e**, **4f**). The biorelevant sulfonamide group was also compatible with the reaction conditions (**3h**). Trimethylsilyl-protected 4-bromophenylacetylene underwent successful formylation in 53% yield (**4i**); the unprotected terminal alkyne led to a complex mixture. Fluorine- and chlorine-substituted bromobenzenes reacted with high chemoselectivity (**4n**–**o**). The Boc-protected dipeptide Boc-(4-Br)Phe-Val-OMe was efficiently formylated with no evidence of deprotection. Heteroaryl bromides such as 3- and 4-bromopyridines were smoothly converted, as was 5-bromopyrimidine. In contrast, 2-bromopyridines, imines, and 5-bromobenzotriazol led to complex mixtures, whereas 2-bromo-5-methylthiazol and β-bromostyrene showed only minimal conversion under the reaction conditions.

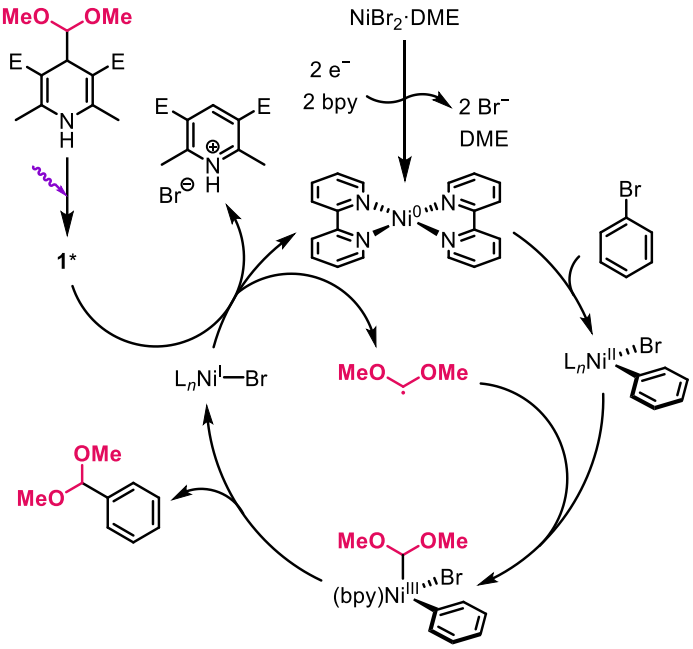
For aryl bromides bearing electron-donating groups in the *ortho* or *para* position, we observed a pronounced decrease in product yield (<30%); such reactivity patterns are well-documented for electron-rich substrates in free-radical nickel-catalyzed cross-couplings.[28,30–33] We observed substantial formation of the hydrodebrominated aromatic core as a side product. Hydrodehalogenation side reactions have been proposed to mainly affect the oxidative addition product [L$_n$NiArX], either via protodemetallation[34] or through photochemical Ni-C bond homolysis[35,36] followed by hydrogen atom transfer (HAT) onto the aryl radical. We performed deuterium labeling experiments which suggest that approximately half of the hydrodebromination arises from protodemetallation mediated by collidinium. Roughly 20% is presumed to result from Ni-C bond homolysis followed by HAT from acetonitrile, while the remaining 30% is attributed to HAT from other positions, presumably mainly within the Hantzsch ester. Both side

reactions have been shown to decelerate with increasing electron density on the Ni center.[34,35] Indeed, upon employing the more electron-rich ligand 4,4'-dimethoxy-2,2'-bipyridine (dMeObpy), the yield of the acetal **4v** was improved from 25 to 50% in the case of 4-bromoanisol (full optimization in the experimental section). It is worth noting that the use of dMeObpy in reactions with non-electron-rich substrates typically offers no improvement (e.g. **3k**, 48% with either ligand) and may even be detrimental to the product yield (e.g. **3a**, 83% vs. 63%). Encouraged by these findings, we subjected a broader set of electron-rich aryl bromides to these optimized conditions. We observed an up to two-fold increase in yields as compared to bpy for O-, S-, and N-substituted bromobenzenes. Dibrominated BINOL **2aa** was successfully bisformylated to yield **4aa** in good yield.



Scheme 3. *Substrate scope. 100 µmol scale reactions, ^{1}H NMR yields vs. 1,3,5,-trimethoxybenzene for known products, isolated yields in parentheses.* ***A****: Addition of 0.3 mL 4 M HCl, 2 h, r.t.,* ***B****: Addition of 100 mg Dowex 50W X2 (dried) or Amberlyst 15(H) (dry) and 1 mL acetone, 2 h, r.t.,* ***C****: Addition of 20 mol% p-TsOH·H_2O and 1 mL acetone, 16 h, r.t., [d] 50 µmol starting material ≙ 100 µmol Br atoms.*

Based on comprehensive previous works on light-driven nickel-catalyzed cross-couplings, including computational studies,[25,37–42] we propose the following simplified mechanism (Scheme 4): In the presence of 2,2'-bipyridine, the Ni^{II} precatalyst $NiBr_2$·DME is reduced ($E(Ni^{II}/Ni^0)$ = −1.51 V vs. SCE for [$NiBr_2$(dtbbpy)])[43] by photoexcited Hantzsch ester **1*** ($E(\mathbf{1}^{\cdot+}/\mathbf{1}^*)$ = −2.43 V vs. SCE)[44] to generate [$Ni^0(bpy)_2$], which enters the catalytic cycle. The observed requirement for a 2:1 ligand/nickel ratio and the formation of metallic nickel in its absence are consistent with the involvement of this bisligated Ni^0 species. Subsequent oxidative addition of the aryl bromide affords [$Ni^{II}ArBr(bpy)_2$][45,46] or [$Ni^{II}ArBr(bpy)$]. This Ni^{II} species is a competent radical acceptor[42,47] which may imply a predominant inner-sphere mechanism via dimethoxymethyl radical addition. The resulting Ni^{III} intermediate is prone to rapid reductive elimination[41] to yield the aryl acetal product and a Ni^{I}-Br species. The catalytic cycle is turned over by a single-electron transfer from the excited Hantzsch ester **1***, which generates the dimethoxymethyl radical. An alternative contemporaneous mechanism might be operative in which the radical adds first to [$Ni^0(bpy)_2$], followed then by oxidative addition of ArBr.[42,43]



Scheme 4. *Proposed mechanism and catalytic cycle.*

In summary, we have developed a photocatalyst-free nickel-catalyzed photoformylation of (hetero)aryl bromides, offering a mild, efficient, and operationally straightforward route to aromatic aldehydes. This protocol proceeds under ambient conditions using inexpensive reagents, without the need for cryogenic temperatures, organometallic reagents, expensive catalysts, or toxic carbon monoxide. This reaction demonstrates excellent tolerance of a multitude of important functional groups. Optimal yields are obtained with electron-deficient aryl bromides; traditionally challenging electron-rich substrates are also effectively converted with a substituted ligand. Advantageously, the aldehydes are initially obtained in a protected acetal form, facilitating downstream reactions, but can be readily deprotected in the same pot.

Literature References

[1] A. Vilsmeier, A. Haack, *Ber. Dtsch. Chem. Ges.* **1927**, *60*, 119–122.

[2] R. M. Garbaccio, S. J. Stachel, D. K. Baeschlin, S. J. Danishefsky, *J. Am. Chem. Soc.* **2001**, *123*, 10903–10908.

[3] K. C. Nicolaou, Q. Kang, S. Y. Ng, D. Y. K. Chen, *J. Am. Chem. Soc.* **2010**, *132*, 8219–8222.

[4] C. A. Kuttruff, H. Zipse, D. Trauner, *Angew. Chem. Int. Ed.* **2011**, *50*, 1402–1405.

[5] J. C. Duff, E. J. Bills, *J. Chem. Soc.* **1932**, 1987–1988.

[6] J. C. Duff, E. J. Bills, *J. Chem. Soc.* **1934**, 1305–1308.

[7] J. F. Larrow, E. N. Jacobsen, Y. Gao, Y. Hong, X. Nie, C. M. Zepp, *J. Org. Chem.* **1994**, *59*, 1939–1942.

[8] A. A. Anderson, T. Goetzen, S. A. Shackelford, S. Tsank, *Synth. Commun.* **2000**, *30*, 3227–3232.

[9] L. Gattermann, J. A. Koch, *Ber. Dtsch. Chem. Ges.* **1897**, *30*, 1622–1624.

[10] L. Gattermann, W. Berchelmann, *Ber. Dtsch. Chem. Ges.* **1898**, *31*, 1765–1769.

[11] A. Rieche, H. Gross, E. Höft, *Chem. Ber.* **1960**, *93*, 88–94.

[12] I. Ramos-Tomillero, M. Paradís-Bas, I. De Pinho Ribeiro Moreira, J. Bofill, E. Nicolás, F. Albericio, *Molecules* **2015**, *20*, 5409–5422.

[13] L. Bouveault, *Bull. Soc. Chim. Paris* **1904**, 1306–1322.

[14] D. L. Comins, H. Hong, G. Jianhua, *Tetrahedron Lett.* **1994**, *35*, 5331–5334.

[15] X. Lin, R. W. Kavash, P. S. Mariano, *J. Org. Chem.* **1996**, *61*, 7335–7347.

[16] H. Weinstabl, M. Suhartono, Z. Qureshi, M. Lautens, *Angew. Chem. Int. Ed.* **2013**, *52*, 5305–5308.

[17] A. Schoenberg, R. F. Heck, *J. Am. Chem. Soc.* **1974**, *96*, 7761–7764.

[18] V. P. Baillargeon, J. K. Stille, *J. Am. Chem. Soc.* **1983**, *105*, 7175–7176.

[19] V. P. Baillargeon, J. K. Stille, *J. Am. Chem. Soc.* **1986**, *108*, 452–461.

[20] L. Ashfield, C. F. J. Barnard, *Org. Process Res. Dev.* **2007**, *11*, 39–43.

[21] K. L. Skubi, T. R. Blum, T. P. Yoon, *Chem. Rev.* **2016**, *116*, 10035–10074.

[22] C. Zhu, H. Yue, L. Chu, M. Rueping, *Chem. Sci.* **2020**, *11*, 4051–4064.

[23] L. Mantry, R. Maayuri, V. Kumar, P. Gandeepan, *Beilstein J. Org. Chem.* **2021**, *17*, 2209–2259.

[24] M. Marchi, G. Gentile, C. Rosso, M. Melchionna, P. Fornasiero, G. Filippini, M. Prato, *ChemSusChem* **2022**, *15*, e202201094.

[25] H. Wang, T. XU, *Chem Catal.* **2024**, *4*, 100952.

[26] V. M. Chernyshev, V. P. Ananikov, *ACS Catal.* **2022**, *12*, 1180–1200.

[27] K. Nakajima, S. Nojima, Y. Nishibayashi, *Angew. Chem. Int. Ed.* **2016**, *55*, 14106–14110.

[28] L. Buzzetti, A. Prieto, S. R. Roy, P. Melchiorre, *Angew. Chem. Int. Ed.* **2017**, *56*, 15039–15043.

[29] L. Pitzer, F. Schäfers, F. Glorius, *Angew. Chem. Int. Ed.* **2019**, *58*, 8572–8576.

[30] M. K. Nielsen, B. J. Shields, J. Liu, M. J. Williams, M. J. Zacuto, A. G. Doyle, *Angew. Chem. Int. Ed.* **2017**, *56*, 7191–7194.

[31] L. Huang, M. Rueping, *Angew. Chem. Int. Ed.* **2018**, *57*, 10333–10337.

[32] H. Li, L. Guo, X. Feng, L. Huo, S. Zhu, L. Chu, *Chem. Sci.* **2020**, *11*, 4904–4910.

[33] C. N. Prieto Kullmer, J. A. Kautzky, S. W. Krska, T. Nowak, S. D. Dreher, D. W. C. MacMillan, *Science* **2022**, *376*, 532–539.

[34] P. E. Piszel, B. J. Orzolek, A. K. Olszewski, M. E. Rotella, A. M. Spiewak, M. C. Kozlowski, D. J. Weix, *J. Am. Chem. Soc.* **2023**, *145*, 8528.

[35] D. A. Cagan, D. Bim, B. Silva, N. P. Kazmierczak, B. J. McNicholas, R. G. Hadt, *J. Am. Chem. Soc.* **2022**, *144*, 6516–6531.

[36] E. Sutcliffe, D. A. Cagan, R. G. Hadt, *J. Am. Chem. Soc.* **2024**, *146*, 15506–15514.

[37] C. Zhu, H. Yue, L. Chu, M. Rueping, *Chem. Sci.* **2020**, *11*, 4051–4064.

[38] N. A. Till, L. Tian, Z. Dong, G. D. Scholes, D. W. C. MacMillan, *J. Am. Chem. Soc.* **2020**, *142*, 15830–15841.

[39] Y. Ben-Tal, G. C. Lloyd-Jones, *J. Am. Chem. Soc.* **2022**, *144*, 15372–15382.

[40] K. Jaouadi, M. Abdellaoui, E. Levernier, P. A. Payard, E. Derat, T. Le Saux, C. Ollivier, S. Torelli, L. Jullien, R. Plasson, L. Fensterbank, L. Grimaud, *Chem. Eur. J.* **2023**, *29*, e202301780.

[41] D. A. Cagan, D. Bím, N. P. Kazmierczak, R. G. Hadt, *ACS Catal.* **2024**, *14*, 9055–9076.

[42] O. Gutierrez, J. C. Tellis, D. N. Primer, G. A. Molander, M. C. Kozlowski, *J. Am. Chem. Soc.* **2015**, *137*, 4896–4899.

[43] I. B. Perry, T. F. Brewer, P. J. Sarver, D. M. Schultz, D. A. DiRocco, D. W. C. MacMillan, *Nature* **2018**, *560*, 70–75.

[44] Chapter 3 of this work.

[45] Y. G. Budnikova, Y. M. Kargin, *Russ. J. Gen. Chem.* **2001**, *71*, 128–131.

[46] D. G. Yakhvarov, E. G. Samieva, D. I. Tazeev, Y. G. Budnikova, *Russ. Chem. Bull.* **2002**, *51*, 796–804.

[47] Q. Lin, E. H. Spielvogel, T. Diao, *Chem* **2023**, *9*, 1295–1308.

Experimental Section

General Information

Nuclear magnetic resonance (NMR) spectroscopy: ^{1}H NMR spectra (300 MHz) and ^{13}C-NMR spectra (75.5 MHz) were recorded on a *Bruker Fourier HD 300.* ^{1}H NMR spectra (400 MHz) and ^{13}C-NMR spectra (101 MHz) were recorded on a *Bruker Avance III HD 400*. ^{1}H NMR spectra (600 MHz), ^{13}C-NMR spectra (151 MHz), and ^{19}F-NMR spectra (565 MHz) were recorded on a *Bruker Avance III HD 600*. All spectra were recorded at 25 °C unless otherwise stated. Chemical shifts δ are reported in parts per million (ppm) relative to tetramethylsilane for ^{1}H and ^{13}C NMR spectra, relative to $CFCl_3$ for ^{19}F NMR spectra, and relative to $BF_3{\cdot}OEt_2$ for ^{11}B NMR spectra. Coupling constants *J* are given in Hertz (Hz). *MestReNova 14* (Mnova) by *Mestrelab* was used for analysis of the NMR spectra. Abbreviations used for NMR data: s = singlet; br. s = broad singlet; d = doublet; t = triplet; q = quartet; and combinations thereof.

Infrared (IR) spectroscopy: Infrared spectra were recorded using a *Bruker VERTEX 70* FTIR spectrometer using a *Specac Golden Gate* ATR unit.

UV-Vis spectroscopy: UV-Vis spectra were measured at room temperature on an *Agilent Cary 5000* UV-Vis-NIR Spectrophotometer in double-beam mode using 10 mm SUPRASIL quartz cuvettes by *Hellma*.

Fluorescence spectroscopy: Fluorescence spectra were measured at room temperature on an *Agilent Cary Eclipse Fluorescence Spectrophotometer* at a 90° angle using 10 mm SUPRASIL quartz fluorescence cuvettes by *Hellma*.

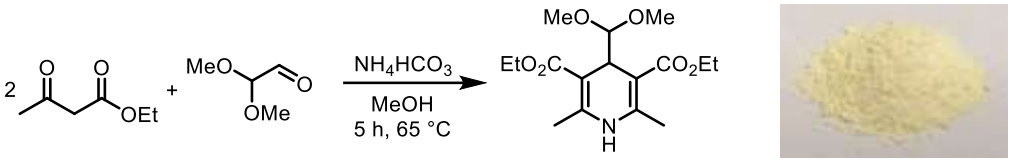
Mass spectrometry (MS): High-resolution mass spectra (electrospray ionization, ESI) were measured using an *Agilent 6224 ESI-TOF* or a *Bruker maXis ESI-Q-TOF* by direct injection in positive or negative ion mode. Abbreviations used for MS data: *m/z* = mass-to-charge ratio; M = exact mass of the target compound. *MestReNova 14* (Mnova) by *Mestrelab* was used for analysis of the MS spectra.

Melting points: Melting points (m.p.) were measured using a *DigiMelt MPA160* by *Stanford Research Systems*.

Thin-layer chromatography (TLC) and column chromatography: TLC was performed using aluminium plates coated with UV-fluorescence-indicator-doped stationary phase by *Macherey-Nagel* (*ALUGRAM® Xtra Sil G/UV$_{254}$* for SiO_2, *ALUGRAM® ALOX N / UV254* for neutral Al_2O_3). Preparative column chromatography was performed using silica by *Acros Organics* (35–70 µm, 60 Å pore size) or neutral alumina by *Macherey-Nagel* (50–200 µm, 90 Å pore size) using distilled technical grade solvents.

Synthesis of Compounds

Diethyl 4-(dimethoxymethyl)-2,6-dimethyl-1,4-dihydropyridin-3,5-dicarboxylate (**1**)



A suspension of ammonium bicarbonate (2.37 g, 30.0 mmol, 1.0 equiv.), ethyl acetoacetate (7.81 g, 60.0 mmol, 2.0 equiv.) and 2,2-dimethoxyacetaldehyde (60 wt.% soln. in water, 5.21 g, 30.0 mmol, 1.0 equiv.) in methanol (30 mL) was refluxed. Within 10–20 minutes the solid ammonium bicarbonate dissolves and the mixture turns homogeneous and bright yellow. After 5 h of reflux, the solvent was removed and the orange syrupy residue was thoroughly dried *in vacuo*, during which slow solidification to a waxy solid eventually occurs (scratching the flask wall is often required to induce crystallization). The product crystallizes slowly (after ~30 min) from boiling diethyl ether (~25–30 mL) upon cooling to r.t., then to −25 °C overnight, initially as small pale-yellow needles which merge into solid clumps. **1** is obtained as a pale-yellow solid after filtration and washing with cold diethyl ether and room-temperature pentane until the distinct odor of ethyl acetoacetate is no longer perceptible (5.37 g, 16.4 mmol, 55 %). The solid thus obtained melts at 88–89 °C and is sufficiently pure for the photoreaction. A purer, almost colorless product melting at 90–91 °C is obtained after a second recrystallization or careful silica column chromatography (SiO_2, PE/EtOAc 3:2). This synthesis was also conducted several times on a 5.0, 60, and 150 mmol scale with consistent yields (50–60 %).

^{1}H NMR (600 MHz, $CDCl_3$): δ [ppm] = 5.85 (s, 1H), 4.34 (d, J = 5.2 Hz, 1H), 4.25 – 4.11 (m, 4H), 3.94 (d, J = 5.2 Hz, 1H), 3.29 (s, 6H), 2.27 (s, 6H), 1.28 (t, J = 7.2 Hz, 6H).

^{13}C{^{1}H} NMR (151 MHz, $CDCl_3$): δ [ppm] = 168.4, 145.1, 107.9, 99.2, 59.8, 55.3, 36.9, 19.4, 14.5.

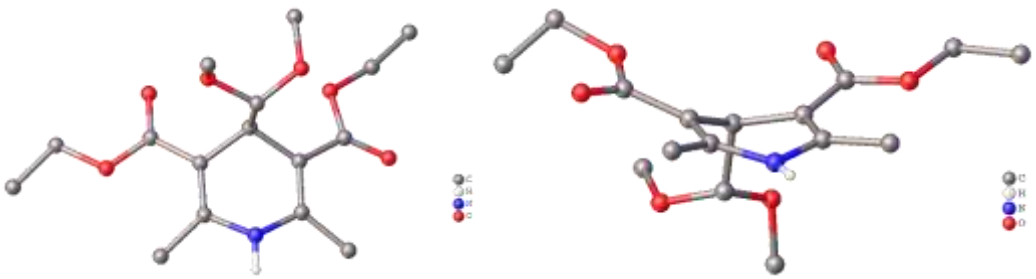
IR (ATR): $\tilde{\nu}$ [cm^{-1}] = 3346 (N–H), 2990, 2938, 2889, 2837, 1699, 1649 (C=O), 1484, 1474, 1448, 1391, 1368, 1335, 1321, 1291, 1272, 1258, 1210 (C–O–C), 1166, 1150, 1122, 1099, 1044, 1016, 981, 916, 863, 776, 741, 711, 699, 643, 628.

UV-Vis (MeCN): λ_{max} [nm] (ε [$L \cdot mol^{-1} \cdot cm^{-1}$]) = 230, 248, 332 (6496).

HRMS (ESI): *m/z* = calcd. for $C_{16}H_{25}NNaO_6^+$ ([M+Na]$^+$): 350.1574, found.: 350.1571; calcd. for $C_{32}H_{50}N_2NaO_{12}^+$ ([2M+Na]$^+$): 677.3256, found.: 677.3260.

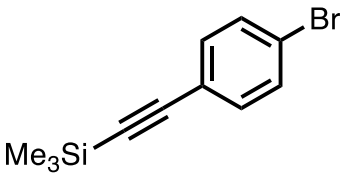
m.p. = 90–91 °C.

XRD (Non heteroatom-bonded hydrogen atoms omitted for clarity):



Synthesis of Aryl Bromides

((4-Bromophenyl)ethynyl)trimethylsilane (**2i**)



To a solution of 4-bromophenylacetylene (543 mg, 3.00 mmol, 1.0 equiv.) in CH_2Cl_2 (12 mL) was added NEt_3 (627 µL, 4.50 mmol, 1.5 equiv.) and $Zn(OTf)_2$ (54.5 mg, 150 µmol, 5.0 mol%). Trimethylsilyl triflate (814 µL, 4.50 mmol, 1.5 equiv.) was added dropwise and the mixture was stirred for 24 h at ambient temperature. Sat. aq. NH_4Cl (20 mL) was added and the aqueous phase was extracted with CH_2Cl_2 (3× 10 mL). The combined organic phases were dried over Na_2SO_4, filtered, and concentrated. The residue was re-dissolved in a small amount of CH_2Cl_2 and passed through a silica plug deactivated with NEt_3, eluting with further CH_2Cl_2.

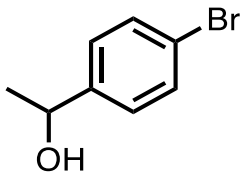
Yield: 93% (706 mg, 2.80 mmol).

Appearance: Colorless solid.

^{1}H NMR (300 MHz, $CDCl_3$): δ [ppm] = 7.47 – 7.39 (m, 2H), 7.36 – 7.28 (m, 2H), 0.24 (s, 9H)

Literature: R. J. Rahaim, J. T. Shaw, *J. Org. Chem.* **2008**, *73*, 2912–2915.

1-(4-Bromophenyl)ethanol (**2j**)



A solution of 4'-bromoacetophenone (1.99 g, 10.0 mmol, 1.0 equiv.) in a dry mixture of MeOH (7 mL) and THF (7 mL) was cooled to 0 °C. $NaBH_4$ (567 mg, 15.0 mmol, 1.5 equiv.) was added portionwise. After complete addition, the mixture was slowly warmed to room temperature, and stirred for 2 h. Sat. aq. NH_4Cl (5 mL) was added and the mixture was partitioned between water (10 mL) and EtOAc (50 mL). The aq. phase was extracted with EtOAc (3× 10 mL). The combined organic phases were washed with brine (20 mL), dried over Na_2SO_4, filtered, and concentrated. The residue was purified by column chromatography (SiO_2, PE/Et_2O 2:1).

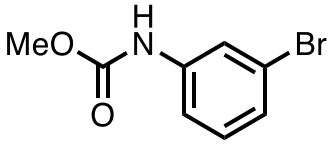
Yield: 85% (1.71 g, 8.50 mmol).

Appearance: Colorless solid.

^{1}H NMR (300 MHz, $CDCl_3$): δ [ppm] = 7.52 – 7.42 (m, 2H), 7.30 – 7.19 (m, 2H), 4.86 (qd, J = 6.4, 3.5 Hz, 1H), 1.84 (d, J = 3.6 Hz, 1H), 1.47 (d, J = 6.5 Hz, 3H).

Literature: B. Zoller, T. Stach, P. H. Huy, *ChemCatChem* **2020**, *12*, 5637–5643.

Methyl (3-bromophenyl)carbamate (**2m**)



A solution of 3-bromoaniline (860 mg, 5.00 mmol, 1.0 equiv.) and pyridine (600 µL, 7.50 mmol, 1.5 equiv.) in CH_2Cl_2 (25 mL) was cooled to 0 °C using an ice bath. Methyl chloroformate (460 µL, 6.00 mmol, 1.2 equiv.) was added dropwise. After complete addition, the mixture was slowly warmed to room temperature and stirred for 16 h. Water (20 mL) was added to the pale-brown mixture and the aqueous phase was extracted with CH_2Cl_2 (3× 10 mL). The combined org. phases were washed with water (20 mL), dried over Na_2SO_4, filtered, and concentrated.

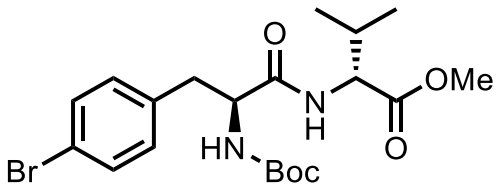
Yield: 98% (1.12 g, 4.89 mmol).

Appearance: Pale-brown solid.

^{1}H NMR (300 MHz, $CDCl_3$): δ [ppm] = 7.72 – 7.56 (m, 1H), 7.32 – 7.23 (m, 1H), 7.23 – 7.11 (m, 2H), 6.68 (br. s, 1H), 3.78 (s, 3H).

Literature: N. Uhlig, C.-J. Li, *Chem. Eur. J.* **2014**, *20*, 12066–12070.

Methyl ((*S*)-3-(4-bromophenyl)-2-((*tert*-butoxycarbonyl)amino)propanoyl)-D-valinate (**2r**)



A suspension of Boc-Phe(4-Br)-OH (3.44 g, 10.0 mmol, 1.0 equiv.), H-Val-OMe hydrochloride (2.01 g, 12.0 mmol, 1.2 equiv.), and HBTU (5.69 g, 15.0 mmol, 1.5 equiv.) in CH_2Cl_2 (50 mL) was cooled to 0 °C using an ice bath. DIPEA (5.1 mL, 30 mmol, 3.0 equiv.) was added dropwise. After complete addition, the ice bath was removed and the mixture was slowly warmed to room temperature, then stirred for 20 h. The mixture was washed with aq. HCl (1 M, 50 mL), sat. aq. $NaHCO_3$ (50 mL), and water (50 mL), dried over Na_2SO_4, filtered, and concentrated. The residual solid was recrystallized from MeCN/H_2O. The product initially separated as brownish oil droplets. As soon as this was observed, the flask was vigorously shaken in an ice bath, upon which lush small colorless needles appeared. Crystallization was completed by storage at 3 °C overnight.

Yield: 70% (3.20 g, 7.01 mmol).

Appearance: Colorless needles.

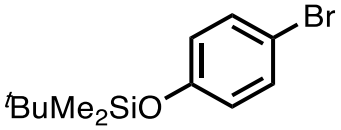
^{1}H NMR (600 MHz, $CDCl_3$): δ [ppm] = 7.43 – 7.38 (m, 2H), 7.11 – 7.06 (m, 2H), 6.33 (d, *J* = 9.3 Hz, 1H), 5.00 (br. s, 1H), 4.45 (dd, *J* = 8.7, 5.0 Hz, 1H), 4.34 – 4.28 (m, 3H), 3.06 – 2.98 (m, 2H), 2.15 – 2.07 (m, 1H), 1.42 (s, 9H), 0.86 (dd, *J* = 17.5, 6.9 Hz, 6H).

^{13}C{^{1}H} NMR (101 MHz, $CDCl_3$): δ [ppm] = 171.9, 170.9, 135.7, 131.8, 131.2, 121.1, 57.3, 55.8, 52.4, 37.5, 31.4, 28.4, 19.0, 17.8.

HRMS (ESI): *m/z* = calcd. for $C_{20}H_{29}BrN_2NaO_5^+$: 479.1152, found: 479.1156.

m.p. = 132–133 °C.

(4-Bromophenoxy)(*tert*-butyl)dimethylsilane (**2w**)



To a solution of 4-bromophenol (943 mg, 5.45 mmol, 1.0 equiv.) and imidazole (742 mg, 10.9 mmol, 2.0 equiv.) in *N*,*N*-dimethylformamide (15 mL) was added *tert*-Butyldimethylsilyl chloride (838 mg, 5.56 mmol, 1.02 equiv.) in portions. The mixture was stirred for 16 h, then partitioned between water (50 mL) and Et_2O (50 mL). The aqueous phase was extracted with Et_2O (2× 50 mL). The combined organic phases were washed with brine (2× 50 mL), dried over Na_2SO_4, filtered, and concentrated.

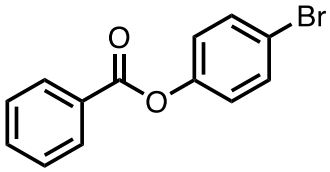
Yield: 66% (1.49 g, 3.62 mmol).

Appearance: Colorless oil.

^{1}H NMR (300 MHz, $CDCl_3$): δ [ppm] = 7.35 – 7.28 (m, 2H), 6.76 – 6.67 (m, 2H), 0.97 (s, 9H), 0.18 (s, 6H).

Literature: G. R. Pettit, M. P. Grealish, M. K. Jung, E. Hamel, R. K. Pettit, J.-C. Chapuis, J. M. Schmidt, *J. Med. Chem.* **2002**, *45*, 2349–2674.

4-Bromophenyl benzoate (**2x**)



To a solution of 4-bromophenol (1.73 g, 10.0 mmol) and triethylamine (2.1 mL, 15 mmol, 1.5 equiv.) in CH_2Cl_2 (100 mL) was added benzoyl chloride (1.21 mL, 10.5 mmol, 1.05 equiv.) dropwise. The mixture was stirred for 16 h at room temperature, then washed with water (50 mL). The aqueous phase was extracted with CH_2Cl_2 (2× 30 mL) and the combined organic phases were washed with brine (50 mL), dried over Na_2SO_4, filtered, and concentrated. The residue was recrystallized from EtOH/H_2O 4:1; crystallization was completed at 3 °C overnight.

Yield: 87% (2.42 g, 8.73 mmol).

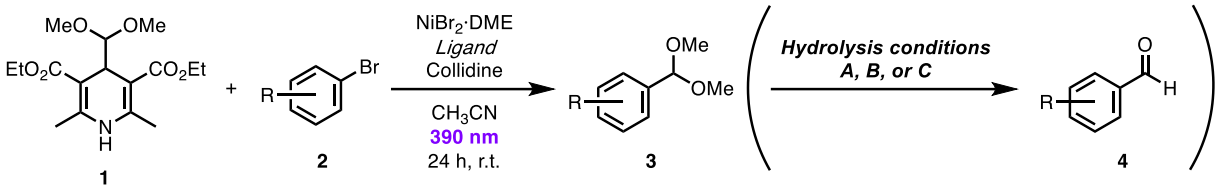
Appearance: Colorless crystal plates.

^{1}H NMR (300 MHz, $CDCl_3$): δ [ppm] = 8.24 – 8.15 (m, 2H), 7.71 – 7.60 (m, 1H), 7.59 – 7.47 (m, 4H), 7.14 – 7.08 (m, 2H).

Literature: X. Liu, J. Yi, Z.-Q. Zhang, J.-J. Dai, J.-H. Liu, B. Xiao, Y. Fu, L. Liu, *Chem. Eur. J.* **2014**, *20*, 15339–15343.

Synthesis of Aromatic Dimethyl Acetals

General procedure for the light-driven cross-coupling of aryl bromides (GP1)



Inside an argon-filled glove box, Hantzsch ester **1** (49.1 mg, 150 µmol, 1.5 equiv.), the corresponding aryl bromide if solid (100 µmol, 1.0 equiv.), nickel(II) bromide dimethoxyethane adduct (1.5 mg, 5.0 µmol, 5 mol%), and **either** 2,2'-bipyridine (bpy, 1.6 mg, 10 µmol, 10 mol%) **or** 4,4'-dimethoxy-2,2'-bipyridine (dMeObpy, 2.2 mg, 10 µmol, 10 mol%) were weighed into a 4 mL glass vial. Collidine (13 µL, 100 µmol, 1.0 equiv.), the corresponding aryl bromide if liquid (100 µmol, 1.0 equiv.), acetonitrile (dried and degassed, 1.0 mL), and a magnetic stir bar were added. The vial was closed with a septum screw cap, transferred out of the glove box, and placed inside the photoreactor *(EvoluChem PhotoRedOx Box*). The mixture was stirred for 24 h under air cooling and irradiation at 390 nm (*EvoluChem LED 390PF*). If applicable, the obtained aryl dimethyl acetal was directly deprotected by one of three conditions:

Hydrolysis conditons A: Aqueous hydrochlorid acid (4 M, 0.3 mL) was added to the mixture, followed by stirring for 2 h at room temperature. The mixture was neutralized with solid Na_2CO_3, then further treated as described below.

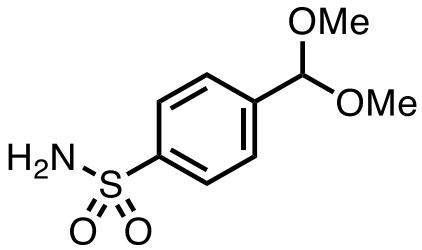
Hydrolysis conditons B: Acetone (1.0 mL) and 100 mg of a dry acidic ion exchange resin (*Amberlyst 15* and *Dowex 50W X2* were used interchangeably) were added to the mixture, followed by stirring for 2 h at room temperature. The mixture was then further treated as described below.

Hydrolysis conditons C: Acetone (1.0 mL) and *para*-toluenesulfonic acid monohydrate (3.8 mg, 20 µmol, 20 mol%) were added to the mixture, followed by stirring for 16 h at room temperature. The mixture was then further treated as described below.

NMR yield determination: An exactly weighed amount of methyl phenyl sulfone (>99 % purity, 1.50–3.00 mg) was added and the vial was shaken well. The mixture was filtered through a sand plug (if no hydrolysis had been conducted the sand plug was topped with a short silica plug) and concentrated. The residue was taken up in $CDCl_3$ and a ^1H NMR spectrum was recorded. By integration of a suitable product signal in comparison with the signal of the internal standard, the amount of substance and thus the yield was determined. Known products were quantified by ^1H NMR yield.

Product isolation: The mixture was filtered through a sand plug (if no hydrolysis had been conducted the sand plug is topped with a short silica plug) and Celite® (~100 mg) was added. The solvent was removed and the crude product adsorbed on Celite® was purified by column chromatography on silica or neutral alumina using an appropriate solvent mixture as determined by TLC. Unknown products were isolated and fully characterized.

4-(Dimethoxymethyl)benzenesulfonamide (**3h**)



By GP1 starting from 4-bromobenzenesulfonamide (23.6 mg). Isolated by column chromatography (SiO_2, Pentane/Et_2O 1:4).

Yield: 87% (20.2 mg, 87.3 µmol).

Appearance: Off-white solid.

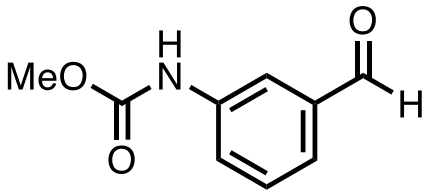
^{1}H NMR (300 MHz, DMSO-d_6): δ [ppm] = 7.91 – 7.79 (m, 2H), 7.63 – 7.50 (m, 2H), 7.38 (s, 2H), 5.46 (s, 1H), 3.26 (s, 6H).

^{13}C{^{1}H} NMR (75.5 MHz, $CDCl_3$): δ [ppm] = 144.1, 141.8, 127.1, 125.6, 101.8, 52.7.

HRMS (ESI): *m/z* = calcd. for $C_9H_{13}NNaO_4S^+$: 254.0457, found: 254.0465.

m.p. = 156–157°C.

Methyl (3-(dimethoxymethyl)phenyl)carbamate (**4m**)



By GP1 starting from methyl (3-bromophenyl)carbamate **2m** (23.0 mg) with hydrolysis conditions B. Isolated by column chromatography (SiO_2, Pentane/Et_2O 2:1).

Yield: 78% (14.0 mg, 78.1 µmol).

Appearance: Pale-yellow crystals.

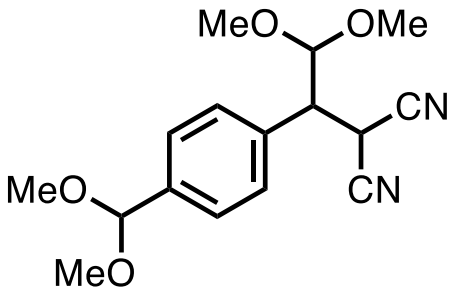
^{1}H NMR (300 MHz, $CDCl_3$): δ [ppm] = 9.99 (s, 1H), 7.94 – 7.82 (m, 1H), 7.76 – 7.66 (m, 1H), 7.66 – 7.55 (m, 1H), 7.55 – 7.40 (m, 1H), 6.84 (br. s, 1H), 3.81 (s, 3H).

^{13}C{^{1}H} NMR (151 MHz, $CDCl_3$): δ [ppm] = 192.1, 154.0, 139.0, 137.4, 130.0, 124.9, 124.4, 119.3, 52.8.

HRMS (ESI): *m/z* = calcd. for $C_9H_{10}NO_3^+$: 180.0655, found: 180.0665.

m.p. = 99–101 °C.

Methyl (3-(dimethoxymethyl)phenyl)carbamate (**3q**)



By GP1 starting from 2-(4-bromophenyl)-2-dicyanomethylacetaldehyde dimethyl acetal (30.9 mg). Isolated by column chromatography (Neutral Al_2O_3, Pentane/EtOAc 4:1).

Yield: 60% (18.2 mg, 59.8 µmol).

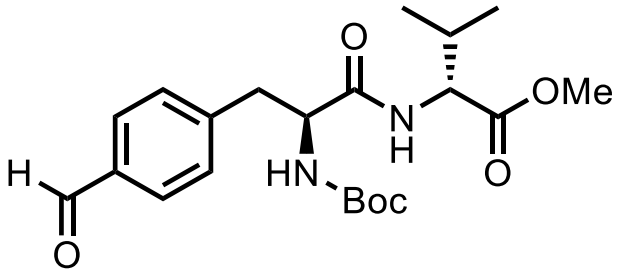
Appearance: Pale-yellow syrup.

^{1}H NMR (300 MHz, $CDCl_3$): δ [ppm] = 7.54 – 7.48 (m, 2H), 7.44 – 7.39 (m, 2H), 5.41 (s, 1H), 4.79 (d, *J* = 6.6 Hz, 1H), 4.34 (d, *J* = 5.6 Hz, 1H), 3.52 (s, 3H), 3.43 (dd, *J* = 6.7, 5.6 Hz, 1H), 3.34 (s, 6H), 3.30 (s, 3H).

^{13}C{^{1}H} NMR (75.5 MHz, $CDCl_3$): δ [ppm] = 139.3, 133.7, 128.8, 127.7, 112.0, 111.9, 104.4, 102.8, 56.5, 55.2, 52.98, 52.95, 49.1, 25.9.

HRMS (ESI): *m/z* = calcd. for $C_{16}H_{20}N_2NaO_4^+$: 327.1315, found: 327.1320.

Methyl ((*S*)-2-((*tert*-butoxycarbonyl)amino)-3-(4-formylphenyl)propanoyl)-D-valinate (**4r**)



By GP1 starting from methyl ((*S*)-3-(4-bromophenyl)-2-((*tert*-butoxycarbonyl)-amino)propanoyl)-D-valinate **2r** (45.7 mg) with hydrolysis conditions C. Isolated by column chromatography (SiO_2, Pentane/Et_2O 2:1).

Yield: 64% (26.1 mg, 64.2 µmol).

Appearance: Colorless solid.

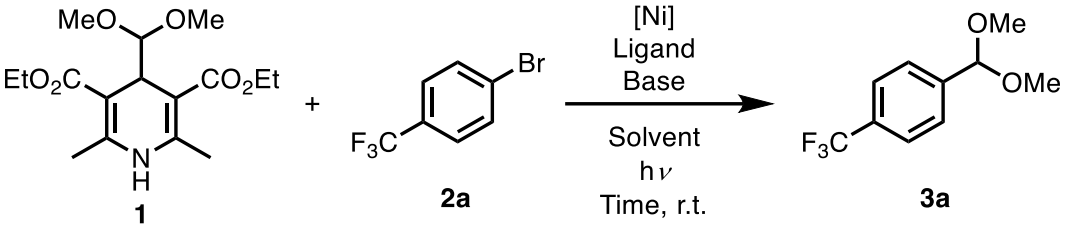
^{1}H NMR (600 MHz, $CDCl_3$): δ [ppm] = 9.98 (s, 1H), 7.80 (d, J = 8.2 Hz, 2H), 7.38 (d, J = 8.2 Hz, 2H), 6.43 (d, J = 8.4 Hz, 1H), 5.07 (d, J = 7.1 Hz, 1H), 4.46 (dd, J = 8.7, 5.0 Hz, 1H), 4.43 – 4.37 (m, 1H), 3.68 (s, 3H), 3.20 (dd, J = 13.9, 6.8 Hz, 1H), 3.11 (dd, J = 13.9, 7.1 Hz, 1H), 2.16 – 2.08 (m, 1H), 1.40 (s, 9H), 0.88 (d, J = 6.9 Hz, 3H), 0.85 (d, J = 6.9 Hz, 3H).

^{13}C{^{1}H} NMR (75.5 MHz, $CDCl_3$): δ [ppm] = 192.0, 171.9, 170.8, 155.5, 144.1, 135.4, 130.2, 130.2, 80.7, 57.3, 55.7, 52.3, 38.3, 31.4, 28.4, 19.0, 17.8.

HRMS (ESI): *m/z* = calcd. for $C_{21}H_{30}N_2NaO_6^+$: 429.1996, found: 429.1992.

m.p. = 102–104 °C.

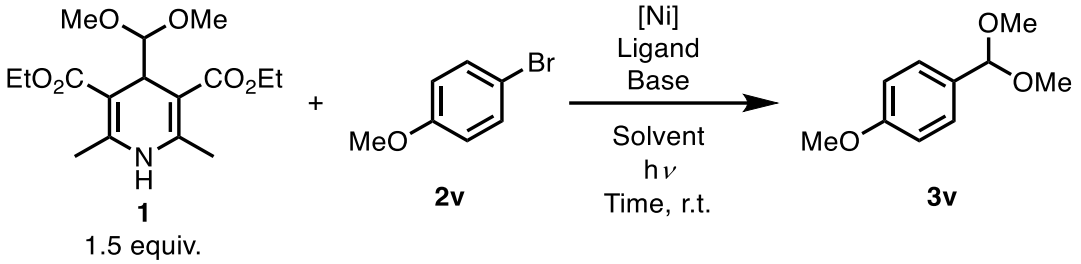
Optimization Experiments



Entry	[Ni] (mol%)	Ligand (mol%)	Base	Solvent	Wavelength [nm]	Time [h]	Yield[a] [%]
1	$NiCl_2$·DME (10)	bpy (20)	Collidine	MeCN	365	16	<5
2	$NiCl_2$·DME (10)	bpy (20)	Collidine	MeCN	405	24	60
3	$NiCl_2$·DME (10)	dtbbpy (20)	Collidine	MeCN	405	24	52
4	$NiBr_2$·DME (10)	dtbbpy (20)	Collidine	DMF	405	24	18
5	$NiBr_2$·DME (10)	bpy (20)	Collidine	Acetone	405	24	31
6	$NiBr_2$·DME (10)	bpy (20)	Collidine	MeCN	405	24	83
7	$NiBr_2$·DME (10)	phen (20)	Collidine	MeCN	405	24	35
8	$NiBr_2$·DME (10)	dMeObpy (20)	Collidine	MeCN	405	24	63
9	$NiBr_2$·DME (10)	$dMeO_2C$bpy (20)	Collidine	MeCN	405	24	20
10	$NiCl_2$·DME (10)	phen (20)	Collidine	MeCN	405	24	56
11	$NiCl_2$·DME (10)	dMeObpy (20)	Collidine	MeCN	405	24	69
12	$NiCl_2$·DME (10)	$dMeO_2C$bpy (20)	Collidine	MeCN	405	24	19
13	$NiBr_2$·DME (10)	bpy (20)	Lutidine	MeCN	405	24	74
14	$NiBr_2$·DME (10)	bpy (20)	DTBMP	MeCN	405	24	36
15	$NiBr_2$·DME (10)	bpy (20)	DIPEA	MeCN	405	24	67
16	$NiBr_2$·DME (10)	bpy (20)	NEt_3	MeCN	405	24	20
17	$NiBr_2$·DME (10)	bpy (20)	Cs_2CO_3	MeCN	405	24	6
18	$NiBr_2$·DME (10)	bpy (20)	K_2CO_3	MeCN	405	24	56
19	$NiBr_2$·DME (10)	bpy (20)	K_3PO_4	MeCN	405	24	61
20	$NiBr_2$·DME (10)	bpy (20)	K_2HPO_4	MeCN	405	24	65
21	$NiBr_2$·DME (10)	bpy (20)	KH_2PO_4	MeCN	405	24	15
22	$NiBr_2$·DME (10)	bpy (20)	–	MeCN	405	24	12
23	$NiBr_2$·DME (10)	bpy (20)	Collidine	MeCN	405	24	5[b]
24	$NiBr_2$·DME (10)	bpy (20)	Collidine	MeCN	405	24	16[c]
25	$NiBr_2$·DME (10)	bpy (10)	Collidine	MeCN	405	24	42
26	$NiBr_2$·DME (5)	bpy (10)	Collidine	MeCN	405	24	22
27	$NiBr_2$·DME (5)	bpy (10)	Collidine	MeCN	405	48	78
28	**$NiBr_2$·DME (5)**	**bpy (10)**	**Collidine**	**MeCN**	**390**	**24**	**83**

[a] ^{1}H NMR yield vs. 1,3,5-trimethoxybenzene, [b] 4-Chlorobenzotrifluoride instead of **2a**, [c] 4-Iodobenzotrifluoride instead of **2a**. bpy = 2,2'-bipyridine, dtbbpy = 4,4'-di-*tert*-butyl-2,2'-bipyridine, phen = 1,10-phenanthroline, dMeObpy = 4,4'-dimethoxy-2,2'-bipyridine, $dMeO_2C$bpy = dimethyl 2,2′-bipyridine-4,4′-dicarboxylate, DTBMP = 2,6-di-*tert*-butyl-4-methylpyridine, DIPEA = diisopropyl-ethylamine.

Further Optimization Experiments for Electron-Rich Substrate 2v



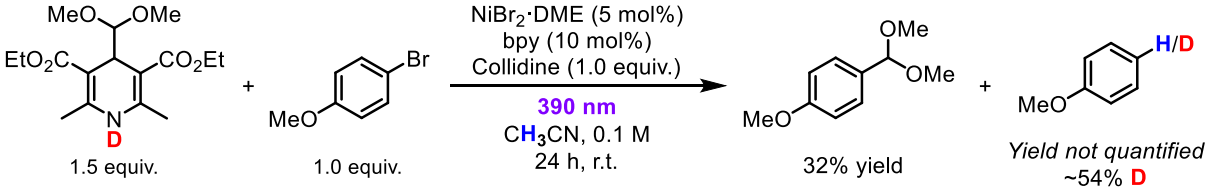
Entry	[Ni] (mol%)	Ligand (mol%)	Base	Solvent	Wavelength [nm]	Time [h]	Yield[a] [%]
1	$NiBr_2$·DME (5)	bpy (10)	Collidine	MeCN	390	24	25
2	$NiBr_2$·DME (10)	bpy (20)	Collidine	MeCN	390	24	26
3	$NiBr_2$·DME (15)	bpy (30)	Collidine	MeCN	390	24	24
4	$NiBr_2$·DME (10)	bpy (20)	Collidine	MeCN	405	24	8
5	$NiBr_2$·DME (15)	bpy (30)	Collidine	MeCN	405	24	12
6	$NiBr_2$·DME (10)	dtbbpy (20)	Collidine	MeCN	390	24	21
7	$NiBr_2$·DME (10)	$dMeO_2Cbpy$ (20)	Collidine	MeCN	390	24	8
8	$NiBr_2$·DME (10)	dCF_3bpy (20)	Collidine	MeCN	390	24	6
9	$NiBr_2$·DME (10)	dppf (20)	Collidine	MeCN	390	24	<5
10	$NiBr_2$·DME (10)	dppe (20)	Collidine	MeCN	390	24	<5
11	**$NiBr_2$·DME (5)**	**dMeObpy (10)**	**Collidine**	**MeCN**	**390**	**24**	**50**
12	$NiBr_2$·DME (5)	dMe_2Nbpy (10)	Collidine	MeCN	390	24	22
13	$Ni(acac)_2$ (10)	–	Collidine	MeCN	390	24	<5
14	$Ni(dpm)_2$ (10)	–	Collidine	MeCN	390	24	<5
15	$NiBr_2$·DME (5)	bpy (10)	Collidine	MeCN	390	24	<5[b]
16	$NiBr_2$·DME (5)	bpy (10)	Barton	MeCN	390	24	<5
17	$NiBr_2$·DME (5)	dMeObpy (10)	Barton	MeCN	390	24	<5

[a] ^{1}H NMR yield vs. 1,3,5-trimethoxybenzene, [b] 4-Methoxyphenyl triflate instead of **2v**. dppf = 1,1'-bis(diphenylphosphino)ferrocene, dppe = 1,2-bis(diphenylphosphino)ethane, dCF_3bpy = 4,4'-bis(trifluoromethyl)-2,2'-bipyridine, dMe_2Nbpy = 4,4'-bis(dimethylamino)-2,2'-bipyridine, acac = acetylacetone, dpm = dipivaloylmethane, Barton = 2-*tert*-butyl-1,1,3,3-tetramethylguanidine.

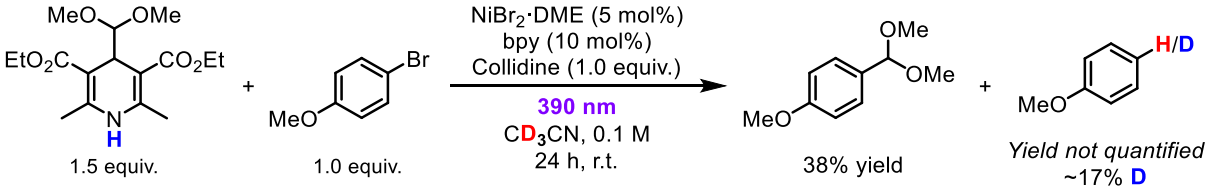
Deuteration Experiments

The deuterated Hantzsch ester **1-*d*$_1$** was synthesized by keeping **1** in methanol-d_4 (0.1 M) for 16 h, followed by evaporation. ^{1}H NMR showed a deuteration degree of >95%. A regular photoreaction as described above was set up. The yields of the acetal were determined by ^{1}H NMR spectroscopy with 1,3,5-trimethoxybenzene as internal standard. The degree of deuteration of the anisole was determined by GC-MS and comparison of the peaks at *m/z* = 108 and 109.

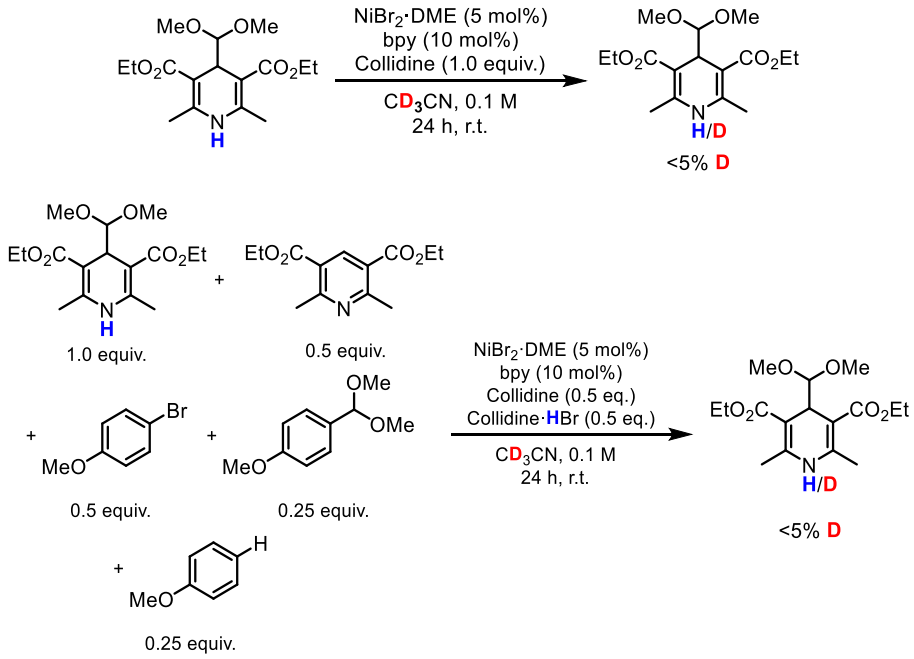
When **1** is substituted by **1-*d*$_1$**, a degree of deuteration of ~54% is obtained for the anisole. This likely results from protodemetallation.



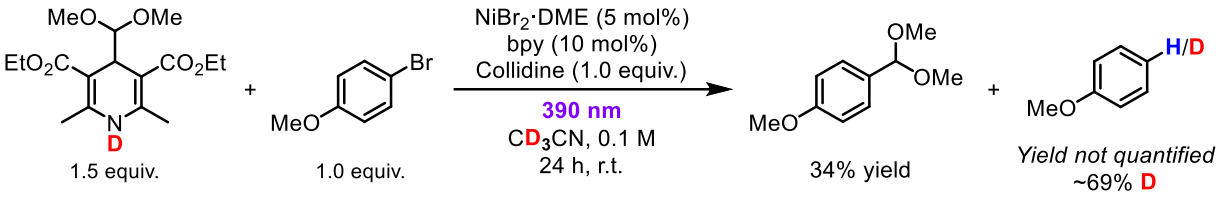
When MeCN is substituted with CD_3CN, the anisole degree of deuteration is ~17%. This likely results from a hydrogen-atom abstraction from the solvent by an intermediate aryl radical.



The incorporated deuterium must originate from the CD_3CN, as no scrambling between **1** and CD_3CN is observed, neither under conditions at the beginning of the photoreaction nor under conditions emulating a conversion of 50%:



The deuteration incorporation from **1-*d*$_1$** (~54%) and from CD_3CN (~17%) is additive:

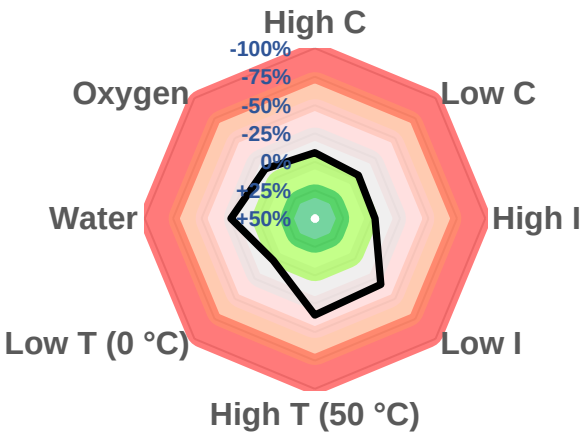


The remaining ~30% of hydrogen atoms in the anisole-forming side reaction must originate from other sites, likely from other positions within the Hantzsch ester. These are also likely abstracted by an aryl radical.

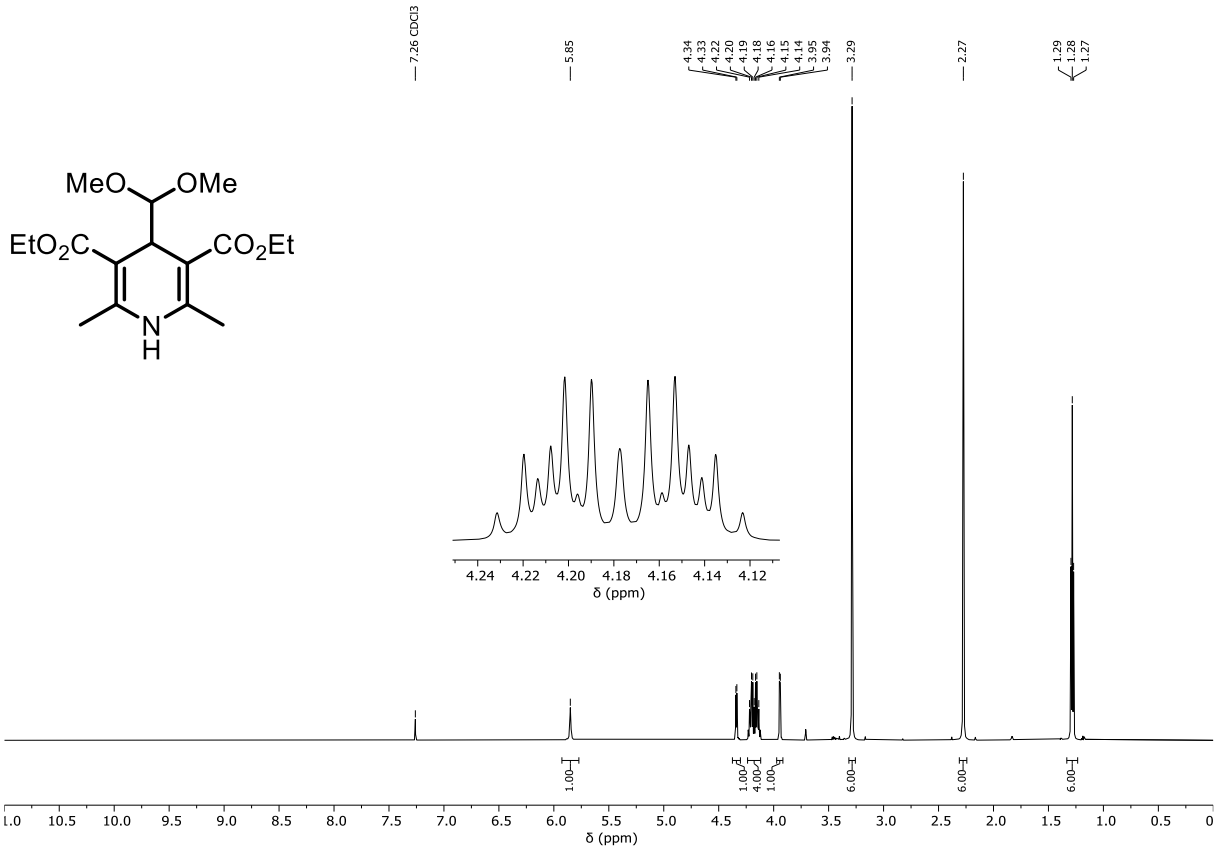
Sensitivity assessment

The reactions were set up using the standard conditions described above, on a 0.10 mmol scale in combination with the deviations shown below. The yields were determined via ^{1}H NMR spectroscopy using 1,3,5-trimethoxybenzene as the standard.

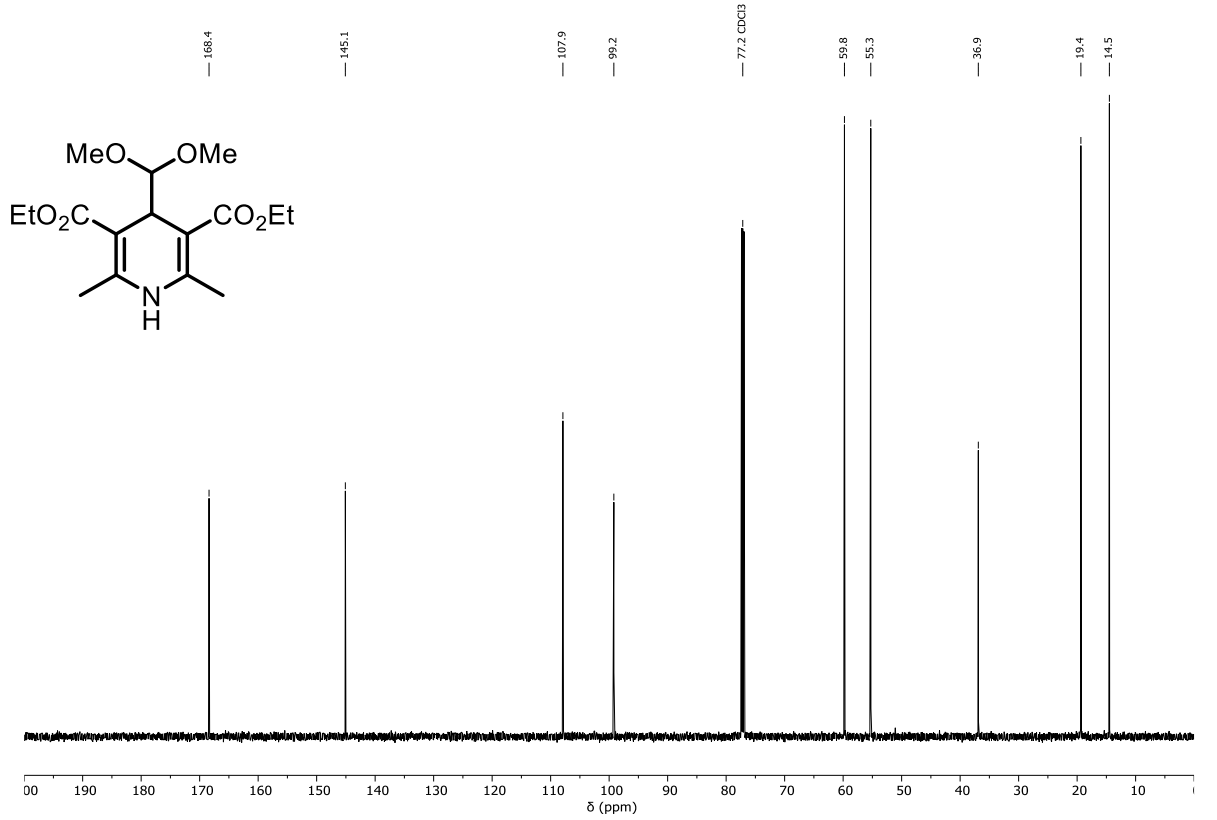
Entry	Deviations from standard conditions	Yield of 3a [%]	Difference in yield to standard conditions (83%) [%]
High *c*	0.2 M	75	−8
Low *c*	0.05 M	79	−4
High *I*	Vial placed ~1 cm in front of the LED, cooled by a desk fan	80	−3
Low *I*	Placed in the furthest corner of the PhotoRedOx Box	51	−32
High *T*	50 °C	48	−35
Low *T*	0 °C	81	−2
Water	+ 1 vol.% degassed water	59	−24
Oxygen	+ 2 mL of dry air added	71	−12



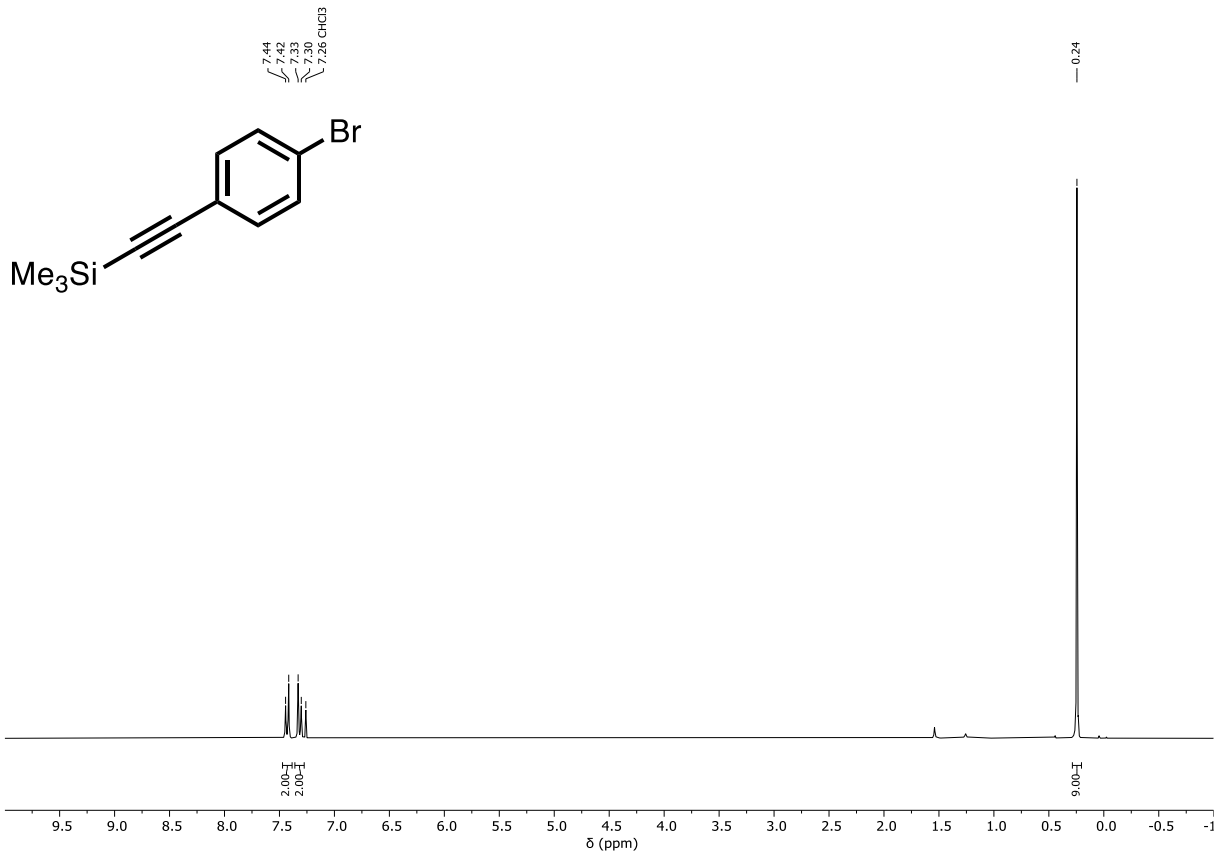
NMR Spectra of all Compounds



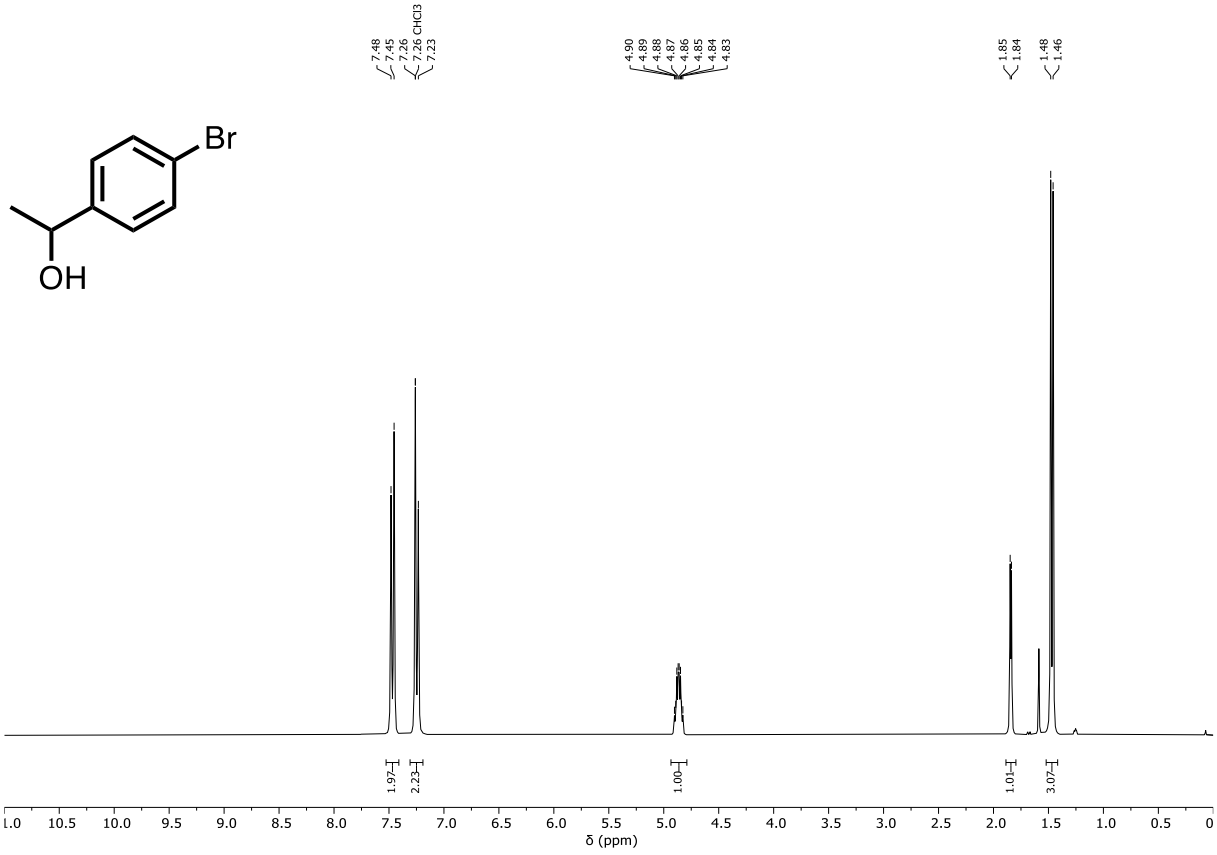
^{1}H NMR spectrum (600 MHz, $CDCl_3$) of **1**



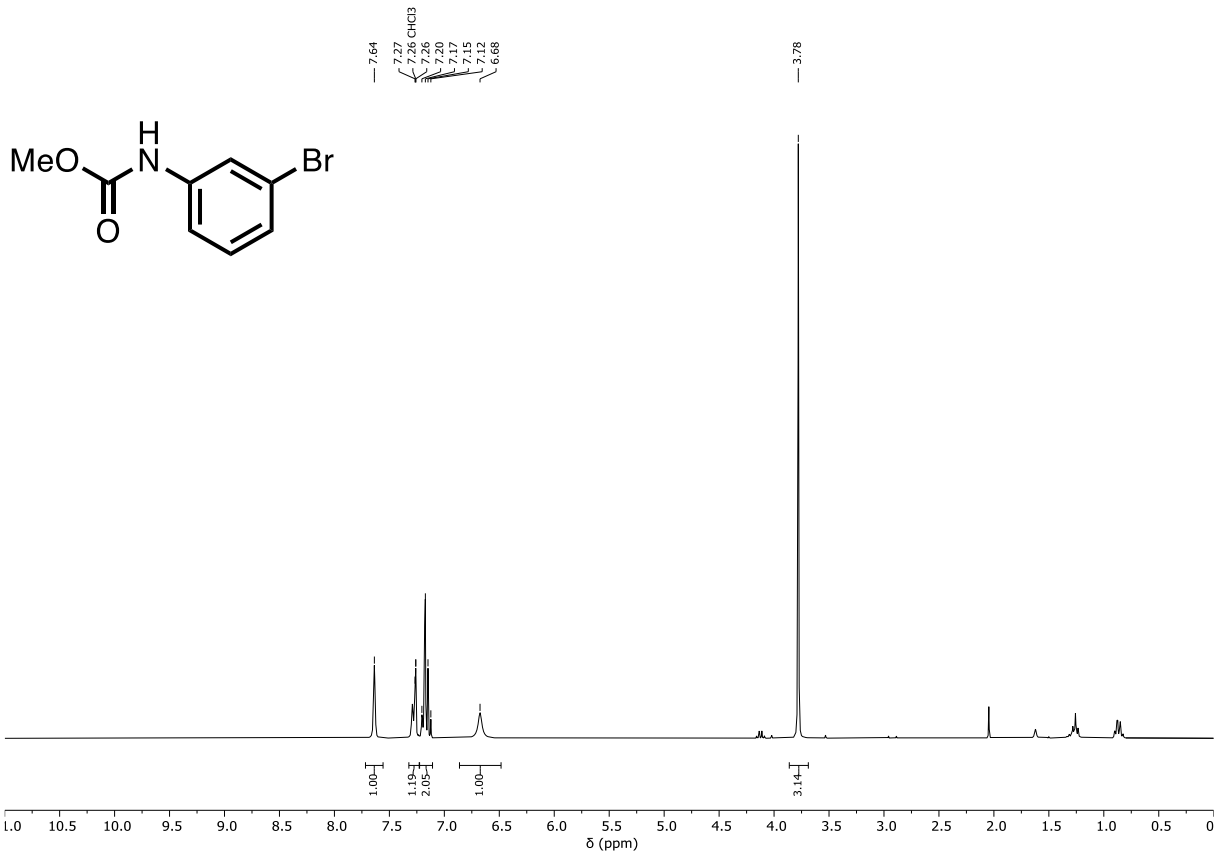
^{13}C NMR spectrum (151 MHz, $CDCl_3$) of **1**



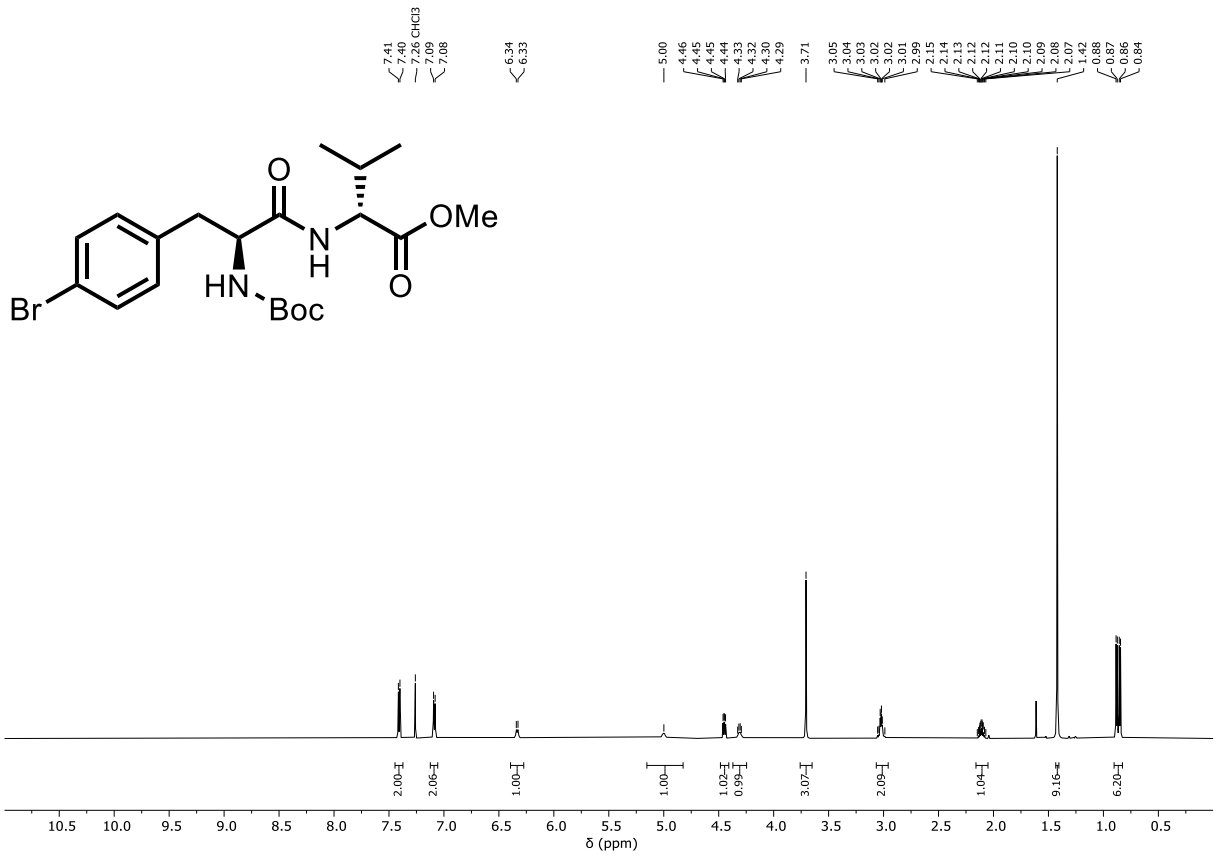
^{1}H NMR spectrum (300 MHz, $CDCl_3$) of **2i**



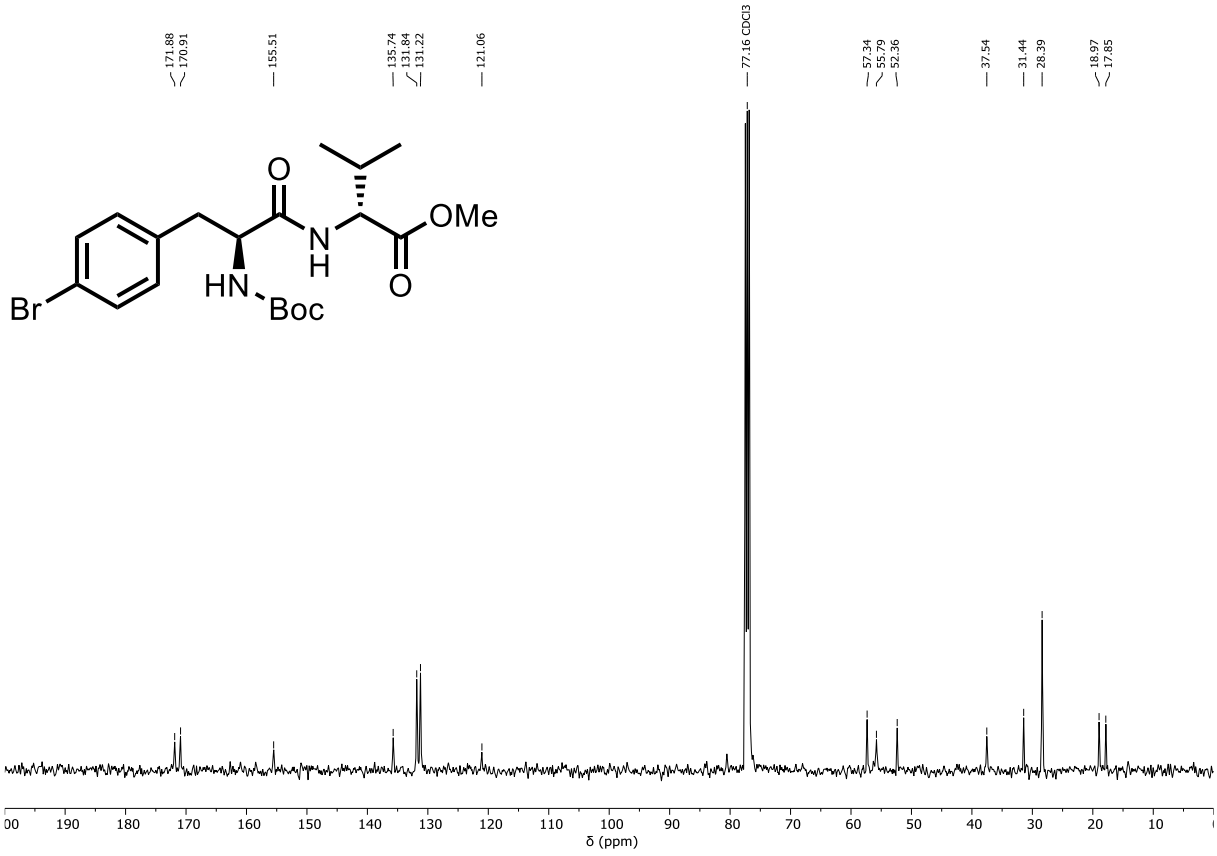
^{1}H NMR spectrum (300 MHz, $CDCl_3$) of **2j**



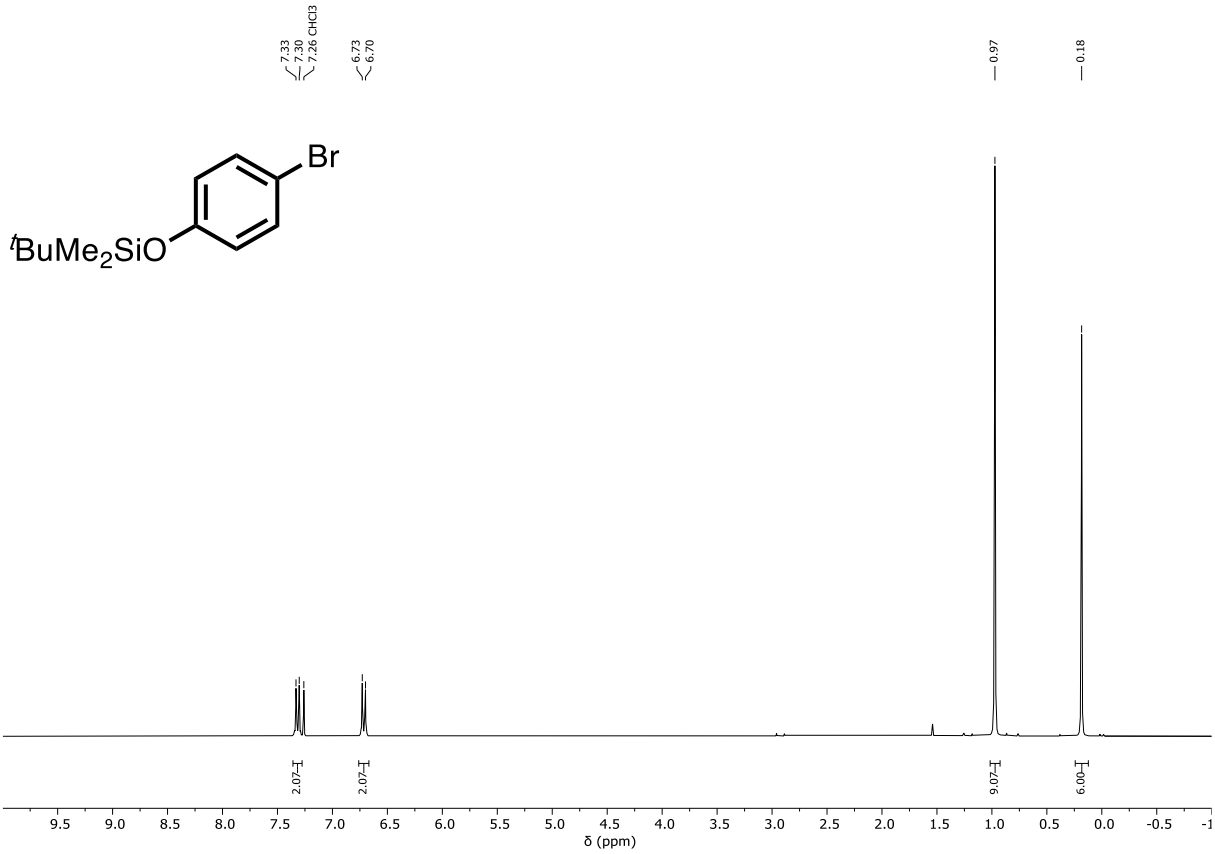
^{1}H NMR spectrum (300 MHz, $CDCl_3$) of **2m**



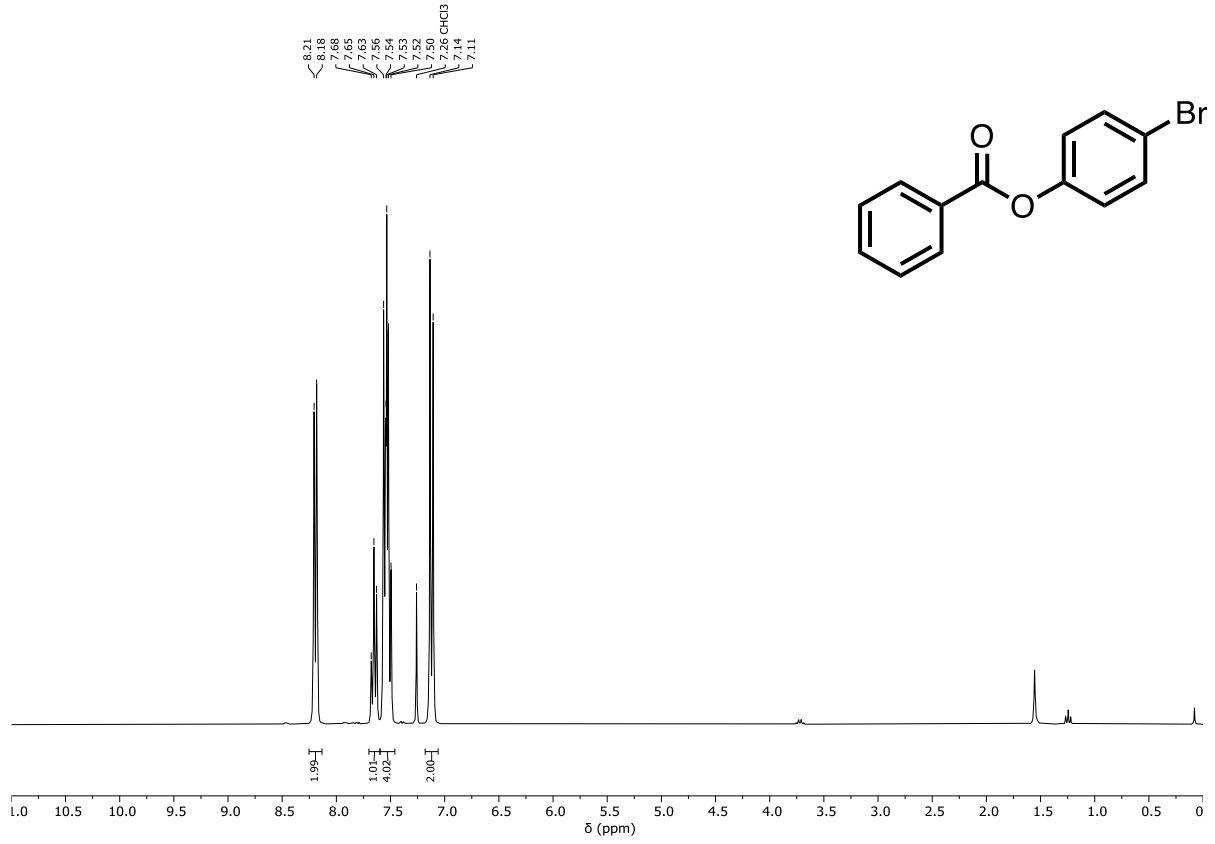
^{1}H NMR spectrum (600 MHz, $CDCl_3$) of **2r**



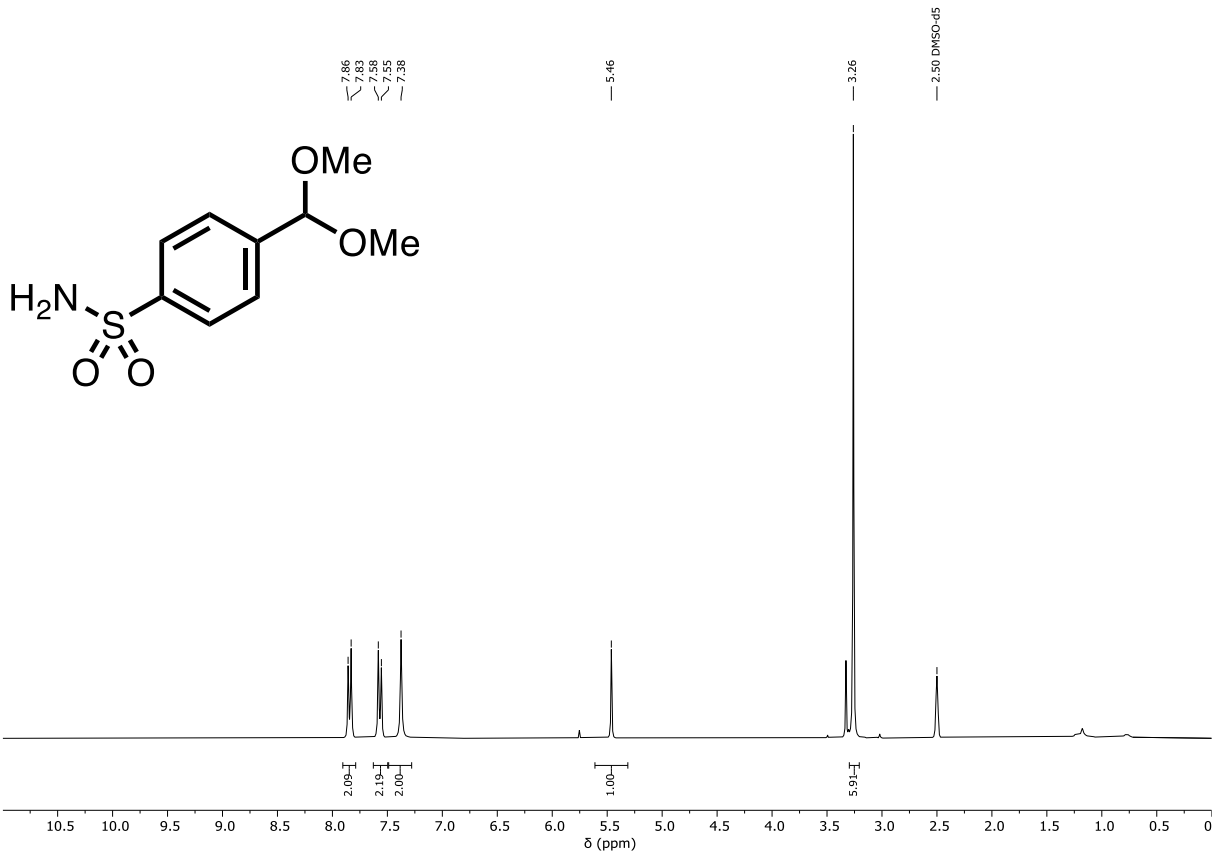
^{13}C{^{1}H} NMR spectrum (101 MHz, $CDCl_3$) of **2r**



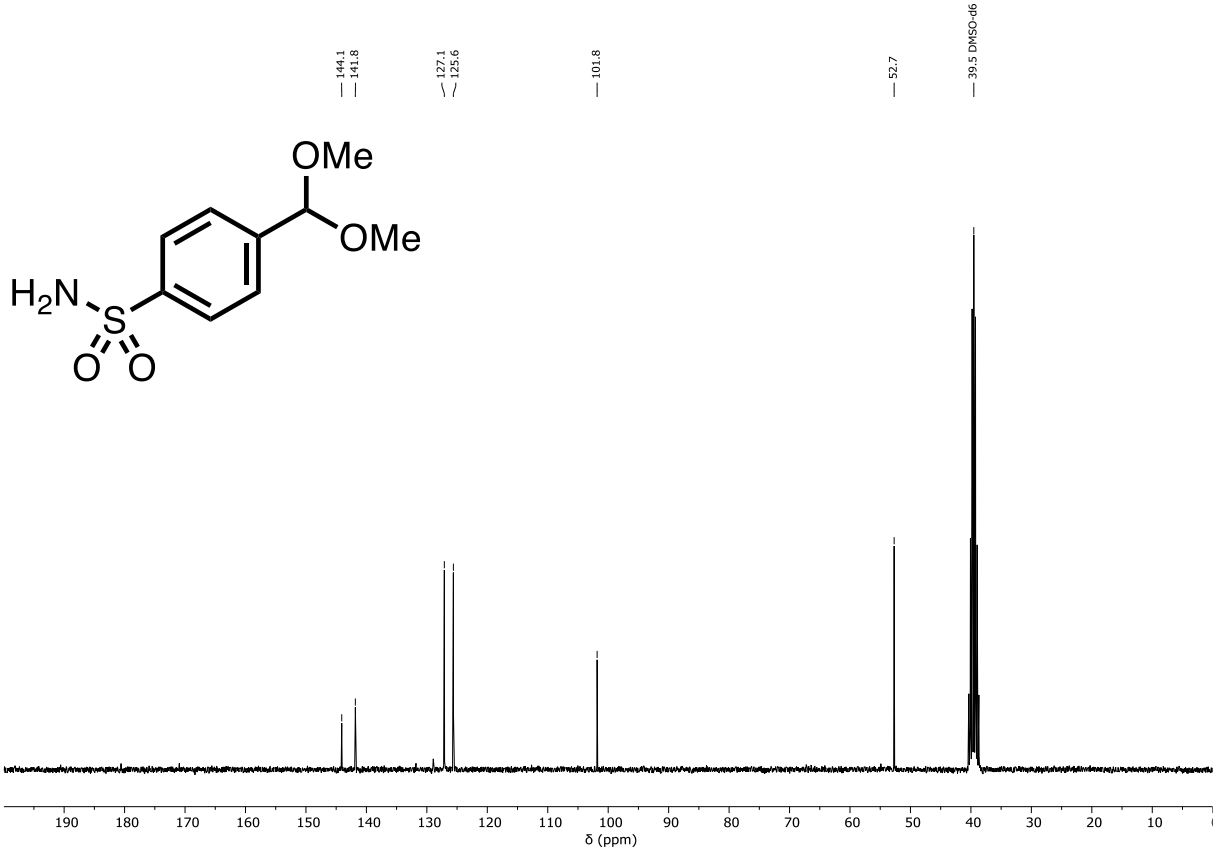
^{1}H NMR spectrum (300 MHz, $CDCl_3$) of **2w**



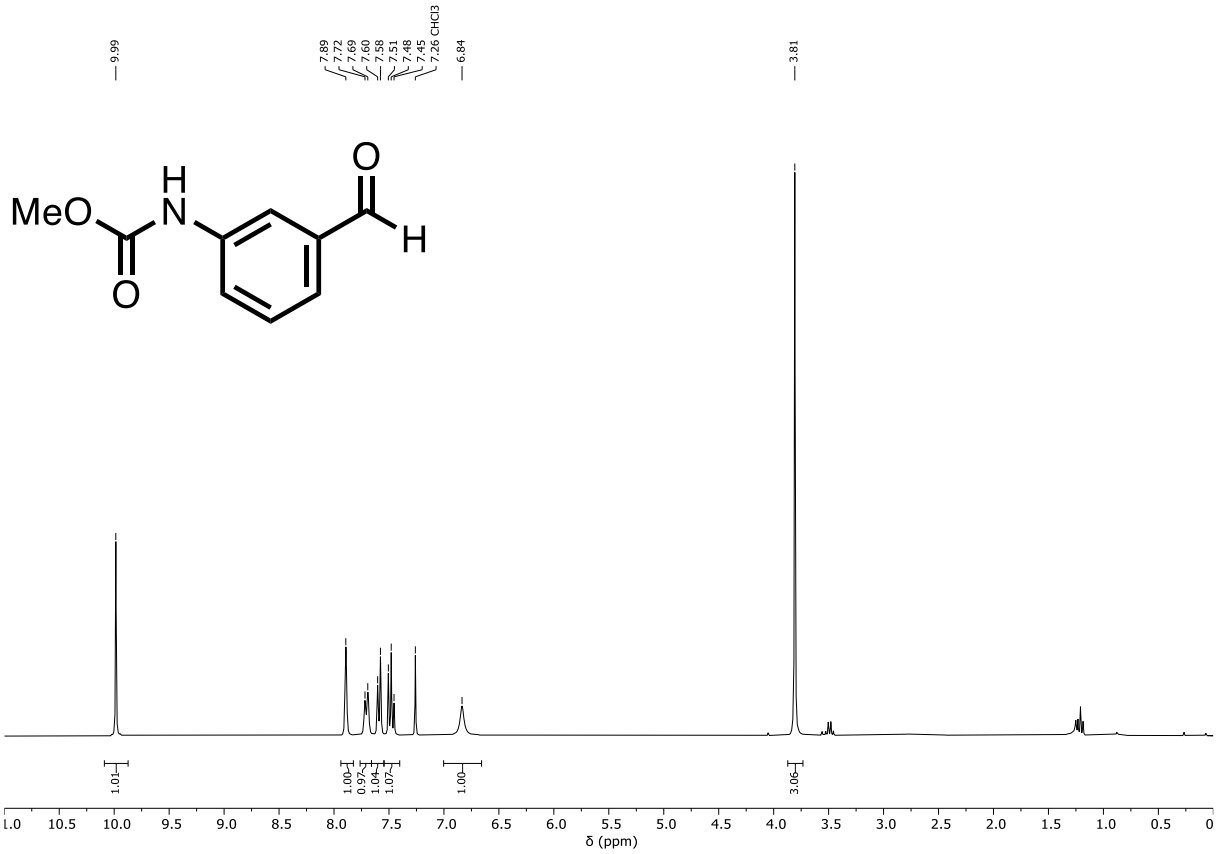
^{1}H NMR spectrum (300 MHz, $CDCl_3$) of **2x**



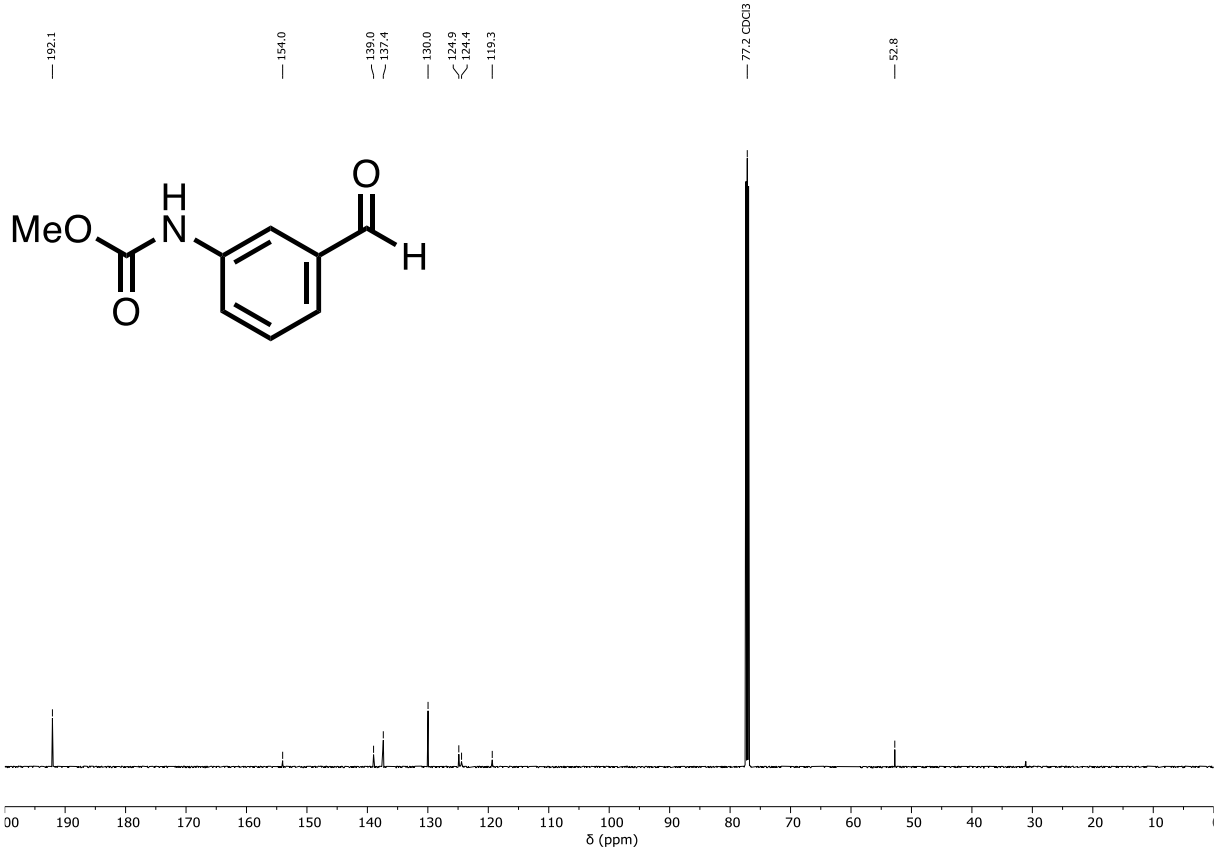
^{1}H NMR spectrum (300 MHz, DMSO-d_6) of **3h**



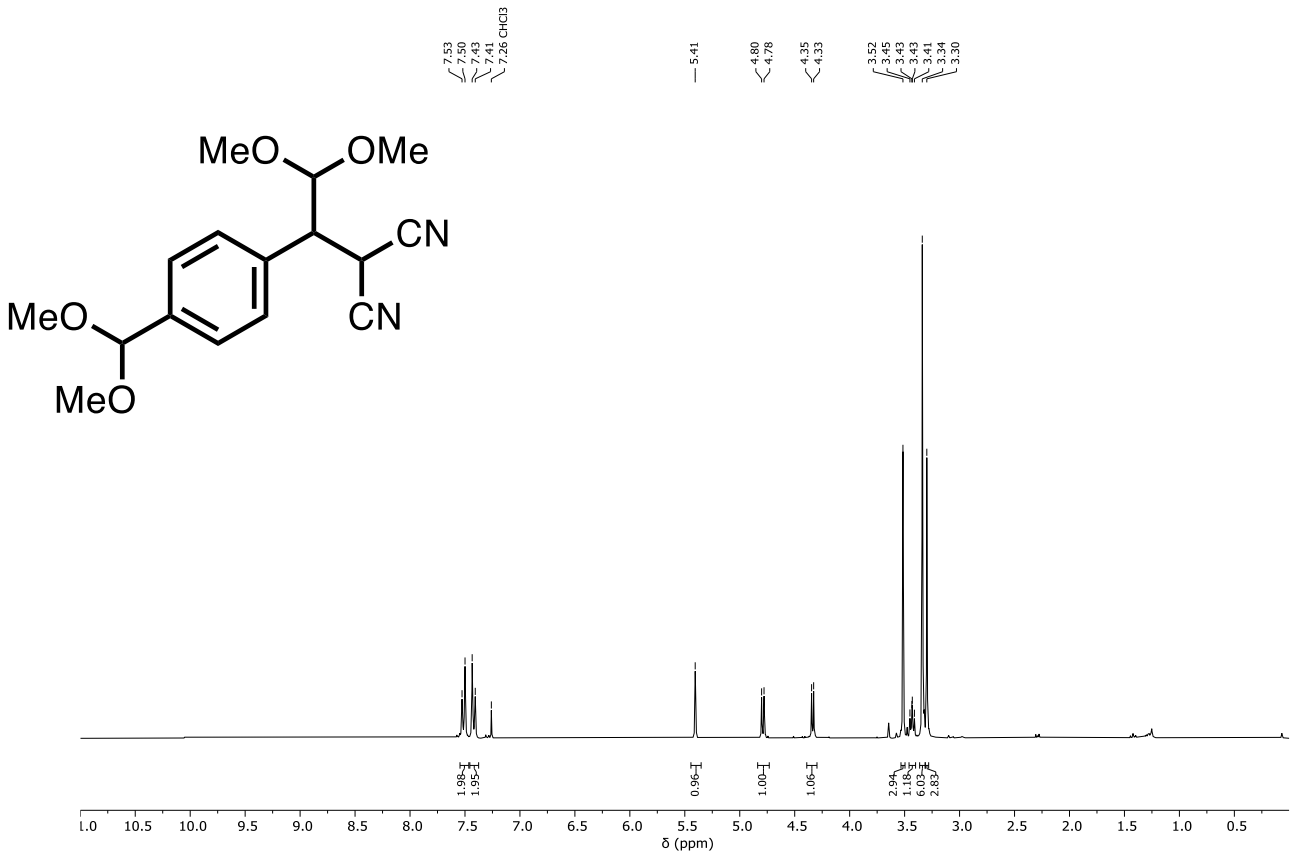
^{13}C{^{1}H} NMR spectrum (75.5 MHz, DMSO-d_6) of **3h**



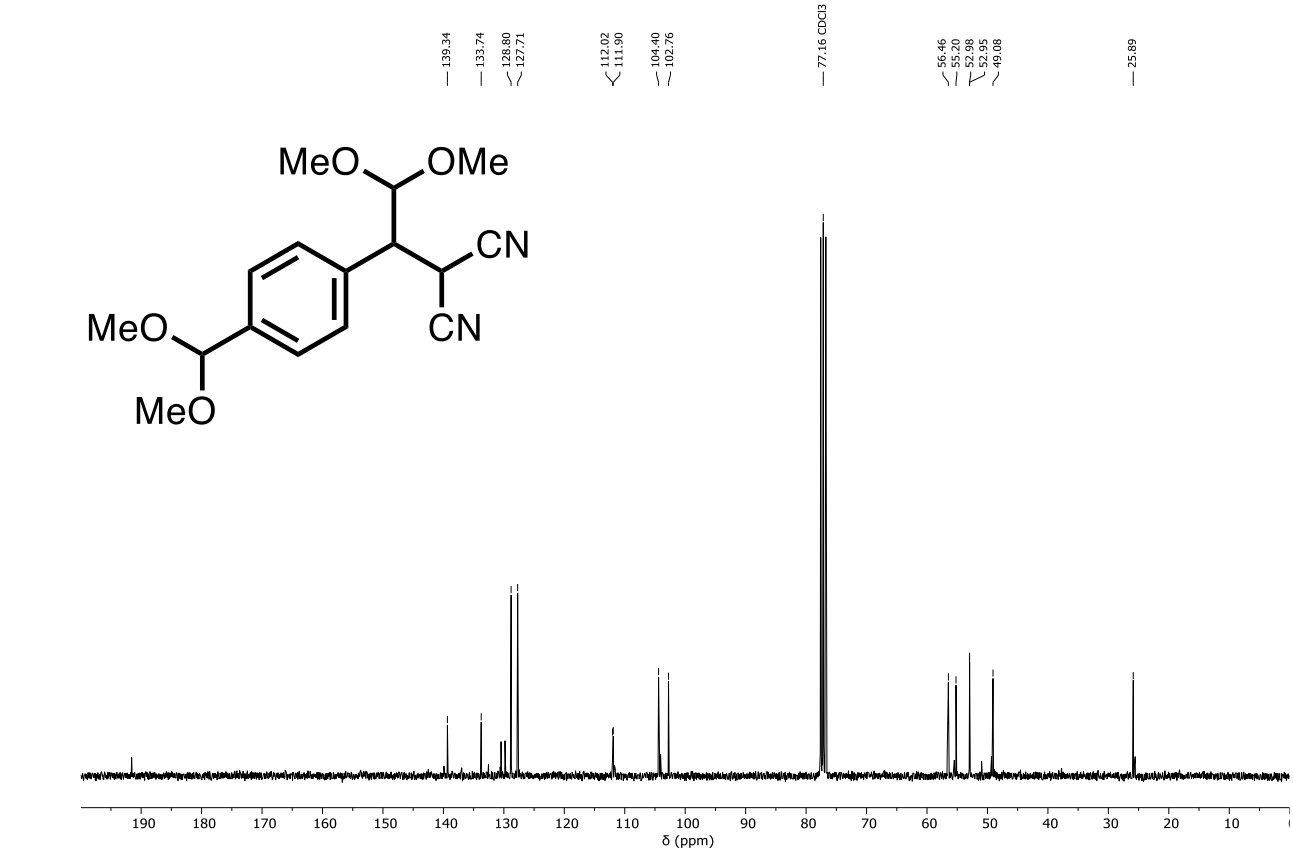
^{1}H NMR spectrum (300 MHz, $CDCl_3$) of **4m**



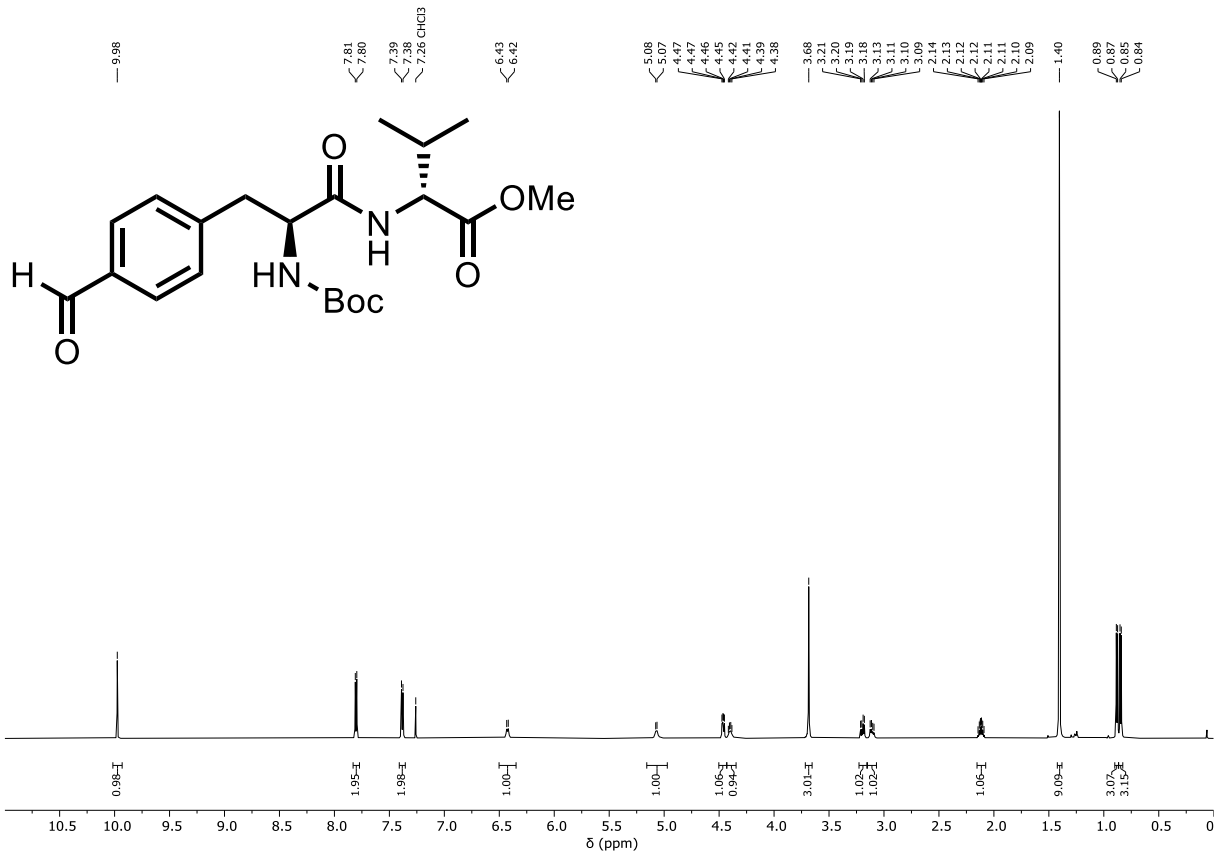
^{13}C{^{1}H} NMR spectrum (151 MHz, $CDCl_3$) of **4m**



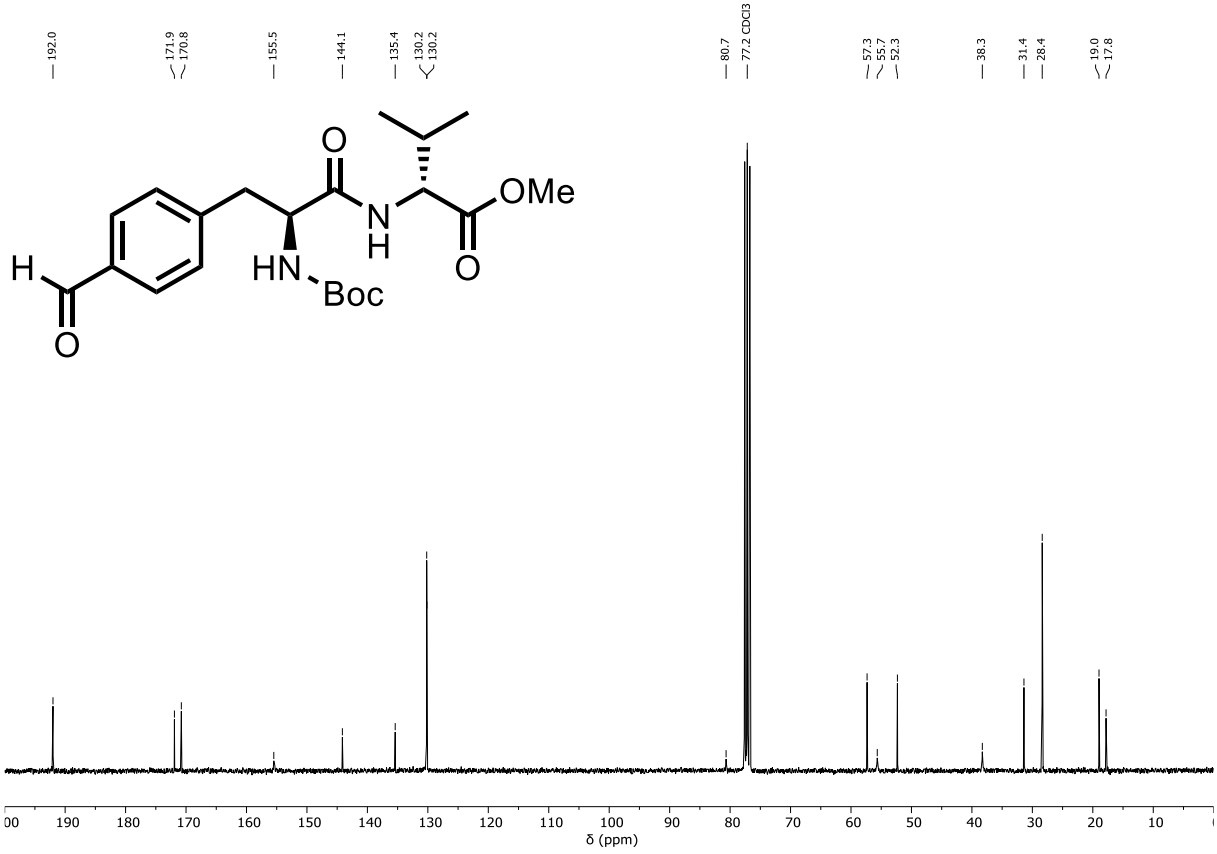
^{1}H NMR spectrum (300 MHz, $CDCl_3$) of **3q**



^{13}C{^{1}H} NMR spectrum (75.5 MHz, $CDCl_3$) of **3q**. Contaminated with the free aromatic aldehyde due to hydrolysis within the NMR tube.

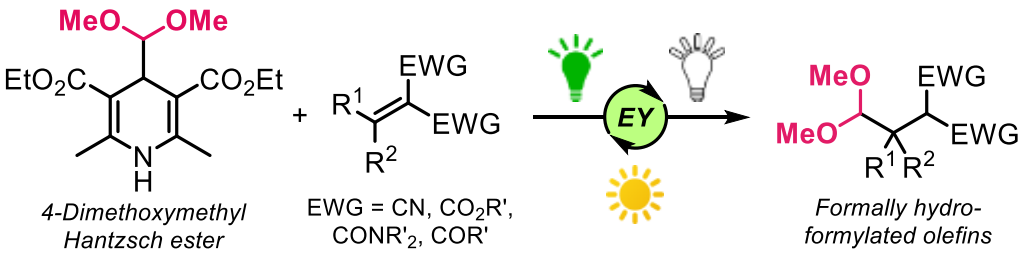


^{1}H NMR spectrum (600 MHz, $CDCl_3$) of **4r**



^{13}C{^{1}H} NMR spectrum (75.5 MHz, $CDCl_3$) of **4r**

Chapter 5



★ *Photoredox catalysis driven by **green light** and a cheap organic dye*

★ ***Mild** conditions, high chemoselectivity, broad functional group tolerance*

★ *Conveniently scalable in **batch** and **continuous flow***

★ ***No** stoichiometric additives* ★ ***Quaternary** centers possible*

Hydroformylation of Electron-Deficient Olefins by Photoredox Catalysis

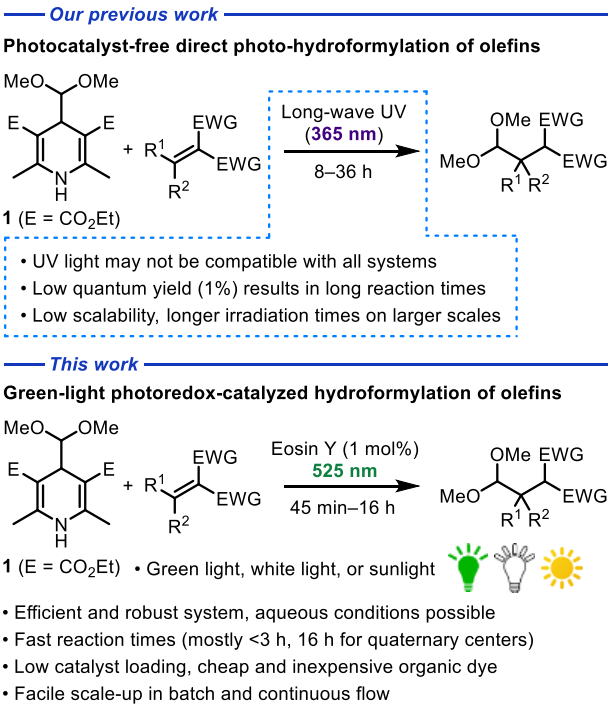
Abstract: *We report a formal hydroformylation of electron-deficient olefins using a bench-stable, easily synthesized 1,4-dihydropyridine derivative. The reaction proceeds under green-light irradiation using the common and inexpensive dye Eosin Y as the photocatalyst and sole additive. The reaction conditions are exceptionally mild and tolerate a broad array of synthetically important functional groups. The reaction is fast, high-yielding, efficient, robust, scalable in batch and continuous flow, and can even be conducted in sunlight. Mechanistic studies suggest the occurrence of intermediate dimethoxymethyl radicals.*

The work outlined in this chapter is scheduled for publication.

Part of this work is part of the master thesis “Hantzsch Esters as Formylation Agents under Photochemical Conditions”, Dorottya Mikóczi, **2022**.

Author contributions: **Mattis-Ole W. S. Schmotz** wrote the manuscript and performed experimental work, **Dorottya Mikóczi** performed experimental work, **Axel Jacobi von Wangelin** supervised this work.

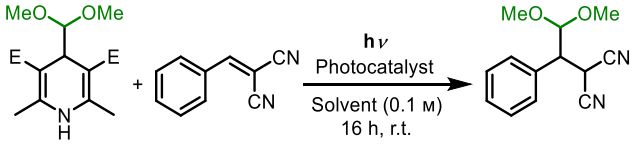
Photoredox catalysis has fundamentally reshaped the landscape of modern organic synthesis, of which it has become a cornerstone. Novel pathways toward old and new molecules have been enabled by providing mild and efficient access to single-electron chemistry. The ability to harness visible light to drive selective chemical transformations under mild conditions is attractive from synthetic, economic, and environmental viewpoints. Originating from first sporadic reports from as far back as the 1970s,[1,2] countless key developments have emerged in a "photoredox hype" over the last 15–20 years.[3–6] Due to the vital importance of aldehyde functionalities in organic synthesis, their light-driven photocatalytic synthesis is a highly researched field.[7] The most common protocols involve photocatalytic decarboxylation of glyoxylic acid derivatives in combination with a base like cesium carbonate,[8–17] but other precursors such as *N*-hydroxyphthalimide derivatives,[18,19] or dioxolane via H-atom abstraction[20,21] have been reported. In a preceding report,[22] we observed that the Hantzsch ester **1** transfers its dimethoxymethyl unit onto electron-deficient olefins under direct ultraviolet irradiation (365 nm) in a formal hydroformylation, in the absence of any photocatalyst or additive (Scheme 1, top). This method, while useful, suffers from long reaction times which are highly dependent on the electronics of the substrate, and associated difficulties in scaling up, which may impede practical utility. Additionally, the employed ultraviolet radiation may not be compatible with all systems. In order to address these issues, and based on our previous reports on photoredox-catalyzed transformations of Hantzsch esters,[23,24] we anticipated that this method could be adapted into a photoredox-catalyzed protocol using visible light, while avoiding stoichiometric additives and catalysts based on expensive precious metals such as iridium or ruthenium (Scheme 1, bottom).



***Scheme 1**. Photo-hydroformylation of electron-deficient olefins using a substituted Hantzsch ester.*

We commenced our exploration by mirroring the model reaction of **1** and **2a** under visible-light irradiation in the presence of different organic photoredox catalysts (Scheme 2). To our delight, we found that irradiation with blue light (450 nm) in the presence of the organic photocatalyst 3DPAFIPN gave the desired acetal **5a** in 58% yield in acetonitrile (entry 1). The product yield was increased to 81% when the disodium salt of Eosin Y (hereinafter abbreviated as Na_2-Eosin Y or EY) was employed under green light irradiation (525 nm, entry 5). Using acetone as solvent gave a consistently increased yield of 89% and was additionally deemed more optimal due to its superior benignity as a "greener" solvent (entry 6). Notably, we found the reaction to be reasonably fast, with complete conversion of **2a** after only 45 minutes. Control experiments showed that both Na_2-Eosin Y and light are crucial for product formation (entries 7–8).

Scheme 2. Optimization of Reaction Conditions.



1 (E = CO_2Et) **2a** **5a**

№	Photocat. (mol%)	Solvent	Wavelength	Yield [%][a]
1	3DPAFIPN (2.5)	MeCN	450 nm	58
2	3DPA2FBN (2.5)	MeCN	450 nm	60
3	4CzIPN (2.5)	MeCN	450 nm	56
4	Rhodamine B (2.5)	MeCN	525 nm	38
5	Na_2-Eosin Y (2.5)	MeCN	525 nm	81
6	Na_2-Eosin Y (1.0)	Acetone	525 nm	89[b]
7	Na_2-Eosin Y (1.0)	Acetone	–	0
8	–	Acetone	525 nm	0

0.10 mmol scale reactions, 1.2 equiv. of **1**, under Ar/N_2 in dry solvents, [a] Yields determined by ^{1}H NMR *vs.* 1,3,5-trimethoxybenzene. [b] Both at 16 h and 45 min of reaction time. 3DPAFIPN = 2,4,6-Tris(diphenylamino)-5-fluoroisophthalonitrile, 3DPA2FBN = 2,4,6-Tris(diphenylamino)-3,5-difluorobenzonitrile, 4CzIPN = 1,2,3,5-Tetrakis-(9*H*-carbazol-9-yl)isophthalonitrile.

A robustness screening[25] (Figure 1) revealed that the yield of **5a** remains unaffected by the presence of water; the reaction could even be performed in a 1:1 mixture of acetone/water with similar yields. A lower concentration (½×) as well as increased light intensity likewise had no discernible effect. The reaction is robust toward stark differences in temperature (0–50 °C). Decreased yields were observed in the presence of oxygen (−41%), upon doubling the concentration (−25%), and with lower light intensity (−52% due to incomplete conversion of **2a**).

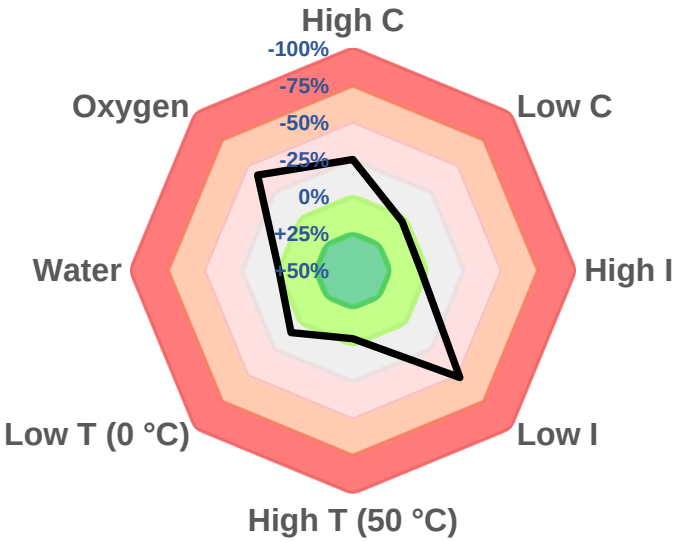
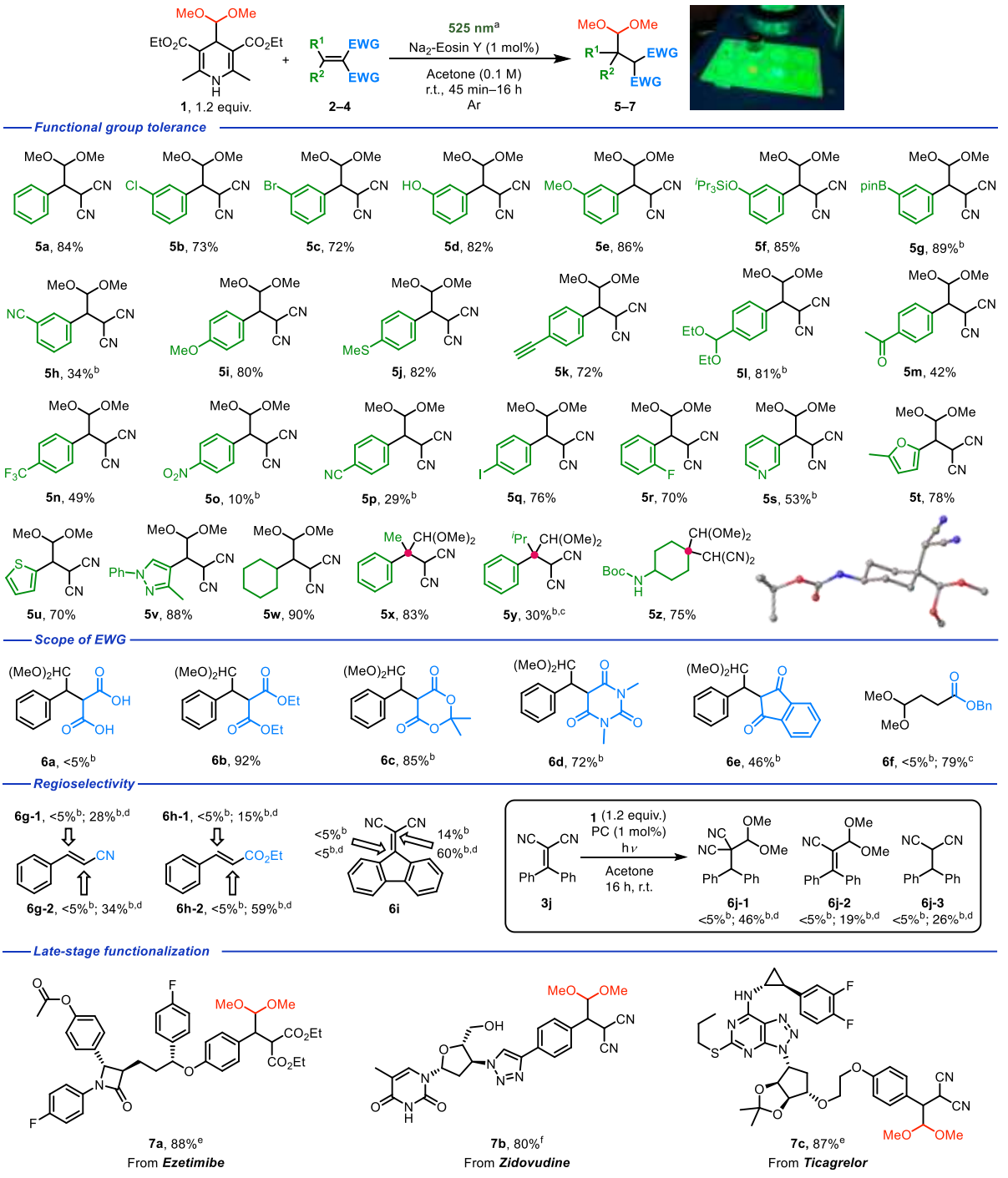


***Figure 1**. Robustness screening.*

We proceeded to explore the substrate scope of our reaction employing the optimized conditions (Scheme 3). A broad range of arylidene malononitrile successfully afforded the dimethyl acetals in good to excellent yields. Critical functional groups such as (thio)ethers (**5e**, **5j**), silyl ethers (**5f**), phenols (**5d**), boronates (**5g**), terminal alkynes (**5k**), or aromatic acetals (**5l**) are fully accommodated by the reaction conditions. Halogenated substrates (F, Cl, Br, I) underwent smooth formylation in high yields (**5b**–**c**, **5q**–**r**) without any evidence of hydrogehalogenation as we have previously observed for iodides in our UV protocol upon prolonged irradiation.[22] Substrates bearing additional electron-withdrawing groups generally exhibited diminished yields, likely due to competitive side reactions at the aromatic core or radical-initiated polymerization. The same result is observed irrespective of the position of the group on the aromatic ring (e.g. *meta*-CN in **5h**, *para*-CN in **5o**). O-, S-, and N-heterocycles were well tolerated (**5s**–**v**), and a non-aromatic alkylidenemalononitrile furnished **5w** in excellent yield. Quaternary carbon centers could be obtained from ketone-derived malononitriles, both aromatic or aliphatic (**5x**–**z**). The presence of a quaternary carbon was confirmed by single-crystal X-ray diffraction of **5z**. However, upon substantial steric hindrance (^{i}Pr), the reaction is decelerated with a decrease in yield (**5y**). Benzylidenemalonic acid remained unconverted under the standard conditions, likely due to catalyst deactivation by protonation. This is corroborated by the rapid decolorization of the reaction mixture. Diester substrates, including the valuable Meldrum's acid synthon, were smoothly converted to the acetals (**6b**–**c**), as was a barbituric acid derivative (**6d**). An indanedione-derived substrate gave a somewhat diminished yield with a substantial amount of colored side products (**6e**). Olefins bearing only a single electron-withdrawing group showed no conversion under the standard conditions (**6f**–**h**). Alternative conditions employing the organic dye 4CzIPN under blue-light irradiation enabled product formation

despite inferior performance in the case of **2a** (see optimization; Scheme 2). Notably, benzyl acrylate, typically prone to free-radical polymerization, was formylated in excellent yield using



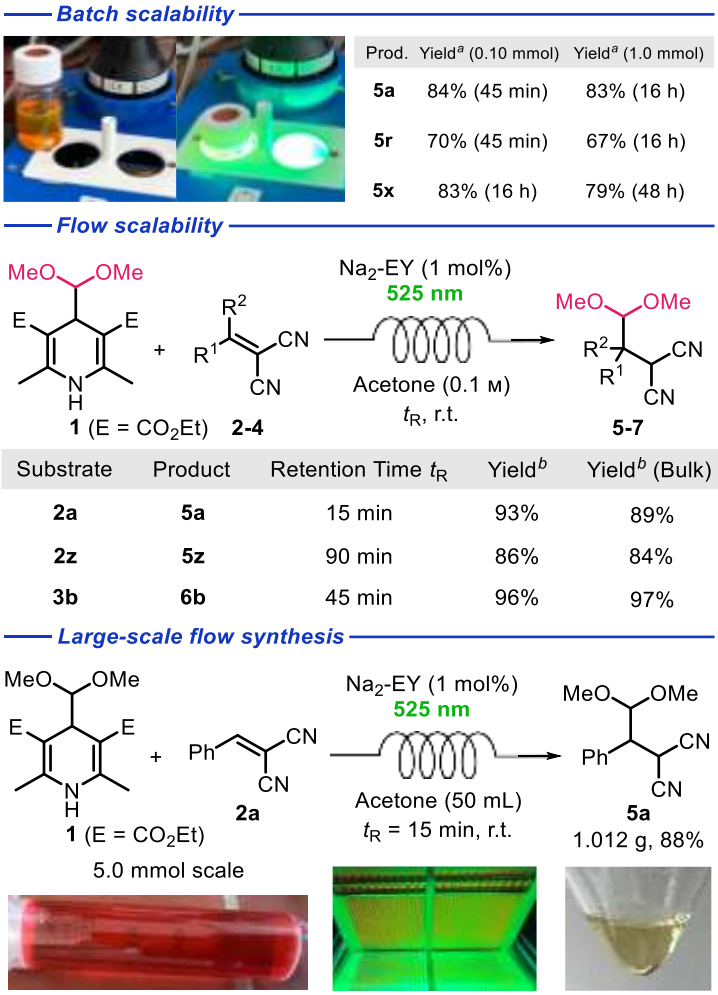
***Scheme 3**. Substrate scope. 100 µmol scale reactions, isolated yields are given. [a] EvoluChem 525PF LED, [b] ^{1}H NMR yield vs. 1,3,5-trimethoxybenzene. [c] 24 h of irradiation time. [d] 1 mol% 4CzIPN, 450 nm, 16 h. [e] Isolated yield on a 50 µmol scale. [f] Isolated yield on a 20 µmol scale.*

these conditions (91% by ^{1}H NMR; **6f**). In the case of cinnamonitrile and ethyl cinnamate, similar results and isomeric distributions as previously detected for the photocatalyst-free approach[22] were observed using the 4CzIPN method, with homobenzylic formylation

predominating (**6g**–**h**). Diaryl malononitriles also showed little conversion under Eosin Y conditions, but under 4CzIPN conditions likewise afforded similar yields and (side) product distributions with inversion of regioselectivity as in the photocatalyst-free approach (**6i**–**j**). The mechanistic implications of these observations are discussed below. Remarkably, our protocol accommodated structurally complex substrates bearing medicinally relevant motifs: An Ezetimibe-derived diester (**7a**), a Zidovudine (AZT)-based alkyne-azide cycloadduct (**7b**), and a Ticagrelor-derived malononitrile (**7c**) were converted efficiently with yields >80%, underscoring the exceptional mildness and functional group tolerance of this reaction. Compared to our previously reported photocatalyst-free UV-mediated protocol, the yields and reaction times are superior in nearly all cases. The properties and synthetic utility of the resulting dimethyl acetals have been described in **Chapter 3**.

We next evaluated the scalability of our system. The reaction was successfully scaled up by a factor of 10 for three different substrates with minimal difference in yield (**5a**, **5r**, **5x**; Scheme 4, top). To further enhance productivity, we explored photo-flow chemistry, which has emerged as a powerful tool in photochemical transformations due to greater light penetration as a result of the small tube diameter, superior mass transfer, and theoretically infinite scalability due to a continuous substrate input and product output (Scheme 4, bottom). Under continuous flow conditions, **5a** was obtained after 15 min of retention time in unchanged yields compared to the batch method (45 min on a 0.10 mmol scale). This corresponds to a space-time-yield (STY) of 0.37 $mmol \cdot h^{-1} \cdot mL^{-1}$, exceeding the batch productivity of 0.12 $mmol \cdot h^{-1}$ (lower on bigger scales) by over threefold. Even the slowest-reacting substrates that require up to 16 h in batch even on small scales (e.g. **3z**) were fully converted within 90 min of retention time. Using these optimized continuous flow conditions, we were able to obtain **5a** on a gram-scale.

Remarkably, the reaction proceeds efficiently under sunlight without the need for specialized light sources (Figure 2). Under standard conditions and scale, the reaction reached completion (90% yield of **5a** by ^{1}H NMR) within 4 h of direct solar irradiation. This underscores the operational simplicity and robustness of the transformation, highlighting its potential for sustainable and environmentally benign applications.

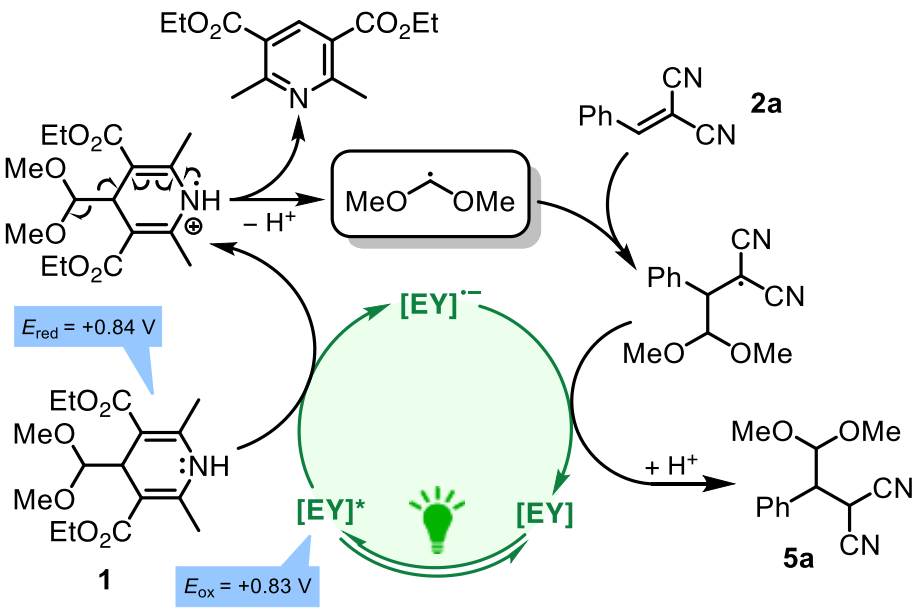


Scheme 4. *Investigations into upscaling in batch and continuous flow.*



Figure 2. *Formylation of* ***2a*** *using direct sunlight, with the skyline of Hamburg in the background. The reaction was performed in July 2024 with uninterrupted solar irradiation through an open window for 4 h (Latitude: 53.6° N).*

Trapping experiments using the radical scavenger CHANT[26] revealed the formation of free TEMPO, which is eliminated upon reaction of CHANT with free radicals. This demonstrates that a free-radical mechanism is operative. A long-lived light-initiated radical chain mechanism may be excluded on the basis of a reaction quantum yield of Φ_R = 8.4%. Based on our mechanistic investigations, reactivity observations, and preceding literature, we propose the following reaction pathway (Scheme 5): Hantzsch ester **1** (E(**1**$^{\bullet+}$/**1**) = +0.84 V vs. SCE in MeCN)[22] undergoes single-electron oxidation by the excited-state Eosin Y (and E(EY*/EY$^{\bullet-}$) = +0.83 V vs. SCE in MeOH),[27] generating the radical cation **1**$^{\bullet+}$ and EY$^{\bullet-}$. Rapid aromatization-driven fragmentation releases a dimethoxymethyl radical, which adds to the activated double bond of **2a** in a Giese-type fashion. Subsequent single-electron reduction by EY$^{\bullet-}$ and protonation completes the photocatalytic cycle and furnishes the formylated product **5a**. A triplet sensitization of **1** by EY* is thermodynamically unfeasible based on a triplet energy of E(^{3}EY) = 182 kJ·mol^{-1} [28] compared to the triplet energies of 4-aryl Hantzsch esters of E(^{3}HE) ≈ 250 kJ·mol^{-1};[29] E(^{3}**1**) should be even higher. However, an alternative mechanism involving initial reduction of **2a** followed by oxidation of **1**, fragmentation of **1**$^{\bullet+}$, and radical recombination (analogous to the UV-mediated hydroformylation) cannot be excluded. Both the oxidation of **1** and reduction of **2a** by EY* are slightly endergonic (E(**2a**/**2a**$^{\bullet-}$) = −1.16 V vs. SCE).[22] To gain further insight, we attempted to determine the fluorescence quenching constants of **1** and **2a** with regard to EY via Stern-Volmer studies. **1** displayed an expected linear quenching profile; in contrast, a mixture of EY and **2a** usually exhibited a pronounced decrease of fluorescence intensity and an overall bathochromic shift. This suggests a strong interaction between EY and **2a** of unknown nature, possibly formation of an EDA complex.[30] UV-Vis and fluorescence experiments of these mixtures were hampered by the low solubility of EY in most organic solvents and gave irreproducible results, which appear to be strongly influenced by the presence of trace amounts of water. Definitive mechanistic conclusions from these data remain elusive. We believe that the rapid and irreversible fragmentation of **1**$^{\bullet+}$ likely drives the equilibrium toward the proposed reaction pathway, but concomitant operation of both pathways cannot be excluded. The inability of the EY system to convert diaryl malononitriles and cinnamate/cinnamonitrile indicate a differing mechanism from the previously reported photocatalyst-free method, in which initial reduction of the olefin seems likely.[22] Similar yields and product distributions between the latter and the 4CzIPN system suggest similar mechanisms in this case and further hints at dissimilarity between the EY- and UV-mediated systems.



Scheme 5. *Proposed mechanism and photocatalytic cycle.*

In conclusion, we have developed a photoredox-catalyzed protocol for the hydroformylation of electron-deficient olefins using the easily accessible dimethoxymethyl-substituted Hantzsch ester **1**. The reaction is robust and highly efficient, and gives superior yields to our previously re-ported photocatalyst-free protocol. The reaction proceeds rapidly and tolerates a broad ar-ray of functional groups. Multiple examples of late-stage functionalization were demonstrated. Mechanistic studies suggest the intermediacy of nucleophilic free dimethoxymethyl radicals, which efficiently add to electron-deficient olefins.

Literature References

[1] D. M. Hedstrand, W. H. Kruizinga, R. M. Kellogg, *Tetrahedron Lett.* **1978**, *19*, 1255–1258.

[2] T. J. van Bergen, D. M. Hedstrand, W. H. Kruizinga, R. M. Kellogg, *J. Org. Chem.* **1979**, *44*, 4953–4962.

[3] C. K. Prier, D. A. Rankic, D. W. C. MacMillan, *Chem. Rev.* **2013**, *113*, 5322–5363.

[4] N. A. Romero, D. A. Nicewicz, *Chem. Rev.* **2016**, *116*, 10075–10166.

[5] A. Y. Chan, I. B. Perry, N. B. Bissonnette, B. F. Buksh, G. A. Edwards, L. I. Frye, O. L. Garry, M. N. Lavagnino, B. X. Li, Y. Liang, E. Mao, A. Millet, J. V. Oakley, N. L. Reed, H. A. Sakai, C. P. Seath, D. W. C. MacMillan, *Chem. Rev.* **2022**, *122*, 1485–1542.

[6] D. C. Cabanero, T. Rovis, *Nat. Rev. Chem.* **2024**, *9*, 28–45.

[7] Y. Wang, X. F. Liu, W. M. He, *Org. Chem. Front.* **2023**, *10*, 4198–4210.

[8] H. Huang, X. Li, C. Yu, Y. Zhang, P. S. Mariano, W. Wang, *Angew. Chem. Int. Ed.* **2017**, *56*, 1500–1505.

[9] H. Huang, C. Yu, Y. Zhang, Y. Zhang, P. S. Mariano, W. Wang, *J. Am. Chem. Soc.* **2017**, *139*, 9799–9802.

[10] S. Zhang, Z. Tan, H. Zhang, J. Liu, W. Xu, K. Xu, R. Li, *Chem. Commun.* **2017**, *53*, 11642.

[11] B. Zhao, R. Shang, W. M. Cheng, Y. Fu, *Org. Chem. Front.* **2018**, *5*, 1782–1786.

[12] W. Jia, Y. Jian, B. Huang, C. Yang, W. Xia, *Synlett* **2018**, *29*, 1881–1886.

[13] X. L. Lyu, S. S. Huang, H. J. Song, Y. X. Liu, Q. M. Wang, *RSC Adv.* **2019**, *9*, 36213–36216.

[14] P. Xiang, L. He, H. Li, Z. Qi, M. Zhang, Q. Fu, J. Wei, X. Du, D. Yi, S. Wei, *Tetrahedron Lett.* **2020**, *61*, 152369.

[15] C. H. Ma, Y. Ji, J. Zhao, X. He, S. T. Zhang, Y. Q. Jiang, *Chin. J. Catal.* **2022**, *43*, 571–583.

[16] Y. Dong, X. Li, P. Ji, F. Gao, X. Meng, W. Wang, *Org. Lett.* **2022**, *24*, 5034–5039.

[17] C. Ma, H. Meng, J. Li, X. Yang, Y. Jiang, B. Yu, *Chin. J. Chem.* **2022**, *40*, 2655–2662.

[18] J. Dong, X. Wang, H. Song, Y. Liu, Q. Wang, *Adv. Synth. Catal.* **2020**, *362*, 2155–2159.

[19] D. Liu, K. Yang, D. Fang, S.-J. Li, Y. Lan, Y. Chen, *Angew. Chem. Int. Ed.* **2023**, *62*, e202213686.

[20] M. K. Nielsen, B. J. Shields, J. Liu, M. J. Williams, M. J. Zacuto, A. G. Doyle, *Angew. Chem. Int. Ed.* **2017**, *56*, 7191–7194.

[21] W. Ou, G. Zhang, J. Wu, C. Su, *ACS Catal.* **2019**, *9*, 5178–5183.

[22] Chapter 3 of this work.

[23] L. Cardinale, M. O. Konev, A. Jacobi von Wangelin, *Chem. Eur. J.* **2020**, *26*, 8239–8243.

[24] L. Cardinale, M.-O. W. S. Schmotz, M. O. Konev, A. Jacobi von Wangelin, *Org. Lett.* **2022**, *24*, 506–510.

[25] L. Pitzer, F. Schäfers, F. Glorius, *Angew. Chem. Int. Ed.* **2019**, *58*, 8572–8576.

[26] P. J. H. Williams, G. A. Boustead, D. E. Heard, P. W. Seakins, A. R. Rickard, V. Chechik, *J. Am. Chem. Soc.* **2022**, *144*, 15969–15976.

[27] T. Shen, Z. G. Zhao, Q. Yu, H. J. Xu, *J. Photochem. Photobiol. A Chem.* **1989**, *47*, 203–212.

[28] M. Majek, F. Filace, A. J. von Wangelin, *Beilstein J. Org. Chem.* **2014**, *10*, 981–989.

[29] A. J. Jimenez, M. Fagnoni, M. Mella, A. Albini, *J. Org. Chem.* **2009**, *74*, 6615–6622.

[30] V. Quint, F. Morlet-Savary, J. F. Lohier, J. Lalevée, A. C. Gaumont, S. Lakhdar, *J. Am. Chem. Soc.* **2016**, *138*, 7436–7441.

Experimental Section

General Information

Nuclear magnetic resonance (NMR) spectroscopy: ^{1}H NMR spectra (300 MHz) and ^{13}C-NMR spectra (75.5 MHz) were recorded on a *Bruker Fourier HD 300.* ^{1}H NMR spectra (400 MHz) and ^{13}C-NMR spectra (101 MHz) were recorded on a *Bruker Avance III HD 400*. ^{1}H NMR spectra (600 MHz), ^{13}C-NMR spectra (151 MHz), and ^{19}F-NMR spectra (565 MHz) were recorded on a *Bruker Avance III HD 600*. All spectra were recorded at 25 °C unless otherwise stated. Chemical shifts δ are reported in parts per million (ppm) relative to tetramethylsilane for ^{1}H and ^{13}C NMR spectra, relative to $CFCl_3$ for ^{19}F NMR spectra, and relative to $BF_3{\cdot}OEt_2$ for ^{11}B NMR spectra. Coupling constants *J* are given in Hertz (Hz). *MestReNova 14* (Mnova) by *Mestrelab* was used for analysis of the NMR spectra. Abbreviations used for NMR data: s = singlet; br. s = broad singlet; d = doublet; t = triplet; q = quartet; and combinations thereof.

Infrared (IR) spectroscopy: Infrared spectra were recorded using a *Bruker VERTEX 70* FTIR spectrometer using a *Specac Golden Gate* ATR unit.

UV-Vis spectroscopy: UV-Vis spectra were measured at room temperature on an *Agilent Cary 5000* UV-Vis-NIR Spectrophotometer in double-beam mode using 10 mm SUPRASIL quartz cuvettes by *Hellma*.

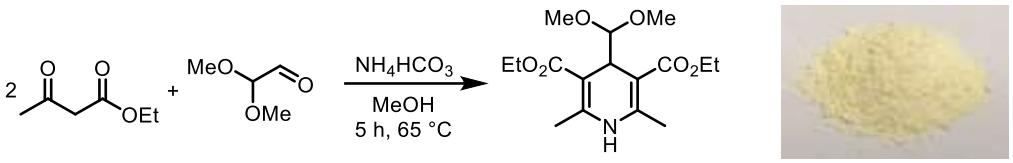
Mass spectrometry (MS): High-resolution mass spectra (electrospray ionization, ESI) were measured using an *Agilent 6224 ESI-TOF* or a *Bruker maXis ESI-Q-TOF* by direct injection in positive or negative ion mode. Abbreviations used for MS data: *m/z* mass-to-charge ratio; M = exact mass of the target compound. *MestReNova 14* (Mnova) by *Mestrelab* was used for analysis of the MS spectra.

Melting points: Melting points (m.p.) were measured using a *DigiMelt MPA160* by *Stanford Research Systems*.

Thin-layer chromatography (TLC) and column chromatography: TLC was performed using aluminium plates coated with UV-fluorescence-indicator-doped stationary phase by *Macherey-Nagel* (*ALUGRAM® Xtra Sil G/UV$_{254}$* for SiO_2, *ALUGRAM® ALOX N / UV254* for neutral Al_2O_3). Preparative column chromatography was performed using silica by *Acros Organics* (35–70 µm, 60 Å pore size) or neutral alumina by *Macherey-Nagel* (50–200 µm, 90 Å pore size) using distilled technical grade solvents.

Synthesis of Compounds

Diethyl 4-(dimethoxymethyl)-2,6-dimethyl-1,4-dihydropyridin-3,5-dicarboxylate (**1**)



A suspension of ammonium bicarbonate (2.37 g, 30.0 mmol, 1.0 equiv.), ethyl acetoacetate (7.81 g, 60.0 mmol, 2.0 equiv.) and 2,2-dimethoxyacetaldehyde (60 wt.% soln. in water, 5.21 g, 30.0 mmol, 1.0 equiv.) in methanol (30 mL) was refluxed. Within 10–20 minutes the solid ammonium bicarbonate dissolves and the mixture turns homogeneous and bright yellow. After 5 h of reflux, the solvent was removed and the orange syrupy residue was thoroughly dried *in vacuo*, during which slow solidification to a waxy solid eventually occurs (scratching the flask wall is often required to induce crystallization). The product crystallizes slowly (after ~30 min) from boiling diethyl ether (~25–30 mL) upon cooling to r.t., then to −25 °C overnight, initially as small pale-yellow needles which merge into solid clumps. **1** is obtained as a pale-yellow solid after filtration and washing with cold diethyl ether and room-temperature pentane until the distinct odor of ethyl acetoacetate is no longer perceptible (5.37 g, 16.4 mmol, 55 %). The solid thus obtained melts at 88–89 °C and is sufficiently pure for the photoreaction. A purer, almost colorless product melting at 90–91 °C is obtained after a second recrystallization or careful silica column chromatography (SiO_2, Pentane/EtOAc 3:2). This synthesis was also conducted several times on a 5.0, 60, and 150 mmol scale with consistent yields (50–60 %).

^{1}H NMR (600 MHz, $CDCl_3$): δ [ppm] = 5.85 (s, 1H), 4.34 (d, J = 5.2 Hz, 1H), 4.25 – 4.11 (m, 4H), 3.94 (d, J = 5.2 Hz, 1H), 3.29 (s, 6H), 2.27 (s, 6H), 1.28 (t, J = 7.2 Hz, 6H).

^{13}C{^{1}H} NMR (151 MHz, $CDCl_3$): δ [ppm] = 168.4, 145.1, 107.9, 99.2, 59.8, 55.3, 36.9, 19.4, 14.5.

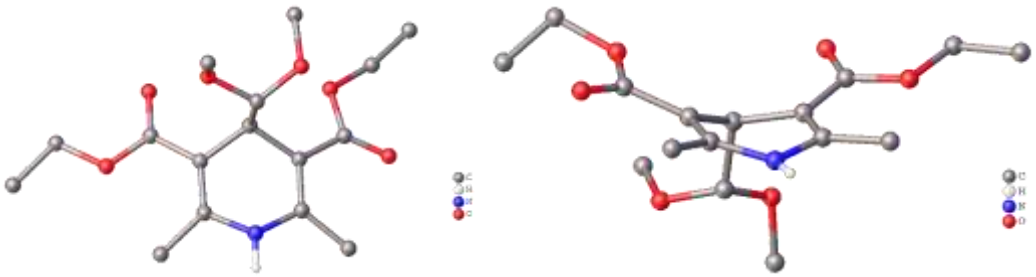
IR (ATR): $\tilde{\upsilon}$ [cm^{-1}] = 3346 (ν(N–H)), 2990, 2938, 2889, 2837, 1699, 1649 (ν(C=O)), 1484, 1474, 1448, 1391, 1368, 1335, 1321, 1291, 1272, 1258, 1210 (ν(C–O–C)), 1166, 1150, 1122, 1099, 1044, 1016, 981, 916, 863, 776, 741, 711, 699, 643, 628.

UV-Vis (MeCN): λ_{max} [nm] (ε [$L \cdot mol^{-1} \cdot cm^{-1}$]) = 230, 248, 332 (6496).

HRMS (ESI): *m/z* calcd. for $C_{16}H_{25}NNaO_6^+$ ([M+Na]$^+$): 350.1574, found.: 350.1571; calcd. for $C_{32}H_{50}N_2NaO_{12}^+$ ([2M+Na]$^+$): 677.3256, found.: 677.3260.

m.p. = 90–91 °C.

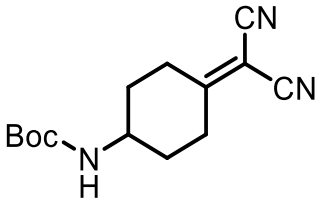
XRD (Non heteroatom-bonded hydrogen atoms omitted for clarity):



Synthesis of Electron-Deficient Olefins

The synthesis of starting materials **2a**–**y**, **3a**–**j**, and **4a**–**c** is described in **Chapter 3** of this work.

Tert-butyl (4-(dicyanomethylene)cyclohexyl)carbamate (**2z**)



N-Boc-4-Aminocyclohexanone (1.60 g, 7.50 mmol, 1.0 equiv.), malononitrile (495 mg, 7.50 mg, 1.0 equiv.), and β-alanine (134 mg, 1.50 mmol, 20 mol%) were suspended in toluene (75 mL). The mixture was refluxed for 16 h in a Soxhlet apparatus with $CaCl_2$ in the extraction thimble. The mixture was then washed with water (30 mL) and the aqueous phase was extracted with ethyl acetate (2× 50 mL). The combined organic phases were washed with brine (50 mL), dried over Na_2SO_4, filtered, and concentrated. The residual solid was recrystallized from ethanol/water.

Yield: 85% (1.66 g, 6.36 mmol).

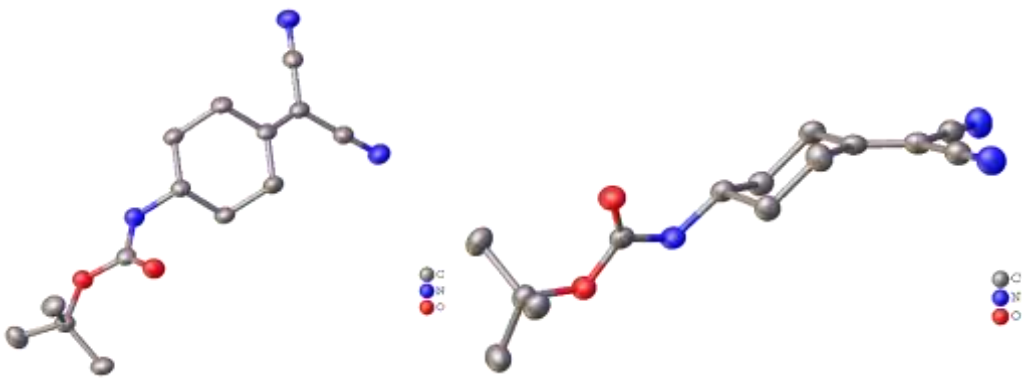
Appearance: Long thin colorless needles.

^{1}H NMR (400 MHz, $CDCl_3$): δ [ppm] = 4.49 (br. s, 1H), 3.86 – 3.68 (m, 1H), 3.04 – 2.90 (m, 2H), 2.50 (ddd, J = 14.9, 11.7, 5.1 Hz, 2H), 2.29 – 2.14 (m, 2H), 1.56 – 1.39 (m, 11H).

^{13}C{^{1}H} NMR (101 MHz, $CDCl_3$): δ [ppm] = 181.8, 155.2, 111.5, 84.0, 80.1, 47.6, 32.9, 32.4, 28.5.

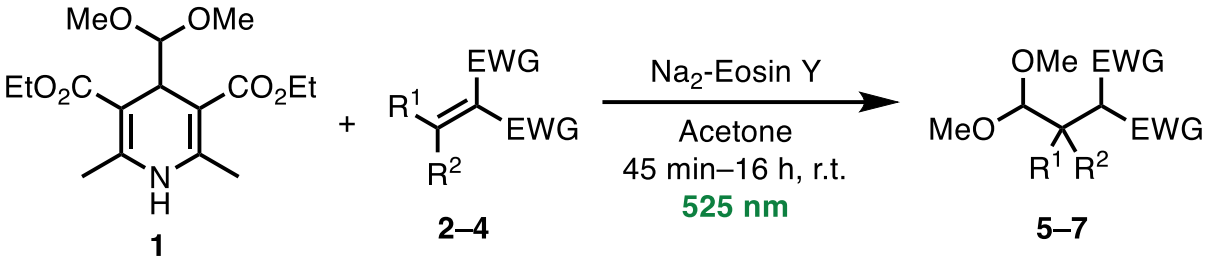
m.p. = 159–160 °C.

As both ESI(+) and elemental analysis gave dissatisfactory results (presumably due to decomposition of the Boc group), the constitution of the product was proven *via* X-ray diffraction analysis (hydrogen atoms have been omitted for clarity):



Synthesis of Substituted Acetaldehyde Dimethyl Acetals

General procedure for the Eosin Y photoredox-catalyzed synthesis of substituted acetaldehyde dimethyl acetals (GP1)



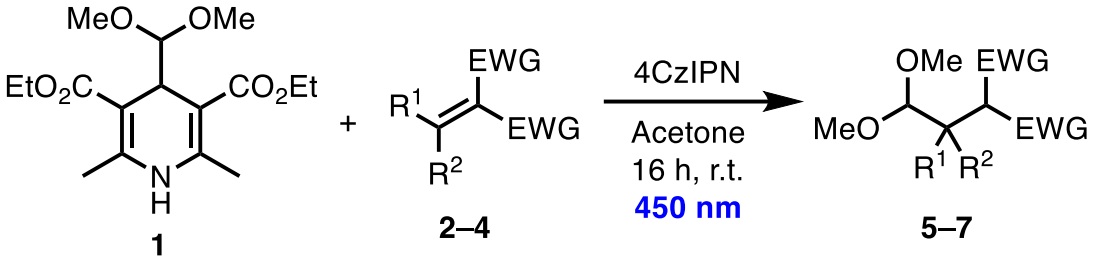
The corresponding olefin (100 µmol, 1.0 equiv.), Hantzsch ester **1** (39.2 mg, 120 µmol, 1.2 equiv.), and Eosin Y disodium salt (0.69 mg, 1.0 µmol, 1.0 mol%) were weighed into a 4 mL glass vial, equipped with a stir bar and closed with a septum screw cap which was punctured by a cannula. The vial was transferred into an argon-filled glove box and acetone[a] (1.0 mL, 0.1 M) was added. The vial was closed, removed from the glove box, and placed into an *EvoluChem PhotoRedOx Box* with fan cooling. The mixture was vigorously stirred under irradiation (**525 nm**, *EvoluChem LED 525PF*) for the corresponding time.

NMR yield determination: An exactly weighed amount of 1,3,5-trimethoxybenzene (>99 % purity, 1.50–5.00 mg) was added to the reaction mixture after complete irradiation and the vial was shaken well. The mixture was transferred to a round-bottom flask, the solvent was removed, the residue was dissolved in $CDCl_3$, and a ^1H NMR spectrum was recorded. By integration of a suitable product signal in comparison with the signal of the internal standard, the amount of substance and thus the yield was determined.

Isolation of the product: The mixture after complete irradiation was directly transferred to a round-bottom flask and Celite® (~100 mg) was added. The solvent was removed and the crude product adsorbed on Celite® was purified by column chromatography on silica or neutral alumina using an appropriate solvent mixture as determined by TLC (generally pentane/ethyl acetate).

[a] Acetone (technical grade) was stirred over activated 3 Å molecular sieves for a maximum of **16 hours**, distilled off, and degassed using the Freeze-Pump-Thaw technique under nitrogen (3–4 cycles). The solvent was stored in an argon-filled glove box.

General procedure for the 4CzIPN photoredox-catalyzed synthesis of substituted acetaldehyde dimethyl acetals (GP2)

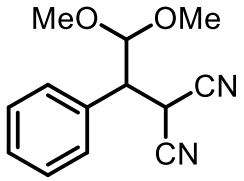


The corresponding olefin (100 µmol, 1.0 equiv.), Hantzsch ester **1** (39.2 mg, 120 µmol, 1.2 equiv.), and 4CzIPN (0.79 mg, 1.0 µmol, 1.0 mol%) were weighed into a 4 mL glass vial, equipped with a stir bar and closed with a septum screw cap which was punctured by a cannula. The vial was transferred into an argon-filled glove box and acetone[a] (1.0 mL, 0.1 M) was added. The vial was closed, removed from the glove box, and placed into an *EvoluChem PhotoRedOx Box* with fan cooling. The mixture was vigorously stirred under irradiation (**450 nm**, *EvoluChem LED 450PF*) for 16 h. The mixtures were then treated as described in GP1.

The products **5a**–**l**, **5n**–**y**, **6a**–**e**, **6g-1**, **6g-2**, **6h-1**, **6h-2**, **6i**, **6j-1**, **6j-2**, **6j-3**, and **7a**–**c** have been synthesized and, if applicable, isolated and fully characterized in **Chapter 3** of this work.

[a] Acetone (technical grade) was stirred over activated 3 Å molecular sieves for a maximum of **16 hours**, distilled off, and degassed using the Freeze-Pump-Thaw technique under nitrogen (3–4 cycles). The solvent was stored in an argon-filled glove box.

2-(Dicyanomethyl)-2-phenylacetaldehyde dimethyl acetal (**5a**)



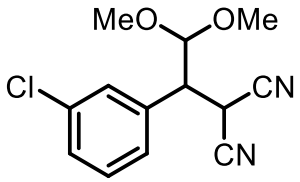
By GP1 starting from benzylidenemalononitrile (**2a**, 15.4 mg) with an irradiation time of 45 min. Purified by column chromatography (Neutral Al_2O_3, Pentane/EtOAc 5:1).

Yield: 84% (19.3 mg, 83.8 µmol).

Appearance: Pale-yellow oil.

^{1}H NMR (400 MHz, $CDCl_3$): δ [ppm] = 7.50 – 7.34 (m, 5H), 4.81 (d, J = 6.6 Hz, 1H), 4.34 (d, J = 5.6 Hz, 1H), 3.52 (s, 3H), 3.43 (t, J = 6.1 Hz, 1H), 3.31 (s, 3H).

2-(3-Chlorophenyl)-2-dicyanomethylacetaldehyde dimethyl acetal (**5b**)



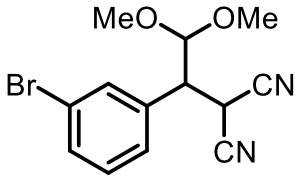
By GP1 starting from (3-chlorobenzylidene)malononitrile (**2b**, 18.9 mg) with an irradiation time of 45 min. Purified by column chromatography (Neutral Al_2O_3, Pentane/EtOAc 4:1).

Yield: 73% (19.3 mg, 72.9 µmol).

Appearance: Colorless oil.

^{1}H NMR (300 MHz, $CDCl_3$): δ [ppm] = 7.45 – 7.27 (m, 4H), 4.76 (d, J = 6.4 Hz, 1H), 4.33 (d, J = 6.0 Hz, 1H), 3.53 (s, 3H), 3.40 (t, J = 6.2 Hz, 3H), 3.35 (s, 3H).

2-(3-Bromophenyl)-2-dicyanomethylacetaldehyde dimethyl acetal (**5c**)



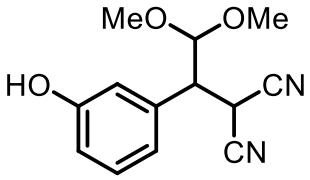
By GP1 starting from (3-bromobenzylidene)malononitrile (**2c**, 23.3 mg) with an irradiation time of 45 min. Purified by column chromatography (Neutral Al_2O_3, Pentane/EtOAc 4:1).

Yield: 72% (22.4 mg, 72.4 µmol).

Appearance: Colorless oil.

^{1}H NMR (400 MHz, $CDCl_3$): δ [ppm] = 7.61 – 7.50 (m, 2H), 7.40 – 7.28 (m, 2H), 4.76 (d, J = 6.3 Hz, 1H), 4.33 (d, J = 5.9 Hz, 1H), 3.52 (s, 3H), 3.39 (t, J = 6.2 Hz, 1H), 3.34 (s, 3H).

2-(Dicyanomethyl)-2-(3-hydroxyphenyl)acetaldehyde dimethyl acetal (**5d**)



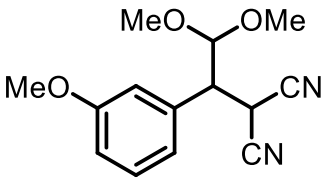
By GP1 starting from (3-hydroxybenzylidene)malononitrile (**2d**, 17.0 mg) with an irradiation time of 60 min. Purified by column chromatography (SiO_2, Pentane/EtOAc 2:1).

Yield: 82% (20.1 mg, 81.6 µmol).

Appearance: Colorless gum.

^{1}H NMR (300 MHz, $CDCl_3$): δ [ppm] = 7.32 – 7.23 (m, 1H), 7.01 – 6.93 (m, 1H), 6.93 – 6.81 (m, 2H), 5.23 (s, 1H), 4.77 (d, J = 6.6 Hz, 1H), 4.32 (d, J = 5.7 Hz, 1H), 3.52 (s, 3H), 3.36 (t, J = 6.1 Hz, 1H), 3.33 (s, 3H).

2-(Dicyanomethyl)-2-(3-methoxyphenyl)acetaldehyde dimethyl acetal (**5e**)



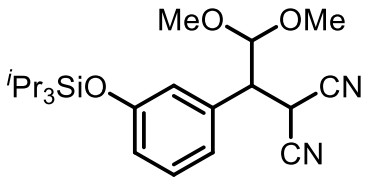
By GP1 starting from (3-methoxybenzylidene)malononitrile (**2e**, 18.4 mg) with an irradiation time of 45 min. Purified by column chromatography (Neutral Al_2O_3, Pentane/EtOAc 4:1).

Yield: 86% (22.5 mg, 86.4 µmol).

Appearance: Colorless oil.

^{1}H NMR (500 MHz, $CDCl_3$): δ [ppm] = 7.40 – 7.30 (m, 1H), 7.03 – 6.97 (m, 1H), 6.97 – 6.87 (m, 2H), 4.78 (d, *J* = 6.6 Hz, 1H), 4.32 (d, *J* = 5.6 Hz, 1H), 3.83 (s, 3H), 3.52 (s, 3H), 3.39 (t, *J* = 6.2 Hz, 1H), 3.32 (s, 3H).

2-(Dicyanomethyl)-2-(3-((triisopropylsilyl)oxy)phenyl)acetaldehyde dimethyl acetal (**5f**)



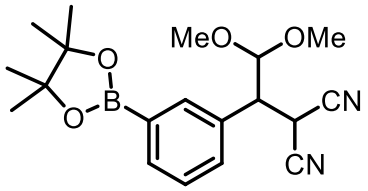
By GP1 starting from (3-((triisopropylsilyl)oxy)benzylidene)malononitrile (**2f**, 32.7 mg) with an irradiation time of 45 min. Purified by column chromatography (Neutral Al_2O_3, Pentane/EtOAc 10:1).

Yield: 85% (37.9 mg, 85.3 µmol).

Appearance: Colorless oil.

^{1}H NMR 500 MHz, $CDCl_3$): δ [ppm] = 7.31 – 7.19 (m, 1H), 7.01 – 6.95 (m, 1H), 6.95 – 6.89 (m, 2H), 4.73 (d, *J* = 6.6 Hz, 1H), 4.30 (d, *J* = 5.7 Hz, 1H), 3.50 (s, 3H), 3.34 (*pseudo*-t, *J* = 6.2 Hz, 1H), 3.29 (s, 3H), 1.31 – 1.21 (m, 3H), 1.18 – 0.94 (m, 18H).

2-(Dicyanomethyl)-2-(3-(4,4,5,5-tetramethyl-1,3,2-dioxaborolan-2-yl)phenyl)acetaldehyde dimethyl acetal (**5g**)



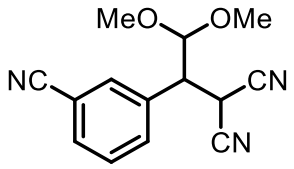
By GP1 starting from (3-(2,2-dicyanovinyl)phenylboronic acid pinacol ester (**2g**, 28.0 mg) with an irradiation time of 45 min. An analytical sample was obtained by column chromatography (SiO_2, Pentane/Et_2O 5:1 → 1:1).

Yield: 89% (^{1}H NMR yield *vs.* 1,3,5-trimethoxybenzene).

Appearance: Colorless oil.

^{1}H NMR (400 MHz, $CDCl_3$): δ [ppm] = 7.88 – 7.80 (m, 1H), 7.80 – 7.71 (m, 1H), 7.58 – 7.49 (m, 1H), 7.47 – 7.38 (m, 1H), 4.81 (d, *J* = 6.5 Hz, 1H), 4.33 (d, *J* = 6.0 Hz, 1H), 3.52 (s, 3H), 3.46 (t, *J* = 6.2 Hz, 1H), 3.31 (s, 3H), 1.35 (s, 12H).

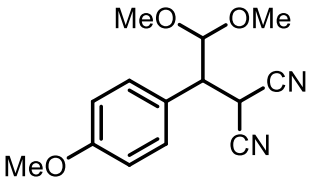
2-(Dicyanomethyl)-2-(3-cyanophenyl)acetaldehyde dimethyl acetal (**5h**)



By GP1 starting from (3-cyanobenzylidene)malononitrile (**2h**, 17.9 mg) with an irradiation time of 45 min.

Yield: 34% (^{1}H NMR yield *vs.* 1,3,5-trimethoxybenzene).

2-(Dicyanomethyl)-2-(4-methoxyphenyl)acetaldehyde dimethyl acetal (**5i**)



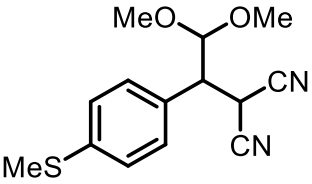
By GP1 starting from (4-methoxybenzylidene)malononitrile (**2i**, 18.4 mg) with an irradiation time of 45 min. Purified by column chromatography (Neutral Al_2O_3, Pentane/EtOAc 5:1).

Yield: 80% (20.7 mg, 79.5 µmol).

Appearance: Off-white solid.

^{1}H NMR (500 MHz, $CDCl_3$): δ [ppm] = 7.34 (d, *J* = 8.7 Hz, 2H), 6.94 (d, *J* = 8.7 Hz, 2H), 4.76 (d, *J* = 6.7 Hz, 1H), 4.31 (d, *J* = 5.5 Hz, 1H), 3.82 (s, 3H), 3.51 (s, 3H), 3.38 (dd, *J* = 6.7, 5.6 Hz, 1H), 3.31 (s, 3H).

2-(Dicyanomethyl)-2-(4-(methylthio)phenyl)acetaldehyde dimethyl acetal (**5j**)



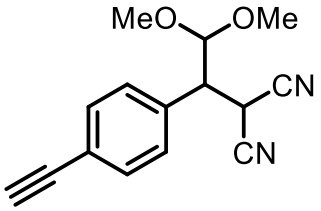
By GP1 starting from (4-(methylthio)benzylidene)malononitrile (**2j**, 20.0 mg) with an irradiation time of 60 min. Purified by column chromatography (Neutral Al_2O_3, Pentane/EtOAc 4:1).

Yield: 82% (22.7 mg, 82.1 µmol).

Appearance: Pale-yellow solid.

^{1}H NMR (400 MHz, $CDCl_3$): δ [ppm] = 7.37 – 7.26 (m, 4H), 4.77 (d, *J* = 6.6 Hz, 1H), 4.32 (d, *J* = 5.6 Hz, 1H), 3.51 (s, 3H), 3.38 (dd, *J* = 6.7, 5.6 Hz, 1H), 3.31 (s, 3H), 2.49 (s, 3H).

2-(Dicyanomethyl)-2-(4-ethynylphenyl)acetaldehyde dimethyl acetal (**5k**)



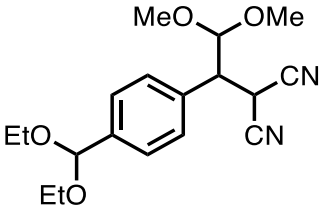
By GP1 starting from (4-ethynylbenzylidene)malononitrile (**2k**, 17.8 mg) with an irradiation time of 45 min. Purified by column chromatography (Neutral Al_2O_3, Pentane/EtOAc 4:1).

Yield: 72% (18.3 mg, 72.0 µmol).

Appearance: Colorless oil.

^{1}H NMR (400 MHz, $CDCl_3$): δ [ppm] = 7.55 (d, *J* = 8.4 Hz, 2H), 7.39 (d, *J* = 8.3 Hz, 2H), 4.78 (d, *J* = 6.6 Hz, 1H), 4.34 (d, *J* = 5.7 Hz, 1H), 3.52 (s, 3H), 3.42 (*pseudo*-t, *J* = 6.2 Hz, 1H), 3.31 (s, 3H), 3.13 (s, 1H).

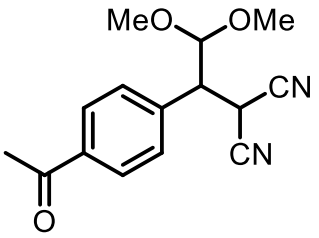
2-(Dicyanomethyl)-2-(4-(diethoxymethyl)phenyl)acetaldehyde dimethyl acetal (**5l**)



By GP1 starting from (4-acetylbenzylidene)malononitrile (**2l**, 19.6 mg) with an irradiation time of 45 min.

Yield: 81% (^{1}H NMR yield *vs.* 1,3,5-trimethoxybenzene).

2-(Dicyanomethyl)-2-(4-acetylphenyl)acetaldehyde dimethyl acetal (**5m**)



By GP1 starting from (4-acetylbenzylidene)malononitrile (**2m**, 19.6 mg) with an irradiation time of 45 min.

Yield: 42% (11.4 mg, 41.9 µmol).

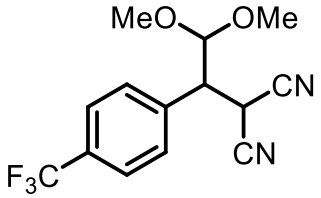
Appearance: Colorless gum.

^{1}H NMR (300 MHz, $CDCl_3$): δ [ppm] = 8.07 – 7.94 (m, 2H), 7.60 – 7.47 (m, 2H), 4.82 (d, *J* = 6.6 Hz, 1H), 4.37 (d, *J* = 5.9 Hz, 1H), 3.53 (s, 3H), 3.50 (t, *J* = 5.7 Hz, 1H), 3.33 (s, 3H), 2.62 (s, 3H).

^{13}C{^{1}H} NMR (75.5 MHz, $CDCl_3$): δ [ppm] = 197.5, 138.5, 137.8, 129.3, 129.2, 111.8, 111.6, 104.1, 56.6, 55.4, 49.2, 26.8, 25.6.

HRMS (ESI): *m/z* calcd. for $C_{15}H_{17}N_2O_3^+$: 273.1234, found: 273.1229.

2-(Dicyanomethyl)-2-(4-(trifluoromethyl)phenyl)acetaldehyde dimethyl acetal (**5n**)



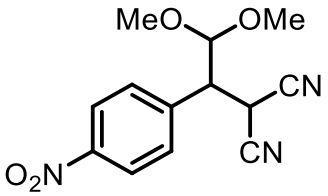
By GP1 starting from (4-(trifluoromethyl)benzylidene)malononitrile (**2n**, 22.2 mg) with an irradiation time of 45 min. Purified by column chromatography (Neutral Al_2O_3, Pentane/EtOAc 6:1).

Yield: 49% (14.6 mg, 48.9 µmol).

Appearance: Pale-yellow oil.

^{1}H NMR (300 MHz, $CDCl_3$): δ [ppm] = 7.74 – 7.66 (m, 2H), 7.60 – 7.52 (m, 2H), 4.81 (d, *J* = 6.4 Hz, 1H), 4.37 (d, *J* = 5.9 Hz, 1H), 3.53 (s, 3H), 3.50 (t, *J* = 6.1 Hz, 1H), 3.34 (s, 3H).

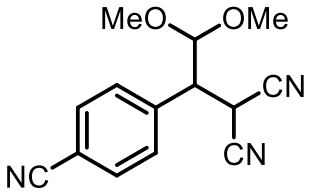
2-(Dicyanomethyl)-2-(4-nitrophenyl)acetaldehyde dimethyl acetal (**5o**)



By GP1 starting from (4-nitrobenzylidene)malononitrile (**2o**, 19.9 mg) with an irradiation time of 45 min.

Yield: 10% (^{1}H NMR yield *vs.* 1,3,5-trimethoxybenzene).

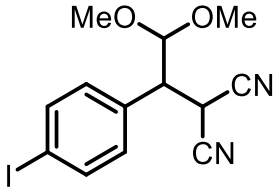
2-(Dicyanomethyl)-2-(4-cyanophenyl)acetaldehyde dimethyl acetal (**5p**)



By GP1 starting from (4-cyanobenzylidene)malononitrile (**2p**, 17.9 mg) with an irradiation time of 45 min.

Yield: 31% (^{1}H NMR yield *vs.* 1,3,5-trimethoxybenzene).

2-(Dicyanomethyl)-2-(4-iodophenyl)acetaldehyde dimethyl acetal (**5q**)



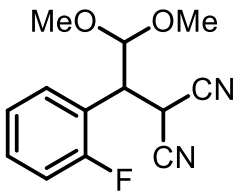
By GP1 starting from (4-iodobenzylidene)malononitrile (**2q**, 28.0 mg) with an irradiation time of 45 min. Purified by column chromatography (Neutral Al_2O_3, Pentane/EtOAc 4:1).

Yield: 78% (27.9 mg, 78.3 µmol).

Appearance: Pale-yellow solid.

^{1}H NMR (400 MHz, $CDCl_3$): δ [ppm] = 7.81 – 7.73 (m, 2H), 7.19 – 7.14 (m, 2H), 4.75 (d, *J* = 6.5 Hz, 1H), 4.32 (d, *J* = 5.7 Hz, 1H), 3.51 (s, 3H), 3.37 (-t, *J* = 6.1 Hz, 1H), 3.32 (s, 3H).

2-(Dicyanomethyl)-2-(2-fluorophenyl)acetaldehyde dimethyl acetal (**5r**)



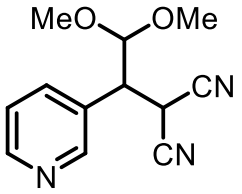
By GP1 starting from (2-fluorobenzylidene)malononitrile (**2r**, 17.2 mg) with an irradiation time of 45 min. Purified by column chromatography (Neutral Al_2O_3, Pentane/EtOAc 5:1).

Yield: 60% (15.0 mg, 60.4 µmol).

Appearance: Colorless syrup.

^{1}H NMR (400 MHz, $CDCl_3$): δ [ppm] = 7.59 – 7.47 (m, 1H), 7.43 – 7.36 (m, 1H), 7.25 – 7.13 (m, 2H), 4.83 (d, *J* = 6.7 Hz, 1H), 4.34 (d, *J* = 6.2 Hz, 1H), 3.96 (t, *J* = 6.5 Hz, 1H), 3.52 (s, 3H), 3.33 (s, 3H).

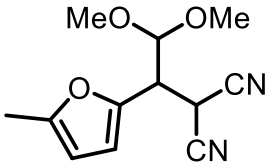
2-(Dicyanomethyl)-2-(pyridin-3-yl)acetaldehyde dimethyl acetal (**5s**)



By GP1 starting from (pyridin-3-ylmethylidene)malononitrile (**2s**, 15.5 mg) with an irradiation time of 45 min.

Yield: 53% (^{1}H NMR yield *vs.* 1,3,5-trimethoxybenzene).

2-(Dicyanomethyl)-2-(5-methylfuran-2-yl)acetaldehyde dimethyl acetal (**5t**)



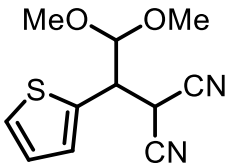
By GP1 starting from ((5-methylfuran-2-yl)methylidene)malononitrile (**2t**, 15.8 mg) with an irradiation time of 3 h. Purified by column chromatography (Neutral Al_2O_3, Pentane/EtOAc 5:1).

Yield: 77% (18.1 mg, 77.2 µmol).

Appearance: Colorless oil.

^{1}H NMR (500 MHz, $CDCl_3$): δ [ppm] = 6.35 (d, J = 3.2 Hz, 1H), 5.99 (dd, J = 3.2, 1.2 Hz, 1H), 4.76 (d, J = 7.0 Hz, 1H), 4.29 (d, J = 5.0 Hz, 1H), 3.55 (dd, J = 7.0, 5.0 Hz, 1H), 3.50 (s, 3H), 3.35 (s, 3H), 2.31 (d, J = 1.1 Hz, 3H).

2-(Dicyanomethyl)-2-(thiophen-2-yl)acetaldehyde dimethyl acetal (**5u**)



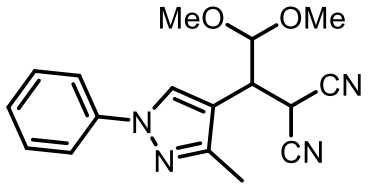
By GP1 starting from (thiophen-2-ylmethylidene)malononitrile (**2u**, 16.0 mg) with an irradiation time of 3 h. Purified by column chromatography (Neutral Al_2O_3, Pentane/EtOAc 5:1).

Yield: 77% (18.1 mg, 77.2 µmol).

Appearance: Pale-yellow oil.

^{1}H NMR (500 MHz, $CDCl_3$): δ [ppm] = 7.37 (dd, J = 5.2, 1.2 Hz, 1H), 7.21 (dd, J = 3.6, 1.2 Hz, 1H), 7.07 (dd, J = 5.2, 3.6 Hz, 1H), 4.70 (d, J = 5.7 Hz, 1H), 4.35 (d, J = 5.5 Hz, 1H), 3.78 (t, J = 5.6 Hz, 1H), 3.54 (s, 3H), 3.41 (s, 3H).

2-(Dicyanomethyl)-2-(3-methyl-1-phenyl-1*H*-pyrazol-4-yl)acetaldehyde dimethyl acetal (**5v**)



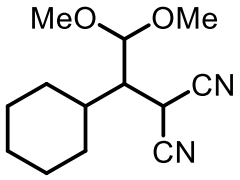
By GP1 starting from ((3-methyl-1-phenyl-1*H*-pyrazol-4-yl)methylene)malononitrile (**2v**, 23.4 mg) with an irradiation time of 3 h. Purified by column chromatography (Neutral Al_2O_3, Pentane/EtOAc 5:1).

Yield: 87% (27.1 mg, 87.3 µmol).

Appearance: Pale-yellow oil.

^{1}H NMR (500 MHz, $CDCl_3$): δ [ppm] = 8.07 (s, 1H), 7.70 – 7.64 (m, 2H), 7.50 – 7.39 (m, 2H), 7.35 – 7.25 (m, 1H), 4.61 (d, *J* = 5.8 Hz, 1H), 4.32 (d, *J* = 4.8 Hz, 1H), 3.52 (s, 3H), 3.50 (dd, *J* = 5.9, 4.8 Hz, 1H), 3.39 (s, 3H), 2.40 (s, 3H).

2-(Dicyanomethyl)-2-cyclohexylacetaldehyde dimethyl acetal (**5w**)



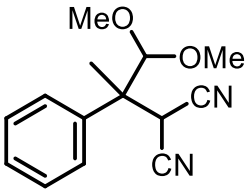
By GP1 starting from cyclohexylmethylidenemalononitrile (**2w**, 16.0 mg) with an irradiation time of 3 h. Purified by column chromatography (Neutral Al_2O_3, Pentane/Et_2O 2:1).

Yield: 64% (15.2 mg, 64.3 µmol).

Appearance: Colorless oil.

^{1}H NMR (500 MHz, $CDCl_3$): δ [ppm] = 4.49 (d, *J* = 4.2 Hz, 1H), 4.20 (d, *J* = 2.7 Hz, 1H), 3.48 (s, 3H), 3.41 (s, 3H), 2.04 (ddd, *J* = 7.0, 4.2, 2.7 Hz, 1H), 1.97 – 1.92 (m, 1H), 1.86 – 1.76 (m, 4H), 1.74 – 1.68 (m, 1H), 1.36 – 1.27 (m, 2H), 1.23 – 1.08 (m, 3H).

2-(Dicyanomethyl)-2-phenylpropionaldehyde dimethyl acetal (**5x**)



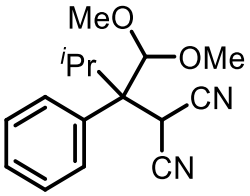
By GP1 starting from (1-phenylethylidene)malononitrile (**2x**, 16.8 mg) with an irradiation time of 16 h. Purified by column chromatography (Neutral Al_2O_3, Pentane/EtOAc 5:1).

Yield: 84% (20.5 mg, 83.9 µmol).

Appearance: Colorless oil.

^{1}H NMR (500 MHz, $CDCl_3$): δ [ppm] = 7.57 – 7.47 (m, 2H), 7.44 – 7.40 (m, 2H), 7.39 – 7.34 (m, 1H), 4.64 (s, 1H), 4.36 (s, 1H), 3.54 (s, 3H), 3.42 (s, 3H), 1.72 (s, 3H).

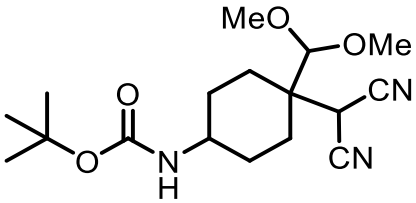
2-(Dicyanomethyl)-2-phenyl-3-methylbutyraldehyde dimethyl acetal (**5y**)



By GP1 starting from (2-methyl-1-phenylpropylidene)malononitrile (**2y**, 19.6 mg) with an irradiation time of 24 h.

Yield: 30% (^{1}H NMR yield *vs.* 1,3,5-trimethoxybenzene).

tert-Butyl (4-(dicyanomethyl)-4-(dimethoxymethyl)cyclohexyl)carbamate (**5z**)



By GP1 starting from *tert*-butyl (4-(dicyanomethylene)cyclohexyl)carbamate (**2z**, 26.1 mg) with an irradiation time of 16 h. Purified by column chromatography (SiO_2 deactivated with NEt_3, Pentane/EtOAc 3:1).

Yield: 77% (26.1 mg, 77.4 µmol).

Appearance: Colorless solid.

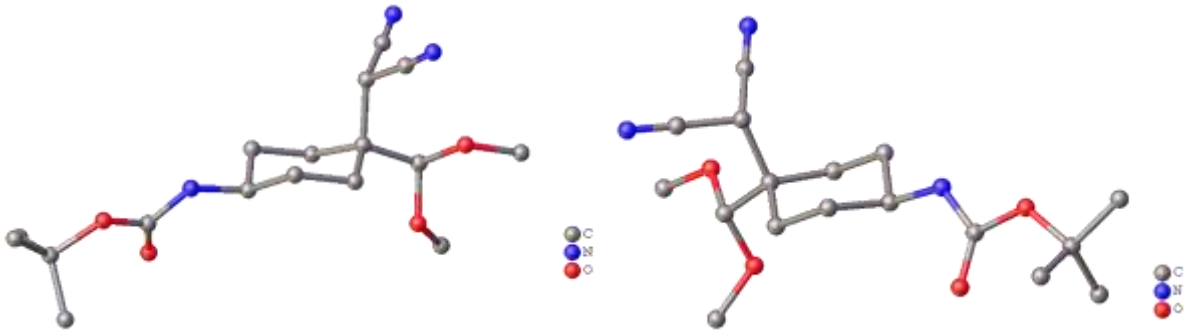
^{1}H NMR (600 MHz, $CDCl_3$): δ [ppm] = 4.49 (br. s, 1H), 4.24 (s, 1H), 4.05 (s, 1H), 3.59 (s, 6H), 3.54 – 3.43 (m, 1H), 1.96 (dqd, J = 13.6, 4.7, 1.5 Hz, 2H), 1.82 (dd, J = 8.1, 4.6 Hz, 4H), 1.44 (s, 9H), 1.32 – 1.23 (m, 2H).

$^{13}C\{^{1}H\}$ NMR (151 MHz, $CDCl_3$): δ [ppm] = 155.1, 111.9, 108.8, 79.6, 59.0, 47.9, 45.1, 28.4, 27.5, 26.6, 26.3.

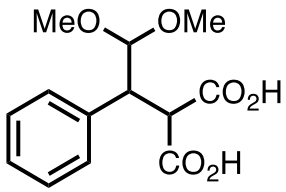
HRMS (ESI): *m/z* calcd. for $C_{17}H_{27}N_3NaO_4^+$: 360.1894, found: 360.1899.

m.p. = 120–123 °C.

XRD (hydrogen atoms omitted for clarity):



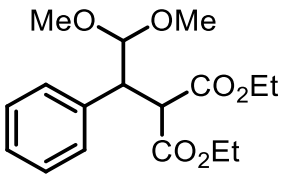
(2,2-Dimethoxy-1-phenylethyl)malonic acid (**6a**)



By GP1 starting from benzylidenemalonic acid (**3a**, 19.2 mg) with an irradiation time of 6 h.

Yield: <5% (^{1}H NMR yield *vs.* 1,3,5-trimethoxybenzene).

Diethyl (2,2-dimethoxy-1-phenylethyl)malonate (**6b**)



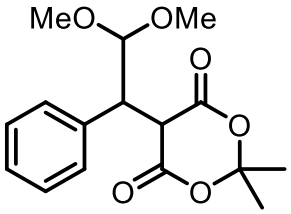
By GP1 starting from diethyl benzylidenemalonate (**3b**, 24.8 mg) with an irradiation time of 6 h. Purified by column chromatography (Neutral Al_2O_3, Pentane/EtOAc 8:1).

Yield: 92% (29.8 mg, 91.9 µmol).

Appearance: Colorless oil.

^{1}H NMR (500 MHz, $CDCl_3$): δ [ppm] = 7.30 – 7.15 (m, 5H), 4.59 (d, *J* = 6.0 Hz, 1H), 4.25 – 4.12 (m, 2H), 4.04 – 3.80 (m, 3H), 3.76 (dd, *J* = 10.3, 6.0 Hz, 1H), 3.34 (s, 3H), 3.24 (s, 3H), 1.26 (t, *J* = 7.1 Hz, 3H), 0.92 (t, *J* = 7.1 Hz, 3H).

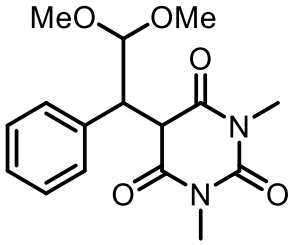
5-(2,2-Dimethoxy-1-phenylethyl)-2,2-dimethyl-1,3-dioxane-4,6-dione (**6c**)



By GP1 starting from 5-benzylidene-2,2-dimethyl-1,3-dioxane-4,6-dione (**3c**, 23.2 mg) with an irradiation time of 6 h.

Yield: 85% (^{1}H NMR yield *vs.* 1,3,5-trimethoxybenzene).

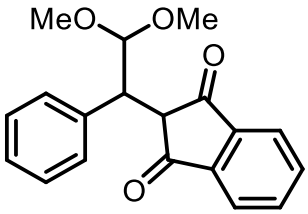
N,*N'*-Dimethyl-5-(2,2-dimethoxy-1-phenylethyl)barbituric acid (**6d**)



By GP1 starting from *N*,*N'*-dimethyl-4-benzylidenebarbituric acid (**3d**, 24.4 mg) with an irradiation time of 6 h. Purified by automated flash chromatography (C_{18}-SiO_2, 10% MeCN in H_2O → 100% MeCN).

Yield: 72% (^{1}H NMR yield *vs.* 1,3,5-trimethoxybenzene).

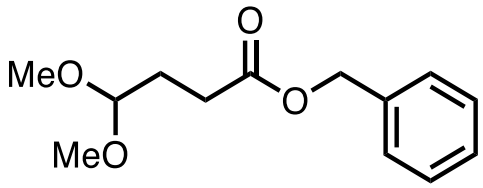
2-(2,2-Dimethoxy-1-phenylethyl)indane-1,3-dione (**6e**)



By GP1 starting from 2-benzylideneindane-1,3-dione (**3e**, 23.4 mg) with an irradiation time of 6 h. Attempts at separating the product from side products were unsuccessful.

Yield: 46% (^{1}H NMR yield *vs.* 1,3,5-trimethoxybenzene).

Benzyl 4,4-dimethoxybutanoate (**6f**)



By GP1 starting from benzyl acrylate (**3f**, 16.2 mg) with an irradiation time of 6 h.

Yield: <5% (^{1}H NMR yield *vs.* 1,3,5-trimethoxybenzene).

By GP2 on a 300 µmol scale starting form benzyl acrylate (3f, 48.7 mg), **1** (118 mg, 360 µmol), and 4CzIPN (2.4 mg, 3.0 µmol) in acetone (3.0 mL). Purified by column chromatography

Yield: 79% (56.4 mg, 237 µmol).

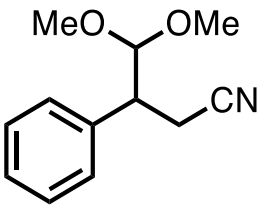
Appearance: Colorless oil.

^{1}H NMR (300 MHz, $CDCl_3$): δ [ppm] = 7.42 – 7.27 (m, 5H), 5.12 (s, 2H), 4.39 (t, *J* = 5.6 Hz, 1H), 3.31 (s, 6H), 2.43 (t, *J* = 7.5 Hz, 2H), 1.95 (td, *J* = 7.5, 5.6 Hz, 2H).

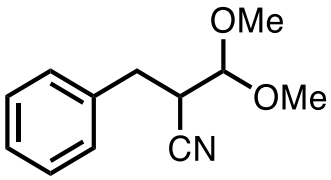
^{13}C{^{1}H} NMR (75.5 MHz, $CDCl_3$): δ [ppm] = 173.19, 136.13, 128.69, 128.34, 103.75, 66.41, 53.33, 29.50, 27.95.

HRMS (ESI): *m/z* calcd. for $C_{13}H_{18}NaO_4^+$: 261.1097, found: 261.1107.

2-(Cyanomethyl)-2-phenylacetaldehyde dimethyl acetal (**6g-1**) and 2-Cyano-3-phenyl-2-propionaldehyde dimethyl acetal (**6g-2**)



6g-1



6g-2

By GP1 starting from cinnamonitrile (**3g**, 12.9 mg) with an irradiation time of 16 h:

*2-(Cyanomethyl)-2-phenylacetaldehyde dimethyl acetal (**6g-1**)*

Yield: <5% (^{1}H NMR yield *vs.* 1,3,5-trimethoxybenzene).

*2-Cyano-3-phenyl-2-propionaldehyde dimethyl acetal (**6g-2**)*

Yield: <5% (^{1}H NMR yield *vs.* 1,3,5-trimethoxybenzene).

By GP2 starting from cinnamonitrile (**3g**, 12.9 mg):

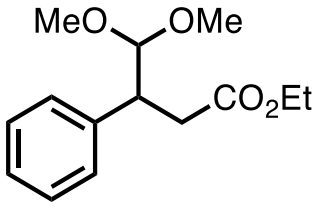
*2-(Cyanomethyl)-2-phenylacetaldehyde dimethyl acetal (**6g-1**)*

Yield: 28% (^{1}H NMR yield *vs.* 1,3,5-trimethoxybenzene).

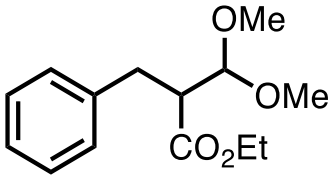
*2-Cyano-3-phenyl-2-propionaldehyde dimethyl acetal (**6g-2**)*

Yield: 34% (^{1}H NMR yield *vs.* 1,3,5-trimethoxybenzene).

Ethyl 4,4-dimethoxy-3-phenylbutanoate (**6h-1**) and Ethyl 2-benzyl-3,3-dimethoxypropanoate (**6h-2**)



6h-1



6h-2

By GP1 starting from ethyl cinnamate (**3h**, 17.6 mg) with an irradiation time of 16 h.

*Ethyl 4,4-dimethoxy-3-phenylbutanoate (**6h-1**)*

Yield: <5% (^{1}H NMR yield *vs.* 1,3,5-trimethoxybenzene).

*Ethyl 2-benzyl-3,3-dimethoxypropanoate (**6h-2**)*

Yield: <5% (^{1}H NMR yield *vs.* 1,3,5-trimethoxybenzene).

By GP2 starting from ethyl cinnamate (**3h**, 17.6 mg).

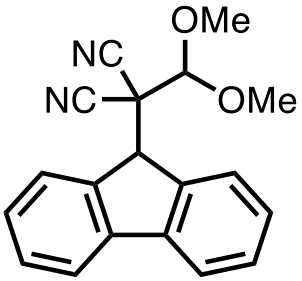
*Ethyl 4,4-dimethoxy-3-phenylbutanoate (**6h-1**)*

Yield: 15% (^{1}H NMR yield *vs.* 1,3,5-trimethoxybenzene).

*Ethyl 2-benzyl-3,3-dimethoxypropanoate (**6h-2**)*

Yield: 59% (^{1}H NMR yield *vs.* 1,3,5-trimethoxybenzene).

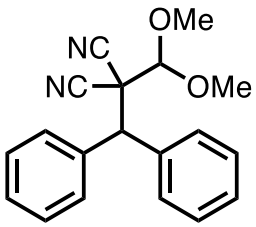
2,2-Dicyano-2-(9*H*-fluoren-9-yl)acetaldehyde dimethyl acetal (**6i**)



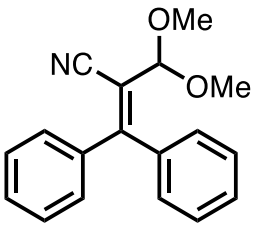
By GP1 starting from (9*H*-fluoren-9-yl)malononitrile (**3i**, 22.8 mg) with an irradiation time of 16 h.

Yield: 60% (^{1}H NMR yield *vs.* 1,3,5-trimethoxybenzene).

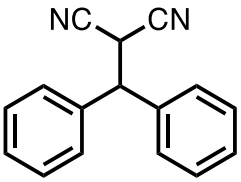
2,2-Dicyano-3,3-diphenylpropionaldehyde dimethyl acetal (**6j-1**), 2-Cyano-3,3-diphenyl-acrolein dimethyl acetal (**6j-2**), and Benzhydrylmalononitrile (**6j-3**)



6j-1



6j-2



6j-3

By GP1 starting from (diphenylmethylidene)malononitrile (**6j**, 23.0 mg) with an irradiation time of 16 h.

*2,2-Dicyano-3,3-diphenylpropionaldehyde dimethyl acetal (**6j-1**)*

Yield: <5% (^{1}H NMR yield *vs.* 1,3,5-trimethoxybenzene after 24 h on a 100 µmol scale).

*2-Cyano-3,3-diphenylacrolein dimethyl acetal (**6j-2**)*

Yield: <5% (^{1}H NMR yield *vs.* 1,3,5-trimethoxybenzene after 24 h on a 100 µmol scale).

*Benzhydrylmalononitrile (**6j-3**)*

Yield: <5% (^{1}H NMR yield *vs.* 1,3,5-trimethoxybenzene after 24 h on a 100 µmol scale).

By GP2 starting from (diphenylmethylidene)malononitrile (**6j**, 23.0 mg).

*2,2-Dicyano-3,3-diphenylpropionaldehyde dimethyl acetal (**6j-1**)*

Yield: 53% (^{1}H NMR yield *vs.* 1,3,5-trimethoxybenzene after 24 h on a 100 µmol scale).

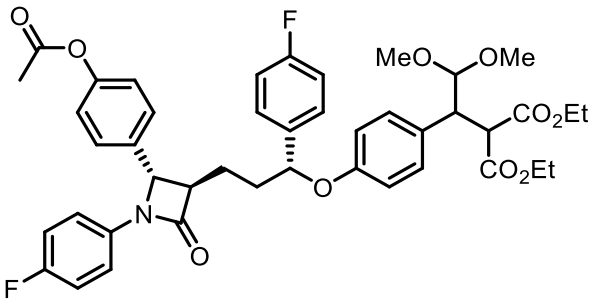
*2-Cyano-3,3-diphenylacrolein dimethyl acetal (**6j-2**)*

Yield: 22% (^{1}H NMR yield *vs.* 1,3,5-trimethoxybenzene after 24 h on a 100 µmol scale).

*Benzhydrylmalononitrile (**6j-3**)*

Yield: 20% (^{1}H NMR yield *vs.* 1,3,5-trimethoxybenzene after 24 h on a 100 µmol scale).

Diethyl 2-(1-(4-((*R*)-3-((2*S*,3*R*)-2-(4-acetoxyphenyl)-1-(4-fluorophenyl)-4-oxoazetidin-3-yl)-1-(4-fluorophenyl)propoxy)phenyl)-2,2-dimethoxyethyl)malonate (**7a**)



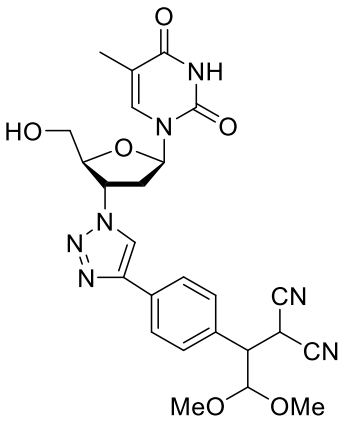
By GP1 on a 50 µmol scale starting from **4a** (34.9 mg) with an irradiation time of 60 min. Purified by automated flash chromatography (C_{18}-SiO_2, 20% MeCN in H_2O → 100% MeCN).

Yield: 34.2 mg (44.2 µmol, 88%).

Appearance: Fluffy colorless solid (lyophilisate).

^{1}H NMR (600 MHz, C_6D_6): δ [ppm] = 7.31 – 7.26 (m, 2H), 7.26 – 7.20 (m, 1H), 7.00 – 6.91 (m, 4H), 6.89 – 6.83 (m, 2H), 6.82 – 6.73 (m, 2H), 6.74 – 6.68 (m, 2H), 6.64 – 6.58 (m, 1H), 4.85 (ddd, *J* = 7.2, 4.8, 2.1 Hz, 1H), 4.61 (t, *J* = 5.9 Hz, 1H), 4.23 (dd, *J* = 10.0, 5.5 Hz, 1H), 4.11 – 4.04 (m, 2H), 4.05 – 3.96 (m, 1H), 3.78 – 3.65 (m, 2H), 3.11 (d, *J* = 2.7 Hz, 3H), 3.03 (d, *J* = 3.2 Hz, 3H), 2.76 (td, *J* = 7.9, 4.0 Hz, 1H), 2.09 – 2.00 (m, 1H), 1.95 – 1.85 (m, 0H), 1.80 – 1.72 (m, 1H), 1.72 (s, 3H), 1.70 – 1.60 (m, 0H), 0.95 (td, *J* = 7.1, 1.5 Hz, 3H), 0.65 (td, *J* = 7.1, 6.1 Hz, 3H).

2-(1-(4-(1-((2*S*,3*S*,5*R*)-2-(Hydroxymethyl)-5-(5-methyl-2,4-dioxo-3,4-dihydropyrimidin-1(2*H*)-yl)tetrahydrofuran-3-yl)-1*H*-1,2,3-triazol-4-yl)phenyl)-2,2-dimethoxyethyl)malononitrile (**7b**)



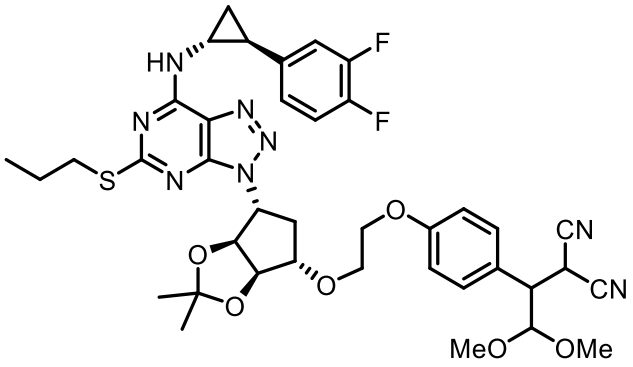
By GP1 on a 20 µmol scale starting from **4b** (8.9 mg) with an irradiation time of 60 min. Purified by automated flash chromatography (C_{18}-SiO_2, 10% MeCN in H_2O → 100% MeCN).

Yield: 8.3 mg (16 µmol, 80%).

Appearance: Fluffy colorless solid (lyophilisate).

^{1}H NMR (600 MHz, DMSO-d_6): δ [ppm] = 11.37 (s, 1H), 8.80 (s, 1H), 7.90 – 7.85 (m, 2H), 7.86 – 7.82 (m, 1H), 7.58 – 7.45 (m, 2H), 6.45 (t, *J* = 6.6 Hz, 1H), 5.42 (dt, *J* = 8.7, 5.5 Hz, 1H), 5.31 (t, *J* = 5.3 Hz, 1H), 4.83 (d, *J* = 6.6 Hz, 1H), 4.28 (dt, *J* = 5.6, 3.6 Hz, 1H), 3.87 (t, *J* = 5.7 Hz, 1H), 3.77 – 3.70 (m, 1H), 3.70 – 3.63 (m, 1H), 3.41 (s, 3H), 3.25 (s, 3H), 2.81 (ddd, *J* = 14.0, 6.9, 5.4 Hz, 1H), 2.71 (ddd, *J* = 13.8, 8.6, 6.3 Hz, 1H), 1.82 (d, *J* = 1.2 Hz, 3H).

2-(1-(4-(2-(((3a*R*,4*S*,6*R*,6a*S*)-6-(7-(((1*R*,2*S*)-2-(3,4-Difluorophenyl)cyclopropyl)amino)-5-(propylthio)-3*H*-[1,2,3]triazolo[4,5-*d*]pyrimidin-3-yl)-2,2-dimethyltetrahydro-4*H*-cyclopenta[*d*]-[1,3]dioxol-4-yl)oxy)ethoxy)phenyl)-2,2-dimethoxyethyl)malononitrile (**7c**)



By GP1 on a 50 µmol scale starting from **4c** (35.7 mg) with an irradiation time of 60 min. Purified by automated flash chromatography (C_{18}-SiO_2, 20% MeCN in H_2O → 100% MeCN).

Yield: 25.1 mg (31.7 µmol, 63%).

Appearance: Fluffy colorless solid (lyophilisate).

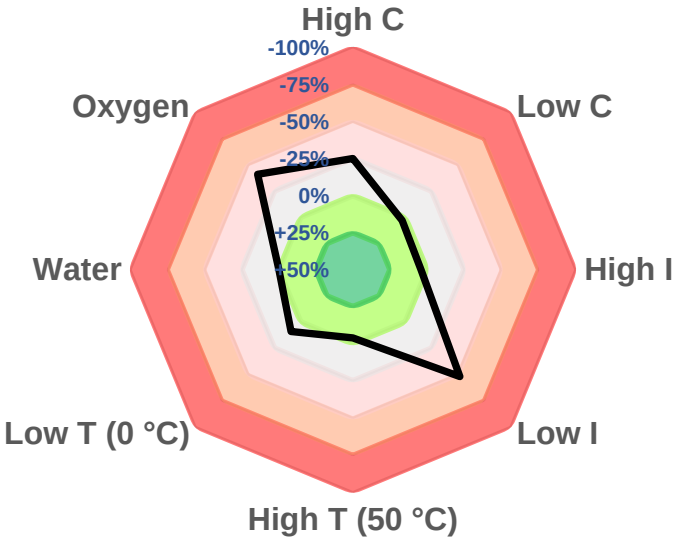
The product is a mixture of two rotamers in DMSO-d_6 solution (Ratio 80%/20%), as is known for Ticagrelor and its derivatives, including this compound.

^{1}H NMR (600 MHz, DMSO-d_6): δ [ppm] = 9.39 (d, *J* = 4.1 Hz, 0.8H), 8.99 (d, *J* = 5.0 Hz, 0.2H), 7.35 – 7.27 (m, 3.8H), 7.25 – 7.20 (m, 0.2H), 7.08 – 7.04 (m, 0.8H), 7.01 – 6.98 (m, 0.2H), 6.95 – 6.91 (m, 2H), 5.24 (dd, *J* = 7.3, 4.6 Hz, 0.8H), 5.19 (dd, *J* = 7.5, 4.6 Hz, 0.2H), 5.15 (d, *J* = 6.6 Hz, 1H), 5.03 (ddd, *J* = 9.6, 6.9, 4.5 Hz, 1H), 4.74 – 4.70 (m, 1.8H), 4.68 (dd, *J* = 3.4 Hz, 0.2H), 4.11 – 4.00 (m, 3H), 3.80 (ddd, *J* = 11.1, 5.5, 3.7 Hz, 1H), 3.76 – 3.70 (m, 2.2H), 3.38 (s, 3H), 3.21 (s, 3H), 3.16 – 3.12 (m, 0.8H), 3.11 – 3.08 (m, 0.2H), 3.07 – 3.02 (m, 0.2H), 2.96 – 2.84 (m, 1.6H), 2.68 (dt, *J* = 13.0, 6.5 Hz, 1H), 2.61 – 2.56 (m, 1H), 2.25 – 2.21 (m, 0.2H), 2.11 (ddd, *J* = 9.6, 6.4, 3.3 Hz, 0.8H), 1.72 – 1.67 (m, 0.4H), 1.56 – 1.50 (m, 2.4H), 1.49 (s, 3H), 1.45 – 1.42 (m, 0.2H), 1.40 – 1.34 (m, 1H), 1.26 (s, 2.4H), 1.25 (s, 0.6H), 0.98 (t, *J* = 7.5 Hz, 0.6H), 0.83 (t, *J* = 7.3 Hz, 2.4H).

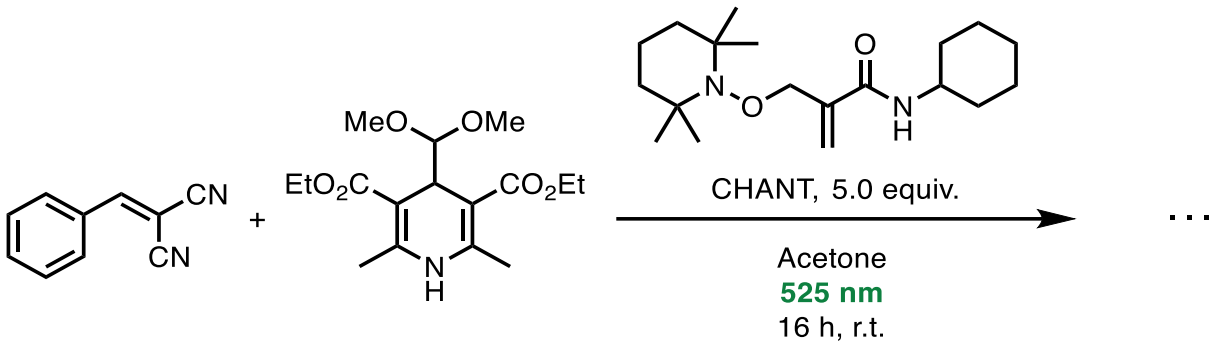
Sensitivity Assessment

The reactions were set up using the standard conditions (0.10 mmol scale, 1.0 equiv. **2a**, 1.2 equiv. **1**, 1 mol% Na_2-Eosin Y, Acetone (0.1 M), 525 nm, 45 min, r.t.) in combination with the deviations shown below. The yields were determined *via* ^{1}H NMR spectroscopy using 1,3,5-trimethoxybenzene as the standard.

Entry	Deviations from standard conditions	Yield of 5a [%]	Difference in yield to standard conditions (89%) [%]
High *c*	0.2 M	64	−25
Low *c*	0.05 M	92	+3
High *I*	Vial placed ~1 cm in front of the LED, cooled by a desk fan	93	+4
Low *I*	Placed in the furthest corner of the PhotoRedOx Box	37	−52
High *T*	50 °C	93	+4
Low *T*	0 °C	80	−9
Water	10 vol.% of degassed water added	89	±0
Oxygen	2 mL of dry air added	48	−41



Radical-Trapping Experiments



A standard reaction on a 100 µmol scale according to GP1 was set up using benzylidenemalononitrile with the addition of *N*-cyclohexyl-2-(((2,2,6,6-tetramethylpiperidin-1-yl)oxy)methyl)acrylamide (CHANT, 161 mg, 500 µmol, 5.0 equiv.) with an irradiation time of 16 h. The crude reaction mixture after irradiation for 16 h was analyzed by GC-MS (Fig. 3). Free TEMPO was detected, which is eliminated from the intermediate formed when a radical adds to the conjugated double bond of CHANT. However, no radical adducts of CHANT or TEMPO could be detected unequivocally.

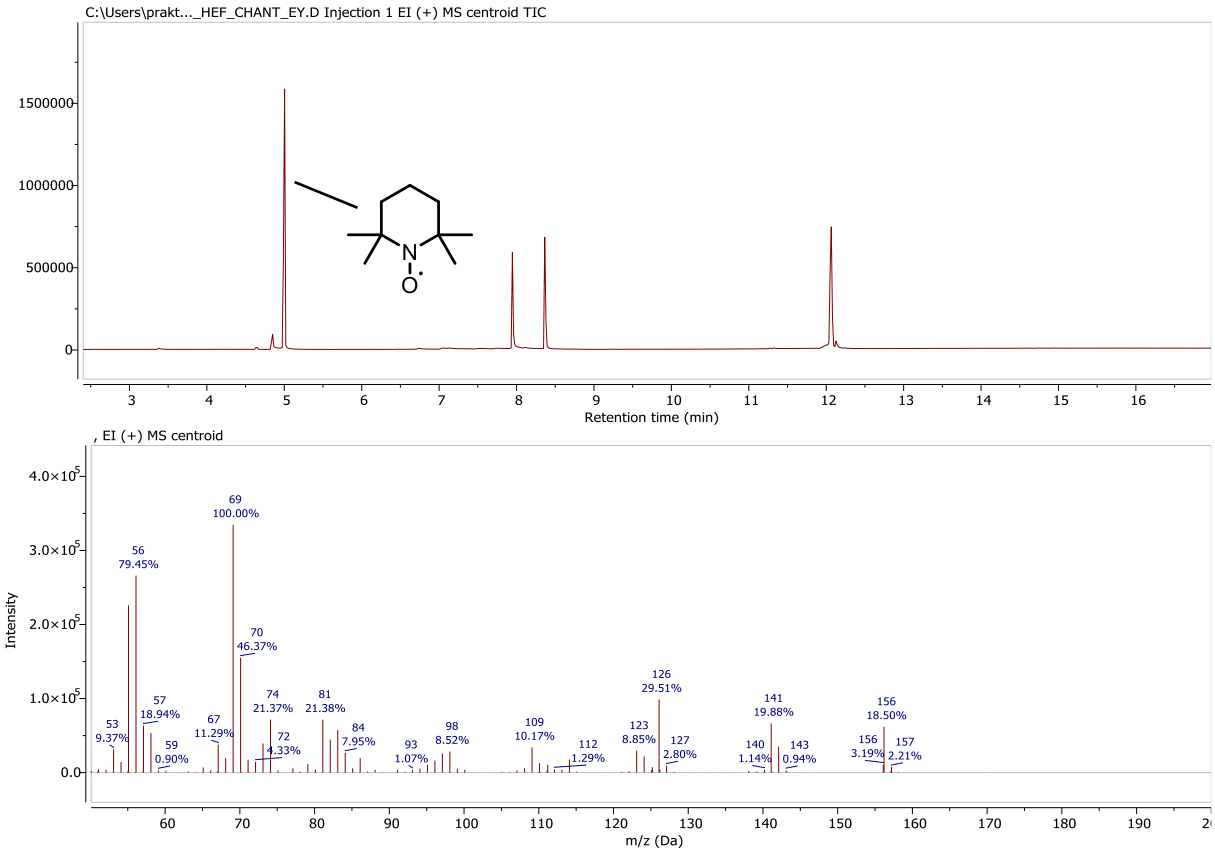


Figure 3. *GC-MS chromatogram of the crude reaction mixture and the EI-mass spectrum of detected TEMPO.*

Quantum Yield Measurements

The reaction quantum yield Φ_{R} was measured using a *Quantum Yield Determination Setup* (*QYDS*) by Eberhard Riedle *et al.* (U. Megerle, R. Lechner, B. König, E. Riedle, Photochem. Photobiol. Sci. **2010**, 9, 1400–1406, see www.qyds.info for further details). The setup is shown schematically in Figure 4 below. The LED light source (*Osram* GT-CS8PM1.13) is powered by a *Korad* KA3005P DC Power Supply. The light is passed through a sample cuvette onto a standard solar cell. The voltage is read by a *PicoScope* 2204A USB Oscilloscope and converted to a power reading after prior calibration using a *Coherent* PowerMax USB PS19Q.

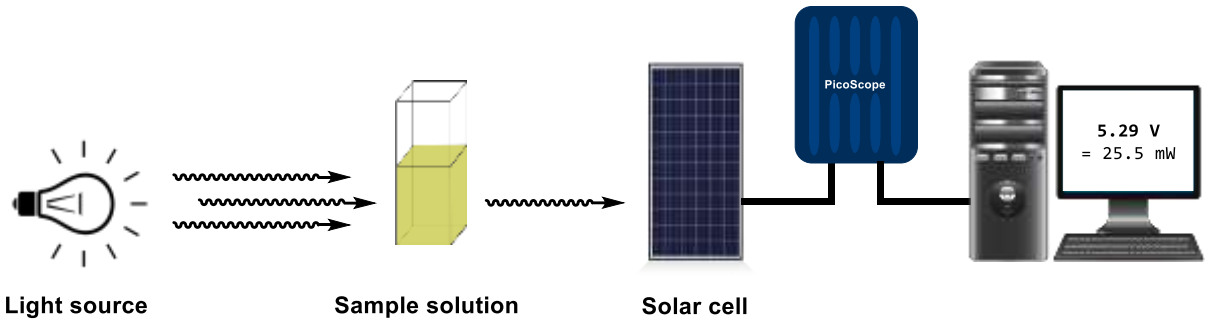


Figure 4. *Schematic depiction of the setup used for quantum yield determination.*

The energy of the light that has been absorbed by the reaction mixture is

$$E_{abs} = \mathrm{h}\upsilon \cdot N_{\mathrm{Photons}} = \frac{\mathrm{hc}}{\lambda} \cdot N_{\mathrm{Photons}} \tag{1}$$

and also

$$E_{abs} = P_{\mathrm{beam}} t - \int_{t=0}^{t} P(t)\, dt \tag{2}$$

with P_{beam} being the radiant flux of the beam itself and $P(t)$ being the power of the solar cell measured over time throughout the irradiation of the sample. This leads to

$$N_{\mathrm{Photons}} = \frac{\lambda}{\mathrm{hc}} \left(P_{\mathrm{beam}} t - \int_{t=0}^{t} P(t)\, dt \right) \tag{3}$$

Using the definition of the reaction quantum yield

$$\Phi_{\mathrm{R}} = \frac{N_{\mathrm{Molecules}}}{N_{\mathrm{Photons}}} \tag{4}$$

results in

$$\Phi_{\mathrm{R}} = \frac{\mathrm{hc} \cdot N_{\mathrm{Molecules}}}{\lambda \left(P_{\mathrm{beam}} t - \int_{t=0}^{t} P(t)\, dt \right)} \tag{5}$$

Combining the constants, including the unit conversions, and using $N_{\mathrm{Molecules}} = n \cdot \mathrm{N_A}$:

$$\Phi_{\mathrm{R}} = 1994000 \cdot \frac{n}{\lambda \left(P_{\mathrm{beam}} t - \int_{t=0}^{t} P(t)\, dt \right)} \tag{6}$$

with n being the amount of product in **mmol**, λ being the wavelength of the light in **nm**, P_{beam} being the radiant flux of the light beam in **mW**, t being the irradiation time in **min**, and $\int_{t=0}^{t} P(t)\, dt$ being the integral of the radiant flux vs. time plot in **mW·min**.

Illumination was performed at λ = 521 nm at a constant current of 58.0 mA and a voltage of 2.92 V. The radiant flux of the beam after passing through the cuvette containing the solvent P_{beam} was found to be 27.89 mW with a voltage of 10.58 V being measured (calibration factor: 2.636 mW·V^{-1} at 520 nm).

The reaction between **1** and **2a** was set up under standard conditions on a scale of 200 µmol in a *Hellma* QS Transmission Cuvette (10 mm, screw cap) equipped with a stir bar. The reaction was irradiated for t = 30.0 min in total while stirring and measuring the radiant flux of the light beam after passing through the reaction mixture. The plot of the measured radiant flux vs. time is shown in Figure 5 below. The integral was found to be $\int_{t=0}^{t} P(t)\, dt = 17.2\ \mathrm{mW} \cdot \mathrm{min}$.

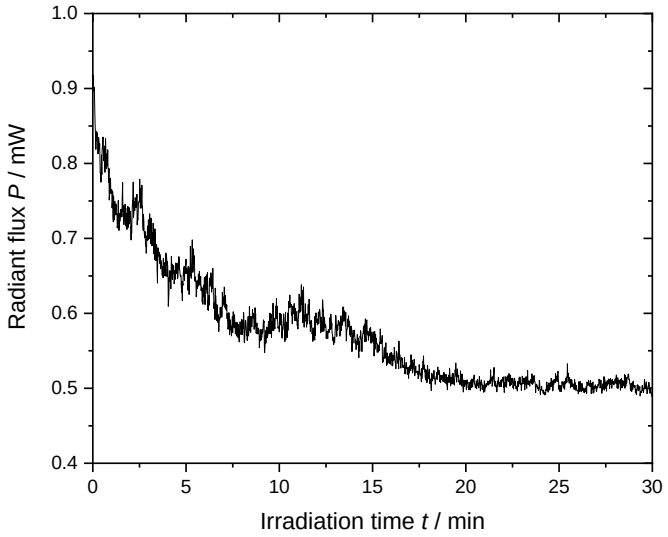
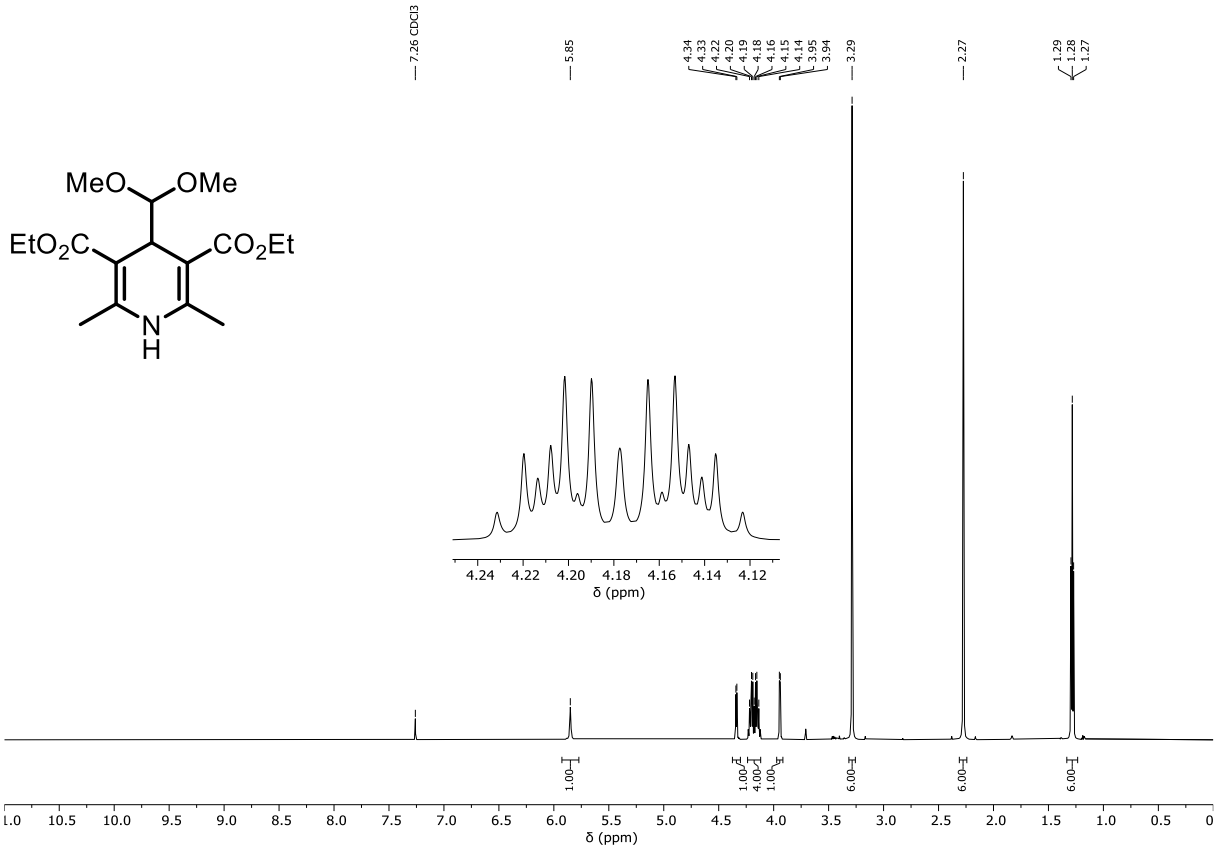


Figure 5. *Radiant flux detected by the solar cell during the irradiation period.*

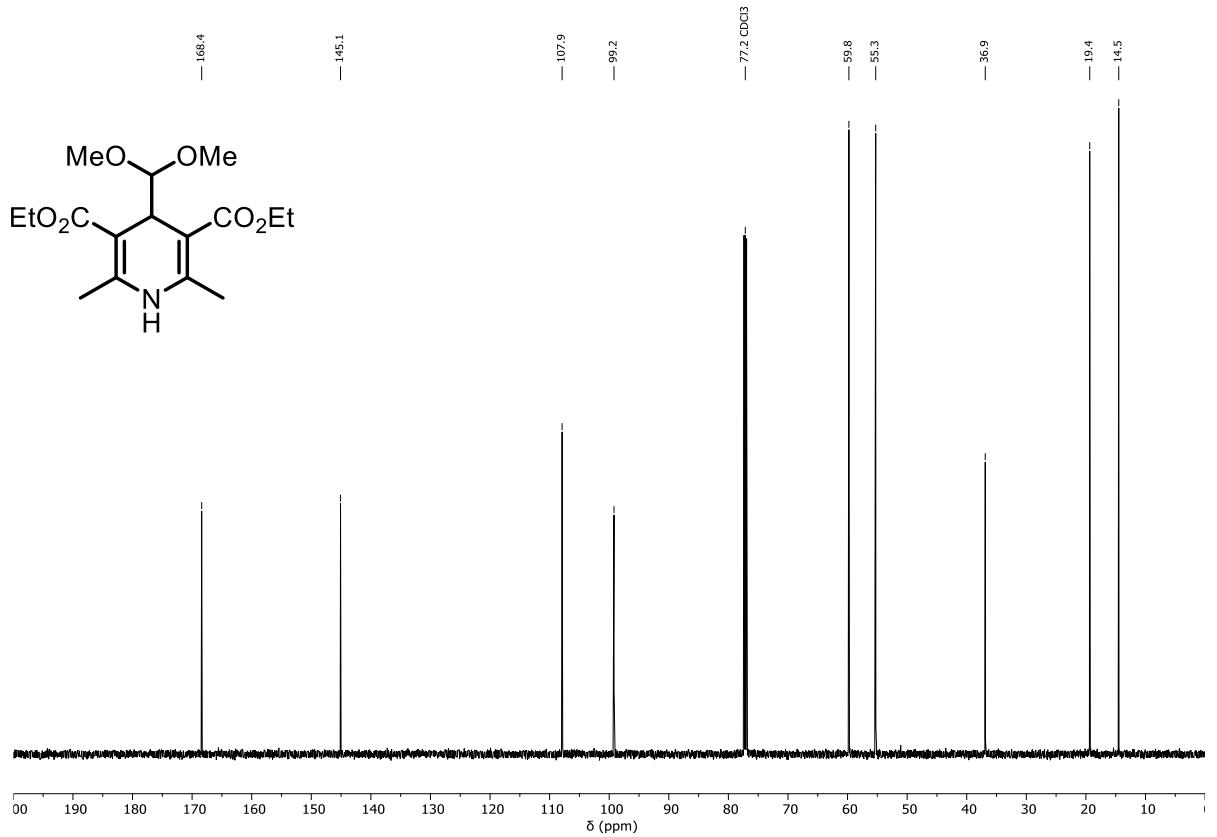
After irradiation, 1,3,5-trimethoxybenzene was added to the mixture as a standard and the yield was determined by ^{1}H NMR. A yield of 8.8% was found, that is 18·10^{-3} mmol.

According to equation 6: $\Phi_{\mathrm{R}} = 8.4\%$.

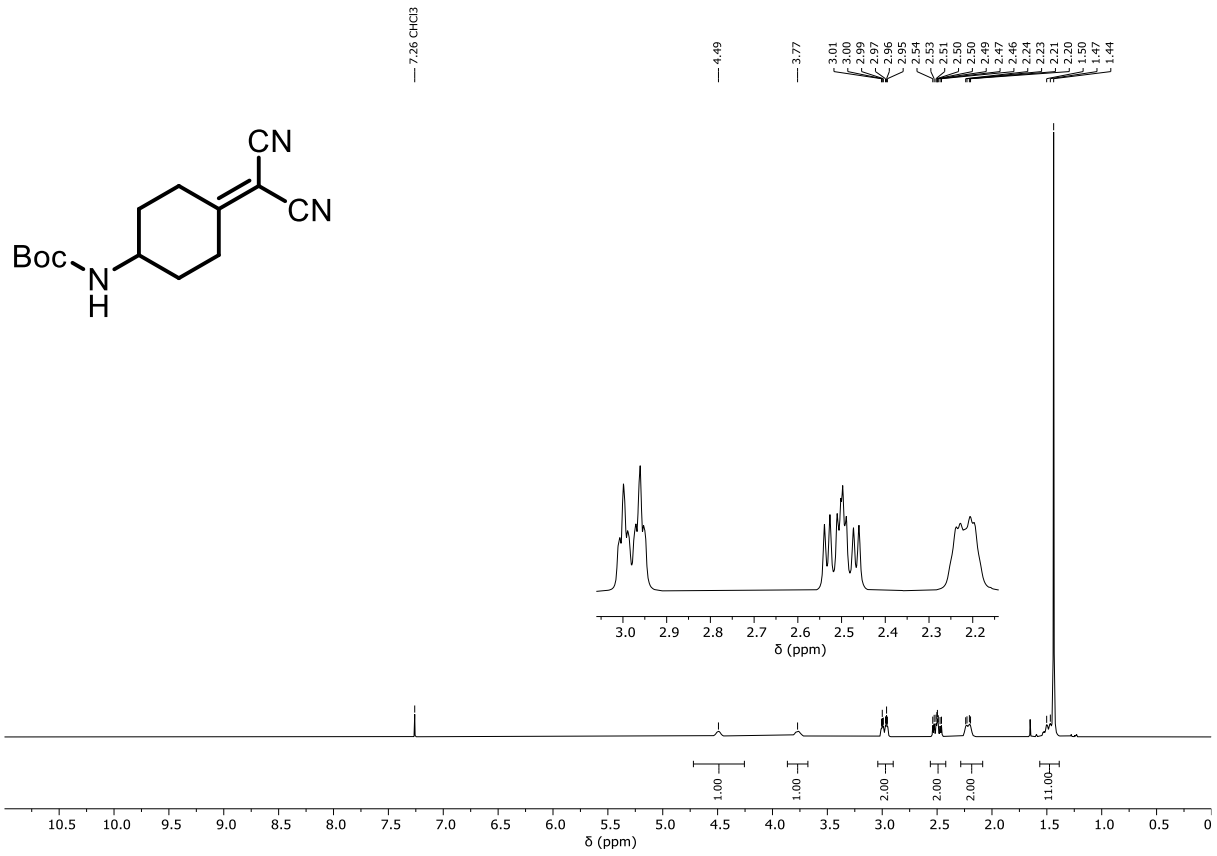
NMR Spectra of all Compounds



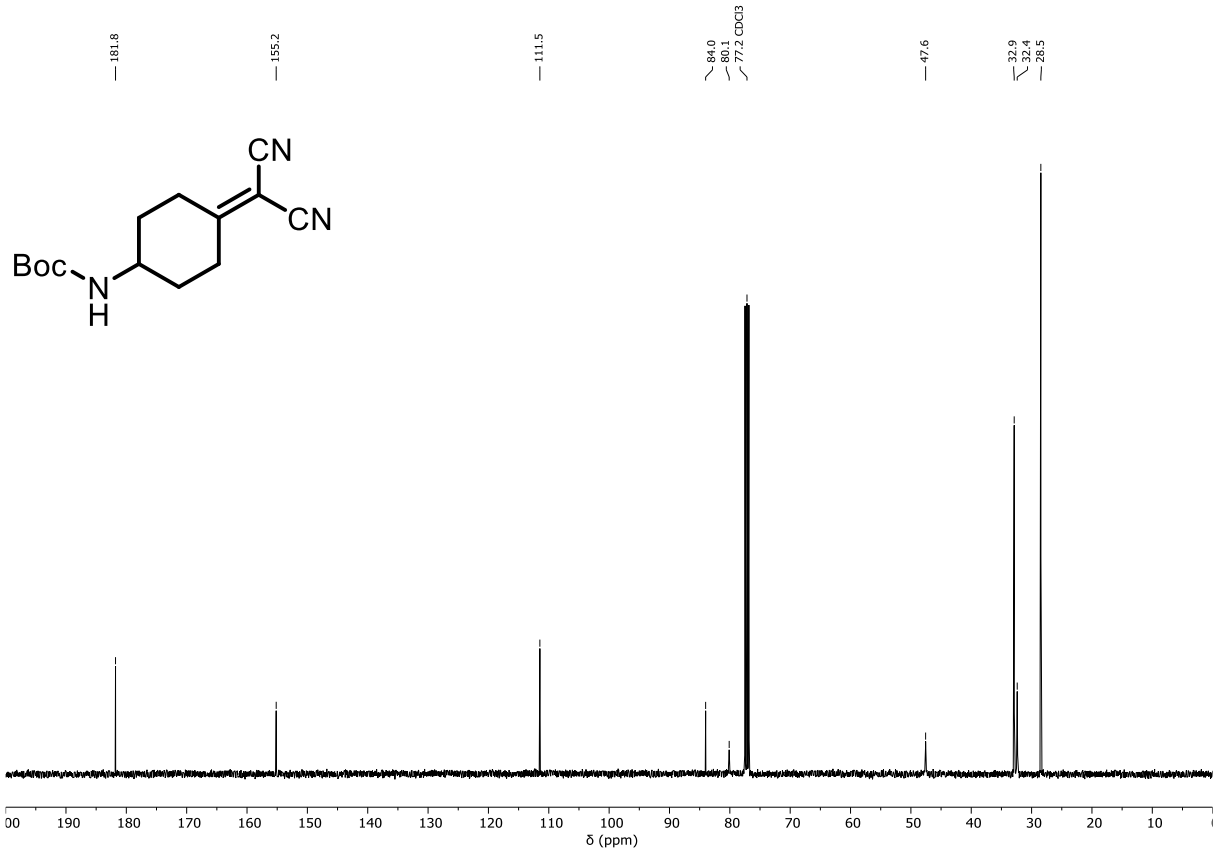
^{1}H NMR spectrum (600 MHz, $CDCl_3$) of **1**



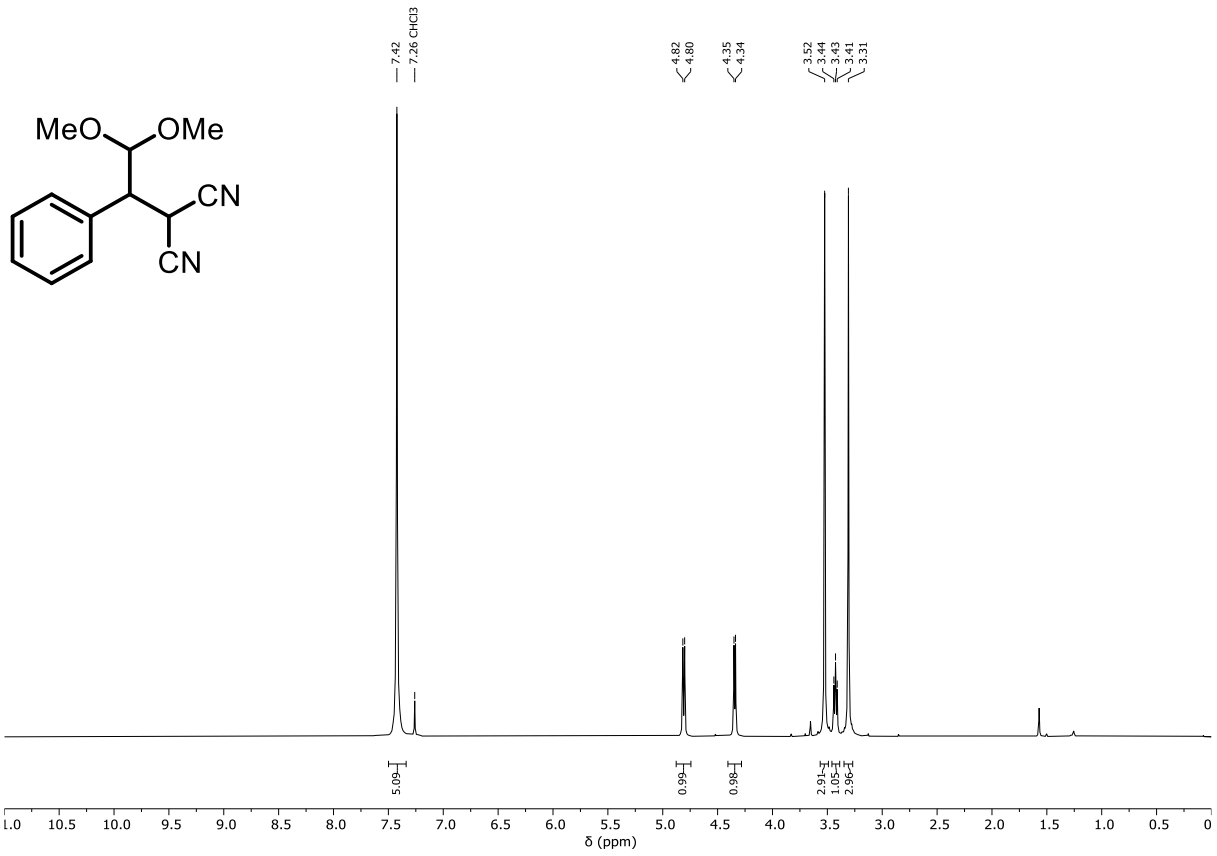
^{13}C NMR spectrum (151 MHz, $CDCl_3$) of **1**



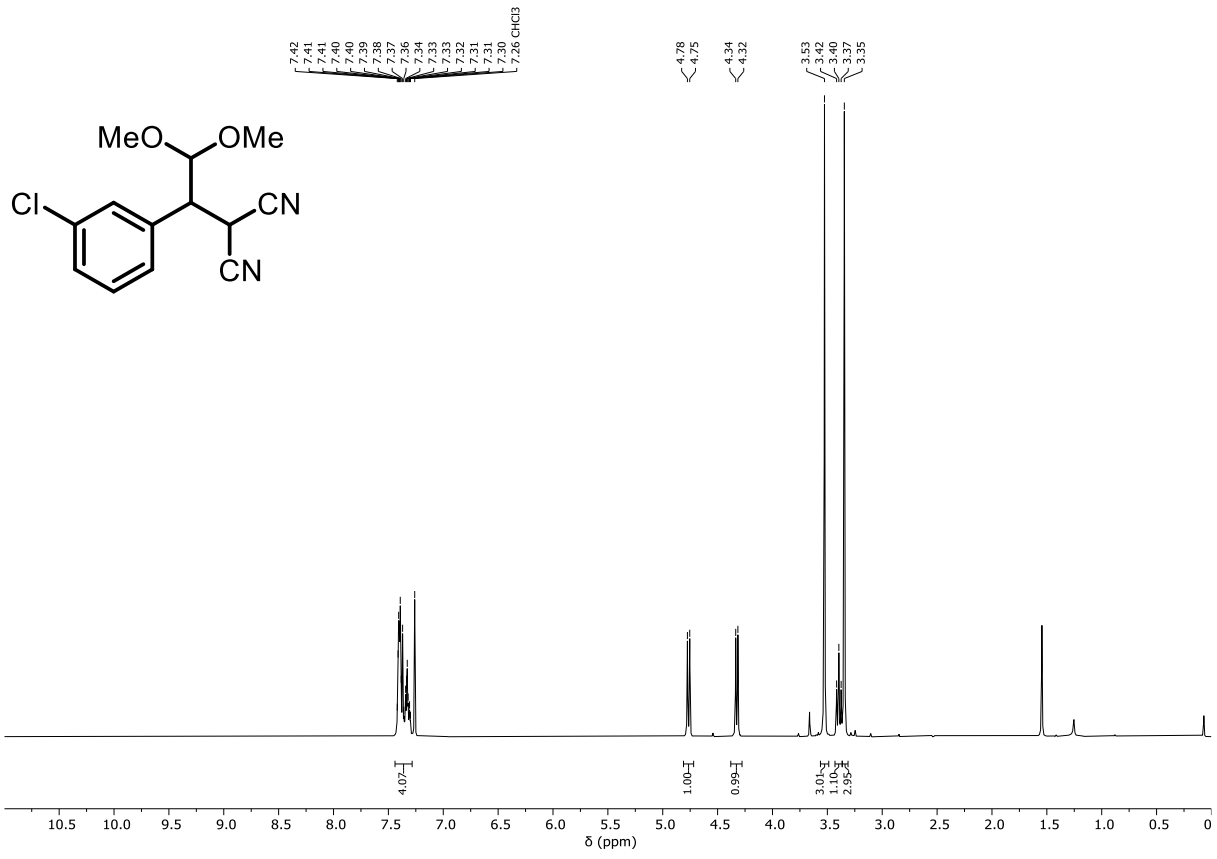
^{1}H NMR spectrum (400 MHz, $CDCl_3$) of **2z**



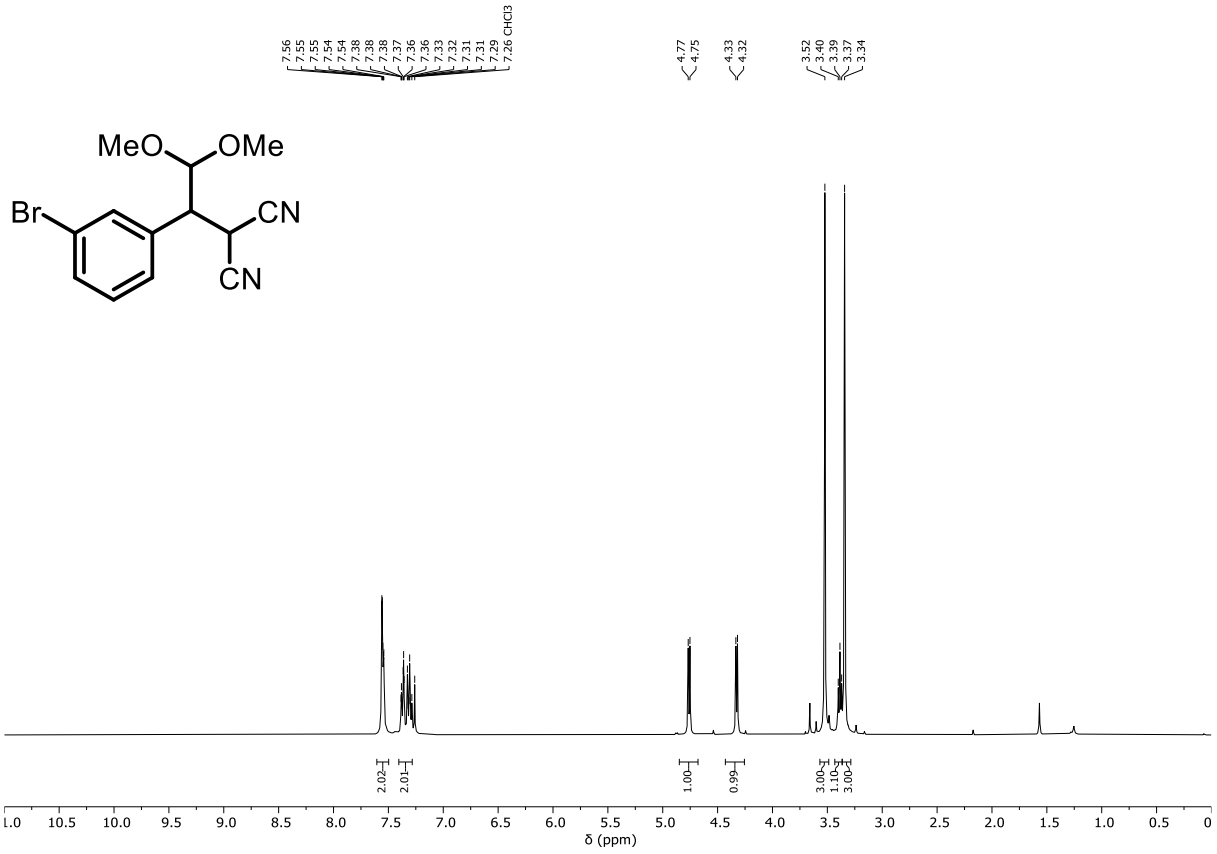
^{13}C NMR spectrum (101 MHz, $CDCl_3$) of **2z**



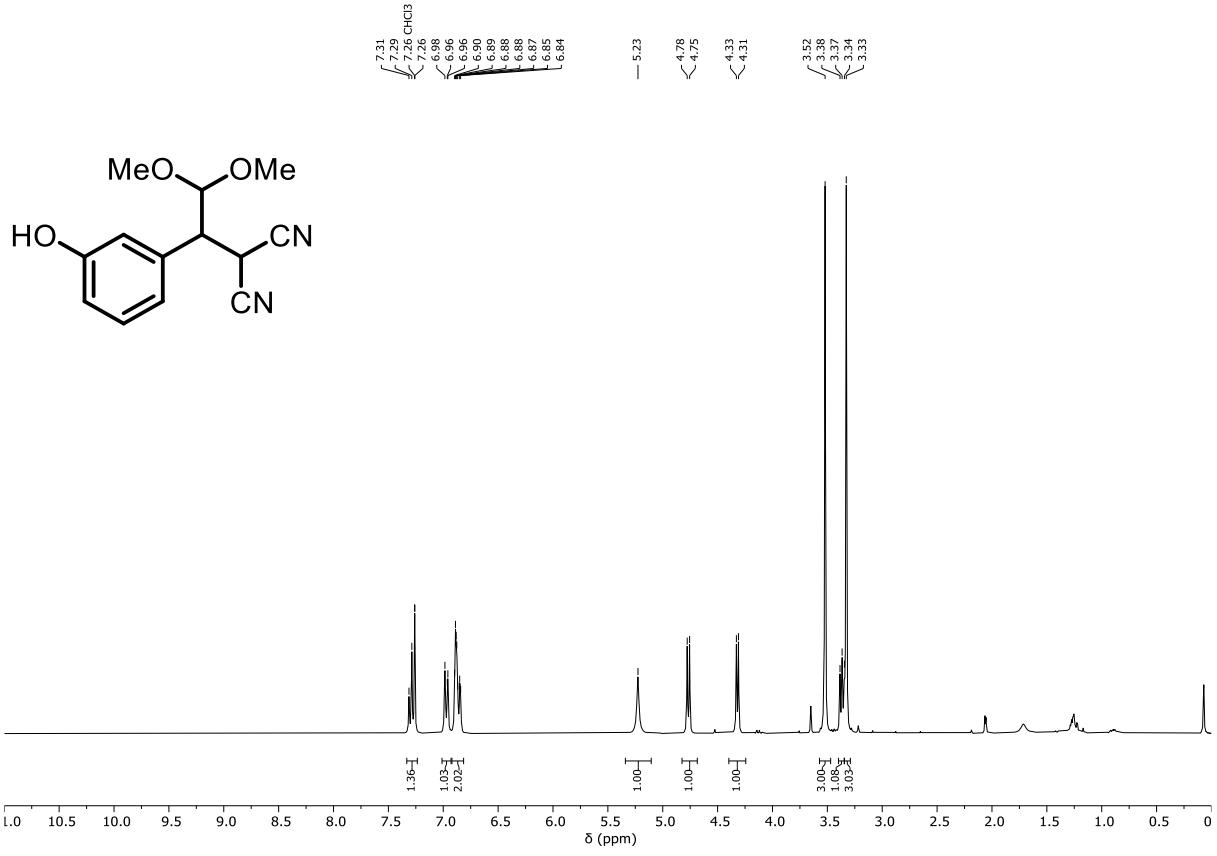
^{1}H NMR spectrum (400 MHz, $CDCl_3$) of **5a**



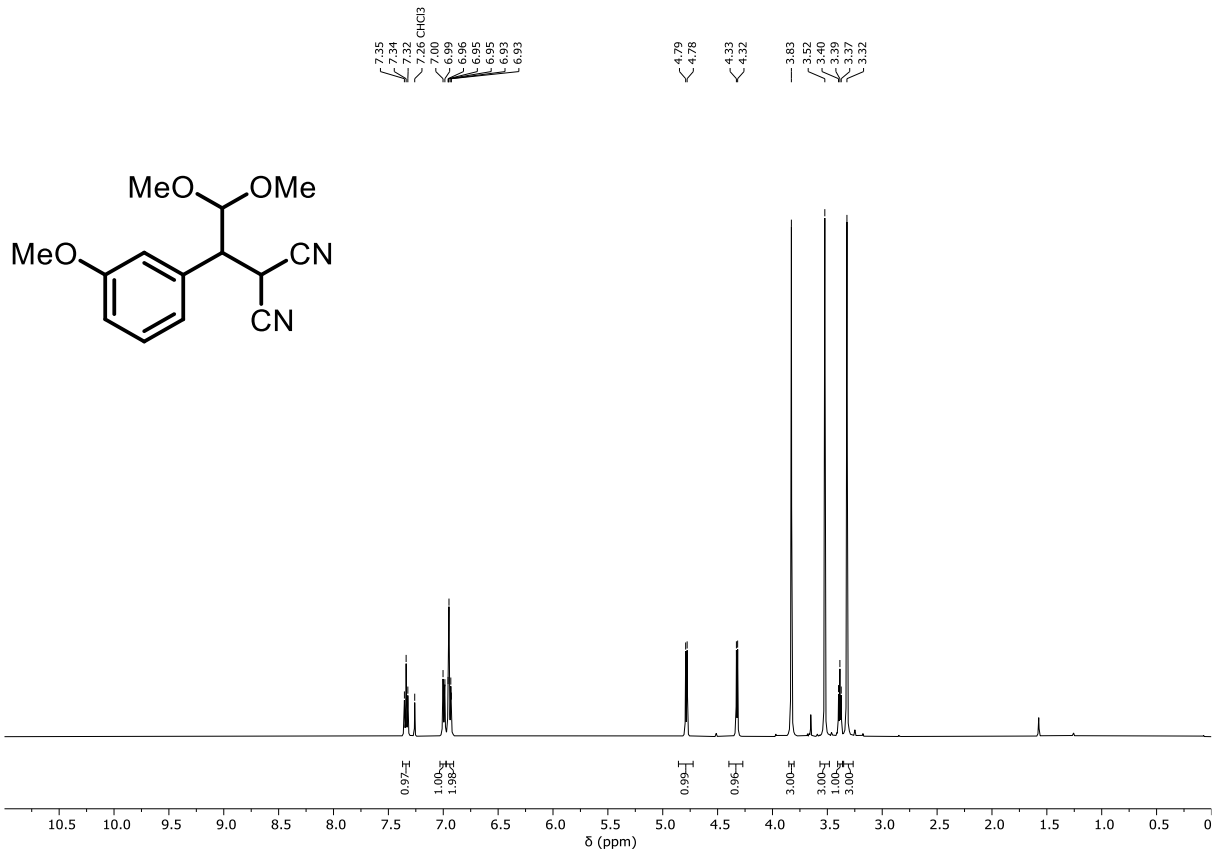
^{1}H NMR spectrum (300 MHz, $CDCl_3$) of **5b**



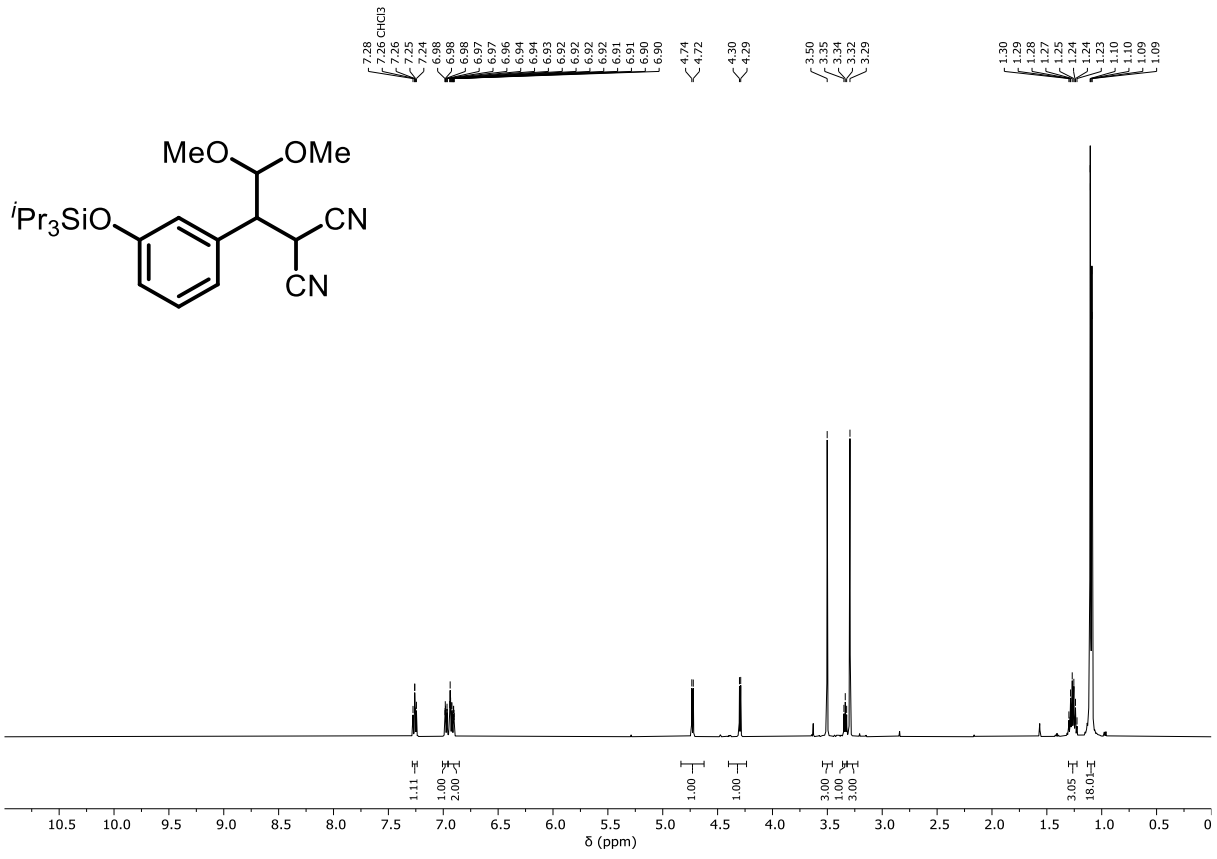
^{1}H NMR spectrum (400 MHz, $CDCl_3$) of **5c**



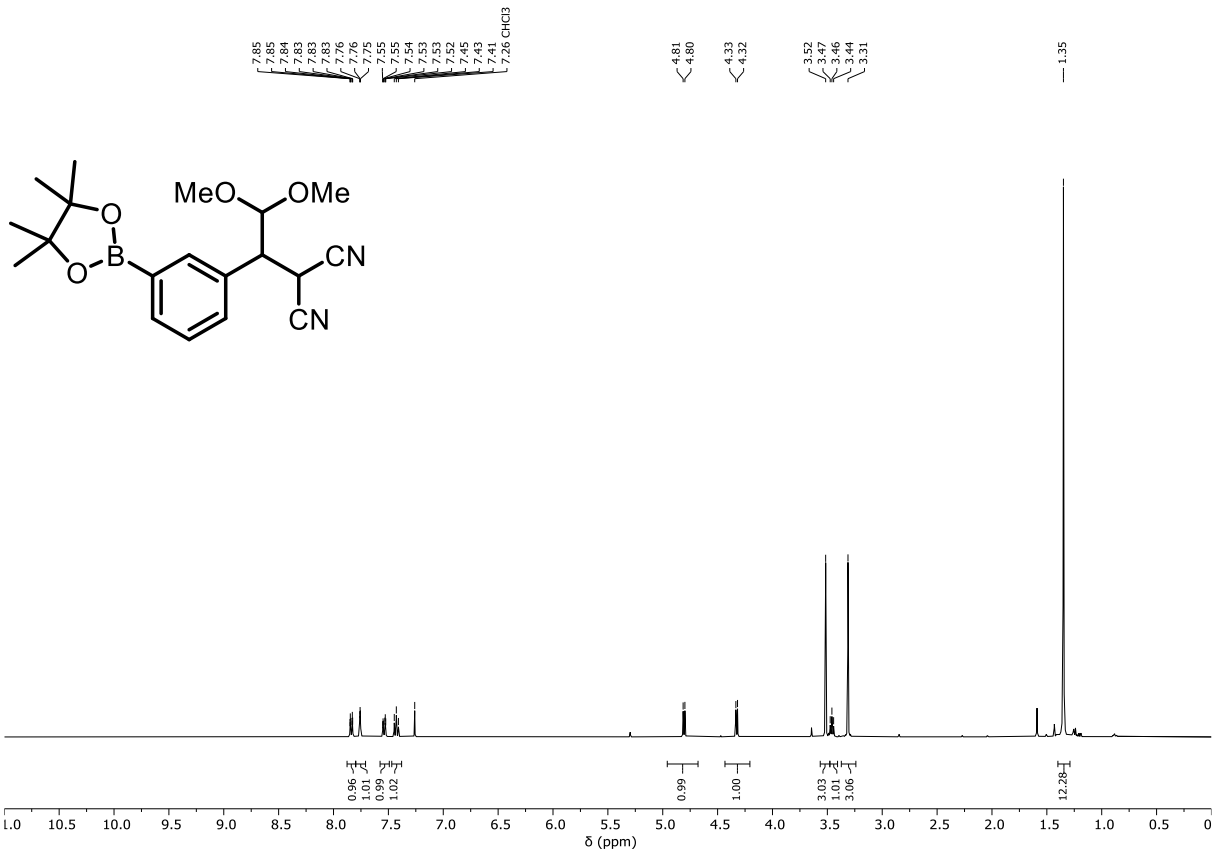
^{1}H NMR spectrum (300 MHz, $CDCl_3$) of **5d**



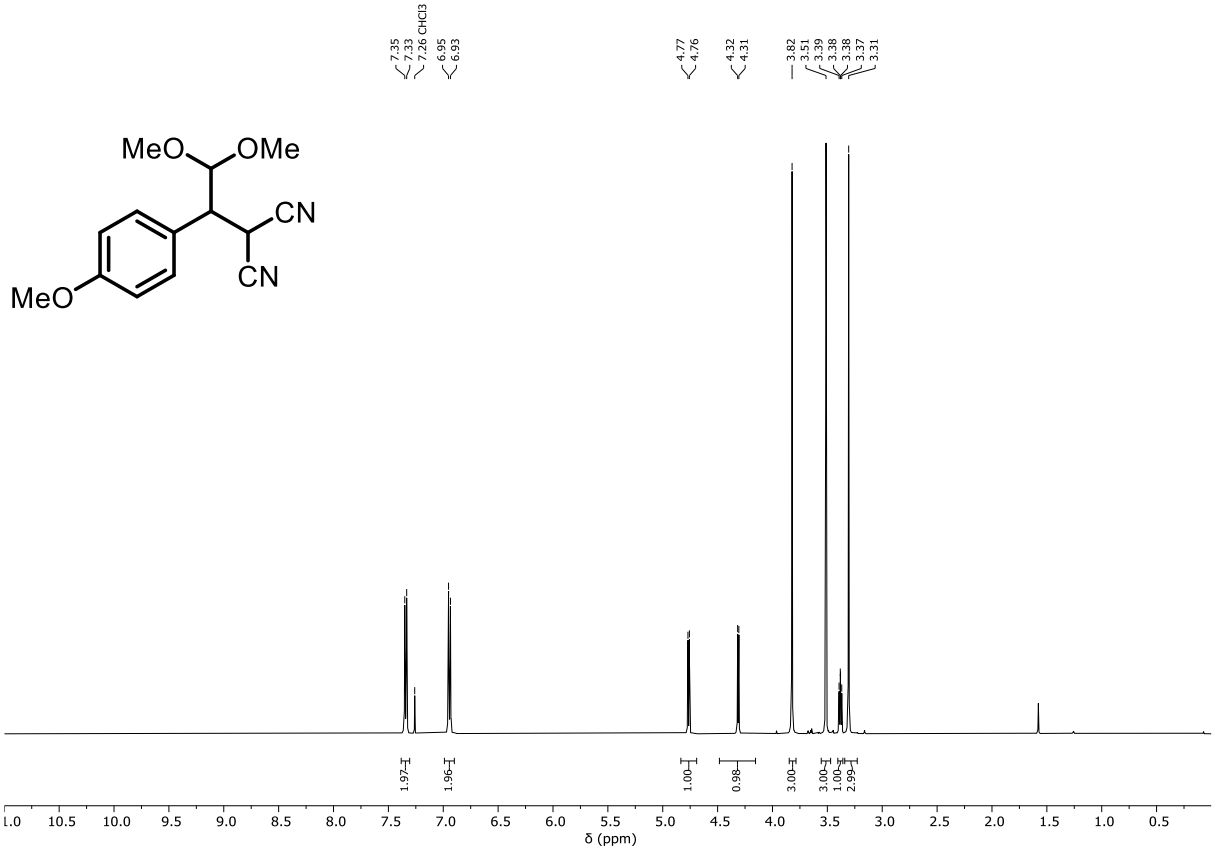
^{1}H NMR spectrum (500 MHz, $CDCl_3$) of **5e**



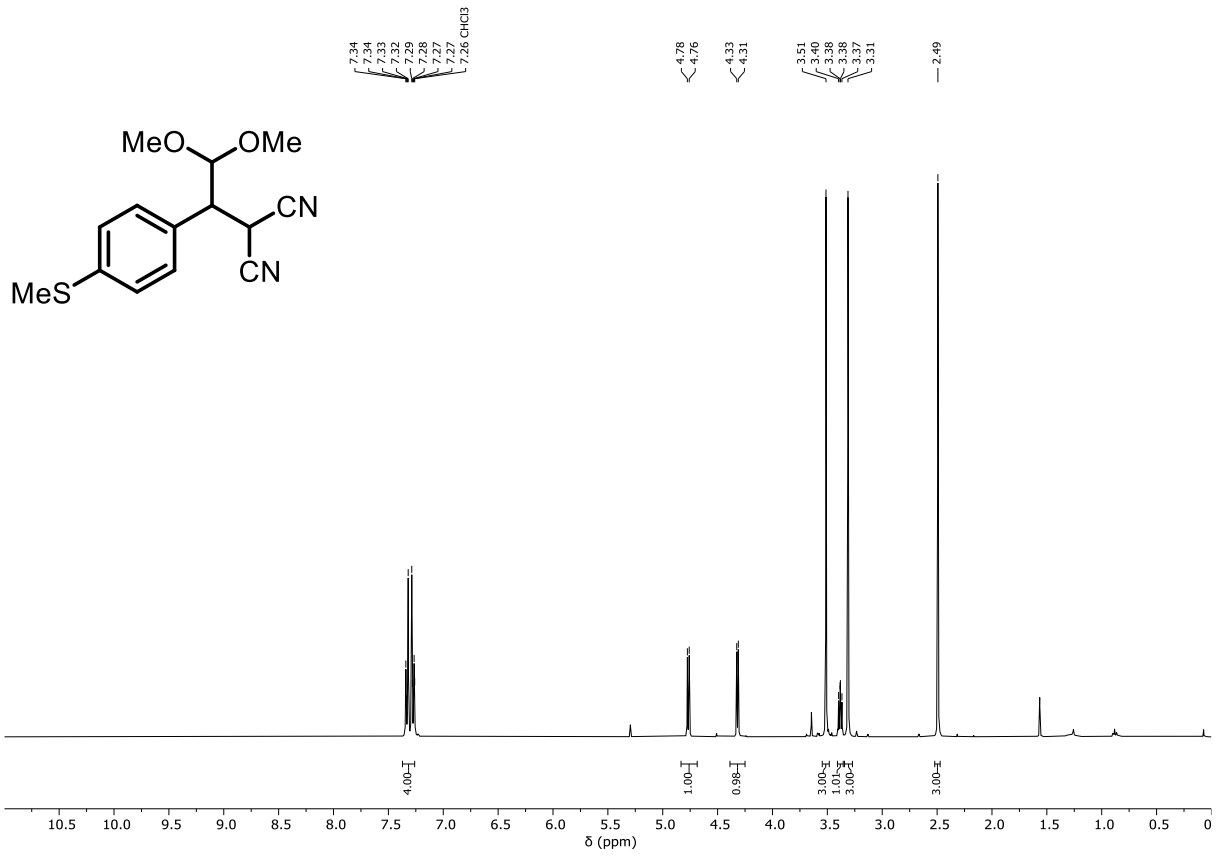
^{1}H NMR spectrum (500 MHz, $CDCl_3$) of **5f**



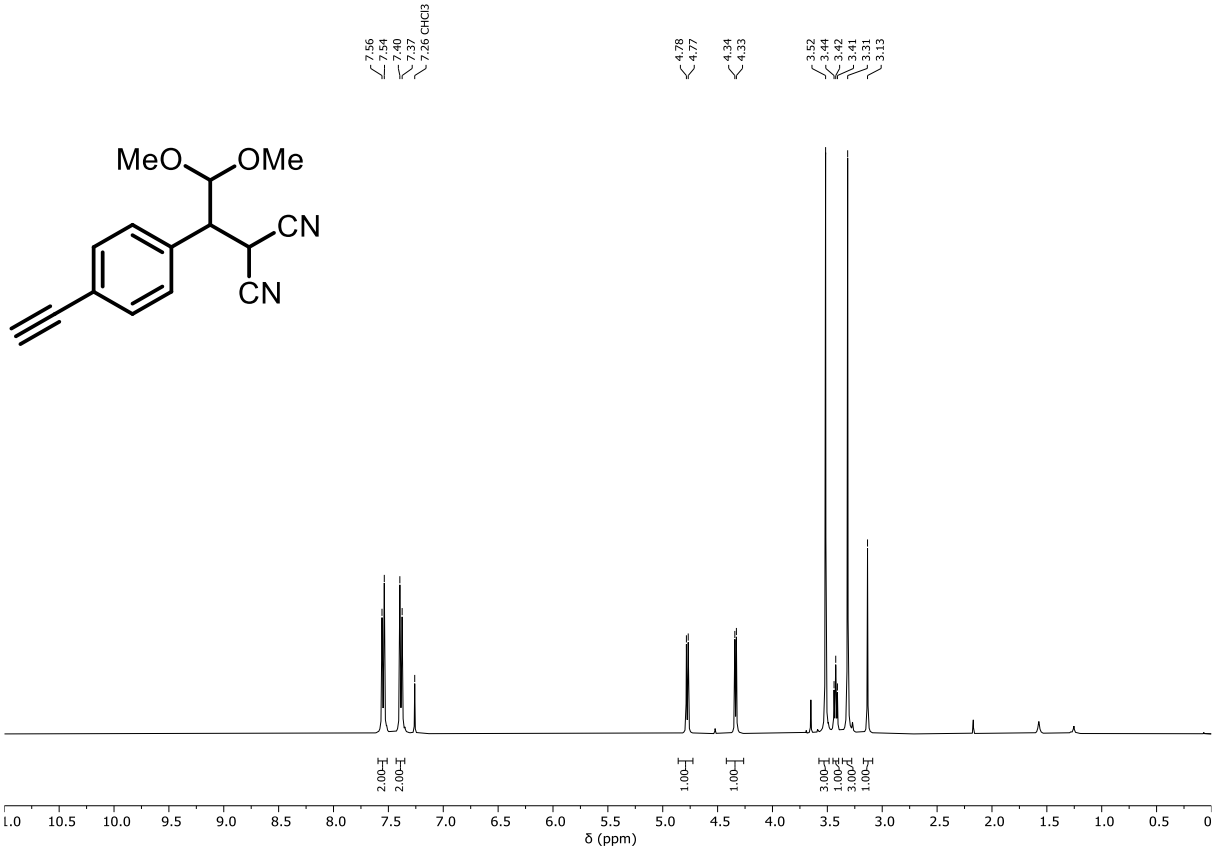
^{1}H NMR spectrum (400 MHz, $CDCl_3$) of **5g**



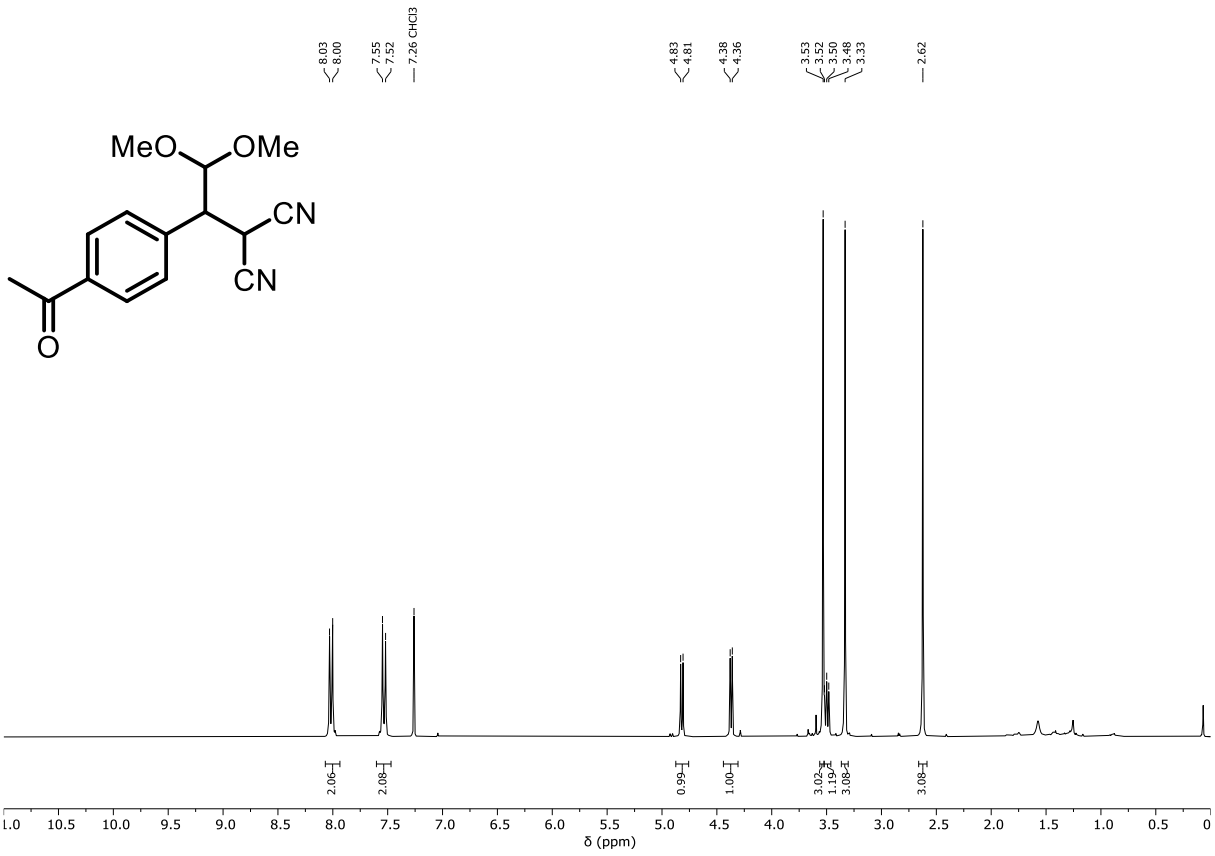
^{1}H NMR spectrum (500 MHz, $CDCl_3$) of **5i**



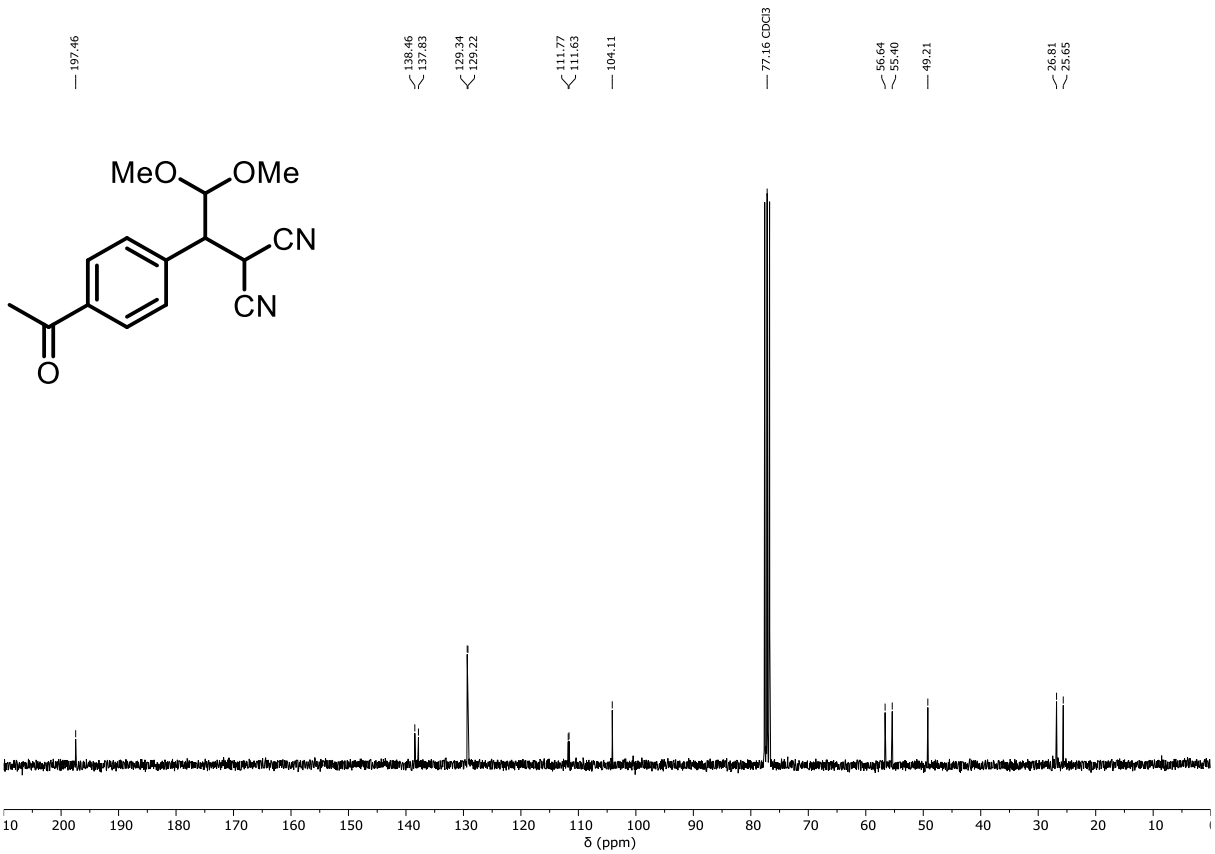
^{1}H NMR spectrum (400 MHz, $CDCl_3$) of **5j**



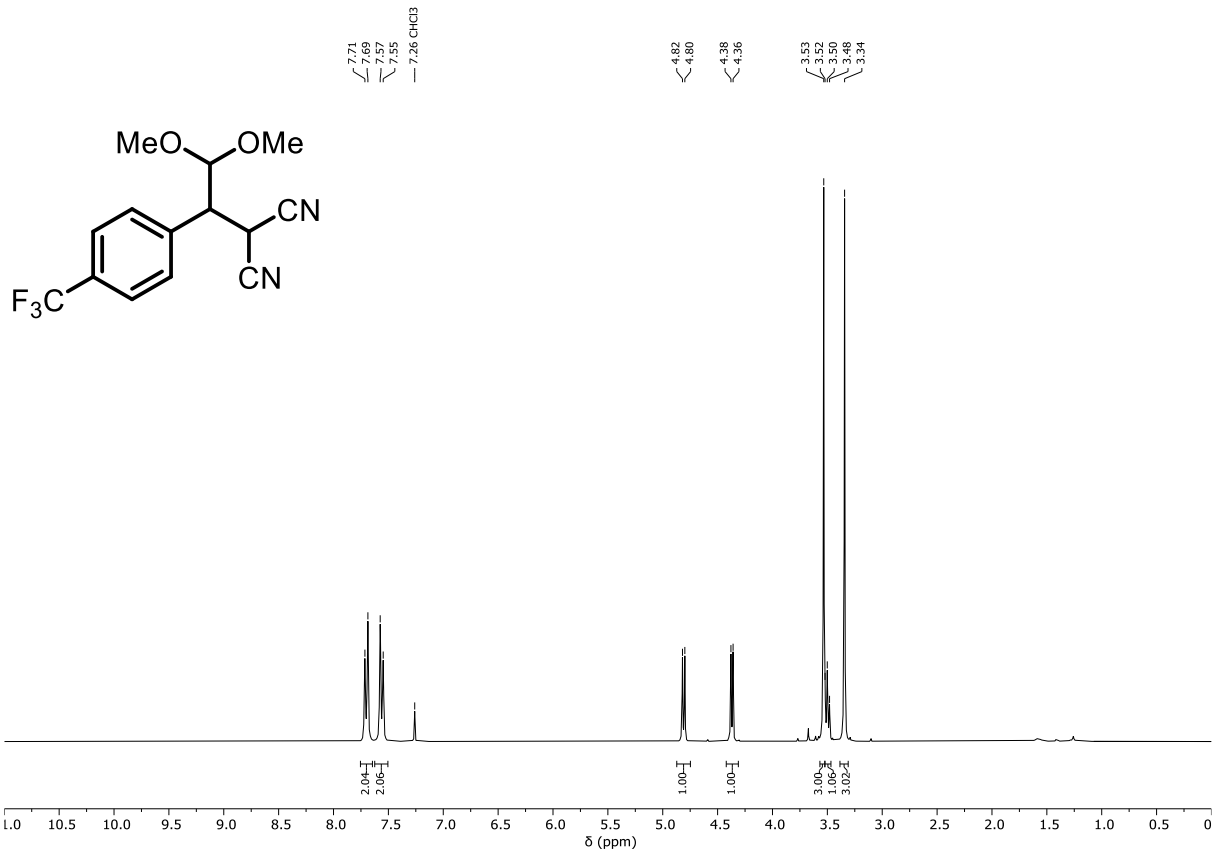
^{1}H NMR spectrum (400 MHz, $CDCl_3$) of **5k**



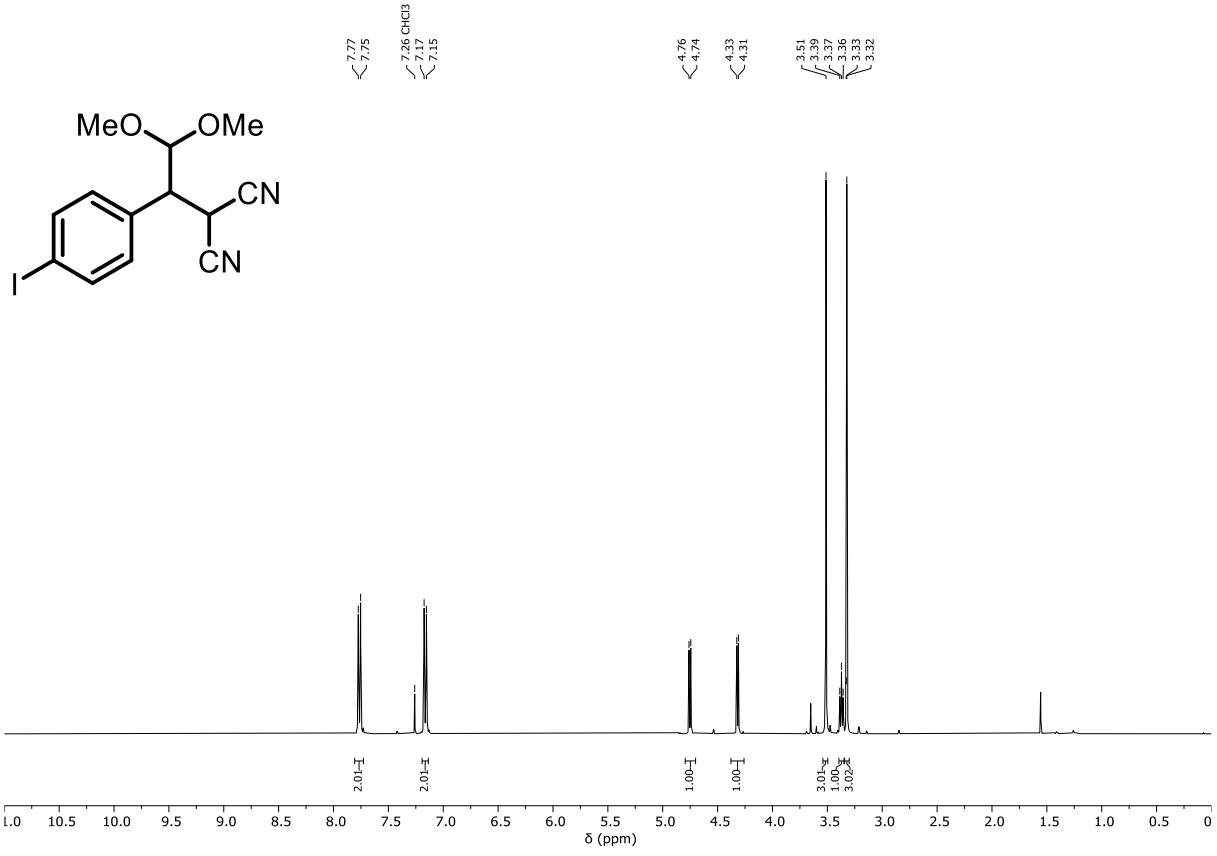
^{1}H NMR spectrum (300 MHz, $CDCl_3$) of **5m**



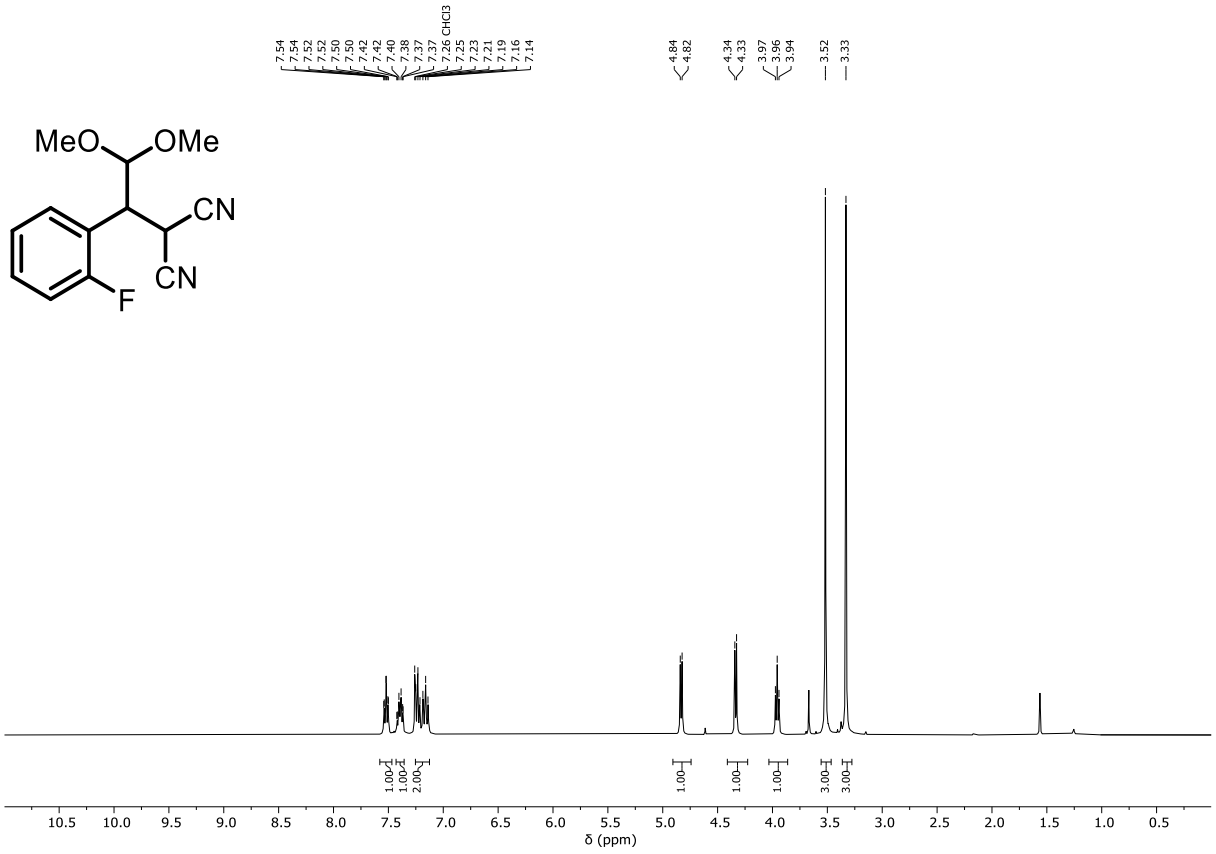
^{13}C NMR spectrum (75.5 MHz, $CDCl_3$) of **5m**



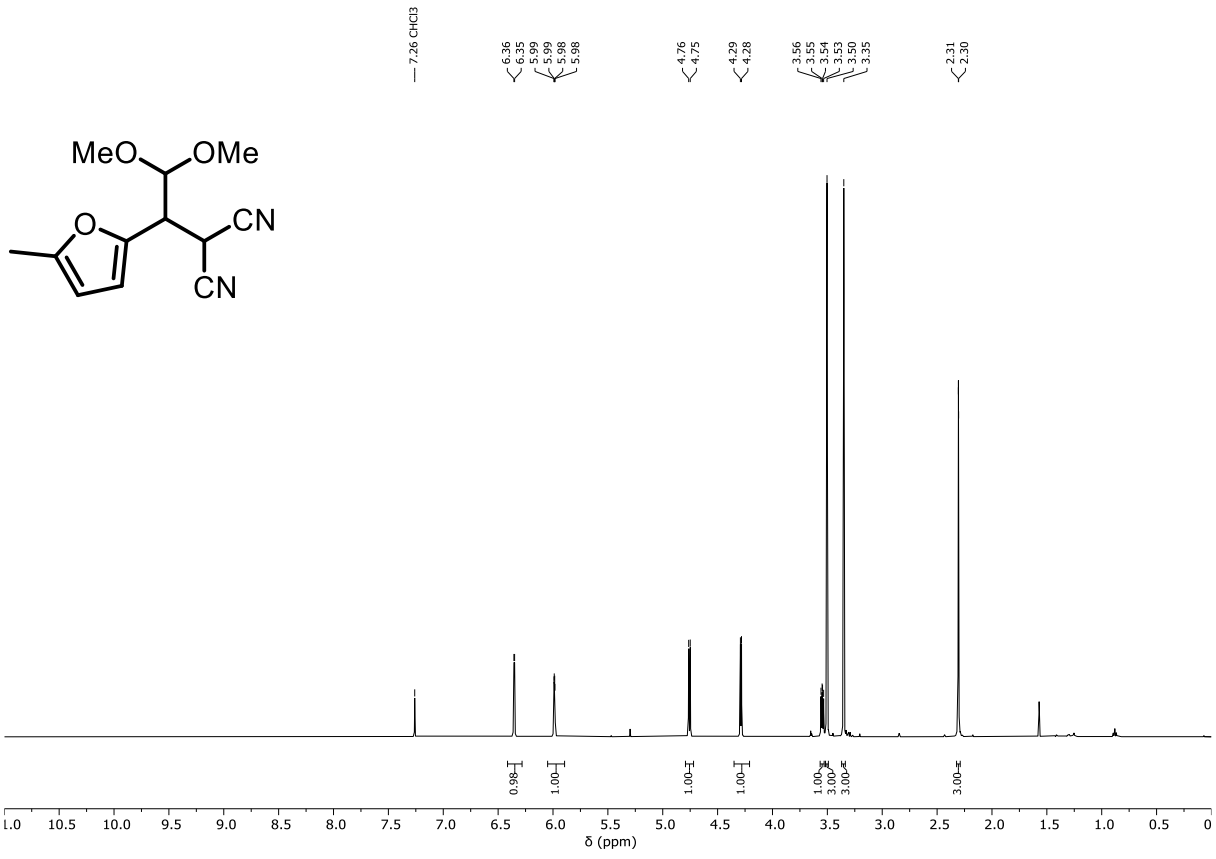
^{1}H NMR spectrum (300 MHz, $CDCl_3$) of **5n**



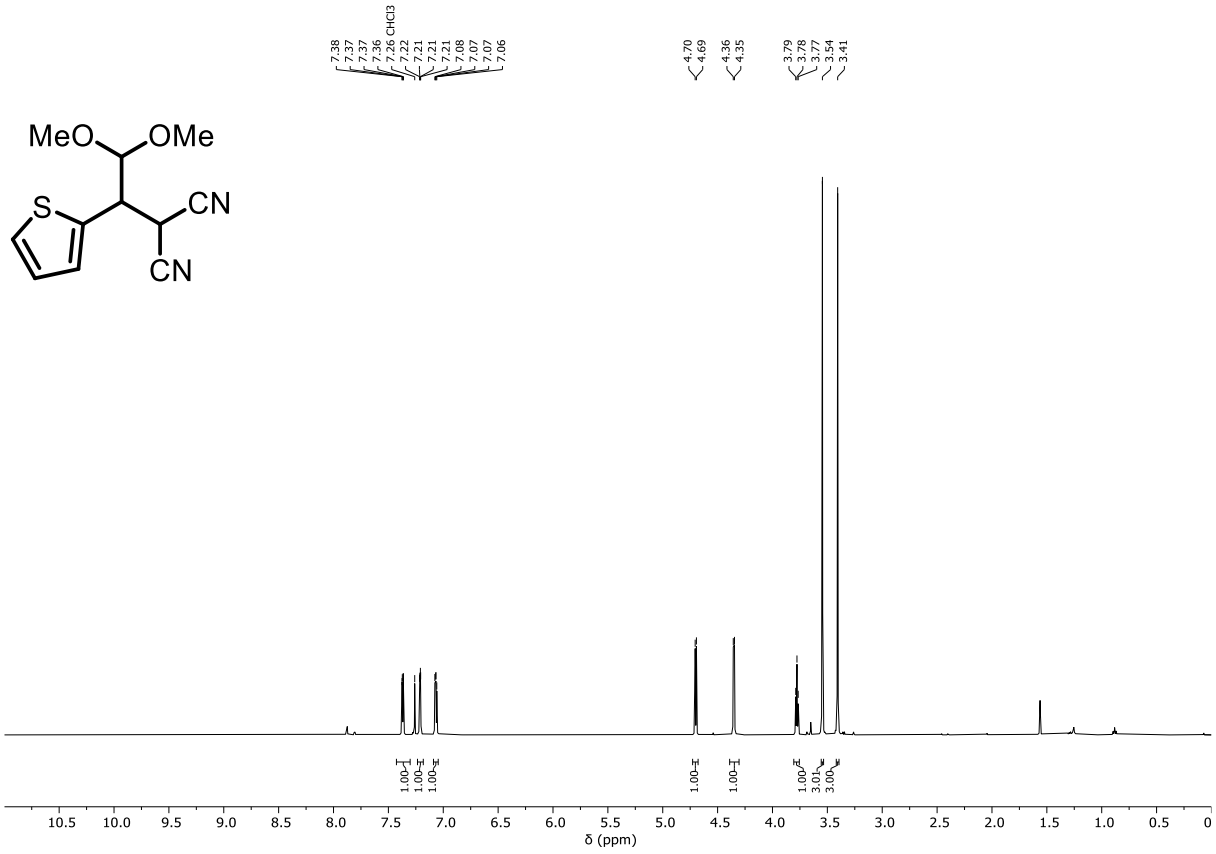
^{1}H NMR spectrum (400 MHz, $CDCl_3$) of **5q**



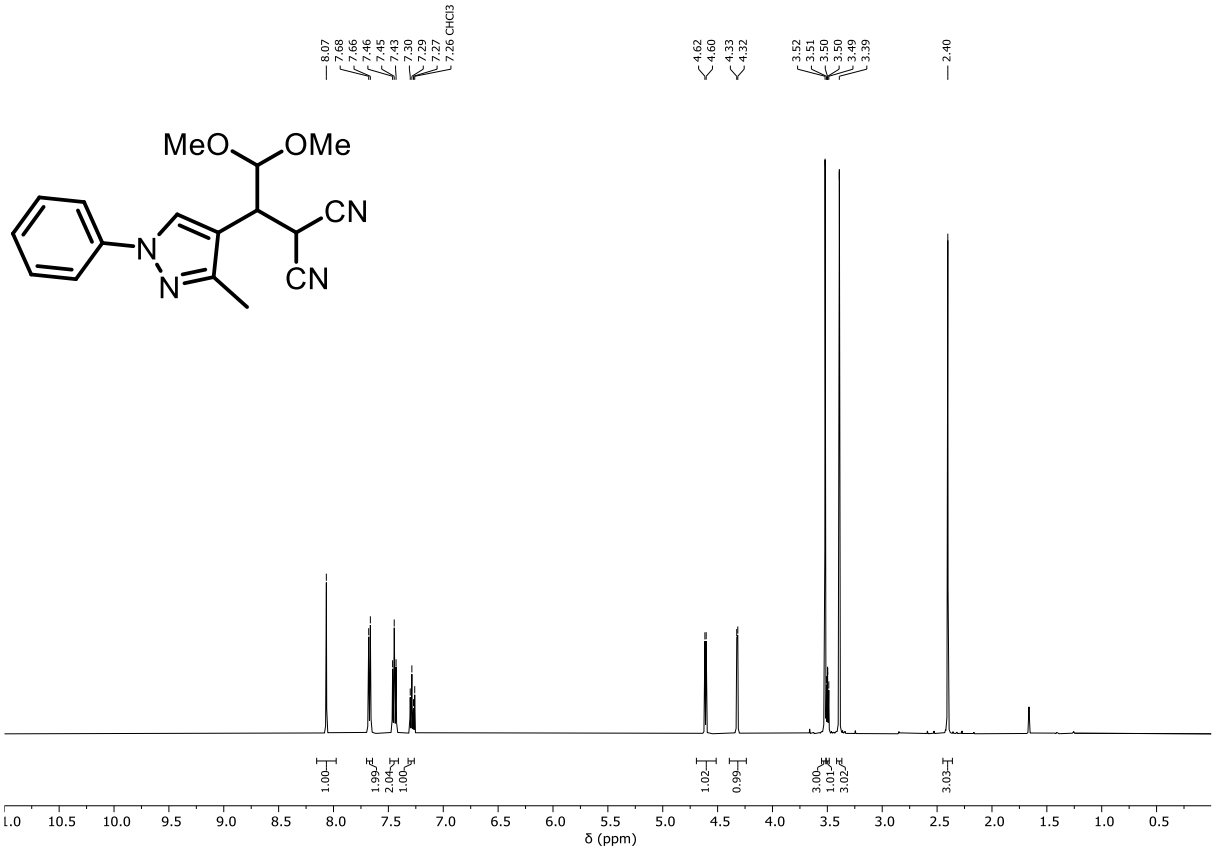
^{1}H NMR spectrum (400 MHz, $CDCl_3$) of **5r**



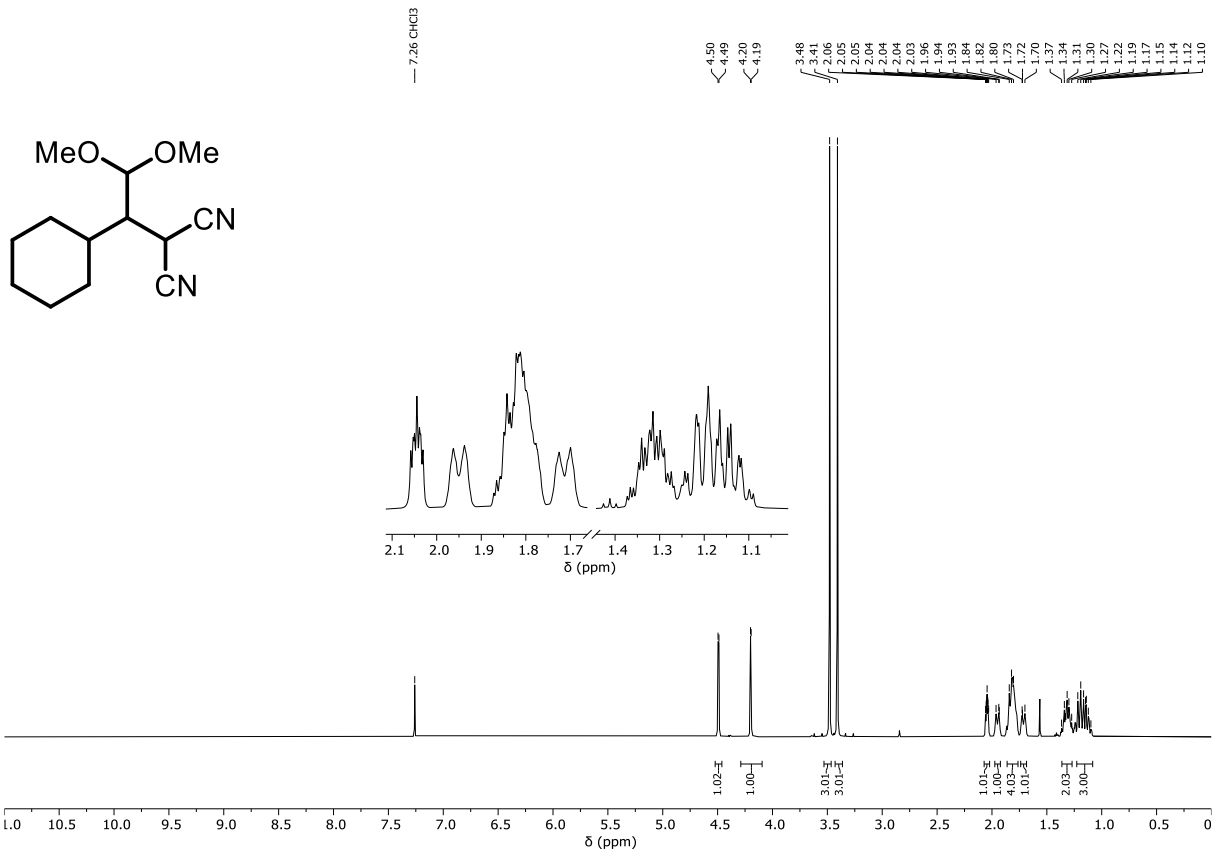
^{1}H NMR spectrum (500 MHz, $CDCl_3$) of **5t**



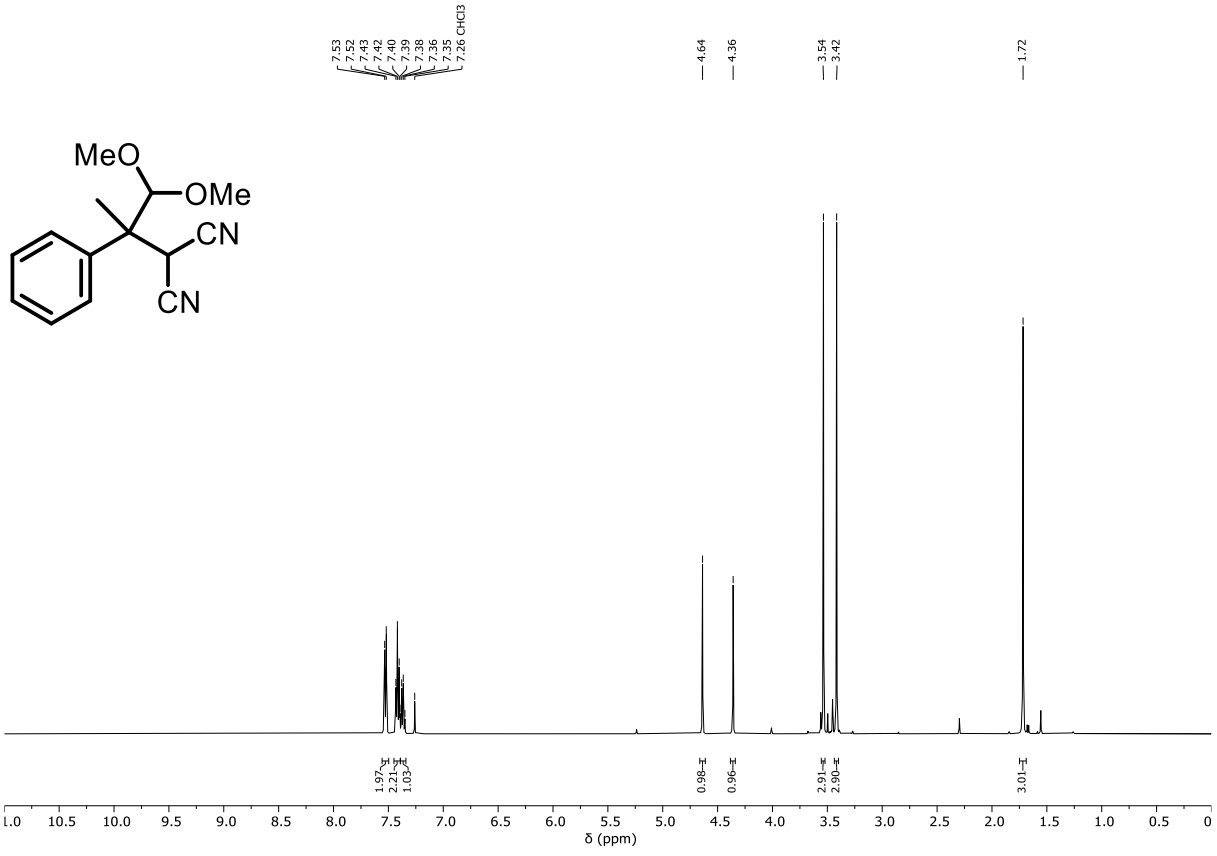
^{1}H NMR spectrum (500 MHz, $CDCl_3$) of **5u**



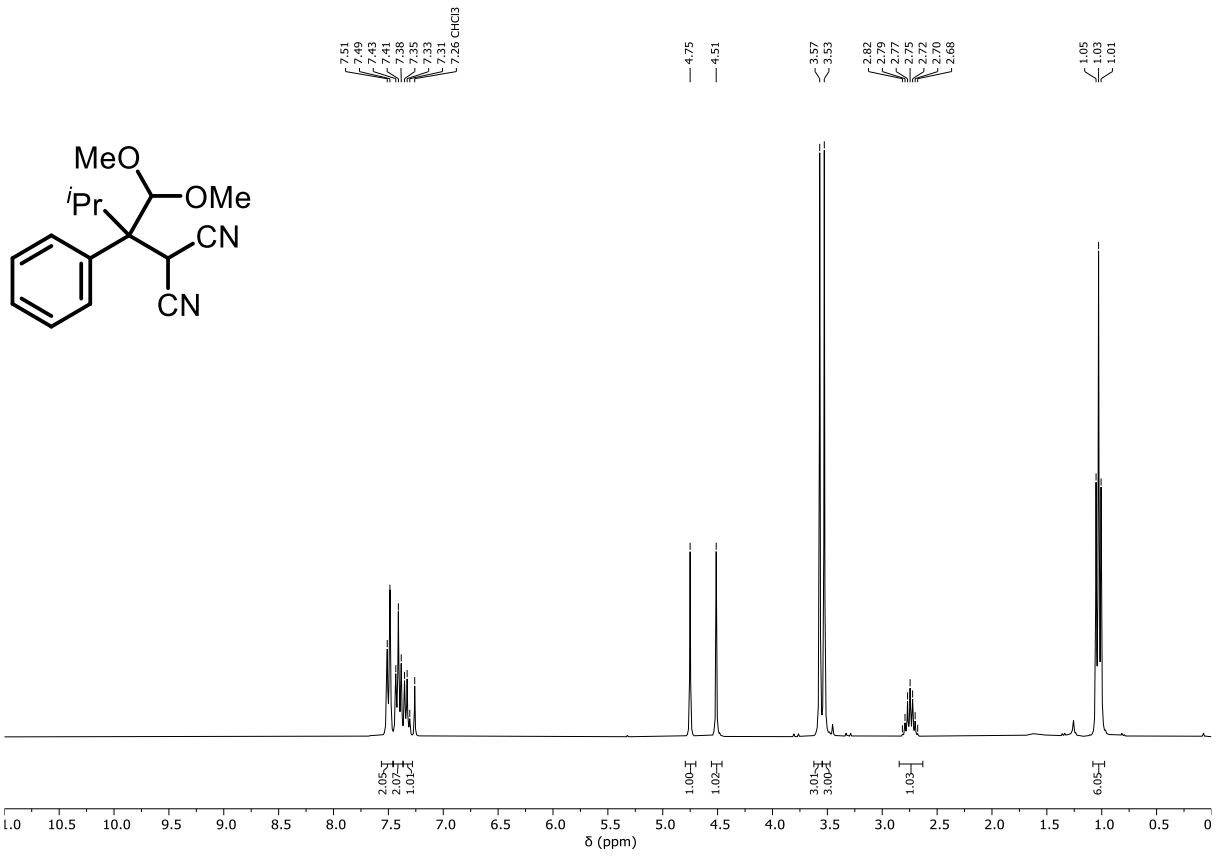
^{1}H NMR spectrum (500 MHz, $CDCl_3$) of **5v**



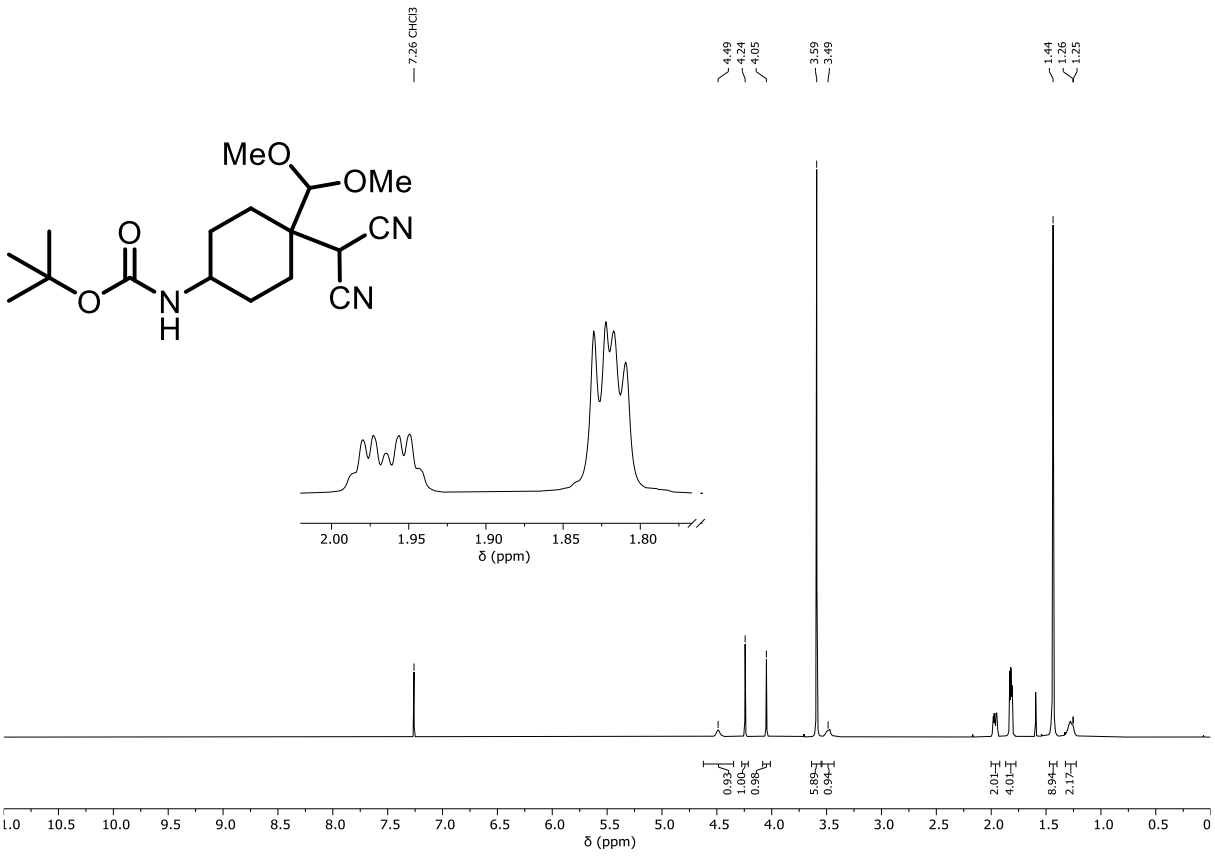
^{1}H NMR spectrum (600 MHz, $CDCl_3$) of **5v**



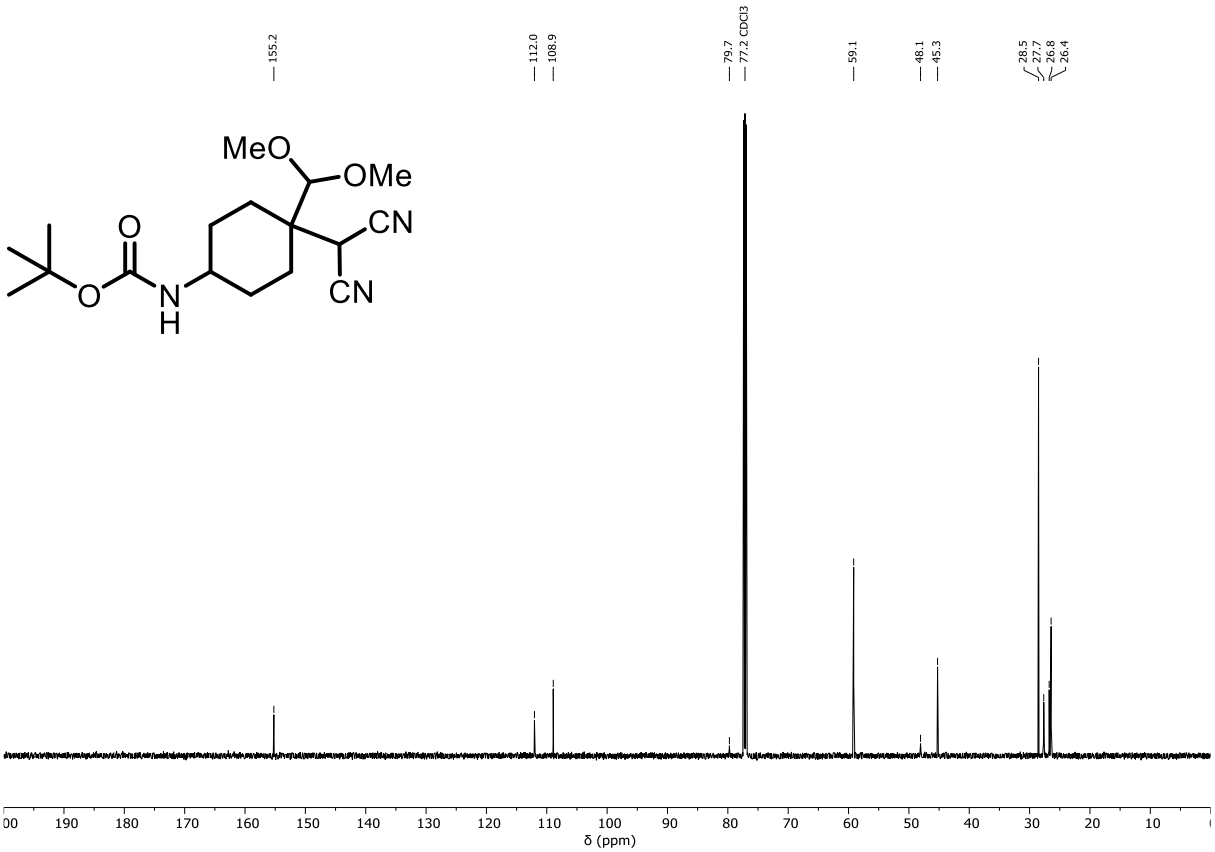
^{1}H NMR spectrum (500 MHz, $CDCl_3$) of **5w**



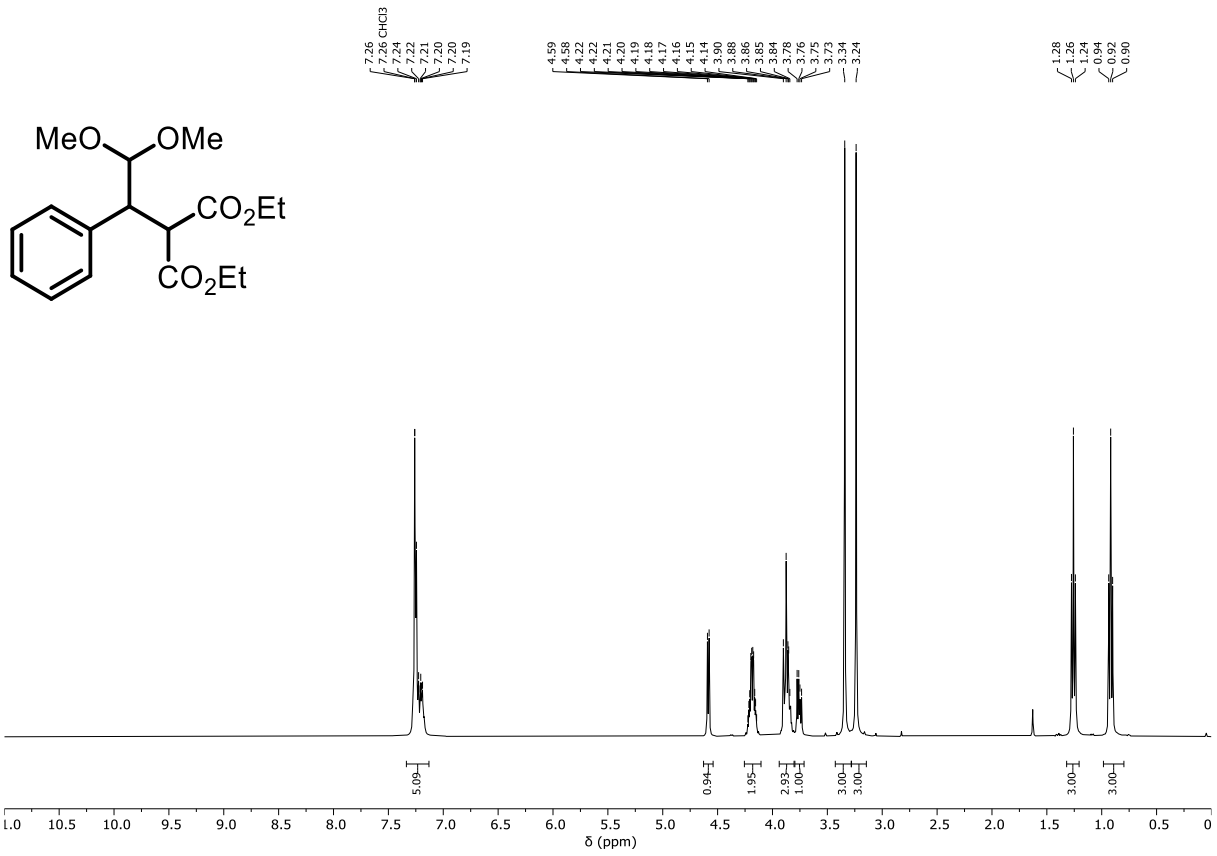
^{1}H NMR spectrum (300 MHz, $CDCl_3$) of **5x**



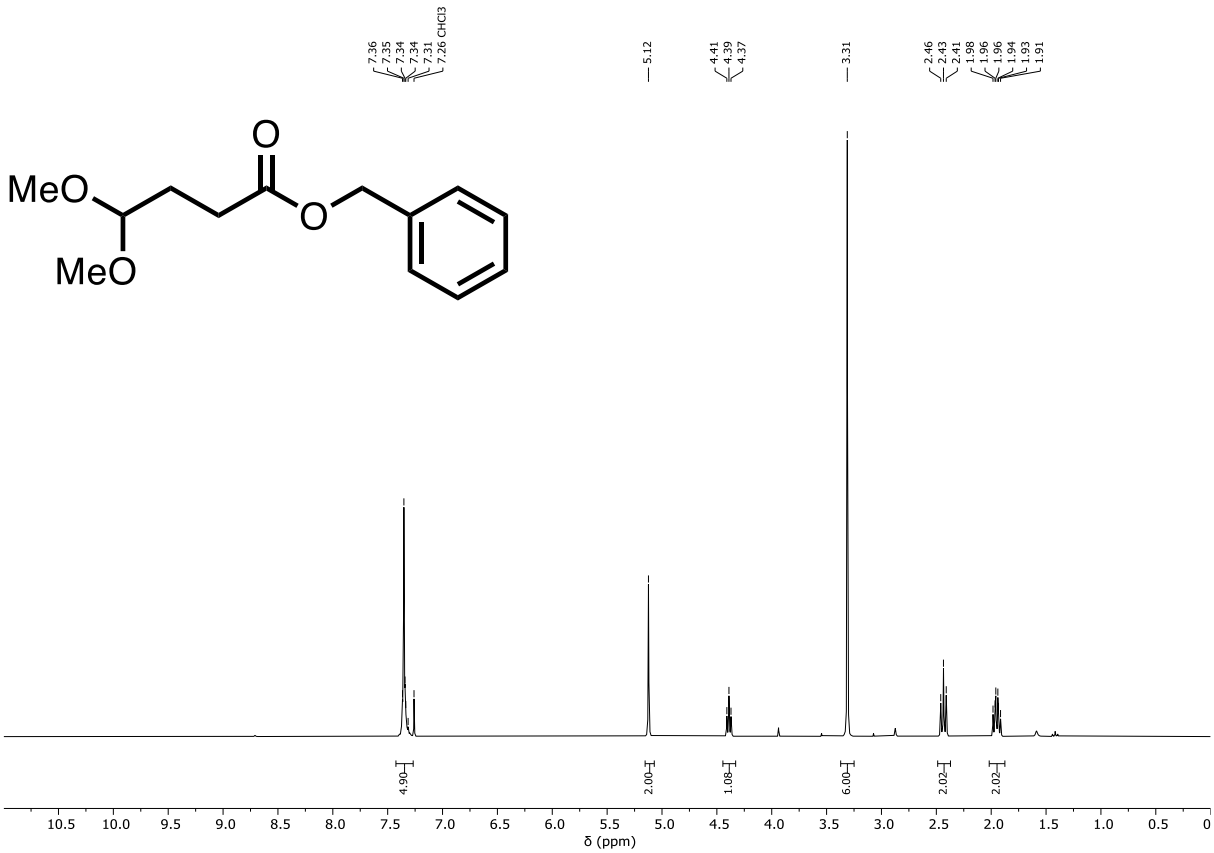
^{1}H NMR spectrum (600 MHz, $CDCl_3$) of **5z**



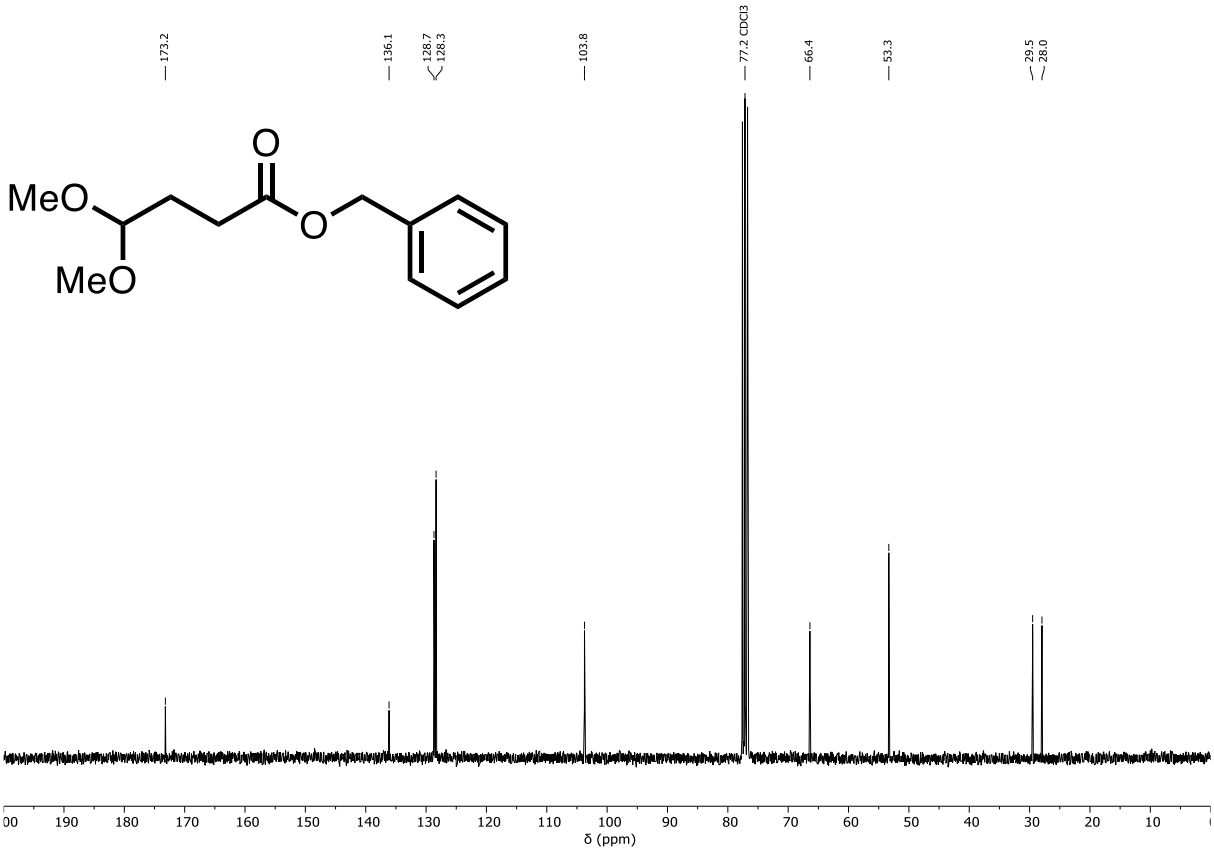
^{13}C NMR spectrum (151 MHz, $CDCl_3$) of **5z**



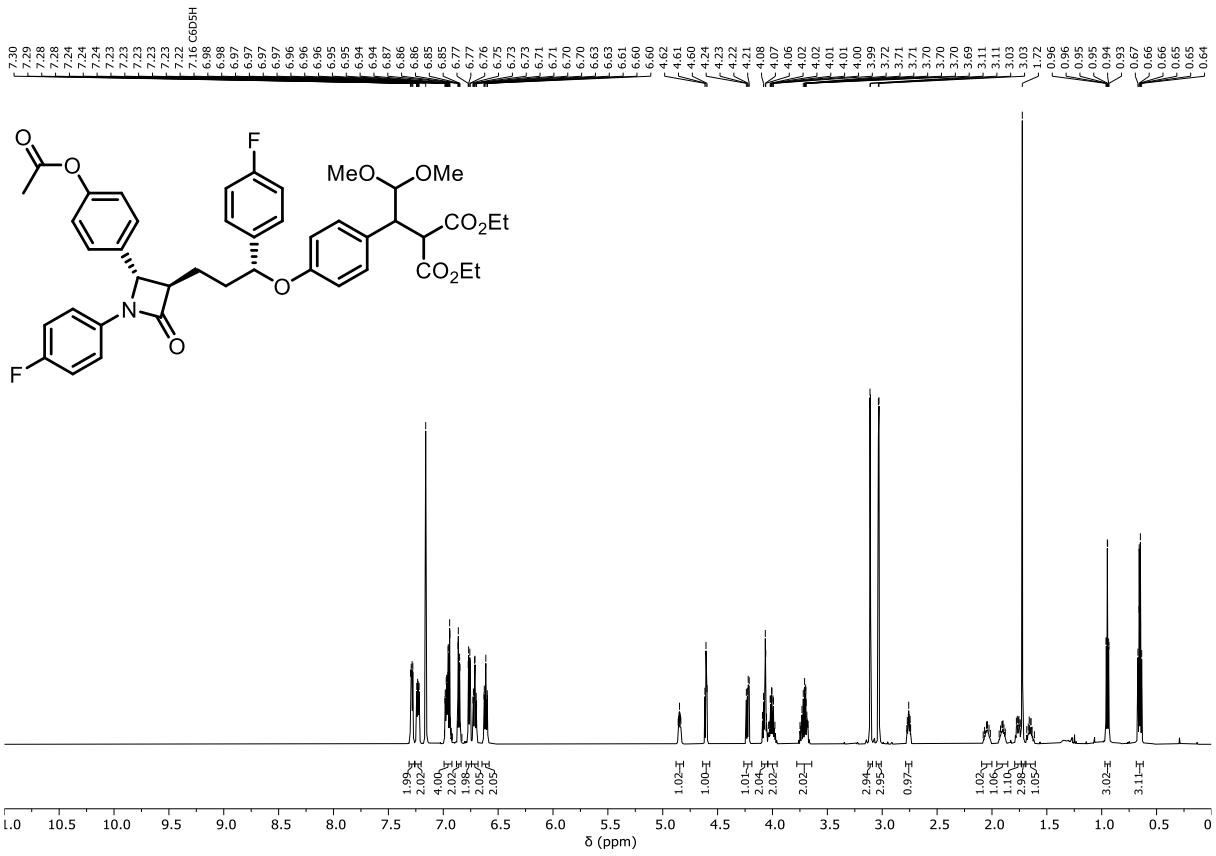
^{1}H NMR spectrum (500 MHz, $CDCl_3$) of **6b**



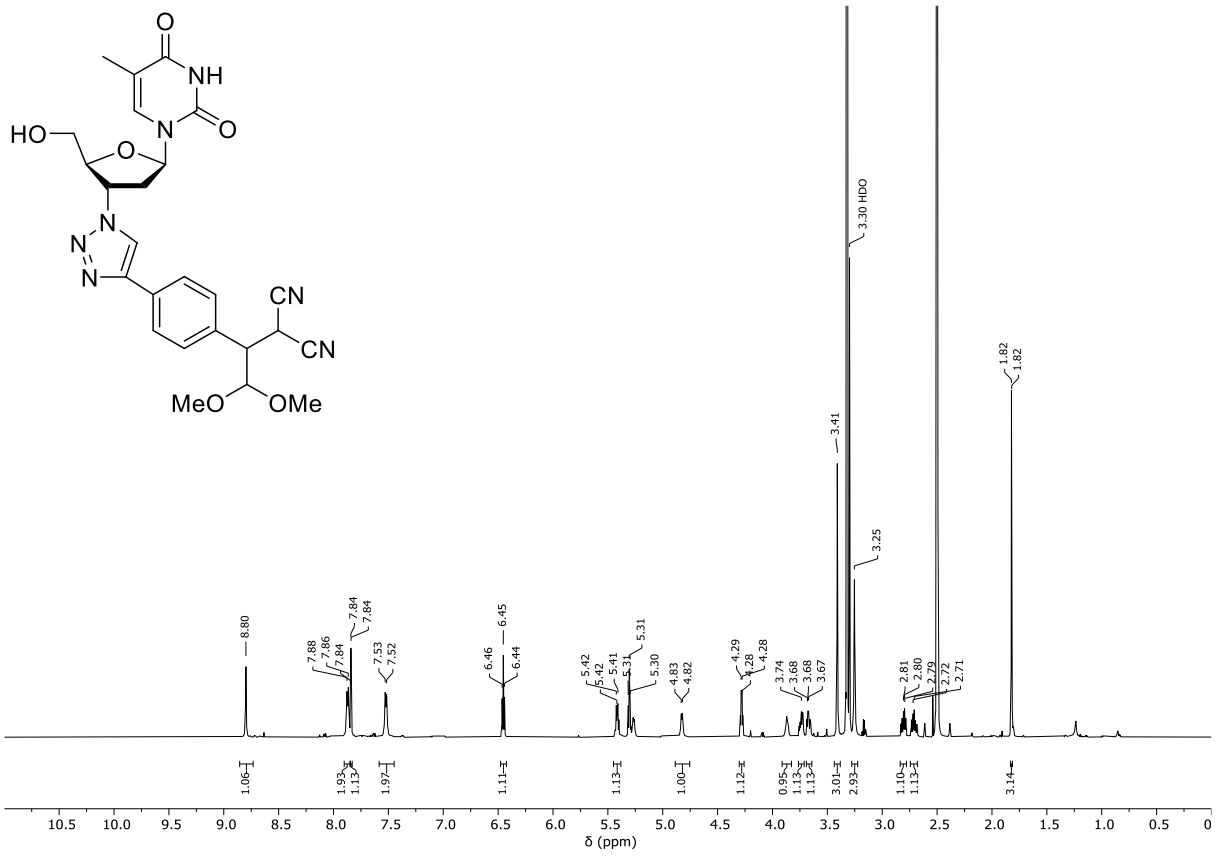
^{1}H NMR spectrum (300 MHz, $CDCl_3$) of **6f**



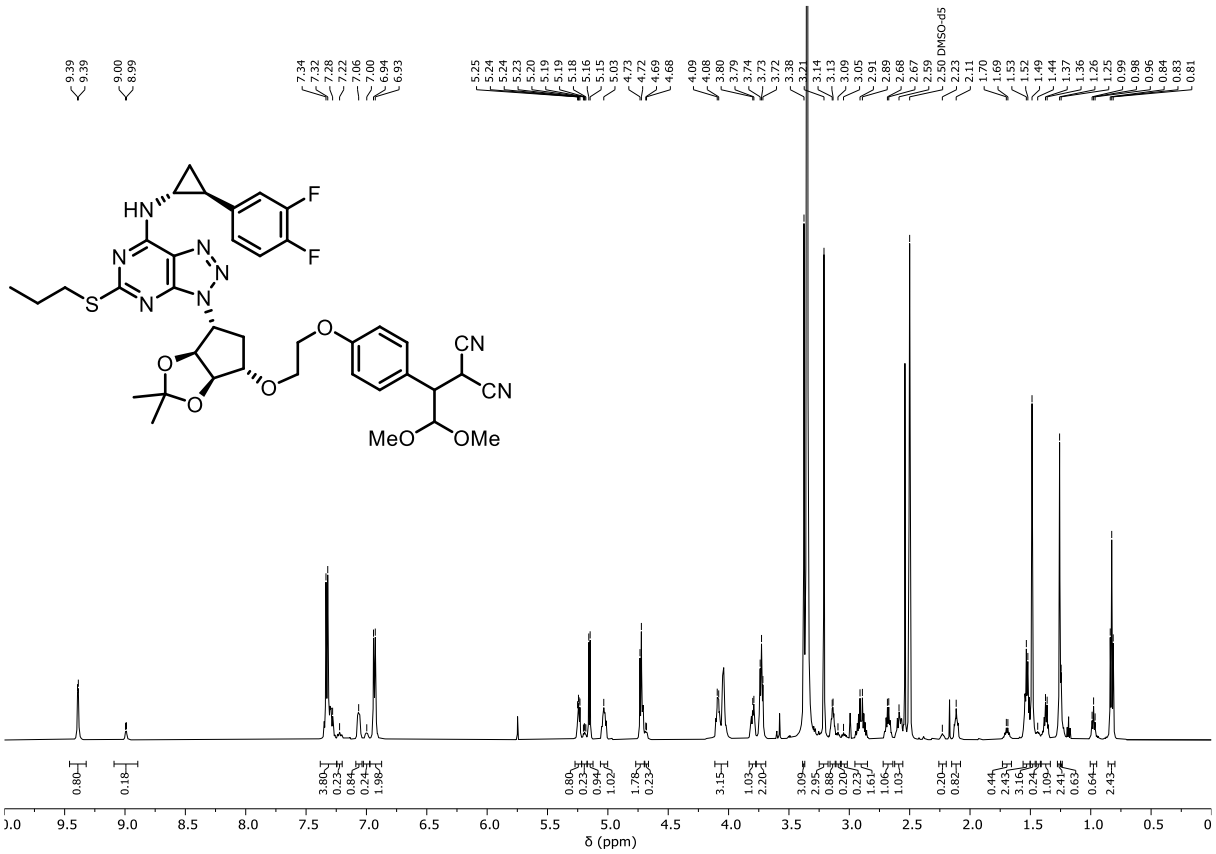
^{13}C NMR spectrum (75.5 MHz, $CDCl_3$) of **6f**



^{1}H NMR spectrum (600 MHz, C_6D_6) of **7a**

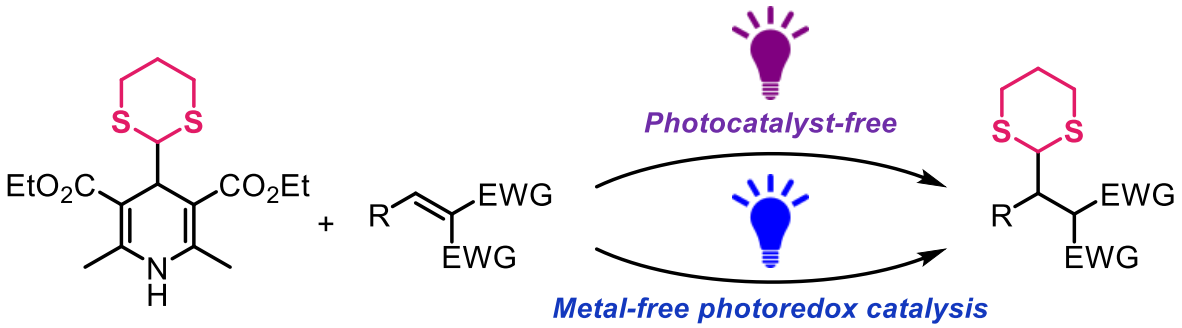


^{1}H NMR spectrum (600 MHz, DMSO-d_6) of **7b**



^{1}H NMR spectrum (600 MHz, DMSO-d_6) of **7c** (major + minor rotamer signals highlighted)

Chapter 6



★ ***2 Methods in 1:*** *Photocatalyst-free* ***and*** *photoredox approach*

★ *Mild conditions with high chemoselectivity* ★ *Broad functional group tolerance*

★ *Smooth conversion, up to near-quant. yields* ★ *Bench-stable crystalline precursor*

Hydroformylation of Electron-Deficient Olefins via Thioacetal Intermediates

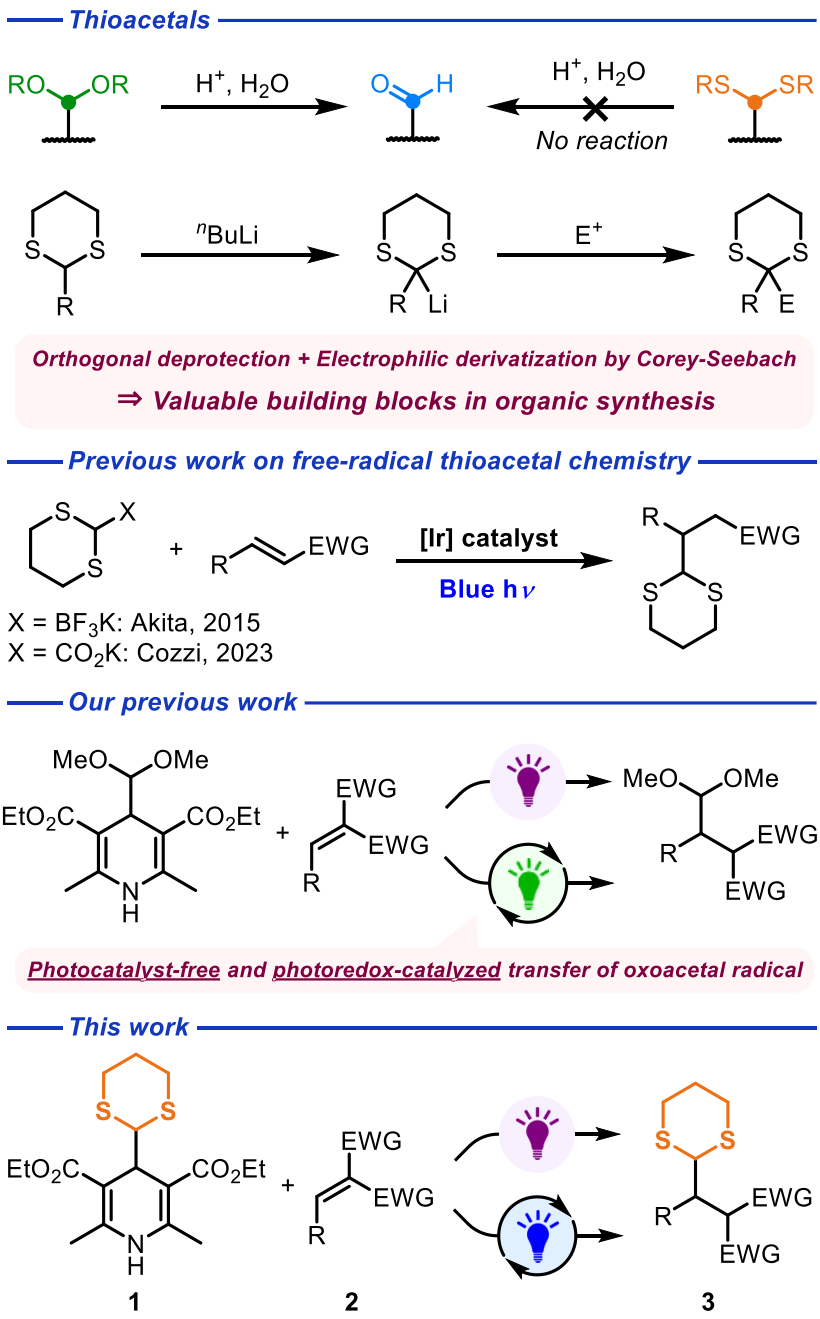
Abstract: *An alternative method of formal hydroformylation of electron-deficient olefins using a readily accessible 4-dithianyl Hantzsch ester (**1**) is reported. We show that under both photocatalyst-free direct irradiation as well as metal-free blue-light photoredox catalysis, a dithianyl moiety is smoothly transferred under mild conditions onto a diverse set of olefins, yielding aldehyde thioacetals in up to near-quantitative yields. Mechanistic studies suggest involvement of the free heteroatom-stabilized dithianyl radical.*

The work outlined in this chapter is scheduled for publication.

Part of this work is part of the master thesis “Hantzsch Esters as Formylation Agents under Photochemical Conditions”, Dorottya Mikóczi, **2022**.

Author contributions: **Mattis-Ole W. S. Schmotz** wrote the manuscript and performed experimental work, **Dorottya Mikóczi** performed experimental work, **Axel Jacobi von Wangelin** supervised this work.

While the use of oxoacetals as protecting groups is well-established in organic synthesis, the structurally analogous thioacetals offer various advantages. Notably, they are robust under acidic conditions and typically require alternative deprotection strategies,[1] such as aqueous treatment with large, soft metal ions (most commonly Hg^{2+}), oxidants (e.g. Ag^{+}, NBS, PIFA, DMP), or alkylating agents (e.g. MeI). This provides orthogonal stability profiles that are highly valuable in multi-step syntheses. In addition, they are precursors to nucleophilic carbonyl synthons as part of the Corey-Seebach reaction, which presents an expedient addition to the toolbox of carbonyl syntheses: Deprotonation between the two sulfur atoms by strong bases leads to a stable dithianyl anion, which reacts effortlessly with electrophiles (e.g. alkyl halides, epoxides, ketones and aldehydes, imines).[2,3] We previously reported a photochemical strategy towards formal hydroformylation of electron-deficient olefins using a dimethoxymethyl-substituted Hantzsch ester, both under photocatalyst-free conditions in **Chapter 3** and via Eosin Y photoredox catalysis in **Chapter 5**. This method furnished dimethyl acetals, which could be readily deprotected under acidic conditions to furnish the corresponding free aldehydes. In stark contrast to well-established free-radical oxoacetylation methods,[4] similar reactions via free thioacetalyl radicals remain scarce. The most common approach is homolysis of 2-substituted dithiane precursors (–SePh,[5] –S(C=S)OEt,[6] –TEMPO,[7] –Cl[8]) under thermal or photochemical conditions. A hydrogen-atom abstraction methodology for the dithianylation of styrenes using $FeCl_3$ was reported in 2014 by Tang and co-workers.[9] Photoredox approaches are limited to a 2014 report from the Akita group featuring an iridium-photoredox-catalyzed Giese addition of dithianyl radicals generated from potassium dithianyltrifluoroborate to unsaturated carbonyl groups,[10] and a 2023 report featuring a similar reaction by Cozzi and coworkers, generating dithianyl radicals from oxidative decarboxylation of dithiane-2-carboxylates.[11] Although these methodologies represent efficient dithianylation protocols, they often rely on harsh conditions, laborious preparation of precursors, or catalysts containing iridium, one of the rarest and most expensive metals on earth.[12] Motivated by the vast synthetic potential and relative underexploration of thioacetals in photochemistry, we wondered if our free-radical acetalyl transfer methodology could be extended to the direct installation of thioacetal groups using a corresponding Hantzsch ester in a photocatalyst-free and metal-free photoredox catalysis approach. To the best of our knowledge, no thioacetal-containing Hantzsch ester motifs have been synthesized to date.

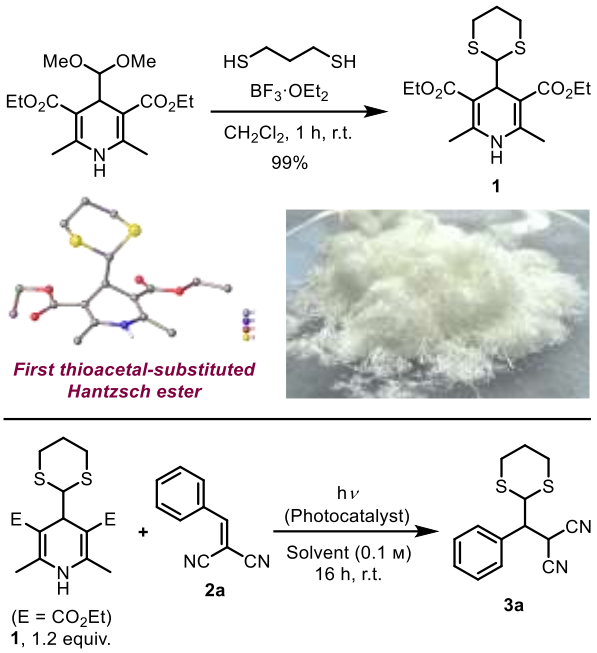


***Scheme 1**. Thioacetals vs. oxoacetals in organic synthesis and in free-radical formylation chemistry.*

Attempts to obtain **1** via a direct Hantzsch dihydropyridine synthesis of 2,2-dithioalkyl acetaldehydes proved infeasible due to the instability of such aldehydes. Fortunately, a transacetalization approach from the previously reported dimethoxymethyl-substituted Hantzsch ester afforded **1** in near-quantitative yield as a crystalline solid (Scheme 2, top). We then assessed its reaction with benzylidenemalononitrile **2a** under various conditions (Scheme 2, bottom). We were pleased to find that **1** smoothly transferred its thioacetalyl moiety under direct photocatalyst-free ultraviolet radiation, with similar yields in acetonitrile and acetone (entries 1–2). The reaction likewise proceeded well under photoredox catalysis. In contrast to our previous results regarding the dimethoxymethyl-substituted Hantzsch ester,[13] 4CzIPN (1,2,3,5-tetrakis(9*H*-

carbazol-9-yl)-4,6-dicyanobenzene)[14] emerged as the optimal catalyst (entries 5–6) with Eosin Y performing slightly inferior (entry 3). Again, acetonitrile and acetone gave comparable results. Control experiments revealed that light irradiation is required for product formation in both cases (entries 7–8)

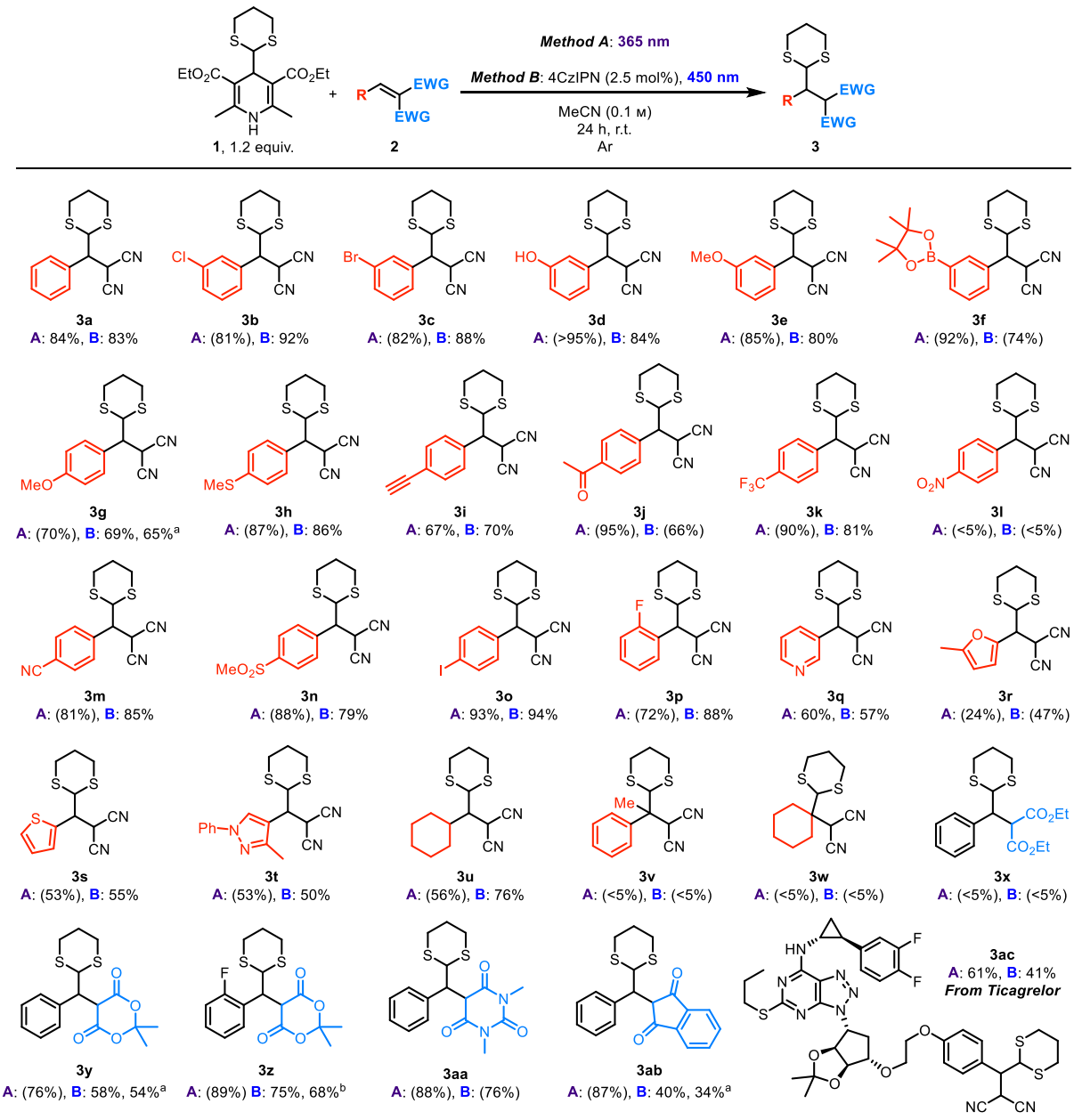
Scheme 2. *Top: Synthesis of* ***1*** *via trans-thioacetalization. Bottom: Optimization experiments.*



№	Solvent	[PC] (mol%)	λ / nm	Yield[a] / %
1	MeCN	–	365	88
2	Acetone	–	365	85
3	MeCN	Na_2-EY (2.5)	525	79
4	MeCN	3DPA2FBN (2.5)	450	81
5	MeCN	4CzIPN (2.5)	450	89
6	Acetone	4CzIPN (2.5)	450	89
7	MeCN	–	–	0
8	MeCN	4CzIPN (2.5)	–	0

[a] ^{1}H NMR yields *vs.* 1,3,5-trimethoxybenzene. Na_2-EY = Eosin Y disodium salt, 3DPA2FBN = 2,4,6-Tris(diphenylamino)-3,5-difluorobenzonitrile, 4CzIPN = 1,2,3,5-tetrakis(carbazol-9-yl)-4,6-dicyanobenzene.

Next, we explored the scope of this reaction (Scheme 3). A diverse array of functional groups is tolerated by the mild conditions, with good to excellent yields using both direct UV irradiation (Method A) and blue-light photoredox catalysis (Method B). Halogens (F, Cl, Br, I) were well tolerated with no signs of hydrodehalogenation, a known side reaction under similar conditions (**3b**–**c**, **3o**–**p**). Importantly, substrates bearing additional electron-withdrawing groups on the aromatic ring or electron-deficient heterocycles afforded good yields using both methods. These substrates have been shown to be problematic under our previously reported conditions



Scheme 3. *Substrate scope.100 µmol scale reactions, isolated yields are given, yields in parentheses represent ^{1}H NMR yields vs. 1,3,5-trimethoxybenzene. [a] Isolated yield on a 1.0 mmol scale (36 h of irradiation). [b] Isolated yield on a 4.0 mmol scale (two parallel 2.0 mmol scale reactions, 36 h of irradiation).*

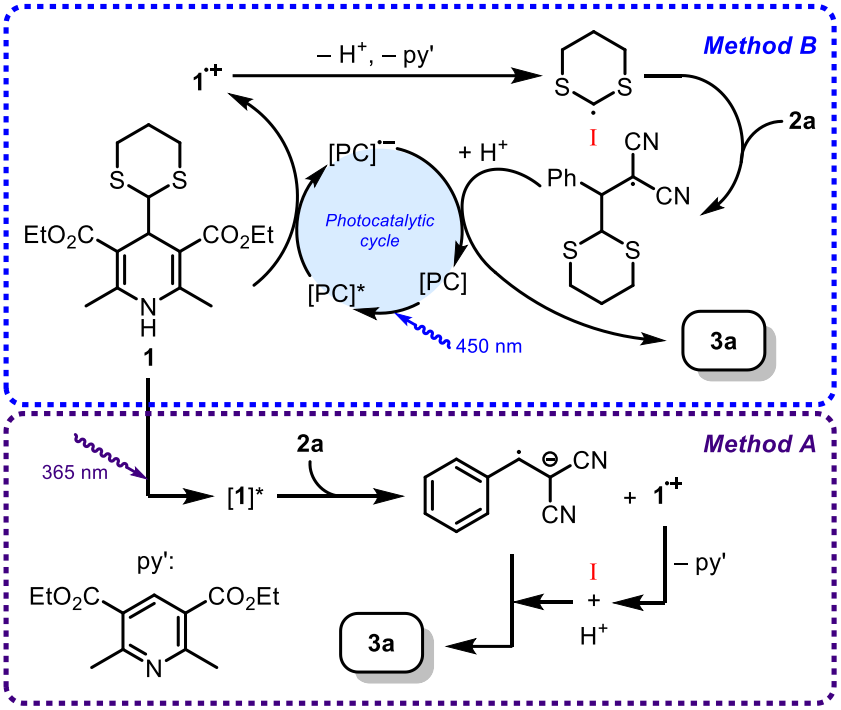
employing a dimethoxymethyl-substituted Hantzsch ester under UV irradiation or Eosin Y photoredox catalysis. In contrast, electron-rich substituents afforded lower yield and/or conversion, for example the furan-substituted olefin (**3r**); again contrary to our previously reported conditions. Nitro groups led to a complex mixture (**3l**). Ketone-derived malononitriles showed no conversion under the reaction conditions (**3v**, **3w**). Substitution of the nitrile groups on the olefin for ester functionalities hampered conversion under both conditions (**3x**). The origin of this effect is currently unknown, as diethyl benzylidenemalonate lies well within the redox window of excited-state **1*** (E(**2x**/**2x**$^{\bullet-}$) = −1.6 V vs. SCE),[15] as well as being a known substrate

for conjugate addition of dithianyl radicals[11] (see mechanistic discussion below). On the contrary, the structurally similar Meldrum's acid-derived substrates showed good yields (**3y**–**z**). This is likely a result of their distinct electronic structure arising from the conformation of the six-membered ring, which greatly stabilizes anions or radicals; the same effect grants Meldrum's acid its unusually high acidity.[16,17] Barbiturate- and indanedione-derived substrates likewise afforded product in both cases (**3aa**–**ab**), with higher yields for the UV method. A highly functionalized Ticagrelor derivative was successfully converted to the respective thioacetal, showcasing the chemoselectivity and potential applicability to late-stage functionalizaton (**3ac**). Method B could conveniently be scaled by a factor of 10 for **3g**, **3y**, and **3ab**, as well as by a factor of 20–40 for **3z**, with more than 1 g of **3z** being obtained in one operation via two parallel reactions.

Previous studies on the photocatalyst-free dimethoxymethyl Hantzsch ester-mediated formylation strongly supported a free-radical mechanism initiated by reduction of the olefin by excited Hantzsch ester.[13] Here, we propose a comparable mechanism. (Scheme 4, bottom) Cyclic voltammetry experiments revealed two irreversible oxidation processes of **1** at E = +1.06 V as well as E = +1.18 V vs. SCE, which may be attributed to the oxidation of the dihydropyridine core and the dithianyl unit, respectively. The energy of the singlet state S_1 of the dihydropyridine core was approximated from UV-Vis absorption and fluorescence spectra via the intersection method, and was found to be 3.38 eV (326 kJ·mol^{-1}, corresponding to 367 nm), Accordingly, the excited-state redox potential in S_1 is $E(\mathbf{1}^{\bullet+}/{}^1\mathbf{1}) \approx -2.32$ V vs. SCE, which is nearly identical to the dimethoxymethyl Hantzsch ester (E = −2.43 V vs. SCE).[13] Single-electron reduction of **2a** (E(**2a**/**2a**$^{\bullet-}$) = −1.16 V vs. SCE)[13] by excited **1** is thus thermodynamically feasible. The concomitantly formed radical cation **1**$^{\bullet+}$ rapidly fragmentates under aromatization to release the dithianyl radical **I**, which recombines with the spatially close benzylic radical **2a**$^{\bullet-}$. Product **3a** is then formed upon protonation. UV-Vis spectroscopy revealed no persistent EDA complex between **1** and **2a** due to the absence of a bathochromic shift, however, transient complex formation with a small equilibrium constant cannot be ruled out.

We propose the photoredox-catalyzed variant to operate via initial excitation of 4CzIPN (PC) by blue light (450 nm; Scheme 4, top). Oxidation of **1** by PC* (E(PC*/PC$^{\bullet-}$) = +1.43 V vs. SCE)[14] is the thermodynamically favored next step. In contrast, reduction of **2a** is only marginally accessible (E(PC$^{\bullet+}$/PC*) = −1.18 V vs. SCE),[14] making it a less likely initial step, especially in the case of substrates bearing additional electron-donating groups. The oxidation of **1** analogously yields **1**$^{\bullet+}$, which likewise fragmentates to release the free dithianyl radical **I**. This radical undergoes a Giese-type conjugate addition to the olefin **2a**. Subsequent reduction of the α,α-dinitrile radical by PC$^{\bullet-}$ completes the photocatalytic cycle and yields the product **3a** after protonation. Remarkably, the oxidation of the dithianyl moiety on **1** lies well within the

redox window of PC* (see above). Thioacetal deprotection protocols under photoredox or photochemical conditions have been described;[18–20] despite this, no significant side reactions involving the dithianyl moiety were detected, underscoring the high chemoselectivity of this reaction.



Scheme 4. *Proposed reaction mechanisms for the catalyst-free (Method A) and photoredox-catalyzed (Method B) reactions.*

In conclusion, we have developed two practical methods for the hydroformylation of electron-deficient olefins using a novel dithianyl-substituted Hantzsch ester: A photocatalyst- and additive-free approach via long-wave ultraviolet irradiation, and a metal-free blue-light photoredox-catalyzed approach employing the organic dye 4CzIPN. Both methods yield thioacetals, which show orthogonal reactivity compared to oxoacetals. We propose the presence of a dithianyl radical at the heart of both mechanisms.

Literature References

[1] P. G. M. Wuts, *Greene's Protective Groups in Organic Synthesis*, Wiley, **2014**.

[2] E. J. Corey, D. Seebach, *Angew. Chem. Int. Ed. Engl.* **1965**, *4*, 1077–1078.

[3] M. Haroon, A. F. Zahoor, S. Ahmad, A. Mansha, M. Irfan, A. Mushtaq, R. Akhtar, A. Irfan, K. Kotwica-Mojzych, M. Mojzych, *Molecules* **2023**, *28*, 4367.

[4] K. L. Samony, D. K. Kim, *ChemCatChem* **2023**, *15*, e202301091.

[5] J. H. Byers, C. C. Whitehead, M. E. Duff, *Tetrahedron Lett.* **1996**, *37*, 2743–2744.

[6] M. De Greef, S. Z. Zard, *Tetrahedron* **2004**, *60*, 7781–7791.

[7] A. J. Herrera, A. Studer, *Synthesis* **2005**, *2005*, 1389–1396.

[8] W. Du, J. Lai, L. Tian, X. Xie, X. She, S. Tang, *Chem. Commun.* **2014**, *50*, 14017–14020.

[9] W. Du, L. Tian, J. Lai, X. Huo, X. Xie, X. She, S. Tang, *Org. Lett.* **2014**, *16*, 2470–2473.

[10] Y. Li, K. Miyazawa, T. Koike, M. Akita, *Org. Chem. Front.* **2015**, *2*, 319–323.

[11] A. Gualandi, E. Matteucci, F. Monti, A. Baschieri, N. Armaroli, L. Sambri, P. G. Cozzi, *Chem. Sci.* **2017**, *8*, 1613–1620.

[12] W. M. Haynes, Ed. , *CRC Handbook of Chemistry and Physics*, CRC Press, Boca Raton, **2016**.

[13] Chapter 3 of this work.

[14] E. Speckmeier, T. G. Fischer, K. Zeitler, *J. Am. Chem. Soc.* **2018**, *140*, 15353–15365.

[15] B. R. McDonald, K. A. Scheidt, *Org. Lett.* **2018**, *20*, 6877–6881.

[16] K. Byun, Y. Mo, J. Gao, *J. Am. Chem. Soc.* **2001**, *123*, 3974–3979.

[17] S. Nakamura, H. Hirao, T. Ohwada, *J. Org. Chem.* **2004**, *69*, 4309–4316.

[18] G. A. Epling, Q. Wang, *Tetrahedron Lett.* **1992**, *33*, 5909–5912.

[19] M. Krumb, L. M. Kammer, R. Forster, C. Grundke, T. Opatz, *ChemPhotoChem* **2020**, *4*, 101–104.

[20] P. D. Dharpure, A. Bhowmick, P. K. Warghude, R. G. Bhat, *Tetrahedron Lett.* **2020**, *61*, 151407

Experimental Section

General Information

Nuclear magnetic resonance (NMR) spectroscopy: ^{1}H NMR spectra (300 MHz) and ^{13}C-NMR spectra (75.5 MHz) were recorded on a *Bruker Fourier HD 300.* ^{1}H NMR spectra (400 MHz) and ^{13}C-NMR spectra (101 MHz) were recorded on a *Bruker Avance III HD 400*. ^{1}H NMR spectra (600 MHz), ^{13}C-NMR spectra (151 MHz), and ^{19}F-NMR spectra (565 MHz) were recorded on a *Bruker Avance III HD 600*. All spectra were recorded at 25 °C unless otherwise stated. Chemical shifts δ are reported in parts per million (ppm) relative to tetramethylsilane for ^{1}H and ^{13}C NMR spectra, and relative to $CFCl_3$ for ^{19}F NMR spectra. Coupling constants *J* are given in Hertz (Hz). *MestReNova 14* (Mnova) by *Mestrelab* was used for analysis of the NMR spectra. Abbreviations used for NMR data: s = singlet; br. s = broad singlet; d = doublet; t = triplet; q = quartet; m = multiplet, and combinations thereof.

Infrared (IR) spectroscopy: Infrared spectra were recorded using a *Bruker VERTEX 70* FTIR spectrometer using a *Specac Golden Gate* ATR unit.

UV-Vis spectroscopy: UV-Vis spectra were measured at room temperature on an *Agilent Cary 5000* UV-Vis-NIR Spectrophotometer in double-beam mode using 10 mm SUPRASIL quartz cuvettes by *Hellma*.

Fluorescence spectroscopy: Fluorescence spectra were measured at room temperature on an *Agilent Cary Eclipse Fluorescence Spectrophotometer* at a 90° angle using 10 mm SUPRASIL quartz fluorescence cuvettes by *Hellma*.

Mass spectrometry (MS): High-resolution mass spectra (electrospray ionization, ESI) were measured using an *Agilent 6224 ESI-TOF* or a *Bruker maXis ESI-Q-TOF* by direct injection in positive or negative ion mode. Abbreviations used for MS data: *m/z* mass-to-charge ratio; M = exact mass of the target compound. *MestReNova 14* (Mnova) by *Mestrelab* was used for analysis of the MS spectra.

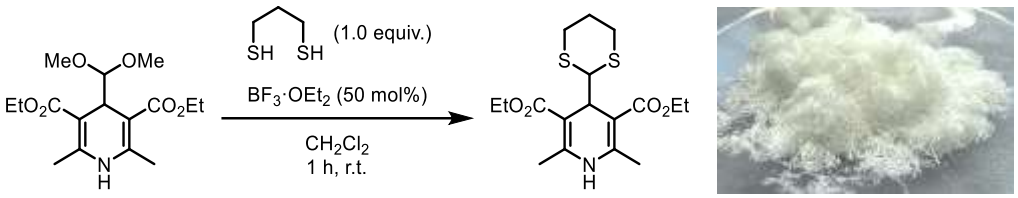
Melting points: Melting points (m.p.) were measured using a *DigiMelt MPA160* by *Stanford Research Systems*.

Cyclic voltammetry (CV): CV measurements were performed with a potentiostat galvanostat *PGSTAT101* from *Metrohm Autolab* using a glassy carbon working electrode, a platinum wire counter electrode, a silver/silver(I) chloride reference electrode and $N(n\text{-}Bu)_4PF_6$ (0.1 M) as supporting electrolyte.

Thin-layer chromatography (TLC) and column chromatography: TLC was performed using aluminium plates coated with UV-fluorescence-indicator-doped stationary phase by *Macherey-Nagel* (*ALUGRAM® Xtra Sil G/UV$_{254}$* for SiO_2, *ALUGRAM® ALOX N / UV254* for neutral Al_2O_3). Preparative column chromatography was performed using silica by *Acros Organics* (35–70 µm, 60 Å pore size) or neutral alumina by *Macherey-Nagel* (50–200 µm, 90 Å pore size) using distilled technical grade solvents.

Synthesis of Compounds

Diethyl 4-(1,3-dithian-2-yl)-2,6-dimethyl-1,4-dihydropyridine-3,5-dicarboxylate (**1**)



Diethyl 4-(dimethoxymethyl)-2,6-dimethyl-1,4-dihydropyridine-3,5-dicarboxylate (1.64 g, 5.00 mmol, 1.0 equiv.) was dissolved in dichloromethane (50 mL, 0.1 M) and 1,3-propanedithiol (0.50 mL, 5.0 mmol, 1.0 equiv.) was added in one portion. Boron trifluoride diethyl etherate (0.31 mL, 2.5 mmol, 50 mol%) was added dropwise, resulting in a yellow coloration of the mixture and a mild exotherm. The mixture was stirred at room temperature for 1 hour[a] then washed with water (50 mL). The aqueous phase was separated and extracted with dichloromethane (3× 25 mL). The combined organic phases were dried over Na_2SO_4, filtered, and concentrated to yield **1** as an off-white solid (1.84 g, 4.95 mmol, 99%). Further purification is usually not necessary. If desired, the product may be recrystallized from boiling (aqueous) acetonitrile (ca. 30–35 mL of MeCN/H_2O 1:1 per gram of crude product), from which it readily crystallizes as odorless, colorless, transparent needles. The recovery is about 85% if the mother liquor is stored overnight at 4 °C.

^{1}H NMR (600 MHz, $CDCl_3$): 6.22 (s, 1H), 4.63 (d, *J* = 8.5 Hz, 1H), 4.20 (q, *J* = 7.1 Hz, 4H), 3.31 (d, *J* = 8.6 Hz, 1H), 2.97 (ddd, *J* = 14.2, 8.1, 3.6 Hz, 2H), 2.55 (ddd, *J* = 14.1, 7.2, 3.5 Hz, 2H), 2.35 (s, 6H), 2.00 – 1.93 (m, 2H), 1.30 (t, *J* = 7.2 Hz, 6H).

^{13}C{^{1}H} NMR (151 MHz, $CDCl_3$): 168.1, 144.2, 102.5, 60.0, 36.7, 28.1, 26.2, 19.6, 19.5, 14.5.

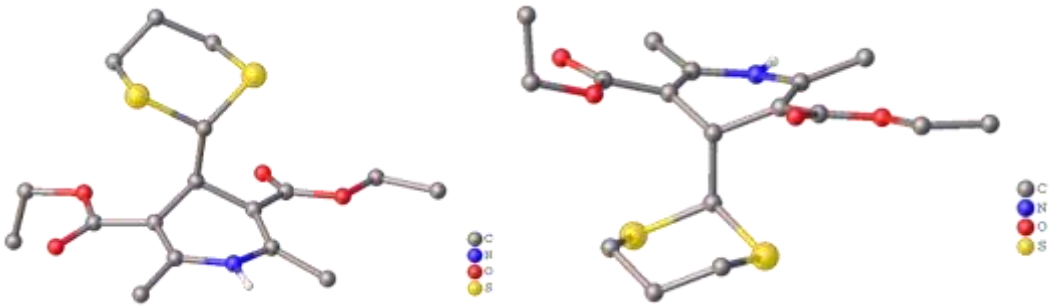
IR (ATR): 3326 (N–H), 2985, 2934, 2891, 1652 (C=O), 1621, 1490, 1443, 1389, 1368, 1326, 1296, 1259, 1245, 1212, 1185, 1163, 1122, 1109, 1090, 1047, 1018, 964, 912, 778, 763, 750, 716, 687, 681, 661, 649.

UV-Vis (MeCN): λ_{max} [nm] (ε [L·mol^{-1}·cm^{-1}]) = 225, 248, 326 (6020).

HRMS (ESI): *m/z* calcd. for $C_{17}H_{25}NNaO_4S_2^+$ $[M+Na]^+$: 394.1117, found: 394.1129; calcd. for $C_{17}H_{25}KNO_4S_2^+$ $[M+K]^+$: 410.0857, found: 410.0860; calcd. for $C_{34}H_{50}N_2NaO_8S_4^+$ $[2M+Na]^+$: 765.2342, found: 765.2352.

m.p. = 179–180 °C.

XRD (Non heteroatom-bonded hydrogen atoms omitted for clarity):

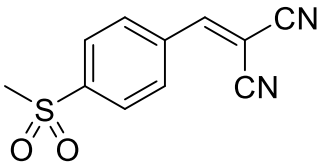


[a] Longer reaction times lead to lower purity and an increasingly yellow discoloration of the product.

Synthesis of Electron-Deficient Olefins

The synthesis of **2a**–**m**, **2o**–**y**, and **2aa**–**ac** is described in **Chapter 3** of this work.

(4-(Methylsulfonyl)benzylidene)malononitrile (**2n**)



To a suspension of 4-(methylsulfonyl)benzaldehyde (387 mg, 2.10 mmol, 1.0 equiv.) and malononitrile (139 mg, 2.10 mmol, 1.0 equiv.) in ethanol (5 mL) was added a spatula tip of 1,4-diazabicyclo[2.2.2]octane (DABCO). The heterogeneous mixture was stirred for 3 h at room temperature, diluted with water, and filtered. The solid was washed with plenty of water and once with cold (−25 °C) ethanol. No further purification was required.

Yield: 85% (414 mg, 1.78 mmol).

Appearance: Pale-brown solid.

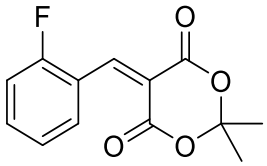
^{1}H NMR (300 MHz, DMSO-d_6): δ [ppm] = 8.70 (s, 1H), 8.20 – 8.08 (m, 4H), 3.31 (s, 3H).

^{13}C{^{1}H} NMR (75.5 MHz, DMSO-d_6): δ [ppm] = 159.9, 144.5, 135.5, 130.9, 127.9, 113.7, 112.6, 85.5, 43.1.

HRMS (ESI): *m/z* calcd. for $C_{11}H_9N_2O_2S^+$: 233.0379, found: 233.0392.

m.p. = 193–195°C.

5-(2-Fluorobenzylidene)-2,2-dimethyl-1,3-dioxane-4,6-dione (**2z**)



Meldrum's acid (8.91 g, 61.8 mmol, 1.0 equiv.), freshly distilled 2-fluorobenzaldehyde (8.05 g, 64.9 mmol, 1.05 equiv.), pyrrolidine (0.50 mL, 620 µmol, 10 mol%), and acetic acid (0.30 mL, 620 µmol, 10 mol%) were suspended in benzene (300 mL). Excess 4 Å molecular sieves were added and the mixture was stirred for 24 h at 60 °C. The mixture was filtered and washed with sat. aq. $NaHCO_3$ (200 mL). The aqueous phase was extracted with ethyl acetate (2× 100 mL) and the combined phases were dried over $MgSO_4$, filtered, and concentrated. The residual solid was recrystallized from boiling methanol (~250 mL).

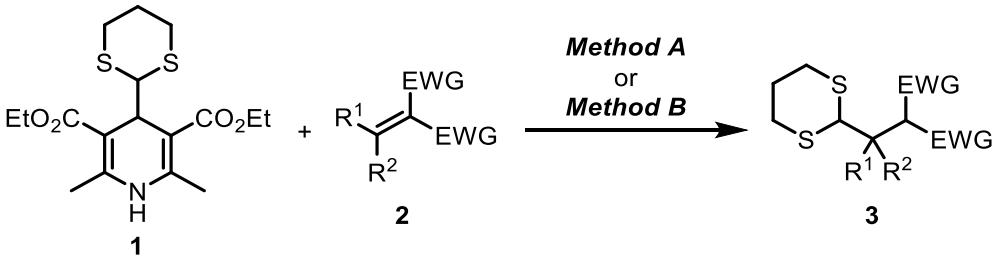
Yield: 80% (12.34 g, 49.3 mmol).

Appearance: Large colorless crystals

^{1}H NMR (300 MHz, $CDCl_3$): δ [ppm] = 8.50 (s, 1H), 8.00 – 7.88 (m, 1H), 7.58 – 7.45 (m, 1H), 7.28 – 7.19 (m, 1H), 7.19 – 7.08 (m, 1H), 1.82 (s, 6H).

Literature: A. M. Dumas, E. Fillion, *Org. Lett.* **2009**, *11*, 1919–1922.

Synthesis of Substituted Acetaldehyde Thioacetals



Method A: The corresponding olefin (100 µmol, 1.0 equiv.), Hantzsch ester **1** (39.2 mg, 120 µmol, 1.2 equiv.) and, if applicable, 4CzIPN (2.0 mg, 2.5 µmol, 2.5 mol%) were weighed into a 4 mL glass vial equipped with a stir bar and a septum screw cap. The septum was punctured by a cannula and the vial was transferred into an argon-filled glove box. Dry, degassed acetonitrile (1.0 mL) was added.[a] The vials were transferred out of the glove box and placed inside the photoreactor (*EvoluChem PhotoRedOx Box TC*) filled with silicone oil that was kept at 25.0 °C. The mixture was vigorously stirred under irradiation (**365 nm**, *EvoluChem LED 365DX*) for 24 h.

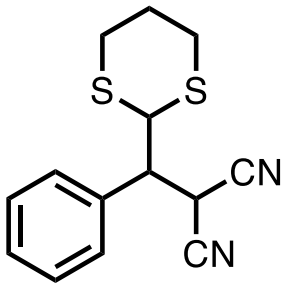
Method B: As above, with 4CzIPN (2.0 mg, 2.5 µmol, 2.5 mol%) additionally weighed into the vial. Irradiation was conducted at **450 nm** (*EvoluChem 450PF*) for 24 h.

Determination of NMR yields: An exactly weighed amount of 1,3,5-trimethoxybenzene (1.5 – 5.0 mg) was added to the reaction mixture after irradiation. The solvent was removed and the residue dissolved in $CDCl_3$. A ^{1}H NMR spectrum (300 MHz) was recorded and a suitable product signal (generally the thioacetal proton between the two sulfur atoms at ~4.7–4.8 ppm) was integrated against the signal of 1,3,5-trimethoxybenzene (3H, 6.08 ppm).

Isolation of products: The mixture was transferred to a round-bottom flask and either 1.) evaporated to dryness onto Celite® (~100 mg) and purified by regular column chromatography (SiO_2 or neutral alumina) or 2.) evaporated to dryness, dissolved in a minimal amount of DMSO, and purified by automated flash chromatography on C_{18}-SiO_2 (gradient from H_2O/MeCN 8:2 to MeCN), followed by lyophilization and repeated coevaporation with $CHCl_3$ to remove residual acetonitrile.

[a] The mixture starts off as a suspension due to the low solubility of **1** in acetonitrile and eventually becomes homogeneous as **1** is consumed during the reaction.

2-((1,3-Dithian-2-yl)(phenyl)methyl)malononitrile (**3a**)



By GP1 starting from benzylidenemalononitrile (**2a**, 15.4 mg). Purified by column chromatography (SiO_2, Pentane/CH_2Cl_2 1:2).

Yield (Method A): 84% (23.1 mg, 84.1 µmol).

Yield (Method B): 83% (22.7 mg, 82.7 µmol).

Appearance: Colorless solid.

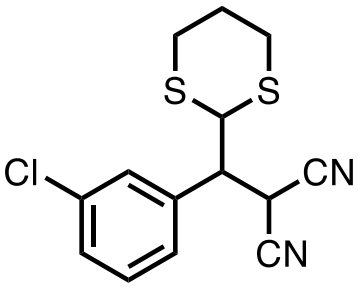
^{1}H NMR (300 MHz, $CDCl_3$): δ [ppm] = 7.50 – 7.35 (m, 5H), 4.75 (d, *J* = 5.8 Hz, 1H), 4.52 (d, *J* = 10.1 Hz, 1H), 3.58 (dd, *J* = 10.1, 5.8 Hz, 1H), 3.00 – 2.90 (m, 2H), 2.88 – 2.73 (m, 2H), 2.21 – 2.05 (m, 1H), 2.02 – 1.81 (m, 1H).

^{13}C{^{1}H} NMR (75.5 MHz, $CDCl_3$): δ [ppm] = 133.6, 129.9, 129.3, 128.7, 111.8, 111.2, 50.4, 47.6, 29.6, 29.4, 27.9, 25.2.

HRMS (ESI): *m/z* calcd. for $C_{14}H_{15}N_2S_2^+$: 275.0671, found: 275.0684.

m.p. = 102–103 °C.

2-((1,3-Dithian-2-yl)(3-chlorophenyl)methyl)malononitrile (**3b**)



By GP1 starting from (3-chlorobenzylidene)malononitrile (**2b**, 18.9 mg). Purified by column chromatography (SiO_2, Pentane/CH_2Cl_2 1:2).

Yield (Method A): 81% (^{1}H NMR yield vs. 1,3,5-trimethoxybenzene).

Yield (Method B): 92% (28.3 mg, 91.6 µmol).

Appearance: Colorless solid.

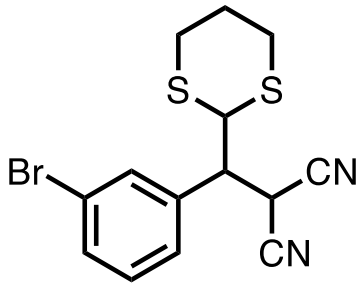
^{1}H NMR (300 MHz, $CDCl_3$): *δ* [ppm] = 7.47 – 7.33 (m, 3H), 7.34 – 7.26 (m, 1H), 4.74 (d, *J* = 5.8 Hz, 1H), 4.46 (d, *J* = 10.1 Hz, 1H), 3.55 (dd, *J* = 10.0, 5.8 Hz, 1H), 3.01 – 2.89 (m, 2H), 2.90 – 2.73 (m, 2H), 2.21 – 2.04 (m, 1H), 2.02 – 1.83 (m, 1H).

^{13}C{^{1}H} NMR (75.5 MHz, $CDCl_3$): *δ* [ppm] = 135.5, 135.2, 130.6, 130.1, 128.9, 126.8, 111.5, 111.0, 49.9, 47.2, 29.5, 29.3, 27.7, 25.1.

HRMS (ESI): *m/z* calcd. for $C_{14}H_{14}ClN_2S_2^+$: 309.0282, found: 309.0285.

m.p. = 84–86 °C.

2-((1,3-Dithian-2-yl)(3-bromophenyl)methyl)malononitrile (**3c**)



By GP1 starting from (3-bromobenzylidene)malononitrile (**2c**, 23.3 mg). Purified by column chromatography (SiO_2, Pentane/CH_2Cl_2 1:2).

Yield (Method A): 82% (^{1}H NMR yield vs. 1,3,5-trimethoxybenzene).

Yield (Method B): 88% (31.2 mg, 88.3 µmol).

Appearance: Off-white solid.

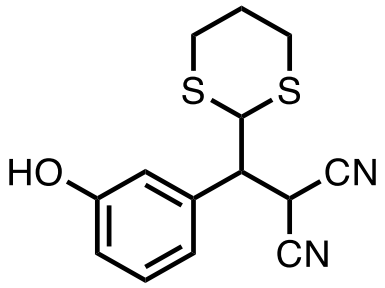
^{1}H NMR (300 MHz, $CDCl_3$): *δ* [ppm] = 7.64 – 7.52 (m, 2H), 7.40 – 7.26 (m, 2H), 4.74 (d, *J* = 5.9 Hz, 1H), 4.46 (d, *J* = 10.1 Hz, 1H), 3.54 (dd, *J* = 10.0, 5.8 Hz, 1H), 3.00 – 2.89 (m, 2H), 2.89 – 2.73 (m, 2H), 2.21 – 2.04 (m, 1H), 2.00 – 1.82 (m, 1H).

^{13}C{^{1}H} NMR (75.5 MHz, $CDCl_3$): *δ* [ppm] = 135.8, 133.1, 131.8, 130.8, 127.2, 123.3, 111.5, 110.9, 49.9, 47.2, 29.5, 29.3, 27.7, 25.1.

HRMS (ESI): *m/z* calcd. for $C_{14}H_{14}BrN_2S_2^+$: 352.9777, found: 352.9776.

m.p. = 108–109 °C.

2-((1,3-Dithian-2-yl)(3-hydroxyphenyl)methyl)malononitrile (**3d**)



By GP1 starting from (3-hydroxybenzylidene)malononitrile (**2d**, 17.0 mg). Purified by automated flash column chromatography (C_{18}-SiO_2, 20% MeCN in H_2O → 100% MeCN).

Yield (Method A): >95% (^{1}H NMR yield vs. 1,3,5-trimethoxybenzene).

Yield (Method B): 84% (24.5 mg, 84.3 µmol).

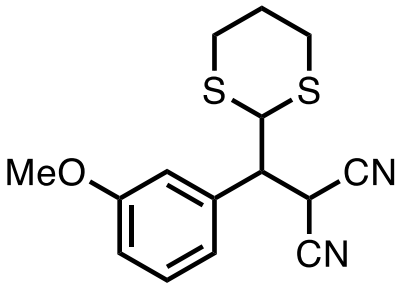
Appearance: Colorless sticky foam.

^{1}H NMR (300 MHz, $CDCl_3$): δ [ppm] = 7.74 – 7.61 (m, 1H), 7.35 (d, *J* = 7.8 Hz, 1H), 7.30 – 7.22 (m, 2H), 5.81 (s, 1H), 5.11 (d, *J* = 5.8 Hz, 1H), 4.83 (d, *J* = 10.2 Hz, 1H), 3.92 (dd, *J* = 10.2, 5.8 Hz, 1H), 3.37 – 3.26 (m, 2H), 3.26 – 3.11 (m, 2H), 2.55 – 2.42 (m, 1H), 2.37 – 2.22 (m, 1H).

^{13}C{^{1}H} NMR (75.5 MHz, $CDCl_3$): δ [ppm] = 156.2, 135.4, 130.6, 120.9, 117.1, 115.5, 111.8, 111.3, 49.9, 47.4, 29.4, 29.3, 27.9, 25.1.

HRMS (ESI): *m/z* calcd. for $C_{14}H_{13}N_2OS_2^-$: 289.0475, found: 289.0467.

2-((1,3-Dithian-2-yl)(3-methoxyphenyl)methyl)malononitrile (**3e**)



By GP1 starting from (3-methoxybenzylidene)malononitrile (**2e**, 18.4 mg). Purified by column chromatography (SiO_2, Pentane/CH_2Cl_2 1:2).

Yield (Method A): 85% (^{1}H NMR yield vs. 1,3,5-trimethoxybenzene).

Yield (Method B): 80% (24.3 mg, 79.8 µmol).

Appearance: Off-white solid.

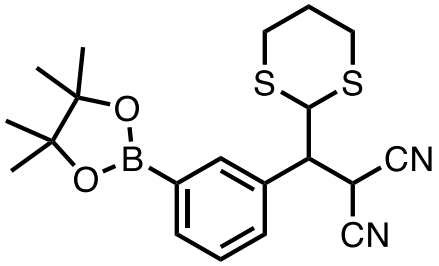
^{1}H NMR (300 MHz, $CDCl_3$): δ [ppm] = 7.40 – 7.30 (m, 1H), 7.02 – 6.89 (m, 3H), 4.72 (d, *J* = 6.0 Hz, 1H), 4.48 (d, *J* = 10.0 Hz, 1H), 3.83 (s, 3H), 3.54 (dd, *J* = 10.0, 5.9 Hz, 1H), 2.99 – 2.89 (m, 2H), 2.89 – 2.74 (m, 2H), 2.19 – 2.05 (m, 1H), 2.00 – 1.83 (m, 1H).

^{13}C{^{1}H} NMR (75.5 MHz, $CDCl_3$): δ [ppm] = 160.1, 135.1, 130.4, 120.7, 115.0, 114.6, 111.8, 111.3, 55.4, 50.3, 47.6, 29.6, 29.4, 27.8, 25.2.

HRMS (ESI): *m/z* calcd. for $C_{15}H_{17}N_2OS_2^+$: 305.0777, found: 305.0775.

m.p. = 143–144 °C.

2-((1,3-Dithian-2-yl)(3-(4,4,5,5-tetramethyl-1,3,2-dioxaborolan-2-yl)phenyl)methyl)malononitrile (**3f**)

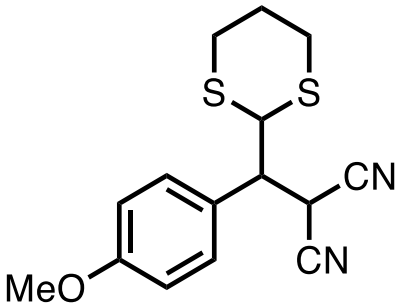


By GP1 starting from (3-(2,2-Dicyanovinyl)phenylboronic acid pinacol ester (**2g**, 28.0 mg).

Yield (Method A): 92% (^{1}H NMR yield vs. 1,3,5-trimethoxybenzene).

Yield (Method B): 74% (^{1}H NMR yield vs. 1,3,5-trimethoxybenzene).

2-((1,3-Dithian-2-yl)(4-methoxyphenyl)methyl)malononitrile (**3g**)



By GP1 starting from (4-methoxybenzylidene)malononitrile (**2g**, 18.4 mg). Purified by column chromatography (SiO_2, Pentane/CH_2Cl_2 1:2).

Yield (Method A): 70% (^{1}H NMR yield vs. 1,3,5-trimethoxybenzene).

Yield (Method B): 69% (20.9 mg, 68.7 µmol).

Appearance: Pale-yellow solid.

^{1}H NMR (300 MHz, $CDCl_3$): δ [ppm] = 7.37 – 7.28 (m, 2H), 7.00 – 6.91 (m, 2H), 4.71 (d, *J* = 5.8 Hz, 1H), 4.49 (d, *J* = 10.0 Hz, 1H), 3.52 (dd, *J* = 10.0, 5.8 Hz, 1H), 2.98 – 2.90 (m, 2H), 2.87 – 2.75 (m, 2H), 2.20 – 2.05 (m, 1H), 1.98 – 1.81 (m, 1H).

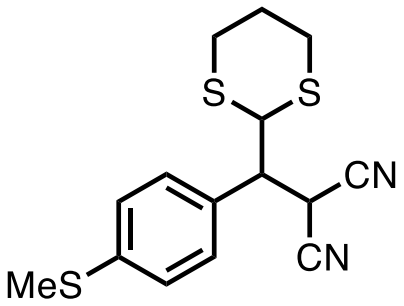
$^{13}C\{^{1}H\}$ NMR (75.5 MHz, $CDCl_3$): δ [ppm] = 160.6, 129.9, 125.3, 114.6, 111.9, 111.3, 55.4, 49.8, 48.0, 29.8, 29.6, 28.0, 25.2.

HRMS (ESI): *m/z* calcd. for $C_{15}H_{17}N_2OS_2^+$: 305.0777, found:305.0790.

m.p. = 116–117 °C.

This product was also obtained via Method B on a 1.00 mmol scale with an irradiation time of 36 h. Yield: 65% (198 mg, 650 µmol).

2-((1,3-Dithian-2-yl)(4-(methylthio)phenyl)methyl)malononitrile (**3h**)



By GP1 starting from (4-(methylthio)benzylidene)malononitrile (**2h**, 20.0 mg). Purified by column chromatography (SiO_2, Pentane/EtOAc 2:1).

Yield (Method A): 87% (^{1}H NMR yield vs. 1,3,5-trimethoxybenzene).

Yield (Method B): 86% (27.7 mg, 86.4 µmol).

Appearance: Pale-orange solid.

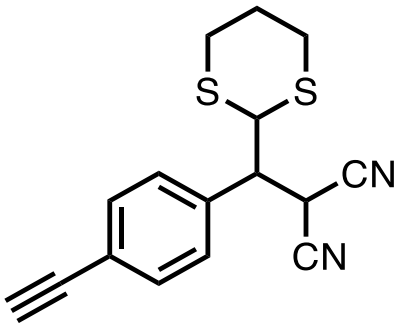
^{1}H NMR (300 MHz, $CDCl_3$): δ [ppm] = 7.35 – 7.26 (m, 4H), 4.73 (d, *J* = 5.8 Hz, 1H), 4.49 (d, *J* = 10.0 Hz, 1H), 3.53 (dd, *J* = 10.1, 5.8 Hz, 1H), 2.98 – 2.90 (m, 2H), 2.88 – 2.75 (m, 2H), 2.49 (s, 3H), 2.19 – 2.06 (m, 1H), 1.99 – 1.82 (m, 2H).

$^{13}C\{^{1}H\}$ NMR (75.5 MHz, $CDCl_3$): δ [ppm] = 141.1, 129.7, 129.0, 126.5, 111.8, 111.2, 50.0, 47.6, 29.7, 29.5, 27.9, 25.2, 15.3.

HRMS (ESI): *m/z* calcd. for $C_{15}H_{17}N_2S_3^+$: 321.0548, found: 321.0550.

m.p. = 101–103 °C.

2-((1,3-Dithian-2-yl)(4-ethynylphenyl)methyl)malononitrile (**3i**)



By GP1 starting from (4-ethynylbenzylidene)malononitrile (**2i**, 17.8 mg). Purified by column chromatography (SiO_2, Pentane/CH_2Cl_2 1:2).

Yield (Method A): 67% (20.0 mg, 67.0 µmol).

Yield (Method B): 70% (21.0 mg, 70.3 µmol).

Appearance: Off-white solid.

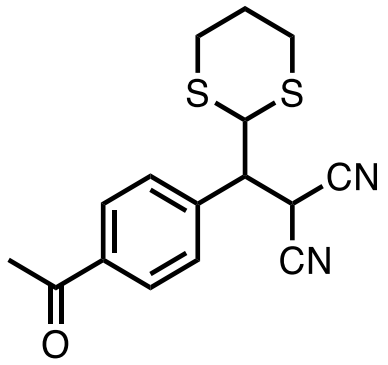
^{1}H NMR (300 MHz, $CDCl_3$): δ [ppm] = 7.63 – 7.50 (m, 2H), 7.43 – 7.31 (m, 2H), 4.75 (d, J = 5.8 Hz, 1H), 4.48 (d, J = 10.1 Hz, 1H), 3.58 (dd, J = 10.1, 5.8 Hz, 1H), 3.14 (s, 1H), 3.01 – 2.90 (m, 2H), 2.88 – 2.73 (m, 2H), 2.21 – 2.04 (m, 1H), 2.00 – 1.82 (m, 1H).

^{13}C{^{1}H} NMR (75.5 MHz, $CDCl_3$): δ [ppm] = 134.1, 133.0, 128.7, 123.9, 111.6, 111.0, 82.8, 78.9, 50.1, 47.2, 29.5, 29.4, 27.7, 25.1.

HRMS (ESI): *m/z* calcd. for $C_{16}H_{15}N_2S_2^+$: 299.0671, found: 299.0694.

m.p. = 123–124 °C.

2-((1,3-Dithian-2-yl)(4-acetylphenyl)methyl)malononitrile (**3j**)

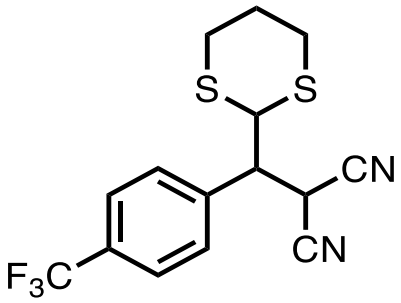


By GP1 starting from (4-acetylbenzylidene)malononitrile (**2j**, 19.6 mg).

Yield (Method A): 96% (^{1}H NMR yield vs. 1,3,5-trimethoxybenzene).

Yield (Method B): 66% (^{1}H NMR yield vs. 1,3,5-trimethoxybenzene).

2-((1,3-Dithian-2-yl)(4-(trifluoromethyl)phenyl)methyl)malononitrile (**3k**)



By GP1 starting from (4-(trifluoromethyl)benzylidene)malononitrile (**2k**, 22.2 mg). Purified by column chromatography (SiO_2, Pentane/CH_2Cl_2 1:2).

Yield (Method A): 90% (^{1}H NMR yield vs. 1,3,5-trimethoxybenzene).

Yield (Method B): 81% (27.7 mg, 80.1 µmol).

Appearance: Off-white solid.

^{1}H NMR (600 MHz, $CDCl_3$): *δ* [ppm] = 7.77 – 7.65 (m, 2H), 7.60 – 7.50 (m, 2H), 4.79 (d, *J* = 5.7 Hz, 1H), 4.51 (d, *J* = 10.2 Hz, 1H), 3.65 (dd, *J* = 10.2, 5.6 Hz, 1H), 3.02 – 2.90 (m, 2H), 2.90 – 2.77 (m, 2H), 2.17 – 2.09 (m, 1H), 1.97 – 1.88 (m, 1H).

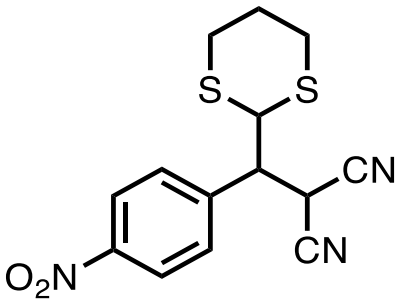
^{19}F NMR (565 MHz, $CDCl_3$): *δ* [ppm] = −62.83.

^{13}C{^{1}H} NMR (151 MHz, $CDCl_3$): *δ* [ppm] = 137.4, 132.0 (q, *J* = 32.8 Hz), 129.3, 126.3 (q, *J* = 4.0 Hz), 123.8 (q, *J* = 272.7 Hz), 111.5, 110.9, 50.0, 47.0, 29.5, 29.3, 27.7, 25.0.

HRMS (ESI): *m/z* calcd. for $C_{15}H_{14}F_3N_2S_2^+$: 343.0545, found: 343.0567.

m.p. = 140–141 °C.

2-((1,3-Dithian-2-yl)(4-nitrophenyl)methyl)malononitrile (**3l**)

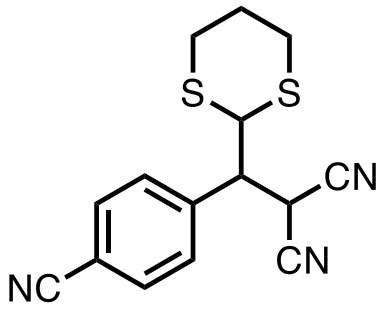


By GP1 starting from (4-nitrobenzylidene)malononitrile (**2l**, 19.9 mg).

Yield (Method A): <5% (^{1}H NMR yield vs. 1,3,5-trimethoxybenzene).

Yield (Method B): <5% (^{1}H NMR yield vs. 1,3,5-trimethoxybenzene).

2-((1,3-Dithian-2-yl)(4-cyanophenyl)methyl)malononitrile (**3m**)



By GP1 starting from (4-cyanobenzylidene)malononitrile (**2m**, 17.9 mg). Purified by column chromatography (SiO_2, CH_2Cl_2).

Yield (Method A): 81% (^{1}H NMR yield vs. 1,3,5-trimethoxybenzene).

Yield (Method B): 85% (25.3 mg, 84.5 µmol).

Appearance: Off-white solid.

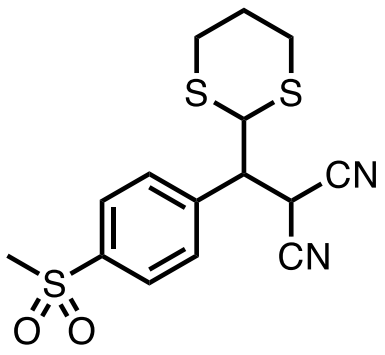
^{1}H NMR (300 MHz, $CDCl_3$): δ [ppm] = 7.82 – 7.69 (m, 2H), 7.61 – 7.48 (m, 2H), 4.79 (d, J = 5.7 Hz, 1H), 4.48 (d, J = 10.3 Hz, 1H), 3.64 (dd, J = 10.2, 5.6 Hz, 1H), 3.04 – 2.90 (m, 2H), 2.88 – 2.75 (m, 2H), 2.20 – 2.07 (m, 1H), 2.01 – 1.84 (m, 1H).

^{13}C{^{1}H} NMR (75.5 MHz, $CDCl_3$): δ [ppm] = 138.6, 133.0, 129.7, 118.1, 114.0, 111.3, 110.7, 50.2, 46.7, 29.4, 29.3, 27.5, 25.0.

HRMS (ESI): *m/z* calcd. for $C_{15}H_{14}N_2S_2^+$: 300.0624, found: 300.0645.

m.p. = 140–142 °C.

2-((1,3-Dithian-2-yl)(4-(methylsulfonyl)phenyl)methyl)malononitrile (**3n**)



By GP1 starting from (4-(methylsulfonyl)benzylidene)malononitrile (**2n**, 23.2 mg). Purified by automated flash column chromatography (C_{18}-SiO_2, 20% MeCN in H_2O → 100% MeCN).

Yield (Method A): 90% (^{1}H NMR yield vs. 1,3,5-trimethoxybenzene).

Yield (Method B): 79% (27.7 mg, 78.9 µmol).

Appearance: Beige solid.

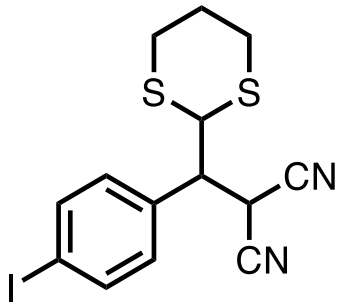
^{1}H NMR (400 MHz, $CDCl_3$): δ [ppm] = 8.12 – 7.92 (m, 2H), 7.70 – 7.51 (m, 2H), 4.82 (d, *J* = 5.5 Hz, 1H), 4.50 (d, *J* = 10.3 Hz, 1H), 3.69 (dd, *J* = 10.3, 5.6 Hz, 1H), 3.11 (s, 3H), 3.04 – 2.89 (m, 2H), 2.89 – 2.74 (m, 2H), 2.20 – 2.07 (m, 1H), 2.00 – 1.85 (m, 1H).

^{13}C{^{1}H} NMR (75.5 MHz, $CDCl_3$): δ [ppm] = 141.9, 139.6, 130.0, 128.3, 111.4, 110.7, 50.0, 46.6, 44.6, 29.3, 29.2, 27.6, 24.9.

HRMS (ESI): *m/z* calcd. for $C_{15}H_{17}N_2O_2S_3^+$: 353.0447, found: 353.0470.

m.p. = 185–186 °C.

2-((1,3-Dithian-2-yl)(4-iodophenyl)methyl)malononitrile (**3o**)



By GP1 starting from (4-iodobenzylidene)malononitrile (**2o**, 28.0 mg). Purified by column chromatography (SiO_2, Pentane/CH_2Cl_2 1:2).

Yield (Method A): 93% (37.1 mg, 92.7 µmol).

Yield (Method B): 94% (37.7 mg, 94.1 µmol).

Appearance: Colorless solid.

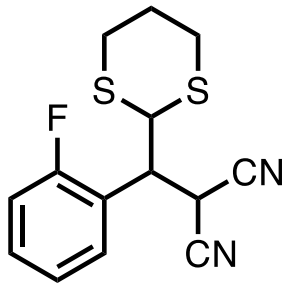
^{1}H NMR (300 MHz, $CDCl_3$): δ [ppm] = 7.89 – 7.68 (m, 2H), 7.23 – 7.06 (m, 2H), 4.74 (d, *J* = 5.8 Hz, 1H), 4.46 (d, *J* = 10.1 Hz, 1H), 3.53 (dd, *J* = 10.1, 5.7 Hz, 1H), 3.01 – 2.88 (m, 2H), 2.88 – 2.74 (m, 2H), 2.22 – 2.03 (m, 1H), 1.99 – 1.82 (m, 1H).

^{13}C{^{1}H} NMR (75.5 MHz, $CDCl_3$): δ [ppm] = 138.5, 133.1, 130.4, 111.6, 111.0, 96.1, 50.0, 47.2, 29.6, 29.4, 27.6, 25.1.

HRMS (ESI): *m/z* calcd. for $C_{14}H_{14}IN_2S_2^+$: 400.9638, found: 400.9651.

m.p. = 118–119 °C.

2-((1,3-Dithian-2-yl)(2-fluorophenyl)methyl)malononitrile (**3p**)



By GP1 starting from (2-fluorobenzylidene)malononitrile (**2p**, 17.2 mg). Purified by column chromatography (SiO_2, Pentane/CH_2Cl_2 1:2).

Yield (Method A): 72% (^{1}H NMR yield vs. 1,3,5-trimethoxybenzene).

Yield (Method B): 88% (25.7 mg, 87.9 µmol).

Appearance: Colorless solid.

^{1}H NMR (300 MHz, $CDCl_3$): *δ* [ppm] = 7.58 – 7.47 (m, 1H), 7.47 – 7.37 (m, 1H), 7.31 – 7.10 (m, 2H), 4.79 (d, *J* = 5.5 Hz, 1H), 4.39 (d, *J* = 10.7 Hz, 1H), 4.21 (dd, *J* = 10.7, 5.5 Hz, 1H), 3.08 – 2.81 (m, 3H), 2.81 – 2.67 (m, 1H), 2.18 – 1.91 (m, 2H).

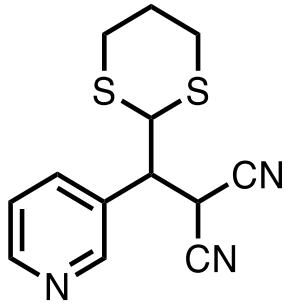
^{19}F NMR (282 MHz, $CDCl_3$): *δ* [ppm] = −115.47.

^{13}C{^{1}H} NMR (75.5 MHz, $CDCl_3$): *δ* [ppm] = 161.2 (d, *J* = 247.4 Hz), 131.3 (d, *J* = 8.6 Hz), 128.5 (d, *J* = 2.8 Hz), 125.1 (d, *J* = 3.9 Hz), 121.7 (d, *J* = 13.5 Hz), 116.3 (d, *J* = 22.9 Hz), 111.5, 111.2, 46.1, 41.9 (d, *J* = 2.8 Hz), 28.2, 28.0, 27.5, 25.0.

HRMS (ESI): *m/z* calcd. for $C_{14}H_{14}FN_2S_2^+$: 293.0577, found: 293.0588.

m.p. = 135–136 °C.

2-((1,3-Dithian-2-yl)(pyridin-3-yl)malononitrile (**3q**)



By GP1 starting from (pyridin-3-ylmethylidene)malononitrile (**2q**, 15.5 mg). Purified by automated flash column chromatography (C_{18}-SiO_2, 20% MeCN in H_2O → 100% MeCN).

Yield (Method A): 64% (^{1}H NMR yield vs. 1,3,5-trimethoxybenzene).

Yield (Method B): 57% (15.8 mg, 57.7 µmol).

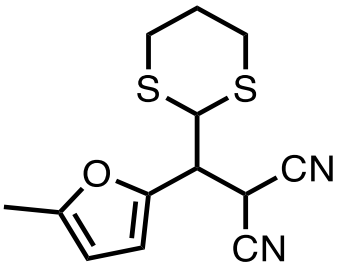
Appearance: Yellow fluffy solid (lyophilisate).

^{1}H NMR (300 MHz, $CDCl_3$): δ [ppm] = 8.78 – 8.58 (m, 2H), 7.80 (dt, *J* = 8.0, 2.0 Hz, 1H), 7.40 (dd, *J* = 8.1, 4.9 Hz, 1H), 4.82 (d, *J* = 5.7 Hz, 1H), 4.49 (d, *J* = 10.2 Hz, 1H), 3.66 (dd, *J* = 10.2, 5.6 Hz, 1H), 3.02 – 2.90 (m, 2H), 2.88 – 2.74 (m, 2H), 2.20 – 2.05 (m, 1H), 2.00 – 1.83 (m, 1H).

^{13}C{^{1}H} NMR (75.5 MHz, $CDCl_3$): δ [ppm] = 151.0, 150.1, 135.9, 129.7, 124.0, 111.4, 110.8, 48.0, 46.8, 29.3, 29.1, 27.7, 25.0.

HRMS (ESI): *m/z* calcd. for $C_{13}H_{14}N_3S_2^+$: 276.0624, found: 276.0635.

2-((1,3-Dithian-2-yl)(5-methylfuran-2-yl)methyl)malononitrile (**3r**)

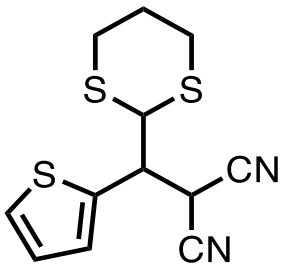


By GP1 starting from ((5-methylfuran-2-yl)methylidene)malononitrile (**2r**, 15.8 mg).

Yield (Method A): 24% (^{1}H NMR yield vs. 1,3,5-trimethoxybenzene).

Yield (Method B): 47% (^{1}H NMR yield vs. 1,3,5-trimethoxybenzene).

2-((1,3-Dithian-2-yl)(thiophen-2-yl)methyl)malononitrile (**3s**)



By GP1 starting from (thiophen-2-ylmethylidene)malononitrile (**2s**, 16.0 mg). Purified by column chromatography (SiO_2, Pentane/CH_2Cl_2 1:2).

Yield (Method A): 53% (^{1}H NMR yield vs. 1,3,5-trimethoxybenzene).

Yield (Method B): 55% (15.5 mg, 55.2 µmol).

Appearance: Off-white solid.

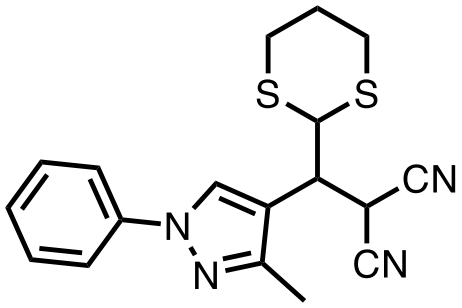
^{1}H NMR (300 MHz, $CDCl_3$): δ [ppm] = 7.40 (d, *J* = 5.2 Hz, 1H), 7.22 (d, *J* = 3.9 Hz, 1H), 7.08 (dd, *J* = 5.2, 3.5 Hz, 1H), 4.70 (d, *J* = 6.1 Hz, 1H), 4.43 (d, *J* = 9.4 Hz, 1H), 3.96 (dd, *J* = 9.4, 6.1 Hz, 1H), 3.00 – 2.75 (m, 4H), 2.20 – 2.06 (m, 1H), 2.01 – 1.85 (m, 1H).

$^{13}C\{^{1}H\}$ NMR (75.5 MHz, $CDCl_3$): δ [ppm] = 135.4, 128.7, 127.4, 127.1, 111.6, 111.1, 48.7, 46.3, 29.5, 29.4, 28.8, 25.1.

HRMS (ESI): *m/z* calcd. for $C_{12}H_{13}N_2S_3^+$: 281.0236, found: 281.0258.

m.p. = 94–96 °C.

(1,3-Dithian-2-yl)(3-methyl-1-phenyl-1*H*-pyrazol-4-yl)methyl)malononitrile (**3t**)



By GP1 starting from ((3-methyl-1-phenyl-1*H*-pyrazol-4-yl)methylene)malononitrile (**2t**, 23.4 mg). Purified by column chromatography (SiO_2, Pentane/EtOAc 3:1).

Yield (Method A): 53% (^{1}H NMR yield vs. 1,3,5-trimethoxybenzene).

Yield (Method B): 50% (17.9 mg, 50.4 µmol).

Appearance: Pale-brown solid.

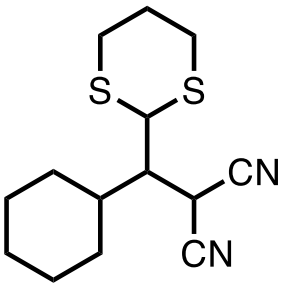
^{1}H NMR (300 MHz, $CDCl_3$): δ [ppm] = 8.09 (s, 1H), 7.74 – 7.63 (m, 2H), 7.50 – 7.39 (m, 2H), 7.33 – 7.26 (m, 1H), 4.65 (d, *J* = 5.5 Hz, 1H), 4.41 (d, *J* = 9.4 Hz, 1H), 3.67 (dd, *J* = 9.4, 5.5 Hz, 1H), 2.98 – 2.91 (m, 2H), 2.91 – 2.84 (m, 2H), 2.42 (s, 3H), 2.21 – 2.08 (m, 1H), 1.99 – 1.83 (m, 1H).

$^{13}C\{^{1}H\}$ NMR (75.5 MHz, $CDCl_3$): δ [ppm] = 150.2, 139.8, 129.6, 126.8, 125.8, 119.3, 114.6, 111.9, 111.6, 49.3, 41.7, 29.9, 29.7, 28.3, 25.1, 12.2.

HRMS (ESI): *m/z* calcd. for $C_{18}H_{19}N_4S_2^+$: 355.1046, found: 355.1042.

m.p. = 154–155 °C.

(Cyclohexyl(1,3-dithian-2-yl)methyl)malononitrile (**3u**)



By GP1 starting from cyclohexylmethylidenemalononitrile (**2u**, 16.0 mg). Purified by column chromatography (Neutral Al_2O_3, Pentane/EtOAc 8:1).

Yield (Method A): 56% (^{1}H NMR yield vs. 1,3,5-trimethoxybenzene).

Yield (Method B): 76% (21.4 mg, 76.3 µmol).

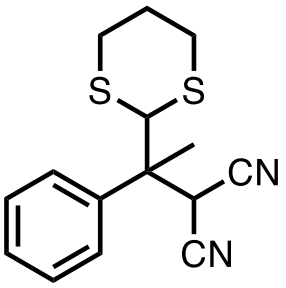
Appearance: Colorless gum.

^{1}H NMR (600 MHz, $CDCl_3$): *δ* [ppm] = 4.52 (d, *J* = 2.2 Hz, 1H), 4.46 (d, *J* = 4.4 Hz, 1H), 2.97 (ddd, *J* = 14.2, 11.6, 2.7 Hz, 1H), 2.93 – 2.85 (m, 2H), 2.83 (ddd, *J* = 14.2, 11.4, 2.6 Hz, 1H), 2.18 (ddd, *J* = 8.6, 4.6, 2.3 Hz, 1H), 2.16 – 2.05 (m, 2H), 2.05 – 2.00 (m, 1H), 1.93 – 1.78 (m, 3H), 1.75 – 1.68 (m, 1H), 1.39 – 1.30 (m, 2H), 1.24 – 1.12 (m, 3H).

^{13}C{^{1}H} NMR (151 MHz, $CDCl_3$): *δ* [ppm] = 113.6, 112.3, 51.4, 48.0, 37.9, 31.0, 30.9, 30.3, 29.9, 26.04, 25.99, 25.9, 25.3, 22.8.

HRMS (ESI): *m/z* calcd. for $C_{14}H_{21}N_2S_2^+$: 281.1141, found: 281.1142.

(1-(1,3-Dithian-2-yl)-1-phenylethyl)malononitrile (**3v**)

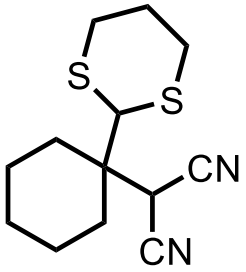


By GP1 starting from (1-phenylethylidene)malononitrile (**2v**, 16.8 mg).

Yield (Method A): <5% (^{1}H NMR yield vs. 1,3,5-trimethoxybenzene).

Yield (Method B): <5% (^{1}H NMR yield vs. 1,3,5-trimethoxybenzene).

(1-(1,3-Dithian-2-yl)cyclohexyl)malononitrile (**3w**)

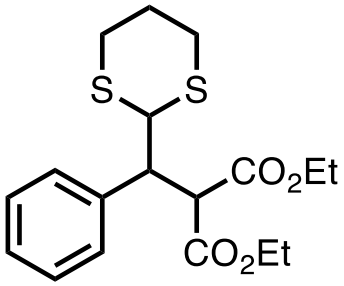


By GP1 starting from cyclohexylidenemalononitrile (**2w**, 14.6 mg).

Yield (Method A): <5% (^{1}H NMR yield vs. 1,3,5-trimethoxybenzene).

Yield (Method B): <5% (^{1}H NMR yield vs. 1,3,5-trimethoxybenzene).

Diethyl ((1,3-dithian-2-yl)(phenyl)methyl)malonate (**3x**)

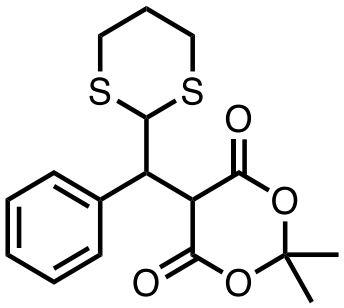


By GP1 starting from diethyl benzylidenemalonate (**2x**, 24.8 mg).

Yield (Method A): <5% (^{1}H NMR yield vs. 1,3,5-trimethoxybenzene).

Yield (Method B): <5% (^{1}H NMR yield vs. 1,3,5-trimethoxybenzene).

5-((1,3-Dithian-2-yl)(phenyl)methyl)-2,2-dimethyl-1,3-dioxane-4,6-dione (**3y**)



By GP1 starting from 5-benzylidene-2,2-dimethyl-1,3-dioxane-4,6-dione (**2y**, 23.2 mg). Purified by column chromatography (SiO_2, CH_2Cl_2 → CH_2Cl_2 + 0.1% AcOH).

Yield (Method A): 76% (^{1}H NMR yield vs. 1,3,5-trimethoxybenzene).

Yield (Method B): 58% (57.6 µmol).

Appearance: Colorless sticky foam.

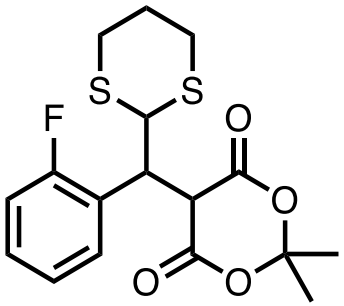
^{1}H NMR (600 MHz, $CDCl_3$): δ [ppm] = 7.42 – 7.37 (m, 2H), 7.35 – 7.27 (m, 3H), 4.93 (d, *J* = 12.3 Hz, 1H), 4.54 – 4.45 (m, 1H), 4.41 (dd, *J* = 12.3, 2.6 Hz, 1H), 3.06 (ddd, *J* = 14.3, 8.6, 3.9 Hz, 1H), 2.91 (ddd, *J* = 14.4, 8.3, 3.9 Hz, 1H), 2.74 (ddd, *J* = 14.2, 6.8, 3.7 Hz, 1H), 2.61 (ddd, *J* = 14.2, 7.0, 3.7 Hz, 1H), 2.07 – 2.00 (m, 2H), 1.67 (s, 3H), 1.29 (s, 3H).

^{13}C{^{1}H} NMR (151 MHz, $CDCl_3$): δ [ppm] = 165.5, 164.7, 137.9, 129.6, 129.0, 128.4, 105.6, 49.6, 48.7, 45.3, 28.4, 28.0, 27.1, 26.7, 25.4.

HRMS (ESI): *m/z* calcd. for $C_{17}H_{19}O_4S_2^-$: 351.0730, found: 351.0747.

This product was also obtained via Method B on a 1.00 mmol scale with an irradiation time of 24 h. Yield: 54% (189 mg, 536 µmol).

5-((1,3-Dithian-2-yl)(2-fluorophenyl)methyl)-2,2-dimethyl-1,3-dioxane-4,6-dione (**3z**)



By GP1 starting from 5-(2-fluorobenzylidene)-2,2-dimethyl-1,3-dioxane-4,6-dione (**2z**, 25.0 mg). Purified by column chromatography (SiO_2, CH_2Cl_2 → CH_2Cl_2 + 0.1% AcOH).

Yield (Method A): 89% (^{1}H NMR yield vs. 1,3,5-trimethoxybenzene).

Yield (Method B): 75% (27.7 mg, 74.8 µmol).

Appearance: Colorless solid.

^{1}H NMR (300 MHz, $CDCl_3$): δ [ppm] = 7.78 – 7.56 (m, 1H), 7.33 – 7.26 (m, 1H), 7.20 – 7.00 (m, 2H), 5.13 (dd, *J* = 12.2, 2.1 Hz, 1H), 4.70 (d, *J* = 12.1 Hz, 1H), 4.09 (d, *J* = 2.0 Hz, 1H), 3.05 (ddt, *J* = 14.1, 10.7, 3.2 Hz, 2H), 2.56 (tdd, *J* = 13.8, 5.9, 3.0 Hz, 2H), 2.14 – 1.91 (m, 2H), 1.71 (s, 3H), 1.60 (s, 3H).

^{19}F NMR (282 MHz, $CDCl_3$): δ [ppm] = −115.68.

^{13}C{^{1}H} NMR (151 MHz, $CDCl_3$): δ [ppm] = 164.7, 164.6, 161.1 (d, *J* = 246.4 Hz), 129.6 (d, *J* = 7.3 Hz), 129.5 (d, *J* = 19.2 Hz), 127.1 (d, *J* = 13.6 Hz), 124.8 (d, *J* = 4.0 Hz), 115.6 (d, *J* = 23.2 Hz), 105.4, 49.9, 43.2, 39.1 (d, *J* = 3.4 Hz), 28.3, 27.6, 26.1, 25.3, 25.0.

HRMS (ESI): *m/z* calcd. for $C_{17}H_{19}FNaO_4S_2^+$: 393.0601, found: 393.0598.

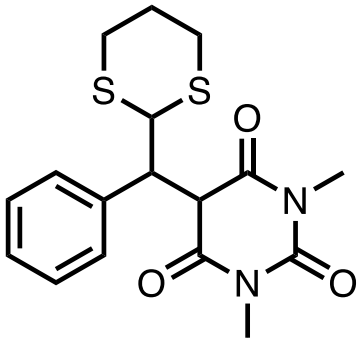
m.p. = 145–146 °C.

This product was also obtained via Method B on a 4.00 mmol scale via two parallel 2.00 mmol scale reactions with an irradiation time of 36 h (Fig. 1). The mixtures were combined after irradiation and treated as one reaction. Yield: 68% (1.01 g, 2.73 mmol).



***Figure 1**. Large-scale synthesis of **3z**.*

5-((1,3-Dithian-2-yl)(phenyl)methyl)-1,3-dimethylpyrimidine-2,4,6(1H,3H,5H)-trione (**3aa**)

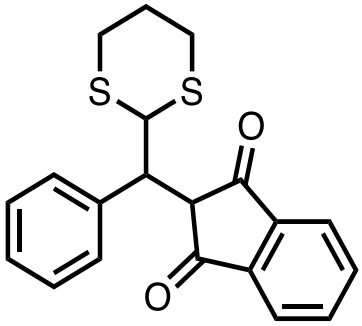


By GP1 starting from *N*,*N'*-dimethyl-4-benzylidenebarbituric acid (**3c**, 24.4 mg).

Yield (Method A): 88% (^{1}H NMR yield vs. 1,3,5-trimethoxybenzene).

Yield (Method B): 76% (^{1}H NMR yield vs. 1,3,5-trimethoxybenzene).

2-((1,3-Dithian-2-yl)(phenyl)methyl)-1*H*-indene-1,3(2*H*)-dione (**3ab**)



By GP1 starting from 2-benzylideneindane-1,3-dione (**3d**, 23.4 mg). Purified by column chromatography (SiO_2, Pentane/CH_2Cl_2 1:3).

Yield (Method A): 87% (^{1}H NMR yield vs. 1,3,5-trimethoxybenzene).

Yield (Method B): 40% (14.2 mg, 40.1 µmol).

Appearance: Off-white solid.

^{1}H NMR (300 MHz, $CDCl_3$): δ [ppm] = 7.93 – 7.81 (m, 2H), 7.79 – 7.69 (m, 2H), 7.42 – 7.33 (m, 2H), 7.26 – 7.10 (m, 3H), 4.83 (d, *J* = 12.1 Hz, 1H), 4.13 (dd, *J* = 12.2, 2.7 Hz, 1H), 3.88 (d, *J* = 2.6 Hz, 1H), 2.99 – 2.85 (m, 2H), 2.77 – 2.60 (m, 2H), 2.11 – 1.88 (m, 2H).

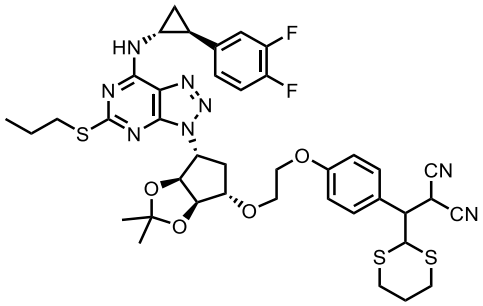
^{13}C{^{1}H} NMR (75.5 MHz, $CDCl_3$): δ [ppm] = 198.9, 198.6, 142.3, 142.0, 139.1, 135.5, 135.4, 129.2, 128.6, 127.7, 123.2, 123.1, 57.5, 48.3, 46.6, 28.2, 27.7, 25.5.

HRMS (ESI): *m/z* calcd. for $C_{20}H_{18}NaO_2S_2^+$: 377.0640, found: 377.0650.

m.p. = 154–155 °C.

This product was also obtained via Method B on a 1.00 mmol scale with an irradiation time of 36 h. Yield: 34% (122 mg, 344 µmol).

2-((4-(2-(((3aR,4S,6R,6aS)-6-(7-(((1R,2S)-2-(3,4-Difluorophenyl)cyclopropyl)amino)-5-(propylthio)-3H-[1,2,3]triazolo[4,5-d]pyrimidin-3-yl)-2,2-dimethyltetrahydro-4H-cyclopenta[d][1,3]dioxol-4-yl)oxy)ethoxy)phenyl)(1,3-dithian-2-yl)methyl)malononitrile (**3ac**)



By GP1 on a 50 µmol scale starting from **4c** (35.7 mg). Purified by automated flash column chromatography (C_{18}-SiO_2, 20% MeCN in H_2O → 100% MeCN).

Yield (Method A): 62% (25.8 mg, 30.9 µmol).

Yield (Method B): 41% (17.0 mg, 20.4 µmol).

Appearance: Colorless fluffy solid (lyophilisate)

The product is a mixture of two rotamers in DMSO-d_6 solution (Ratio 80%/20%), as is known for Ticagrelor and its derivatives.

^{1}H NMR (300 MHz, DMSO-d_6): δ [ppm] = 9.39 (d, J = 4.1 Hz, 0.8H), 9.00 (d, J = 5.0 Hz, 0.2H), 7.38 – 7.26 (m, 3.8H), 7.25 – 7.19 (m, 0.2H), 7.09 – 7.04 (m, 0.8H), 7.02 – 6.98 (m, 0.2H), 6.96 – 6.91 (m, 2H), 5.40 (d, J = 6.1 Hz, 1H), 5.24 (ddd, J = 6.9, 4.6, 1.4 Hz, 0.8H), 5.19 (dd, J = 7.4, 4.8 Hz, 0.2H), 5.03 (ddd, J = 9.6, 6.9, 4.5 Hz, 1H), 4.72 (dd, J = 7.3, 3.2 Hz, 0.8H), 4.69 (dd, J = 7.0, 3.5 Hz, 0.2H), 4.45 (d, J = 10.3 Hz, 1H), 4.14 – 4.01 (m, 4H), 3.84 – 3.77 (m, 1H), 3.77 – 3.70 (m, 1.2H), 3.14 (dq, J = 8.3, 4.1 Hz, 0.8H), 3.11 – 3.08 (m, 0.2H), 3.07 – 3.00 (m, 1.2H), 2.96 – 2.85 (m, 2.6H), 2.81 (ddd, J = 14.1, 8.7, 2.9 Hz, 1H), 2.73 – 2.65 (m, 2H), 2.58 (dt, J = 13.1, 8.7 Hz, 1H), 2.26 – 2.21 (m, 0.2H), 2.14 – 2.10 (m, 0.8H), 1.95 – 1.87 (m, 1H), 1.83 – 1.75 (m, 1H), 1.73 – 1.65 (m, 0.4H), 1.57 – 1.50 (m, 2.4H), 1.49 (s, 3H), 1.46 – 1.42 (m, 0.2H), 1.37 (dt, J = 7.9, 6.0 Hz, 1H), 1.26 (s, 2.4H), 1.25 (s, 0.6H), 0.98 (t, J = 7.3 Hz, 0.6H), 0.83 (t, J = 7.4 Hz, 2.4H).

^{19}F NMR (565 MHz, DMSO-d_6): δ [ppm] = −139.28 – −139.45 (m), −143.03 – −143.26 (m).

^{13}C{^{1}H} NMR (151 MHz, DMSO-d_6, only major signals): δ [ppm] = 169.5, 158.5, 153.9, 149.4 (dd, J = 244.1, 12.4 Hz), 149.1, 147.8 (dd, J = 241.0, 12.7 Hz), 139.3 – 139.2 (m), 129.7, 128.0, 123.2, 123.0 – 122.8 (m), 117.0 (d, J = 16.4 Hz, 114.9 (d, J = 17.5 Hz), 114.4, 113.5, 113.0, 112.5, 83.7, 82.2, 81.9, 67.4, 66.8, 61.4, 46.6, 46.0, 42.1, 40.4, 35.2, 34.0, 32.4, 28.6, 26.9, 26.8, 25.0, 24.7, 24.0, 22.4, 15.0, 13.1.

HRMS (ESI): *m/z* calcd. for $C_{40}H_{45}F_2N_8O_4S_3^+$: 835.2688, found: 835.2729.

Determination of the Excited-State Redox Potential of 1

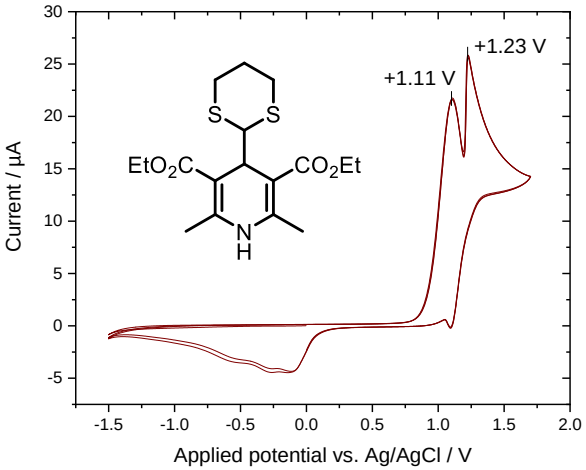


Figure 2. *Cyclic voltammogram (CV) of* ***1*** *in (1.0 mM) in 0.10 M Bu_4NPF_6 in MeCN (7.0 mL). ±0.00 V → −1.50 V → +1.70 V → ±0.00 V, 3 cycles. Scan rate 100 mV·s^{-1}.*

Hantzsch ester **1** shows an irreversible oxidation with an anodic peak potential of E_{pa} = +1.11 V *vs.* Ag/AgCl, which is attributed to oxidation of the dihydropyridine core (Fig. 2). Upon conversion, this is $\underline{E(\mathbf{1}^{\cdot+}/\mathbf{1})}$ = +1.06 V vs. SCE. To approximate the redox potential of **1** in its singlet excited state, the equation $\underline{E(\mathbf{1}^{\cdot+}/\mathbf{1}^*) = E(\mathbf{1}^{\cdot+}/\mathbf{1}) - E_{0\text{-}0}}$,where $E_{0\text{-}0}$ is the singlet energy, also known as the zero-zero-transition energy (that is the energy of the lowest vibrational state of the first singlet excited state), was used. $E_{0\text{-}0}$ is approximated from the UV-Vis (absorption) and fluorescence (emission) spectrum according to the mirror image rule as the intersection of the normalized curves (Fig. 3).

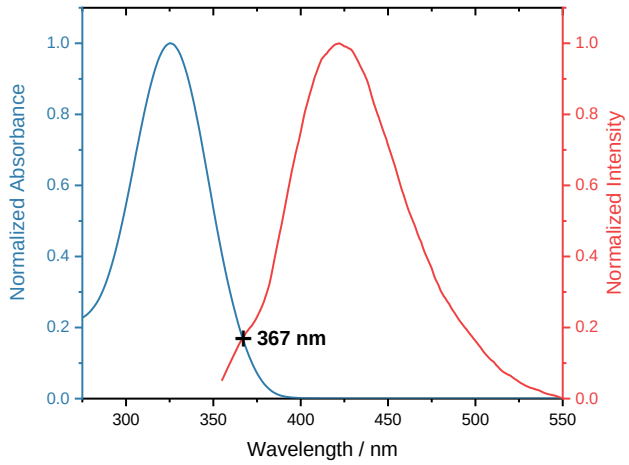
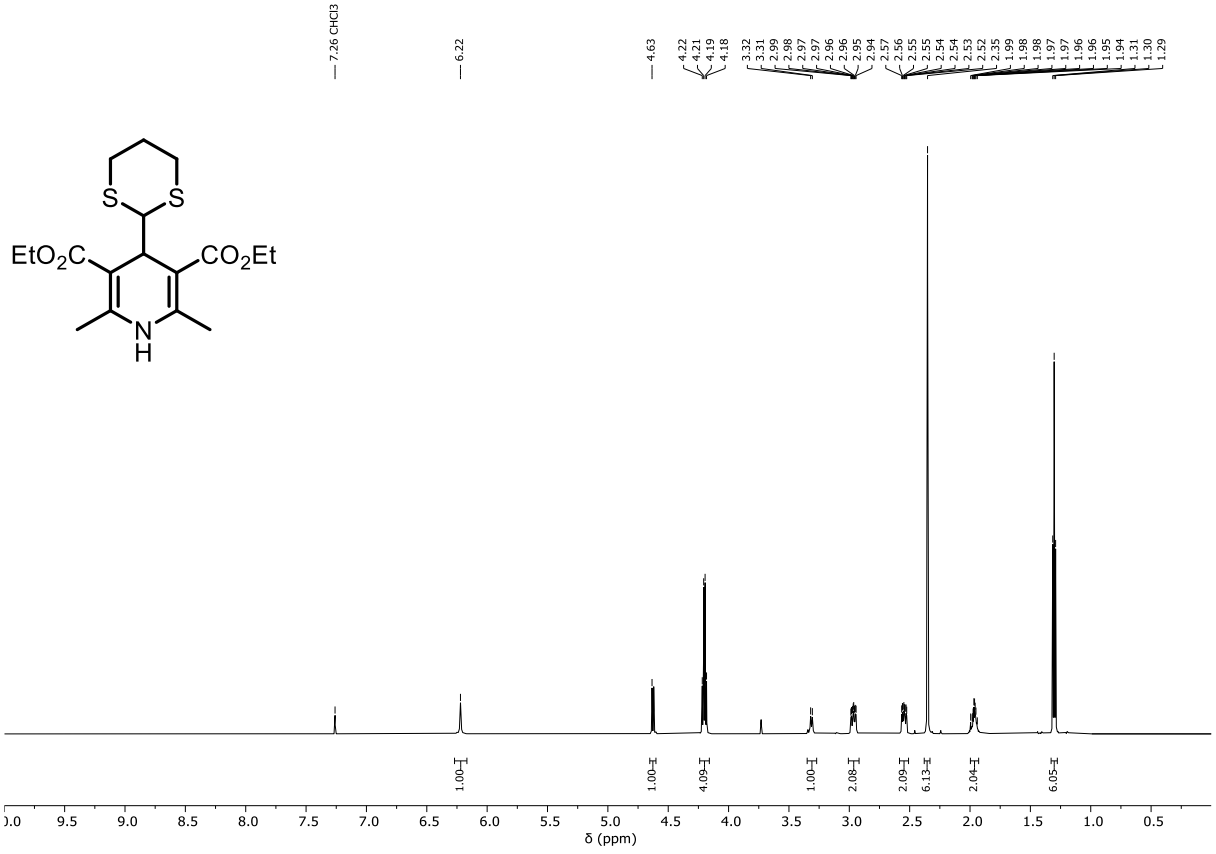


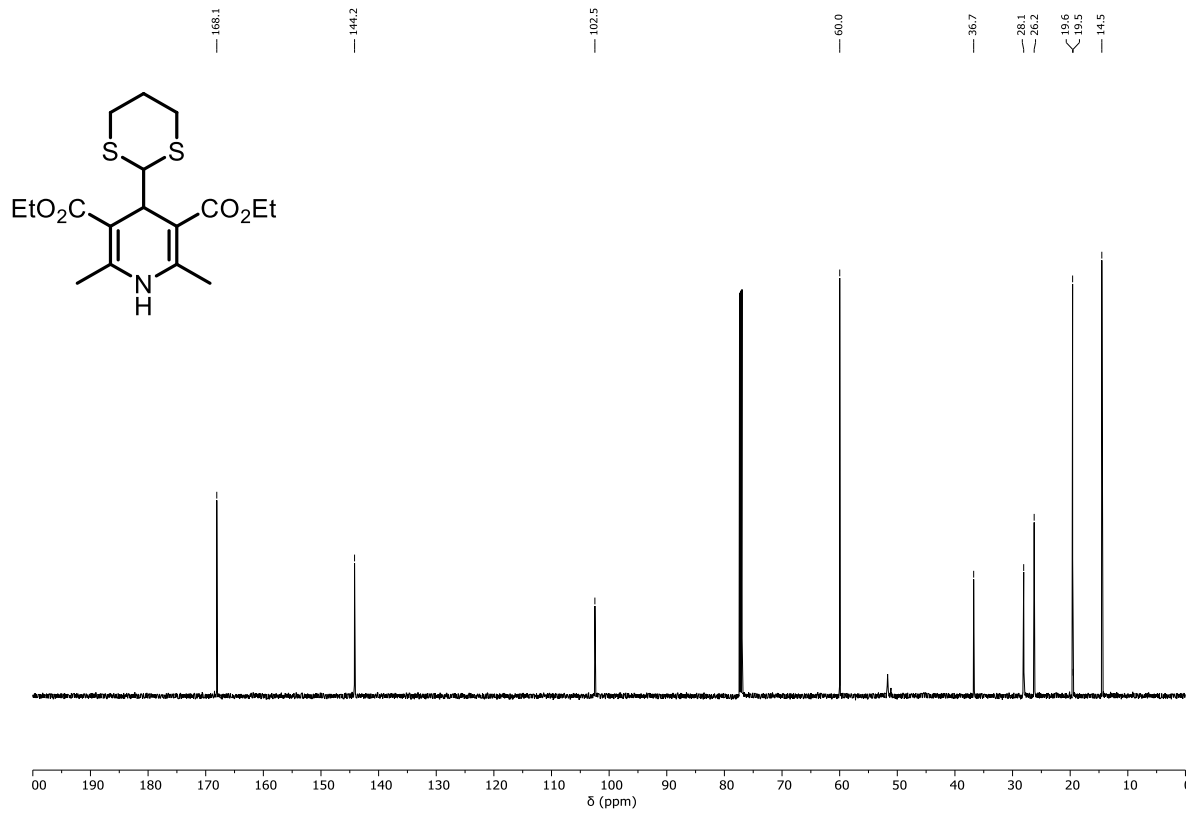
Figure 3. *Blue: Normalized UV-Vis absorption spectrum of* ***1****, 0.3 mM in MeCN, path length 10 mm. Red: Normalized fluorescence spectrum of* ***1****, 90 degree mode, 0.3 mM in MeCN, 10 mm cuvette, excitation wavelength: 340 nm, excitation slit: 10 nm, emission slit: 10 nm.*

The intersection was found to be 367 nm, which corresponds to an energy of 77.9 kcal·mol^{-1}, or 326 kJ·mol^{-1}, or 3.38 eV (≙ 3.38 V for one electron). The excited state redox potential in the singlet state S_1 is thus approximately $E(\mathbf{1}^{\cdot+}/\mathbf{1}^*)$ = 1.06 V – 3.38 V = $\underline{-2.32 \text{ V vs. SCE}}$.

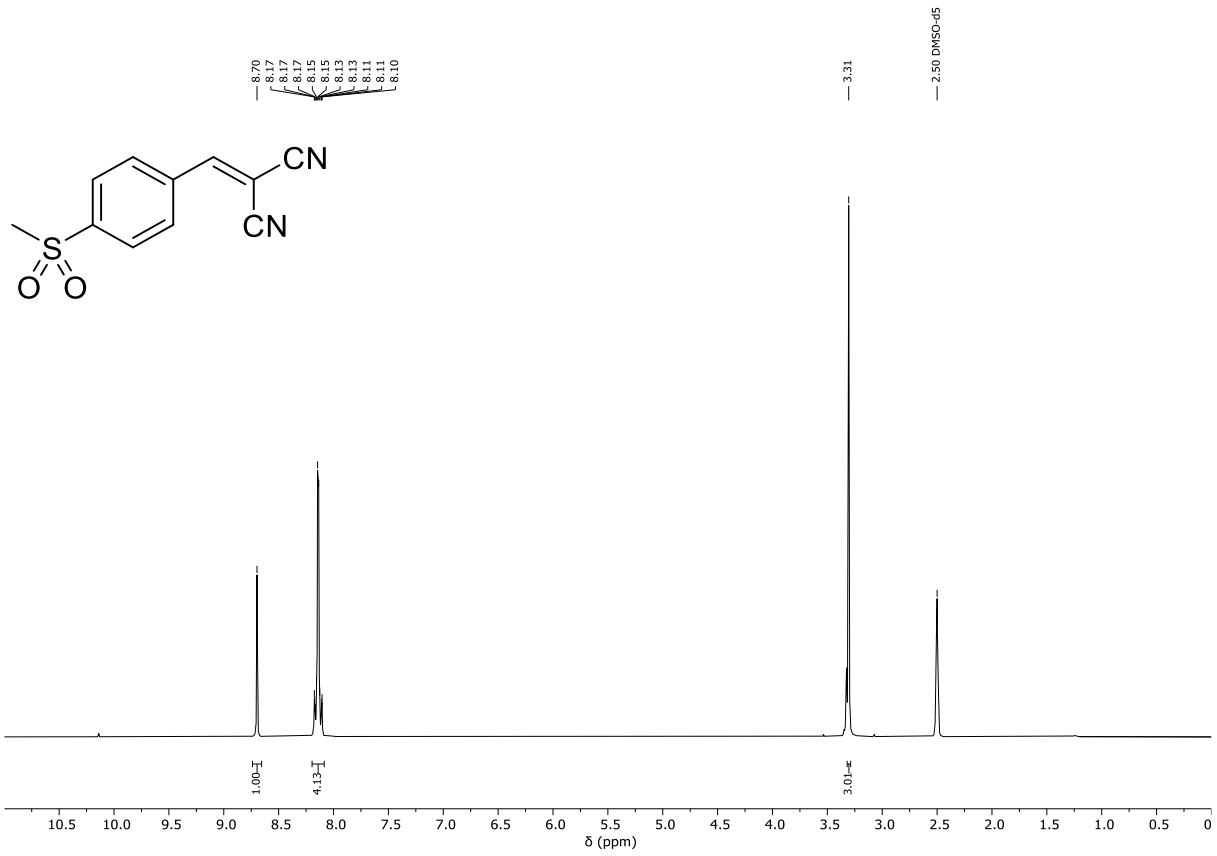
NMR Spectra of all Compounds



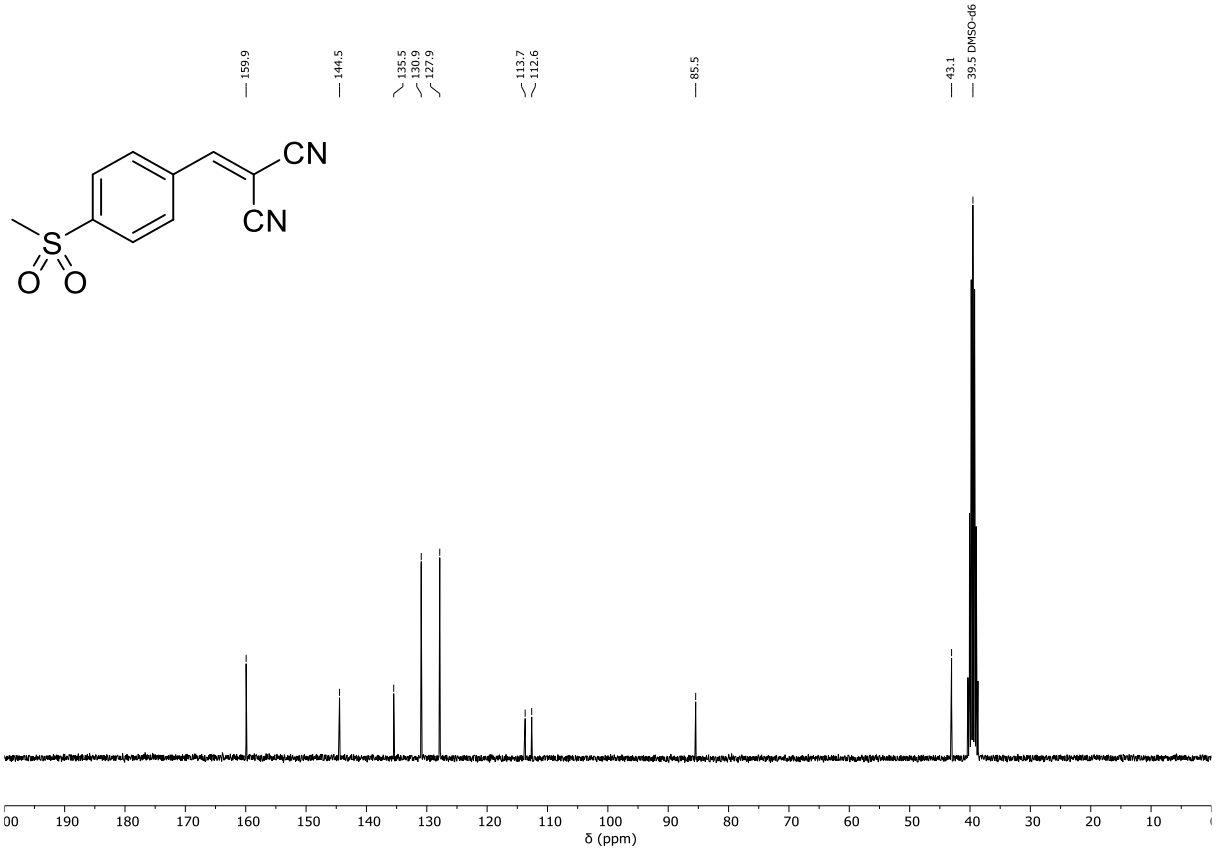
^{1}H NMR spectrum (600 MHz, $CDCl_3$) of **1**



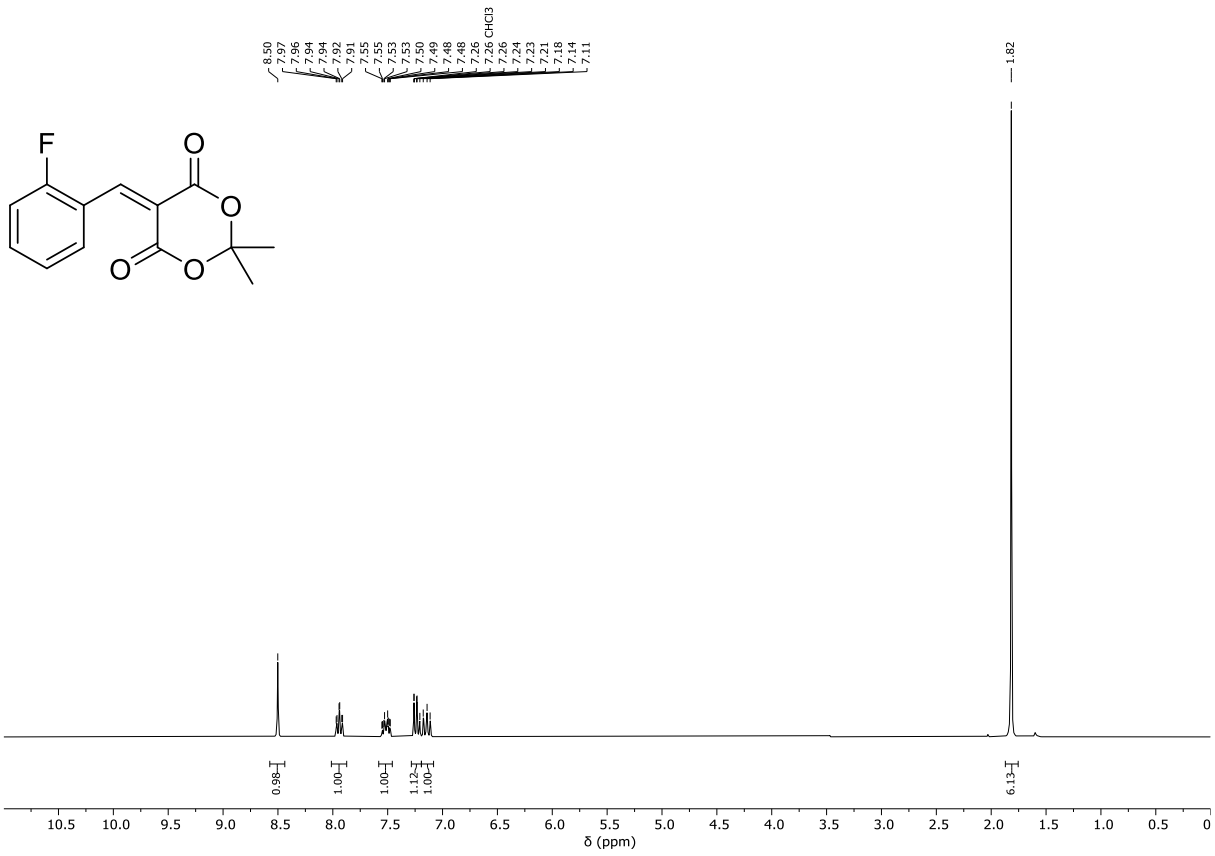
^{13}C NMR spectrum (151 MHz, $CDCl_3$) of **1**



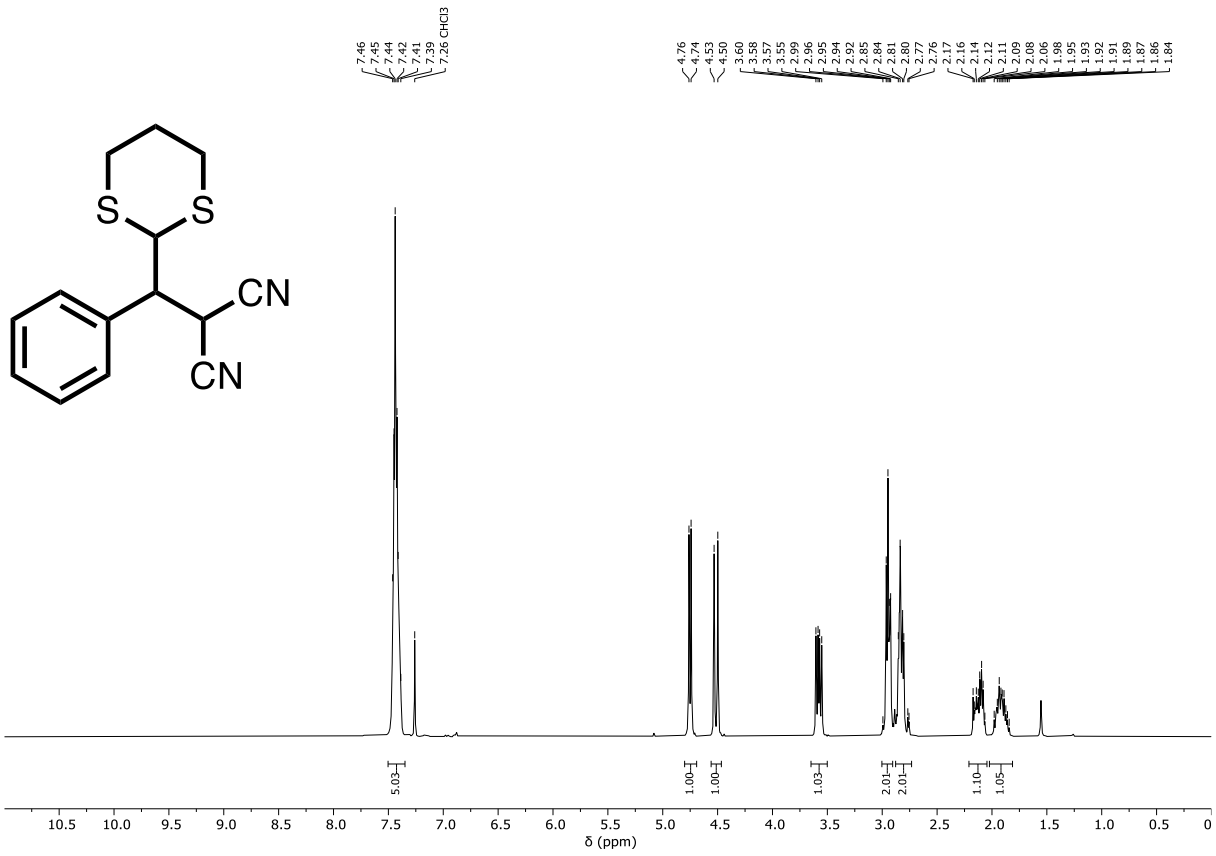
^{1}H NMR spectrum (300 MHz, DMSO-d_6) of **2n**



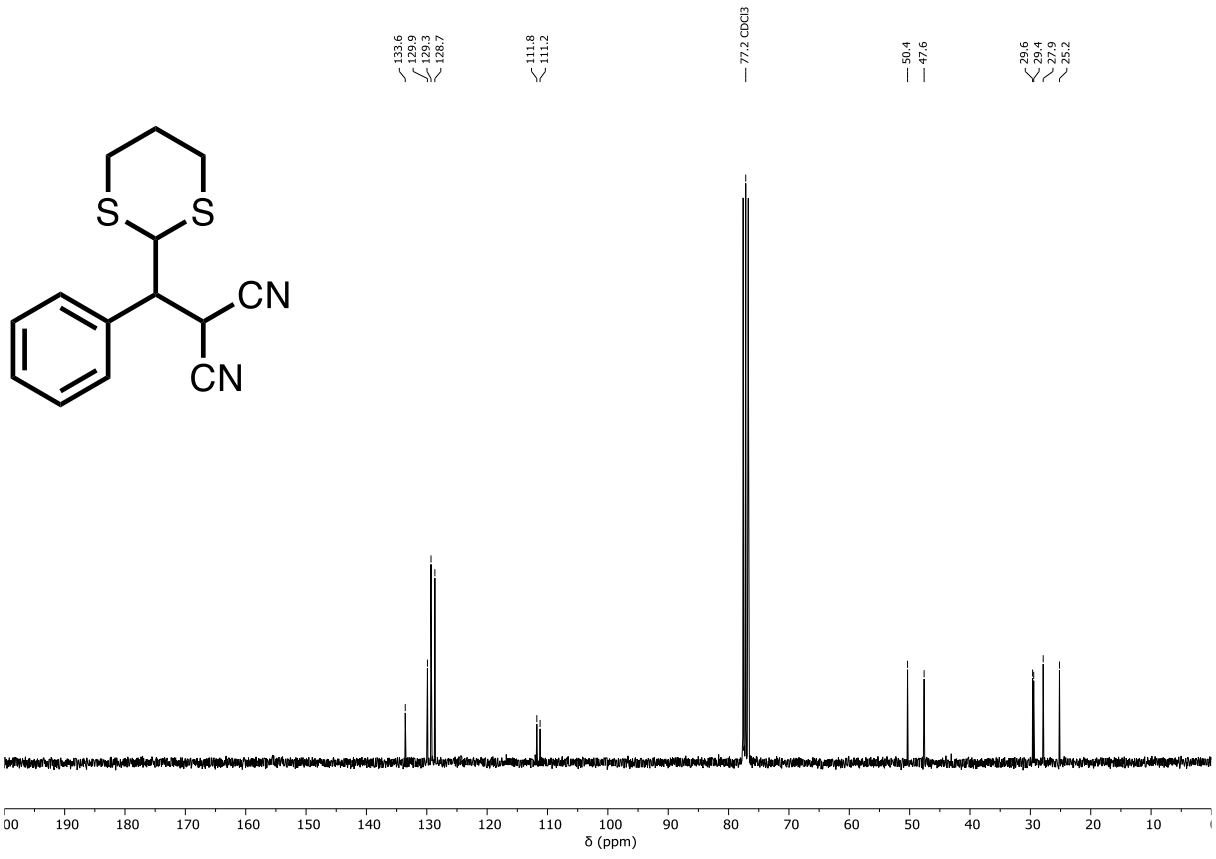
^{13}C{^{1}H} NMR spectrum (75.5 MHz, DMSO-d_6) of **2n**



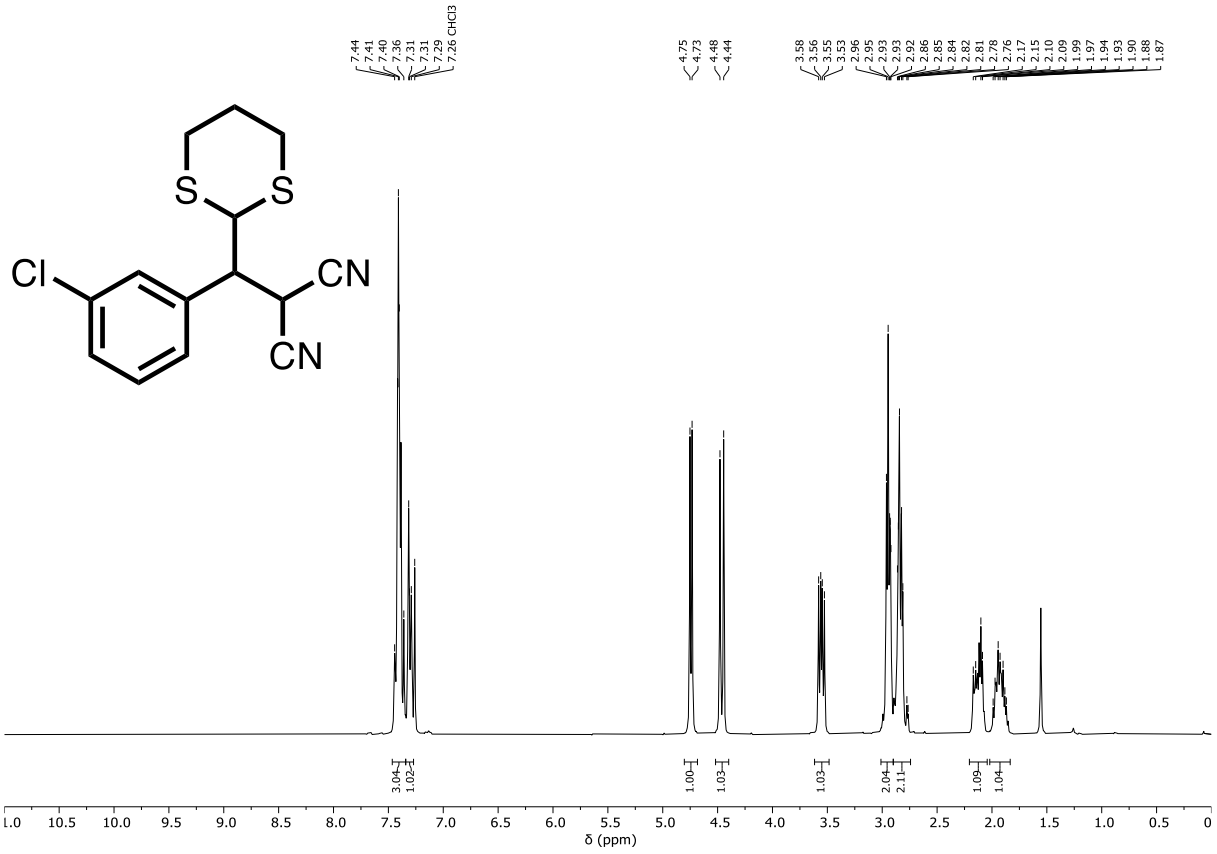
^{1}H NMR spectrum (300 MHz, $CDCl_3$) of **2z**



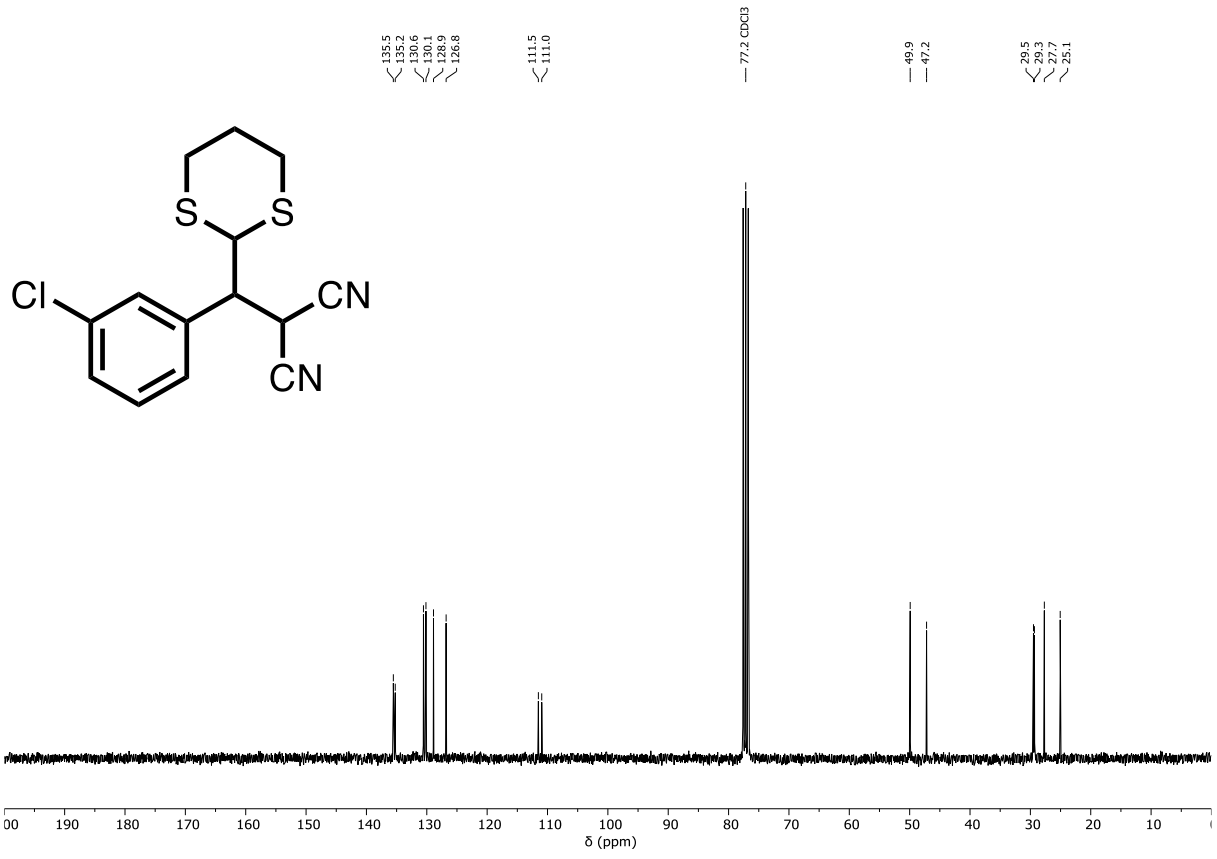
^{1}H NMR spectrum (300 MHz, $CDCl_3$) of **3a**



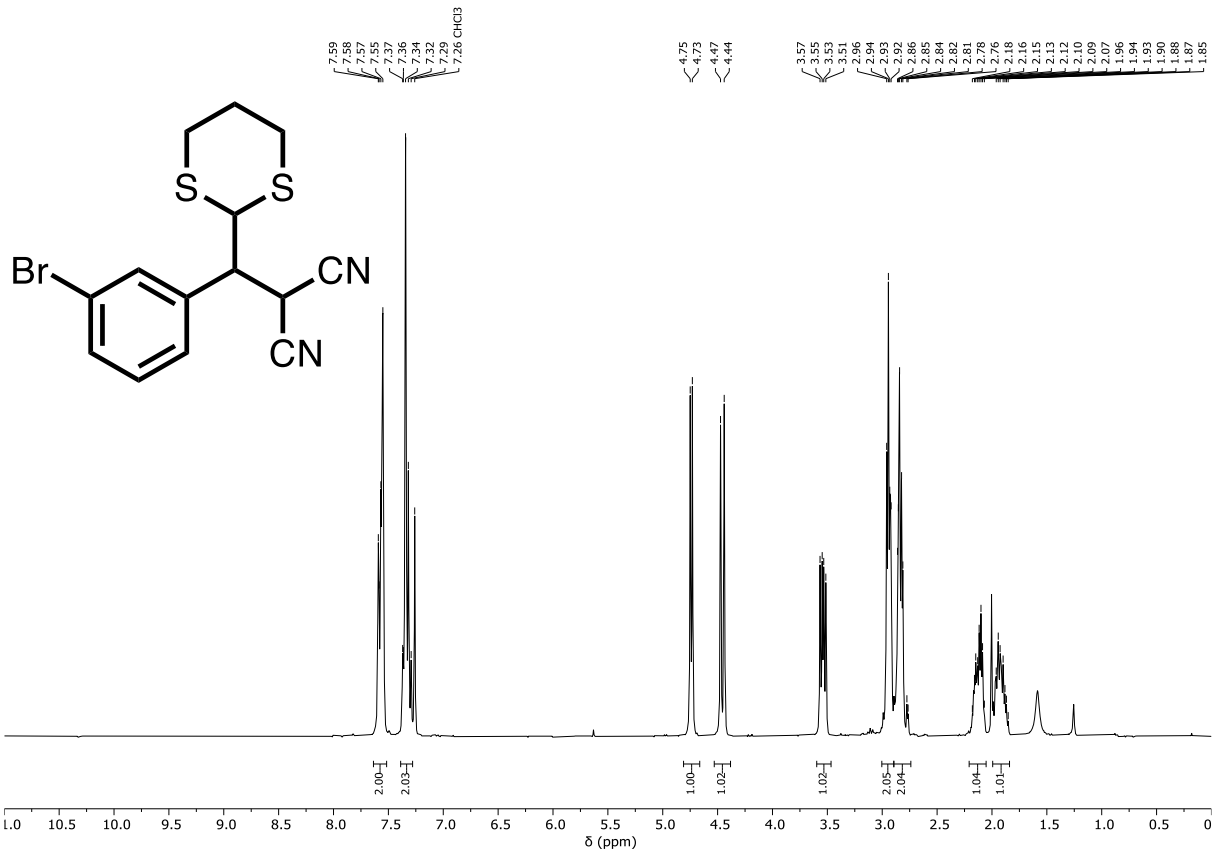
^{13}C{^{1}H} NMR spectrum (75.5 MHz, $CDCl_3$) of **3a**



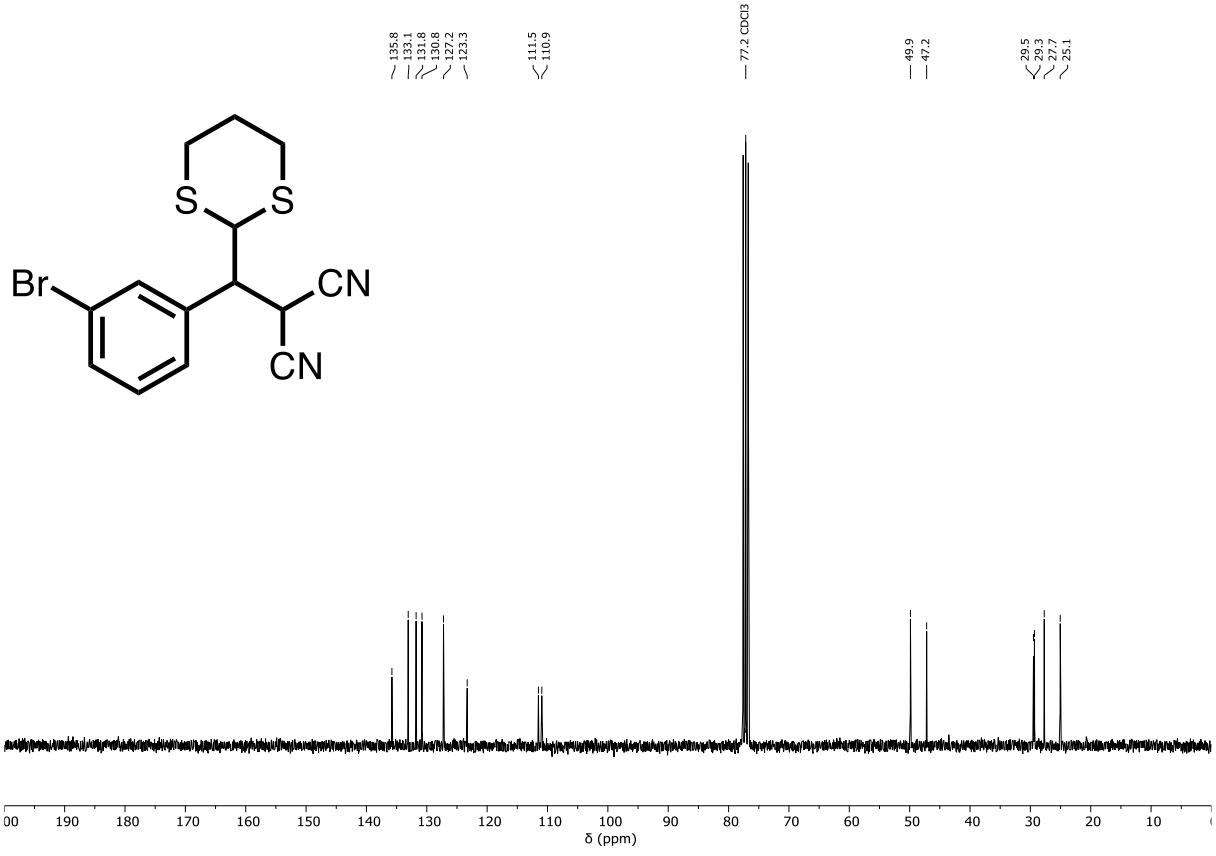
^{1}H NMR spectrum (300 MHz, $CDCl_3$) of **3b**



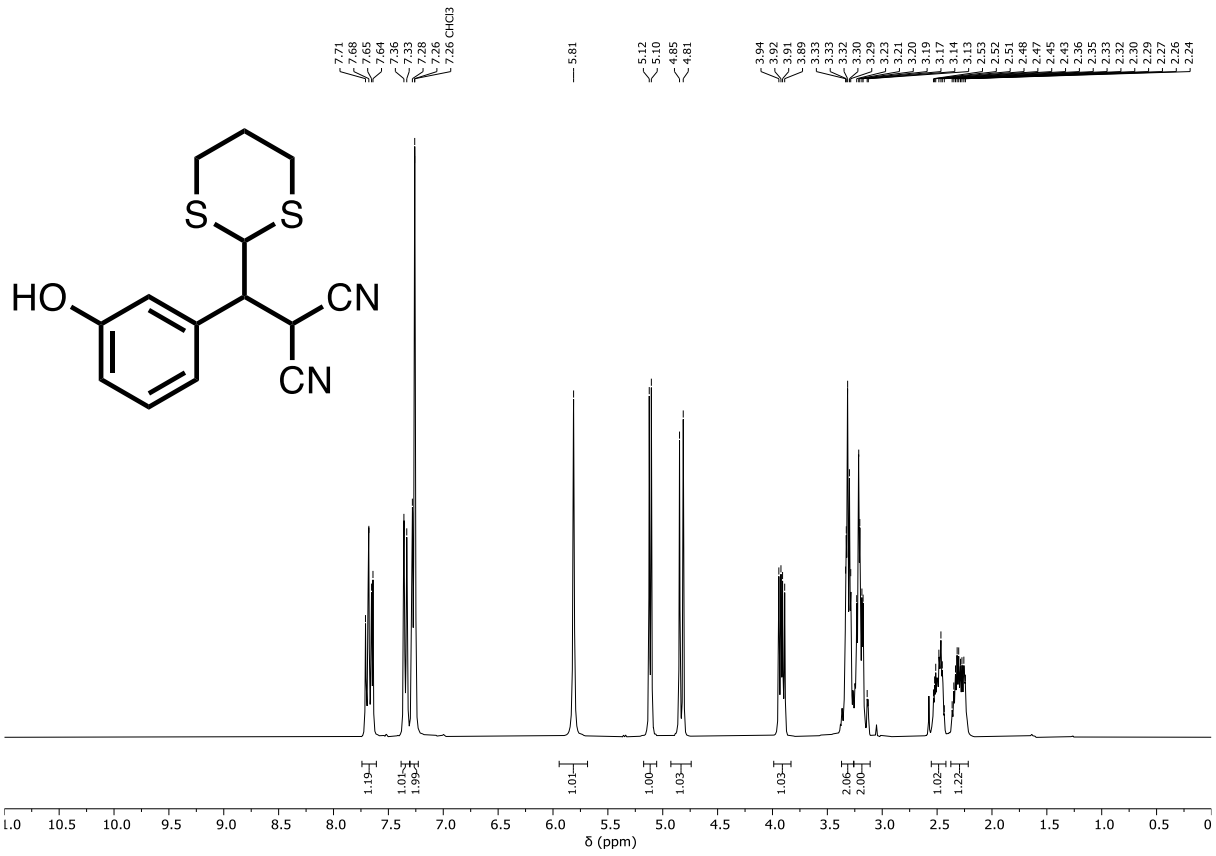
^{13}C{^{1}H} NMR spectrum (75.5 MHz, $CDCl_3$) of **3b**



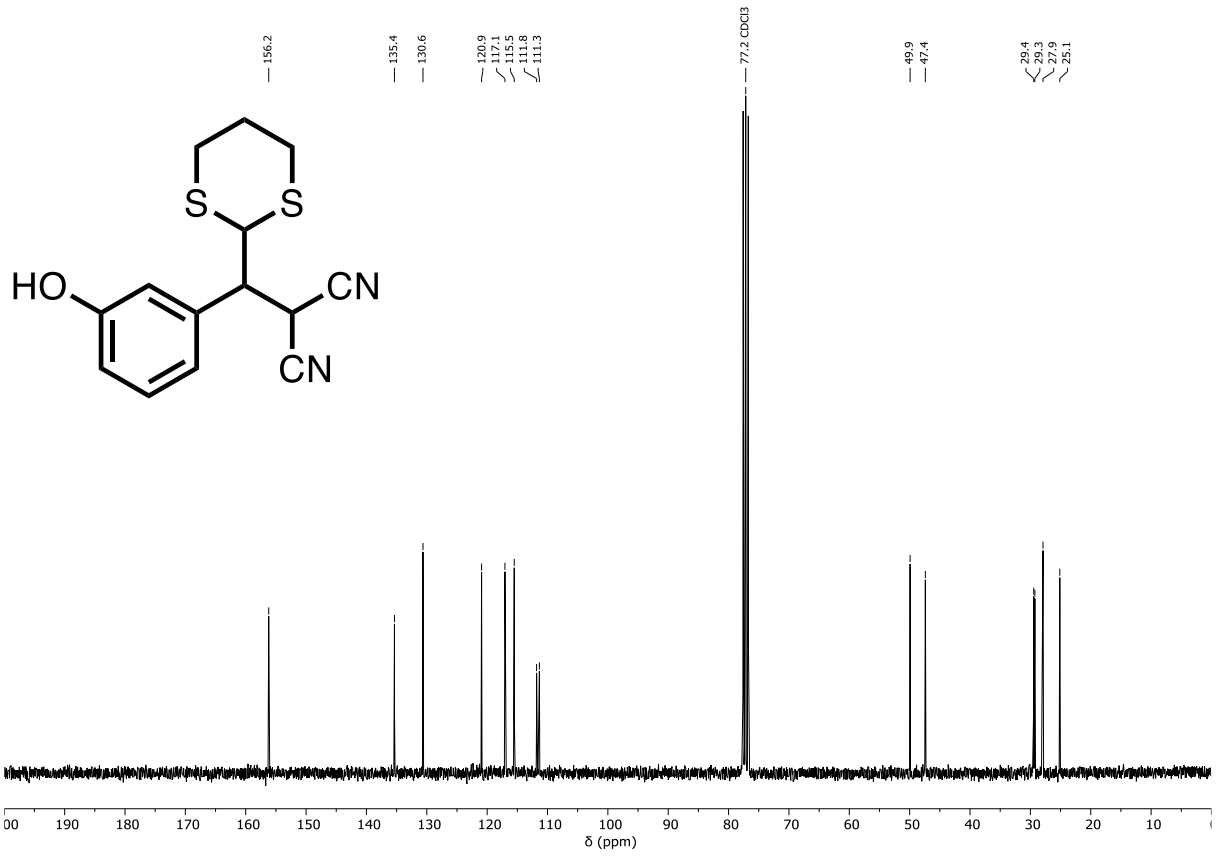
^{1}H NMR spectrum (300 MHz, $CDCl_3$) of **3c**



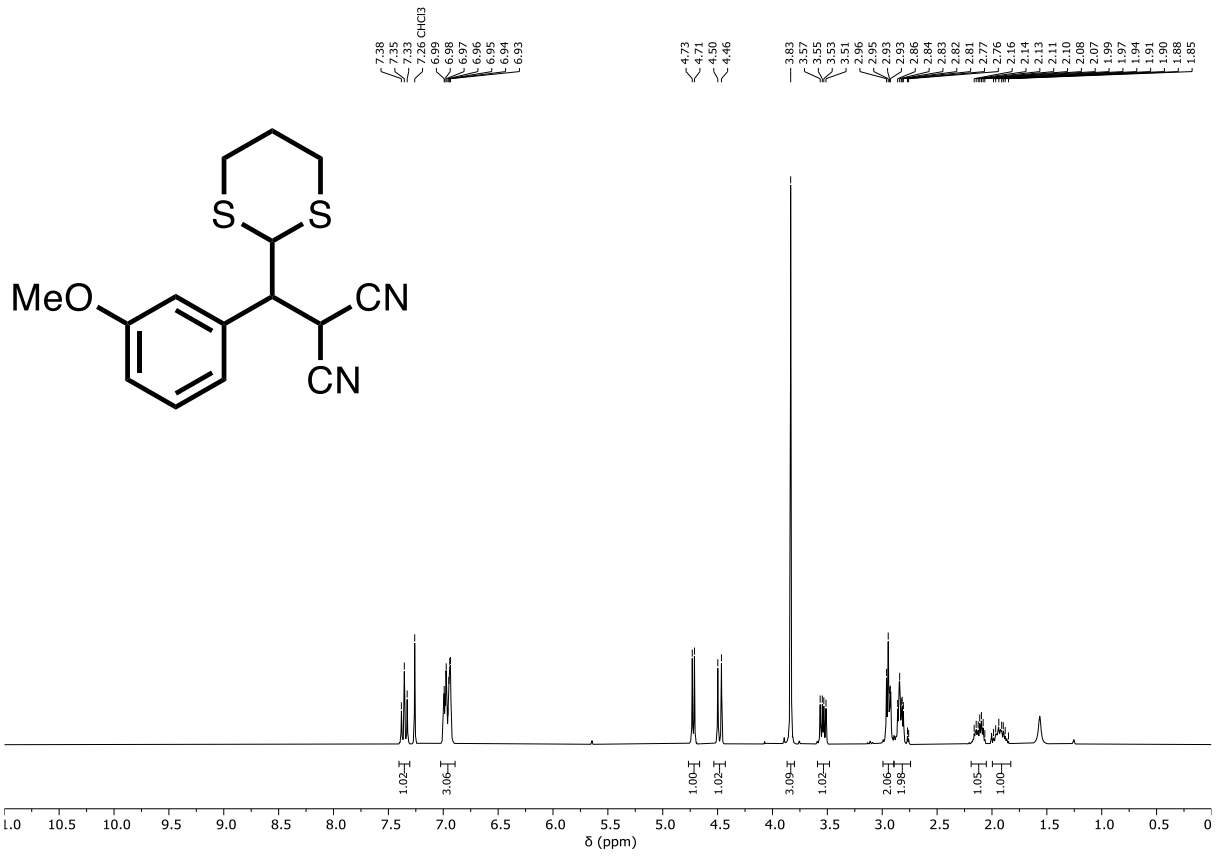
^{13}C{^{1}H} NMR spectrum (75.5 MHz, $CDCl_3$) of **3c**



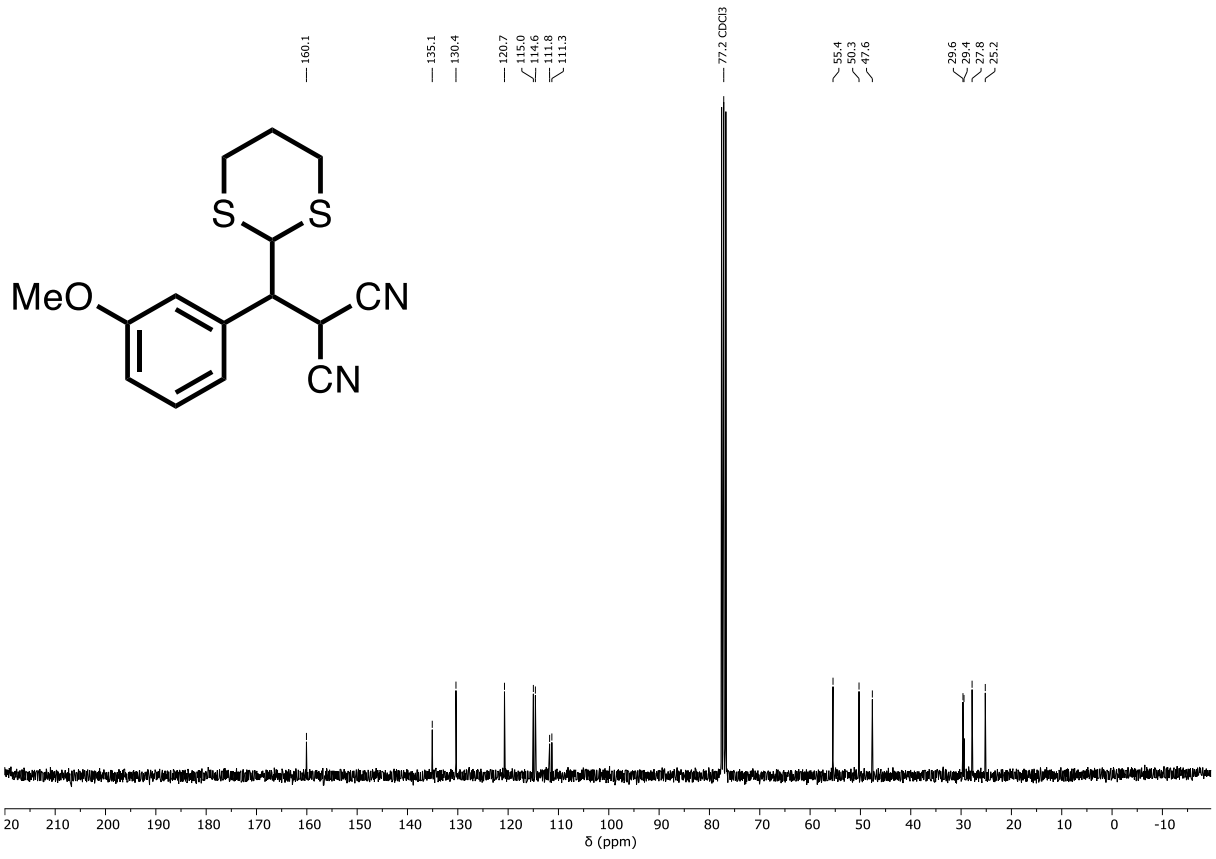
^{1}H NMR spectrum (300 MHz, $CDCl_3$) of **3d**



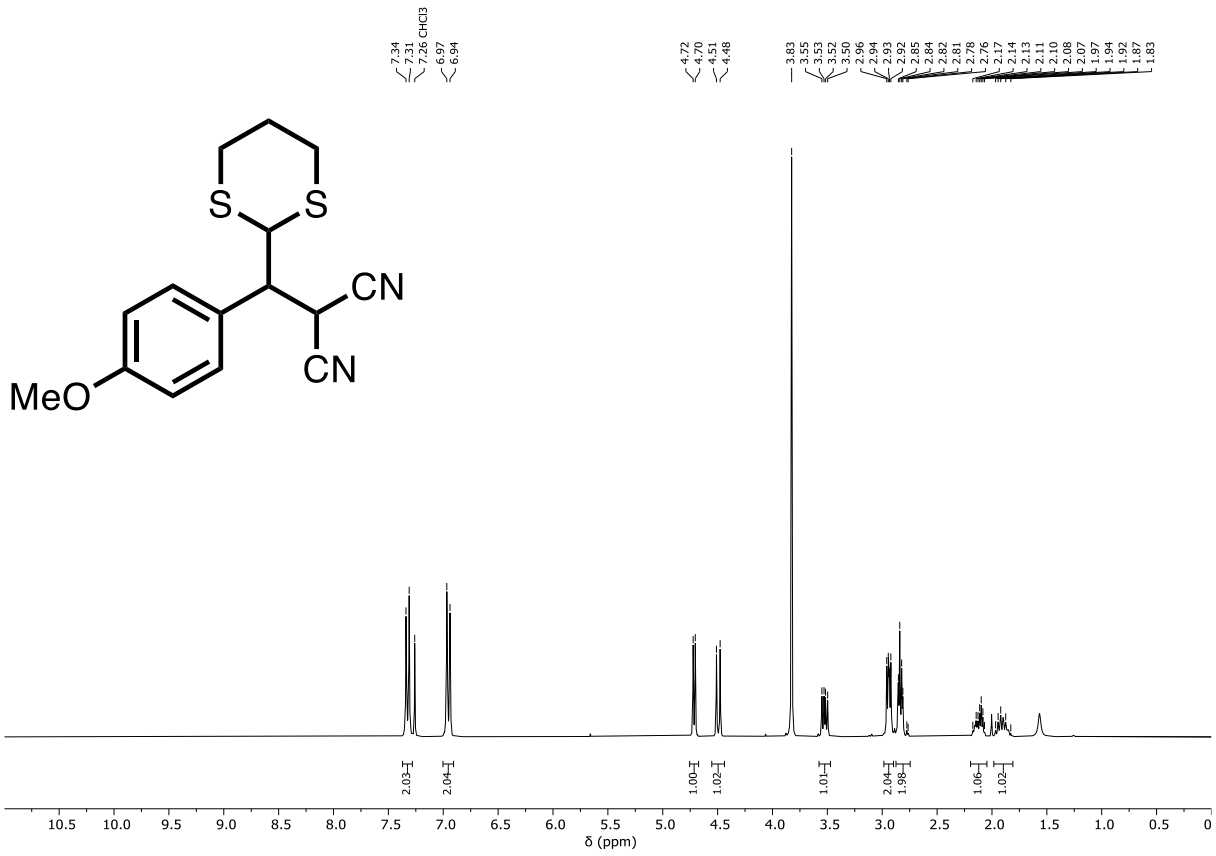
$^{13}C\{^{1}H\}$ NMR spectrum (75.5 MHz, $CDCl_3$) of **3d**



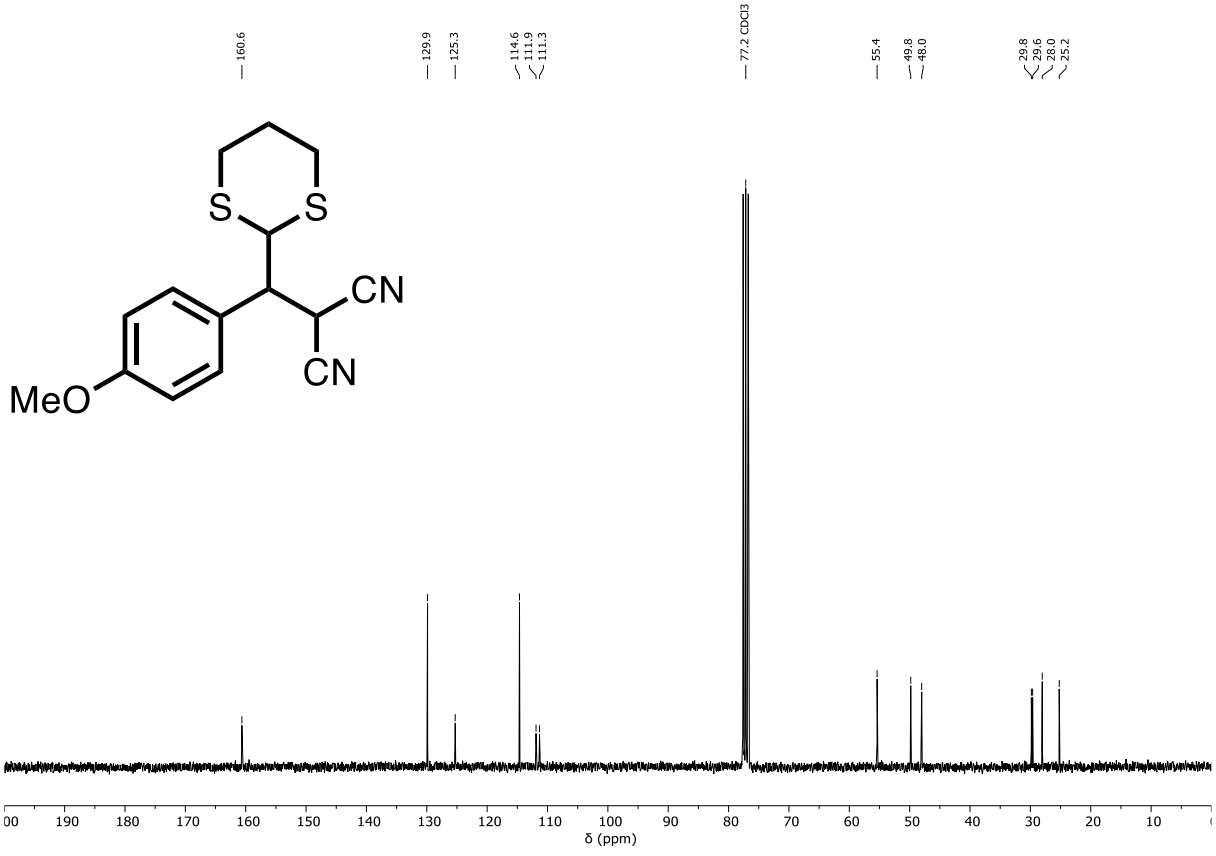
^{1}H NMR spectrum (300 MHz, $CDCl_3$) of **3e**



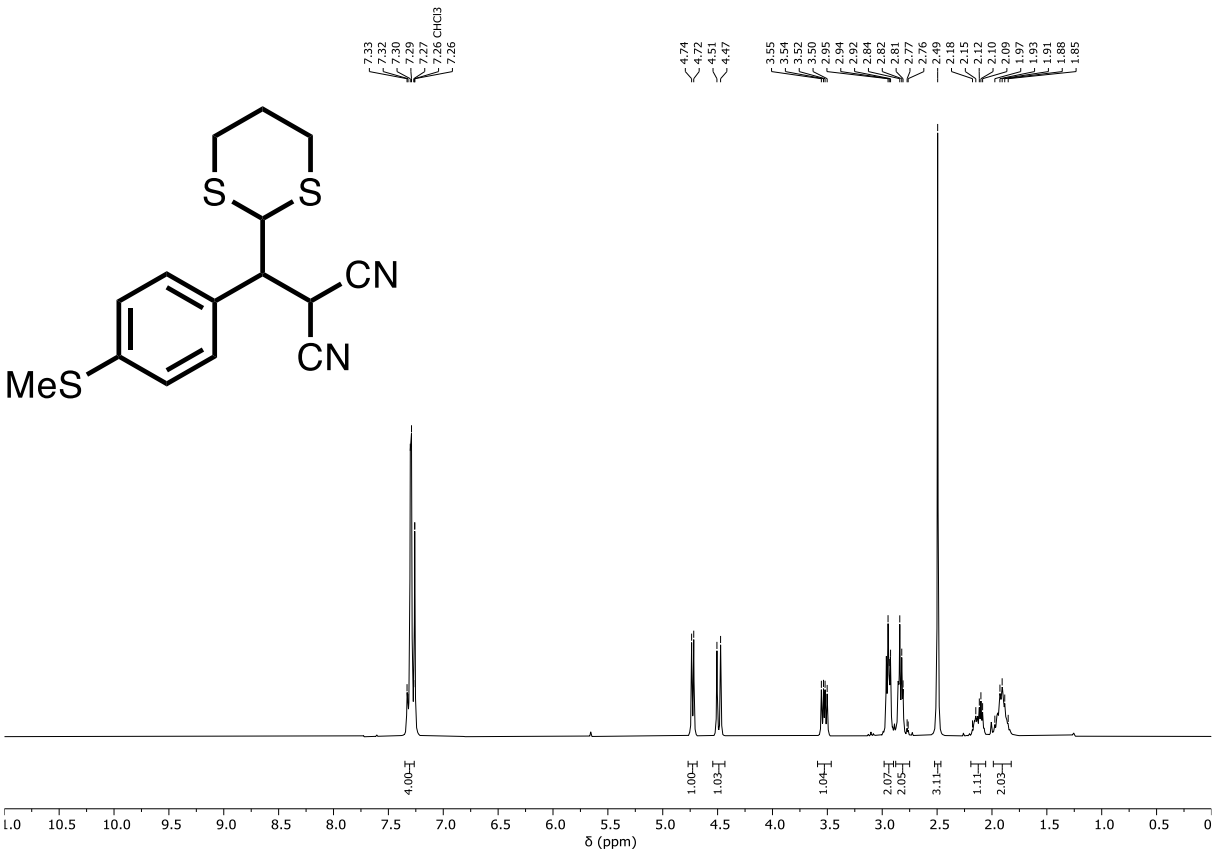
$^{13}C\{^{1}H\}$ NMR spectrum (75.5 MHz, $CDCl_3$) of **3e**



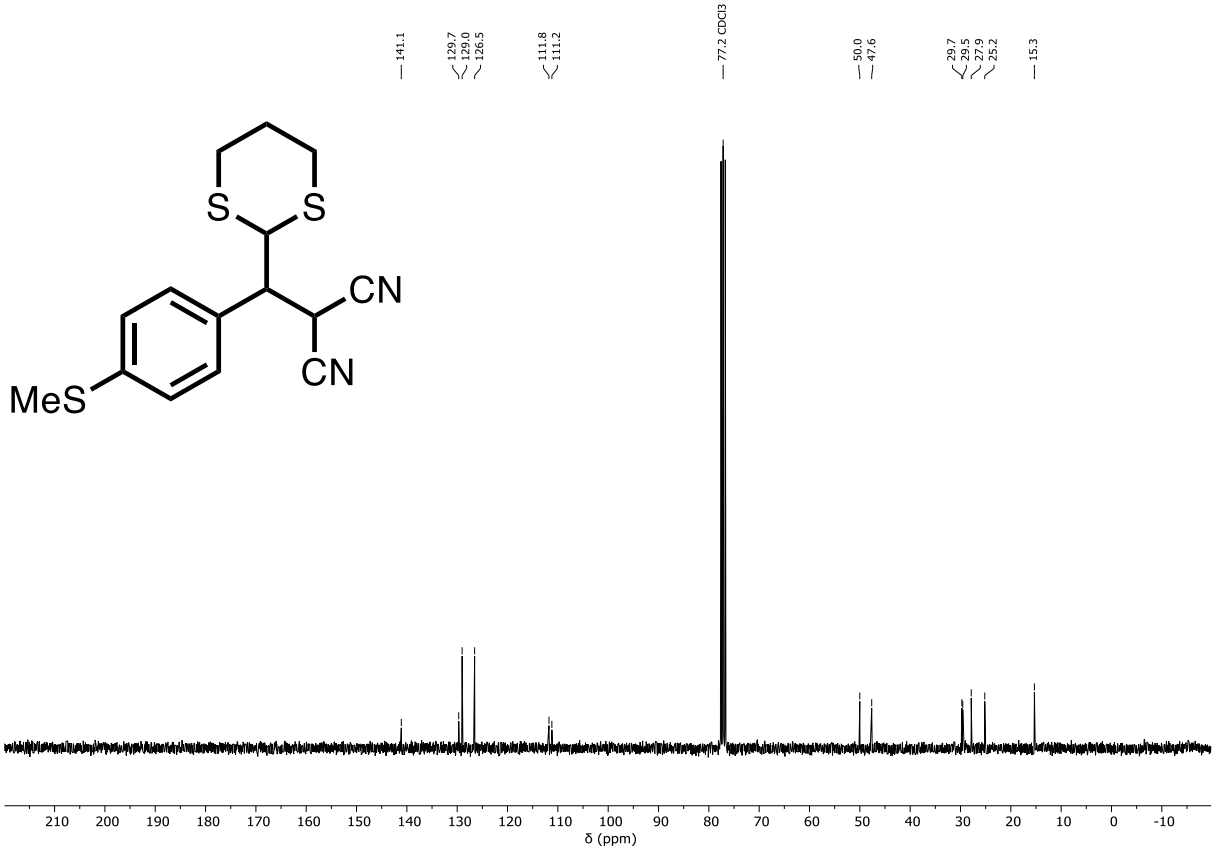
^{1}H NMR spectrum (300 MHz, $CDCl_3$) of **3g**



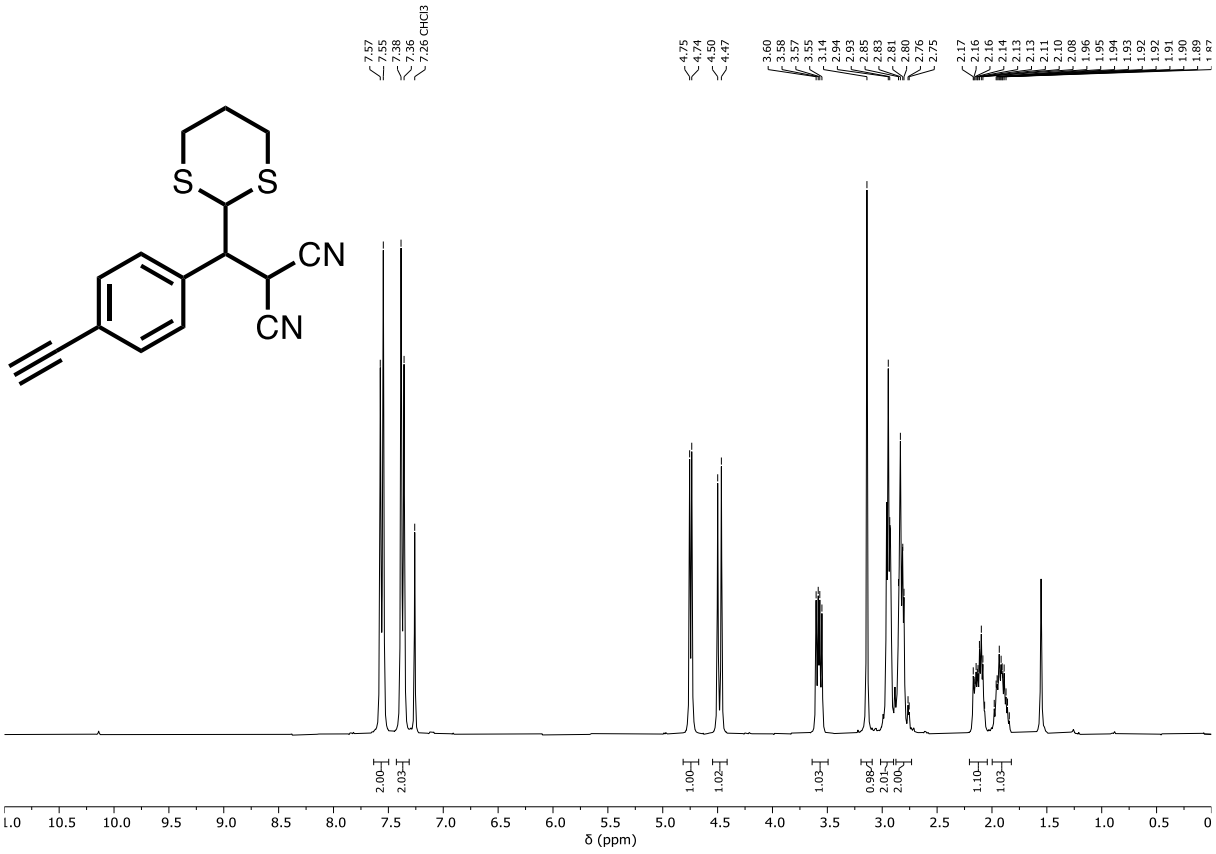
^{13}C{^{1}H} NMR spectrum (75.5 MHz, $CDCl_3$) of **3g**



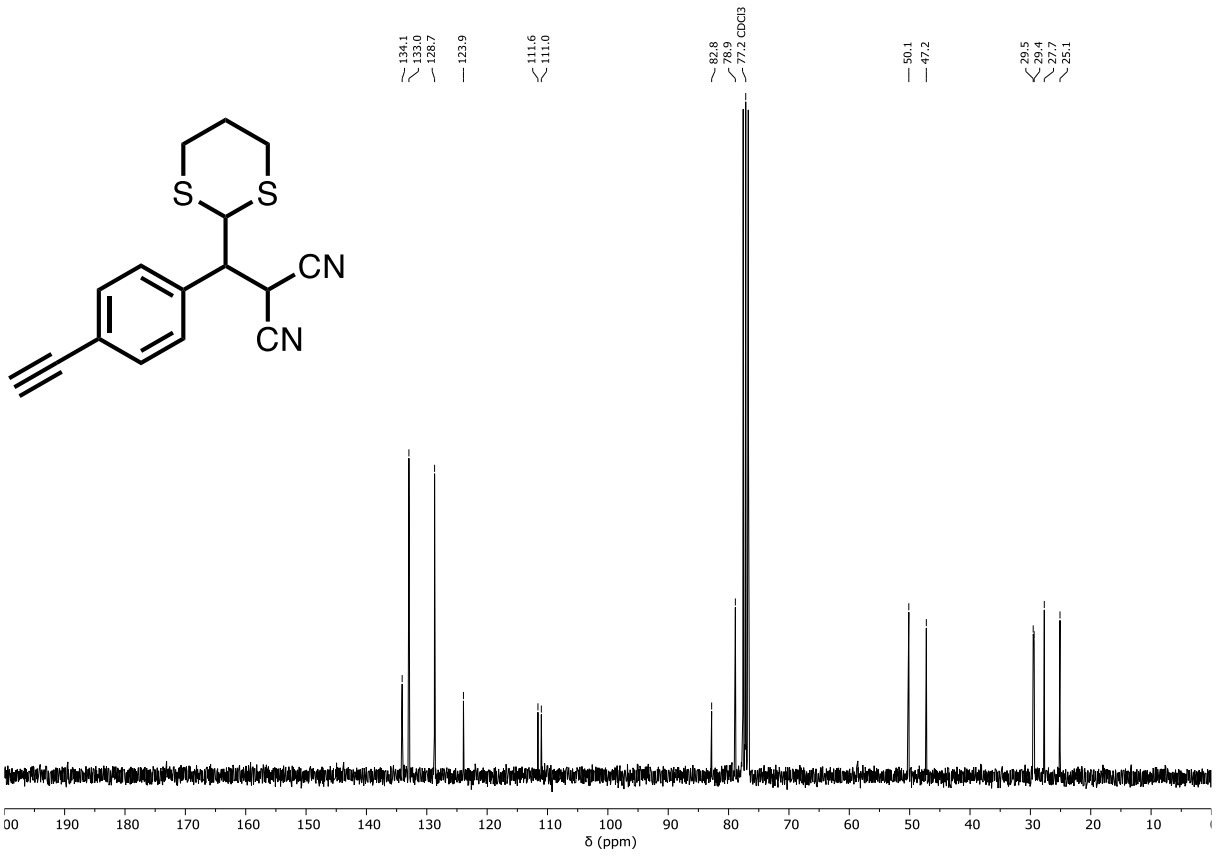
^{1}H NMR spectrum (300 MHz, $CDCl_3$) of **3h**



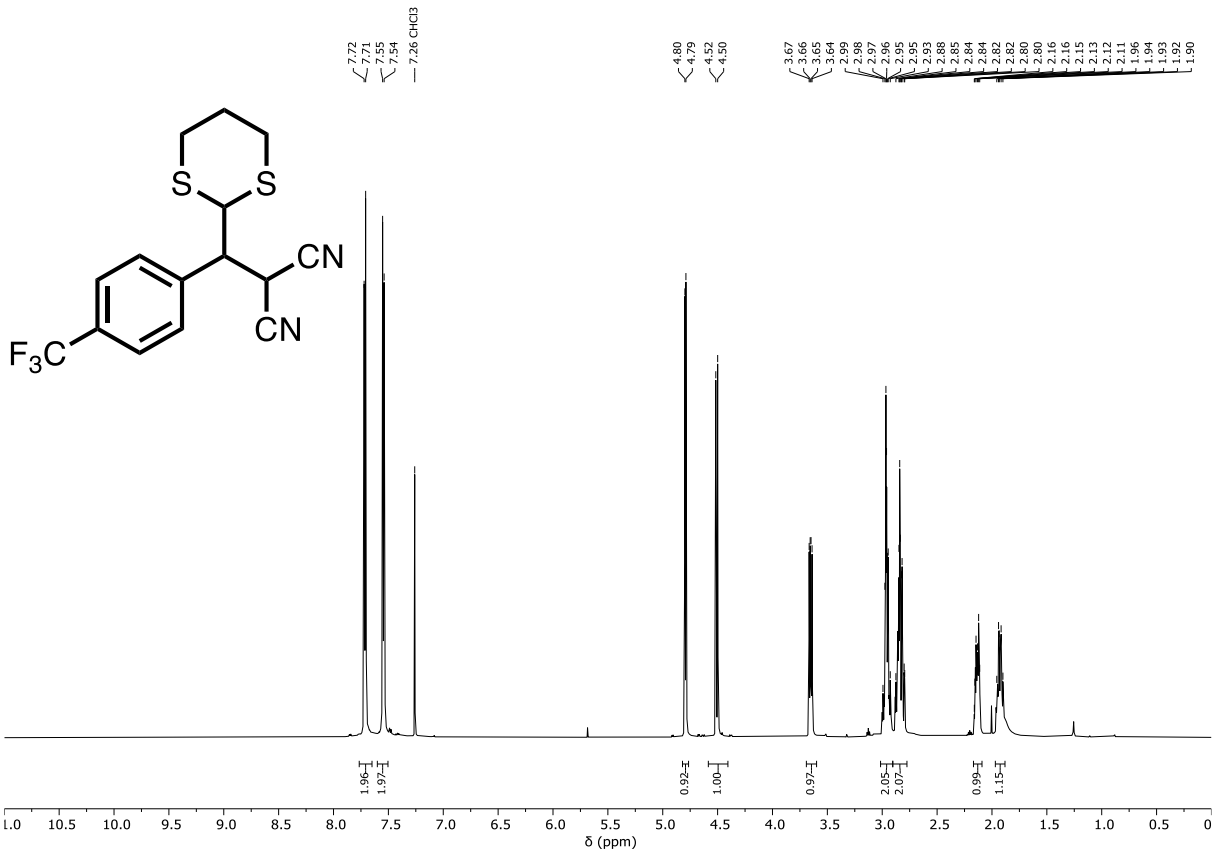
^{13}C{^{1}H} NMR spectrum (75.5 MHz, $CDCl_3$) of **3h**



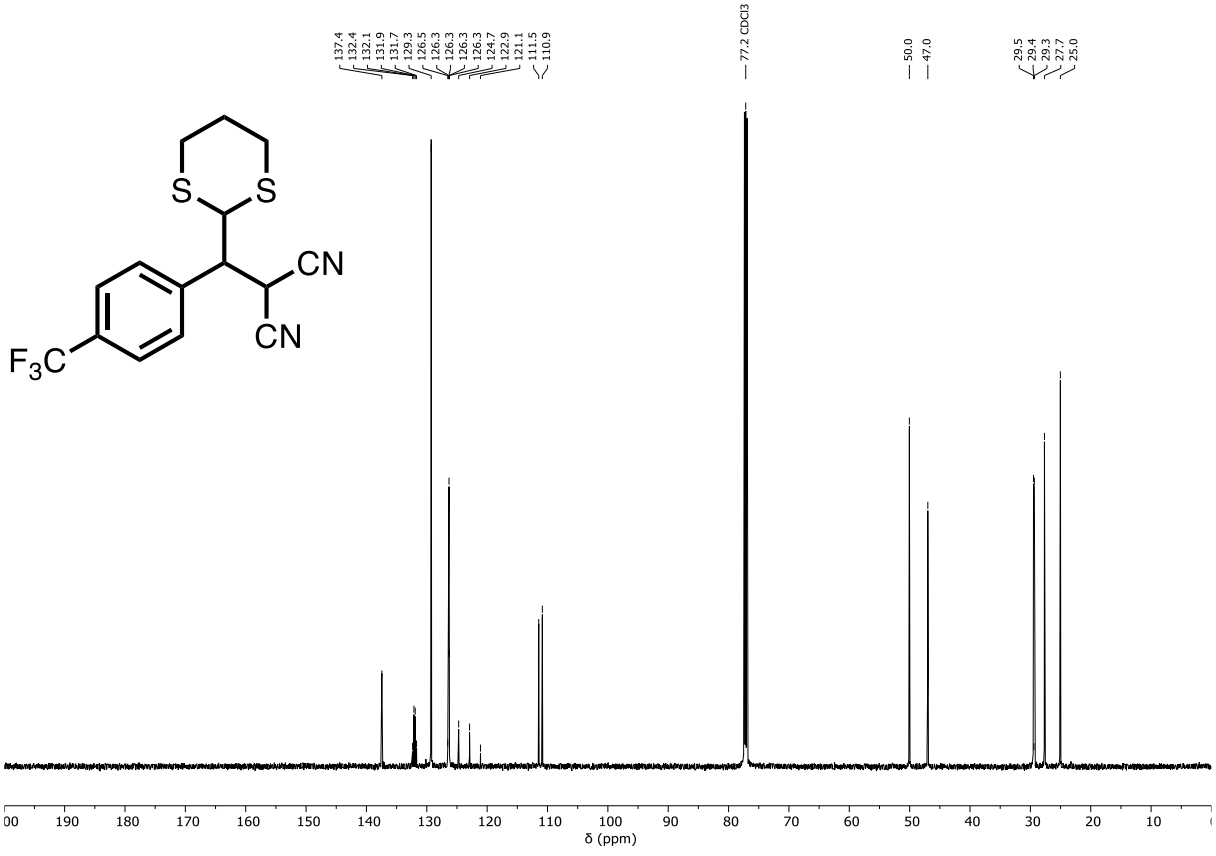
^{1}H NMR spectrum (300 MHz, $CDCl_3$) of **3i**



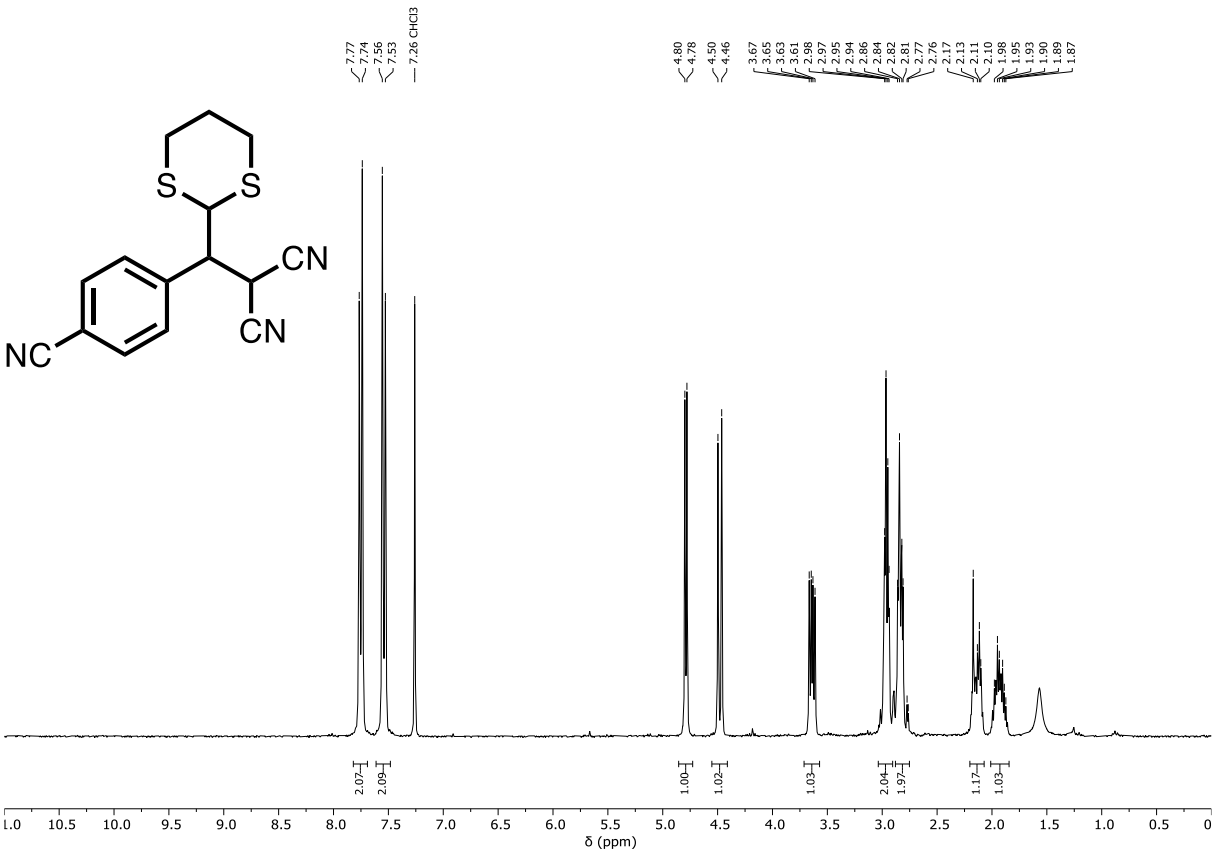
^{13}C{^{1}H} NMR spectrum (75.5 MHz, $CDCl_3$) of **3i**



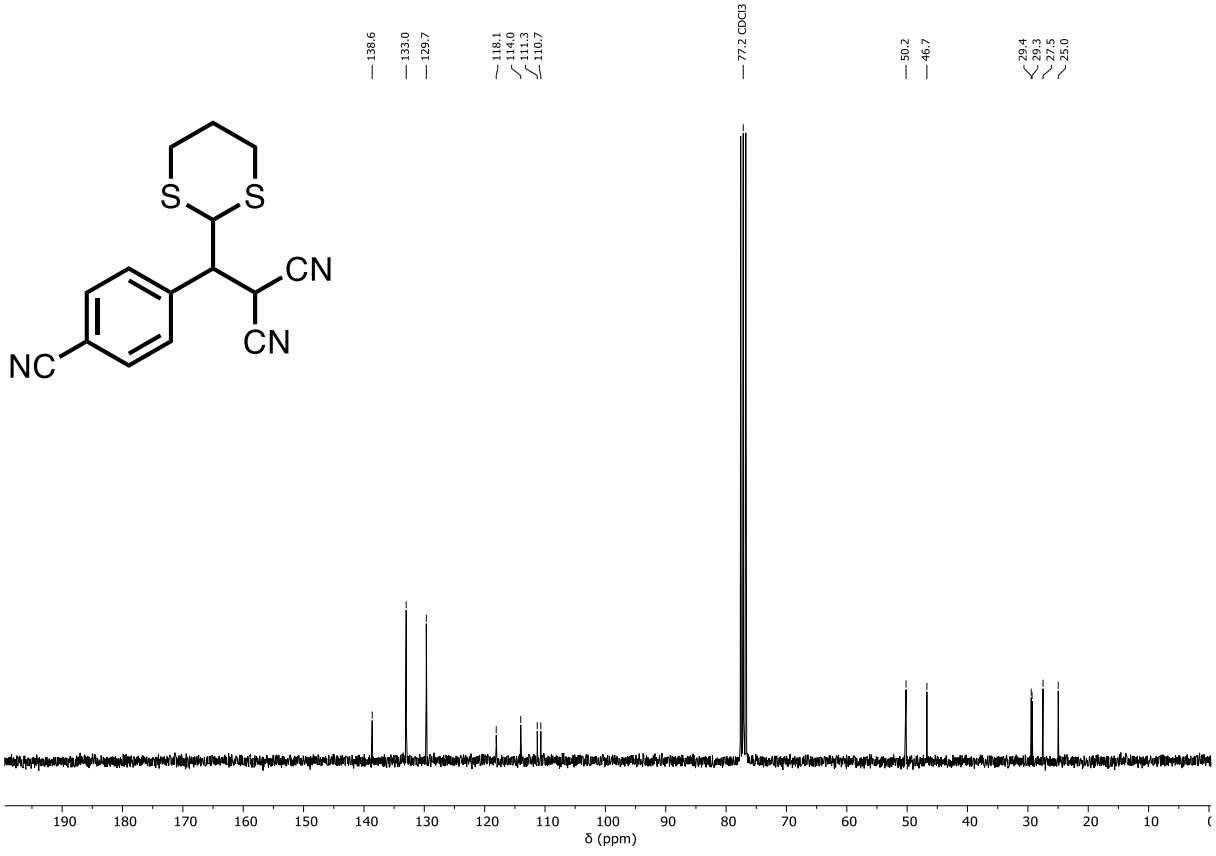
^{1}H NMR spectrum (600 MHz, $CDCl_3$) of **3k**



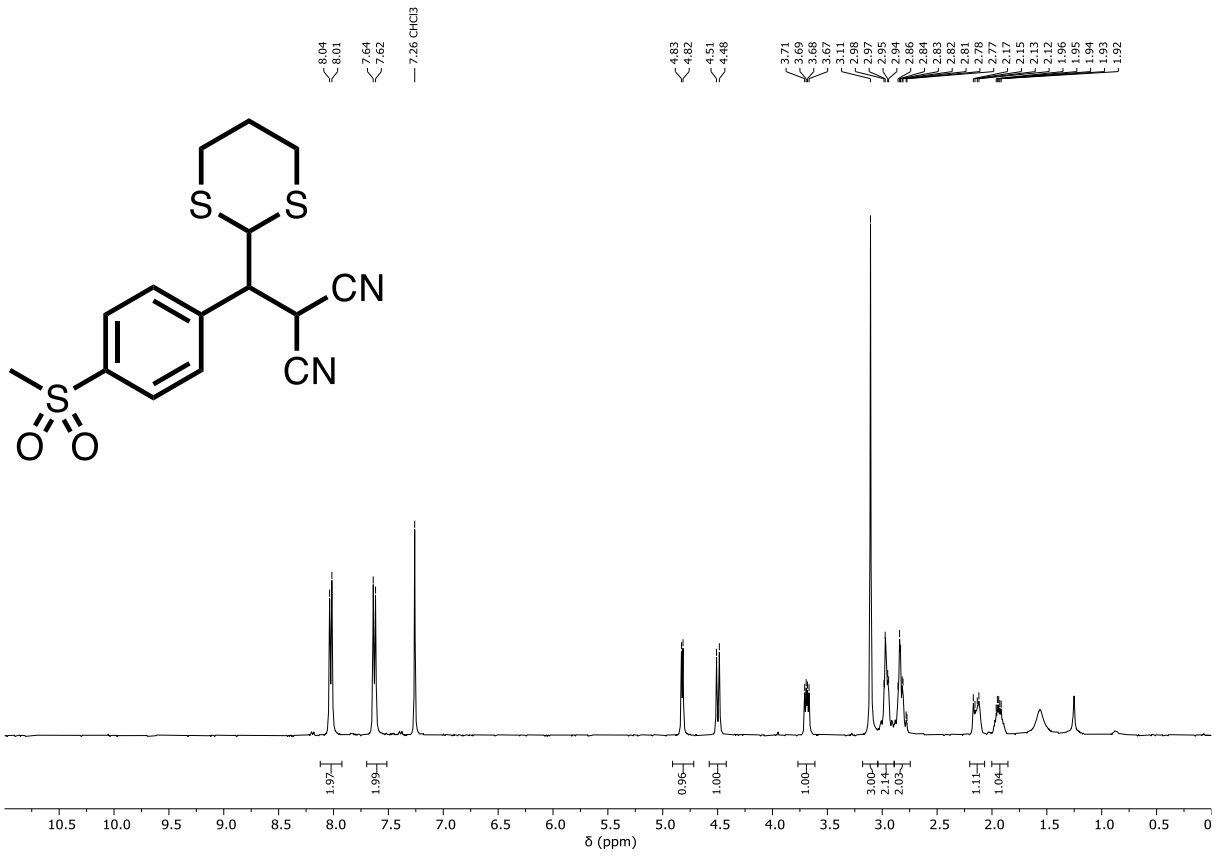
^{13}C{^{1}H} NMR spectrum (151 MHz, $CDCl_3$) of **3k**



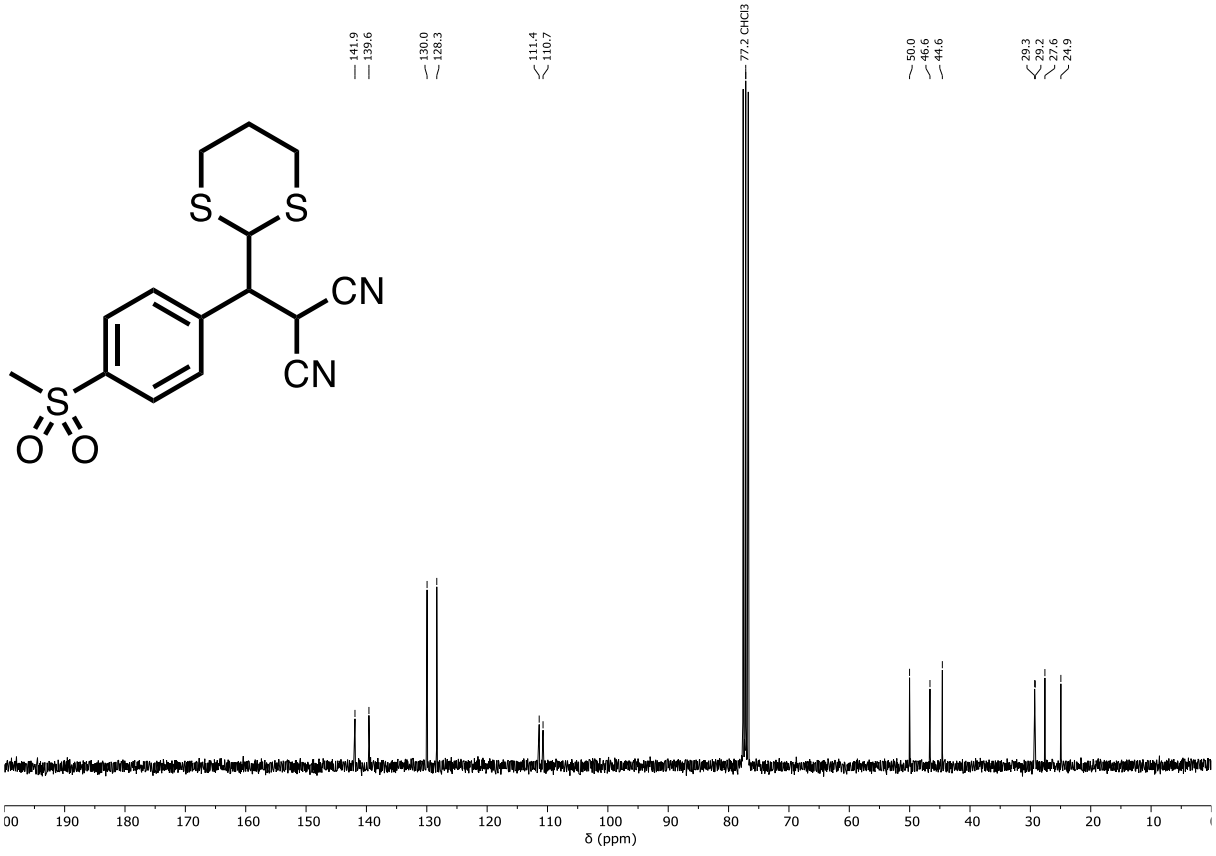
^{1}H NMR spectrum (300 MHz, $CDCl_3$) of **3m**



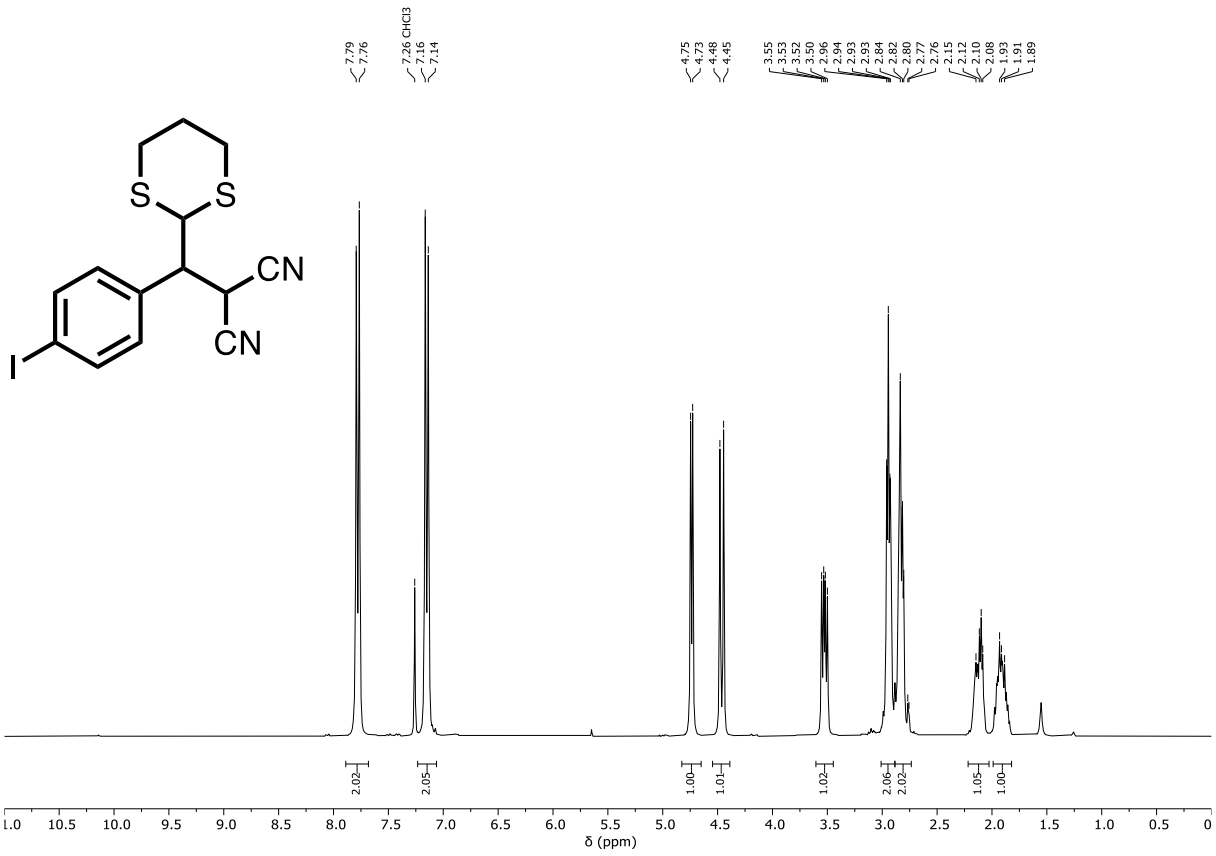
^{13}C{^{1}H} NMR spectrum (75.5 MHz, $CDCl_3$) of **3m**



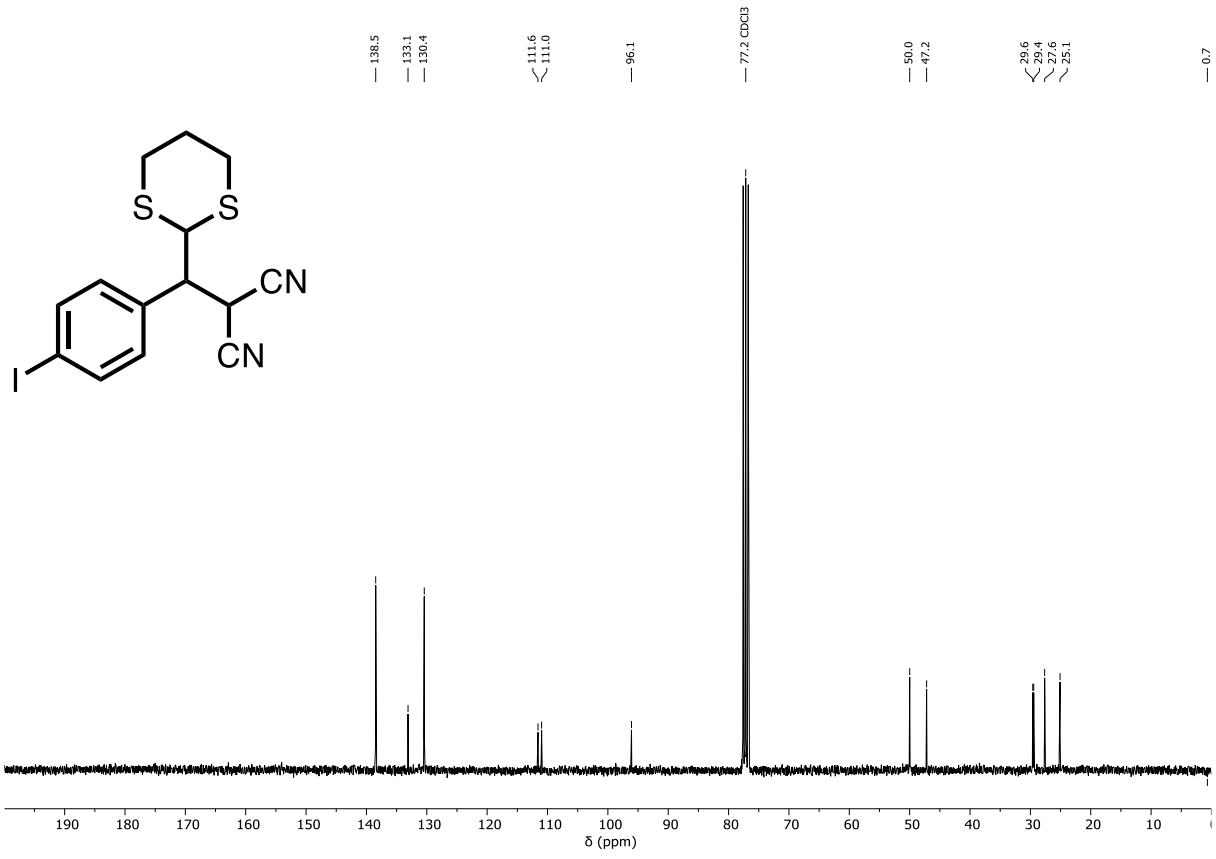
^{1}H NMR spectrum (300 MHz, $CDCl_3$) of **3n**



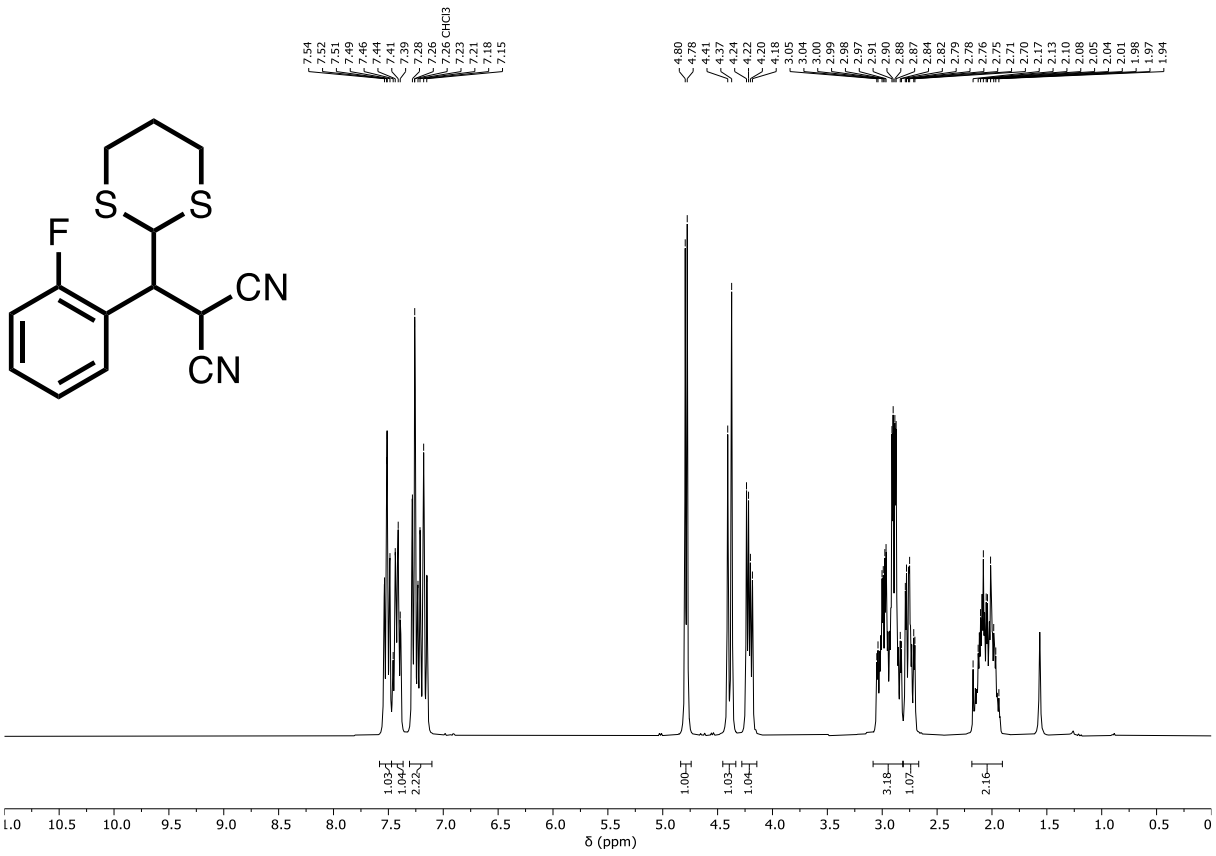
^{13}C{^{1}H} NMR spectrum (75.5 MHz, $CDCl_3$) of **3n**



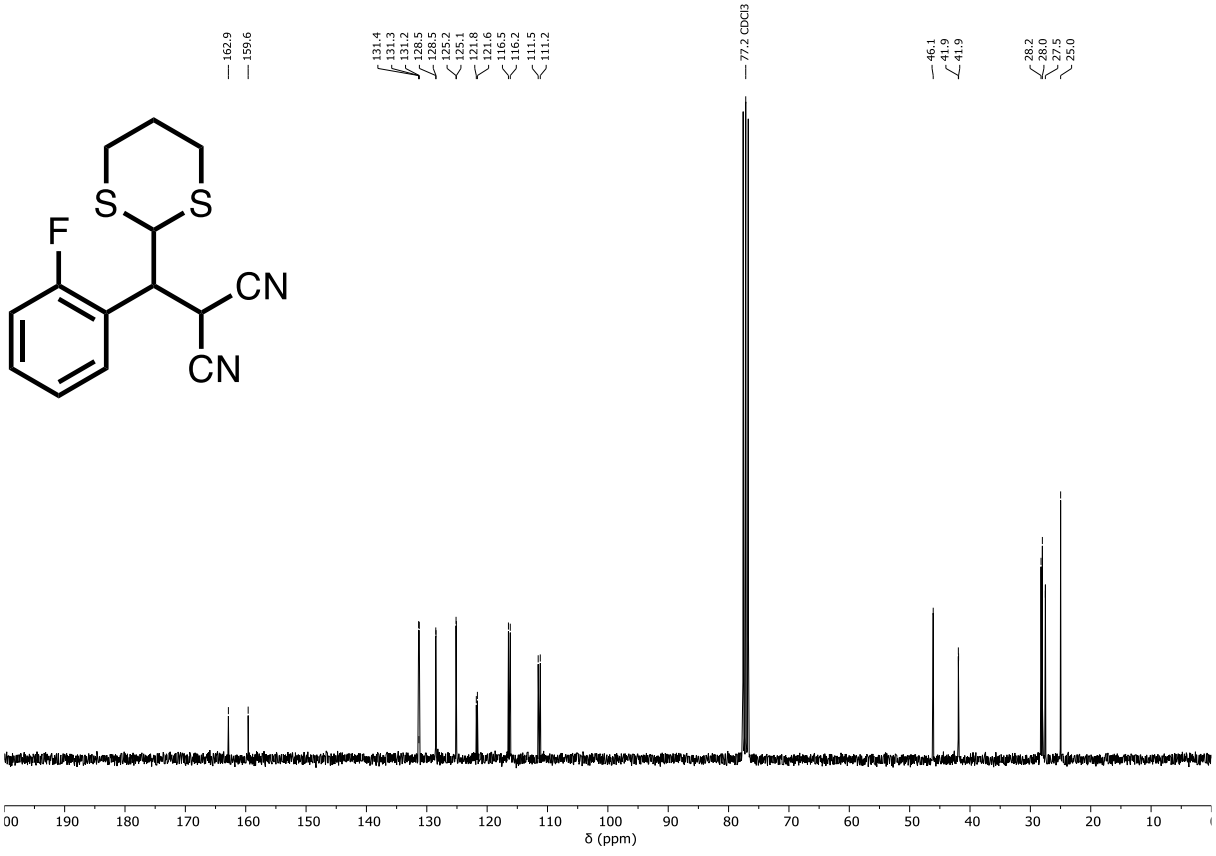
^{1}H NMR spectrum (300 MHz, $CDCl_3$) of **3o**



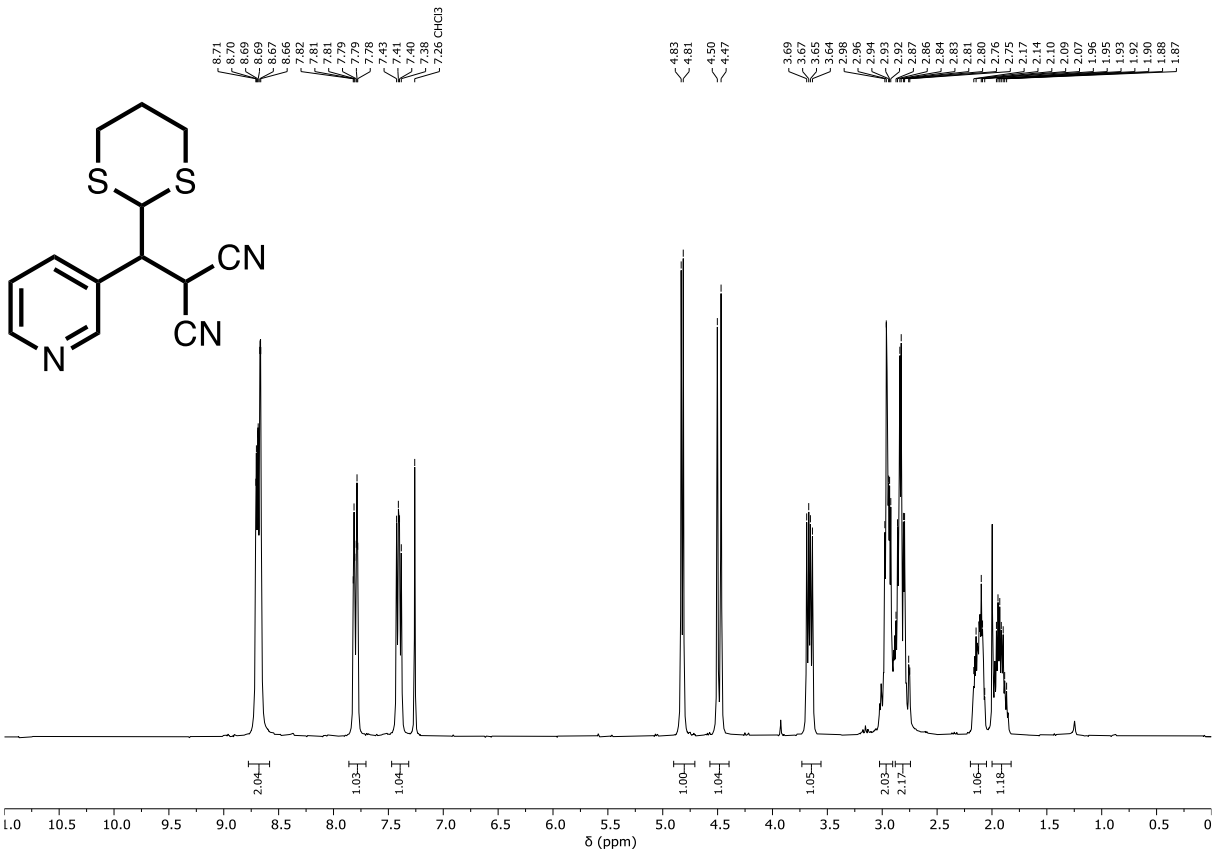
^{13}C{^{1}H} NMR spectrum (75.5 MHz, $CDCl_3$) of **3o**



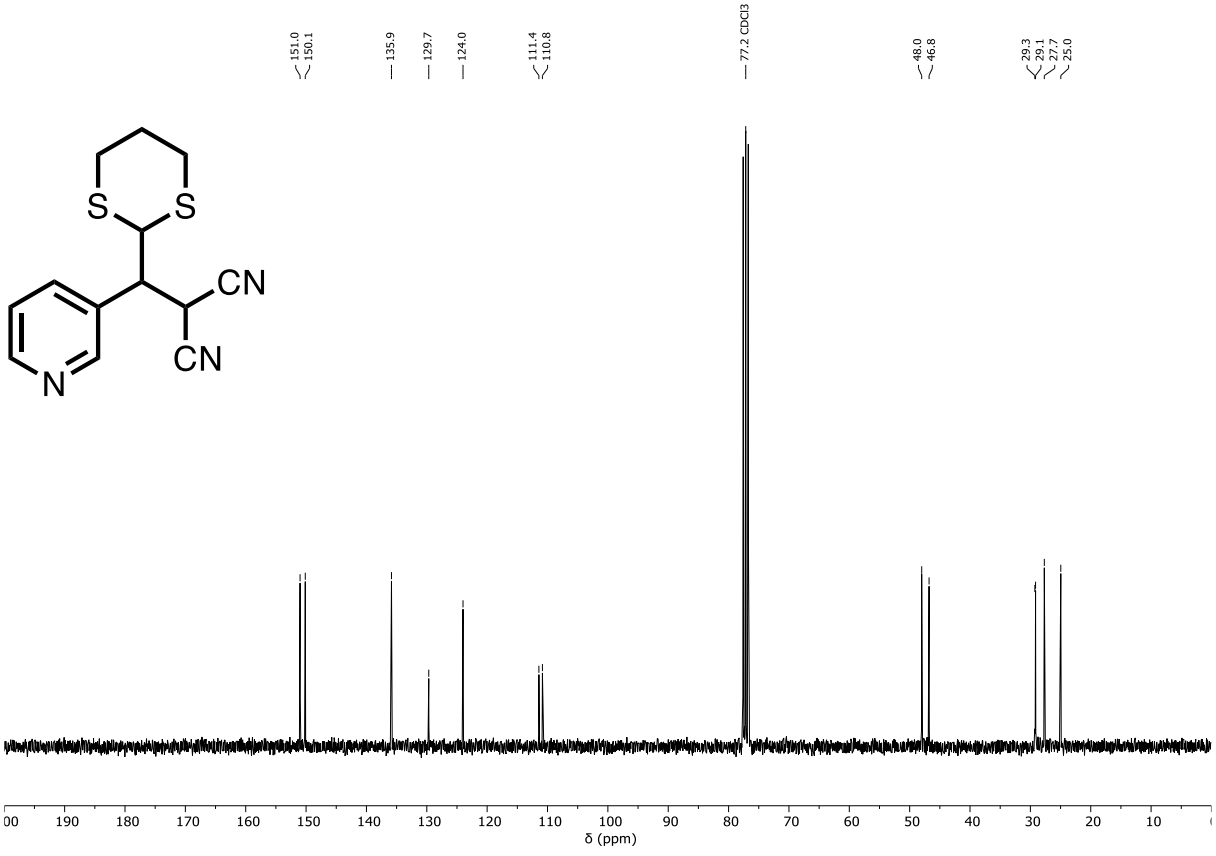
^{1}H NMR spectrum (300 MHz, $CDCl_3$) of **3p**



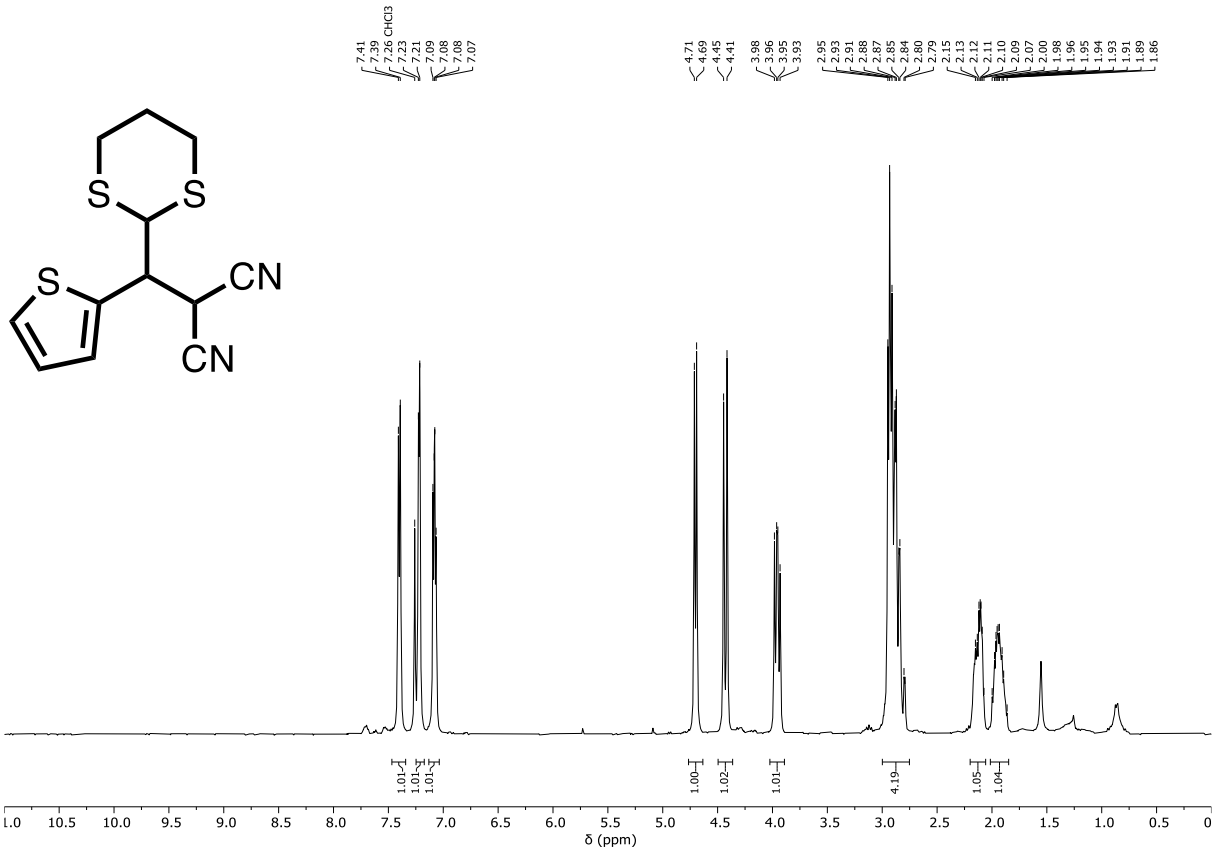
$^{13}C\{^{1}H\}$ NMR spectrum (75.5 MHz, $CDCl_3$) of **3p**



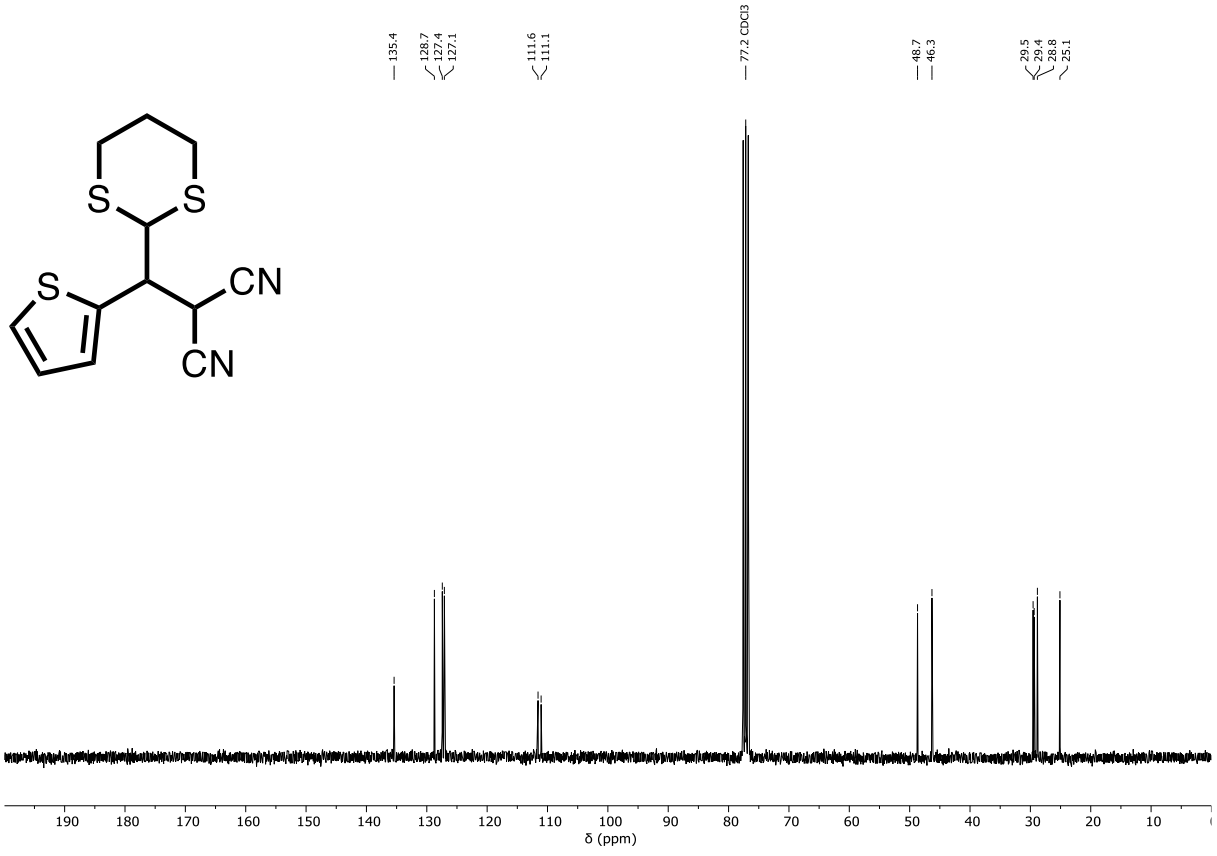
^{1}H NMR spectrum (300 MHz, $CDCl_3$) of **3q**



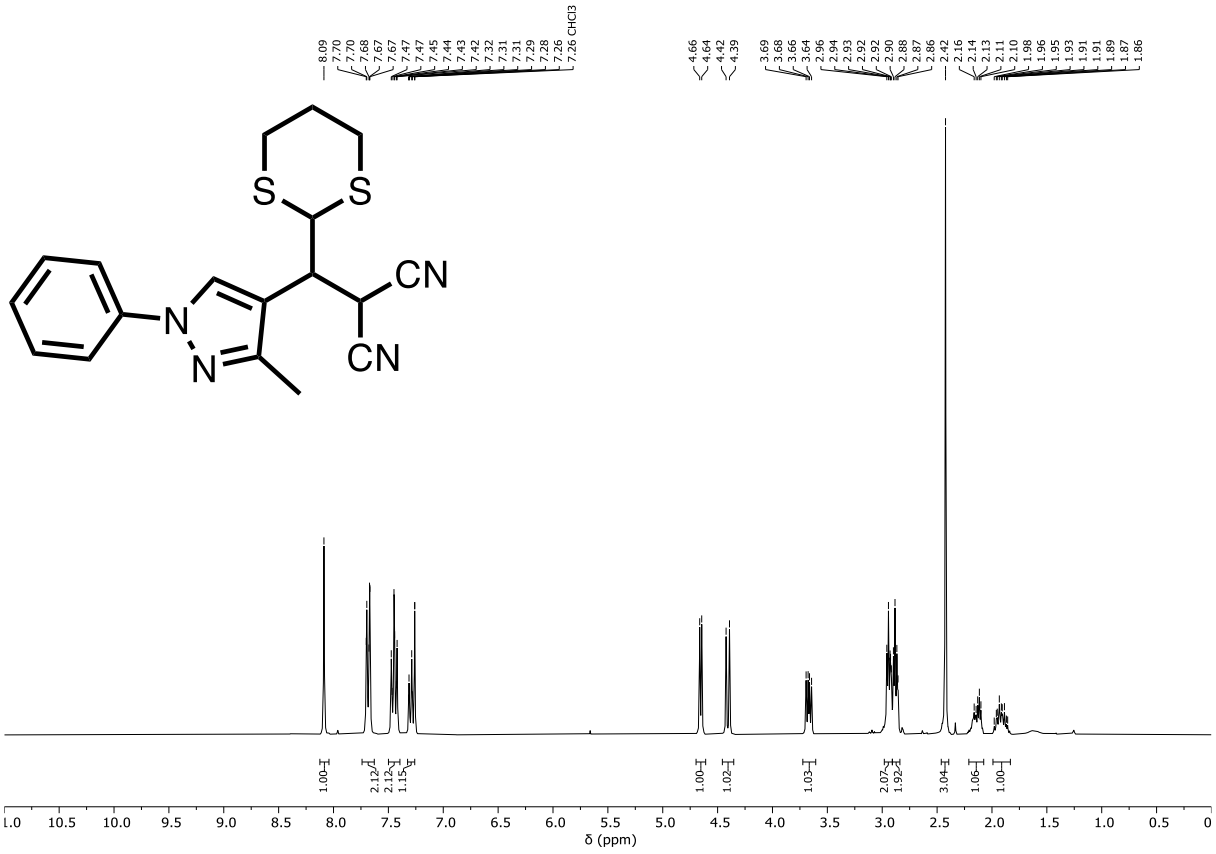
^{13}C{^{1}H} NMR spectrum (75.5 MHz, $CDCl_3$) of **3q**



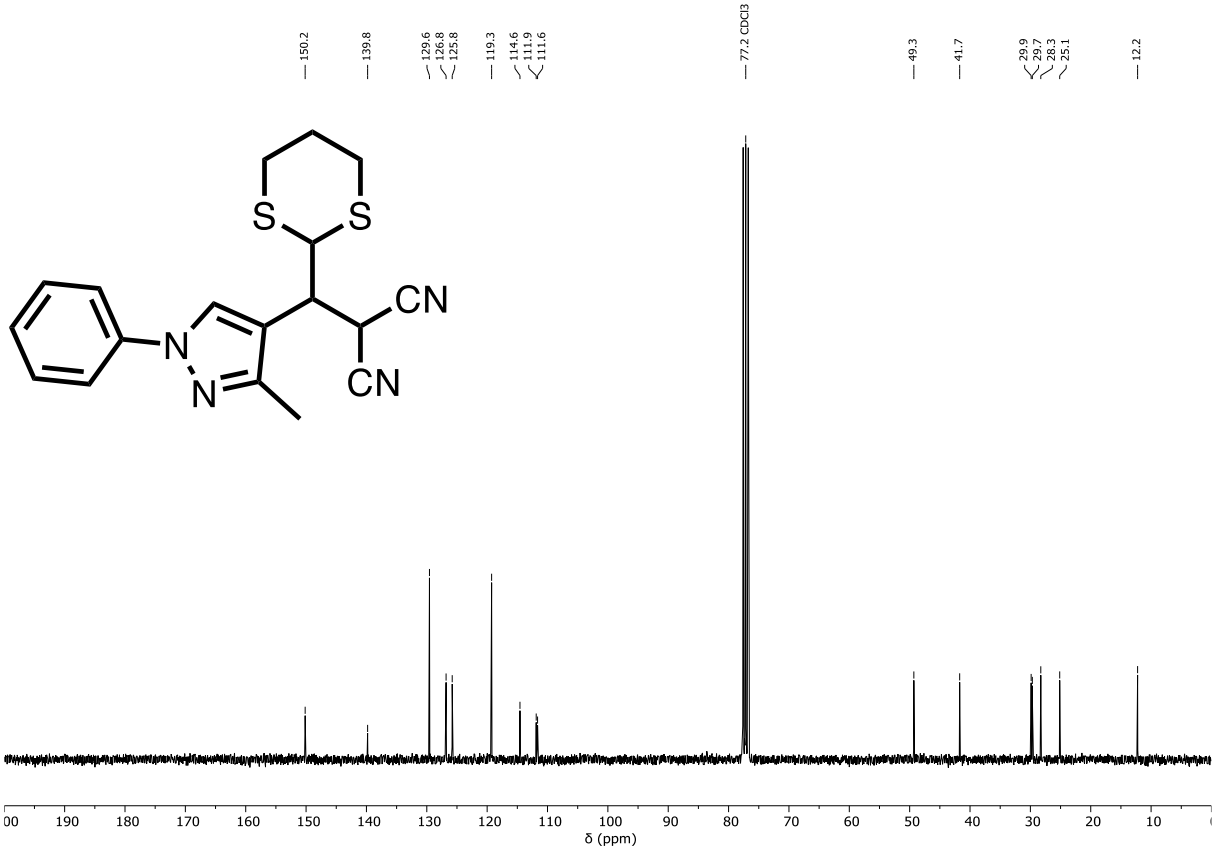
^{1}H NMR spectrum (300 MHz, $CDCl_3$) of **3s**



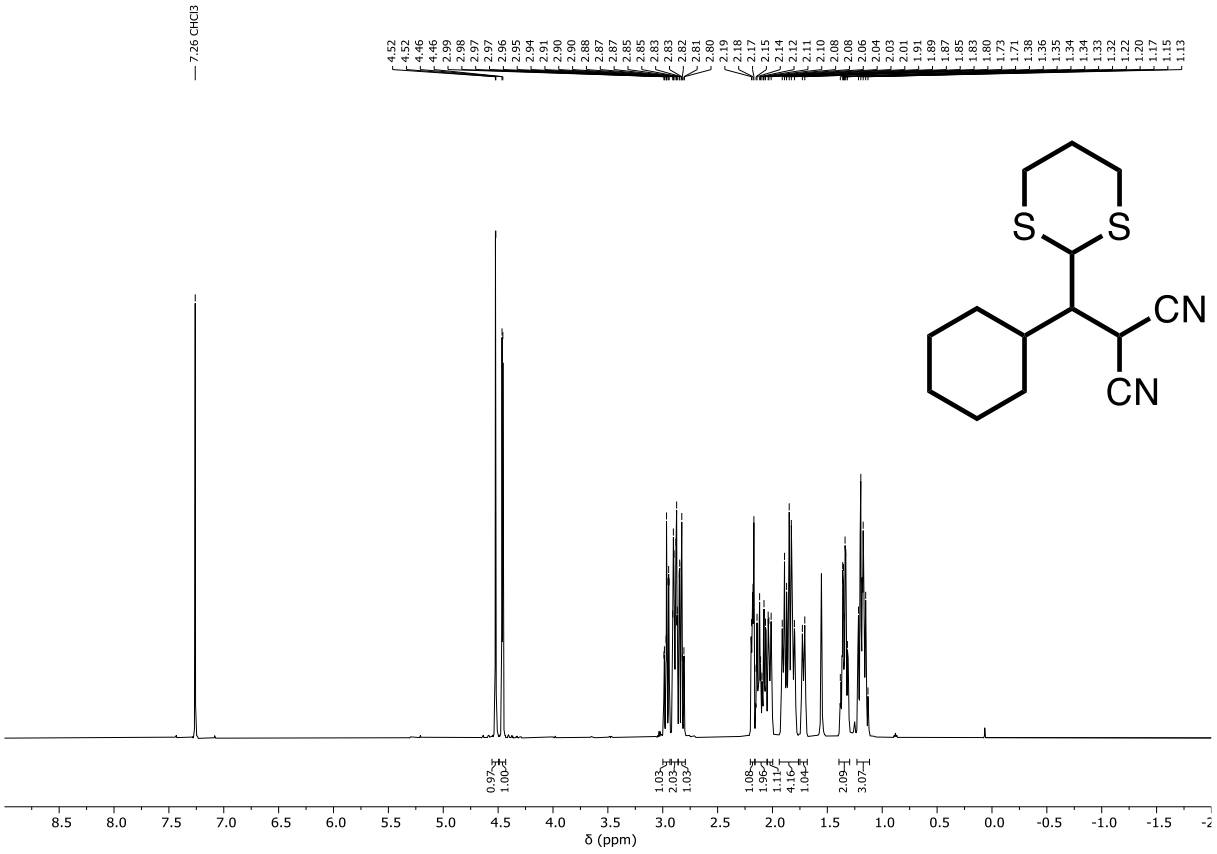
$^{13}C\{^{1}H\}$ NMR spectrum (75.5 MHz, $CDCl_3$) of **3s**



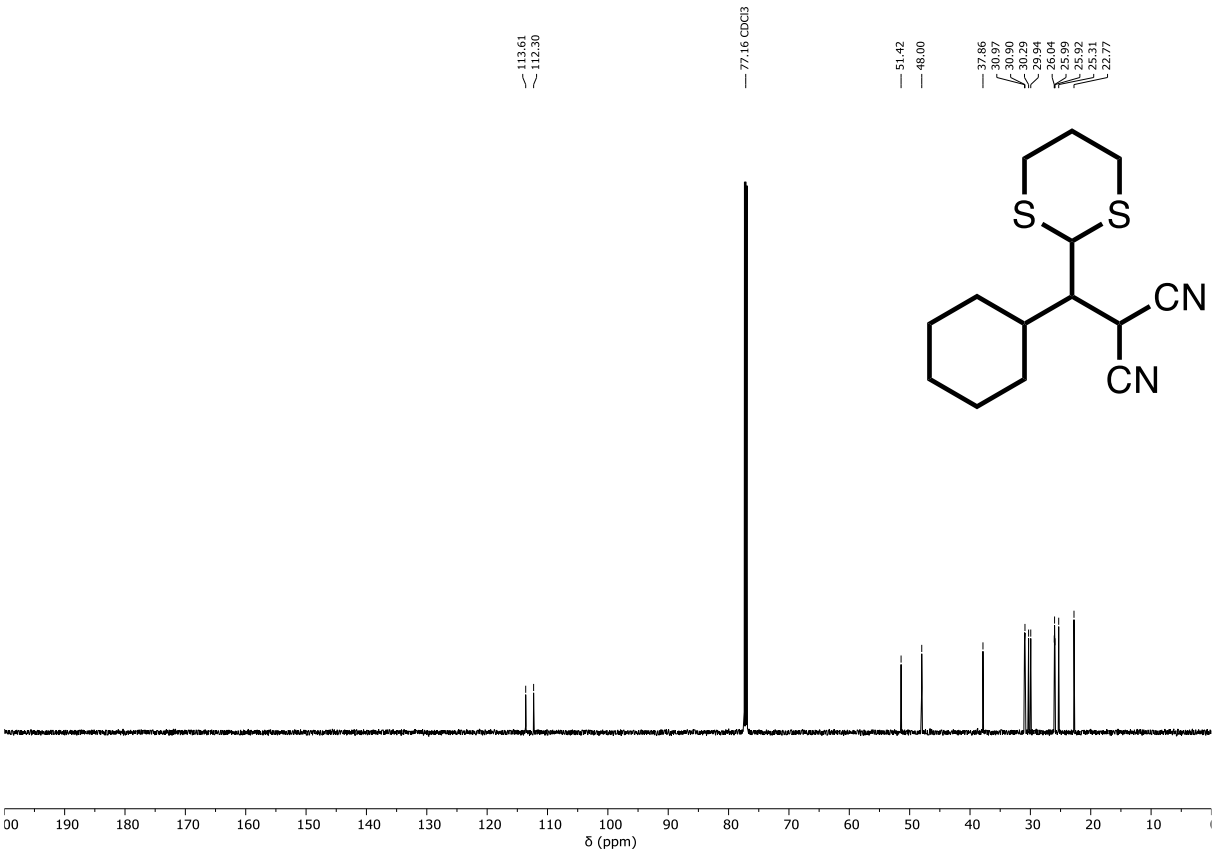
^{1}H NMR spectrum (300 MHz, $CDCl_3$) of **3t**



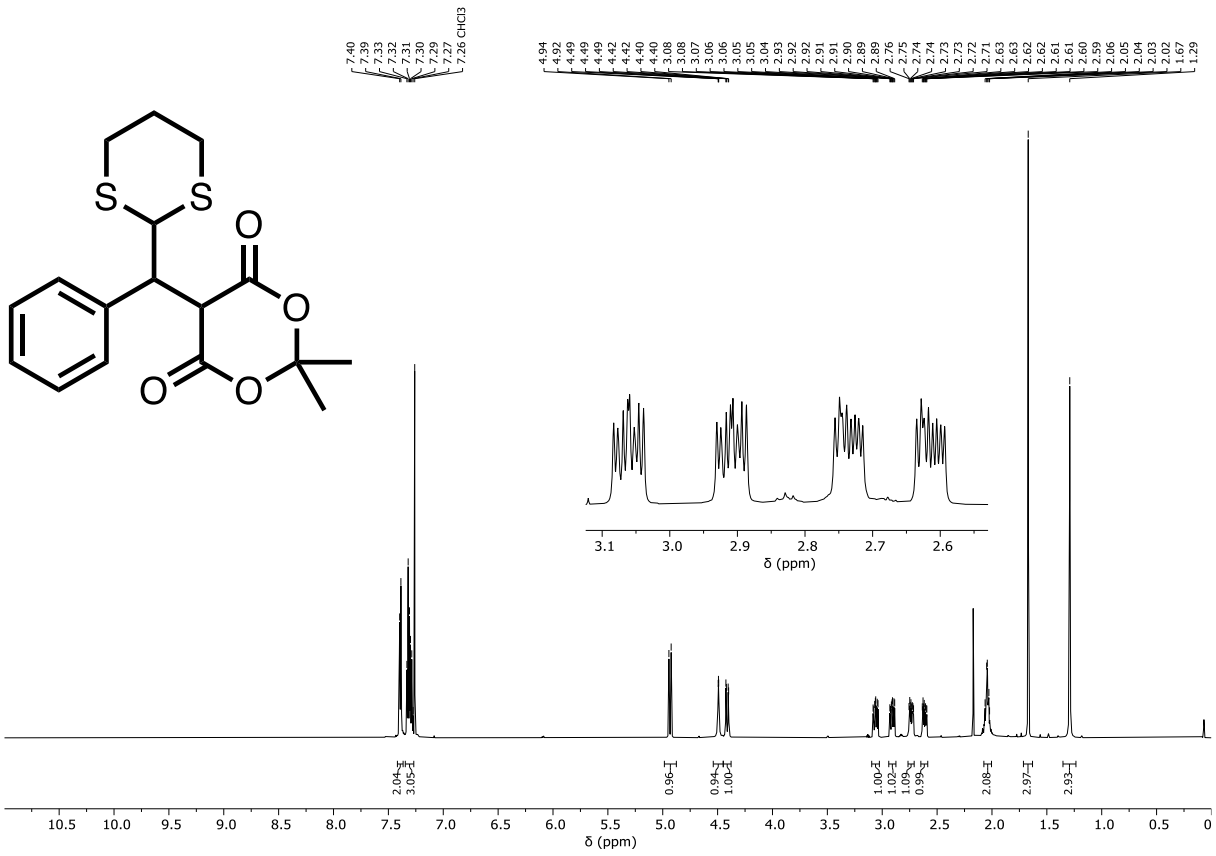
^{13}C{^{1}H} NMR spectrum (75.5 MHz, $CDCl_3$) of **3t**



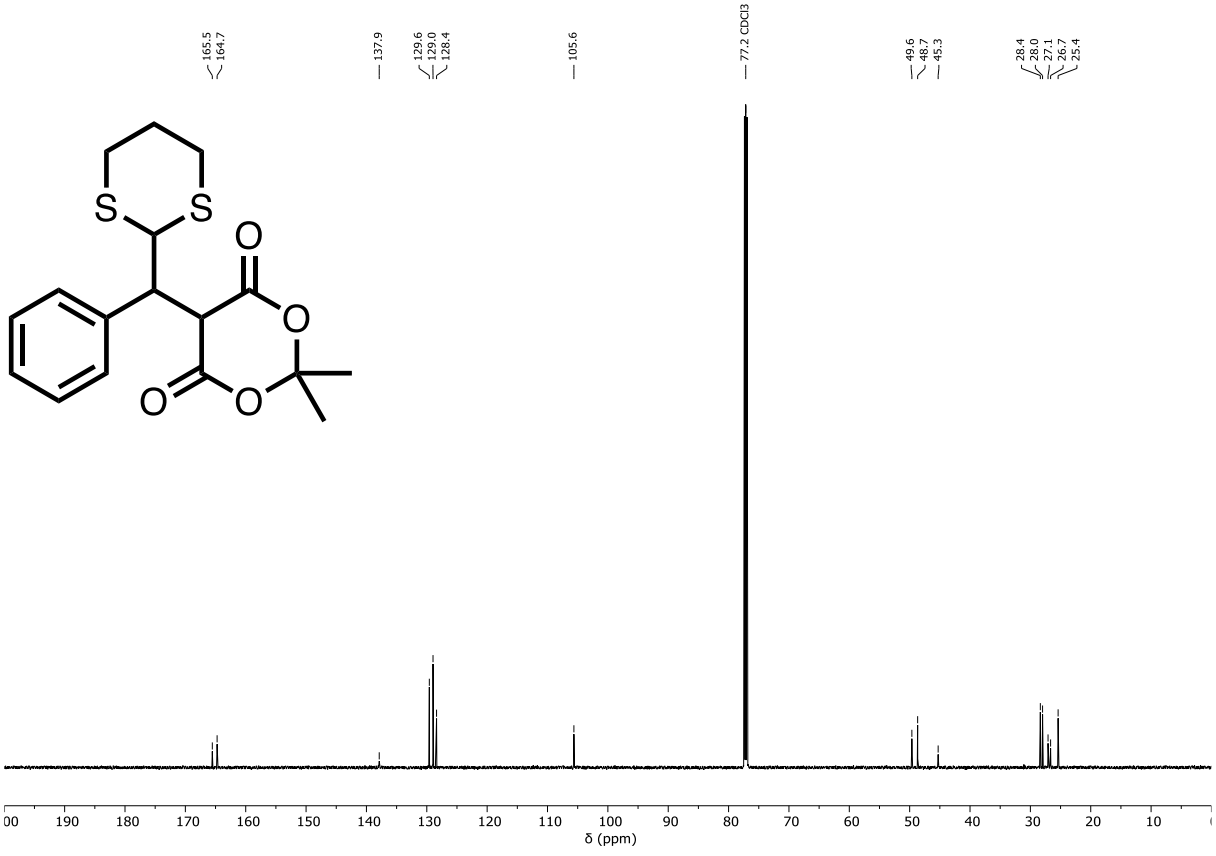
^{1}H NMR spectrum (300 MHz, $CDCl_3$) of **3u**



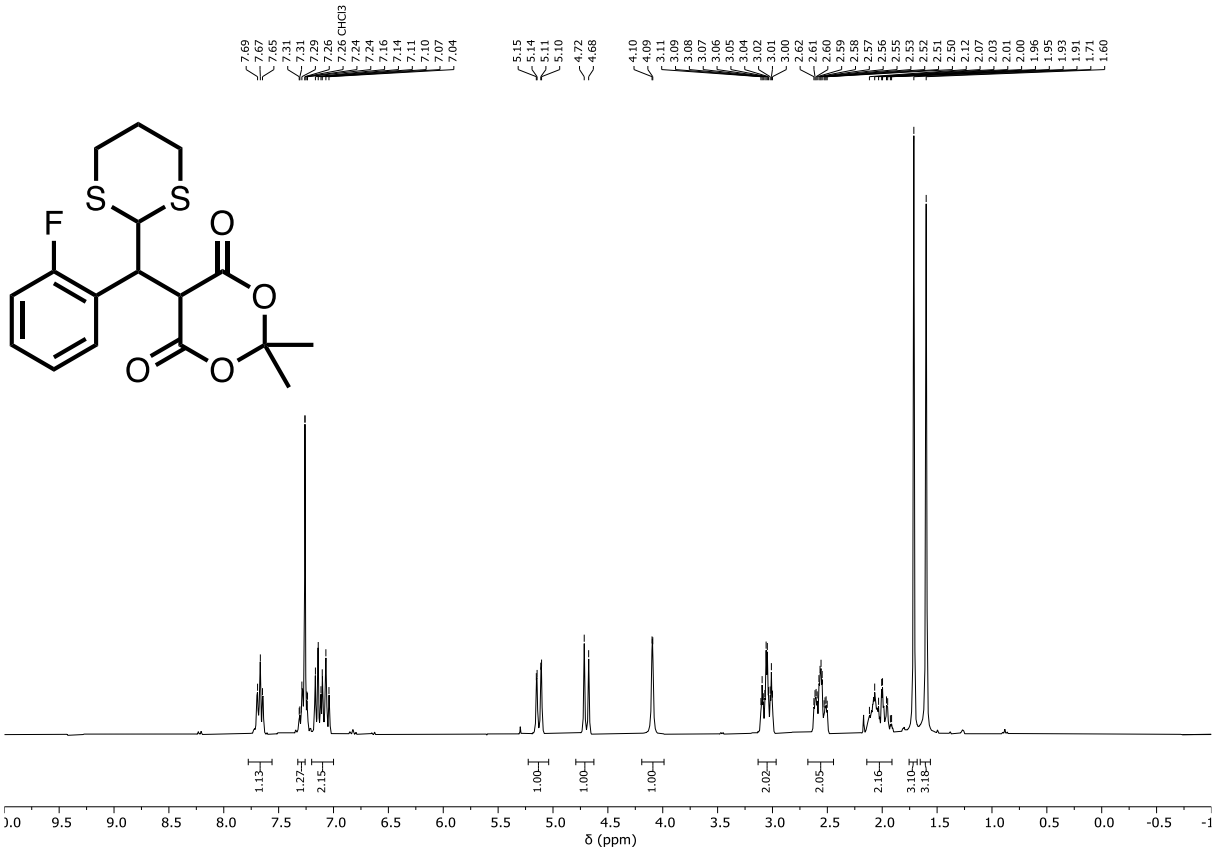
^{13}C{^{1}H} NMR spectrum (75.5 MHz, $CDCl_3$) of **3u**



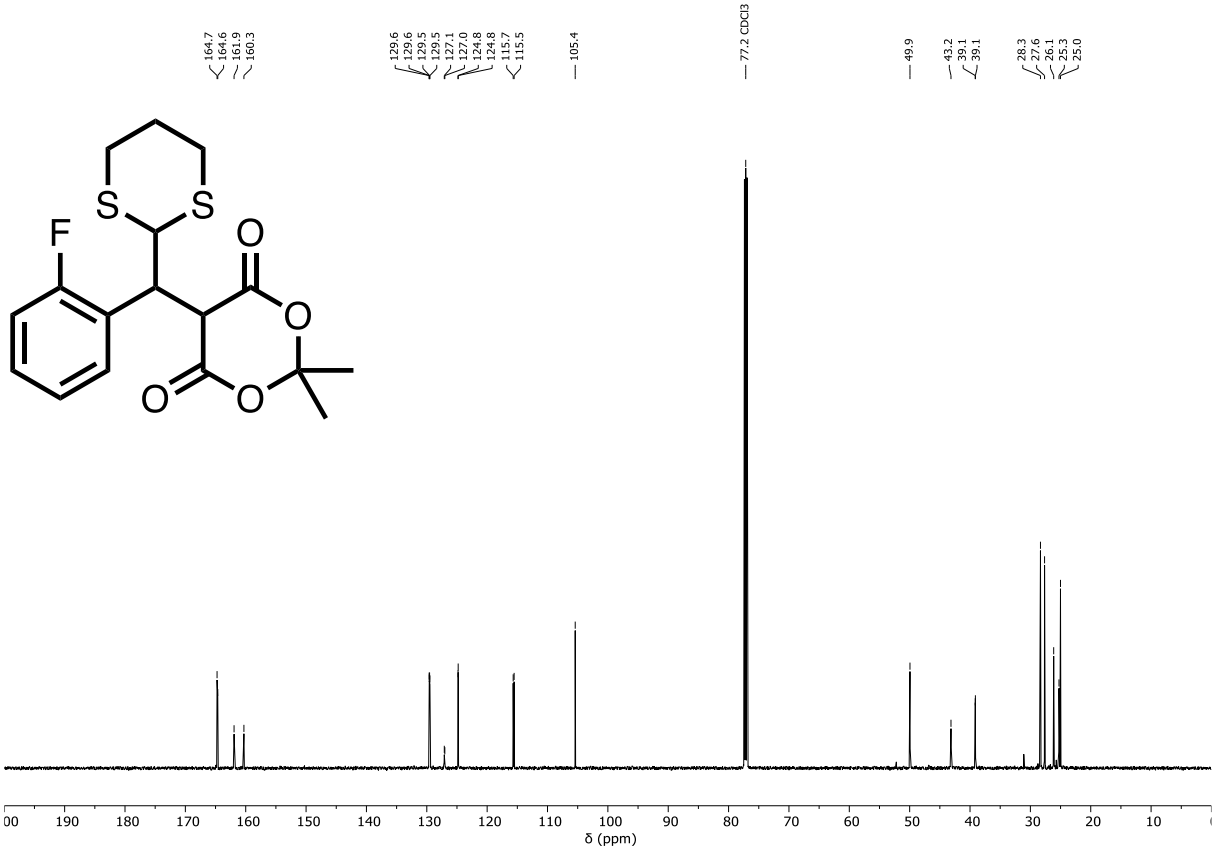
^{1}H NMR spectrum (600 MHz, $CDCl_3$) of **3y**



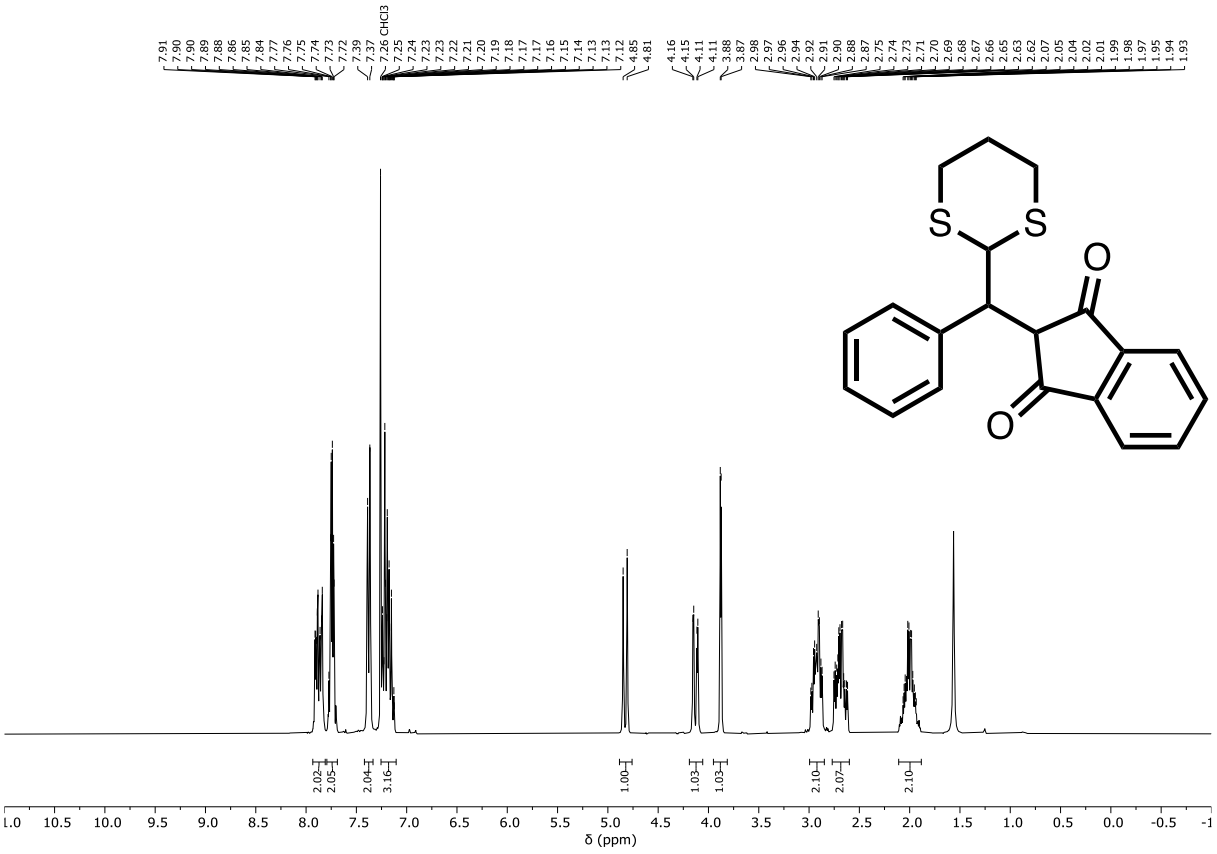
^{13}C{^{1}H} NMR spectrum (75.5 MHz, $CDCl_3$) of **3y**



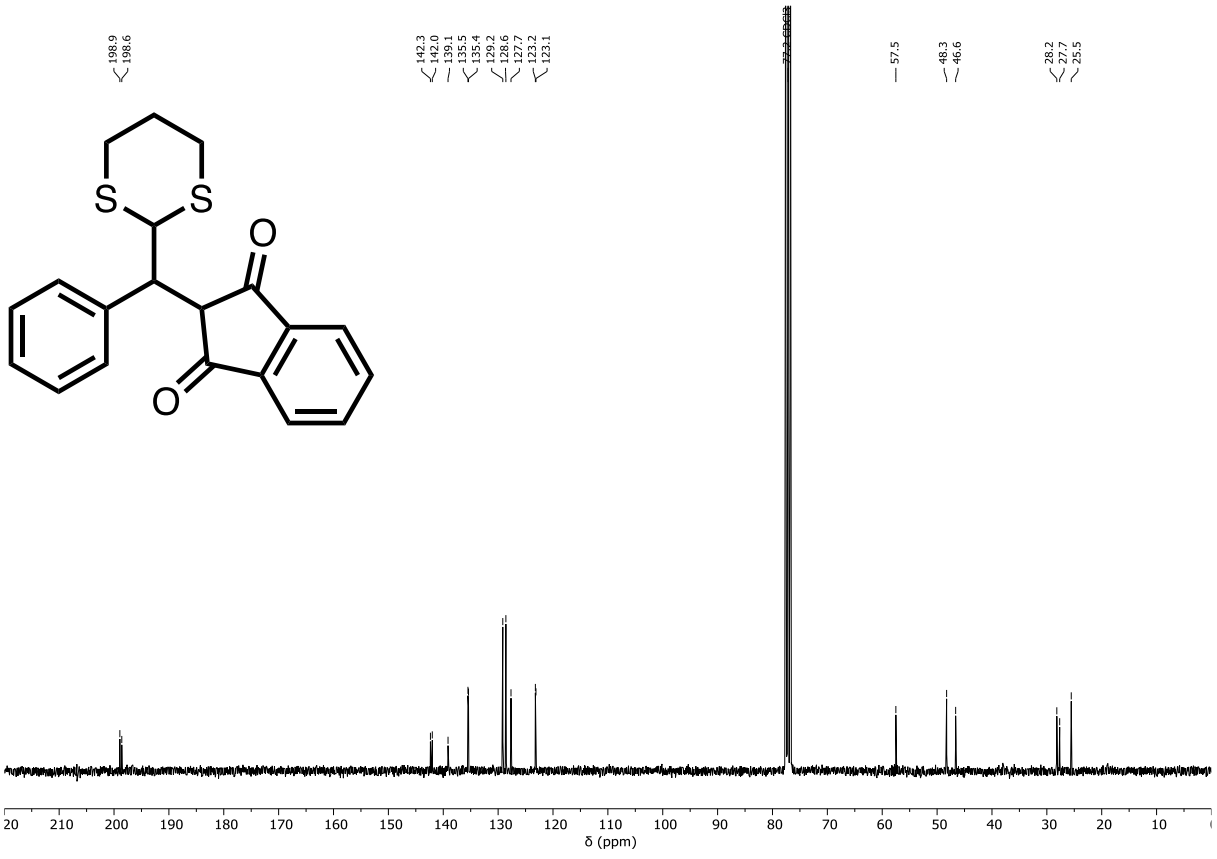
^{1}H NMR spectrum (300 MHz, $CDCl_3$) of **3z**



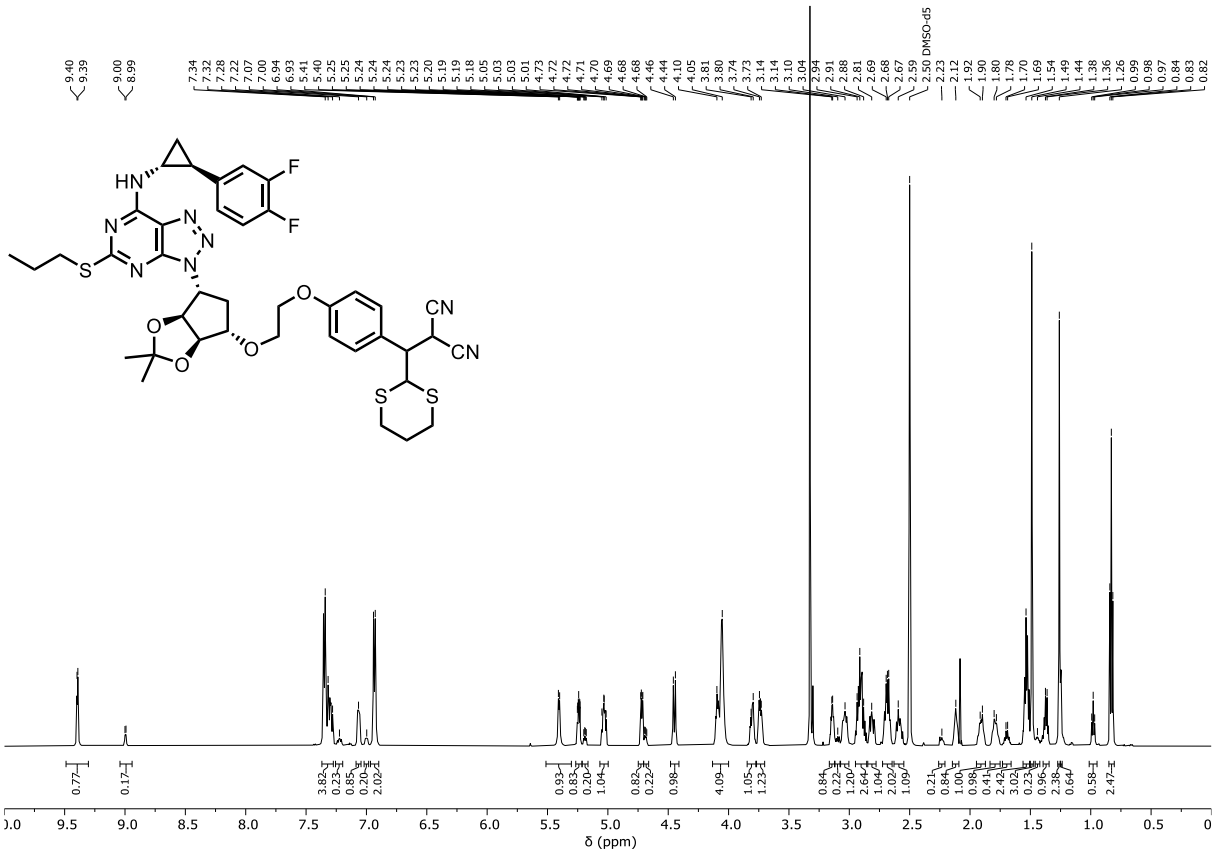
^{13}C{^{1}H} NMR spectrum (151 MHz, $CDCl_3$) of **3z**



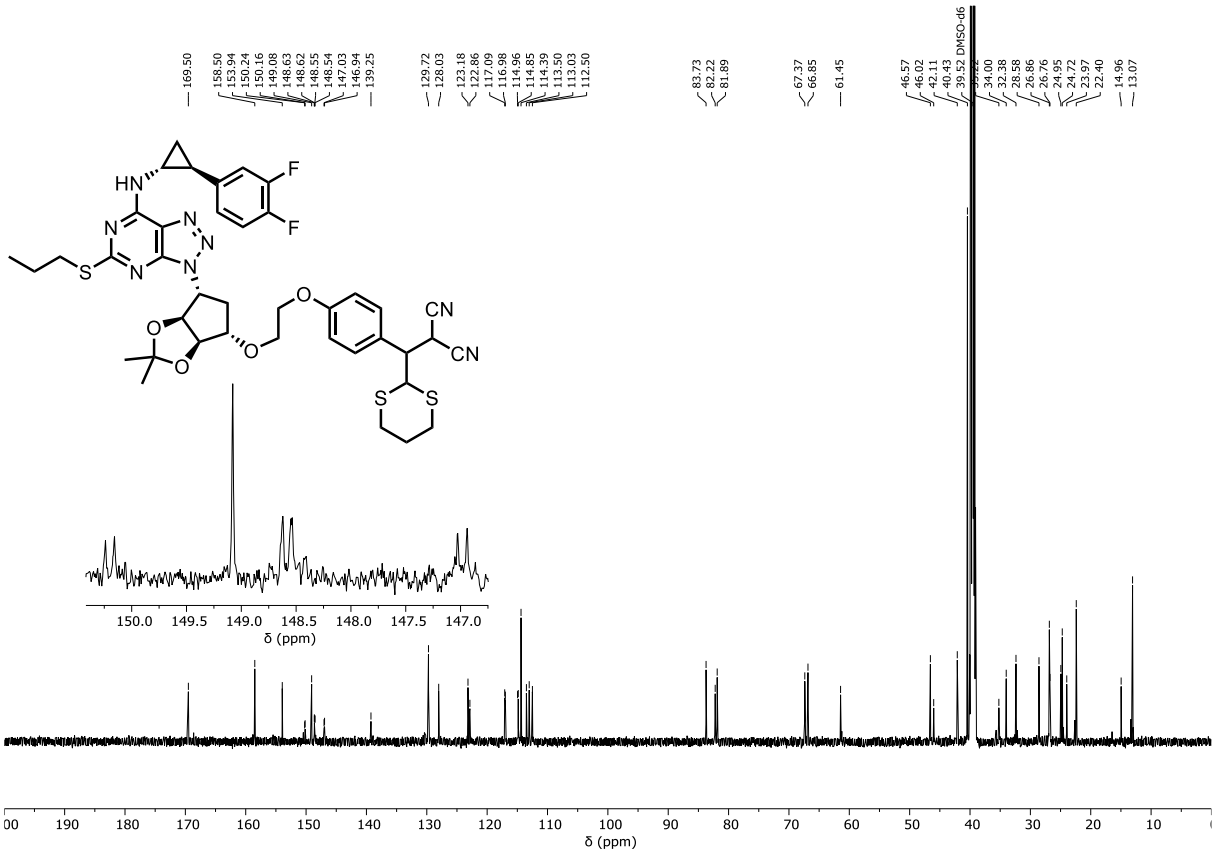
^{1}H NMR spectrum (300 MHz, $CDCl_3$) of **3ab**



^{13}C{^{1}H} NMR spectrum (75.5 MHz, $CDCl_3$) of **3ab**



^{1}H NMR spectrum (600 MHz, DMSO-d_6) of **3ac** (major + minor rotamer signals highlighted)

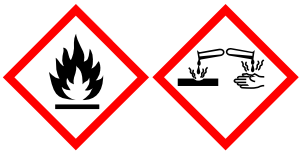


^{13}C{^{1}H} NMR spectrum (151 MHz, DMSO-d_6) of **3ac** (only minor rotamer signals highlighted)

Appendix

List of Used Chemicals

An alphabetical list of the chemicals used in this work as well as their GHS pictograms, signal words, hazard statements, and precautionary statements is given below. Safety information was obtained from the GESTIS Substance Database of the IFA (available online) or directly from vendors (Sigma-Aldrich, TCI Chemicals). All chemicals which appear in this work but are not listed in the table below are unknown substances which have not yet been classified according to Regulation (EC) No 1272/2008.

Name	Pictograms and Signal Words	Hazard Statements	Precautionary Statements
Acetic acid	 Danger	226, 314	210, 280, 301+330+331, 303+361+353, 305+351+338, 310
Acetic anhydride	 Danger	226, 302, 331, 314, 335	210, 260, 280, 303+361+353, 305+351+338, 312
Acetone, Acetone-d_6	 Danger	225, 319, 336, EUH066	210, 233, 240, 241, 242, 305+351+338
Acetonitrile, Acetonitrile-d_3	 Danger	225, 302+312+332, 319	210, 280, 301+312, 303+361+353, 304+340+312, 305+351+338
4-Acetyl-benzaldehyde	Not a hazardous substance or mixture according to Regulation (EC) No 1272/2008.		
4-Acetylbenzoic acid	Not a hazardous substance or mixture according to Regulation (EC) No 1272/2008.		

Name	Pictograms and Signal Words	Hazard Statements	Precautionary Statements
Acetyl chloride	 Danger	225, 314, EUH014, EUH071	210, 260, 280, 303+361+353, 305+351+338, P310
β-Alanine	Not a hazardous substance or mixture according to Regulation (EC) No 1272/2008.		
Ammonium bicarbonate	 Warning	302	301+312+330
Anisole	 Warning	226, 315, 319	210, 233, 241, 243, 280, 305+351+338
Benzaldehyde	 Danger	302, 332, 315, 319, 335, 360D, 411	273, 301+312, 302+352, 304+340+312, 305+351+338, 308+313
Benzene	 Danger	225, 304, 315, 319, 340, 350, 372 (Blood), 412	201, 210, 273, 301+330+331, 302+352, 308+313
Benzophenone imine	 Warning	315, 319, 335	261, 264, 271, 280, 302+352, 305+351+338

Name	Pictograms and Signal Words	Hazard Statements	Precautionary Statements
2-(1H-Benzotri-azol-1-yl)-1,1,3,3-tetramethyluronium hexafluorophosphate (HBTU)	 Warning	317	261, 272, 280, 302+352, 333+313, 362+364
Benzoyl chloride	 Danger	302+312, 332, 314, 317	280, 301+330+331, 303+361+353, 304+340, 305+351+338, 310
Benzyl acrylate	 Warning	315, 335, 411	261, 264, 271, 273, 280, 302+352
Benzylidene-malononitrile	 Warning	302+312+332, 315, 319, 335	261, 280, 301+312, 302+352+312, 304+340+312, 305+351+338
2,2'-Bipyridine	 Danger	301+311	264, 270, 280, 301+310, 302+352+312, 361+364
4,4'-Bis-(dimethylamino)-2,2'-bipyridine	 Warning	302+312+332, 315, 319	501, 261, 270, 271, 264, 280, 337+313, 305+351+338, 362+364, 332+313, 301+312+330, 302+352+312, 304+340+312,

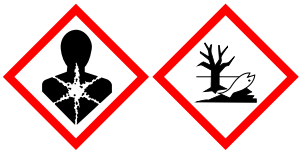
Name	Pictograms and Signal Words	Hazard Statements	Precautionary Statements
1,2-Bis(diphenyl-phosphino)ethane	 Warning	335	261, 271, 304+340+312, 403+233, 405, 501
1,1'-Bis(diphenyl-phosphino)ferrocene	 Warning	302+312+332	501, 261, 264, 280, 302+352+312, 304+340+312
4,4'-Bis-(trifluoromethyl)-2,2'-bipyridine	Not a hazardous substance or mixture according to Regulation (EC) No 1272/2008.		
Boc-Phe(4-Br)-OH	Not a hazardous substance or mixture according to Regulation (EC) No 1272/2008.		
Borane (1 M in THF)	 Danger	225, 260, 302, 318, 335, 336, 351	210, 231, 232, 280, 301+312, 305+351+338, 308+313
Boron trifluoride diethyl etherate	 Danger	226, 302+332, 314, 372 (Kidneys), 412	210, 273, 280, 303+361+353, 304+340+310, 305+351+338

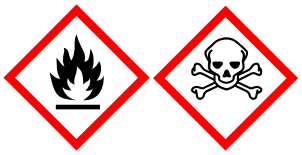
Name	Pictograms and Signal Words	Hazard Statements	Precautionary Statements
2-Bromo-4-*tert*-butylpyridine	 Warning	302, 315, 319, 332, 335	261, 280, 305+351+338
2-Bromo-5-methylthiazol	 Warning	315, 319	264, 280, 302+352, 337+313, 362+364, 332+313
2-Bromobenzonitrile	 Danger	301, 312, 319, 412	264, 273, 280, 301+310, 302+352+312, 305+351+338
2-Bromoquinoline	 Danger	302, 315, 318, 335	261, 264, 280, 301+312, 302+352, 305+351+338
2-*tert*-Butyl-1,1,3,3-tetramethylguanidine	 Danger	314	501, 280, 303+361+353, 301+330+331, 304+340+310, 305+351+338
4-Bromoacetanilide	Not a hazardous substance or mixture according to Regulation (EC) No 1272/2008.		
4'-Bromoacetophenone	 Warning	315, 319, 335	261, 264, 271, 280, 302+352, 305+351+338
3-Bromoaniline	 Danger	302, 312, 332, 315, 319, 335	261, 280, 301+312, 302+352, 304+340, 305+351+338

Name	Pictograms and Signal Words	Hazard Statements	Precautionary Statements
3-Bromoanisole	None	412	273
4-Bromoanisole	 Warning	302, 315	264, 270, 280, 301+312, 302+352, 332+313
3-Bromo-benzaldehyde	 Warning	302, 315, 319	501, 270, 264, 280, 302+352, 337+313, 305+351+338, 362+364, 332+313, 301+312+330
4-Bromo-benzaldehyde	 Warning	302, 315, 317, 319, 335	261, 264, 280, 301+312, 302+352, 305+351+338
4-Bromobenzene-sulfonamide	 Warning	302	None
4-Bromobenzonitrile	 Warning	302+312, 319, 412	264, 273, 280, 301+312, 302+352+312, 305+351+338
5-Bromo-1*H*-benzotriazole	 Warning	302	264, 270, 301+312, 501
4-Bromobenzo-trifluoride	 Warning	226, 315, 319	210, 302+352, 305+351+338

Name	Pictograms and Signal Words	Hazard Statements	Precautionary Statements
1-Bromo-2-chlorobenzene	 Warning	302+312+332, 315, 319	261, 264, 280, 337+313, 302+352+312, 304+340+312
1-Bromo-2-fluorobenzene	 Warning	226	210, 233, 240, 241, 242, 243
4-Bromo-2-fluoropyridine	 Danger	302, 315, 318, 335	261, 264, 280, 301+312, 302+352, 305+351+338
4-Bromo-*N*-methoxy-*N*-methylbenzamide	 Warning	315, 319	264, 280, 302+352, 337+313, 362+364, 332+313
9-Bromo-phenanthrene	Not a hazardous substance or mixture according to Regulation (EC) No 1272/2008.		
4-Bromophenol	 Warning	302, 315	264, 270, 280, 301+312, 302+352, 332+313
(4-Bromo-phenyl)acetylene	 Warning	302, 411	264, 270, 273, 301+312, 391, 501
4-Bromo-phenylboronic acid pinacol ester	Not a hazardous substance or mixture according to Regulation (EC) No 1272/2008.		
4-Bromophenyl trifluoromethane-sulfonate	 Danger	302, 318	264, 270, 280, 301+312, 305+351+338, 310, 330, 501

Name	Pictograms and Signal Words	Hazard Statements	Precautionary Statements
5-Bromopyrimidine	 Warning	315, 319, 335	261, 264, 271, 280, 302+352, 305+351+338
β-Bromostyrene	 Warning	302	501, 270, 264, 301+312+330
4-Bromothioanisole	 Warning	302	264, 270, 301+312, 501
5-Bromo-2-trifluoro-methyl-pyridine	 Danger	301, 315, 319	501, 270, 264, 280, 337+313, 301+310+330
tert-Butanol	 Danger	225, 332, 319, 335, 336	210, 233, 240, 241, 304+340+312, 305+351+338
4-(*tert*-Butoxy-carbonylamino)-cyclohexanone	 Warning	400	273
tert-Butyldimethylsi-lyl chloride	 Danger	228, 314, 411	210, 260, 273, 280, 303+361+353, 305+351+338, 310

Name	Pictograms and Signal Words	Hazard Statements	Precautionary Statements
Calcium chloride	 Warning	319	264, 280, 305+351+338, 337+313
Carbazole	 Warning	315, 319, 335, 351, 410	280, 332+313, 337+313, 261, 273, 305+351+338
Cesium carbonate	 Danger	318, 361f, 373	202, 260, 280, 305+351+338, 308+313+405
3-Chloro-benzaldehyde	 Warning	315, 319, 335	261, 264, 271, 280, 302+352, 305+351+338
4-Chloro-benzotrifluoride	 Warning	226, 317, 411	210, 233, 240, 273, 280, 303+361+353
Chloroform, Chloroform-*d*	 Danger	302, 331, 315, 319, 351, 361d, 336, 372 (Liver, Kidneys), 412	201, 273, 301+312+330, 302+352, 304+340+311, 308+313
Cinnamonitrile	 Warning	302+312+332, 315, 319	261, 264, 280, 337+313, 302+352+312, 304+340+312

Name	Pictograms and Signal Words	Hazard Statements	Precautionary Statements
2,4,6-Collidine	 Danger	226, 302+332, 311, 315, 319, 335	210, 280, 301+312, 303+361+353, 304+340+312, 305+351+338
Copper(II) sulfate	 Warning	302, 315, 319, 410	264, 270, 273, 301+312, 302+352, 305+351+338
3-Cyano-benzaldehyde	 Warning	315, 319, 335	261, 264, 271, 280, 302+352, 305+351+338
4-Cyano-benzaldehyde	 Warning	302+312+332	261, 264, 280, 301+312, 302+352+312, 304+340+312
Cyclohexanone	 Warning	226, 301+312+332, 315, 318	210, 280, 301+312+330, 302+352+312, 304+340+312, 305+351+338
Cyclohexyl-carboxaldehyde	 Warning	226, 315, 319, 335	210, 233, 240, 241, 303+361+353, 305+351+338
1,4-Diazabicyclo-[2.2.2]octane	 Danger	228, 302, 315, 318	210, 240, 280, 301+312, 302+352, 305+351+338

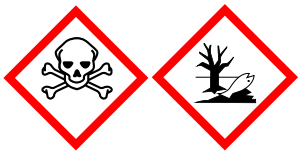
Name	Pictograms and Signal Words	Hazard Statements	Precautionary Statements
(*R*)-3,3'-Dibromo-2,2'-dimethoxy-1,1'-binaphthyl	 Warning	319, 335	261, 264, 271, 280, 304+340+312, 305+351+338
Dichloromethane	 Warning	315, 319, 336, 351	201, 302+352, 305+351+338, 308+313
Diethyl 2,6-dimethylpyridine-3,5-dicarboxylate	Not a hazardous substance or mixture according to Regulation (EC) No 1272/2008.		
Diethyl benzylidenemalonate	Not a hazardous substance or mixture according to Regulation (EC) No 1272/2008.		
Diethyl ether	 Danger	224, 302, 336, EUH019, EUH066	210, 233, 240, 241, 301+312, 403+233
Diethyl malonate	 Warning	319	264, 280, 305+351+338, 337+313
Dihydropyran	 Danger	225, 315, 317, 319, 412, EUH019	210, 233, 273, 280, 303+361+353, 305+351+338
Diisopropyl azodicarboxylate	 Warning	315, 319, 335, 351, 373, 411	202, 260, 273, 302+352, 305+351+338, 308+313

Name	Pictograms and Signal Words	Hazard Statements	Precautionary Statements
Diisopropyl-ethylamine	 Danger	225, 302, 318, 331, 335, 411	210, 273, 280, 301+312, 304+340+311, 305+351+338
2,2-Dimethoxy-acetaldehyde (60 wt.% in water)	 Warning	317	261, 272, 280, 302+352, 333+313, 362+364
4,4'-Dimethoxy-2,2'-bipyridine	 Warning	315, 319	264, 280, 302+352, 337+313, 362+364, 332+313
2,2-Dimethoxy-propane	 Danger	225, 319	210, 233, 240, 241, 242, 305+351+338
N,*N*-Dimethyl-acetamide	 Danger	312+332, 319, 360D	202, 280, 302+352+312, 304+340+312, 305+351+338, 38+313
Dimethyl 2,2'-bipyridine-4,4'-dicarboxylate	 Danger	315, 318, 335	261, 264, 271, 280, 302+352, 305+351+338

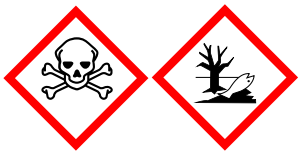
Name	Pictograms and Signal Words	Hazard Statements	Precautionary Statements
N,*N*-Dimethyl-formamide	 Warning	226, 312+332, 319, 360D	201, 210, 302+352, 305+351+338, 308+313
Dimethyl sulfoxide-d_6	Not a hazardous substance or mixture according to Regulation (EC) No 1272/2008.		
Dipivaloylmethane	Not a hazardous substance or mixture according to Regulation (EC) No 1272/2008.		
4,4'-Di-*tert*-butyl-2,2'-bipyridine	 Danger	301+311	264, 280, 301+310, 302+352+312, 361+364, 405
2,6-Di-*tert*-butyl-4-methylpyridine	 Warning	302, 315, 319, 335	261, 264, 270, 301+312, 302+352, 305+351+338
Eosin Y disodium salt	 Warning	317, 319	261, 264, 272, 280, 302+352, 305+351+338
Ethanol	 Danger	225, 319	210, 233, 240, 241, 242, 305+351+338
Ethyl acetate	 Danger	225, 319, 336, EUH066	210, 233, 240, 241, 242, 305+351+338

Name	Pictograms and Signal Words	Hazard Statements	Precautionary Statements
Ethyl acetoacetate	Not a hazardous substance or mixture according to Regulation (EC) No 1272/2008.		
Ethyl cinnamate	Not a hazardous substance or mixture according to Regulation (EC) No 1272/2008.		
4-Ethynyl-benzaldehyde	 Warning	315, 319	264, 280, 302+352, 337+313, 362+364, 332+313
Ezetimibe	Not a hazardous substance or mixture according to Regulation (EC) No 1272/2008.		
Fluorenone	 Warning	319, 411	264, 273, 280, 305+351+338, 337+313, 391
2-Fluoro-benzaldehyde	 Warning	315, 319, 226	210, 264, 280, 370+378, 337+313, 303+361+353
3-Formylphenyl boronic acid	 Danger	314	280, 305+351+338, 310
Hydrochloric acid (37%)	 Danger	290, 314, 335	234, 261, 271, 280, 303+361+353, 305+351+338
4-Hydroxy-benzaldehyde	 Danger	318	280, 305+351+338

Name	Pictograms and Signal Words	Hazard Statements	Precautionary Statements
3-Hydroxy-benzaldehyde	 Warning	315, 319	264, 280, 302+352, 305+351+338, 332+313, 337+313
Imidazole	 Danger	302, 314, 360D	260, 280, 301+312, 303+361+353, 304+340+310, 305+351+338
4-Iodobenzaldehyde	 Warning	315, 319	264, 280, 302+352, 337+313, 362+364, 332+313
4-Iodo-benzotrifluoride	 Warning	315, 319	264, 280, 302+352, 337+313, 362+364, 332+313
Isobutyrophenone	 Warning	315, 319	264, 280, 302+352, 337+313, 362+364, 332+313
Isopropanol	 Danger	225, 319, 336	210, 233, 240, 241, 242, 305+351+338
2,6-Lutidine	 Warning	226, 302, 315, 319	210, 233, 240, 301+312, 303+361+353, 305+351+338
Magnesium sulfate	Not a hazardous substance or mixture according to Regulation (EC) No 1272/2008.		

Name	Pictograms and Signal Words	Hazard Statements	Precautionary Statements
Malonic acid	 Danger	318	280, 305+351+338
Malononitrile	 Danger	300, 311, 331, 317, 319, 410	273, 280, 304+340, 305+351+338, 311
Meldrum's acid (2,2-Dimethyl-1,3-dioxane-4,6-dione)	Not a hazardous substance or mixture according to Regulation (EC) No 1272/2008.		
Methanol	 Danger	225, 301+311+331, 370 (Eyes)	210, 233, 280, 301+310, 303+361+353, 304+340+311
4-Methoxyphenyl tri-fluoromethane-sulfonate	 Warning	315, 319	264, 280, 337+313, 305+351+338, 302+352, 332+313, 362
Methyl chloroformate	 Danger	225, 302+312, 314, 330	210, 280, 301+312, 303+361+353, 304+340+310, 305+351+338
3-Methyl-1-phenyl-1*H*-pyrazole-4-carboxaldehyde	Not a hazardous substance or mixture according to Regulation (EC) No 1272/2008.		
Methyl phenyl sulfone	 Warning	302	501, 270, 264, 301+312+330

Name	Pictograms and Signal Words	Hazard Statements	Precautionary Statements
4-(Methylsulfonyl)-benzaldehyde	 Warning	302, 315, 319, 335	261, 264, 270, 301+312, 302+352, 305+351+338
4-(Methylthio)-benzaldehyde	Not a hazardous substance or mixture according to Regulation (EC) No 1272/2008.		
Nickel(II) 2,2,6,6-tetramethyl-3,5-heptanedionate	 Danger	302+312+332, 350	202, 280, 301+312, 302+352+312, 304+340+312, 308+313
Nickel(II) acetylacetonate	 Danger	302+312, 317, 334, 341, 350	202, 261, 280, 301+312, 302+352+312, 308+313
Nickel(II) bromide dimethoxyethane adduct	 Danger	228, 317, 332, 334, 341, 351, 361f, 372, 410	202, 210, 273, 280, 302+352, 308+313
Nickel(II) chloride dimethoxyethane adduct	 Danger	261, 301, 315, 319, 334, 350, 400	202, 231+232, 273, 301+310, 302+352, 305+351+338

Name	Pictograms and Signal Words	Hazard Statements	Precautionary Statements
4-Nitrobenzaldehyde	 Warning	317, 319	261, 264, 272, 280, 302+352, 305+351+338
Pentane	 Danger	225, 304, 336, 411, EUH066	210, 233, 240, 273, 301+310, 331
1,10-Phenanthroline	 Danger	301, 410	264, 270, 273, 301+310, 391, 405
Pinacol	 Warning	315, 319	264, 280, 302+352, 337+313, 362+364, 332+313
Piperidine	 Danger	225, 302, 311+331, 314	210, 280, 301+312, 303+361+353, 304+340+310, 305+351+338
Potassium carbonate	 Warning	315, 319, 335	261, 264, 271, 280, 302+352, 305+351+338
Potassium dihydrogen phosphate	Not a hazardous substance or mixture according to Regulation (EC) No 1272/2008.		

Name	Pictograms and Signal Words	Hazard Statements	Precautionary Statements
Potassium hydrogen phosphate	Not a hazardous substance or mixture according to Regulation (EC) No 1272/2008.		
Potassium phosphate	 Danger	318, 335	261, 271, 280, 304+340+312, 305+351+338, 403+233
1,3-Propanedithiol	 Warning	302, 315, 319	501, 270, 264, 280, 337+313, 301+312+330
Pyridine	 Danger	225, 302+312+332, 315, 319	210, 280, 301+312, 303+361+353, 304+340+312, 305+351+338
Rhodamine B	 Danger	302, 318, 412	264, 273, 280, 301+312, 305+351+338, 501
Sodium ascorbate	Not a hazardous substance or mixture according to Regulation (EC) No 1272/2008.		
Sodium bicarbonate	Not a hazardous substance or mixture according to Regulation (EC) No 1272/2008.		
Sodium borohydride	 Danger	260, 301, 314, 360FD, EUH014	231+232, 260, 280, 303+361+353, 304+340+310, 305+351+338

Name	Pictograms and Signal Words	Hazard Statements	Precautionary Statements
Sodium hydroxide	 Danger	290, 314	234, 260, 280, 303+361+353, 304+340+310, 305+351+338
Sodium sulfate	Not a hazardous substance or mixture according to Regulation (EC) No 1272/2008.		
Terephthalaldehyde mono(diethyl acetal)	 Warning	319, 315, 335	261, 302+352, 280, 305+351+338
Tetrahydrofuran	 Danger	225, 302, 319, 335, 336, 351, EUH019	210, 280, 301+312+330, 305+351+338, 370+378, 403+235
2,4,5,6-Tetrakis(9*H*-carbazol-9-yl)-isophthalonitrile (4CzIPN)	Not a hazardous substance or mixture according to Regulation (EC) No 1272/2008.		
Ticagrelor	Not a hazardous substance or mixture according to Regulation (EC) No 1272/2008.		
Titanium tetrachloride	 Danger	314, 330, 335, EUH014	260, 271, 280, 303+361+353, 304+340+310, 305+351+338
Toluene	 Danger	225, 315, 361d, 336, 373 (Central Nervous System), 304, 412	202, 210, 273, 301+310, 303+361+353, 331

Name	Pictograms and Signal Words	Hazard Statements	Precautionary Statements
para-Toluene-sulfonic acid monohydrate	 Warning	315, 319, 335	261, 264, 271, 280, 302+352, 305+351+338
Triethylamine	 Danger	225, 301+311+331, 314, 335	210, 280, 301+312, 303+361+353, 304+340+310, 305+351+338
Triethylsilane	 Danger	225, 410	210, 303+361+353, 403+233
Trifluoroacetic acid	 Danger	290, 331, 314, 412, EUH071	260, 273, 280, 303+361+353, 305+351+338, 312
4-(Trifluoromethyl)-benzaldehyde	 Warning	302, 315, 319, 227	501, 270, 210, 264, 280, 302+352, 370+378, 337+313, 305+351+338, 362+364, 332+313, 301+312+330, 403+235
Triisopropylsilyl chloride	 Danger	314	280, 303+361+353, 304+340+310, 305+351+338, 363, 405
1,3,5-Trimethox-ybenzene	 Warning	302	264, 270, 301+312, 501

Name	Pictograms and Signal Words	Hazard Statements	Precautionary Statements
Triphenylphosphine	 Danger	302, 317, 318, 372 (Central Nervous System, Peripheral Nervous System)	260, 280, 301+312, 302+352, 305+351+338, 314
2,4,6-Tris(diphenylamino)-3,5-difluorobenzonitrile (3DPA2FBN)	Not a hazardous substance or mixture according to Regulation (EC) No 1272/2008.		
2,4,6-Tris(diphenylamino)-5-fluoroisophthalonitrile (3DPAFIPN)	Not a hazardous substance or mixture according to Regulation (EC) No 1272/2008.		
L-Valine methyl ester hydrochloride	Not a hazardous substance or mixture according to Regulation (EC) No 1272/2008.		
Zidovudine (AZT)	 Warning	341, 351	201, 202, 280, 308+313, 405, 501

Acknowledgements

My biggest thanks of course go to Prof. Dr. Axel Jacobi von Wangelin, not only for believing in me and urging me to seek the *Fast Track* scholarship of the Hamburg Research Academy which allowed me to start my PhD directly after finishing my bachelor thesis in this group, but also for your constant input and ideas, countless (late-night) chemical discussions, and unwaivering support also regarding my future!

Special thanks are in order for Dr. Dieter Schaarschmidt for your tireless efforts in making sure things run smoothly in our group, like ordering chemicals and new equipment.

I'm tremendously grateful to Dr. Luana Cardinale for taking me as your bachelor student and being my lab mate and mentor throughout the first year of my PhD. You taught me everything I know about practical photoredox catalysis and much more, and this work wouldn't have been possible without you!

Of course, I thank each and every current and former member of this group: Dr. Yannik Appiarius, Thilo Baggendorf, Ben Bimberg, Dr. Uttam Chakraborty, Dr. Andrey Fedulin, Dr. Pradip Ghosh, Dr. Bernhard Gregori, Ankita Haldar, Finn Höeg, Till Jahny, Tim-Oliver "TOK" Kindler, Dr. Mikhail Konev, Gleb Kubrin, Chiara Looks, Lea Luxenberger, Roderich Meißner, Constanze von Meyenn, Jie Qi "Jackie" Ng, Nils Nun, Stefano Piacentini, Dr. Jennifer "Jenny" Pölker, Dr. Javier Recio Ramos, Dr. Ursula Rastetter, Dr. Sebastian Sandl, Dr. Carl Schiller, Dr. Robin Stuhr, and Dr. Ignacio Erazo Valdés. These past five years have been a blast!

Special thanks to Fabian Lüttchens, and "my" master student Dorottya "Dorka" Mikoczi for your considerable support during this work. Your contributions are indispensable and have more than enabled some of the projects in this thesis!

I also thank Margarethe "Maggie" Fritz, Thomas Schuld, and Martin Stürminger – lab technicians are the unsung heroes of any working group! No less important are our secretaries Charlotte Navitzkas, Sofia Paleari, and Christina Redlbeck.

This work was generously financially supported by the Hamburg Research Academy as part of the Fast-Track Program (2020–2022) and by the Evonik Stiftung as part of the Werner-Schwarze-Stipendium (2022–2024). Big thanks to all the friendly people involved for making this work possible at all, including the opportunity for meet-ups with other scholarship holders and much more!

Last but not least I would like to thank Prof. Dr. Gerrit Luinstra as well as Prof. Dr. Ralph Holl and Prof. Dr. Lisa Vondung for kindly agreeing to be my examiners.

Eidesstattliche Erklärung

„Hiermit versichere ich an Eides statt, die vorliegende Dissertationsschrift selbst verfasst und keine anderen als die angegebenen Quellen und Hilfsmittel benutzt zu haben. Sofern im Zuge der Erstellung der vorliegenden Dissertationsschrift generative Künstliche Intelligenz (gKI) basierte elektronische Hilfsmittel verwendet wurden, versichere ich, dass meine eigene Leistung im Vordergrund stand und dass eine vollständige Dokumentation aller verwendeten Hilfsmittel gemäß der Guten wissenschaftlichen Praxis vorliegt. Ich trage die Verantwortung für eventuell durch die gKI generierte fehlerhafte oder verzerrte Inhalte, fehlerhafte Referenzen, Verstöße gegen das Datenschutz- und Urheberrecht oder Plagiate."

Hamburg, den 15.09.2025

Mattis-Ole Schmotz